Backward Erosion Piping

Author:
Allan, Rebecca

Publication Date:
2018

DOI:
https://doi.org/10.26190/unsworks/3441

Backward Erosion Piping

Rebecca Jane Allan

A thesis in fulfillment of the requirements for the degree of

Doctor of Philosophy

School of Civil and Environmental Engineering

Faculty of Engineering

The University of New South Wales

April 12, 2018

THE UNIVERSITY OF NEW SOUTH WALES
Thesis/Dissertation Sheet

Surname or Family name: **Allan**

First name: **Rebecca** Other name/s: **Jane**

Abbreviation for degree as given in the University calendar: **PhD**

School: **School of Civil and Environmental Engineering** Faculty: **Faculty of Engineering**

Title: **Backward Erosion Piping**

Abstract 350 words maximum

Backward Erosion Piping is an internal erosion mechanism which occurs beneath embankment dams and levees founded on soil. When the foundation contains uniform sand, backward erosion becomes the major cause of incidents and failures. Yet, despite extensive research over the past century, a robust and accurate method for predicting backward erosion has been elusive. This study provides new insights into many aspects of backward erosion and provides improvements to existing prediction methods, with the use of a comprehensive suite of 92 large-scale laboratory flume experiments.

For the first time, the four exit geometries of slope, plane, slot and circle were tested in otherwise identical flumes. Experimental results and complementary numerical modelling demonstrated that exit geometries with more confined outflow areas required both lower initiation and critical gradients because these exits caused higher seepage velocities at both the exit and channel tip, thus needing less gradient to generate necessary erosive forces.

Few studies had investigated internally stable soils with uniformity coefficients above 3, therefore, seven of these soils were tested. Critical gradients increased exponentially with increase in uniformity and with decrease in permeability at a constant tip width. Additionally, the tip width increased linearly with d_{50}. The latter two findings were combined to form a new empirical model with a coefficient of correlation of 0.95.

To investigate the industry's concern that critical gradient decreases with subsequent floods, novel tests were loaded in cycles. The critical gradient did decrease in experiments by 2-13% but not due to cyclic loading. In fact, gradients needed under cyclic loading were higher than under constant loading. It was due to an increase in permeability as the channel lengthened.

An unprecedented investigation into the rate of backward erosion revealed an average channel advance rate of 3mm/minute at critical gradient and a 3-fold increase in this rate with each 10% increment in gradient above critical (in 0.3mm uniform sand).

Using experimental results from both this present study and those undertaken by others, an assessment was made of the two most widely used prediction methods- Schmertmann (2000) and Sellmeijer et al. (2011). In doing so, modifications are recommended to improve model performance in forms suitable for industry use.

Originality Statement

'I hereby declare that this submission is my own work and to the best of my knowledge it contains no materials previously published or written by another person, or substantial proportions of material which have been accepted for the award of any other degree or diploma at UNSW or any other educational institution, except where due acknowledgement is made in the thesis. Any contribution made to the research by others, with whom I have worked at UNSW or elsewhere, is explicitly acknowledged in the thesis. I also declare that the intellectual content of this thesis is the product of my own work, except to the extent that assistance from others in the project's design and conception or in style, presentation and linguistic expression is acknowledged.'

Rebecca Jane Allan
April 12, 2018

Copyright Statement

Authenticity Statement

'I certify that the Library deposit digital copy is a direct equivalent of the final officially approved version of my thesis. No emendation of content has occurred and if there are any minor variations in formatting, they are the result of the conversion to digital format.'

Rebecca Jane Allan
April 12, 2018

Acknowledgements

Firstly, acknowledgement and thanks must go to my supervisors, Dr. Kurt Douglas and A/Prof. Bill Peirson for their guidance, support and patience. I am particularly grateful for Kurt's practical ideas in the laboratory and his concern for my well-being as well as Bill's insight into numerical modelling and his continual encouragement despite my often low spirits. I am also thankful for both meeting with me at the Water Research Laboratory (WRL), especially considering the long drive required.

To E/Prof. Robin Fell, for initiating this research project, encouraging me to apply for this valuable opportunity and accommodating my sensitive nature. And to the sponsors of this project and their representatives who attended committee meetings: Dr. Mark Foster, Chris Topham, Malcolm Barker, David Jeffery, Brian Cooper, Steve Knight, David Ryan, Michael Somerford, Michael Smith, Dr. Robert Wilson, Dr. Gamini Adikari, Mark Arnold, Thomas Kuen, Cristian Andersson and Hans Rönnqvist. Thank you for your attendance, technical feedback and support.

Larry Paice and Robert Jenkins laboured over fabrication and construction of laboratory equipment with much skill and care- thank you. Hamish Studholme not only ran and documented many experiments but also provided good company in the laboratory. Honour students Bronson Forward, Edmund Han and Angela Greenlees assisted with experiments and, through supporting them, encouraged me to see that I had learnt things and could still be passionate about backward erosion piping. Thanks also go to my fellow PhD candidates at WRL, for sharing this challenging journey with me with friendship and laughs (and many languages).

I very much treasure the love and support I receive from my family; they are my rock. And I could not have crossed the finish line without the love and encouragement (and hours of proof reading) from my fiancé, Elliott. Thank you. I also received invaluable reassurance and prayers from my church family and friends. Lastly, yet most significantly, I give thanks to God. *"For we are God's handiwork, created in Christ Jesus to do good works, which God prepared in advance for us to do."* Ephesians 2:10

This research was undertaken in partnership between:

Australian Research Council; UNSW Australia; Department of Public Works, New South Wales; Dam Safety Committee of New South Wales; Murray Darling Basin Authority, ACT; Water Corporation, Western Australia; Southern Water, Tasmania; Hydro Tasmania, Tasmania; Melbourne Water, Victoria; Goulburn-Murray Water, Victoria; Sunwater, Queensland; URS Australia; GHD Australia; SMEC Australia; Elforsk, Sweden.

Abstract

Backward Erosion Piping is an internal erosion mechanism which occurs beneath embankment dams and levees founded on soil. When the foundation contains uniform sand, backward erosion becomes the major cause of incidents and failures. Yet, despite extensive research over the past century, a robust and accurate method for predicting backward erosion has been elusive. This study provides new insights into many aspects of backward erosion and provides improvements to existing prediction methods, with the use of a comprehensive suite of 92 large-scale laboratory flume experiments.

For the first time, the four exit geometries of slope, plane, slot and circle were tested in otherwise identical flumes. Experimental results and complementary numerical modelling demonstrated that exit geometries with more confined outflow areas required both lower initiation and critical gradients because these exits caused higher seepage velocities at both the exit and channel tip, thus needing less gradient to generate necessary erosive forces.

Few studies had investigated internally stable soils with uniformity coefficients above 3, therefore, seven of these soils were tested. Critical gradients increased exponentially with increase in uniformity and with decrease in permeability at a constant tip width. Additionally, the tip width increased linearly with d_{50}. The latter two findings were combined to form a new empirical model with a coefficient of correlation of 0.95.

To investigate the industry's concern that critical gradient decreases with subsequent floods, novel tests were loaded in cycles. The critical gradient did decrease in experiments by 2-13% but not due to cyclic loading. In fact, gradients needed under cyclic loading were higher than under constant loading. It was due to an increase in permeability as the channel lengthened.

An unprecedented investigation into the rate of backward erosion revealed an average channel advance rate of 3mm/minute at critical gradient and a 3-fold increase in this rate with each 10% increment in gradient above critical (in 0.3mm uniform sand).

Using experimental results from both this present study and those undertaken by others, an assessment was made of the two most widely used prediction methods- Schmertmann (2000) and Sellmeijer et al. (2011). In doing so, modifications are recommended to improve model performance in forms suitable for industry use.

Contents

Chapter 1

Introduction

1.1 Backward Erosion Piping

Backward Erosion Piping is an internal erosion mechanism which occurs either within or beneath embankment dams and levees. It initiates during flood events when seepage forces exiting the downstream face/toe transport cohesionless soil out from the embankment or foundation. If a structure or cohesive soil which can support the roof of a pipe is present, erosion continues and forms a small pipe which progresses toward the upstream end, opposite to the direction of flow, i.e. backwards. If the pipe reaches the upstream end then pipe enlargement leading to dam/levee failure is likely (ICOLD, 2015). The backward erosion piping process in a foundation is shown in Figure 1.1.

1.2 Problem statement

When embankment dams and levees are founded on uniform sand, Backward Erosion Piping becomes the major cause of incidents and failures (van Beek et al., 2013). These foundation conditions are common for levee systems along major rivers such as the Mississippi River in the United States, the Yangtze River in China and main rivers in The Netherlands (van Beek et al., 2013). As an example, the U.S. Bureau of Reclamation, who manage over 220 embankment dams, have attributed 16 of their internal erosion incidents and failures (out of 99) to backward erosion piping (U.S. Department of the Interior

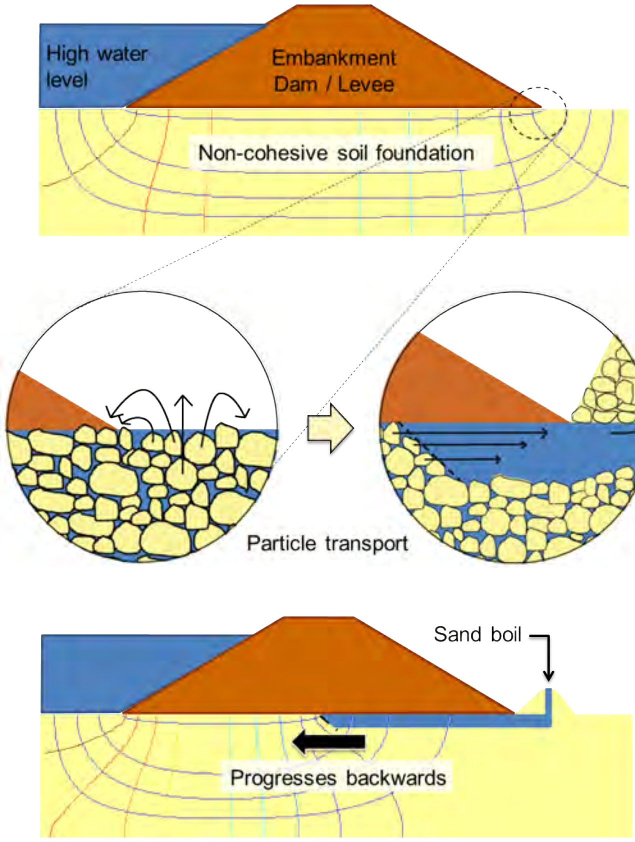

Figure 1.1: The process of backward erosion piping through a foundation (not to scale)

Bureau of Reclamation and U.S. Army Corps of Engineers, 2015). These incidents and failures would have undoubtedly caused great social and financial loss, including risk to life.

When backward erosion piping occurs from the foundation, sand boils usually form along the downstream toe, sometimes in the order of hundreds in any given flood (Fell, 2012). Authorities responsible for the levees respond by placing sand bags around sand boils in order to raise the water level in the boil and slow erosion down (referred to as 'flood fighting'). They are usually successful in preventing failures (ICOLD, 2015) however, it is a resource-intensive reactive measure which is dangerous for personnel and carries a high risk of missing significant sand boils along kilometres of levee systems.

Backward Erosion Piping is a complex internal erosion mechanism which proves to be sensitive to a vast range of factors. *"Most likely everyone who has studied the piping problem realises its complexity and difficulty. It involves the interaction of soil mechanics, fluid mechanics and sediment transport."* (Schmertmann, 2000, pg. 9). So whilst much research has been carried out on backward erosion piping, there still remains much the dam engineering community do not yet understand. For instance, the effect of exit geometry on the critical gradient has not been quantified or modelled; current prediction methods are ill-equipped to predict backward erosion in soils other than fine to medium uniform sand; it is not known what effect successive flood events have on the critical gradient; and there is little information on the rate of backward erosion, particularly at gradients above critical; just to name a few gaps in understanding.

The aim of this study was to fill these gaps in understanding with the use of laboratory experiments and subsidiary numerical modelling; in order to better equip engineers to design against and assess the risk of backward erosion piping.

1.3 Objectives

The main objective of this study was to extend knowledge on backward erosion piping with an extensive laboratory testing programme designed to fill significant gaps in understanding by testing variables not addressed previously. Specific objectives were as follows.

1. To verify the exit geometry effect reported by van Beek et al. (2013) whereby an increase in exit outflow area causes an increase in initiation and critical gradients. Then to quantify this effect with a more extensive suite of experiments not previously available, including all four exits in otherwise identical flumes. Lastly, to support the exit geometry effect hypothesis with the use of numerical modelling.

2. To investigate the influence experimental set-up had on the initiation and critical gradients in order to make informed decisions when selecting set-up variables and to aid in the interpretation of results. In particular, the aim was to quantify the effect soil density and seepage length had on gradients as well as investigate whether bladder pressure affected gradients and whether the uneven distribution of pressure imposed by the bladder influenced where backward erosion would occur.

3. To examine backward erosion piping in soils with uniformity coefficients (C_u) greater than 3 with the aims to:

- determine initiation and critical gradients in poorly and well graded soils;
- test well graded soils which are also internally stable in order to isolate the possible interference of internal instability from backward erosion;
- ascertain the maximum C_u at which soil no longer fails by backward erosion in the laboratory;
- review the Schmertmann (2000) relation between local critical gradient and C_u; and
- explore other possible relations between soil properties and the critical gradient.

4. To test industry's concern that the critical gradient decreases with subsequent flood events by applying head to experiments in cycles. If the critical gradient does decrease, provide an explanation as to why and determine whether dams and levees are under greater risk when imposed by a series of flood events than when imposed by one longer-sustained flood.

5. To determine the rate of erosion at critical head and whether this rate increases with increase in gradient above critical in order to inform engineers on possible times to failure.

6. To review the current most widely used methods for predicting backward erosion-the Schmertmann (2000) and the Sellmeijer et al. (2011) methods. In doing so, the intention was to identify opportunities for improvement, particularly improvements which came to light as a result of having tested soils not previously tested (such as internally stable, well graded soils). Then develop these improvements in forms suitable for industry use.

1.4 Thesis overview

A brief overview of the structure and contents of this thesis is listed in Table 1.1.

Table 1.1: Thesis overview

Chapter		Contents
1	Introduction	Topic, problem statement, objectives and overview.
2	Literature review	A comprehensive review of literature on backward erosion piping. The review includes the types of internal erosion and what distinguishes backward erosion piping; observations of backward erosion in the field; laboratory experiments; empirical and numerical models; and current practices for estimating the risk of backward erosion in Australia. Lastly, a summary of the gaps in understanding is given.
3	Experimental method	Description of the new apparatus and methodology used to carry out laboratory experiments. Summary tables of set-up variables used in each test are provided, printed on coloured paper for easy reference.
4	Experimental observations	A detailed account of experimental observations which were universal across the various testing groups. Observations such as the stages of backward erosion piping, sand boils and channel behaviour. Also includes measurements such as soil density, flow rate, soil permeability and water temperature. Summary tables of observations, measurements and results (gradients) are provided, printed on coloured paper for easy reference.
5	Group 1: Replicate Townsend et al. (1981) testing	Group 1 gradients which verify the experimental set-up and procedures produce results similar to those obtained in an independent study. Also includes discussion on the impact of using a starter channel.

Table 1.1: Thesis overview (continued)

Chapter		Contents
6	Group 2: Exit geometry	Group 2 gradients which quantify the effect of exit geometry. Also includes a comparison of findings with those from other studies as well as a discussion on why the exit geometry affects the initiation and critical gradients, as indicated by the numerical model. Lastly, suggestions on how to account for exit geometry in design and risk assessment.
7	Group 3: Set-up variables	Group 3 gradients which demonstrate the effect of soil density, bladder pressure and seepage length. Also includes discussion on how to account for these attributes in design.
8	Group 4: Soil grading	Group 4 gradients which quantify the effect of 10 different soils. Also includes an analysis and discussion on the relationships between critical gradient and soil uniformity, permeability and particle size as well as how to account for soil grading in design.
9	Group 5: Cyclic and above critical loading	Group 5 gradients which indicate the effect of cyclic loading and tip progression speeds, at both critical and above critical gradients. Also includes a discussion on these attributes.
10	Numerical model	A description of how the model was formulated as well as output from the model including seepage velocity through the flume both before and after a channel had formed. These seepage velocities explained the exit geometry effect. Also includes evidence of and discussion on a singularity at the exit as well as method for minimising its effect by increasing permeability of soil at the exit. Lastly, a discussion on the ways in which the model could be further developed is given.

Table 1.1: Thesis overview (continued)

Chapter		Contents
11	Review of existing models	A review of the two most widely used methods for predicting the critical gradient- the Schmertmann (2000) and Sellmeijer et al. (2011) methods. The review includes an analysis of how well the two models predicted experimental results, from both this study and the studies of others. Also includes newly developed improvements to the models, for industry and research use.
12	Summary & recommendations	A summary of findings as well as recommendations for industry and recommendations for further research.

Chapter 2

Literature Review

2.1 Introduction and structure

The purpose of the literature review is to learn, evaluate and consolidate the research that has been carried out on the topic of backward erosion piping. In doing so the objectives are to ascertain the progress in the field, identify current gaps in understanding and provide justification for further research.

An outline of this literature review is as follows - firstly a description of what internal erosion is, including its four modes of initiation, of which backward erosion piping is one. This will be followed by an explanation of what backward erosion piping is. Then an account of the observations of backward erosion in the field will be given to illustrate its impact. Next is a discussion on the research carried out. The discussion on the research includes:

- an overview of the laboratory experiments researchers have conducted;
- a recollection of the observations they have made;
- a breakdown of the modelling techniques they have used for the separable components; and
- a presentation of the predictive models they offer to bring the components together and calculate the conditions which are likely to initiate and progress backward

erosion.

Following on from this is a list of what is thought to be the current gaps in understanding on backward erosion. Next a description of what the current practice is for designing against and assessing the risk of backward erosion piping is given. Lastly a conclusion is made.

2.2 Internal Erosion and Backward Erosion Piping

Internal erosion is the transport of soil particles within an embankment dam or its foundation. Transport of the soil particles starts when the erosive forces imposed by the hydraulic loads exceed the resistance of the materials. The transport continues if the seepage flow can carry the soil particles downstream (ICOLD, 2015).

The terms internal erosion and piping are often used interchangeably however piping only strictly refers to 2 of the 4 types of internal erosion initiation mechanisms - concentrated leak and backward erosion both which form pipes.

From the results of a statistical analysis of world-wide large embankment dams it was found that internal erosion was the cause of about half of the failures (Foster et al., 2000b). In fact, for dams in Australia, USA, Canada and New Zealand design and constructed after 1930 about 90% of failures were related to internal erosion (Foster et al. 1998, 2000a,b; cited in Fell et al. 2005). Therefore it is plain to see that internal erosion is the most significant challenge for dam engineers.

The process of internal erosion can be broadly broken into four phases (ICOLD, 2015):

1. Initiation - detachment of particles;
2. Continuation - the filter is too coarse to allow the eroded base material to seal the filter allowing unrestricted erosion of the base soil;
3. Progression - where hydraulic shear stresses within the eroding soil may lead to ongoing erosion and, in the case of backward and concentrated leak erosion, form

a pipe. The main issues are whether the pipe will collapse, or whether upstream zones may control the erosion process by flow limitation; and

4. Breach initiation - an uncontrolled release of water from the reservoir.

The first phase, initiation, can occur by four different mechanisms (ICOLD, 2015):

1. Concentrated leaks - where there is an opening, through which concentrated leakage occurs, the walls of the opening may be eroded by the leaking water;
2. Contact erosion - selective erosion of fine particles from the contact with a coarser layer, caused by the flow passing through the coarser layer;
3. Suffusion - erosion of internally unstable soils whereby seepage flow carries the finer particles of a soil through the voids between coarser particles because the voids are under-filled. The effective stresses are largely carried by the coarse particles. Whilst suffusion usually causes little or no change in the volume of soil mass, a soil skeleton of coarser particles is left behind; and
4. Backward erosion - the detachment of soil particles by seepage forces from an unfiltered surface downstream of a water retaining structure. The detached particles are carried away by the seepage flow and more soil particles are detached until a pipe is formed. The pipe progresses in a ‘backwards’ manner, opposite to the direction of flow, from downstream to upstream, until a continuous pipe is formed.

This literature review focuses only on backward erosion.

There are two types of backward erosion (ICOLD, 2015):

1. Backward erosion piping - horizontal or near-horizontal piping that requires the soil above to form a ‘roof’ and usually in the foundation, but can also occur within the embankment; and
2. Global Backward Erosion - near-vertical or inclined piping that does not need a ‘roof’ to form and occurs within the core.

This literature review focuses only on the first type, backward erosion piping. For the remainder of this literature review when the term 'backward erosion' is used it is intended to refer to 'backward erosion piping' only.

The four phases of internal erosion leading to failure, for backward erosion in the foundation, are sketched in Figure 2.1.

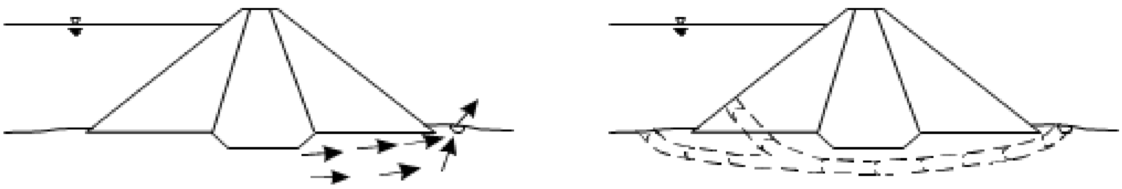

INITIATION	➔	CONTINUATION	➔	PROGRESSION	➔	BREACH/FAILURE
Leakage exits on d/s side of core and backward erosion initiates		Continuation of erosion		Backward erosion progresses back to the reservoir		Breach mechanism forms

Figure 2.1: Model for the development of failure by backward erosion in the foundation (Foster and Fell, 1999)

Soils which are at greatest risk of backward erosion appear to be fine to medium sands with uniformity coefficients less than 3 in the foundations of dams/levees/dikes, based on experience in the USA and Europe (ICOLD, 2015). Participants at the Aussois Workshop (37 international experts on internal erosion) came to a consensus that soils which are subject to backward erosion are probably restricted to non-plastic soils or soils with low plasticity, which for practical purposes have been defined as soils with a plasticity index of less than 7, based on experience and judgement (although not systematically proven) (Fell and Fry, 2007; ICOLD, 2015).

The unfiltered surface where the backward erosion process begins may be a (ICOLD, 2015):

- Ditch;
- Crack within a cohesive strata formed as a result of heave;
- Seeping surface on the downstream face of the embankment; or
- The stream bed.

The pipe that forms with backward erosion can form either within the embankment, within in the foundation or form from the embankment into the foundation. The most common location for the pipe to form is in the foundation (ICOLD, 2015).

For a pipe to form, the soil or structure directly above the pipe needs to be self-supportive and form a roof. Soils which are capable of supporting a roof are those which contain fines ($\geq$15% passing the 0.075mm sieve is likely to be able to support a roof regardless of the plasticity of the fines) and are moist or saturated (ICOLD, 2015). In most cases a homogeneous embankment or core material would fall in this category and could support a roof enabling a pipe to form beneath it. However if an embankment contains non-plastic shoulders then the shoulders may collapse and pipe formation would be inhibited. In the case of a pipe forming within the embankment the roof would need to be formed by either a more cohesive strata layered into the core or at the phreatic surface when the partially saturated soil above the surface is silty (ICOLD, 2015).

Backward erosion piping is often exhibited by the presence of sand boils downstream of the embankment. Sand boils can also indicate suffusion, but sand boils due to backward erosion are more likely (ICOLD, 2015). Examples of sand boils are pictured in Figure 2.2.

2.3 Field observations

Most internal erosion failures and accidents occur due to concentrated leak erosion however 20% of failures and 15% of accidents due to internal erosion have occurred in soil types prone to backward erosion (Foster et al., 1998, 2000a,b, cited in Fell, 2012).

In countries such as The Netherlands, the United States and China where there are levees founded on fine uniform sandy soils along river systems, the issue of backward erosion becomes more pronounced and becomes the major cause of failures and accidents (van Beek et al., 2012b).

The United States Army Corps of Engineers (USACE) who manage the levee system along major USA rivers, including the Mississippi, are required to manage sand boils and the risk of backward erosion during floods (Sills and Vroman, 2007). As a result they have carried out extensive studies and made many observations of backward erosion over many years. In any one flood they observe hundreds of sand boils along a levee system (examples of sand boils are given in Figure 2.2). However the sand boils rarely lead to failures partly due to their "flood fighting" response. The "flood fighting" response is the building of sand bags and sometimes sub-levees around the sand boils to raise the downstream water head (thereby reducing the hydraulic gradient) and decrease flow rate (ICOLD, 2015).

(a) In Australia (Fell, 2012)

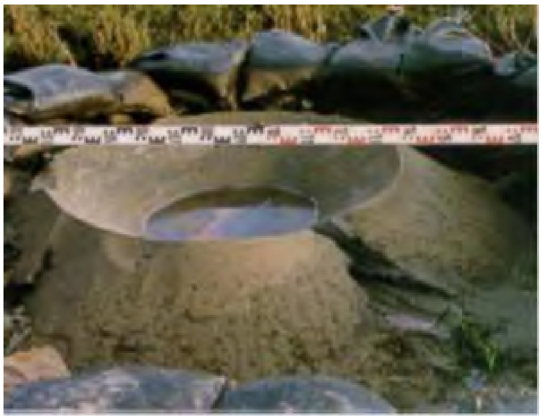

(b) In The Netherlands (Sellmeijer, 2009)

(c) In The United States (Dennee, 2011)

Figure 2.2: Examples of sand boils

The USACE have also observed cases of sand boils occurring at levees at successively lower flood levels (Glynn and Kuszmaul, 2004). For example Glynn and Kuszmaul (2004) showed that greater sand boil activity occurred during the 1995 flood than the 1993 flood even though the flood level was lower in the 1995 flood. This phenomenon points to the possibility of an ever-increasing weakening of the levee system (Sills and Vroman, 2007). Sills and Vroman (2007) suggested that pipes remain open between flood events, allowing for progressive erosion in subsequent floods thereby increasing the porosity/permeability with each event leading to lower factors-of-safety. This poses the unanswered question of 'how many more flood events can a levee take before the pipe reaches the upstream end and causes failure?' (Sills and Vroman, 2007).

Additionally, Wolff (2002) showed that local geology has an important influence of the occurrence of sand boils (ICOLD, 2015) in that they are more likely to occur where swales from point bar deposits cross the levee at an angle which causes seepage to concentrate at the toe.

2.4 Laboratory Experiments

2.4.1 Introduction

Many researchers have used laboratory experiments to investigate backward erosion. Table 2.1 is a list of these experiments found in the literature along with some of the variables studied.

Most of the laboratory experiments have the following attributes in common:

- Soil (usually sand) is placed into a flume/box (or built as an embankment for real-scale tests) and subjected to a horizontal hydraulic gradient;
- The flume or embankment incorporates an exit which allows sand grains to be moved at the downstream side;
- A top horizontal cover to confine the sand and create the roof of the pipe (either a cohesive or impermeable cover); and
- An experimental method that involves increasing the gradient in increments until backward erosion initiates. Sometimes the channel(s) stop progressing and the gradient needs to be increased further for the channels to progress to the upstream side. The gradients required for initiation and progression to the upstream side are recorded.

Table 2.1: Experimental research from reviewed literature

Publication	outlet	seepage length (m)	soil d_{50}	soil C_u	soil placement	cover type
Miesel (1978)	plane, circle	1.36	unknown	unknown	unknown	scaled zoned dam, perspex
Müller-Kirchenbauer (1978)	circle	0.73	0.27	2	unknown	Perspex
de Wit et al. (1981)	plane, slot, circle	0.8, 1.2, 2.4, 4.5	0.16, 0.38 & 0.8	1.43, 2.05 & 4	wet pluviation, varied densities	clay cover
Pietrus (1981)	slope	1.5	0.2	1.5	dry pluviation, loose	Perspex
de Wit (1984)	plane, slot, circle	0.8, 1.2, 2.4, 2.7 4.5	0.19, 0.2, 0.4, 0.365 & 0.75	1.48, 1.33, 2.3, 2.1 & 3.85	wet pluviation, varied densities	clay cover
Hanses et al. (1985)	circle	0.72, 0.66, 2.64	0.32	1.3	unknown	Perspex
Townsend and Shiau (1986)	slope	1.5	0.2, 0.93, 1.6, 1.42, 0.5, 0.6	1.5, 1.6, 2.1, 6.7, 5.6, 6.1	dry pluviation, loose	Perspex
Silvis (1991)	slot	6, 9, 12	0.21	1.6	unknown	Perspex & steel plate
Müller-Kirchenbauer et al. (1993)	circle	0.72	0.18, 0.3, 0.7, 1.3	1.5, 1.1, 1.3, 1.6	unknown	Perspex
Ding et al. (2007)	circle	1.4	0.24, 15	3.5, 11.4	unknown	Perspex
Yao et al. (2007)	plane & circle	1.4	0.24	3.5	unknown	Perspex
van Beek et al. (2008)	slope	0.3	0.13, 0.22, 0.47	1.55, 1.53, 2.7	wet pluviation, varied densities	Perspex
van der Zee (2011)	slope	0.5	0.38	1.6	compacted	Perspex
van Beek et al. (2011a)	slope & plane	0.3, 1.4, 15	0.15, 0.22, 0.32, 0.16, 0.37, 0.17, 0.15, 0.13, 0.16, 0.29, 0.34, 0.15, 2.0	2.6, 2.1, 1.6, 2.2, 1.3, 1.6, 1.5, 2.2, 1.6, 1.7, 2.1, 2.6, 1.6, 1.8	wet pluviation, varied densities & moist compaction by plant to RD > 50%	Perspex & Clay levee
van Beek et al. (2012b)	slope, circle	0.3	0.13, 0.36	1.6, 1.5	wet pluviation, RD= 90%	Perspex
van Beek et al. (2012a)	slope	0.3	0.13	1.6	dry pluviation, RD=18–47%	Perspex
van Beek (2015)	plane, circle	0.3, 1.3	0.38, 0.13, 0.34, 0.23, 0.22, 0.16, 0.14	1.6, 1.54, 1.58, 2.06, 1.71, 2.43, 3.17, 2.25, 1.5	wet pluviation, varied densities	Perspex

However the laboratory experiments differ with variations in inlet geometry, outlet/exit configuration, scale, soil, preparation method, cover type, imposed vertical stress and measured parameters. Present evidence is that the exit condition, scale and soil have the most effect on the critical gradient. Therefore, each of these critical variations will be considered in turn in the following sections. There are also concerns regarding the effect of soil density and total stress and these will also be discussed in preparation for the experimental program.

2.4.2 Set-up variables

Outlet/Exit

Of the backward erosion experiments found in the literature reviewed there are five different geometries used at the downstream exit (where the soil is transported out of the channel). These different exit geometries are used to model different scenarios found in the field. They are sketched in Figure 2.3 and include:

Slope: a non-cohesive soil foundation sloping down at the downstream toe of the embankment to meet a river bed;

Plane: a non-cohesive soil foundation;

Slot: a foundation consisting of both a top cohesive soil layer and a lower non-cohesive soil layer where a slot/ditch has been cut into the top cohesive layer deep enough to reach the underlying non-cohesive layer. This is found where drains have been installed along the downstream toe to manage seepage and surface run-off flow.

Circle: a foundation consisting of both a top cohesive soil layer and a lower non-cohesive soil layer where a shaft/crack has formed through the top cohesive layer deep enough to reach the underlying non-cohesive layer. This is found where the top cohesive soil layer has cracked due to heave of the underlying non-cohesive layer, or where a local anomaly in the top cohesive layer exists (possibly a sandy shaft/lens).

Vertical structure: a foundation consisting of both a top cohesive soil layer and a lower non-cohesive soil layer where the downstream/landward toe of the embankment has been constructed with a cut-off which directs flow vertically upwards.

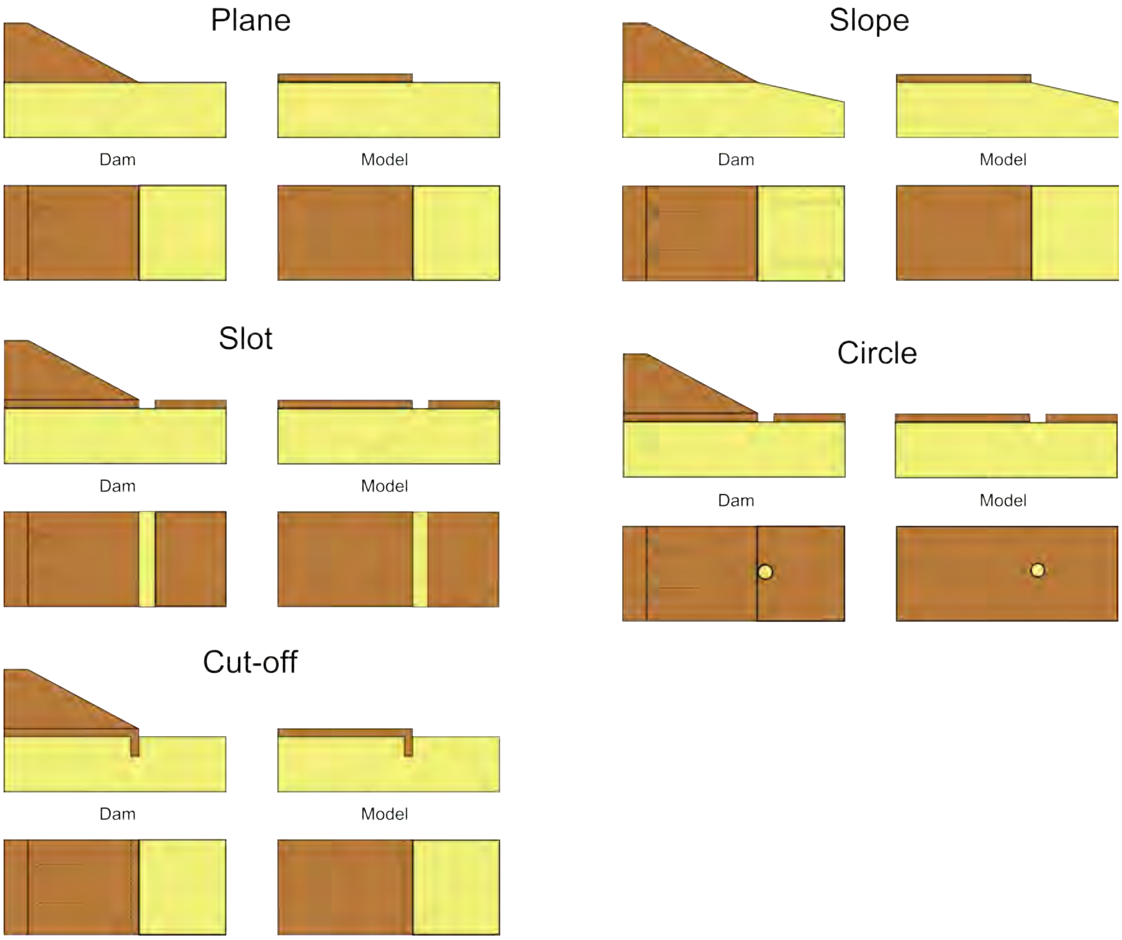

Figure 2.3: Sketch of exit geometries (water flows from left to right)

The exit geometries previously tested are as listed in Table 2.1. However the cut-off exit is not included in the table because an additional mechanism is added to the erosion process, erosion in the vertical direction. This condition has not been considered during this study.

Major experimental studies focusing on different exit geometries include:

De Wit et al. (1981) Plane and circle exits (L=2.4 and 4.5m), but observations on the effect of exit geometry were not reported and results were not presented in a way which facilitated comparison.

De Wit (1984) Plane and circle exits (L=2.4 and 4.5m) as sketched in Figure 2.4. A shortcoming of this study was the circular exit contained a taller shaft due to the 120mm thick clay layer over the sand. This relatively tall shaft meant that additional head difference was required to raise sand in the shaft high enough to reach the top of the clay layer and deposit on top of the clay layer, only then would channel initiation occur. This additional head difference made for higher critical heads than would be necessary for a thin roof layer. Another shortcoming of this study was the eroding channel was not visible due to the clay cover. This meant that observations were limited to boiling and volume of soil at the exit and determination of the initiation and critical gradients were unreliable.

A slot exit (also referred to as a ditch) was also tested by de Wit (1984) however, it was tested with a different seepage length of 2.7m. This meant slot results could not be compared with plane and circle results due to the added influence of seepage length. Additionally, the slot exit was a different width (0.05m) to the circle diameter (0.04m and 0.1m), again adding an additional influence, this time being exit area, and inhibiting study of the exit effect alone.

Van Beek (2015) summarised the effect exit geometry had on the *initiation* gradients found by de Wit (1984) in Figure 2.5.

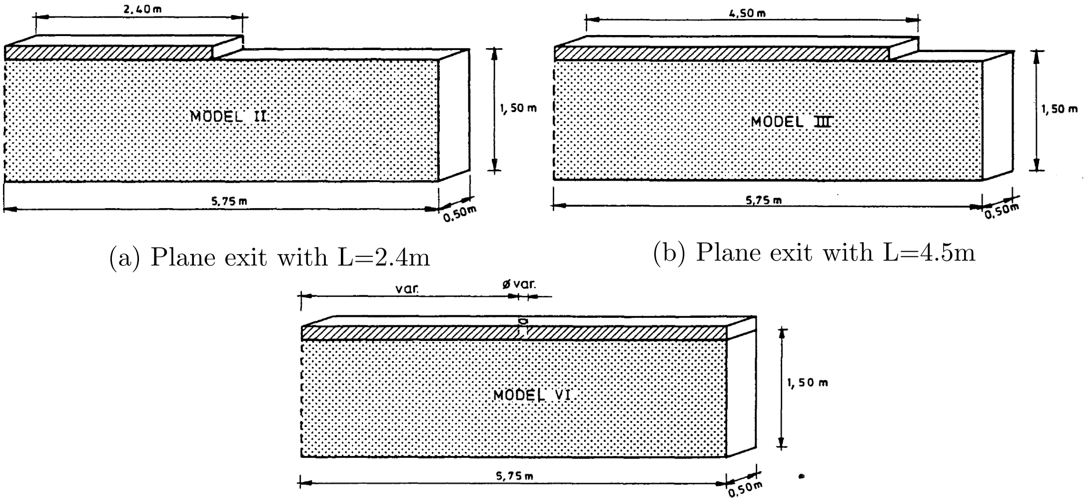

(a) Plane exit with L=2.4m (b) Plane exit with L=4.5m

(c) Circle exit

Figure 2.4: Plane and circle exit set-ups used by de Wit (1984)

Van Beek et al. (2012b) Slope and circle exits (L≈0.35m) as shown in Figure 2.6. The results are shown in Figure 2.7 as critical head with ratios of soil layers (this study considered the effect of two layers of different sands).

Van Beek (2015) Slope and circle exits (L=0.3m–0.35m for slope and 0.344m for circle) drawn in Figure 2.6. The experiments were loaded in a similar manner to the cyclic loading procedure used in this present study (described in detail in Subsection 3.3.4)

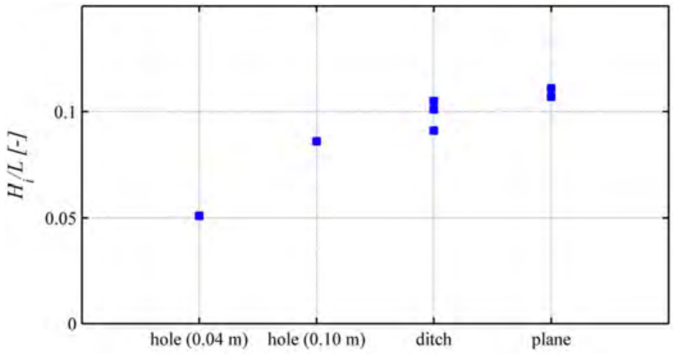

Figure 2.5: Effect of exit geometry on initiation gradient (de Wit, 1984; van Beek, 2015)

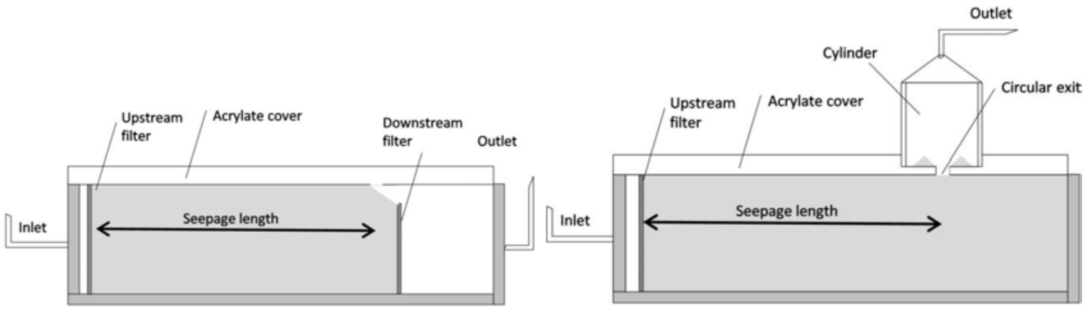

(a) Slope exit with L=0.3m–0.35mm (b) Circle exit with L=0.344m

Figure 2.6: Slope and circle exit set-ups used by van Beek (2015)

whereby once the channel had progressed a small distance, the head was dropped back to zero and then raised again in small increments until the tip re-initiated. The van Beek (2015) results are shown in Figure 2.8.

Yao et al. (2007) Plane and circle exits with a seepage length of 1.4m. The critical gradient was lower for the hole exit (0.214m) than the plane exit (0.278m) (van Beek, 2015).

In summary, all studies demonstrate that the exit geometry affects the initiation and critical gradients. Van Beek (2015) showed that the initiation gradient increased in the order of hole, ditch and plane exits. Van Beek et al. (2012b) showed that the critical gradient increased in the order of hole and slope exits. Yao et al. (2007) showed that critical gradient increased in the order of hole and plane exits. Therefore, it could be hypothesised that the more an exit geometry concentrates seepage flow, the lower the global gradient required to both initiate and progress the eroding channel.

In addition, van Beek (2015) demonstrated that experiments using the circle exit required

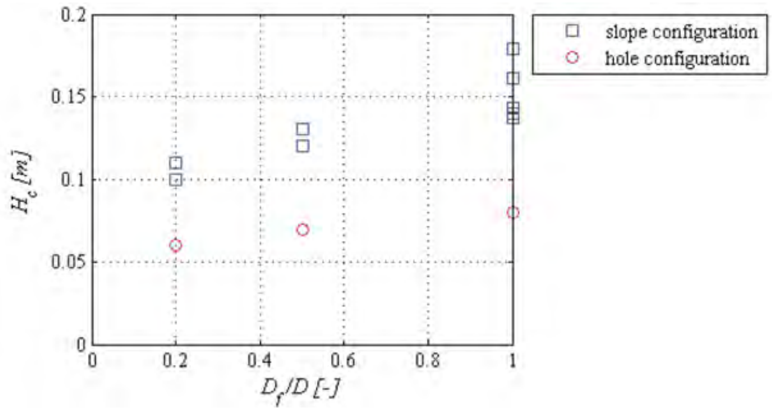

Figure 2.7: Critical head for ratios of fine sand layer thickness to total thickness (van Beek et al., 2012b)

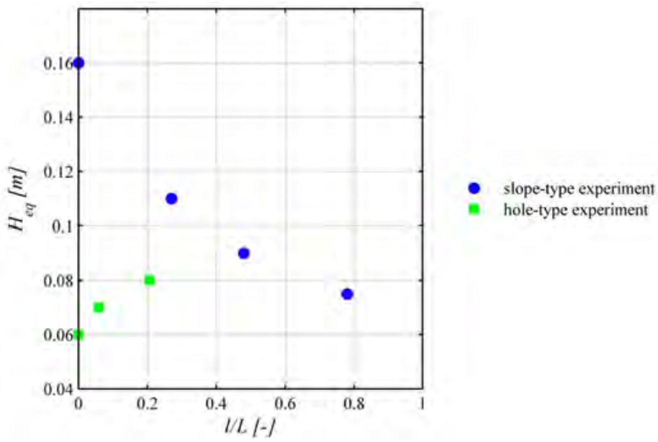

Figure 2.8: Effect of exit geometry on initiation and progression gradients (van Beek, 2015)

incremental increases in head to maintain channel progression whereas experiments using the slope exit did not, but would in fact continue progressing with lower heads. In other words, in circle exit experiments, the critical gradient > initiation gradient, but in slope exit experiments, the critical gradient = initiation gradient. Van Beek (2015) described critical gradients in circular exits as being 'progression dominated' and critical gradients in slope exits as being 'initiation dominated'.

A consequence of initiation-dominated exit geometries was that, when head was kept constant after initiation, equilibrium would not be observed. Equilibrium was a phase of backward erosion identified by van Beek et al. (2011a) in which the tip of the eroding channel would become stationary and remain so until the head was increased. This means that the exit geometry also influences which phases of backward erosion occur. The phases of backward erosion identified by van Beek et al. (2011a) are subsequently defined in Subsection 2.4.3.

An exception to a slope-type exit skipping the equilibrium phase was the experiments run by the University of Florida (Townsend and Shiau, 1986). This is due to the use of a starter dowel, a semi-circular rod placed into the sand to create the beginnings of a channel. This pre-formed channel concentrates the seepage flow and therefore the gradient required for initiation is less than the gradient required for progression and equilibrium of the channels can be observed. However it should be noted that the gradient required for initiation is not initiation in a true sense because the channel had already been artificially initiated.

Despite these findings, no study to date has systematically carried out experiments on, and compared, all four exit geometries. Although the de Wit (1984) study compared three exit geometries, there were short-comings with his study, as previously outlined. Therefore this present study aimed to confidently verify the exit geometry affect by carrying out experiments on all four exit geometries in otherwise identical tests.

Soil density

Van Beek (2015) placed soil into experimental flumes using wet pluviation with the flume rotated 90°(with the closed flow inlet facing downwards). Loose to medium-dense soils were achieved by applying pulses to the flume (lifting and dropping) after filling and dense soils were achieved with continuous tamping during filling (Rietdijk et al., 2010). The flume was rotated to the horizontal alignment prior to testing.

Bulk density of the soil was calculated by measuring the mass of the flume filled with water and the mass of the flume once sand had been drizzled in and compacted. The difference in mass gave the dry soil mass. Then, assuming the sand particle density and knowing the volume of the flume, the bulk soil density was calculated (Rietdijk et al., 2010).

In order to measure soil density specifically in the top layer of sand where backward erosion occurred, van Beek (2015) used 'the electrical density method'. This method involved the insertion 4 of electrods into the sample through the lid (and some into the side of the flume). An electrical current was applied across two outer electrodes and the resistance was measured between the two inner electrodes. This electrical resistance was then related to porosity with an empirical equation containing constants unique to each soil (van Beek, 2015).

Van Beek (2015) reports that both the initiation head and critical head increased with decreasing porosity. Given porosity is inversely proportional to density, this result can be interpreted as an increase in initiation head and critical head with increasing density.

Van Beek (2015) used data from the studies of de Wit (1984) (plane exit experiments) and van Beek et al. (2011a) (slope exit experiments) to plot Figure 2.9a which illustrates the relation between the initiation gradient and porosity. Van Beek (2015) points out that role played by porosity may differ in slope exit experiments because the slope angle and friction angle, which determine the onset of grain movement on the slope, may also affect the initiation gradient.

Van Beek (2015) plotted Figure 2.9b to illustrate the relation between the critical gradient and density.

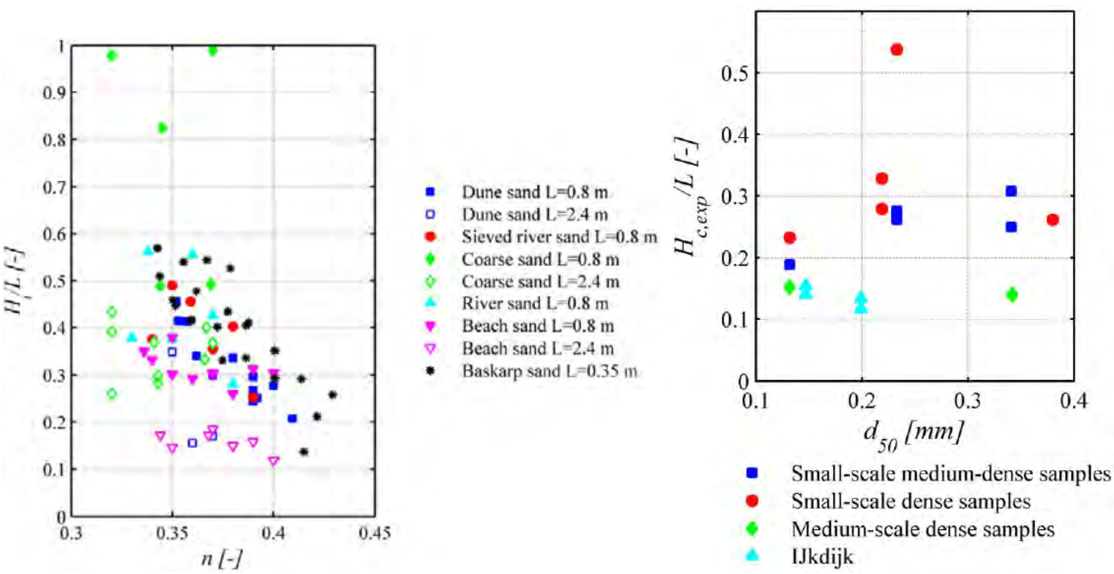

(a) Initiation gradients as a function of porosity

(b) Critical gradients as a function of d_{50} for varying soil-density series

Figure 2.9: Effect of soil porosity (van Beek, 2015)

The influence of soil density/porosity on the initiation and critical gradients is likely to be due to the related change in permeability, friction angle and angle of repose (van Beek, 2015). With an increase in permeability, less head is required to generate the seepage forces needed to initiate and progress the backward eroding channel.

Total stress

The studies of de Wit (1984), Townsend et al. (1981) and van Beek et al. (2011b) investigated the effect of total stress on the critical gradient. De Wit (1984) varied the total stress in experiments by applying different surcharge loads on top of the clay layer. Load on the clay was increased threefold from the load used in standard experiments (although the magnitude of this standard load was not provided) so that a load ranging from 8.8 to 16.2kPa was imposed from the downstream to upstream sides (van Beek, 2015). Townsend et al. (1981) varied the total stress in experiments by inflating a bladder pressure with pressures of approximately 34 to 69kPa. The pressure bladder was a 1/4 inch thick rubber membrane on the base of the flume which when inflated with water pressure, expanded pushing the sand sample up against the Perspex lid. Van Beek et al. (2011b) varied the total stress in their experiments using a compressible strip placed between the box and Perspex lid. As bolts around the edge were tightened the strip compressed allowing the lid to impose pressure on the sand. Total stress applied was reported to be between 8 to 15kPa, with an effective stress at initiation between 0 to 12.7kPa (van Beek, 2015).

Studies to date have concluded that varying total stress has no impact on the critical gradient. The only reported impact of total stress was prevention of forward erosion (van Beek et al., 2011b). Forward erosion occurred when no stress was applied and soil was loose (with a relative density <50%) and occurred at lower heads than backward erosion. Once significant stress was applied, forward erosion was prevented and backward erosion occurred instead, even whilst the soil was still loose (soil was still at a relative density <50%) (van Beek et al., 2011b).

Van Beek (2015) concluded that effective stress (added to by total stress applied) does not impact the critical gradient because the backward eroding process is governed by conditions at the channel tip where effective stress are zero or close to zero, regardless of whether total stress was added to the system or not. Van Beek (2015) verified that the effective stresses at the channel tip approached zero with readings from stress sensors. Van Beek (2015) concluded that the role of applied stress was to ensure good contact between the sand and roof. This contact prevented higher porosity along the interface than the porosity within the sand and enabled build-up of effective stress in the sand.

Scale

A variety of different lengths, depths and widths have been used in backward erosion experiments. Lengths range from 0.35m (Figure 2.10) to 15m (Figure 2.11) in the one study by van Beek et al. (2011a).

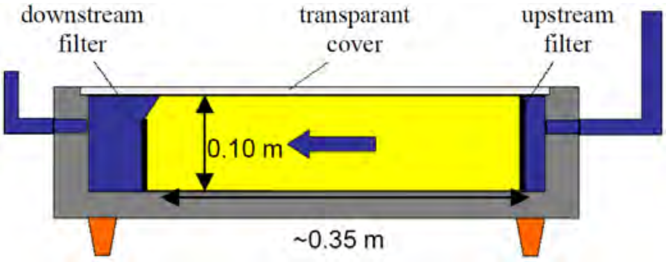

Figure 2.10: Small-scale experiments (van Beek et al., 2011a)

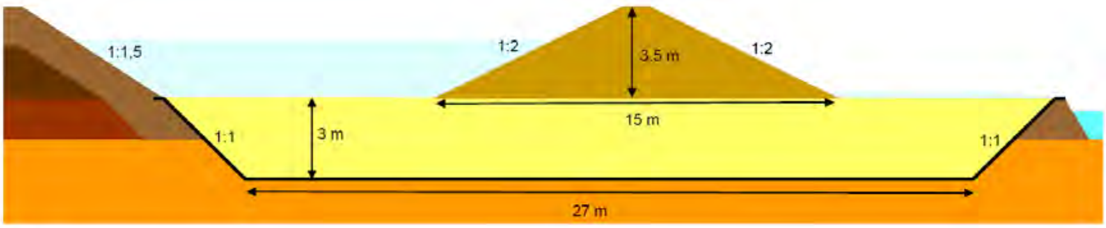

Figure 2.11: Large-scale experiments (van Beek et al., 2011a)

When experiments with equal length, depth and width ratios were used, it could be seen that both the initiation and critical gradients decreased with increasing scale. This was illustrated by van Beek (2015) with Figure 2.12.

This means that initiation and critical gradients observed in the laboratory will not be the same as those occurring in the field. In other words, laboratory-found gradients are not directly transferable to field predictions.

Studies of the scale effect (e.g. Bezuijen and Steedman (2010)), have not revealed the cause for the scale effects. The large correction factors required for scale effects generates uncertainties in the suitability of the models for application to the backward erosion problem (Fell, 2012).

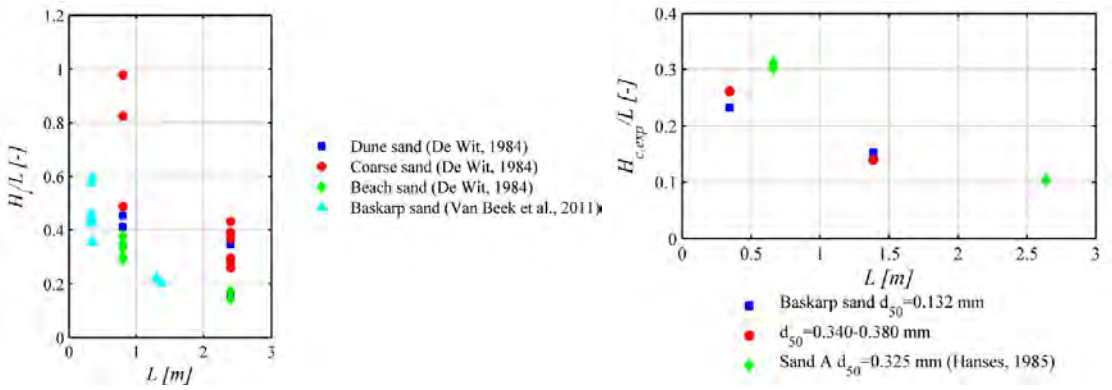

(a) Initiation gradients (b) Critical gradients

Figure 2.12: Effect of scale in experiments with constant D/L ratios(van Beek, 2015)

Given scale is expressed as seepage length in Figure 2.12 it gives the impression that the critical gradient is inversely proportional to seepage length. However, to maintain a constant D/L ratio, the data plotted in Figure 2.12 also varies in depth and it is depth that is inversely proportional to the critical gradient, not length. Van Beek (2015) demonstrates that initiation and critical gradients are not dependent on seepage length and yet investigates the exponent $i \propto L^x$ for both initiation and gradient because the Sellmeijer model contains $i \propto L^{-1/3}$.

Vandenboer et al. (2014a) demonstrated that width is also inversely proportional to critical gradient however, van Beek (2015) points out that width does not appear to affect the critical gradient at larger scales (for 2D exit geometries), on the basis that large-scale experiments were well predicted by the two-dimensional Sellmeijer model.

Soil gradation

Particle size distributions of soils tested by others have been plotted in Figure 2.13. This shows that all soils are sand with most being uniform to poorly graded. To examine grading uniformities, the uniformity coefficients of soils have been plotted in Figure 2.14 over a scale marking the definition of 'well graded' soils. As can be seen, most soils tested are within uniformity coefficients of 1 to 3.

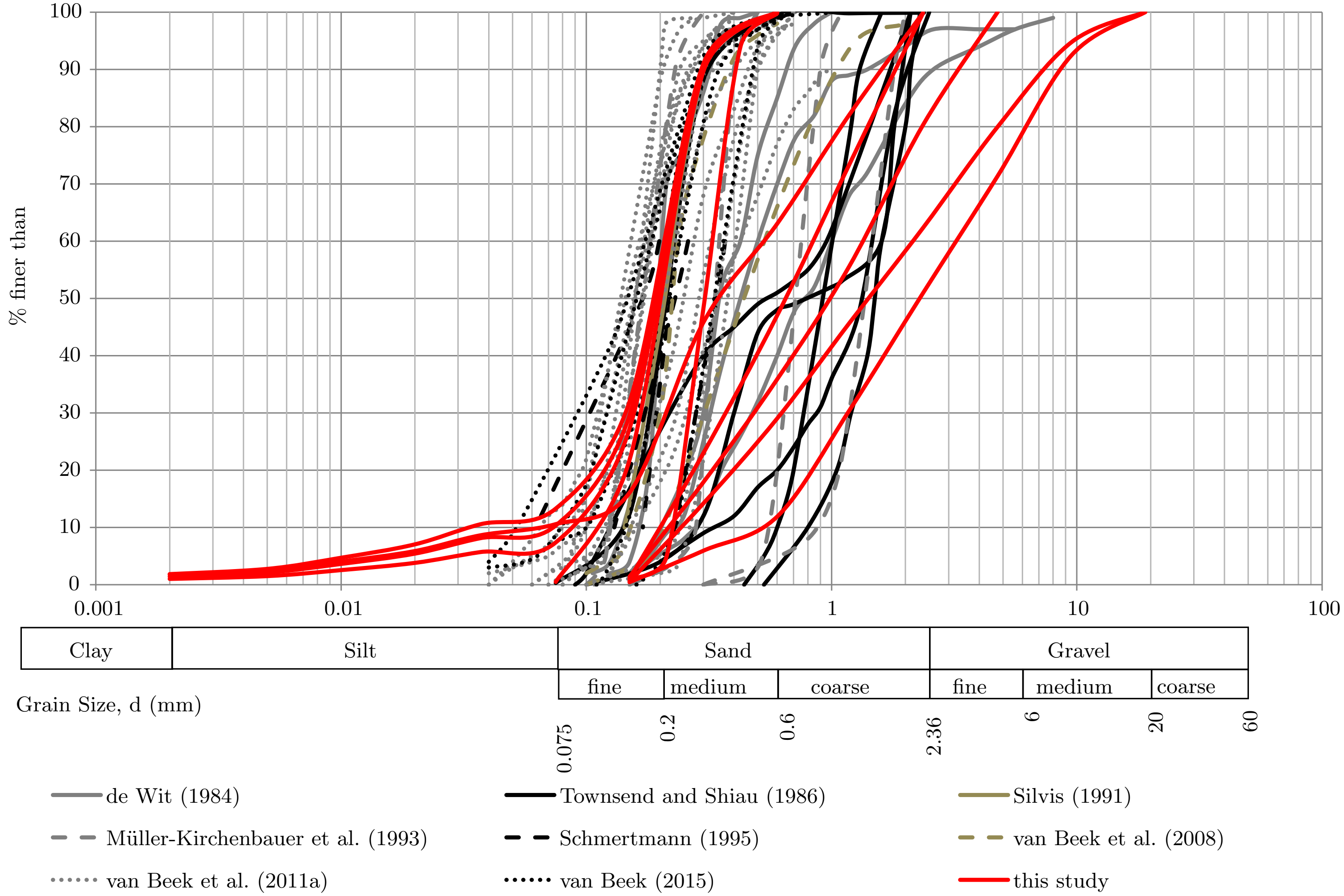

Figure 2.13: Particle size distribution of soils tested by others and soils tested in this study

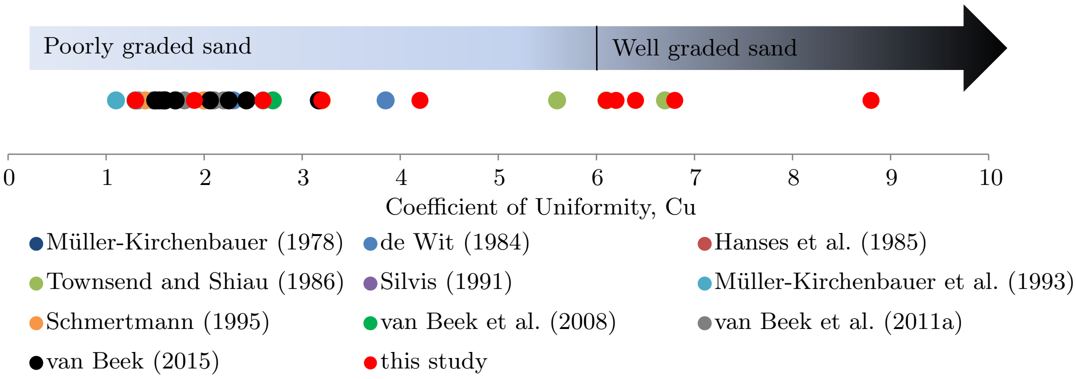

Figure 2.14: Uniformity coefficient of soils tested by others and soils tested in this study

Evidence is critical gradient increases with uniformity coefficient. Schmertmann (2000) illustrates this with Figure 2.34 in which he relates an increasing coefficient of uniformity with an increasing critical gradient. Although when ICOLD (2015) and Fell et al. (2008) present the Schmertmann (2000) findings, including the suggested equation relating critical gradient with uniformity coefficient, they do so with caution for soils with uniformity coefficients greater than 3 because "is it based on little data in the larger uniformity coefficient range, and some of these may be affected by internal instability". An assessment of the internal stability of soils with uniformity coefficients greater than 3 was carried out and is reported on in Subsection 3.2.2. This assessment indicated that of the 5 soils whose C_u values were greater than 3, 4 had probabilities of internal instability $\geq 40\%$ (assessed using the method of Wan and Fell (2007)).

One of the aims of this study was to test more well graded soils which are also internally stable because no soils of this nature have been tested before and to assess the Schmertmann (2000) critical gradient with uniformity coefficient relation.

2.4.3 Observations of the BE process

Van Beek et al. (2011a) identified four phases to the backward erosion process which are pictured in Figure 2.15 and described below.

Phase 1 Seepage Seepage occurs in the permeable strata

Phase 2 Backward Erosion van Beek et al. (2011a) identify a gradient referred to as the critical gradient that delineates the behaviour of the backward erosion process.

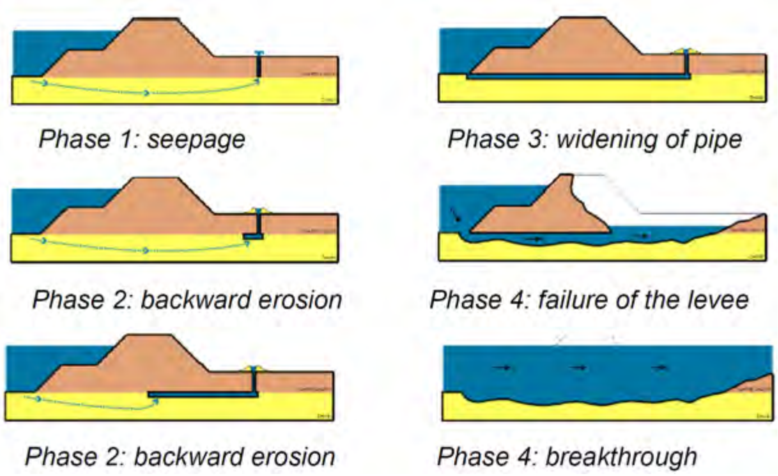

Figure 2.15: Phases of backward erosion (van Beek et al., 2011a)

- Gradient < critical gradient

  At the start of backward erosion phase there is rearrangement of grains and formation of preferential flow paths through small channels. The height of these channels is typically 4 to 10 times d_{15}, i.e. often less than 2mm (Fell, 2012). The channels start to progress towards the upstream side and small amounts of sand are transported. The transport of sand is indicted by sand boils (if the geometry of the experimental setup allows formation of sand boils). However before long the channels stop progressing and the erosion process reaches a state of equilibrium (discussed in the next section).

- Gradient = critical gradient

  With an increase in gradient to the critical gradient, equilibrium is no longer possible and the channel progress to the upstream side without any additional increase in gradient.

- Gradient > critical gradient

  The rate of erosion increases with increase in gradient.

Phase 3 Widening Once the channels reach the upstream side, the pressure gradient along the channel increases significantly and the channels widen to form a traditional pipe. The widening progresses forwards (from upstream to downstream). Flow and sand transport at the exit point do not increase significantly until the widened pipe almost reaches the downstream side at which point it increases suddenly. The situation can change from sand boils to rapid flow and sand transport without warning.

Phase 4 Breakthrough Failure occurs soon after the widening phase is complete, but can be delayed due to collapse of the embankment causing the pipes to close. If the pipe does collapse then the backward erosion and widening phases repeat to reopen the pipe, which may occur several times before the embankment fails.

2.4.4 Equilibrium

The backward erosion process can reach a state of equilibrium for a given gradient. In other words, the channels, having initiated and progressed for a given length, can stop. Once stopped the hydraulic gradient needs to be increased to recommence progression. In fact, the gradient needs to be continually increased to maintain channel growth until the channels reach a length of between 30 to 50% of the seepage length (Schmertmann, 2000); 50% of the seepage length for an infinitely deep foundation (Sellmeijer and Koenders, 1991) and 30% of the seepage length when the foundation is shallow (in the order of D/L= 1/3) (Hoffmans, 2009).

Once the channels reach this critical length of between 30 to 50% of the seepage length, no further increase in gradient is required, and the channels progress through to the upstream side. Actually, when the channels exceed the 30 to 50% seepage length, the gradient required for progression gradually decreases as illustrated in Figure 2.16. The maximum gradient required for progression is known as the critical gradient.

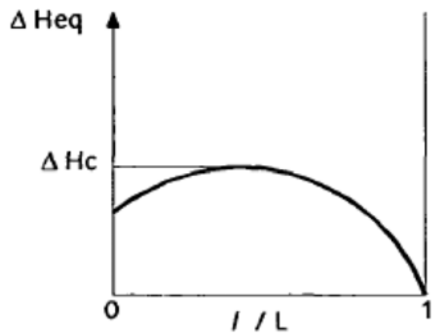

Figure 2.16: Head required to advance the channel with location of tip along seepage path (van Beek et al., 2013)

Explanations as to why the channels stop differ. In Technical Advisory Committee on Flood Defences (1999) the reason given for channel arrest is weakening of the flow gradient to such a degree that grains on the edge of the fissure are able to resist the drag forces.

It is unclear whether the 'edge of the fissure' refers to the channel tip or the channel bed and whether the 'flow gradient' is the local flow gradient at the tip or across the length of the channel. The Technical Advisory Committee on Flood Defences (1999) uses Figure 2.17 to illustrate the weakening of the flow gradient.

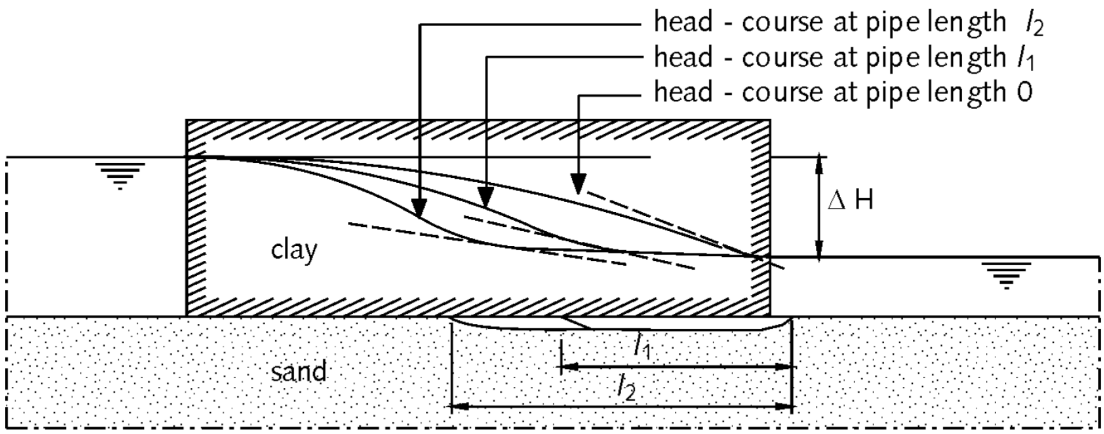

Figure 2.17: Weakening of flow gradients as piping is created (Technical Advisory Committee on Flood Defences, 1999)

Figure 2.17 should be treated with caution given the decreasing gradients appear to be an artefact of the shape used to draw the head curves, i.e. the curves for l1 and l2 are drawn using more of an 's' shape for no apparent reason.

Sellmeijer and Koenders (1991) suggest that because the permeability in the channel is much greater than that of the surrounding soil, the hydraulic gradients are damped down and thus equilibrium may be reached. This is understood in terms of Darcy's Law in that if $v = ki$ and velocity of the flow is kept continuous over sand and channel boundary then the increase in 'k' in the channel must mean 'i' decreases and this is what is meant by "the hydraulic gradients and damped down". However this explanation does not explain the influence of channel length on equilibrium or why the behaviour in Figure 2.16 is observed.

Hoffmans (2009) proposes that channels will stop when the gradient along the channel falls below the gradient required for particle detachment (to be more accurate, the gradient controls the velocity of the water in the channel, which if large enough, overcomes the shear strength of the soil particles along the bed of the channel). The gradient across the channel reduces because the length of the channel is increasing given by $(H1 - H2)/l$ (H1 is the head at the channel tip and H2 is the downstream head). However it is possible that the gradient along the channel that controls the velocity of the water in the channel is not the sole factor. Seepage entering the channel through the bed (an injection boundary) could also be significant. Seepage entering the channel through the bed increases the flow and continues to increase it from the tip to the downstream exit (there is an accumulation of flow entering the channel). This means that whilst the increasing length of the channel may decrease the gradient and hence decrease the velocity of water flowing in the channel, the seepage entering the channel through the bed may counteract the drop in velocity and it is therefore unknown whether the velocity decreases, remains the same or increases - it would depend on the relative influence of channel length increase and channel bed seepage inflow.

This theory (that channels stop when the gradient along the channel decreases and does so because the channel lengths) suggests that the head required to prevent channels from stopping would continue to increase as the channel lengthens. However, this is not the case illustrated in Figure 2.16. In Figure 2.16, the head required to maintain tip progression decreases once the channel is longer than half the seepage length.

Schmertmann (2000) is of the opinion that it is the local gradient at the tip of the channel that determines whether the channel will advance or stop. As the channel tip advances from the downstream side towards the centre of the embankment, the local gradient decreases as can be seen in the flownet shown in Figure 2.18. The equipotential lines become less concentrated in the middle regions beneath the embankment and this is why, as Schmertmann suggests, the highest global gradients are required to advance the channel through this region. Although it is noted that Figure 2.18 neglects any impact the channel has on the flow net.

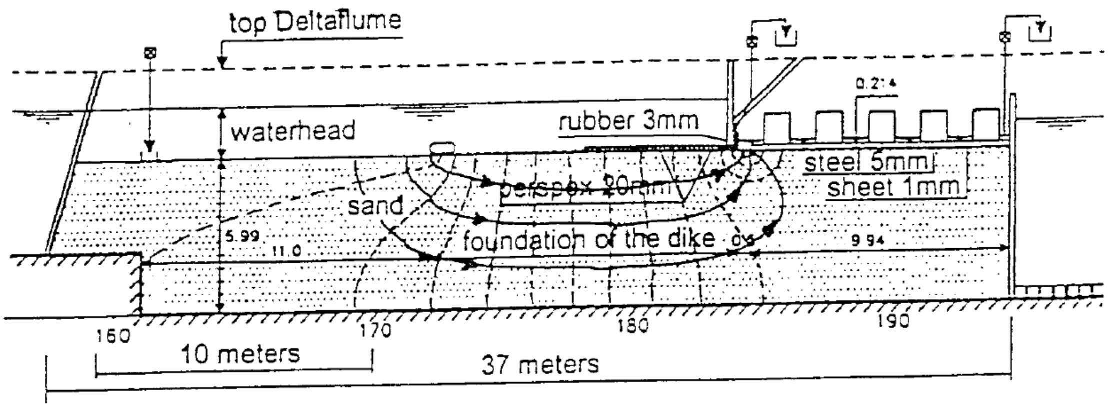

Figure 2.18: Flownet through BEP experiment (Schmertmann, 2000)

Schmertmann's explanation that the channels stop because the local gradient at the tip decreases in the middle region beneath the embankment appears to explain the observed behaviour of Figure 2.16 whereas the other explanations do not. However, it is acknowledged that both Schmertmann's and Sellmeijer's methods are able to model the observed behaviour and produce figures like Figure 2.16.

Whether it is more accurate to explain equilibrium by a drop in local gradient at the tip or gradient across the channel depends on whether it is particle detachment at the tip or the bed which drives progression (or a combination of the two). If progression is driven by particle detachment at the tip of the channel, referred to as primary erosion by Hanses (1985), then it seems likely that it is the local gradient at the tip that drives advancement. However conversely, if progression is driven by particle detachment along the bed of the channel (secondary erosion (Hanses, 1985)) then it's likely to be the gradient along the channel that drives advancement.

2.5 Modelling

This section describes the different ways researchers have modelled backward erosion. Table 2.2 lists the models reviewed. This list demonstrates the vast time over which backward erosion has been studied, the need for a prediction method and the complexity of backward erosion given the number of attempts made. Despite the many number of models formulated, there appears to be no predictive method that is a) applicable to all the scenarios required and b) is suitable for robust engineering practice.

Table 2.2 lists the method used to model each of the separable mechanics involved in backward erosion: seepage flow, channel flow and particle detachment. These mechanics are elaborated on in Sections 2.5.1 to 2.5.3. The completed models pull together the various mechanics of backward erosion to provide a prediction of what conditions are likely to bring about initiation or complete progression of backward erosion. Table 2.2 also summaries the main strengths and weaknesses of each model and provides relevant things to note on each. The most popular and widely used models are expanded on in their own respective sections in Section 2.5.6.

Table 2.2: Backward Erosion Piping Models

Reference	Type	Seepage flow	Channel flow	Particle detachment	Strengths	Weaknesses	Note
Bligh (1910)	empirical	-	-	-	easy-to-use and widely used	over conservative, over simplified	-
Lane (1935)	empirical	-	-	-	easy-to-use, widely used and accomodates vertical seepage paths	over conservative, over simplified	-
Terzaghi and Peck (1948)	analytical	pore pressure	-	when $\sigma = u$ so that $\sigma' = 0$	easy-to-use, widely used and $i_c \approx 1$	applies to vertical flow only	more applicable to heave than BEP
Schmertmann (2000)	empirical	Darcy's Law and Laplace equation	-	vertical gradient at channel tip leading to liquefaction	accessible, widely used, validated with experiments	few soils with higher Cu's tested and susceptible to suffusion, can not be used for 3D-flow exits	-
Ojha et al. (2003)	analytical	Carmen-Kozeny	-	Critical tractive stress	only model to give a critical velocity	no channel included, presumably 2D exits only	As no channel is included perhaps Hcrit and Vcrit given are actually initiation limits (not critical)
Sellmeijer (2006)	numerical-2D FEM	Darcy's Law and Laplace equation	Navier-stokes	Force equilibrium on bed particles (using White (1940))	With use of an artifical network, expressions can be derived for any 2D geometry, validated with experiments	only 2D exits and flow, not applicable for soils with Cu >3 or d_{70} >0.43mm, not readily available to industry	Program called Mseep
Sellmeijer et al. (2011)	empirical	Darcy's Law and Laplace equation	Navier-stokes	Force equilibrium on bed particles (using White (1940))	accessible, widely used, validated with experiments	only applicable to 'standard configuration' and not applicable for soils with Cu >3 or d_{70} >0.43mm	Conformal mapping used to solve Laplace equation
Zhou et al. (2012)	numerical-2D FEM	Darcy's law	"pipe flow theory"	force analysis on soil particle in horizontal direction (Han, 2000)* and settling velocity in vertical direction (Wu, 2000)*	validated with experiments	2D, unknown exit geometry, not readily available to industry	"element free Galerkin method (EFG) was employed to faciliate the efficiency of coupling iteration".
Liang et al. (2013)	numerical-3D finite volume method	Navier-stokes	Navier-stokes	particle erosion law derived from Sterpi (2003)* and empirical equation for liquid-solid interaction forces from Ergun (1952)*	validated with experiments, includes empirical erosion rate law by Sterpi (2003)*	not readily available to industry	"pseudo-liquid" assumption used to simulate particle movement.
Hoffmans (2016)	analytical	Darcy's Law	Hagen-Poiseuille	Shields (1936) adapted for laminar flow	uses the traditional Shield's diagram, validated with experiments	only 2D exits and flow, allows for circular channels only	-
Vandenboer et al. (2014b)	numerical-3D FEM	Darcy's Law and Laplace equation	porous flow with greater permeability	-	validated with experiments including 3D-flow exit geoemtry (circle)	Does not include particle detachment or predict critical gradient, not readily available to industry	models flow conditions when channel present
Fujisawa et al. (2014)	numerical-2D FEM	Darcy's law	Navier-stokes	empirical formula (Fujisawa et al., 2012)*		2D, unusual exit geometry (plane with 90° notch) and not compared with experimental data, not readily available to industry	Darcy and Navier-stokes solved simultanously using Darcy-Brinkman. Tracking of interface using phase-field equation modified by Sun & Beckermann (2007)*
van Beek et al. (2014b)	analytical	Darcy's law and conformal mapping	-	heave of a group of particles sized 20 x mean grain diameter	accessible, validated with experiments	initiation only, plane and slot exits only	initiation gradient only
Kramer (2014)	combination	Darcy's Law and Laplace equation	Navier-stokes	Force equilibrium on bed particles (using White (1940))	includes rate of progression, predicted time to critical situation and sand transport rate of full-scale experiments	same as Sellmeijer et al. (2011)	Sellmeijer et al. (2011) model extended to include erosion velocity formula of Wang et al. (2014)* to account for time and variable head difference. Required neural networks.

* citation not included in reference list, please refer to source paper for reference

2.5.1 Seepage flow

Seepage flow (i.e. flow through the foundation as groundwater) has been modelled using Darcy's Law and Laplace equation, Carman-Kozeny and Navier Stokes. A description and discussion of the first two techniques is given below under their respective headings.

Darcy's Law and Laplace Equation

Darcy's Law (Equation 10.2) is used to model flow through the foundation. When spatial distribution of head was needed, researchers used the steady flow Laplacean equation (Equation 10.1) in homogeneous and isotropic material.

To solve Laplace's equation Sellmeijer (1988) used complex variable theory which reduces to determination of the boundary conditions using conformal mapping (or the Cauchy integral formula).

Schmertmann (2000) used 3D and 2D flownets (generated by computer programs and hand-drawn) formulated using Darcys Law and the Laplace equation. However Schmertmann (2000) assumed the pre-channel flownet was sufficient to determine local gradients even after a channel was present, i.e. a channel made only small and local alterations to the flownet which could be ignored for model purposes.

Liang et al. (2013) claims that Darcy's law is inappropriate for backward erosion applications due to the high Reynolds number of flowing water caused by the continuous particle erosion and increasing porosity. Instead, Liang et al. (2013) use an averaged Navier-Stokes equation to model the seepage flow.

Carman-Kozeny

Ojha et al. (2003) model flow through the soil using the Carman-Kozeny head loss model. This model assumes flow through a porous media can be idealised as flow through a network of parallel pipes whose diameters are equal to the mean grain size. Modelling the flow as flow through pipes enables use of the Darcy-Weisbach equation, but with modifications applicable to the porous flow geometry, to be:

$$H_L = f\left(\frac{L}{\varnothing d_{50}}\right)\left(\frac{1-n}{n^3}\right)\left(\frac{v^2}{g}\right) \tag{2.1}$$

where $f = 150\dfrac{1-n}{Re} + 1.75$

where $Re = \dfrac{\varnothing d_{50} v}{\nu}$

$\varnothing$ = shape factor = 1 for spherical particles

It is understood Ojha et al. (2003) used the Carman-Kozeny head loss model, instead of Darcy's model, so as to facilitate calculation of shear stress acting through the soil to determine when critical tractive force may be overcome, leading to initiation.

2.5.2 Channel flow

Flow through the channel was modelled by researchers using the Navier-Stokes equation and Hagen-Poiseuille flow. Other researchers do not model channel flow at all. A description and discussion of these techniques is given below under their respective headings.

Navier-Stokes equation

Most researchers used the equation of continuity and steady-state laminar flow governed by the Navier-Stokes equation. For steady flow, incompressible water and small Reynolds numbers (so the convection term can be neglected) the Navier-Stokes equation simplifies to:

$$\frac{\partial h}{\partial x} = \frac{v}{g}\left(\frac{\partial^2 v_x}{\partial x^2} + \frac{\partial^2 v_x}{\partial y^2}\right) \tag{2.2}$$

And

$$\frac{\partial h}{\partial y} = \frac{v}{g}\left(\frac{\partial^2 v_y}{\partial x^2} + \frac{\partial^2 v_y}{\partial y^2}\right) \tag{2.3}$$

To solve the flow pattern Sellmeijer (1988) used complex calculus. Since both the real (piezometric head) and imaginary parts of the complex field are harmonic and obey the Cauchy-Riemann conditions the Navier-Stokes equations can be rearrange into two Laplace equations and solved.

The result is the continuity of flow and is given by:

$$12\kappa Q = C_d^3 i_{channel} \tag{2.4}$$

where C_d = channel depth

$i_{channel}$ = gradient in the channel

Hagen-Poiseuille flow

Hoffmans (2016) used Hagen-Poiseuille flow assuming a parabolic laminar velocity profile (and circular channels/pipes) given by:

$$\overline{v_x} = \frac{g}{4\nu} i_{channel} \left((C_d/2)^2 - {}^1\!/\!{}_4 C_d^2\right) \tag{2.5}$$

and therefore,

$$Q = -\frac{\pi g C_d^4}{128\nu} i_{channel} \tag{2.6}$$

C_d = channel depth

$i_{channel}$ = gradient in the channel

Channel dynamics ignored

Schmertmann (2000) assumes a channel will progress through zones of higher local gradient with lower global gradients and zones of lower local gradient with higher global gradients, all before the channel enters the area and locally distorts the gradients and flow conditions. In other words, Schmertmann (2000) assumes that local gradients present before the channel exists can be used to predict backward erosion.

As support for this approach, Schmertmann (2000) reports that a conservative interpretation of flownet studies and flume tests indicate a negligible effect of the channel on the flownet when one considers a point 80 radii in any direction from the channel with a semi-circular cross-section. In addition, Schmertmann (2000) argues that a flow entering a channel which was able to detach the particles is more than sufficient to move the particles through the channel.

Therefore, Schmertmann (2000) does not model flow in the channel.

2.5.3 Particle Detachment

Particle detachment is the movement of particles from the soil matrix into the channel and can occur from three places: the channel tip, the channel bed and the channel sides; however detachment from the tip is needed for channel progression to occur.

There are different theories and criteria used within the literature to explain and predict when and from where particle detachment will occur. The most influential theories and criteria on particle detachment include:

- Force equilibrium on bed grains using the White (1940) model;
- Critical shear stress on bed grains using the Shields (1936) model;
- Critical local gradients at the tip (Schmertmann, 2000; Hanses, 1985)
- Slope stability with outward-seepage (van Rhee and Bezuijen, 1992)

Each of these theories/criteria are discussed below. Following on from this is a presentation of the ideas of Vandenboer and van Beek (2013) on whether scour or seepage forces drive particle detachment. Lastly, a discussion of the current author's opinions on continuum versus discrete mechanics, and their applicability to the modelling of particle detachment is given.

Force equilibrium on bed grains using the White (1940) model

Sellmeijer (1988) assumes that particle detachment will start along the bed of the channel due to shear stress applied by water flowing through the channel. Sellmeijer (1988) also assumes that detachment of material from the channel bed will lead to detachment from the channel tip, thereby causing tip progression (van Beek et al., 2013).

Sellmeijer (1988) uses the White (1940) model to determine when particles will detach from the channel bed. White (1940) used experiments to calibrate the theoretical equilibrium of forces on a particle for three different types of flow: viscous steady, steady inviscid and turbulent flows (van der Zee, 2011). Sellmeijer assumes viscous steady flow in the context of backward erosion piping and so uses White's model for this case. However the viscous steady flow assumption only holds for cases when tangential forces are more significant than pressure gradient forces (relatively slow speeds and small grains). According to Nikuradse (1933), tangential forces are more significant when the particle Reynolds number $Re_p^* = v^* d/\nu \leq 3.5$ (where v^* is the shear velocity $= \sqrt{\tau/\rho_w}$) (White, 1940).

The White (1940) model for force equilibrium of grains subjected to viscous steady flow included the weight of the particle and the drag force, as sketched in Figure 2.19. The two forces are in equilibrium when their components transverse to the angle of repose are equal and opposite and occurs when the shear stress is equal to:

$$\tau_c = \alpha \eta \frac{\pi}{6} \gamma_p' d \tan \theta \tag{2.7}$$

where α = eccentricity coefficient

η = packing coefficient

θ = angle of repose

White (1940) used experimental calibration to derive both the 'packing coefficient' η (accounts for the fact that the drag force isnt applied equally to all particles but is concentrated on exposed particles) and the eccentricity coefficient α (account for the eccentricity of the drag force) and suggested a combined coefficient value of 0.31.

Sellmeijer did not take α into account (due to its uncertainty); instead he used a

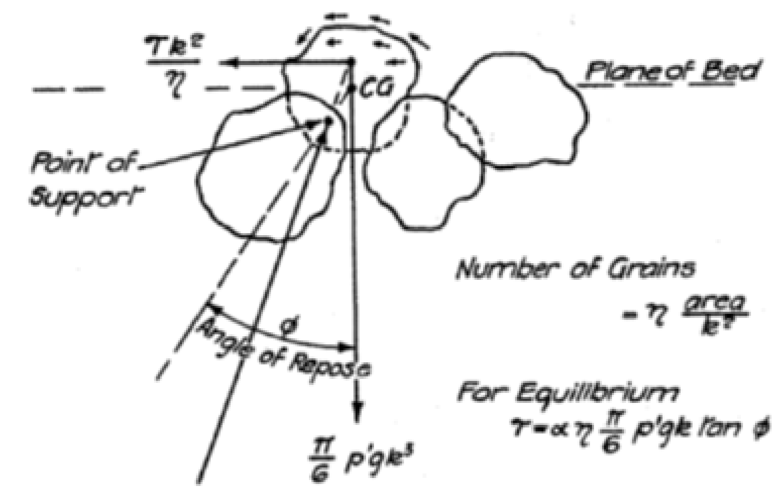

Figure 2.19: Forces on a soil particle according to White (1940)

conservative value of 0.25 for η based on two experiments for laminar flow (van Beek et al., 2013; van der Zee, 2011).

It is of particular interest that the White (1940) model does not include the uplift force, especially considering the context of backward erosion piping where flow is likely to be entering up into the channel through its bed. White argues that the lift component would be negligibly small because open spaces between loosely packed grains would allow pressure equalisation (van der Zee, 2011). White demonstrated this with a model grain made of wax (lighter than sand) which did not rise. However the uplift force White was considering was only due to pressure distribution, not upward flow as is the case in backward erosion piping (White's experiment didn't include an upward flow, it was simply a sloping open channel lined with sand) (van der Zee, 2011). Therefore van der Zee (2011) suggests White's assumption of negligible uplift may not be applicable to the bed of a backward eroding channel.

Sellmeijer et al. (2011) did not include an uplift force either because it was considered that a sand particle at limit equilibrium would protrude (because the smaller particles would have already eroded away) and so flow forces would not affect it.

Baldock and Nielsen (2010), who study sediment transport in the context of beach erosion, also report findings of no impact on incipient motion under injection boundary loading causing bed fluidisation (from Baldock and Holmes (1999)). This supports not including an uplift force. Baldock and Nielsen (2010) explain this lack of impact by suggesting that the uplift force only acts *within* the soil matrix and once a particle begins to lift out of its bed recess it is no longer subjected to this uplift force. It is also pointed out that the vertical flow velocity out of a bed which causes fludisation is generally two orders of magnitude smaller than the settling velocity, indicating it is insufficient to counteract the particle's weight and lift it from its recess (Baldock and Holmes, 1999).

Van der Zee (2011) argued against the use of White's model based on his observation of detachment occurring in groups of mass erosion instead of individual grains, as White's model assumes. Van der Zee (2011) was also concerned that White's model was based on only a few experiments, on grains that were barely visible and in flumes with no injection boundaries (a backward eroding channel does have injection boundaries). Furthermore van der Zee (2011) questions the analytical assumptions of spherical grains, larger more prominent grains transferring all shear to the bed, a purely horizontal resultant force and the shear stress being equally shared between the bed and top of the channel. Moreover van der Zee (2011) points out that the $\alpha\eta$ value of 0.31 is only based on two experiments on coarse-grained sand, so it is not a robust calibration, and it does not vary with the particle Reynolds number which contradicts the Shields (1936) findings (that $\tau/\rho' gd$ varies inversely with the particle Reynolds number).

The Hoffmans (2016) concerns with the Sellmeijer (1988) use of the White (1940) model includes use of too high an angle of repose (between 37° to 41° when Hoffmans (2016) cites a recommendation to use angles between 30° to 35°), excessively high critical wall stress predicted for coarse sands and no relation between White's critical shear stress and grain size (Hoffmans, 2016).

Critical shear stress on bed grains using the Shields (1936) model

Shear stress required to mobilise particles on a bed subjected to parallel flow can be estimated using the work of Shields (1936) and Mantz (1977). Shields carried out experiments in open rectangular flumes lined with sediment with an aim to investigate the influence of weight and shape of grains on the movement of river beds. The experiments provided information on what flows were required to immobilise river bed sediments of different sizes. Shields plotted the experimental results on a graph (Figure 2.20) whose axes were obtained using dimensional analysis on the shear stress of the water flow imposed on the particles and its relation to the relative density of the grains and fluid (Henderson, 1966).

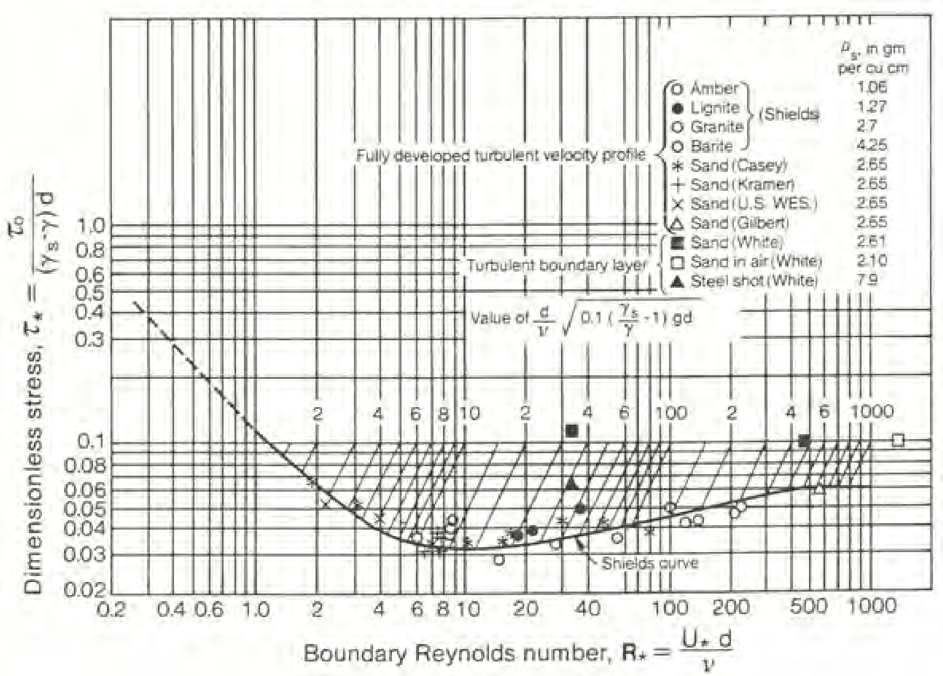

Figure 2.20: Shields diagram ($U_* = \sqrt{\tau/\rho_w}$ for shear velocity)

Hoffmans (2016) uses Shields' critical dimensionless stress to model when particles along the channel bed will detach but uses the empirical relation for laminar flow (Mantz, 1977; Yalin and Karahan, 1979):

$$\tau_{*,c,lam} = 0.2\,(d_*)^{-1/3} \qquad \text{for } 2 \leq d_* \leq 15 \tag{2.8}$$

Where $d_* = d_{50}\left(\left(\rho_p/\rho_w - 1\right)g/\nu^2\right)^{1/3}$ is a dimensionless particle diameter (for 0.15mm $< d_{50}$ <0.75mm).

Hoffmans (2016) assumes that particle detachment from the channel bed will automatically lead to detachment from the channel tip and hence lead to tip progression.

Cheng and Chiew (2010) warn that the Shields diagram is only applicable to uniform soil with horizontal (or near-horizontal) bed slopes and unidirectional flows. In the case of backward erosion piping, flow is not unidirectional because in addition to flow along the channel there is also flow entering the channel from its tip and bed (injection boundaries).

Consideration of the uplift force (imposed as flow enters the channel from below) was discussed in the previous section on force equilibrium of bed particles. Here it was pointed out that neither White (1940) nor Sellmeijer et al. (2011) took uplift into account and that this omittance was supported by the experimental findings of Baldock and Holmes (1999) (Baldock and Nielsen, 2010). Yet, other researchers have considered the effect of uplift relevant, as evident by the studies cited by Baldock and Nielsen (2010) which offer modifications to the effective weight of a grain within a bed subject to fluidisation, including Baldock himself in Baldock and Holmes (1999). These modifications reduce the effective weight of a grain thereby reducing the critical Shields parameter. However these modifications resulted in predictions of incipient motion for fluidised beds at very low free stream flow rates which contradicted experimental observations. Therefore, Baldock and Nielsen (2010) conclude that modifications to the Shields parameter for beds experiencing uplift forces is not required and explains this by pointing out *"that the Shields parameter represents a force balance on grains outside the fluid-sediment matrix, whereas the seepage forces acts only within the fluid-sediment matrix"* (Baldock and Nielsen, 2010, pg. 79).

Furthermore, van der Zee (2011) claims that the Shields diagram is not valid for water depths less than 100 grain diameters, but does not provide a reference of evidence for this.

Critical local gradients at the tip (Schmertmann, 2000; Hanses, 1985)

Schmertmann (2000) suggests particle detachment occurs at the tip due to some complicated combination of horizontal and vertical seepage gradients and flows but seeks to simplify it by separating the two directions into two different mechanisms - horizontal gradients leading to regressive slope failure and vertical gradients leading to fluidisation.

Schmertmann (2000) describes the mechanism of horizontal gradients leading to regressive slope failure as very high horizontal gradients into the channel tip causing slumping slope failures. It's suggested that after the slump occurs, *"perhaps there exists a temporary disruption in the gradients, a temporary steeper slope exits for a short time until the material moves away from the slope and the gradients re-establish themselves and the process continues in a series of regressive, micro-slope failures that advance the pipe"* (Schmertmann, 2000, pg.10). A sketch of the current author's understanding of this mechanism is given in Figure 2.21.

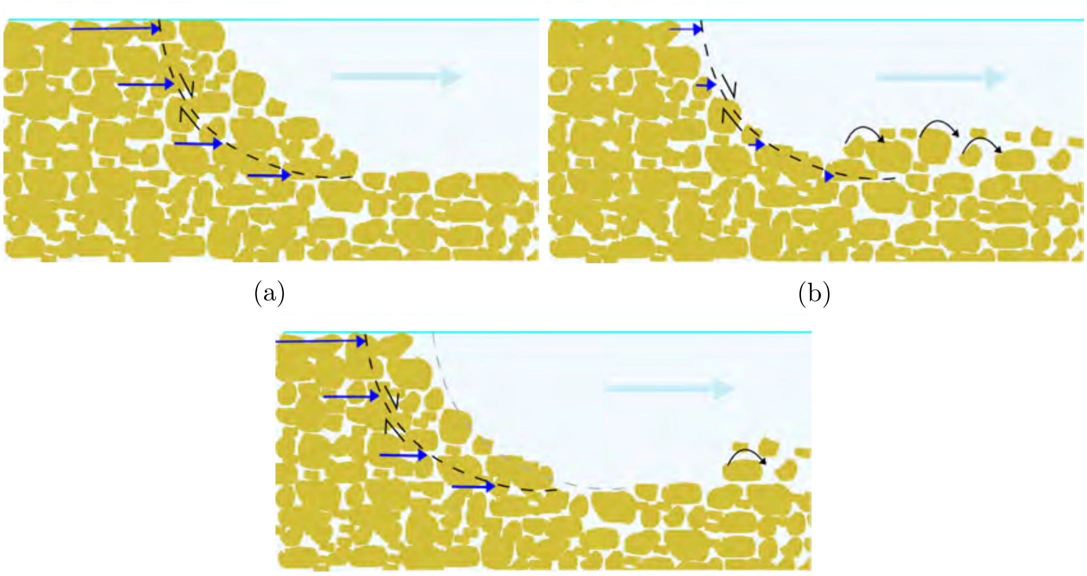

(a) (b) (c)

Figure 2.21: Sketch of slope failure of tip due to horizontal gradients

This mechanism of regressive slope failures supports the observations of Hanses (1985); Townsend et al. (1988); van der Zee (2011) in which intermittent groups of grains slide into the channel. These groups of particles are washed away by the channel flow, leaving a new slope which in time also slumps (van Beek et al., 2013). This cycle of slope failure and erosion continues resulting in propagation of the channel.

The mechanism of vertical gradients leading to fluidisation, suggested by Schmertmann (2000), is understood as the process sketched in Figure 2.22.

In Figure 2.22a and Figure 2.22b the local vertical hydraulic gradient at the toe of the tip slope is great enough to suspend the particle. Schmertmann refers to Martin (1970) who suggests that the vertical gradient needed to suspend a particle from the bed is 2 to 3 times that of the classical heave gradient of, $i_c = \rho'/\rho_w \approx 1$ because as the particle lifts the gradient reduces (indicated by the smaller arrows in Figure 2.22b). Schmertmann reports that his flownet studies demonstrate that the high local vertical gradients required to suspend the particle are easily obtainable due to flow concentration into the tip, even at global gradients typical for dams/levees.

In Figure 2.22c, because the particles are suspended they easily roll along the bed and move downstream. This removes particles from the toe of the tip slope causing particles

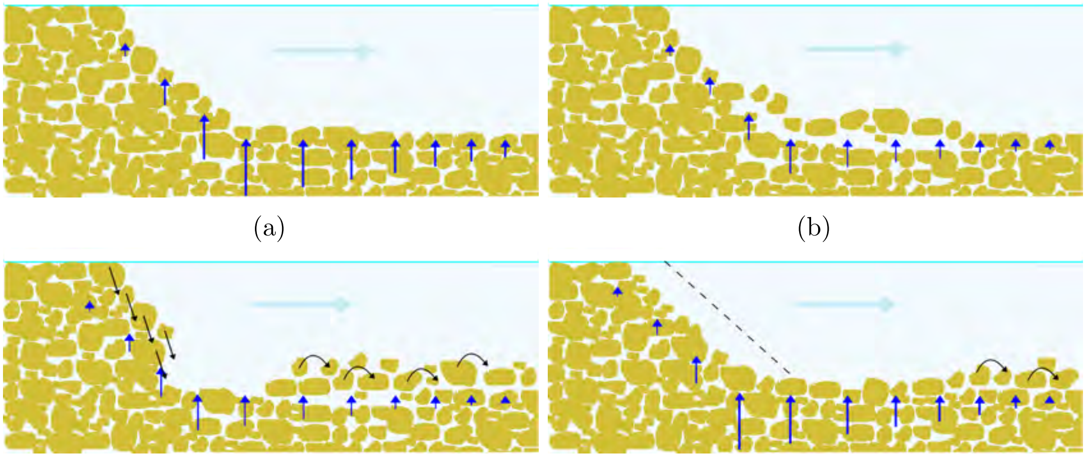
(a) (b) (c) (d)

Figure 2.22: Sketch of fluidisation at tip due to vertical gradients

above to slide down the slope and replace those removed. The sliding of the particles down to the bed causes the slope to retreat as shown in Figure 2.22d. With particles at the toe of slope now replaced the local vertical gradients build-up until they're again high enough to suspend the new particles.

There appears to be contention within the literature as to whether vertical gradients (or uplift forces) cause/influence particle detachment. The general consensus amongst White (1940); Sellmeijer et al. (2011); Baldock and Nielsen (2010) is that uplift forces need not be considered because they do no affect incipient motion and uplift forces only act within the sand matrix, not at the channel bed surface. Schmertmann (2000) acknowledges that gradients significantly reduce at the bed surface by citing the work of Martin (1970) who stated that gradients needed to suspend a particle were 2 to 3 times greater than the classical heave gradient of close to one. But Schmertmann (2000) still considers the uplift force to be the driver behind particle detachment where as White (1940); Sellmeijer et al. (2011); Baldock and Nielsen (2010) all consider it to be the drag force.

Interestingly, Schmertmann (2000) notes that a study of 2D flownets and 3D numerical modelling indicates that horizontal gradients were approximately 30% greater than vertical gradients. Yet, of the two mechanisms, Schmertmann (2000) chose the vertical gradient mechanism, for convenience, when developing the various gradient correction factors. However it is unclear how vertical gradients were used especially when pre-channel gradients were used and they would have been near-zero along the base of the dam/levee.

Hanses (1985) studied the erosion mechanism in detail and distinguished two types of particle detachment, primary and secondary erosion. Primary erosion referred to detachment from the channel tip due to local vertical gradients into the tip causing fluidisation (van Beek et al., 2013). Secondary erosion referred to detachment from the channel bed and sides due to drag forces imposed by flow through the channel. It appears that Hanses (1985) used a numerical model to calculate critical vertical gradients at the channel tip, but no method for others to calculate these was given.

Slope stability with outward-seepage

Van Rhee and Bezuijen (1992) analysed the stability of a sandy slope with inward or outward seepage. It was carried out in the context of dredging activities or slope stability in the tidal zone, but their work could be useful in considering initiation from a sloping exit or, if the channel tip is considered a small slope, then detachment from the channel tip.

Van Rhee and Bezuijen (1992) firstly considered two theoretical formulations of the critical gradient out of or into a sandy slope. These formulations used a continuum mode and a single-particle mode. Laboratory experiments were then carried out to verify the theoretical formulations. These experiments consisted of a transparent rectangular tank containing soil with flow passing either into or out of the top surface (shown in Figure 2.23a. With a head difference applied across the tank to drive flow, the tank was tilted until movement of grains at the surface occurred.

Results from experiments are plotted on Figure 2.23b along with the two theoretical modes of continuum and single-particle. It was found that results correlated with the continuum mode more when flow was directed outward through the slope (negative gradient). And given that seepage flows 'out' of the slope at the channel tip, this is considered the scenario most comparable to backward erosion piping.

The continuum mode considers a rectangular slice along the slope's surface and uses force equilibrium acting on the slice to arrive at a critical gradient of:

$$i_c = -\left(1 - n\right)\Delta\frac{\sin\left(\phi - \beta\right)}{sin\phi} \tag{2.9}$$

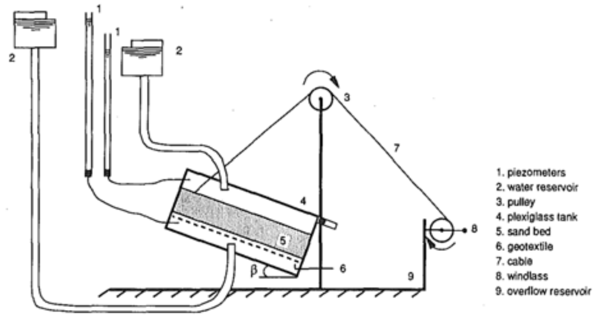

(a) Experimental set-up

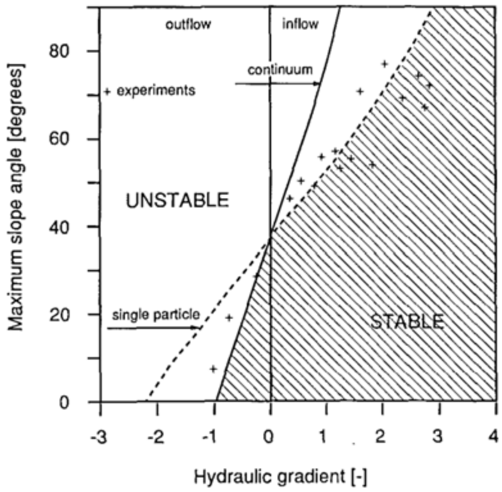

(b) Relation between maximum slope angle and hydraulic gradient

Figure 2.23: Testing and analysis of slope stability with seepage by van Rhee and Bezuijen (1992)

where n = porosity

Δ = relative grain density = $(\rho_s - \rho_w)/\rho_w$

ϕ = internal friction angle

β = slope angle

An alternate study on the stability of a slope with outward seepage is Keizer et al. (2016). In this study, the global gradient required to initiate first movement (i_m) across a range of different soils and slope angles were recorded and plotted as shown in Figure 2.24. On this plot, the gradient required to initiate first movement (i_m) is normalised to the Terzaghi and Peck (1948) heave gradient (Equation 2.13) and PAOR, on the x-axis, is the percentage of the loose angle of repose whereby $PAOR = \frac{Exit\ face\ slope\ angle}{Loose\ angle\ of\ repose} \times 100$.

The resulting proposed model was expressed as:

$$
\begin{aligned}
& i_{cr} = a \times PAOR^2 + b \times PAOR + c \qquad \text{(for PAOR} \geq 8.8\text{)} \\
& a = -1.8 \times 10^{-6}\,(\gamma) + 1.16 \times 10^{-4} \\
& b = 1.9748 \times 10^{-5}\,(\gamma) - 0.0016 \\
& c = \frac{\gamma_b}{\gamma_w}
\end{aligned}
\tag{2.10}
$$

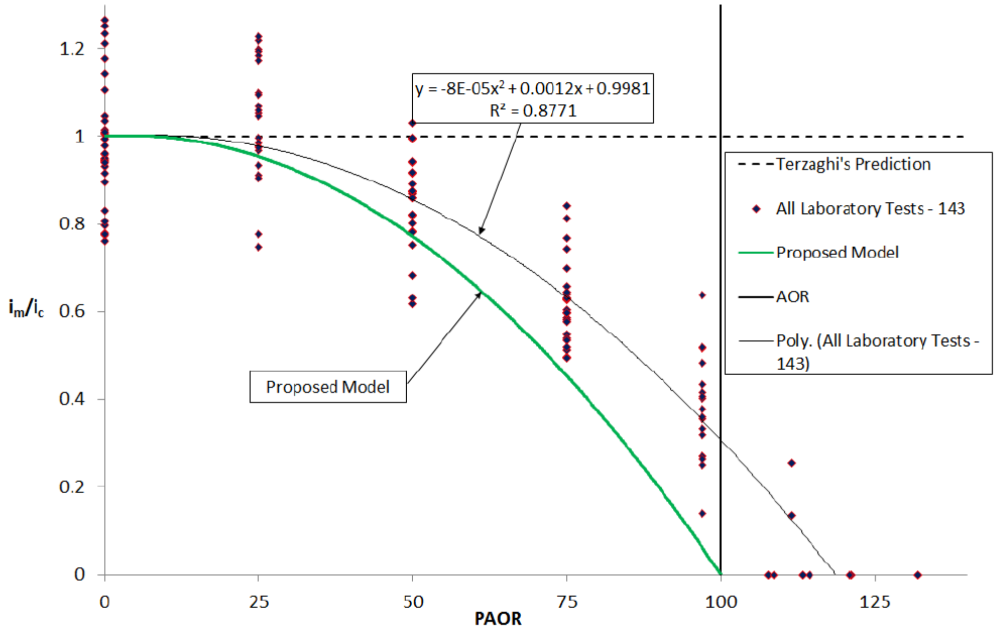

Figure 2.24: Experimental results and proposed model from Keizer et al. (2016) study

Scour versus seepage forces

Vandenboer and van Beek (2013) demonstrated that erosion from the channel bed is more likely to occur due to seepage forces than scour forces. They did this firstly by assuming erosion by seepage forces occurs when the local gradient is close to one (the Terzaghi and Peck (1948) vertical heave criteria). This meant that, according to Darcy's Law Equation 10.2, when the gradient was near one, the velocity was close to the permeability of the soil, which was 2.4 x 10^{-4}m/s in their example. Then they estimated the seepage velocity required for erosion by scour as the average of the velocities from the Hjulstrm's diagram (Figure 2.25) and a method for assessing contact erosion, which was 7.3 x 10^{-2}m/s in their example. Given the velocity required for erosion by seepage was much smaller than the velocity required for erosion by scour, it was concluded that erosion from the channel bed was more likely to occur by seepage than scour.

However, Vandenboer and van Beek (2013) also note that experiments indicate the channel depth remains somewhat constant and therefore erosion must not be occurring from the channel bed.

Vandenboer and van Beek (2013) then went on to show that erosion by seepage was more likely to occur from the channel tip and sides than the channel bed because, as expressed by van Rhee and Bezuijen (1992) in Equation 2.9, the critical gradient reduces on slopes and the tip and sides are slopped whereas the channel bed is not.

Assessment of particle detachment models

The presented particle detachment models can be classified into discrete and continuum approaches and further classified into where detachment is assumed to occur. Discrete mechanics consider forces on individual grains. Both White (1940) and Shields (1936) use discrete mechanics and assume detachment occurs from the channel bed.

Continuum mechanics considers the soil-water-air matrix as one material with averaged properties. Models which use local gradients, Darcy's Law and the Terzaghi and Peck (1948) vertical heave criteria, such as Schmertmann (2000), Hanses (1985) and van Rhee and Bezuijen (1992), use continuum mechanics. Both Schmertmann (2000) and Hanses (1985) assume detachment occurs from the channel tip, where as van Rhee and Bezuijen (1992) wasn't developed for a backward eroding channel specifically, but is likely to be applicable to any sloping sandy surface (such as the tip and sides).

At the soil-channel interface, Darcy's Law is no longer applicable because the velocity is a superficial velocity, not the actual seepage velocity of the fluid; the permeability relates only to the superficial velocity through the porous media and the head loss (or gradient) across the interface is some complicated transitional value between that within the porous media and that along the channel. In fact, the calculation of local gradients at the soil-channel interface is problematic given that gradients across infinitesimally small distances start to become erroneously high at best or meaningless at worst. Making particle detachment models which use continuum mechanics questionable.

The fact that Baldock and Nielsen (2010) found that vertical seepage forces/gradients do not affect incipient motion supports the idea that gradients occurring within the soil matrix are not occurring at the soil-channel interface.

As for the Terzaghi and Peck (1948) vertical heave criteria of $i_c = \rho'/\rho_w \approx 1$, this is a measure of when effective stress *throughout* a vertical shaft of soil is zero. It occurs when, at the base of a vertical shaft of soil, the weight of soil above it is equal and opposite to the seepage force below it. Yet at the soil-channel interface, there is no weight of soil above, so effective stress is no longer a function of soil weight and is likely to already be quite low. In other words, zero effective stress could occur at local gradients much less than one.

The current author is of the opinion that modelling particle detachment would be most accurate using a discrete mechanism which considers forces on individual particles.

As for where each model assumes particle detachment is occurring from, the channel bed, tip and/or walls, the current author prefers models which assume detachment from the channel tip because it is detachment from the tip that causes tip progression, not detachment from the bed as Sellmeijer (1988); Hoffmans (2016) assume. If detachment were occurring from the channel bed then one would expect the channel to become deeper with length yet channel depths are observed as remaining fairly constant (see Subsection 4.5.1 and Vandenboer and van Beek (2013)). It is likely particle detachment is occurring from the sides as well, however this detachment results in channel meandering more than tip progression. Currently, there are no particle detachment models which use discrete mechanics at the channel tip.

2.5.4 Particle Transport

If particle transport is differentiated from particle detachment and defined as the carrying of soil particles through the channel and out of the system (perhaps through a sand boil) then it appears that particle transport is not modelled amongst the reviewed models.

Both Townsend et al. (1988) and Schmertmann (2000) believe larger water velocities are needed to detach particles from the tip than needed to transport the particles out of the channel. Therefore if water velocities are sufficient for detachment they are more than sufficient for transport and detachment becomes the governing mechanism. To support this Schmertmann (2000) refers to Hjulstroms diagram (Figure 2.25) (Krumbein and Sloss, 1963) which shows higher velocities needed for erosion (detachment) than transport.

Schmertmann (2000) acknowledges that he does not model particle transport because he suggests that the gradients and water velocities required to detach the particles are more than sufficient to transport the particles and so it is particle detachment that is the limiting process of backward erosion. When responding to the possible criticism that his method

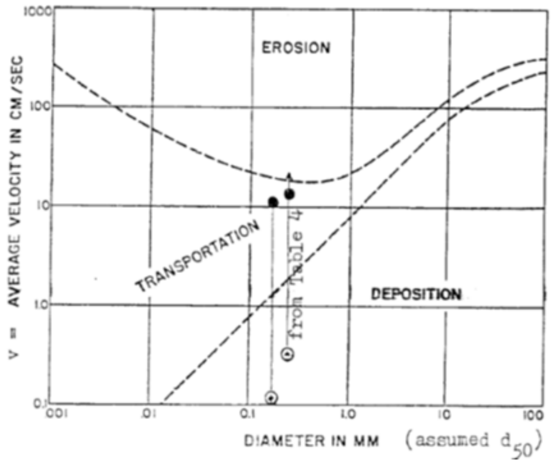

Figure 2.25: Hjulstrom's diagram of erosion, transport and deposition of sedimentary particles (Krumbein and Sloss, 1963)

does not consider how sand gets carried to the discharge point Schmertmann (2000) responds with "In this respect the method produces conservative results by considering only the requirements for advancing the pipehead. However, the experiments themselves which underpin the new method at least partially include the discharge requirements."

The observation of channels blocking may challenge the principle of water velocities sufficient for detachment will be more than sufficient to transport particles out of the system (if blocking occurs due to sediments settling and depositing out from the channel flow). Townsend et al. (1981) and van der Zee (2011) observed channel blockages.

Townsend et al. (1981) reported that as the channel progressed, the area of the channel increased, thereby reducing flow velocities in the channel to an extent which permitted particle deposition. Particles deposited in the downstream portion of the channel and caused the channel to stop progressing. The head was further increased until progression recommenced.

van der Zee (2011) also reported a deposition of sand at downstream portion of the channel leading to blockage but in this instance, did so without an increase in channel area. The area of the channel was restricted due to a test set-up only 10mm wide. Like Townsend et al. (1981), blocking was overcome by raising the head until the blockage cleared.

Considering the vast number of backward erosion testing (listed in Table 2.1) these reports represent only a small portion of experiments and therefore blocking doesn't appear to be common. However, blocking was observed in 40% of experiments carried out as part of this study (see Subsection 4.5.4), although only 26% of these experiments required an increase in head above critical to maintain tip progression.

Given that channel blocking was not common across backward eroding testing and when it did occur it only resulted in *higher* global critical gradients, it is considered acceptable and conservative to not include the resistance offered by channel blocking. Therefore it is also considered acceptable and conservative to not include particle transport in predictive models.

2.5.5 Erosion rate

The rate of backward erosion is the speed at which the channel tip progresses. Neither of the most widely used prediction models, the Schmertmann (2000) method or the Sellmeijer et al. (2011) method, include the speed of channel progression. Nor does the most recent research of van Beek (2015) include consideration of erosion rate.

Schmertmann (2000) does report that the length of time over which a head is maintained does not affect the initiation or critical head (i.e. no time effect). For instance, allowing additional time for a channel to initiate did not reduce the initiation head. Also reported was that increases in gradient above critical resulted in an increase in channel progression rate. Schmertmann (2000) provided a single tip progression rate of 5mm/min. Müller-Kirchenbauer et al. (1993) provided a range of tip progression rates from 6mm/min to 42mm/min and reported that this rate increased with increase in channel length.

Hoffmans (2016) refers to Bonelli et al. (2007) and van Rijn (2014) for time-scale relations. However Bonelli et al. (2007) is more applicable to concentrate leak erosion and the time to enlargement of a crack resulting in failure. Van Rijn (2014) is applicable to backward erosion piping and puts forward two techniques for estimating the time-scale of channel progression. One is the bed-load transport model of Paintal (1971) which is designed for estimates in turbulent flow but also produces realistic results in laminar flow with some turbulence (van Rijn, 2014). The other technique is also a bed-load transport model but by Girgus (1977) for laminar flow, although van Rijn (2014) warns his results may not be valid for very small bed-shear stresses around incipient motion. Van Rijn (2014) graphs a set of time-scales for a full-sized example however no experimental or field-based validation appears to be have been made. Also, both of the time-scale models assume bed-load transport which concerns the current author given that transport from the channel tip is considered more likely than bed-load transport.

The rate of backward erosion piping would enable comparison of the time required for a channel to reach the upstream side with anticipated flood duration (taken from flood hydrographs). This comparison could lead to reducing the risk of failure if time for complete progression was less than flood duration or could lead to increasing the risk of failure if flood levels above the critical head reduced the time for complete progression thereby equating it or making it less than flood duration. Rate information could also give an indication of how many more flood events a given dam/levee system could withstand, if past flood levels and durations are known. There is currently no way to estimate this (Sills and Vroman, 2007).

2.5.6 Predictive Models

Predictive models are formulations which bring together the various mechanics of backward erosion discussed above. These predictive models provide the critical gradient which will lead to progression of a continuous pipe and eventually failure of the dam/levee (with exception of the Terzaghi method which provides the initiation gradient).

The account to follow is not an exhaustive one of all predictive models available but is restricted to the most well-known methods used in industry.

Bligh

The predictive model of Bligh (1910) appears to be one of the first methods developed for backward erosion prediction and has been a popular, widely used method. It is an empirical relationship developed from having analysed a large number of failures from field studies (Technical Advisory Committee on Flood Defences, 1999). The method relates the hydraulic gradient to an erosion coefficient 'c' which is unique to different sands as per Table 2.3. Griffith (1913) suggested a similar approach and called it the 'line of creep method' (Sellmeijer et al., 2011). The relationship is given by Equation 2.11 (Sellmeijer et al., 2011).

Table 2.3: Bligh and Lane erosion coefficients (Technical Advisory Committee on Flood Defences, 1999)

Soil type	Median grain diameter (μm)	c (Bligh, 1910)	c (Lane, 1935)
Extremely fine sand	<105		8.5
Very fine sand	105-150	18	
Very fine sand (mica)		18	7
Moderately fine sand (quartz)	150-210	15	7
Moderately coarse sand	210-300		6
Very/extremely coarse sand	300-2000	12	5
Fine shingle	2000-5600	9	4
Moderately coarse shingle	5600-16000		3.5
Very coarse shingle	>16000	4	3

$$\frac{H_c}{L} = \frac{1}{c} \tag{2.11}$$

Lane

If a seepage length contained a vertical section Bligh (1910) was of the opinion that the length of the vertical sections should be included in the seepage length along with the horizontal sections. However Lane (1935) proposed that vertical sections contribute more to the erosion resistance than the horizontal sections do (Technical Advisory Committee on Flood Defences, 1999). Therefore Lane (1935) provided an alternate empirical rule, called the weighted seepage method, whose erosion coefficients are given in Table 2.3. The relationship is (Technical Advisory Committee on Flood Defences, 1999):

$$\frac{H_c}{{}^1\!/_3 L_h + L_v} = \frac{1}{c} \tag{2.12}$$

where L_h = horizontal seepage length
L_v = vertical seepage length

Whilst the methods of Bligh and Lane are easy-to-use and have been widely used, they are quite conservative methods often leading to rather wide dams and levees (which are often space or cost inhibitive). Therefore research was initiated to devise less conservative methods (Weijers and Sellmeijer, 1993).

Terzaghi

Terzaghi and Peck (1948) provided a vertical critical gradient that will lead to heave. Heave occurs when effective stress *throughout* a vertical shaft of soil is zero. This occurs when, at the base of a vertical shaft of soil, the weight of soil above it is equal and opposite to the seepage force below it (Holtz et al., 2011).

The critical heave gradient is given by (Holtz et al., 2011):

$$\frac{H_c}{L} = \frac{\gamma_p - \gamma_w}{\gamma_w}(1-n) = \frac{\rho'}{\rho_w} \approx 1 \tag{2.13}$$

Table 2.4 lists typical values of the critical heave gradient for soil containing particles with density = 2680 kg/m^3. As the table suggests, the critical heave gradient is usually close to one.

Table 2.4: Typical values of critical heave gradient for ρ_s = 2680 kg/m^3 (Holtz et al., 2011)

Void Ratio	Approximate Relative Density	i_c
0.5	Dense	1.12
0.75	Medium	0.96
1	Loose	0.84

Terzaghi and Peck (1948) show that backward erosion piping will initiate when a heave or zero effective stress condition occurs in cohesionless soils at the downstream toe of an embankment (ICOLD, 2015). Though Pabst et al. (2013) challenge this, stating that backward erosion or the creation of an unfiltered surface will not necessarily occur due to heave.

Nevertheless, it is common practice to use the critical heave gradient to determine when backward erosion piping will initiate (ICOLD, 2015). Though it is important that only the vertical component of the exit gradient is considered given the Terzaghi and Peck

(1948) critical heave gradient is only applicable to vertical seepage gradients (Pabst et al., 2013).

Sellmeijer

Sellmeijer and his colleagues at Deltares in The Netherlands have produced two predictive models. One is a mathematical model which is solved with the use of computer programs and the other is a formula for a 'standard dike' configuration. Both models started with Sellmeijers PhD thesis (Sellmeijer, 1988).

Mathematical & Numerical model

In order to combine the various components on the backward erosion mechanism, such as seepage flow in the eroding soil layer, flow in the channel and particle detachment (described in their respective sections above), a mathematical model is used and solved by a computer program. In essence the mathematical model is a linear groundwater flow problem with unusual boundary conditions (Koenders and Sellmeijer, 1992). Boundary conditions of the groundwater flow as well boundary conditions of the sand particles at equilibrium in the sand boil (Coulomb equilibrium) and in the channel (rolling equilibrium) (Koenders and Sellmeijer, 1992).

Output from the program is in the form of Figure 2.26 which are curves of H/L as a function of l/L for 3 different particle sizes. The curves show that H/L is at a maximum at approximately $l/L = 1/2$. The maximum H/L is the critical gradient for progression and is commonly obtained once the channels reach halfway across the foundation (Sellmeijer and Koenders, 1991). This is for an infinite foundation depth but as the foundation depth reduces to a finite value the critical gradient is reached sooner, e.g. for $D/L = 1/3$, $l/L = 1/3$ (Hoffmans, 2009).

Whilst the mathematical model could handle multiple geometries, it was still restricted to simple geometries due to the restrictive nature of the analytical technique of conformal mapping - the method used by the mathematical model to solve Laplace's flow equation (Sellmeijer, 2006). Therefore a numerical model was required to allow for more complicated geometries.

This numerical model was an extension of the 2D-FEM seepage program MSEEP with code

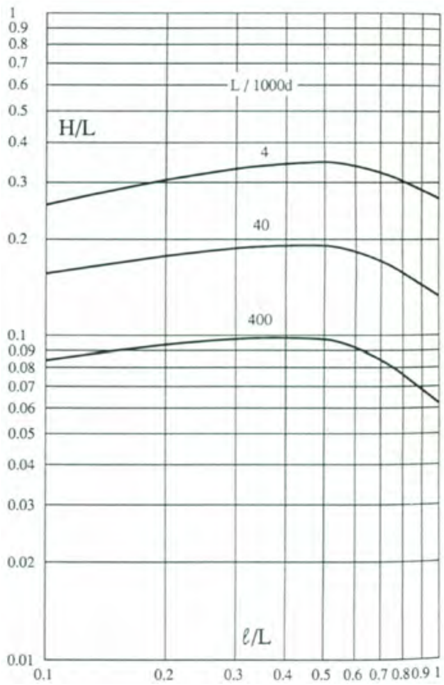

Figure 2.26: Output from mathematical model (Sellmeijer and Koenders, 1991)

added to include Sellmeijer's model (van Beek et al., 2008). MSEEP can accommodate more complicated geometries, such as a sloping levee base; multiple foundation layers including gravel; and foundation layers of varying thickness. MSEEP also features in the literature as the means for determining the geometrical factor (van Beek et al., 2010b) and developing the formula for a standard dike configuration (van Beek et al., 2012b) (which is described in the following section).

In Sellmeijer (2006) amendments were made to the model including omission of the vertical and horizontal flow forces. The flow forces were omitted because it was considered that a particle at equilibrium would be protruding out of the soil surface as a result of the smaller particles around it having already been eroded away and so the flow forces would not affect the particle.

Sellmeijer (2006) demonstrates the numerical model can also be used with an Artificial Neural Network to develop formulas for configurations more complicated than the 'standard dike' configuration. This is demonstrated by providing a formula for the critical head and critical levee width of a sloping dike with two granular foundation layers of varying width. This formula can be readily used by industry.

Van Beek et al. (2012b) compared MSEEP calculations with small-scale experimental results for single and multi-layer foundations using sloping and circular exits. The result of this comparison is shown in Figure 2.27. This comparison indicated good agreement between experimental observations and MSEEP predictions for single and multi-layer foundations with a slope exit (note: for a single-layer foundation, $D_f/D = 1$). However, this was not the case for circular exits for which critical heads in experiments were approximately half of the MSEEP predictions. This is because MSEEP is a 2-dimensional model and is therefore unable to model exit geometries which create 3D flow patterns (van Beek et al., 2012b).

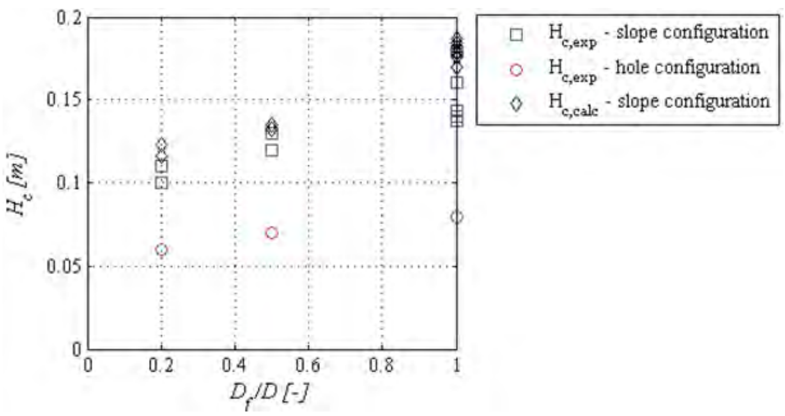

Figure 2.27: Comparison of experimental results ($H_{c,exp}$) with MSEEP calculations ($H_{c,calc}$) for critical head difference (van Beek et al., 2012b) (D_f/D is the depth of top fine layer divided by total foundation depth)

Formula for 'standard dike'

The formula for a standard dike was developed to provide a design engineering tool for practising engineers (Sellmeijer, 1988). The model was formed as an equation for the critical gradient which would provide engineers the maximum water level difference permissible for a given dam/dike/levee cross-sectional length. The equation was constructed by clustering related terms, making approximations and curve-fitting results obtained from the mathematical model (Sellmeijer, 1988). The 'standard dike' is a flat (non-sloping) levee on a single-layer foundation of uniform sand with a slot/ditch exit as depicted in Figure 2.28.

The first standard dike formula in Sellmeijer (1988) was for a semi-infinite foundation then in Sellmeijer et al. (1989) the standard dike formula was amended to include a finite foundation thickness and a clay cover over the landside. The accuracy of the standard dike formula is illustrated by Weijers and Sellmeijer (1993) for both small-scale (Figure 2.29) and large-scale tests (Figure 2.30). The small-scale test comparisons indicated a very

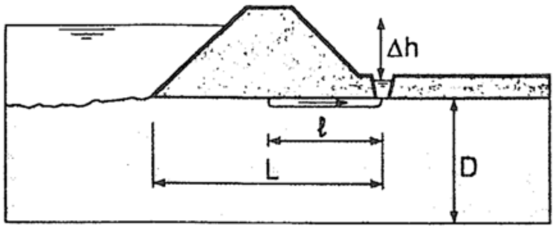

Figure 2.28: Standard dike configuration (Weijers and Sellmeijer, 1993)

good match for fine sands but for coarse sands the results were more erratic and the agreement was less satisfactory. A suggested reason for this is the model assumes the flow in the channel is laminar, which for fine sands is a reliable assumption, however for coarse sands the flow becomes turbulent (Weijers and Sellmeijer, 1993). Sellmeijer et al. (2011) also suggests the poor model performance for coarse sands is related to the width of the channel, which increases with increasing grain size (van Beek, 2015) and is not considered in the model (the model assumes an infinitely wide channel, given it is a 2D model). Additionally, Sellmeijer et al. (2011) suggests that channels in fine sands develop as a front while channels in coarse sands erode in smaller strips.

As for the large-scale test comparisons, comparisons indicated a good match (note: the large-scale tests were carried out in fine sand).

The standard dike formula was first written in terms of three factors by van Beek et al. (2010a) to distinguish different features of the backward erosion model. The resistance factor, F_R is related to the equilibrium of forces on grains in the bed of the channel. The scale factor, F_S is a function of the ratio of grain size to seepage length. The geometrical factor, F_G is a function of the effect of aquifer shape on groundwater flow (van Beek, 2015).

In Sellmeijer et al. (2011) further amendments were made to the standard dike formula to include the 2-force limit equilibrium of bed particles; further development of the three factors; and inclusion of sand characteristics not previously considered including relative density, uniformity, roundness and d_{70}. The influence of these sand characteristics were incorporated by means of a multivariate regression analysis carried out on results from the small-scale experiments (there were insufficient medium and large-scale tests for statistical analyses).

The revised standard dike formula was validated with full-scale test levees with a seepage

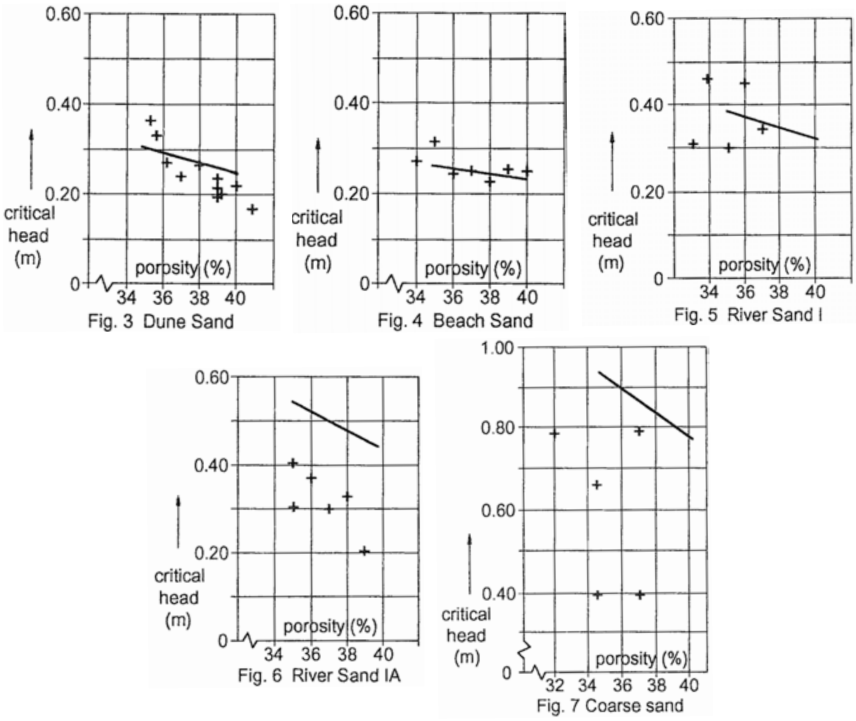

Figure 2.29: Model (indicated by lines) and experimental results (indicated by + symbols) for small-scale tests (Weijers and Sellmeijer, 1993)

length of 15m (van Beek et al., 2011a). These test levees were constructed in north-east Netherlands and referred to in literature as the IJkdijk testing (which roughly translates from Dutch to 'test dike' according to personal correspondence with Dr van Beek). Two of the IJkdijk tests were carried out in fine sand ($d_{70} = 180\mu$m) and another test in coarse sand ($d_{70} = 260\mu$m) (Sellmeijer et al., 2011). Experimental results in the fine sand were well predicted by the standard dike formula but were not in the coarse sand which saw a deviation of 25% (Sellmeijer et al., 2011). This is similar to the comparison in Weijers and Sellmeijer (1993) which showed good predictions for fine sands but not for coarse sands.

In van Beek et al. (2012b) the intrinsic permeability was amended to account for multiple sand layers in the foundation. In van Beek et al. (2013) the geometrical factor was slightly amended to eliminate a singularity which presented when depth to length ratios outside the calibrated range. The standard dike formula in van Beek (2015) is the most current

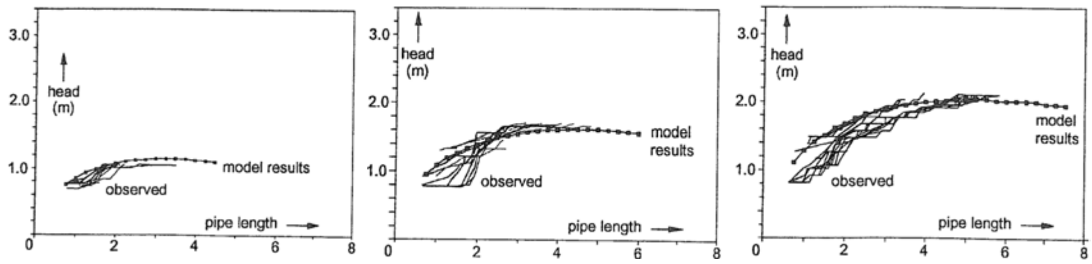

(a) 6m seepage length (b) 9m seepage length (c) 12m seepage length

Figure 2.30: Model (indicated by dotted lines) and experimental results (indicated by stepped lines) for large-scale tests (Weijers and Sellmeijer, 1993)

version that the current author is aware of and is given by:

$$\begin{aligned}
\frac{H_c}{L} &= \frac{1}{c} = F_R F_S F_G \\
F_R &= \eta \frac{\gamma_p'}{\gamma_w} \tan\theta_r \left(\frac{RD}{RD_m}\right)^{0.35} \left(\frac{C_u}{C_{u,m}}\right)^{0.13} \left(\frac{KAS}{KAS_m}\right)^{-0.02} \\
F_S &= \frac{d_{70}}{\sqrt[3]{\kappa L}} \left(\frac{d_{70,m}}{d_{70}}\right)^{0.6} \\
F_G &= 0.91 \left(\frac{D}{L}\right)^{\frac{0.24}{\left(\frac{D}{L}\right)^{2.8}-1}}
\end{aligned} \tag{2.14}$$

where F_R = resistance factor [-]

F_S = scale factor [-]

F_G = geometrical factor [-]

η = White's coefficient [-]

γ_p' = effective unit weight of particle [N/m^3]

θ_r = angle of repose [°]

RD = relative density [-]

C_u = coefficient of uniformity [-]

KAS = roundness of particle [-]

κ = intrinsic permeability [m^2]

subscript$_m$ = mean value of experimental data set

For multi-layered foundations with horizontal layers of constant thickness, $D/L < 0.3$ and $K_{coarsesand}/K_{finesand} < 10$, the intrinsic permeability may be altered to according to van Beek et al. (2012b):

$$\kappa_{horizontal,average} = \sum_{m=1}^{n} \frac{\kappa_{horizontal,m} D_m}{D_{total}} \tag{2.15}$$

Given that much of the standard dike formula is empirical in its adaptation with little physical foundation, it is recommended the formula only be used for geometries and soils similar to those tested (Sellmeijer et al., 2011), i.e. within the limits listed in Table 2.5.

Table 2.5: Parameter limits of standard dike formula

parameter	minimum	maximum	mean
Relative density, RD	50%	100%	72.50%
Coefficient of uniformity, C_u [-]	1.3	2.6	1.81
Roundness, KAS	35%	70%	49.8%
d_{70}	150 μm	430 μm	208 μm
D/L for multiple foundation layers [-]	0.1	1	not needed
$k_{coarse.sand}/k_{fine.sand}$ for multiple foundation layers [-]	1.5	100	not needed
D_{fine}/D for multiple foundation layers [-]	0.1	1	not needed

Van Beek (2015) provided comparison of experimental results with predictions from the latest standard dike formula given in Equation 2.14. Figure 2.31a shows model comparison for experiments with 2-dimensional exit geometries (slot and plane exits) in fine and uniform sands. In this instance, predictions provided by the standard dike formula performed well, although slightly higher (slightly non-conservative).

Figure 2.31b shows model comparison with experiments containing 3-dimensional exit geometries (circle exit) in fine, uniform sands. This shows model predictions were twice as large as critical gradients observed in experiments, leading to Van Beek (2015) suggesting predictions be halved for 3D exits. Poor performance of the model in this instance is attributed to the effect 3D groundwater flow conditions on the critical graident which can no be captured by the standard dike formula given it's derived from the 2D numerical model (van Beek, 2015).

Figure 2.31c shows model comparison with experiments in which soil type and relative density were varied (using a circular exit). This shows model predictions were again, twice as large as critical gradients observed in experiments, for Baskarp sand (another fine, uniform sand) (again, as a result of the circular exit). However model predictions for coarser soils (Sterskel, Oostelijke and Waalre sands) were considerably different to experimental findings. One reason for this, suggested by van Beek (2015), is the model does not take the increase of erosion resistance due to increase in fines into account.

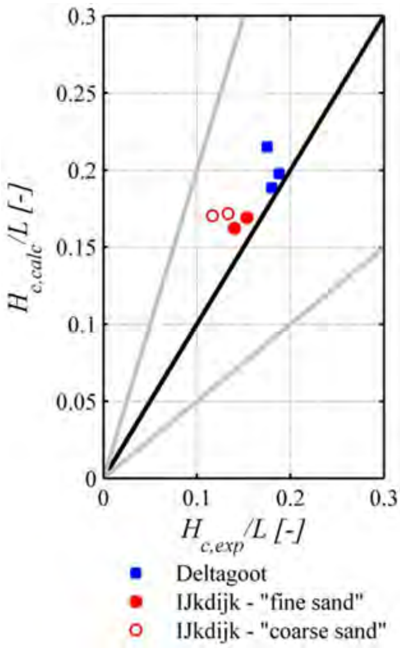

(a) 2D exits and fine, uniform sands

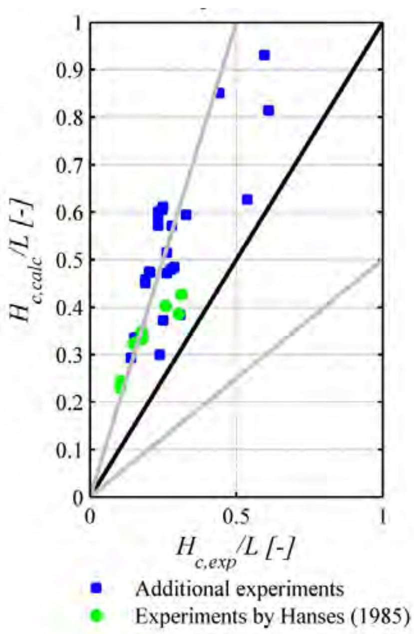

(b) 3D exits and fine, uniform sands

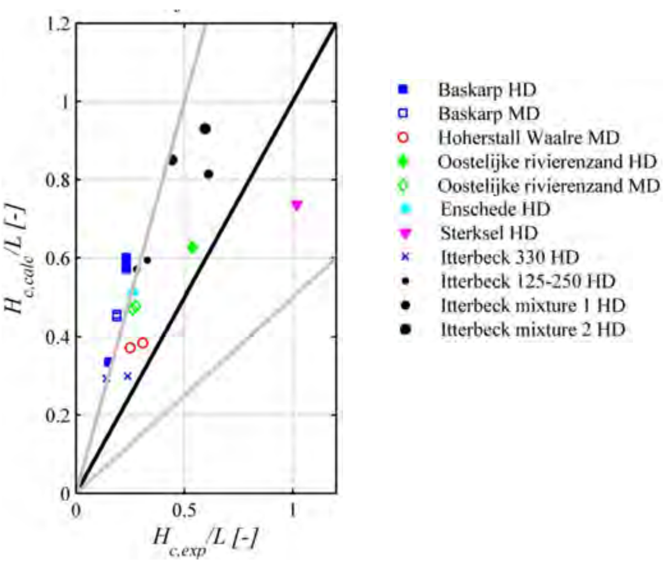

(c) 3D exits and fine to coarse sands with $C_u < 3.17$

Figure 2.31: Comparison of model predictions with experimental results by van Beek (2015). Black line indicates perfect agreement and grey lines indicate differences by a factor of 2.

In summary, van Beek (2015) concludes the standard dike formula performs well for 2D exit-geometries in fine uniform sands. It also accounts well for changes in permeability, scale and depth:length ratios. However the formula over-predicts the critical gradient when 3D exit-geometries are used, by a factor of 2. Although this factor can be used to compensate for differences. Also, the standard dike formula does not perform well for coarse or well graded soils.

Concerns with the Sellmeijer et al. (2011) model, according to Hoffmans (2016), begin with the premise that whilst it includes all relevant parameters, it does not give insight into physical processes. In addition, it is non-conservative for coarse sands, likely to be a result of using White's equilibrium of forces on a bed grain, which for coarse sand, over-predicts the critical shear stress. Furthermore, the White (1940) theory does not take grain size into account which lead Sellmeijer et al. (2011) to use a constant critical Shields parameter for all sediment sizes, yet the Shields curve demonstrates the parameter is dependent on sediment size. Related to this is the use of a single angle of repose for all soils in the Sellmeijer et al. (2011) model of between 37° to 41°, which Hoffmans (2016) considers to be too high and cites references stating that the angle of repose should lie in the range of 30° (for fines) to 35° (for coarse sand) for 0.15mm $<d_{50}$ <0.75mm.

In response to the erroneous independence of the White (1940) model on particle size, van Beek (2015) suggested an amendment to the calculation of critical shear stress used within the Sellmeijer model. The amendment came about after having collated the critical Shields parameter across a number of various studies looking at incipient motion in laminar flow. This collation led to a new fit in the data which when expressed in terms of critical shear stress and parameters related to the grain equilibrium (particle density and size), provided a relationship between d_{50} and the angle of repose given in Equation 11.8.

$$\theta_r = -8.125 \ln d_{50} - 38.777 \tag{2.16}$$

This defines a decrease in angle of repose with increase in particle diameter. Van Beek (2015) states that the reason behind this relationship is unclear but does refer to other researchers who have reported the same trend. Therefore, instead of using a constant angle of repose of 37°, as done by Sellmeijer et al. (2011), the angle of repose ought to be calculated using Equation 11.8, before use in the resistance factor of Equation 2.14. Van

Beek (2015) also recommended using an $\eta = 0.3$ (instead of 0.25) to be consistent with the findings of White (1940).

This amendment is reported to still be based on the equilibrium of forces by White (1940) but also complies with the Shields approach and was calibrated using an array of incipient motion experiments in laminar flow (van Beek, 2015).

In examining the improvement this amendment makes to predictions calculated by the standard dike formula, (van Beek, 2015) provides Figure 2.32 which shows that the difference between model predictions and experimental observations reduced when the amendment was used, as indicated by the green data points clustered closer to the zero difference line. Note that “cal. White” in the figure legend refers to ‘calibrated White model’, the label which (van Beek, 2015) used to refer to her suggested amendment.

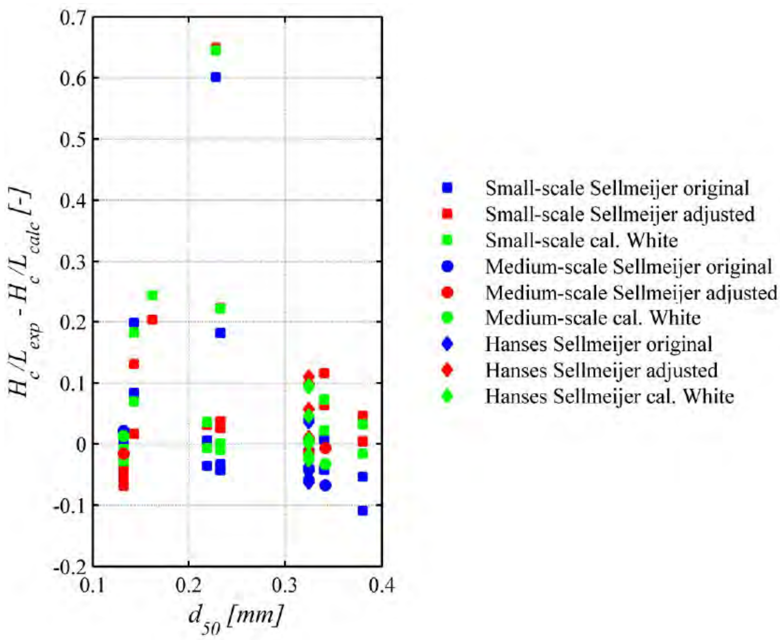

Figure 2.32: Difference between model predictions and experimental results using critical shear stress amendments suggested by (van Beek, 2015) (green data points)

A review of the Sellmeijer et al. (2011) standard dike formula, along with the (van Beek, 2015) amendment to the critical shear stress calculation, is given in Section 11.3 whereby its predictions are compared to results both from this study and other studies. Also given in Section 11.3 are recommendations for amendments to the standard dike formula to improve model predictions.

Hoffmans

Hoffmans (2014) formulated a model called the 'Shields-Darcy model', which as the name suggests, is a combination of Darcy's Law (used to evaluate head loss as flow seeps through the sand) and the Shields (1936) diagram (used to ascertain incipient motion due to shear stress imposed by flow). Hoffmans (2014) also uses the Hagen-Poiseuille equation to determine channel flow.

Figure 2.33a is a schematisation of flows used in the model and Figure 2.33c is a diagram of the simplified approach whereby the hydraulic gradient is divided into two straight lines, the upstream line for the gradient through the sand and the downstream line for the gradient through the sand. Symbols used in these figures include Q_1 = horizontal groundwater discharge on river side, Q_2 = horizontal groundwater discharge on landside, $Q_{T,p}$ = pipe discharge at channel tip, $Q_{T,s}$ = vertical inflow towards the channel, $Q_{p,m}$ = pipe discharge on landside.

The critical hydraulic gradient is the sum of the critical Shields gradient and the critical Darcy's gradient as illustrated in Figure 2.33b. The equation for the critical (global) hydraulic gradient is given in Equation 2.17.

$$\frac{(H_1 - H_2)_c}{L} = \frac{\sqrt{g}\left(\tau_{*,c,lam}\Delta d_{15}\right)^{3/2}}{\nu\sqrt{\alpha_{Re,l}}} + \left(1 - \frac{l_c}{L}\right)\frac{d_{50}\nu}{l_{Re}kD} \tag{2.17}$$

where $\tau_{*,c,lam}$ = critical Shields parameter for laminar flow $= 0.2\left(d_*\right)^{-1/3}$ for $2 \leqslant d_* \leqslant 15$

where d_* = dimensionless particle diameter $= d_{50}\left(\Delta g/\nu^2\right)^{1/3}$

Δ = relative density $= \rho_s/\rho - 1$

ν = kinematic viscosity

$\alpha_{Re,l}$ = geometrical pipe coefficient = 6

$$\frac{l_c}{L} = \exp\left(-\left(\frac{\alpha_f D}{L}\right)^2 \frac{\sqrt{g}\left(\tau_{*,c,lam}\Delta d_{15}\right)^{3/2}}{\nu\sqrt{\alpha_{Re,l}}}\right)$$

where α_f = geometrical groundwater coefficient = 5

l_{Re} = length scale $= 18 \times 10^{-6}$m

k = hydraulic conductivity of sand $= \dfrac{g}{160\nu}\dfrac{n^3 d_{15}^2}{(1-n)^2}$

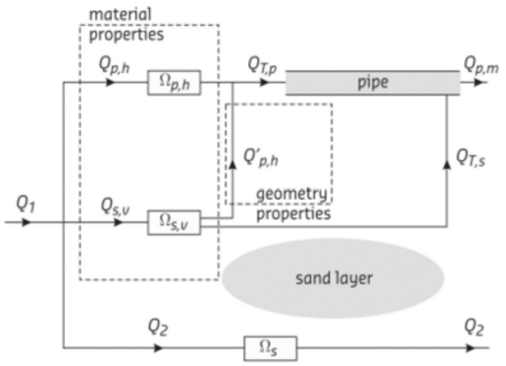

(a) Simplification of the distribution of the hydraulic gradient

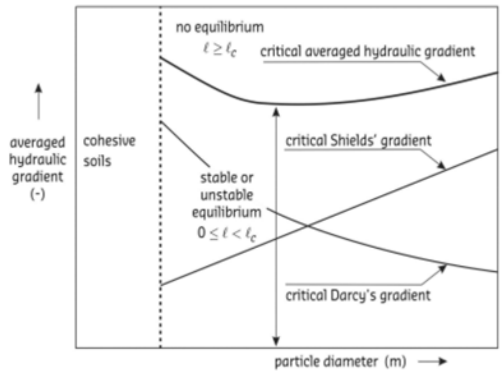

(b) Critical averaged hydraulic gradient is the sum of critical Shields gradient and critical Darcy's gradient

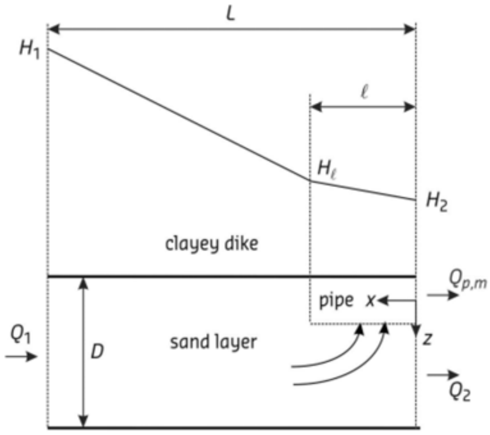

(c) Simplification of the distribution of the hydraulic gradient

Figure 2.33: Diagrams explaining the Shields-Darcy Model (Hoffmans, 2014)

Schmertmann

Schmertmann (2000) predicts the *local* gradient at the channel tip required to progress a channel by taking critical global gradients found in experiments and then converting these to an equivalent local gradient in the field, at some point 'x' along the seepage path, with a series of correction factors.

These correction factors are listed in Equation 2.18 whereby the numerator is the local gradient at the channel tip required to progress the channel and the denominator is the local gradient expected at the channel tip. This fraction gives the factor of safety against backward erosion.

$$F_{px} = (i_p/i)_{xf} = \left\{ \frac{(C_D C_L C_S C_K C_Z C_\gamma)\left(C_G \bar{i}_{pm}\right)_t C_\alpha}{\left(C_G \bar{i} C_R\right)_f} \right\}_x \tag{2.18}$$

where i_{pxf} = local gradient at pipe tip needed to drive piping; in the field at some point 'x' along the seepage path

i_{xf} = local gradient at pipe tip; in the field at some point 'x' along the seepage path

C_D = depth/length factor

C_L = length factor = $(L_t/L_f)^{0.2}$

C_S = grain size factor = $(d_{10}/0.2)^{0.2}$

C_K = anisotropic permeability factor

C_Z = underlayer factor

C_γ = density factor

C_G = gradient factor for parallel flow

$\bar{i}_{pmt}$ = critical global gradient in laboratory test

C_α = pipe inclination correction

C_R = gradient factor for convergent/divergent flow

$\bar{i}_f$ = global gradient in the field

$_p$ = piping

$_x$ = point 'x' along seepage path

$_f$ = field

$_t$ = test

Schmertmann (2000) assumes a channel will progress through zones of higher local gradient with lower global gradients and zones of lower local gradient with higher global gradients, all before the channel enters the area and locally distorts the gradients and flow conditions. In other words, Schmertmann (2000) assumes that local gradients present before the channel exists can be used to predict backward erosion. As support for this approach, Schmertmann (2000) reports that a conservative interpretation of flownet studies and flume tests indicate a negligible effect of the channel on the flownet when one considers a point 80 radii in any direction from the channel with a semi-circular cross-section.

Schmertmann (2000) calculates local gradients by multiplying the global critical gradient with the gradient factor for parallel flow, C_G. The C_G factor is calculated using 2D flownets, which, due to the above assumption, can be flownets drawn without the channel. These 2D flownets provide the local gradient at the point of interest.

In the numerator, the point of interest is where the tip would be located when the maximum head difference would be required, usually when l/L = 30–50% in Delft tests and 20% in University of Florida tests (Schmertmann, 2000). Note that the maximum global gradient will be required where the local gradient is at its minimum (i.e. highest head needed when seepage velocities at the tip are at their slowest). The local gradient (where the tip would be located when the maximum head difference would be required) is divided by the critical global gradient to give the C_G factor.

In the denominator, the point of interest is the position along the seepage page at which the factor of safety is being calculated, i.e. at point 'x'. In this case, the C_G factor would be the local gradient at point 'x' divided by the global gradient for the flood level under consideration. Alternatively though, the local gradient itself could be directly input into the dominator of Equation 2.18 and the C_G factor would not be needed.

If seepage modelling or flownets of the dam/levee under consideration is not available then Schmertmann (2000) provides a method for calculating the average factor of safety, referred to as the 'average method'. Note that the more detailed method, considering factors of safety at numerous points along the seepage path, is referred to as the 'point method'. The average method is over-conservative and is intended as a first-pass method used to determine whether the point method is necessary.

Schmertmann (2000) does not appear to consider the ramifications of exit geometries which create 3D flow, such as a circular exit. Otherwise it would have been recognised that calculating local gradients using 2D transverse flownets would be insufficient in these instances. For example, if flow through a circular exit is modelled using either a hand-drawn 2D transverse flownet or a 2D seepage program, then the circular exit is reduced to a slot exit and any distinction between the two exit geometries is lost. Schmertmann (2000) does include a C_R factor, a gradient factor for convergent/divergent flow, however this factor is only included on the denominator (excluding the possibility of testing in circular exits) and seems to be only relevant to convergent/divergent flows caused by dam axis curvature, although this is not clear. The current author speculates that the Schmertmann (2000) method could still be used when 3D exits are used, however local gradients (and therefore the C_G factor) would need to be calculated using 3-dimensional seepage programs.

Ideally, experimental tests would be carried out on foundation soil of the dam/levee being designed/reviewed. However if this is not feasible then Schmertmann (2000) offers a method for predicting what the critical local gradient would be in the University of Florida testing by relating the soil's coefficient of uniformity to the critical local gradient as shown in Figure 2.34. This relation was developed by plotting results from numerous studies and suggesting a conservative trend-line whereby $i_{pmt} = 0.05 + 0.183\,(C_u - 1)$.

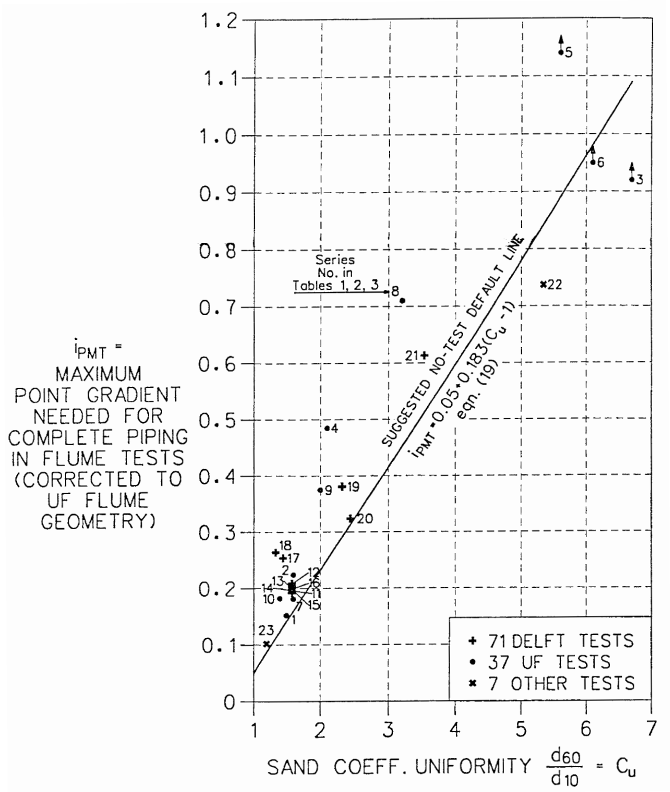

Figure 2.34: Critical local gradient at channel tip with uniformity (Schmertmann, 2000)

Before Schmertmann (2000) plotted results from other studies onto Figure 2.34, he adjusted their critical global gradients to equivalent local gradients at the tip which would have occurred in the University of Florida flume. To do so, he used three correction factors: the depth/length factor (C_D), the length factor (C_L) and the gradient factor for parallel flow (C_G) resulting in Equation 2.19.

$$i_{pmt} = C_D C_L \cdot C_G \overline{i_{pmt}} \tag{2.19}$$

It is noted Schmertmann (2000) did not apply the particle size factor, C_S or the density factor, C_γ to results before plotting them onto Figure 2.34 (neither the University of Florida results or the results from other studies). Schmertmann's justification for not using C_S was the d_{10} sizes of the tests plotted, ranged between 0.15–0.28mm whose average was 0.2mm. Therefore, with an average value of 0.2mm, C_S became equal to one given that $C_S = (d_{10}/0.2)^{0.2}$. However review reveals that d_{10} sizes actually ranged between 0.062mm and 0.8mm, raising questions about this decision. A similar justification was given for not using C_γ, that the averaged test results plotted on Figure 2.34 had an average relative density of 60%, so C_γ became equal to one given that $C_\gamma = 1 + 0.4(RD - 0.6)$. However upon inspection of source literature, relative densities varied between 16 to 95% (from among the Dutch testing), with averages not equal to 60% for each of the test series data points. Given this large range of values, the robustness of C_γ is questionable.

Recommended minimum factors of safety for design are 2 when the seepage path contains filter protection and 3 when it does not. These factors of safety relate to the maximum factor of safety when the 'point method' is used. Lower minimum factors of safety are given for the 'average method'.

Schmertmann (2000) makes reference to using vertical gradients to develop the various correction factors. It is unclear how vertical gradients were used especially when pre-channel vertical gradients would be zero along the mid-base of the dam/levee.

The Schmertmann (2000) method is referred to in both the ICOLD Bulletin No. 164 on internal erosion (ICOLD, 2015) and the Unified Piping Toolbox (Fell et al., 2008) (a popular guidance document in Australia and the United States). However in both of these documents, caution is called for when using this method for soils with uniformity coefficients greater than 3 because *"is it based on little data in the larger uniformity coefficient range, and some of these may be affected by internal instability"* (ICOLD, 2015, p. 50).

Given that soils tested in this study had uniformity coefficients greater than 3 and were designed to be internally stable, experimental results from this study provided an opportunity to review the Schmertmann (2000) method. This review can be found in Section 11.2 and considers not only results from this study but also those from other studies that either Schmertmann (2000) did not consider or have been carried out since. Section 11.2 also includes suggested amendments to improve the performance of the Schmertmann (2000) model.

2.6 Current Australian Practice

In this chapter the current practice for design against and assessing the risk of backward erosion in Australia is considered. This has been done to gain an appreciation for what method(s) the industry is using and identify what research they have drawn from to form their methods. It may also help to identify any gaps or shortcomings in methods used by the industry that this current research could aim to fill/overcome.

In Australia the most widely accepted practice in design and risk assessment of dams is to follow The Australian National Committee on Large Dams' Guidelines. The guideline pertaining to internal erosion is the Guidelines on Risk Assessment (Australian National Committee on Large Dams, 2003). This guideline suggests using the method of event tress to estimate the probability of failure by internal erosion. This method can also provide indirect guidance when designing a dam/levee to protect against backward erosion. The guideline makes reference to literature available at the time of its printing which provides guidance on the event tree method and suggests engineers consult this literature. The authors of the referred to literature later combined their knowledge and methodology to form a guidance document titled "Risk Analysis for Dam Safety: A Unified Method for Estimating Probabilities of Failure of Embankment Dams by Internal Erosion and Piping" (Fell et al., 2008). This guidance document, referred to in shorthand as the 'Piping Toolbox', is currently the most widely accepted practice used to estimate the risk of internal erosion in Australia (in the current author's experience).

The Piping Toolbox (Fell et al., 2008) categorises failure by internal erosion into three failure modes: erosion through the embankment, erosion through the foundation and erosion of the embankment into or at the foundation. For the sake of simplicity, only backward erosion through the foundation will be considered here, which this study focuses on. In any rate, estimating the probably of backward erosion initiation and progression in the other two failures models are very similar.

Firstly, all potential failure paths are identified and those which are identified as having negligible contribution to the probability of failure can be screened out. Failure paths through the foundation being considered for backward erosion can be screened out if the soil foundation is isolated by a cut-off trench founded into non-erodible rock or if it has a plasticity index >7 or if it is not continuous, i.e it terminates beneath the dam. Otherwise, the failure path requires assessment and an event tree is needed.

The Piping Toolbox (Fell et al., 2008) suggests that for a dam to fail due to internal erosion the following sequence of events must occur: the reservoir rises, a continuous zone of cohesionless soil exists in the foundation, backward erosion initiates, erosion continues because the exit is unfiltered (or inadequately filtered), piping progresses, intervention fails and the dam breaches. It is these events which form the branches of an event tree.

Of the branches on the event tree it is the initiation branch which contains an estimate of the probability of backward erosion to occur. It should be noted that whilst in some instances backward erosion will initiate but not progress through to the upstream side, and hence the two events may be assigned different probabilities, both initiation and progression of the backward eroding pipe is contained within the 'initiation' branch on the event tree. This is because 'progression' on the event tree has a slightly different meaning to progression/advancement of a backward eroding tip. Progression on the event tree is related to whether a pipe will enlarge dependent on the probability of the roof of the pipe supporting itself, the probability of crack filing action fails to prevent pipe enlargement and the probability of the upstream zone failing to limit flows.

The probability of initiation and progression of backward erosion in the foundation is given by:

$$P_I BEP = P_{CL} \times [P_H \times P_{IH} + (1 - P_H) \times P_{INH}] \tag{2.20}$$

Where:

P_{CL} is the probability of a continuous layer from upstream to downstream. This layer need not be exposed downstream, it may be underlain by a top cohesive layer. If the layer is not continuous then the probability is zero and backward erosion need no longer be considered. If there is uncertainty then a probability may be chosen, usually between 0.1 and 1, based on geotechnical investigations, understanding of the depositional environment and piezometer data.

P_H is the probability of heave. Three methods are given to estimate the probability: using the factor of safety against heave based on peizometric data; using the factor of safety against heave based on a flownet analysis and the Terzaghi and Peck (1948) criteria for zero effective stress (Equation 2.13); and an approximation based on finite element seepage modelling for standard dam geometries. The standard dam geometries include a plane exit with embankments of different slopes, a circular exit and no exit (a foundation with a top cohesive layer before a crack or discontinuity exits).

P_{IH} is the probability of initiation and progression of backward erosion given heave has occurred. If boils have been observed then the probability is one. If boils have not been observed then instruction is given to use the Schmertmann (2000) method which is described in Section 2.5.6. The Schmertmann (2000) method provides a prediction of the local gradient at the tip when the critical head is needed, referred to here as $(i_{pmt})_{corrected}$. Recommended probabilities are then provided for given $(i_{pmt})_{corrected}$ values and average (global) gradients.

If C_u >6 then it is suggested to also calculate the Terzaghi and Peck (1948) criteria for zero effective stress (Equation 2.13) and adopt this gradient if smaller than $(i_{pmt})_{corrected}$.

P_{INH} is the probability of initiation and progression of backward erosion where heave is not predicted. This probability is evaluated the same way as P_{IH}, where one takes the global gradient and compares it with $(i_{pmt})_{corrected}$ (determined using the Schmertmann (2000) method described in Section 2.5.6) and compares the two on a table which provides probabilities, only this time, the probabilities are lower than those given in the table for P_{IH}.

2.7 Summary

Internal erosion is the transport of soil particles from within or beneath an embankment dam or levee (ICOLD, 2015). Backward Erosion piping is a type of internal erosion whereby seepage forces exiting from the downstream face or foundation are sufficient enough to detach and transport soil particles out through an unfiltered surface. This creates a small void which exposes a new surface of soil particles to the strong seepage forces which are also ejected until a small pipe or channel forms. Formation of this channel requires either a structure or a cohesive soil above it to support its roof. If the process of detachment of soil particles from the leading tip of the channel continues, and flow through the channel is sufficient enough to transport detached particles out, then the channel tip will progress towards the upstream side of the embankment, opposite to the direction of flow, i.e. backwards. If the channel tip reaches the upstream end then the channel will widen and deepen and eventually lead to failure of the dam/levee (ICOLD, 2015).

When embankment dams and levees are founded on fine uniform sand, backward erosion piping becomes the major cause of failures and incidents (van Beek et al., 2013). These foundation conditions are common for levee systems along major rivers such as the Mississippi River in the United States, the Yangtze and Nenjiang Rivers in China and lowlands in the Netherlands (van Beek et al., 2013). When backward erosion is in progress, sand boils form downstream/landward of the dam/levee. During floods, several, sometimes hundreds, of sand boils are observed along levees (van Beek et al., 2013). Owners and operators respond by 'flood-fighting' which involves placing rings of sand bags around boils to raise the downstream head, thereby reducing the hydraulic gradient and slowing the erosion process down (Sills and Vroman, 2007). This is a high risk and resource-intensive reactive measure to manage a somewhat undefined risk which could (and does) have catastrophic consequences.

Backward Erosion Piping is a complex internal erosion mechanism which proves to be sensitive to a vast range of factors. *"Most likely everyone who has studied the piping problem realises its complexity and difficulty. It involves the interaction of soil mechanics, fluid mechanics and sediment transport."* (Schmertmann, 2000, pg. 9). There are prediction methods available, the most widely used being Bligh (1910) and Lane (1935) in the first half of the previous century, and more recently the methods of Terzaghi and Peck (1948), Sellmeijer et al. (2011) and Schmertmann (2000). However none of these methods are applicable to all the scenarios required and there are still many aspects of backward erosion piping that the dam engineering community do not yet understand.

This literature review has revealed the following eight major gaps in the understanding of backward erosion piping.

1. The influence of grain size on the critical gradient(Sellmeijer et al., 2011). Whilst the general trend is known - that an increase in grain size will result in an increase in critical gradient (Schmertmann, 2000) - this trend is not yet well modelled in prediction methods.

   The (Sellmeijer et al., 2011) model is able to predict the critical gradient of *fine* uniform sands, but it is unable to predict the critical gradient of *coarse* uniform sands (Sellmeijer et al., 2011). Schmertmann (2000) seeks to model the influence of the grain size using the grain size factor, $C_S = (d_{10}/0.2)^{0.2}$. However, Schmertmann (2000) states that the comparisons used to determine the power of 0.2 were not ideal and proposal of the C_S factor was *"tentatively"* proposed.

   van Beek (2015) suggests critical gradient is not greatly affected by grain size in uniform sands because the increase in critical gradient due to wider channels in coarse sands is in effect 'cancelled out' by the decrease in critical gradient due to a higher local gradient immediately upstream of the channel tip.

2. Prediction of the critical gradient in well graded soils. The standard dike formula by Sellmeijer et al. (2011) should only be used for soils with uniformity coefficients of less than 2.6 as limited by soils included in the multivariate analysis. The Schmertmann (2000) method is developed using soils with a wider range of C_u values (up to $C_u = 6.7$) however, caution is called for when using this method for soils with uniformity coefficients greater than 3 because *"is it based on little data in the larger uniformity coefficient range, and some of these may be affected by internal instability"* (ICOLD, 2015, p. 50).

3. The particle detachment mechanism including why/how it occurs, where it occurs from (from the channel bed, sides or tip) and how to model it. Sellmeijer (1988)

and Hoffmans (2016) assume that particle detachment starts from the channel bed which in turn triggers detachment from the tip causing tip progression. Although Sellmeijer (1988) uses the White (1940) model to determine incipient motion and Hoffmans (2016) uses Shields (1936). Schmertmann (2000), Hanses (1985) and van Beek (2015) assume particle detachment occurs from the channel tip as a result of high local gradients causing high seepage forces at the tip which leads to either liquefaction and/or micro-slope failures. Although van Beek (2015) also considers scour to play a roll in which scour (or secondary erosion) influences the cross-sectional area of the channel, which affects the gradient through the channel, that in turn controls the amount of flow entering the channel and therefore the local gradient at the tip.

Then there is the matter of whether vertical uplift from flow emerging underneath the channel affects detachment. The general consensus amongst White (1940), Sellmeijer et al. (2011) and Baldock and Nielsen (2010) is that uplift forces need not be considered because they do no affect incipient motion and uplift forces only act within the sand matrix, not at the channel bed surface. Schmertmann (2000) acknowledges that gradients significantly reduce at the bed surface by citing the work of Martin (1970) who stated that gradients needed to suspend a particle were 2 to 3 times greater than the classical heave gradient of close to one. But Schmertmann (2000) still considers the uplift force to be the driver behind particle detachment where as Sellmeijer et al. (2011) and Hoffmans (2016) consider it to be the horizontal drag force.

These differing opinions can be summarised as discrete mechanic models of particles on the bed of the channel which do not consider uplift seepage forces and continuum mechanic models of particles at the channel tip which do consider uplift seepage forces. Given there is differing opinions amongst researchers on the location and mechanism of particle detachment, it seems this is not yet well understood.

4. Inclusion of both 3-dimensional flow effects into the channel and particle detachment in a predictive model. Three-dimensional flow is important because, as demonstrated by Vandenboer et al. (2014b), backward erosion piping is a 3-dimensional phenomenon (as flow converges into the channel), circular exit geometries cause 3D flow and 2D models are insufficient. Vandenboer et al. (2014b) has constructed

a 3D FEM model of the groundwater but does not include particle detachment criteria. The most widely used predictive methods of Schmertmann (2000) and Sellmeijer et al. (2011) do include particle detachment criteria but model 2D flow only. Notably, Schmertmann (2000) does report to have referred to 3D numerical modelling of seepage into a channel by Wong (Townsend et al., 1981), however Schmertmann (2000) still appears to rely on 2D pre-channel flownets.

5. The rate of backward erosion piping. It appears that no backward erosion model provides the speed of channel progression. The extent of erosion rate information in the literature includes some indicative tip progression speeds observed in experiments by Schmertmann (2000) and Müller-Kirchenbauer et al. (1993). Schmertmann (2000) also observed an increase in erosion rate with gradients above critical and Müller-Kirchenbauer et al. (1993) observed an increase in erosion rate with channel length. Therefore, it appears there are no insights available into the effect of soil, scale or geometry on the rate of backward erosion.

   Sills and Vroman (2007) confirms the lack of understanding in erosion rate and points to the need for an understanding of erosion rate in order to predict how many more flood events a dam/levee could withstand, particularly dams and levees which have experienced sand boils (and hence backward erosion) in the past.

6. The exit geometry effect. Prior to the commencement of this study, there was little in the literature regarding the effect of the exit geometry. De Wit (1984) tested plane, slot and circle exits and Yao et al. (2007) tested plane and circle exits, however their publications lacked clear comparison on the effect of the exit and were not well known or cited within the literature. Although, Schmertmann (2000) did recognise that different exit geometries resulted in different flownets and compensated for this with the C_G factor.

   Since the commencement of this study, van Beek et al. (2012b, 2013) have reported that an increase in the exit flow area results in an increase in both the initiation and critical gradients. Van Beek et al. (2013) also observed that equilibrium occurred when circular exit were used but not when sloping exits were used.

   Yet, no study has investigated all four of the possible exit geometries presented in Section 2.4.2, in otherwise identical test set-ups. Therefore the effect all possible exit geometries have on the initiation and critical gradients have not yet been quantified.

7. The effect repeated flood events has on the initiation and critical gradients. The United States Army Corps of Engineers have observed an increase in sand boil activity during subsequent flood events, even when subsequent floods reach lower levels (Glynn and Kuszmaul, 2004; Sills and Vroman, 2007). The concern is that perhaps the critical gradient is decreasing with each flood event. Furthermore, with each flood, the existing channel tip is progressed further toward the upstream end with no indication or estimation technique of how far along it is and how many more flood events the levee could withstand before failing (Sills and Vroman, 2007).

8. The plasticity index at which soils are no longer susceptible to backward erosion (at gradients likely to be present in dams and levees) (Fell and Fry, 2007). Fell and Fry (2007) cite studies (Marot et al., 2005; Sun, 1989) which showed that whilst cohesive soils are susceptible to backward erosion they are only susceptible at high hydraulic gradients that are unlikely to occur across dams and levees. For practical purposes, Fell et al. (2008) concluded that soils with a plasticity index >7 may be considered not subject to backward erosion piping at gradients experienced in dam and levees (based on available data, experience and judgement) (ICOLD, 2015). However, little to no backward erosion testing has been carried on soils with low plasticity.

This present study will investigate some of these gaps in understanding, predominately with the use of laboratory experiments but will also make use of some numerical modelling. Findings of this study will inform and equip practising engineers to better design against and assess the risk of backward erosion piping.

Chapter 3

Experimental Method

3.1 Apparatus

3.1.1 Flume

The experimental flume was a rectangular aluminium box with a clear Perspex lid. Soil placed in the flume represented the foundation of a dam/levee and the lid represented the underside of a dam/levee (which could support the roof of a channel). A hydraulic head difference was applied across the flume to drive seepage through the soil. Once the seepage was sufficient Backward Erosion Piping would occur at the top of the soil and be observed through the Perspex lid. A drawing of the flume designed and constructed for this study is given in Figure 3.1a and a photo in Figure 3.1b.

The design of the flume was based on a flume used by Townsend et al. (1981). This provided an opportunity for comparison and validation of results. It is known that different sized and proportioned flumes give different results (van Beek et al., 2013). The size of the Townsend et al. (1981) flume was considered to be the best balance between a flume as large as possible (to minimise scale effects) and a size that was practical to load and unload with soil repeatedly.

The box was fabricated with structural grade aluminium to have internal dimensions 2237mm long, 310mm deep and 450mm wide. An isometric sketch of the flume walls and base is given in Figure 3.2 and an elevation of the end plate and lid detail is given

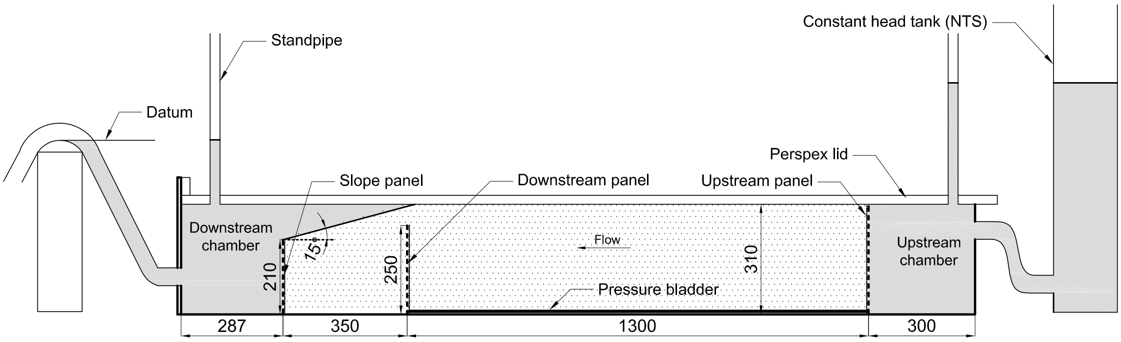

(a) Longitudinal section through centreline

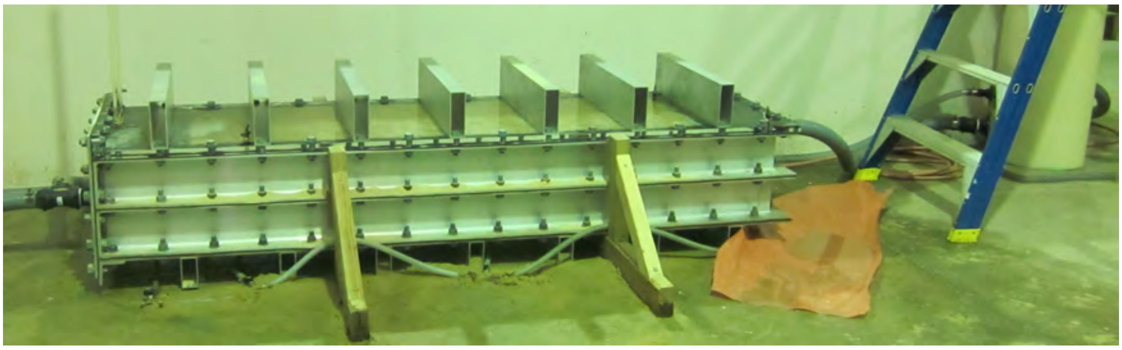

(b) Photo

Figure 3.1: Flume used for tests 1-18 (all dimensions in mm) (direction of flow from right to left)

in Figure 3.3. The flume walls were made from two 152 x 63mm channel sections with 6.3mm thick web and 8mm thick flange. The grade and thickness of the aluminium was chosen to restrict maximum deflection to 1mm under design loads. The channels were cut and welded into frames, machined with 20mm bolt holes along the flanges spaced at approximately 150mm, equipped with end tabs (to make a flat surface for the end gasket and plate) and bolted together. The base was 10mm thick, also machined with 20mm bolt holes at 150mm spacing and equipped with rectangular hollow sections welded onto its underside (100 x 50 x 3mm) at 300mm spacing as well as a tab onto its end (to make a flat surface for the end gasket and plate). The end plate was also 10mm thick and machined with 20mm bolt holes. A 3mm gasket was placed between the channel flanges; between the box rim and lid; and up against the end plate (with Silicone). The flume components were manufactured by a local commercial sheet-metal work fabricator and assembled in-house.

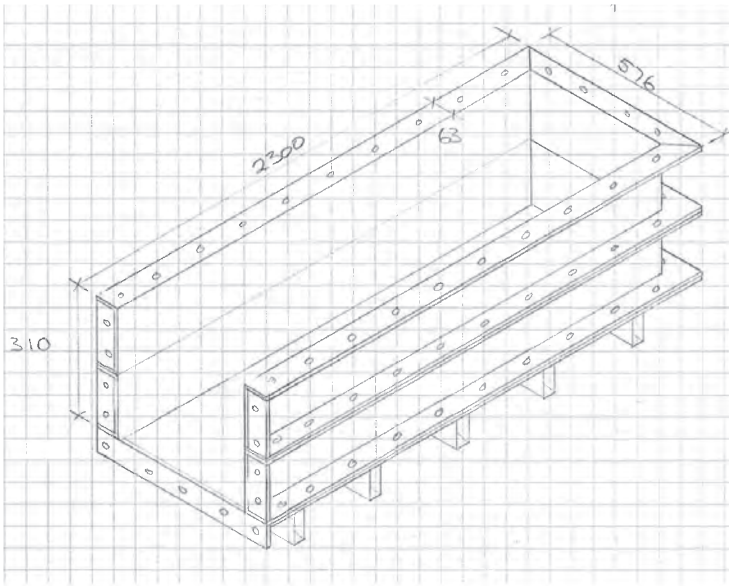

Figure 3.2: Isometric sketch of flume walls and base (end-plate, gasket, lid and bolts not shown) (dimensions in mm)

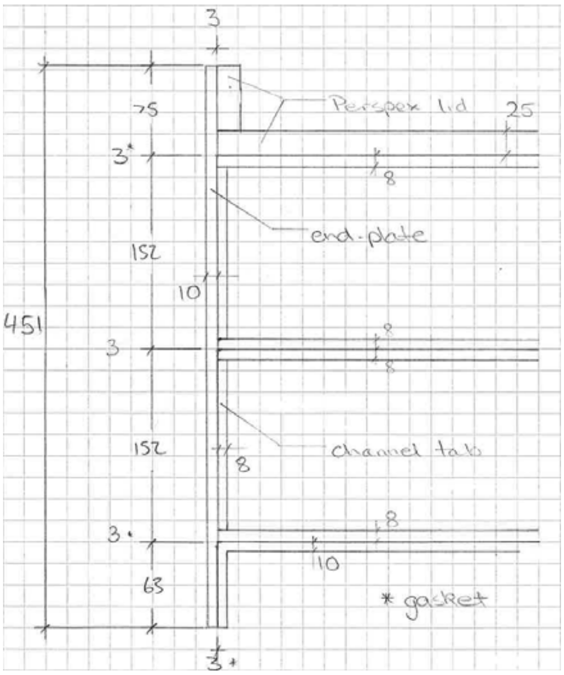

Figure 3.3: Elevation of flume end detail (bolts not shown) (dimensions in mm)

A 'pressure bladder' was added to the flume by lining the base with a 3mm thick rubber sheet and bolting down and sealing (with silicon) its edges to make it water tight. A 17mm diameter inlet was cut into the flume base and connected to a hose. This was used to fill the space between the rubber sheet and flume base with water which, with sufficient pressure, would cause the rubber sheet to expand and in turn push the soil up against the lid. The pressure bladder had two functions: to prevent gaps between the soil and lid and to impose a total stress on the soil representative of the weight of the overlying embankment (except the stress is applied from the bottom-up instead of the top-down). A photo of the pressure bladder inflated without soil is shown in Figure 3.4. In the photo a white flexible sheet can be seen placed over the bladder in order to show the inflated shape of the bladder. The tanks used to provide pressure head to the bladders were 100mm diameter PVC pipes pictured in Figure 3.5. These pressure tanks could provide heads up to 5m (the height of the roof in the laboratory).

Figure 3.4: Empty flume showing inflated pressure bladder and internal panels lined with geofabric

Three internal panels were added to the flume to contain the soil and separate it from the end water chambers. These panels were 4mm thick aluminium plates perforated with 6mm diameter holes at 20mm spacing. They were lined with a nonwoven, needle-punched geotextile commercially referred to as *Bidim* with an average maximum pore space of 0.12mm and an average minimum flow rate of 50 $l/m^2/s$. These panels would contain soil but allow water flow. The three panels are shown in the photo in Figure 3.4 and in the drawing of Figure 3.1a.

Figure 3.5: 5m pressure bladder tanks

Tests were carried out in which standpipes were positioned either side of the geotextile-lined panels and flow passed through, to measure for head-loss. The head-loss was so small it was difficult to detect and measure, therefore it was considered negligible for the remainder of the study.

As labelled in the drawing, the three panels have been designated upstream panel, downstream panel and slope panel. The function of the downstream panel was to keep pressure applied by the bladder from deforming the slope. The downstream panel did not need lining with geotextile. It was made shorter than the depth of the flume (250mm) to allow for the backward erosion process to occur at the top of the slope.

Initially the slope panel was 150mm in height (based on the 6 inch high slope panel in Schmertmann (2000)) creating a slope angle of 23.2° . However, this angle created an unstable slope which would retreat during saturation. Therefore, from Test 4 onwards, the height of the slope panel was increased to 210mm creating a slope of 15° .

The panels were slotted into small (7mm wide) aluminium channels screwed into the flume walls and base. This meant that a) the panels could be removed and reinserted as needed and b) the pressure bladder was pinned to the base where panels were placed, hence restricting pressure to between the upstream and downstream panels. This was not an issue because the backward eroding channel was confined to this region.

Both the inlet and outlet on the flume were 50mm in diameter (large enough to keep any head loss between the constant head tank and upstream chamber negligible). Ball valves were added to both so that both ends could be closed off during CO_2 flushing and the flow of water into the flume during saturation could be controlled and kept small. Refer to Subsection 3.2.8 Saturation for explanation of CO_2 flushing.

The downstream hose was elevated above the top of the flume so as to keep the downstream chamber full (to keep the sand saturated). This elevated height became datum.

The Perspex lid was a 25mm thick sheet of clear acrylic cut to the outer size of the flume (2300 x 575mm) and machined with bolt holes to match the flume. A concern with the lid was the surface was too smooth to model erosion along a soil to soil interface and that the lack of friction may alter the backward eroding mechanism. To compensate for this the underside of the lid was coated with a flowable silicon sealant (commercial name: *Dow Corning 734*). The flowable sealant self-levelled and provided a roughness more typical of field conditions. On first application it appeared to impede the transparency of the Perspex, but once it was pressed up against sand and the sand was saturated, the transparency was acceptable.

To prevent the lid from deflecting upwards (due to pressure from the bladder) it was restrained with aluminium rectangular hollow sections of 150 x 50 x 3mm at 300mm spacing (every second bolt hole). This size and spacing was chosen to ensure deflection at the midpoint remained less than 1mm (under 50kPa of pressure from the bladder). The restraints were cut through the base at either end to allow for fixing to the flume with bolts. The restraints are not shown in Figure 3.1a but are shown in Figure 3.1b.

A standpipe was added to the upstream chamber to check for head loss between the constant head tank and the flume. This was done to check the head level being applied to the sand was the same (or very close to) the head level in the constant head tank. The standpipe added to the downstream chamber showed any head loss along the downstream hose as height above datum. These standpipes required plugs during CO_2 flushing to keep the CO_2 contained.

Small inlets and outlets were added to the flume and lid for the CO_2 system. These are discussed in Subsection 3.1.12.

The sides of the flume were restrained by 1 or 2 wooden frames (seen in Figure 3.1b). These frames prevented the side-walls from deflecting out under the load of the soil and pressure bladder so that the lid could be bolted onto the flume walls and the volume inside the flume be kept constant, lest the sand void ratio increase and/or the sand settle and create a gap under the lid. The wooden frames were adjusted to keep the width of flume to 450mm +/–2mm.

After test 18, a series of modifications were made to the flume including moving the internal panels, adding a box onto the downstream-end of the lid (over the exit) and cutting different exit geometries into the lid.

Additionally, after test 18, three more flumes were constructed including the new modifications (making 4 flumes in total). Multiple flumes were constructed so experiments could be run simultaneously (to maximise the number of tests).

The internal panels were moved to the positions shown in Figure 3.6a. They were moved to facilitate the joining of two flumes. The ability to join two flumes together was made possible by the detachable end-plate and lid upstand. This was a feature not included in the Townsend et al. (1981) design but was added in this study so that seepage length effects could be investigated. Figure 3.6b shows a photo of two flumes joined together.

The internal panels were moved so that individual flumes could be used in either flow direction without having to move the panels again. The flow direction needed to be mirrored because once a flume was joined to another its downstream end would need to become its upstream end and vice versa. The new panel positions allowed for 3 different seepage lengths, the standard 1300mm, double the standard at 2600mm, and triple the standard at 3900mm. Additionally, as a result of having moved the downstream and slope panels closer (to a spacing of 230mm instead of 350mm) the slope panel height was increased to 250mm, the same as the downstream panel, to maintain a slope angle of approximately 15°.

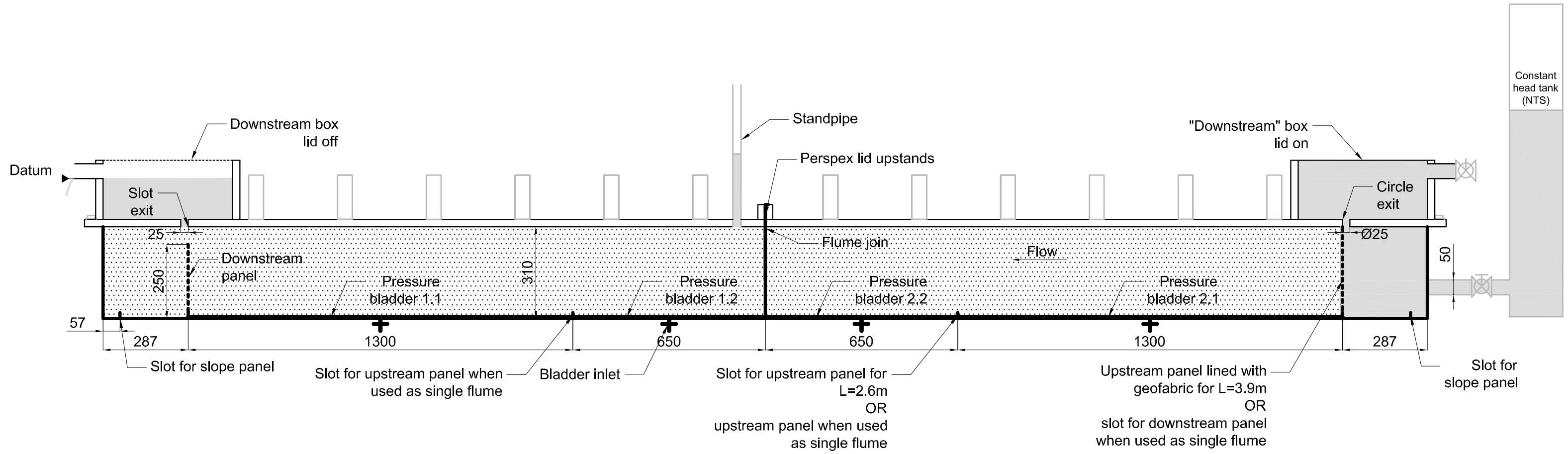

(a) Longitudinal section through centreline showing slot positions for multiple panel positions to enable the joining of two flumes (all dimensions in mm)

(b) Photo

Figure 3.6: Double flume (direction of flow from right to left)

As the pressure bladder was now separated into independent sections (by either the panel slots or flume join) each section needed its own inlet and hose to the bladder tank. Each inlet was equipped with a valve so portions of the bladder not in use could be closed off from the head tank. All hoses were joined upstream of the valves so that all bladder portions were filled from one tank at the same head. The bladder inlet positions are shown in Figure 3.6a diagrammatically as crosses.

A box was added to the downstream end of the lid over the exit so that the plane, slot and circle exit geometries could be kept submerged (to keep the soil saturated). The box was made large enough to allow sand boils to form unhindered. The left, right and downstream edges were placed next to the edges of the flume and the upstream edge was placed 150mm upstream of the exit. The box was fitted with a lid that was fastened during CO_2 saturation but removed during the experiment (so the exit could be seen clearly). The exception to this was when a flume was rotated to attach to another flume, in which case the end with the box became the upstream end, and the lid remained on throughout the experiment (as shown in Figure 3.6b). An outlet, 50mm in diameter, was cut into the downstream wall of the box and fitted with a ball valve. The ball valve served to close the outlet during CO_2 flushing. The invert of this outlet became the datum level from which all constant head tank and standpipe levels were measured from. The outlet was installed so its invert was 120mm above the flume lid.

Different exit geometries were cut into the lid to model different scenarios found in the field. The different scenarios found in the field are discussed in Section 2.4.2 and include the slope, plane, slot, circle and vertical structure. The first four of these were cut into the lid as shown in Figures 3.7 and 3.8 (the vertical structure was not included in this study). Note: only the slope exit was used in the Townsend et al. (1981) study, three additional exit geomtries were added in this study to investigate the exit geometry effect.

A diameter of 25mm for the circle exit and a spacing of 25mm for the slot exit were chosen because, after having reviewed dimensions used by other researchers, it was found that the average diameter to seepage length ratio was 1:50 and so a ratio of 25:1300 was selected.

The seepage length was kept at 1.3m for each exit. Given the bladder pressure was terminated at 1.3m for the slope exit (in line with the top of the slope), so as to not

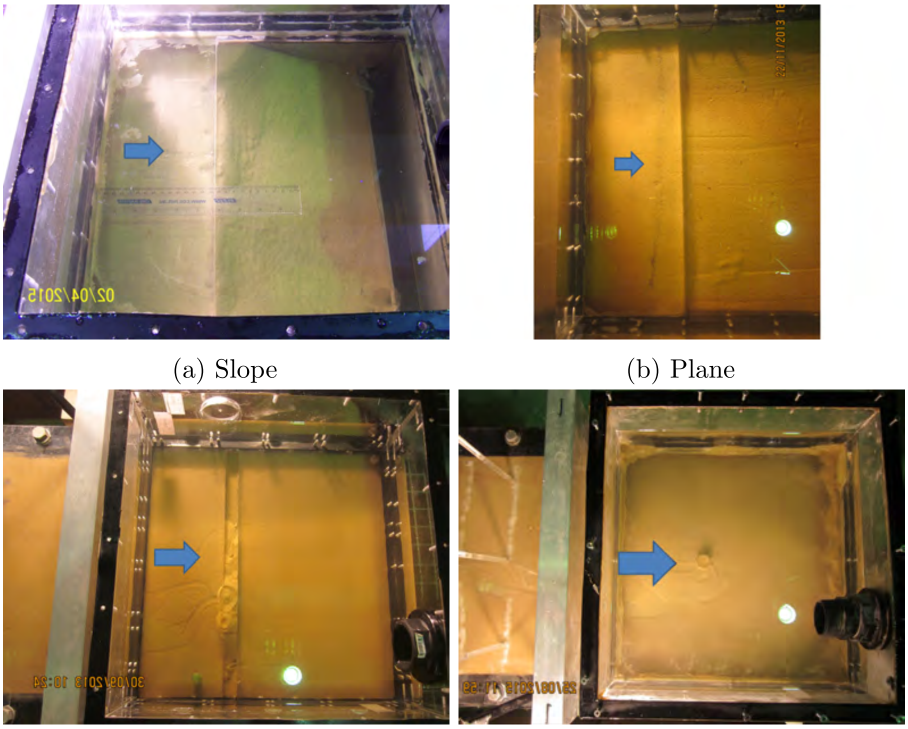

(a) Slope (b) Plane

(c) Slot (d) Circle

Figure 3.7: Photos of exit geometries (blue arrows indicate direction of flow)

damage the slope, it was practical to maintain this terminating position for all other exits (so a new pressure bladder, with repositioned panel slots, weren't required for each exit). This meant that soil downstream of the exit did not have direct pressure from the bladder applied to it. This was not expected to have any impact on results, even in the case of slot and circle exits, because the backward eroding channel did not occur here (it always progressed upstream of the exit).

After test 46 an additional modification was made: the installation of standpipes above the soil. A total of 9 standpipes were added to a lid (configured with the circle exit), 3 between each restraining bar, as shown in Figure 3.9.

The purpose of these standpipes was to measure the total head through the sand as well as next to and/or within the channel (if the channel occurred directly beneath a standpipe). The standpipe levels provided insight into head losses and were used to calibrate the numerical model. Datum was marked on the standpipes (level with the invert of the flume outlet) with use of a dumpy level. Measurement tapes with 1mm increments were stuck to each of the standpipes and light coloured beads were inserted to indicate the water levels more clearly.

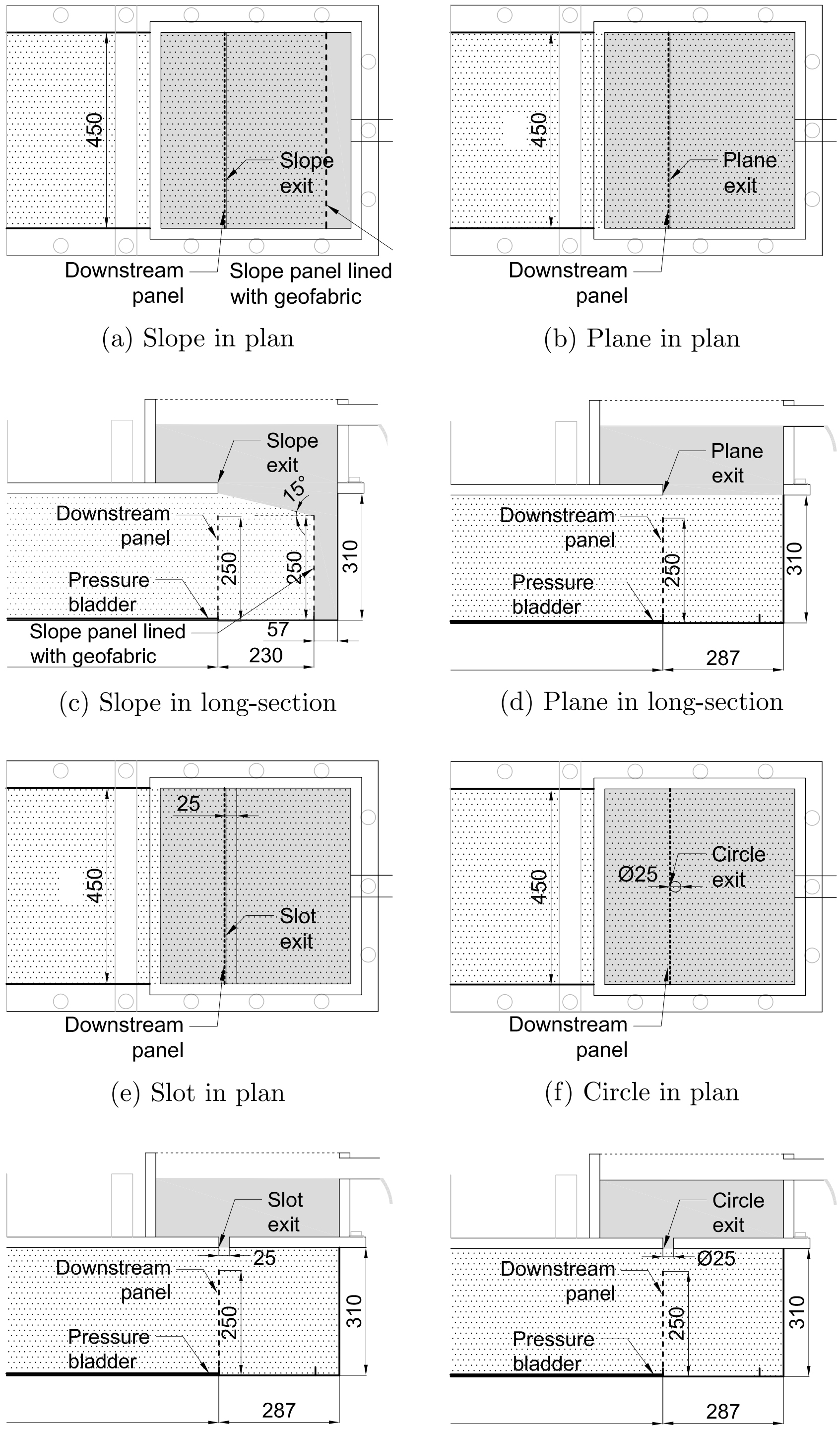

(a) Slope in plan

(b) Plane in plan

(c) Slope in long-section

(d) Plane in long-section

(e) Slot in plan

(f) Circle in plan

(g) Slot in long-section

(h) Circle in long-section

Figure 3.8: Exit geometries in flume (all dimensions in mm and direction of flow is left to right)

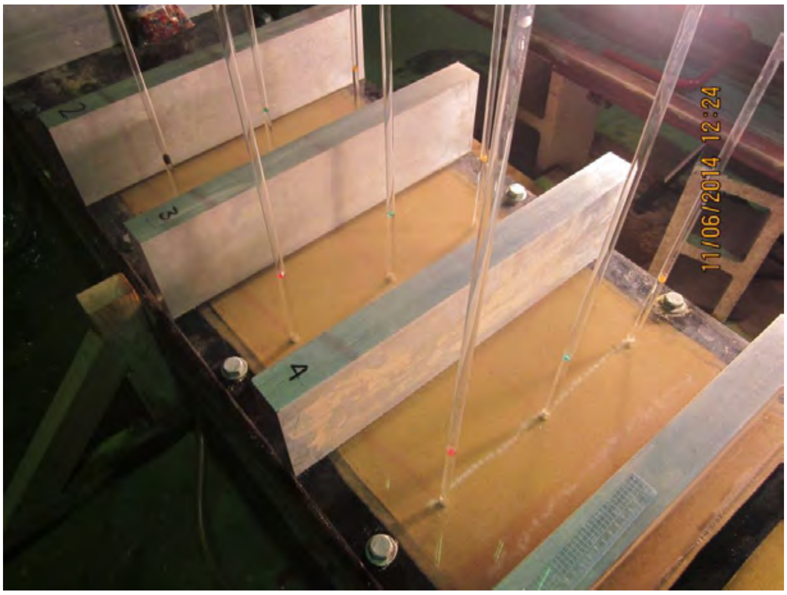

Figure 3.9: Standpipes

To prevent erosion from occurring into the standpipes, tensiometers were cut from polypropylene sediment water filters made to snugly fit into the base of the standpipe hole. The tensiometer allowed water but prevented sand from entering the standpipe. It was important that the base of tensiometer sat flush with the underside of the lid to prevent indents or extrusions that could interfere with the eroding process.

Small rubber plugs were pushed into the top of the standpipes during CO_2 flushing but removed for the experiment.

Initially standpipes were only in one of the four lids but later they were added to a second lid, also with the circle exit. No lids configured with the other exit geometries included standpipes.

As a summary, Figure 3.10 illustrates the flumes used for tests 19 onwards including modifications to the internal panel positions and the exit geometry as well as addition of the downstream box and standpipes.

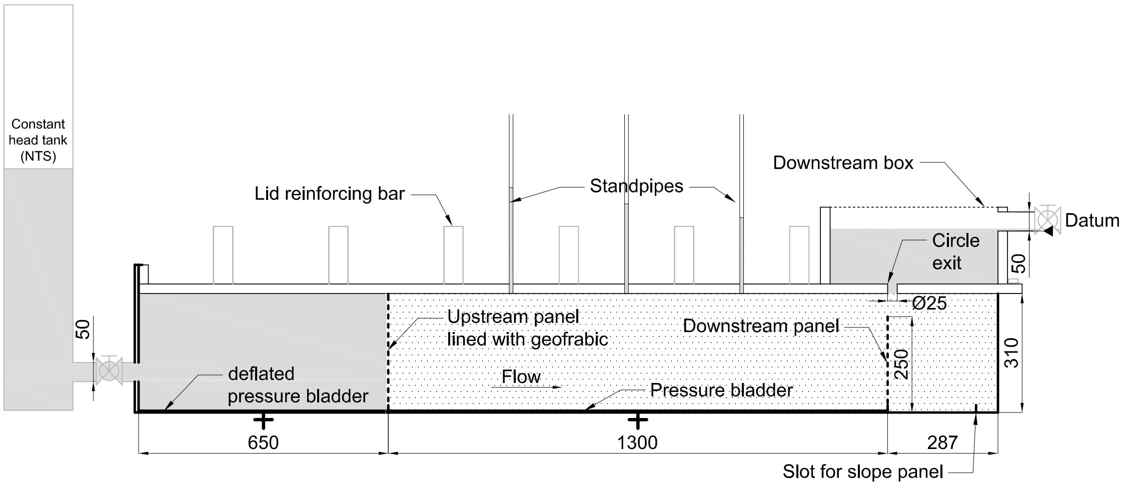

(a) Longitudical section though centreline with circle exit

(b) Photo

(c) Photo of oblique close-up (Note: there was only one sand boil, two can be seen due to refraction)

Figure 3.10: Flume used for test 19 onwards including modifications to the internal panel positions and the exit geometry as well as addition of the downstream box and standpipes. (Direction of flow is left to right)

3.1.2 Flume open-top tank

The soil-placement technique of 'wet pluviation' was trialled for reasons which will be explained in Subsection 3.2.3. To do so, the top of the flume was required to be submerged and hence an open-top tank was constructed around one of the flumes (flume 3) as shown in Figure 3.11a. The open-top tank was built with 17mm thick formply and dimensions in plan of 2570 x 1220mm and a height of 620mm. The height provided a water depth of 140mm above the flume lid so that there was enough space to reach in under the lid and remove air bubbles (whilst the lid was suspended in the water, above the flume) (as discussed in Subsection 3.2.3). The width of the tank provided enough room to tighten the bolts while submerged (enough room for a spanner and socket wrench set to fit between the flume and tank walls).

(a) Elevation view

(b) Struts supporting flume inside

Figure 3.11: Flume open-top tank

New wooden side-supports were built to span the width of the tank and, in order to support the flume within the tank, struts were wedged in between the flume and tank in-line with the side-supports, as shown in Figure 3.11b. The tank base was suspended above the ground so that the base of the side-supports could be placed underneath. Additional planks of wood, the same height of the side-support bases, were also placed underneath the tank to support it.

Holes were cut into the tank ends to accommodate the 50mm diameter inlet and outlet hoses and sealed using a tank connector (the hole for the outlet can be seen in Figure 3.11a.

3.1.3 Constant head tank

It was necessary to provide a hydraulic head to the experiment which could be held constant at a specified height of between 300mm (the height of the flume) and 4000mm and could be adjusted in small increments (order of 1 to 5mm). It was also necessary that the head be kept constant even if flow through the flume changed and continue to be provided over long periods of time (typically 1 to 7 days) unsupervised.

To do this a constant head tank was designed comprising of a 3m long, 375mm diameter, PVC pipe standing on its end with a smaller PVC pipe (250mm in diameter and 150mm long) suspended inside. A drawing of the design is given in Figure 3.12a and a photo in Figure 3.12b.

The outer pipe contained the water whilst the inner pipe controlled the water level. The height of the inner pipe was lowered and raised with a winch to control the head provided to the flume. A sight-tube/standpipe was installed on the outside of the tank to indicate the water level inside (and hence the height of the inner pipe). A measurement tape was attached along side the standpipe with its zero at datum (determined using a dumpy level).

The rate of flow entering the constant head tank was controlled with a 25mm diameter gate valve and was kept greater than the rate of flow through the flume so that there was always an excess of flow over-topping into the inner pipe.

To prevent the inner pipe from floating its base was lined with ballasts. Figure 3.13 is a photo taken from the top of the head tank looking down. The ballasts can be seen in the base of the inner pipe.

Note that the diameter of the inner pipe photographed in Figure 3.13 is 100mm and not the 250mm drawn in Figure 3.12a. This is because the inner pipe was changed to a 250mm diameter pipe later on in the project. It was changed so that the inner pipe could be made shorter whilst still containing the same volume. The advantage of making

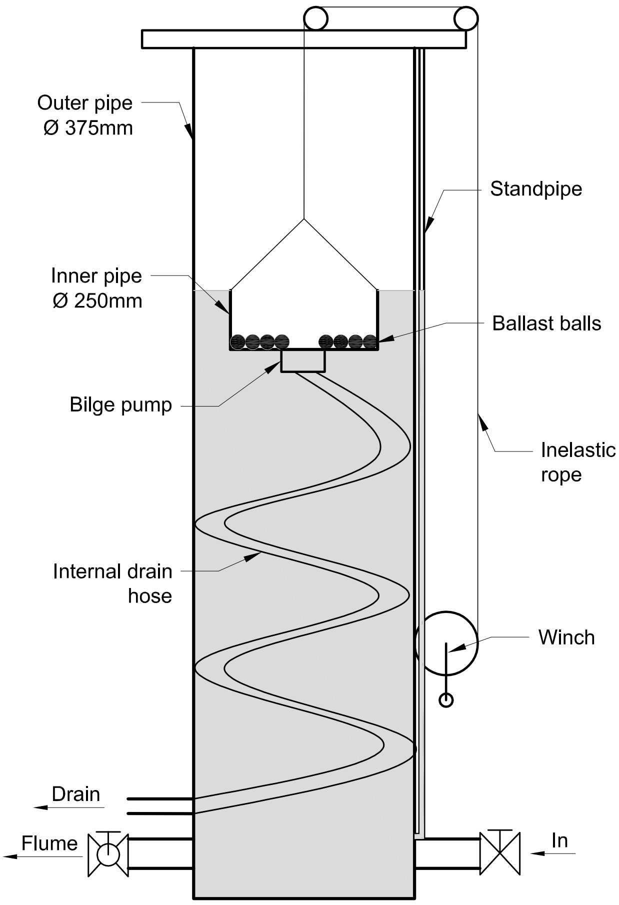

(a) Transparent side elevation

(b) Photo of tank 3(left) and 4(right)

Figure 3.12: Constant head tank

it shorter was achieving lower heads. The lowest height the inner pipe could be lowered to was restricted by the coiled internal drain hose beneath it.

What can also be seen in Figure 3.13 are fins attached to the inner pipe and a portion of the inner drain hose protruding above the water surface. The fins were designed to reach the edge of the outer pipe and served to prevent the inner pipe from tipping.

The protruding portion of the inner drain hose was evidence of air trapped in the drain hose. This air prevented the inner pipe from draining under the action of gravity alone, as was the initial intention. The hose couldn't prime itself because the height of water required to push the air out was greater than the height of the inner pipe, and so the inner pipe would become fully submerged. To overcome this a small bilge pump was

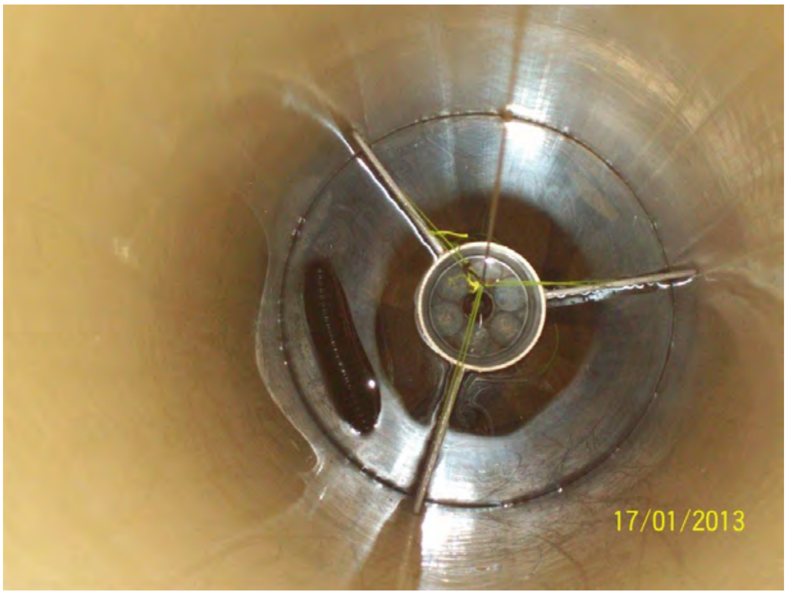

Figure 3.13: Photo taken from top looking down into constant head tank showing inner drain cylinder, fins attached to inner drain cylinder, ballast balls and portion of drain hose protruding above water surface

installed to the under-side of the inner pipe (the pump was always submerged to keep it from overheating). The bilge pump was able to keep the inner pipe drained (or at least kept from becoming submerged) as long as the flow rate entering the constant head tank was adjusted to be less than the capacity of the bilge pump (30l/min). It was beneficial to set the flow rate entering the tank as close as possible to the capacity of the bilge pump so that when flow through the flume increased (as the channel progressed) there was reserve flow available. In summary, $Q_{\text{in}} \approx Q_{\text{bilge.capacity}} >> Q_{\text{experiment}}$.

After test 18, an additional 3 constant head tanks were built to accompany each of the new flumes.

The maximum head the constant head tanks could provide was approximately 1900mm (equivalent to a gradient of approximately 1.5). This was sufficient until soils with lower permeabilities were used. Soils with lower permeabilities required heads greater than 1900mm to (sometimes) initiate and progress the backward eroding channel. Therefore a second PVC pipe (also 3000mm long and 375mm in diameter) was inserted and glued into the top to make the tank twice as tall (the pipes came with spigot and socket connections). With the tank raised a maximum head of approximately 3900mm was made available. Only one tank was raised- tank 3 which is shown in Figure 3.12b on the left and in Figure 3.11a. It was prudent to restrain the tank from tipping by anchoring it to adjacent reliable structures (yellow and orange straps seen in top of Figure 3.12b).

3.1.4 Water supply

Water was initially supplied to the constant head tank directly from a local dam (Manly Dam) providing approximately 8m of head.

During initial tests a build-up of organic matter was seen along the downstream slope (in the form of froth) as shown in Figure 3.14. The concern was this organic matter may have been affecting the backward eroding process. Therefore the dam water was filtered (from test 8 onwards) with a 5 micron polypropylene sediment filter, fitted upstream of the constant head tank. The filter housing can be seen in Figure 3.12b as the blue cylinders at the base of the head tanks. The filters were replaced when in flow to the head tank was inhibited or the required head could not be reached.

Figure 3.14: Plan view of organic build-up along downstream slope (along right-hand-side of photo) (blue arrow indicates direction of flow)

Whilst these filters did stop the froth from forming, they didn't remove all organic material from the dam water. The remaining organics caused a different issue which was noticed once an experiment had been running for three to four days. The sand became darker in colour along the upstream edge and, if a channel had reached the upstream end, along the channel(s), as shown in Figures 3.15 and 4.6.

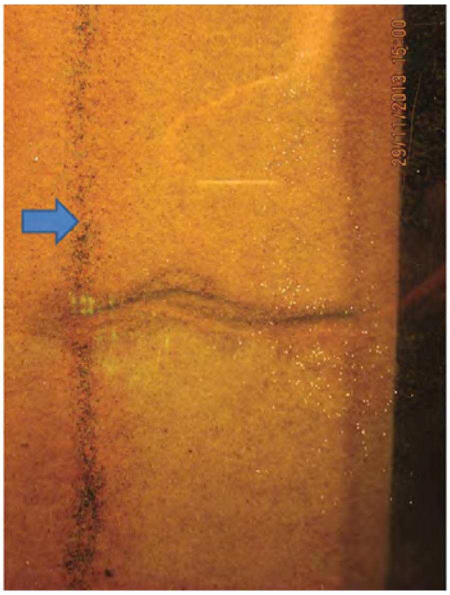

Figure 3.15: Plan view of dark sand along upstream edge (right-hand-side) and along channel indicating bio-clogging. Can also see coloured-sand tracer particles in line along left-hand-side. Blue arrow indicates direction of flow.

The darker sand was an issue because it did not erode (where it had been eroding previously). This meant that the final two stages of backward erosion (forward deepening and failure) did not occur (refer to Section 4.3 for explanation of the backward erosion stages). This observation has not been reported by other researchers.

Investigation into this phenomenon revealed the discolouration to be bio-clogging. Bio-clogging occurs when biofilm grows on sand particles as bacteria grows. Bacteria grew because it was feeding on nutrients in the untreated water from Manly Dam. When bio-film grows on the sand particles it fills up voids (reduces the permeability) and reduces the critical erosion velocity (Fang et al., 2014). In fact, the use of bio-clogging as a method of ground improvement has been researched and used over the past decade in many civil engineering applications, called biosealing (Molendijk et al., 2009). However in these experiments bio-clogging was undesirable.

To prevent bio-clogging (by preventing bacteria growth) the water was treated with chlorine to a concentration a little less than a common swimming pool- about 3 parts per million. As an extra measure, potable tap water was used instead of water from Manly Dam. This method was employed from test 41 onwards and was successful in minimising sand discolouration and preventing bio-clogging.

Given the large volume of potable tap water to be used over time (and the cost of potable water), the water was recycled through the experiments. To do so a 2700l pit in the laboratory floor was used to contain the potable water and treat with chlorine. Inside the pit a submersible pump was placed to pump water from the pit up into the manifold box. The submersible pump was chosen on the basis of the maximum head it could provide so there would be sufficient head to run multiple experiments at the same time. The pump chosen was a 'high volume shrouded impeller' pump with model number 'SP500' from the Australian pump manufacturer 'Orange Pumps'. It could provide a maximum head of 13m. The manifold box was constructed to distribute the one water supply to four different constant head tanks, shown in Figure 3.16. A one-way valve was installed upstream of the manifold box to prevent back-flow from the constant head tanks into the pit in the event the submersible pump turned off (due to power cut or the water level dropping too low in the pit). Prior to installing the one-way valve, a few experiments became irreparable when the pump turned off because the back-flow caused the experiments to desaturate.

Figure 3.16: Manifold box used to split treated water from pit to four constant head tanks

In order to return used water from the experiment back to the pit, a 60L container was placed below the flume outlet and fitted with a float-activated bilge pump (pictured in Figure 3.32). Also, to send the overflow water being pumped out of the constant head tank back to the pit, the hoses were extended to reach back to the pit. Figure 3.17

shows the network of hoses feeding to and from each of the four flumes (two hoses per flume). The photo also (partly) shows the pit which is under the grate and plywood cover (the plywood cover was used to prevent sand and other debris from falling into the pit). Figure 3.18 is a sketch of the experimental set-up illustrating the water recirculation cycle (as well as 3D schematic diagram of the flume).

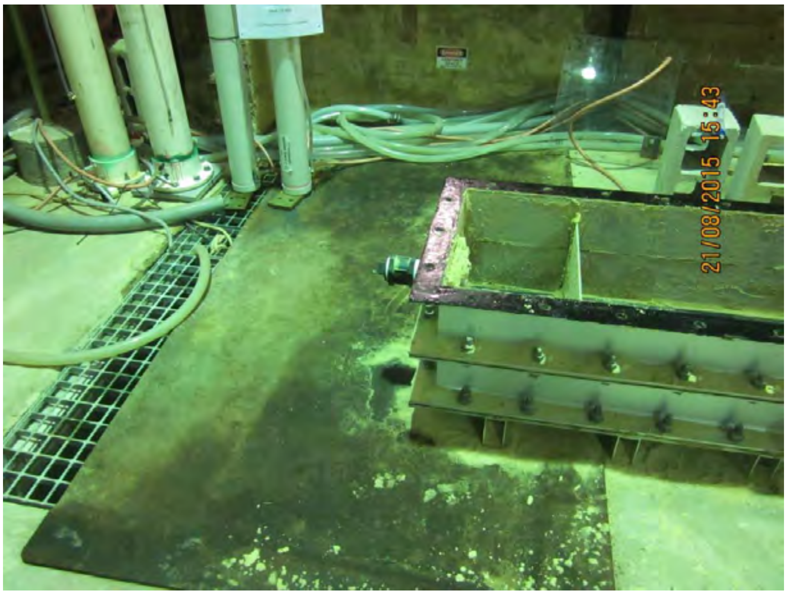

Figure 3.17: Network of hoses in background running to and from experiments and water supply pit (under plywood)

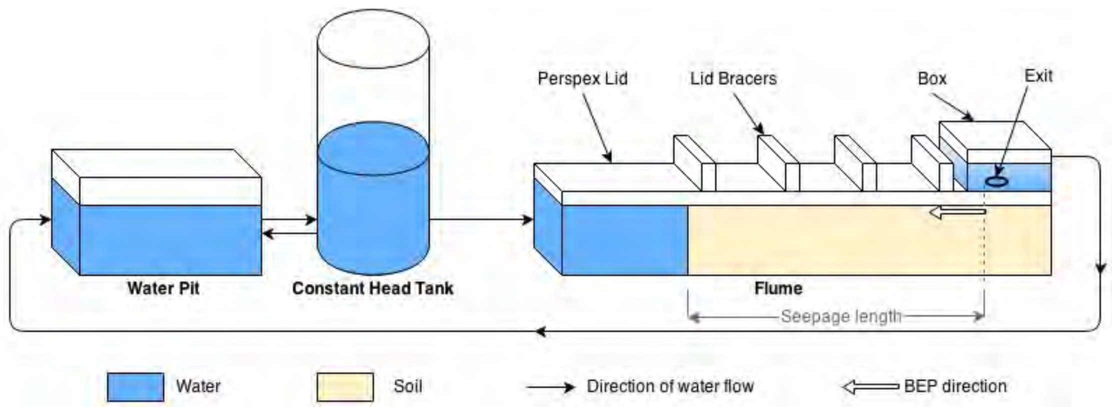

Figure 3.18: Water recirculation cycle and 3D schematic diagram of flume (Forward, 2014)

Outflow from experiments on soils containing the fine-grained soil (referred to as 'Sibelco 300g' described in Subsection 3.1.5) could not be recycled because the fine-grained soil would become suspended in the water (and could affect subsequent tests). In these cases the water was disposed of into the sewer system.

3.1.5 Soil

Ten different soils were tested, either as is, or added to a mix to make a more well graded soil. The soils were commercially available products from distributors in Sydney and Melbourne. As commercially available products, soils were processed (i.e. uniform) and often contained angular to sub-angular shaped particles. The soils are listed and described below in Table 3.1, plotted on a particle size distribution graph in Figure 3.19 and photographed in Figure 3.20.

Sydney Sand and Sibelco 50n were tested as they were, without mixing; all other products were used in soil mixes.

Sydney Sand was tested because it was similar to the Reid-Bedford Sand tested by Townsend et al. (1981). The d_{50} of Sydney Sand was 0.3mm and the d_{50} of Reid-Bedford Sand was 0.21mm. The C_u of both soils were the same at 1.3. Testing similar sands meant similar experimental results could be used to verify the test set-up and method.

Sibelco 50n was tested to investigate the influence of permeability without the effect of C_u by comparing its results with those in Sydney Sand. Both soils had similar C_u values but different d_{10} sizes (and d_{10} is a key determinate of a soil's permeability according to the Hazen formula (Fell et al., 2005)).

For details on soil mixes refer to Subsection 3.2.2.

Table 3.1: Supply soil products

Product name	Supplier	Soil type	USCS* symbol	Particle size or plasticity	d50 (mm)	Colour
EJ Shaw 10mm	EJ Shaw & Son, Mona Vale	Gravel	GP	medium	7.3	brown
Boral 5mm	Brookvale Sand, Brookvale	Gravel with some sand	GP	fine	3.3	white-yellow
Sibelco Silica Sand 8/16	Lang Lang Sands, Lang Lang	Gravelly Sand	SP	coarse	1.7	white-brown
Boral 1mm	Brookvale Sand, Brookvale	Sand with some gravel	SP	coarse	0.9	yellow
Sydney sand	Brookvale Sand, Brookvale	Sand	SP	medium	0.3	yellow
Sibelco Silica Sand 50n	Lang Lang Sands, Lang Lang	Sand	SP	fine	0.2	white
Sibelco Silica Flour 300g	Lang Lang Sands, Lang Lang	Silt with a trace of clay	ML	non-plastic	0.02	white

* Unified Soil Classification System

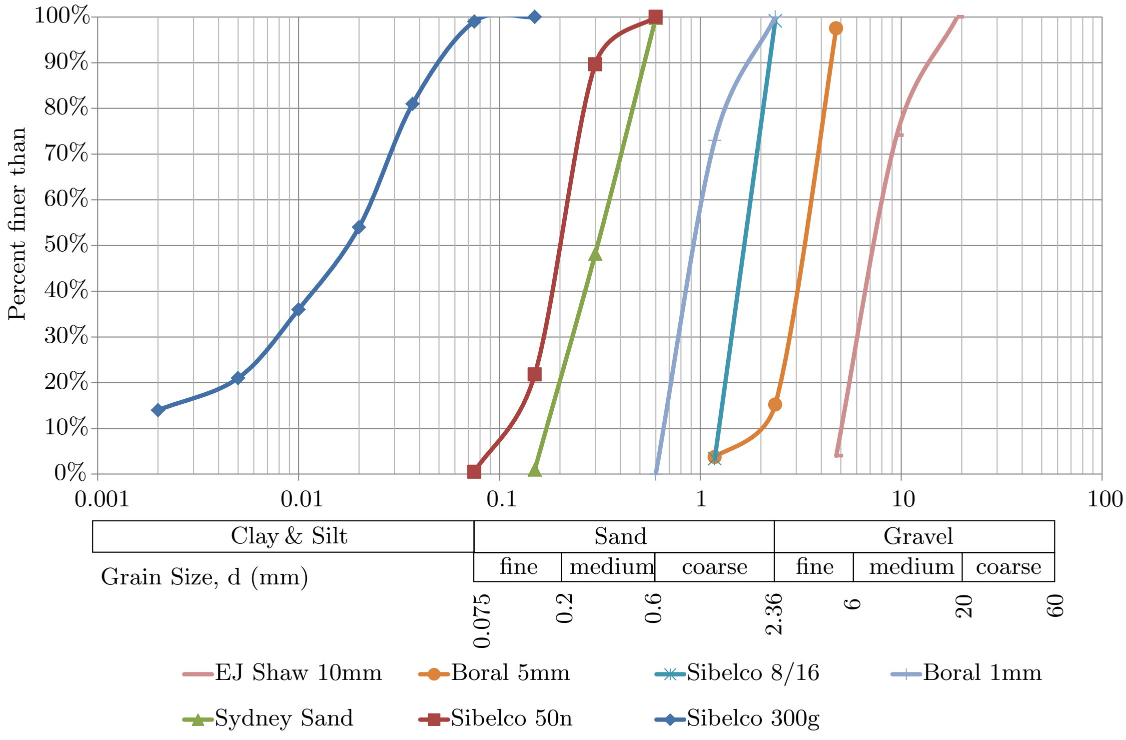

Figure 3.19: Particle Size Distribution of soil products

Figure 3.20: Photo of soil products

3.1.6 Soil mixer

A 300L 'force action cement mortar mixer' was used to mix the soil products. The mixer was manufactured by Baron with model name 'M300'. It contained paddles which moved soil around the base of the mixer as shown in Figure 3.21. The paddles were powered by a 4KW motor and a chute in the base of the mixer allowed for easy unloading of the soil.

(a) Overall unit

(b) Paddles inside mixer

Figure 3.21: Soil mixer

3.1.7 Sand Rainer

A 'sand rainer' was designed and constructed to achieve consistent and uniform placement of *loose* sand. The design was largely based on the design developed by Townsend et al. (1981) in that it was a hopper-shaped box held above the flume from a controlled height which released sand through a slot. The rainer was constructed from plywood with its base split and angled down at 45°to create a 25mm wide slot as shown in Figure 3.22.

3.1.8 Tamper and vibrator

A tamper and vibrator were used to achieve consistent and uniform placement of *dense* sand.

The tamper was a rectangular steel plate 215 x 155mm attached to the end of a 1500mm steel rod as shown in Figure 3.23. The tamper weighed approximately 6kg. However

(a) From above (b) From underneath (showing slot)

Figure 3.22: Sand rainer

tamping proved to be time consuming and difficult to standardise, as density would vary across experiments and between users. Therefore an alternate method of compaction by vibration was sought.

Figure 3.23: Tamper used to compact sample

A variety of different vibrators and methods of vibrating were trialled. These trials included:

- Clamping an internal concrete vibrator onto the flume but this produce hazardous noise levels.
- A vibrating table motor fixed to a plank of wood (pictured in Figure 3.24a) but this method did not transmit vibrations laterally and so only a small area of sand

was compacted.

- And an off-hand grinder modified with an eccentric load to produce vibrations and attached to a larger wooden plank which covered most of the sand's surface (pictured in Figure 3.24b). However, only a shallow depth of sand directly beneath the plank was compacted, leaving the remaining sand underneath loose. This could have been compensated for by placing sand in thin lifts and compacting each lift at a time, but a more time-efficient method was being sought.

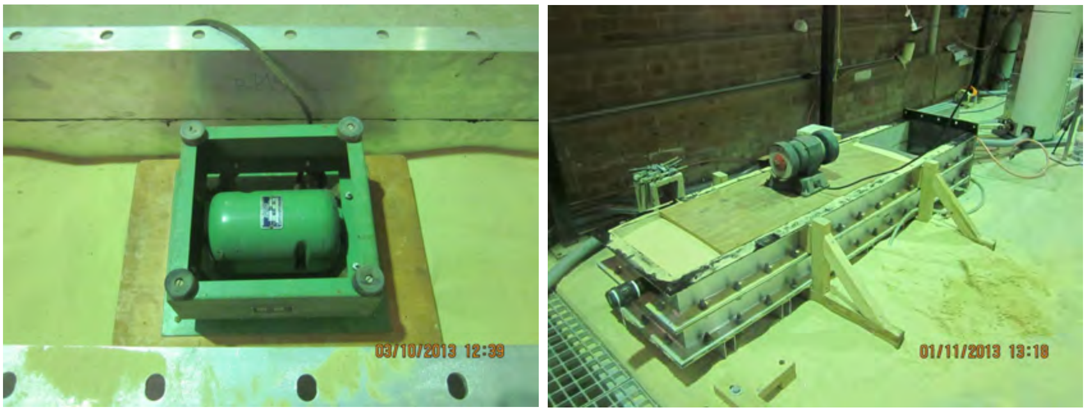

(a) Vibrating table motor on wooden plank (b) Modified off-hand grinder on larger wooden plank

Figure 3.24: Vibrator trials

Eventually an external concrete formwork vibrator fixed to the flume via a stiff steel frame was found to be successful (shown in Figure 3.25a). The external formwork vibrator was model AR 36/3/240W purchased from Wacker Neuson. It vibrated at 3000rpm with a standard centrifugal force of 2.61kN. After approximately a minute of operation, sand settled between 20 to 60mm as shown in Figure 3.25b.

3.1.9 Screed

A 3mm thick PVC sheet was cut to make a surfacing screed. The screed was cut 570mm wide so that it spanned the width of the flume but 6mm shorter (the flume was 576mm wide) to keep it from hitting the wooden frames (which restrained the flume rim from expanding outwards). One edge of the screed was cut with a 3mm indent and the other edge with a 1mm indent, both across the middle 485mm span so it would span the flume's

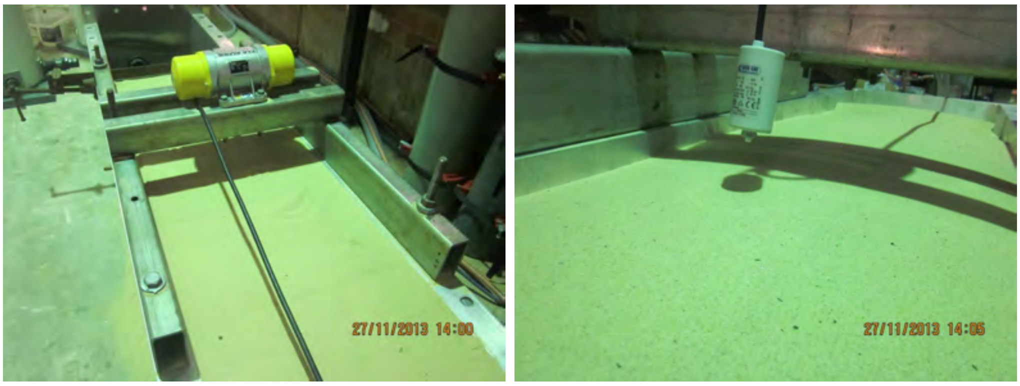

(a) Vibrator on steel frame (b) Sand settled between 20 to 60mm

Figure 3.25: External formwork vibrator used to compact sample

inner width of 450mm with some excess. The idea was the edges of the screed were dragged along the flume rim and the indent levelled the sand's surface to be 1mm higher than the flume rim. Photos of the screed are given in Figure 3.26.

(a) General view showing screed spanning full inner width of flume (b) Edge used for first pass showing close-up of 3mm indent

Figure 3.26: Screed used to level soil surface

3.1.10 Starter dowel

Group 1 tests required a 6-inch-long channel be pre-formed prior to testing in order to repeat the Townsend et al. (1981) experiments (refer to Subsection 3.2.11 for an explanation of Group 1 tests). From Test 5 onwards the starter channel was formed with a dowel. The first dowel was made out of wooden dowelling and shaped as a semicircular rod, 6.35mm (1/4 inch) in diameter and 152.4mm (6 inches) in length, to match the dowel used by Townsend et al. (1981). The dowel was pulled out of the sand sample via a string tied to its end but upon first extraction, the end of the wooden dowel broke, leaving the dowel in place as shown in Figure 3.27a (and in Figure 3.14). Therefore a second dowel was made from delrin rod with the same dimensions, pictured in Figure 3.27b. This dowel did not break and proved successful for the remainder of the Group 1 tests.

(a) Wooden dowel which broke at its tip where string was tied

(b) Delrin dowel which replaced wooden dowel

Figure 3.27: Starter dowel used in Tests 5-18 (prior to extraction) (blue arrows indicate direction of flow)

3.1.11 Tracer particles

To understand and predict the particle detachment and transport mechanisms it was informative to measure the speed of water flow through the channel. This was a challenge because the channels were small (between 2 to 25mm wide), inaccessible (under the Perspex lid) and unpredictable in their position (because they meandered). The method employed was to lace the soil's surface with traceable particles and take high-speed photos of the moving particles as they left the soil matrix and travelled along the channel. The choice of tracer particles was important. A few alternatives were trialled including glass beads, granulated pvc, tyre shreddings, a synthetic powder colourant (DayGlo ZQ-17 Saturn Yellow Pigment) and coloured sand (all shown in Figure 3.28 except for the coloured sand which can be seen in Figure 3.15). When coloured sand was photographed and analysed it was noticed that distance travelled between frames varied suggesting (an unlikely) sporadic unsteady flow (as shown in Figure 3.29). Also noticed was the shape of particles varying between frames suggesting the sub-angular particles were rolling. This suggested the coloured sand particles were rolling along the bed of the channel, i.e. were bed-load, and were likely to be moving slower than the surrounding flow. Therefore a lighter tracer particle which would suspend in and move with the channel flow was needed, i.e. a particle with a density similar to water.

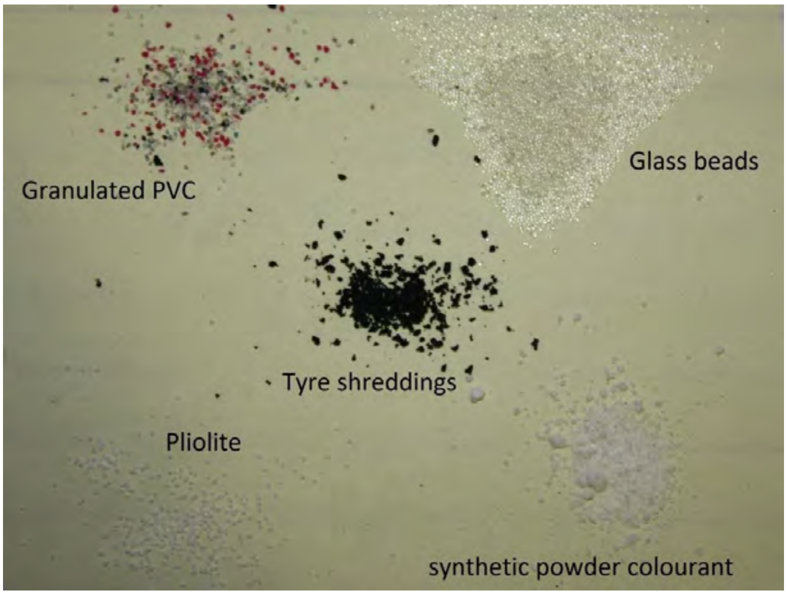

Figure 3.28: Tracer particles trialled

A white granular material, commercially referred to as *Pliolite VTAC-L* demonstrated to be neutrally buoyant and travelled with the channel flow. This was evident by the uniform spacing between position markers from previous frames as shown by the blue and red lines in Figure 3.29 (the markers were uniformly spaced once the Pliolite VTAC-L had entered the centre of the channel).

Pliolite VTAC-L (referred to as just Pliolite from here on) is a *"highly soluble vinyl toluene acrylate copolymer"* used as a *"solvent based newtonian resin designed for intumescent coatings and flat or textured masonry paints"* (Omnova Solutions, 2017).

The Pliolite had been sieved down to particle sizes between 0.25 to 0.355mm (similar size to Sydney sand particles) before use.

3.1.12 Carbon Dioxide system

As will be discussed in Subsection 3.2.8 Carbon Dioxide (CO_2) was used to improve saturation of the sand. The CO_2 was purchased from a local gas supplier (BOC) in bottles containing approximately 15kg of pressurised CO_2 (15kg when at 15°C and atmospheric pressure). A gas regulator and rotameter were attached to the bottle to control and measure the flow rate as shown in Figure 3.30a.

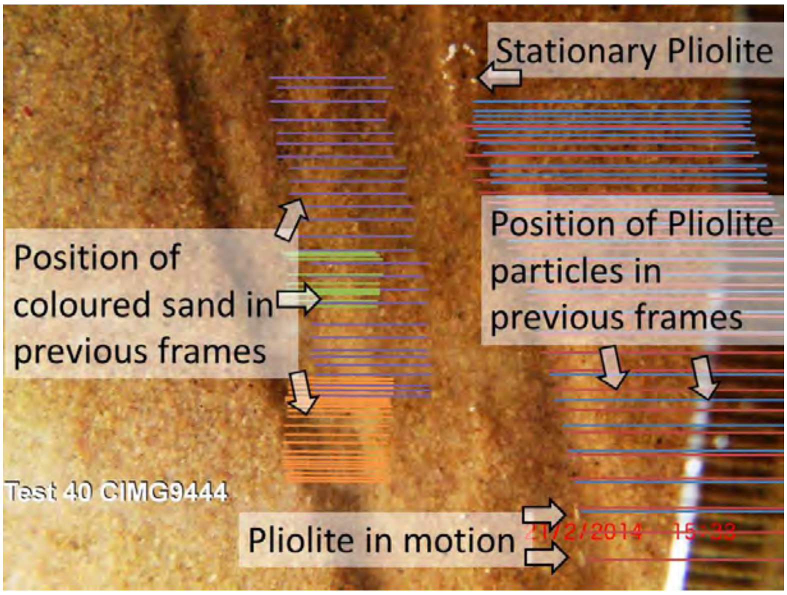

Figure 3.29: Lines indicate position of particles in previous frames. Distances between lines on the left varied indicating unsteady speed of coloured sand particles. Distances between lines on the right become constant indicating constant speed of Pliolite particles.

CO_2 was sent via a 5mm diameter welding hose (1.2MPa) into a 12mm (internal) diameter valve cut into the upstream-end wall of the flumes. Two release valves were drilled into the lid of the flume, one into the downstream box lid and the other into the lid above the upstream chamber. These release values were connected with a 12mm (internal) diameter hose (as shown in Figure 3.30d), so that air and later CO_2 could be contained and sent to a manifold tube. This manifold tube was fitted with four valves, one for each flume (as shown in Figure 3.30b) and was used to direct CO_2 to a second rotameter before being send outside through another hose.

To monitor CO_2 levels in the laboratory a meter was purchased from CO2Meter.com, with model number TIM10, pictured in Figure 3.30c. The meter provided CO_2 levels up to 5000ppm with an alarm that sounded at a user-specified limit.

3.1.13 Cameras and lighting

Four different cameras were used to photograph the experiments including:

- A Canon IXUS 105, used to capture observations of interest through-out the experiment.

(a) CO_2 rotameter, regulator and bottle

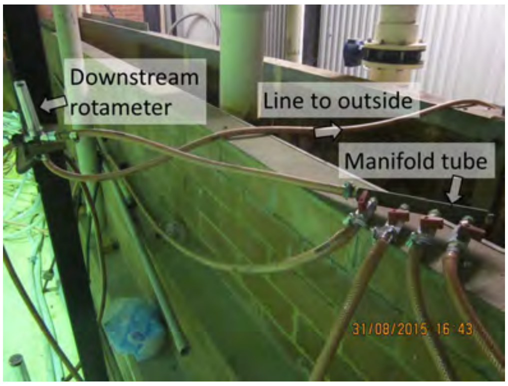

(b) Gas manifold tube

(c) CO_2 meter

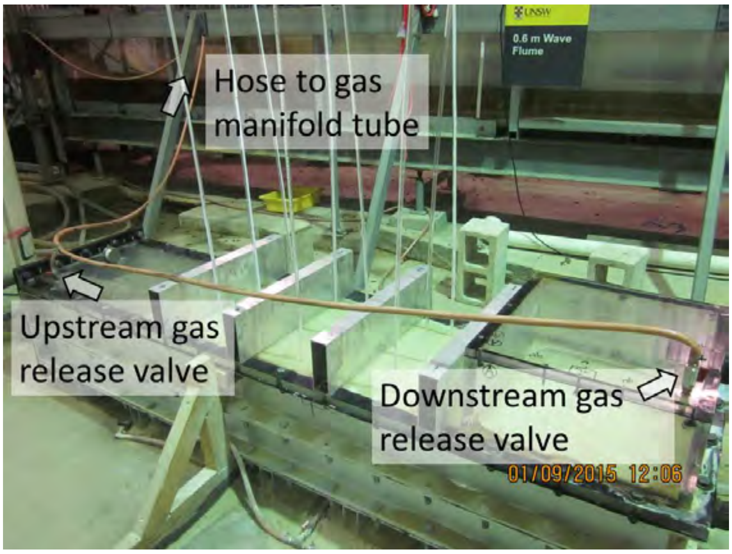

(d) Gas pressure release valves and hoses

Figure 3.30: Carbon Dioxide System

- A Canon EOS 1000D, used to take plan-view shots of the backward eroding channel through the flume lid. The camera was set above the flume with a tripod (as can be seen in Figure 3.10b) and triggered by a wireless timer remote: a Hähnel Giga T Pro II.
- A Casio Exilim EX-F1 high-speed camera used to measure the speed of Pliolite particles travelling through channels.
- A Sony HandyCam DCR-SX40E video camera used to watch tip progression and other processes.

Whilst the laboratory building was reasonably lit, it was difficult to see the backward eroding process (and photograph it). Initially torches were used to illuminate the experiments and aid in photo taking (example shown in Figure 3.31). Combinations of different LED lights were also used. However by test 12 500W Halogen flood lights, already present at the laboratory, were used and proved far more effective. The halogen flood lights can be seen in Figure 3.10 and were used for all remaining experiments.

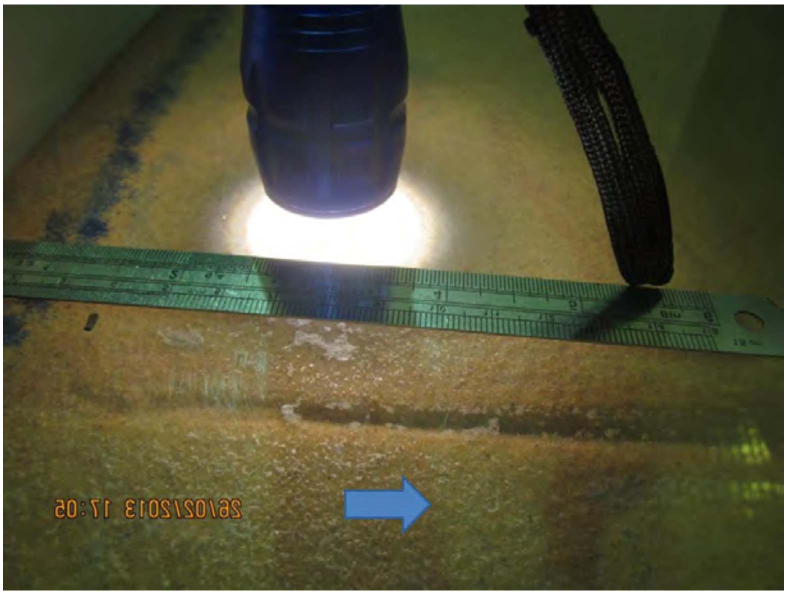

Figure 3.31: Using a torch for experiment illumination (viewing starter channel) (blue arrow indicates direction of flow)

3.1.14 Flow rate scales and computer

Initially the rate of flow leaving the flume was measured with a stop-watch and beaker when the head difference was 100mm. However it was of interest to see whether the bulk permeability increased over time with either loss of fines or increasing channel length. Therefore a method for continually measuring the flow rate throughout the experiment was sought. To do this a digital scale, which could transmit weight measurements to a computer, was used to weigh the 60L container capturing flow leaving the flume. The scale was a make and model of A&D SE-60KAL with capacity of 60kg in 0.01kg increments. The software used to time and record the weights was R&D's 'RsCom' Ver.2.49. The scales, 60L container and computer are shown in Figure 3.32.

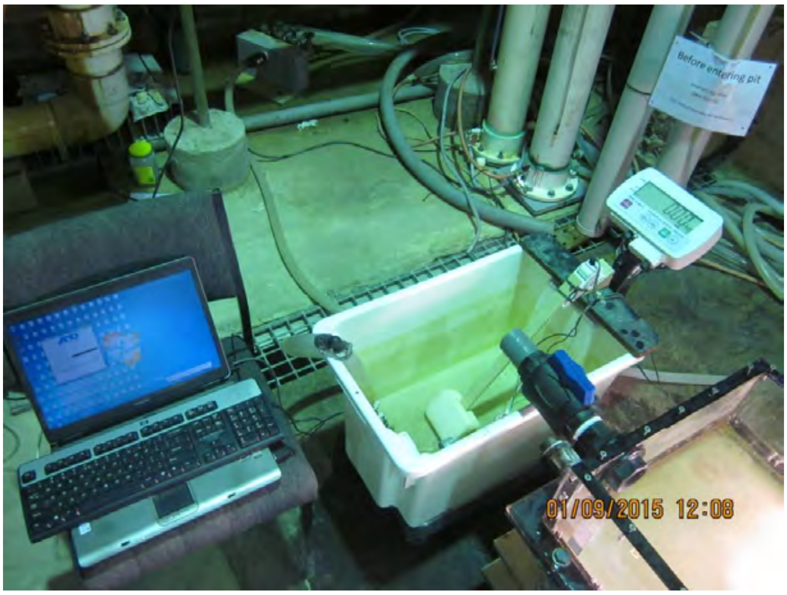

Figure 3.32: Scales, 60L container and computer used for flow rate measurement

3.1.15 Density push tubes

In order to measure the density of soil in the flume (after a test) small thin-walled push-tubes were made in-house. The tubes were cut from a stainless steel pipe of outer diameter 60.3mm and 1.85mm thick to make tubes 50mm long. The penetrating end of the tubes were bevelled as per the specification AS1289.1.3.1 for thin-walled samplers. To lift full push tubes up out of the soil, and to screed the top and bottom surfaces, a thin 'L' shaped piece of galvanised iron was used. Both the push tubes and 'L' shaped iron are shown in Figure 3.33.

3.1.16 Sand drying bays

It was economical to reuse the same sand from one experiment to the next but this meant that approximately 400kg of wet sand needed to be dried between tests and done so in as little time as possible (to maximise the number of tests). Sand needed to be dry before reuse for 3 reasons, 1) so it would fall through the sand rainer (when loose density was required) 2) to aid in compaction by vibrations (when compact density was required) and 3) to allow CO_2 to reach all air voids for successful saturation.

Many different methods of drying sand were trialled but the most successful method involved placing sand on top of a raised perforated plate. The perforated plate was a 1.2

Figure 3.33: Density push tubes and 'L' shaped iron

by 2.5m galvanised steel plate, 1.5mm thick, with 3mm diameter holes spaced 6mm in one direction and 10mm in the other (centre-to-centre). When the sand was wet it had sufficient cohesion to keep it from falling through the perforated holes but when it dried it fell through the perforations and waited dry underneath (as shown in Figure 3.34b). The sand was dried by placing heaters underneath, but around the edge of the raised perforated plate. The plate was raised with Besser Blocks. The Besser Blocks also served to contain the heat underneath by creating 'windows' just large enough for the heaters to be placed in, as shown in Figure 3.34c. Most of the heaters were inexpensive radiant heaters but one was a 3-phase 5kW convection heater (the orange circular heater shown in Figure 3.34d). The convection heater was used to circulate hot air around and up through the perforations (drying more sand as it passed by). An advantage of this method was that sand could be placed in a thick layer (as thick as the perforated plate could support) because drying occurred from beneath and as sand dried and fell through the perforations, new moist sand would be exposed to the heat. An example of the sand layer thickness placed on the drying bays is shown in Figure 3.34a (along with an inquisitive Water Dragon).

(a) Thick sand layer on plate (and water dragon in background)

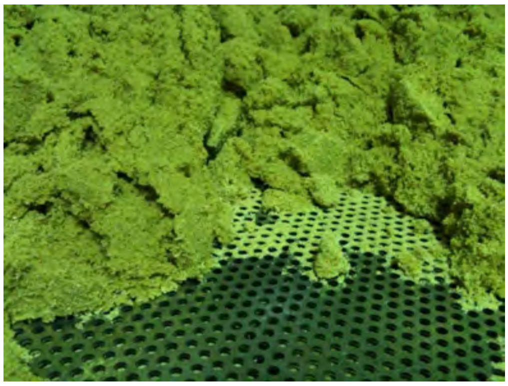

(b) Close up of wet sand on top of perforated plate

(c) Underneath perforated plate before sand has fallen through perforations

(d) General view once drying almost complete

Figure 3.34: Sand drying bays

3.2 Test set-up

This section describes the test set-up procedure used, from mixing the soil through to the start of an experiment. A chronological list is given to outline the steps taken. This is followed by a subsection describing each step. Lastly a list of all the set-up variables used for each experiment is presented.

3.2.1 Chronological list

A chronological list of the steps required to set-up an experiment are listed in Table 3.2.

Table 3.2: Chronological list of test set-up

	Step	Description reference
1	Mix soil	Subsection 3.2.2
2	Place soil	Subsection 3.2.3
3	Attach lid	Subsection 3.2.5
4	Inflate Pressure Bladder	Subsection 3.2.6
5	Flush with CO_2	Subsection 3.2.7
6	Saturate	Subsection 3.2.8
7	Remove downstream box lid	Subsection 3.2.9
8	Set-up cameras and lighting	Subsection 3.2.10

3.2.2 Soil mixing

Of the ten different soils tested in this study, eight were produced by mixing different soils together. This section details the mix portions used and why, as well as how the soils were mixed.

The mixed soils were created by mixing the soil products described in Subsection 3.1.5. They were created by mixing, as opposed to sourcing natural soils, to avoid the arduous task of sourcing and transporting large volumes of soil that did not vary in composition. It also meant that the labour-intensive tasks of drying and removing clay fractions could be avoided. Furthermore, creating soils by mixing products provided the ability to isolate and investigate particular soil properties, such as fixing d_{10} to fix permeability whilst increasing C_u to isolate the effect of uniformity.

The disadvantage with using processed products is the particle shapes are typically more angular than natural soils. However, the influence of angularity on backward erosion is considered negligible when compared to the influence of other soil attributes. As evidence for this, Sellmeijer et al. (2011) found, through the use of a multivariate analysis, that the roundness of particles (as measured by the KAS scale, pictured in Figure 11.25) required an exponent of only -0.02. When compared with exponents required for other soil attributes of between 0.13 and 0.4 for relative density, intrinsic permeability, d_{70} and uniformity coefficient, one can see how relatively unimportant particle roundness worked out to be. Therefore, the influence of angular particles on test results were considered to be negligible.

To design the soil mixes a spreadsheet was set-up which constructed a particle size distribution from mix percentages of each product. An initial mix design was calculated by comparing the distribution of the ideal soil with the distribution achieved by the mix and using the 'method of least squares' to bring the two into alignment (as much as possible). On occasion the percentages of products needed manual adjustments to meet all requirements.

Broadly speaking, the aim of testing soil mixes was to investigate well graded soils with consideration of how particle size, uniformity and silt fractions affected the critical gradient. Soil mix designs were characterised by target values of either d_{50} and C_u, d_{10} and C_u or the fraction of silt. These target values for each soil mix are listed in Table 3.3 followed by an explanation of why these values were targeted.

Table 3.3: Target values for soil mix designs

Mix	d_{50} (mm)	d_{10} (mm)	C_u	% of Silt
1	0.3	-	7	-
2	-	0.24	4	-
3	-	0.24	6	-
4	-	0.24	8	-
5	-	0.5	6	-
6	-	-	-	7
7	-	-	-	10
8	-	-	-	13

Mix 1 was designed to investigate a soil at the upper range of C_u on the Schmertmann (2000) graph of critical gradient with C_u whilst being fixed at a d_{50} similar to Sydney Sand (0.3mm).

Mix 1 did not backward erode at a global gradient of up to 1.4 and because gradients above 1 are unlikely in most dams/levees, the C_u of the next soil, Mix 2, was reduced (in an effort to reduce the critical gradient). For Mix 2, instead of fixing the d_{50} similar to Sydney Sand again, the d_{10} was fixed similar to Sydney Sand (0.24mm). This was done to create a soil with similar permeability as Sydney Sand but with a larger C_u so that the effect of increasing C_u could be investigated without change in permeability. In other words, the affect of C_u could be partially isolated from the affect of permeability.

The concept of keeping permeability similar by fixing d_{10} is based on Hazen's formula of $k = Cd_{10}^2$, where C is a factor (usually taken as 0.01) and k is the permeability in m/sec (Fell et al., 2005). It is recognised that Hazen's formula is only an estimate and only for clean sands with d_{10} between 0.1 and 3mm (Fell et al., 2005), but it was considered a helpful guide in designing soils to be of similar permeability. Refer to Section 4.10 for presentation of the permeability values achieved.

Tests carried out in Mix 2 did backward erode so C_u was increased to a target value of 6 in order to find the upper C_u limit, whilst maintaining the d_{10}. Mix 3 backward eroded as well, albeit at high heads, so C_u was increased again to 8. Mix 4 did not completely backward erode. Channels did form, and reached a maximum length of 1040mm (80% of the seepage length), but never reached the upstream end. Therefore a maximum C_u of 8 was considered to have spanned the full range of C_u values susceptible to backward erosion.

The next soil, mix 5, was designed to have the same C_u as Mix 3 (around 6) but with a larger d_{10} (more permeable) to investigate the influence of permeability without the effect of C_u. The soil product Sibelco 50n was also tested as is, for the same reason: to investigate the influence of permeability without the effect of C_u by comparing its results to Sydney Sand's results (both have similar C_u values but different d_{10}).

Mix 6 was designed to model fine to medium silty sands found at two Australian dams, Atkinson and Ewen Maddock Dams, as advised by Emeritus Professor Fell. Whilst these dams have not experienced backward erosion piping, it is an active issue that requires estimation of probability (which, if made using the prediction methods of Sellmeijer and Schmertmann would be subject to much uncertainty given these methods do not cover silty sands such as these).

Mixes 7 and 8 were slight alterations of Mix 6 to contain more of the Sibelco 300g product so that the effect of fines could be investigated. The four soils of Sibelco 50n, Mix 6, 7 and 8 provided a 'family' of results on soils containing 0%, 7%, 10% and 13% of silty fines. It was of interest to see what effect fines would have on the progression gradient and on the Schmertmann (2000) method.

In addition to the target values, each soil mix needed to be designed to be internally stable. Using internally stable soils reduced the chance of soil eroding by suffusion, lest the two erosion mechanisms occur simultaneously and their interaction contaminate the results and understanding of the backward eroding process. The method used to check for internal stability was the method of Burenkova (1993) adapted by Wan and Fell (2007) by designing soils to plot as high on Figure 3.35 as possible.

As can be seen in Figure 3.35, probabilities of internal instability for soil mixes 1–5 were all less than 20%. This was an improvement over the well graded soils tested by Townsend and Shiau (1986) and van Beek (2015) whose probabilities of internal instability ranged between 40–80%.

The resulting soil mix portions are listed in Table 3.4 and the final soil properties and descriptions are listed in Table 3.5. Particle size distributions are graphed in Figure 3.36. A photo of the soil mixes is shown in Figure 3.37.

It was considered that these ten soils (the two uniforms sands and the eight mixed soils) provided a good range and even spread of C_u and permeability values. To illustrate this, Figure 3.38 indicates the C_u values of each soil superimposed over the boundary between 'poorly' and 'well' graded sands according to the Unified Soil Classification System (a C_u of 6). Figure 4.40 illustrates the range of permeabilities tested and shows that a good range of permeabilities was achieved covering 2 orders of magnitude within the sand range (for a description of the methods used to measure permeability refer to Subsection 3.4.5, for individual permeability measurements refer to Table 4.3 and for permeability comparisons refer to Section 4.10). Figure 4.40 also shows that soils with similar d_{10} sizes had similar permeabilities as can be seen by the group of Mix 1, 6, 7 and 8; and the group of Sydney Sand, Mix 2, 3 and 4. This illustrates the intention of testing soils with similar permeabilities but different uniformity coefficients was somewhat successful.

The procedure for mixing the soils was to weigh the soil products (not to rely on bag-labelled weights) and place into the soil mixer starting with the largest-grained soil and working down-in-size (so fine grains moved through coarser-grained soils). The soil mixer could contain approximately 350kg of soil, but the flume required between 400–450kg (depending on the mix), so 300kg of the mix was produced first, then a second batch was made based on how much of the flume the first batch filled.

The mixer was run for approximately 2 minutes at 32 revolutions per minute until the mixture appeared well mixed. The soil mix was emptied from the base of the mixer through a chute into a wheel barrow. The barrow was then wheeled to the flume ready for soil placement.

The challenge with mixing well graded soils was to avoid segregation. Care was taken to avoid segregation by:

1. Making an excess of soil mix (approximately 10kg over) so that the last of the soil to be taken from the mixer was not the finer material that sometimes remained underneath the mixer paddles. This was particularly important given the last of the soil to be the taken from the mixer was the top layer of the soil to be placed in the flume- where backward erosion occurred.

2. Aligning the chute from the base of the mixer with the top of the wheel barrow to minimise fall height to the base of the barrow (was <0.5m- the depth of the wheel barrow).

3. Then when placing the soil (as discussed in the next section), shovelling out small volumes at a time, lowering the shovel to the soil's surface so soil was not being dropped and keeping the soil's slide out of the shovel slow with a shallow angle.

4. And when compacting the soil (as discussed in the next section), using only the tamping method (no vibrations) in thin, 50mm thick layers.

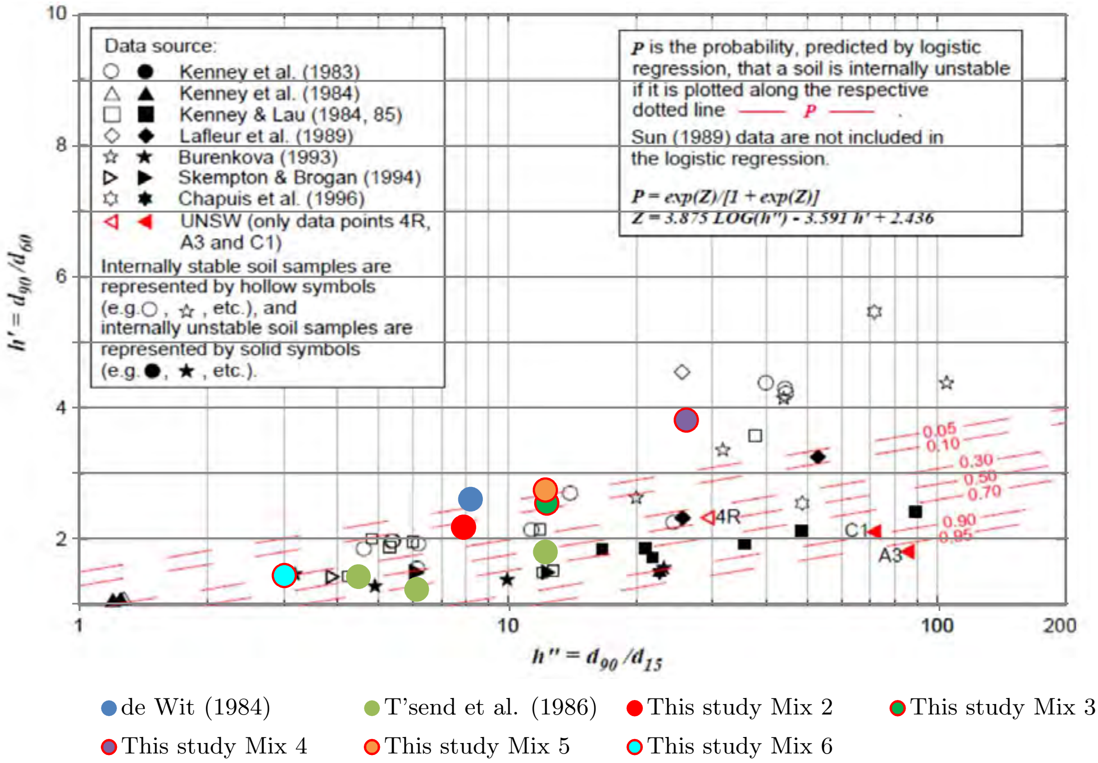

(a) Sand-gravel soils with <10% finer than 0.075mm

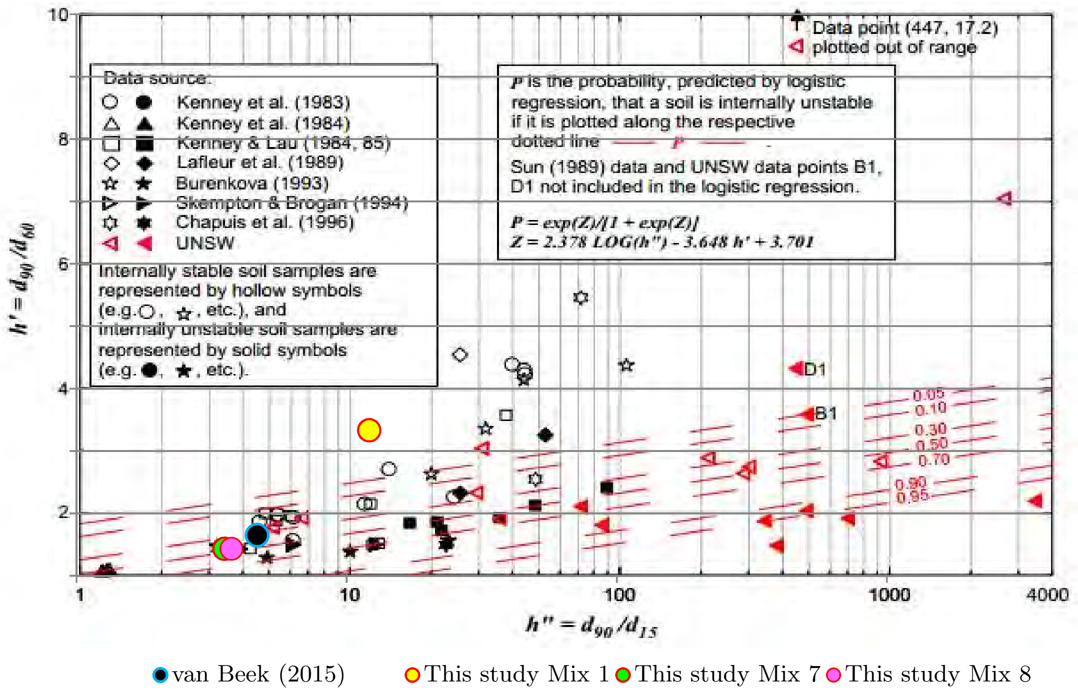

(b) Silt-sand-gravel soils and clay-silt-sand-gravel soils of limited clay content and plasticity

Figure 3.35: Soils from both this study and from others over contours of probability of internal instability (Wan and Fell, 2007) showing most soils from this study are less susceptible to internal instability

Table 3.4: Soil mix proportions

	Mix 1	Mix 2	Mix 3	Mix 4	Mix 5	Mix 6	Mix 7	Mix 8
EJ Shaw 10mm				20.35%	29.24%			
Boral 5mm			23.77%	20.33%	23.25%			
Sibelco 8/16	11.30%	17.50%	15.51%	8.68%	11.69%			
Boral 1mm	26.00%	36.00%	26.39%	22.28%	24.76%			
Sydney sand	28.50%	46.50%	34.34%	28.36%	11.07%			
Sibelco 50n	24.00%					93.00%	90.00%	87.00%
Sibelco 300g	10.20%					7.00%	10.00%	13.00%

Table 3.5: Soil descriptions and properties

	Soil	PSD & grading	Secondary component	d_{10}	d_{50}	C_u	Suffusion P.
Sydney Sand	Sand (SP)	medium, uniform	-	0.24	0.30	1.3	<0.05
Sibelco 50n	Sand (SP)	fine to medium, poorly graded	-	0.11	0.20	1.9	<0.05
Mix 1	Sand (SM)	fine to coarse, well graded	some low plasticity silt	0.075	0.35	6.8	<0.05
Mix 2	Sand (SP)	medium to coarse, poorly graded	-	0.20	0.64	4.2	0.1–0.3
Mix 3	Gravelly Sand (SW)	medium to coarse, well graded	fine gravel	0.27	1.00	6.2	0.05–0.1
Mix 4	Gravelly Sand (SW)	medium to coarse, well graded	fine gravel	0.24	1.40	8.8	<0.05
Mix 5	Sandy Gravel (GW)	fine to medium, well graded	medium to coarse sand	0.51	2.36	6.1	<0.05
Mix 6	Sand (SP)	fine to medium, poorly graded	some low plasticity silt	0.080	0.19	2.6	0.1–0.3
Mix 7	Sand (SP)	fine to medium, poorly graded	some low plasticity silt	0.065	0.18	3.2	0.3–0.5
Mix 8	Sand (SP)	fine to medium, poorly graded	some low plasticity silt	0.033	0.18	6.4	0.3–0.5

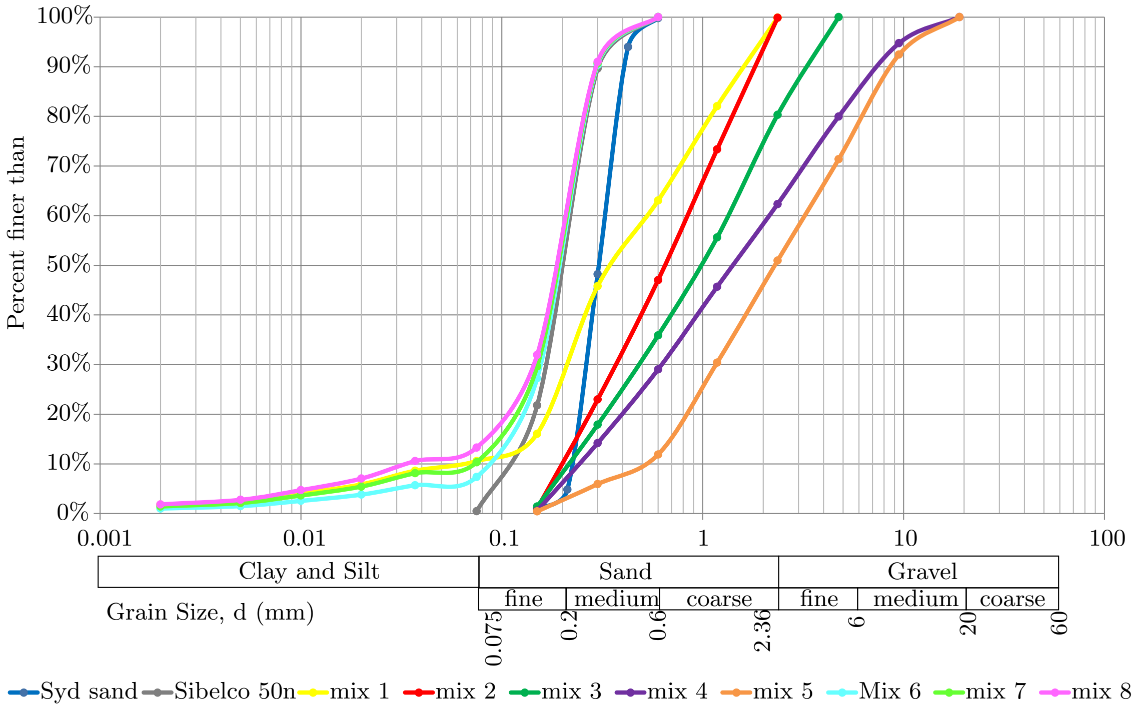

Figure 3.36: Particle Size Distributions of soils tested

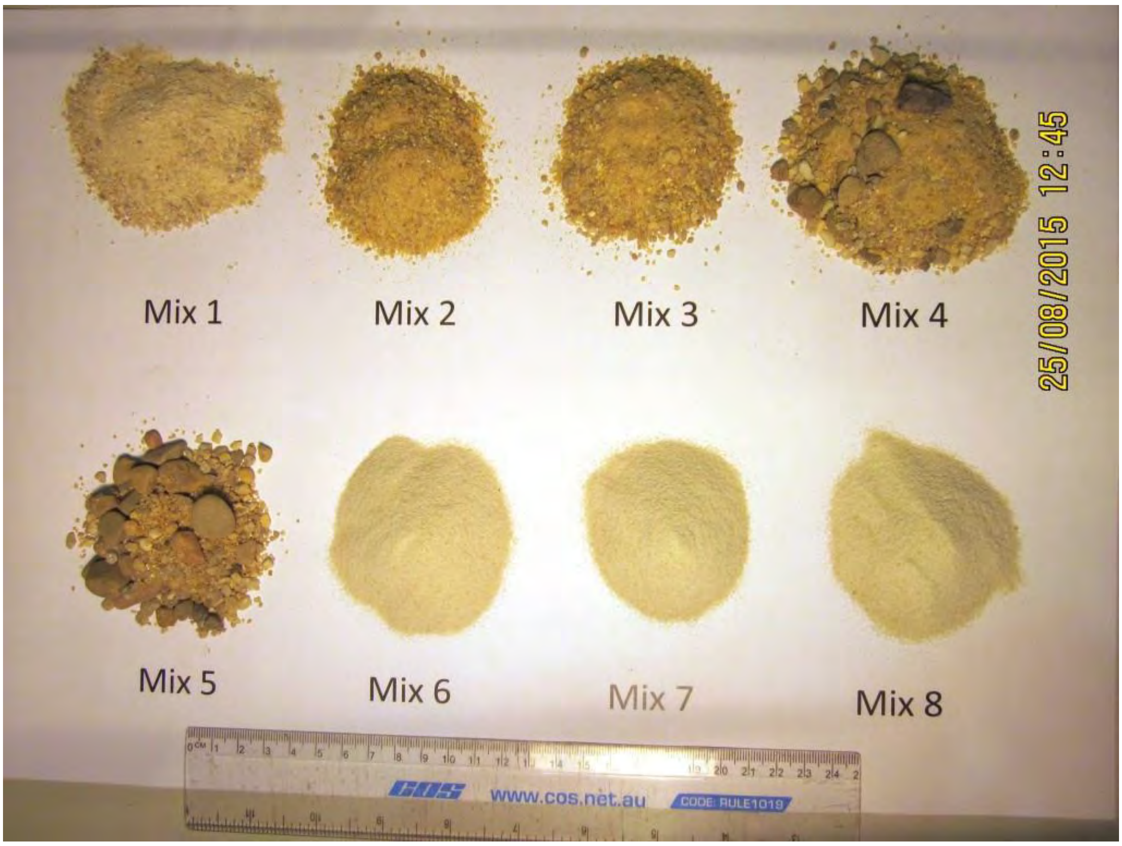

Figure 3.37: Photo of soil mix samples

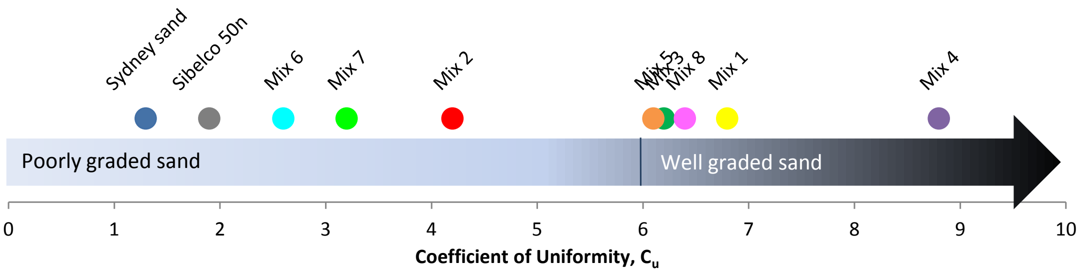

Figure 3.38: C_u values of soils tested

3.2.3 Soil placement

Four different techniques were used to place soil into the flumes. These techniques were used to place soil at either loose or medium dense densities in such a way that produced a uniform density throughout, especially throughout the top layer of soil. These four techniques included dry pluviation (raining), wet pluviation, tamping and vibrating. Each of these techniques are described below.

Rained

Tests 1–13 required loose sand in order to recreate the test set-up used by Townsend et al. (1981). Tests 14–18 also required loose sand for the same reason, but were not placed loosely for reasons to follow. Test 46 required loose sand in order to investigate the effect of sand density by comparing its results with otherwise identical tests carried out on medium density and dense sands.

Van Beek et al. (2011a) achieved a loose sand density by placing the sand using 'wet pluviation' (which is described in Section 3.2.3). However when the flume was rotated from a vertical to horizontal position prior to testing (using hydraulic rams), the sand settled and created a small gap between the sand and lid. Given that lifting equipment which could rotate the flume were not available in this study, and that this method resulted in collapsed settlement, it was not used.

Townsend et al. (1981) used 'dry pluviation' by dropping sand into the flume from a hopper-shaped box which was held above the flume on a wheeled steel frame and fitted with a steel shutter plate, this was called a 'sand rainer'. For this study a similar sand rainer was constructed as described in Subsection 3.1.7.

Prior to loading the rainer with sand, the slot was covered over with plastic sheeting to prevent sand falling through prematurely. Once the rainer was full, with approximately 0.12m^3 per load, it was raised off the ground with an overhead crane (capable of lifting 1000kg) and driven from the sand bays to the flume. The crane was positioned along the centreline of the laboratory building, so both the loading position and the flume had to be located along the building centreline. However there was an existing structure on the centreline next to the flume so lifting slings were used to pull the rainer a small distance out from the centre of the building to be over the flume. Figure 3.39 shows the rainer suspended from the crane next to the flume.

Figure 3.39: Sand rainer suspended by crane above flume

The height of the rainer was adjusted to keep the sand fall-height at approximately 1.1m (a similar height used by Townsend et al. (1981)). With the rainer in position the plastic sheeting was pulled out through the slot allowing the sand to fall into the flume. It was necessary to ensure the sand was dry as practical, otherwise it would not fall through the slot. On occasion a piece of PVC sheet similar to the screed (described in Subsection 3.1.9) was used to encourage sand to continue to fall though the slot by pushing it up into the slot to loosen the sand.

Two to three sand rainer loads were required to over-fill a flume.

When sand was rained in, the sloping exit would often slip and scarp during saturation. This was not ideal as it would cause the top of the slope to retreat leaving the starter dowel sticking out (and reducing the length of the starter channel) and reducing the sample's seepage length. Initially it was thought this slipping was due to too steep a slope and loosing sand down the sides of the slope, and these were indeed causes, but once they were fixed the slope continued to slip, particularly from Test 9 when CO_2 flushing started to be used. So the next speculated cause for slope slipping was the loose density of the sand. To investigate this possibility, Test 14 was tamped in to achieve a denser sand. With a denser sand the slope no longer slipped or retreated. Another advantage was a reduction in the frequency of channels forming along the edges of the flume. Therefore raining in the sand was abandoned from Test 14 onwards. Except for Test 46, where sand was rained in again, however this test was on a circle exit, so slope slipping was not a concern.

Tamped

Tests were required in medium dense to dense sands in order to investigate soils at densities more likely to exist in the field (more likely than loose sands). To achieve medium dense to dense sands, sand was compacted in the flume using either a tamper (described in Subsection 3.1.8) or a vibrator.

The tamper was used before the vibrator was purchased, in Test 49 when the maximum density was sought (by using both the vibrator and tamper) and on graded soils (when the vibrator could not be used due to segregation).

Soil was slowly and carefully placed into the flume with a shovel to minimise segregation and make 50mm thick layers. Each soil layer was tamped by dropping the tamper from approximately 100mm above the soil's surface. Every effort was made to keep the compaction effort consistent by standardising the drop-height, number of drops and tamping pattern over the surface of the soil however the method was more susceptible to variation than the vibratory method. It was also more time consuming.

When soils containing the fine Sibelco 300g product were tamped into flumes, care had to be taken to reduce the risk of inhaling it. According to the Material Safety Data Sheet for the Sibelco 300g product, it is toxic if exposed to prolonged inhalation due to the respirable ($\leq 7\mu$m) crystalline silica dust it contains. Therefore half-face respirators were worn with dust filters of class P2 certified to AS1716. In addition, the laboratory was closed during soil placement, preventing unprotected personnel from entering. Figure 3.40 shows the Sibelco 300g product becoming air-born during tamping.

Figure 3.40: Air-born Sibelco 300g during tamping (and respirator use)

Vibrated

For tests that required sand be placed to form a medium dense to dense density, sand was compacted in the flume using either a tamper or a vibrator (described in Subsection 3.1.8).

The vibrator was used from test 32 onwards (it was purchased after test 31) on Sydney Sand only.

With the flume over-full of soil (at least 60mm above the top of the flume), the vibrator frame was fastened to the flume and the vibrator was turned on for 2 minutes. The vibrator always operated at 3000rpm with a standard centrifugal force of 2.61kN. This prescribed run time and power meant that compaction effort across tests could be kept more consistent than the tamping method. The vibrations caused the soil's surface to settle between 20 and 60mm. Often the sand would settle more along the edges of the flume than the centre. In some instances, when the sand settled to below the flume rim (particularly in the corners where the most vibrations were experienced), additional sand had to be poured in whilst the vibrator was still operating. It was important that any newly placed soil was also subjected to a vibrator run-time of 2 minutes in an effort to achieve uniform density.

Wet pluviation

Wet pluviation occurs when soil is scattered into water and allowed to settle under its own submerged weight. The result is loose, saturated soil. The advantage of wet pluviation was that soil need not be dried between tests as CO_2 flushing was not required. Not needing to dry soil was not only a time-saver but it was necessary when using soils containing the fine Sibelco 300g product (because it was hazardous when placed onto drying bays and handled/relocated dry). For this reason, underwater soil placement was trialled.

In order to scatter the top soil layer into water, the top of the flume needed to be submerged. To achieve this, an open-top tank, described in Subsection 3.1.2, was constructed. This open-top tank surrounded and submerged the entire flume.

Wet pluviation was trialled in three tests: 47, 48 and 54 as shown in Figure 3.41. In Test 47, sand was scattered into water in three lifts, vibrating to compact between each lift. However, the fine-grained Sibelco 300g material became suspended almost immediately upon contact with water and vibrations caused segregation, evident by small boils of fine-grained material across the surface. As a result of the loss of fines, a gap was left between the soil and lid and the test failed by concentrated leak erosion. Tests 48 and 54 were modified by scattering sand through more shallow columns of water and either compacting by tamping underwater or not compacting at all. However, these tests failed suddenly when a corridor of soil slipped along the top surface along the full length of the flume. And whilst both tests did this at rather different heads, it was decided that these 'surface slips' occurred because the soil was too loose and will slip before it backward erodes. Therefore, the method of wet pluviation was abandoned.

This meant that all soil had to be dried between tests because soil had to be placed dry for CO_2 flushing (the only remaining method of successful saturation). As the Sibelco 300g product could not be dried (because it was hazardous to do so) all soil mixes containing it (Mix 1, 6, 7 and 8) could only be used once. When these mixes were excavated out of a flume after a test (wet) they were disposed of. Subsequent soil samples were mixed with new dry material.

(a) Placing soil into water (b) Screeding surface underwater

Figure 3.41: Wet pluviation

3.2.4 Surface preparation

Surface preparation included screeding the soil's surface, forming the slope exit (for slope-exit tests), placing the starter channel/starter dowel (for group 1 tests) and lining the surface with tracer particles (for select Sydney sand tests).

Surface screeding

The surface was levelled using the screed described in Subsection 3.1.9. It was used by firstly dragging the screed across the flume with the 3mm indented edge in order to remove the bulk of the excess soil and any foreign objects. Then the screed was used a second time but with the 1mm indented edge in order to leave the soil's surface approximately 1mm above the flume's rim. This was done to reduce the possibility of gaps being left behind and to ensure good contact with the lid. It was important to drag the screed in one continuous motion from one end to the next so as to prevent additional undulations where the screeding started/stopped.

Often foreign objects and/or gravel pieces in the mix would create streaks/lines along the soils surface as it got caught under the screed and dragged along. In these instances effort was made to fill-in the lines with soil but it is recognised that this soil was unlikely to be at the same density as the soil surrounding it.

Slope exit formation

When the slope exit was required, a dust-pan was used to 'cut' a slope into the sand starting from the downstream-panel-position (which was buried at the time so it's position was marked on the gasket prior to filling the flume in) and sloped down to the top of the slope panel. Thick foam was pushed into the gap between the slope panel and flume-end to prevent sand from falling in and filling the gap during vibration and whilst the slope was formed. When forming the slope, it was found that if the sides of the slope were formed with a steeper slope, so as to form a kind of 3-dimensional corner fillet of sand (shown in Figure 3.42), then a channel was less likely to form along the edge of the flume because the seepage length was being slightly increased along this flow path. A channel forming along the edge of the flume was not ideal because factors such as void ratio, total stress and friction were different along the edge than elsewhere. However this technique of filleting the slope corners was not used until test 36.

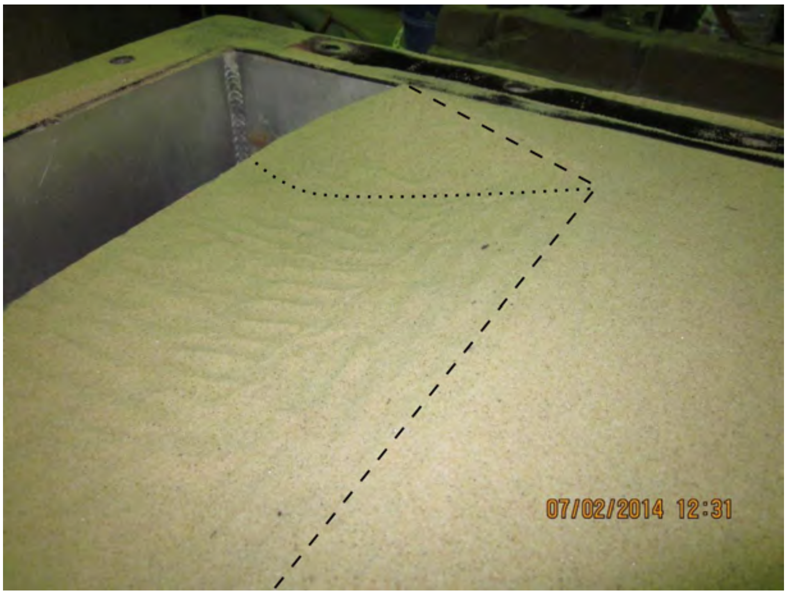

Figure 3.42: Corner fillet when forming slope exit to extend seepage length along edge (so that channel was less likely to form along edge)

Starter channel formation

In the study by Townsend et al. (1981) the beginnings of an eroding channel was cut into the sand sample prior to testing. This 'starter channel' was formed with a 6 inch long dowel which was carefully extracted once the experiment was ready to begin. Townsend et al. (1981) do not appear to explain why they formed a starter channel but perhaps it was done to avoid a channel from forming along the edge of the flume. Regardless of the reason, a starter channel was also needed in this study if the results of Townsend et al. (1981) were to be replicated (as was the aim of the Group 1 experiments).

The starter channel was carefully excavated with a spade bit and small paint brush to be 6 inches long and approximately 1/4 inch deep and 1/4 inch wide. The excavation was placed at the top of the sloping exit in the middle of the flume.

For tests 1-4, sugar was delicately sprinkled into the excavation to fill it to be level with the surrounding sand. The idea was once the sand was saturated the sugar would dissolve leaving an open starter channel behind. Sugar was used instead of a dowel, as Townsend et al. (1981) had done, because unlike their lid, the lid in this study did not allow access to reach in and pull the dowel out. The sugar-lined starter channel is shown in Figure 3.43 (after the lid was attached but before saturation). However it was found that the sugar dissolved too quickly and the downstream end of the starter channel closed before saturation was complete.

Therefore, from test 5 onwards, the idea of a dowel was adopted after all. Except instead of reaching in to pull the dowel out, a piece of string was tied to the end of the starter dowel and fed up out of the downstream-end standpipe, allowing for dowel extraction by pulling on the string. The circular face of the dowel was placed into the excavated starter channel and the flat side of the dowel was up against the lid. The string was fed up through the standpipe as the lid was being lifted and placed into position.

Tracer particle placement

Tracer particles were placed on the sand's surface for a select number of Sydney sand tests (as listed in Table 4.3) for reasons explained and with particles described in

Figure 3.43: Sugar designed to dissolve upon saturation and leave open starter channel behind but starter channel collapsed upon dissolving (blue arrow indicates direction of flow)

Subsection 3.1.11. The tracer particles were sprinkled in 3 sets of 3 thin lines on top of the sand's screeded surface. The lines spanned almost the full width of the flume and were placed in-between lid restraint positions so that particles could be seen as they moved into the channel (instead of being hidden underneath the restraints). Multiple lines provided more opportunities to photograph newly dislodged tracer particles. Figure 3.44 shows the lines of tracer particles before the Perspex lid was placed onto test 39. In test 39 different types of tracer particles were being trialled as use of coloured sand was transitioned to Pliolite particles. The first three lines (in the photo-foreground) are a synthetic powder colourant and the next two sets of triple lines follow the order of tyre shreddings, glass beads and Pliolite.

(a) General view (b) Close-up

Figure 3.44: Tracer particles placed (ready for Test 39) in three lines between each lid reinforcing bar

3.2.5 Lid attachment

Prior to placing the lid on the flume it was cleaned with methylated spirits to ensure most sand and previously placed silicon grease was removed (with focus around the edge), as was the gasket around the top rim of the flume. Then a continuous thick line of silicon grease was smudged along the gasket between the sand and bolt holes. This served to improve the chances of an air-tight seal. When the lid was lifted and lowered into position with the engine crane, small metal ballast balls (same as those used in the inner pipe on the constant head tank) were placed in/on bolt holes so that the lid could rest on the ballast balls whilst being suspended above the flume just high enough to enable removal of lifting slings. Then the ballast balls were removed and the lid carefully lowered to rest on the soil (keeping soil disturbance to a minimum). Next, lid restraints were placed at every second bolt hole and bolts were inserted and tightened until no gaps could be seen between the gasket and lid (which were visible as light-black zones between darker-black zones where the silicon grease spread).

3.2.6 Pressure bladder inflation

With the valves open to the bladder portions requiring inflation, the bladder head tanks were filled to the required height. The default height was 5m but in some experiments the height was 2.5m or not inflated at all. Refer to Table 3.8 for a listing of what bladder pressures were used for each experiment.

3.2.7 Carbon Dioxide flushing

Carbon Dioxide (CO_2) flushing was used to improve saturation of the sand from Test 9 onwards.

With all valves into and out of the flume closed, except for the CO_2 inlet and the gas release valve in the downstream-box-lid, CO_2 was flushed through the flume at a rate of 5L/min for 5 hours. This rate and time period were somewhat arbitrary in that they were chosen to deliver a volume which would replace the void space (in the flume and within the sand) approximately 10 times to ensure full air replacement and done so slowly to keep flow laminar. A rotameter attached to the CO_2 bottle regulator was used to adjust the flow to 5L/min.

Because CO_2 is heavier than air, it would sink and replace air in voids from the base of the flume, up. Displaced air, and later excess CO_2, was released out through the valve in the downstream-box-lid and sent outside through hoses via a second rotameter. The second rotameter provided a measure of how much CO_2 was leaking from connections and the flume and so entering the laboratory (as the difference of its reading from 5L/min).

Replacing air in voids with CO_2 aided in saturation because CO_2 is more soluble in water than air. This meant that as water slowly infiltrated the voids, the CO_2 would dissolve and go into solution thereby filling all voids with water. Theoretically air would also dissolve, given enough time, but the time required for full saturation of air was impractical.

For CO_2 to reach all/most of the void spaces it was necessary for soil to be dry, otherwise water in pores could prevent CO_2 from reaching some seepage paths. Hence all soils were placed into flumes dry. Whilst a method for drying soils was developed (described in Subsection 3.4.3) this method could not be used on soils containing the fine-grained Sibelco 300g product. Therefore flushing wet unsaturated sand with CO_2 was trialled in Test 43. Whilst CO_2 was being pushed through the wet sand, the pressure pushed water from voids to the sand's surface, as pictured in Figure 3.45a (there was no free water above the sand before the CO_2 flushing). In addition a network of channels formed from the exit for a lengths around 350mm as pictured in Figure 3.45b. The channels may have formed as preferred flow paths as pore water flowed to the surface or formed not-unlike backward eroding channels under the pore pressure gradient. Regardless, the channels meant that the initiation gradient could not be determined because channels were already formed. The experiment was carried out anyway but progressed at global gradients approximately 25% lower than previous experiments.

An alternate method was trialled whereby wet sand from a previous test was left in the flume except for the top 1/4 of the flume which I removed and replaced with dry sand. This was test 44. The idea was, whilst CO_2 flushing wet sand didn't work, perhaps it would be acceptable to have only the top of the sand dry, thereby saving work/time by not having to empty the entire flume between each test. This did mean that no

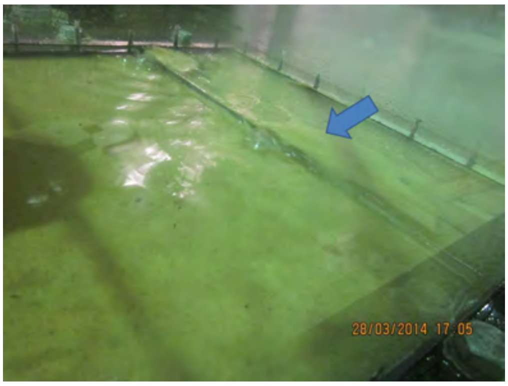

(a) Water pushed to surface by pressure imposed from CO_2 entering (there was no free water above the sand before CO_2 flushing)

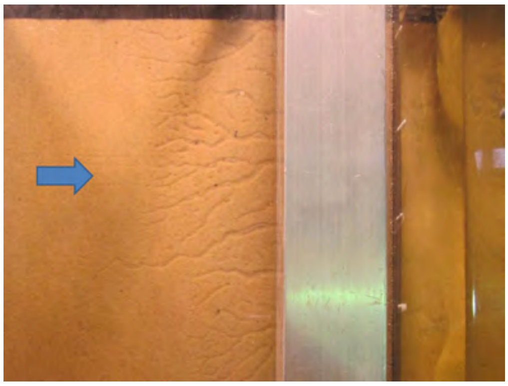

(b) Channels formed during CO_2 flushing as water pushed out by CO_2 established preferred flow paths

Figure 3.45: Trial of flushing CO_2 through wet/moist sand- Test 43 (blue arrows indicate direction of flow)

channels formed during CO_2 flushing, as was the case in Test 43, and the top sand did look consistent and saturated (no gas bubbles). However the progression gradient was found to be around 25% less than other tests (same happened in Test 43). A possible explanation for this is the lower 3/4 of the sand was less permeable than the upper 1/4 meaning that more flow was directed through the upper 1/4 and so a lower head was required to produce eroding seepage velocities. The lower 3/4 of the sand may have been less permeable because it had already been compacted in a previous test.

Given both Test 43 and 44 produced lower progression gradients than previous tests it was decided that CO_2 flushing the entire or portions of wet/moist soil was inexpedient.

It is acknowledged that dissolving CO_2 into water produces Carbonic Acid however it is considered the acid produced would be too weak and too diluted to affect the backward eroding experiments or damage the flume or connections. And indeed no corrosion was observed during the testing program.

Given that CO_2 has the capacity to displace air, using it in an enclosed laboratory posed a health and safety risk, especially given CO_2 is an odourless and colourless gas thereby offering no warning of its presence. Over exposure to CO_2 can cause symptoms ranging from shortness of breath and deep breathing (at 30 000 parts per million (ppm)) to death by asphyxiation (at 300 000 ppm).

The national exposure standards stipulate a time weighted average (TWA) limit of 5000 parts per million (ppm) and a short term exposure limit (STEL) of 30000 ppm. The TWA is the average exposure level not to be exceeded over a working day (usually 8 hours) and the STEL is the average exposure level not to be exceeded over a 15 minute period.

The CO_2 meter described in Subsection 3.1.12 was set to alarm at a concentration of 2000 ppm. If the alarm sounded the source of the leak was searched for by brushing water containing detergent on suspect leakage points (bolts, joins, connections and valves). Leaking CO_2 would reveal itself as expanding bubbles of detergent. With the CO_2 flow stopped, leaks would be sealed and CO_2 flushing recommenced.

3.2.8 Saturation

It took many trials and errors to refine the saturation process. Issues encountered included inability to control and slow the rate of infilling and the presence of air bubbles as shown in Figure 3.46. Inability to slow the rate of infilling resulted in damage to the sand sample- particularly to the slope exit and air bubbles resulted in channel tips stopping and requiring gradients higher than critical to circumnavigate the bubbles.

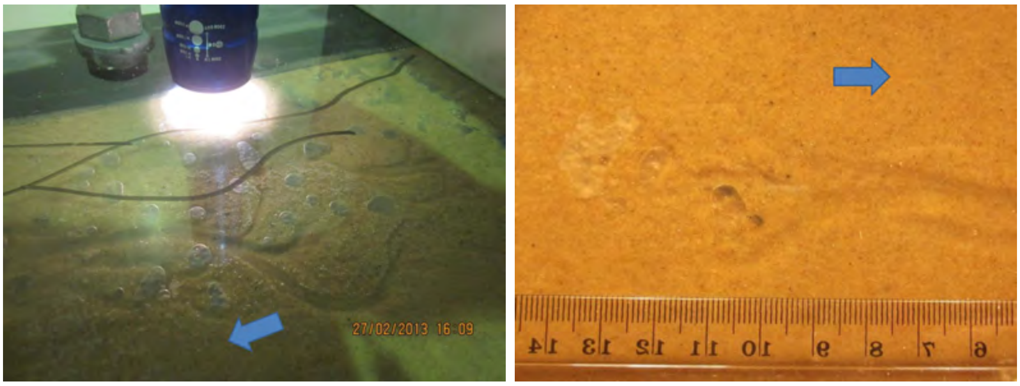

(a) Example showing density of air bubbles (b) Example of tip stopping on air bubble

Figure 3.46: Air bubbles prior to use of CO_2 (blue arrows indicate direction of flow)

As discussed previously, air bubbles were removed by flushing the sample with CO_2 prior to saturation. Once flushing was complete, the CO_2 value into the flume was closed and the gas pressure release valve in the upstream chamber was opened. This release valve allowed for release of gas from the upstream chamber as water entered the flume.

Without the upstream release valve, water would not reach the lid but stop short due to gas pressure build-up within the chamber.

The flow of water into the flume was controlled and slowed by improving the constant head tank and opening the ball-valve into the flume only a fraction. A bypass hose was also fitted, which sent some flow to the downstream chamber causing saturation from both ends of the flume, but this was later disregarded. Improvements to the constant head tank included addition of an upstream gate valve which was opened to only $^3/_4$ of a turn and addition of a bilge pump onto the base of the inner drain cylinder. With the ball-valve into the flume opened only a fraction, water inflow was reduced to just a 'trickle'. At this flow rate, approximately 12 hours was required to fill the flume (i.e. overnight). This slow flow rate was successful in minimising disturbance to the sand and resulted in full saturation (by observation- i.e. no air bubbles).

Slowing the inflow rate during saturation did prevent damage to the slope exit however, once CO_2 flushing was used, using even the slowest of inflow rates could not prevent damage to the slope. The slope still scarped and retreated as shown in Figure 3.47. This was put down to a combination of a higher degree of saturation resulting in a reduction of the sand's shear strength and the loose soil. Therefore, from Test 14, sand was compacted in by tamping, and whilst this was not ideal as it was different from the loose rained-in sand used by Townsend et al. (1981), it was necessary to keep the slope exit intact.

Saturation was complete once the downstream chamber was full or, from Test 19 onwards, once the water level in the downstream box had reached datum (the invert of the outflow ball-valve). Before testing, both the inflow and outflow ball-valves were fully opened. Full opening of the inflow ball-valve was important to prevent head loss across the valve.

3.2.9 Downstream box lid removal

For Test 19 onwards, when the flume was equipped with the downstream box, the lid of the downstream box was unscrewed and removed after saturation, prior to testing. This was done so view of the exit and eroding channel was unobstructed (condensation built up on the underside of the downstream-box-lid during saturation, making it difficult to see through).

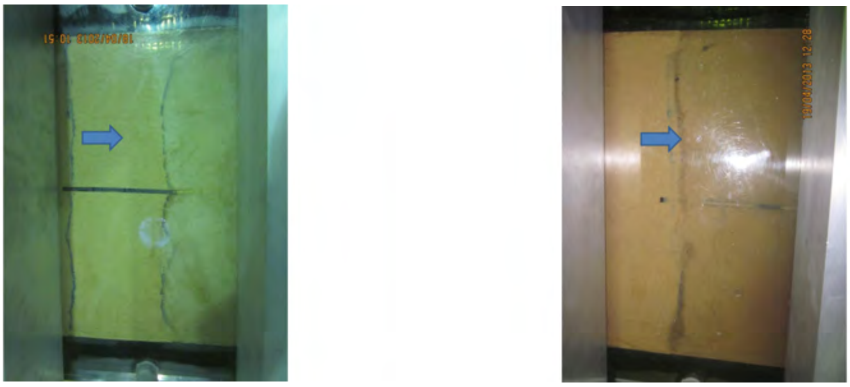

(a) Scarping

(b) Slope retreated and starter dowel pushed downstream (top of slope started in lower half of photo and dowel started further up)

Figure 3.47: Slope exit scarping and retreating during saturation due to combination of loose sand and full saturation- Test 11 (blue arrows indicate direction of flow)

3.2.10 Camera and lighting setup

The last step in setting up a test was to arrange lighting and cameras. The Canon EOS 1000D camera was set up on a tripod and positioned so that the length from the exit to the upstream edge of the soil could be seen (and the full flume width could be seen). It was advantageous to tilt the tripod legs so that the camera could be positioned as close to over the flume as possible (without the tripod tipping) so that the least degree of perspective distortion possible would affect the photos. When the open-top flume tank was used the Canon EOS 1000D camera was fixed to a metal frame built purposely to span across the tank width (the camera frame can be seen over the left-hand-side of the tank in Figure 3.11a).

The three halogen flood lights were placed along side the flume on a wooden plank (which was suspended across two besser blocks). The plank was positioned so that the lights were as close to the edge of the lid as possible. The lights were positioned to minimise shadows cast by the restraining bars: one light was placed in line with bar 1 (see Figure A.1 for a sketch denoting bar numbering convention) to illuminate the exit and between bars 1 and 2, the second light was placed in between bars 2 and 3 and the third light in line with bar 4 to illuminate between bars 3 and 4 and upstream of bar 4. The lights were also tilted down towards the lid, on a shallow angle, to reduce reflection off the lid (otherwise points of concentrated reflection would obscure details in photos).

3.2.11 Experimental program groups

Experimental set-up variables included exit geometry, soil density, seepage length, bladder pressure, soil grading and hydraulic loading sequence. These variables were categorised into 5 groups, each designed to investigate a different variable and achieve a unique project objective, as listed in Table 3.6.

Table 3.6: Experimental program groups

Group	Investigate	Objective	Variables
1	Townsend et al. (1981) results	Verify the experimental setup and procedure can reproduce the same results obtained by Townsend et al. (1981)	-
2	Exit geometry	Quantify the effect exit geometry has on the initiation and progression gradients	Slope, plane, slot, circle
3	Setup	Assess the influence changes in experimental setup has on the initiation and progression gradients	Bladder pressure Soil placement Seepage length
4	Soil	Investigate the effect soil grading has on the initiation and progression gradients	Soil grading
5	Loading	Investigate whether cyclic loading reduces the progression gradient and time effects	Cyclic & amplified loading

3.2.12 Set-up summary table

Each test used the default test configuration except for the one variable under consideration. The default test configuration was a circular exit with a seepage length of 1.3m, a bladder pressure head of 5m (50kPa) and Sydney Sand vibrated in.

Table 3.7 lists which variable was the variable under consideration for each test.

Table 3.7: Test set-ups

Group	Variable	No. of tests	Test numbers
1	same as Townsend et al. (1981)	18	1–18
2	Slope	3	33, 35, 36
	Plane	3	28, 30, 32
	Slot	6	21, 23, 25, 26, 29, 37
	Circle	7	19, 20, 22, 24, 27, 31, 34
	Group 2 total	19	
3	Bladder pressure 0m	1	42
	Bladder pressure 2.5m	5	39, 40, 66, 70, 76
	Rained (loose)	1	46
	Vibrated & tamped (dense)	1	49
	Seepage length 2.6m	2	41, 55
	Seepage length 3.9m	3	45, 65, 68
	Trial CO_2 flushing of wet sand	2	43, 44
	Group 3 total	15	
4	Mix 1	6	38, 47, 48, 54, 56, 71
	Mix 2	2	50, 61
	Mix 3	3	51, 53, 63
	Mix 4	2	52, 73
	Mix 5	2	58, 74
	Mix 6	3	59, 72, 78
	Mix 7	2	67, 69
	Mix 8	3	62, 64, 75
	50n	2	57, 60
	Group 4 total	25	
5	Cyclic loading on Sydney Sand	3	77, 79, 80
	Cyclic loading on Mix 6	2	81, 82
	Above critical loading on Sydney Sand	10	83–92
	Group 5 total	15	
	Grand total	92	

3.2.13 Set-up detailed table

Table 3.8 lists the set-up configuration for each test.

Table 3.8: Test set-ups ordered by test number

Test	Group	L	Soil	Placement	Starter channel	Exit	BP	CO_2	Loading procedure
1	1	1.3	Syd sand	Rained	Yes	Slope*	5	No	Increase only
2	1	1.3	Syd sand	Rained	Yes	Slope*	5	No	Increase only
3	1	1.3	Syd sand	Rained	Yes	Slope*	5	No	Increase only
4	1	1.3	Syd sand	Rained	Yes	Slope*	5	No	Increase only
5	1	1.3	Syd sand	Rained	Yes	Slope*	5	No	Increase only
6	1	1.3	Syd sand	Rained	Yes	Slope*	5	No	Increase only
7	1	1.3	Syd sand	Rained	Yes	Slope*	5	No	Increase only
8	1	1.3	Syd sand	Rained	Yes	Slope*	5	No	Increase only
9	1	1.3	Syd sand	Rained	Yes	Slope*	5	Yes	Increase only
10	1	1.3	Syd sand	Rained	Yes	Slope*	5	Yes	Increase only
11	1	1.3	Syd sand	Rained	Yes	Slope*	5	Yes	Increase only
12	1	1.3	Syd sand	Rained	Yes	Slope*	5	Yes	Increase only
13	1	1.3	Syd sand	Rained	Yes	Slope*	5	Yes	Increase only
14	1	1.3	Syd sand	Tamped	Yes	Slope*	5	Yes	Increase only
15	1	1.3	Syd sand	Tamped	Yes	Slope*	5	Yes	Increase only
16	1	1.3	Syd sand	Tamped	Yes	Slope*	5	Yes	Increase only
17	1	1.3	Syd sand	Tamped	Yes	Slope*	5	Yes	Increase only
18	1	1.3	Syd sand	Tamped	Yes	Slope*	5	Yes	Increase only
19	2	1.3	Syd sand	Tamped	No	Circle	5	Yes	Increase only
20	2	1.3	Syd sand	Tamped	No	Circle	5	Yes	Increase only
21	2	1.3	Syd sand	Tamped	No	Slot	5	Yes	Increase only
22	2	1.3	Syd sand	Tamped	No	Circle	5	Yes	Increase only
23	2	1.3	Syd sand	Tamped	No	Slot	5	Yes	Increase only
24	2	1.3	Syd sand	Tamped	No	Circle	5	Yes	Increase only
25	2	1.3	Syd sand	Tamped	No	Slot	5	Yes	Increase only
26	2	1.3	Syd sand	Tamped	No	Slot	5	Yes	Increase only
27	2	1.3	Syd sand	Tamped	No	Circle	5	Yes	Increase only
28	2	1.3	Syd sand	Tamped	No	Plane	5	Yes	Increase only
29	2	1.3	Syd sand	Tamped	No	Slot	5	Yes	Increase only
30	2	1.3	Syd sand	Tamped	No	Plane	5	Yes	Increase only
31	2	1.3	Syd sand	Tamped	No	Circle	5	Yes	Decrease at POI
32	2	1.3	Syd sand	Vibrated	No	Plane	5	Yes	Increase only

Table 3.8: (continued)

Test	Group	L	Soil	Placement	Starter channel	Exit	BP	CO_2	Loading procedure
33	2	1.3	Syd sand	Vibrated	No	Slope	5	Yes	Increase only
34	2	1.3	Syd sand	Vibrated	No	Circle	5	Yes	Decrease at POI
35	2	1.3	Syd sand	Vibrated	No	Slope	5	Yes	Increase only
36	2	1.3	Syd sand	Vibrated	No	Slope	5	Yes	Increase only
37	2	1.3	Syd sand	Vibrated	No	Slot	5	Yes	Decrease at POI
38	4	1.3	Mix 1	Tamped	No	Circle	5	Yes	Decrease at POI
39	3	1.3	Syd sand	Vibrated	No	Slope	2.5	Yes	Decrease at POI
40	3	1.3	Syd sand	Vibrated	No	Slot	2.5	Yes	Decrease at POI
41	3	2.6	Syd sand	Vibrated	No	Slot	5	Yes	Decrease at POI
42	3	1.3	Syd sand	Vibrated	No	Circle	0	Yes	Decrease at POI
43	3	1.3	Syd sand	Vibrated	No	Plane	5	Yes^	Decrease at POI
44	3	1.3	Syd sand	Vibrated#	No	Plane	5	Yes	Decrease at POI
45	3	3.9	Syd sand	Vibrated	No	Slot	5	Yes	Decrease at POI
46	3	1.3	Syd sand	Rained	No	Circle	5	Yes	Decrease at POI
47	4	1.3	Mix 1	Wet pluviation	No	Plane	5	No	Decrease at POI
48	4	1.3	Mix 1	Wet pluviation	No	Plane	5	No	Decrease at POI
49	3	1.3	Syd sand	Vibrated & tamped	No	Circle	5	Yes	Decrease at POI
50	4	1.3	Mix 2	Tamped	No	Circle	5	Yes	Decrease at POI
51	4	1.3	Mix 3	Tamped	No	Circle	5	Yes	Decrease at POI
52	4	1.3	Mix 4	Tamped	No	Circle	5	Yes	Decrease at POI
53	4	1.3	Mix 3	Tamped	No	Circle	5	Yes	Decrease at POI
54	4	1.3	Mix 1	Wet pluviation	No	Circle	5	No	Decrease at POI
55	3	2.6	Syd sand	Vibrated	No	Slot	5	Yes	Decrease at POI
56	4	1.3	Mix 1	Tamped	No	Circle	5	Yes	Decrease at POI
57	4	1.3	50n	Tamped	No	Circle	5	Yes	Decrease at POI
58	4	1.3	Mix 5	Tamped	No	Circle	5	Yes	Decrease at POI
59	4	1.3	Mix 6	Tamped	No	Circle	5	Yes	Decrease at POI
60	4	1.3	50n	Tamped	No	Circle	5	Yes	Decrease at POI
61	4	1.3	Mix 2	Tamped	No	Circle	5	Yes	Decrease at POI
62	4	1.3	Mix 8	Tamped	No	Circle	5	Yes	Decrease at POI
63	4	1.3	Mix 3	Tamped	No	Circle	5	Yes	Decrease at POI
64	4	1.3	Mix 8	Tamped	No	Circle	5	Yes	Decrease at POI

Table 3.8: (continued)

Test	Group	L	Soil	Placement	Starter channel	Exit	BP	CO_2	Loading procedure
65	3	3.9	Syd sand	Vibrated	No	Slot	5	Yes	Decrease at POI
66	3	1.3	Syd sand	Vibrated	No	Slope	2.5	Yes	Decrease at POI
67	4	1.3	Mix 7	Tamped	No	Circle	5	Yes	Decrease at POI
68	3	3.9	Syd sand	Vibrated	No	Slot	5	Yes	Decrease at POI
69	4	1.3	Mix 7	Tamped	No	Circle	5	Yes	Decrease at POI
70	3	1.3	Syd sand	Vibrated	No	Slope	2.5	Yes	Decrease at POI
71	4	1.3	Mix 1	Tamped	No	Circle	5	Yes	Decrease at POI
72	4	1.3	Mix 6	Tamped	No	Circle	5	Yes	Decrease at POI
73	4	1.3	Mix 4	Tamped	No	Circle	5	Yes	Decrease at POI
74	4	1.3	Mix 5	Tamped	No	Circle	5	Yes	Decrease at POI
75	4	1.3	Mix 8	Tamped	No	Circle	5	Yes	Decrease at POI
76	3	1.3	Syd sand	Vibrated	No	Slope	2.5	Yes	Decrease at POI
77	5	1.3	Syd sand	Vibrated	No	Circle	5	Yes	Cyclic
78	4	1.3	Mix 6	Tamped	No	Circle	5	Yes	Decrease at POI
79	5	1.3	Syd sand	Vibrated	No	Circle	5	Yes	Cyclic
80	5	1.3	Syd sand	Vibrated	No	Circle	5	Yes	Cyclic
81	5	1.3	Mix 6	Tamped	No	Circle	5	Yes	Cyclic
82	5	1.3	Mix 6	Tamped	No	Circle	5	Yes	Cyclic
83	5	1.3	Syd sand	Vibrated	No	Circle	5	Yes	Above critical
84	5	1.3	Syd sand	Vibrated	No	Circle	5	Yes	Above critical
85	5	1.3	Syd sand	Vibrated	No	Circle	5	Yes	Above critical
86	5	1.3	Syd sand	Vibrated	No	Circle	5	Yes	Above critical
87	5	1.3	Syd sand	Vibrated	No	Circle	5	Yes	Above critical
88	5	1.3	Syd sand	Vibrated	No	Circle	5	Yes	Above critical
89	5	1.3	Syd sand	Vibrated	No	Circle	5	Yes	Above critical
90	5	1.3	Syd sand	Vibrated	No	Circle	5	Yes	Above critical
91	5	1.3	Syd sand	Vibrated	No	Circle	5	Yes	Above critical
92	5	1.3	Syd sand	Vibrated	No	Circle	5	Yes	Above critical

L Seepage length (m)

BP Bladder Pressure (m)

POI Points of interest (defined Subsection 3.3.4)

Vibrated top 1/4 of sand (btm 3/4 had been left from previous test)

* Slope exit without downstream box on top

ˆ Flushed wet sand with CO_2

3.3 Test Procedure

3.3.1 Note taking

During experiments, notes of head levels and observations were made, with the time, on test data sheets. Observations made often included (but were not limited to):

- start of sand boiling
- particle movement seen prior to initiation
- initiation
- tip and channel location
- tip and channel size
- information on any secondary channels/tips
- flow measurements
- channel blockages
- complete progression (i.e. when the channel reached the upstream end)
- sample failure (sudden washout of channel)

All test data sheets are included in Appendix A.

3.3.2 Starter dowel extraction

When a starter dowel was used to form a starter channel (Group 1 tests from Test 5 onwards), the starter dowel required extraction before starting the test. The dowel was extracted by pulling on its string which had been fed up through the downstream-end standpipe (shown in Figure 3.48a). If the dowel came out suddenly the sudden movement would often cause sand to fall into the starter channel, so it was important to pull on the string slowly and gradually. Once the dowel was pulled out of the sand sample it was left floating in the downstream chamber where it remained during the experiment.

The starter channel left behind once the dowel was pulled out is shown in Figure 3.48b (and in Figure 3.31).

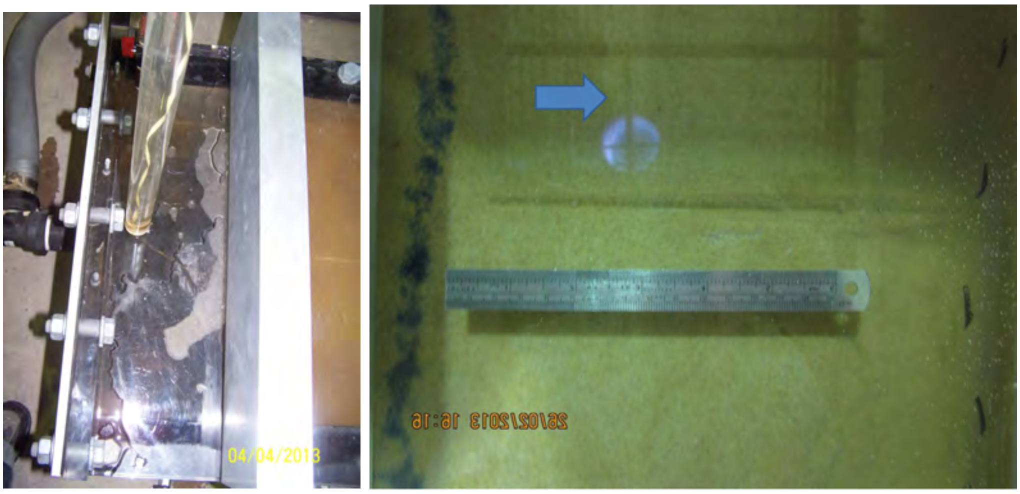

(a) String from dowel up through standpipe

(b) Starter channel left behind once dowel removed

Figure 3.48: Starter dowel extraction (blue arrow indicates direction of flow)

3.3.3 Channel initiation

At the start of a test the hydraulic head was raised in increments until initiation was observed. The increments of head increase were up to 50mm if the head was well below the expected initiation head and in smaller increments (down to 12mm) as the expected initiation head was approached. The exception to this was Group 5 tests when the start of sand boiling at the exit was measured. In these instances the head was increased in very small increments until boiling was observed (5-12mm at a time).

One revolution of the constant head tank winch equated 50mm of head increase. A head increment was maintained for at least 15 minutes before increasing, although this was subject to judgement (for example, if with experience the initiation head could be predicted with confidence then either the head was increased again without waiting for the full 15 minutes to pass or the head was increased in larger increments).

Often a small number of grains (between 5-50) would rearrange near the exit at heads approaching the initiation head. If this occurred it was noted and the full 15 minutes, if not longer, was allowed to pass before raising the head again (to make sure initiation would not start at this head given enough time). Although experience showed that initiation usually occurred as soon as the initiation head was reached.

When starter channels were used (Group 1 tests) initiation occurred from the upstream end of the starter channel. However often about 50% of the starter channel's cross-sectional area became filled in with the sand, for its entire length, before the tip began to progress.

When initiation occurred at an exit it usually did so quite clearly, i.e. it was not subject to interpretation but could easily been seen with a well defined channel (albeit short in the case of circle and slot exit tests). Often 2-3 points of initiation would develop but one channel would usually dominate and progress faster than the others.

The head, time and location of initiation was noted and often photographed.

3.3.4 Hydraulic loading procedures

There were four different procedures used to load the flume with hydraulic head difference. These procedures are referred to as 'increase only', 'decrease at points of interest', 'cyclic loading' and 'above critical loading' and are described below.

Increase only

Only increasing the head (never decreasing) so that once the channel continued to progress without need for further head increases the head was left constant until the channel reached the upstream end. This method did not provide the progression head because without reducing the head it was unknown whether the tip would continue to progress at lower heads or not. This procedure was used for Tests 1–30, 32, 33, 35 and 36.

When a tip stopped progressing (i.e. when a test had reached equilibrium), the head was not increased until waiting for at least 15 minutes. This 15-minute-delay was used to make sure the tip had indeed stopped eroding and not just significantly slowed down or momentarily stopped. This decision was made once enough tests had been observed that a judgement could be made on the length of time over which tips would not re-initiate by themselves. In coming to this judgement some experiments were left running with a stationary tip for up to 2–3 days, without the tip re-initiating on its own.

It is not intended this 15-minute time-step be representative of any time-step or delay in field scenarios. It was only chosen for this laboratory testing application because, firstly, there is no single time-step of hydraulic loading in the field which could be modelled in the laboratory. The rate and rate-of-change in hydraulic loading in field scenarios vary greatly depending on a host of hydrological, volumetric and hydraulic variables. Secondly, even if there was a single time-step of hydraulic loading in the field, it is likely it would need to be scaled appropriate to the laboratory size-scale, adding an unnecessary complication. For argument sake, these 15-minute time-steps could be considered representative of either short-term time-steps during normal seasonal fluctuations or a single flood event or they could be long-term steps between floods.

Decrease at points of interest

'Points of interest' included 25, 50, 70, 80 and 90% of the seepage length. The first point at 25% was chosen because that was often where channels from the circle exit continued to progress without need for further head increases (as seen in previous tests). 50 and 70% were chosen somewhat arbitrarily as points along the flume. 80 and 90% were chosen as points closer together as the upstream end was approached because in previous tests, it had been noticed that the rate of channel progression increased close to the upstream end, suggesting the progression head dropped substantially here. When the tip reached a point of interest the head was lowered by 25mm. If the tip continued to progress for more than 150mm the head was lowered by another 25mm. However if the tip progressed but stopped or didn't progress at all and remained stationary for more than 15 minutes, the head was raised by 12mm. The intention with this method was to determine whether the progression head remained constant or decreased with increasing channel length and in a way that was consistent and repeatable across experiments. This procedure was used for Tests 31, 34, 37 and all of Groups 3 and 4.

Cyclic loading

Once the channel had progressed 130mm the head was taken back to datum (zero head difference) and left there for at least 24 hours. Then the head was increased in small increments to measure the start of sand boiling and once boiling was observed, increased in larger increments until tip progression recommenced. The channel was then allowed to progress another 130mm after which the procedure was repeated. This method was used to model repeated loading events such as reoccurring floods. This was done to investigate whether sand boiling would start at and/or increase in size with successively lower heads as reported by Glynn and Kuszmaul (2004) and test the concern that the progression gradient decreases with repeated loading events. This procedure was used for Group 5 Tests 77 and 79–82.

Above critical loading

Above critical loading involved raising the head directly to a head higher than the critical head. The head was raised straight to the target level at the beginning of a test and maintained for the full duration of the test, until failure. Given this loading procedure was used in tests on Sydney Sand using the circle exit, the critical head was taken to be 206mm which was the average critical head from Group 2 testing on Sydney Sand in circle exits (average excluding the outlying Test 19).

Target head levels chosen were between approximately 105–180% of the critical head. The head level was raised straight to the target level by dividing the target level by 50mm and turning the winch this number of revolutions (one revolution of the winch equated to raising the inner cylinder in the constant head tank by approximately 50mm). This method rarely achieved the exact target level but given precision was not needed and all of the operator's attention was usually required at the flume at this point (give the rapid erosion usually occurring), the head was not adjusted once it reached the inner cylinder. This is why actual head levels imposed, reported in Chapter 9, are unusual percentages of critical head, such as 103.8% and 176.4% (instead of 105% and 180% as were the targets).

This loading procedure was used to investigate the effect of above critical loading. In particular, it was interest to investigate whether the rate of erosion increased with heads above critical. This loading procedure was used in Group 5 tests from Test 83 to Test 92.

3.3.5 Standpipe levels

Once standpipes had been installed on some lids, water levels within in them were recorded 3–4 times a day, particularly when a channel was directly beneath a standpipe.

Refer to Table 4.3 for a list of which tests included standpipe level measurements.

3.3.6 Photography

As mentioned previously, four different cameras were used to photograph the experiments. The Canon IXUS 105 camera was used to capture observations of interest and photos taken were noted in the test data sheet. The timer on the Canon EOS 1000D camera was set to take a photo each minute to track the location and behaviour of the eroding channel. The timer was started at the start of each test and stopped once the samples failed (washed-out).

The Casio Exilim EX-F1 camera was used to measure the speed of Pliolite particles. Close-up high resolution photos were taken at 60 frames per second (fps) with a ruler included in the photo. On average about 50 photos were taken in each set. The camera was supported by a purpose made mini-tripod and positioned over a section of the channel containing Pliolite particles travelling through it. It was necessary to record when and where the photos were taken so that the speed of flow measured could be analysed in light of the head difference and channel length at the time as well as the position along the channel measured. It was necessary to pose ready to take a set of photos and press the shutter when Pliolite particles were seen travelling under the camera lens. If Pliolite particles were not travelling through the channel it helped to knock the Perspex lid above groups of stationary Pliolite particles positioned along the channel to release some.

The Sony HandyCam DCR-SX40E video camera was used to record various events/processes such as removing starter dowels and channel blocking/unblocking. The most recorded process was the progression of the tip. If the video camera was placed on the Perspex lid, lens down, close-up video recording of the particle detachment process at the tip was possible.

3.3.7 Total flow

Total flow through the flume was measured in two ways. Initially flow was measured once for each experiment by measuring the time it took to fill a graded beaker when the head difference across the flume was 100mm. This head difference of 100mm was arbitrarily chosen but was kept as a consistent point-in-time to measure the flow so that change in permeability could be isolated from change in head difference. This measurement was taken 4–5 times (to find an average) and recorded on the test data sheet.

The other method of measuring total flow was to weigh the 60L container capturing flow leaving the flume by sitting it on a digital scale and setting up a laptop, connected to the scales, to read the weight every minute. The 60L container was fitted with a float-switch activated bilge pump so that it would empty prior to overfilling but switch off once the water level was low enough. The scales and software are described and pictured in Subsection 3.1.14.

Refer to Table 4.3 for a list of which tests the total flow was measured in by the 'beaker' and 'scales' methods.

3.3.8 Water temperature

The temperature of water in the downstream box was measured at least once every 4–5 tests. It was not needed frequently because it was found the temperature remained fairly constant until change in seasons. The water temperature was of interest in case water viscosity was needed later during the data analysis stage.

Refer to Table 4.3 for a list of the average water temperatures measured (and by inference, which tests the water temperature was measured in).

3.3.9 Sand boil size

For Group 5 tests the sand boil was collected after each 130mm long channel segment. This was done to help estimate the volume of the channel; provide insight into the proportion of primary and secondary erosion; and measure sand boil size relative to channel length. Sand boil size relative to channel length was of interest due to observations made by American authors of sand boil activity increasing with smaller successive floods along the Mississippi River (such as Glynn and Kuszmaul (2004)). Sand boil samples were oven dried and weighed for their dry-soil weight.

3.3.10 Perspex lid marking

Whiteboard markers were used to label observations on the Perspex lid such as multiple channels with letters used to identify them in test notes, locations at which the head needed to be reduced and channel outlines.

3.3.11 Channel geometry

The width of the channel was measured during experiments with a ruler placed on top of the Perspex lid. However the channel widths were not measured as often as they should have been and do not represent typical widths because were often made when a wider-than-normal channel width was observed. The depth of the channel was estimated by judging the number of particles stacked in the channel side walls, however these judgements were subjective with large ranges. Therefore there weren't many channel widths and depths measured/estimated using these methods and more accurate methods were used post-experiment, discussed in Subsection 3.4.2.

Refer to Table 4.3 for a list of which tests the channel width was measured in by the 'ruler on lid' method and the channel depth by the 'depth by sight' method.

3.3.12 Forward deepening and failure

During forward deepening (explained in Subsection 4.3.4) the hydraulic head was kept constant at the head applied when the channel tip reached the upstream end until the forward deepening reached the downstream end and the sampled failed (washed-out). Although not all tests were left running to forward deepen for a number of reasons such as timing, desaturation and bio-clogging. Forward deepening was investigated from Test 19 onwards, refer to Table 4.3 for a listing of which tests were left to forward deepen.

Once the sample had failed (channel washed-out) the test was ended by closing the valve into the constant head (to stop water flow). Refer to Subsection 4.3.5 for an explanation of what 'failure' entailed.

3.4 Post test activities

3.4.1 Test disassemble

Tests were disassembled by firstly deflating the pressure bladder, then removing the lid and emptying the soil. It was important to deflate the bladder before attempting to undo the lid bolts, otherwise the lid would bow from the stress of the bladder without restraint from bolts and bars. Water could be partly drained from the flume by lowering the inner pipe in the constant head tank to as low possible and keeping the inner bilge pump on. However the flume inlet was not low enough to drain it all, so remaining water was pumped out with a portable bilge pump.

Soil was then dug out from the flume and either moved to the sand drying bays or disposed of (if it contained the fine grained Sibelco 300g product). Care was needed to not puncture the pressure bladder with the shovel.

As mentioned previously, removing only the top 1/4 of the sand and leaving the lower 3/4 of sand in place, wet, for the next test was tried (thereby saving time and effort in emptying the entire flume) (Test 44). However the progression gradient was found to be around 25% less than other tests therefore emptying only a portion of the soil was considered unsuitable (refer to Subsection 3.2.7 for more information).

3.4.2 Channel geometry

Channel width

Channel widths were measured post-test using photos which included a ruler. This involved drawing rectangles across the channel and using the ruler in the photo to measure their widths. In some instances, when the photos used were photos taken by the Casio Exilim EX-F1 camera, successive frames showed sediment transport along a 'corridor' which was less wide than the width of the disturbed zone. In this scenario the channel width was taken to be the full width of the disturbed zone, an example of which is shown in Figure 3.49. This was because it was likely to be the full width of the disturbed zone which influenced flow speed through the channel. However it is noteworthy that mobilised bed load did not always occur across the full width of the channel.

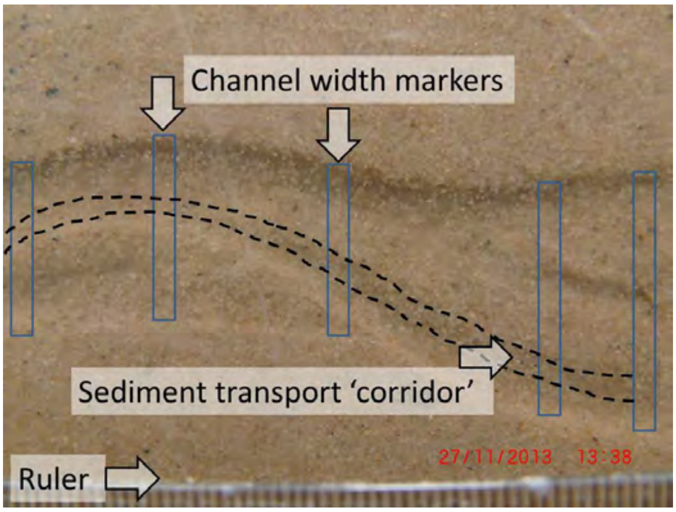

Figure 3.49: Example of using photo to measure channel width

Refer to Table 4.3 for a list of which tests the channel width was measured in by the 'ruler in photo' method.

Channel depth

Channel depths were measured/estimated post-test using wax moulds, a caliper and sand boil weights.

Wax was melted and poured into a standpipe hole (once the standpipe was pulled out) to fill a portion of the channel (a standpipe hole that had the channel erode beneath it). The idea was that once the Perspex lid was removed, the wax would have set to the shape of the channel providing a mould which could be measured with more accuracy. However the wax was too viscous to allow air to pass out as wax flowed in, so the wax didn't flow further than the standpipe hole. Therefore the Perspex lid was removed and the wax simply poured into the channel. This was less ideal as the depth of the wax was less representative of the channel depth without the lid containing it. So as an alternative, restraining bars were placed over the channel and wax was poured into the channel where it would flow beneath the bar, as shown in Figure 3.50a. This way the restraining bar would provide a top boundary instead of the lid. In some instances, where wax had been able to flow over the top of the sand, the depth of the channel could be measured with more accuracy by deducting the depth of the overflow from the total mould depth (example in Figure 3.50b). A caliper was used to measure the depth and width of the wax mould.

The caliper was also used to measure the channel as it was (without wax), however this was difficult given the light-touch needed to extend the caliper stem to the bed of the channel without 'under or over shooting' it (Figure 3.50c).

(a) Poured wax into channel under restraining bar (b) Wax mould of channel (c) Measuring channel with caliper

Figure 3.50: Measuring depth of channel

Refer to Table 4.3 for a list of which tests the channel depth was measured in by the 'caliper + wax' method.

As was outlined in Subsection 3.3.9, sand boils were collected after every 130mm channel segment in the cyclic tests of Group 5 and dried and weighed. The depth of the first channel segment was estimated by first trialling depths from 1 to 5mm then, knowing the channel segment length and assuming a rectangular cross-section, calculated channel widths necessary to contain the volume of sand contained within the first boil. The range of channel depths which gave sensible channel widths became the estimated depths.

3.4.3 Soil drying

It was necessary to dry soil between tests for reasons explained in Subsection 3.1.16. To do so, soil was excavated out of the flume and wheelbarrowed to the sand drying bays where soil was shovelled onto the perforated plates from the back corner and filled towards the front. The thickness of soil placed on the plates was limited by the weight the suspended plates could support (and not the drying process because it dried from underneath and dropped out once dry revealing more wet sand). The plates could support a layer up to approximately 200mm thick. It was advantageous to 'toss' soil onto the bays loosely with an irregular surface, without packing the soils surface, to encourage heat to pass through the layer. An example of sand placed on the drying bays is shown in Figure 3.34a (along with an inquisitive Water Dragon).

A full flumes-worth of sand was dried over two plates (i.e. an area of 1.2 by 4.8m) in under 48 hours.

3.4.4 Soil density measurement

Three different methods were used to measure the density of the soil, the 'can', 'total sand' and 'push tubes' methods. These are described below.

Refer to Table 4.3 for a list of which tests were measured for soil density and by which method.

Use of a nuclear densometer was also investigated but not used for reasons discussed below.

Volumetric

The 'volumetric' method involved placing a tin can into a partially filled flume and continuing to rain sand into the flume. The can would theoretically be filled with sand to the same density as the rest of the flume. The can was then removed from the flume, the top screeded off for a flat, level surface of sand and weighed. This gave the weight of the dry sand, which when divided by the volume the can contains, would give the density of the soil. The can volume was determined from the weigh of water it could contain (and adjusting water density for the measured temperature).

This method was not used past Test 12 because it was eventually found that results were unreliable.

Total sand

The 'total sand' method involved weighing all the sand once it had been dug out of the flume and dried. Whilst the sand drying bays almost completely dried the sand, the moisture content was still measured and corrected for (from 3 small, random samples). The weight of dry sand was then divided by the volume of the flume to obtain the dry density. The volume of the flume was calculated using flume dimensions. Strictly speaking the volume the pressure bladder expanded by should have been deducted from the flume volume however it was not for two reasons, 1) whilst an estimate of how much the bladder expanded by could be made (by opening its tap when the bladder tank was full and noting how much the water level in the tank dropped, thereby ascertaining how much volume of water entered the bladder) it was not accurate and 2) deducting the bladder volume would have increased the soil densities calculated when they were already too high (as explained in Section 4.8).

Push tubes

The 'push tubes' method involved pushing purpose-built tubes (described in Subsection 3.1.15) into the sand (once the flume lid had been removed). The hollow tubes were buried into the sand so that the top rim of the tube was a few millimetres below the surface. Then sand adjacent to the tube was dug out to below the base of the tube to enable the thin 'L' shaped piece of galvanised iron to be lowered down next to the tube and pushed into the sand below it. This way the tube could be lifted out from beneath it (to prevent sand within the tube falling out). Sand at both ends of the tube were screeded off to leave flat, level surfaces and any sand stuck to the outside of the tube was brushed off. The tubes were then placed into a soil oven to dry the soil before weighing it. The dry-soil weight was then divided by the volume each tube contained to obtain the soil's dry density. The volume each tube contained was calculated from each tube's dimensions measured carefully with a caliper. Whilst every effort went into fabricating the push tubes to be consistent in sizing, there were small variations.

Nuclear densometer

Using a nuclear densometer to determine soil densities was investigated but not used. It was not used because, to do so, the bladder and lid would need to have been deflated/removed thereby increasing the soil density from what it would have been during testing. Additionally, it is likely the nuclear signal would have bounced-off and been distorted by the neighbouring flume walls/base resulting in inaccurate readings.

3.4.5 Permeability

Four different methods were used to determine the permeability of the soil. They included:

1. Use of the flow rate measured by the beaker (as described in Subsection 3.3.7) and Darcy's law:

   $$k = \frac{QL}{HA} \tag{3.1}$$

   where k = coefficient of permeability

   H = global head difference

   L = seepage length of 1.3m

   A = cross-sectional area of flume of 0.31 x 0.45m

   Refer to Table 4.3 for a list of which tests the 'beaker' method was used in to measure permeability.

2. Use of the flow rate measured by the electronic scales (as described in Subsection 3.3.7) and Darcy's Law as $v = ki$. The Darcy velocity as plotted with global hydraulic gradient and the slope of the line-of-best-fit was taken to be the coefficient of permeability (example of which is shown in Figure 3.51). Because the "apparent permeability" increased with increasing channel length (discussed in Section 4.9)

it was important to only use flow data during the initial stages of the test before the channel was long enough to affect permeability. Refer to Table 4.3 for a list of which tests the 'scales' method was used in to measure permeability.

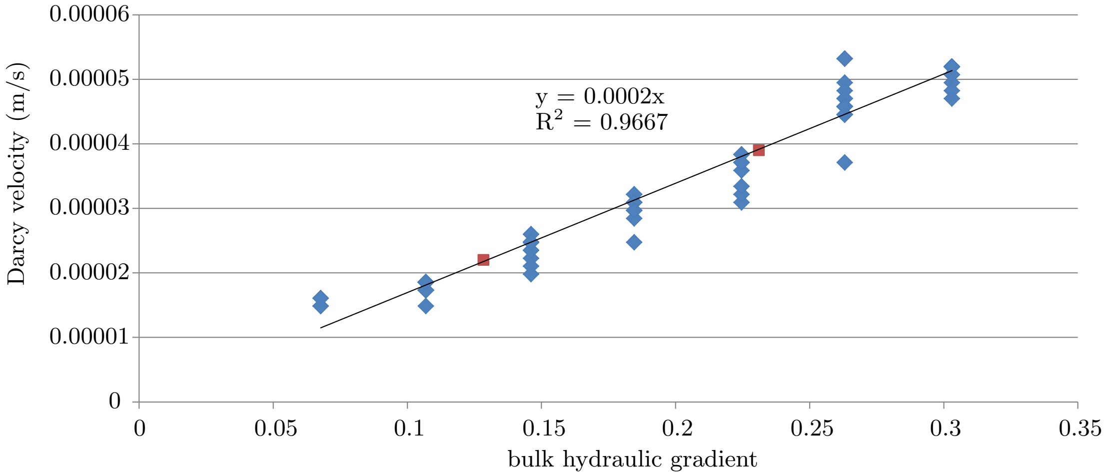

Figure 3.51: Example of how scale data was used to calculate coefficient of permeability

3. Use of the flow rate measured by the electronic scales, Darcy's Law and levels in standpipes. It was assumed that the total flow was also the flow moving between two rows of standpipes (by continuity of flow) so that in Equation 3.1:

   H = difference in head between two standpipes; and

   L = length between two standpipes of 0.302m

   Because the channel altered levels in standpipes it passed under, it was important to only use standpipe levels prior to a channel existing or at least levels of standpipes a reasonable distance away from the channel. Refer to Table 4.3 for a list of which tests the 'scales + standpipes' method was used in to measure permeability.

4. Sending soil samples to a NATA accredited soils laboratory for permeability testing. Sydney sand was tested for permeability using the constant head permeability test to AS1289 6.7.1 at both its minimum and maximum densities (to gauge the range of permeability values possible). Mixes 4, 5 and 8 were tested using the falling head permeability test to AS1289 6.7.2. Mix 4 was also tested at both its minimum and maximum densities but Mixes 5 and 8 were only tested at their maximum densities. Mixes 5 and 8 were chosen for testing because they were the most and least permeable soils used where as Mix 4 was chosen (and tested at both its maximum and minimum densities) because it had the largest coefficient of

uniformity. The remaining soils (Sibelco 50n and Mixes 1–3, 6 & 7) were not tested by the soils laboratory.

Another possible method to determine the soil's permeability could have been to measure the soil's void ratio and relate it to permeability with use of the Kozeny-Carman equation (Ren et al., 2016) whereby:

$$k = C_F \frac{1}{S_p^2} \frac{\gamma_w}{\mu \rho_p^2} \frac{e^3}{1+e} \tag{3.2}$$

where k = coefficient of permeability (m/s)

C_F = dimensionless shape constant (≈ 0.2)

S_p = specific surface area of particles (m^2/g)

γ_w = unit weight of fluid N/m^3)

μ = fluid viscosity (Ns/m^2)

ρ_p = particle density of soil (kg/m^3)

e = void ratio of soil

However, it was not possible to measure the soil's void ratio at the density it was tested at (whilst inside the test flume). The best that could be achieved was to measure void ratio once the Perspex lid was removed (with push-tubes, as discussed in the previous section, Subsection 3.4.4). With the Perspex lid removed (and pressure bladder deflated- which had to be done to remove the lid), soil partially rebounded to a greater void ratio. Therefore, if Equation 3.2 had of been used to determine permeability with void ratios measured using the push-tubes, permeabilities greater than the soil permeability during testing would have been returned.

3.4.6 Photo processing

After each experiment photos were used to make a time-lapse video, document observations, measure the speed of flow through the channel and closely observe processes of interest.

Photos taken with the Canon EOS 1000D camera were used to make a time-lapse video of the entire experiment. Firstly the freeware graphic viewer 'Irfanview' was used to label each photo with the date and time of the photo as well as the test number and file name.

This could be done as a batch process labelling all photos from an experiment in a matter of minutes. Then ‘Windows Movie Maker’ (version 2012) was used to compile the photos into a time-lapse video, usually showing each photo for 0.01 seconds and compressing a 2-day test into 2 minutes (in the order of).

Photos taken with the Canon IXUS 105 camera were used to document observations of interest in test reports. Test reports are explained in the next section, Subsection 3.4.7.

Photos taken with the Casio Exilim EX-F1 camera were used to measure the speed of flow through the channel. Firstly the freeware graphic viewer ‘Irfanview’ was used to label each photo with the file name (to distinguish photos and check for correct order). Then photos were inserted into a Microsoft PowerPoint presentation, one photo per slide, so the time-line of photos could be advanced through quickly/easily and so lines could be drawn over the photos marking pliolite positions (and copy and pasted onto subsequent photos indicating the position in previous frames).

Figure 3.52 is an example of a high-speed photo. The channel runs through the centre of the photo, at a slight angle, with the flow-direction down the photo. Each coloured line marks the position of a particular Pliolite particle in previous frames. The last line of each colour is on the Pliolite particle. The particles are also pointed to by corresponding coloured arrows and may be seen, with difficulty, as a blurred, short, white line. White dots around the photo are stationary Pliolite particles. The ruler (shown along the left of the photo) is used to measure the distance between lines. As there are 60 frames per second, there must be 0.0167s between frames and so the average distance between lines gives a Pliolite speed (examples of speed calculations are shown in Figure 3.52). This method, tracking the distance of particular particles between known time intervals, is known as ‘Particle tracking velocimetry’.

It is recognised that the speed of a Pliolite particle will depend on where the particle is relative to the channel boundary and lid because there would be a parabolic distribution of velocity due to laminar flow in a viscous fluid. However by considering the speed of many Pliolite particles a range of velocities can be seen with the fastest likely to be moving through the centre of the channel.

Refer to Table 4.3 for a list of which tests high-speed photos were taken in, including

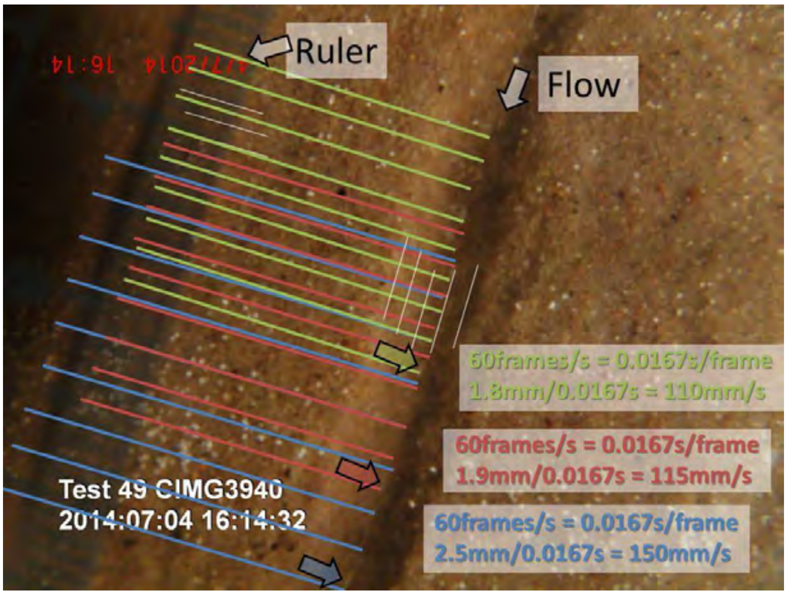

Figure 3.52: Example of high-speed photo processed for Pliolite particle speed

mention of the tracer particles used. Also note that no Pliolite speeds have been reported in this thesis. Some photos were analysed for Pliolite speeds to compare speeds with those measured by coloured-sand particles, thereby verifying the suitability of Pliolite use. However, most photos were not analysed due to the numerical model not having been developed to the stage where flow through the channel could be compared and calibrated. In other words, channel flow estimates were not required in the end but are available for subsequent studies.

3.4.7 Data analysis & reporting

After each experiment a report was written documenting the key results and any noteworthy observations, often with photos. The report provided a succinct summary of the experiment without having to re-interpret and analyse the test data sheet.

Reports often included two key graphs. The first being a scatter plot of head difference and channel length with time, an example of which is shown in Figure 3.53. This graph showed the hydraulic loading procedure used as well as the tip progression over time. The slope of the channel length line provided the tip progression speed. The other graph was the channel length against global head difference, often plotted with results from other experiments in order to show the relationship being investigated, an example of which is shown in Figure 3.54. To plot these graphs it was necessary to input results into a Microsoft Excel spreadsheet, an example of which is shown in Figure 3.55. Some additional data points were added to the plots where they included sloped (instead of stepped) lines. A sloped line would have suggested the head was increasing whilst the tip was progressing, but this was not the case, head increase was relatively instantaneous. These additional data points contained the previous head but the proceeding time and channel length to show the tip progressed at a constant head.

Another graph which was often included in the test report was the critical gradient with coefficient of uniformity to progressively test the relationship of the two suggested by Schmertmann (2000).

Test reports are included in Appendix A.

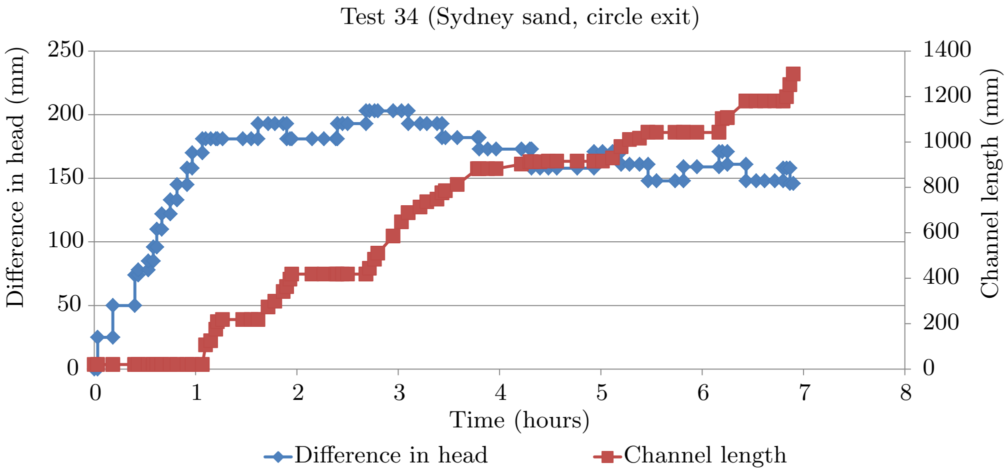

Figure 3.53: Example of head difference and channel length with time graph

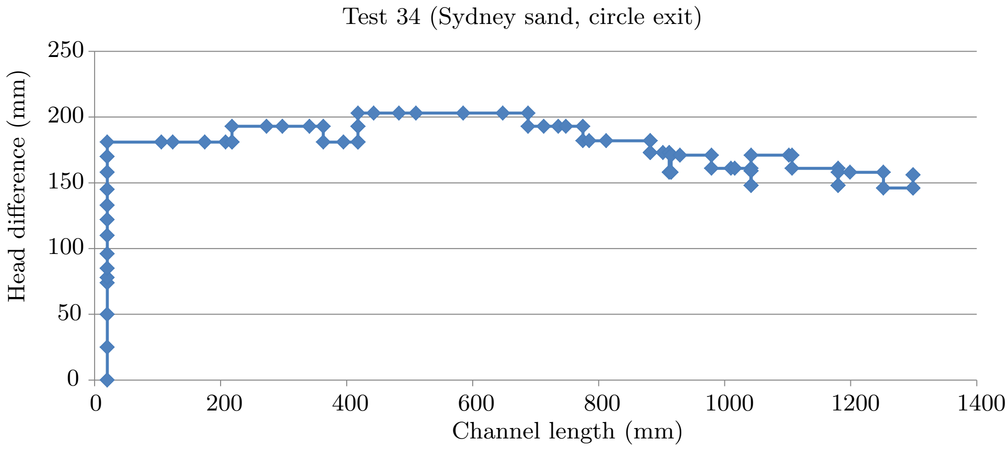

Figure 3.54: Example of channel length with head difference graph

Flume	4
Exit	circle

			Tip position		
Head (mm)	Date/Time	Time (hours)	mm	position	channel length (mm)
0	17/01/2014 10:53		20	ae	20
25	17/01/2014 10:55	0.03	20	ae	20
50	17/01/2014 11:04	0.18	20	ae	20
74	17/01/2014 11:17	0.40	20	ae	20
78	17/01/2014 11:19	0.43	20	ae	20
85	17/01/2014 11:25	0.53	20	ae	20
96	17/01/2014 11:28	0.58	20	ae	20
110	17/01/2014 11:30	0.62	20	ae	20
122	17/01/2014 11:33	0.67	20	ae	20
133	17/01/2014 11:38	0.75	20	ae	20
145	17/01/2014 11:42	0.82	20	ae	20
158	17/01/2014 11:48	0.92	20	ae	20
170	17/01/2014 11:51	0.97	20	ae	20
181	17/01/2014 11:57	1.07	20	ae	20
181	17/01/2014 11:59	1.10	106	ae	106
181	17/01/2014 12:02	1.15	124	ae	124
181	17/01/2014 12:05	1.20	175	ae	175
181	17/01/2014 12:06	1.22	208	ae	208
181	17/01/2014 12:09	1.27	218	ae	218
181	17/01/2014 12:21	1.47	218	ae	218
181	17/01/2014 12:26	1.55	218	ae	218
193	17/01/2014 12:30	1.62	218	ae	218
193	17/01/2014 12:36	1.72	15	ab1	273
193	17/01/2014 12:40	1.78	40	ab1	298
193	17/01/2014 12:45	1.87	83	ab1	341
181	17/01/2014 12:47	1.90	105	ab1	363
181	17/01/2014 12:49	1.93	137	ab1	395
181	17/01/2014 12:50	1.95	160	ab1	418
181	17/01/2014 13:02	2.15	160	ab1	418
181	17/01/2014 13:09	2.27	160	ab1	418
181	17/01/2014 13:16	2.38	160	ab1	418
193	17/01/2014 13:17	2.40	160	ab1	418
193	17/01/2014 13:20	2.45	160	ab1	418
193	17/01/2014 13:23	2.50	160	ab1	418
203	17/01/2014 13:34	2.68	160	ab1	418
203	17/01/2014 13:36	2.72	185	ab1	443
203	17/01/2014 13:39	2.77	225	ab1	483
203	17/01/2014 13:41	2.80	252	ab1	510
203	17/01/2014 13:50	2.95	25	ab2	585
203	17/01/2014 13:55	3.03	88	ab2	648
193	17/01/2014 13:59	3.10	128	ab2	688
193	17/01/2014 14:06	3.22	153	ab2	713
193	17/01/2014 14:10	3.28	176	ab2	736
193	17/01/2014 14:16	3.38	188	ab2	748
182	17/01/2014 14:19	3.43	215	ab2	775

Figure 3.55: Example of results speadsheet (position acronyms defined in Appendix A)

Chapter 4

Experimental Observations

4.1 Introduction

This chapter describes experimental observations which were common to all tests, i.e. they were not unique to a particular experimental group. These observations include the universal behaviour of backward erosion as well as measurements of a particular attribute, such as soil density, across all experiments. Towards the end of the chapter, Table 4.3 is given which lists key observations and measurements made in each test. Experimental *results* are presented in terms of the initiation and critical heads/gradients at the end of this chapter, listed in Table 4.4.

Note that hydraulic loading is referred to through-out this and the next 5 chapters as the hydraulic 'head', not 'gradient', because it is the head that is varied in experiments, whilst the seepage length is kept constant. The exception to this is Subsection 7.2.3 which does refer to the gradient because the seepage length was varied. Other chapters will refer to the hydraulic loading as the hydraulic 'gradient'. This distinction will be made in their respective introductions.

4.2 Experimental program

A total of 92 experiments were carried out across five distinct focus groups, as listed in Table 3.7. The first experiment was carried out on the 14th December 2012 and the last on the 6th April 2016. The majority of experiments were carried out by the current author, however some were carried out by a laboratory assistant, Hamish Studholme; an honours student, Bronson Forward; and another honours student, Angela Greenlees (who carried out the last 10 experiments). Test data sheets and reports can be found in Appendix A.

4.3 Backward Erosion Piping stages

Observations of the backward erosion process can be grouped into 5 stages- boiling, tip progression, equilibrium, forward deepening and failure. These stages are shaded over an idealised test plot of head difference and tip position with time in Figure 4.1. They are also described below.

These observed stages are consistent with those observed by other studies and are similar to those reported by van Beek et al. (2011a).

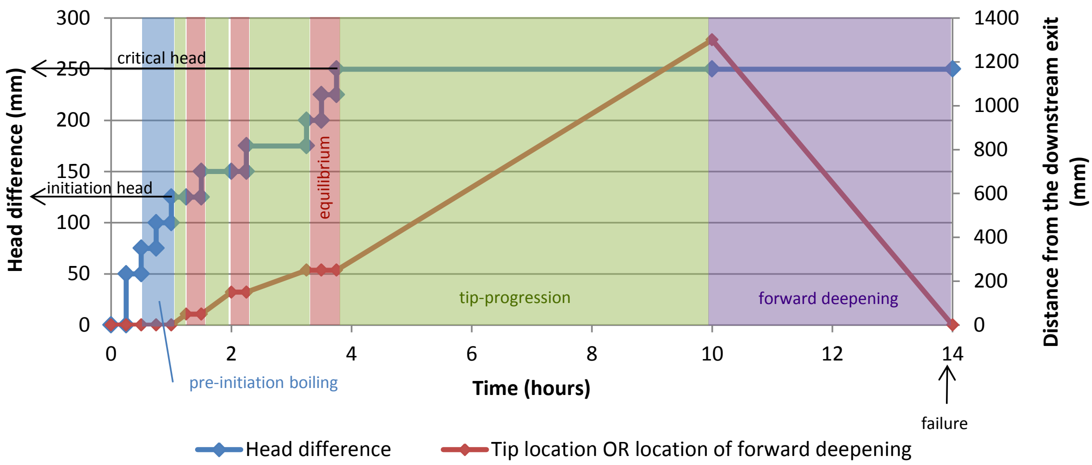

Figure 4.1: Idealised experimental result in a circle exit showing the stages of backward erosion piping and initiation and critical heads

4.3.1 Boiling

The first sign of movement in an experiment was small boils of fluidised sand at the exit in which particles would continually rise (slightly) and fall. This would occur when the local pore pressure became equal to the effective stress. These boils were usually semi-circular in shape with a diameter of about 10–20 particles. It would occur at exits of all geometries except the slope geometry and often occur at 2–3 locations simultaneously.

Figure 4.2 contains photos of these small boils. These boils were referred to as 'pre-initiation boils' to distinguish them from larger boils which accumulated after initiation during tip progression. Figure 4.2b of pre-initiation boils in the slot exit show them on the downstream edge of the slot. This is because the pre-initiation boils would form on both sides of the slot exit and this photo was taken after initiation, once a channel had formed. Prior to initiation there would have been pre-initiation boils on the upstream edge of the slot as well. In fact channels initiated from one of the upstream pre-initiation boils. This was also the case for plane and circle exits, channels started at these pre-initiation boils.

What can also be seen in Figure 4.2b is a strip of raised sand along the downstream edge. Perhaps this is the group of particles which require uplifting in order to initiate backward erosion as suggested by van Beek et al. (2014b) (a group approximately 20 particles wide as a minimum).

In cases where there was a small gap between the lid/exit and the soil (like the sketch in Figure 6.11a), pre-initiation boils did not occur. Boiling only began once a channel had initiated and transported enough soil to fill the gap. Test 79 was an example of this photographed in Figure 9.3b and graphed in Figure 9.1.

Pre-initiation boiling was less apparent in well-graded soils. This may be because they did not occur, or because they were just more difficult to see on account of fine material becoming suspended. Figure 4.2d is evidence of pre-initiation boiling in more well-graded soils by way of a plume of Sibelco 300g prior to initiation.

Whilst the head difference required to cause pre-initiation boiling was not recorded in Group 3 tests (varying exit geometries), it was evident that the more an exit geometry concentrated the flow, the lower the required head difference was to cause pre-initiation

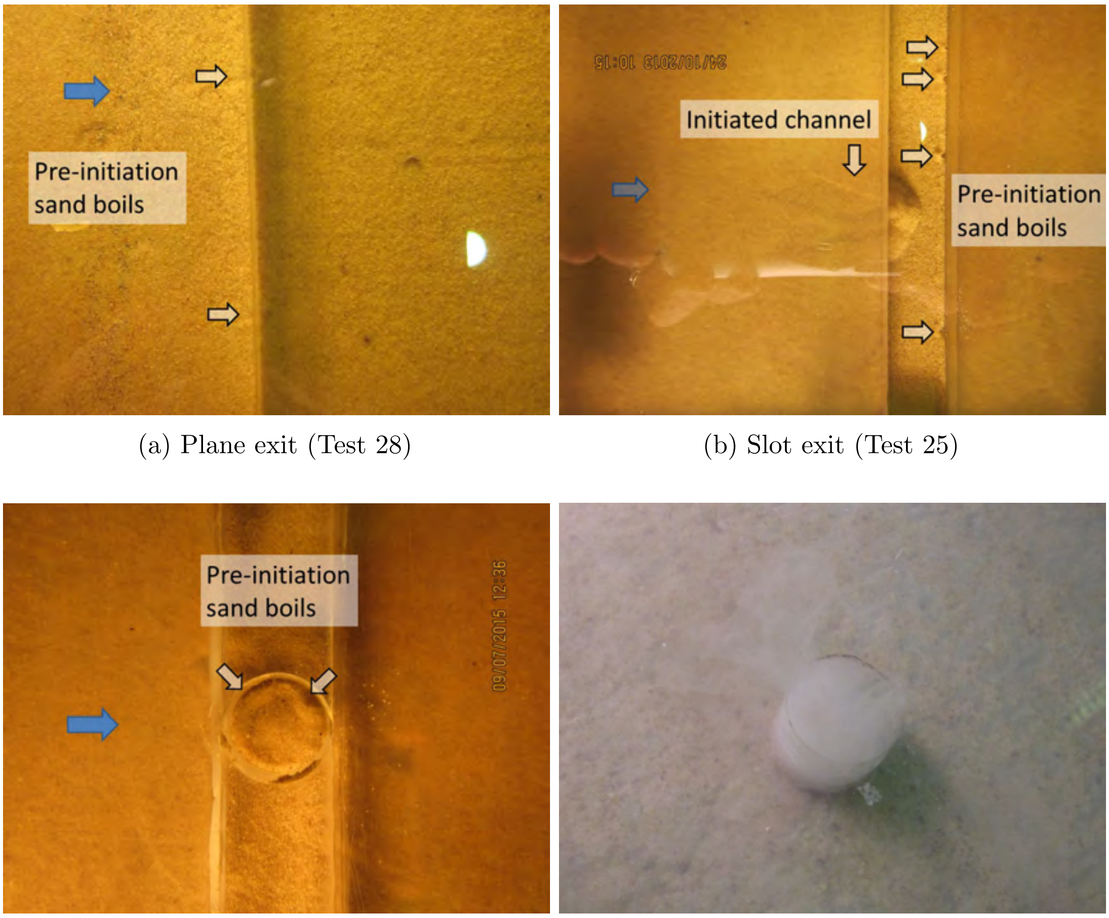

(a) Plane exit (Test 28)

(b) Slot exit (Test 25)

(c) Circle exit (Test 79)

(d) Possible boil indicated by plume of Sibelco 300g (Test 38)

Figure 4.2: Pre-initiation boils (blue arrows indicate direction of flow)

boiling.

The head difference required to cause pre-initiation boiling was recorded in Group 5 cyclic tests. Test 80 began boiling at a head of 8mm but didn't initiate until a head of 177mm (see Figure 9.1) and Test 81 began boiling at a head of 84mm but initiated at 314mm (see Figure 9.2).

Boiling at the exit was also the first movement observed when an experiment was being continued on subsequent days, when a channel was already present. If the head was raised in very small increments, boiling was seen at the channel exit before any other movement in the channel. The head difference at which this first boiling occurred remained fairly constant throughout the test, as discussed and graphed in Subsection 9.2.1.

Boiling at the exit continued throughout the experiment during all stages of the backward eroding process. Discussion on boiling during later stages can be found in Section 4.6.

4.3.2 Tip progression

With further increases in head the 'initiation head' was reached, marked by the onset of particles leaving the sand matrix at the exit. The leaving of particles exposes new particles to seepage forces without restraint and so they too were detached and transported out, resulting in formation of a channel. This process continually repeated causing the channel tip to progress toward the upstream end. With sufficient seepage forces, eventually the tip reached the upstream end. Therefore the 'tip progression' stage started at initiation and completed once the tip reached the upstream end.

The tip progressed when soil eroded from the tip (primary erosion). Particle detachment from the tip was observed as starting with a group of grains, about 5–10 particles upstream of the tip, rearranging themselves into downstream void spaces. Moments later a group of particles, approximately between 10–50 grains, would suddenly slide/slip downstream into the channel together. These grains would then be transported away along the channel as bed load. The tip would then remain stationary for a time until the process repeated. In this way the tip would progress in a stop-start, intermittent fashion. Primary erosion is elaborated on in Subsection 4.5.2.

During tip progression the channel would meander and sometimes widen, block and unblock. These behaviours are discussed in Subsections 4.5.3 and 4.5.4. Also during tip progression, flow through the flume increased, this is discussed in Section 4.9.

4.3.3 Equilibrium

In some instances the tip stopped progressing, this was referred to as the equilibrium stage. Whilst in equilibrium there may have still been transport of particles through the channel and out the exit and channel meandering, but the channel length remained fairly constant and the tip stayed in the same position indefinitely.

With sufficient increase in head, equilibrium could be overcome and tip progression re-initiated. From there the tip either continued to progress through to the upstream end or it progressed for a short distance before reverting back to equilibrium, possibly many times before the ‘critical head’ was reached.

Equilibrium did not always occur. In fact, equilibrium was less likely to occur in tests on slope and plane exit geometries as evident by the lack of ‘steps’ in the results plotted in Figure 6.12. In contrast, the circle geometry caused equilibrium often.

When equilibrium did occur, the head was kept constant for at least 15 minutes, before raising. This 15-minute-delay was used to make sure the tip had indeed stopped eroding and not just significantly slowed down or momentarily stopped. The basis for choosing 15 minutes is discussed in Subsection 3.3.4 on hydraulic loading procedures.

There were instances when the channel would become blocked when the tip stopped. Of the 20 instances of the channel blocking and needing an increase in head to re-initiate the tip, 12 of those saw the tip stopping and the blocking occur practically at the same time (refer to Figure 4.19). It’s not clear whether it was the tip stopping that caused the blocking or the blocking that caused the tip to stop, but regardless, there did appear to be an interaction between the two.

4.3.4 Forward deepening

Once the tip reached the upstream end, the ‘forward deepening’ stage began. Forward deepening is the deepening (and widening) of the channel in a forward direction, i.e. the same direction as the flow. When the channel reached the upstream end it became ‘connected’ to the higher upstream head which pushed into the channel and enlarged it. However, this sudden enlarging of the channel resulted in sediment being pushed into the regular channel causing a blockage between the regular channel and the deepened channel (shown in Figure 4.3b). Yet as backward erosion continued in the regular portion of the channel, sediment from the blockage was removed and transported downstream. This occurred until enough of the blockage was removed that it slipped from the pressure of the upstream head, which allowed more of the channel to be enlarged but also resulted in a new blockage. This process repeated until the enlarged channel reached the downstream end.

As the forward deepening process enlarged the channel it would typically remove/reduce its meandering shape and somewhat straighten. However scouring and meandering continued (and often increased) in the regular downstream portion of the channel. Figure 4.3 shows examples of the forward deepening process.

During forward deepening the hydraulic head was kept constant at the head applied when the channel tip reached the upstream end. This head was nearly always sufficient enough to drive the forward deepening process to completion (i.e. to drive the forward deepening to the downstream end). It is not known whether forward deepening could have continued at lower heads as this was not tested. Once forward deepening reached the downstream end, failure (i.e. washout) of the sample was imminent. Failure is discussed in the next section.

Forward deepening was first observed in Test 7 and then again in Test 19 when the test was left running overnight. However, the tests were terminated before the forward deepening completed as it was not yet realised that its completion would lead to sample failure. However Test 21 was left running long enough for failure to occur which was unintentional and unexpected. From Test 21 onwards most tests were left running to observe and time how long forward deepening would take to complete and lead to failure. Table 4.3 lists which tests were left to forward deepen and fail.

When forward deepening occurred beneath standpipes, levels would quickly rise to heads similar to the upstream head thereby supporting the explanation offered above that the channel became exposed to the higher upstream head when it reached the upstream end. Unfortunately there are no recorded standpipes levels which document this observation as standpipes levels were usually only taken during the tip progression stage. There is however a set of photos, shown in Figure 4.29.

Total flow measured by the digital scales showed that flow through the flume increased slightly during forward deepening even with the head kept constant. This slight flow increase was likely due to the deepened channel increasing the effective bulk permeability of the sample. This is discussed further in Section 4.9.

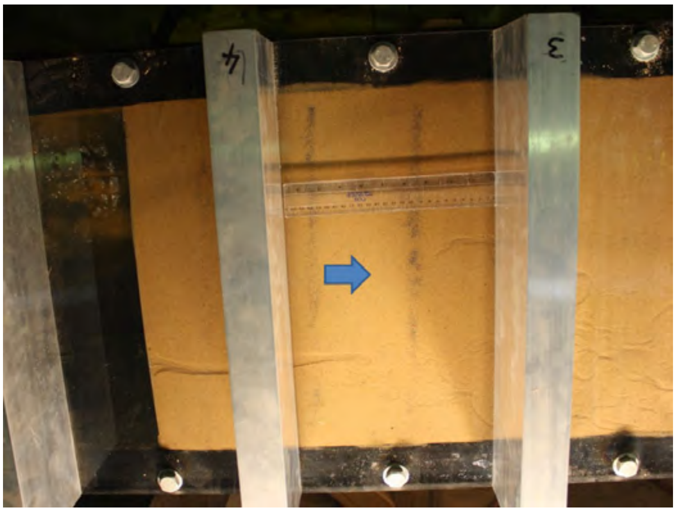

(a) Forward deepening approaching midway between bars 3 and 4 (Test 33 in Sydney Sand)

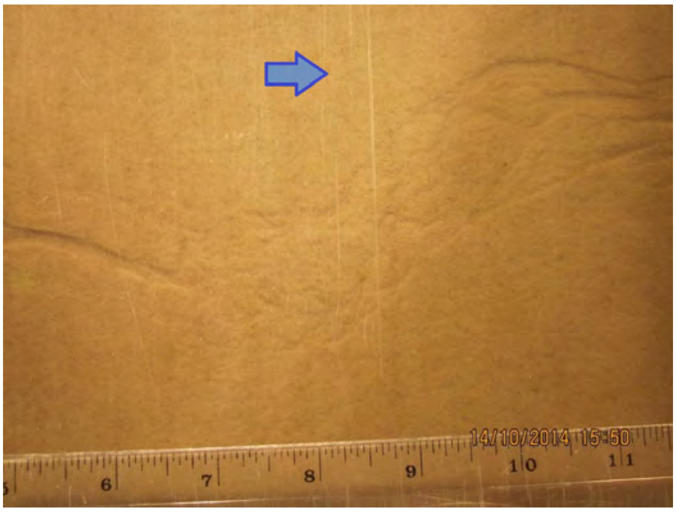

(b) Close up of blockage between enlarged and regular channels (Test 57 in Sibelco 50n)

(c) Forward deepening had reached halfway before Test 25 was stopped; shown once lid removed

Figure 4.3: Forward deepening examples (blue arrows indicate direction of flow)

Forward deepening occurred in all soils except for Mixes 1 and 4 whose channels did not reach the upstream end. It is also unclear whether Mix 3 exhibited forward deepening because there was so little time between the channel reaching the upstream end and the sample failing (1 to 4 minutes) that it was neither seen nor photographed. However, failure of the sample looked similar to other experiments so it is assumed that forward deepening did occur (i.e. assumed failure occurred as a result of forward deepening completion as opposed to surface slip or failure by other mechanisms). The forward deepening behaviour was similar in all soils relative to their behaviour during tip progression. As the channel width increased with increasing coefficient of uniformity (as discussed in Subsection 4.5.1), so did the enlarged channel width. Examples of this can be seen in Figures 4.4 and 4.5 whereby the enlarged channel in the Sibelco 50n test is within 10–30mm wide and almost half the width of the flume in the Mix 5 test. Note that arrows in Figures 4.4 and 4.5 indicate where forward deepening had reached. What is also interesting in Figure 4.5 is the rippled and ragged shape to the enlarged channel not observed in other soils.

As previously discussed in Subsection 3.1.4, once an experiment had been running for 3 to 4 days, biofilm would grow on sand particles resulting in a reduction of permeability and additional resistance against erosion (though biofilm was prevented from Test 41 onwards with the use of potable, chlorinated water). When bio-clogging occurred during forward deepening, it would discolour and bind particles around the enlarged channel and stop the forward deepening process, examples of which are given in Figures 3.15 and 4.6.

In Test 30 an attempt was made to re-initiate forward deepening despite bio-clogging Figure 4.6, by continuing to raise the head. The head was raised from 313mm to 782mm but forward deepening did not re-initiate. Instead, the downstream portion of the sampled failed by surface slip.

In addition to tests not completing forward deepening due to bio-clogging, some tests did not complete forward deepening due to excessive blocking in the regular channel. This occurred in Tests 41, 45 and 46. These tests were in Sydney Sand. Tests 41 and 45 were 2600mm and 3900mm long tests and Test 46 was a regular 1300mm long test but in loose (rained in) sand. These tests were left running 2, 5 and 1 day(s) respectively after the channel had reached the upstream end but the forward deepening process didn't extend past the first 100mm. In all three tests there was extensive blockages within

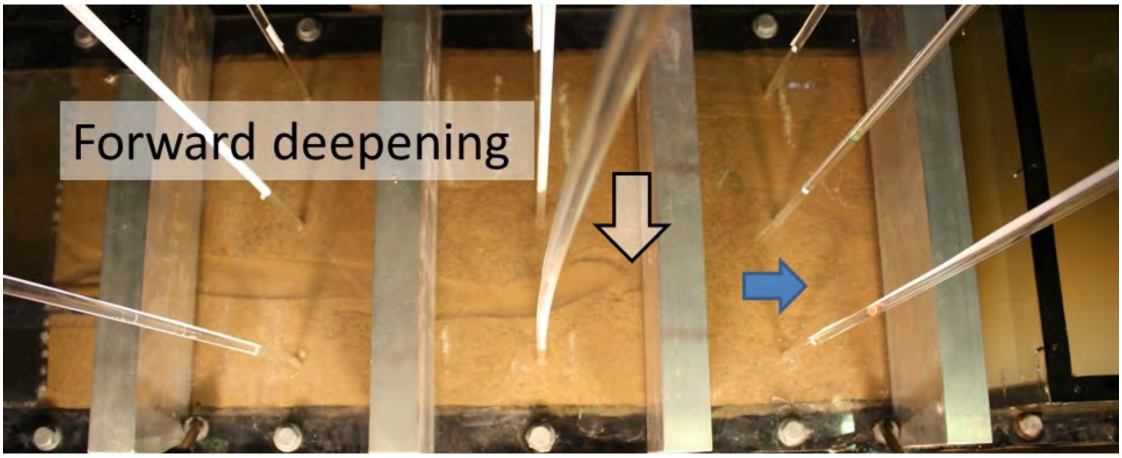

(a) Test 50 in Mix 2

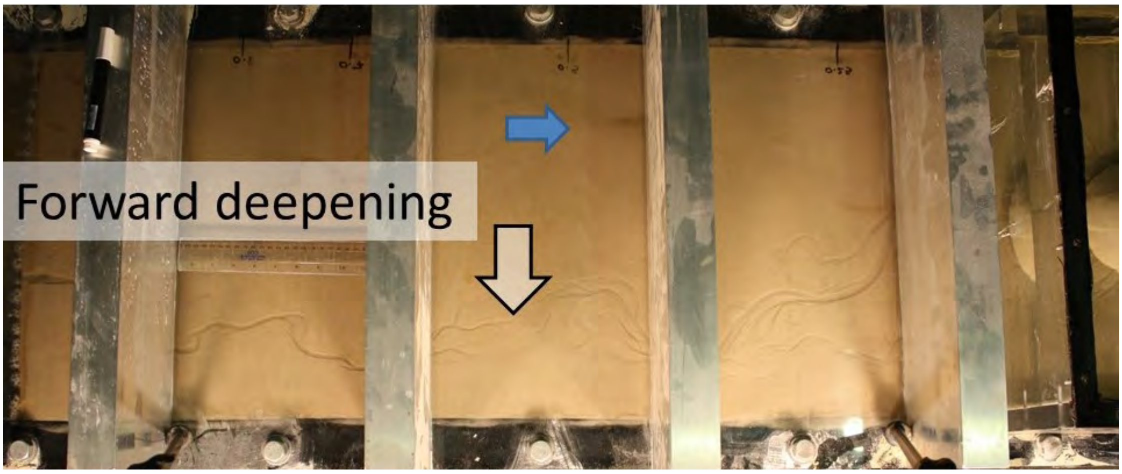

(b) Test 57 in Sibelco 50n

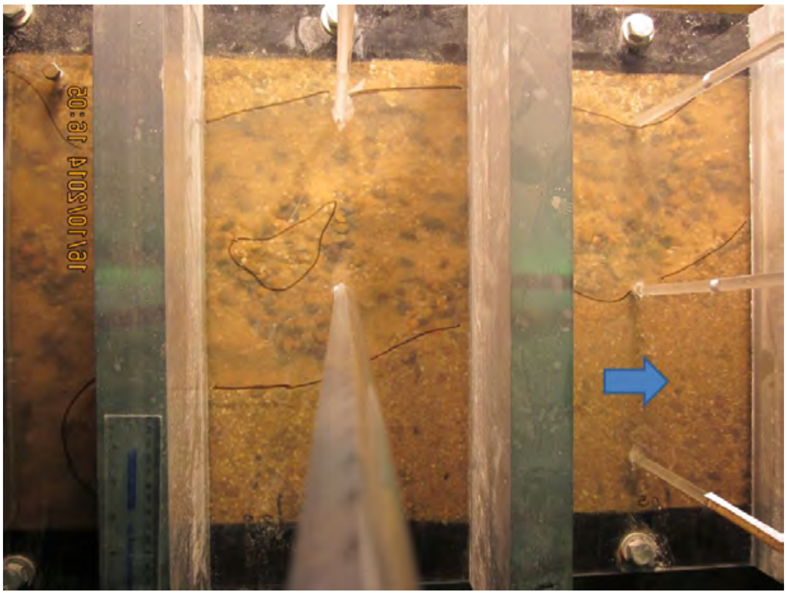

(c) Test 58 in Mix 5

Figure 4.4: Forward deepening in Sibelco 50n and Mixes 2 & 5 (blue arrow indicates direction of flow)

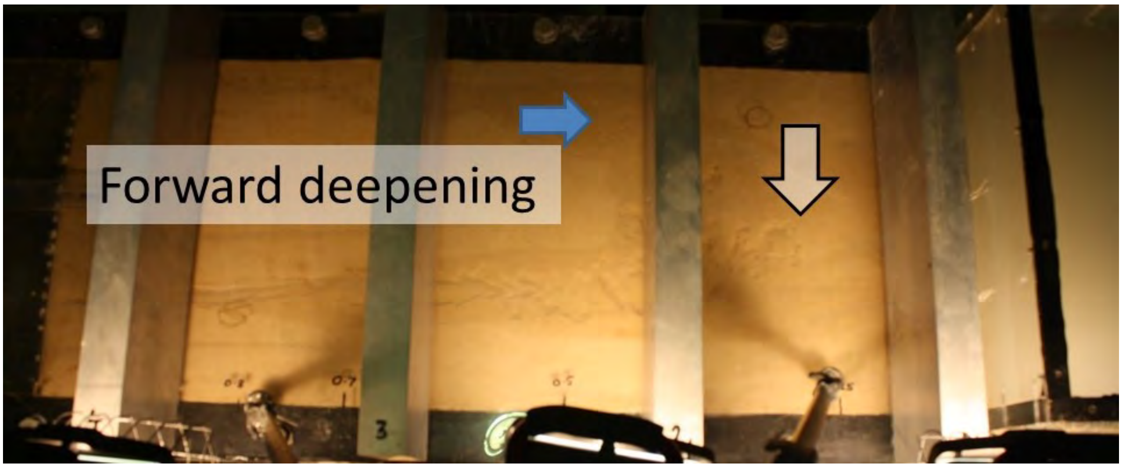

(a) Test 72 in Mix 6

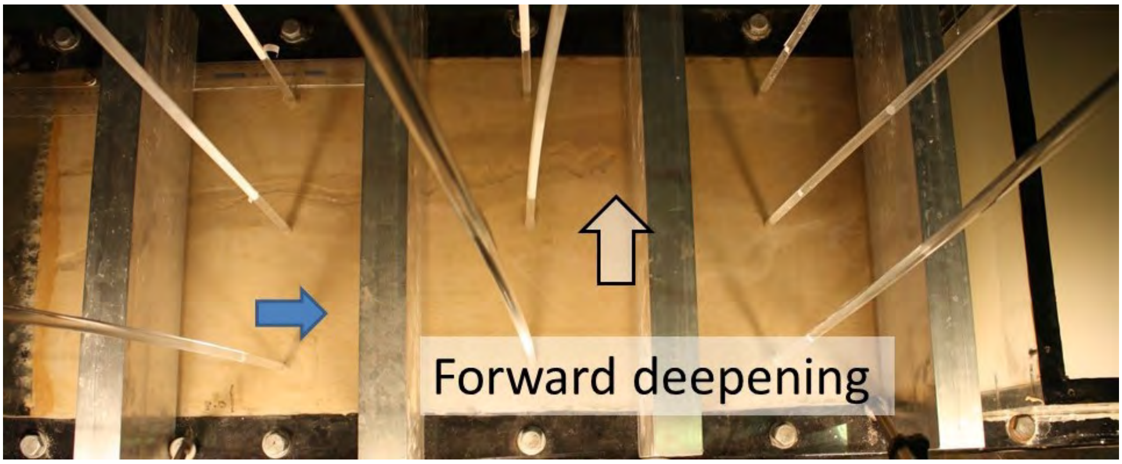

(b) Test 67 in Mix 7

Figure 4.5: Forward deepening in Mixes 6 & 7 (blue arrow indicates direction of flow)

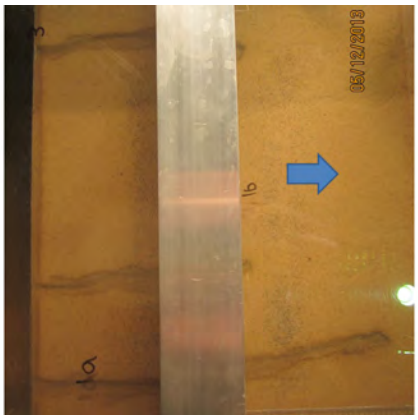

(a) Three enlarged channels arrested in Test 30

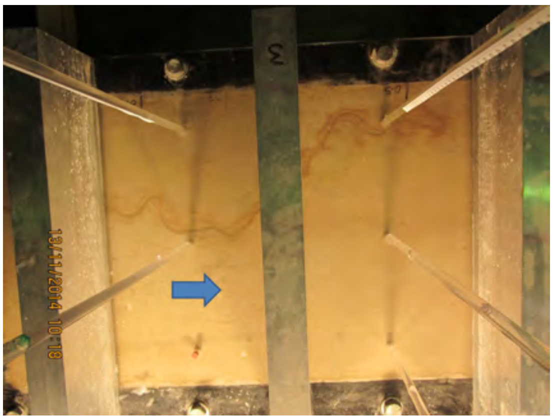

(b) Enlarged channel arrested in Test 59

Figure 4.6: Forward deepening stopped due to bio-clogging (blue arrow indicates direction of flow)

the regular channel. New channels formed in an effort to bypass the blocked channel but tests were ended before these new channels reached the upstream end (which may have lead to full forward deepening if allowed enough time). The hypothesis is that forward deepening did not continue in these tests because the extensive channel blockages prevented backward erosion from removing sediment from the smaller blockage between the regular and enlarged channels.

However, there were other tests which contained blockages within the regular channel but still managed to completely forward deepen and fail. Test 68 which was a 3900mm long test, also contained channel blockages but completely forward deepened in under 24 hours. So perhaps there exists a critical volume or location of channel blockages which prevent further erosion. This possibility is explored in Subsection 4.5.4.

4.3.5 Failure

Failure occurred as soon as the forward deepening process reached the downstream end. It was marked by a large and sudden surge of sand movement resulting in removal of the top layer of sand across about a 1/3 of the flume's width. This removal of sand resulted in a large increase in water flow because the system now behaved like pipe flow rather than seepage flow. See Figures 4.36 and 4.37 for plots and photos of the sudden jump in flow.

Figures 4.7 and 4.8 show examples of tests after failure, the same tests which are shown in Figures 4.4 and 4.5.

There was another 'mode' or mechanism of failure (sample-wash-out) observed in some experiments where by sand flowed over large areas without being restricted to channels (even often 'washing' the channel away). The sand appeared to flow as a thin 'sheet' so this movement has been referred to as 'sheet flow'. It is also sometimes referred to as 'surface slip' because the hypothesis is this movement occurs when the hydraulic forces overcome friction between the sand and Perspex lid, causing the surface of the sand to slip en masse.

Sheet flow/surface slip often occurred when the hydraulic head was excessively high such as when soils of high uniformity coefficients were loaded with the maximum head or

(a) Test 50 in Mix 2 1 minute after Figure 4.4a

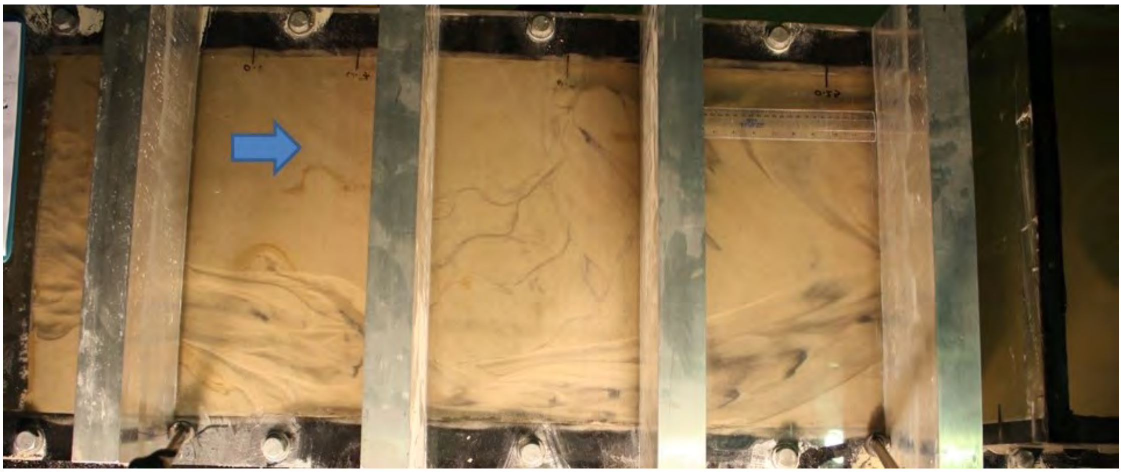

(b) Test 57 in Sibelco 50n

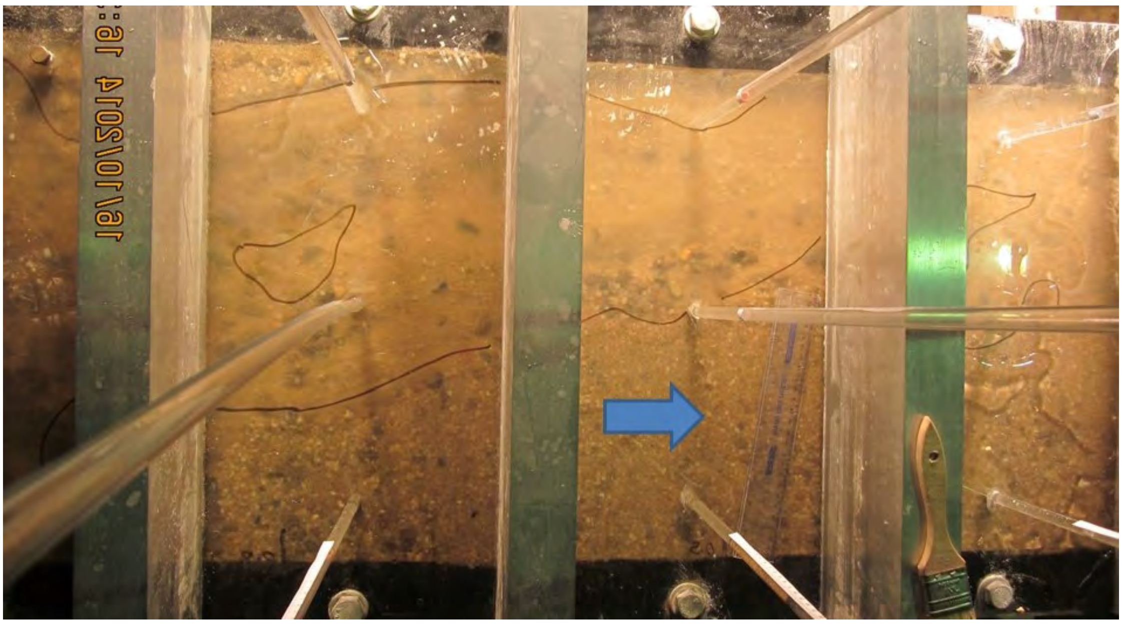

(c) Test 58 in Mix 5

Figure 4.7: Failure in Sibelco 50n and Mixes 2 & 5 (blue arrow indicates direction of flow)

(a) Test 72 in Mix 6 1 minute after Figure 4.5a

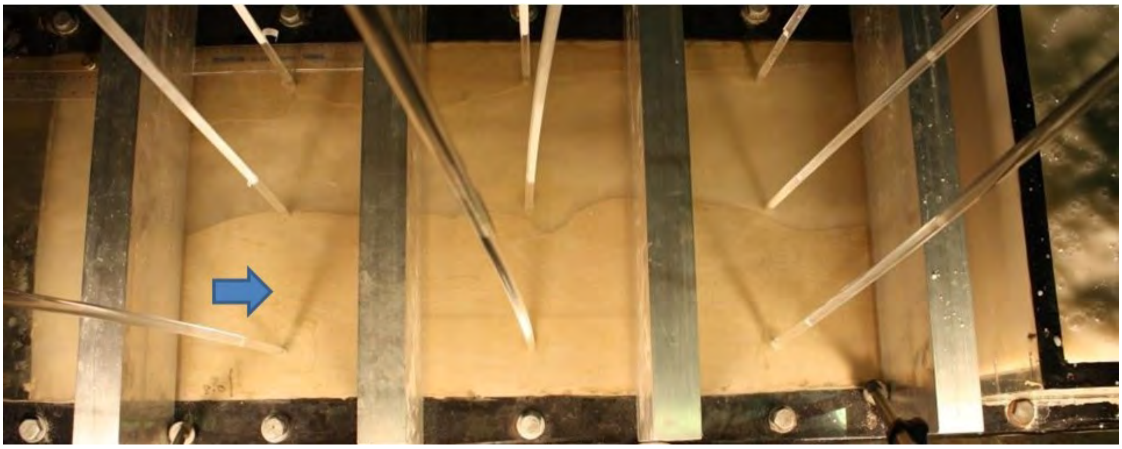

(b) Test 67 in Mix 7 1 minute after Figure 4.5b

Figure 4.8: Failure in Mixes 6 & 7 (blue arrow indicates direction of flow)

when the head was unusually high in attempt to overcome blockages or bio-clogging. It was considered whether a small deflection of the Perspex lid could also be a factor in the initiation of sheet flow/surface slip but it was thought to be unlikely given sheet flow/surface slips only occurred under excessively high heads whereas initiation due to lid deflections could have occurred at any head. Sheet flow/surface slip was not considered a stage of backward erosion.

4.4 Initiation, critical and progression heads

The initiation, critical and progression heads are indicators of hydraulic loading which activate and/or maintain the backward erosion process.

The initiation head marks the onset of particles leaving the sand matrix at the exit. The leaving of these first particles triggers a continuous cycle of erosion which creates (and progresses) a channel. Therefore the initiation head also marks the start of a channel, i.e. the start of the 'tip progression' stage. The 'initiation head' was influenced by the presence of a starter channel and the exit geometry. A starter channel caused a lower initiation head and exit geometries which concentrated the flow more (i.e. circle and slot exits) also caused lower initiation heads. These influences are demonstrated in Sections 5.3 and 6.2.

The critical head was the minimum head required to overcome equilibrium and keep the tip progressing through to the upstream end. In situations where equilibrium did not occur, the critical head was the initiation head since once the channel initiated it continued to progress through to the upstream end without need for further head increase. Either way, the critical head was the maximum head applied throughout the test.

The critical head was influenced by:

1. A starter channel which lowered the critical head (see Section 5.3);
2. The exit geometry- the more an exit concentrated the flow, the lower the critical head (see Section 6.2); and

3. The soil grading- the more uniform the soil the lower the critical head (see Section 8.2).

The progression head was the minimum head required to continue tip progression at a given location. Therefore the progression head varied with channel length. To determine the progression head, either the 'decrease at points of interest' (POI) or cyclic loading procedures were needed so that it could be seen whether heads required after the maximum (critical) head reduced or stayed the same.

The 'decrease at points of interest' (POI) loading procedure was used in tests belonging to both Groups 2, 3 and 4. In these tests, heads required after critical usually decreased, i.e. the progression head usually decreased with channel length (as opposed to remaining constant). Decreases from critical to progression heads were between 0.5–94%, though most decreases (80%) were between 10–30%.

4.5 Channel behaviour

4.5.1 Geometry

Channel width

The majority of channel width measurements were made post-test using high-speed photos intended for measuring Pliolite particle speeds. Given that Pliolite particles were only used in Sydney Sand tests, most channel width measurements were in Sydney Sand. Therefore the focus will be on channel widths in Sydney sand before considering widths in other soils.

Figure 4.9a is a plot of channel widths in Sydney Sand by test number. Tests beyond Test 38 were not measured for channel widths (post test using photos) because it was a time-intensive task and widths were remaining within the same range across tests.

Figure 4.9a revealed:

1. All widths were between 1 to 40mm;

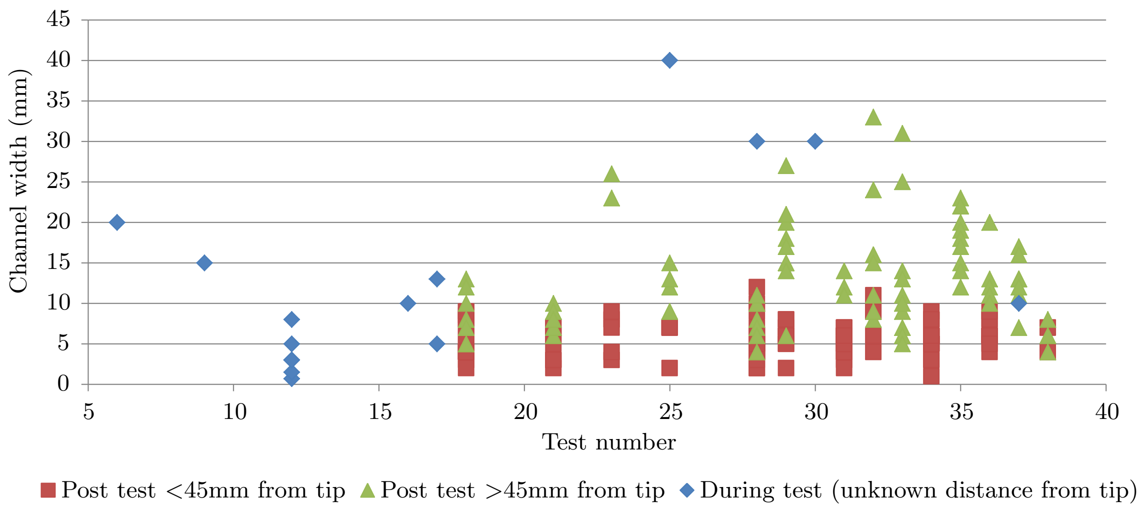

(a) Channel widths by test number, method and proximity to tip

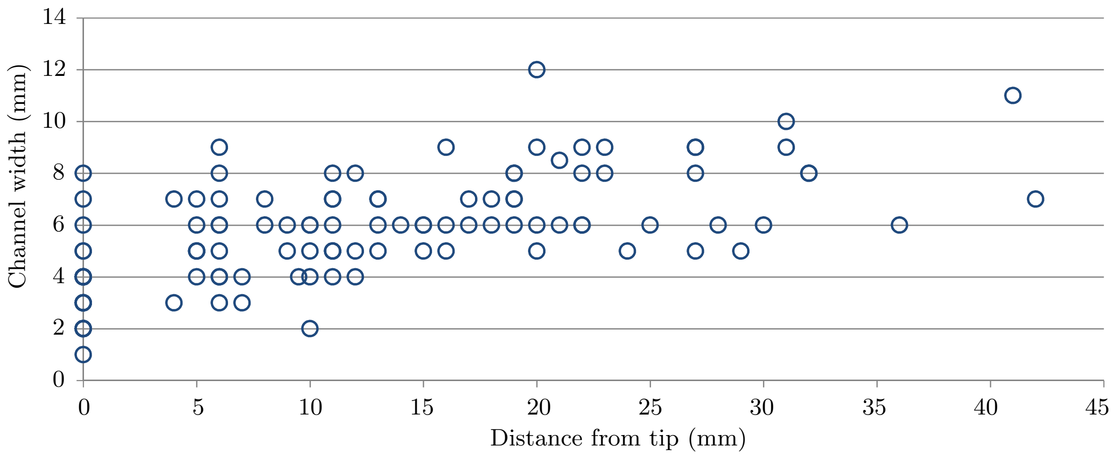

(b) Channel widths with distance from tip

Figure 4.9: Channel widths in Sydney Sand

2. On average, widths measured within 45mm of the tip were less than widths measured elsewhere;

3. Widths varied significantly within one test covering a range up to 38mm; and

4. Measurements taken during the test were more likely to be wider (because wider-than-normal widths were more likely to be noticed and measured).

A data analysis of the widths taken >45mm from the tip produced the histogram shown in Figure 4.10a and calculated an average value of 13mm and standard deviation of 7mm. This average width expressed as a number of sand grains is 43 grains (given Sydney Sand is uniform with a d_{50} of 0.3mm).

Figure 4.9b is the widths measured within 45mm of the tip plotted against distance from the tip. This plot shows:

1. Widths at the tip ranged between 1 to 7mm;
2. There was an overall trend of increasing channel width with distance from the tip; and
3. There was a reasonable spread in widths at any given distance from the tip, up to 7mm.

A data analysis of the widths taken at the tip produced the histogram shown in Figure 4.10b and calculated an average value of 4mm. This average width expressed as a number of sand grains is 13 grains (given Sydney Sand is uniform with a d_{50} of 0.3mm).

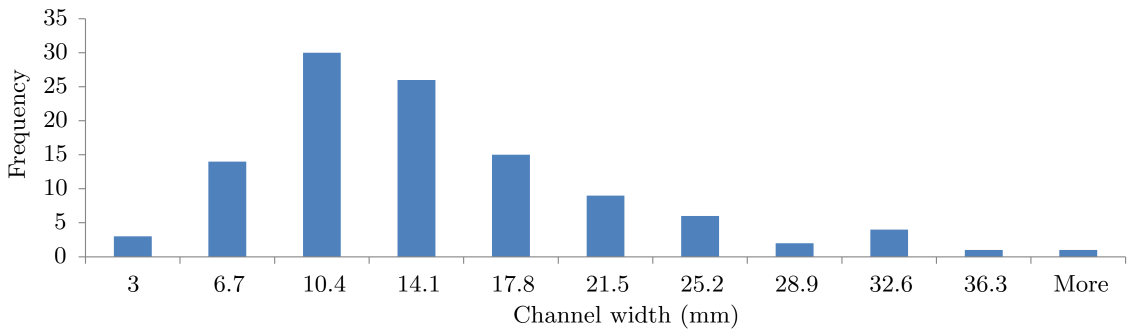

(a) Channel widths at distances >45mm from the tip

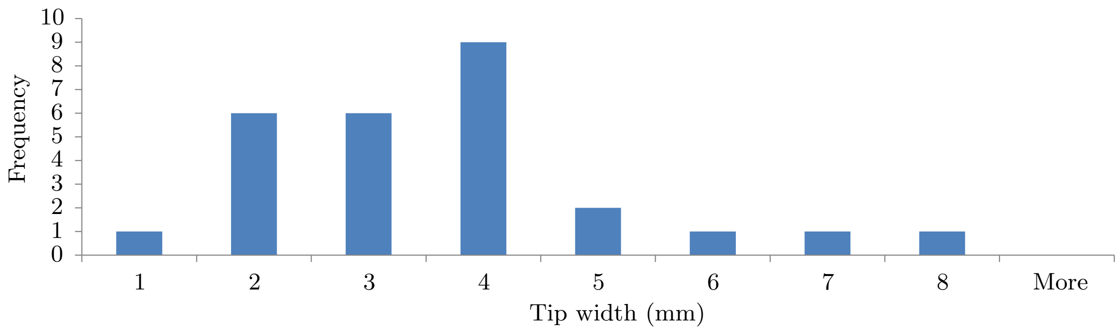

(b) Tip widths

Figure 4.10: Histograms of channel widths in Sydney Sand

To consider channel widths in other soils, Figure 4.11 is a plot of average tip width measured in each test, against d_{50}. Note: the region of the 'tip' was was defined as being between the first sign of soil disturbance to 20mm downstream of this disturbance. Only tip widths were plotted because tip widths were considered more influential over the critical gradient than other widths along the length of the channel. Tip width was considered more influential because it is seepage velocities into the tip that are considered to be the driver of backward erosion, and seepage velocities into the tip are partly determined by the tip width. Other widths along the length of the channel did often increase like they did in Sydney Sand, as illustrated in Figure 4.9b, but also like in Sydney Sand, increase of channel width did not always occur and when it did, was often only a subtle increase.

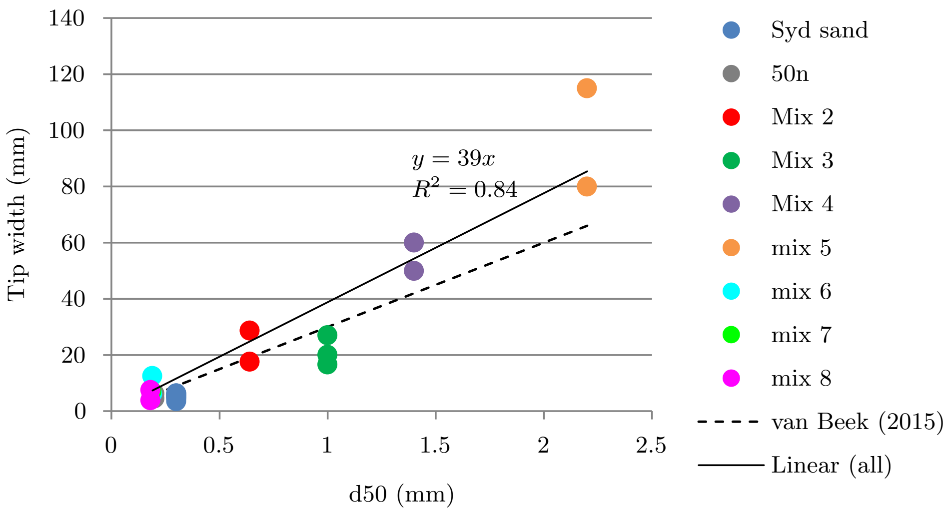

Figure 4.11: Tip width with d_{50}

Figure 4.11 shows a linear proportional relationship between tip width and the soil's d_{50}. This relationship can be generalised as 40 times d_{50} as shown by the line-of-best fit. Van Beek (2015) also reported a similar relationship but suggested 30 times d_{50}, indicated by the dashed line.

Characterising channel width as a function of d_{50} was somewhat arbitrary however, when the same relationship against d_{70} was plotted, the R^2 value of the line-of-best-fit was a little lower.

Channel depth

The channel depth was estimated during tests by judging the number of particles stacked in the channel side walls, but this was done infrequently and was subjective with large ranges. After tests, the channel depths were measured/estimated using wax moulds, a caliper and sand boil weights. A list of tests that had their channel depths measured, and by which method, is given in Table 4.3.

Three estimations of channel depth were made during tests. These included 5 to 10 particles in Test 16 and 10 to 20 particles in Test 17 (twice). Both these tests were in Sydney Sand and given Sydney Sand was uniform with a d_{50} of 0.3mm, these depths equated to 1.5mm to 3mm in Test 16 and 3mm to 6mm in Test 17.

Depths measured using the caliper and wax moulds are plotted in Figure 4.12 as a histogram. These measurements were made in Tests 79 and 80, also in Sydney Sand. Most depths were between 1.5 to 3mm with an average (from across all depths) of 2.4mm. These depth measurements are considered more reliable than depths estimated by observation and depths estimated by boil mass.

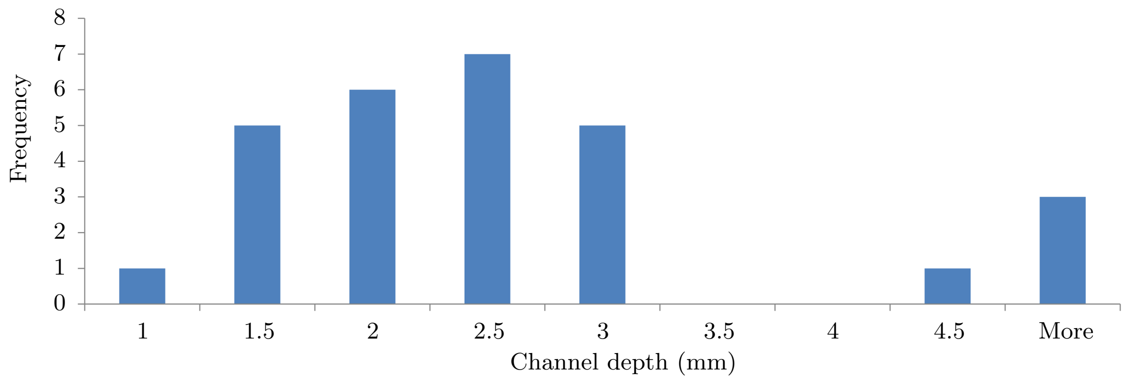

Figure 4.12: Histogram of channel depths measured in Sydney Sand using caliper and wax moulds

Depths using sand boil masses were approximated by dividing the estimated channel area by the average width of 13mm. Depths ranged between 4–7mm in Test 77, 11–15mm in Test 79 and 4–9mm in Test 80 (refer to Section 4.6 for these calculations). These depths are based on many assumptions (such as sand density) and are therefore considered the least reliable but are still provided to offer an 'order of magnitude' check.

It is interesting to note that some tests carried out using the starter dowel partially filled in with sand for its full length before traditional tip progression commenced, namely Tests 8, 12, 14, 16 & 17. A discussion on this is given in Section 5.2 along with a photo of an example. This partial infilling of the starter channel suggests that the diameter of the starter (6.35mm) was greater than the natural channel depth (for reasons explained in Section 5.2). This suggestion supports these depth measurements of between 1 to 5mm.

There was insufficient information to determine whether the channel increased in depth with distance from the tip. However, based on general test observations the channel depth appeared to remain fairly constant and a channel was more likely to widen than deepen with distance from the tip.

No channel depth measurements were made in soils other than Sydney sand. Therefore it is not known what effect soil grading has on channel depth.

Channel cross-sectional shape

Whilst the cross-sectional shape of the channel has not been determined with certainty, observations made during the tests suggest the channel is a trapezoidal shape, with sloping walls, rounded corners and a near-flat bed. This observation can be seen in the wax moulds shown in Figure 4.13. It is likely the walls were sloped close to the angle of repose, but this was not confirmed. Also, as mentioned previously, a channel was more likely to widen than deepen with distance from the tip.

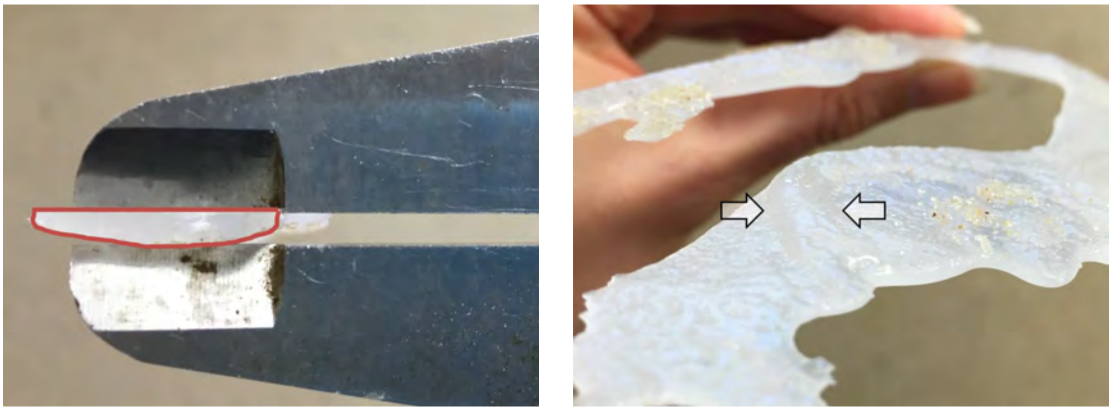

(a) Wax mould held in calliper with channel cross-section outlined

(b) Underside of wax mould (arrows indicate edge of channel)

Figure 4.13: Wax moulds taken after Test 79 showing cross-sectional channel shapes

Number of channels

In the majority of experiments only one channel formed from the exit (not including channels which had branched off the primary channel or channels abandoned by braiding).

Experiments which included more than one channel were experiments in plane exit tests.

All three of the tests contained three independent channels, an example of which is shown in Figure 4.14a. Most of the time all three tips would progress simultaneously. In two out of the three tests it was the third channel to initiate which reached the upstream end first; in the other test it was the first channel to reach upstream first.

As a detailed example of multiple channels, Figure 4.14b shows channel progression with time in Test 30. The slope of the channel length lines indicate the speed of tip progression. It shows channel 1 (the first channel to initiate) progressing quite fast until it splits into 2 branches, channels 1a and 1b, after which the progression slows. It also shows that at about the same time channel 1 split, channel 3 initiated. Channel 3 progressed at a reasonably consistent speed (although did slow down slightly) and reached the upstream end before channels 1a and 1b. There was also a channel 2 but it stopped progressing before too long.

There was also 1 (out of 7) tests using the slope exit which had 2 independent channels (Test 36) and 1 (out of 6) tests using the slot exit which had 3 independent channels (Test 21).

Furthermore, many circle-exit tests in uniform sands started with 2-3 channels from the exit, an example of which is shown in Figure 6.9 (often having formed during CO_2 flushing and/or saturation). And whilst these channels sometimes progressed to lengths of up to 100mm, only the channel closest to the upstream direction progressed further.

It was difficult to tell how many channels were present in tests in Mixes 1 and 5 as channels were difficult to see and define in these soils. Channels appeared to be more like a network of disconnected channels or an eroded ‘region’ rather than an obvious channel.

In Group 5 testing when heads above critical were applied, it was common for multiple channels to branch from the main channel at the circle exit and progress simultaneously. Often, once the longest channel was approximately up to bar 3, other channels arrested and the longest proceeded to progress to the upstream end.

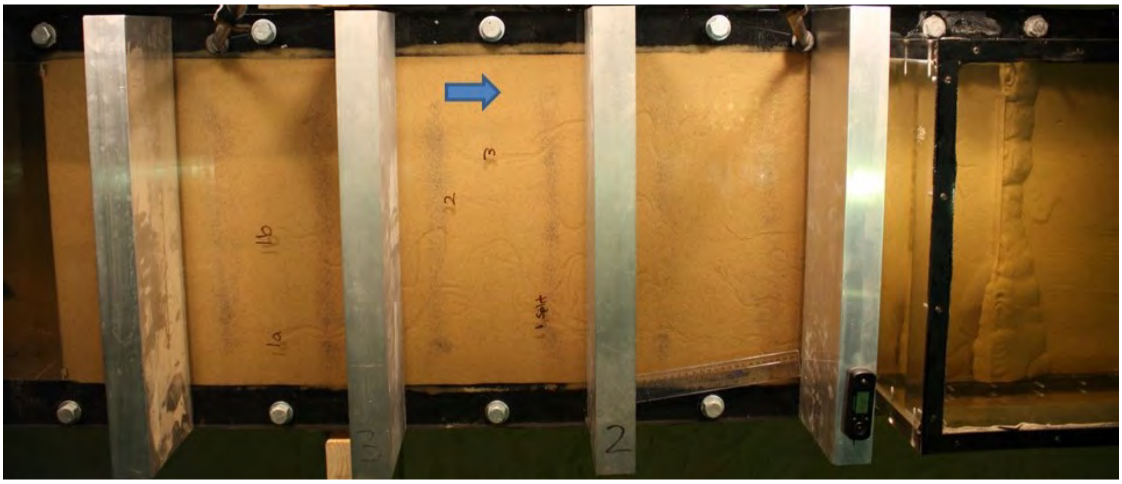

(a) Photo with channels labelled on lid (blue arrow indicates direction of flow)

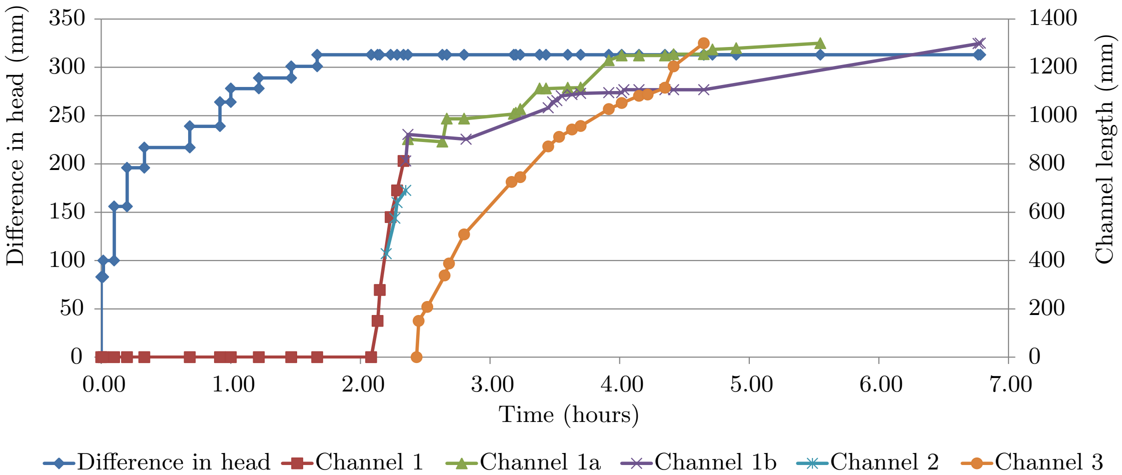

(b) Head and channel lengths with time

Figure 4.14: Three channels in Test 30

4.5.2 Primary erosion

Primary erosion is a term coined by Hanses et al. (1985). It is used to refer to particle detachment from the channel tip resulting in tip progression.

Mechanism

In uniform soils (Sydney sand and Sieblco 50n) particle detachment from the channel tip appeared to start as a select few grains, perhaps 5-10 grains upstream of the tip, moved downstream to fill void spaces before stopping on downstream grains. Moments later a group of particles, maybe between 10-50 grains, would suddenly move downstream into the channel together. These grains would then be transported away, along the channel, as bed load. The tip would then remain stationary for a time until the process repeated. In this way the tip would progress in a stop-start, intermittent fashion.

The time between particle group detachment appeared to be influenced by how close the hydraulic head was to critical. If the head applied was above critical, the time between group detachments was small and almost undetectable (particle detachment was continuous) but if the head was reduced in fine increments to approach critical, the time between group detachments increased so much that it was challenging to determine whether tip progression had stopped or not. Sometimes time between group detachments was as much as 15 to 20 minutes.

In addition, the number of particles contained within each detaching group was also influenced by how close the hydraulic head was to critical. The closer the head was to critical the fewer the number of grains which detached together.

This process was well captured with close-up video at 29 frames/second. Two frames from one of these videos, is given in Figure 4.15. However the tip erosion process can not be seen in these images (enough to support the above description) because extracted frames were only 0.4 megapixels (so insufficient resolution to see individual grains) and successive frames are needed to see the movement. The process was also captured with the high-speed casio camera however it could not focus into the tip as close as the video camera (without a specialised lens).

In cyclic tests where the head was increased in small increments as the critical head was approached, it was often observed that at one head increment prior to critical, sediment transport, as bed load, commenced in the downstream portion of the channel only (usually contained within the last 150mm of the channel). This transport did not affect the upstream portions of the channel or the tip. With the next increase in head the extent of bed mobilisation would work its way towards the tip. Once bed mobilisation reached the tip, erosion from the tip and hence tip progression, would recommence.

In short, it was possible to see sediment transport through the channel without erosion from the tip but it was not possible to see erosion from the tip without sediment transport throughout the channel (so particles detached from the tip could be transported away).

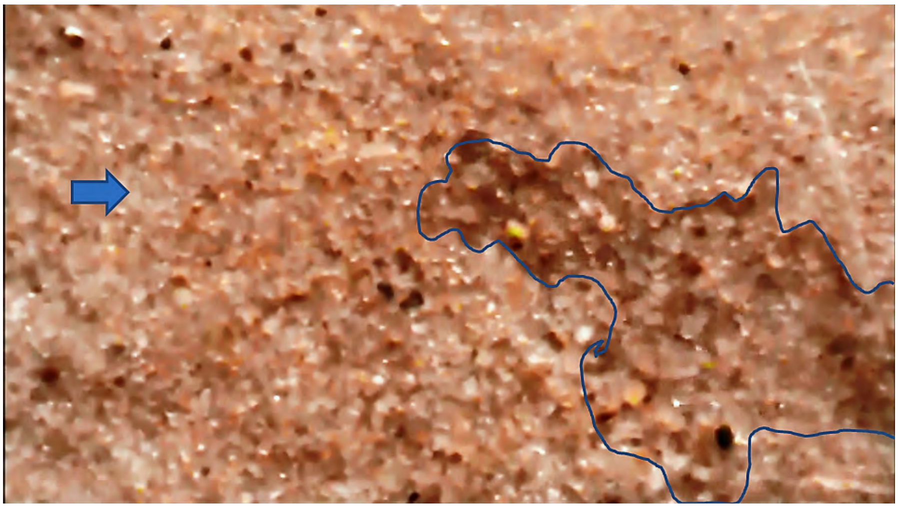

(a) First frame extracted (blue outline)

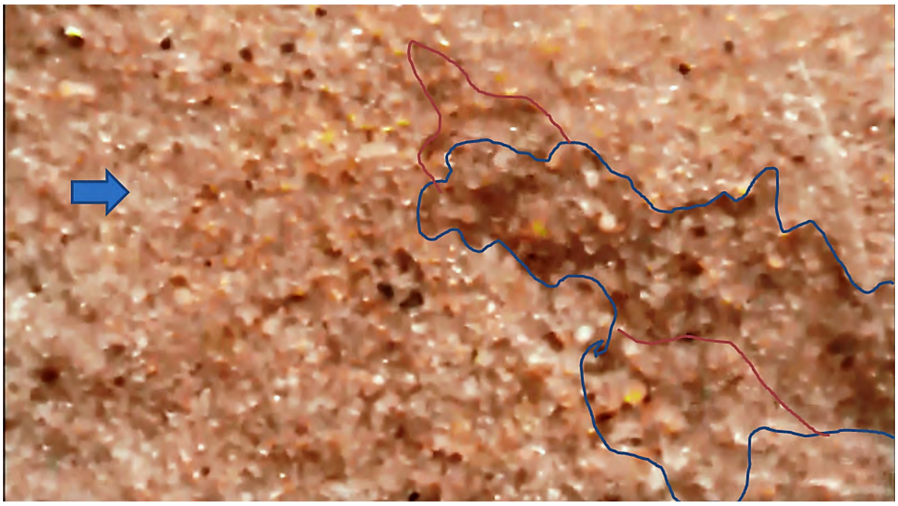

(b) 0.6 of a second after (a) (red outline shows difference)

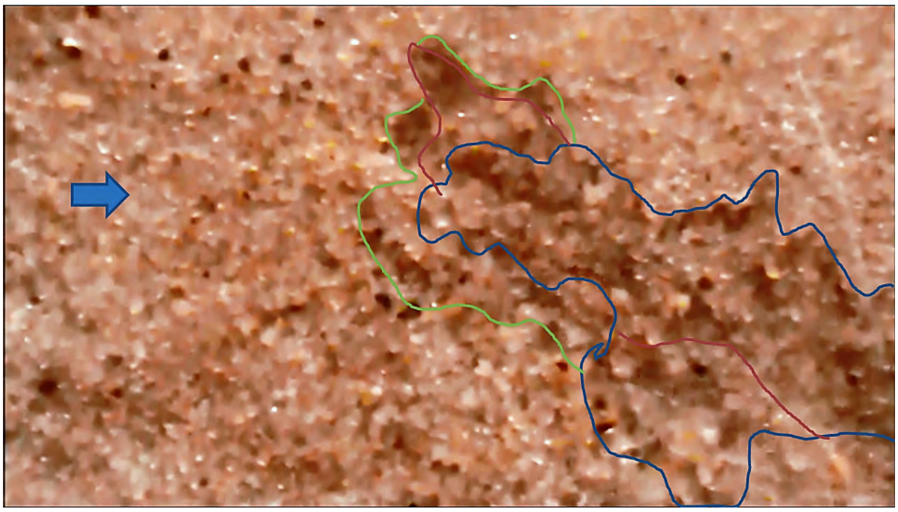

(c) 2 seconds after (b) (green line shows difference)

Figure 4.15: Frames extracted from video of tip progression with lines outlining channel (blue arrows indicate direction of flow)

Branching

On occasion a new channel tip would form off an existing channel creating a channel branch. This new tip would then progress towards the upstream end. Most of the time branching occurred when the original tip slowed or stopped due to either the channel becoming blocked or the tip came into contact with an obstacle. Although sometimes branching occurred for no apparent reason.

When a channel became blocked and branching occurred, the new tip formed downstream of the blockage and progressed toward the upstream end alongside the blocked channel. Sometimes the new tip would eventually join up with the original channel upstream of the blockage but other times it would remain independent. Figure 4.16a is an example of channel branching as a result of channel blockage. Figure 8.12 is another example, only in this occasion, channel blockage occurred due to bubbles entering the channel.

When a tip came into contact with an obstacle and branching occurred, the new tip formed downstream of the obstacle and progressed toward the upstream end around the obstacle. Obstacles included bubbles, a void between the sand's surface and Perspex lid or a zone of apparent additional erosion resistance (perhaps a zone of more denser soil). Figure 4.16c is an example of channel branching due to a void and Figure 4.16d an example due to a zone of apparent additional erosion resistance.

Figure 4.14b presented in Subsection 4.5.1 on the number of channels shows the influence of channel branching on the speed of tip progression. It shows that once channel 1 split into 2 channels (1a and 1b), the tip progression slowed (shown as the reduced slope of the line). It also shows that when channel 1 split, a new channel, 'channel 2' formed. These observations were not present at all channel branching occurrences, so this chart is not included to represent typical behaviour due to branching, but to demonstrate that channel branching can have an effect on these attributes.

Channel branching was less likely to occur in well graded soils which backward eroded in sudden bursts with wide channels.

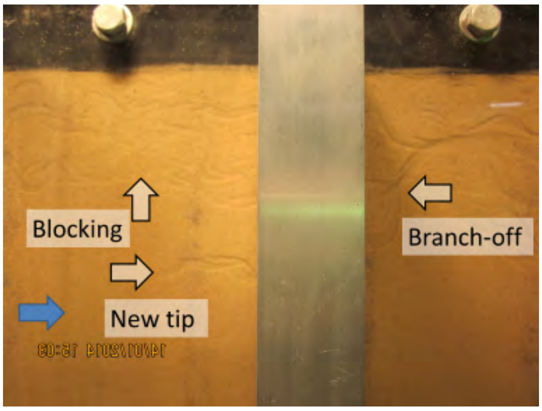

(a) Due to channel blockage (Test 33)

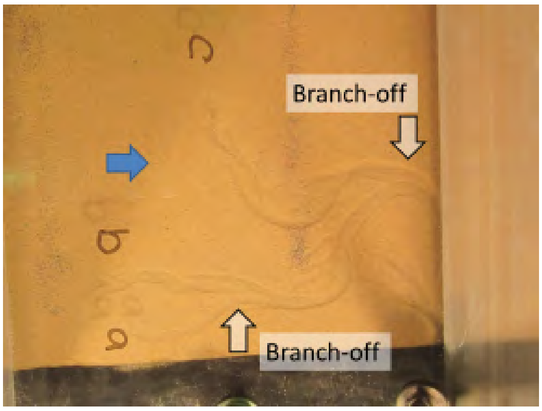

(b) Branched twice for no visible reason (Test 35) resulting in 3 active tips

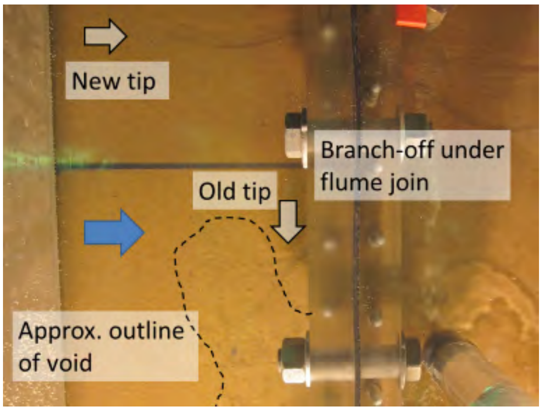

(c) Due to tip having come in contact with a void (Test 45)

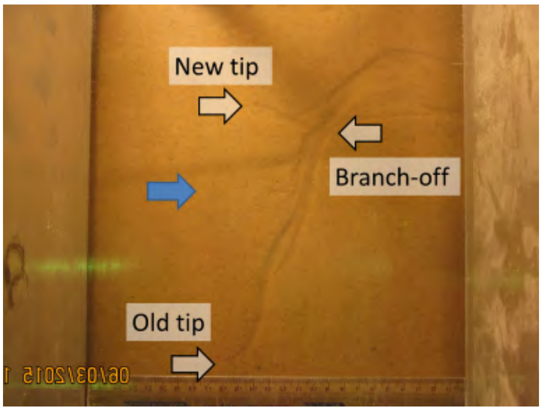

(d) Due to tip having come in contact with erosion resistance (Test 68)

Figure 4.16: Channel branching (blue arrows indicate direction of flow)

4.5.3 Secondary erosion

Secondary erosion is a term coined by Hanses et al. (1985). It is used to refer to transport of particles along the channel as well as particle detachment from the channel bed and walls. Secondary erosion results in clearing of the tip and channel from detached sediment and moving it out through the downstream exit as well as meandering and scour of the channel.

Bed load

Of the two main modes of sediment transport: bed load and suspended load, it looked as if sediment being transported along the channel was done so as bed load. It looked this way because when coloured sand was photographed and analysed with the close-up high-speed photos, it was noticed that the distance travelled between frames varied (as shown in Figure 3.29). If the coloured sand had of been moving as suspended load then this varying distance between frames would have suggested a sporadic unsteady flow, which was unlikely. It was also noticed that the shape of particles varied between frames suggesting the sub-angular particles were rolling, most likely along the bed of the channel. This theory of bed load was supported when Pliolite particles were used instead of coloured sand. The Pliolite particles moved considerably faster than the coloured particles because they moved as suspended load (since they were a similar density to water). This confirmed that the coloured sand (and therefore regular sand) was moving slower than the water flow, a unique characteristic of bed load.

Meandering & scour

Channels always meandered similar to river systems with a sinuous pattern of eroding sediments from the outside of bends and depositing them on the inside.

It is thought that initial channel meandering occurred as the tip followed micro variations in soil erodibility thereby tracing out a sinuous path of least resistance. Figure 4.17a is an example of a tip progressing laterally as it moves around a zone of extra resistance (perhaps a zone of denser soil). Eventually the tip turned again to progress upstream but this temporary lateral divergence created an initial meander in the channel.

Additional channel meandering, which moved downstream portions of the channel, is considered to have occurred due to variations in hydraulics along the channel. Hydraulic variations such as faster flows colliding with channel walls resulting in the scour of sediments around to slower flow positions where sediments settled out and deposited.

In general, there was more meandering activity towards the downstream end of the channel than the upstream end (example of which can seen in Figure 4.17c).

The meandering action was well captured in time-lapse videos.

No measurements were made to quantify the meander amplitude or wavelength given the complexity and ever-changing position. However the degree or shape of meandering did not appear to influence the head difference required to progress the tip, so it did not

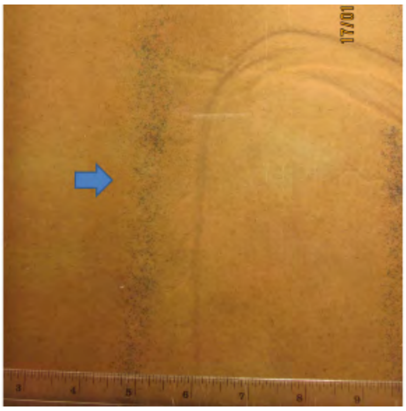

(a) Tip progressed laterally at region of extra resistance resulting in channel meandering (Test 34 in Sydney Sand)

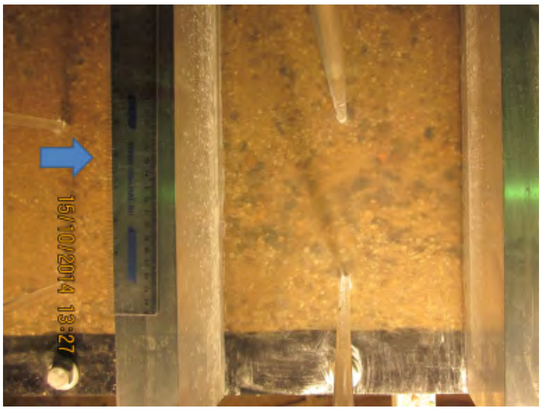

(b) Example of less channel meandering in well graded soils (Test 58 in Mix 5)

(c) Example of more channel meandering in uniform soil and more meandering and braiding toward downstream end (Test 57 in Sibelco 50n)

Figure 4.17: Channel meandering (blue arrows indicate direction of flow)

appear to influence the initiation or critical heads. It is noted that channel lengths and distances from the tip presented throughout this thesis are linear distances; they do not take the sinuosity into account.

As discussed in Subsection 4.5.1 on channel geometry, the width of the channel in Sydney Sand appeared to increase from an average 4mm at the tip to 13mm at distances greater than 45mm from the tip. Meandering, scour and braiding are the most likely cause of this channel widening. Although given the extent of channel meandering and movement it is surprising the degree of channel widening is not greater. This suggests that perhaps the channel widening is somewhat self-limiting; that perhaps the interaction between channel flows and sediment weight/falling velocity maintain a channel shape instead of allowing continual lateral spreading.

As for channel depth, also discussed in Subsection 4.5.1, it appeared to remain fairly constant, although there weren't sufficient measurements to verify this. A constant depth suggests that meandering, scour and braiding was more likely to erode channel walls instead of the channel bed. Perhaps the continual transport of detached sediments along the bed of the channel replaced any sediments removed from the bed, hence maintaining a constant depth.

The exit geometry appeared to have an influence on meandering because more meandering (and braiding) occurred in slope, plane and slot exits than circle exits. This is likely to be due to the downstream end of the channel having more freedom with these exit shapes. And in fact, the channel at the downstream end was observed to move from one side of the flume to other in some slope, plane and slot exit tests.

Soils which were well graded with higher coefficients of uniformity such as Mix 1, 3, 4 and 5, meandered less than more uniform soils. Figure 4.17b shows an example of Test 58 in Mix 5 whose channel meandering was less pronounced than the example of Test 57 in Sibelco 50n in Figure 4.17c.

There are three possible reasons as to why the soil grading influenced the degree of channel meandering. One reason is the speed of tip progression. Well graded soils exhibited fast tip progression, often backward eroding in sudden bursts. This suggests that the faster the tip progressed the less the channel meandered. This also played-out as variations in same-soiled tests whereby tips which were slowed down on bubbles, cemented sediments (due to bio-clogging) or (presumably) zones of denser soils exhibited more channel meandering downstream.

A second reason is variations in the erodibility and settling velocity of fine compared to coarse sediments where larger and heavier sediments were less likely to be eroded from outer meander bends.

Thirdly, because the soil grading affected the channel width and the channel width would affect hydraulics within the channel, then wider channels resulted in slower flow velocities and less eddies driving less channel meandering. This holds with the fact that larger, more well graded soils, resulted in wider channels (as discussed in Subsection 4.5.1) which coincided with less channel meandering.

4.5.4 Blocking

Blocking refers to a build-up of sediment in a channel which prevented particle transport through the channel. Figures 4.3b and 8.10b show examples of channel blocking.

Blocking also occurred as part of the forward deepening process, between the regular and deepened channels. However this blocking is treated separately in Subsection 4.3.4. This section is limited to discussion of blocking which occurred during tip progression and equilibrium.

Table 4.3 indicates which tests included channel blockages (prior to forward deepening). Approximately 40% of the tests included some channel blockage. Blocking occurred in Sydney Sand tests with all exit geometries and all seepage lengths. Blocking did not occur in Sydney Sand tests which were rained in, imposed by bladder pressures less than 50kPa or loaded in cycles. In soils other than Sydney Sand, blocking occurred in Mixes 3 to 8. This means blocking did not occur in tests on Mixes 1, 2 or Sibelco 50n.

In Sydney Sand tests, blockages first occurred when the channels were between 685mm to 1112mm long, i.e. between 53% to 85% of the seepage length. This is shown in Figure 4.18a (note only first blockages are plotted, there were often subsequent blockages which are not plotted). Also shown in Figure 4.18a are the approximate extents of the initial blockage (very approximate- so for instance if a blockage was observed between bars 1 and 2 then the position of these bars are plotted on Figure 4.18a, even though the blockage may not have spanned the full bar spacing). The approximate extents show the position of blockages varied, i.e. blockages occurred somewhere different each time. The tests plotted in Figure 4.18a included the four different exit geometries and there does not appear to be a correlation between exit geometry and how long the channel was when it blocked.

Figure 4.18b shows the same data but for Sydney Sand tests with seepage lengths greater than 1.3m, i.e. 2.6 and 3.9m. It shows blockages first occurred when channels were about 50% of their respective seepage lengths (i.e. the tip was halfway to the upstream end). Also, as before, the position of blockages varied. It is worth noting that all of the 5 tests which were carried out on seepage lengths greater than 1.3m included channel blockages. This suggests that the likelihood of channel blocking increases with increasing seepage length.

Figure 4.18c shows the same data but for tests in soils other than Sydney Sand. It shows a larger variation in channel lengths at first blockage: between 70mm to 1164mm i.e. between 5% to 90% of the seepage length. Therefore it appears that blockage behaviour is much less predictable in well graded soils. Also, as before, the position of blockages varied.

Of the 42 instances of recorded blockages (some of which occurred in the same test), 22 (52%) reached the upstream end without need for head increase and 20 (48%) stopped before reaching the upstream end and did need a head increase. This demonstrates that there was no pattern or typical behaviour as to how the tip responded to blocking.

Figure 4.19 graphically illustrates this almost 50/50 split of needing a head increase upon blocking. It also shows the breakdown of tip and channel behaviours exhibited within each group. Behaviours such as the channel unblocking itself, remaining blocked and a new tip branching off to bypass the blockage. Again, the lack of consistent behaviour suggests there was no pattern to the consequences of channel blockage.

For 17 of the 42 instances of recorded blockages, a plot of the channel distance with time was graphed in order to see whether the blockage influenced the speed of tip progression. It was speculated that blockages occurred when tip progression had sped up, thereby increasing the flow rate of sediment to be transported through the channel leading to a blockage. It was also expected that tip progression slowed once blocking occurred. However this was observed in only 2 of the 17 instances. In most instances (11) channel blocking appeared to have no effect on the speed of tip progression, neither before or after blocking. Of the remaining 4 instances each of the three possibilities for before and after blocking were included (slowed down, remained unchanged and sped up). Figure 4.20 shows an example of constant tip progression speed before and after first blockage.

Of the 20 recorded instances of having to raise the head to re-initiate the tip after blocking, 8 resulted in unblocking of the channel (either once or repeatedly in cycles of blocking and unblocking), 7 remained blocked (but still progressed), 4 caused a new tip to form

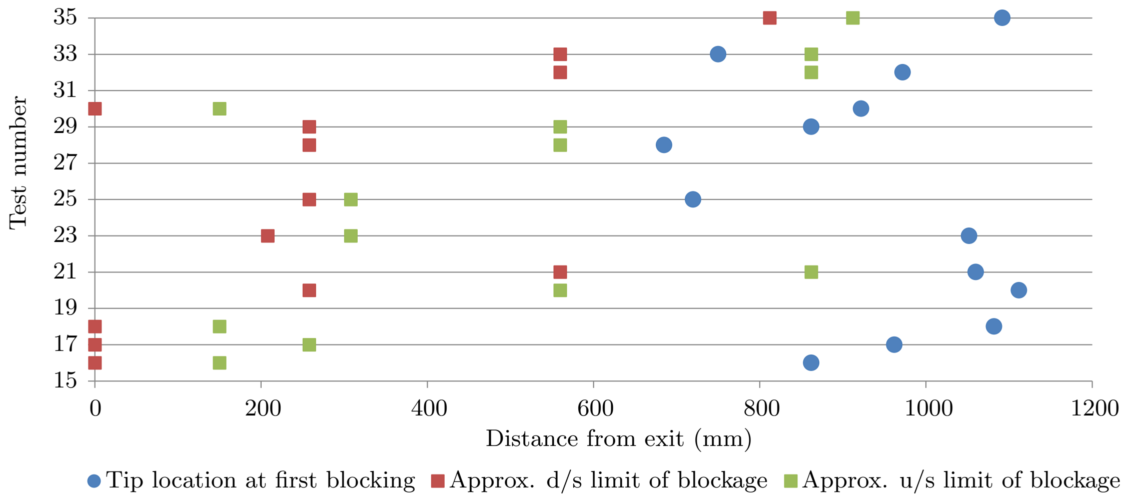

(a) Sydney Sand tests with seepage length of 1.3m

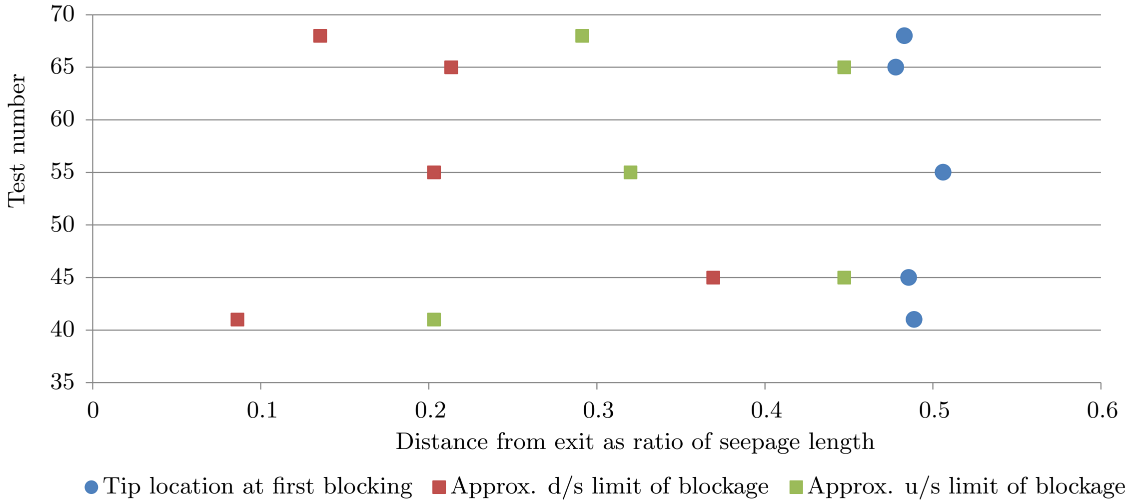

(b) Sydney Sand tests with seepage lengths of 2.6 and 3.9m

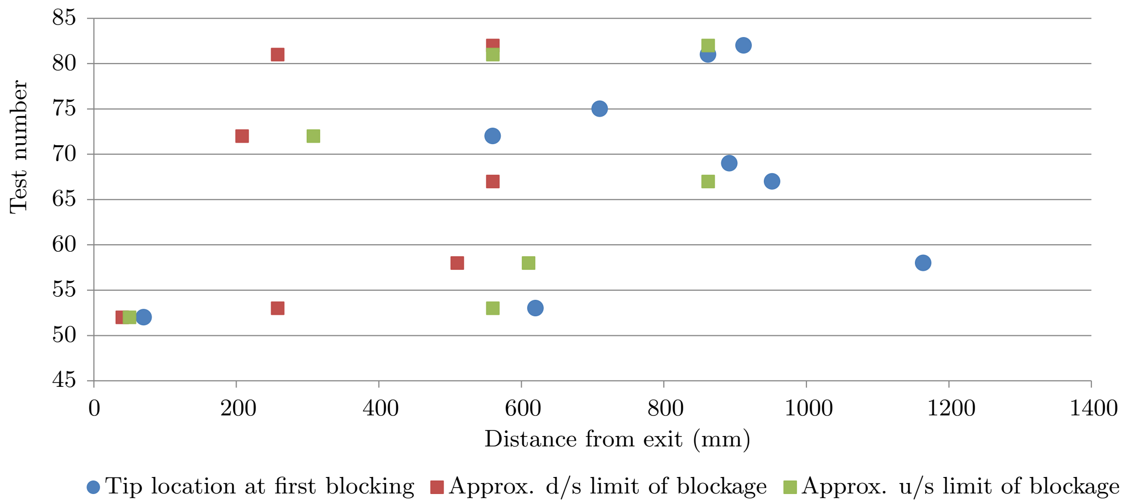

(c) Other soil tests with seepage length of 1.3m

Figure 4.18: Positions of tip when first blockage occurred and extent of blockage

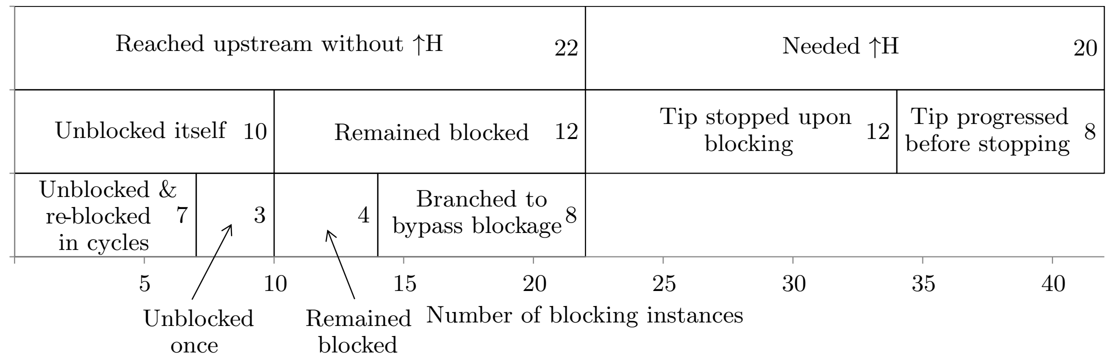

Figure 4.19: Tip and channel response upon blocking

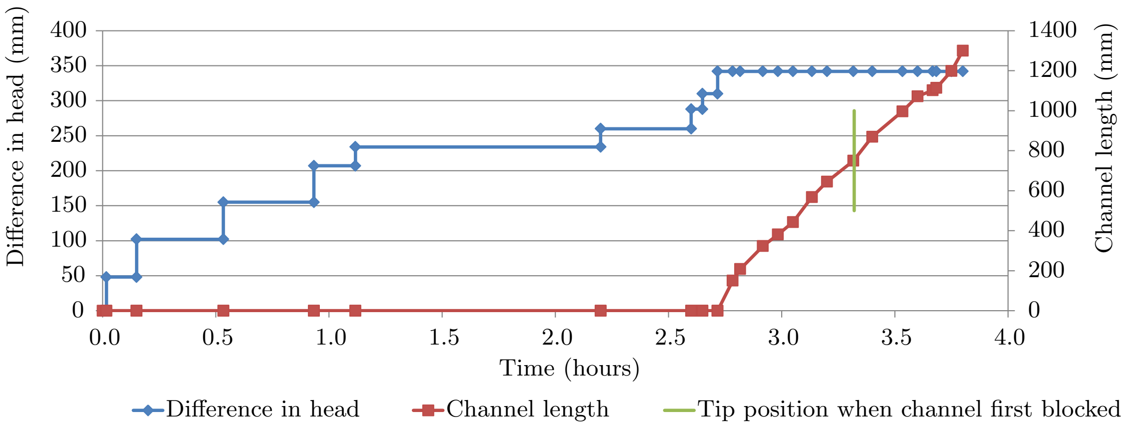

Figure 4.20: Head difference and channel length with time showing constant tip progression speed (line slope) before and after first channel blockage

from branches off the main channel and 1 progressed but then stopped again needing a further increase in head. Therefore, again, there was no clear pattern or typical behaviour as to what occurred when the head was increased when the tip stopped due to blocking.

The length of time allowed for the tip to re-initiate on its own before raising the head ranged from 7 minutes to over a weekend, with most being greater than 30 minutes. Greater than 30 minutes is considered enough time to wait for a tip to re-initiate based on experiment experience.

Raising the head in response to blocking did not always mean the critical head was being increased. Sometimes the head was below critical when it needed raising and didn't need to be raised above critical to re-initiate the tip. Of the 20 recorded instances of having to raise the head to re-initiate the tip, 11 resulted in raising the head above the previous maximum, i.e. resulted in increasing the critical head, and 8 did not (and 1 instance was indeterminate). Amongst the 11 instances that resulted in an increase of the critical head, the critical head was raised between approximately 10% to 60%.

In summary, of the total 42 recorded instances of channel blocking, only 11 (26%) resulted in an increase of the critical head (increases ranging between 10% to 60%).

4.6 Sand boils

In all exit geometries except the slope exit, soil which had been transported out of the channel was deposited outside the exit in such a way that sediment was concentrated into a mound with a column of fluidised particles in its centre. New sediment was added to the mound by being transported up and out of the centre fluidised column. This mound is typically referred to as a sand boil. In some literature it is also referred to as a sand volcano.

Figure 4.21 shows typical examples of sand boils in plane, slot and circle exits. Figure 4.21d shows an example of what the centre column of fluidised particles is likely to look like. It was taken when the boil had moved to the side of the downstream box, being able to do so because it was a slot exit. The sides of the boil formed at the angle of repose of the soil.

Sand boils ranged in size from very small to large enough to fill the entire downstream box which was 450mm by 450mm in plan (**??**). As expected the boil increased in size as the channel lengthened.

There were a number of questions posed in considering the impact of sand boils and their narrative. These questions included:

1. Did boils add to erosive resistance? In other words, could a tip which had stopped be reactivated by removing the boil instead of raising the head? Did removing boils keep the head from being raised, resulting in a lower critical head?
2. Did particle sizes of boiled material reveal a disproportionate representation of eroded soil? In other words, when well graded soils were tested, were larger particles not in early boils, indicating a head larger than the initiation head was needed to transport larger particles? Were the largest particles transported out at all?

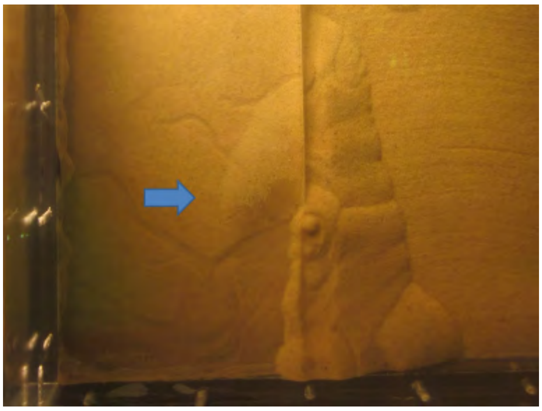

(a) Plane exit (Test 30)

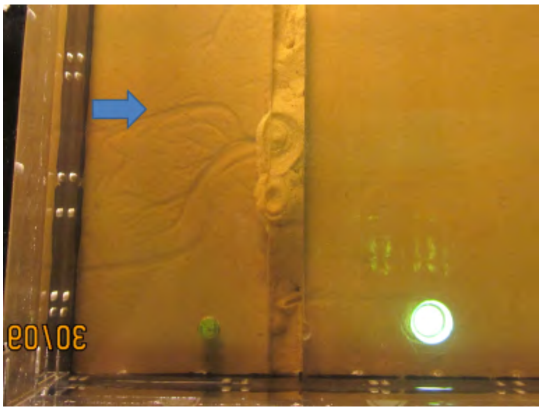

(b) Slot exit

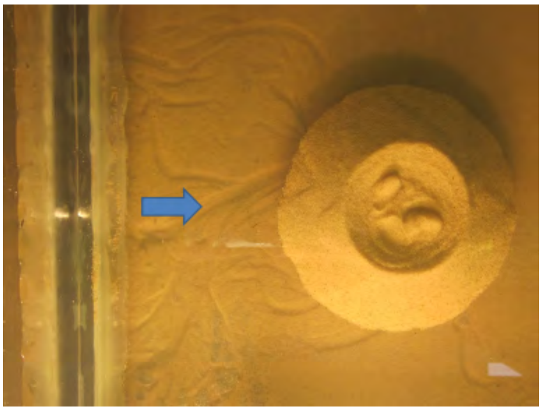

(c) Circle exit (Test 20)

(d) Slot exit- showing centre shaft of boil (Test 68)

Figure 4.21: Sand boil examples (blue arrows indicate direction of flow)

3. Did boils increase in size for successive fixed-length channel segments?

4. Could boil-volume be used to infer channel geometry?

5. Could boil-volume be used to estimate the portion of primary to secondary erosion?

6. Did boiling re-commence at lower heads for each successive loading cycle?

Question 6 is addressed in Subsection 9.2.1 on Group 5 cyclic-loaded test results. The rest of the questions are addressed in turn below.

These questions were addressed by routinely removing sand boils during tests. In Tests 53 (Mix 3) and 58 (Mix 5) the sand boil was collected each time the tip stopped. The boil material was then dried and sifted to assess particle sizes.

In Tests 65 and 68, which were both double-flume tests in Sydney Sand, the boiled material was pushed away from the slot exit but left inside the downstream box. In Test 65 it was pushed away only towards the end of the test when the tip had been stationary for an long time and the head had already been raised significantly. In Test 68, the boil was pushed away more frequently, especially before raising the head or when boiling stopped. Boils in Test 69 (Mix 7) were also pushed away before raising the head or when boiling stopped. In all these tests the times when boiled material was moved was recorded.

Boiled material was also pushed away from the exit in Tests 71, 73, 74 and 75 however the reasons for, and times of, removal were not recorded (the only record is photos showing the boil pushed aside).

Group 5 cyclic tests, Tests 77, 79 and 80 in Sydney Sand and Tests 81 and 82 in Mix 6, had their boils removed and collected between each loading cycle, i.e. after each 130mm-long channel segment. These boils were dried and weighed but not sifted.

Erosion resistance of boils

In order to determine whether sand boils added to erosion resistance, tests which did and didn't have boils removed are compared in Figure 4.22. Tests shown in grey did not have boils removed.

Sand boils were considered to resist erosion if, when a boil was removed, the channel progressed at heads lower than heads needed in tests without boil removal. In other words, if the coloured lines were below the grey lines in Figure 4.22. As can be seen, the channel in Tests 68 and 69 progressed at heads slightly lower than tests with no boil-removal (coloured slightly lower than grey) whereas in Test 53, the channel progressed at heads slightly higher than tests with no boil-removal (coloured slightly higher than grey). Therefore, there is no clear indication as to whether sand boils resist erosion, but if they do, the increase in critical gradient they cause is no more than 10%.

Test 65 (in Figure 4.22a) was an exception. When the channel was 83% of the seepage length, boiling action in the centre of the boil stopped and the tip stopped progressing. It is likely boiling action stopped because the height of the boil had become too tall for fluidisation to be maintained for its full depth. As a result of discontinued boiling, more

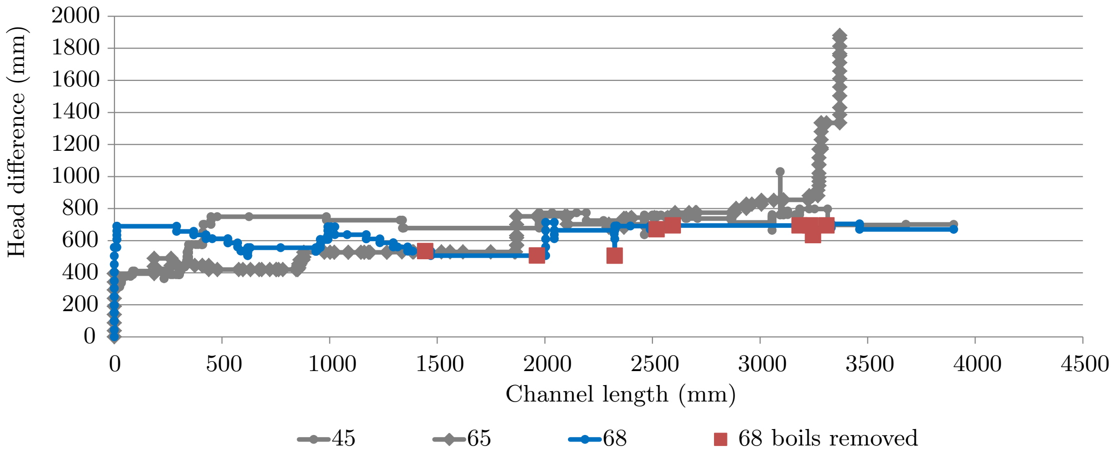

(a) Sydney Sand tests with 3.9m seepage length

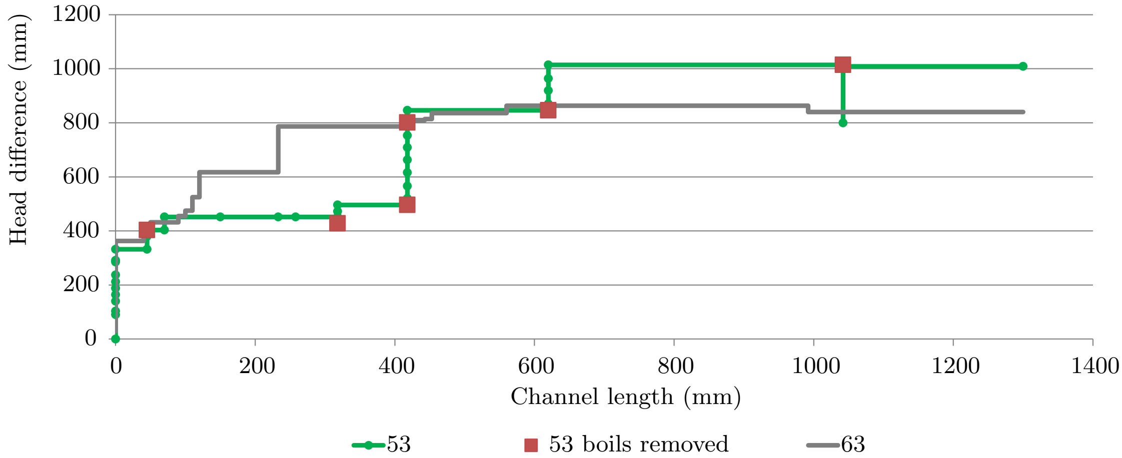

(b) Mix 3 tests

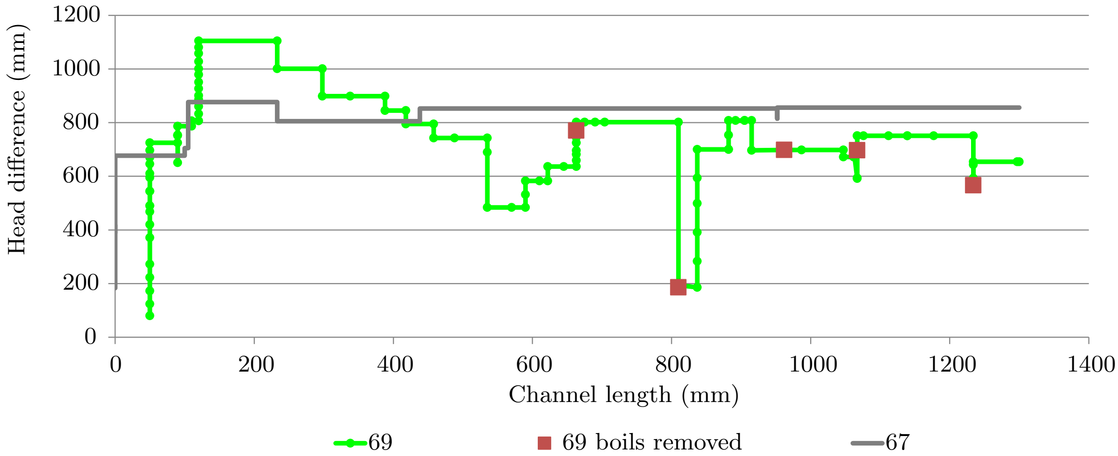

(c) Mix 7 tests

Figure 4.22: Comparing tests with and without boil removal

head loss was now occurring at the exit, hence reducing the gradient along the flume. Therefore, it appears sand boils are capable of resisting erosion if they become tall enough that the weight of the soil column through the centre becomes heavier than the pore pressure beneath it.

Selective particle-size erosion

Figure 4.23 is a particle size distribution of boiled material from Test 53. It shows that boil material did reveal a disproportionate representation of eroded soil. The first boil was missing 40% of the particles larger than 1mm and no particles larger than 2.36mm where present (which makes up 20% of Mix 3).

Each successive boil contained more of the larger fractions, although boils 2 and 3 did not contain any particles larger than 2.36mm. By boils 4, 5 and 6, all particle sizes were included, just less of the larger sizes. Interestingly the boils which contained all sizes (4, 5 and 6) were collected when the head was either at or above critical head (see Figure 4.22b). This suggests the critical head is needed to transport all particle sizes and perhaps this is what determines the critical head (but this theory would only stand for well graded materials- all sizes of uniform soils were transported at heads lower than critical).

Also of interest is the size distribution of boils 2 and 3 and boils 4 and 5 were similar and that both of these sets of boils were collected at similar heads (again see Figure 4.22b). This suggests that the particle sizes eroded is related to the head applied.

Unfortunately boiled material from Test 58 was not sifted so Figure 4.23 of Test 53 is the only data on particle sizes of boiled material available.

Increasing boil size

It was evident that sand boils grew in size as channels lengthened. This was expected because for the channel to lengthen, more sediment needed eroding, adding to the size of the boil. However, what was also of interest was whether the sand boil increased in size for successive fixed-length channel segments. This was of interest because Glynn

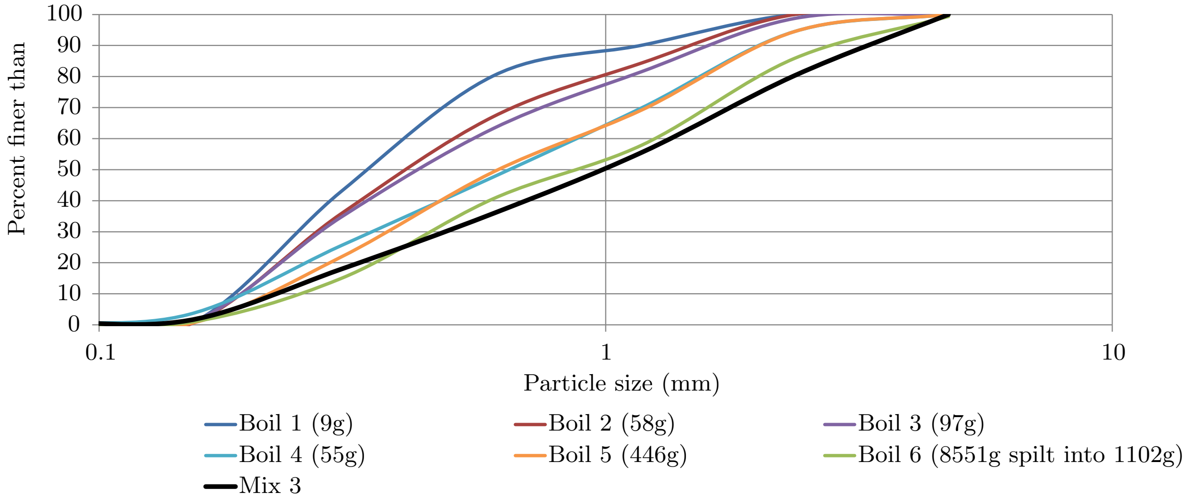

Figure 4.23: Particle size distributions of boiled material- Test 53

and Kuszmaul (2004) reported an increase in the size of sand boils (downstream of Mississippi River levees) with subsequent floods even when subsequent floods were lower. The author's hypothesis was sand boils increased in size with subsequent floods, regardless of the relative levels of floods, because the channel formed in the previous flood remained under the dam/levee; the new flood lengthened the channel, exposing more channel sides/bed to scour, and hence more scoured sediment was transported to boils (so larger boils). To test this hypothesis, sand boils were collected, dried and weighed after each 130mm long channel segment (in the Group 5 cyclic tests only). If it could be shown that the sand boil increased in size with each 130mm long channel segment, then this hypothesis would be supported.

Figure 4.24a is a plot of the sand boil weights once dried for Sydney Sand tests. Also plotted is the length of the segment of channel which preceded each sand boil. The intention was to keep each channel segment 130mm long but factors such as positions of the restraining bars and timing meant that segment lengths were not always exactly 130mm. On first inspection it appears that the sand boils both increased and decreased, exhibiting no overall trend. However, it can also be seen that sand boil size was sensitive to the channel segment length. Therefore, the sand boil weight was expressed as a ratio of the channel segment length to standardise it. The result is Figure 4.24b (with one outlier removed: a boil from Test 79 at 1102mm with a ratio of 2). It's possible there was a slight increasing trend in this plot, however the trend is disputable. The results show that successive sand boils will not always increase in size and if they do, the increase will only be slight. Though it is possible that increases in sand boil size may be more apparent at the field scale.

Figure 4.25 is a plot of the sand boil weights once dried, for Mix 6 tests. It is plotted as a ratio of the channel segment length against total channel length. As with the Sydney Sand results, it is possible there is a slight increasing trend, however the trend is not clear and there are some exceptions.

One of these exceptions is the first point of Test 81 at a channel length of approximately 190mm and a boil mass to segment length ratio of 0.32, which despite being the first boil is almost the largest boil to segment length ratio. This data point is called into question because the recorded mass was 37g even though a) all other first boils were between 2-11g, b) the channel segment when the boil was removed was much shorter than all other tests (170mm where others were around 300mm) c) it doesn't look like 37g worth- see Figure 4.26 and d) when 37g was used to infer a channel width (using the method described previously) widths of between 25 to 128mm were achieved which are unrealistically wide.

In summary, it is possible there is a slight increasing trend in boil size with successive fixed-length channel segments. However, the trend is not clear and there are exceptions. The apparent increasing trend is not significant enough to identify with certainty. Therefore, boil sizes with successive fixed-length channel segments were not able to conclusively explain the Glynn and Kuszmaul (2004) observation of larger boils in subsequent floods.

Channel geometry inferred by boil-mass

Mass of the boiled material could be used to estimate the cross-sectional area of the channel if assumptions regarding the density of the soil were made. Table 4.1 is an example of this estimate using boil masses from Test 77. It was assumed that sand in boils was at the minimum dry density of 1.475 x 10^{-3}g/mm^3 (determined from the minimum dry density test according to AS1289 5.5.1) and sand in the sample, before it was eroded out through the channel, was at a uniform density of 1.6 x 10^{-3}g/mm^3 (a density close to the maximum density of 1.64 x 10^{-3}g/mm^3). It was also assumed that the first boil was missing 18g of sand because sand which had accumulated in the 25mm

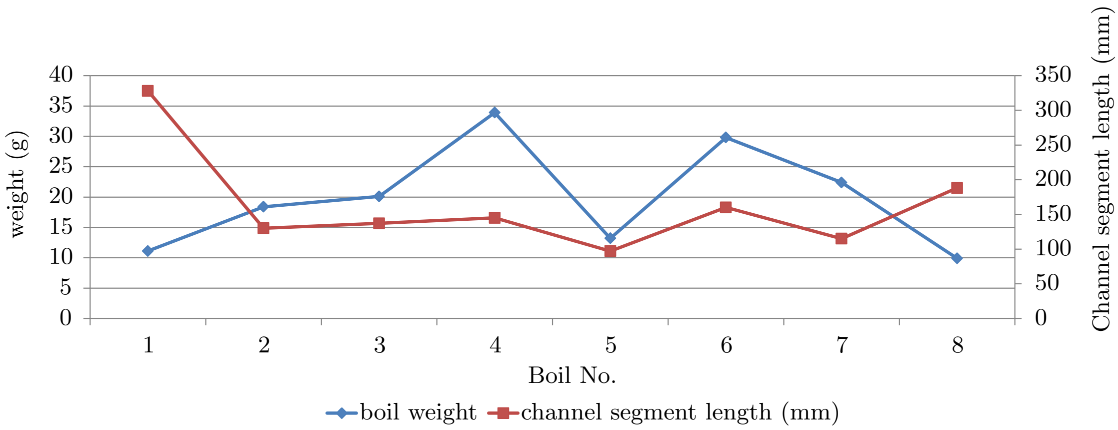

(a) Dry mass of sand boils removed from Test 77 with channel segment lengths

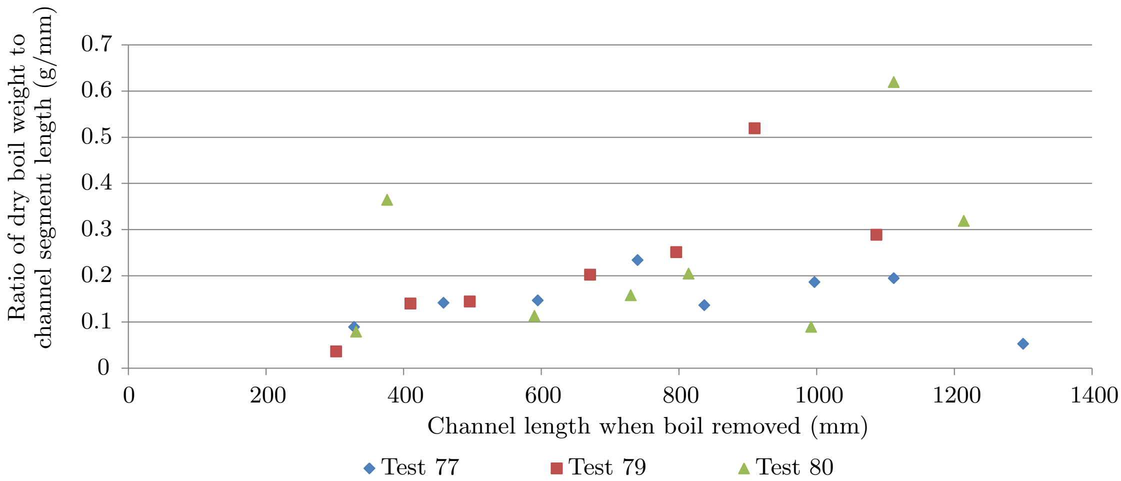

(b) Dry mass of sand boil as a ratio of channel segment length with total channel length

Figure 4.24: Mass of sand boils taken from cyclic loading tests on Sydney Sand

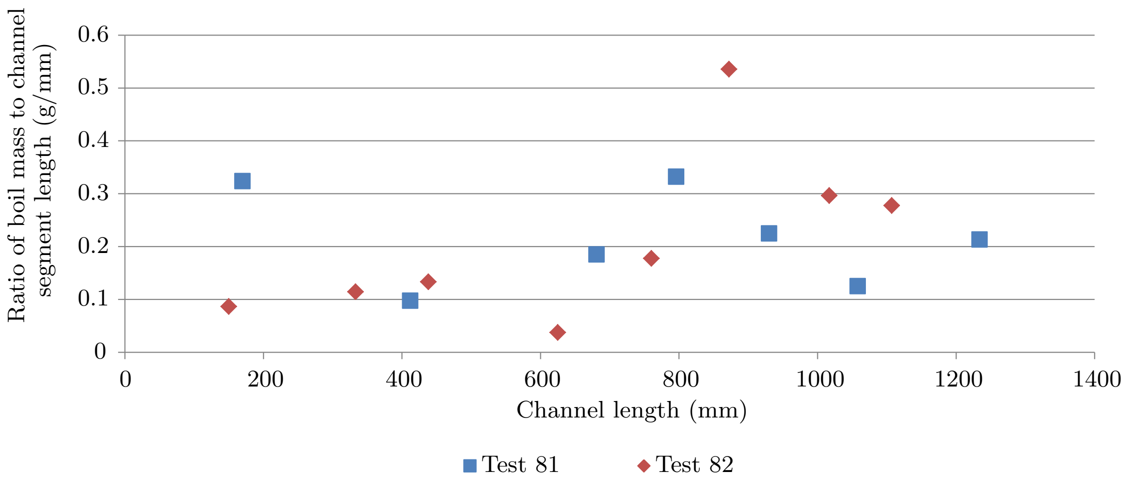

Figure 4.25: Dry mass of sand boil as a ratio of channel segment length with total channel length for Mix 6 tests

Figure 4.26: First boil prior to removal- unlikely to be 37g

tall hole shaft had been left behind.

Table 4.1: Channel cross-sectional areas estimated using boil masses from Test 77

boil	boil mass (g)	cumulative boil mass (g)	volume (mm^3)	segment length (mm)	cumulative length (mm)	channel area (mm^2)
1	11.1	29.1	18188	328	328	55.4
2	18.4	47.5	29688	130	458	64.8
3	20.1	67.6	42250	137	595	71.0
4	33.9	101.5	63438	145	740	85.7
5	13.2	114.7	71688	97	837	85.6
6	29.8	144.5	90313	160	997	90.6
7	22.4	166.9	104313	115	1112	93.8
8	9.9	176.8	110500	188	1300	85.0

Table 4.1 shows the channel's cross-sectional area to increase over the first 4 boils and then remain around an average value of 88mm^2. This increase in channel area is most likely due to secondary erosion as discussed in the next section.

Whilst these cross-sectional areas did not explicitly provide the channel's width and depth, they were compared to measured widths and depths to provide a basic 'sanity check'. Measured channel widths (plotted in Figure 4.10a) had an average width of 13mm with a standard deviation of 7mm. If it was assumed that the channel was rectangular (even though a trapezoidal shape was more likely, as discussed in Subsection 4.5.1) then the calculated channel area divided by the average width of 13mm gave channel depths of between 4–7mm in Test 77, 11–15mm in Test 79 and 4–9mm in Test 80. Actual measured depths ranged between 1.5 to 6mm (presented in Subsection 4.5.1). Whilst these inferred and measured channel depths did differ, they were considered close enough to verify the calculated channel areas were sensible (especially considering the extensive assumptions and simplifications required to arrive at these inferred depths).

4.7 Standpipe levels

Water levels in standpipes were used to measure pressure head through the sand as well as next to and/or within the channel (if the channel occurred directly beneath a standpipe). Standpipe water level records are included in Appendix A.

These water levels appropriately rose and fell as the upstream head was raised and dropped. They also demonstrated the expected successive head loss as water seeped through the sand. Figure 4.27 shows an example of water levels successively dropping along the flume from upstream to downstream.

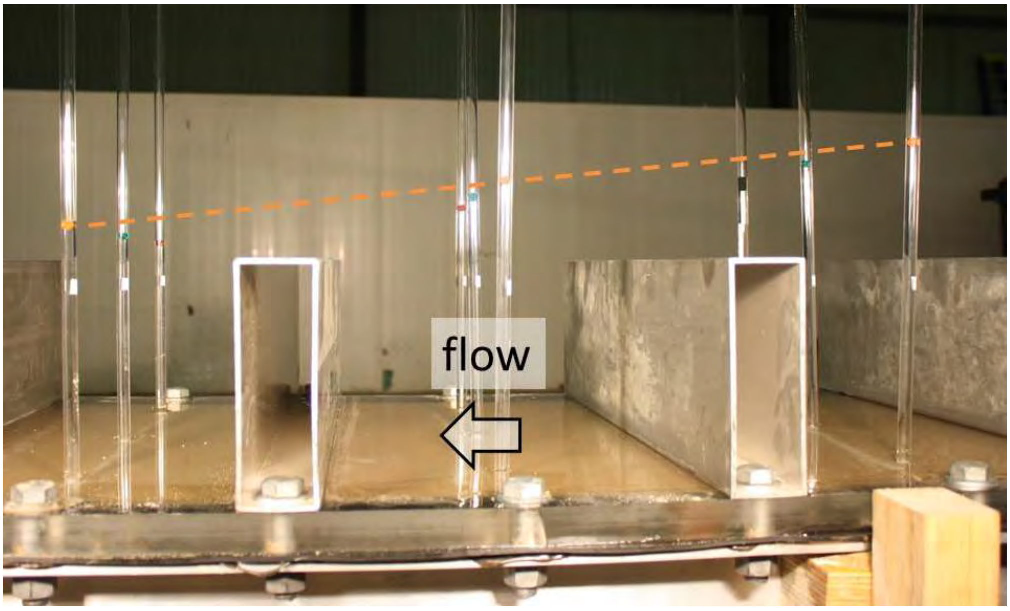

Figure 4.27: Example of water levels in standpipes successively dropping due to head loss through sand (Test 46)

When a channel positioned itself beneath the base of a standpipe the water level dropped. This demonstrated that head loss along the channel was less than head loss though the sand thereby causing head in the channel to be closer to the downstream head. The distance by which the water levels dropped varied but could be characterised as falling between 5–20% of the pre-channel water level. Figure 4.28 is an example of the water level dropping due to a channel, including both a photo showing the channel positioned beneath the left-hand-side standpipe in the 2nd row and a chart of the standpipe water levels at that time.

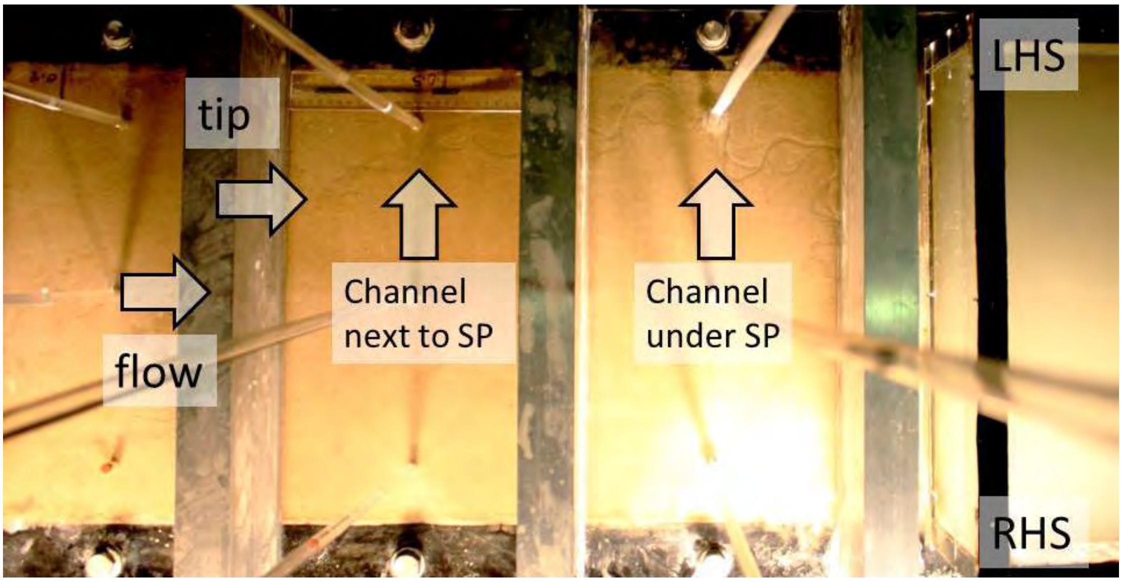

(a) Photo

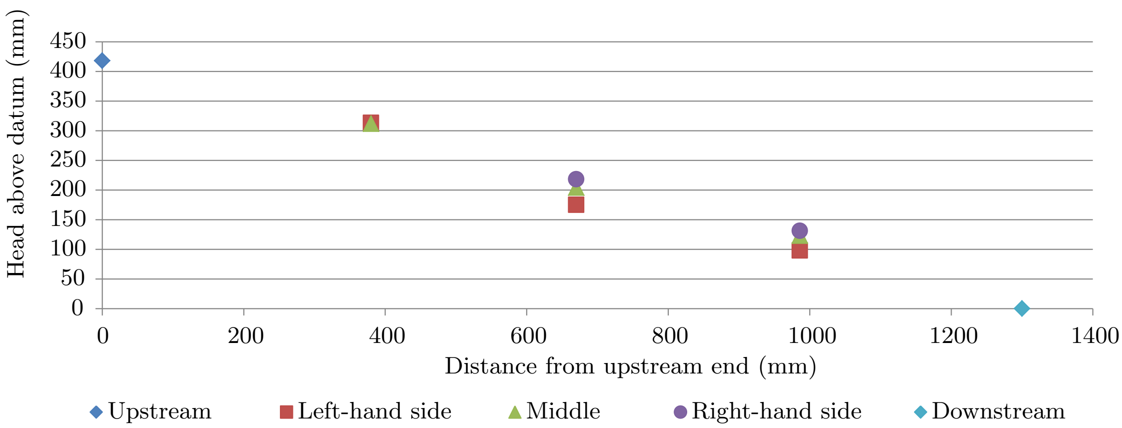

(b) Standpipe levels plotted with distance from upstream end

Figure 4.28: Example of water levels in standpipes when channel positions itself beneath a standpipe

During forward deepening, when the deepened channel positioned itself beneath a standpipe the water level rose. This again demonstrated the small degree of head loss through the channel. It also demonstrated that the deepened channel was 'linked' to the upstream end and brought a higher head directly through the flume thereby increasing the gradient in the regular channel and surrounding soil downstream of it. Figure 4.29 is an example of the raising standpipe levels due to a deepened channel.

On two occasions, namely Test 58 and Test 71, non-linear standpipe levels revealed unusual behaviours which were interpreted as gravel blocking the exit and an indicator of suffusion as described in their respective Subsections 8.2.5 and 8.2.1. The non-linear levels in Test 71 are shown in Figure 8.3.

Standpipe levels were also used to calibrate the numerical model. This is discussed in Chapter 10.

4.8 Soil density

As explained in Subsection 3.4.4, three different methods were used to measure the density of the soil, the 'can', 'total sand' and 'push tubes' methods.

Soil densities found using the can method were found to be 12.8, 14.3, 14.1 and 14.5kN/m^3 for Tests 1, 2, 7 and 12 respectively, and are plotted on Figure 4.30. These results were considered unreliable since they are less dense than the minimum density determined in a NATA accredited soils laboratory tested to AS1289 5.5.1 of 14.47kN/m^3. This is not to say that the sand density in the can couldn't be less than the minimum found by AS1289 5.5.1, it could be, it just seems unlikely given the larger mass and fall height of rained-in sand compared to the method used to obtain loose sand in AS1289 5.5.1.

Of the 13 soil densities found using the 'total sand' method (plotted on Figure 4.30), 10 were more dense than the maximum density found by a NATA accredited soils laboratory using test standard AS1289 5.5.1 (of 16.13kN/m^3). It is unlikely sand in the flume was more dense than soil prepared according to AS1289 5.5.1. Therefore, these density results are likely to be incorrect. The most probable reason for this error is the volume of the flume. The density calculation is quite sensitive to the flume volume and yet it is difficult to measure it accurately. The flume walls expand and distort slightly which would increase the volume enough to alter the density calculated.

Soil densities found using the push tubes ranged from 14.9 to 15.4kN/m^3 and are plotted on Figure 4.30. These densities are more likely than those found using the 'can' and

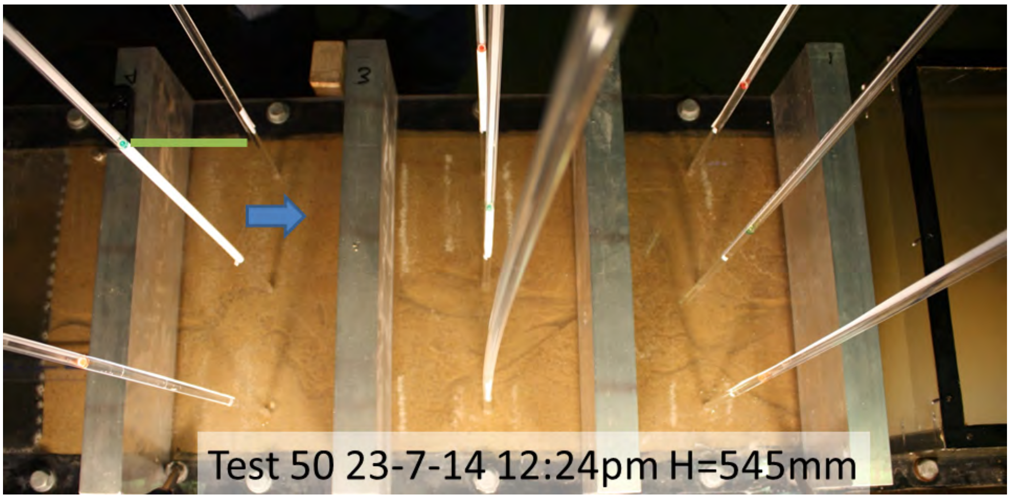

(a) Test 50 23-7-14 12:24pm H=545mm

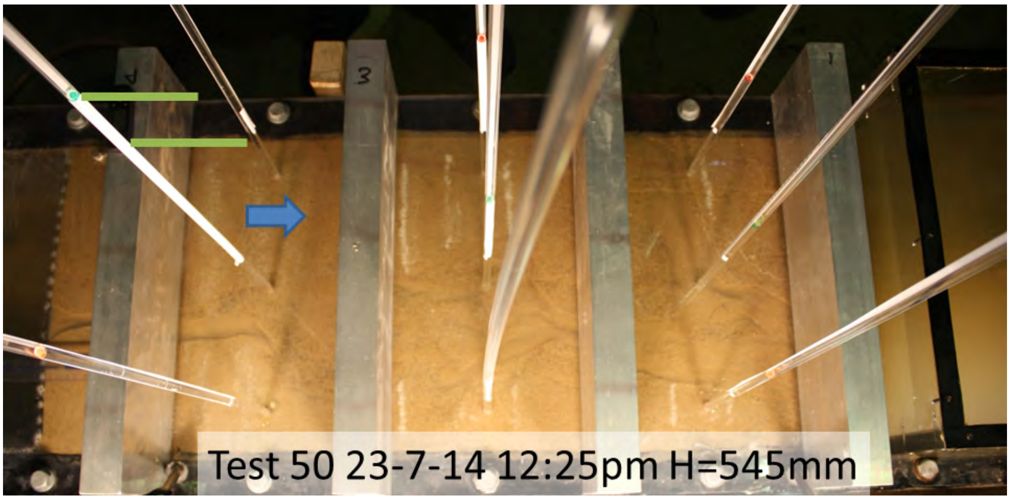

(b) 1 minute after (a)

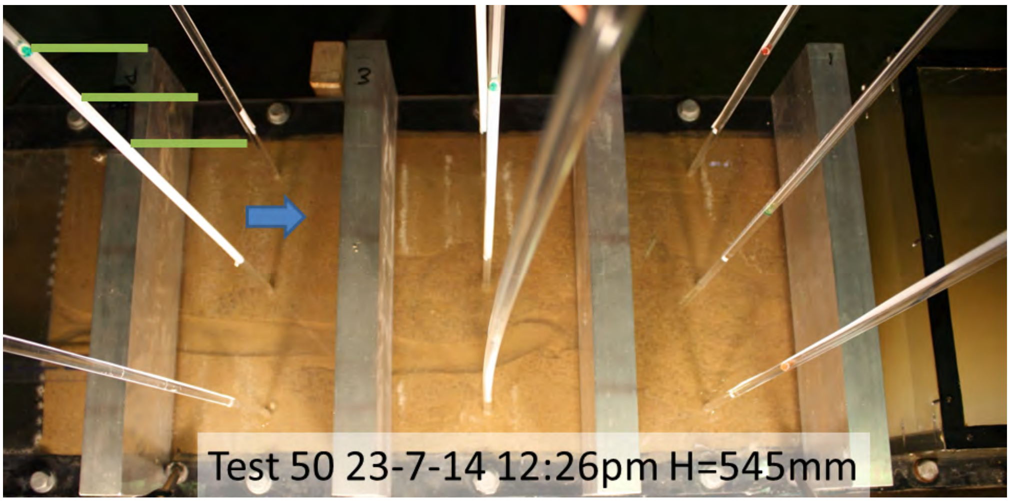

(c) 1 minute after (b)

Figure 4.29: Example of water levels in standpipes rising during forward deepening, indicated by green lines (blue arrows indicate direction of flow)

'total sand' methods as they are in between the minimum and maximum densities found using AS1289 5.5.1. However, no difference in density can be seen between the different soil placement methods even though it was expected that densities would increase in the order of 'rained in', 'vibrated' and 'vibrated & tamped'. This suggests that perhaps the 'push-tube' density-measurement method still lacks accuracy. This and the range of variable densities found within one test (see range of results for Tests 45, 46 and 49).

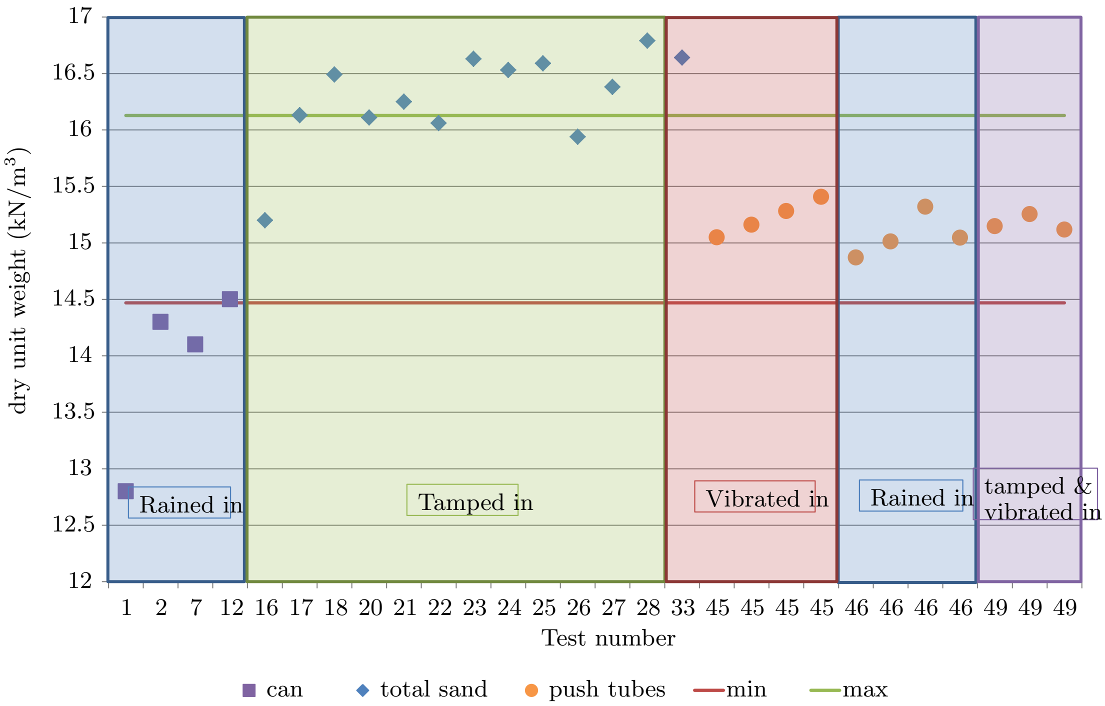

Figure 4.30: Dry unit weight of soils

It's noted that once the bladder is deflated and the lid removed, the sand would expand slightly and no longer be at the same density it was during the experiment. Therefore, it is likely that densities measured were less than the density during testing and so measurements are taken as lower-bound estimates.

It is acknowledged a sand cone test (according to AS1289.5.3.1) could have been used instead of the push-tubes however, sand cone tests were considered to give no significant advantage over the push-tubes. This was because the sand cone testing also needed the bladder to be deflated and the lid to be removed, hence allowing the sand to expand from its tested state. Therefore, both methods were unable to test the density of sand contained in the flume during backward erosion.

Considering the inaccuracies, these results have only been used to give an indication of

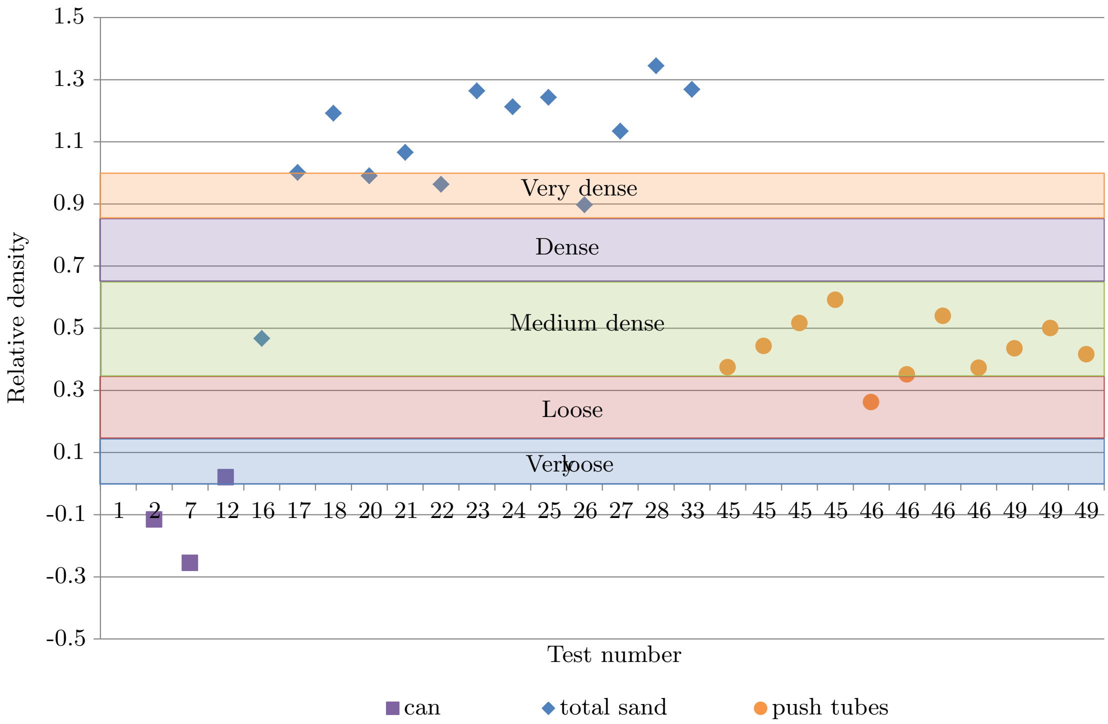

Figure 4.31: Relative density of soils

probable density range and density classification (as opposed to precise densities). If the dry unit weights are converted to void ratios (assuming a specific gravity of sand particles of 2.65) and compared with the minimum/maximum densities found using test AS1289 5.5.1., then relative densities can be plotted, as shown in Figure 4.31. With AS1726 classifications of density (based on relative density) shaded over Figure 4.31 it can be seen that 'push tube' results lay within the loose and medium dense classifications. Also, if the fact that dilation when the bladder was deflated and lid removed would have occurred, then it is considered sand would likely have been within the medium dense to dense classifications during testing.

4.9 Flow rate

Total flow through the flume was measured by either timing how long it took to fill a beaker whilst the head was at 100mm or recording the weight of a 60L container capturing the downstream outflow every minute with digital scales connected to a laptop. These methods are described in more detail in Subsection 3.3.7.

To firstly consider flows through Sydney Sand, Figure 4.32 shows flows ranged between $1.3\text{x}10^{-6}\text{m}^3/\text{s}$ and $8.5\text{x}10^{-6}\text{m}^3/\text{s}$ when the head difference was 100mm. It also shows flow was not influenced by exit geometry, except that perhaps the plane exit was more likely to produce larger flows.

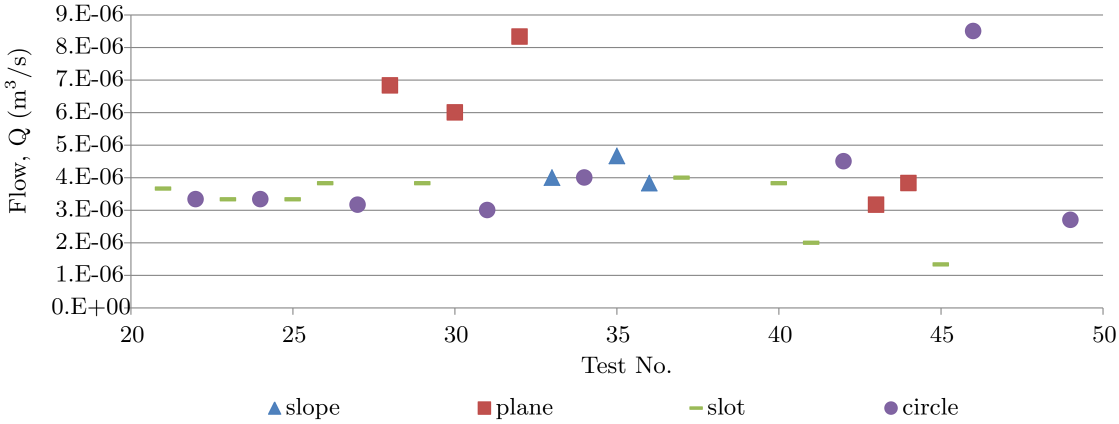

Figure 4.32: Total flow through flume containing Sydney Sand when H=100mm

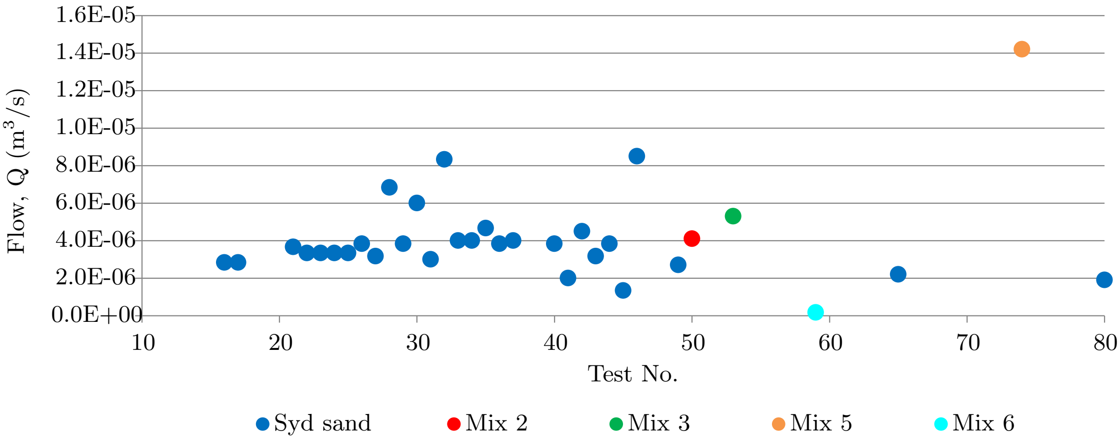

Figure 4.33: Total flow through flume when H=100mm

Total flow was measured in only four tests other than Sydney Sand when the head difference was 100mm. These four points are added to Figure 4.33 which shows Mix 5 to be the most permeable, permitting a flow of $1.4\text{x}10^{-5}\text{m}^3/\text{s}$ and Mix 6 to be the least permeable amongst the flow records (at H=100mm) permitting a flow of $1.7\text{x}10^{-7}\text{m}^3/\text{s}$. It also shows Mixes 2 and 3 permitting slightly higher flows than the average Sydney Sand flow, at $4.1\text{x}10^{-6}\text{m}^3/\text{s}$ and $5.3\text{x}10^{-6}\text{m}^3/\text{s}$, as expected.

Flow data from Group 5 tests loaded with the 'above critical' loading procedure provided the opportunity to observe any changes in flow without influence from changes in head (because the head was kept constant). The flow data, plotted in Figure 4.34a, shows that flow increased during the experiment, whilst head was kept constant at the labelled heights.

This increase in flow as the channel progressed was also observed in experiments with loading procedures of 'decrease at points of interest' and cyclic loading as can be seen in Figure 4.34b. As head difference was varied in these tests (and flow is proportional to head difference), the flow had to be expressed as a ratio of the head difference. Test 80 was an exception to the trend which actually *decreased* as the channel progressed. It is not known why this is, but Test 80 has been considered erroneous previously, as discussed in Subsection 9.2.1.

Furthermore, this increase in flow as the channel progressed was observed in experiments other than Sydney Sand as can be seen in Figure 4.34c. It was helpful to standardise the flow with head difference ratio against the soil's permeability to superimpose the data.

This increasing total flow with channel length suggests the channel increased the bulk permeability of the sample as it progressed. It is conceivable that this increase in bulk permeability with increasing channel length resulted in more flow entering the channel tip/bed and therefore required less head to maintain channel progression. However, the increase in flow was only slight and given the variability of backward erosion testing, it would have been difficult to observe and quantify this slight effect.

Total flow continued to increase slightly once the tip reached the upstream end during forward deepening. Examples are shown in Figure 4.35. Flow in Figure 4.35a increased only very slightly because it was Mix 7 whose permeability was relatively small and the scales lacked the sensitivity required.

This slight increase in flow during forward deepening has been attributed to the same reason that flow increased during tip progression- that the channel, now forward deepening, was increasing the sample's bulk permeability.

Upon failure, the flow would suddenly jump significantly, examples of which are shown in Figure 4.36. This jump in flow occurred because removal of the top layer of sand (across about 1/3 of the flume's width) resulted in a flow regime more like pipe flow rather than seepage flow (as water was now free to flow along the top of the sample). Figure 4.37 is photos only 3 minutes apart, either side of failure, showing the large increase in flow.

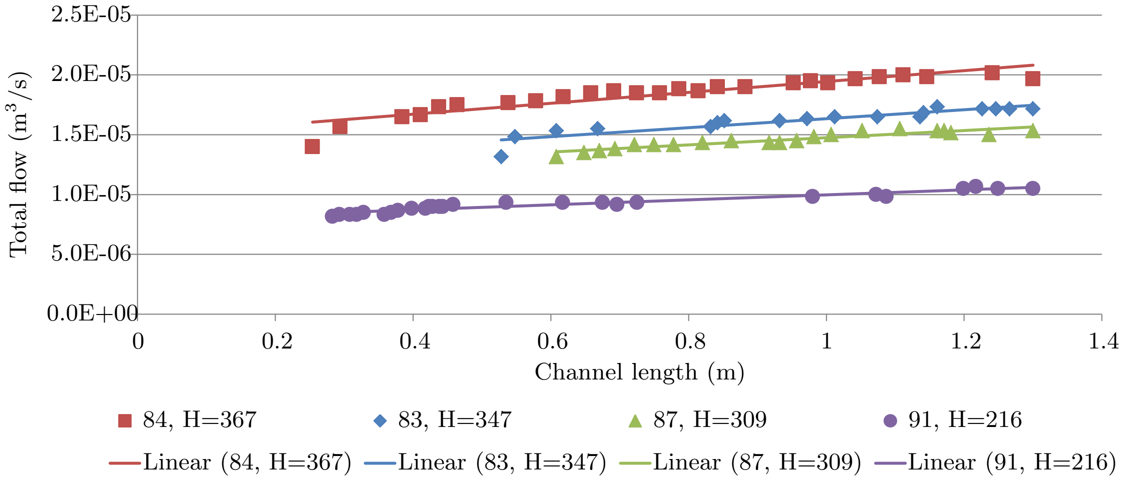

(a) Above critical loading (with constant head) on Sydney Sand

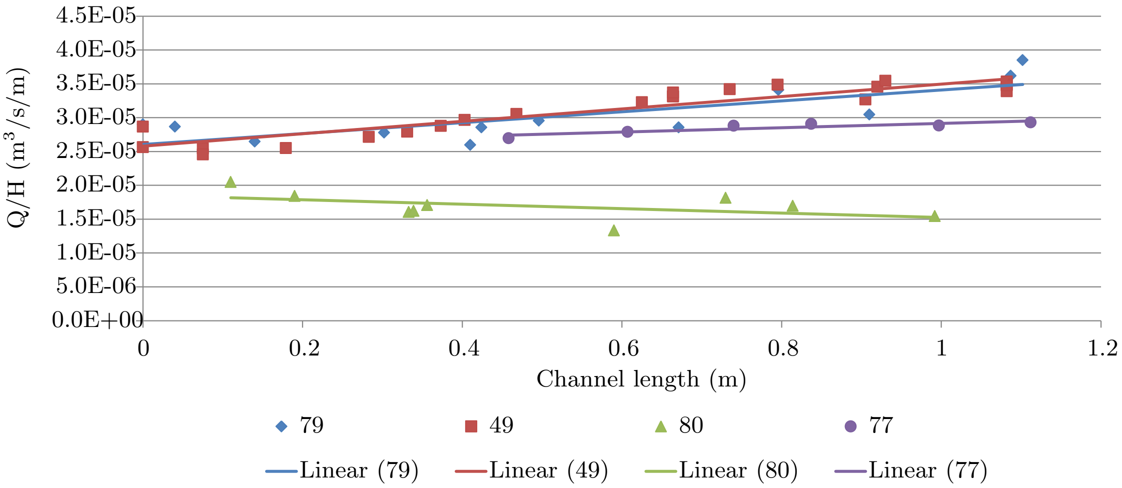

(b) Decrease at 'points of interest' and cyclic loading on Sydney Sand standardised against head difference

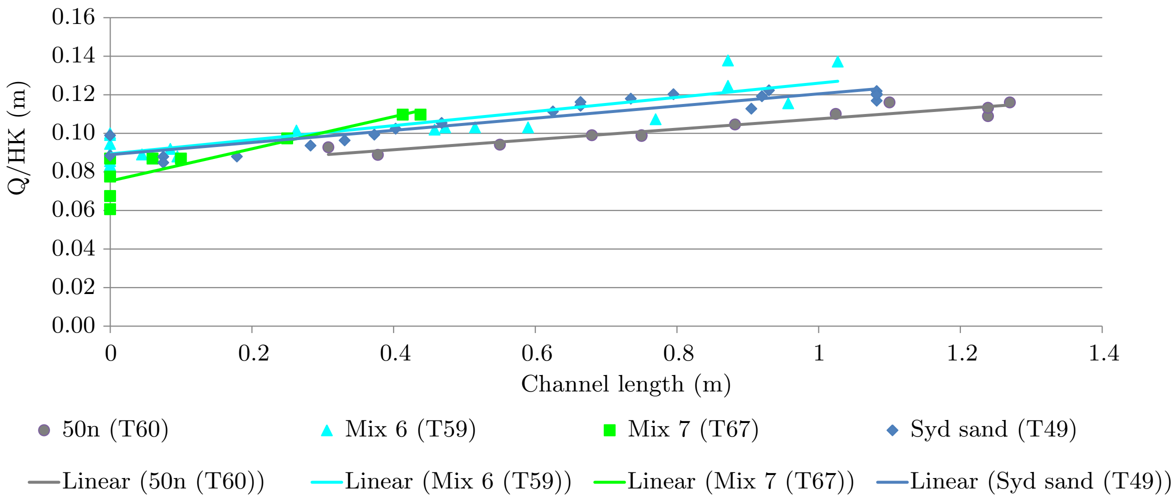

(c) Decrease at 'points of interest' on various soils standardised against head difference and permeability

Figure 4.34: Total flow with channel length

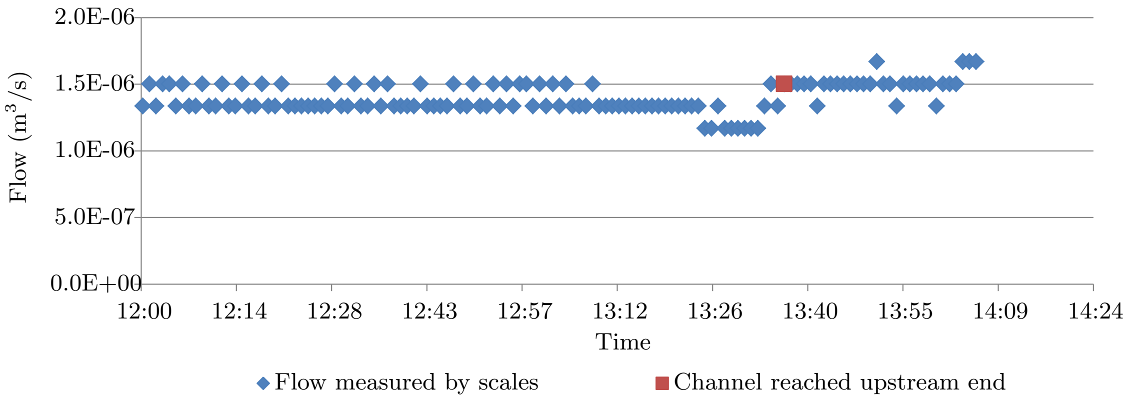

(a) Test 69 (Mix 7)

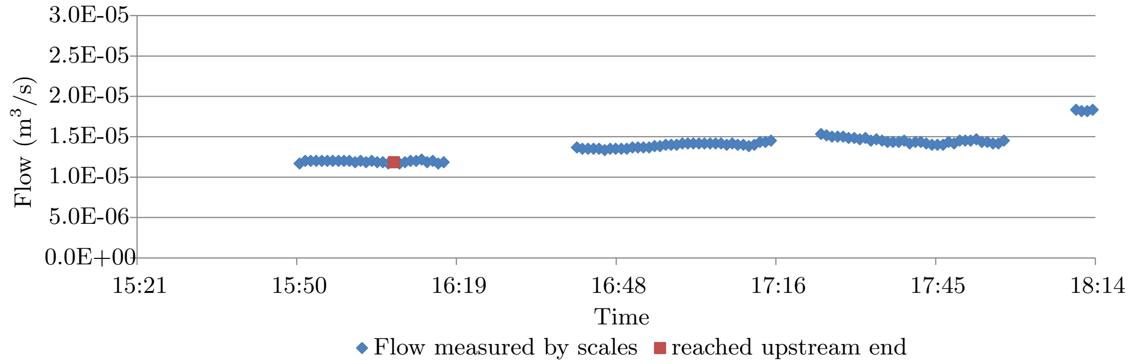

(b) Test 92 (Sydney Sand)

Figure 4.35: Flow during forward deepening (head kept constant)

Often, once failure had occurred, the bilge pump inside the constant head tank could be heard running dry. This meant that the flow rate through the experiment after failure was often larger than the flow rate into the constant head tank.

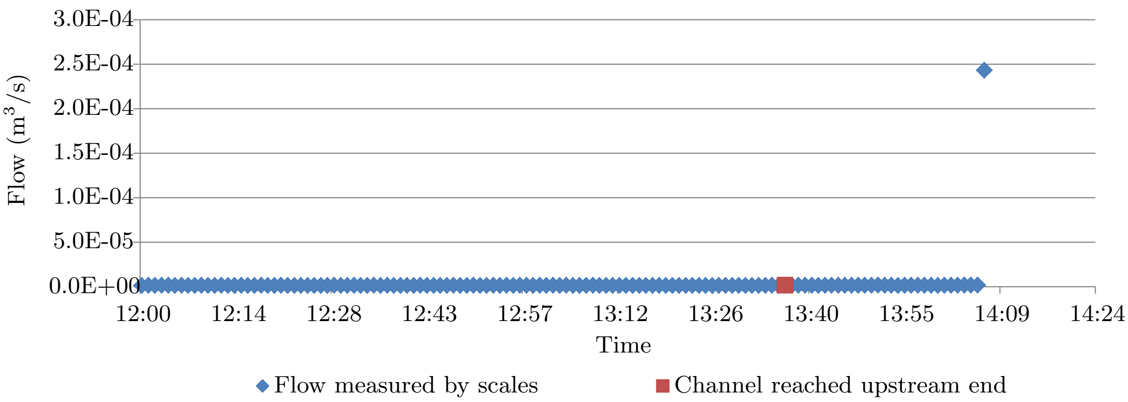

Figure 4.36: Sudden jump in total flow at failure: Test 69 (Mix 7)

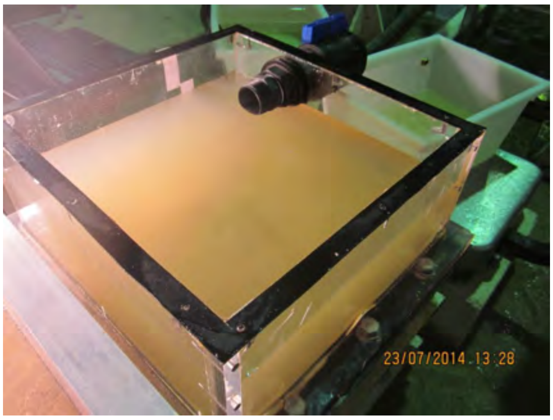

(a) Flow before failure

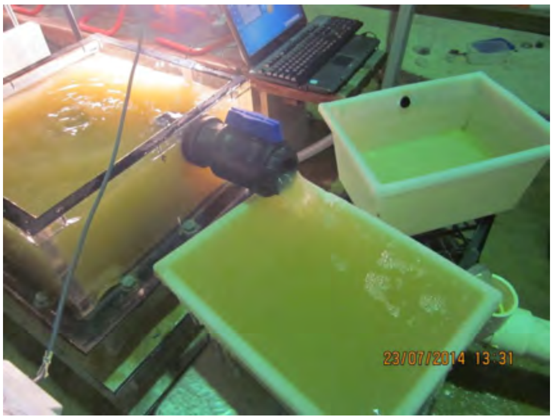

(b) Flow after failure

Figure 4.37: Photos 3 minutes apart showing increase in flow after failure (Test 50)

4.10 Soil permeability

Coefficients of permeability measured in various Sydney Sand tests are plotted in Figure 4.38 according to the different methods of measurement used (methods are described in Subsection 3.4.5).

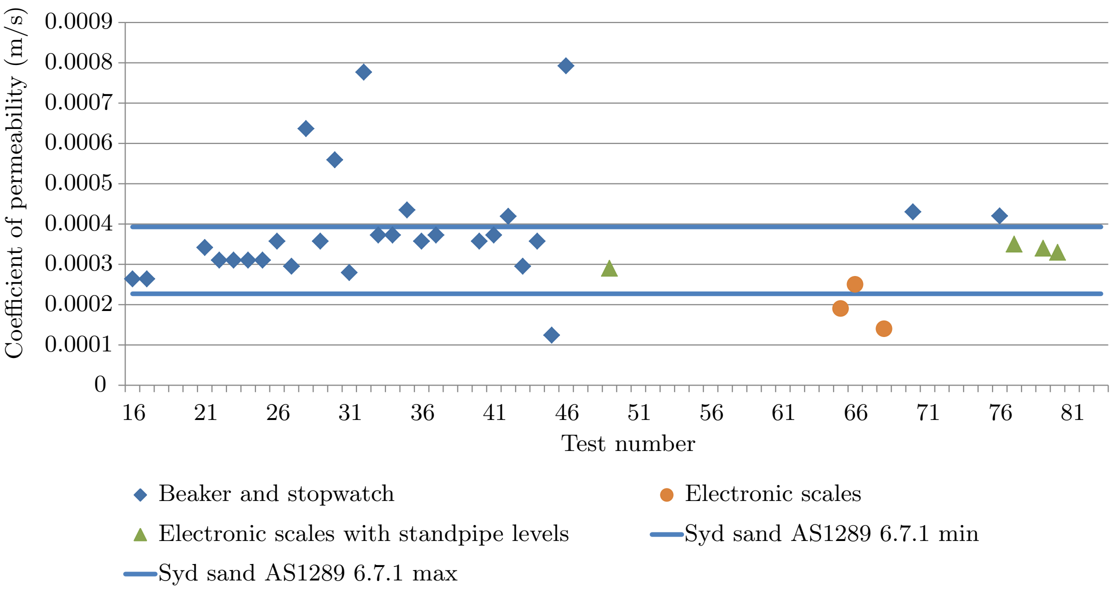

Figure 4.38: Permeability of Sydney Sand with method used

Figure 4.38 shows that 30% of the permeability coefficients were either greater or less than the minimum and maximum permeabilities obtained by the NATA accredited soils laboratory, according to AS1289 6.7.1 permeability testing. It is unlikely that permeabilities outside the minimum/maximum range defined by AS1289 are correct. This demonstrates the vulnerability and error associated with the measurement methods used. The only measurement method to provide permeabilities within the AS1289 range was the electronic scales with standpipe levels method. Therefore, this method was considered the most reliable.

Coefficients of permeability measured in all soils are plotted in Figure 4.39a and Figure 4.39b (replotted to a maximum permeability of 0.00008m/s). It is noted that permeabilities measured in flume tests for Mixes 4, 5 and 8 were larger than permeabilities measured using AS1283 and AS1289. Permeabilities measured in flumes are considered more representative of testing conditions.

Coefficients of permeability listed in Table 4.2 are average results taken as representative values.

Table 4.2: Averaged or estimated permeability of each soil

Soil	Permeability (m/s)
Sydney Sand	3.3 x 10^{-4}
Sibelco 50n	1.3 x 10^{-4}
Mix 1	3.0 x 10^{-5}
Mix 2	3.9 x 10^{-4}
Mix 3	7.1 x 10^{-4}
Mix 4	6.3 x 10^{-4}
Mix 5	2.7 x 10^{-3}
Mix 6	2.4 x 10^{-5}
Mix 7	1.8 x 10^{-5}
Mix 8	1.5 x 10^{-5}

Permeability coefficients listed in Table 4.2 have been plotted over a figure illustrating and characterising the full range of possible permeabilities in Figure 4.40. This figure shows that a good range of permeabilities covering 2 orders of magnitude have been tested within the sand range. It also shows that soils with similar d_{10} sizes have similar permeabilities as can be seen by the group of Mix 1, 6, 7 and 8; and the group of Sydney Sand, Mix 2, 3 and 4. This illustrates the intention of testing soils with similar permeabilities but different uniformity coefficients was somewhat successful (done in order to isolate the effect of permeability from uniformity).

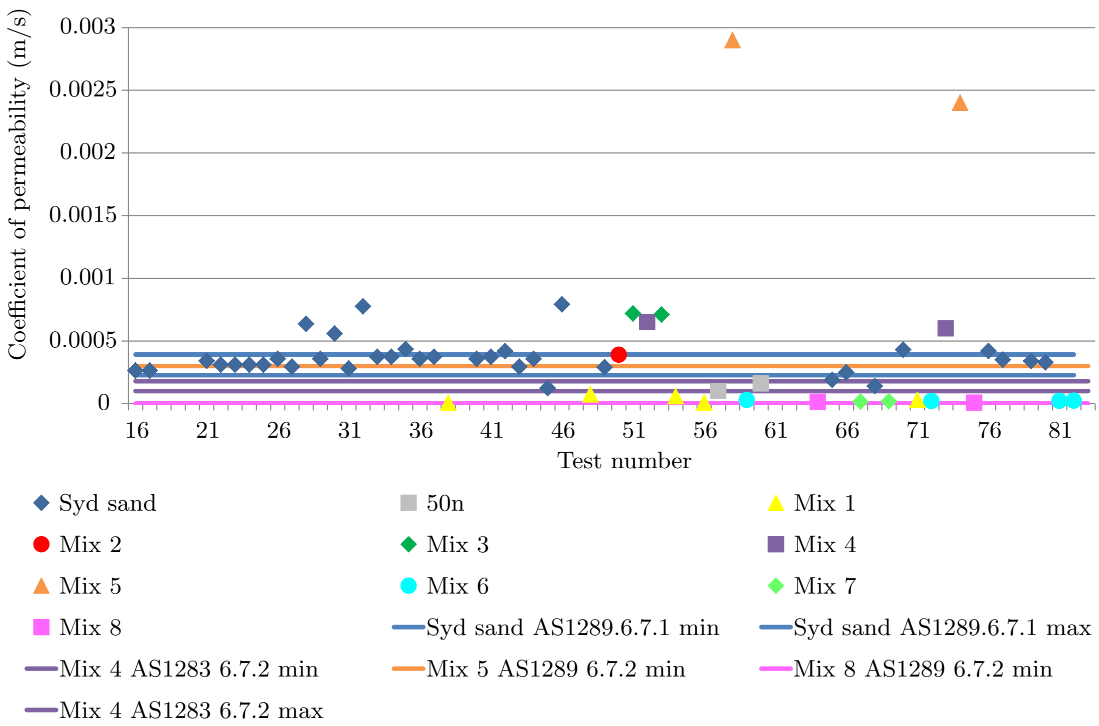

(a) Automatic y-axis max

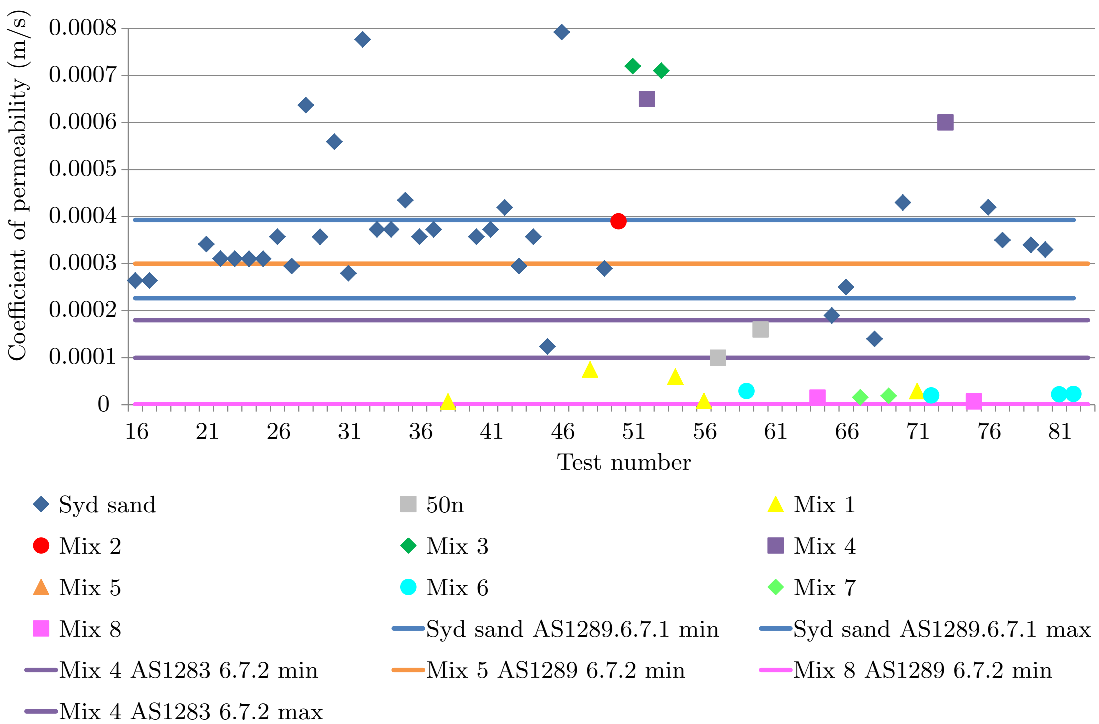

(b) Y-axis max at 0.0008m/s

Figure 4.39: Permeability of all soils

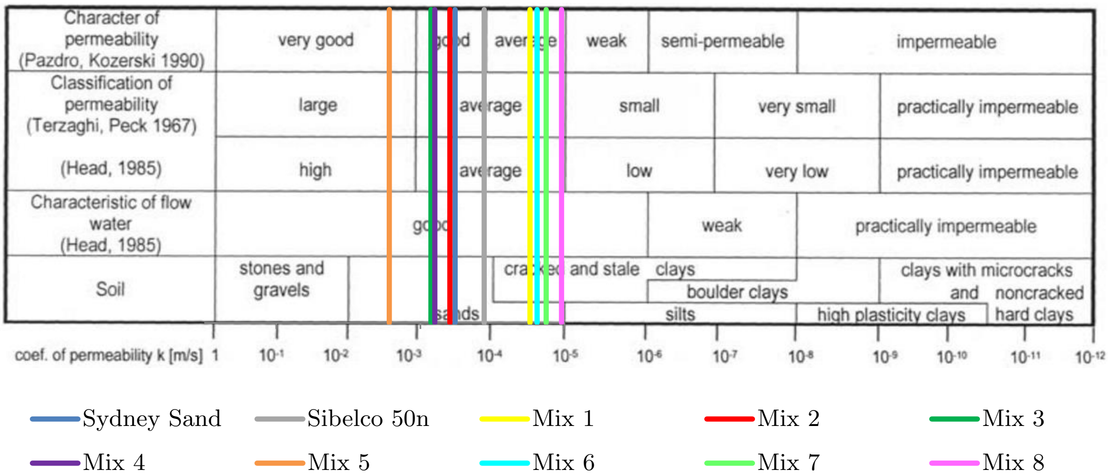

Figure 4.40: Soil permeability over indicative ranges (chart from Sobolewski (2002))

4.11 Water temperature

In a select few tests (identified in Table 4.3) the temperate of water in the downstream box was measured with a mercury-in-glass thermometer. The water temperature was measured in case the viscosity of water was required in later calculations/models.

Water temperatures are plotted in Figure 4.41 against the month of the year. The minimum water temperature was 10°C (corresponding to a dynamic viscosity of 1.3×10^{-3}Pa.s) and the maximum was 25°C (corresponding to a dynamic viscosity of 8.9×10^{-4}Pa.s). The month of June, in which several temperatures were measured, indicated a possible variance of 6°C in a given month.

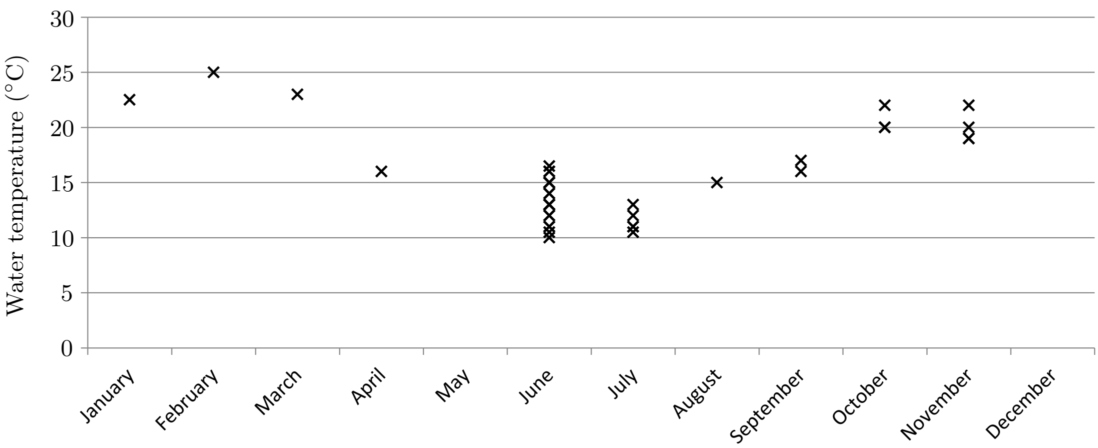

Figure 4.41: Temperature of water in downstream box with month

4.12 Table of observations & measurements

Table 4.3 is a list of observations and measurements taken during experiments.

Table 4.3: Observations made and measurements taken during experiments

Test	Soil	Soil density measurement	γ_{dry} (kN/m^3)	Flow	Total flow when H=100mm (m^3/s)	Standpipe levels	Permeability, k (m/s)	Channel depth/width method	Channel width [depth] (mm)	Tracer particles photographed	Sand boil	Water temp. (°C)	Blocked	Forward deepened	Failed*	Test
1	Syd sand	can	12.8													1
2	Syd sand	can	14.3													2
3	Syd sand															3
4	Syd sand															4
5	Syd sand												✓			5
6	Syd sand							Ruler on lid	20				✓			6
7	Syd sand	can	14.1										✓			7
8	Syd sand															8
9	Syd sand							Ruler on lid	15							9
10	Syd sand															10
11	Syd sand															11
12	Syd sand	can	14.5					Ruler on lid	0.7–8				✓			12
13	Syd sand															13
14	Syd sand												✓			14
15	Syd sand															15
16	Syd sand	total sand	15.2	beaker	2.8E-06		2.6E-04	Ruler on lid + depth by sight	10 [1.5–3]				✓			16
17	Syd sand	total sand	16.1	beaker	2.8E-06		2.6E-04	Ruler on lid + depth by sight	5–13 [3–6]				✓			17
18	Syd sand	total sand	16.5					Ruler in photo	2–13	coloured sand			✓			18
19	Syd sand													✓		19
20	Syd sand	total sand	16.1										✓			20
21	Syd sand	total sand	16.3	beaker	3.7E-06		3.4E-04	Ruler in photo	2–10	coloured sand			✓	✓	✓	21
22	Syd sand	total sand	16.1	beaker	3.3E-06		3.1E-04			coloured sand				✓	✓ 7hr	22
23	Syd sand	total sand	16.6	beaker	3.3E-06		3.1E-04	Ruler in photo	3–26	no tracer			✓	✓		23
24	Syd sand	total sand	16.5	beaker	3.3E-06		3.1E-04									24
25	Syd sand	total sand	16.6	beaker	3.3E-06		3.1E-04	Ruler on lid and in photo	2–15	coloured sand			✓	✓		25
26	Syd sand	total sand	15.9	beaker	3.8E-06		3.6E-04							✓		26
27	Syd sand	total sand	16.4	beaker	3.2E-06		3.0E-04									27
28	Syd sand	total sand	16.8	beaker	6.8E-06		6.4E-04	Ruler on lid and in photo	2–30	coloured sand			✓	✓	✓ 53min	28
29	Syd sand			beaker	3.8E-06		3.6E-04	Ruler in photo	2–27	coloured sand			✓	✓		29
30	Syd sand			beaker	6.0E-06		5.6E-04	Ruler on lid	30	coloured sand			✓	✓		30

Table 4.3: (continued)

Test	Soil	Soil density measurement	γ_{dry} (kN/m^3)	Flow	Total flow when H=100mm (m^3/s)	Standpipe levels	Permeability, k (m/s)	Channel depth/width method	Channel width [depth] (mm)	Tracer particles photographed	Sand boil	Water temp. (°C)	Blocked	Forward deepened	Failed*	Test
31	Syd sand			beaker	3.0E-06		2.8E-04	Ruler in photo	2–14	coloured sand						31
32	Syd sand			beaker	8.3E-06		7.8E-04	Ruler in photo	4–33	coloured sand			✓			32
33	Syd sand	total sand	16.6	beaker	4.0E-06		3.7E-04	Ruler in photo	5–31	coloured sand			✓	✓	✓ 24min	33
34	Syd sand			beaker	4.0E-06		3.7E-04	Ruler in photo	1–9	coloured sand						34
35	Syd sand			beaker	4.7E-06		4.3E-04	Ruler in photo	12–23	coloured sand			✓	✓	✓	35
36	Syd sand			beaker	3.8E-06		3.6E-04	Ruler in photo	4–20	coloured sand			✓	✓	✓ 2hr12min	36
37	Syd sand			beaker	4.0E-06		3.7E-04	Ruler on lid and in photo	7–17	no tracer			✓	✓		37
38	Mix 1			beaker			7.1E-06	Ruler in photo	4–8							38
39	Syd sand									Pliolite				✓	✓	39
40	Syd sand			beaker	3.8E-06		3.6E-04			PVC and tyre shreddings				✓	✓ 1hr42min	40
41	Syd sand			beaker	2.0E-06		3.7E-04						✓	✓		41
42	Syd sand			beaker	4.5E-06		4.2E-04			Pliolite				✓		42
43	Syd sand			beaker	3.2E-06		3.0E-04									43
44	Syd sand			beaker	3.8E-06		3.6E-04							✓		44
45	Syd sand	push tubes	15.0–15.4	beaker	1.3E-06		1.2E-04			Pliolite		12–15	✓	✓		45
46	Syd sand	push tubes	14.9–15.3	beaker	8.5E-06	✓	7.9E-04			Pliolite		13–16				46
47	Mix 1	push tubes														47
48	Mix 1			scale			7.5E-05					10				48
49	Syd sand	push tubes	15.1–15.3	scale		✓	2.9E-04			Pliolite		11–13				49
50	Mix 2			beaker	4.1E-06	✓	3.9E-04	Ruler on lid	30–60	Pliolite but no ruler				✓	✓ 6min	50
51	Mix 3			scale		✓	7.2E-04	Ruler on lid	20			15		✓	✓ 1min	51
52	Mix 4			scale		✓	6.5E-04	Ruler on lid	20–400			16–17	✓			52
53	Mix 3			scale	5.3E-06	✓	7.1E-04				collected		✓	✓	✓ 1min	53
54	Mix 1			scale			6.0E-05									54
55	Syd sand												✓			55
56	Mix 1			beaker		✓	8.0E-06									56
57	50n			scale			1.0E-04							✓	✓ 2.5day	57
58	Mix 5			beaker		✓	2.9E-03	Ruler on lid	60–220		collected	20–22	✓	✓	✓	58
59	Mix 6			scale	1.7E-07	✓	2.9E-05	Ruler in photo	11–90			20–22		✓		59
60	50n			scale		✓	1.6E-04	Ruler in photo	5–23							60
61	Mix 2			scale										✓	✓ 10min	61
62	Mix 8					✓								✓	✓	62
63	Mix 3													✓	✓ 4min	63
64	Mix 8			beaker		✓	1.5E-05	Ruler in photo	3–9					✓	✓ 2hr11min	64

Table 4.3: (continued)

Test	Soil	Soil density measurement	γ_{dry} (kN/m^3)	Flow	Total flow when H=100mm (m^3/s)	Standpipe levels	Permeability, k (m/s)	Channel depth/width method	Channel width [depth] (mm)	Tracer particles photographed	Sand boil	Water temp. (°C)	Blocked	Forward deepened	Failed*	Test
65	Syd sand			scale	2.2E-06		1.9E-04				moved		✓			65
66	Syd sand			scale			2.5E-04									66
67	Mix 7			scale		✓	1.6E-05	Ruler on lid	70			25	✓	✓	✓ 55min	67
68	Syd sand			scale			1.4E-04	Ruler on lid	15–30		moved	23	✓	✓	✓	68
69	Mix 7			scale		✓	1.9E-05	Ruler on lid and in photo	3–13				✓	✓	✓ 1hr	69
70	Syd sand			beaker			4.3E-04							✓	✓	70
71	Mix 1			scale		✓	2.9E-05	Ruler in photo	3–11		moved	16				71
72	Mix 6			scale			2.0E-05						✓	✓	✓ 30min	72
73	Mix 4			scale		✓	6.0E-04	Ruler on lid	50		moved					73
74	Mix 5			beaker	1.4E-05		2.4E-03	Ruler on lid	100–200		moved					74
75	Mix 8			scale			7.0E-06	Ruler in photo	3–12		moved	13	✓	✓	✓ 5min	75
76	Syd sand			beaker			4.2E-04							✓	✓ 1hr42min	76
77	Syd sand			scale		✓	3.5E-04				collected			✓	✓ 1hr6min	77
78	Mix 6											11		✓		78
79	Syd sand			scale		✓	3.4E-04	Caliper + wax	[1.1–5.1]	Pliolite	collected	11				79
80	Syd sand			scale	1.9E-06	✓	3.3E-04	Caliper + wax	[0.8–4.1]	Pliolite	collected					80
81	Mix 6			scale		✓	2.2E-05	Ruler on lid	30–40		collected		✓			81
82	Mix 6			scale		✓	2.3E-05				collected		✓			82
83	Syd sand			scale		✓				Pliolite				✓	✓ 3hr36min	83
84	Syd sand			scale		✓								✓	✓ 1hr36min	84
85	Syd sand			scale		✓				Pliolite			✓	✓	✓ 1hr5min	85
86	Syd sand									Pliolite				✓	✓ 1hr16min	86
87	Syd sand			scale		✓				Pliolite				✓	✓ 1hr13min	87
88	Syd sand					✓								✓	✓ 2hr24min	88
89	Syd sand			scale		✓								✓	✓ 1hr25min	89
90	Syd sand			scale		✓		Ruler on lid	1–10	Pliolite				✓		90
91	Syd sand			scale		✓		Ruler on lid	1–7	Pliolite			✓	✓		91
92	Syd sand			scale		✓								✓		92

* time refers to 'time to failure', i.e. duration of forward deepening (when known)

4.13 Table of results

Table 4.4 is a list of experimental results and relevant notes.

Table 4.4: Experimental results

Test	Soil	Initiation		Critical		Note
		head (mm)	gradient	head (mm)	gradient	
1	Syd sand	-	-	-	-	sample damaged
2	Syd sand	-	-	-	-	sample damaged
3	Syd sand	-	-	-	-	sample damaged
4	Syd sand	268	0.21	615	0.47	inadequate head control
5	Syd sand	263	0.20	?	?	Did not reach u/s
6	Syd sand	180	0.14	?	?	Did not reach u/s
7	Syd sand	258	0.20	523	0.40	obstruction by air bubbles
8	Syd sand	253	0.19	410	0.32	obstruction by air bubbles
9	Syd sand	156	0.12	156	0.12	sample damaged
10	Syd sand	142	0.11	?	?	sample damaged
11	Syd sand	94	0.07	?	?	sample damaged
12	Syd sand	389	0.30	446	0.34	sample damaged
13	Syd sand	486	0.37	486	0.37	issue with starter channel
14	Syd sand	1105	0.85	1626	1.25	
15	Syd sand	$<$1863	$<$1.43	?	?	Flow restricted
16	Syd sand	202	0.16	270	0.21	
17	Syd sand	199	0.15	283	0.22	
18	Syd sand	260	0.20	322	0.25	
19	Syd sand	92	0.07	140	0.11	incorrect datum
20	Syd sand	98	0.08	233	0.18	
21	Syd sand	271	0.21	271	0.21	faulty slot
22	Syd sand	146	0.11	195	0.15	
23	Syd sand	212	0.16	256	0.20	
24	Syd sand	236	0.18	236	0.18	initiated u/s of exit
25	Syd sand	271	0.21	271	0.21	
26	Syd sand	171	0.13	171	0.13	inadequate compaction
27	Syd sand	134	0.10	213	0.16	
28	Syd sand	268	0.21	293	0.23	
29	Syd sand	234	0.18	234	0.18	
30	Syd sand	313	0.24	313	0.24	
31	Syd sand	170	0.13	195	0.15	
32	Syd sand	331	0.25	331	0.25	

Table 4.4: (continued)

Test	Soil	Initiation head (mm)	gradient	Critical head (mm)	gradient	Note
33	Syd sand	342	0.26	342	0.26	
34	Syd sand	181	0.14	203	0.16	
35	Syd sand	253	0.19	307	0.24	
36	Syd sand	306	0.24	335	0.26	
37	Syd sand	152	0.12	237	0.18	
38	Mix 1	-	-	-	-	Did not BE
39	Syd sand	236	0.18	265	0.20	incorrect bladder inflation
40	Syd sand	207	0.16	273	0.21	
41	Syd sand	270	0.10	481	0.19	
42	Syd sand	190	0.15	186	0.14	
43	Syd sand	233	0.18	170	0.13	
44	Syd sand	240	0.18	162	0.12	
45	Syd sand	312	0.08	730	0.19	
46	Syd sand	163	0.13	174	0.13	
47	Mix 1	-	-	-	-	Did not BE
48	Mix 1	-	-	-	-	Surface slip
49	Syd sand	144	0.11	196	0.15	
50	Mix 2	100	0.08	661	0.51	
51	Mix 3	147	0.11	1277	0.98	
52	Mix 4	222	0.17	3577	2.75	
53	Mix 3	379	0.29	1014	0.78	
54	Mix 1	-	-	-	-	Surface slip
55	Syd sand	439	0.17	439	0.17	
56	Mix 1	-	-	-	-	Surface slip
57	50n	126	0.10	324	0.25	
58	Mix 5	419	0.32	1280	0.98	max H= 1610 but not critical
59	Mix 6	465	0.36	510	0.39	
60	50n	90	0.07	225	0.17	
61	Mix 2	510	0.39	651	0.50	
62	Mix 8	1315	1.01	1315	1.01	soil desaturated
63	Mix 3	407	0.31	863	0.66	
64	Mix 8	1028	0.79	1028	0.79	
65	Syd sand	342	0.09	-	-	Surface slip
66	Syd sand	386	0.30	386	0.30	soil desaturated
67	Mix 7	677	0.52	853	0.66	
68	Syd sand	690	0.18	690	0.18	

Table 4.4: (continued)

Test	Soil	Initiation head (mm)	Initiation gradient	Critical head (mm)	Critical gradient	Note
69	Mix 7	725	0.56	1105	0.85	
70	Syd sand	204	0.16	204	0.16	incorrect bladder inflation
71	Mix 1	1043	0.80	3710	2.85	
72	Mix 6	258	0.20	847	0.65	
73	Mix 4	537	0.41	3975	3.06	
74	Mix 5	652	0.50	1020	0.78	
75	Mix 8	1072	0.82	1640	1.26	
76	Syd sand	366	0.28	366	0.28	
77	Syd sand	98	0.08	269	0.21	
78	Mix 6	460	0.35	475	0.37	
79	Syd sand	260	0.20	239	0.18	
80	Syd sand	177	0.14	409	0.31	
81	Mix 6	346	0.27	667	0.51	
82	Mix 6	403	0.31	741	0.57	
83	Syd sand	N/A	N/A	347*	0.27*	167% critical
84	Syd sand	N/A	N/A	367*	0.28*	176% critical
85	Syd sand	N/A	N/A	313*	0.24*	150% critical
86	Syd sand	N/A	N/A	305*	0.23*	147% critical
87	Syd sand	N/A	N/A	309*	0.24*	149% critical
88	Syd sand	N/A	N/A	271*	0.21*	130% critical
89	Syd sand	N/A	N/A	259*	0.20*	125% critical
90	Syd sand	N/A	N/A	230*	0.18*	111% critical
91	Syd sand	N/A	N/A	216*	0.17*	104% critical
92	Syd sand	N/A	N/A	225*	0.17*	108% critical

* applied head/gradient which was greater than critical as indicated in notes

Chapter 5

Group 1: Replicate Townsend (1981) testing

5.1 Introduction and aim

The aim of the first group of experiments was to verify the experimental setup and procedure could replicate results achieved by other researchers. In particular, results obtained by Townsend et al. (1981) were the replicable target because the flume built for this study was the same size as theirs (nullifying scale and shape effects). Every attempt was made to replicate the Townsend et al. (1981) experiments including use of a slope exit, a starter dowel, loose sand (placed with a sand rainer) and a uniform sand with similar grading. Sand used by Townsend et al. (1981) was referred to as 'Reid Bedford' sand with $d_{50} = 0.21$mm and a coefficient of uniformity of 1.5. Sydney Sand used in this study had a $d_{50} = 0.3$mm and a coefficient of uniformity of 1.3.

The target results of Townsend et al. (1981) were their test numbers 2 and 3 which initiated at gradients of 0.13 and 0.131 respectively, and progressed at gradients of 0.2 and 0.16 respectively. These were targeted because they tested the same starter channel diameter and length used in this study (6.35mm diameter and 152.4mm long). Given the seepage length in this study was 1.3m, the Townsend et al. (1981) results are equivalent to an initiation head of 170mm and a critical head of between 200–260mm.

Tests carried out to replicate the Townsend et al. (1981) results were numbered 1-18 and were classified as 'Group 1' of the experimental program.

5.2 Experimental results

Tests 1–15 either did not work or produced results significantly different to those obtained by Townsend et al. (1981). Table A (found in Appendix A) lists what went wrong, what improvements were made and the results obtained, for tests 1–15.

Test 16 was a repeat of Tests 14 and 15 (using denser tamped in sand) but with the geofabric removed from the downstream outlet. This time the initiation head (i.e. the head when the tip of the starter channel began to progress) was 202mm which was much less than Tests 14 and 15 and was closer to the initiation head obtained by Townsend et al. (1981) of 170mm. It's thought that the geofabric over the downstream outlet had been causing significant head loss.

It ought to be noted though that the starter channel partially filled in with sand before the tip began to progress. Sand left the tip of the starter channel and deposited in the channel, and deposited from the tip to the downstream exit (in a forwards direction). An example is shown in Figure 5.1: the starter channel is parallel to the ruler and the flow direction is towards the bottom-left of the photo. The in-filling of the channel can be seen at the 17cm mark on the ruler in that one half of the channel appears deeper than the other.

Strictly speaking the tip did progress during this process, but did so only for only a short distance (perhaps about 10–20mm) and sand transported from the tip did not reach the exit (but instead was deposited in the channel where the in-filling was up to). This process did stop and required increases in head difference to complete. Once the channel was partially filled for its entire length, traditional tip progression commenced. This occurred in Tests 8, 12, 14, 16 & 17.

The hypothesis for why the starter channel partially filled-in with sand prior to progressing is the diameter of the starter dowel was greater than the natural depth a channel would form in these conditions. Because the starter channel was relatively deep, flow velocity through the channel was insufficient to transport particles along and out the exit. Therefore, instead, particles would settle as soon as they detached. Where the channel had been partially filled-in, and hence had its depth reduced, flow velocity increased enough to transport particles along the channel until the portion of deeper channel was reached, where it settled. If this theory is correct then this suggests that channel depths are likely to be less than 6.35mm (the diameter of the starter dowel) in Sydney Sand experiments. This suggestion is supported by the channel depth measurements and estimates of between 1–5mm presented in Subsection 4.5.1.

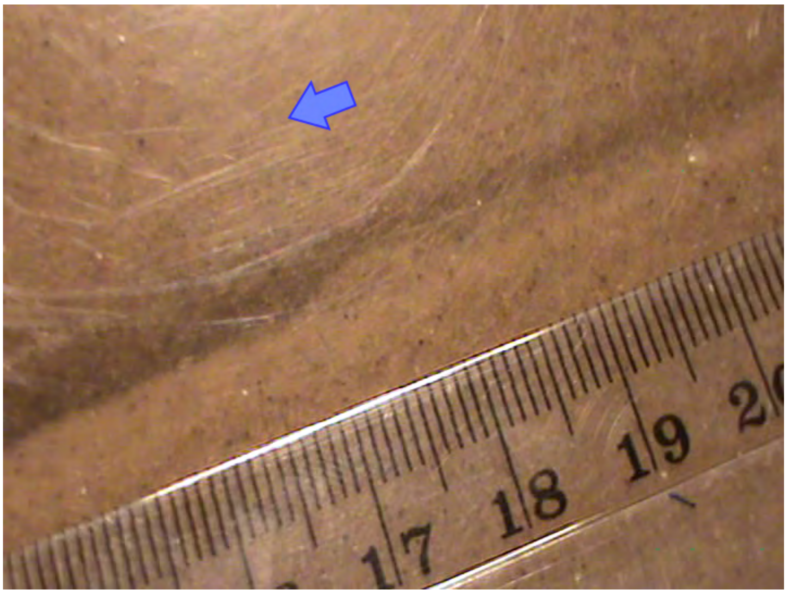

Figure 5.1: Sand deposition in starter channel up to 17cm mark (blue arrow indicates direction of flow)

In Test 16 the tip continued to progress at the initiation head (202mm) until the tip reached bar 3 (1057mm) when the channel blocked at the downstream end. With increases in head the tip re-initiated even though the downstream end was still blocked. Sand which detached from the tip would be transported downstream until it stopped on the blockage, causing the area of blockage to grow upstream. The tip reached the upstream end at a head of 270mm.

Test 17 was a repeat of Test 16 with the exception of how long a head difference was maintained before increasing, i.e. more time was left for the channel to unblock itself and/or the tip to continue progressing (heads were maintained over full weekends in some instances). Test 16 took 2 days to complete where as Test 17 took 6 days. Despite this, the initiation and progression heads were similar to Test 16 results, suggesting the rate of head increase has no effect.

Test 18 was also a repeat of Tests 16 and 17, however at the start of the test, the starter channel was suddenly filled in with sand. It's not clear why but may have been when the downstream hose was knocked and fell, causing a sudden surge of flow back into the flume. Yet, at a head of 260mm the starter channel re-opened and behaved much like Tests 16 and 17.

Figure 5.2 is a plot of channel length with head difference required to progress the channel to the given length. The results of Townsend et al. (1981) test numbers 2 and 3 are also plotted on Figure 5.2 but are done so as a shaded region indicating the minimum initiation head and maximum progression head. It's plotted like this because Townsend et al. (1981) did not report the channel length with head difference.

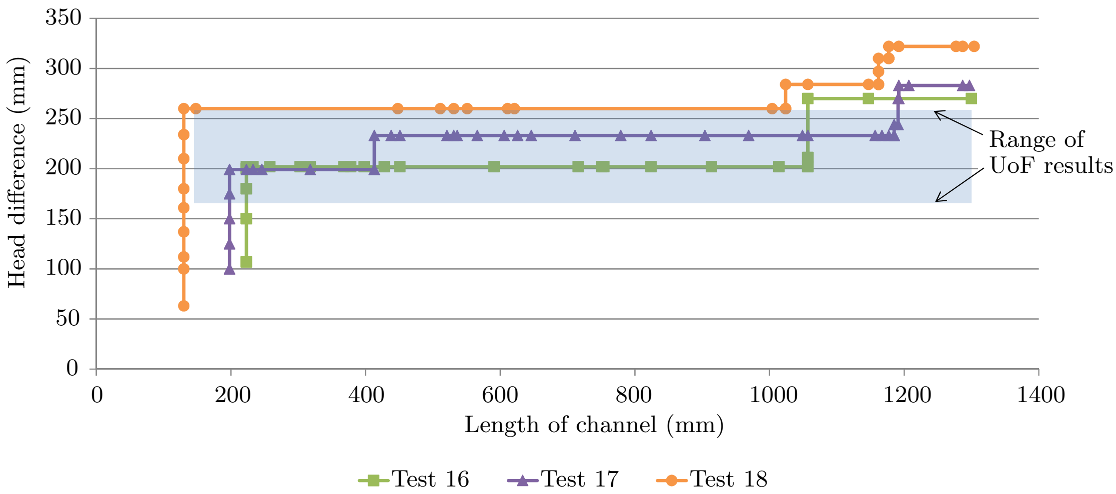

Figure 5.2: Group 1 test results

As can be seen the results from this study fall within the range of results achieved by Townsend et al. (1981). The exception is in the last 0.3m where the heads required to progress the tip were greater in this study.

Higher heads were required in the last 0.3m because when the channel was long it would become blocked with transported sand. This caused the tip to stop progressing and the only way to re-initiate the tip was to raise the head. Whilst Townsend et al. (1981) also report channel blockage, they state: *"Sand buildup at downstream slope was cleared to continue piping. Pipes rerouted at exit point due to buildup."* (Pietrus, 1981, pg. 89). It is not clear whether this means the channels cleared themselves or they reached in and physically cleared the blockage themselves. If it is the later then they wouldn't have needed to increase the head because the tip would have probably continued to progress when they cleared the blockage. In this study it was not possible to reach in and clear a blockage because the channel was inaccessible under the Perspex lid, so the head had to be raised instead. This would explain the discrepancy in the last 0.3m.

Results from Tests 16–18 were considered to verify the experimental set-up and procedure could replicate results achieved by other researchers.

5.3 Impact of using a starter channel

In Group 2 experiments, the slope exit was tested again but this time without a starter channel. By comparing results from the two sets of experiments, the impact of using a starter channel can be seen.

Results of the two sets of experiments are plotted in Figure 5.3. A starter channel was used in Tests 16, 17 and 18 but not in Tests 33, 35 and 36. From the plot it can be seen that the starter channel reduced the initiation head by an average of 26%. The starter channel also reduced the critical head, but by how much depends on what head is interpreted as critical in Tests 16–18. If the critical head is taken to be the head which produced the most channel tip progression, prior to channel blockage, then the starter channel resulted in a 30% reduction in critical head. If however the critical head is taken to be the maximum head required to progression the channel through to the upstream end, and 'push' through channel blockages, then the starter channel resulted in an 11% reduction in critical head.

Note: Tests 33, 35 and 36 are presented and discussed in Subsection 6.2.1.

It is thought that the starter channel reduced the initiation head because it concentrated flow, in a 3-dimensional fashion, toward the channel tip, generating higher seepage velocities and therefore requiring a lower head to generate velocities sufficient for particle detachment. However this lower head was insufficient for particle transport once the channel reached between 80–90% of the seepage length, as evident by channel blockages. When the channels blocked, heads were raised to similar heights as the critical heads in

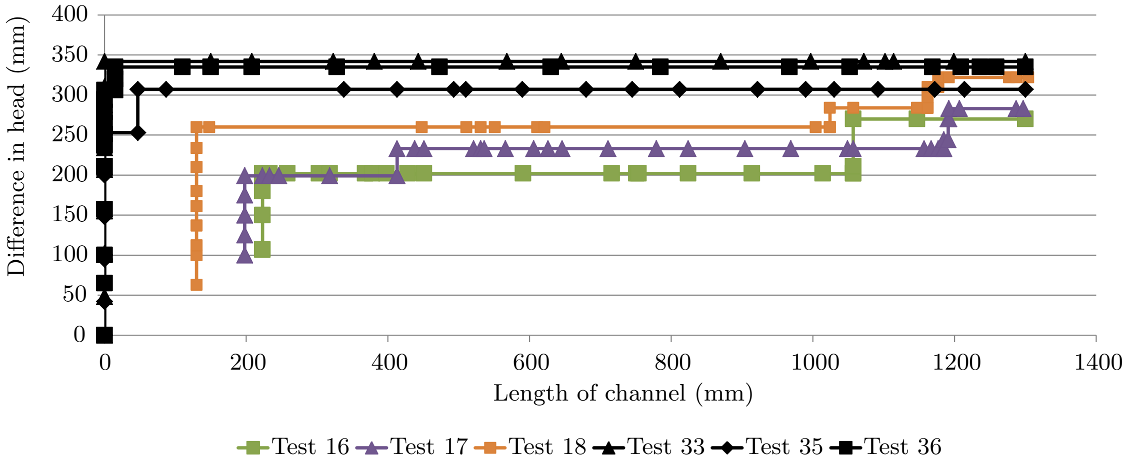

Figure 5.3: Comparison of test results with a starter channel (Tests 16–18) and without (Tests 33, 35 and 36)

tests without a starter channel. This suggests that once the channel is sufficiently long, the effect of the starter channel is lost and the scenario reverts to the no-starter-channel case, where particle transport is the critical mechanism.

Given that a starter channel reduced critical heads by approximately 30% then it is possible that critical heads used by Schmertmann (2000) (from the Townsend et al. (1981) and Townsend and Shiau (1986) studies) to construct the critical head with coefficient of uniformity relationship, were too low (i.e. over conservative). Particularly given it is unlikely for a 'starter channel' to exist in the field.

Chapter 6

Group 2: Exit geometry

6.1 Introduction and aims

The exit is the outlet at the downstream end where particles are transported out and where the backward eroding channel starts. Different foundation conditions create different exit geometries including the slope, plane, slot and circle exits. The foundation conditions which create these exits are described and sketched in Section 2.4.2.

Researchers have reported that the initiation and critical heads increase with increasing exit flow area (van Beek et al., 2013) (as discussed in Section 2.4.2). However none of these studies carried out experiments on all four exits on otherwise identical set-ups to verify or quantify the effect of the exit. Therefore the aim of the work reported in the chapter was to fill this gap. A secondary aim was to provide the background information necessary to investigate the exit effect with the numerical model described in Chapter 10.

The slope, plane, slot and circle exit geometries were cut into the Perspex lid, as described and drawn in Subsection 3.1.1. Tests on the four exits were classified as 'Group 2' of the experimental program and included 19 tests as listed in Table 3.7. The default set-up of Group 2 tests included a single flume with a seepage length of 1.3m, Sydney Sand tamped or vibrated in, saturated with the use of CO_2 flushing and a bladder pressured to 50kPa (5m).

6.2 Experimental results

To follow is an account of the experimental results, firstly for each exit geometry separately and then all exits together to compare. Results are expressed as channel length with head difference.

6.2.1 Slope

The slope exit is used to model a non-cohesive soil foundation sloping down at the downstream toe of the embankment where it meets the river bed. Figure 6.1 is a sketch, drawing and photo of the slope exit.

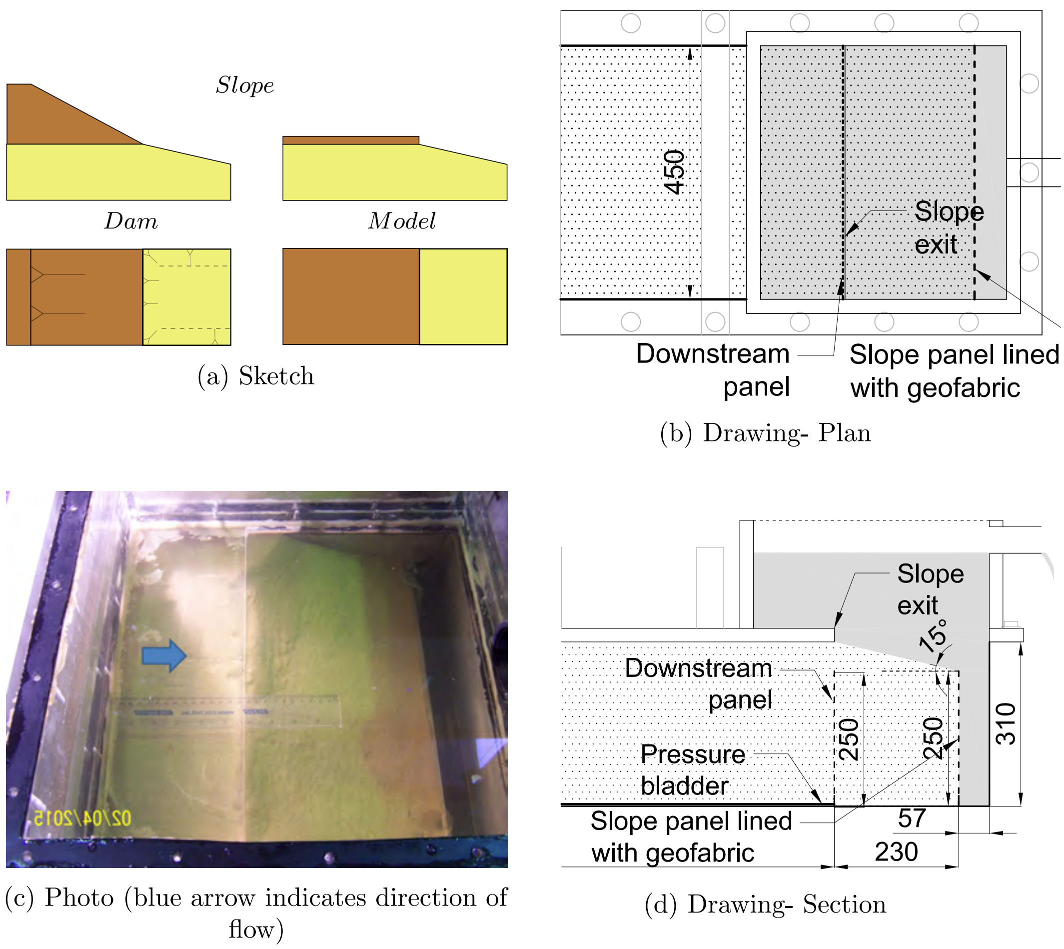

(a) Sketch

(b) Drawing- Plan

(c) Photo (blue arrow indicates direction of flow)

(d) Drawing- Section

Figure 6.1: Slope exit

Tests carried out on the slope exit included 33, 35 and 36. Tests 1–18 were also carried out on the slope exit but were done so using a starter channel which affected the results, therefore these results are not included here. Tests 39, 66, 70 and 76 were also carried out on the slope exit but were done so using a bladder pressure of 2.5m, i.e. less than the standard 5m, therefore these results are not included here either but can be found in Section 7.2.

All three slope tests were loaded with the 'Increase only' procedure. The consequence of this is these experiments do not provide information on the head required to continue tip progression, i.e. whether it decreased with channel length or remained constant.

Plotted in Figure 6.2 is the head difference with channel length and listed in Table 6.1 are the initiation and critical heads with a measure of variability.

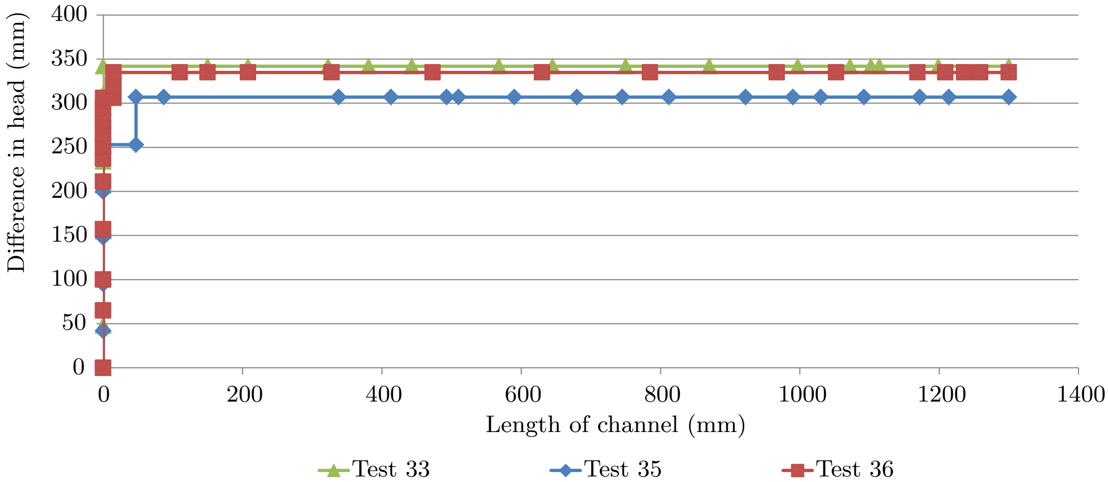

Figure 6.2: Group 2 test results- Slope exit

Table 6.1: Group 2 test results- Slope exit

	Initiation head (mm)	Critical head (mm)	Critical channel length (mm)
Test 33	342	342	0
Test 35	253	307	47
Test 36	306	335	15
average	300	328	21
range	89	35	47
standard error	26	11	14

There were variations in when and how the channels initiated. The range in initiation heads was 89mm and Tests 35 and 36 progressed 15 and 47mm before stopping (requiring 1 to 2 increases in head before the tip progressed continually) where as Test 33 never stopped but continued to progress from initiation. However, with experimental experience, this degree of variability was found to be common and was considered to be within regular experimental variability.

Critical channel lengths were relatively short, with an average of 21mm, and initiation to critical head ratios were high. This implies that the likelihood of a channel, once initiated, will continue to progress through to the upstream end at the same head is likely.

It is noticed the longer the channel was when the critical head was reached, the lower the critical head was. This suggests that when a channel has formed, less head difference is needed to progress the tip because the channel draws more flow (and causes higher seepage velocities).

6.2.2 Plane

The plane exit is used to model a non-cohesive soil foundation. Figure 6.3 is a sketch, drawing and photo of the plane exit.

Tests carried out on the plane exit included 28, 30 and 32. Tests 43 and 44 were also carried out on the plane exit but were done so to test different soil placement methods (CO_2 flushing wet and replacing only the top 1/4 of soil) which affected the results, therefore these results are not included here but are discussed in Subsection 3.2.7 instead.

All three plane tests were loaded with the 'Increase only' procedure. The consequence of this is these experiments do not provide information on the head required to continue tip progression, i.e. whether it decreased with channel length or remained constant.

Plotted in Figure 6.4 is the head difference with channel length and listed in Table 6.2 are the initiation and critical heads with a measure of variability.

The results show that initiation occurred at an average head of 304mm and that once a channel initiated it usually continued to progress without need for further head increases. The channel in Test 28, did stop and require head increases, but it stopped when the channel was only 12mm long, therefore this is considered a small local deformity within expected and accepted experimental variability.

Again it was noticed that the longer the channel was when the critical head was reached,

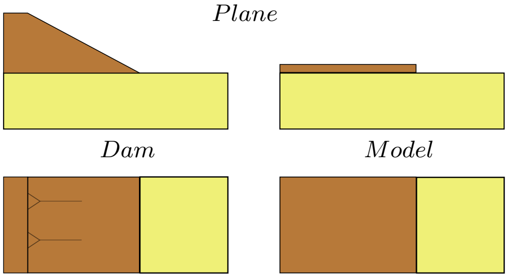

(a) Sketch

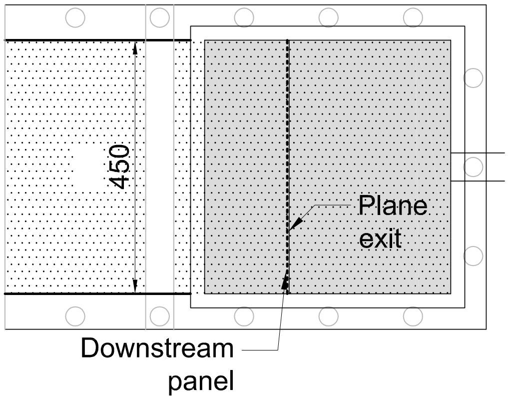

(b) Drawing- Plan

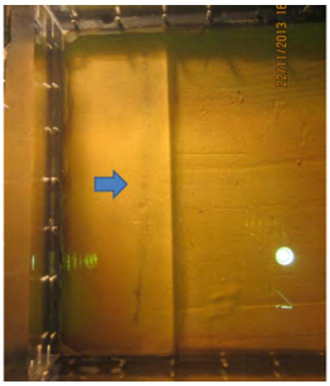

(c) Photo (blue arrow indicates direction of flow)

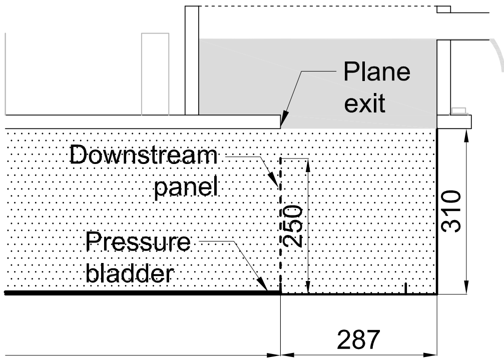

(d) Drawing- Section

Figure 6.3: Plane exit

the lower the critical head was.

6.2.3 Slot

The slot exit is used to model a foundation consisting of both a top cohesive soil layer and a lower non-cohesive soil layer where a slot/ditch has been cut into the top cohesive layer deep enough to reach the underlying non-cohesive layer. This is found where drains have been installed along the downstream toe to manage seepage and surface run-off flow. Figure 6.5 is a sketch, drawing and photo of the slot exit.

Tests carried out on the slot exit included 21, 23, 25, 26, 29 and 37. Test 40 was also carried out on the slot exit but was done so using a bladder pressure of 2.5m, i.e. less than the standard 5m, therefore this result is not included here, it can be found in Section 7.2 instead. Tests 41, 45, 55, 65 and 68 were also carried out on the slot exit but were done

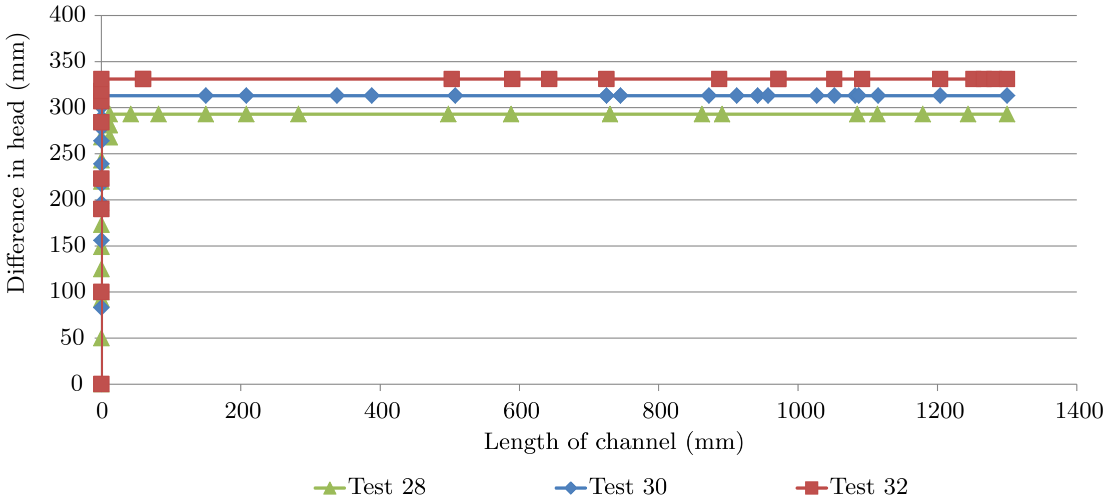

Figure 6.4: Group 2 test results- Plane exit

Table 6.2: Group 2 test results- Plane exit

	Initiation head (mm)	Critical head (mm)	Critical channel length (mm)
Test 28	268	293	12
Test 30	313	313	0
Test 32	331	331	0
average	304	312	4
range	63	38	12
standard error	19	11	4

so using longer seepage lengths of 2.6 and 3.9m, therefore these results are not included here either but are also discussed in Section 7.2.

The first five of the slot tests were loaded with the ‘Increase only’ procedure. The consequence of this is these experiments do not provide information on the head required to continue tip progression, i.e. whether it decreased with channel length or remained constant.

The last slot test, Test 37 was loaded with the ‘Decrease at points of interest’ procedure to determine whether the head required to continue tip progression would remain constant or decrease with channel length.

Plotted in Figure 6.6 is the head difference with channel length and listed in Table 6.3 are the initiation and critical heads with a measure of variability.

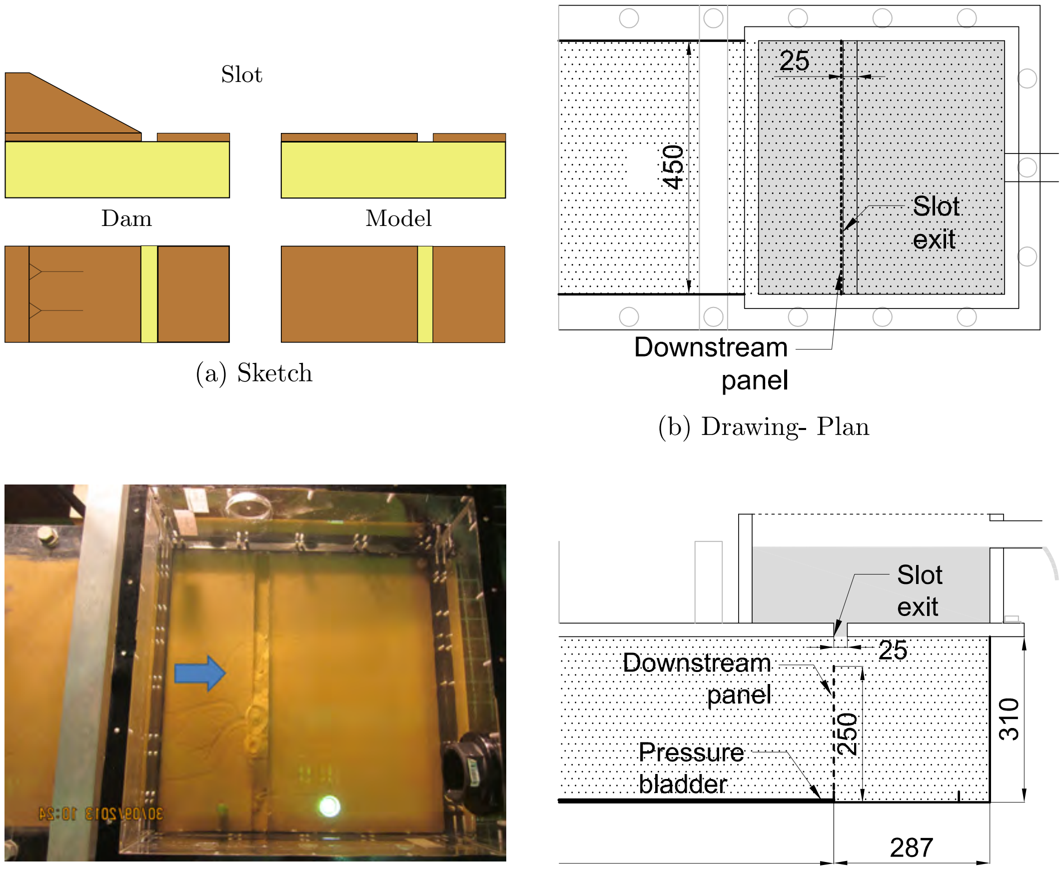

(a) Sketch

(b) Drawing- Plan

(c) Photo (blue arrow indicates direction of flow)

(d) Drawing- Section

Figure 6.5: Slot exit

The first observation made of the results is that Test 26 is significantly lower than the other tests (33% less than the average of the remaining tests at 254mm). It is possible this is due to less compaction of the soil as it was tamped using less passes. Soil density measurements confirmed a lower density in this test. If Test 26 is omitted from the record of results the range of the critical head reduces from 100mm to 37mm, the standard error reduces from 15 to 8mm and the average becomes 254mm.

Channels in 4 of these tests continued to progress from initiation where as the other 2 stopped and required increases in head to continue progression. This suggests it is more likely for channels to continue from initiation. However, if slot tests from other groups of testing are considered, namely Test 40 (imposed by less pressure from the bladder at 2.5m) and those used to investigate seepage length, channels in 5 of these 6 tests stopped after initiation. Therefore, when from all slot tests it appears there is just over a 50% chance channels will stop after initiation and require increases in head.

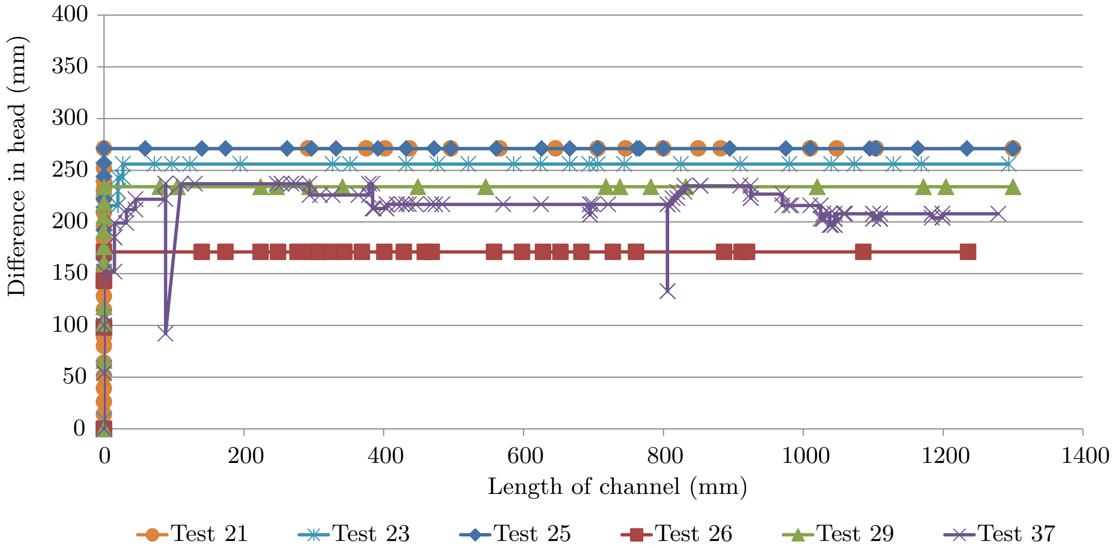

Figure 6.6: Group 2 test results- Slot exit

Table 6.3: Group 2 test results- Slot exit

	Initiation head (mm)	Critical head (mm)	Critical channel length (mm)
Test 21	271	271	0
Test 23	212	256	27
Test 25	271	271	0
Test 26	171	171	0
Test 29	234	234	0
Test 37	152	237	88
average	219	240	19
range	119	100	88
standard error	20	15	14

6.2.4 Circle

The circle exit is used to model a foundation consisting of both a top cohesive soil layer and a lower non-cohesive soil layer where a crack or defect has formed through the top cohesive layer deep enough to reach the underlying non-cohesive layer. This is found where the top cohesive soil layer has cracked due to uplift and blowout, or where a local defect in the top cohesive layer exists (possibly a sandy shaft/lense or rotting tree roots and animal borrows). Figure 6.7 is a sketch, drawing and photo of the circle exit.

Tests carried out on the circle exit included 19, 20, 22, 24, 27, 31 and 34. Tests 42, 46 and 49 were also carried out on the circle exit but were done so using no bladder pressure

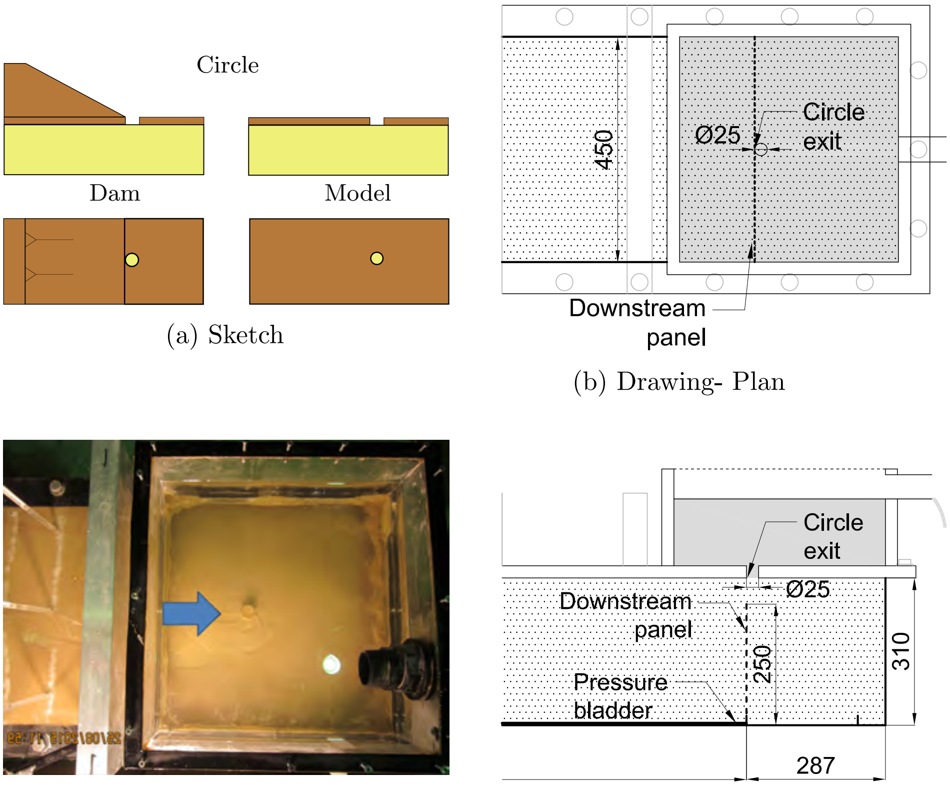

(a) Sketch

(b) Drawing- Plan

(c) Photo (blue arrow indicates direction of flow)

(d) Drawing- Section

Figure 6.7: Circle exit

or alternative densities, therefore these results are not included here but can be found in Section 7.2 instead. Tests in Groups 4 and 5 were also carried out on the circle exit but these results are presented in Section 8.2 and Section 9.2 respectively.

The first five of the circle tests were loaded with the ‘Increase only’ procedure. The consequence of this is these experiments do not provide information on the head required to continue tip progression, i.e. whether it decreased with channel length or remained constant.

The last two circle tests were loaded with the ‘Decrease at points of interest’ procedure to determine whether the head required to continue tip progression would remain constant or decrease with channel length.

Plotted in Figure 6.8 is the head difference with channel length and listed in Table 6.4 are the initiation and critical heads with a measure of variability.

Channel lengths are often greater than zero to begin with because small channels form during CO_2 flushing and/or saturation. Figure 6.9 is an example of this and due to the high gas and water pore pressures that occur as flow is concentrated towards the circle exit.

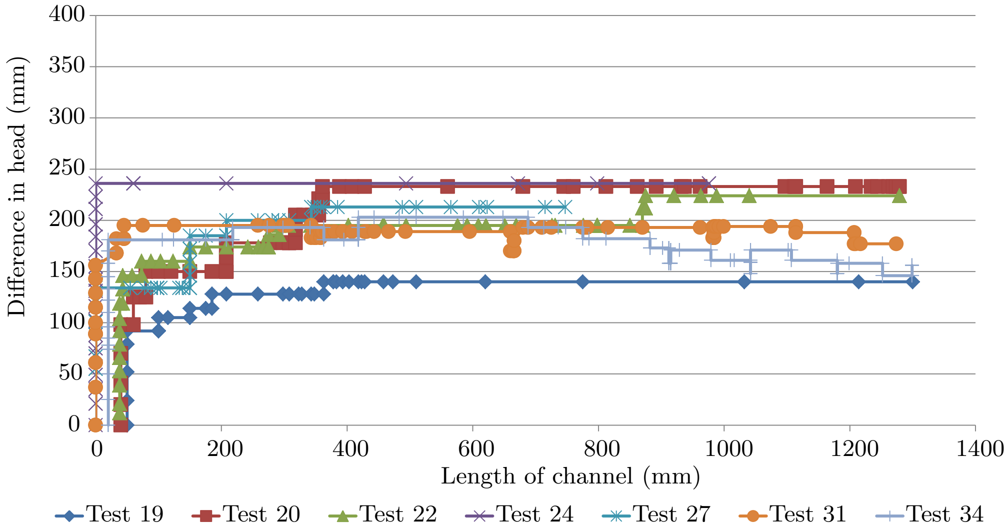

Figure 6.8: Group 2 test results- Circle exit

The critical head of Test 19 is 34% less than the average of the remainder of critical heads however, datum was likely to be incorrect given it had not yet been established with the dumpy level. Datum was established using the dumpy level for all remaining tests.

For Test 22, whilst a critical head of 195mm and a critical channel length of 292mm was reported in Table 6.4, the channel did actually stop beyond this, when it was 875mm long and required a 29mm increase in head to progress the tip. However, in hindsight, perhaps the head shouldn't have been increased at 875mm because, if channel length is plotted with time as done in Figure 6.10 then it can be seen that the tip was still progressing, albeit slowly (20mm overnight) as indicated by the slope of the red 'channel length with time' line.

Table 6.4: Group 2 test results- Circle exit

	Initiation head (mm)	Critical head (mm)	Critical channel length (mm)
Test 19	92	140	363
Test 20	98	233	361
Test 22	146	195	292
Test 24	236	236	0
Test 27	134	213	343
Test 31	170	195	45
Test 34	181	203	418
average	151	202	260
range	144	96	418
standard error	19	12	63

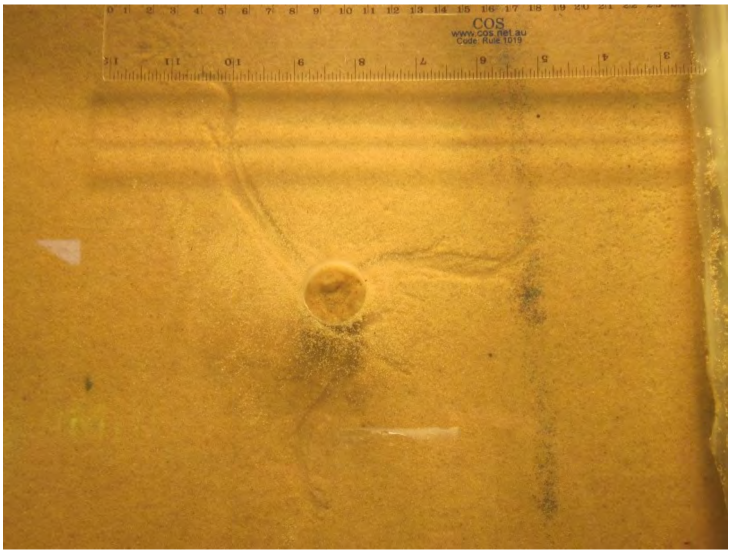

Figure 6.9: Channels which form around circular exit during CO_2 flushing and/or saturation (Test 20)

Test 24 behaved differently as it initiated at a head 70% higher than the average of the other tests and once initiated, didn't stop progressing. This is because there was a gap between the sand and lid in a region around the circular exit, as sketched in Figure 6.11a. The gap meant that seepage velocities/forces were reduced because there was now a larger flux area and the highest seepage forces causing initiation were now at the edge of the gap instead of the circular exit. Therefore initiation occurred at the edge of the gap as shown in Figure 6.11b. This meant that the experiment behaved more like a plane or slope exit than a circular exit in that once it initiated it continue to progress without stopping. Sand transported from the tip of the channel would be deposited at the downstream end

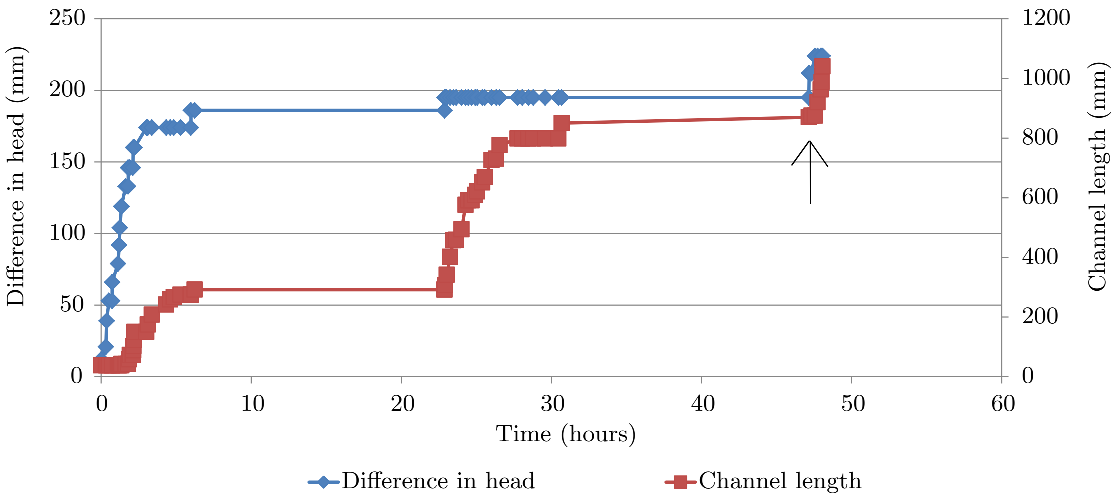

Figure 6.10: Test 22 with time: tip was still progressing when head was increased

of the channel, moving the end progressively closer to the exit. Once the downstream end of the channel reached the exit it began to behave more like a circular exit. This gap was likely to have been caused by not overfilling the flume sufficiently or poor screeding.

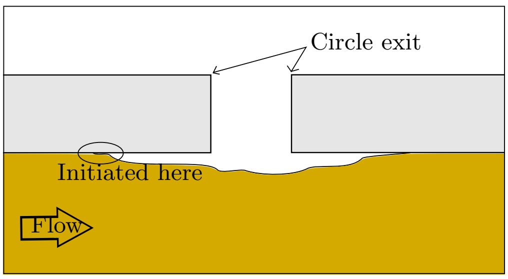

(a) Longitudinal sketch

(b) Plan photo (blue arrow indicates direction of flow)

Figure 6.11: Gap between sand and lid around circular exit (Test 24)

Furthermore, Test 24 was terminated before the channel reached the upstream end because air entered the sample approximately 8.5 hours after the test started. The air probably entered via gaps between the flume and rim gasket amongst build-up of sand and silicon grease from previous tests. This is why it became important to clean the gasket and lid, and re-grease, between each test.

Test 27 was also terminated before the channel reached the upstream end because power to laboratory was going to be turned off over the weekend which would have meant the bilge pump inside the constant head tank would have been turned off. In preparation for the power outage the bilge pump was turned to off to check if the drainage hose was primed and could siphon itself and not need the pump. But the water level in the constant head tank rose to twice it's previous head level without siphoning. At this point the experiment was abandoned because a) the experiment could not run unattended without power and b) the sand sample was damaged when the head was doubled (failed as 'sheet flow').

If Tests 19 and 24 were omitted from the results record, because they were unreliable or compromised results, as explained above, then the range and standard error of critical heads would reduce/improve from values listed in Table 6.4 to an average of 208mm with a range of 38mm and a standard error of 7mm.

In Figure 6.8, it can be seen that most tests required no more increases in head once the channel was approximately 400mm long, or 30% of the seepage length.

6.2.5 All exits

If all exit geometry results are plotted on the one graph then the effect of the exit on the initiation and critical heads can be seen. However before doing so, Test 26 was omitted from the slot exit results and Tests 24 and 19 were omitted from the circle exit results because they were unreliable and/or compromised, as discussed above. Also, tests that were loading using the 'Decrease at points of interest' procedure were altered to look like 'Increase only' tests in that all data points after the critical head were plotted at the critical head. This was done for the sake of clarity and consistency. The erroneous head rise in Test 22 was also omitted for clarity. Figure 6.12 is the result.

Three key findings can be taken from Figure 6.12.

1. Both the initiation and critical heads decreased in the order of slope, plane, slot and circle. In other words, the more an exit concentrated the flow the lower both the initiation and critical heads were.

2. Once a channel started in the plane and slope exits, the channel usually continued to progress without need for further head increases (i.e. initiation head $\approx$ critical head). However for the slot and circle exits, the channel progressed a short distance and then stopped until the head was increased again. Several increases in head

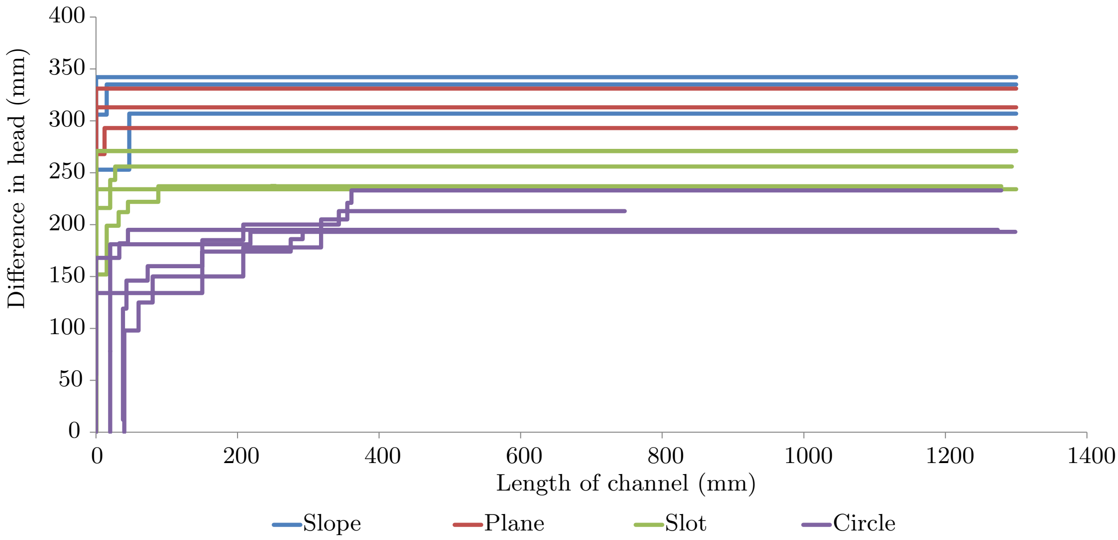

Figure 6.12: Group 2 results- all exits

were required to progress the channel through to the upstream end (i.e. initiation head < critical head).

3. In the slot and circle exit tests the critical head was reached when the channels were approximately 5% and 30% of the seepage length respectively.

6.3 Discussion

6.3.1 Comparison of results with other studies

As discussed in Section 2.4.2, there have been four other studies which have investigated the effect of exit geometry- de Wit (1984), van Beek et al. (2012b), van Beek (2015) and Yao et al. (2007). Van Beek et al. (2013) summarised the findings of these studies with the observation that both the global initiation and critical heads increase with increasing exit flow area. Additionally, van Beek et al. (2013) demonstrated that in circle exit experiments, the critical head > initiation head, which they described as being a 'progression dominated' exit. Where as, in slope exit experiments, the critical head = initiation head and was therefore described as being an 'initiation dominated' exit. A repercussion of initiation-dominated exit geometries was that, when head was kept constant after initiation, equilibrium would not be observed.

These findings from other studies were supported by observations made in this study, namely observations numbered 1 and 2 in Subsection 6.2.5 above. Therefore this study has verified the previously speculated exit geometry effect. This study has also added to these findings in that the slot has also been identified as a 'progression dominated' exit and the plane also an 'initiation dominated' exit.

However observation number 3 listed in Subsection 6.2.5 (reaching of the critical head at channel lengths approximately 5% and 30% of the seepage lengths for the slot and circle exits respectively) was slightly different. Van Beek et al. (2013) state that when the critical head is reached, the channel length is approximately 1/2 of the seepage length for infinitely deep foundations and decreases in percentage of seepage length with decreasing (erodible) foundation thickness. Whilst this study confirmed that the channel length was indeed less than 1/2 when the critical head was reached, it also showed that despite the foundation depth being kept constant, the channel length at critical head changed depending on the exit geometry. From this observation it is suggested that the channel length at critical head is also a function of exit geometry.

Furthermore, the slot and circle results suggest that the larger the difference between initiation and critical heads, the longer the channel will be when critical head is reached. As a consequence of this, it is quite possible the length of the channel when critical head is reached is influenced by the size of the exit. To explain, wider slot exits or larger diameter circles exits would require higher heads for initiation, resulting in less different between initiation and critical heads and therefore shorter channel lengths when critical is reached, and the reverse for smaller exits.

Whilst this could be not confirmed in this study (because only one slot width and one circle diameter was tested), a study by Miesel (1978) did test a variety of circular exit diameters and demonstrated that larger diameter circular exits did indeed need higher heads to initiate (as indicated by the solid black circles in Figure 6.13) yet quite similar critical heads were needed (as indicated by the solid black triangles in Figure 6.13) (van Beek, 2015). Therefore, Miesel (1978) demonstrated a larger difference between initiation and critical heads for smaller circular exits and the current author takes this a step further to suggest that smaller circular exits therefore result in longer channel lengths when critical head is reached.

Though it should be noted that Miesel (1978) also demonstrated bounds to this behaviour whereby very small circular exits (less than 2.56mm) would not allow any backward erosion to occur (due to bridging across the exit) and large circular exits (greater than 13mm) would prevent equilibrium (and hence no channel length at critical head) (van Beek, 2015).

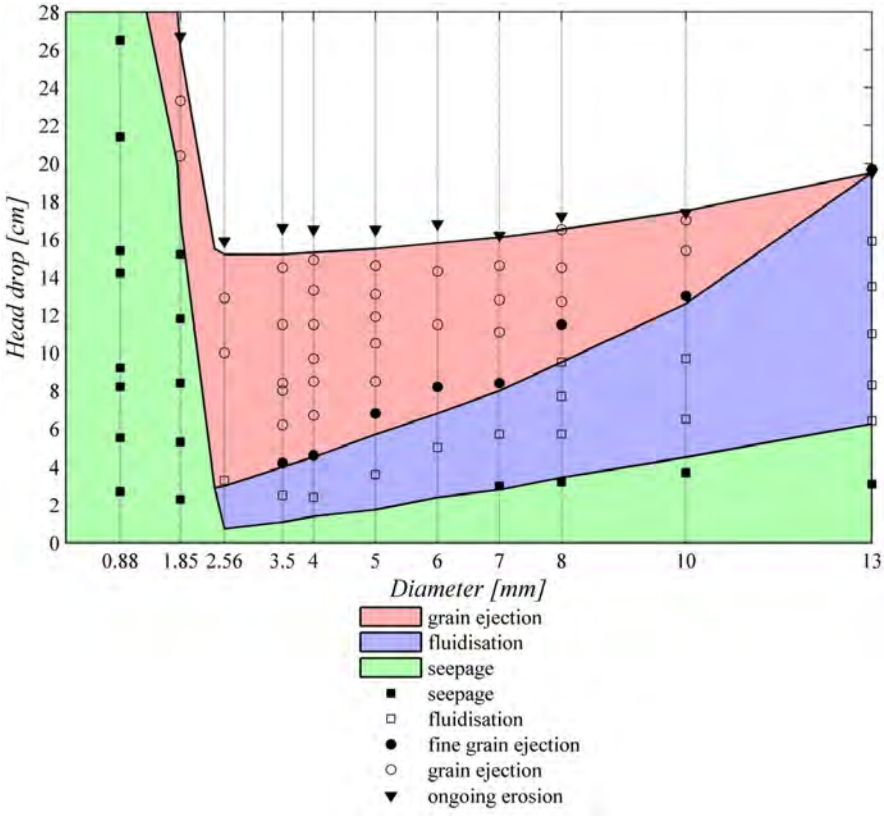

Figure 6.13: Effect of circular exit diameter on piping process (van Beek, 2015, adapted from Miesel (1978))

6.3.2 Understanding the exit geometry effect with the numerical model

Numerical modelling was carried out to investigate why the exit geometry might affect the initiation and critical heads. The numerical model is described in Chapter 10 and provided the distribution of head throughout the flume which, by extension, also gave head gradients and seepage velocities throughout the flume. The numerical model was used to compare the head distribution produced by different exit geometries.

Figure 10.10 is a plot of seepage velocity along the top centreline of the flume for each of the four exits. This plot indicates seepage velocity is constant throughout the flume until it approaches the exit where it rapidly increases. Exit geometries affect maximum seepage velocity at the exits differently such that they ascend in the order of slope, plane, slot and circle.

This order of increasing maximum seepage velocity at the exit is the inverse order of increasing head required to initiate channels in experiments (which can be seen in Figure 6.12). Therefore, the greater the exit velocity the lower the head required to initiate a channel.

Given initiation is thought to occur when seepage velocity at the exit is sufficient enough to fluidise sand and transport particles out, it is expected there is a minimum exit velocity which triggers initiation. If this is the case then the numerical model has explained why the exit geometry affects the global initiation gradient- because the exit geometry affects exit velocity and exit velocity triggers initiation. Or in other words, exit geometries which cause higher local gradients at the exit require lower global gradients to reach the minimum seepage velocity required to initiate a channel.

As for the critical gradient, the numerical model demonstrated that a circle exit results in higher seepage velocity into the channel tip than the slot exit does (higher local gradients into the tip due to circle exits can be seen in the flownets and head profile in Figure 10.12). Therefore, the numerical model explained why the circle exit needed a lower critical gradient than the slot exit- because the circle exit caused a higher local gradient at the tip of the channel, resulting in the need for a lower global gradient to generate the minimum seepage velocity at the channel tip needed to maintain tip progression.

Interestingly, given the slot width and circle diameter where the same, the different critical gradients resulting from these two exits demonstrate the effect of 2-dimensional versus 3-dimensional flow. The slot exit concentrates flow in the longitudinal direction (2D) whereas the circle exit concentrates the flow both in longitudinal and transverse directions (3D) (as shown in Figure 10.12 as flownets and a head profile). And both physical and numerical modelling have demonstrated that 3D flow results in faster seepage velocity into the tip of the channel and therefore lower critical gradients. This indicates that configurations which cause 3-dimensional flow are likely to backward erode at lower gradients than traditional design methods, which assume 2-dimensional flow, would predict (such as the Schmertmann (2000) and Sellmeijer et al. (2011) methods).

Note, this comparison of seepage velocity into the channel tip excluded the slope and plane exits because their critical gradients occurred at initiation, before a channel was present.

6.3.3 Accounting for exit geometry in design

Chapter 11 contains a review of the two most popular methods of design against backward erosion piping- the Schmertmann (2000) and Sellmeijer et al. (2011) methods. This review considers how accurately these methods predicted experimental results from both this study and the studies of others and suggests amendments which improves the accuracy. Within this review consideration is given to the methods' ability to account for the effect of exit geometry- a summary of which is given here.

Schmertmann (2000) accounts for different exit geometries with a correction factor referred to as the gradient factor for parallel flow, C_G. The C_G factor is the minimum local gradient divided by the global critical gradient. The minimum local gradient is found using 2D flownets without a channel. These 2D flownets capture the effect exit geometries have on local gradients and hence the different seepage velocities through-out.

The numerical model described in Chapter 10 was used to determine C_G factors in flumes and exits used in this study. They were found to be 0.92, 0.90, 0.83 and 0.83 for the slope, plane, slot and circle exits respectively. The same C_G value was used for both the slot and circle exits because the circle exit was modelled as a slot to produce a 2D seepage flownet.

Schmertmann (2000) does not appear to consider the ramifications of exit geometries which create 3D flow, such as a circular exit. The current author speculates that the Schmertmann (2000) method could still be used when a 3D exits are used, however local gradients (and therefore the C_G factor) would need to be calculated using 3-dimensional seepage programs. Although, caution is advised when using 3-dimensional seepage programs to model head distribution toward a circular exit because flow concentration towards the exit causes fluidisation of the soil increasing its permeability locally. This local fluidisation affects the head distribution and local gradients throughout and needs to be compensated for when using a 3D model to calculate the C_G factor.

Figure 6.14 is a plot of both experimental results and model predictions for tests carried out in Sydney Sand across the different exit geometries. Experimental results are denoted by the black data points (in shapes representing the different exit geometries) and model predictions are denoted by the green data points- open data points for the predicted local gradients and close data points for the equivalent global gradients. Considering the C_G factor is used to convert the predicted local gradient to the global gradient, Figure 6.14 can be used to illustrate the effectiveness of the C_G factor. Assuming the predicted local gradients are correct, then the C_G factor would be effective if it increased the local gradient up to the global gradients observed in experiments.

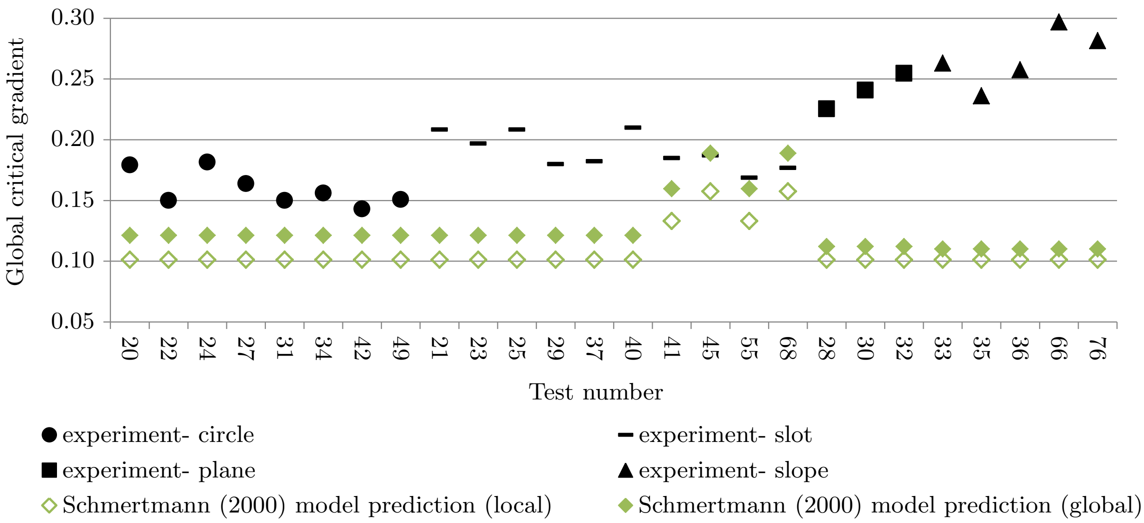

Figure 6.14: Sydney Sand tests from this study across all exit geometries showing inability of C_G factor to model exit-effect

If one were to assume the local critical gradient predictions for seepage lengths of 1.3m were correct (L=1.3m in all tests except 41, 45, 55 and 68), it can be seen that the C_G factors were not large enough to increase predictions up to global critical gradients observed in experiments. It can also be seen that plane and slope global critical gradient predictions were *less than* slot global critical gradient predictions, not greater than as observed in experiments. Therefore, the C_G factors were unable to model both the changes in magnitude and the order of increasing global gradients due to exit geometries.

Possible reasons for inaccuracy of the C_G factor include not compensating for fluidisation and dilation of sand at the exit when using models to calculate the minimum local gradient; using the incorrect local gradient when calculating the C_G factor for slope and plane exits (perhaps the local exit gradient ought to be used instead of the minimum local gradient); and using pre-channel flownets to determine local gradients at the tip for slot and circle exits when these local gradients would be affected by the presence of the channel. These possible reasons are discussed in more detail in Subsection 11.2.3.

The Sellmeijer et al. (2011) formula for a 'standard dike' configuration assumes a slot exit. It does not account for other exit geometries. However, in Subsection 11.3.3 the method of least squares was used to determine a correction factor for each exit which would bring predictions more in-line with experimental results. These exit-correction factors were based on results from both this study and the studies of others. The resulting correction factors were 0.8 for the circle exit and 1.2 for plane exit.

The correction factor for the slope exit depended on what data was considered; when results from this study were considered, the correction factor was 1.4 but when results from the van Beek et al. (2011a) study were included, the correction factor reduced to 0.8. This reduction was unexpected, particularly to <1 which would factor model predictions down instead of up. A factoring up of model predictions was expected because the model assumes a slot exit and, according to critical gradients in this study, slope critical gradients ought to be higher than slot critical gradients, not lower. It was investigated whether there was a distinct difference(s) between the slope testing in this study and the slope testing in the van Beek et al. (2011a) study which would account for the significant reduction in the slope-exit correction factor. Differences identified included the height, length and angle of the slope; the presence of a panel beneath the top of the slope and a pressure bladder; and whether the lid terminated at the slope top or spanned over the slope. It's possible these differences could explain the different slope correction factors needed. Further research into the effect of slope geometry is recommended before a universal slope correction factor can be offered. Where possible, slope exits are not recommended.

Figure 6.15 is a plot of both experimental results and model predictions for tests carried out in Sydney Sand across the different exit geometries. Experimental results are denoted by the black data points (in shapes representing the different exit geometries) and model predictions are denoted by the blue data points before exit corrections are made and in red after exit corrections are made. Note that a slope correction factor of 1.4 was used here.

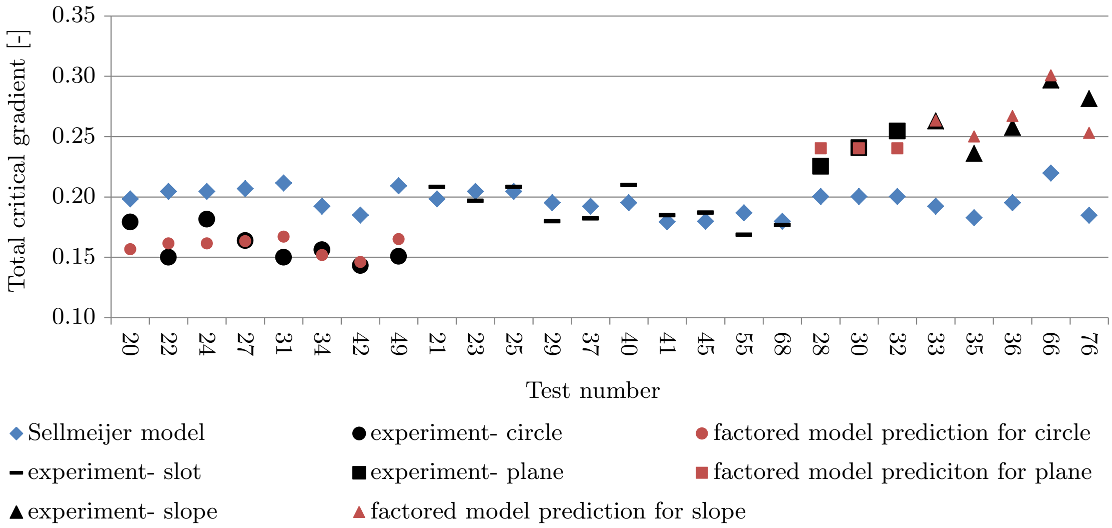

Figure 6.15: Total critical gradient with test number

These model predictions included the amendment suggested by van Beek (2015) whereby Equation 11.8 was used to determine the angle of repose and $\eta = 0.3$. They also included the best-estimate values of relative density = 50% and KAS = 49.8 (essentially removing KAS from the model).

As can be seen in Figure 6.15, the exit-correction factors brought model predictions closer to experimental results- to within 12%.

In conclusion, with the addition of the newly suggested exit-correction factors for the Sellmeijer et al. (2011) 'standard dike' formula, both popular design methods take exit geometry into account but the Sellmeijer et al. (2011) 'standard dike' formula with the new exit-correction factors appears to model the exit effect more accurately.

6.3.4 Accounting for exit geometry in risk assessment

Observations from this study of the behaviour of backward erosion in different exit geometries has the potential to inform and improve current risk assessment and management practices. Identifying which exit geometry is present may assist with estimating the likelihood of backward erosion piping because it is more likely for backward erosion piping to initiate at circle and slot exits than it is at plane and slope exits (because it occurs at lower global hydraulic gradients). Additionally, if backward erosion piping has started (i.e. if a sandboil is present), complete piping progression (leading to dam/levee failure) is more likely for plane and slope exits than it is for slot and circle exits as there is less difference between the initiation and progression gradients (based on experimental evidence).

It is acknowledged that identifying the exit geometry in the field may be challenging given geological and foundation condition uncertainties. In such cases it may be prudent to assume the worst-case scenario (a circle/slot exit before a sandboil is present and a plane/slope exit once it is).

6.4 Summary

This summary brings together the findings on the effects of exit geometry from both Chapter 4 and this chapter. From experimental observations reported in Chapter 4, it was found that the exit geometry significantly impacted the backward eroding process as follows.

1. Boiling (mobilisation of the soil particles at the exit) did not occur in the presence of a slope exit.
2. Equilibrium (a state in which particle mobilisation is observed with channel progression) did not generally occur in the presence of slope and plane exits but did occur in the presence of circle and slot exits.
3. Multiple channels were more likely to occur in the presence of a plane exit. The other exit types did not tend to form multiple channels.
4. Tip speeds were slower in circle and slot exits tests than plane and slope exit tests (and so it took longer for tip to progress through to the upstream end: in the order of a few days compared to a few hours for slope and plane tests).

From experimental results reported in this chapter, it was found that the exit geometry affected the initiation and critical heads. The initiation heads increased in the order of circle, slot, plane and slope with a 103% increase from the circle to the slope exit (in Sydney Sand tests). The critical heads increased in the same order with a 58% increase from the circle to the slope exit (in Sydney Sand tests). Generally speaking, the more an exit concentrated the flow the lower both the initiation and critical heads were. This observation was similar to the observations made by other researchers, thereby confirming the previously speculated exit geometry effect.

Experimental results also indicated that the exit geometry influenced at which point the maximum head (critical head) was required. Critical head was required at initiation in slope and plane tests but required once the channel was approximately 5% and 30% of the seepage length in slot and circle exits respectively. The slot and circle results suggest, the larger the difference between the initiation and critical heads, the longer the channel will be once critical head is reached. As a consequence of this, it is quite possible the length of the channel when critical head is reached is influenced by the size of the exit. To explain, wider slot exits or larger diameter circles exits would require higher heads for initiation, resulting in less different between initiation and critical heads and therefore result in shorter channel lengths when critical is reached, and the reverse for smaller exits. Though, given only one size slot and circle exits were tested, this was not verified.

Van Beek et al. (2013) state the length of the channel when the critical head is reached is a function of soil depth (approximately 1/2 of the seepage length for infinitely deep foundations and decreases in percentage of seepage length with decreasing foundation thickness). However, this study has shown the length of the channel when the critical head is reached is also influenced by exit geometry.

Numerical modelling of the 4 exit geometries has explained why the exit geometry affects the initiation and critical heads and why they increased in the order of circle, slot, plane and slope. With respect to the initiation head, the numerical model demonstrated that the exit geometry alters the local gradient at the exit and it is likely that the local gradient at the exit determines when initiation will occur. The order of increasing local gradient at the exit was the inverse of the order of increasing global initiation gradient. Therefore, exit geometries which cause higher local gradients at the exit require lower global gradients to reach the minimum seepage velocity required to initiate a channel.

With respect to the critical head, the numerical model demonstrated why the circle and slot exits affect the global critical gradient- because the exit geometry affects the local gradient at the tip of the channel and the local gradient at the tip of the channel drives tip progression. Or in other words, because the circle exit causes a higher local gradient at the tip of the channel, it requires a lower global gradient to generate the minimum seepage velocity at the channel tip needed to maintain tip progression.

Having reviewed the two most popular methods for design against Backward Erosion Piping in Chapter 11, it was found that the Schmertmann (2000) model included the C_G factor to account for exit geometry but that the Sellmeijer et al. (2011) 'standard dike' formula did not account for exit geometry as it assumes the 'standard dike' configuration of a slot exit. However, using the sum of least squares method, factors for each exit which increased/decreased the Sellmeijer et al. (2011) 'standard dike' formula predictions closer to experimental results were offered. The exit-correction factors offered were 0.8 for the circle exit and 1.2 for the plane exit. More research into the effect of slope geometry is required before a universal slope correction factor can be offered. With these exit-correction factors, the Sellmeijer et al. (2011) 'standard dike' formula modelled the exit-geometry effect with more accuracy than the Schmertmann (2000) C_G factor.

Chapter 7

Group 3: Set-up variables

7.1 Introduction and aims

It was of interest to investigate the effect variations in experimental set-up had on the backward erosion process. Understanding these effects enabled informed decision making when choosing set-up variables and also provided additional insight into the backward erosion mechanism. Experimental set-up variables of interest included soil density, bladder pressure and seepage length. In particular the following questions were posed:

1. Did the soil placement method affect the initiation and/or critical head?
2. Did the pressure head used to inflate the pressure bladder affect the initiation and/or critical head? Additionally, did the 'pillow' shape of the bladder impose an uneven pressure and did this influence where the backward eroding channel occurred?
3. Are there seepage length effects? I.e. did the length of the flume affect the initiation and/or critical gradient?

The aim of this chapter was to answer these questions.

The default set-up of Group 3 tests included a single flume with a seepage length of 1.3m, Sydney Sand vibrated in, saturated with the use of CO_2 flushing and a bladder pressure of 50kPa (5m of water pressure). In order to investigate the effect of soil placement, two additional soil placement methods were tested- rained in (more loose than the standard vibrate) and vibrated with tamping (more dense than the standard vibrate alone). To investigate the effect of surcharge, two additional bladder pressures were tested- 0kPa and 25kPa (less pressure than the standard 50kPa). And to investigate seepage length, two additional lengths were tested- 2.6m and 3.9m (longer than the standard 1.3m). These tests were classified as 'Group 3' of the experimental program and included 15 tests as listed in Table 3.7.

7.2 Experimental results

7.2.1 Soil density

As discussed in Section 2.4.2 researchers have shown that both initiation heads and critical heads increase with increasing soil density. So whilst the effect of soil density on backward erosion has been tested before, it was still of interest to see how the particular placement methods used in this study would affect the results.

As described in Subsection 3.2.3, four different methods were used to place soil which, in order of expected soil density, included wet pluviation, raining, tamping and vibration. Wet pluviation proved to be unsuccessful so was not considered further.

Tests carried out to investigate the effect of soil density used the default set-up (single flume with a seepage length of 1.3m, Sydney Sand, saturated with the use of CO_2 flushing, circle exit and a bladder pressured of 50kPa) but with two different placement methods. As results would be compared with Group 2 circle-exit results which were either tamped or vibrated in and considered to achieve a medium dense to dense sand (see Section 4.8), the two different densities aimed for were loose and very dense sand. The method of sand raining was used in an effort to produce loose sand and a combination of both tamping and vibrating (in numerous 50mm layers) was used in an effort to produce very dense sand. It was difficult to determine whether loose and very dense sand was achieved (despite considerable effort- see Section 4.8) but it is expected that at least relatively speaking, the targeted densities ought to have been achieved.

Test 46 was rained in to achieve a loose density and Test 49 was both tamped and vibrated in to achieve a dense density. Both tests were loaded with the 'Decrease at points on interest' procedure. Results are plotted in Figure 7.1 along with all circle tests from Group 2 in soils of medium density.

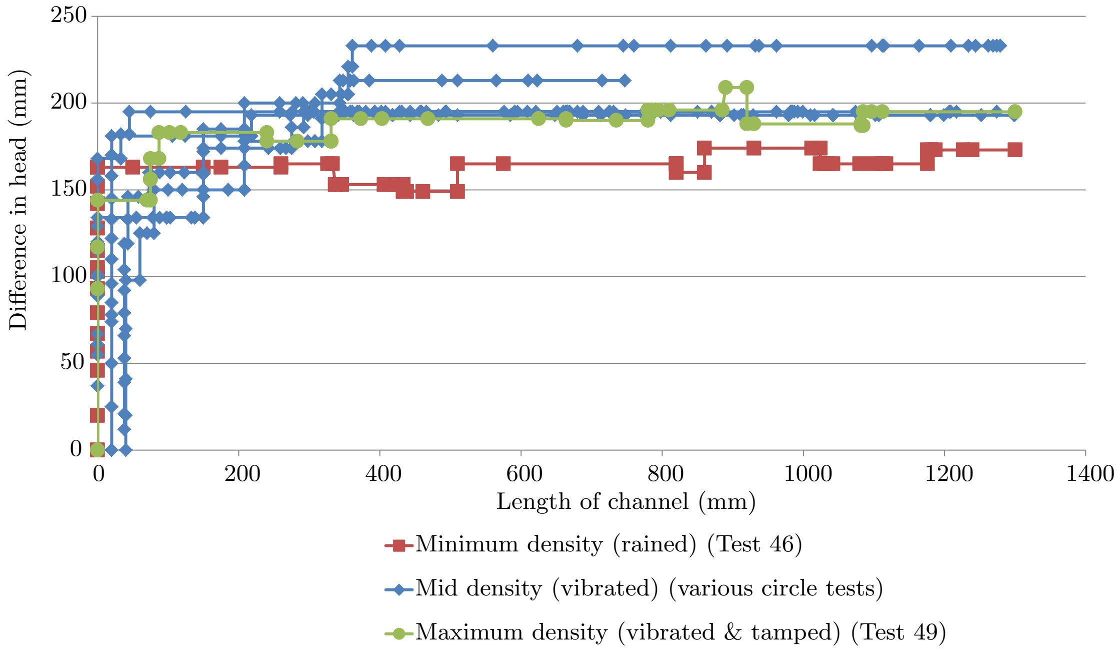

Figure 7.1: Group 3 results- soil density

As shown in Figure 7.1, initiation gradients remained unchanged across the three different soil placement methods. Critical gradient also remained unchanged when soil was compacted with maximum effort (Test 49) but reduced by 20% when soil was rained in (Test 46). Therefore a proportional relationship between initiation/critical gradients and soil density was not observed in experiments.

It is possible there was no increase in critical gradient with increase in compaction effort because the maximum compaction effort did not result in an increase in soil density. This is suggested by soil density measurements plotted in Figure 4.30 in which soil density was similar across all three compaction methods. Whilst this is unlikely, it can not be ruled out given uncertainties with the method of soil density measurement available.

7.2.2 Surcharge

Where backward erosion piping occurs, it will always occur in a confined soil experiencing a significant surcharge load (because backward erosion piping is an internal erosion process, occurring within or beneath a water-retaining embankment). Surcharge will be applied to the eroding soil by the weight of the embankment above it.

As outlined in Chapter 2, other researchers, namely de Wit et al. (1981), Townsend et al. (1981) and van Beek et al. (2011b), have investigated the influence of the surcharge on the soil by applying different surcharges to the soil being tested and looking for changes in the initiation and critical gradients. Both studies report the change in surcharge had no effect on either the initiation or critical gradients.

Surcharge was applied to soil in this study by way of a rubber membrane fixed across the base of the flume. This rubber membrane is referred to as the 'pressure bladder' and is described in Subsection 3.1.1. The pressure bladder was inflated with water pressure, usually with a pressure head of 5m.

To test the effect of bladder pressure, Test 42 was tested without inflating the bladder and Tests 39, 40, 66, 70 and 76 were tested with half of the regular pressure head at 2.5m. Test 42 was carried out using the circle exit, Tests 39, 66, 70 and 76 using the slope exit and Test 40 the slot. Figure 7.2 is a plot of the results. Dark colours are results from the standard 50kPa tests where as bright colours are results from less-than-standard bladder pressures (either 25 or 0kPa). However Figure 7.2a has more colours which are explained below.

In Figure 7.2a Tests 39, 66 and 70 are plotted with grey lines because they were compromised. Both Tests 39 and 70 were compromised when the bladder was inflated incorrectly. Out of habit or miscommunication with laboratory assistance, the bladder was first inflated to 5m of water pressure head before being reduced to the target head of 2.5m. This is likely to have caused a small gap to form between the soil and lid.

To explain why this gap probably formed it is necessary to recognise that when the bladder was inflated its increase in volume was limited by the decrease of soil volume. Therefore the change in volume during bladder inflation could be characterised by one-dimensional

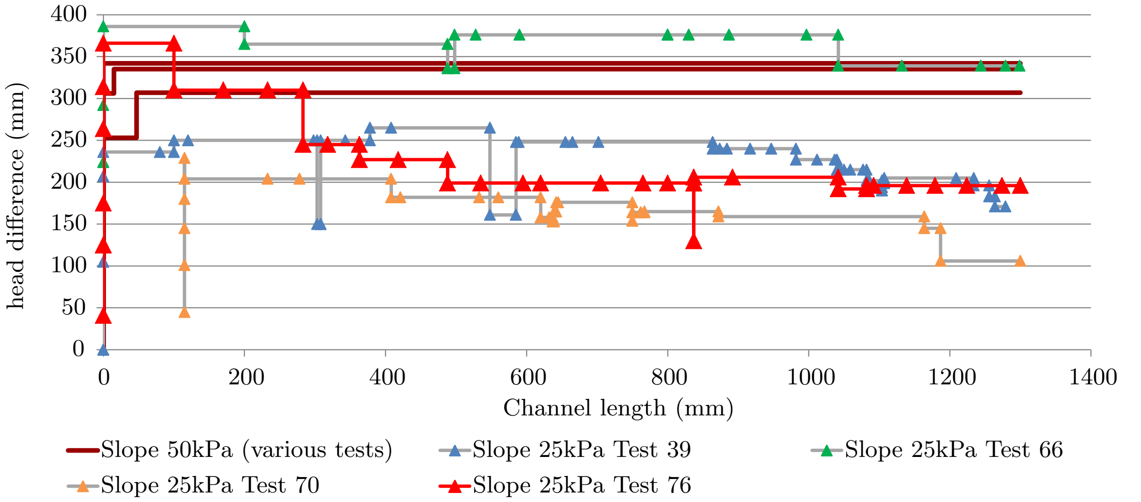

(a) Slope exit

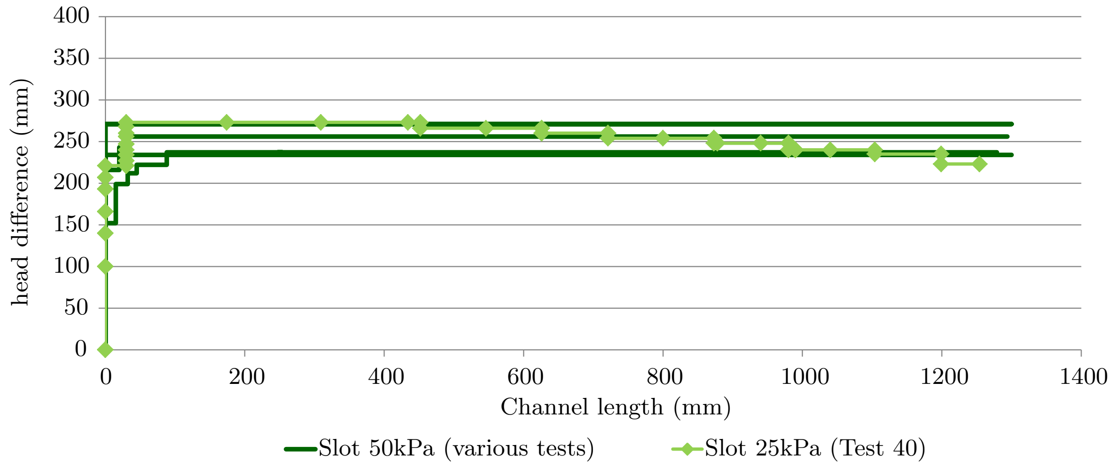

(b) Slot exit

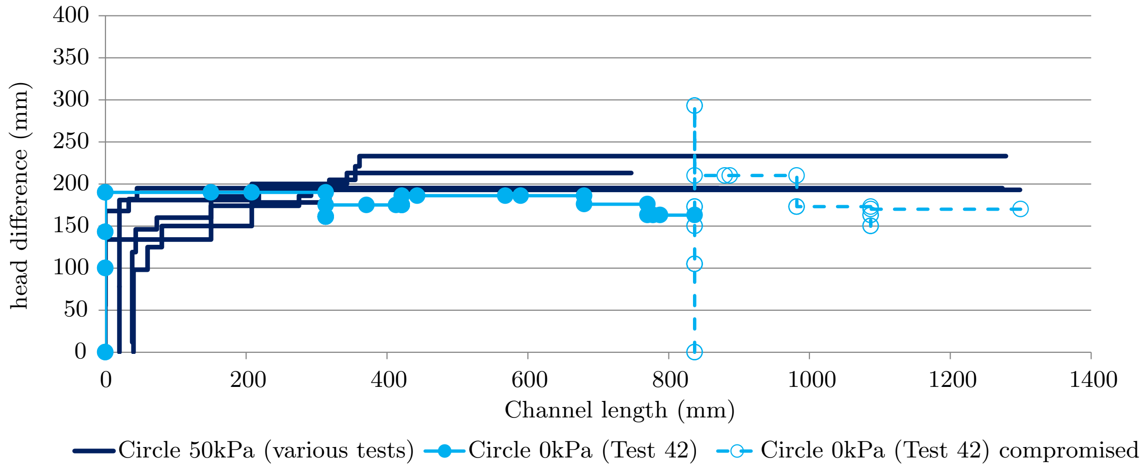

(c) Circle exit

Figure 7.2: Effect of bladder pressure on initiation and critical heads

consolidation of normally-consolidated soil. However when the bladder was deflated, its decrease in volume had little relation to the soil. The bladder volume simply decreased as a result of the drop in pressure and did so elastically. Due to the drop in total stress the soil expanded but did so in the elastic-plastic manner of an over-consolidated soil. This meant the decrease in bladder volume was greater than the increase in soil volume. In other words, the soil did not expand enough to compensate for and fill the space left by the deflated bladder. This is likely to have created a small gap. Pressure measured by earth pressure cells (described later in this section) verified that pressure dropped below pre-bladder-inflation values when the bladder was deflated, indicating the sand did not expand to its pre-bladder volume.

This gap between the soil and lid could have a number of consequences including less stress on the top grains; less friction between the sand and lid; and a zone of higher permeability along the sand-lid interface. All of these consequences would result in less head difference needed to initiate and progress a backward eroding channel and this is what was observed in Tests 39 and 70. The initiation heads were 21 and 22% lower and the critical heads were 19 and 38% lower.

Test 66 was compromised when it became unsaturated overnight (for unknown reasons). The result was higher than normal heads were needed to drive the tip around bubbles which is why the initiation head was 29% higher and critical head was 18% higher.

Test 76 was successful. Its initiation and critical head was 366mm which was only 11% higher than the average critical head of standard tests (within experimental variability). It's acknowledged that the Test 76 line on Figure 7.2a looks quite different to the standard 50kPa lines but this is only due to different loading procedures used for each. The standard 50kPa tests were loaded using the 'increase only' procedure where as Test 76 was loaded using the 'decrease at points-of-interest' procedure. If Test 76 had of been loaded using the 'increase only' procedure as well, it would have simply continued at 366mm for the full length of the flume and looked similar to the standard 50kPa results.

A slot test was also run at a lower bladder pressure- at 25kPa, and gave results similar to the standard 50kPa tests as shown in Figure 7.2b. The only difference was Test 40 decreased in head with channel length because the 'decrease at points of interest' loading procedure was used instead of the 'increase only' procedure.

A circle test was also run at a lower bladder pressure but this time it was no pressure, i.e. the bladder was left deflated. Yet it too produced results similar to the standard 50kPa tests as shown in Figure 7.2c. There were subtle differences in results but none of which were a result of no bladder pressure. The subtle differences were a) not stopping after initiating, because there was a gap between the sand and circular exit as sketched in Figure 6.11a (like there was in Test 24) b) the 'decrease at points of interest' procedure was used instead of the 'increase only' procedure and c) Test 42 was compromised when the channel was 837mm long because the test became unsaturated when the sump pump turned off (because the water level in the pit became too low, switching the sump pump off via its float switch).

In summary, the results show that similar initiation and critical heads were achieved regardless of whether 25kPa or no bladder pressure was applied. Therefore it was confirmed that the magnitude of surcharge applied does not affect backward erosion piping. What is important is that there is sufficient pressure to ensure there is contact between the soil and lid. This contact needs to be sufficient enough to ensure the void ratio along the interface is similar to the void ratio within the sand matrix so that there isn't less friction or more flow where backward erosion occurs.

An additional question was posed when considering the effect of the pressure bladder on the backward eroding process: did the 'pillow' shape of the bladder impose an uneven pressure and did this influence where the backward eroding channel positioned itself? For instance, when channels positioned themselves along the edges of the flume did it do so because there was less effective stress in these areas and so initiation and critical heads observed in these tests were compromised and not reliable as the backward eroding mechanism was being influenced by experimental artefacts (i.e. differential stress not present in the field)? This question is sketched in Figure 7.3b.

The 'pillow' shape of the pressure bladder can be seen in Figure 7.3a, although the shape is likely to be far less pronounced when soil is confined in the flume above it. This shape is also shown in Figure 7.3c but as wet soil pushed up out of the flume by the bladder pressure (without constraint of the lid). Usually the bladder was deflated before the Perspex lid was removed but in this scenario (after Test 40) it was not.

Given the results above indicating that bladder pressure does not effect the initiation or

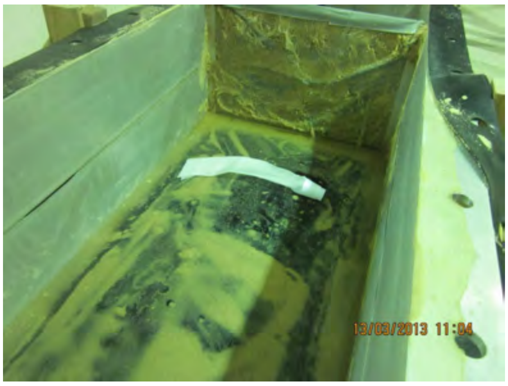

(a) Empty flume showing pillow shape of inflated pressure bladder

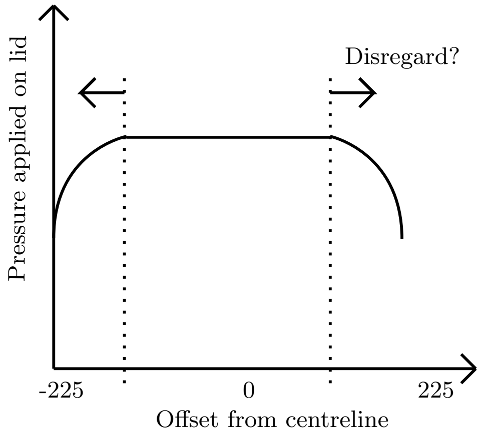

(b) Sketch of 'pillow' effect concern

(c) Sand pushed up out of flume by bladder after Test 40

Figure 7.3: Bladder 'Pillow' effect

critical heads then it is unlikely that differential stress would effect the heads either, but it was still worth investigating.

To investigate this, three earth pressure cells were placed on the underside of the Perspex lid across the flume width in the centre. Cell number 4 was placed in the middle, cell number 3 next to the edge and cell number 12 midway between the centre and edge (these positions are sketched in Figure 7.4a). All cells were placed beneath a restraining bar where deflection would be at a minimum. It was interest to see whether cells placed in the centre would read more pressure than cells near the outer edge.

Sand was dry during bladder inflation and then slowly inundated with water. Saturation of the sand was not achieved because CO_2 flushing was not possible on account of not being able to seal the flume with pressure cell cables protruding.

Cell readings are plotted in Figure 7.4a over time. The plot includes indicators of when the lid bolts were fastened; when the infilling of water commenced; and the inflation and deflation of the bladder. Figure 7.4b is an interpretation of the results as the approximate cell reading against bladder pressure applied. The number labels denote the order where 1 was before the lid was fastened (the bladder pressure of -10kPa has no meaning, it was done just to position these data points to the left of the 2nd data points), 2 was once the lid was bolted down, 3 was once the bladder pressure was applied to 50kPa and 4 was once the bladder was deflated. The pressure increase labels donate the change in pressure from before and after the bladder pressure was applied. Figure 7.4c is the same results just presented as the increase in pressure due to bladder inflation across the width of the flume- to show spatial variation.

As can be seen in Figure 7.4a cells 3, 4 and 12 gave initial pressure readings of 25, 10 and 10kPa respectively but then increased to about 30, 18 and 47kPa respectively when the bolts where tightened down. Then, as the pressure bladder was inflated to 50kPa the cell readings increased to 60, 50 and 80kPa respectively. Because the cells were detecting pressure before the bladder was inflated (due to having the lid bolted down on top of them) it was necessary to take the change in pressure to measure the pressure applied by the bladder (as opposed to absolute pressure readings).

The change in pressures at cells 3, 4 and 12 were 30, 33 and 33kPa respectively and are plotted on Figure 7.4c against the spacial distance of each cell location with respect to the flume's centreline. Even though there were only 3 cells, 5 pressure readings have been plotted on Figure 7.4c assuming readings would have been symmetrical across the flume width. Figure 7.4c indicates the 'pillow' effect was minimal. There was only 3kPa difference between the centre and edges of the flume, therefore the bladder pressure was applied reasonably even and is unlikely to influence where the backward eroding channel positioned itself. This meant that initiation and critical heads observed need not be disregarded when the channel occurred along the flume's edges.

It is interesting to also note that when the bladder was deflated, pressure readings dropped to about 30, 13 and 18kPa at cells 3, 4 and 12 respectively. These pressure readings were lower than the pre-bladder-inflation readings by 30, 37 and 62kPa indicating the elastic-plastic behaviour of the sand in that it didn't expand back to it's original volume.

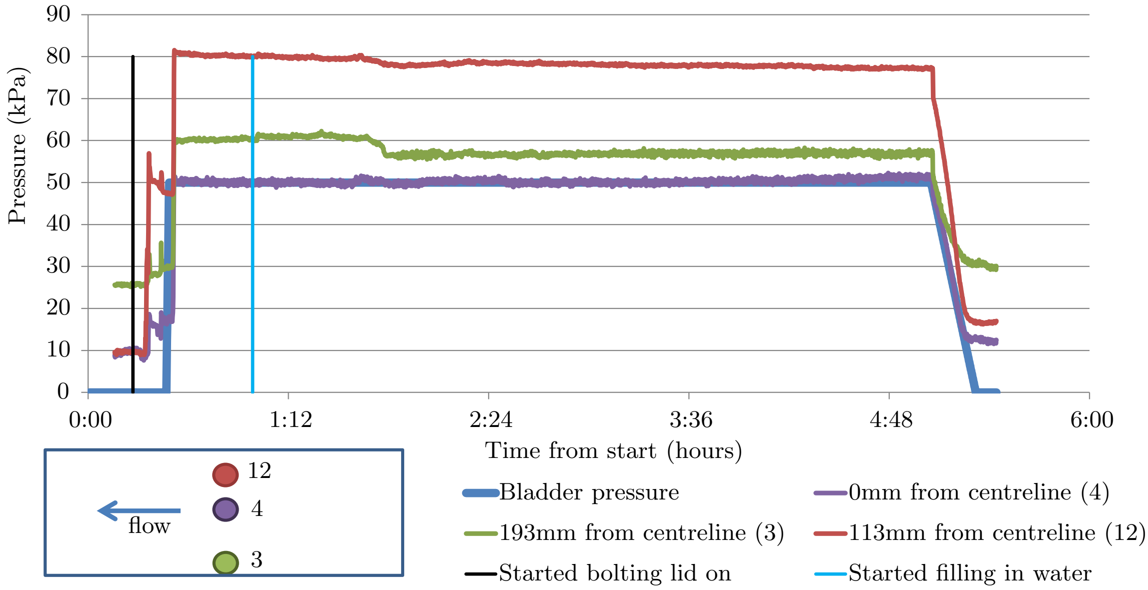

(a) Earth pressure cell data with time

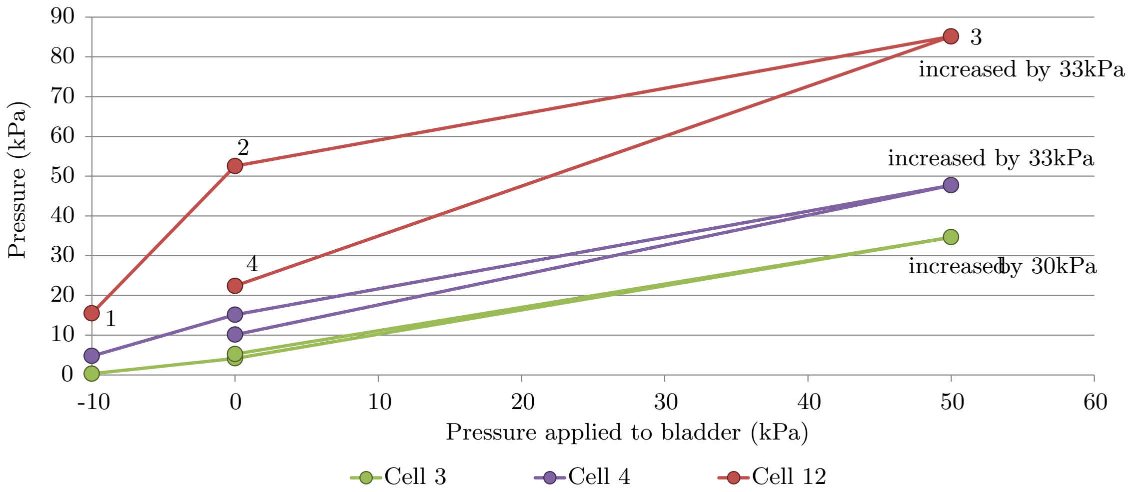

(b) Approximate cell pressure readings against bladder pressure applied

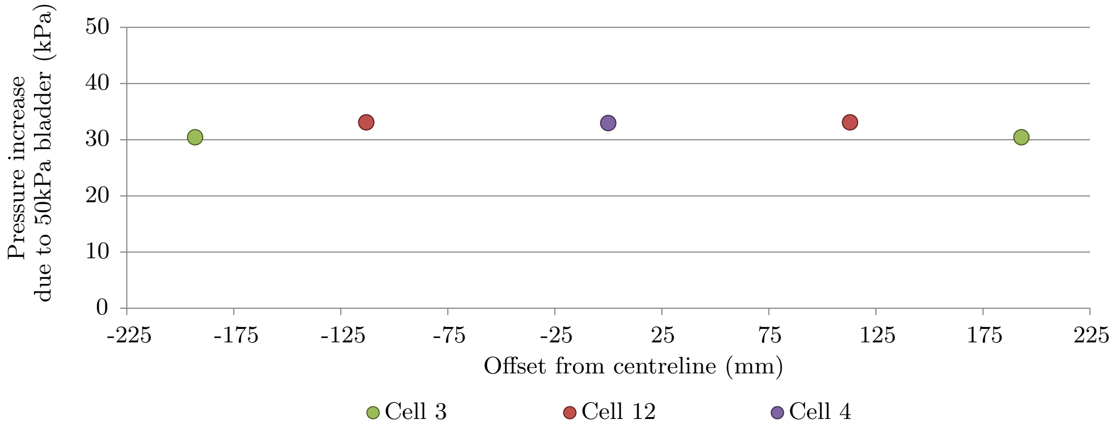

(c) Change in pressure due to bladder inflation across width of flume

Figure 7.4: Earth pressure cell Test 5 results

This supports the theory discussed above that incorrect bladder inflation, i.e. to 50kPa before bringing back down to 25kPa, produced a gap between the sand and lid.

7.2.3 Seepage length

The seepage length is the distance from the downstream exit where the channel starts to the upstream end where the channel connects to the reservoir/river. It is the distance the overall head difference is divided by to obtain the global hydraulic gradient.

The influence of the seepage length was investigated by de Wit (1984) (with experiments in flumes 2.4 and 4.5m long) and Silvis (1991) (with experiments in flumes 6, 9 and 12m long). Both investigations found that seepage length did not affect the initiation or progression gradients so long as the depth of the eroding soil was kept constant.

This study also investigated the influence of the seepage length by joining two flumes together and moving the upstream panel to create three different seepage lengths, 1.3, 2.6 and 3.9m, as discussed in Subsection 3.1.1 and drawn and photographed in Figure 3.6. Tests 41 and 55 were carried out on a seepage length of 2.6m and Tests 45, 65 and 68 were carried out on a seepage length of 3.9m. All these tests were carried on Sydney sand vibrated in, with a bladder pressure of 50kPa (5m water pressure head) and a slot exit.

Experiments showed the seepage length affected the backward eroding piping process in the following ways:

1. A channels susceptibility to blocking. The longer the seepage length the more frequently channels became blocked. This is elaborated on in Subsection 4.5.4.
2. The speed of tip progression. The longer the seepage length the slower tip progression was likely to be on account of channel blocking.
3. The magnitude of the initiation and critical heads. This is elaborated on below.

The results are presented in Figure 7.5 as the head difference required to achieve the given channel length in both (a) and (b) however Test 65 was omitted from results presented in (b) for reasons to follow. The results are non-dimensionalised in (c) as the global hydraulic gradient required to progress the channel to the given length, expressed as a percentage of the total seepage length. Results are also listed in Table 7.1.

Table 7.1: Group 3 test results- Seepage length effects

	Seepage length (mm)	Initiation head (mm)	Critical head (mm)	Initiation gradient (-)	Critical gradient (-)
Group 2 slot	1300	219	240	0.17	0.18
Test 41	2600	270	481	0.10	0.19
Test 55	2600	439	439	0.17	0.17
Test 45	3900	324	798	0.08	0.20
Test 65	3900	394	?	0.10	-
Test 68	3900	690	705	0.18	0.18
average	-	-	-	0.13	0.18
range	-	-	-	0.09	0.04
standard error	-	-	-	0.02	0.006

To follow are comments on results in sequential test order.

Test 41 required a 119mm increase in head when the channel was near 2m long. This was unusual behaviour- usually the maximum head was needed when the channel was relatively short (within the first 10% of the seepage length). However in the case of Test 41, the maximum head was when the channel was about 75% of the seepage length. This position coincided with the flume joins. Therefore it is likely this unexpected rise in head is an experimental artefact, possibly due to a small gap between the lid ends where the rubber gasket didn't extend all the way down to the sand's surface. This rise in head needed at the flumes join was also seen in Tests 45 and 68. In these tests, once the head was high enough to drive the tip past the join it was quickly lowered to a head difference similar to what it was before the tip reached the join. For this reason, maximum heads reached at the flume join were not considered to be the critical head but were disregarded as an experimental artefact.

Test 45 initiated at a rather low head of 324mm. This was considered low because it was less than or similar to heads the 2.6m tests initiated at and it was expected that longer seepage lengths would require higher initiation heads. However the expected critical gradient, i.e. double that of 2.6m tests, was reached. This large difference in initiation and critical heads is why the critical channel length is relatively long at about 500mm. There is no indication in test notes as to why it initiated at such a low head.

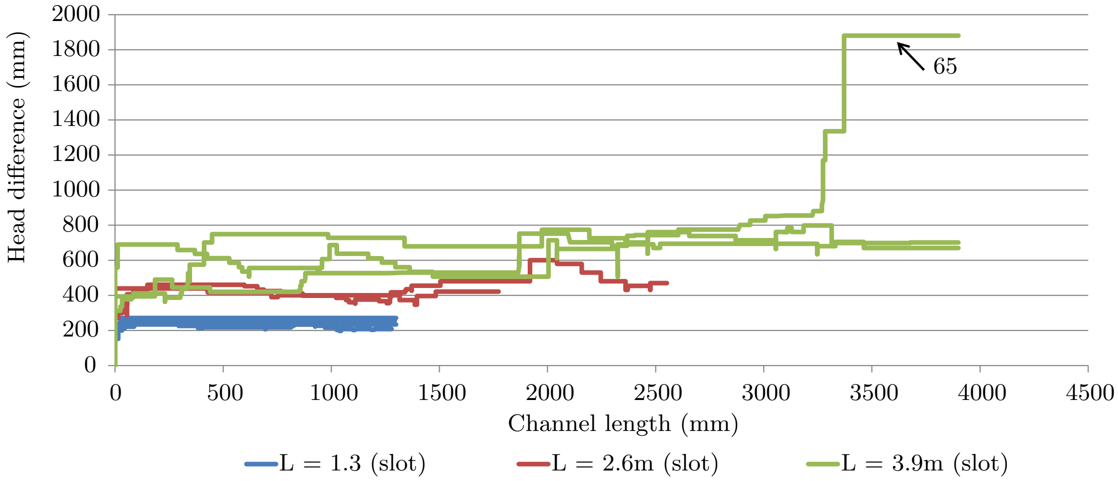

(a) Head difference required to achieve channel length for different seepage lengths

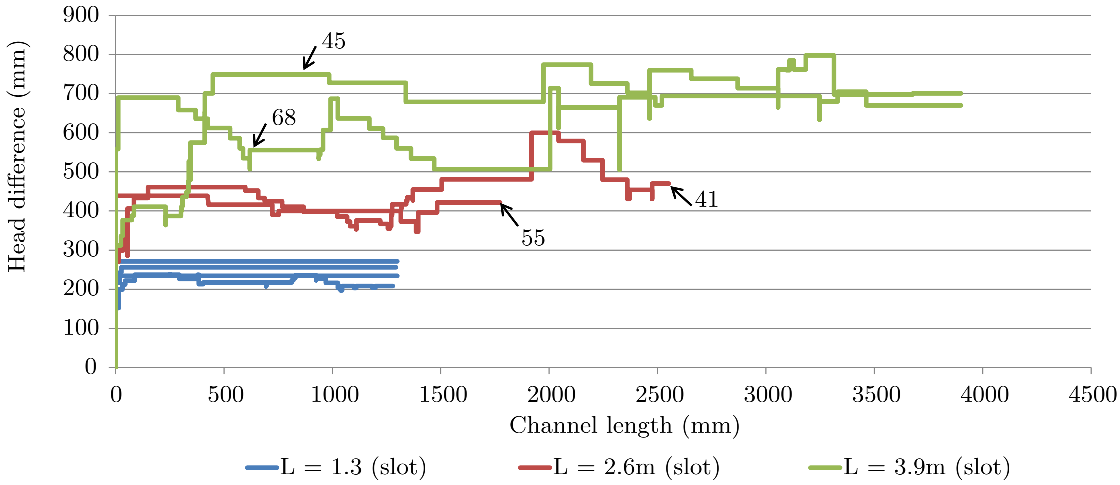

(b) Head difference required to achieve channel length for different seepage lengths with Test 65 omitted

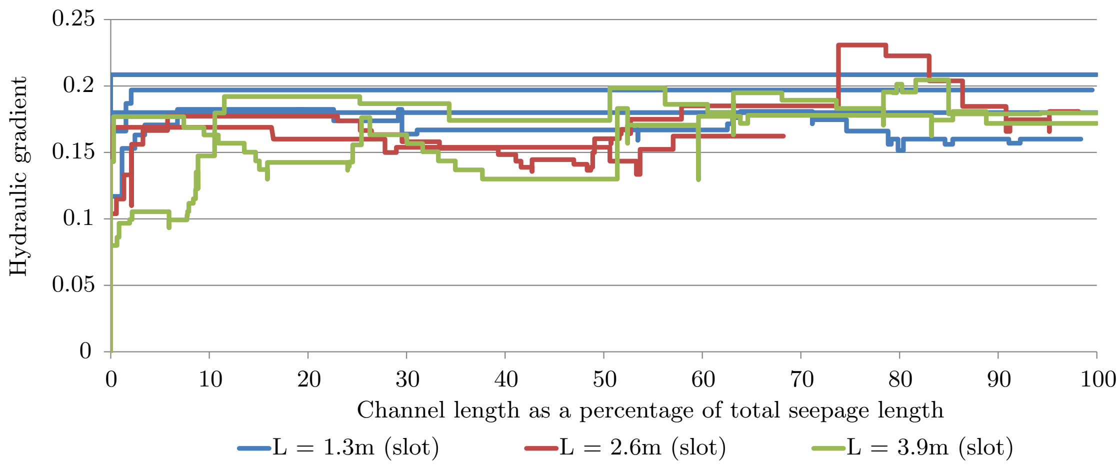

(c) Non-dimensionalised results: Global hydraulic gradient required to achieve channel length as a % of seepage lengths for different seepage lengths (Test 65 omitted)

Figure 7.5: Effect of seepage length

Test 55 did not reach the upstream end at 2600mm because the tip intercepted a large air bubble at 1774mm. Air from the bubble entered the channel. For this reason, and because larger still air bubbles were present further upstream, the test was terminated. Bubbles entered the sample when the submersible pump turned off allowing water to flow back down into the pit which lowered the water level to below the flume lid. It was not known why the submersible pump turned off.

Test 65 is shown in Figure 7.5a but was removed for Figure 7.5b so that other tests could be seen more clearly (more appropriate y-axis scale). When the head difference was 880mm boiling at the exit stopped. The hypothesis is boiling stopped on account of a tall sand boil. The weight of the soil column through the centre of the boil was now heavier than the pore pressure beneath it. Because boiling had stopped at the exit, more head loss was now occurring at the exit, hence reducing the gradient along the flume. This is why the tip stopped progressing. In hindsight it would have been better to remove the sand boil, then the tip may have re-initiated and continued to progress to the upstream end at the same head, however this wasn't thought of at the time, instead the head was continually raised.

Test 68 was carried out slightly differently in that:

1. The head wasn't lowered only at points of interest but was lowered repeatedly, usually in 25mm increments (half a turn of the constant head tank winch), until the tip stopped.

2. Instead of waiting approximately 15 minutes before raising the head after tip arrest, a minimum of 60 minutes was allowed to pass, during which the tip was stationary, before deciding to raised the head.

3. The sand boil was removed periodically, especially before raising the head or when boiling ceased.

This change in procedure resulted in a plot that was lower than the other 3900mm seepage length test, Test 45, as can be seen in Figure 7.5b. Yet the critical heads were still similar and so Test 68 was considered to have demonstrated repeatability of 3900mm long tests.

Whilst removing the sand boil did on occasion enable the tip to progress a little further, it didn't keep from having to raise the head. In other words, removing the sand boil didn't reduce the critical head. More discussion on the sand boil, such as its size, is given in Section 4.6.

Experimental artefacts aside, the results generally show that the initiation and critical heads were directly proportional to the seepage length, that is, if the seepage length was doubled so were the initiation and critical heads. This meant that the global initiation and critical *gradients* remained unchanged. This is shown in Figure 7.5c as results overlying each other and in Table 7.1 as a small range and standard error in critical gradients. It is acknowledged that the 1.3m results in Figure 7.5c (the blue lines) appear slightly higher than results associated with other the two lengths, however, this is only due to the different loading procedures used, of 'increase only' in the 1.3m flumes and 'decrease at points of interest' in the other flumes.

7.3 Discussion

7.3.1 Soil density

Effect of soil density from other studies

Whilst experimental results from this study we not able to demonstrate the relationship between soil density and initiation or critical gradients (because a reliable method of measuring density was not available), it was still possible to use experiential data from de Wit (1984), van Beek et al. (2011a) and van Beek (2015) as these studies provided relative density measurements.

As discussed in the literature review in Section 2.4.2, van Beek et al. (2011a); van Beek (2015) measured relative density by either weighing the entire flume full of sand (then with an assumed sand particle density and flume volume calculated the bulk soil density) or using an electrical density method where by electrical resistance was related to porosity using a soil-specific empirical equation.

Van Beek (2015) plotted Figure 2.9a to illustrate the relation between the initiation gradient and porosity (inversely proportional to density) and Figure 2.9b to illustrate the relation between the critical gradient and density. Here, Figure 7.6 is plotted to further illustrate the effect of soil density. Each data series delineates sets of experiments which were the same apart from soil density. In all but one case, the critical gradient did increase with increase in relative density. This makes sense as an increase in density would result in a decrease in permeability which would therefore require a higher head to generate the necessary erosive forces. Although the proportional relationship was somewhat weak in that there was much scatter and variability around the trend-lines and the angle of trend-lines varied (i.e. the density had more affect in some soils than others).

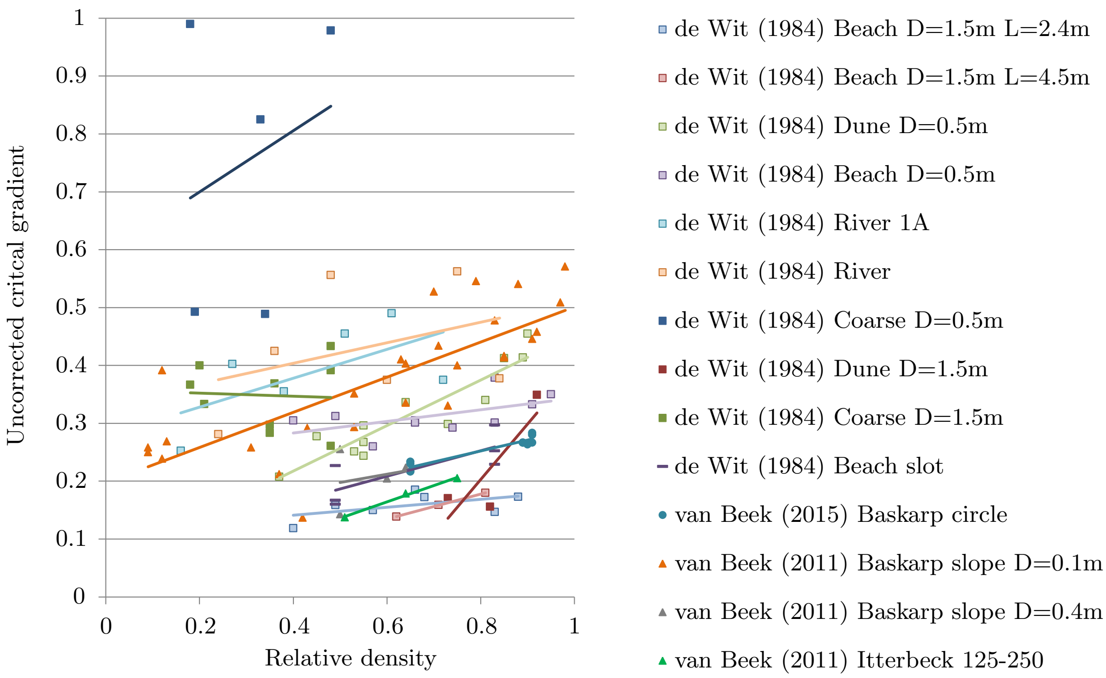

Figure 7.6: Uncorrected critical gradient of experiments against relative density showing slight but varied proportional relationship

Accounting for soil density in design

Chapter 11 contains a review of the two most popular methods of design against backward erosion piping- the Schmertmann (2000) and Sellmeijer et al. (2011) methods. This review considers how accurately these methods predicted experimental results from both this study and the studies of others and suggests amendments which improves the accuracy. Here a summary is given on how these two design methods account for soil density and, with the use of data from other studies, a judgement is made on which design method more accurately accounts for changes in soil density.

The Schmertmann (2000) model account for soil density with the density factor, C_γ whereby

$$C_\gamma = 1 + 0.4\,(RD - RD_{UoF}) \tag{7.1}$$

Where $RD_{UoF} = 0.6$ on the basis that experimental data used to form the model had an average relative density of 0.6. Equation 7.1 means that the critical gradient change by 20% over the full range of relative density, or in other words, a 10% change in relative density will produce a 4% change in critical gradient.

To illustrate the effectiveness of the C_γ factor, Figure 7.7a is a plot of normalised gradient with relative density. Experimental gradients were normalised using the gradient expected at the relative density of 60% (the RD_{UoF}). To determine the expected gradient at RD=60%, a line-of-best-fit was fitted through experimental results and it's equation was used to provide the gradient expected at RD=60%.

Normalised gradients at or near a relative density of 60% should now ≈ 1 whilst C_γ also ≈ 1. When $C_\gamma \approx 1$, no adjustment is made on account of soil density. When experiments within each series vary only in relative density, any trend in the normalised gradients should be modelled by C_γ.

Figure 7.7a shows 2 of the 4 linear lines of best fit align with the C_γ line and of the 2 which do not, vary only in slight slope changes. Though it is noted that their R^2 values were low (with the exception of the de Wit (1984) data in Dune sand). Therefore, it appears that experimental variability is so significant that subtle changes in gradient due to soil density is difficult to model and predict.

In addition, as demonstrated and discussed in Subsection 11.2.3, the C_γ factor was unable to capture the linear increase in gradient with relative density because the slope of this relationship varied across the different soils. In other words, it was possible that soil density affected the gradient more in some soils than others and so one relationship for all soils did not suffice.

Furthermore, inclusion of the C_γ factor did not improve the coefficient of determination R^2 of the Schmertmann (2000) model, it marginally reduced it from 0.64 to 0.56 (see Table 11.1). Therefore, the author suggests to not use the C_γ factor.

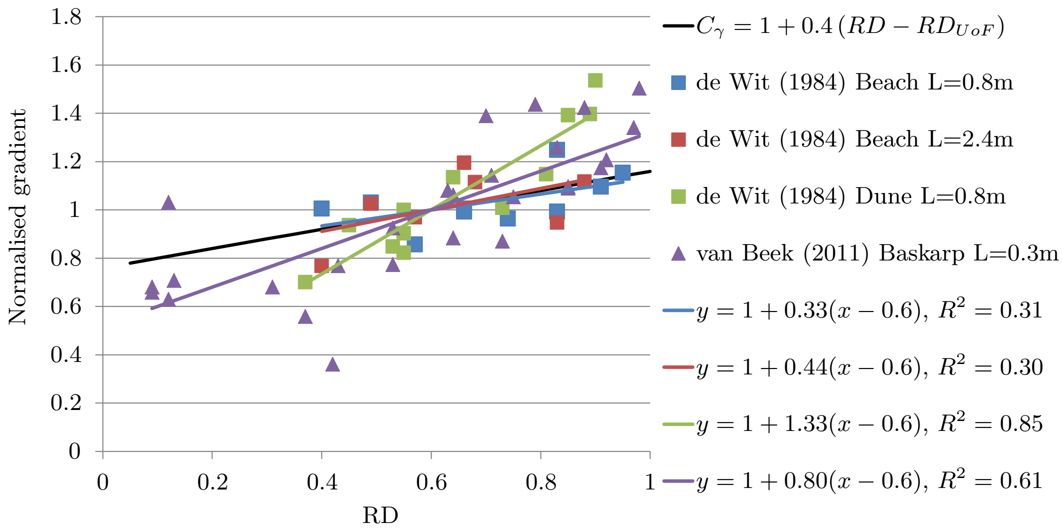

(a) Ability of C_γ factor (in Schmertmann (2000) model) to model relative density effect (reference relative density = 60%)

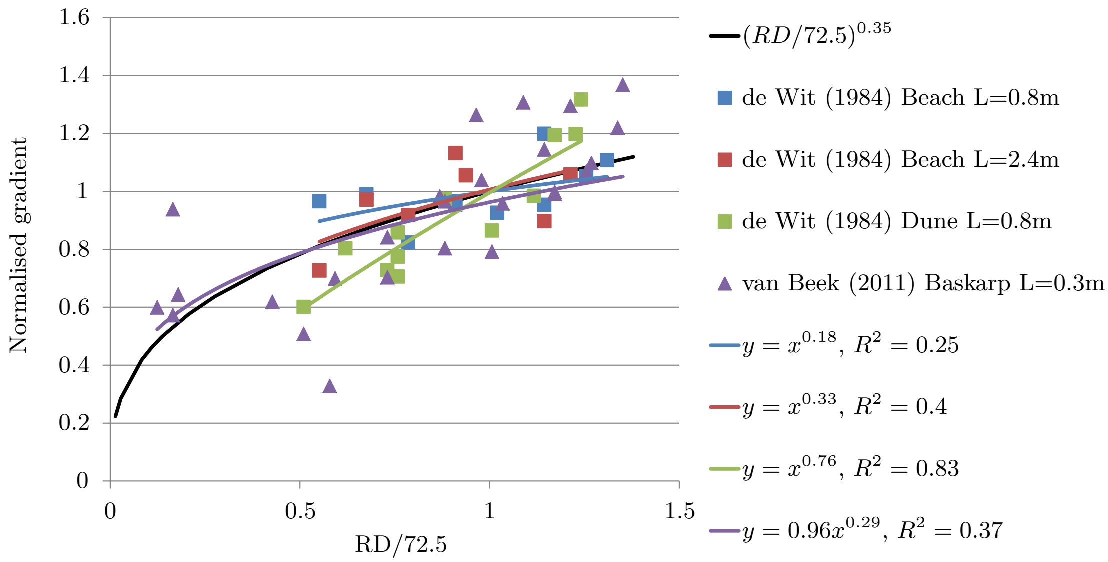

(b) Ability of $(RD/RD_m)^{0.35}$ term (in Sellmeijer et al. (2011) model) to model relative density effect (reference relative density = 72.5%)

Figure 7.7: Ability of each model to capture the effect of relative density- gradients normalised using gradient at reference relative density

As for the Sellmeijer et al. (2011) model, relative density was incorporated into the model via a multivariate analysis which produced a relation of $(RD/RD_{mean})^{0.35}$ where RD_{mean} was the average relative density amongst the tests in van Beek et al. (2011a) equal to 72.5%.

To illustrate the effectiveness of the $(RD/RD_m)^{0.35}$ term, Figure 7.7b is a plot of normalised gradient with RD/RD_m. This plot was constructed in the same way Figure 7.7a was except that gradients were normalised using the gradient expected at a relative density of $RD_m = 72.5\%$ (instead of 60%).

Figure 7.7b shows power lines-of-best-fit did align with the $= (RD/RD_m)^{0.35}$ term, with the exception of the de Wit (1984) data in Dune sand, which plotted with a higher exponent. However, the lines-of-best-fit which aligned with the $= (RD/RD_m)^{0.35}$ term had low R^2 values (between 0.25–0.4). As was the case for the C_γ factor, it appears that experimental variability is so significant that subtle changes in gradient due to soil density is difficult to model and predict.

The Sellmeijer et al. (2011) model with the $(RD/RD_m)^{0.35}$ term models the effect of relative density only marginally better than the C_γ factor in the Schmertmann (2000) model with an R^2 value of 0.49 as compared to an R^2 value of 0.44. But clearly neither do well on account of experimental variability. Note these R^2 values are based only on the data plotted in Figure 7.7, additional experimental data was available to plot but this additional data did not contain as many data points or covered as large a range in RD.

Relative density of soil foundations beneath dams and levees in the field is difficult to measure. One would have to either expose the foundation and test with a nuclear densitometer or use geophysical survey or borehole investigations (using a cone penetrometer or standard penetration tests), all of which provide average estimates only. Furthermore, relative density would vary in a far greater manner within the foundation than within experimental flumes with controlled soil placement. Construction records may be available with foundation densification specification and/or test records, but again, the engineer would still need to make estimations across probable ranges. Considering this, and given the effect of density on the critical gradient is relatively small and experimental repeatability is relatively large, it is suggested that the density of soil need not be incorporated in prediction models but instead be accommodated for with the use of sensible factors of safety in design.

7.3.2 Surcharge

The findings of this study were in agreement with the findings of de Wit (1984), Townsend et al. (1981) and van Beek et al. (2011b) in that surcharge applied to experiments did not affect the critical gradient. Application of a surcharge served only to ensure a good contact between the sand and lid.

Examples of poor contact between the sand and lid were tests in van Beek et al. (2011a) which eroded forwards and Tests 39 and 70 in this study which eroded at lower initiation and critical gradients.

Forward erosion suggests a poor contact because it behaved more as concentrated leak erosion through a gap rather than backward erosion. Van Beek (2015) also gave evidence of this gap as exceptionally high porosity (around 0.7) (as indicated by electrical resistance measurements) and visual observation.

Lower initiation and critical gradients suggest a poor contact because less head is needed to reach erosive forces which suggests higher flow gradients are present. Higher gradients suggest a preferential flow path exists along the interface where backward erosion occurs which suggests a higher void ratio between the lid and sand than within the sand. The incorrect bladder inflation could explain the higher void ratio because when the bladder was inflated to 50kPa and then partially deflated to 25kPa, it is likely that the bladder deflated more (elastically) than the soil rebounded (as elastic-plastic material) causing a larger void ratio (or even a gap) at the sand-lid interface. However, there no measurements available to verify this larger void ratio or gap. Note that when the bladder was inflated correctly in Test 76- straight to 25kPa and kept constant, the initiation (and critical) gradient was between 55–79% higher than those in Tests 39 and 70 and were similar to the initiation (and critical) gradients in standard tests (with a bladder pressure of 50kPa).

It is not clear why Tests 39 and 70 in this study did not forward erode like tests in the van Beek et al. (2011a) study. Both sets of experiments are likely to have gaps or a larger void ratio between the lid and sand yet the behaviour of both were different. Perhaps there is a spectrum of resulting behaviours from a gap- the smallest of gaps, just large enough to create a larger void ratio resulting in slight flow preferential but soil is fixed enough to still enable backward erosion, where as larger gaps behave more like concentrate leak erosion and push erosion forwards first.

The theory of van Beek (2015) as to why additional surcharge does not affect the critical gradient appears reasonable- because there is zero or near zero effective stress at the channel tip and it's conditions at the channel tip which drives progression. The addition of surcharge is of no consequence once a channel opens a void and allows neighbouring sand particles to dissipate effective stress. Van Beek (2015) confirms effective stresses at the channel tip approached zero with readings from stress sensors.

There is likely to be good contact between the soil foundation and cohesive embankment in the field given the weight of the embankment pressing down on the foundation. Therefore forward erosion or erosion at lower gradients due to a higher void ratio along the interface is unlikely.

It is noted that neither the Schmertmann (2000) or Sellmeijer et al. (2011) methods incorporate total or effective stress which agrees with these experimental observations.

7.3.3 Seepage length

Experimental results indicate that seepage length does not affect the initiation or critical gradients. This is in agreement with the findings of de Wit (1984) and Silvis (1991) as indicated by Figure 7.8. Data plotted in Figure 7.8 were restricted to test series which were identical in all ways except for seepage length. Of particular importance was these test series were tested in flumes with constant depth and width (otherwise the gradient would not have remained constant). This plot illustrates that gradients remained somewhat constant across a range of different seepage lengths (with the exception of two high outliers).

Accounting for seepage length in design

Chapter 11 contains a review of the two most popular methods of design against backward erosion piping- the Schmertmann (2000) and Sellmeijer et al. (2011) methods. This review

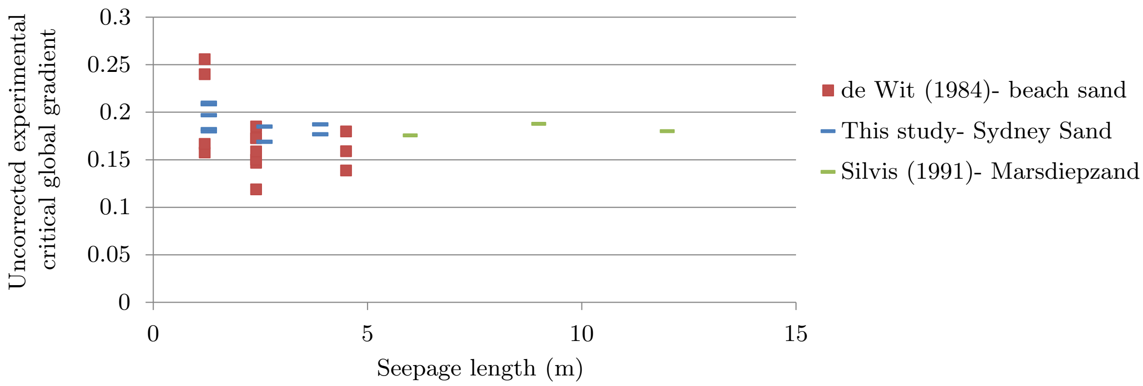

Figure 7.8: Tests carried out in flumes of the same depth but across different seepage lengths showing independence between gradient and seepage length

considers how accurately these methods predicted experimental results from both this study and the studies of others and suggests amendments which improves the accuracy. Here a summary is given on how these two design methods account for seepage length.

The Schmertmann (2000) model accounts for seepage length with the length factor:

$$C_L = (L_t/L_f)^{0.2} \tag{7.2}$$

where L_t is the seepage length in the University of Florida testing (1.524m) and L_f is the seepage length being considered.

Given Figure 7.8 demonstrates that seepage length does not affect the critical gradient, it is suggested a correction factor for seepage length is not needed. However, as C_D the correction for depth, was evaluated in terms of a D/L ratio, C_L is required to compensate for the scenario when both L and D increase whilst keeping D/L constant, so no correction is provided by C_D factor, yet the gradient still decreases. Hence, C_L is required when C_D is a function of D/L. If C_D were to be altered to be a function of depth only, then C_L could be omitted.

Schmertmann (2000) used Figure 11.14 to verify C_L was required and to determine the exponent in Equation 7.2 of 0.2. Although errors in the data points on this graph were identified (discussed in Subsection 11.2.3) and an exponent of 0.1 worked better for the de Wit (1984) data; data from this study verified the original 0.2 exponent and the original 0.2 exponent still resulted in the best improvement to the overall R^2 value, from 0.51 before C_L was applied to 0.64 after C_L was applied.

As for the Sellmeijer et al. (2011) model, seepage length is incorporated into the model within the scale factor where by $i_c \propto 1/\sqrt[3]{L}$.

To illustrate accuracy of both C_L and the $1/\sqrt[3]{L}$ term, experimental results of tests which varied in seepage length only, were used to back-calculate the C_L factor and the $1/\sqrt[3]{L}$ term required to align model predictions. These back-calculated C_L factors and $1/\sqrt[3]{L}$ terms are plotted in Figure 7.9 along with the curves of $C_L = (1.524/L)^{0.2}$ and $1/\sqrt[3]{L}$. When back-calculated values do not lie over the curve, this does not necessarily mean a discrepancy or error in C_L or the $1/\sqrt[3]{L}$ term as the back-calculated values contain other discrepancies and errors contained within the model. However, given experimental results used were restricted to tests series which varied in seepage length only, other components of the models would remain constant within a data series so that even if they contained errors, the errors would remain constant and any trends should only be due to the effect of seepage length. In other words, even if data points lie above or below the C_L factor and $1/\sqrt[3]{L}$ curves, they should at least lie along similar, 'parallel', curves.

As can be seen in Figure 7.9, most data points are positioned along trends similar to the C_L factor and $1/\sqrt[3]{L}$ curves. Therefore both the C_L factor and $1/\sqrt[3]{L}$ terms do appear to capture the seepage length effect with reasonable accuracy, although experimental variability makes verifying the relationship with certainty, difficult. Experimental variability also makes it difficult to assess which model captures the seepage length affect more accurately, as do other errors/discrepancies in the models.

As discussed previously, critical gradient is independent of seepage length, however, because scale is quantified in terms of the D/L ratio, then a correction for seepage length is still required to, in effect, 'decouple' the influence of depth from length. If scale was not quantified in terms of the D/L ratio then a correction for seepage length would not be required. In fact, the seepage flux area, DW, would be a more suitable measure of scale given it is this area which controls the volume of flow, This volume of flow controls the volume of flow entering the channel which in turn determines seepage velocities entering the channel and it is these seepage velocities which drive erosion and ascertain the hydraulic head (or gradient) required. Notably though, the 'width' in field applications would need to be based on research into the lateral influence of erosion channels.

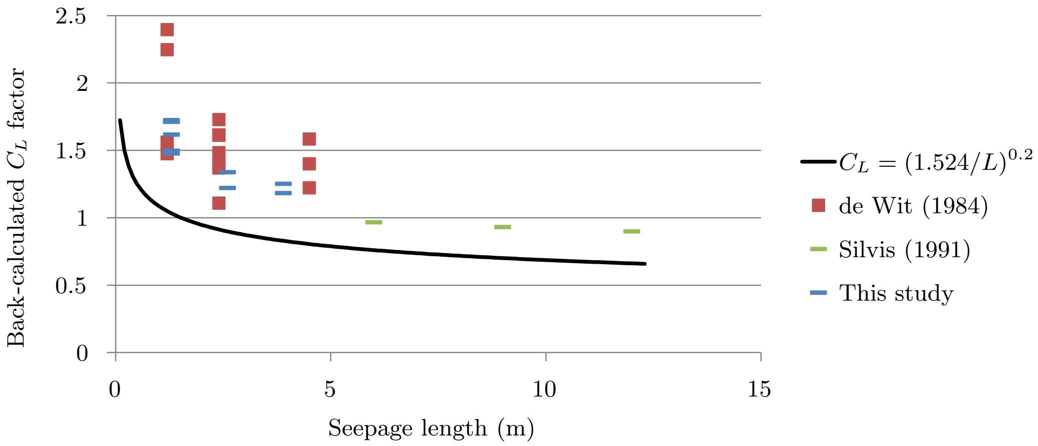

(a) C_L factor in Schmertmann (2000) model

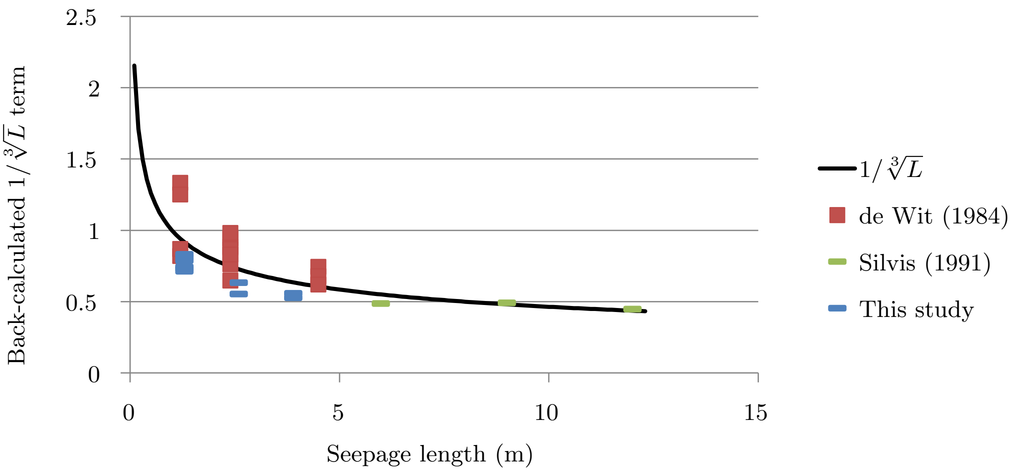

(b) $1/\sqrt[3]{L}$ term in Sellmeijer et al. (2011) model

Figure 7.9: Back-calculated seepage-length terms showing ability of each model to capture the effect of seepage length

7.4 Summary

7.4.1 Soil density

In answer to the question posed at the start of this chapter, "Did the soil placement method affect the initiation and/or critical head?" the answer was yes. Two experiments in less-dense soils resulted in lower initiation and critical gradients. And whilst an experiment in more-dense soil was not able to verify a higher initiation and critical gradient, experimental results from the studies of de Wit (1984), van Beek et al. (2011a) and van Beek (2015) were able to. Additional testing into the effect of soil density was not pursued given the impracticality of measuring soil density in the enclosed system of the flume.

Results from the studies of de Wit (1984), van Beek et al. (2011a) and van Beek (2015) indicated a proportional relationship between soil density and critical gradient, however the relationship appeared to vary across different soil types and the extent of experimental variability made it difficult to define density-gradient relationships with certainty.

The Schmertmann (2000) model accounts for soil density with the C_γ factor. When the C_γ factor was included in model predictions of all experiments the coefficient of determination, R^2, reduced instead of increasing. Therefore it is not considered worthwhile to include C_γ when using the Schmertmann (2000) model. The Sellmeijer et al. (2011) model accounts for soil density with the $(RD/RD_m)^{0.35}$ term. Whilst both the C_γ factor and the $(RD/RD_m)^{0.35}$ term did model the general trend in increase in gradient with density, experimental variability prevented assessment or improvement of its accuracy.

Considering experimental variability is relatively large compared to the effect of soil density and given uncertainty in measuring and determining relative density in the field, as well as its likely variation throughout a given site, it is suggested that the density of soil need not be incorporated in prediction models but instead be accommodated for with the use of sensible factors of safety in design.

7.4.2 Surcharge

In answer to the question posed at the start of this chapter, "Did the pressure head used to inflate the pressure bladder affect the initiation and/or critical head?" the answer was no. Initiation and complete progression occurred at similar heads when the bladder was inflated with 5m of water pressure, 2.5m of water pressure and not inflated at all.

However, the bladder pressure was not all together unnecessary, it served to ensure good contact between the sand and lid. If a higher void ratio exists between the sand and lid, a preferential flow path is established causing higher seepage velocities along the interface and therefore lower heads are needed to reach erosive forces.

The second question posed at the start of this chapter was, "did the 'pillow' shape of the bladder impose an uneven pressure and did this influence where the backward eroding channel occurred?" The answer to this was yes, the bladder did impose slightly less pressure in the vicinity of its perimeter, but seeing as the magnitude of total stress did not effect the backward erosion mechanism, less pressure around the perimeter did not influence where the backward eroding channel progressed to, as long as there was good contact between the sand and lid everywhere.

7.4.3 Seepage length

In answer to the question posed at the start of this chapter, "Are there seepage length effects? I.e. did the length of the flume affect the initiation and/or critical gradient?" the answer was no. Both initiation and critical gradients remained the same (within normal experimental variability) regardless of the seepage length used.

Whilst the seepage length did not appear to affect the initiation or critical gradients, it was observed that longer channels became more susceptible to blocking and often resulted in slower tip progression speeds.

Despite seepage length having no affect on the initiation and critical gradients, both the Schmertmann (2000) and Sellmeijer et al. (2011) models included adjustments for seepage length. It is understood that these adjustments are needed because scale, another component of the models, is expressed as the ratio of depth to length, and the length adjustment is needed to 'decouple' the depth effect from the seepage length. It was suggested that the seepage flux area (depth × width) would be better a measure of scale and that if scale was defined this way, no adjustment for seepage length would be required.

Chapter 8

Group 4: Soil grading

8.1 Introduction and aims

Most soils tested in backward erosion piping studies have been uniform to poorly graded soils with uniformity coefficients less than 3, as illustrated in Figure 2.14. Of the 6 soils identified from other studies with uniformity coefficients greater than 3, only 3 soils were well graded, i.e. had uniformity coefficients greater than or close to 6. These soils were tested in the Townsend and Shiau (1986) study and were either gap graded or had some sizes poorly represented, making them susceptible to internal instability. In fact, the Wan and Fell (2007) method suggests probabilities of internal instability for these soils between 0.4–0.8. If a soil being tested for backward erosion is also undergoing suffusion/suffosion, then the two internal erosion mechanisms may interact and lead to misleading results.

Given so few well graded soils had been tested for backward erosion piping and those which were, were susceptible to internal instability, it was necessary to test well graded, internally stable soils for backward erosion piping. This was particularly important given dams and levees founded on non-uniform and well graded soils are present in Australia (Fell, 2012).

The design method currently best suited for use when well graded soils are present is the Schmertmann (2000) method. Given the Schmertmann (2000) method relates the soil's uniformity coefficient to the local critical gradient, it was of interest to assess this relationship, particularly considering it was based on the 3, possibly internally unstable soils referred to above.

It was also of interest to investigate whether other soil properties influenced the critical gradient. Correlations with other soil properties had the potential to lead to a greater understanding as to why the soil grading affects the critical gradients and lead to alternate predictive models.

Therefore, the aims in this chapter were to test a range of different soils in order to investigate:

- the behaviour of well graded, internally stable soils to fill this gap in understanding;
- the accuracy of the critical gradient with C_u relation offered by Schmertmann (2000); and
- other relations which may exist between the critical gradient and soil properties.

Tests on the ten different soils were classified as 'Group 4' of the experimental program and included 25 tests as listed in Table 3.7.

8.2 Experimental results

Ten different soils were tested. These soils were all commercially available processed products either tested as they were or mixed together with designed portions to create specific grading curves. The soil products used are described in Subsection 3.1.5, the soil mixer is described in Subsection 3.1.6 and the soil mixes, including why they were chosen, their designed portions, their properties, how they were mixed and photos of each are all included in Subsection 3.2.2.

To follow is an account of the experimental results, firstly for each soil separately and then all soils together to compare. Results are expressed as channel length with head difference. Note that colours used to plot each soil in Figure 3.36 are maintained throughout this section. For example, Sydney Sand is always plotted with a blue line, Sibelco 50n with a grey line, etc.

8.2.1 Mix 1

Mix 1 was a well graded fine to coarse sand with some low plasticity silt. It had a coefficient of uniformity of 6.8 and a d_{10} of 0.075mm.

Tests 38, 56, and 71 were carried out on Mix 1. These tests were tamped in, tested with a circle exit, saturated after flushing with CO_2, pressurised with 5m of pressure head in the bladder and loaded with the 'decrease at points of interest' procedure. Tests 47, 48 and 54 were also carried out on Mix 1 but were placed using the wet pluviation method which affected the results. Therefore these tests are discussed in Section 3.2.3.

Test 38 did not initiate despite the head being raised to its maximum (at the time) of 1865mm and left at the head overnight. Therefore the constant head tank was modified to provide higher heads.

Test 56 was compromised when the submersible pump stopped. This allowed water to drop back into the pit and lowered the head to below the level of the flume lid which brought air into the sample (hence was no longer saturated).

Test 71 is plotted in Figure 8.1 as the head difference with channel length and its initiation head is listed in Table 8.1.

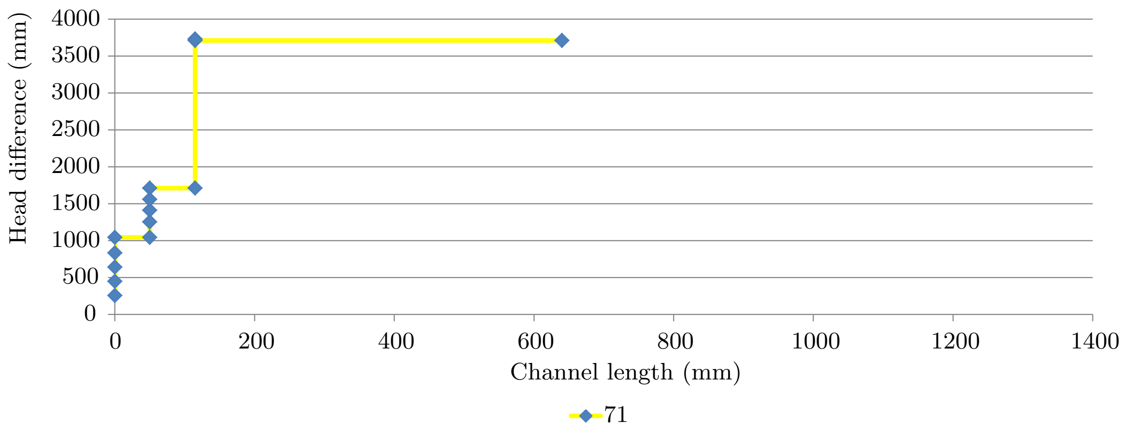

Figure 8.1: Group 4 test results- Mix 1

Test 71 initiated at 1043mm and with increases in head up to 1710mm, progressed to a channel length of 115mm. The tip then remained stationary despite having raised the hydraulic head to its maximum of 3710mm. This maximum head was maintained for 4 days. On the 5th day of testing a possible channel with a tip at 640mm was observed, although the channel was not clear, it appeared more like a network of disconnected channels. 1.5 hours after having observed the possible channel tip at 640mm, the sample failed by a sudden surface slip.

There was evidence suggesting fines (the Sibelco 300g product) in the soil were being transported downstream within the soil matrix leading to suffosion. This evidence included settlement of upstream portions of the sample and variable gradients through the sample. Settlement of upstream portions of the sample was observed as soil no longer pressed up against the Perspex lid and tension cracks which progressively formed across the width of flume as shown in Figure 8.2. This settlement suggests a loss in soil volume as fines were removed from the sample. Variable gradients through the sample are shown in Figure 8.3 as blue, red and green lines which connect water levels in standpipes and down to the head at the circle exit (i.e. the water level in the downstream box). These lines show a drastic increase in head loss through the soil as it approaches the downstream end. This suggests soil downstream is less permeable, supporting the hypothesis of transport of fines downstream.

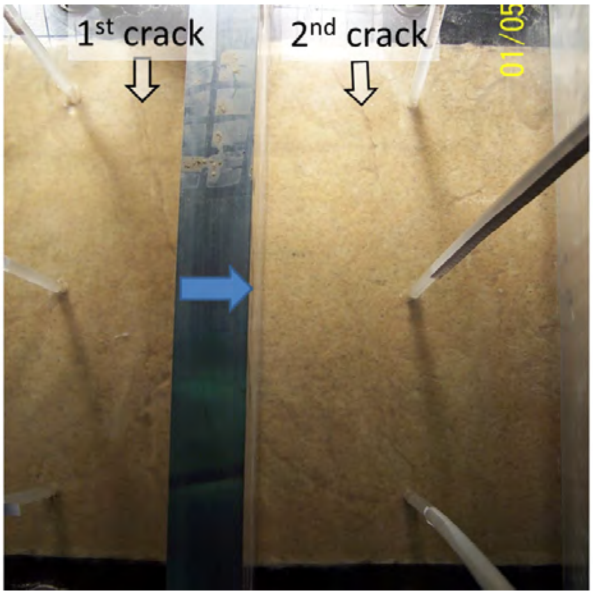

Figure 8.2: Tension cracks as evidence of settlement (blue arrow indicates direction of flow)

Suffosion would inhibit backward erosion piping as fines transported downstream would decrease permeability of the soil surrounding the channel tip. This decrease in permeability would mean higher gradients would be required to generate erosive seepage velocity into the channel tip.

Figure 8.3: Non-linear head loss in Test 71

8.2.2 Mix 2

Mix 2 was a poorly graded medium to coarse sand with a coefficient of uniformity of 4.2 and a d_{10} of 0.2mm. Tests 50 and 61 were carried out on Mix 2 and were tamped in, tested with a circle exit, saturated after flushing with CO_2, pressurised with 5m of pressure head in the bladder and loaded with the 'decrease at points of interest' procedure.

Plotted in Figure 8.4 are the results as the head difference with channel length and listed in Table 8.1 are the average initiation and critical heads.

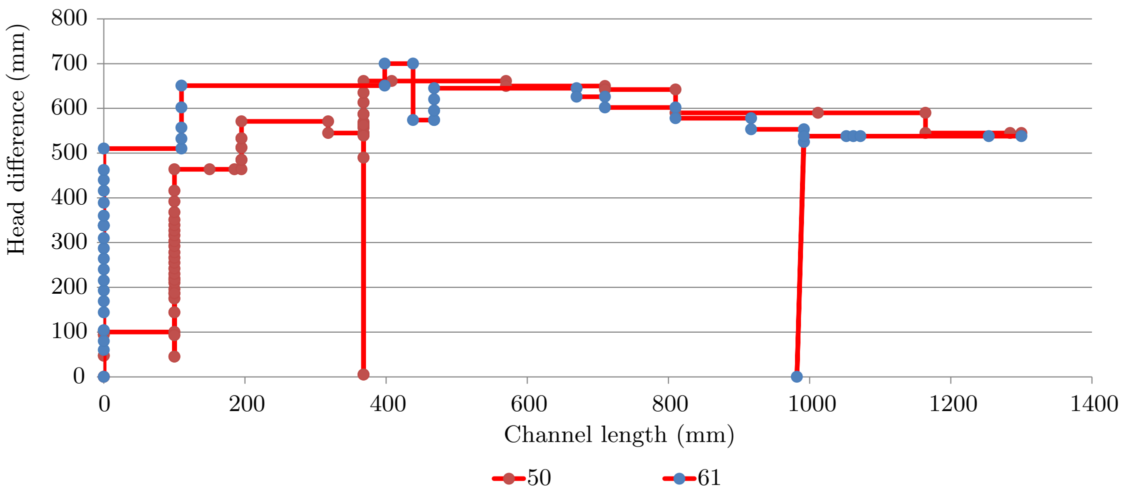

Figure 8.4: Group 4 test results- Mix 2

Test 50 initiated at 100mm and reached a critical head of 661mm when the channel was

368mm long (28% L). The initiation head was unusually low, in fact it was 33% lower than the average initiation head for Sydney sand.

Test 61 initiated at 510mm and reached a critical head of 651mm when the channel was 110mm long (8% L). Technically the maximum head imposed was 700mm however not enough time was allowed to pass between the tip apparently stopping and raising the head to 700mm (only 5 minutes). The head was dropped back down only 1 minute later because the progression was too fast. Therefore the critical head has been taken as 651mm.

8.2.3 Mix 3

Mix 3 was a well graded medium to coarse sand with fine gravel. It had a coefficient of uniformity of 6.2 and a d_{10} of 0.27mm.

Tests 51, 53 and 63 were carried out on Mix 3. These tests were tamped in, tested with a circle exit, saturated after flushing with CO_2, pressurised with 5m of pressure head in the bladder and loaded with the 'decrease at points of interest' procedure.

Plotted in Figure 8.5 are the results as the head difference with channel length and listed in Table 8.1 are the average initiation and critical heads.

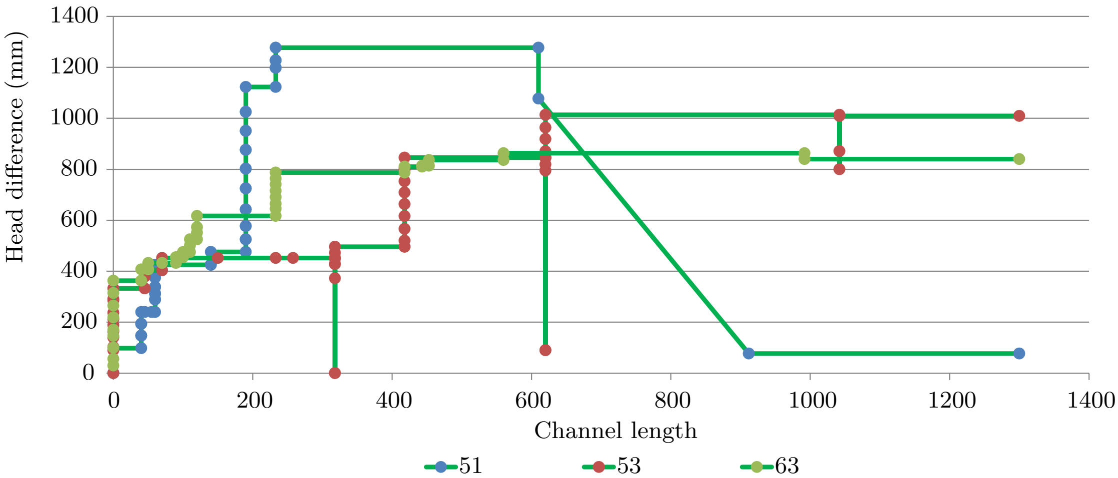

Figure 8.5: Group 4 test results- Mix 3

Test 51 initiated at 98mm and reached a critical head of 1277mm when the channel was 233mm long (18% L). The initiation head was unusually low, in fact it was 35% lower than the average initiation head for Sydney sand. Once critical head had been reached the tip progressed very fast. Effort was made to slow it down by reducing the head twice, the second time the head reduction was drastic, from 1077mm to 77mm (a 93% decrease), but the tip progression could not be stopped.

Test 53 initiated at 379mm and reached a critical head of 1014mm when the channel was 620mm long (48% L). This critical channel length was unusually long.

Test 63 initiated at 407mm and reached a critical head of 836mm when the channel was 560mm long (43% L). This was also an unusually long critical channel length.

8.2.4 Mix 4

Mix 4 was a well graded, medium to coarse sand with fine gravel. It had a coefficient of uniformity of 8.8 and a d_{10} of 0.24mm.

Tests 52 and 73 were carried out on Mix 4. These tests were tamped in, tested with a circle exit, saturated after flushing with CO_2, pressurised with 5m of pressure head in the bladder and loaded with the 'decrease at points of interest' procedure.

Plotted in Figure 8.6 are the results as the head difference with channel length and listed in Table 8.1 are the average initiation and critical heads.

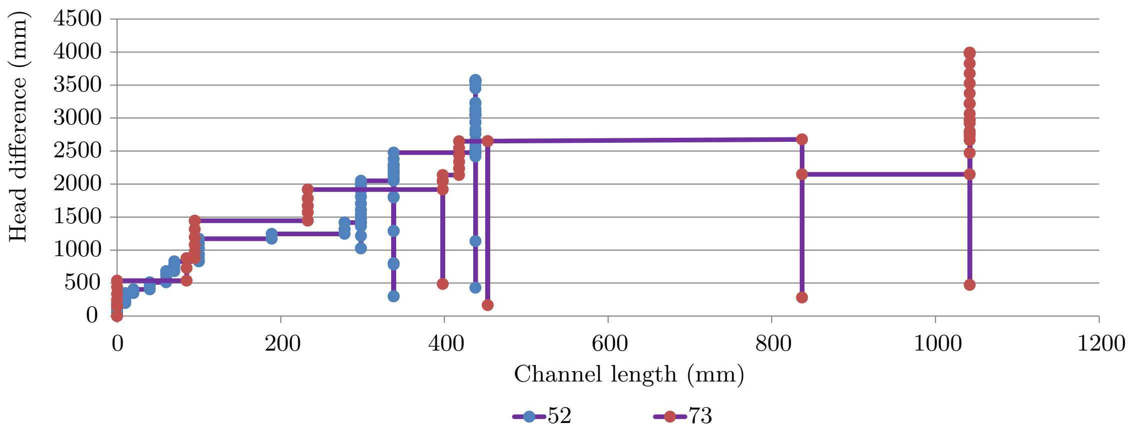

Figure 8.6: Group 4 test results- Mix 4

Test 52 initiated at 222mm and with increases in head to 2476mm progressed the tip to a channel length of 438mm but stopped there. The head was increased to its maximum of 3577mm, and held for almost 5 hours, but the tip remained at 438mm (34% L). The sand boil was cleared from the exit in case the boil was adding resistance but it had no effect on tip progression.

It is possible the tip did not progress past 438mm because gravel at the tip was impeding particle detachment. This gravel formed an usually dense collection (shown in Figure 8.7) which had the potential to resist and/or stop backward erosion by way of reinforcement through interlocking effective stresses. In an attempt to release the gravel barricade, the Perspex lid was knocked several times with a mallet. Whilst this did release material into the channel and doubled the channel width, it did not release the reinforcing gravel at the tip and the tip did not progress any further.

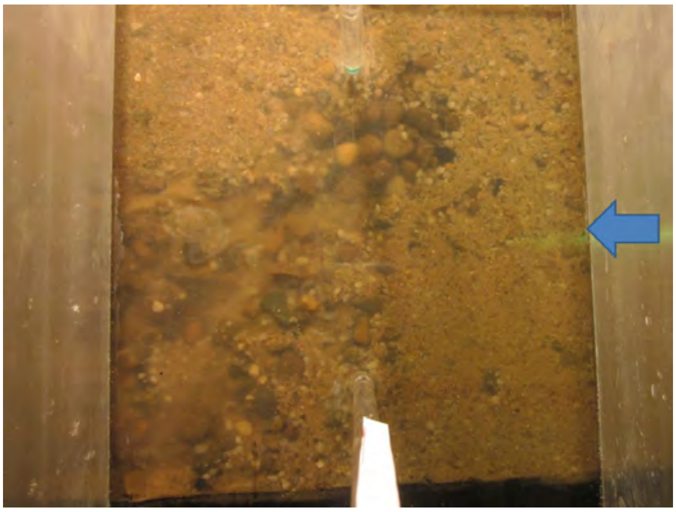

Figure 8.7: Tip at 438mm where it stopped on a group of gravel (blue arrow indicates direction of flow which is opposite to thesis convention due to angle photo was taken)

Test 73 initiated at 537mm and with increases in head to 2675mm progressed the tip to a channel length of 1042mm but stopped there. The head was increased to its maximum of 3988mm, and held for 2 hours, but the tip remained at 1042mm (80% L). The sand boil was cleared from the exit in case the boil was adding resistance but it had no effect on tip progression.

It was difficult to identify the channel and position of the tip because there were many disconnected channel-looking patterns ranging from hair-line passages (where fine-grained particles were seen travelling through) through to 50mm wide voids, shown in Figure 8.8. Therefore, the measurement of the final tip position at 1042mm (80% L) was a matter of judgement. It is possible the tip could not be progressed further (irrespective of where it was) due to the presence of many channels effectively 'sharing' flow concentrations thereby preventing adequate flow concentration (and hence seepage velocity) into the most upstream tip.

Figure 8.8: Channel and tip difficult to identify. Tip identified at dashed line. (blue arrow indicates direction of flow)

It was unusual for channels to be longer than about 30% of the seepage length when the critical head was needed, yet in Mix 4 tests, the channels were 34% and 80% of the seepage length (in Tests 52 and 73 respectively) when the head was raised to the maximum in pursuit of the critical head. Given the channels had exceeded the average critical channel length in these tests, it is possible that the channels could have continued to progress had the tip not intercepted a dense group of gravel (as it did in Test 52) or had multiple voids/channels not formed (as had occurred in Test 73). In other words, it is possible the heads which caused the channels to progress to 34% and 80% of the seepage length were the critical heads for Mix 4 sand but channels stopped for reasons other than insufficient head and perhaps other tests in Mix 4 may have fully progressed at these heads. Assuming so is a conservative and safe approach, especially considering the channel in Test 73 was only 20% short of reaching the upstream end. Therefore, when formulating a new model (as was done in Subsection 8.3.2) and when reviewing existing models (as was done in Chapter 11), the critical head for the Mix 4 tests were taken to be the head which caused the channels to progress to 34% and 80% of the seepage length which was 2.476m in Test 52 and 2.675m in Test 73.

Mix 4 was considered to have identified the C_u cut-off at which backward erosion no longer completed (for soils which 'pivot' at a d_{10} similar to Sydney sand) because the tip couldn't be progressed to the upstream end despite imposing large global hydraulic gradients up to 3.

8.2.5 Mix 5

Mix 5 was a well graded, fine to medium gravel with medium to coarse sand. It had a coefficient of uniformity of 6.1 and a d_{10} of 0.51mm.

Tests 58 and 74 were carried out on Mix 5. These tests were tamped in, tested with a circle exit, saturated after flushing with CO_2, pressurised with 5m of pressure head in the bladder and loaded with the 'decrease at points of interest' procedure.

Plotted in Figure 8.9 are the results as the head difference with channel length and listed in Table 8.1 are the average initiation and critical heads.

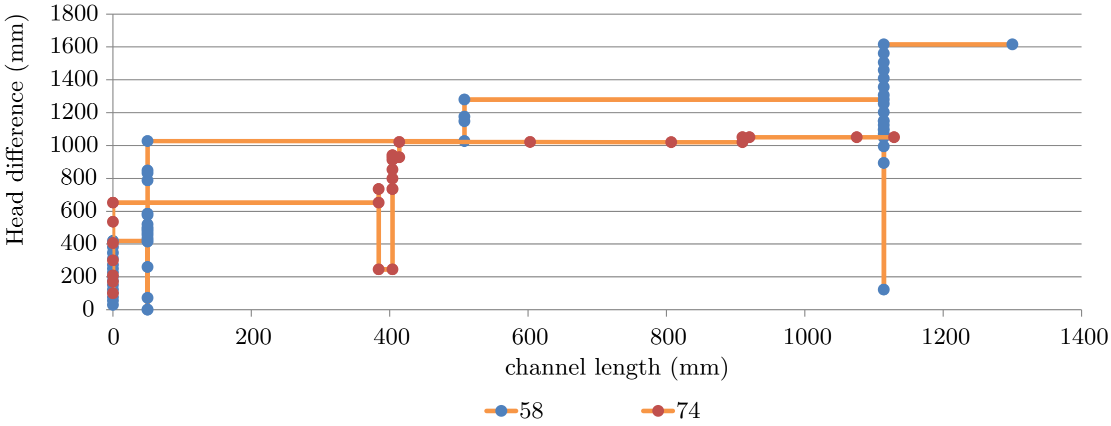

Figure 8.9: Group 4 test results- Mix 5

Test 58 was defined as initiating at a head of 419mm. It was difficult to define because the 'channel' was more of an eroded 'region' than a channel, as shown in Figure 8.10a. Initiation was defined at 419mm because it was the first time when particles of all sizes were transported out, not just fines through the coarser matrix.

Channel progression occurred in three sudden ‘bursts’, each time progressing fast (approximately 200mm/min). After the second burst at a head of 1280mm, the channel was 1114mm long however a blockage occurred below bar 2, as shown in Figure 8.10b. This blockage probably occurred due to the large amount of sediment being transported suddenly, because the channel was wide and tip progression occurred quickly. It is expected that if this blockage had not occurred the tip would have progressed through to the upstream end at this head. However the head needed increasing to 1615mm before the tip reached the upstream end.

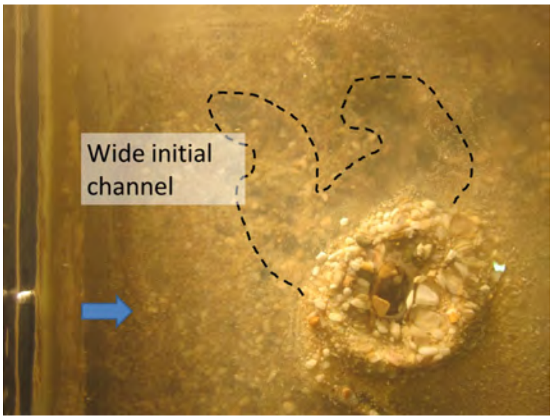

(a) Initial channel was wide and difficult to define

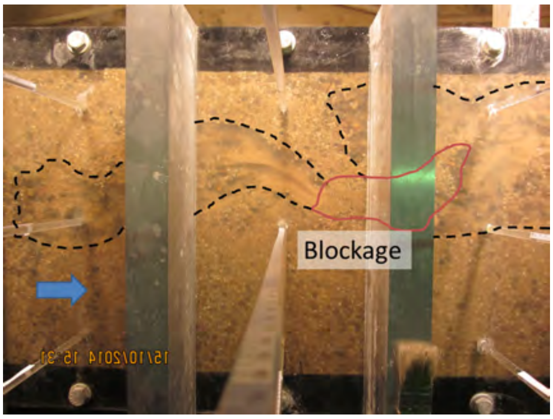

(b) Channel blockage when head 1280mm

Figure 8.10: Test 58 photos (blue arrow indicates direction of flow)

Once the tip reached the upstream end it was expected to fail quickly but it didn’t. Instead flow through the experiment dropped, as evident by the sand boil no longer boiling and a still water surface in the downstream box (after there had been substantial ripples in the surface on account of the high flow). Additionally levels in the standpipes were all similar and close to the water level in the constant head tank. This suggested that the gradient across the sample was low and that there must have been a large head loss at the exit. Having reached in to feel the inside of the boil, large gravel pieces were found to have interlocked and immobilised beneath the exit. Once the jammed gravel pieces were released by hand, flow drastically jumped and the sample failed.

Test 74 initiated at 652mm and reached a critical head of 1020mm when the channel was 414mm long (32% L). As was the case in Test 58, the channel wasn’t well defined and the location of the tip was based on judgement. The test was terminated when the channel tip was at 1129mm because the sample had become desaturated over the weekend (presumably because the submersible pump had been inadvertently turned off).

8.2.6 Mix 6

Mix 6 was a poorly graded, fine to medium sand with some low plasticity silt. It had a coefficient of uniformity of 2.6 and a d_{10} of 0.08mm.

Tests 59, 72 and 78 were carried out on Mix 6. These tests were tamped in, tested with a circle exit, saturated after flushing with CO_2, pressurised with 5m of pressure head in the bladder and loaded with the 'decrease at points of interest' procedure. Tests 81 and 82 were also carried out on Mix 6 but were carried out using the cyclic loading procedure. Therefore these tests are discussed in Section 9.2.

Plotted in Figure 8.11 are the results as the head difference with channel length and listed in Table 8.1 are the average initiation and critical heads.

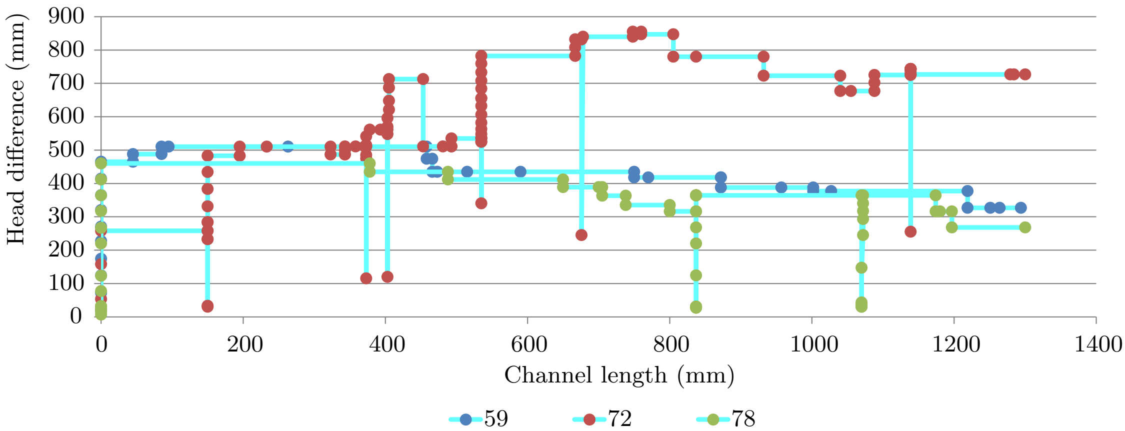

Figure 8.11: Group 4 test results- Mix 6

Test 59 initiated at 465mm and reached a critical head of 510mm when the channel was 85mm long (7% L).

Test 72 initiated at 258mm and reached a critical head of 855mm when the channel was 748mm long (58% L). The initiation head was considerably lower than the initiation head in Test 59 (45% lower). Air bubbles and voids were seen around the exit although it's expected these would cause higher than normal heads, not lower. When the channel was 405mm long, air bubbles appeared alongside the channel. There was no indication as to why or how air bubbles entered. The introduction of air bubbles coincided with a large increase needed in head, leading to a critical head 68% higher than the critical head in Test 59. Therefore, the high critical gradient was attributed to the air bubbles and the result of Test 72 was not included when modelling the behaviour of Mix 6 in Section 8.3 or in Chapter 11.

Test 78 initiated at 460mm. This was the maximum head needed to progress the tip through to the upstream end so it also became the critical head. This was unusual for a circle exit. The high initiation head may be attributed to voids and bubbles observed around the exit.

On the morning of the second day of testing, many bubbles were found in the channel, as they were in Test 72, for reasons unknown. The concern was the bubbles would again cause higher heads so despite the stationary tip, the head was maintained for a full day in the hope the tip would re-initiate without increasing head. By late afternoon a new channel, without air bubbles, branched off the bubble-ridden channel and continued to progress through to the upstream end. Both the bubbles in the channel and the newly branched-off channel are shown in Figure 8.12.

Figure 8.12: Air bubbles in channel and new channel which branched off existing (blue arrow indicates direction of flow)

8.2.7 Mix 7

Mix 7 was a poorly graded, fine to medium sand with some low plasticity silt. It had a coefficient of uniformity of 3.2 and a d_{10} of 0.065mm.

Tests 67 and 69 were carried out on Mix 7. These tests were tamped in, tested with a circle exit, saturated after flushing with CO_2, pressurised with 5m of pressure head in the bladder and loaded with the 'decrease at points of interest' procedure.

Plotted in Figure 8.13 are the results as the head difference with channel length and listed in Table 8.1 are the average initiation and critical heads.

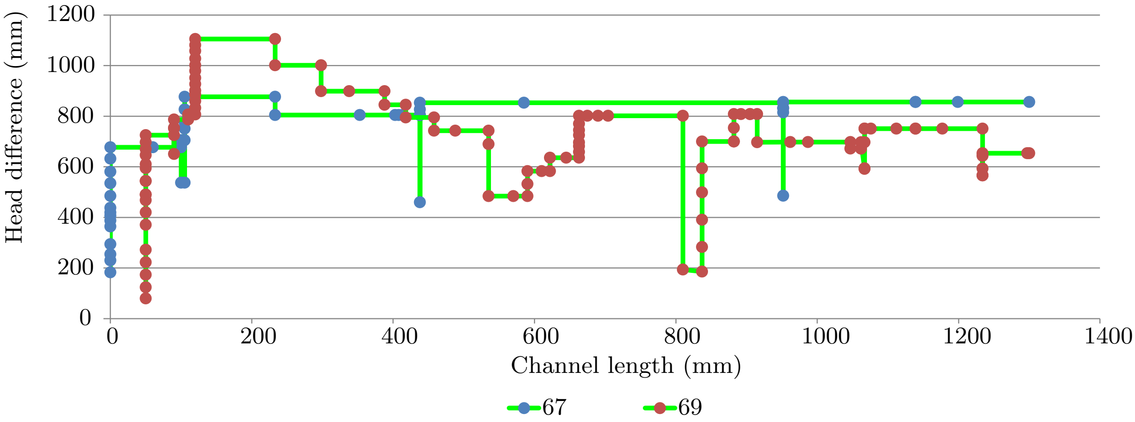

Figure 8.13: Group 4 test results- Mix 7

Test 67 initiated at 677mm and reached a critical head of 877mm when the channel was 105mm long (8% L).

In Test 69, initiation was defined as occurring at 725mm however, it was difficult to determine when a channel had begun to form because it was difficult to see through the turbid water in the downstream box (turbid due to suspended Sibelco 300g product).

The head then needed raising several times before critical was reached at 1150mm when the channel was 120mm long. This was a 25% increase over the critical head in Test 67. There was no indication as to why a higher head was needed, although a large amount of soil had boiled from the exit during the CO_2 flushing which would have left a void around the exit and perhaps altered local gradients enough to affect the critical gradient.

Once the tip re-initiated at a head of 1105mm, the head was frequently reduced in an effort to bring the head down to the critical head found in Test 67. Therefore the head was lowered more often than just at 'points of interest'. This change in procedure accounts for the large reduction in head from 1105mm to 484mm. The channel stopped at a head of 484mm and required increase back up to 802mm to maintain progression. Interestingly, a head of 802mm was similar to the critical head in Test 67.

8.2.8 Mix 8

Mix 8 was a poorly graded, fine to medium sand with some low plasticity silt. It had a coefficient of uniformity of 6.4 and a d_{10} of 0.033mm.

Tests 62, 64 and 75 were carried out on Mix 8. These tests were tamped in, tested with a circle exit, saturated after flushing with CO_2, pressurised with 5m of pressure head in the bladder and loaded with the 'decrease at points of interest' procedure.

Plotted in Figure 8.14 are the results as the head difference with channel length and listed in Table 8.1 are the average initiation and critical heads.

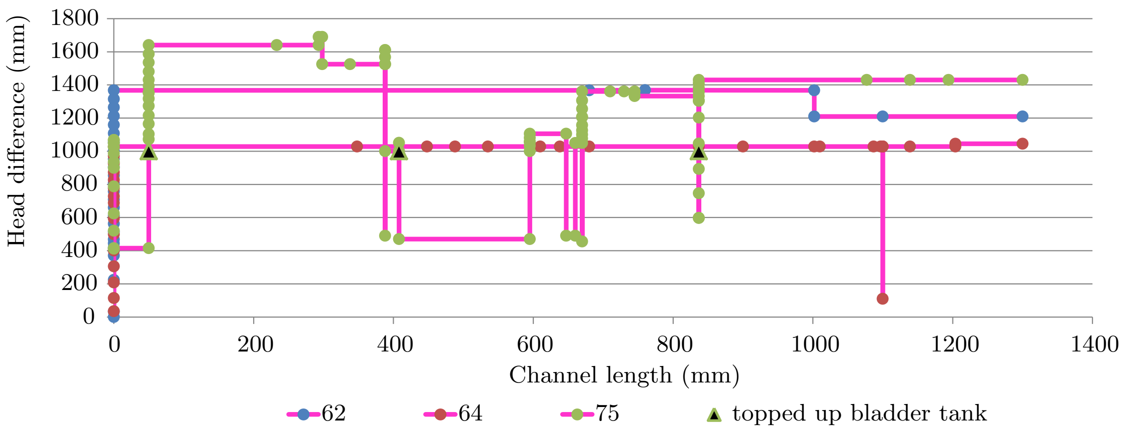

Figure 8.14: Group 4 test results- Mix 8

In all Mix 8 tests, channels could not be seen until they were either past the downstream box (175mm) or past the downstream box and the first restraining bar (224mm) (depending on which flume the test was carried out in). This was because water in the downstream box was opaque as a result of suspended Sibelco 300g fines. This resulted in the inability to determine the initiation head and prior to seeing a channel, the test operator had to wait longer before increasing the head to allow a channel that may exist to progress either 175mm and 224mm long before assuming initiation had not occurred.

Test 62 became desaturated prior to testing (the submersible pump must have been inadvertently turned off over the weekend). This would have been reason to abandon the test but given the time and materials spent to set it up, it was still carried out. The head was initially increased, on average, every 13 minutes and a channel was first observed when the head was at 1367mm. At this head the channel progressed through to the upstream end quickly (in about 15 minutes). It is likely this head was higher than necessary on account of the air bubbles throughout the soil.

In Test 64, the head was initially increased, on average, every 30 minutes and a channel was first observed when the head was at 1028mm. At this head the channel progressed through to the upstream end and at a slower rate than Test 62 (taking about 3 hours to reach the upstream end).

In Test 75, the head was initially increased, on average, every 25 minutes. The head was much higher than the two previous Mix 8 tests when the channel was first observed, at 1640mm. Erosion did not behave as a typical backward eroding channel. Instead, there was often a region, 100-150mm wide, through which many simultaneous flow paths formed as shown in Figure 8.15a. A group of sand particles appeared to suddenly slip downstream together, leaving a void into which a group of upstream particles would slide into moments later. The eroding region would often remain stationary, sometimes for a few hours after several head increases, before repeating the same process of grouped slips. Because there was no distinct channel, there was no path along which detached particles could be transported out and it was difficult to define a tip as illustrated by the multiple possibilities labelled in Figure 8.15a.

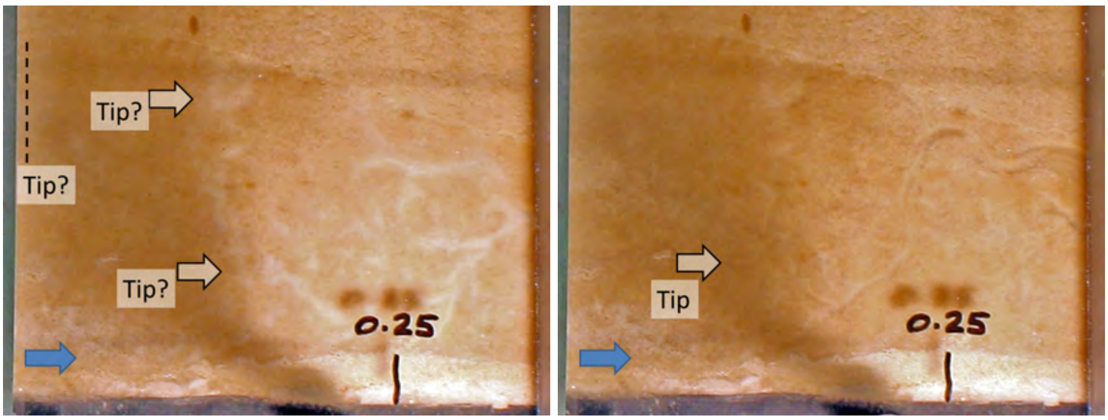

(a) Atypical channel behaviour (b) Typical channel behaviour

Figure 8.15: Test 78 photos (blue arrow indicates direction of flow)

In attempt to return the erosion mechanism to typical backward erosion, the head was reduced from 1610mm down to 470mm. This worked for a short while, the channel became more defined, as shown in Figure 8.15b, and the tip progressed in a more typical fashion until the tip reached 595mm. Here the head required increasing again, but once higher than 1000mm, the channel reverted back to the non-channel-like behaviour observed previously. It is likely the wide eroded zones had increased the sample's permeability and left the sample damaged.

Considering the air bubbles in Test 62 and the excessively high head imposed on Test 75, it is likely these test were compromised. However, with only one reliable test remaining, a judgement on the degree of compromise could not be made. Therefore, all three test results were still used in analysis in Section 8.3 and in Chapter 11.

8.2.9 Sibelco 50n

Sibelco 50n was a poorly graded fine to medium sand with a coefficient of uniformity of 1.9 and a d_{10} of 0.11mm.

Tests 57 and 60 were carried out on Sibelco 50n. These tests were tamped in, tested with a circle exit, saturated after flushing with CO_2, pressurised with 5m of pressure head in the bladder and loaded with the 'decrease at points of interest' procedure.

Plotted in Figure 8.16 is the head difference with channel length and listed in Table 8.1 are the average initiation and critical heads.

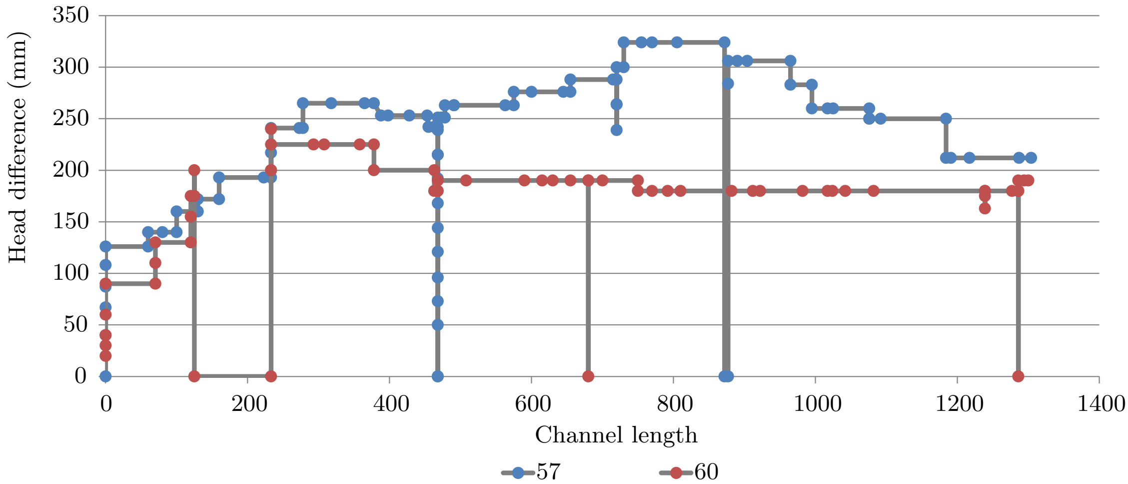

Figure 8.16: Group 4 test results- Sibelco 50n

Test 57 initiated at 126mm and reached a critical head of 324mm when the channel was 730mm long (56% L).

Test 60 initiated at 90mm and reached a critical head of 225mm when the channel was

233mm long (18% L). After the first day of testing, the head was dropped down to datum. This usually meant the tip remained in the same position ready for the next day however, in this instance, the tip was found a further 108mm upstream the next day. It is unlikely this occurred whilst head was at datum so it is expected to have occurred whilst the head was lowering from 200mm down to 0.

There was a 30% difference in critical heads between Tests 57 and 60 and there was no indication given during experiments which would explain this difference. Whilst this difference in critical heads was more than desired, it is within experimental variability of backward erosion testing as indicated by the range of experimental results observed by other researchers.

8.2.10 All soils

Figure 8.17 is a plot of all soil results combined. However this plot is busy so it was modified to make trends more clear by a) not including reductions in head b) plotting only to the maximum (i.e. critical) head and then keeping at the maximum head for the remainder of channel length (in essence, pretending the 'increase only' loading procedure was used) and c) not plotting data points. The result is Figure 8.18.

Average initiation and critical heads for each soil are listed in Table 8.1 along with the average critical channel length and the range of results.

Table 8.1: Group 4 test results

	initiation head (mm)		critical head (mm)		critical channel length (mm)	
Soil	average	range	average	range	average	range
Mix 1	1043	-	> 3710	-	≥ 640	-
Mix 2	305	410	656	10	239	258
Mix 3	393	28	925	178	590	60
Mix 4	380	315	> 3783	-	≥ 740	-
Mix 5	536	233	1318	595	764	700
Mix 6	463	5	485	50	43	85
Mix 7	701	48	991	228	113	15
Mix 8	unknown	-	1345	612	unknown	-
Sibelco 50n	108	36	275	99	482	497
Sydney sand	146	83	208	38	292	373

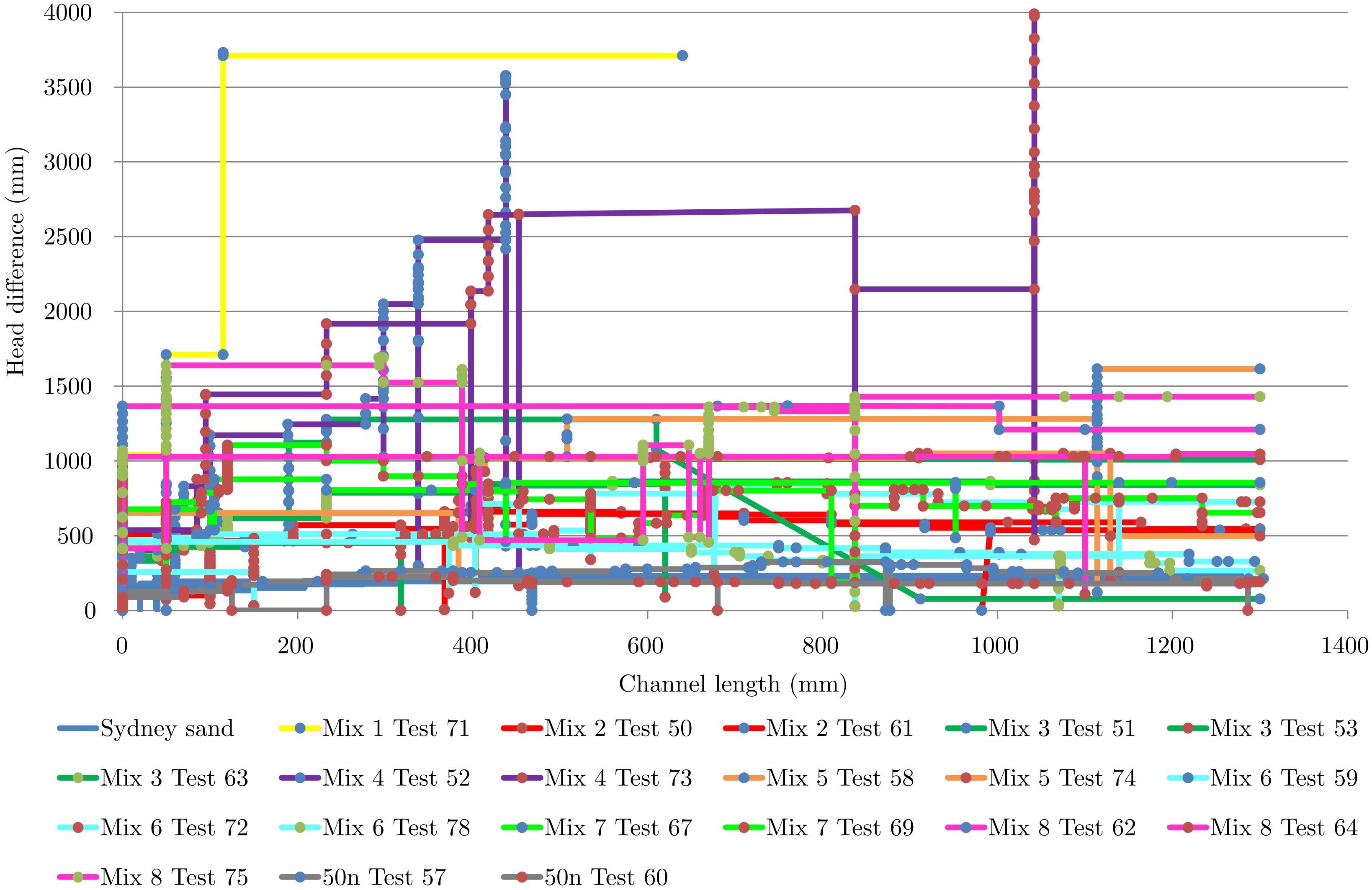

Figure 8.17: Group 4 test results- all soils

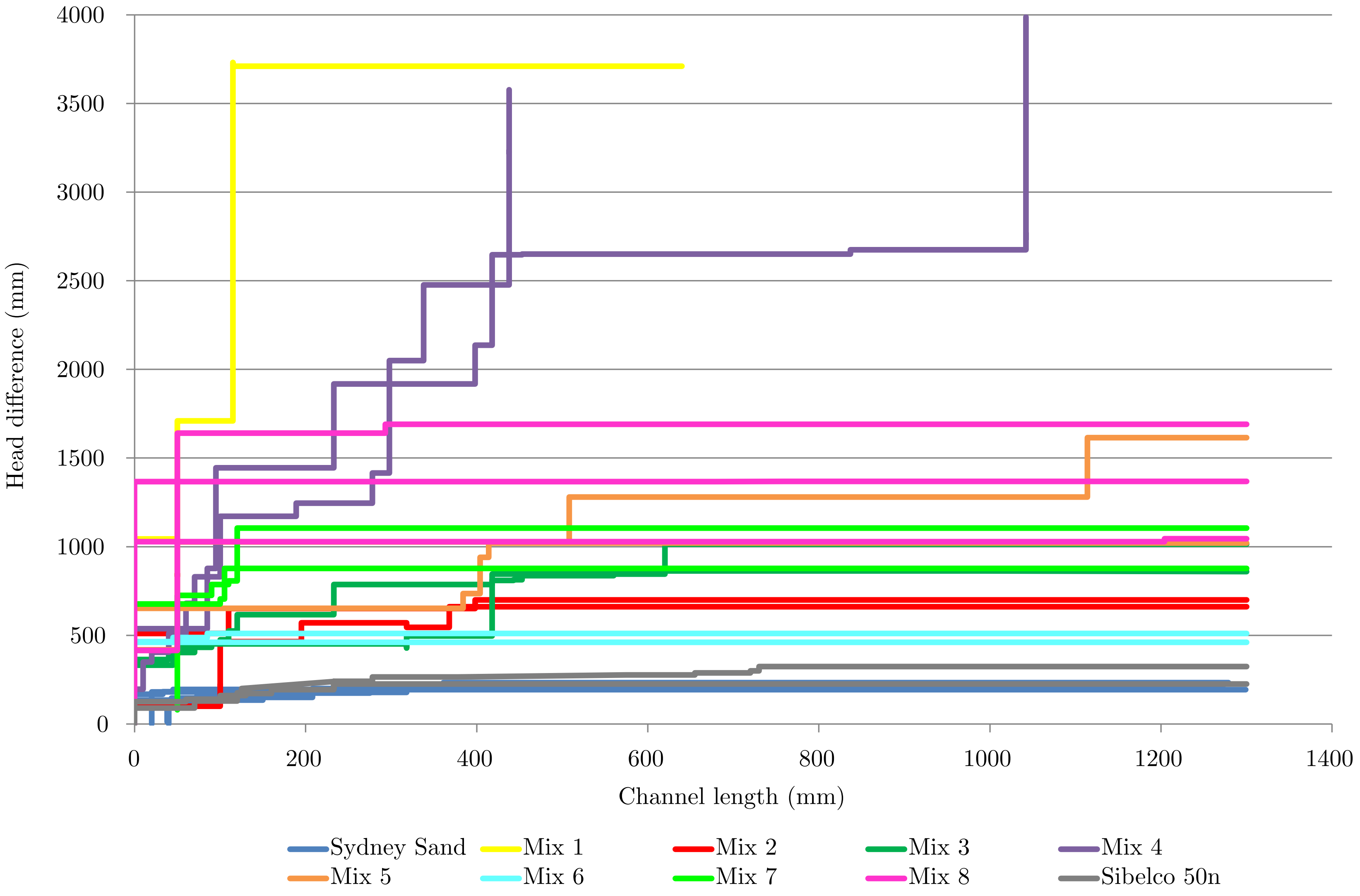

Figure 8.18: Group 4 test results- all soils (modified)

In Figure 8.18 there is an order of increasing critical head of Sydney Sand, Sibelco 50n, Mix 6, Mix 2, Mix 3, Mix 7, Mix 5, Mix 8, Mix 1 and Mix 4. To better depict this order, the average values of critical heads are plotted in Figure 8.19a, ordered in increasing order.

Figure 8.19a shows there is a steadily increasing critical gradient until Mixes 1 and 4 where it significantly jumps. Stems on the plot show the range of results around the average. These stems show that the larger the critical gradient, the larger the range of results. Note that Mix 1 doesn't have a stem because only one test was plotted.

Figure 8.19b is a plot of the average initiation heads, plotted in the same order as Figure 8.19a. This plot shows the initiation head doesn't follow the same order as the critical head. It also shows that the range of initiation heads are smaller than the range of critical heads.

Figure 8.19c is a plot of the average critical channel length, plotted in the same order as Figure 8.19a. This plot shows the critical channel length doesn't follow the same order as the critical head and has no discernible pattern or order. The stems show there was significant scatter in the results.

8.3 Discussion

It was of interest to investigate whether there was a correlation between the soil's uniformity coefficient and the critical gradients observed in experiments because Schmertmann (2000) reported there was a correlation and based his model on it, as shown in Figure 2.34. It was also of interest to investigate whether there were other relationships between the critical gradient and soil properties other than C_u. The findings of these investigations are described in this discussion.

8.3.1 Uniformity

Figure 8.20 is a plot of critical gradients with uniformity coefficients for Group 4 results and Sydney Sand tests in circle exits. However, Test 71 on Mix 1 was omitted because it failed by a surface slip, not backward erosion, and Tests 52 and 73 on Mix 4 were

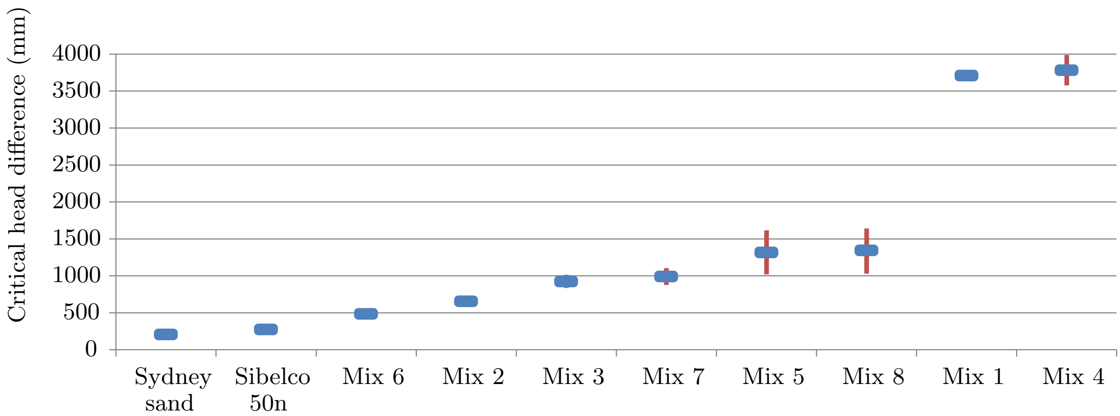

(a) Average critical heads for each soil with stems showing ranges

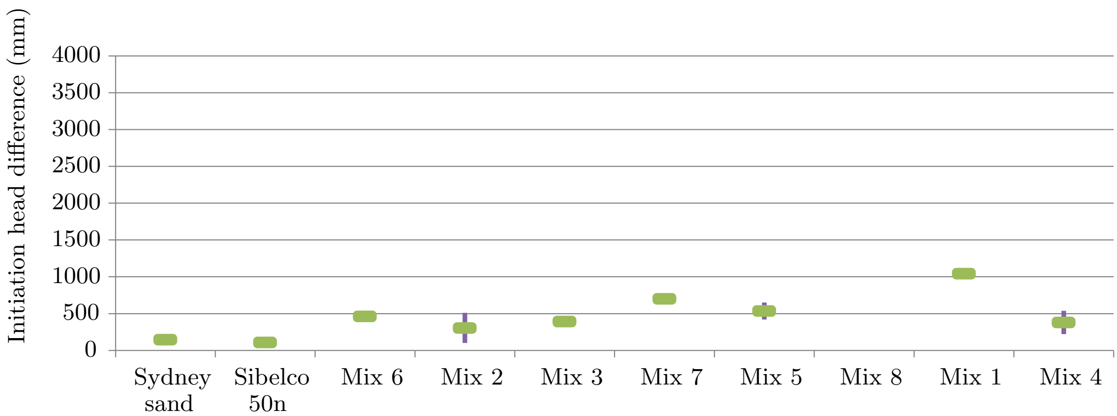

(b) Average initiation heads for each soil with stems showing ranges

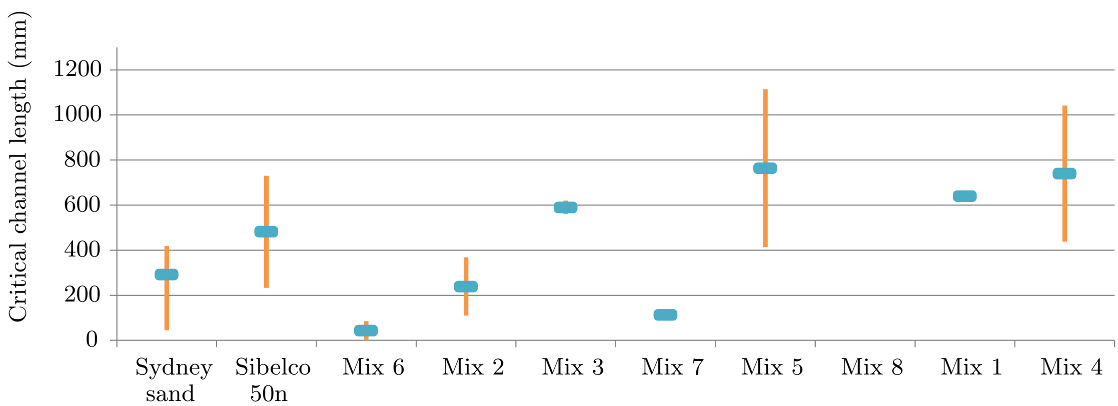

(c) Average critical channel lengths for each soil with stems showing ranges

Figure 8.19: Group 4 test results- average initiation heads, critical heads and critical channel lengths

amended to plot at the gradients prior to the channel tip stopping on groups of gravel because it was expected that the channels would have continued to progress if it weren't for the groups of gravel (this expectation and decision is discussed in more detail in Subsection 11.2.3).

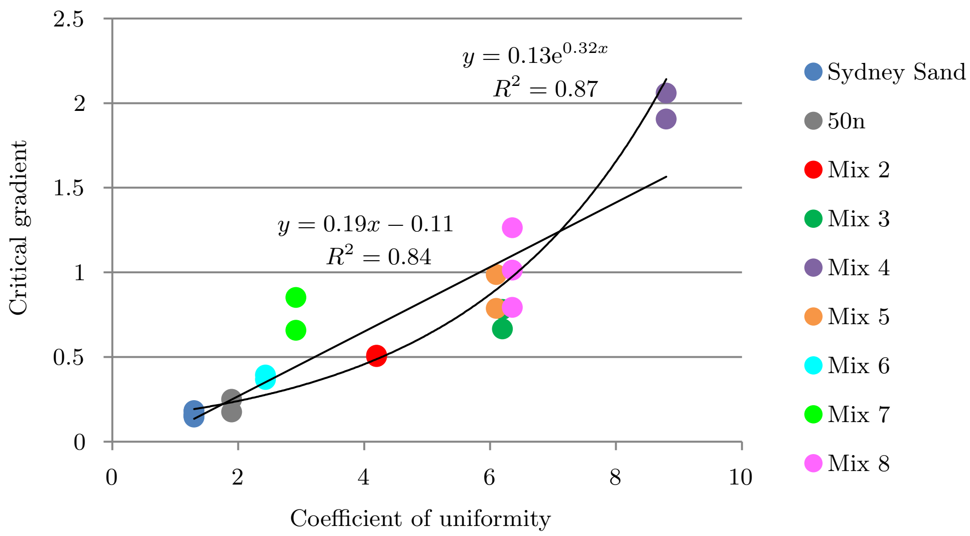

Figure 8.20: Critical gradient with uniformity coefficient for Group 4 tests and Sydney Sand tests in circle exit

Figure 8.20 confirms there is a proportional relationship between critical gradient and coefficient of uniformity, although an exponential line-of-best-fit represents the data with a higher R^2 value than a linear line-of-best-fit.

The Schmertmann (2000) equation of critical gradient with uniformity coefficient can not be drawn onto Figure 8.20 because the Schmertmann (2000) equation only applies to gradients corrected to the University of Florida (UoF) flume (the flume used in Townsend et al. (1981), Townsend and Shiau (1986) and Schmertmann (1995)). However, gradients observed in this study were corrected to the UoF flume (using methods described in Subsection 11.2.3) and plotted over the Schmertmann (1995) figure in Figure 8.21.

Figure 8.21 shows that experiments from this study did follow the approximate trend of the Schmertmann (1995) equation (indicated by the line) but that correlation reduced for soils with a $C_u > 3$, particularly for soils around $C_u = 6$ where the model overestimated the critical gradient by up to 82%. The theory as to why the model overestimated critical gradients around $C_u = 6$ is the model was based on soils here which experienced internal erosion (soils referred to as 'WG' and 'Gap I' and 'Gap II' by Townsend and Shiau (1986)

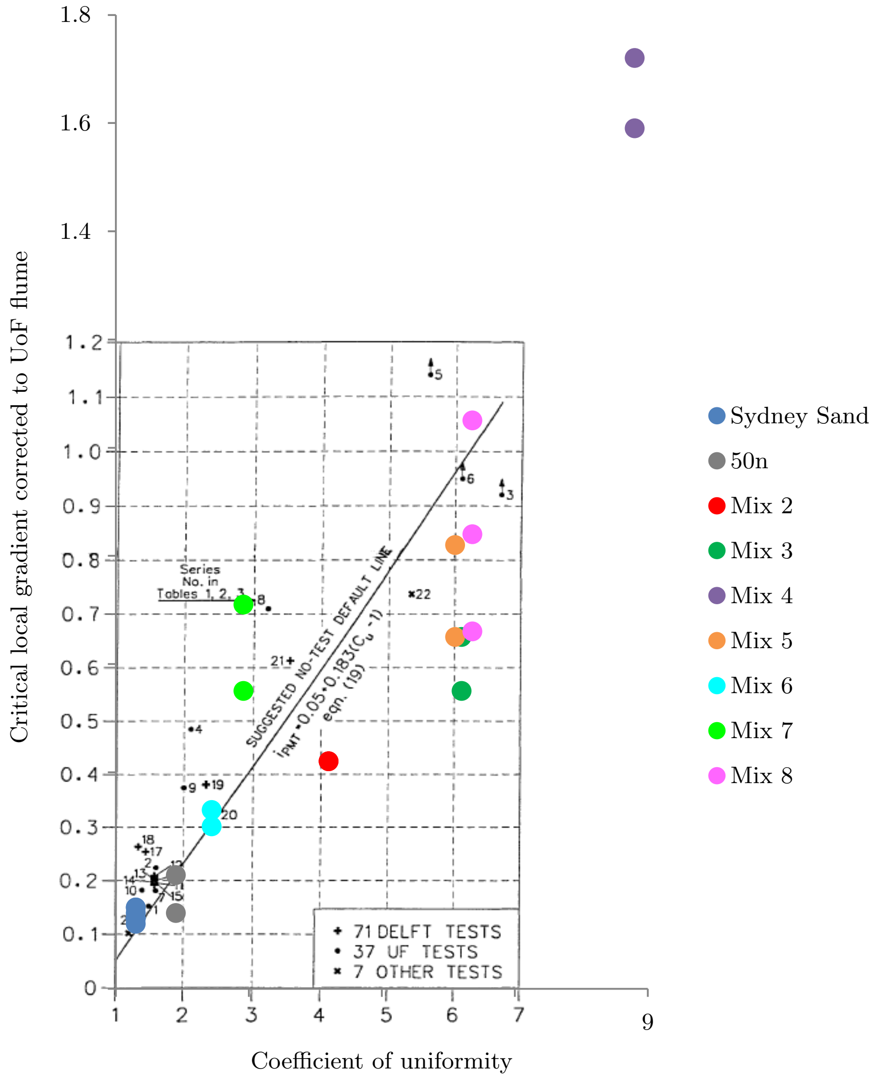

Figure 8.21: Experimental results from this study on the Schmertmann (1995) plot (gradients corrected to local gradients in UoF flume)

and referred to Test series 3, 5 and 6 by Schmertmann (2000)). When soils undergo internal erosion, fine-grained soil is transported downstream, causing a local reduction in permeability where backward erosion initiates and reaches the critical gradient. This local reduction in permeability results in the need for a higher gradient thereby increasing the critical gradient. Evidence for why the soils in Test series 3, 5 and 6 (as labelled by Schmertmann (2000)) are thought to have experienced internal erosion is presented in Subsection 11.2.2. Furthermore, it is worthy to note that the gradients plotted for Test series 3, 5 and 6 were not the critical gradients, but the highest gradient applied during the test which was terminated either before the critical gradient was reached or as a result of the test failing by a mechanism other than backward erosion. So in fact, there is likely to be an even larger difference between Test series 3, 5 and 6 and Mixes 3, 5 and 8 from this study, if higher gradients had of been applied to the Townsend and Shiau (1986) tests.

Note that Figure 8.21 is repeated as Figure 11.20 but contains data from other studies as well, and does not differentiate soil mixes.

8.3.2 Permeability & particle size

Based on the theory that sufficient velocity of fluid moving from soil pores into the channel tip is what drives backward erosion, the soil's permeability ought to be a property which determines the critical gradient. A higher soil permeability would allow more fluid flow through the soil and into the channel tip which, assuming a fixed channel width and depth, would result in faster fluid velocity into the tip and hence greater viscous shear forces leading to the need for lower gradients to maintain backward erosion.

It is acknowledged this increase in viscous shear forces may be offset when the soil has increased in permeability as a result of an increase in grain size. This is because an increase in grain size results in larger pore spaces which, whilst allowing a large volume of flow, also results in less viscous shear forces because there is now more space between the fluid flow and soil grains (the Navier-Stokes phenomenon). Therefore, the question becomes whether the increase in viscous shear forces due to an increase in soil permeability is more or less the decrease in viscous shear forces due to larger pore spaces.

To investigate a possible relationship between the soil's permeability and the critical gradient, Figure 8.22a was plotted. Whilst Figure 8.22a does not reveal a clear trend between critical gradient and permeability across all soils, it does reveal a trend amongst Sydney Sand, 50n and Mixes 6, 7 and 8. This trend is shown in Figure 8.22b with a power trendline. What is unique about these soils is they all exhibited narrow and similar tip widths, as shown in Figure 8.23. The tip widths were narrow because these soils had the lowest d_{50} sizes and similar because their d_{50} sizes were similar. With similar tip widths (and presumably depths), the inversely proportional relationship between permeability and critical gradient, seen in Figure 8.22b, can be explained by the theory described above, that seepage velocity into the channel tip is what drives backward erosion.

Soils which did not follow the power curve in Figure 8.22b- Mixes 2-5, have larger d_{50} sizes and therefore wider tip widths as seen in Figure 8.23. When the width of the tip increases, seepage velocities into the tip slow down and therefore a higher gradient is required to generate erosive forces. This can be seen in Figure 8.24 which shows the gradient increasing with tip width from Sydney Sand to Mix 2, 3 and 4, indicated by the dashed line.

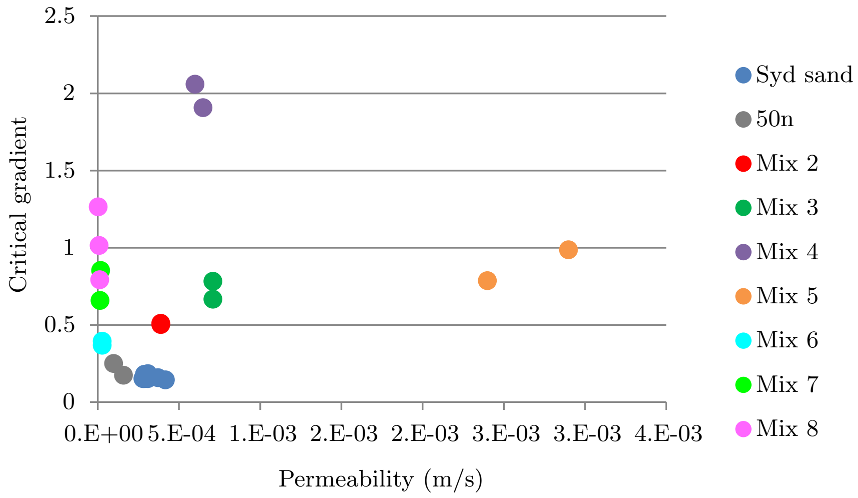

(a) All soils

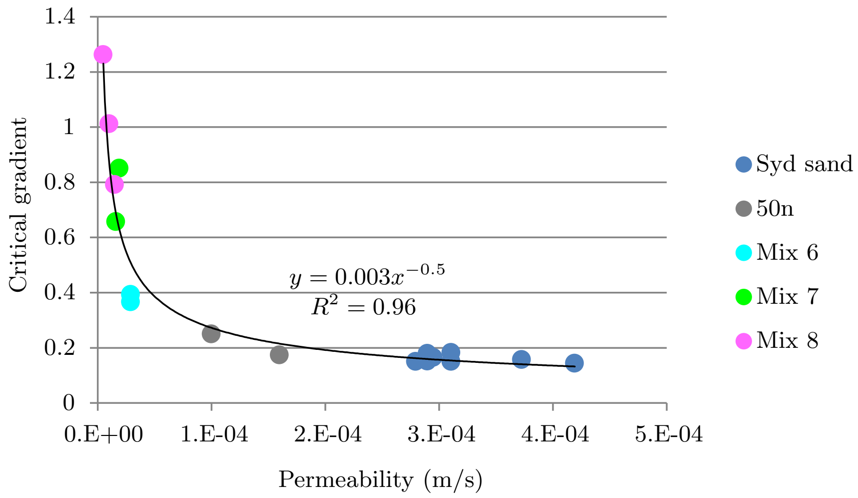

(b) Only soils with $d_{50} = 0.2 - 0.3$mm (hence channel widths <20mm)

Figure 8.22: Critical gradient with soil permeability for all Group 4 tests and Sydney Sand tests in circle exits

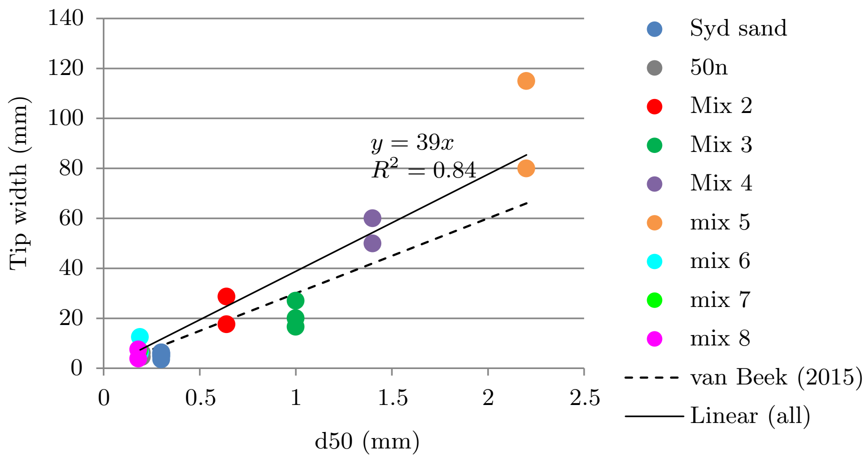

Figure 8.23: Tip width with d_{50}

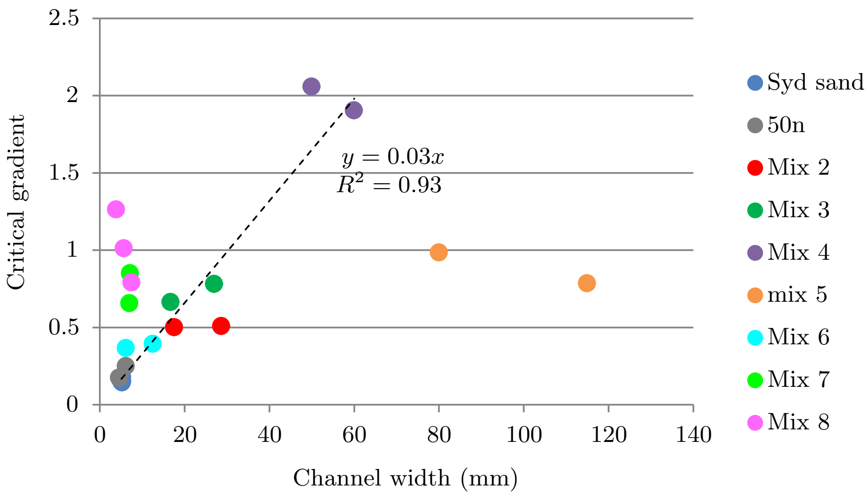

Figure 8.24: Critical gradient with average tip width showing linear increase from Sydney Sand to Mix 2, 3 and 4

However soils with significantly different permeabilities, i.e. the 50n 'family' (50n and Mixes 6–8) and Mix 5, do not lie along the same dashed line, therefore there is not a clear trend between critical gradient and tip width for all soils either.

Given Sydney Sand, 50n and mixes 6–8, all with similar tip widths, laid along a single power curve in the permeability and critical gradient chart, it was speculated that perhaps the other soils laid along similar curves unique to their tip widths. To investigate this, firstly the power trendline in Figure 8.22b was re-evaluated without Sydney Sand because Sydney Sand had a slightly larger d_{50} than 50n and Mixes 6–8 (and a unique power curve for a given tip width was being sought). The re-evaluated power curve was given by $i_c = 0.0009K^{-0.6}$. Secondly, the exponent was increased until curves coincided with results of other soils. Figure 8.25 is a plot of the exponents required and demonstrated a relationship of exponent $= -0.23 \ln d_{50} - 0.96$. Using this relationship, curves were drawn for the d_{50} of each soil, in Figure 8.26. With experimental results also plotted, it can be seen that the curves positioned close to experimental data.

Hence the suggested model is:

$$i_c = 0.0009K^{-0.23 \ln d_{50} - 0.96} \tag{8.1}$$

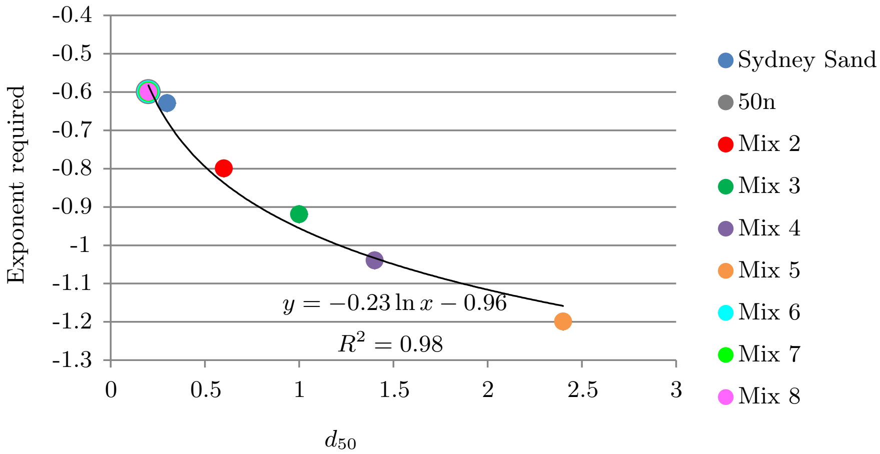

Figure 8.25: The exponent required in Equation 8.1 with d_{50}

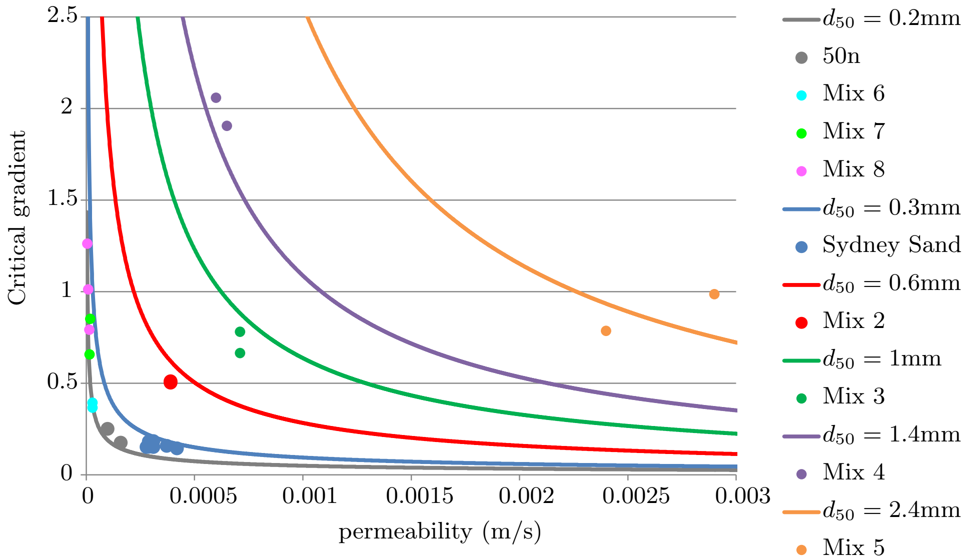

Figure 8.26: Critical gradient with soil permeability showing experimental results and model curves unique to each d_{50}

To demonstrate the effectiveness of this model, Figure 8.27a is a plot of experimental results versus model predictions. The coefficient of determination of the correlation was $R^2 = 0.95$. This model was more accurate than the Schmertmann (2000) and Sellmeijer et al. (2011) models, based on the Group 4 results from this study, as illustrated in Figures 8.27b and 8.27c and demonstrated by their R^2 values of 0.76 and 0.29 respectively.

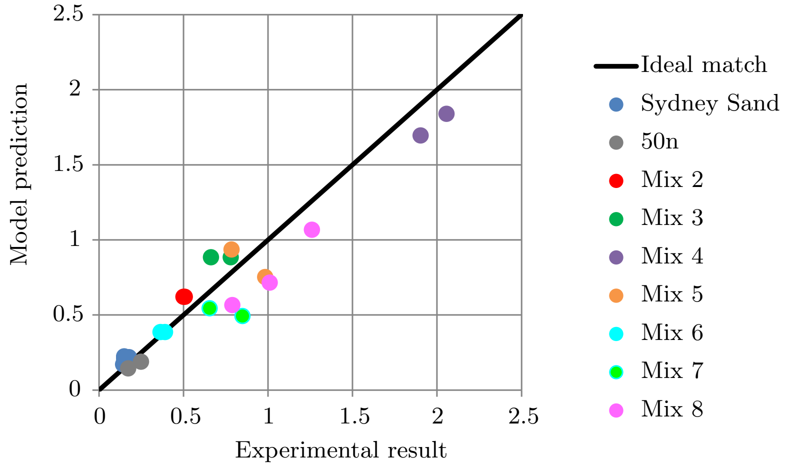

(a) Equation 8.1 model

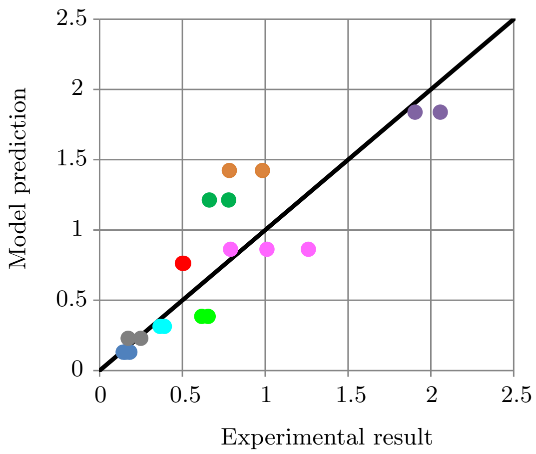

(b) Schmertmann (2000) model

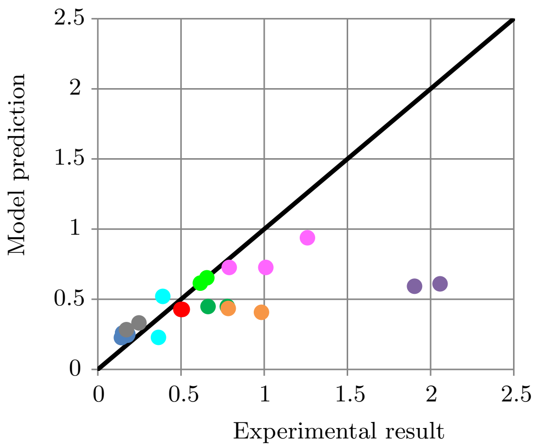

(c) Sellmeijer et al. (2011) model

Figure 8.27: Critical gradients predicted by respective models versus critical gradient observed in Group 4 experiments showing effectiveness of models

It is acknowledged that when considering the correlation of experiments with these models, the model suggested here (Equation 8.1) has the advantage of being compared with the experimental data it was based on, and perhaps the other models would perform just as well if they too were compared to the data they were based on. Ideally, all three models would be compared to all data available (and indeed this was done for the Schmertmann

(2000) and Sellmeijer et al. (2011) models in Chapter 11) however, the model suggested here does not include any scale or exit effects therefore, it can not be compared with data in any flume or exit geometry other than the flume used in this study with the circular exit.

Having demonstrated that critical gradient is a function of soil permeability and size (d_{50}) the question arises of why then does critical gradient also appear to be a function of uniformity coefficient? It is because the three soil properties are inter-related. A low C_u (corresponding to a low critical gradient) keeps permeability high (because uniform sands have higher void ratios) which explains why the critical gradient remains low. A high C_u (corresponding to a high critical gradient) keeps permeability low or d_{50} high which both explain why the critical gradient is high.

However, there are exceptions to these generalisations, such as a uniform coarse-grained sand or fine gravel resulting in a low C_u but wide tip width which drives the critical gradient higher than the Schmertmann (2000) model prediction. Examples of this are soils 20/30 and 8/30 tested in the Townsend and Shiau (1986) study which resulted in average critical gradients of 48% and 93% higher than the Schmertmann (2000) model prediction. Another exception is a poorly or gap graded sand with a silty fraction accounting for less than 10% of the soil. With the silt fraction less than 10%, the d_{10} remains close to the d_{60}, so keeps a low C_u, but the silt reduces the soil's permeability driving the critical gradient higher than the Schmertmann (2000) model prediction. An example of this is Mix 7 from this study which resulted in critical gradients 70–80% higher than the Schmertmann (2000) model prediction. Therefore, there are soils for which the C_u relation won't predict as well. For these soils, a relation incorporating permeability and d_{50}, such as the relation offered in Equation 8.1, is expected to out-perform the C_u relation. Although, this can not be proven yet, not without development of Equation 8.1 to incorporate exit and scale effects. To incorporate scale effect, further experimentation is required to characterise the scale effect with respect to depth and width (instead of with respect to depth and length as Sellmeijer et al. (2011) and Schmertmann (2000) have done).

8.3.3 Accounting for soil grading in design

Chapter 11 contains a review of the two most popular methods of design against backward erosion piping- the Schmertmann (2000) and Sellmeijer et al. (2011) methods. This review considers how accurately these methods predicted experimental results from both this study and the studies of others and suggests amendments which improves the accuracy. Within this review consideration is given to the methods' ability to account for soil grading - a summary of which is given here.

Schmertmann (2000) accounts for the effect of soil grading by relating the local critical gradient to the soil's uniformity coefficient and with a correction factor called the grain size factor, C_S. The accuracy of the relation between local critical gradient to the soil's uniformity coefficient was explored above using the results from this study and in Subsection 11.2.3 using results from other studies. Both Figures 8.20 and 11.22 indicated that experiments did confirm the approximate relation suggested by Schmertmann (2000) but that an exponential curve would predict gradients for more well graded soils more accurately. Yet there is still considerable scatter from the exponential curve and a reason for this is offered above - that C_u alone can not always capture what the current author considers are the two most relevant soil properties, permeability and d_{50}. Two examples of soils for which C_u does not capture the soil's permeability and d_{50} (and therefore result in gradients significantly different from the Schmertmann (2000) prediction) were given above.

Schmertmann (2000) used a grain size correction factor, C_S to compensate for the influence of grain size on the critical gradient whereby finer soils require lower gradients, given by $C_S = (d_{10}/0.2mm)^{0.2}$. However, Figure 11.16 demonstrates no clear relationship between d_{10} and critical gradient and Figure 11.17 demonstrates the C_S factor is inaccurate. Furthermore, a reduction in R^2 between experimental results and model predictions after C_S was applied demonstrated the C_S factor did not add value to the Schmertmann (2000) model. Schmertmann (2000) does not appear to explain why d_{10} was chosen to characterise the soil size.

Sellmeijer et al. (2011) characterises soil grading in the standard dike formula with use of C_u, d_{70} and intrinsic permeability. Whilst d_{50} is usually the representative diameter for modelling incipient motion, Sellmeijer et al. (2011) used d_{70} on the assumption that incipient motion is not sufficient and that larger particles need to be transported as well (van Beek, 2015). Although Sellmeijer et al. (2011) note they do not understand the physical mechanism of the grain size exponent and that the scale factor is purely empirical with no physical foundation.

It's not possible to examine how accurately the model predicts the influence of each soil parameter separately because the parameters are inter-related. However, analysis in Chapter 11 indicated that the model performed better for 'standard dike' soils than non 'standard dike' soils (see autoreffig:sellmeijer-all-soils). 'Standard dike' soils are those which fall within the limits listed in Table 2.5, i.e. reasonably uniform, fine to medium sands. Given the Sellmeijer et al. (2011) standard dike formula was formulated using these 'standard dike' soils, it stands to reason the formula is less accurate for other soils. When results from non 'standard dike' soils were included in a revised multi-variate analysis, the exponents associated with the C_u, d_{70} terms changed. The C_u exponent increased from 0.13 to 0.5 and the d_{70} exponent decreased from 0.6 to 0.04. This suggested C_u has more influence and d_{70} has less influence over the critical gradient than indicated by Sellmeijer et al. (2011).

8.4 Summary

From experimental observations reported in Chapter 4, it was found that for graded soils:

1. The width of the channel increased linearly as a function of d_{50} (Figure 4.11 and repeated as Figure 8.23).
2. The speed of tip progression increased with increasing C_u. In uniform soils, tip progression was approximately steady. In more well graded soils, tip progression usually occurred in sudden bursts.
3. The speed of forward deepening leading to failure increased with increasing C_u.
4. Channel branching and meandering were less likely in well graded soils.

From experimental results reported in this chapter, it was found that:

1. Soil grading affected the critical head such that it increased in the order of Sydney Sand, Sibelco 50n, Mix 6, Mix 2, Mix 3, Mix 7, Mix 5, Mix 8, Mix 1 and Mix 4.

2. As critical gradients increased, so did experimental variability (variation in critical gradients obtained from identical tests increased).

3. There appeared to be no discernible pattern or order to initiation head or critical channel length.

4. The envelope of soils susceptible to backward erosion, in terms of coefficient of uniformity, were covered because channels in Mix 1 and 4 did not backward erode all the way to upstream end despite applying a hydraulic gradient of 3 (gradients in the field rarely exceed 1).

5. Obstacles impeding backward erosion were more likely with increasing C_u. Obstacles such as groups of gravel arresting the tip, multiple small erosion paths making it difficult to identify the eroding tip and regions of slippage instead of a concentrated channel were more likely to occur.

Having analysed critical gradients with C_u, it was found that the critical gradient increased with increasing C_u thereby confirming the trend suggested by Schmertmann (2000). However, a revised trendline was suggested which used an exponential curve instead of linear and resulted in lower critical gradients around $C_u = 6$ but higher gradients past a C_u of 8.

Also having analysed critical gradients with soil permeability, it was observed that critical gradients of fine-grained soils plotted along a power curve but that the more coarse soils did not. Having noticed that the tip width was similar across the fine-grained soils, it was thought that perhaps this power curve was unique to this tip width and that all results might plot over similar power curves unique to their respective tip widths. To investigate this, the exponent of the power curve was amended by trial until curves coincided with the results of the more coarse soils. Equipped with the finding that tip width was a function of d_{50}, the exponents required were plotted against d_{50} revealing a natural log curve. With the equations of both curves combined, a relationship of critical gradient as a function of soil permeability and d_{50} was formed resulting in: $i_c = 0.0009K^{-0.23\ln d_{50}-0.96}$. This relationship predicted the critical gradients observed in experiments with considerable accuracy, as indicated by an R^2 value of 0.95.

It is expected this relationship could predict critical gradients with more accuracy than the Schmertmann (2000) model however, the relationship requires further development to incorporate scale and exit effects before this can be proven.

When accounting for soil grading in design, Schmertmann (2000) characterises the soil grading using C_u and d_{10}. Experimental results from both this study and those of others indicated the Schmertmann (2000) relation between C_u and critical gradient has merit but may be better modelled with an exponential curve instead of a linear one as used by Schmertmann (2000). However, experimental results did not support the d_{10} relation (C_S) suggested by Schmertmann (2000), therefore it is suggested C_S not be used.

Sellmeijer et al. (2011) characterises the soil grading using C_u, d_{70} and intrinsic permeability. Whilst parameters could not be isolated to examine the model's ability to predict the influence of each, a revised multi-variate analysis, using results from this study and others (and therefore a wider variety of soils) indicated C_u has more influence over the critical gradient and d_{70} has less than indicated by Sellmeijer et al. (2011). Revised exponents reflecting this are given in Chapter 11.

Chapter 9

Group 5: Cyclic and above critical loading

9.1 Introduction and aims

Glynn and Kuszmaul (2004) reported an increase in the number and size of sand boils downstream of levees along the Mississippi River with subsequent floods even when subsequent floods were lower. This raised the concern that perhaps the critical gradient reduces with repeated loading events.

To investigate this concern a group of tests were carried out whereby the head applied to the flume was raised and dropped in a series of cycles to model successive flood events, as described in Subsection 9.2.1. This group of tests included Tests 77, 79 and 80 carried out in Sydney Sand and Tests 81 and 82 in Mix 6 (with the default set-up of circle exit, 1.3m seepage length and 50kPa bladder pressure) and were classified as 'Group 5' of the experimental program.

In addition, very little research had been carried out on the rate of backward erosion and the impact of gradients above critical (this is discussed in Section 2.7). Therefore, the rate of backward erosion of previous tests were analysed and an additional group of tests were carried out in which heads above critical were applied, as described in Subsection 3.3.4. This group of tests included Tests 83–92 carried out in Sydney Sand (with the default set-up of circle exit, 1.3m seepage length and 50kPa bladder pressure).

The aims in this chapter were to investigate cyclic and above critical loading in order to answer the following questions:

1. Does the critical gradient reduce with each loading cycle?
2. If the critical gradient does reduce with each cycle, is it due to cyclic loading 'weakening' the experiment? In other words, are critical gradients under cyclic loading lower than critical gradients under regular loading?
3. What is the rate of backward erosion in Sydney Sand using the circle exit and does this rate increase with increasing gradient above critical?

9.2 Experimental Results

9.2.1 Cyclic loading

Results of the Sydney Sand tests are plotted in Figure 9.1 and results of the Mix 6 tests are plotted in Figure 9.2. Note that the term 'regular loading' used throughout this chapter refers to either the 'increase only' or the 'decrease at points of interest' hydraulic loading procedures (or both). See Subsection 3.3.4 for definition of these loading procedures.

There were two findings of interest. The first was whether the head difference required to re-initiate the tip reduced with each successive cycle. The second was whether cyclic loading made the system weaker, that is, whether head differences required under cyclic loading were lower than head differences required under regular loading. A summary of these results are listed in Table 9.1.

The head difference required to re-initiate the tip did reduce with each successive cycle, for 3 out of the 4 cycle tests (disregarding Test 80). Reductions in head required were, on average, quite small at 2% in the Sydney Sand test and a little larger at 5 and 13% in the Mix 6 tests. Although, these were averaged reductions; actual reductions were as great as 30% in Test 82 (from the second to the third cycle).

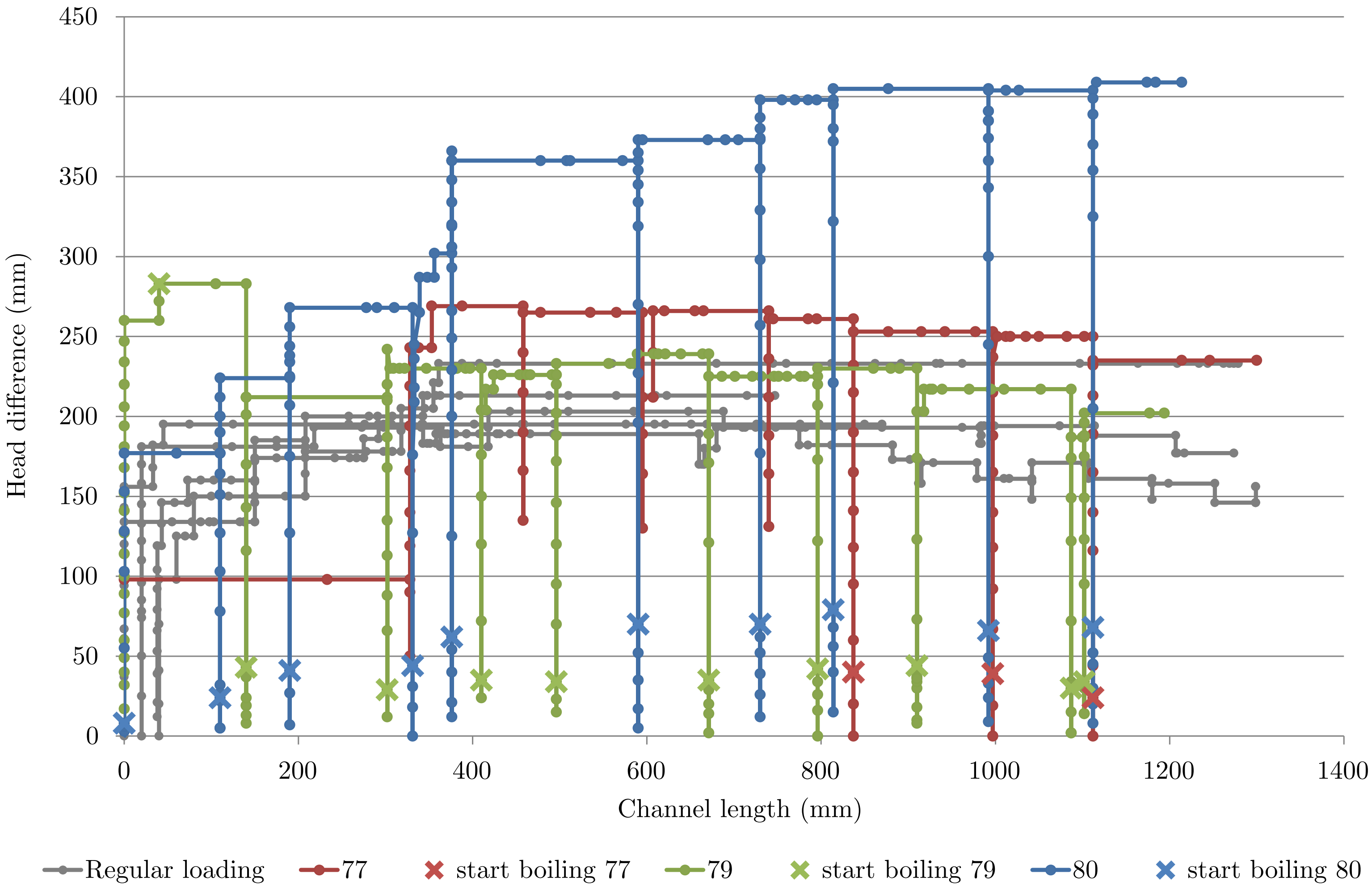

Figure 9.1: Group 5 test results- Cyclic loading on Sydney Sand

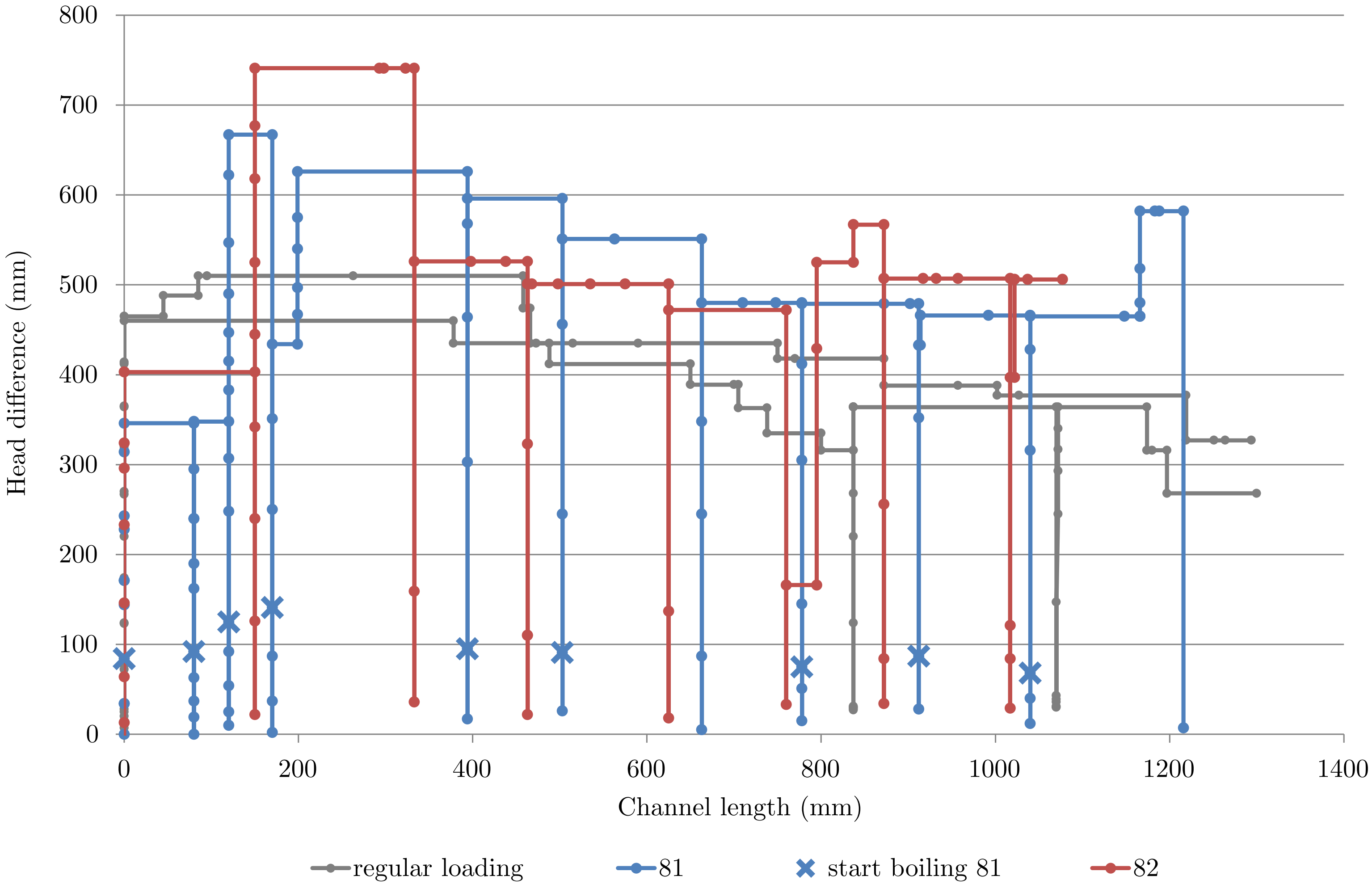

Figure 9.2: Group 5 test results- Cyclic loading on Mix 6

Table 9.1: Summary of cyclic loading test results

Test	Soil	Head required to re-initiate tip with successive cycles (excluding first cycle)	Max. head (mm) (excluding first cycle)	Max. head as % of avg. crit. head for regular loading*
77	Sydney Sand	decreased on average by 2%	269	131
79	Sydney Sand	decreased on average by 0.5% (i.e. near constant)	239	116
80	Sydney Sand	increased on average by 8% (but sample desaturated so result disregarded)	409	199
81	Mix 6	decreased on average by 5% (also excluding second cycle)	667	138
82	Mix 6	decreased on average by 13% (also excluding last 3 cycles)	741	153

* Avg. crit. head for regular loading was 206mm for SS and 485mm for Mix 6

The only test to not reduce in head with each cycle was Test 79. This test saw both reductions and increases in head differences required, resulting in very little net change.

Test 80 was disregarded because air bubbles entered the channel between bars 3 and 4 (for reasons unknown), as shown in Figure 9.3a. Most likely as a result of the air bubbles, critical heads were at least 40% greater than both the previous cyclic and regular tests. This was the only test to see increases in head required for each successive cycle.

As noted in Table 9.1, the first cycle was not included when considering whether the head required for each cycle increased or decreased. The first cycle was also not included when identifying the maximum head. This was because the initiation head (the head for the first cycle) was affected by abnormalities in the sand at the exit. Tests 77 and 79 were good examples of this. Test 77 initiated at a very low head (35% less than the average initiation head of regular tests) and progressed further (25%L) than any other test without need for head increases. There was no visual indication as to why this occurred. Where as Test 79 initiated at a very high head (63% higher than the average initiation head of regular tests). It's understood this occurred because sand wasn't pressed up against the lid in the vicinity of the exit, causing the exit to behave more like a slope

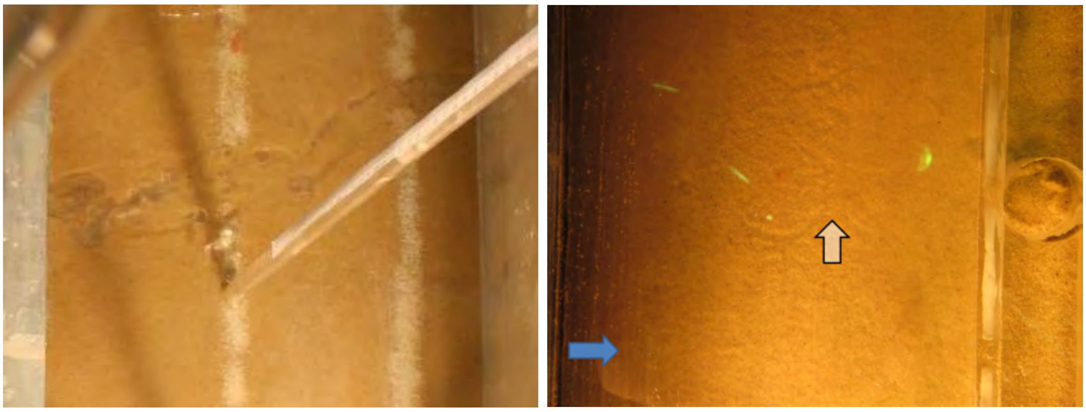

(a) Air bubbles entered channel between bars 3 and 4 in Test 80 (flow direction unknown)

(b) Channel initiated about 50mm upstream of exit due to local void in Test 79

Figure 9.3: Group 5 cyclic test abnormalities (blue arrow indicates direction of flow)

exit. As a result, initiation didn't occur at the exit but some 50mm upstream of the exit where sand came in contact with the lid, as shown in Figure 9.3b.

Also noted in Table 9.1 was the exclusion of the last 3 cycles in Test 82 when considering whether the head increased or decreased between cycles. They were excluded because the heads imposed to re-initiate the tip skipped the critical head of the previous cycle. This meant these cycles could have progressed at lower heads and to include them would be misleading.

Also note that the head increase in the last cycle of Test 81 was not considered significant when considering the impact of cyclic loading because the channel blocked substantially at this time.

With regards to whether cyclic loading made the system weaker than if there was one, long-term flood, experimental results suggest that no, cyclic loading in and of itself, did not make the system weaker. This was indicated by heads required for cyclic loading tests which were higher than heads required for regular loading tests (between 16–53% higher). Therefore, the data implies cyclic loading may have strengthened the system.

Although it should be noted that given the large variability in experimental results and limited number of tests to characterise the variability with confidence, it is still possible that critical gradients of cyclic tests were not higher as a result of cyclic loading but were simply at the higher end of the experimental variability.

Cyclic tests were also used to determine when sand boiling at the exit began. If sand boiling began at successively lower heads then this could explain why Glynn and Kuszmaul (2004) reported an increase in boiling activity with successively lower floods. The crosses on Figures 9.1 and 9.2 mark at what head levels boiling was first observed. The crosses do not appear to decrease but appear to remain at similar head levels which does not explain the Glynn and Kuszmaul (2004) observation.

9.2.2 Above critical loading

In order to determine whether the tip progression speed (i.e. rate of erosion) increased with increasing head above critical, it was necessary to first calculate the average tip speed at the critical head using Group 2 tests (in Sydney Sand using the circle exit). This is done in Table 9.2 which indicates that the average tip speed was 3.2mm/minute.

Table 9.2: Average tip progression speed for Group 2 (non-cyclic) tests in circle exits

Test	Critical head (mm)	End channel length (mm)	Duration of active tip progression (hrs)	Average tip progression speed (mm/minute)
20	233	1279	7.7	2.8
22	195	1279	7.9	2.7
24	236	990	5.1	3.2
27	213	747	7.3	1.7
31	195	1274	13.5	1.6
34	203	1300	2.9	7.5
		average	7.4	3.2

Under the direction of the author, an undergraduate student, Ms Greenless, carried out the majority of the above critical loading tests. Results of the above critical loading tests are listed in Table 9.3. Note that average tip progression speeds listed in Table 9.3 are a little different to those reported in Greenlees (2016) as speeds were calculated by Greenlees (2016) using the slope of a linear line-of-best-fit, whereas speeds were calculated in Table 9.3 using final channel length divided by duration of active tip progression.

With average tip progression speed plotted against head difference applied, the proportional, linear relationship can be seen in Figure 9.4. The tip progression speed (also termed erosion rate) does indeed increase with increase in head difference, albeit with with some scatter in the data and one–two outlier(s) (an R^2 of 0.7).

Table 9.3: Above critical loading results

Test	Head difference (mm)	Head difference % of avg. crit. head of 206mm	End channel length (mm)	Duration of active tip progression (hrs)	Avg. progression speed (mm/minute)	Duration of forward deepening (hrs)
83	347	168	1300	0.35	62	3.60
84	367	178	1300	0.42	51	1.10
85	330	160	1300	0.35	62	1.08
86	305	148	1146	0.57	34	1.27
87	309	150	1300	0.47	46	1.22
88	271	132	1276	1.03	21	2.40
89	259	126	1300	0.75	29	1.42
90	230	112	1112	0.48	39	0.75
91	216	105	1300	4.83	4	-
92	225	109	1300	2.15	10	5.63

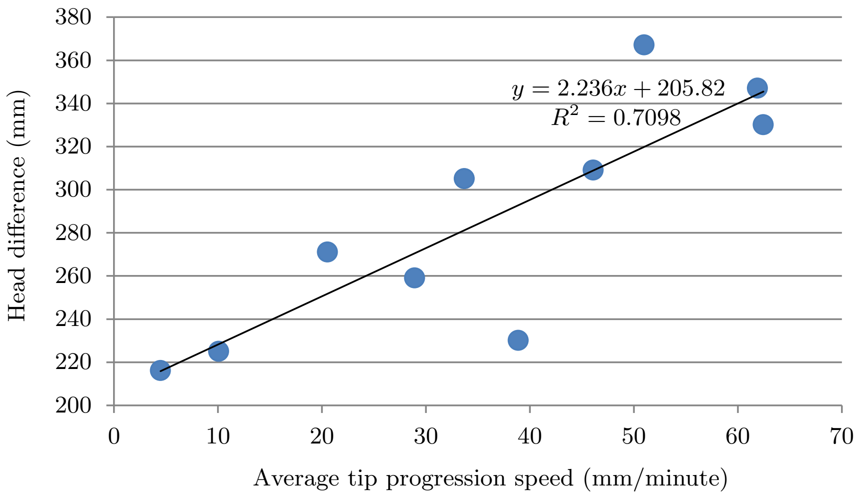

Figure 9.4: Tip progression speed with head difference applied to Group 5 'above critical loading' tests

If the increase in tip progression speed is expressed as a ratio of the average speed observed in regular loading tests and the head difference is expressed as a ratio of the average critical head then a non-dimensionalised, universal relationship can be modelled. Note that the y-intercept of the line of best fit was altered to ensure the line passed through 1,1 (because the average tip speed in tests at critical head ought to correlate with the critical head). This relationship suggests that a 10% increase in head above critical is likely to result in tip progression speed more than three times that of the speed at critical head.

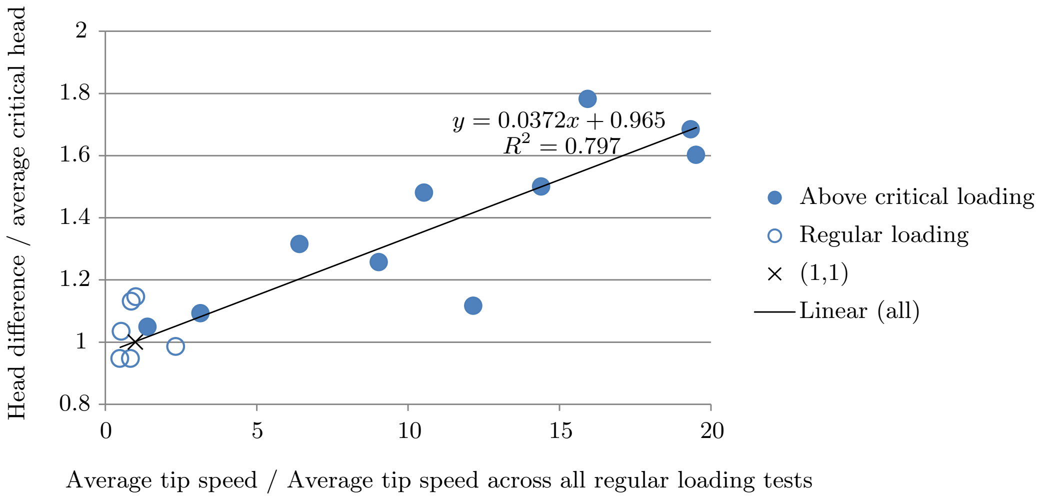

Figure 9.5: Non-dimensionalised to show increase in tip progression speed as ratio of regular average with increase in head difference as ratio of critical

9.3 Discussion

9.3.1 Cyclic loading

Experiments hydraulically loaded in cycles in this study, have confirmed the concern of Sills and Vroman (2007), that the critical gradient reduces with each flood. However, reductions in critical head were moderate (between 0.5 to 13% on average) and were not due to a weakening of the system as a result of cyclic loading. Instead, reductions in critical head are thought to be due to the same reason head could be reduced when the 'decrease at points of interest' loading procedure was used. As the channel lengthens, it causes an increase in the system's bulk permeability (demonstrated in Figure 4.34), resulting in more flow into the channel tip which then needs less head difference to produce erosive seepage forces into the tip.

As evidence for cyclic loading not weakening the system, heads required to re-initiate the tip were usually higher than heads required in regular tests. This suggests that repeated flood loading events throughout the years does not put a dam/levee at greater risk than one flood imposing the critical head over a long period of time.

It is not yet known why cyclic tests required higher heads than regular tests, but perhaps stationary, inactive channel tips require higher gradients to re-activate than progressing, active channel tips require to continue eroding.

In response to the observation made by Glynn and Kuszmaul (2004) whereby sand boils increased in size with subsequent floods, even when subsequent floods were lower, the theory is offered that the channel remains in place between flood events so that it becomes longer with each flood which results in a larger surface area from which scour occurs, resulting in more sand detached and transported to sand boils. In other words, whilst two flood events of the same level and duration would erode the same volume of material from the channel tip (primary erosion), the later flood would erode more material from the longer channel's sides and bed (secondary erosion) and hence result in a larger sand boil.

To test this theory, sand boils were collected after each cycle, dried and weighed. Note that channel length segments contributing to each sand boil were approximately constant at 130mm. The sand boil weights are reported in Section 4.6. It is possible there was a slight increase in boil size with successive cycles, however, the trend was not clear and there were exceptions. Therefore, the observation of increasing sand boils with successive floods could not be clearly reproduced (or explained) with laboratory tests.

9.3.2 Above critical loading

There are two separate, but related findings herein. The first being the tip progression speed at critical head and the second being the increase in tip progression speed at heads above critical.

Tip progression speed at critical head

It is worth noting that the average tip progression speeds listed in Table 9.2 (which are limited to Sydney Sand tests using the circle exit), between 1.6–7.5 mm/minute, are similar to average speeds calculated from time marks listed in laboratory notes by Townsend et al. (1981), between 1.9–15.6mm/minute (these tests were carried out in a similar flume and similar soil but a different exit- the slope exit). Tip speeds provided by Müller-Kirchenbauer et al. (1993) were faster at 6–42mm/min however, it is unclear what soil these speeds were obtained in and the flume geometry was significantly different.

It appears that soil grading affects the speed of tip progression. Tip progression was commonly steady in uniform soils (between 1.6-7.5mm/minute) but fast and intermittent in well graded soils, often eroding in sudden bursts (up to approximately 30mm/min in Mix 5). Tip progression speeds in soils other than Sydney Sand were not evaluated, although this data is available in experimental records for extraction for further research.

It was also clear, from testing different exit geometries, that the exit affected the speed of tip progression. Tip progression was commonly faster when the slope and plane exits were used (with tests typically taking a few hours) than when the circle and slot exits were used (typically taking a few days). It is possible that it was not the exit geometry itself affecting the tip progression speed but the larger heads required to initiate backward erosion in slope and plane exits. Again, tip progression speeds in exits other than circle exits were not evaluated but are available in experimental records for further research.

It is not known whether tip progression speed is affected by scale, i.e. whether a tip progresses at a unique, soil-specific speed when a flume or foundation is loaded by its critical gradient even if their critical gradients are substantially different (on account of scale effects). This means it is not known whether the tip progression speeds obtained at critical head in this study (between 1.6–7.5mm/minute) can be used as an indication of tip progression speed in the field, assuming a similar soil and exit geometry. Further laboratory testing which measures the tip progression speed in set-ups which vary only in depths and widths are required to determine this.

Tip progression speeds in the field would enable comparison of the time required for progression to reach the upstream side (time to failure) with anticipated flood duration (taken from flood hydrographs). This comparison could lead to reducing the estimated risk of failure if time for complete progression was less than flood duration, even if the flood reaches critical level. Tip progression speeds in the field could also provide an indication of warning times required once a flood level has reached critical. They could also provide a way of estimating the length of a channel beneath a dam/levee which has been exposed to critical floods in the past, if past flood levels and durations are known. This would provide an indication of how many more flood events a given dam/levee system could withstand in the future before failing.

Tip progression speeds at heads above critical

Experimental results indicate that not only does tip progression speed increase with increase in head above critical, it does so quite dramatically, with a 10% increase in head above critical resulting in approximately a three-fold increase in tip progression speed. This means that a 10% increase in gradient above critical could cause failure in 1/3 of the time and 20% above critical in 1/6 of the time.

It is not known whether the tip speed would increase as dramatically in the field, though it is expected to still increase (there's no reason to expect this increase in tip speed is an experimental anomaly only). In the field, an increase in tip progression speed with heads above critical would result in the channel reaching the upstream side, leading to failure, faster than anticipated. This would require the estimated risk of failure in assessments to be increased to reflect the fact that now the the time to failure has reduced. Particularly in situations where the risk of backward erosion was considered low at critical head, because time to failure was greater than the expected flood duration, but now with a head above critical, time to failure is reduced, making it less than or equal to the expected flood duration.

It is recommended further experimental work be carried out to measure the increase of tip speeds at heads above critical in other exit geometries, soils and scales. Testing in other scales would be particularly useful to determine whether such large increases in tip speed would be likely to occur in the field as well.

9.4 Summary

In summary, experiments have confirmed that the gradient required to re-initiate backward erosion does reduce when hydraulic loading is applied in cycles (designed to model successive flood events). However, reductions in head with each cycle were moderate (between 0.5 to 13%, on average) and heads required were actually higher than those required for regular experiments (experiments loaded without cycles). Therefore, it was not cyclic loading that was weakening the system (i.e. causing a reduction in the head needed for each cycle). It is thought that the system was weakening as a result of the lengthening channel which increased the system's bulk permeability. This was supported by the fact that head required also decreased when the 'decrease at points of interest' loading procedure was used.

Channel tips progressed at speeds of between 1.6–7.4mm/minute in Sydney Sand at critical head. Similar speeds were calculated using time marks listed in laboratory notes by Townsend et al. (1981). It is not known whether channel tips would progress at this same speed in field (in similar soil and exit geometry) because it is not yet known what effect, if any, scale has on tip progression speed. It is suggested that additional experiments be carried out in flumes with varying depths and widths to determine the effect of scale on tip progression speed. It is also suggested that additional experiments be carried out in other soils and exit geometries to examine the effect of these on tip progression speed.

When head differences above the critical head were applied, the tip progression speed increased significantly. For example, with a 10% increase in head above critical, the tip progression speed increased approximately three-fold. Additional experiments at heads above critical in other scales, soils and exit geometries would go toward informing engineers whether this rate of speed increase for heads above critical is universal or not.

Chapter 10

Numerical model

10.1 Introduction and aims

This chapter describes the numerical model developed as part of this study. A numerical model was formulated with the aim to visualise and quantify the effect exit geometry had on streamlines and local hydraulic gradients. This was done to investigate why the exit geometry affected initiation and critical gradients.

On commencement of this study, none of the literature reviewed contained an explanation for why the exit geometry affected initiation and critical gradients. During this study though, Vandenboer et al. (2014b) used a 3-dimensional finite element program (Abaqus 6.12) to investigate the difference between 2 and 3-dimensional seepage models in both the slot and circle exits. Their investigation led to the conclusion that 2-dimensional models are insufficient for modelling the 3D nature of backward erosion, particularly at circular exits (Vandenboer et al., 2014b). So whilst Vandenboer et al. (2014b) had investigated differences between the slot and circle exits, this was only 2 of the 4 exit geometries and conclusions on why the exit affects initiation and critical gradients were not drawn. For the first time, this study modelled all four exit geometries for the purpose of explaining the exit geometry affect.

Through out this chapter the hydraulic loading is described in terms of the hydraulic gradient (instead of head). In addition, the terms 'global' and 'local' are often used to distinguish gradients across different distances. Refer to the Glossary for definition of these terms.

10.2 Method

The numerical model was written in MATLAB (edition R2015a by The Mathworks, Inc.) from anew (i.e. it was not built upon any existing code/software).

The model consisted of a rectangular domain, discretised into square elements and enclosed by the following boundaries:

- The upstream panel, modelled as an inflow boundary of purely lateral flow with constant, uniform head;
- The exit, modelled as an outflow boundary across which flow is permitted and whose head is uniform and equal to the downstream head;
- Flume walls, base and lid, modelled as an impermeable boundaries by setting the hydraulic gradient to zero (no flow boundary);

The elements were fixed as squares/cubes by keeping grid spacings on all axes equal (or as close to equal as the fixed-flume-geometry would allow). In other words, the aspect ratio of the element grid was kept as close to 1 as possible. This was done to maximise accuracy.

Hydraulic head was distributed through the model using the Laplace equation:

$$\nabla^2\mathbf{H} = \frac{\partial^2 H}{\partial x^2} + \frac{\partial^2 H}{\partial y^2} = 0 \tag{10.1}$$

The Laplace derivatives were approximated using the finite difference method to second order accuracy. Seepage velocity was calculated using Darcy's Law:

$$v = ki \qquad \text{OR} \qquad \frac{Q}{A} = k\frac{\Delta H}{\Delta L} \tag{10.2}$$

and separated into directional-components. The head gradients were also approximated using the finite difference method to second order accuracy. The domain was characterised by a uniform coefficient of permeability (K). Therefore, the soil was assumed to be homogeneous and isotropic.

Water volume flux into and out of the model was calculated using:

$$q = \oint \overrightarrow{v} \cdot \hat{n}\, dA \tag{10.3}$$

where $\overrightarrow{v}$ = velocity vector at surface of interest

$\hat{n}$ = local unit normal vector of surface

dA = elemental area of surface

with the integral approximated using the Simpson's Rule:

$$q = \frac{\Delta y}{3}(vx_{i,1} + 4vx_{i,2} + 2vx_{i,3} + \cdots + 2vx_{i,n-2} + 4vx_{i,n-1} + vx_{i,n}) \tag{10.4}$$

where Δy = spacing between points on y-axis

$vx_{i,1}$ = velocity component in x-direction at (x,y)=(i,1)

Flow was assumed to be steady.

Three different models were produced when the outflow boundary was shaped into the slope, plane and slot exit geometries. Two-dimensional models were adequate in these instances. However in order to model the circle exit, the model was further developed to include a third dimension.

A schematic representation of the 3-dimensional circle model, showing the boundary conditions and nomenclature, is given in Figure 10.1.

Trials were conducted with a range of different grid spacings to investigate model sensitivities and limitations. The head difference applied was 206mm (the average critical gradient for Sydney Sand) and the soil's permeability was set to 3×10^{-4}m/s (the approximate

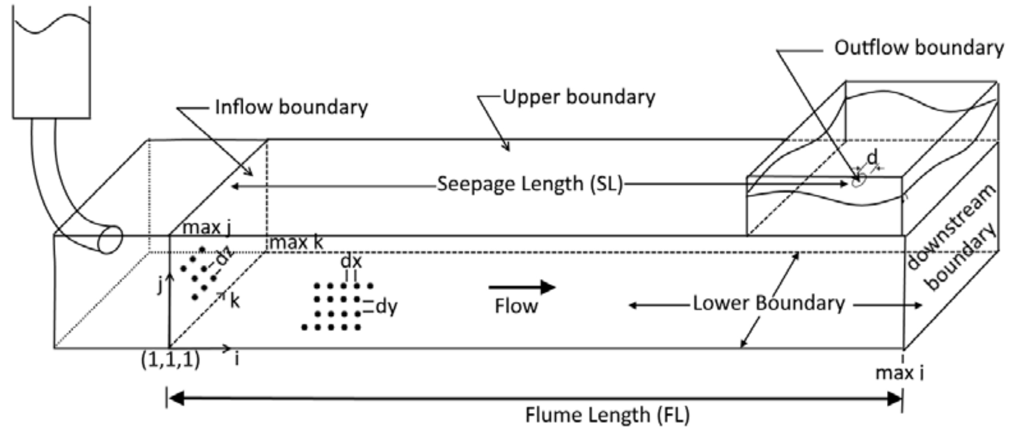

Figure 10.1: Sketch of flow in porous media model (shown with circle exit)

permeability of Sydney Sand). Grid spacings were chosen so that a data point always positioned on the circle-exit edge at 1.3m from upstream. To enable grid points to position on the circle-exit edge at 1.3m, a slight adjustment to the flume length was required, from 1.59m to 1.6m.

Results of these trials are listed in Table 10.1 and show that the computer's Random Access Memory (RAM) was exceeded once the grid spacing was set to 5mm. The computer used had a RAM of 16GB and an Intel Core processor model i7-6650U with speed 2.2GHz.

Table 10.1: Trials of different grid spacings

Kmax	dx (mm)	No. points in exit	Exit area (mm^2)	Max. velocity (m/s)	Flow (m^3/s)	Run time (h:mm:ss)	Max. RAM used (GB)
19	25	2	-	0.0012	2.91E-6	0:00:03	0.47
37	12.5	5	312.5	0.0021	2.57E-6	0:05:02	1.71
55	8.3	8	275.6	0.0032	2.23E-6	1:02:34	13.65
73	6.25	13	317.5	0.0039	2.21E-6	5:56:29	13.71
91	5	22	400.0	unknown	unknown	21:50:58	>available

A minimum grid spacing limited to 6.25mm meant that definition of the 25mm diameter circle-exit was limited to a maximum of 13 points. Using such a coarse square grid to represent a circle resulted in a 35% area discrepancy, as shown in Figure 10.2 (note the circle exit had an area of 490.9mm^2). With this reduction in area, it is expected the model would return faster than actual seepage velocities from the exit.

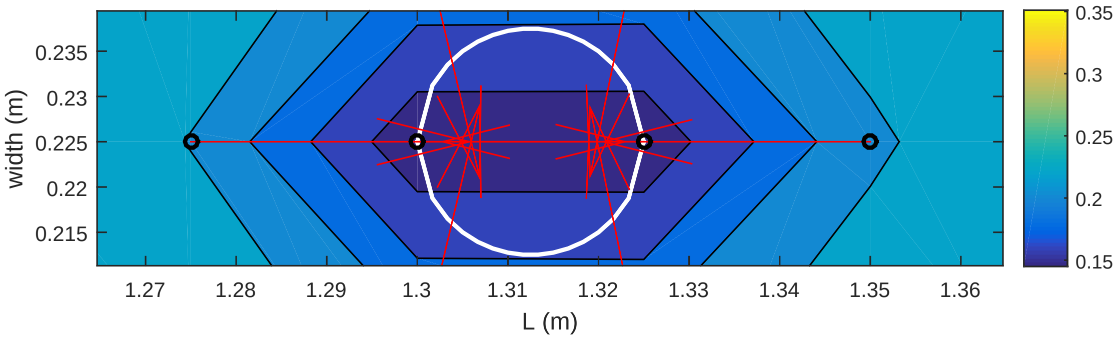

(a) Kmax=19 and dX=25mm resulting in 2 points in exit

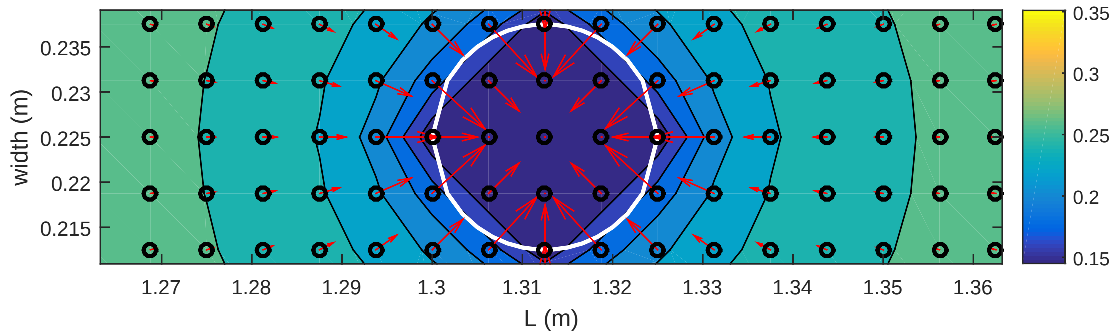

(b) Kmax=73 and dX=6.25mm resulting in 13 points in exit

Figure 10.2: Plan view of circle exit showing number of grid points defining exit

10.3 Results

10.3.1 Singularity

Also shown in Table 10.1 is an ever-increasing maximum seepage velocity with increasing grid resolution. This maximum seepage velocity is plotted with grid spacing in Figure 10.3. The maximum seepage velocity was always located at the exit, on the upstream edge of the circle exit.

This ever-increasing maximum seepage velocity with increasing grid resolution, is evidence of a discontinuity in the hydraulic gradients at the exit, i.e. a singularity (GEO-SLOPE International Ltd, 2016). The maximum seepage velocity continued to increase with increasing grid resolution because the closer grid points became to the singularity, the closer the seepage velocity would become to the infinitely large seepage velocity at the singularity (GEO-SLOPE International Ltd, 2016).

In reality though, seepage velocity at the exit is not infinitely fast. Therefore, seepage

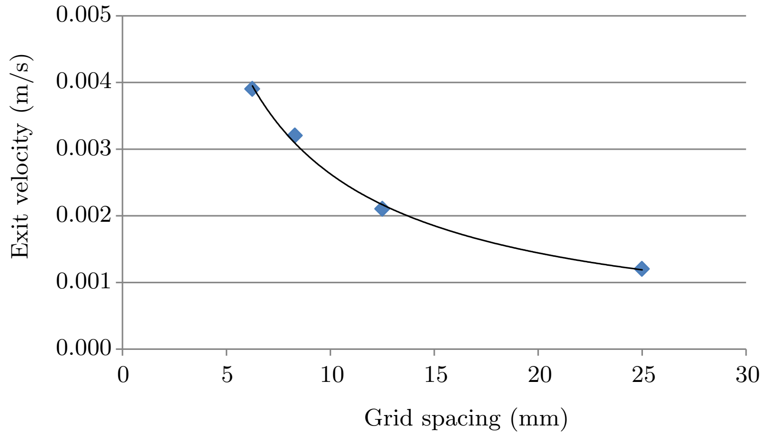

Figure 10.3: Maximum seepage velocity at exit with grid spacing

velocities determined by the numerical model at the exit do not model reality but are a mathematical anomaly, and are a function of grid spacing alone.

Seepage velocity at the exit is crucial because it generates the drag force which is responsible for channel initiation and the highest pressure losses in the aquifer will occur in those regions of highest velocity. Therefore, it was researched whether there were solutions and/or accepted practices within the literature used to compensate for the affect of the singularity so that realistic exit velocities could be obtained. Olsen et al. (2014) reports there is little guidance within the literature on how to compensate for this in a standardised and theoretically-based manner. To demonstrate, Olsen et al. (2014) summarises guidance given by 3 publications: McCook (2011), GEO-SLOPE International Ltd (2016) and Duncan et al. (2011). McCook (2011) suggested selecting an arbitrary distance across which to calculate the exit gradient or an arbitrary head loss but to this Olsen et al. (2014) raise the concern that an arbitrary choice would not provide consistent and reliable exit gradients to predict backward erosion initiation. GEO-SLOPE International Ltd (2016), creators of the commercial seepage model Seep/W, suggest taking an average exit gradient over 1-2 meters however this distance also appears to be chosen arbitrary, without theoretical basis (Olsen et al., 2014) and is also clearly inappropriate for laboratory-sized scale set-ups. Thirdly, a paper referenced as Duncan et al. (2011) (not included in the reference list) was reported to suggest averaging the vertical gradient over a depth of 1 foot beneath the singular point. Whilst Olsen et al. (2014) states that guidance provided by Duncan et al. (2011) is very helpful and the best-supported guidance available, it is still based on judgement of the smallest depth of erosion that would be considered significant. Olsen et al. (2014) make their own suggestion- to calculate the average gradient across the distance of one ‘representative elementary volume’ (REV). The REV is the minimum volume of soil for which the distribution of various-sized voids and a particles remains representative of the larger soil mass. In other words, it’s the minimum volume of soil which would result in a hydraulic conductivity equal to the hydraulic conductivity calculated according to Darcy’s Law (designed for a continuum domain). The Olsen et al. (2014) paper gives no direction on how to calculate the REV but via personal communication, Olsen did suggest using Carrier (2003) to randomly compute permeability for a range of particle sizes (for a given grain-size distribution) and taking the REV to be the minimum number of particles for which change in permeability becomes negligible.

A different method altogether was used in this study. In this study, gradient profiles were plotted for a series of different grid spacings (see Figure 11.8). The exit gradient was taken to be the gradient at which the multiple profiles began to align, the idea being that once profiles began to align, grid points were back far enough from the exit that gradients were no longer influenced by the singularity. Although, this method was only used once, to estimate the exit gradient at the plane exit used by de Wit (1984). In this instance, it was fortunate enough that the gradient profiles began to align quite close to the exit, 20mm away, so adopting this gradient as the exit gradient was reasonable. However, it is likely this method would not be as successful at larger scales or in different exit geometries which concentrate flow more. In these instances, gradient profiles are likely to align further back from the exit, no longer being close, and therefore no longer reasonable to adopt as the exit gradient. Therefore, a consistent and theoretically-based method for calculating the exit gradient, in all geometries, remains elusive.

When circle exits and the flume used in this study were modelled, gradient profiles began to align around 75mm away from the exit, as shown in Figure 10.4. This meant that influence of the singularity was contained within 75mm around the exit and velocities outside this region could be replied upon. Velocities located 75mm away from the exit edges were used to calculate flow out of the exit by creating a control volume, in the form of a box, around the exit. Flux across each face of the control volume was estimated using the Simpson’s Rule (Equation 10.4) and added to calculate the total flow out of the exit. Flow out of the exit was used to check it was equal to flow in through the upstream face, in order to check for flow continuity. Flow was continuous, with flow into and out of the flume remaining within 3% of each other.

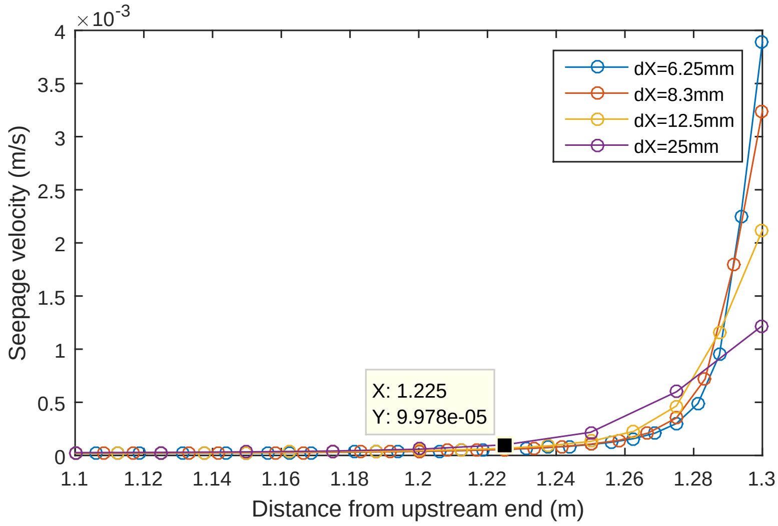

Figure 10.4: Seepage velocity with distance from the upstream end (exit at 1.3m) showing the singularity's zone-of-influence

A consequence of the singularity was head distribution throughout the flume did not match standpipes levels measured in experiments. This is illustrated in Figure 10.5 as a profile of head along the centreline of the flume, produced by the numerical model, and standpipes levels, measured in experiments. The head profile produced by the model was higher than the standpipe levels because amplified gradients at the exit resulted in an exaggerated slope in the head profile at the exit. This exaggerated slope pushed the entire profile higher than the standpipe levels. As evidence for this, Figure 10.5 shows head profiles becoming higher with finer grid resolutions as the affect of the singularity increases. In other words, as grid points became further spaced and further from the exit, the influence of the singularity reduced and the head profile lowered to become closer to the standpipe levels.

Note also that the total flow calculated by the numerical model did not match experimental measurements. In the example of Test 51 at a head of 0.193m, total flow predicted by the numerical model was $4.7 \times 10^{-6}\text{m}^3/\text{s}$ but total flow measured during the experiment was $1.1 \times 10^{-5}\text{m}^3/\text{s}$ (a 57% discrepancy).

The mismatch between numerically modelled heads and experimental measurements was also observed by Ms Vandenboer, although this was not known until after having

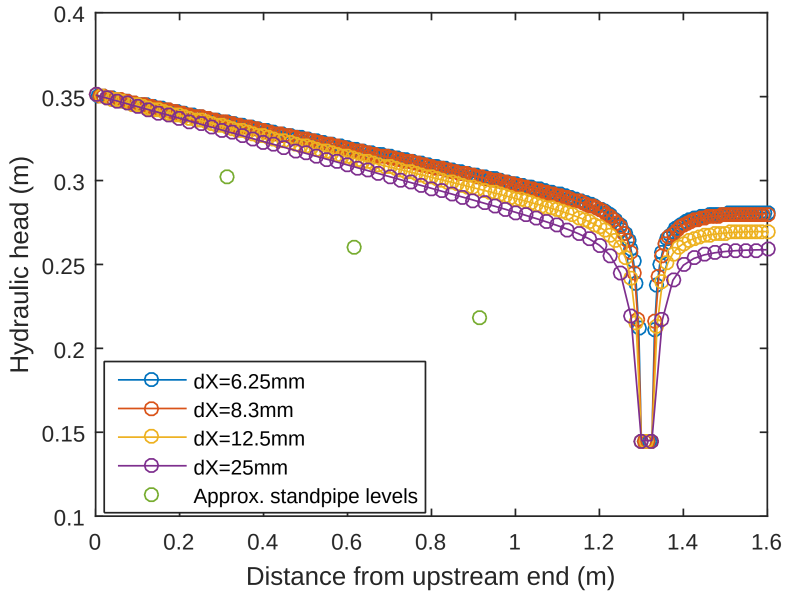

Figure 10.5: Head profile along flume centreline produced by numerical model and standpipe levels measured in experiment showing mismatch

observed the mismatch. Figure 10.6 was received from Ms Vandenboer, via personal communications, illustrating that their 3D finite element model (van Beek et al., 2014a) also produced a head profile higher than pore pressure transducer measurements.

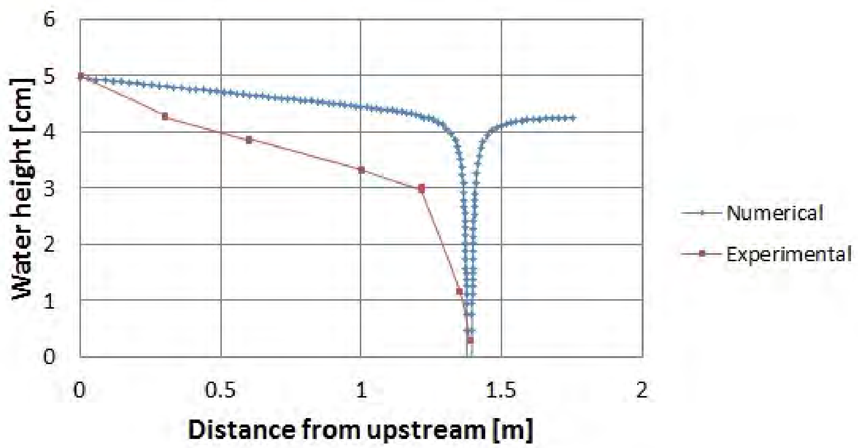

Figure 10.6: Mismatch between numerical model and experimental head measurements also observed by Ms Vandenboer (received via personal communications)

Rice et al. (2016) also reported a difference between numerically modelled heads and experimental measurements, although the difference was only reported for cases once a channel had formed; whereas the differences discussed here are before a channel is present.

The next section describes a method used to compensate for the error caused by the singularity which brought head levels produced by the numerical model down and into alignment with experimental measurements.

10.3.2 Increased permeability at exit

The gradient at the exit, in the numerical model, was artificially reduced, thereby counteracting the affect of the singularity. This was achieved by increasing the permeability locally around the exit. This worked because velocity at the exit was controlled by flow into the upstream face (due to flow continuity) and whilst a reduction in gradient at the exit did result in an increase in gradient at the upstream face (resulting in more flow into the flume and therefore more flow out of the flume, hence faster seepage velocity out of the exit), the change in gradient at the exit was greater than the change in gradient at the upstream face. This meant that velocity at the exit increased less than permeability at the exit increased, so that a decrease in gradient resulted (in line with Darcy's law of $v = Ki$). This is depicted in Figure 10.7.

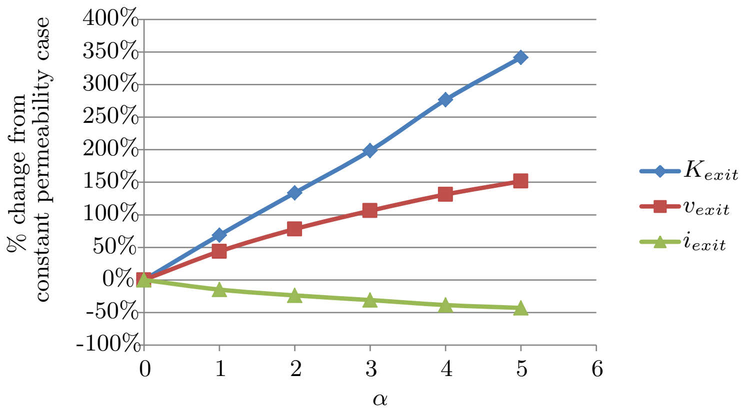

Figure 10.7: Permeability at exit increases more than velocity at exit therefore, the exit gradient decreases

The α on the x-axis of Figure 10.7 refers to a factor by which the permeability at the singularity is multiplied. This factor was exponentially reduced with distance from the singularity as given by:

$$K = K_{true}\left(1 + \alpha e^{-r/\gamma}\right) \tag{10.5}$$

Both α and γ were constants unique to the flume's geometry.

Now that permeability varied through-out the flume, the governing equation used in the numerical model required updating to include a permeability term. Therefore, Equation 10.1 was amended to (for 3 dimensions):

$$\begin{aligned} &-\nabla\mathbf{K}\cdot\nabla\mathbf{H}-\mathbf{K}\nabla^2\mathbf{H} \\ &= -\left(\frac{\partial K}{\partial x}\frac{\partial H}{\partial x}+\frac{\partial K}{\partial y}\frac{\partial H}{\partial y}+\frac{\partial K}{\partial z}\frac{\partial H}{\partial z}\right)-K\left(\frac{\partial^2 H}{\partial x^2}+\frac{\partial^2 H}{\partial y^2}+\frac{\partial^2 H}{\partial z^2}\right)=0 \end{aligned} \tag{10.6}$$

The α and γ constants in Equation 10.5 were varied across a number of different tests in different soils and at different head differences. It was found that an $\alpha = 5$ and a $\gamma = 0.1$ achieved acceptable agreement between the head profile produced by the numerical model and standpipe levels measured in experiments, across all soils and head differences.

Figure 10.8 demonstrates the impact of increasing permeability at the exit using Test 51 in Mix 3 as an example. Figure 10.8a contains two head profiles through the top centreline of the flume, one produced using a constant permeability and the other using an increased permeability at the exit. This shows that once permeability at the exit was increased, the head profile shifted down and came into align with standpipe levels. In this instance, an α value of 4 in Equation 10.5 would have aligned the head profile closer to the standpipes levels, but an α value of 5 was used because it achieved reasonable accuracy across multiple experiments.

Figures 10.8b and 10.8d are contour plots of head values (or flownets) in top plan view. These show changes in head contours were concentrated at the exit when constant permeability was used where as changes in head contours were more evenly spread when permeability was increased at the exit.

Figure 10.8c indicates the variation of permeability along the top centreline of the flume when the permeability was varied using Equation 10.5.

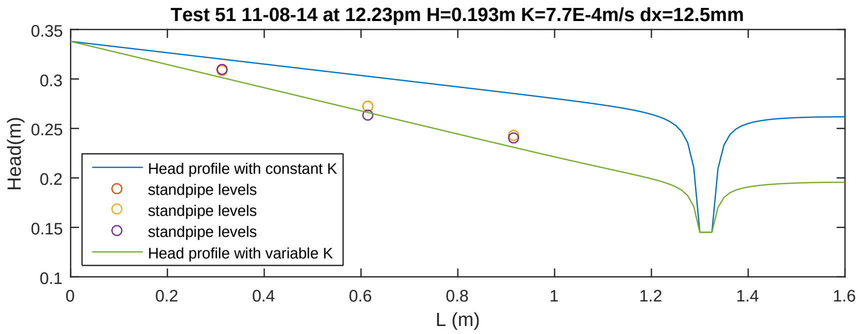

(a) Head profile through top centreline of flume when variable permeability used now matches standpipe levels

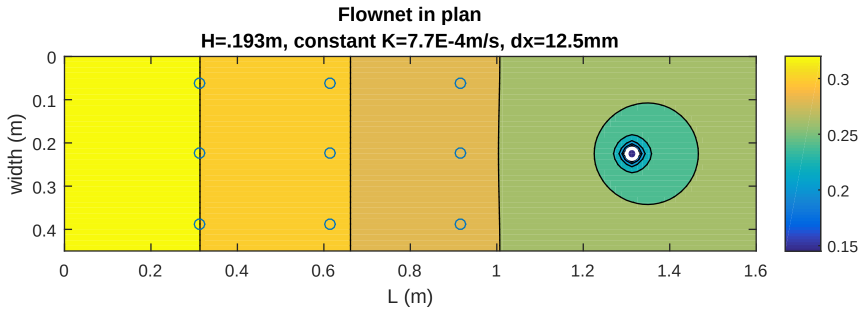

(b) Changes in head contours concentrated around exit when constant permeability used (circles indicate standpipe positions)

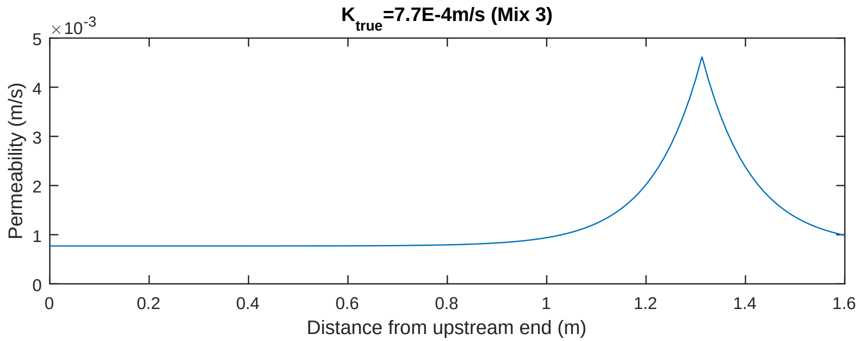

(c) Permeability through top centreline of flume when increased around exit (at 1.3m) according to Equation 10.5

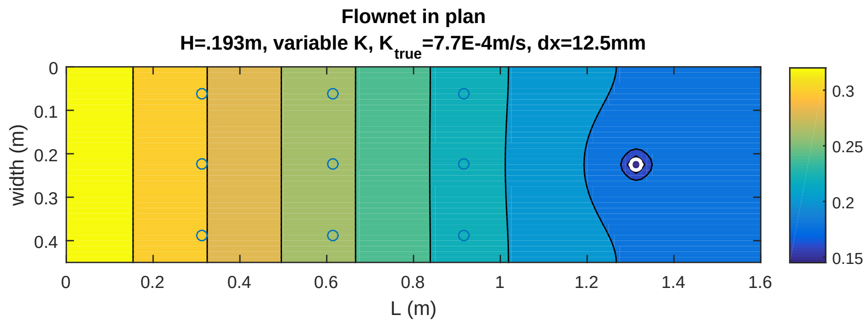

(d) Changes in head contours more evenly spread when permeability increased around exit (circles indicate standpipe positions)

Figure 10.8: Impact of increasing permeability around exit (direction of flow from left to right)

In addition to the head profile now aligning with standpipe levels, the flow calculated by the numerical model now matched the flow measured in experiments. In the example of Test 51 at a head of 0.193m, initially, with a constant permeability, the numerical model predicted a flow of $4.7 \times 10^{-6}\text{m}^3/\text{s}$ however, once permeability was increased at the exit, the numerical model predicted a flow of $1.3 \times 10^{-5}\text{m}^3/\text{s}$. This was now similar to the flow measured in the experiment of $1.1 \times 10^{-5}\text{m}^3/\text{s}$.

Increasing permeability at the exit has physical justification given that convergence of seepage flow is likely to fluidise and dilate the sand, causing an increase in void ratio and therefore an increase in permeability, although this is difficult to prove.

Recently, after having devised this method of increasing permeability at the exit, it was found that Rice et al. (2016) did the same. Rice et al. (2016) identified a region of sand near a circular exit which loosened. Other publications, co-written by Rice, were referred to as having shown that the permeability of this loosened region increased 5-fold. Interestingly, this 5-fold increase is the same as the α factor of 5 (in Equation 10.5) devised in this study. Rice et al. (2016) found that pore pressures evaluated by a FEM model could be matched to sensor measurements when this loosened region, with 5-fold increase in permeability, was introduced into the model (whose extent was determined by trial-and-error until pore pressures matched).

Notably there were differences between the Rice et al. (2016) study and the present study that prevent them from being directly comparable. Namely the use of vertical shaft by Rice et al. (2016) to investigate heave (instead of the horizontal flume used in this study) and inclusion of an additional region in the FEM model to model the backward eroding channel - with a region of 50-fold increase in permeability (whereas this study found need for an increase in permeability at the exit even before a channel had formed). Yet, the similarity in method used is still noteworthy.

Having to always use head level measurements to compensate for the singularity at the exit is impractical, especially when a field scenario is being modelled, because piezometer data may not be available. It appears that the singularity in the Laplace equation at the exit presents a significant challenge in numerical modelling backward erosion piping and further research into how to compensate for this, without the need for head level measurements, is recommended.

10.3.3 Exit geometry effect

Outflow boundary conditions in the numerical model were altered to form the four exit geometries tested in this study. A 2-dimensional model was sufficient for the slope, plane and slots exits but the 3rd dimension was added for the circle exit.

Figure 10.9 contains output from the numerical model presented as contour plots of hydraulic head through the flume's centreline (as a long-section), for each of the four exit geometries. Streamlines were also added to indicate flow patterns. The same head difference of 206mm was applied to all exits and the permeability was set to that of Sydney Sand. Note that permeability was increased at the circle exit using the method described in the previous section but not at the other exits. Permeability was kept constant in the slope, plane and slot exits because standpipe levels were not available in these experiments to evaluate the degree of permeability increase required at the exit (standpipes were added to flumes after the slope, plane and slot experiments had been completed).

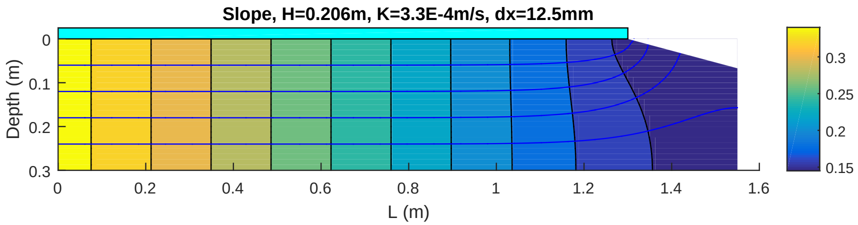

(a) Slope

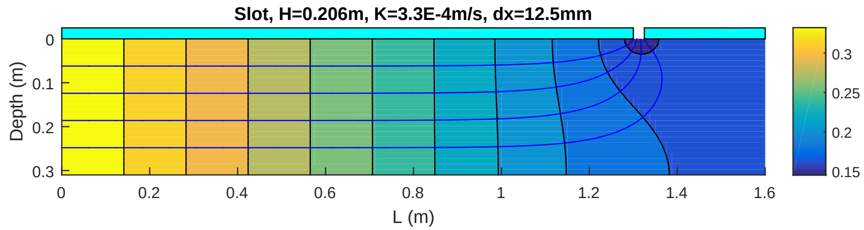

(b) Slot

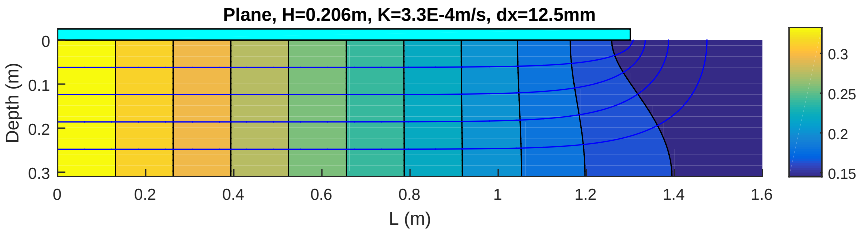

(c) Plane

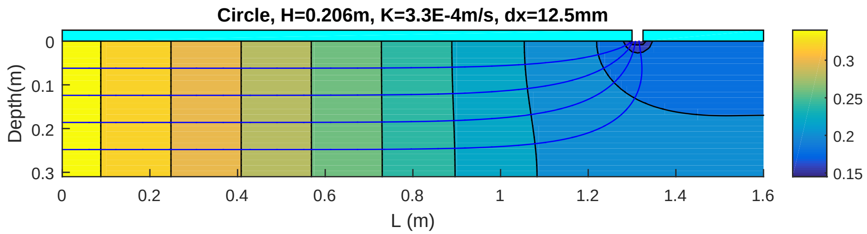

(d) Circle

Figure 10.9: Long-section view along centreline of contour plot of hydraulic head (with streamlines added) for each exit geometry (direction of flow from left to right)

Initiation gradient

Initiation is thought to occur when seepage velocity at the exit is sufficient enough to fluidise sand and transport particles out by drag force. Therefore, to investigate initiation, seepage velocities were obtained from the numerical model for each exit and are plotted in Figure 10.10 along the top centreline of the flume. These velocities were obtained from the same model runs used in Figure 10.9 (with a head difference of 206mm, a permeability of 3.3×10^{-4}m/s for Sydney Sand and permeability increased at the circle exit). Whilst permeability was increased at the circle exit when calculating local gradients, it was kept constant when calculating seepage velocity, otherwise, the correction made by increasing permeability at the exit would have been reversed, returning results to the erroneously high values affected by the singularity.

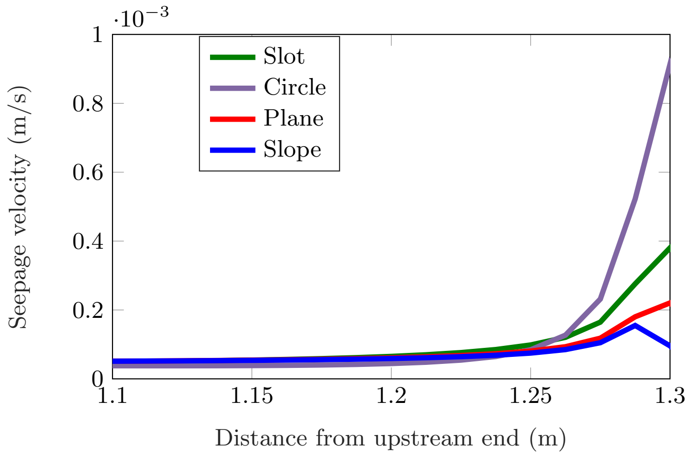

Figure 10.10: Seepage velocity along the top centreline of the flume for each exit geometry (at downstream end)

Figure 10.10 shows seepage velocity is constant through-out the flume until it approaches the exit, where it rapidly increases. It also shows exit geometries cause different maximum velocities at the exits, increasing in the order of slope, plane, slot and circle. These maximum velocities at the exits are affected by the singularity and are therefore unlikely to be absolutely correct however, they're expected to be relatively correct, demonstrating the relative impact each exit geometry has on seepage velocity, especially given each of the models were run at the same grid spacing of 12.5mm and hence equally affected by the singularity.

From the experimental results in Figure 6.12 it can be seen that the *global* gradient required to initiate a channel increased in the order of circle, slot, plane and slope. This is the opposite order of increasing seepage velocity (and *local* gradient) at the exit. Therefore, it appears that the greater the seepage velocity (and local gradient) is at the exit, the lower the global gradient required to initiate a channel.

Given initiation is thought to occur when seepage velocity at the exit is sufficient enough to fluidise sand and transport particles out, it is expected there is a minimum exit velocity which triggers initiation. If this is the case then the numerical model has explained why the exit geometry affects the global initiation gradient- because the exit geometry affects exit velocity and exit velocity triggers initiation. Or in other words, exit geometries which cause higher local gradients at the exit require lower global gradients to reach the minimum seepage velocity required to initiate a channel.

To investigate the possibility of a unique exit gradient which triggers initiation, the numerical model was rerun for each exit at their respective global initiation gradients, the result being Figure 10.11. As can be seen, all velocity profiles (except the slope profile) intersect at a velocity of 1.4×10^{-4}m/s, at a position approximately 36mm upstream of the exit. This suggests that the plane, slot and circle exits had a common velocity near the exit when they initiated and therefore, perhaps this is the unique exit velocity which triggers initiation in Sydney Sand.

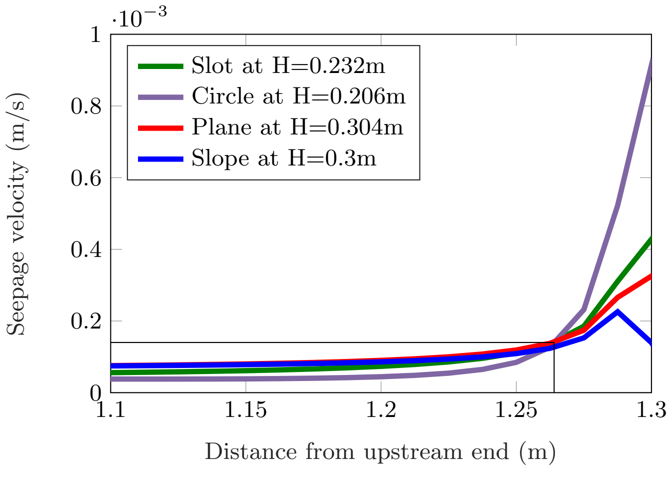

Figure 10.11: Seepage velocity along the top centreline of the flume for each exit geometry (at downstream end) at their respective initiation heads

It is recognised this point of intercept is within the singularity's zone of influence so again, its absolute value should not be relied upon. However, this method of plotting seepage velocity at each of their respective initiation heads and looking for the intercept has potential for determining the exit velocity required for initiation, if a method for compensating for the singularity and determining the exit velocity with more accuracy becomes available.

Critical gradient

From experimental results in Figure 6.12 it can be seen that the critical gradient increased in the order of circle, slot, plane and slope (the same order as the global initiation gradient).

Given the critical gradient in plane and slope exits is also the initiation gradient, the effect of exit geometry on their critical gradients has been covered in discussion on the initiation gradient above. For circle and slot exits however, their critical gradients were reached after initiation, once the channel was approximately 30% and 5% of the seepage length respectively. Therefore, to investigate the effect of exit geometry on the critical gradient in circle and slot exits, a channel was added to the numerical model.

The channel added to the numerical model was simplified to a straight channel with a constant rectangular cross-section and set to the downstream head along its full length. Experimental observations did indicate channels were more complicated than this; channels meandered and varied in cross-sectional shape/size and standpipe levels, when channels run directly beneath them, implied head in the channel was much higher than the downstream head and reduced along the channel (although it was difficult to know whether standpipe levels were measuring head in the channel alone or whether it was measuring an average across the channel and neighbouring sand). However, these simplifications still enabled *relative comparisons* of local gradients at channel tips as a result of different exit geometries.

Given the minimum grid spacing the model could accommodate before exceeding the RAM was 6.25mm and the average channel width and depth in Sydney Sand was 13mm and 2.4mm respectively, there was insufficient grid resolution to model the average channel. To work around this, the small-scale flume used by van Beek (2015) was modelled instead. This flume was only 0.35m long, 0.1m deep and 0.3m wide which meant that using the same number of grid points achieved a finer grid spacing capable of modelling the channel.

Note however that the slot exit was not tested in this small-scale flume, so this model is not a replica of actual testing, but used here for comparative purposes only.

The result of modelling this simplified channel in the van Beek (2015) small-scale flume is shown in Figures 10.12a and 10.12b as a top plan view of head contours of the circle and slot exits respectively, as well as in Figure 10.12c as a profile of the head distribution along the top centreline of the flumes. Figures 10.12a and 10.12b illustrate how the circle exit causes a higher concentration of head contours at the tip of the channel, i.e. a higher local gradient at the tip of the channel, because the downstream head is applied over the smaller area of the circle exit instead of across the full channel width as is the case with the slot exit. Figure 10.12c shows a higher local gradient (steeper head slope) at the channel tip when a circle exit is used.

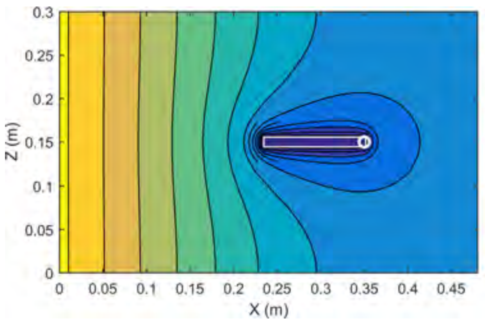

(a) Plan view of head contours- circle exit

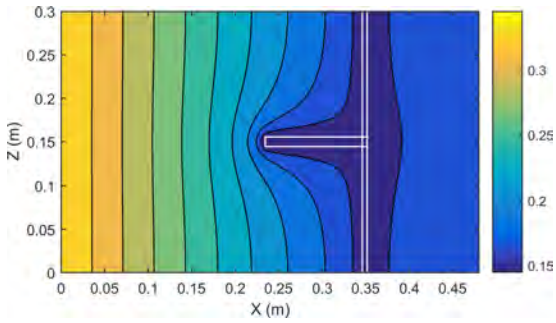

(b) Plan view of head contours- slot exit

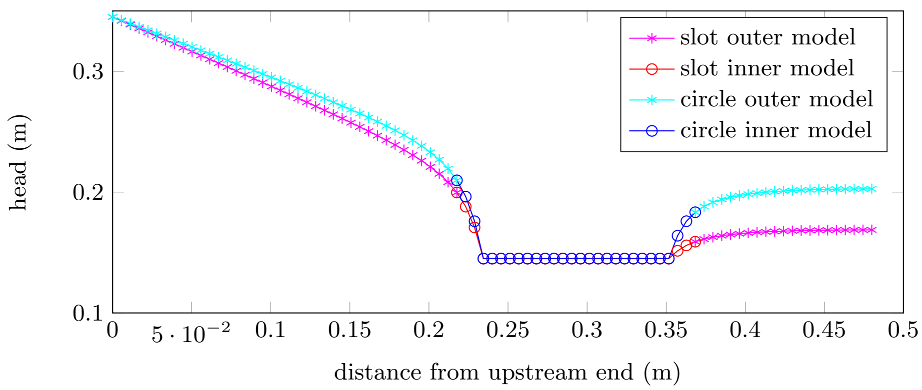

(c) Head profile along top centreline of flumes

Figure 10.12: Steeper gradient at channel tip (at approx. 0.24m) when circle exit used compared to slot exit (direction of flow from left to right and radially toward circle exit)

Therefore, the numerical model has explained why the circle and slot exits affect the global critical gradient - because the exit geometry affects the local gradient at the tip of the channel and the local gradient at the tip of the channel drives tip progression. Or in other words, because the circle exit causes a higher local gradient at the tip of the channel, it requires a lower global gradient to generate the minimum seepage velocity at the channel tip needed to maintain tip progression.

10.4 Further model development

Effort was made to further develop the model to include a more sophisticated representation of the channel by use of the Darcy-Weisbach pipe flow equation to account for friction loss along the channel. However, this time the flume used in this study had to be modelled instead of modelling the small-scale flume used by van Beek (2015), as was done above. The flume used in this study had to be modelled so that numerical results could be compared with experimental measurements such as standpipe levels, total flow and flow velocity through the channel. This meant that the issue of insufficient grid resolution had to be resolved. To do so, the model was developed to include 'nested' models whereby a domain of finer grid spacing was placed around the exit and channel and then nested inside a coarse grid spacing. This way a finer grid spacing could be used to more accurately capture the channel without the total number of grid points creating matrices too large for the computer's memory capacity (because as the fine resolution was increased the coarse resolution was decreased, keeping the same number of points). At the fine-to-coarse model interface, when there was an adjacent point on the coarse grid, central differences with variable grid spacing was used. When there wasn't an adjacent point on the coarse grid, bilinear interpolation of surrounding points was used to estimate head.

Whilst the nested model successfully executed, there was an issue with conservation of flow whereby, despite flow entering the flume matching flow entering the model interface, flow entering a rectangular control volume surrounding the exit was 17% greater. In other words, flow was 'gained' between the model interface and a control volume surrounding the exit. The cause of this discontinuity was not identified and the ambition of modelling with nested models and more sophisticated modelling of the channel was not pursued on account of time restraints and the experimental focus of the research.

It is believed a numerical model which could calculate seepage velocity into the channel tip would be valuable in understanding and predicting backward erosion piping. It would be valuable on the basis that seepage velocity into the tip is responsible for tip progression and therefore determines the critical gradient. It is expected that such a numerical model could determine the critical seepage velocity into the tip by calculating seepage velocity into the tip for both the slot and circle exits at their respective critical heads and respective critical channel lengths. If these seepage velocities are the same/similar then it is likely this is the seepage velocity required to detach particles at the channel tip. Pursuit of a numerical model which could evaluate seepage velocity into the channel tip is recommended for further research.

An additional recommendation for further research is testing all four exit geometries with standpipe levels, ideally with some closer to the exit than they were in this study, so that the degree of permeability increase at the exit required to compensate for the singularity can be determined. This ought to provide realistic exit velocities so that plots of seepage velocity at their respective initiation heads should intercept at the common exit velocity required for initiation (as was attempted in Figure 10.11).

10.5 Summary

A numerical model was written in MATLAB to investigate why the exit geometry affected the initiation and critical gradients. The model provided the distribution of hydraulic head and seepage velocities throughout the flume by approximating Darcy's Law and the Laplace equation with the finite difference method to second order accuracy.

Two-dimensional models were configured to simulate the slope, plane and slot exits and a three-dimensional model was configured to simulate a circle exit. The numerical models demonstrated that the four exit geometries caused different seepage velocities at the exit, increasing in the order of slope, plane, slot and circle. This was the reverse order of increasing gradient required to initiate a channel in experiments. Therefore, it appears that exit geometries which cause faster exit velocities require less gradient to generate the necessary erosive forces to trigger initiation.

The numerical models also demonstrated that the circle exit caused a higher gradient into the channel tip than the slot exit. Considering the critical gradient was lower in circle-exit tests than slot-exit tests, it appears that exit geometries which cause faster seepage velocities into the channel tip require less gradient to generate the necessary erosive forces to maintain tip progression.

When grid resolution was increased in the model it was found that the maximum seepage velocity at the exit also increased without convergence. This is evidence of a singularity at the exit. This singularity caused exaggerated gradients at the exit and therefore higher heads throughout the flume, as evident by a mismatch between the model and standpipe levels measured in experiments. A work-around was formulated whereby permeability at the exit was increased in the model, causing a smaller increase in flow and therefore a decrease in gradient at the exit, according to Darcy's Law. The decrease in exit gradient caused head throughout the flume to lower until the model came into alignment with standpipe levels.

Whilst this 'work-around' was successful, the continual need for such a calibration is impractical, especially when piezometer data is unavailable in field cases. Therefore, further research into how to compensate for the singularity at the exit is recommended. Also recommended is research into the possible need to still increase permeability of soil at the exit, due to sand dilation. Once reliable exit velocities can be determined, the minimum exit velocity required for initiation can be found.

Also recommended for future research is pursuit of a numerical model which can determine seepage velocities into a channel tip. This could provide the minimum seepage velocity into the channel tip required for progression and therefore provide the critical gradient.

Chapter 11

Review of existing models

11.1 Introduction and aims

This chapter contains reviews of current existing models which are used to predict critical gradients. The aim of the reviews is to assess how well the models predict experimental results (both experimental results from this study and the studies of others) so that an assessment of the strengths and weaknesses of each model can be made as well as identify any opportunities for improvement. The second aim is to then develop and offer these improvements for future industry use. Particularly improvements which come to light as a result of having tested soils not previously tested (such as internally stable, well graded soils).

The models reviewed include the Schmertmann (2000) and Sellmeijer et al. (2011) models because these are the most popular models used in industry and both provide critical gradient predictions. There are other models available, the most recent and notable including van Beek et al. (2014b) and Hoffmans (2016). The van Beek et al. (2014b) model was not reviewed because it predicts the initiation gradient only, and whilst this is important, critical gradients are more important to industry. The Hoffmans (2016) model was not reviewed because at the time of writing, it had not yet been publicly published for industry use.

11.2 Schmertmann (2000)

11.2.1 Introduction

The Schmertmann (2000) model is described in Section 2.5.6. It is considered a popular method used by industry because it is presented in the ICOLD (2015) bulletin on internal erosion and is the recommended method in the Fell et al. (2008) piping toolbox. It is also cited by Shewbridge (2016) as being a modern design method available for use when seepage can not be controlled by a landside berm.

11.2.2 Review based on original data

The basis of the Schmertmann (2000) method is a relationship between the soil's coefficient of uniformity and the local critical gradient, as plotted in Figure 2.34 and repeated over the page in Figure 11.1. Schmertmann's plot contains experimental results from a number of other studies however, only average results from across each test series were plotted. When individual test results are plotted, as done in Figure 11.1, more scatter than what was first suggested becomes apparent. In some instances, individual results were plotted at slightly different C_u's from the average plotted by Schmertmann (2000) because the source publication reports a slightly different C_u's than interpreted by Schmertmann (2000).

Robbins and Sharp (2016) recognised that plotting individual results instead of averages illustrated a spread in the results and suggested a linear regression in quantile bands for a qualitative risk approach, as shown in Figure 11.2. Although this approach requires caution because the quantile bands suggest all variability has been captured in the tests plotted, with all possible soil and geometry combinations included and a sufficient number to capture the full possible spread- which is not the case as illustrated in Figure 11.20 when additional data added lead to more spread in the data.

Once experimental results from other studies and from this study were added to the Schmertmann (2000) plot (presented and discussed below in Subsection 11.2.3), it was found that data had a log-normal distribution. Identification of this distribution provided an alternate, more robust way of characterising the spread and probability than the use

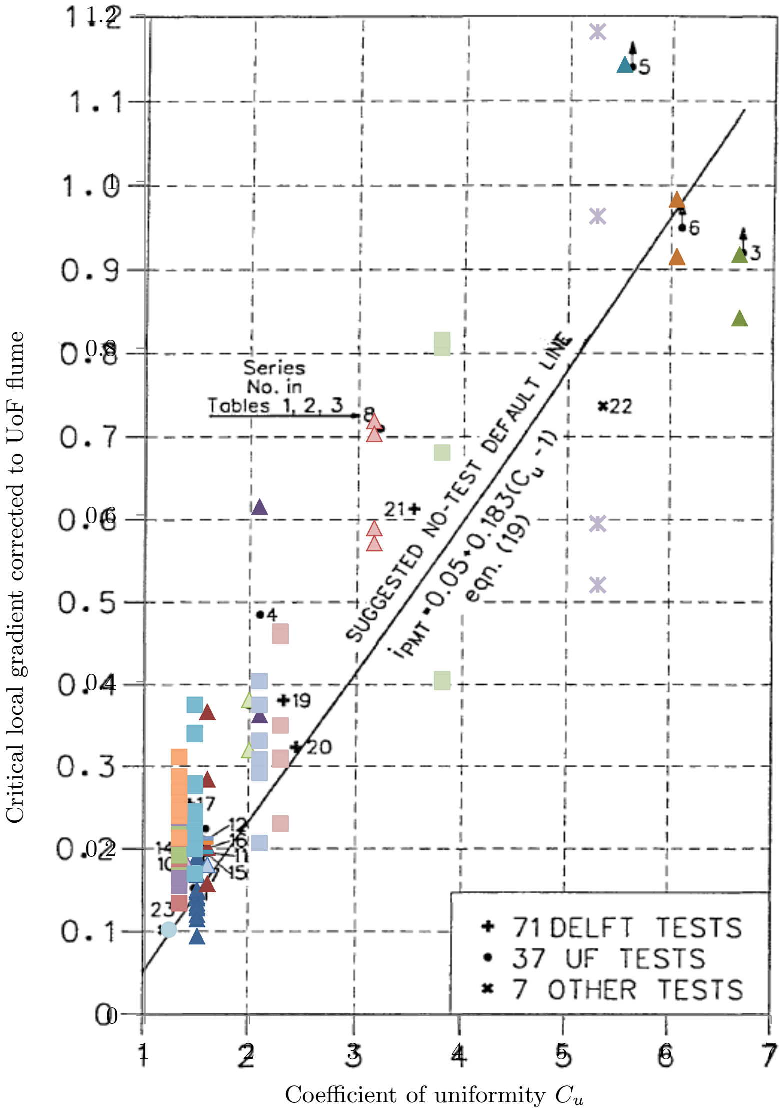

1: Townsend (1986) 2: Towsend (1986) 3: Townsend (1986) 4: Townsend (1986)
5: Townsend (1986) 6: Townsend (1986) 7: unknown 8: Schmertmann (1995)
9: Schmertmann (1995) 10: Schmertmann (1995) 11: Silvis (1991) 12: Silvis (1991)
13: Silvis (1991) 14: de Wit (1984) 15: de Wit (1984) 16: de Wit (1984)
17: de Wit (1984) 18: de Wit (1984) 19: de Wit (1984) 20: de Wit (1984)
21: de Wit (1984) 22: Kohno (1987) 23: Muller-Kirchenbauer (1993)

Figure 11.1: Schmertmann (2000) plot of critical local gradient with C_u but with individual results plotted instead of test averages

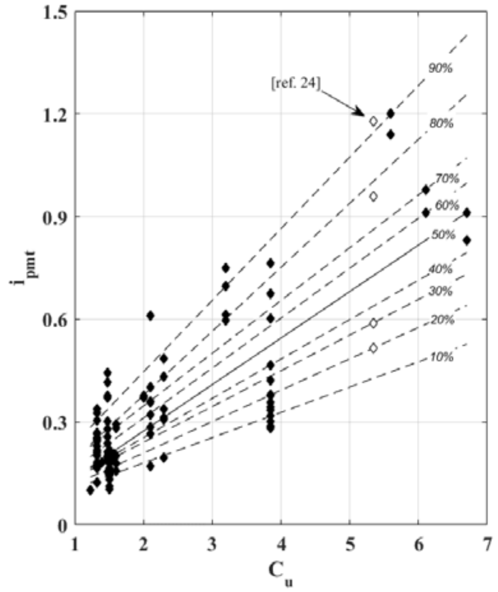

Figure 11.2: Linear regressions of critical gradients divided into quantile bands as suggested by Robbins and Sharp (2016)

of quartile's based on statistical 'bins' offered by Robbins and Sharp (2016).

The current author has concerns with including test results identified by Schmertmann (2000) as Test Series 3, 5, 6 and 22, when developing a predictive model. Test Series 3, 5 and 6 from Townsend and Shiau (1986) either did not initiate (the well graded soil of series 3 and the Gap I soil of series 5) or they could not be progressed further than about 60% of the seepage length, despite tapping on the lid (Gap II soil of series 6). Given these tests did not initiate or reach the upstream end, it is misleading to plot (and fit best-fit lines to) these results as critical gradients when they were not.

Even though the Townsend and Shiau (1986) soils did not initiate or complete, soils tested in this study, with similar uniformity coefficients (Mixes 3, 5 and 8), did initiate and complete at lower gradients. It is believed that what makes the soils tested in this study different from those tested by Townsend and Shiau (1986) is the internal stability of the soil and therefore their susceptibility to suffusion. This is believed because the soils used by Townsend and Shiau (1986) were poorly sorted with gap gradings where as the soils in this study, despite having similar C_u values, were more well graded (see particle size distributions of these soils in Figure 11.3a). The poorly sorted, gap gradings of the Townsend and Shiau (1986) soils made them more susceptible to suffusion, as indicated by plotting lower in Figure 11.3b. Note, it wasn't appropriate to plot Mix 8 on

Figure 11.3b as it contained more than 10% of non-plastic fines. Lastly, as support for this theory, Townsend and Shiau (1986) report fine sands moving through the starter channels without the tip progressing. This suggests fine sands were mobile through the matrix without backward erosion occurring.

It is thought that suffusion hinders and/or prevents backward erosion because fines, having transported downstream, cause a reduction in permeability of the soil at the downstream end. This reduction in permeability means higher heads are needed to generate the necessary erosive forces to initiate and progress the backward eroding channel. It's possible that sufficiently high heads could not be (or simply were not) applied in the laboratory or that failure by other means, under these high hydraulic loads, occurred before backward erosion could, such as sheet flow (or surface slip).

Results from Kohno et al. (1987), referred to as Test Series 22 by Schmertmann (2000), was considered dubious for four reasons:

1. the exit geometry is unlike anything else tested (see Figure 11.4);
2. description of the gradients casts doubt over their relevance (*"the value for the head of the upstream side divided by the length of the specimen <u>before</u> the experiment was begun"* (Kohno et al., 1987, pg. 66));
3. description of the failure does not sound like backward erosion of a channel (*"local failure spread like a fan and became total failure"* (Kohno et al., 1987, pg. 65)) (which sounds similar to the 'sheet failure' observed in this study in Tests 48, 54, 56 and 65); and
4. there was a large variation in results (from 0.7 to 1.6, more than 50% difference).

11.2.3 Review based on additional data

Additional experimental results were available to plot onto Schmertmann's local gradient with uniformity coefficient chart, results that either Schmertmann (2000) did not include or that have been obtained since (including results from this study). Plotting additional data gives further indication of the model's performance and possibly provides opportunity

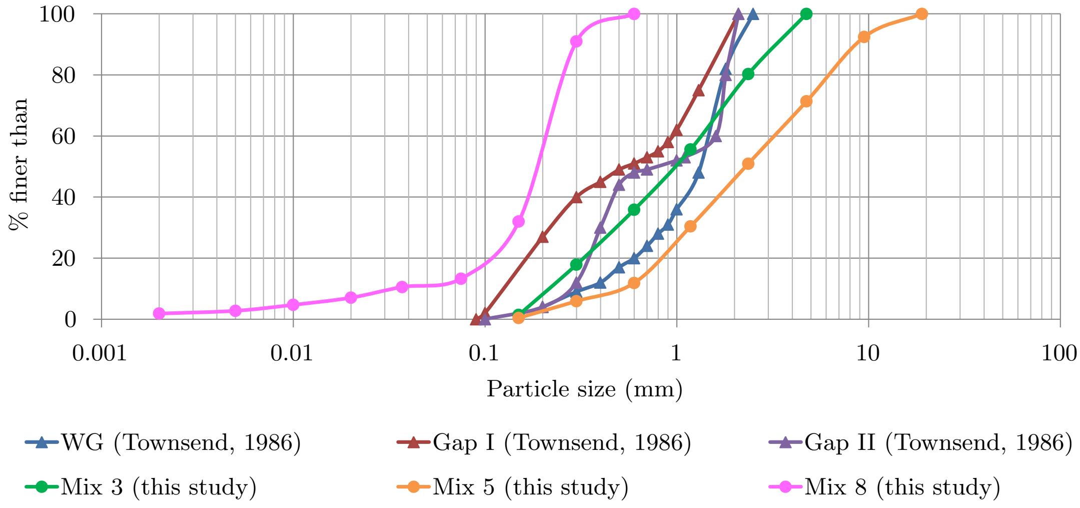

(a) Particle size distributions

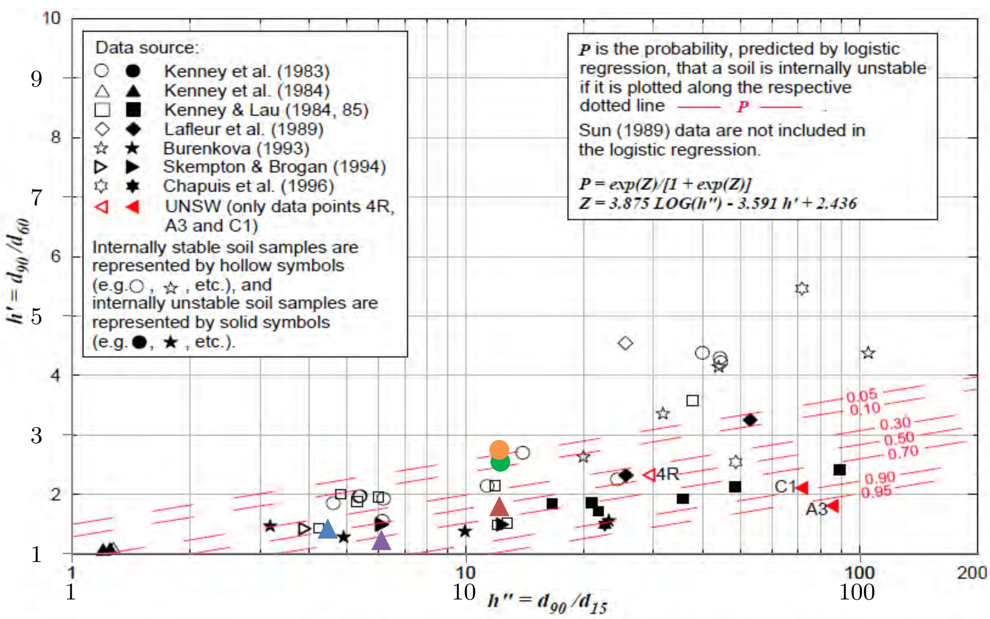

Figure 25. Contours of the probability of internal instability for sand-gravel soils with less than 10% non plastic fines passing 0.075mm (Wan and Fell 2004)

● This study Mix 3 ● This study Mix 5

▲ WG (Townsend, 1986) ▲ Gap I (Townsend, 1986)

▲ Gap II (Townsend, 1986)

(b) Probability of suffusion according to Wan and Fell (2007)

Figure 11.3: Comparing soils testing in this study with those tested by Townsend and Shiau (1986) whose C_u values were between 5.6–6.7

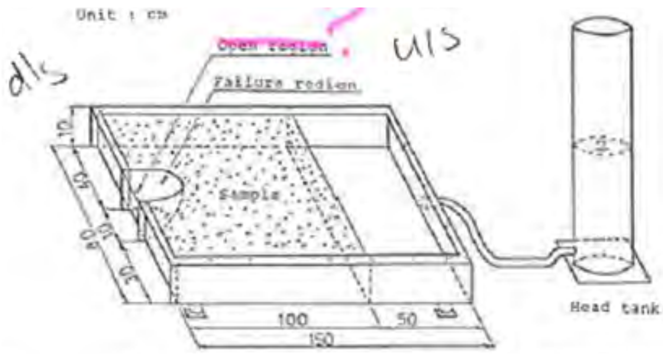

Figure 11.4: Test set-up used by Kohno et al. (1987) with an exit geometry unlike anything else tested

to update the line-of-best-fit. However, before plotting additional data, the global critical gradient observed in experiments required correction by a series of factors which would convert it into a local gradient at the channel tip which would occur in the University of Florida (UoF) flume (testing by Townsend et al. (1981); Townsend and Shiau (1986); Schmertmann (2000)).

Correction of the global critical gradient was made using Equation 11.1:

$$i_{local,UoF} = C_G i_{global} \cdot \frac{1}{C_D} \frac{1}{C_L} \frac{1}{C_S} \frac{1}{C_\gamma} \tag{11.1}$$

where $i_{local,UoF}$ = local gradient at channel tip, in UoF flume, when critical global gradient required. Referred to as i_{pmt} in Schmertmann (2000)

C_G = gradient factor for parallel flow

i_{global} = critical global gradient in laboratory test, referred to as $\overline{i_{pmt}}$ in Schmertmann (2000)

C_D = depth/length factor

C_L = length factor

C_S = grain size factor

C_γ = density factor

These factors were taken from the numerator of Equation 2.18. C_K was not used because it was assumed the test soil was isotropic and C_Z was not used because there was no underlayer (i.e. the base of the flume was impermeable). Additionally, C_α was not used because the channel was horizontal.

The reciprocals of each factor (apart from C_G) were used because the correction factors were designed to convert the local gradient from the gradient expected in the UoF flume to the gradient expected in the field or experiment. When converting in reverse, i.e. from the gradient in the field or experiment to the gradient expected in the UoF flume, the reciprocal was needed. These reciprocals were used by Schmertmann (2000) however it's not made clear. For example, the equation for C_D in his equation 5 is actually the reciprocal and whilst the equation for C_L in his equation 11 is correct, when C_L is calculated in his Tables 1 to 3, they are in fact the reciprocals of C_L, despite not being identified as such.

Each of these factors are considered in turn below. Following on from this is a review of the model once the factors are combined.

Gradient factor for parallel flow, C_G

The gradient factor for parallel flow: C_G, is the ratio of the local gradient where the channel tip would be once the channel reaches its critical length to the global critical gradient, whereby $C_G = i_{local}/i_{global}$. The local gradient where the channel tip would be is calculated using 2D flownets which are drawn/modelled without a channel because Schmertmann (2000) assumes that local gradients present before the channel exists can be used to predict backward erosion.

Once the C_G factor is calculated for a given geometry (i.e. depth to length ratio and exit geometry), it is used to convert any critical global gradient into the equivalent local gradient where the tip was (or expected to be) when maximum head was (or expected to be) needed (but the local gradient before the channel was present). Given the C_G factor quantifies the influence exit geometry has on local gradients, the C_G factor incorporates the effect of the exit geometry into the model.

When Schmertmann (2000) explained the function of the C_G factor he stated it is used *"to correct the global maximum piping test gradient to the appropriate point value when ipt reaches its maximum value (typically when l/L = 30-50% in the Delft tests, 20% in the UF tests)"* (Schmertmann, 2000, pg. 16). However, it is believed there is an error in this statement. It should have read "when ipt reaches its *minimum* value" because maximum head is needed when local gradient (i.e. seepage velocity) is at its minimum.

Minimum local gradients (and therefore C_G factors) were determined for the flumes and exit geometries used in this study using the numerical model described in Chapter 10. Output from the numerical model is shown in Figure 11.5 as local gradient with distance from the upstream end. This output shows local gradients decreased from the exits until they reached their minimum values of 0.92 at 37% of the seepage length (L) from the slope exit, 0.9 at 26%L from the plane exit and 0.83 at 30%L from the slot exit. As the upstream head was chosen to result in a global gradient of 1, the minimum local gradient = C_G. Therefore C_G factors were found to be 0.92, 0.90, 0.83 and 0.83 for the slope, plane, slot and circle exits respectively. The same C_G value was used for both the slot and circle exits because the circle exit was modelled as a slot to keep with the 2D simplification used by Schmertmann (2000).

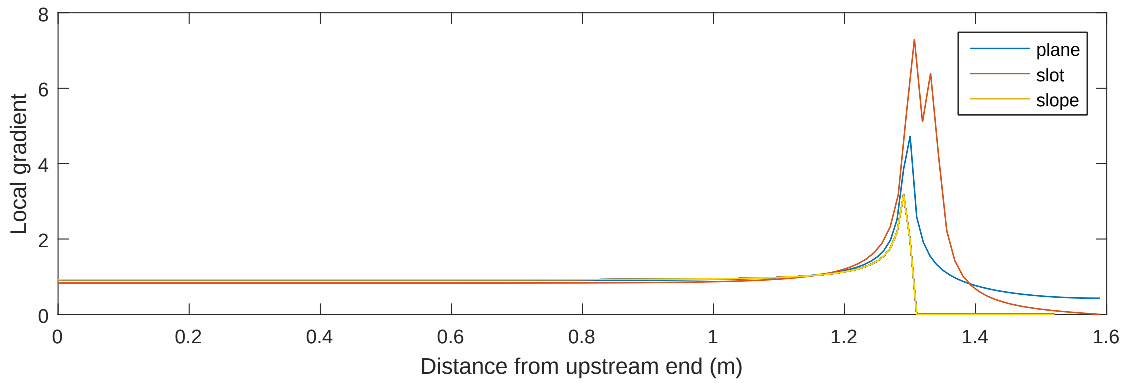

Figure 11.5: Local gradient along top centreline of flume used in this study showing where local gradients reach their minimum (exits at 1.3m)

When the circle exit was modelled in its true 3D configuration (using the 3D model described in Chapter 10), the minimum local gradient was found to be 35% of the global gradient, i.e. $C_G = 0.35$. This drastically reduced critical local gradients and plotted well below the $i_{pmt} = 0.05 + 0.183(C_u - 1)$ line in the Schmertmann (2000) model, suggesting the model is incompatible with 3D exit geometries.

However, it was noticed that this 3D model produced a head profile significantly higher than standpipe levels measured in experiments. This suggested the local gradient at the exit wasn't as high as the model calculated. This erroneously high gradient at the exit is likely to be due to the singularity at the exit which has an infinitely large gradient due to a discontinuity in the Laplace equation at this point. To compensate, permeability at the exit was systematically increased until the head profile lowered and aligned with standpipes levels. This observation and method is presented in Subsection 10.3.2.

When the calibrated 3D model with increased permeability at the exit was used, the minimum local gradient (and therefore the C_G factor) came out to be equivalent to the C_G factor found using the 2D slot model of 0.83. Yet, in reality, minimum local gradients caused by the slot and circle exits would not be the same, the circle exit would still concentrate flow and cause locally higher gradients at the exit than the slot would.

It is likely the 2D slot model was not as accurate as it could be because it too would have been affected by the singularity at the exit. As would the slope and plane exits. Compensation for the singularity at the exit could not be made like it was for the circle exit because flume lids configured with the slot, plane and slope exits were not equipped with standpipes (only circle-exit-lids were equipped with standpipes). Investigating this is suggested for further research.

In conclusion, an identical C_G found using the 2D slot model and the 3D calibrated circle model casts doubt over the accuracy of the minimum local gradient (and therefore the C_G factor) for the slot exit. By extension, this also cast doubt over the C_G factors calculated for plane and slope exits. It is unlikely Schmertmann (2000) encountered the issue of the singularity at the exit because local gradients were obtained with hand-drawn flownets. Of the numerical modelling that Schmertmann (2000) did use (by Wong in Townsend et al. (1981)), it demonstrated agreement between numerically obtained head levels and standpipe levels, suggesting the singularity was not an issue however, this was only in a slope exit in which the effect of the singularity is expected to be at its minimum.

In practice, when calculating the factor of safety against piping for dams and levees in the field, piezometer levels may not be available to calibrate a seepage model with and correct for the singularity at the exit. This uncertainty would need to be taken into account when deciding on an appropriate factor of safety.

Given that C_G was designed to compensate for differences in local gradients due to different exit geometries, accuracy/effectiveness of the C_G factor was assessed by comparing model predictions with experimental results across the four different exit geometries. Comparisons were restricted to tests in Sydney Sand in order to isolate variations due to different soils. This is done in Figure 11.6.

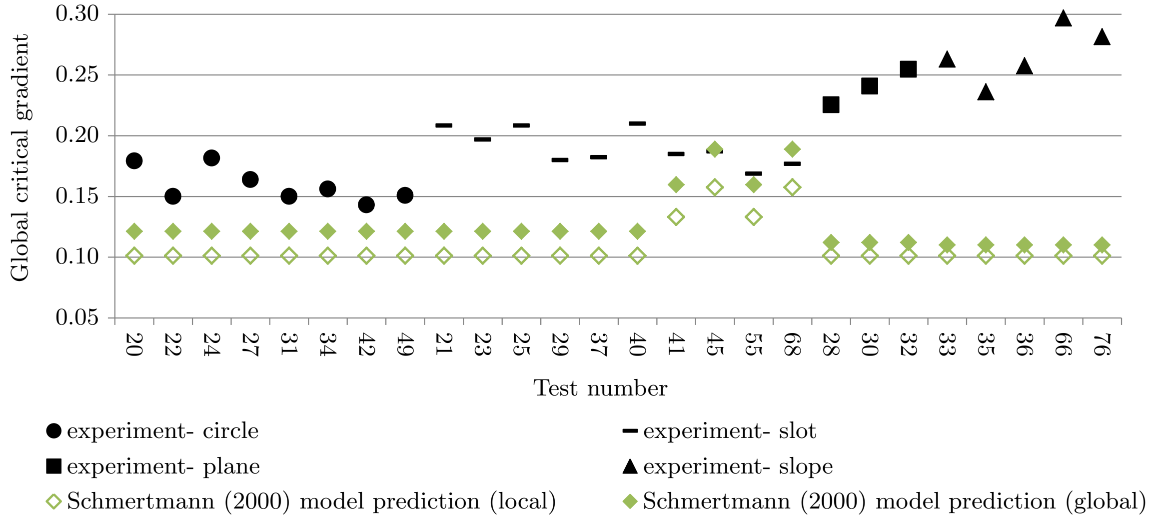

Figure 11.6: Sydney Sand tests from this study across all exit geometries showing inability of C_G factor to model exit-effect

Note that when the local critical gradient prediction was factored to give the global critical gradient, the reciprocal of C_G was required (because $C_G = i_{local}/i_{global}$). Schmertmann (2000) made no mention of using the reciprocal of C_G to convert the local $i_{pmt} = 0.05 + 0.183(C_u - 1)$ prediction into a global one. It's possible this is an oversight of Schmertmann's unless the assumption was made that only local gradients were used to determine factors of safety and conversion into global gradients were not needed.

If one were to assume the local critical gradient predictions for seepage lengths of 1.3m were correct (L=1.3m in all tests except 41, 45, 55 and 68), it can be seen that the C_G factors were not large enough to increase predictions up to global critical gradients observed in experiments. It can also be seen that plane and slope global critical gradient predictions were *less than* slot global critical gradient predictions, not greater than as observed in experiments. Therefore, the C_G factors were unable to model both the changes in magnitude and the order of increasing global gradients due to exit geometries.

Some possible causes for inaccuracy of the C_G factor have already been explained including the effect of the singularity at exit on local gradients nearby and compensating for the singularity in the circle exit (by increasing permeability at the exit) but not in the other exits. Another possible cause for inaccuracy of the C_G factor for plane and slope exits is the local gradient used in the C_G ratio should not be taken as the minimum pre-pipe gradient at about 30% of the seepage length, as Schmertmann (2000) did, because the critical global gradient was not required at this point. The critical global gradient was required at initiation, when the channel was first forming. Therefore the local gradient in the C_G ratio should be taken as the exit gradient.

Schmertmann (2000) did not appear to recognise that some of the data he used experienced critical global gradient at the exit. Namely, the de Wit (1984) plane-exit tests (Schmertmann Test Series 14–21). However it is believed Schmertmann (2000) used the local gradient 30% from the exit to calculate C_G for these tests (pre-channel gradients).

The University of Florida testing (Townsend et al., 1981, 1988) used by Schmertmann (2000), identified as Test series 1–10, were carried out in slope exits. Hence it would be expected that these tests also required exit gradients to be used in the CG calculations. However, Schmertmann (2000) reports to use local gradients at 20% of the seepage length away from the exit. Mention of the critical global gradient being required at 20% of the seepage length away from the exit was not reported in (Townsend et al., 1981, 1988), so it is unclear why Schmertmann (2000) used the local gradient at this position. It is possible this position roughly aligned with the tip of the starter channel used in these experiments. This would coincide with where the current author would expect the maximum head difference would have been required. However, starter channels varied in length ranging from 10% to 50% of the seepage length (Townsend et al., 1988). In any case, the gradient required to progress the tip of the starter channel was not the critical gradient. The starter channel would have concentrated flows into the channel and hence required less head difference than if the starter channel had not been there.

The exit gradient was the maximum gradient, in the pre-channel state. This appears to contradict what was said previously, that the maximum head is needed when local gradient (seepage vel) is at its minimum. However, once a channel forms, flow is concentrated toward the channel, generating higher gradients at the tip of the channel than the original exit gradient. Therefore, the initial pre-channel exit gradient was indeed the minimum local gradient experienced. This is why the maximum head difference was needed at initiation and can then be continuously lowered, without stopping channel progression, in slope (and presumably plane) exits.

Logically this leads to the conclusion that the channel must concentrate flow in plane and slope exits more than the exit does, which is why it's initiation-dominated, when flow concentration is at its minimum at the exit. Conversely, slot and circle exits must concentrate flow more than the channel does, which is why it's progression-dominated, when flow concentration is at its minimum at the channel tip.

Evidence in support of this is Figure 11.7. Assuming head difference required is inversely proportional to the local gradient at either the exit or channel tip, Figure 11.7 demonstrates that higher heads are needed at initiation in slope (and presumably plane) exits (where the exit gradient <tip gradient) and at 10-30% of the seepage length away from the exit in slot and circle exits (where the tip gradient < exit gradient). Note: no plane test are plotted in Figure 11.7 because the head was not reduced in any plane tests (it was only kept constant).

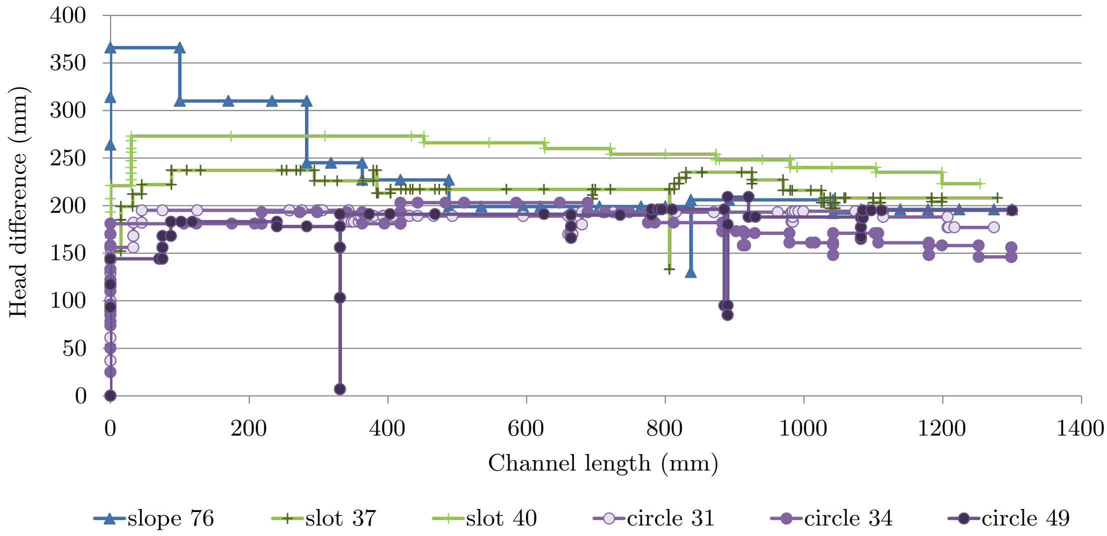

Figure 11.7: Sydney Sand tests from this study in which the head difference was lowered

Ideally C_G factors for plane and slope exits would be recalculated using the exit gradient, where the maximum head difference is required. However, determining the exit gradient is problematic on account of the near-singular anomaly at the exit. The singularity causes erroneously high exit gradients and are a function of grid spacing, yet there is little guidance within the literature on how to compensate for this in a standardised and theoretically-based manner (Olsen et al., 2014). An account of the limited guidance in literature is given in Subsection 10.3.1.

The current author used the numerical model described in Chapter 10 to determine at what distance from the exit, local gradient profiles, calculated using three different grid spacings, began to align.

The local gradient at which gradient profiles began to align was adopted as the local gradient at the exit. The idea being, when profiles began to align they were far enough away from the exit to be less affected by the singularity but still relatively close to the exit, around 20mm away in this case. Figure 11.8 is an example of local gradient profiles of the de Wit (1984) flume with a plane exit and for a 1.2m long seepage length. It can be seen that gradient profiles began to align at a gradient of around 4, which was adopted as the exit gradient.

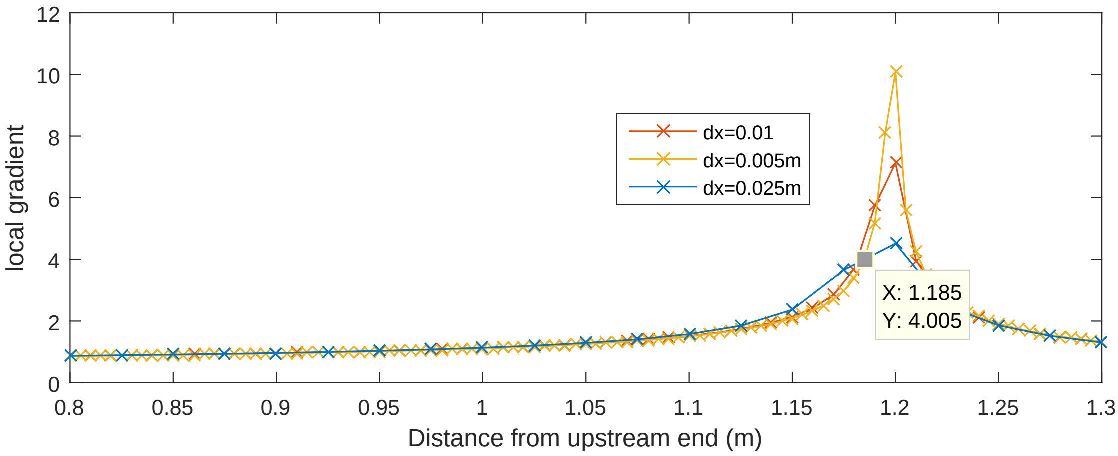

Figure 11.8: Local gradient along top centreline of de Wit (1984) flume with plane exit and 1.2m seepage length. Shows local gradient chosen where profiles begin to diverge. Note global gradient = 1.

Using this method, C_G for seepage lengths 1.2m–4.5m from de Wit (1984) (Schmertmann (2000) test series numbers 14-16) increased approximately 5 fold from 0.8–0.89 to 3.8–5.5 and the C_G for seepage length 0.8m from de Wit (1984) (Schmertmann (2000) test series numbers 17-21) increased approximately 4 fold from 0.775 to 3.

Using these revised C_G values, local critical gradients drastically increase as shown in Figure 11.9. The spread also increases as a C_G >1 amplifies experimental variability. C_G will always be >1 when exit gradients are used because local exit gradients >global gradients.

Therefore, it appears the Schmertmann (2000) model and its line of conservative fit $i_{pmt} = 0.05 + 0.183(C_u - 1)$, only works when C_G is calculated using the pre-channel minimum local gradient (and when C_G <1). Yet this pre-channel, minimum local gradient does not coincide with the critical global gradient in slope and plane exits and so is therefore of little/no significance.

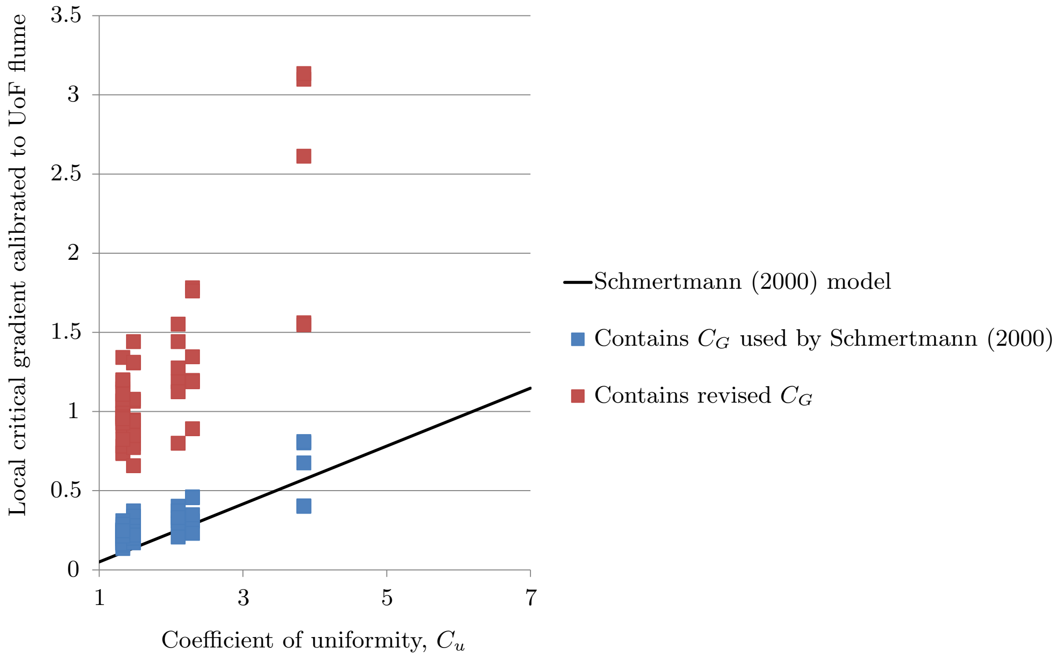

Figure 11.9: Plane-exit tests used by Schmertmann (2000) showing impact of using revised C_G factor

As a final indication of the value the C_G factor adds to the Schmertmann (2000) model, the coefficient of determination (R^2), was calculated for both before and after the C_G factor was applied (but in both cases applying C_L and C_D). For the C_G factor to be worthwhile it would need to increase R^2, which it did marginally. R^2 before the C_G factor was applied was 0.52 and after it was applied it increased to 0.58.

In order to review the performance of the model, using it as intended by Schmertmann (2000), C_G values calculated using the minimum local gradient in 2D models were used throughout the remainder of this subsection.

Depth/length factor, C_D

The depth/length factor, C_D, corrects for the effect of depth whereby depth is inversely related to critical gradient. To investigate whether the critical gradient is indeed inversely proportional to depth, the uncorrected critical gradient against flume depth was plotted in Figure 11.10 using experiments which were the same apart from flume depth by de Wit (1984). These experiments also differed in flume length because de Wit (1984) sought to scale all dimensions and keep the D/L ratio constant.

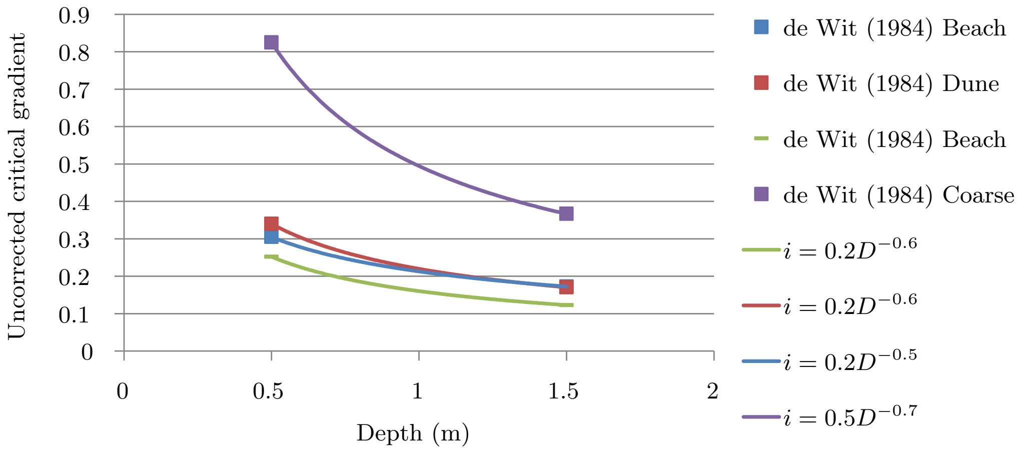

Figure 11.10: Uncorrected critical gradient against depth for experiments which were the same apart from flume depth (also varied in flume length so D/L remained constant at 0.625)

Figure 11.10 verifies the critical gradient is indeed inversely proportional to depth. This makes sense because a deeper foundation would result in more flow and higher gradients into the channel and its tip which therefore requires less global head difference to generate the erosive forces needed.

Best-fit curves in Figure 11.10 were fitted using a power equation because it is expected that the relationship ought to follow this trend whereby the critical gradient becomes infinitely large for infinitely shallow depths and whereby the critical gradient asymptotes to a constant value for deep depths.

Schmertmann (2000) expresses depth as a depth to length ratio and uses this to calculate C_D with. It is not clear why this was done and why C_D was determined based on the D/L ratio instead of depth alone. Especially when tests of constant depth but varying seepage length indicate no change in critical gradient as shown in Figure 7.8 (and repeated in Figure 11.13) (which includes results from both this study and de Wit (1984)). No change in critical gradient across various lengths suggests length does not effect the critical gradient and C_D need not be determined based on the ratio of D/L.

Schmertmann (2000) makes use of Sellmeijer's depth to length correction factor which Schmertmann (2000) reports to be $W = (D/L)^{\left[\frac{2}{(D/L)^{y}-1}\right]}$. Schmertmann (2000) then applies his theory that the horizontal gradient needed to progress the channel tip depends on the vertical gradient at the tip and, for all else being equal, increasing D/L increases

i_{vert}, which proportionally decreases the horizontal gradient needed for tip progression. Schmertmann (2000) expresses the change in D/L and i_{vert} relative to those found in the University of Florida (UoF) flume (in which D/L=0.2), such that:

$$C_D = -\frac{i_{p,UoF}}{i_p} = \frac{i_{vert}}{i_{vert,UoF}} = \frac{W}{W_{UoF}} \tag{11.2}$$

Note that Equation 11.2 has been inverted from Schmertmann's equation 5 so it is in the form to convert the gradient expected in the UoF flume to the gradient expected in the field or experiment.

Equation 11.2 is plotted in Figure 11.11 although it was noticed that when the equation for W was used it did not produce the same curve. Furthermore, Sellmeijer (2006) gave the equation for W as $W = (D/L)^{\left[\frac{0.28}{(D/L)^{2.8}-1}\right]}$. Therefore, it is believed the equation for W given by Schmertmann (2000) contains a typographical error and ought to be:

$$W = (D/L)^{\left[\frac{y}{(D/L)^{2}-1}\right]} \tag{11.3}$$

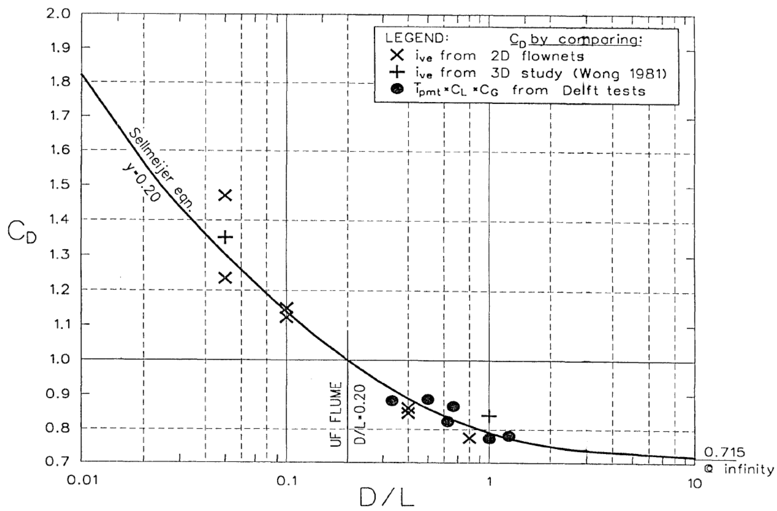

Figure 11.11: The Schmertmann (2000) curve for C_D with respect to D/L

Schmertmann (2000) plots data onto Figure 11.11 and varies 'y' in Equation 11.3 until a fit is achieved, which is reported to be achieved when y=0.2. When Schmertmann (2000) plotted data onto Figure 11.11, he used three different methods. The first method involved use of the 3D study by Wong (in Townsend et al., 1981) to estimate the vertical gradient at the channel tip in the UoF flume and find vertical gradient ratios for the geometries Wong investigated. The second method used hand-drawn longitudinal and transverse-section 2D flownets to approximate 3D conditions and obtained i_{vert} ratios in other geometries. The third method involved back-calculating C_D for tests carried out by de Wit (1984); Silvis (1991). These tests were in similar sands but different D/L ratios. Schmertmann (2000) concluded that three methods of calculating C_D generally agreed, thereby verifying applicability of Figure 11.11.

To assess the suitability/performance of the C_D factor, all experimental results were used to back-calculate the C_D factor using Equation 11.1. In other words, the C_D factor required to bring model predictions in-line with experimental results were calculated. These back-calculated C_D factors are plotted onto Figure 11.12.

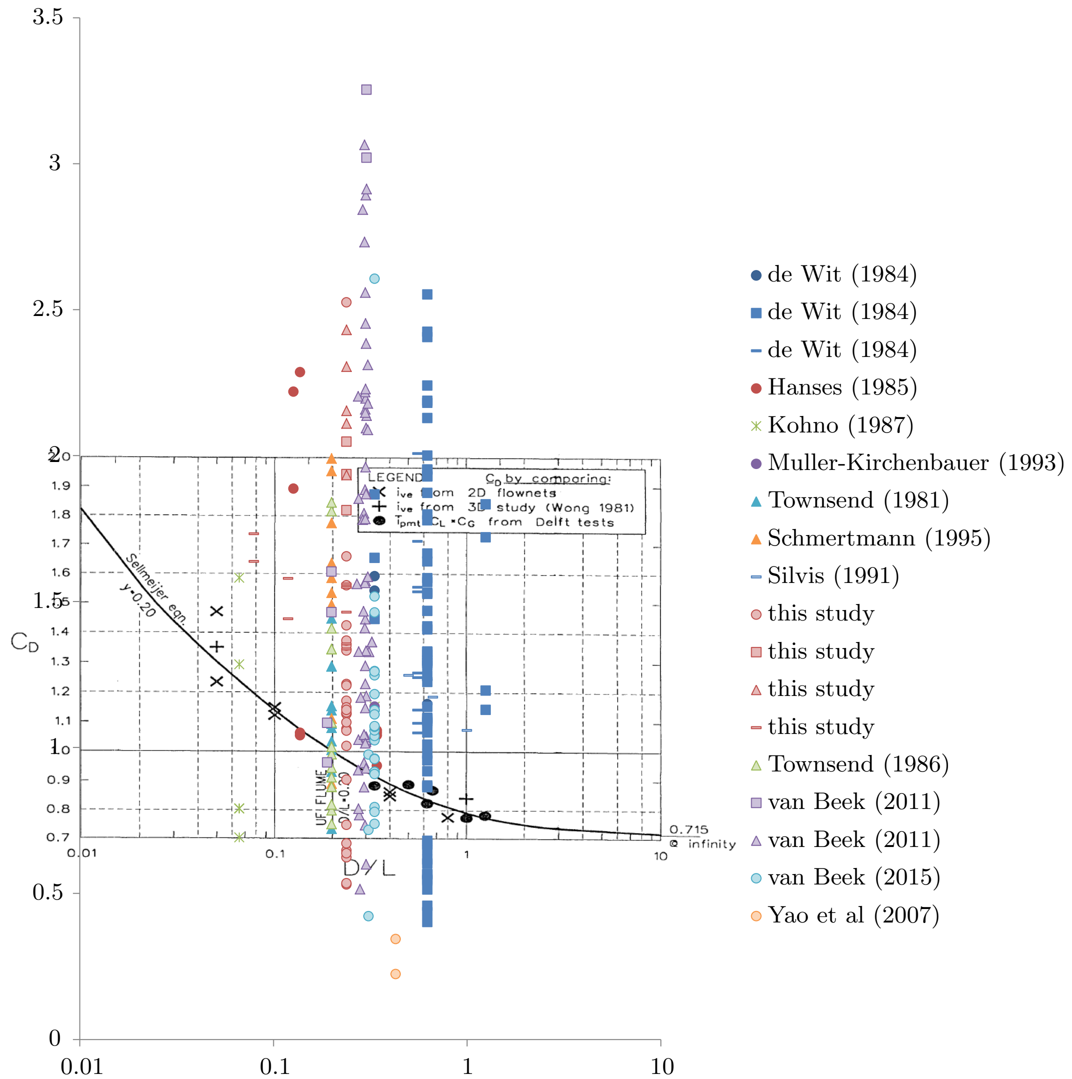

Figure 11.12: Back-calculated C_D factors plotted over the C_D curve suggested by Schmertmann (2000)

Clearly, the back-calculated C_D factors do not match the C_D curve. This suggests the C_D curve is either inappropriate or incorrect. However, the back-calculated C_D factors include other factors and so all error may not be due to inaccuracy of the C_D curve alone.

As a final indication of the value the C_D factor adds to the Schmertmann (2000) model, the coefficient of determination (R^2), was calculated for both before and after the C_D factor was applied (but in both cases applying C_G and C_L). For the C_D factor to be worthwhile it would need to increase R^2, however it did not. R^2 before the C_D factor was applied was 0.68 and after it was applied it decreased marginally to 0.64.

Length factor, C_L

The length factor, C_L compensates for the effect of seepage length however, experimental findings from both this study and the studies of de Wit (1984) and Silvis (1991) indicate that critical gradient is independent of seepage length (as shown in Figure 11.13). This suggests seepage length has no effect of seepage length and a correction factor for seepage length is not required.

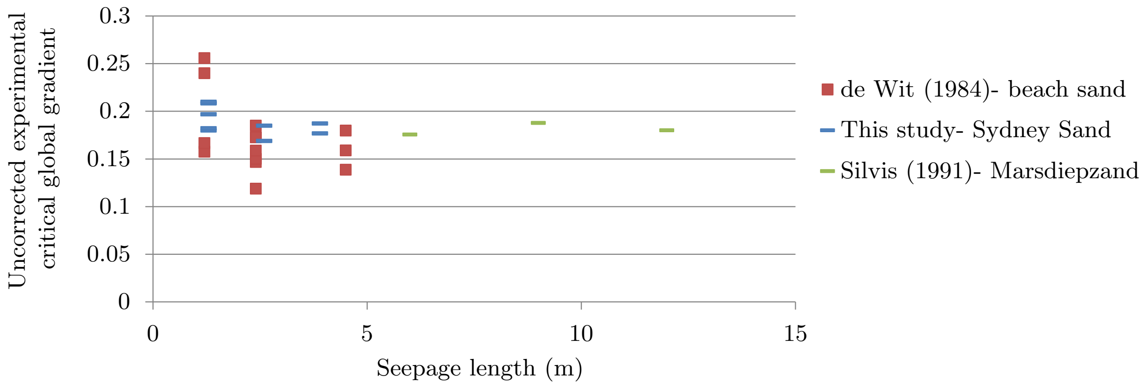

Figure 11.13: Tests carried out in flumes of the same depth but across different seepage lengths showing independence between gradient and seepage length

As evidence for the need for the C_L factor, Schmertmann (2000) points to Figure 11.14 which shows that the case where both L and D increases whilst keeping D/L constant, so no correction is provided by the C_D factor, yet the gradient still decreases. Yet, the only reason Figure 11.14 points to the need for a length correction factor is because C_D is included and C_D incorporates D/L, so the effect of length is 'linked' to effect of depth (and depth does need correcting for). This means that whilst it's been suggested a correction for seepage length is not needed, it is still needed whilst C_D is a function of D/L. If C_D were to be amended to a function of D only, then C_L could be omitted.

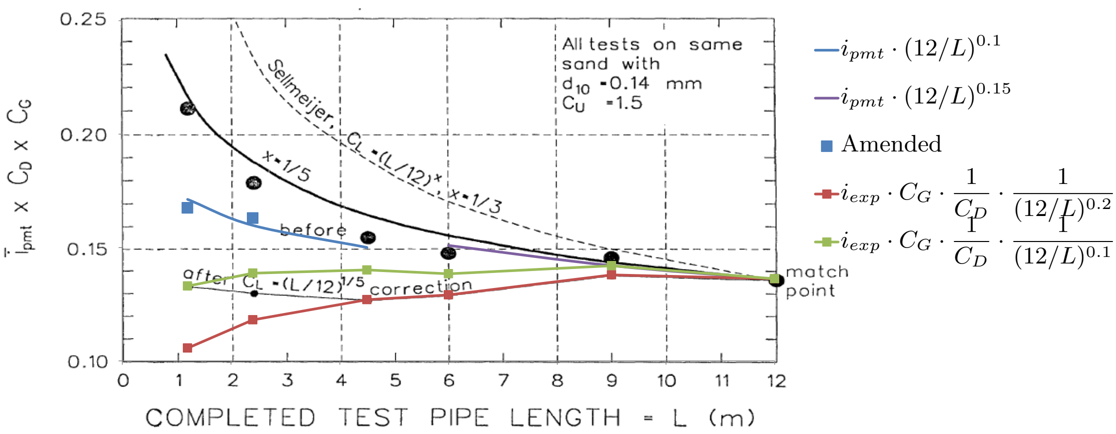

(a) Amended data points added and corrected gradients with exponent of 0.2 suggested by Schmertmann (2000) and newly suggested exponent of 0.1 ($C_u = 1.47$ for all soils)

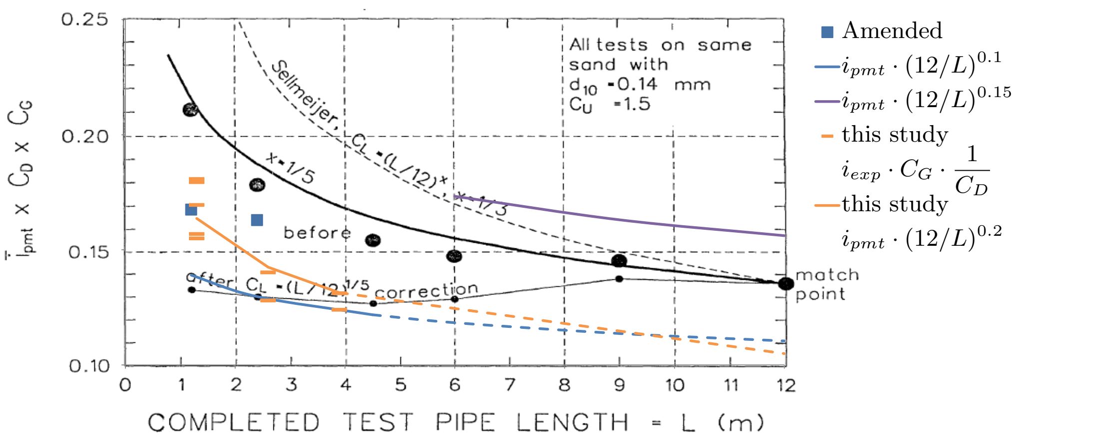

(b) Newly fitted model curves with exponents of 0.1 and 0.15 but evaluated using true uniformity coefficients for beach sand of 1.33 (blue line) and for Marsdiepzand of 1.58 (purple line)

Figure 11.14: Evidence used by Schmertmann (2000) to indicate need for C_L and change in exponent from $1/3$ to $1/5$ with amendments added

Schmertmann (2000) starts with the Sellmeijer (1988) theory that the global critical gradient varies inversely with $L^{1/3}$ but plots data in Figure 11.14 to demonstrate an exponent of 1/5 matches the data more closely. The data plotted in Figure 11.14 are from de Wit (1984) and Silvis (1991) (Schmertmann test series 13–16) which are test series with a fixed flume depth but variable seepage length.

From this, Schmertmann (2000) defines the length factor to be:

$$C_L = (L_t/L_f)^{0.2} \tag{11.4}$$

where L_t is the seepage length in the University of Florida testing (1.524m) and L_f is the seepage length being considered.

To assess performance/accuracy of the C_L factor, C_L factors which brought model predictions in-line with experimental results were back-calculated and plotted onto Figure 11.15. Only experiments which were equivalent in all ways except seepage length were considered. Figure 11.15 shows that whilst all C_L factors did plot above the curve (instead of the ideal over the curve), they did follow the same trend suggested by the C_L equation, suggesting the C_L factor is somewhat successful. All C_L factors plotting above the curve may have been due to an error(s) in the C_G or C_D factors (as they were included in the back-calculation).

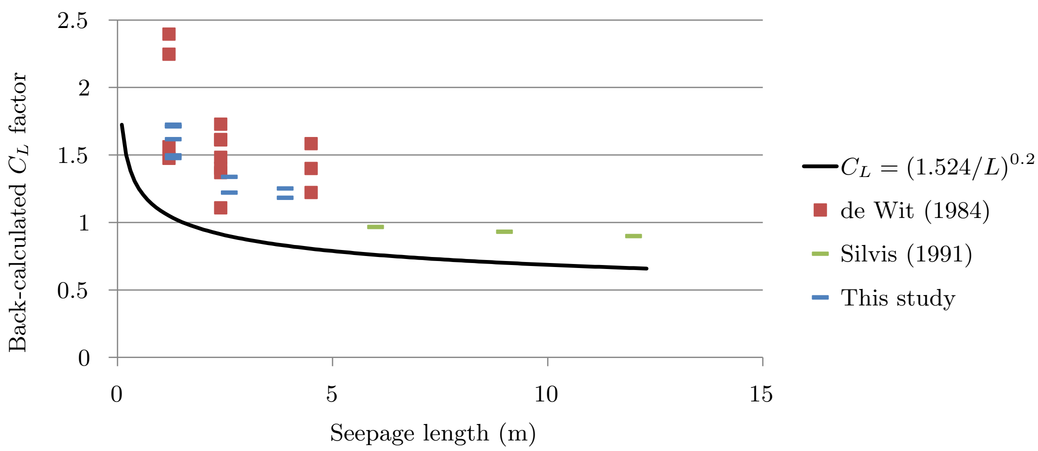

Figure 11.15: Back-calculated C_L factors and suggested C_L factor equation

As a final indication of the value the C_L factor adds to the Schmertmann (2000) model, the coefficient of determination (R^2), was calculated for both before and after the C_L factor was applied (but in both cases applying C_G and C_D). For the C_L factor to be worthwhile it would need to increase R^2, which it did. R^2 before the C_L factor was applied was 0.51 and after it was applied it increased to 0.64.

A possible improvement to Equation 11.4 came to light when Figure 11.14 was considered in more detail. In Figure 11.14 the data point at a seepage length of 2.4m was incorrect.

It appears Schmertmann (2000) was either provided or calculated an incorrect average test result. Schmertmann (2000) had the average test result as 0.174 however, data from van Beek (2015) equates to an average of 0.158. Therefore, this data point was lowered to the position indicated by the blue data point in Figure 11.14. The data point at a seepage length of 1.2m was an average of 4 tests results, two of which were on average 53% greater than the other two. It is unlikely this difference was due to experimental variability alone, and the two higher gradients look to be outliers in Figure 11.13, therefore it is more likely the lower two were more reliable than the higher points and there was an issue with tests resulting in the higher gradients. Therefore, the top two gradients were disregarded and the average of the lower two gradients was added to Figure 11.14 as the other blue data point.

With these two data points lowered, increase in gradients with decreasing seepage length was less pronounced. When C_L was applied to the newly revised averages, using the exponent suggested by Schmertmann (2000) of $1/5$, corrected gradients were no longer constant but decreased with decreasing seepage length, as indicated by the red line on Figure 11.14. Yet, corrected gradients ought to be constant if they are to be predicted by $i_{local,UoF} = 0.05 + 0.183(C_u - 1)$.

For corrected gradients to be near-constant across L, an exponent of 0.1 for the de Wit (1984) results and of 0.15 for the Silvis (1991) results were required. Model calculations using these exponents were shown by the blue and purple lines on Figure 11.14. When an exponent of 0.1 in the C_L factor was used to corrected experimental gradients, the gradients became near-contant as indicated by the green line on Figure 11.14. Yet before recommending a revised exponent, the coefficient of determination (R^2) was calculated across all experimental results using the new exponent. It was found that R^2 was higher when the 0.2 exponent suggested by Schmertmann (2000) was used at 0.64 than when the 0.1 exponent suggested by Figure 11.14 was used at 0.59. Therefore, it appeared that changing the exponent to 0.1 was not worthwhile.

Schmertmann (2000) states that all data in Figure 11.14 was the same soil with $d_{10} = 0.14$mm and $C_u = 1.5$ however, listings of both the de Wit (1984) and Silvis (1991) results in van Beek (2015) suggest otherwise. Soil tested by de Wit (1984) in the 1.2, 2.4 and 4.5m seepage lengths were carried out in Beach sand with $C_u = 1.33$ and soil tested by Silvis (1991) in the 6, 9 and 12m seepage lengths were Marsdiepzand with $C_u = 1.58$. When $i_{local,UoF}$ (or i_{pmt}) was based on the true uniformity values, the model curves shifted up and down to the blue and purple lines shown in Figure 11.14b. However, assuming the relationship between seepage length and the critical gradient remains the same across all C_u values, then it is the shape of the curve (i.e. the exponent) which is more important than the lateral placement of the curve.

Also added to Figure 11.14b are results from this study using the slot exit in Sydney Sand across the 3 different seepage lengths of 1.3, 2.6 and 3.9m. Interestingly, the exponent of 0.2 in C_L matched the data from this study more closely than the 0.1 which matched the de Wit (1984) data. This was another reason to stick with the 0.2 exponent suggested by Schmertmann (2000).

Grain size factor, C_S

The grain size factor, C_S compensates for influence of grain size. Schmertmann (2000) reports that finer soils require lower gradients to backward erode and refers to the methods of Bligh (1910) and Lane (1935) as evidence for this which suggest higher erosion coefficients 'c' for finer soils (note: the inverse of the erosion coefficient is the predicted critical gradient).

To investigate whether the critical gradient is indeed proportional to d_{10}, the uncorrected critical gradient from experiments were plotted against d_{10} in Figure 11.16. Each set of experiments were the same apart from the soil tested and further restricted to soils which had similar uniformity coefficients. Because the gradients are uncorrected, it is expected data series will be different, but considering trends only within a data series, within which the effects of geometry and soil uniformity ought to be the same, one can see the influence of d_{10} alone. Three lines of best-fit are drawn across data sets which span a sizeable range in d_{10}. As can be seen in Figure 11.16, there appears to be no clear relationship between critical gradient and d_{10}.

To derive the grain size factor, Schmertmann (2000) started with the Sellmeijer et al. (2011) theory which states that $F_S = d_{70}/\sqrt[3]{\kappa L}$ (Equation 2.14) and simplifies this to $i \sim d_{10}^{1/3}$. Schmertmann (2000) does not appear to explain why he chose to characterise

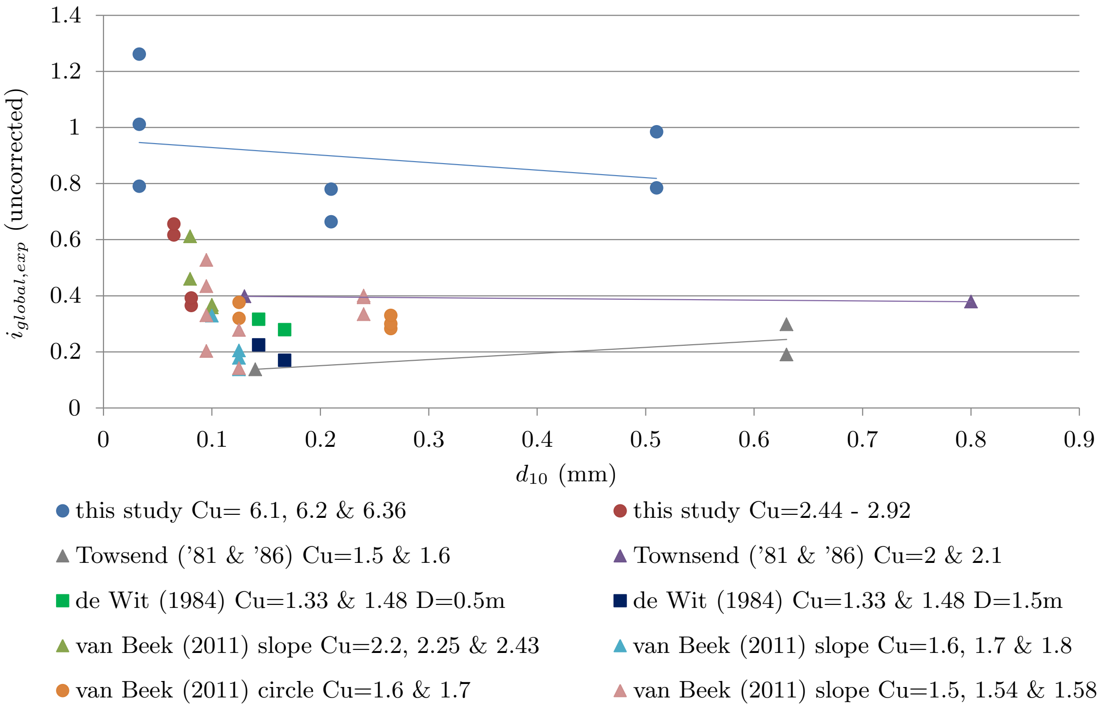

Figure 11.16: Uncorrected global critical gradient of experiments against d_{10} showing lack of relationship

the soil with d_{10} instead of d_{70} as Sellmeijer did.

Schmertmann (2000) suggested that an exponent of 1/5 or 0.2 fits experimental data more closely by calculating the necessary exponent for four of the experimental series. These experimental series were carried out in the same flume and exit geometry but different soils whose uniformity coefficients were similar but d_{10} size was different (tests series 1, 2, 7 and 10 from Townsend et al. (1981), Townsend and Shiau (1986) and Schmertmann (1995)). Schmertmann (2000) also compared test results obtained from Lane (1935) to evaluate the necessary exponent. Across the six exponents calculated, an average of 0.18 was obtained (with a coefficient of variation of 26%). From this Schmertmann (2000) rounded up to 0.2 and suggested a grain size factor of:

$$C_S = (d_{10}/d_{10,ref})^{0.2} \tag{11.5}$$

Where a reference $d_{10,ref}$ of 0.2mm was chosen because it was the average d_{10} across the soils plotted by Schmertmann (2000). It's noted that Schmertmann (2000) reported a range of d_{10} values amongst the plotted results from 0.15–0.28mm, yet the range was indeed 0.062–0.143mm, although this had little effect on the average calculated, 0.22 instead of 0.2mm.

It is noted that Schmertmann (2000) did not use C_S when plotting experimental data onto his plot (Figure 2.34). It is not clear why not.

To assess the applicability/performance of the C_S factor, the same set of experiments (those which were the same apart from soil and similar C_u's) were used to back-calculate the C_S factor required to align the model prediction with experimental result. These back-calculated C_S factors are plotted in Figure 11.17. The relation Schmertmann (2000) suggested for C_S (Equation 11.5) is shown as the curve to illustrate the match between back-calculated and model C_S factors. In addition, 4 of the 6 data points Schmertmann (2000) used to form the relation are plotted as crosses. Also note, that the 6.35/14% or 50% in the legend refer to the starter channel diameter (in mm) and the penetration length as a percentage of seepage length.

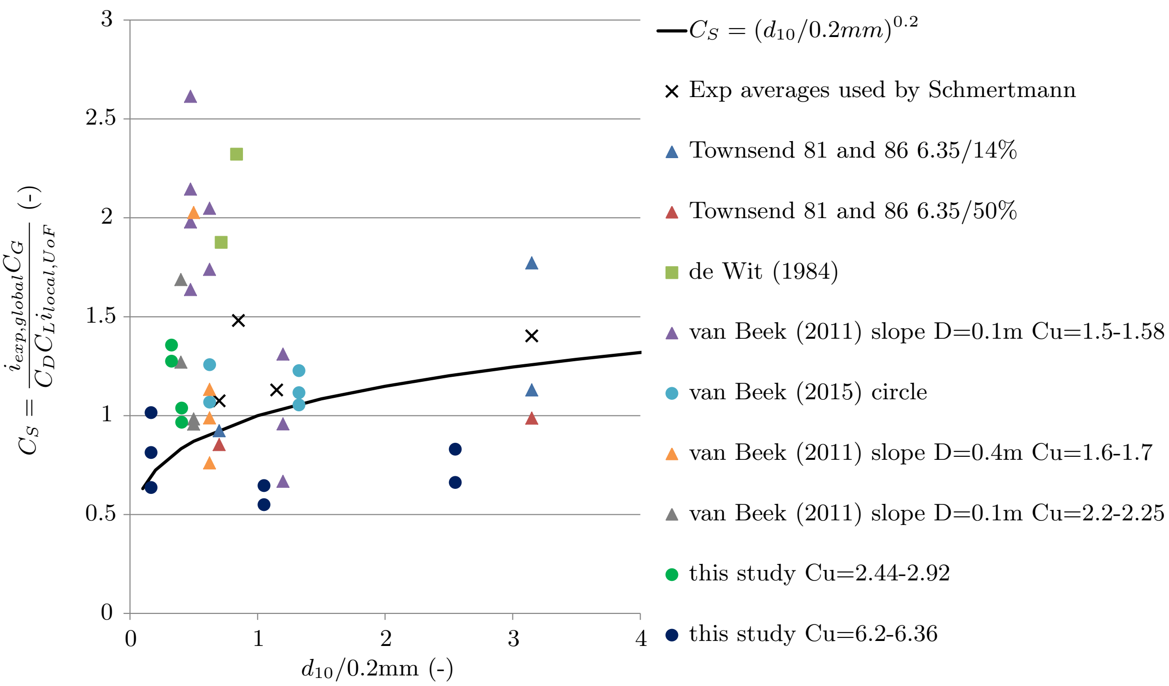

Figure 11.17: C_S factor required to factor experimental global gradient to match the $i_{local,UOF}$ model showing inadequacy of C_S equation

As can be seen in Figure 11.17, the equation for the C_S factor rarely produces the C_S factor required. Errors in other factors are incorporated in the back-calculation of the C_S factor and so all error may not be due to inaccuracy of the C_S equation alone. To isolate out errors from other factors, data series only contained experiments which were the same apart from soil (and restricted to soils of similar C_u's). Other factors are equal within a data series so even if they contained errors, the errors would remain constant and any trends should only be due to the affect of d_{10}. In other words, even if data points are above or below the C_S factor line, they should at least lie along similar, 'parallel', curves. Yet they do not, hence the C_S relation was considered inaccurate.

As a final indication of the value the C_S factor adds to the Schmertmann (2000) model, the coefficient of determination (R^2), was calculated for both before and after the C_S factor was applied (but in both cases applying C_G, C_D and C_L). For the C_S factor to be worthwhile it would need to increase R^2 however, it did not. R^2 before the C_S factor was applied was 0.64 and after it was applied it decreased to 0.56.

Density factor, C_γ

The density factor, C_γ compensates for the effect soil density has on the critical gradient. Schmertmann (2000) reports that, although experimental data does not always demonstrate a density effect, some data does and it makes sense logically that it would, therefore, it is assumed there is a proportional relationship between soil density and critical gradient.

To investigate whether the critical gradient is indeed proportional to soil density, the uncorrected critical gradient from experiments was plotted against relative density in Figure 11.18. This plot shows there was indeed a proportional relationship however it was somewhat weak in that there was much scatter and variability about the trend-lines and the angle of trend-lines varied (i.e. the density had more affect in some soils than others).

Schmertmann (2000) reports that for many sands, the critical gradient increases approximately 20% over the full relative density range however, it was not clear from which tests Schmertmann (2000) drew this conclusion. A 20% increase in critical gradient, over the full relative density range, results in a C_γ factor of:

$$C_\gamma = 1 + 0.4\,(RD - RD_{UoF}) \tag{11.6}$$

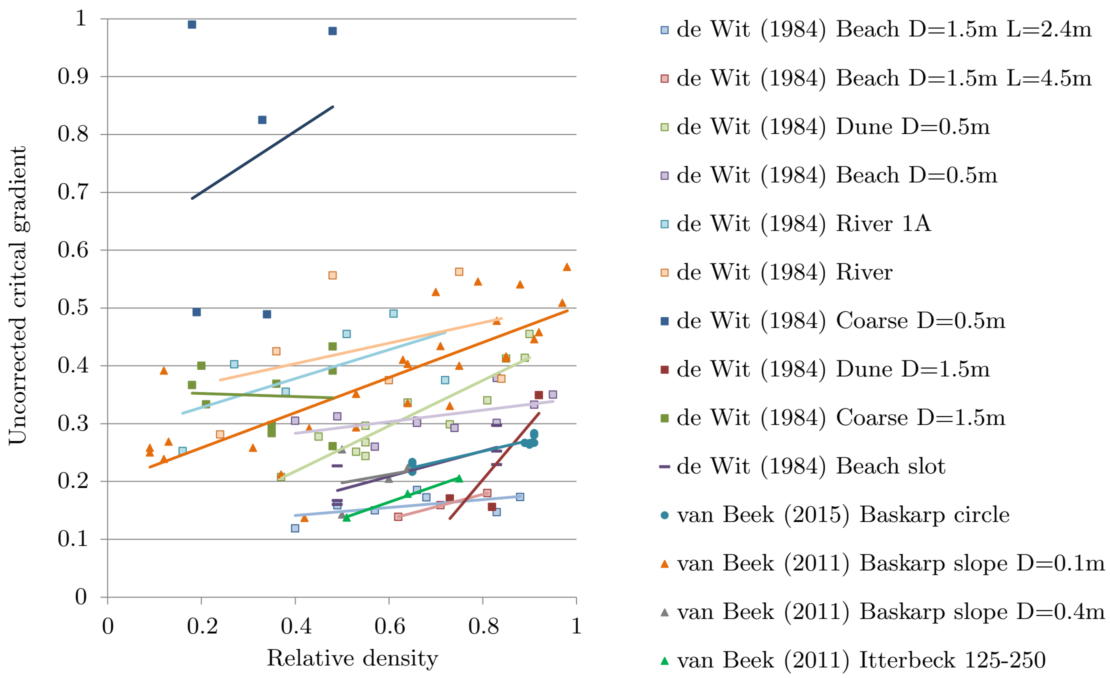

Figure 11.18: Uncorrected critical gradient of experiments against relative density showing slight but varied proportional relationship

Where $RD_{UoF} = 0.6$ on the basis that experimental data used to form the model had an average relative density of 0.6.

It is noted that Schmertmann (2000) did not use C_γ when plotting experimental data onto Figure 2.34. It is not clear why not.

To assess the applicability/performance of the C_γ factor, the same set of experiments (those which were the same apart from soil density) were used to back-calculate the C_γ factor required to align the model prediction with experimental result. These back-calculated C_γ factors are plotted in Figure 11.19 by way of lines of best-fit whose R^2 values varied between 1 to 0.0002 (data points are not shown for the sake of clarity). The equation for C_γ (Equation 11.6) is also plotted on Figure 11.19 to illustrate the match between back-calculated and model C_γ factors.

As can be seen in Figure 11.19, the equation for the C_γ factor rarely produces the C_γ factor required and in most instances, the C_γ equation under estimates the C_γ factor required.

Errors in other factors are incorporated in the back-calculation of the C_γ factor and so all error may not be due to inaccuracy of the C_γ equation alone. To isolate out errors

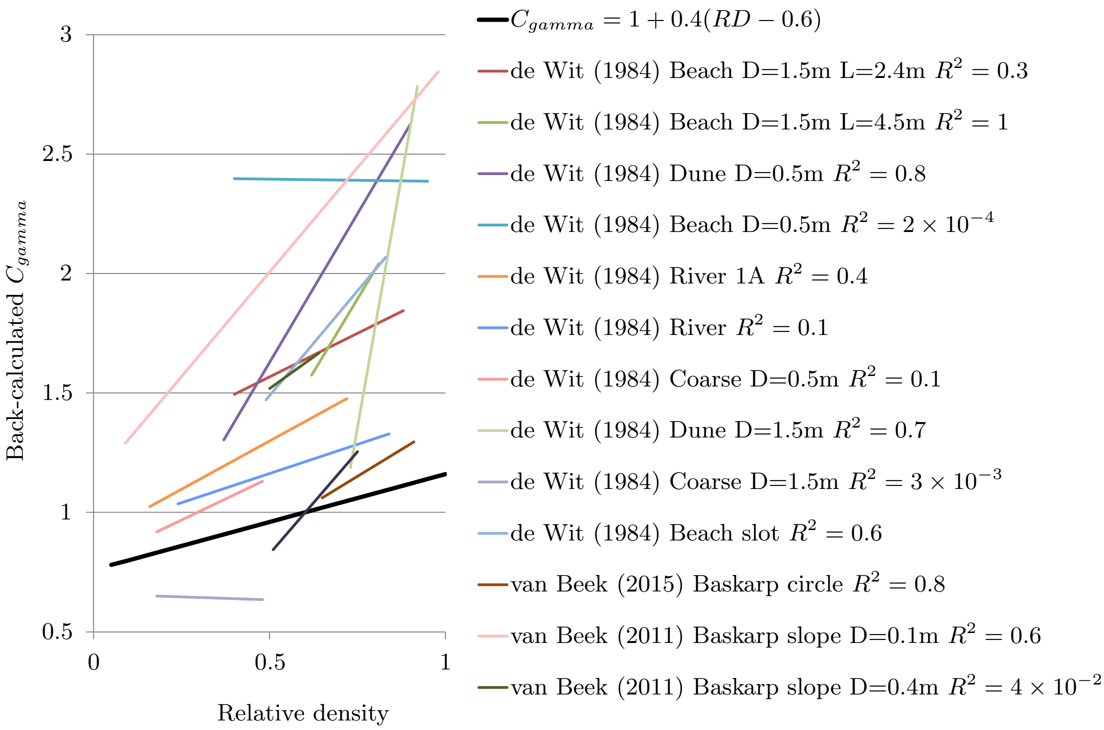

Figure 11.19: Back-calculated C_γ factors and suggested C_γ factor equation

from other factors, data series (and their lines-of-best-fit) only contained experiments which were the same apart from soil density. Other factors are equal within a data series so even if they contain errors, the error ought to remain constant and any trends should only be due to the affect of soil density. In other words, even if lines-of-best-fit are above or below the C_γ factor line, they should at least be parallel. However, the lines-of-best-fit are not parallel to the C_γ factor line because their slopes vary significantly and can not be captured by one C_γ factor line. Note however that slopes are subject to much uncertainty as indicated by the low R^2 values. It is likely that inherent experimental variability plays a part in the low R^2 values. It is possible that soil density has more affect in some soils compared to others.

As a final indication of the value the C_γ factor adds to the Schmertmann (2000) model, the coefficient of determination (R^2), was calculated for both before and after the C_γ factor was applied. For the C_γ factor to be worthwhile it would need to increase R^2, however it did not. R^2 before the C_S factor was applied was 0.64 and after it was applied it decreased to 0.56.

Factors combined

In previous subsections, the coefficient of determination (R^2) before and after a correction factor was applied was compared to assess the value the correction factor adds to the model. A summary of these are listed here in Table 11.1.

Table 11.1: Changes in the coefficient of determination (R^2) quantifying the performance of the model as each correction factor is applied

Factors applied	R^2
-	0.52
C_G	0.58
C_G, C_D & C_L	0.64
C_G, C_D, C_L & C_S	0.56
C_G, C_D, C_L, C_S & C_γ	0.48

C_D and C_L could not be applied without the other as the two are linked via the use of the D/L ratio in the calculation of C_D. In addition, Schmertmann (2000) kept them together when back-calculating or solving for each (see Figures 11.12 and 11.14). Note also, that C_γ was only applied to Dutch studies (de Wit, 1984; Silvis, 1991; van Beek et al., 2011a; van Beek, 2015) as these were the only studies to provide relative densities. C_γ was set to 1 for all other studies.

These R^2 values suggest that the Schmertmann (2000) model is unlikely to perform better than an R^2 of 0.64 and so caution and large factors of safety are required. These R^2 values also suggest that, on average, C_G, C_D and C_L factors add value to the Schmertmann (2000) model where as C_S and C_γ do not. Therefore, C_S and C_γ could be omitted, usually without consequence.

All corrected experimental data are plotted onto Figure 11.20. For this plot, correction factors of C_G, C_D and C_L have been applied, but C_S and C_γ have not.

In order to characterise the apparent random distribution of corrected experimental results across the model line, cumulative distributions were plotted for results in well populated small-windows of C_u values as shown in Figure 11.21.

Whilst the distribution for C_u's of 1.3–1.33 could be interpreted as either a normal or log-normal distribution, a log-normal distribution seems more fitting for C_u's of 1.45–1.54.

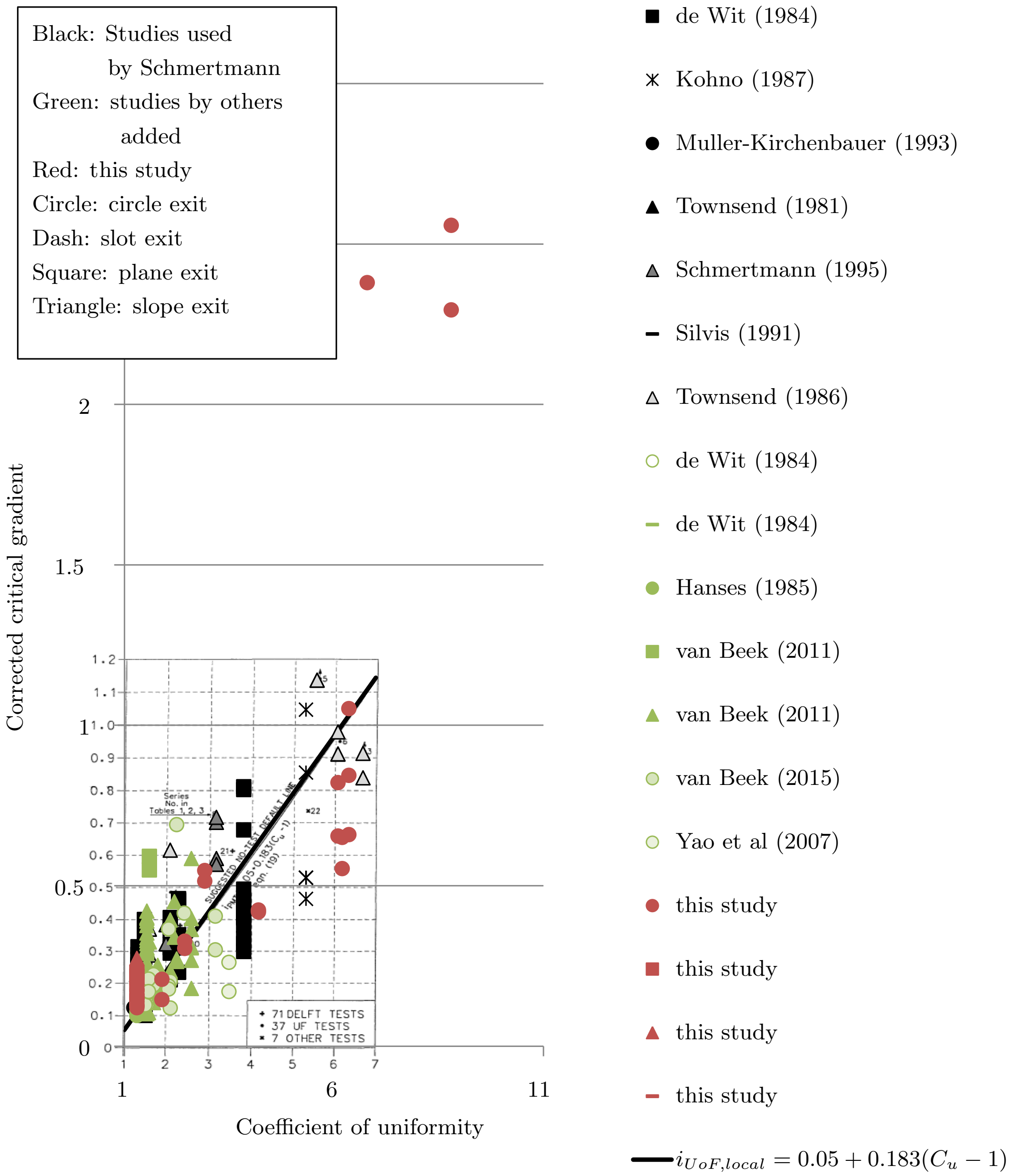

Figure 11.20: Data added to Schmertmann (2000) Figure 2.34

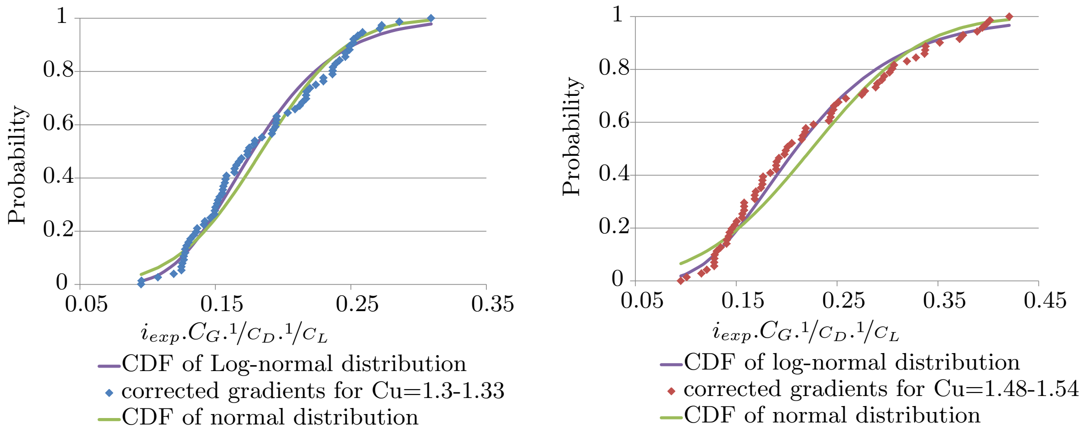

(a) C_u = 1.3–1.33

(b) C_u = 1.48–1.54

Figure 11.21: Cumulative distributions of corrected critical gradients

Therefore, the random distribution of corrected experimental results across the model line are considered to be log-normally distributed.

With all experimental data now added to the plot, the opportunity arose to re-fit a new line-of-best-fit. However, before doing this, some results were either omitted or revised as listed and explained in Table 11.2.

With unreliable data omitted or amended, a new line-of-best-fit was fitted. However, given there were few data points in the higher C_u range, especially once the tests possibly affected by suffusion were disregarded, it was necessary to plot average values (averages of $\ln(i)$) so that when a line of best-fit was fitted, near-equal weighting was given to the higher C_u results.

The average points and new line-of-best-fit are show in Figure 11.22. It was found that an exponential line of best-fit captured the trend in average results better than a linear line. When an exponential line of best-fit was used, the model was lowered to better represent results between C_u's 3–7 (and were therefore more conservative) and the model was raised to better represent the sudden added resistance to backward erosion at C_u's >7.

The equation for the revised best-fit line is:

$$i_{local,UoF} = 0.14\mathrm{e}^{0.28C_u} \tag{11.7}$$

Table 11.2: Test results omitted and amended prior to plotting Figure 11.22

Reference	Test #	Soil		Reason
This study	71	Mix 1	omitted	Influenced by transport of finer grains through sample as evident by settlement of upstream portions of sample, fine-grained plumes continously fed into downstream box and non-linear standpipe levels. Also, failed by surface slip/sheet flow instead of BEP. See Subsection 8.2.1 for more information.
This study	52	Mix 4	amended	Reduced critical head from max. head of 3.577m to 2.476m because channel reached 34%L at 2.476m (more than average critical channel length of 27%L) and then stopped on a group of gravel (channel tip expected to continue if it hadn't of been reinforced by a group of gravel). See Subsection 8.2.4 for more information.
This study	73	Mix 4	amended	Reduced critical head from max. head of 3.988m to 2.675m because channel reached 80%L at 2.675m (more than average critical channel length of 27%L). See Subsection 8.2.4 for more information.
Townsend and Shiau (1986)	7 & 8	WG	omitted	Did not intiate and possibly affected by suffusion. These referred to as Test Series 3 by Schmertmann (2000). See Subsection 11.2.2 for more information.
Townsend and Shiau (1986)	11 & 12	Gap I	omitted	Did not intiate and possibly affected by suffusion. These referred to as Test Series 5 by Schmertmann (2000). See Subsection 11.2.2 for more information.
Townsend and Shiau (1986)	13–15	Gap II	omitted	Did not progress further than 60%L and possibly affected by suffusion. These referred to as Test Series 6 by Schmertmann (2000). See Subsection 11.2.2 for more information.
Kohno et al. (1987)			omitted	Description of failure suggests surface slip or sheet flow instead of backward erosion, there was a large spread in results and exit geometry unlike anything else tested. These referred to as Test Series 22 by Schmertmann (2000). See Subsection 11.2.2 for more information.

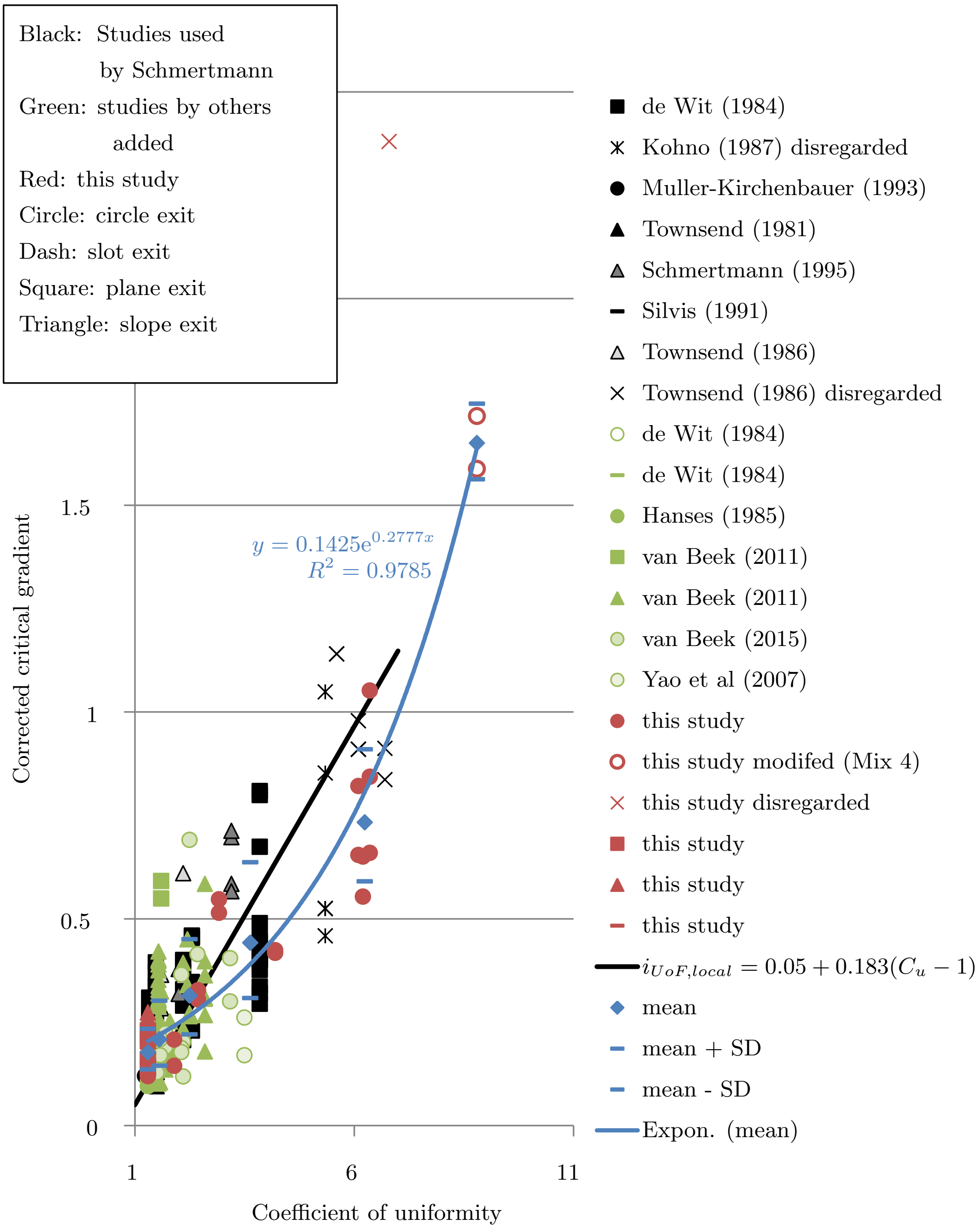

Figure 11.22: Data added to Schmertmann (2000) Figure 2.34 with new suggested line-of-best-fit

Standard deviations of distributions are also plotted on Figure 11.22. The exponential lines-of-best-fit of the standard deviations were $i_{local,UoF} = 0.22\mathrm{e}^{0.24C_u}$ for the mean + standard deviation and $i_{local,UoF} = 0.09\mathrm{e}^{0.31C_u}$ for the mean - standard deviation.

With means and standard deviations, the log-normal distribution at any C_u can be characterised and used to evaluate probability for both design and risk assessments.

11.2.4 Recommendations

When using the Schmertmann (2000) method it is recommended to:

- When determining C_G, calculate the minimum local gradient with a 2-dimensional seepage model. If a circle exit is being considered, model the slot equivalent and factor the resulting critical gradient down using the circle-exit correction factor of 0.8 (discussed and calculated subsequently in Subsection 11.3.3 for use with the Sellmeijer et al. (2011) model).
- Do not apply C_S or C_γ because these factors did not improve performance of the model over the suite of laboratory experiments considered (see Table 11.1).
- Use the exponential relationship for the critical local gradient (expected in the UoF flume) with C_u in Equation 11.7 instead of the linear relationship suggested by Schmertmann (2000).
- Use a factor of safety when using the Schmertmann (2000) model in design. The factor of safety may be chosen to correspond with a probability of acceptable risk by assuming variability can be modelled using a log-normal distribution with a mean = model prediction and $i_{local,UoF} = 0.22\mathrm{e}^{0.24C_u}$ for the mean + standard deviation and $i_{local,UoF} = 0.09\mathrm{e}^{0.31C_u}$ for the mean - standard deviation. This log-normal distribution can also be used to estimate the risk of failure of an existing dam/levee.

11.3 Sellmeijer (2011)

11.3.1 Introduction

The Sellmeijer et al. (2011) model is a tool used to predict the critical gradient of backward erosion piping. It is therefore used to aid in the design and risk assessment of dams and levees. It is the primary design method used in The Netherlands (van Beek, 2015) with Dutch guidelines suggesting the use of 'characteristic parameters' (the mean value plus/minus 1.65 times the standard deviation- whichever is more conservative) and a safety factor of 1.2 applied to the seepage length (Weijers and Sellmeijer, 1993). The Sellmeijer et al. (2011) model is also presented in the ICOLD Bulletin 164 on Internal Erosion (ICOLD, 2015).

A description of the Sellmeijer et al. (2011) model is given in Section 2.5.6. Essentially the model comes in two forms, a 2-dimensional finite element numerical model (as a program called MSeep) and a formula for the 'standard dike' configuration. MSeep is a commercial product which is not available to test against experimental results, however the formula for the 'standard dike' configuration is, therefore this review has been carried out on this formula.

The 'standard dike' configuration consists of the slot configuration as depicted in Figure 11.23 and is limited to fine to medium grained uniform sands whose properties lie within bounds listed in Table 11.3.

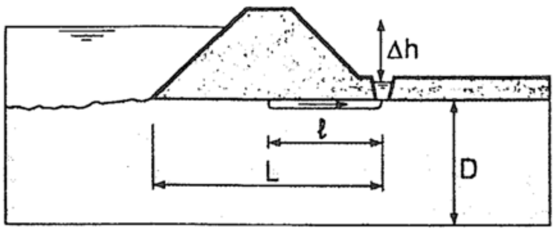

Figure 11.23: Standard dike configuration (Weijers and Sellmeijer, 1993)

This review is divided into two subheadings, the first is a comparison of model predictions with experimental results which were carried out in the 'standard dike' configuration. The second is a comparison of model predictions with experimental results in all exit configurations and soils tested. It is acknowledged that the formula was not intended for these additional exit configurations and soils, however the comparison was carried

Table 11.3: Parameter limits of standard dike formula

parameter	minimum	maximum	mean
Relative density, RD	50%	100%	72.50%
Coefficient of uniformity, C_u [-]	1.3	2.6	1.81
Roundness, KAS	35%	70%	49.8%
d_{70}	150 μm	430 μm	208 μm
D/L for multiple foundation layers [-]	0.1	1	not needed
$k_{coarse.sand}/k_{fine.sand}$ for multiple foundation layers [-]	1.5	100	not needed
D_{fine}/D for multiple foundation layers [-]	0.1	1	not needed

out with the intention to offer amendments which could extend the applicability of the formula to more scenarios.

11.3.2 Model review within 'standard dike' limitations

In this subsection, comparison of experimental results with model predictions are limited to tests carried out in Sydney Sand and slot exits because these are the tests which equate to the 'standard dike' configuration. Nine tests were carried out in Sydney Sand and slot exits including all three seepage lengths of 1.3m, 2.6m and 3.9m.

Experimental results and model predictions are plotted in Figures 11.24a and 11.24b. Predictions using the Sellmeijer model were between 7% – 33% higher (i.e. non-conservative) than experimental results (using best-estimate inputs). Considering the range of possible model predictions did not solely account for the differences.

The following variables were used in the Sellmeijer model predictions:

- White's constant, $\eta = 0.25$ as per Sellmeijer's selection (van Beek et al., 2013; van der Zee, 2011) (see Subsection 2.5.3 for explanation).
- Effective unit weight, $\gamma'_p = 16000$ N/m^3 corresponding to a specific gravity of sand particle, $G_s = 2.65$.
- Angle of repose, $\theta_r = 37$ °. Sellmeijer used a constant angle of repose of 37 degrees regardless of the soil (van Beek, 2015). This angle was chosen by fitting results from experiments carried out at De Deltagoot (experiments reported in Silvis (1991))

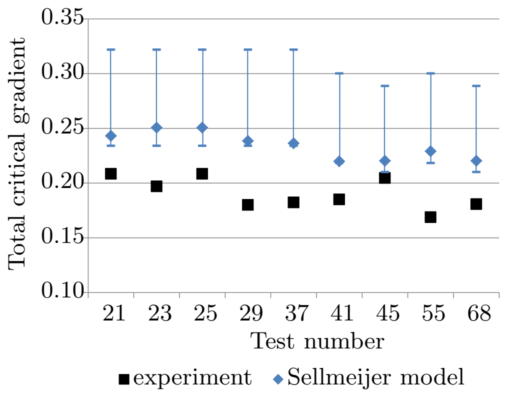

(a) Total critical gradient with test number

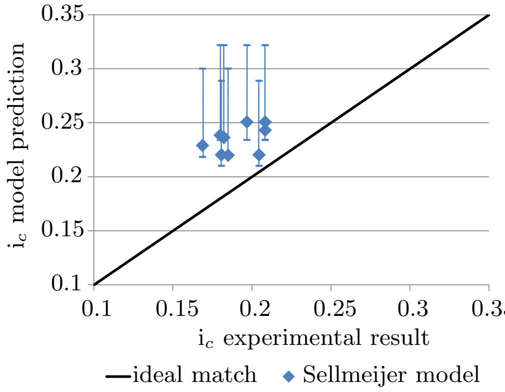

(b) Model prediction versus experimental result

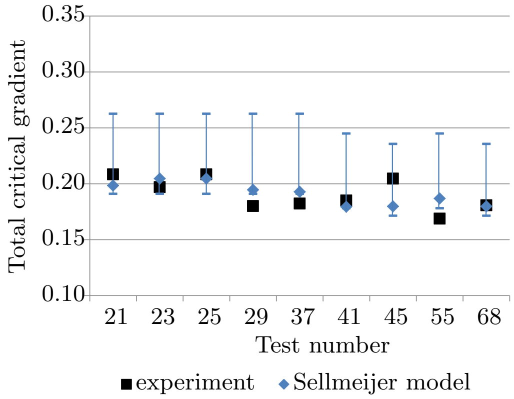

(c) (a) using critical shear stress amendment suggested by van Beek (2015)

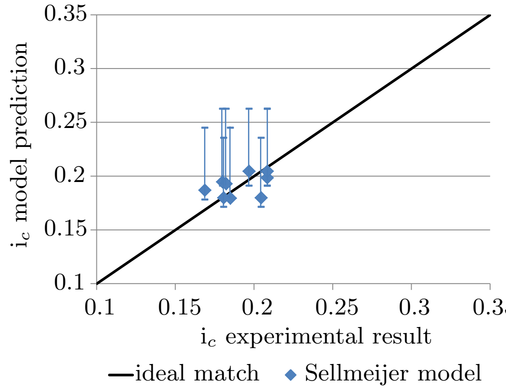

(d) (b) using critical shear stress amendment suggested by van Beek (2015)

Figure 11.24: Comparison of experimental results and Sellmeijer model prediction for tests in Sydney Sand with slot exits

(van der Zee, 2011). Note, this angle is also referred to as the bedding angle in numerous publications and the rolling resistance angle by van der Zee (2011).

- Coefficient of uniformity, C_u = 1.3 for Sydney Sand.
- Particle size for which 70% is finer than, d_{70} = 0.00035m according to the particle size distribution for Sydney Sand.
- Dynamic viscosity, $\mu = 1 \text{ x } 10^{-3}$ Ns/m^2 for water at 20°C.
- Depth, D = 0.31m.
- Length, L = 1.3m for tests 21, 23, 25, 29 & 37; L=2.6m for test 41 & 55; and L=3.9m for tests 45 and 68.

Other variables used in the Sellmeijer model predictions were either not measured in experiments or measured but subject to error. These variables included relative density, roundness of particles and permeability. To capture the possible range across which these variables could affect the model predictions by, error bars in Figure 11.24 span from the most to the least conservative possible predictions resulting from the most to least erosion-resistant variable combinations.

Relative density was not measured in most experiments due to the complexities explained in Section 4.8. Of the few measurements made using push tubes (in Tests 45, 46 and 49), relative densities varied between 26% to 59% (shown in Figure 4.31). However these relative densities were measured after the bladder had been deflated and the Perspex lid removed, allowing for expansion of the soil from its tested state, hence relative densities during testing are likely to have been greater than those measured. In selecting a relative density for tests carried out in this study, it was decided to back-calculate what the relative density ought to be which would bring model predictions in line with experimental results for slot tests in Sydney Sand (the standard dike configuration). A relative density of 50% brought model predictions in line with experimental results for slot tests in Sydney Sand and hence this relative density was adopted for all tests carried out in this study. This relative density of 50% did lie within the range of push tube densities measured. The most resistive and least resistive values of relative density for the error bars were entered as 100% and 50% to coincide with the parameter limits given by Sellmeijer et al. (2011) (listed in Table 11.3).

Roundness of particles, KAS, is an approximate measure using the scale illustrated in Figure 11.25. Given that the ratio of KAS has an exponent of -0.02, it had very little impact of model predictions. Also, given that KAS information was not available for soils tested by others and is quite subjective, a value of 49.8 was given to all tests, whether from this study or others, which was the average value given in Sellmeijer et al. (2011), thereby bringing the KAS ratio to 1 and effectively removing it from the model. The most resistive and least resistive values of KAS for the error bars were entered as 35% and 70% to coincide with the parameter limits given by Sellmeijer et al. (2011) (listed in Table 11.3).

Permeability values for each test were taken from those measured, listed in Table 4.3. Exceptions were Tests 45 and 68 whose measured values were unreliable outliers and

Figure 11.25: Roundness of particles, KAS (van Beek et al., 2009)

were therefore allocated to be the average Sydney Sand permeability. The most resistive and least resistive values of permeability for the error bars were entered as the minimum and maximum values measured from the slot tests (3.1 x 10^{-4}m/s and 3.7 x 10^{-4}m/s respectively).

Model predictions were most sensitive to changes in relative density.

Returning to consideration of the model performance, van Beek (2015) made similar findings when comparing predictions of the Sellmeijer standard dike formula with experimental results (experiments using slot exits in uniform sands). As shown in Figure 11.26, experimental results were over predicted on average by 20% (similar to the over prediction of between 7%–33% of experimental results from this study). What is particularly interesting about the experimental results plotted in Figure 11.26 is that they were large-scale tests, of seepage lengths ranging between 6m–15m. Given the correlation between model and experiment was also good in this instance, it is suggested that the Sellmeijer standard dike formula performs well for changes in depth:length ratio and scale.

Van Beek (2015) suggested an amendment to the calculation of critical shear stress used within the Sellmeijer model. This amendment was suggested in order to overcome the incorrect assumption that critical shear stress is independent of grain size. It was formulated by collating the critical Shields parameter across a number of various studies looking at incipient motion in laminar flow. This collation led to a new fit in the data which, when expressed in terms of critical shear stress and parameters related to the grain equilibrium (particle density and size), provided a relationship between d_{50} and the angle of repose given in Equation 11.8 and plotted in Figure 11.27. This relationship was reported to still be based on the equilibrium of forces by White (1940) but now also complied with the Shields (1936) approach (van Beek, 2015).

$$\theta_r = -8.125 \ln d_{50} - 38.777 \tag{11.8}$$

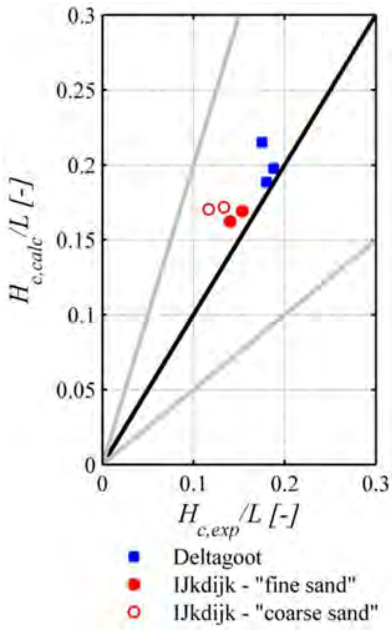

Figure 11.26: Comparison of model predictions with experimental results by van Beek (2015)

Equation 11.8 defines a decrease in angle of repose with increase in particle diameter. Van Beek (2015) states that the reason behind this relationship is unclear but does refer to other researchers who have reported the same trend. Therefore, instead of using a constant angle of repose of 37°, as done by Sellmeijer et al. (2011), van Beek (2015) suggested the angle of repose be calculated using Equation 11.8, before use in the resistance factor in Equation 2.14. Van Beek (2015) also recommended using an $\eta = 0.3$ (instead of 0.25) to be consistent with the findings of White (1940).

Given d_{50} for Sydney Sand is 0.0003m, Equation 11.8 results in an angle of repose of 27°. This angle correlates with the slope of a sand boil of Sydney Sand observed by the author during experiments (measured underwater) as pictured in Figure 11.28.

When an angle of repose of 27° and an η of 0.3 was used, the Sellmeijer model predictions moved closer to the experimental results, as shown in Figures 11.24c and 11.24d. These predictions were between 0.6% – 12% of the experimental results (using best-estimate inputs). Therefore the current author recommends using the (van Beek, 2015) amendment of $\eta = 0.3$ and Equation 11.8.

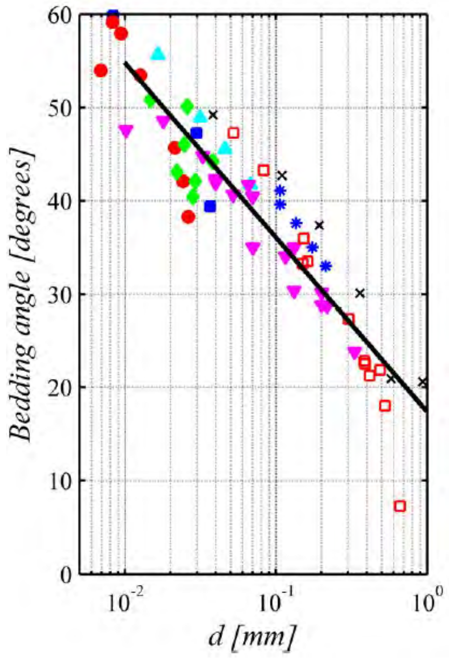

Figure 11.27: Bedding angle with particle size used to determine Equation 11.8 (van Beek, 2015)

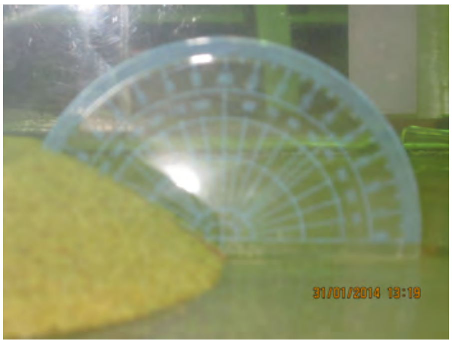

Figure 11.28: Angle of repose of Sydney Sand indicated by submerged sand boil

11.3.3 Model review outside 'standard dike' limitations

In this subsection, comparison of experimental results with model predictions are no longer limited to the 'standard dike' configuration but include all tests in all exit geometries and all soils. It is recognised that the standard dike formula is not designed for exit geometries other than the slot or soils other than fine-medium uniform sands, however comparison has still been made to investigate whether amendments can be offered to extent and improve the formula's versatility.

Non 'standard dike' exit geometries

Here comparisons are limited to tests in 'standard dike' soils which are fine to medium grained uniform sands whose properties are within the limits listed in Table 11.3. However comparisons are made across all exit geometries to investigate (and perhaps improve) the performance of the standard dike formula in exits other than slot exits.

Model predictions and experimental results from this study in Sydney Sand across all exits are plotted in Figures 11.29a and 11.29b. These model predictions included the amendment suggested by van Beek (2015) whereby Equation 11.8 was used to determine the angle of repose and $\eta = 0.3$. They also included the best-estimate values of relative density = 50% and KAS = 49.8 (essentially removing KAS from the model).

Figures 11.29a and 11.29b show that the model worked well for slot exits but overestimated the global critical gradient for circle exits and underestimated for plane and slope exits.

Given that model predictions worked well for slot exits in Sydney Sand, the average change in results for other exits ought to indicate the effect of the exit geometry on the Sellmeijer et al. (2011) model prediction. Using the method of least squares, a factor of 0.8 shifted model predictions to circle exit results, a factor of 1.2 shifted predictions to plane exit results and a factor of 1.4 shifted predictions to slope exit results. Model predictions once factored up or down by these exit correction factors are plotted on Figures 11.29a and 11.29b as red data points.

As discussed in the Literature review, van Beek (2015) suggested an exit correction factor of 0.5 for circular exits because data plotted along the 1:2 line in Figure 11.30a. However model predictions in Figure 11.30a did not include the angle or repose and eta amendment that van Beek (2015) suggested. When the amendment was used, data shifted down towards the 1:1 line, except for Baskarp Sand and Itterbeck Mix 1 and 2 results which shifted up (soils with the smallest d_{70}), see Figure 11.30b.

Given most data shifted down closer to the 1:1 line when the angle of repose and eta amendments were used, the current author is of the opinion that the 0.5 factor is not suitable when these amendments are used.

When the sum of least squares method was used to devise a circle exit correction factor

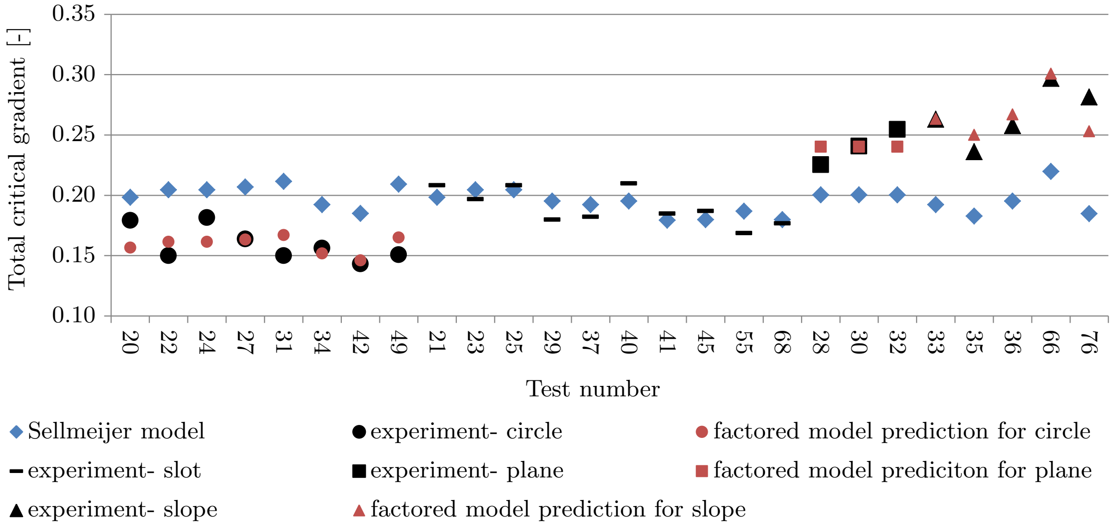

(a) Total critical gradient with test number

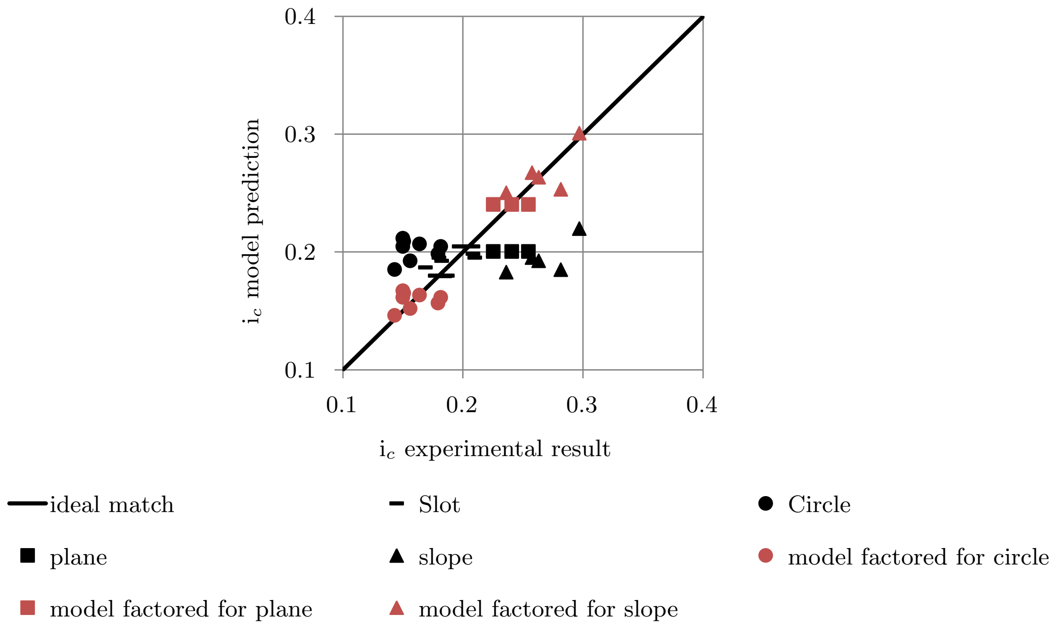

(b) Model prediction versus experimental result

Figure 11.29: Comparison of experimental results and Sellmeijer model prediction for tests in Sydney Sand with all exits (factors developed using sum of least squares)

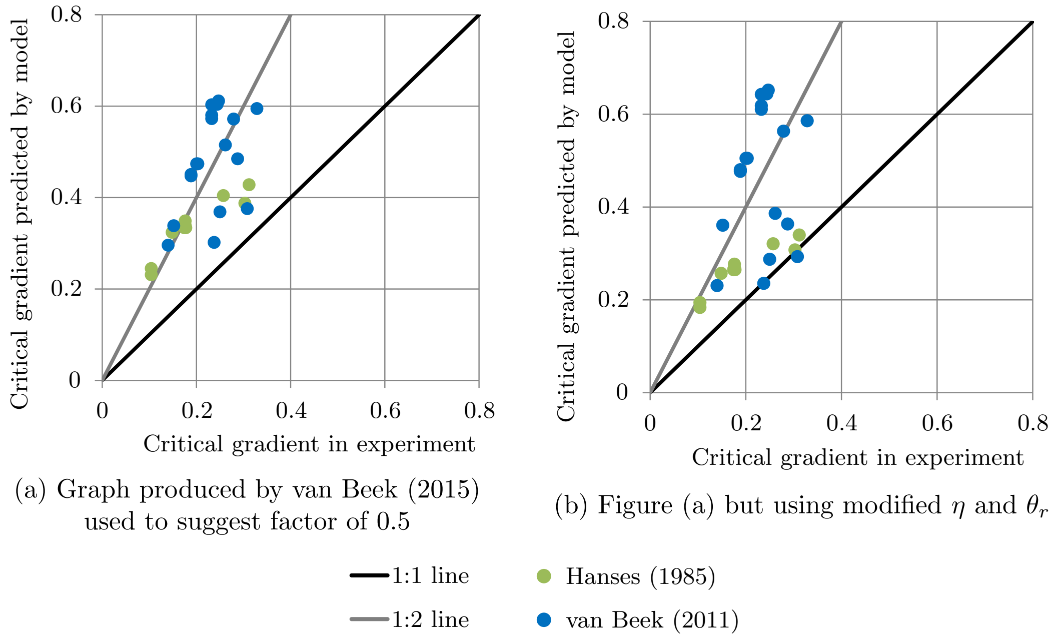

(a) Graph produced by van Beek (2015) used to suggest factor of 0.5

(b) Figure (a) but using modified η and θ_r

Figure 11.30: Effect of using modified η and θ_r on comparison of experimental results with Sellmeijer model predictions (circle exits in 'standard dike' uniform sands)

using results from all studies, not just this study, the circle exit correction factor decreased from 0.79 to 0.65. The main reason the factor decreased was the Baskarp sand results whose model predictions were often double experimental results. Without Baskarp sand results, the factor became 0.83, closer to the original 0.79. Given Baskarp sand was the finest sand tested, it is possible the model's inability to predict its behaviour is a function of the unusually fine sand, not the circular exit. This could be confirmed with experiments in Baskarp sands in slot exits but Dutch researchers did not test this. Given a circle exit correction factor of 0.8 was most appropriate for all soils other than the finest Baskarp sand, it was chosen as the optimal factor.

As for the plane exit, when experimental results from other studies were included in the plane exit correction factor, instead of just results from this study, the factor did not change significantly and still rounded off to 1.2.

The slope exit however, when experimental results from other studies were included in the slope exit correction factor, the factor reduced significantly from 1.4 to 0.8. Note that other studies which tested the slope exit, namely Townsend et al. (1981); Townsend and Shiau (1986); Schmertmann (1995), were not included in this exit-correction-factor calculation because measurements from these studies did not include soil permeability, and soil permeability is required when using the Sellmeijer et al. (2011) model.

This reduction in the slope exit correction factor was unexpected, particularly to a factor less than 1 which would factor model predictions down instead of up. A factoring up of model predictions was expected because the model assumes a slot exit and, according to critical gradients in this study, slope critical gradients ought to be higher than slot critical gradients, not lower.

It was investigated whether there was a distinct difference(s) between the slope testing in this study and the slope testing in the van Beek et al. (2011a) study which would account for the significant reduction in the slope-exit correction factor. Figure 11.31 was plotted to search for a possible difference, by plotting d_{70} against the required, back-calculated, slope-exit correction factor. Firstly, Figure 11.31 shows there was substantial spread in the van Beek et al. (2011a) results, but that 83% of slope tests required a slope correction factor <1. Secondly, Figure 11.31 shows that neither particle size or seepage length appeared to influence the exit correction factor needed, so the plot gives no indication of a distinct difference between the studies that would explain the different slope-exit correction factors needed.

However, the geometry of the slope exits in the two studies were quite different, as pictured in Figure 11.32. The slope used in this study was taller and longer with an additional panel positioned beneath the top of the slope (to reduce deformation due to pressure from the bladder). Also, pressure from the bladder may have imposed different loads onto the slope than the slope set-up used in the van Beek et al. (2011a) study (which did not include a pressure bladder). Furthermore, the lid in this study stopped at the top of the slope whereas it continued across in the van Beek et al. (2011a) study. It's quite possible these differences could explain the different slope correction factors needed, but difficult to prove.

It was also investigated whether having used slope-exit tests to carry out the multivariate analysis in Sellmeijer et al. (2011) could explain why model predictions were higher than experimental results instead of lower expected for slope exits. Perhaps the multivariate analysis had resulted in fitting the model closer to slope results instead of the originally modelled slot configuration. However when contribution of the multivariate analysis was removed (the relative density, coefficient of uniformity and measure of roundness ratios in

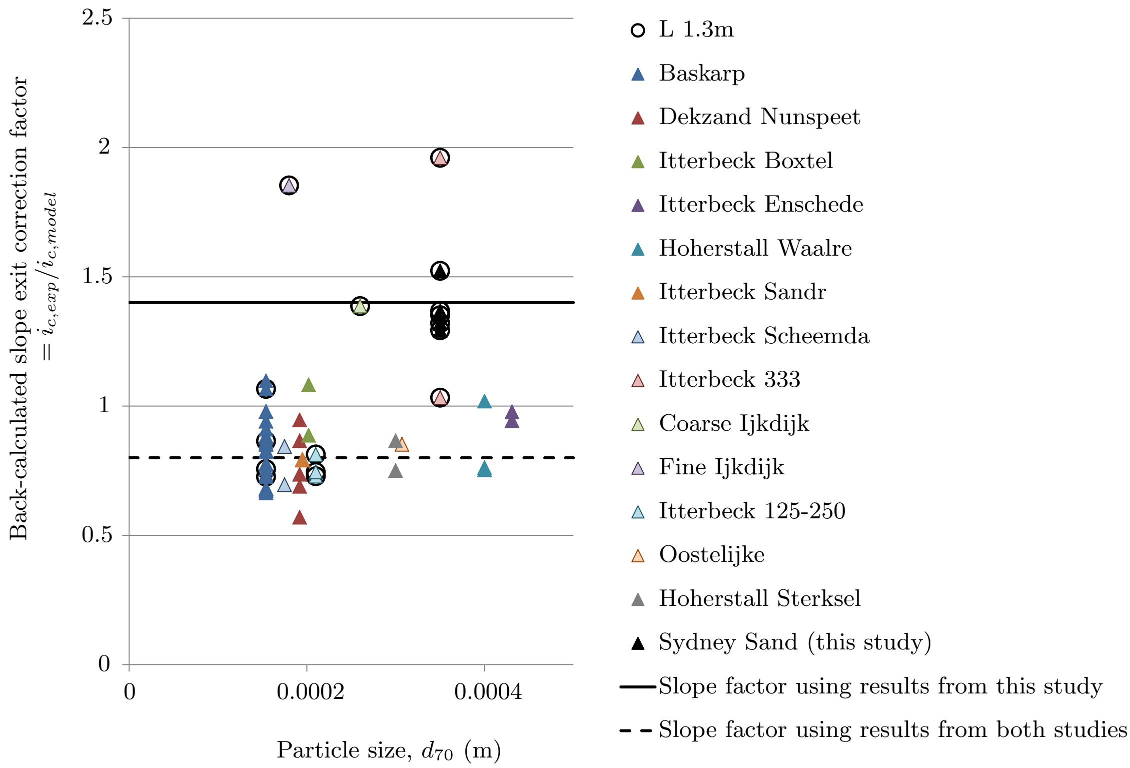

Figure 11.31: Back-calculated slope-exit correction factors against d_{70} for different soils tested in the van Beek et al. (2011a) study and for Sydney Sand in this study

the resistance factor and the d_{70} ratio in the scale factor) the slope-exit correction factor increased only marginally from 0.84 to 0.87. Therefore having used slope-exit tests to carry out the multivariate analysis did not appear to be the issue.

It should be noted though, that whilst the *slope correction factors* needed for this study and the van Beek et al. (2011a) study were quite different, the *critical gradients* observed were not. Figure 11.33 illustrates this below by comparing critical gradients from this study and the van Beek et al. (2011a) study, against permeability. The tests plotted here were only for slope exits with scales similar to the scale used in this study (seepage lengths between 1.3 to 1.46m, depth of 0.4m and width of 0.8m) (the scale in this study was a seepage length of 1.3m, depth of 0.31m and width of 0.45m). It can be seen that critical gradients across the two studies were similar, with 13 out of the 16 critical gradients between 0.15 to 0.3. Therefore, differences needed in the slope correction factors may be more evident of sensitivities in the Sellmeijer et al. (2011) model rather than differences between results across the two studies.

Figure 11.34a is a plot of model predictions with experimental results in all exit geometries

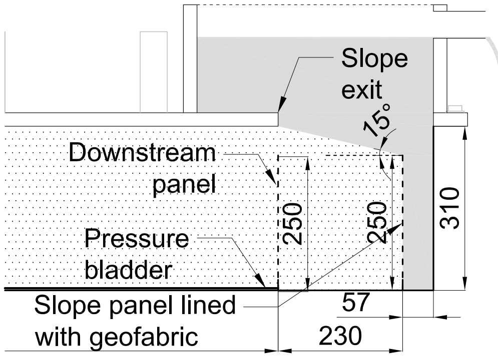

(a) Slope geometry used in this study (direction of flow from left to right)

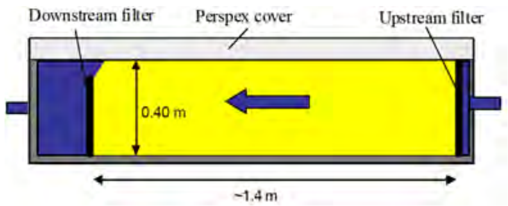

(b) Slope geometry used in van Beek et al. (2011a) study (direction of flow from right to left)

Figure 11.32: Comparing slope geometries used

for 'standard dike' soils before exit-geometry corrections were applied. The coefficient of determination (R^2) before exit-geometry corrections were applied was 0.11. If exit correction factors of 1 for slot, 0.8 for circle, 1.2 for plane and 1.4 for slope were used, R^2 reduced to -0.52. This reduction in model performance was due to difficulty in choosing a suitable slope correction factor for all slope results. As discussed above, results from this study required a factor of 1.4 yet results from the van Beek et al. (2011a) study required a factor of 0.8. When a slope correction factor of 0.8 was applied to all slope results, R^2 increased to 0.51. When a factor of 1.4 was applied to results from this study and 0.8 to results from the van Beek et al. (2011a) study, R^2 further increased to 0.53. The corresponding plot of model predictions with experimental results is given in Figure 11.34b.

It's acknowledged using different slope correction factors for different studies is impractical. Therefore it is recommended that further research be carried out on the affects of slope geometry before a slope correction factor is used in practice. Fortunately, there are few field applications for which the slope exit is required.

It is likely these exit geometry correction factors are dependent on the slot spacing assumed in the original model. For instance, if the assumed slot spacing was wider, then plane and slope corrections are likely to be smaller than the currently suggested 1.2 and 1.4. However without experiments in slot exits with different spacing and corresponding tests in slope and plane exits, this is difficult to verify.

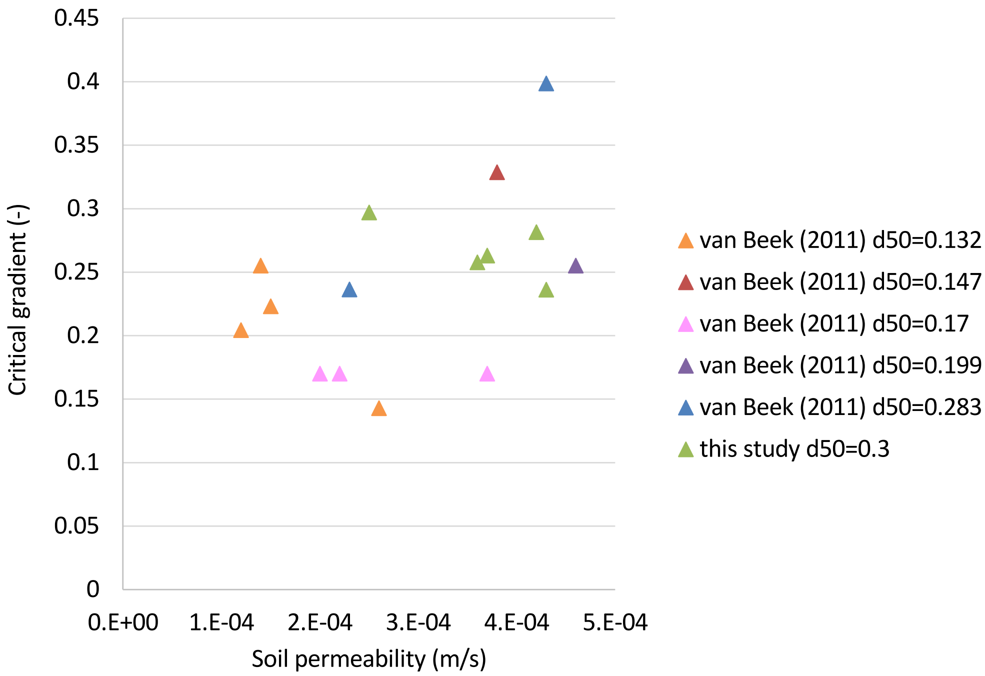

Figure 11.33: Critical gradients against soil permeability for slope exit tests in both this study and the van Beek et al. (2011a) study showing similar results across the two studies

Non 'standard dike' soils

Here comparisons are made for all soils to investigate (and perhaps improve) the performance of the standard dike formula in soils other than 'standard dike' soils. 'Standard dike' soils are fine to medium grained uniform sands whose properties are within the limits listed in Table 11.3, therefore non 'standard dike' soils are either very fine or coarse grained uniform sands or poorly graded and well graded sands.

Figure 11.35a is a plot of experimental results against model predictions for both standard and non standard dike soils. Model predictions include the exit-geometry correction factors discussed above. It shows that non standard soils are less likely to plot near the 1:1 ideal line because model predictions often underestimate the observed critical gradients. The coefficient of determination of the model becomes $R^2 = 0.01$ when non-standard soils are added.

The multivariate analysis carried out by Sellmeijer et al. (2011) covered a C_u range of 1.3–2.6 and a d_{70} range of 0.15–0.43mm. This study extended these ranges with tests on soils ranging in C_u from 1.3 to 8.6 and in d_{70} from 0.24–4.6mm. These extended ranges provided an opportunity to improve the C_u and d_{70} ratio exponents in Equation 2.14.

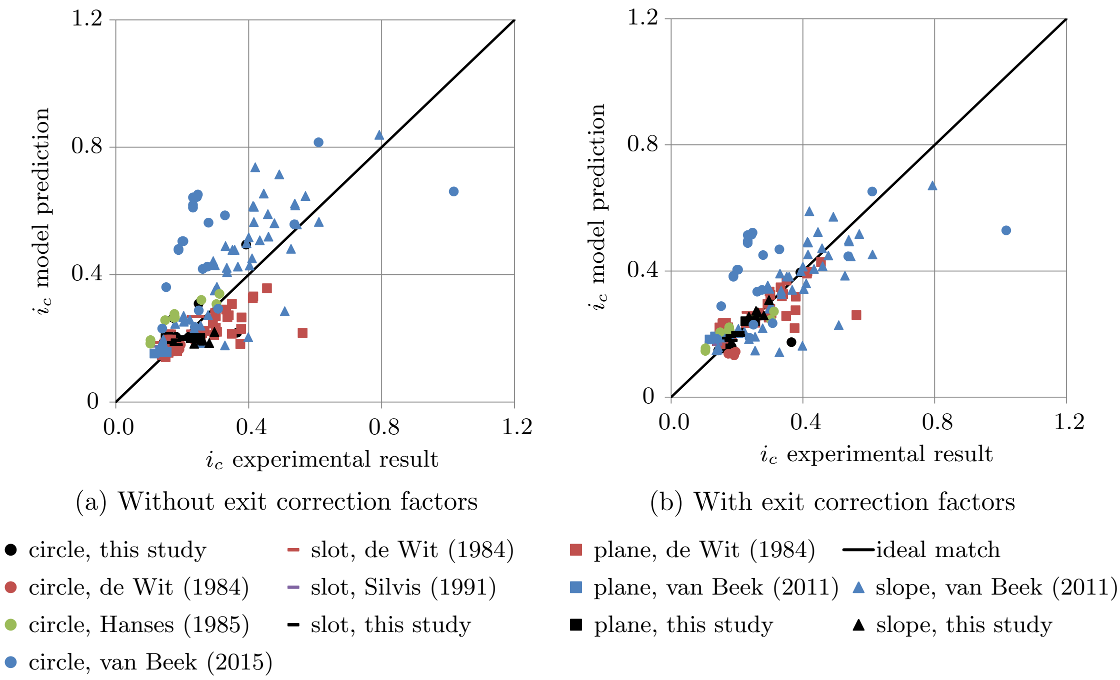

(a) Without exit correction factors

(b) With exit correction factors

Figure 11.34: Comparison of model predictions and experimental results showing improvement made on model predictions when exit-geometry corrections were used (‘standard dike’ soils only)

Exponents of relative density and KAS ratios were not reviewed due to lack of information of these properties.

Using the method of least squares, new exponents of these two ratios were calculated with the non-standard soils included. Doing so saw the C_u exponent increase from 0.13 to 0.5 and the d_{70} exponent decrease from 0.6 to 0.04. This suggests C_u has more influence over the critical gradient and d_{70} has less influence, than indicated by Sellmeijer et al. (2011).

Experimental results are plotted against model predictions found using the newly suggested exponents in Figure 11.35b. This shows model predictions for non-standard soils are now closer to experimental observations as indicated by red data points now closer to the 1:1 ideal line. The coefficient of determination of the model with the newly suggested exponents now becomes $R^2 = 0.75$.

It may not be possible to improve on a R^2 of 0.75 given the inherent variability across experimental results. Examples of this variability can be see in Figure 11.29 from amongst the first 6 circle tests. The 6 circle tests were identical except for slight variations in permeability measurements. These permeability variations caused a 10% variability across model predictions. However experimental observations varied by up to approximately

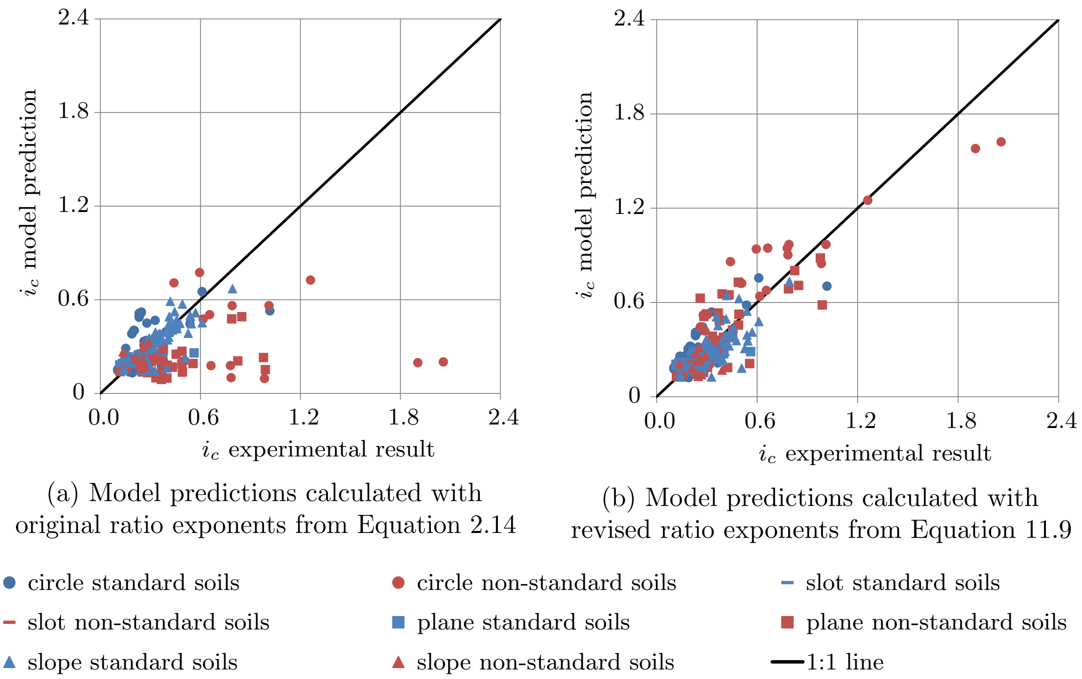

(a) Model predictions calculated with original ratio exponents from Equation 2.14

(b) Model predictions calculated with revised ratio exponents from Equation 11.9

Figure 11.35: Model predictions compared with experimental results for all exits and all soils showing improvement when revised ratio exponents used

20%.

To consider the distribution of this experimental variability around the model prediction, Figure 11.36 contains two cumulative distribution functions of experimental results within a small envelope of model predictions. As can be seen, characterising variability using log-normal distributions ought to provide reasonable approximations for probabilities at high gradients (based on the experimental data available).

Table 11.4 lists the probability of an experimental result being equal to the model prediction and the standard deviation from the experimental mean (assuming log-normal distributions). Figure 11.37 graphs the data listed in the table to illustrate this distribution. This Table and Figure suggest it is reasonable to characterise the log-normal distribution of variability using a mean = model prediction with a standard deviation of 0.3. This distribution can be used to inform the engineer of the probability of deviation from the predicted critical gradient as well as provide guidance on factors of safety needed to reach acceptable risk.

Regardless of the backward erosion piping model used, a sizeable factor of safety will be required, as with most geotechnical engineering design tasks, to account for the inherent

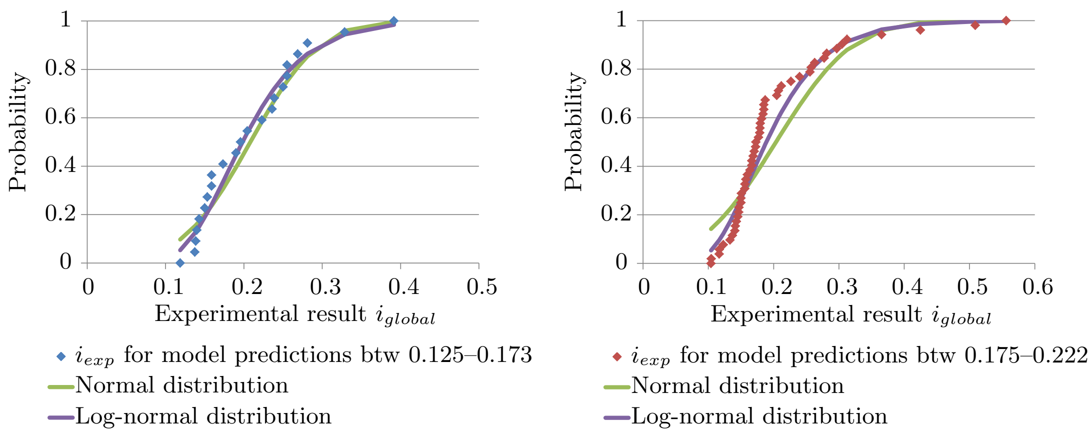

(a) Model predictions within 0.125–0.173 (b) Model predictions within 0.175–0.222

Figure 11.36: Cumulative distributions of experimental results within small envelopes of model predictions

Table 11.4: Distribution of experimental results around model predictions

Range of model predictions	Probability experiment = model	Standard deviation
0.125–0.173	19 %	0.317
0.175–0.222	56 %	0.369
0.226–0.276	56 %	0.276
0.282–0.329	51 %	0.281
0.340–0.390	46 %	0.221
0.392–0.439	71 %	0.377
average	49.8 %	0.3

variability.

11.3.4 Recommendations

When using the Sellmeijer et al. (2011) ‘standard dike’ formula it is recommended to:

- Use a White’s constant, η of 0.3 instead of the 0.25 used by Sellmeijer et al. (2011) as suggested by van Beek (2015) to be consistent with the findings of White (1940). This improved model predictions of slot tests carried out in this study on uniform Sydney Sand.
- Use an angle of repose based on d_{50} calculated using Equation 11.8 instead of the constant 37° as used by Sellmeijer et al. (2011), as suggested by van Beek (2015) to comply with the Shields (1936) approach. This improved model predictions of slot

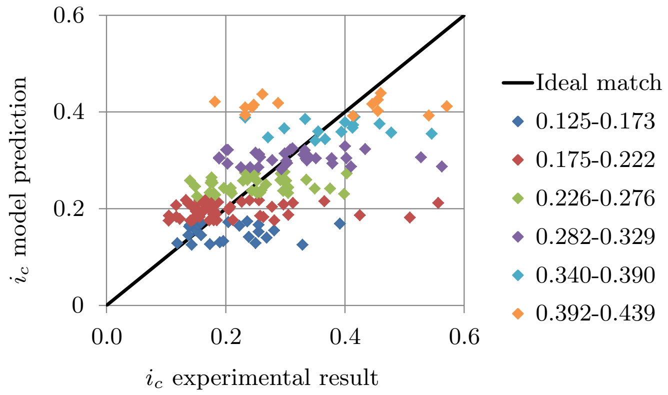

Figure 11.37: Illustration of distribution of experimental results across model predictions (series delineate model predictions within a range of 0.05)

tests carried out in this study on uniform Sydney Sand.

- Multiply model predictions with exit-geometry correction factors of 0.8 for circle exits and 1.2 for plane exits. This decreased/increased model predictions, which are based on the slot exit, closer to experimental results in circle and plane exits. A factor of 0.8 was applied to slope exit results from the van Beek et al. (2011a) study and 1.4 to slope exit results from this study. Further research into the affects of slope geometry is required before a universal correction factor for slope exits can be suggested.

- Use a C_u ratio exponent of 0.5 instead of the 0.13 currently contained within the Sellmeijer et al. (2011) Equation 2.14. This improved model predictions of non 'standard dike' soils.

- Use a d_{70} ratio exponent of 0.04 instead of the 0.6 currently contained within the Sellmeijer et al. (2011) Equation 2.14. This also improved model predictions of non 'standard dike' soils.

With the new exponents, Equation 2.14 becomes:

$$
\begin{aligned}
&\frac{H_c}{L} = \frac{1}{c} = F_R F_S F_G \\
&F_R = \eta \frac{\gamma_p'}{\gamma_w} \tan\theta_r \left(\frac{RD}{RD_m}\right)^{0.35} \left(\frac{C_u}{C_{u,m}}\right)^{0.5} \left(\frac{KAS}{KAS_m}\right)^{-0.02} \\
&F_S = \frac{d_{70}}{\sqrt[3]{\kappa L}} \left(\frac{d_{70,m}}{d_{70}}\right)^{0.04} \\
&F_G = 0.91 \left(\frac{D}{L}\right)^{\frac{0.24}{\left(\frac{D}{L}\right)^{2.8}-1}}
\end{aligned}
\tag{11.9}
$$

where F_R = resistance factor [-]

F_S = scale factor [-]

F_G = geometrical factor [-]

$\eta = 0.3$ = White's coefficient [-]

γ_p' = effective unit weight of particle [N/m^3]

$\theta_r = -8.125 \ln d_{50} - 38.777$ = angle of repose [°]

RD = relative density [-]

C_u = coefficient of uniformity [-]

KAS = roundness of particle [-]

κ = intrinsic permeability [m^2]

subscript$_m$ = mean value of experimental data set in Sellmeijer et al. (2011)

- Use a factor of safety when using the Sellmeijer et al. (2011) model in design. The factor of safety may be chosen to correspond with a probability of acceptable risk by assuming variability can be modelled using a log-normal distribution with a mean = model prediction and a standard deviation of 0.3. This log-normal distribution can also be used to estimate the risk of failure of an existing dam/levee.

11.4 Model comparison & Summary

As a summary and comparison tool, Table 11.5 lists how each model handles each of the attributes that are considered to affect the critical gradient. Also listed are suggested modifications and the coefficient of determination both before and after modifications.

As a final comparison between the two models, Figure 11.38 contains graphs of experimental results to model predictions for both models. When calculating model predictions, the suggested modifications provided herein were applied. When comparing the two models, care was taken to ensure the same data set was used. This meant that results which could not be predicted using the Sellmeijer et al. (2011) model (because permeability was not provided) were not predicted using the Schmertmann (2000) model either. This does leave assessment of the Schmertmann (2000) model at a slight disadvantage- because much of the data used by Schmertmann (2000) to formulate the model was not used in this comparison. However, even when the data used by Schmertmann (2000) was included in the calculation of R^2, it was still less than the R^2 of the Sellmeijer et al. (2011) model.

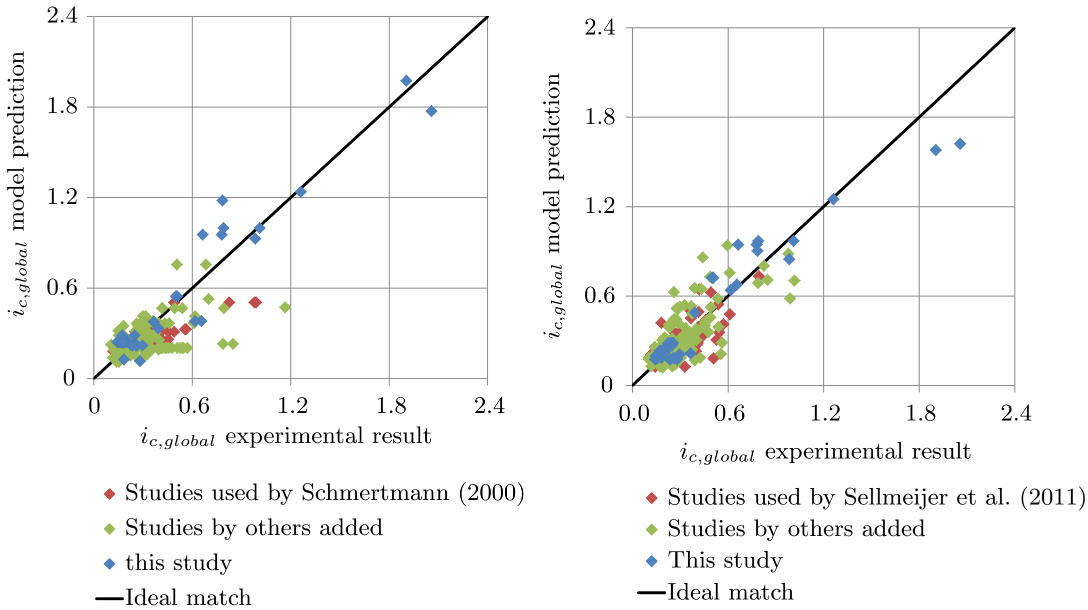

(a) Using the Schmertmann (2000) model (b) Using the Sellmeijer et al. (2011) model

Figure 11.38: Comparison of experimental results and model predictions for the two models

As can be seen in Table 11.5, the coefficient of determination (R^2) of the Schmertmann (2000) model was 0.66 and R^2 of the Sellmeijer et al. (2011) model was 0.75. Therefore the Sellmeijer et al. (2011) model predicted experimental results with more accuracy than the Schmertmann (2000) model. This is not to say that engineers need only use the Sellmeijer et al. (2011) model. Instead, it is suggested engineers determine the critical gradient using both models and assume the lowest gradient to be conservative.

It should be noted that even with use of the suggested corrections herein, engineers need to be aware of the simplifications and limitations of both models and practice engineering judgement accordingly. One such simplification is both models are based on laboratory experiments containing one homogeneous soil and therefore do not take into account anisotropic permeability, layering, soils fining upward, and other geomorphic features that can drastically affect the flow regime and the potential for backward erosion. Such properties have been shown to have great effects on BEP initiation and progression. These geomorphic features are particularly prevalent along meandering rivers (eg Mississippi and Sacramento in USA) but may be less so along the coastal levees of the Netherlands and areas of Florida.

Table 11.5: Comparison of how each variable is modelled and the resulting coefficient of determination before and after suggested amendments

	Sellmeijer et al. (2011)	Suggested revisions	Schmertmann (2000)	Suggested revisions
Depth	$F_G = 0.91\left(\frac{D}{L}\right)^{\frac{0.28}{(D/L)^{0}.28-1}+0.04}$	-	$C_D = \frac{(D/L)^{\left[\frac{0.2}{(D/L)^2-1}\right]}}{0.2^{\frac{0.2}{0.2^2-1}}}$	-
Length*			$C_L = (1.524/L)^{0.2}$	-
Grain size	$F_S = \frac{d_{70}}{\sqrt[3]{\kappa L}}\left(\frac{d_{70,m}}{d_{70}}\right)^{0.6}$	$F_S = \frac{d_{70}}{\sqrt[3]{\kappa L}}\left(\frac{d_{70,m}}{d_{70}}\right)^{0.04}$	$C_S = (d_{10}/0.2\text{mm})^{0.2}$	disregard
Permeability			-	-
Exit geometry	Nil (assumes slot)	Correction for circle and slope exit=0.8 Correction for plane exit=1.2	C_G	-
C_u	$\left(\frac{C_u}{C_{u,m}}\right)^{0.13}$ (contained in F_R)	$\left(\frac{C_u}{C_{u,m}}\right)^{0.5}$ (contained in F_R)	$i_{local,UoF} = 0.05 + 0.183(C_u - 1)$	$i_{local,UoF} = 0.14\mathrm{e}^{0.28C_u}$
Soil density	$\left(\frac{RD}{RD_m}\right)^{0.35}$ (contained in F_R)	-	$C_\gamma = 1 + 0.4(RD - 0.6)$	disregard
Rolling resistance	$\eta\frac{\gamma_p'}{\gamma_w}\tan\theta_r$ (contained in F_R) Where $\eta = 0.25$ and $\theta_r = 37°$	$\eta = 0.3$ and $\theta_r = -8.125\ln d_{50} - 38.777$	-	-
Roundness of particles	$\left(\frac{KAS}{KAS_m}\right)^{-0.02}$ (contained in F_R)	disregard	-	-
$i_{crit,global}$	$F_R F_S F_G$	-	$i_{local,UoF}.C_G.C_D.C_L.C_S.C_\gamma$	$i_{local,UoF}.C_G.C_D.C_L$
Coefficient of determination (R^2)	0.01	0.75	0.48	0.66

* length also incorporated in F_S factor in Sellmeijer et al. (2011) model

See Equations 2.18 and 11.9 for combined equations and symbol listing.

Chapter 12

Summary and recommendations

12.1 Summary of findings

This thesis presents a new comprehensive and extensive experimental programme conducted for backward erosion piping. A total of 92 large scale tests were conducted and explored the following variables, often for the first time in detail:

- Exit geometry;
- Soil density;
- Seepage length;
- Surcharge;
- Average particle size of soils;
- Well graded (and internally stable) soils;
- Silt fraction in soils;
- Cyclic loading;
- Erosion rate at critical gradient; and
- Erosion rate at gradients above critical.

Significant new insights into general backward erosion behaviour and the impact of several key variables have been presented in the preceding chapters. The following summarises the key findings and contributions made. These are organized based on the specific objectives presented in Chapter 1.

12.1.1 Exit Geometry

Objective 1: To verify the exit geometry effect reported by van Beek et al. (2013) whereby an increase in exit outflow area causes an increase in initiation and critical gradients. Then to quantify this effect with a more extensive suite of experiments not previously available, including all four exits in otherwise identical flumes. Lastly, to provide an explanation of the exit geometry effect with the use of numerical modelling.

In experiments, both the initiation and critical heads increased in the order of circle, slot, plane and slope as can be seen in Figure 6.12. This verified the exit geometry effect whereby an increase in exit outflow area causes an increase in gradients required. There was a 103% increase in initiation head and a 58% increase in critical head, from the minimum in the circle exit to the maximum in the slope exit.

It was also found that the maximum head (critical head) was required at initiation in slope and plane exits but required after a channel had formed in slot and circle exits, when the channel was approximately 5% and 30% of the seepage length respectively. This meant that channels in slope and plane exits continued to progress at their initiation gradients but channels in slot and circle exits stopped (i.e. reached equilibrium), requiring a raise in hydraulic head to re-initiate tip erosion.

Numerical modelling of the four exit geometries explained the exit geometry effect. The numerical model demonstrated that an increase in exit outflow area results in a decrease in local gradient at the exit. Therefore, the order of increasing local gradient caused by the exits was the inverse of increasing global initiation gradient needed. Considering local gradient at the exit determines seepage velocity at the exit (Darcy's Law) and seepage velocity at the exit provides the drag force needed for initiation, it was concluded that exit geometries which cause higher local gradients at the exit require lower global gradients to reach the minimum seepage velocity required to initiate a channel.

The numerical model also demonstrated that the circle exit causes a higher local gradient at the tip of the channel than the slot exit. This is why the circle exit requires a lower global critical gradient to generate the minimum seepage velocity at the channel tip needed to maintain tip progression.

12.1.2 Set-up variables

Objective 2: To investigate the influence experimental set-up had on the initiation and critical gradients in order to make informed decisions when selecting set-up variables and to aid in the interpretation of results. In particular, the aim was to quantify the effect soil density and seepage length had on gradients as well as investigate whether bladder pressure affected gradients and whether the uneven distribution of pressure imposed by the bladder influenced where backward erosion would occur.

Given the difficulty in measuring soil density, the effect of soil density on the initiation and critical gradients was not quantified. However, there were two experiments in less-dense soils which indicated lower initiation and critical gradients and experimental data from the studies of others were used to show a proportional relationship. This proportional relationship appeared to vary across different soil types and was often only slight, with variations due to soil density within the degree of expected experimental variability (refer to Figure 7.6).

Seepage length did not effect the initiation or critical gradients. When the seepage length was doubled from 1.3m to 2.6m and again to 3.9m, the initiation and critical heads also doubled each time, resulting in no change in gradients (refer to Figure 7.5).

The magnitude of pressure applied by the bladder did not affect the initiation or critical gradients. However, the pressure was still needed to ensure good contact between the sand and lid. Also, whilst it was confirmed that the bladder imposed less pressure along the edges of the flume (due to the bladder expanding less around the edges of the flume where it was fixed) it did not appear to influence where the channel formed or progressed.

12.1.3 Soil grading

Objective 3: To examine backward erosion piping in soils with uniformity coefficients (C_u) greater than 3 with the aims to:

- Determine initiation and critical gradients in poorly and well graded soils;

Eight poorly and well graded soils, with uniformity coefficients between 2.6 and 8.8, were tested. Initiation and critical gradients in all soils are plotted in Figure 8.18 with average values listed in Table 8.1. There appeared to be no discernible pattern or order in initiation gradients however, critical gradients increased in the order of Sydney Sand, Sibelco 50n, Mix 6, Mix 2, Mix 3, Mix 7, Mix 5, Mix 8, Mix 1 and Mix 4.

- Test well graded soils which are also internally stable in order to isolate the possible interference of internal instability from backward erosion.

Soil Mixes 1–5 were designed to be internally stable by keeping to probabilities of internal instability less than 0.3 as defined by the Wan and Fell (2007) method. Critical gradients observed in these soil mixes were significantly lower (up to 52% lower) than critical gradients in gap graded soils (susceptible to internal instability) tested by Townsend and Shiau (1986). In fact, Townsend and Shiau (1986) ended tests in these gap graded soils before critical gradients were reached, therefore, their true critical gradients are likely to be even higher. Hence, it appears internally stable soils are more susceptible to backward erosion than internally unstable soils. Though, internally unstable soils are more susceptible to other internal erosion issues such as suffusion.

- Ascertain the maximum C_u at which soil no longer fails by backward erosion in the laboratory;

A backward eroding channel did not appear to form in Mix 1 ($C_u = 6.8$) (although a short channel may have formed underneath the downstream box but not been visible through the turbid water) and whilst channels did form in Mix 4 ($C_u = 8.8$), they did not progress through to the upstream end despite high gradients of around 3 being applied for

1–2 days. Eventually the samples failed by sudden slips of the top soil layer. Therefore, it appears that soils with uniformity coefficients greater than 6.8 no longer failed by backward erosion in the laboratory. Notably though, Mixes 3 ($C_u = 6.2$) and 8 ($C_u = 6.4$) with uniformity coefficients similar to Mix 1, did fail by backward erosion, so susceptibility to backward erosion is likely to not be a function of uniformity coefficients alone but a combination of characteristics.

- Review the Schmertmann (2000) relation between local critical gradient and C_u; and

Having analysed critical gradients with C_u, it was found that the critical gradient increased with increasing C_u thereby confirming the trend suggested by Schmertmann (2000). However, a revised trendline which used an exponential curve fitted data more closely than the linear line suggested by Schmertmann (2000). This revised exponential trendline resulted in lower critical gradients around $\mathrm{C}_u = 6$ but higher gradients past a C_u of 8.

- Explore other possible relations between soil properties and the critical gradient.

It was observed that critical gradients increased exponentially with a decrease in permeability, for a constant tip width. It was also observed that the exponent required to shift the exponential curves to align with results in soils of other tip widths could be expressed as a function of tip width with a natural log relation. It was also found that tip width increased linearly with d_{50}. These three relations were combined to form a new empirical model with a coefficient of correlation of 0.95.

When compared with the coefficient of correlations achieved by the Schmertmann (2000) and Sellmeijer et al. (2011) models of 0.76 and 0.29 respectively, it can be seen this new model has potential. Though the model needs incorporation of scale and geometry effects before it can be used for field applications.

12.1.4 Cyclic and above critical loading

Objective 4: To test industry's concern that the critical gradient decreases with subsequent flood events by applying head to experiments in cycles. If the critical gradient does decrease, provide an explanation as to why and determine whether dams and levees are under greater risk when imposed by a series of flood events than when imposed by one longer-sustained flood.

Experiments confirmed the critical gradient did decrease with each loading cycle by averages of 2-13%. However, the critical gradient did not decrease because cyclic loading weakened the system, it decreased because permeability of the system increased as the channel lengthened. This was supported by the fact that head required when the 'decrease at points of interest' loading procedure was used also decreased. Interestingly, critical gradients required to re-initiate the tip with each loading cycle were higher than gradients needed under constant and 'decrease at points of interest' loading procedures.

Objective 5: To determine the rate of erosion at critical gradient and whether this rate increases with increase in gradient above critical in order to inform engineers on possible times to failure.

At critical gradient, the rate of erosion (speed of tip progression) was between 1.6–7.4mm/minute in Sydney Sand. At gradients above critical, this rate of erosion increased by a factor of 3 with each 10% increment in gradient above critical. Additional experiments would be required to determine rates of erosion in different soils, scales and geometries.

12.1.5 Review of existing models

Objective 6: To review the current, most widely used methods for predicting backward erosion- the Schmertmann (2000) and the Sellmeijer et al. (2011) methods. In doing so, the intention is to identify opportunities for improvement, particularly improvements which come to light as a result of having tested soils not previously tested (such as internally stable, well graded soils). Then develop these improvements in forms suitable for industry use.

The coefficient of determination between experimental results (from both this study and the studies of others) and model predictions was 0.48 when predictions were made using the Schmertmann (2000) method and 0.01 when predictions were made using the Sellmeijer et al. (2011) method.

Improvements which industry could readily apply were offered (summarised in the next section). These improvements saw the coefficient of determination increase to 0.66 when predictions were made using the Schmertmann (2000) method and 0.75 when predictions were made using the Sellmeijer et al. (2011) method.

12.2 Recommendations for industry

It is recommended industry use both the Schmertmann (2000) and Sellmeijer et al. (2011) methods to determine the critical gradient but adopt the lowest, more conservative gradient when designing against and assessing the risk of backward erosion piping. When using the Schmertmann (2000) and Sellmeijer et al. (2011) methods, it is recommended industry adopt the improvements suggested herein.

Improvements suggested for the Schmertmann (2000) method were as follows:

1. Use a 2-dimensional seepage model to determine the minimum local gradient (used in the calculation of C_G). If a 3-dimensional circle exit is being considered, model it as a slot exit, then factor the predicted critical gradient down by 0.8.
2. Do not apply C_S or C_γ because these factors did not improve performance of the model over the suite of laboratory experiments considered.
3. Use the exponential relationship for the critical local gradient with C_u in Equation 11.7 instead of the linear relationship suggested by Schmertmann (2000).

Improvements suggested for the Sellmeijer et al. (2011) method were as follows:

1. Use a White's constant, η of 0.3 and an angle of repose based on d_{50}, using Equation 11.8.

2. Multiply model predictions with exit-geometry correction factors of 0.8 for circle exits and 1.2 for plane exits.

3. Use a C_u ratio exponent of 0.5 (instead of 0.13) and a d_{70} ratio exponent of 0.04 (instead of 0.6) in the Sellmeijer et al. (2011) equation for critical gradient (Equation 11.9).

It is also recommended that the log-normal distributions of experimental results across model predictions be used to determine probability when choosing the required factor of safety for design or likelihood of failure. The mean of both log-normal distributions are the critical gradients predicted by the methods and their standard deviations are provided in Chapter 11.

Critical gradients estimated using the Schmertmann (2000) and Sellmeijer et al. (2011) methods are not only sufficient but also conservative under cyclic loading conditions.

Lastly, it is recommended to increase permeability of soil beneath and around the exit when using numerical techniques to evaluate seepage velocity through a foundation. This accounts for the dilation of the soil at the exit when it fluidises and heaves and also reduces the impact of the discontinuity in the Laplace derivatives at the exit. Indication of head levels in the foundation, once a sand boil has formed, are required to determine the degree of permeability increase needed.

12.3 Recommendations for further research

There are five main items recommended for further research: the incorporation of scale and geometry effects into the new empirical model developed in this study (Equation 8.1); investigation into attributes of the slope exit which appear to affect the critical gradient (as evident by varying slope correction factors); development of a method to measure and/or a numerical model to provide seepage velocities at the exit and into the channel tip; understanding of the detachment mechanism both at the exit upon initiation and at the tip of the channel; and quantification of the effect of scale and soil grading on tip progression speed.

Both the Schmertmann (2000) and Sellmeijer et al. (2011) methods factor in the inversely proportional relationship between depth and the critical gradient using the D/L ratio. However, critical gradient is independent of seepage length (see Figure 7.8 and de Wit (1984)) so it is inappropriate to use a D/L ratio when quantifying the influence of depth. In order to determine the relationship between depth and the critical gradient, it is recommended addition experiments be undertaken across a range of different flume depths with all else equal. De Wit (1984) did carry out such experiments (although length was varied to keep a constant D/L ratio) which indicated $i_c \propto D^{-0.6}$ (see Figure 11.10) however, results from this study did not plot along the same curves in Figure 11.10 (at a depth of 0.3m) despite similar flume width, soil and exit geometry. This casts concern with relying on the de Wit (1984) alone for the depth relationship. It is possible gradients from the de Wit (1984) study were abnormally high as the channel could not be seen (due to an overlying clay layer), leaving interpretation of boil activity alone to determine when critical was reached.

It is also recommended addition experiments be undertaken across a range of different flume widths, with all else equal, because scale is also a function of width. Combined, the depth and width quantifies the seepage flux area which controls the volume of flow and therefore the volume of flow (and hence seepage velocities) entering the channel tip. Experiments across 4 different flume widths were carried out by Vandenboer et al. (2014a) which demonstrated $i_c \propto \mathrm{e}^{-3.5W}$. However, a matching set of experiments with a varying depth is also needed (so the two relationships can be combined) and the maximum extent of the flume width which no longer causes a change in critical gradient was not investigated. The maximum extent of width influence is required to determine the lateral zone of influence an eroding channel has on seepage flow. This maximum width of influence would then be used in field assessments. It is noted though that slot-exit-flumes would be needed in such an investigation, because a flume with a circle exit increasing in width would always cause lower gradients as more flow is forced to leave through the only pre-formed exit.

The combined relationship of the influence of depth and width on the critical gradient could then potentially be incorporated into the new empirical model developed in this study (Equation 8.1) to include the effect of scale making it feasible for use in field application.

In Chapter 11 it was demonstrated that the Sellmeijer et al. (2011) equation for a 'standard dike configuration' accurately predicted experimental results in slots exits and by finding the average ratio of results in slots to results in other exit geometries, correction factors for the other three exit geometries could be calculated. However, experimental results in slope exits from this study produced a correction factor of 1.4 but when results from van Beek et al. (2011a) were included, the correction factor reduced to 0.8. Therefore it appears there are attributes of the two different slope set-ups that are affecting the critical gradient which need to be better understood and accounted for before a slope correction factor can be developed.

The current hypothesis is particle detachment occurs when seepage velocity is sufficient enough to impose the necessary drag forces, both at the exit for initiation and at the channel tip for progression. If this is the case then perhaps seepage velocity would be a better indicator of initiation and continued progression rather than the currently used global gradient. The use of a critical seepage velocity would overcome the issue encountered with gradients whereby several correction factors are needed to incorporate effects not captured by the gradient. Whereas all effects would be incorporated into the seepage velocity calculation. However, there is currently no known way to measure seepage velocity at the exit or into the channel tip in experiments, nor is there a known numerical model that provides these velocities. Therefore, it is recommended methods for measuring these velocities and/or a numerical model capable of providing these velocities be pursued and developed as part of further research.

For a numerical model to provide accurate seepage velocities at both the exit and into the channel tip, it would need to be 3-dimensional and include a channel. It would also need to include compensation for the singularity at exits and possibly also at the channel tip or use a different governing equation or method that does not become discontinuous at these locations. Reflections on how the critical seepage velocity could be determined is given in Section 10.4, as is other recommendations for future work on numerical modelling.

Currently, there are numerous theories and practices within the literature when modelling particle detachment. These theories and practices vary in both where detachment is assumed to occur (from the channel bed, sides or tip) and how the detachment is modelled (using continuum or discrete models). There is also contention over whether upward seepage lifts and mobilises particles. Measurement or modelling of the critical seepage velocity would go towards identifying the appropriate detachment mechanism occurring at both the exit for initiation and at the channel tip for progression.

Whilst tip progression speeds (i.e. erosion rates) were determined for Sydney Sand in flumes containing the circle exit at both the critical gradient and at gradients above critical, they were not determined in other soils or in flumes containing other exits. It was observed that tip progression speeds were faster in slope and plane exits than slot and circle exits and it was observed that tip progression speeds were steady in uniform soils but fast and intermittent in well graded soils, often eroding in sudden bursts. However, these changes in tip progression speeds were not quantified but could be done so for further research using laboratory notes included in Appendix A.

It is not known whether tip progression speed is affected by scale, i.e. whether a tip progresses at a unique, soil-specific speed regardless of the critical gradient required. This means it is not known whether the tip progression speeds obtained in this study can be used as an indication of tip progression speed in the field (in similar soil and exit geometry). Therefore, laboratory testing which measures tip progression speed in set-ups of various depth/width ratios and scales is recommended for further research. Estimations of tip progression speeds in the field would enable time-to-failure estimates. They would also enable estimation of the length of channels remaining dormant after past floods (if past flood levels and durations are known) thereby providing an indication of how many more flood events a given dam/levee system could withstand in the future before failing.

Bibliography

Australian National Committee on Large Dams (2003). *Guidelines on Risk Assessment.* Australian National Committee on Large Dam Inc.

Baldock, T. E. and Holmes, P. (1999). Seepage effects on sediment transport by waves and currents. In *Proceedings of the 26th International Conference on Coastal Engineering*, pages 3601–3614, Coppenhagen. ASCE, Reston, VA.

Baldock, T. E. and Nielsen, P. (2010). Discussion of "Effect of Seepage-Induced Nonhydrostratic Pressure Distribution on Bed-Load transport and bed morphodynamics" by Simona Francalanci, Gary Parker, and Luce Solari. *Journal of Hydraulic Engineering*, 136:77–79.

Bezuijen, A. and Steedman, R. (2010). Scaling of hydraulic processes. In Springman, S., Laue, J., and Seward, L., editors, *Physical modelling in geotechnics (ICPMG)*, volume 1, pages 93–98, London. Taylor & Francis Group.

Bligh, W. G. (1910). Dams, barrages and weirs on porous foundations. *Engineering News*, 64(26):708–710.

Bonelli, S., Olivier, B., and Damien, L. (2007). The scaling law of piping erosion. In *18th Congres Francais de Mechanique*, Grenoble.

Burenkova, V. (1993). Assessment of suffusion in non-cohesive and graded soils. In *Filters in Geotechnical and Hydraulic Engineering, Preceedings of the First International Conference "Geo-Filters"*, pages 357–360, Rotterdam. Balkema.

Carrier, W. D. (2003). Goodbye, Hazen; Hello, Kozeny-Carman. *Journal of Geotechnical and Geoenvironmental Engineering*, 129(11):1054–1056.

Cheng, N.-S. and Chiew, Y.-M. (2010). Incipient sediment motion with upward seepage. *Journal of Hydraulic Research*, 37(5):665–681.

de Wit, J. (1984). Onderzoek zandmeevoerende wellen. Report, Laboratorium voor grondmechanica Delft, Delft.

de Wit, J., Sellmeijer, J., and Penning, A. (1981). Laboratory testing on piping. In Publications Committee of X.ICSMFE, editor, *Tenth International Conference on Soil Mechanics and Foundation Engineering*, pages 517–520, Stockholm. A.A. Balkema.

Dennee, S. L. (2011). The Paducah Sun, Washington Post [Accessed: http://www.geologyinmotion.com/2011/06/missouri-levee-boil-forces-evacuations.html].

Ding, L., Yao, Q., and Sun, D. Y. (2007). Experimental studies on piping development in three-stratum dike foundations. *Water Resources and Hydropower Engineering*, 38(2):19–22.

Fang, H., Shang, Q., Chen, M., and He, G. (2014). Changes in the critical erosion velocity for sediment colonized by biofilm. *Sedimentology*, 61(3):648–659.

Fell, R. (2012). Backward erosion piping in cohesionless soils in dams, levees and their foundations, Outline of proposed research.

Fell, R., Foster, M., Cyganiewicz, J., Sills, G. L., Vroman, N., and Davidson, R. (2008). Risk Analysis for Dam Safety. A Unified Method for Estimating Probabilities of Failure of Embankment Dams by Internal Erosion and Piping, Guidance Document, Delta Version, Issue 2, USDI Bureau of Reclamation, USACE, UNSW, URS.

Fell, R. and Fry, J.-J. (2007). The state of the art of assessing the likelihood of internal erosion of embankment dams, water retaining structures and their foundations. In Fell, R. and Fry, J.-J., editors, *Internal erosion of dams and their foundations*, pages 1–23. Taylor & Francis Group, London.

Fell, R., MacGregor, P., Stapledon, D., and Bell, G. (2005). *Geotechnical Engineering of Dams*. Taylor & Francis Group, London.

Forward, B. (2014). *Backward Erosion Piping in well-graded cohesionless soils*. Honours thesis, School of Civil and Environmental Engineering, Faculty of Engineering, UNSW Australia, Sydney.

Foster, M. and Fell, R. (1999). A framework for estimating the probability of failure of embankment dams by internal erosion and piping using event tree methods. Uniciv report no. r-377, The University of New South Wales, Sydney.

Foster, M., Fell, R., and Spannagle, M. (2000a). A method for estimating the relative likelihood of failure of embankment dams by internal erosion and piping. *Canadian Geotechnical Journal*, 37(5):1025–1061.

Foster, M., Fell, R., and Spannagle, M. (2000b). The statistics of embankment dam failures and accidents. *Canadian Geotechnical Journal*, 37(5):1000–1024.

Foster, M., Spannagle, M., and Fell, R. (1998). Report on the analysis of embankment dam incidents. Uniciv report no. r-374, The University of New South Wales, Sydney.

Fujisawa, K., Sakai, K., and Murakami, A. (2014). Numerical analysis of seepage-induced erosion of soils by solving the Darcy-Brinkman equations. In Cheng, L., Draper, S., and An, H., editors, *Proceedings of the 7th International Conference on Scour and Erosion*, pages 381–387, Perth. CRC Press.

GEO-SLOPE International Ltd (2016). Seepage Exit Gradients. Example file, Retrieved from http://downloads.geo-slope.com/geostudioresources/7/examples/exit%20gradient.pdf, Calgary.

Girgus, R. (1977). *Transport of fine bed sand by laminar and turbulent water flows*. PhD thesis, University of London.

Glynn, M. E. and Kuszmaul, J. (2004). Prediction of piping erosion along middle Mississippi River levees-an empirical model. Report ERDC/GSL TR-04-12, USACE, Engineer Reseach and Development Center, Geotechnical and Structures Laboratory, ERDC/GSL TR-04-12.

Greenlees, A. M. (2016). *Backward Erosion Piping*. Honours thesis, School of Civil and Environmental Engineering, University of New South Wales, Sydney.

Griffith, W. M. (1913). The stability of weir foundations on sand and soil subject to hydrostatic pressure. *Minutes of Proceedings, Institute of Civil Engineers*, 197(III):221.

Hanses, U. (1985). *Zur mechanik der entwicklung von erosionskanälen in geschichtetem untergrund unter stauanlagen*. PhD thesis, Grundbauinstitut der Technischen Universität Berlin.

Hanses, U., Müller-Kirchenbauer, H., and Savidis, S. (1985). Mechanics of Backward Erosion Under Dikes and Dams. *Bautechnik*, 62(5):163–168.

Henderson, F. (1966). *Open channel flow*. Macmillan Publishing Co. Inc., New York.

Hoffmans, G. (2009). Backward erosion in cohesionless soils beneath dikes. *Journal of Hydraulic Engineering*, manuscript.

Hoffmans, G. (2014). An overview of piping models. In Cheng, L., Draper, S., and An, H., editors, *Proceedings of the 7th International Conference on Scour and Erosion*, pages 3–18, Perth. CRC Press.

Hoffmans, G. (2016). Shields-Darcy model. Project: 1220240-000, Deltares, Delft.

Holtz, R. D., Kovacs, W. D., and Sheahan, T. C. (2011). *An introduction to geotechnical engineering*. Pearson Education Inc., Upper Saddle River, 2nd edition.

ICOLD (2015). Internal erosion of existing dams, levees, and dikes, and their foundations. Bulletin 164, International Commission on Large Dams, Paris.

Keizer, R., Rice, J., and Jaeger, R. (2016). An empirical model for estimating internal erosion critical gradients for inclined exit face conditions. In *36th Annual USSD Conference*, pages 909–926, Denver, Colorado.

Koenders, M. A. and Sellmeijer, J. (1992). Mathematical Model for Piping. *Journal of Geotechnical Engineering*, 118(6):943–946.

Kohno, I., Nishigaki, M., and Takeshita, Y. (1987). Levee Failure caused by seepage and preventive measures. *Natural Disaster Science*, 9(2):55–76.

Kramer, R. (2014). *Piping under transient conditions*. PhD thesis, University of Twente, Enschede.

Krumbein, W. and Sloss, L. (1963). *Stratigraphy and Sedimentation*. Freeman & Co., 2nd edition.

Lane, E. W. (1935). Security from underseepage- masonry dams on earth foundations. *Transactions of the American Society of Civil Engineers*, 100:1235–1272.

Liang, Y., Wang, J.-j., and Liu, M.-w. (2013). Two-flow model for piping erosion based on liquid-solid coupling. *Journal of Central South University*, 20:2299–2306.

Mantz, P. (1977). Incipient transport of fine grains and flakes by fluids. *Journal of the Hydraulics Division*, 103:601–615.

Marot, D., Alexis, A., and Bendahmane, F. (2005). A specific triaxial device for the study of internal erosion on cohesive soils. In *Workshop on Internal Erosion of Embankment Dams and their Foundations*. Balkema.

Martin, C. (1970). Effect of a porous sand bed on incipient motion. *Water Resources Research*, 6(4):1163.

McCook (2011). A discussion of uplift and exit gradient terminology and factors of safety. In *Dam Safety 2011*, Washington D.C. Association of State Dam Safety Officials, Inc.

Miesel, D. (1978). Rückschreitende erosion unter bindiger deckschicht. In *Baugrundtagung*, pages 599–626.

Molendijk, W., van der Zon, W., and van Meurs, G. (2009). SmartSoils, Adaption of soil properties on demand. In Hamza, M., Shahien, M., and El-Mossallamy, Y., editors, *Proceedings of the 17th International Conference on Soil Mechanics and Geotechnical Engineering*, pages 2443–2446, Alexandria, Egypt. IOS Press.

Müller-Kirchenbauer, H. (1978). Zum zeitlichen verlauf der rückschreitenden erosion in geschichtetem untergrund unter dämmen und stauanlagen. In *Talsperren-Symposium*, pages 1–25.

Müller-Kirchenbauer, H., Rankl, M., and Schlötzer, C. (1993). Mechanism for regressive erosion beneath dams and barrages. In Brauns, J., Heibaun, M. H., and Schuler, U., editors, *Filters in Geotechnical and Hyrdualic Engineering: proceedings of the first international conference "Geo-Filters"*, pages 369–376, Karlsruche Germany. Balkema.

Nikuradse, J. (1933). Tech. Rep. NACA Technical Memorandum 1292. In *Stromungsgesetz in rauhren rohren, VDI Forschungshefte 361 (English translation: Laws of flow in rough pipes)*. USA: National Advisory Commission for Aeronautics. (1950), Washington D.C.

Ojha, C. S. P., Singh, V. P., and Adrian, D. D. (2003). Determination of critical head in soil piping. *Journal of Hydraulic Engineering*, 129(7):511–518.

Olsen, J. A., MacDougall, A. T., and Huzjak, R. J. (2014). REV and exit gradients- using the representative elementary volume to improve the calculation of exit gradients in seepage evaluations. In *Dam Safety 2014*, San Diego. Association of State Dam Safety Officials, Inc.

Omnova Solutions (2017). 'Pliolite VTAC-L'. Retrived from https://www.omnova.com/products/\\ chemicals/pliolite/vtac-l (Feb. 21, 2017).

Pabst, M., Robbins, B. A., Engemoen, W. O., Hannenman, D., Redlinger, C., and Scott, G. (2013). Heave, uplift & piping at the toe of embankment dams. *The Journal of Dam Safety*, 11(2):21–31.

Paintal, A. (1971). Concept of critical shear stress in loose boundary open channels. *Journal of Hydraulic Research*, 9(1).

Pietrus, T. (1981). *An experimental investigation of hydraulic piping in sand.* Masters thesis, Department of Civil Engineering, University of Florida, Gainesville.

Ren, X., Zhao, Y., Deng, Q., Kang, J., Li, D., and Wang, D. (2016). A relation of hydraulic conductivity void ratio for soils based on Kozeny-Carman equation. *Engineering Geology*, 213:89–97.

Rice, J. D., Ibrahim, I. A., Keizer, R. A., and Jaeger, R. A. (2016). Laboratory investigation of backward erosion piping - effects of inclined exit face and constricted seepage exits. In *8th International Conference on Scour and Erosion*, pages 491–497, London. Taylor & Francis Group.

Rietdijk, J., Schenkeveld, F. M., Schaminee, P. E. L., and Bezuijen, A. (2010). The drizzle method for sand sample preparation. In Springman, S., Laue, J., and Seward, L., editors, *Physical modelling in geotechnics (ICPMG)*, volume 1, pages 267–272, London. Taylor & Francis Group.

Robbins, B. A. and Sharp, M. K. (2016). Incorporating uncertainty into Backward Erosion Piping risk assessments. In *3rd European Conference on Flood Risk Management*, Lyon.

Schmertmann, J. (1995). Report on flume tests for piping and scour erosion of HL-2 sands. File no. 966.

Schmertmann, J. (2000). The no-filter factor of safety against piping through sands. In Silva, F. and Kavazanjian, E., editors, *Judgement and innovation: the heritage and future of the geotechnical engineering profession (Geotechnical Special Publication No. 111)*. ASCE, Reston.

Sellmeijer, J. (1988). *On the mechanism of piping under imprevious structures*. PhD thesis, Delft University of Technology, Delft.

Sellmeijer, J. (2006). Numerical computation of seepage erosion below dams (piping). In *Third International Conference on Scour and Erosion*, Gouda. CURNET.

Sellmeijer, J. (2009). Mechanism of piping. (presentation), Deltares, Delft.

Sellmeijer, J., Calle, E., and Sip, J. W. (1989). Influence of aquifier thickness on piping below dikes and dams. In *International Symposium on Analytical Evaluation of Dam Related Safety Problems, Volume 1*, page 357, Copenhagen. Danish National Committee on Large Dams.

Sellmeijer, J. and Koenders, M. A. (1991). A mathematical model for piping. *Appl. Math. Modelling*, 15:646–651.

Sellmeijer, J., Lopez de la Cruz, J., van Beek, V., and Knoeff, J. G. (2011). Fine-tuning of the backward erosion piping model through small-scale, medium-scale and IJkdijk experiments. *European Journal of Environmental and Civil Engineering*, 15(8):1139–1154.

Shewbridge, S. (2016). USACE levee research, design and performance history: internal erosion and risk-informed levee design. In *USSD International Symposium on the mechanics of internal erosion for dams and levees*, Salt Lake City.

Shields, A. (1936). Anwendung der aehnlichkeitsmechanik und der terbulenzforschung auf die geschiebebewegung.

Sills, G. L. and Vroman, N. (2007). A review of Corps of Engineers levee seepage practices in the United States. In Fell, R. and Fry, J.-J., editors, *Internal Erosion of Dams and their Foundations*, pages 209–218. Taylor Francis, London.

Silvis, F. (1991). Verificatie piping model; proeven in de deltagoot. Evaluatierapport, GeoDelft, Delft.

Sobolewski, M. (2002). *Determination of flow water characteristic in cohesive soils on the basis in situ tests.* PhD thesis, Dep. Geoengineering, SGGW, Warsaw.

Sun, B. C.-B. (1989). *Internal stability of clayey to silty sands.* Phd, University of Michigan, Ann Arbor.

Technical Advisory Committee on Flood Defences (1999). Technical report on sand boils (piping). Technical Report draft English version, Delft, The Netherlands.

Terzaghi, K. and Peck, R. (1948). *Soil mechanics in engineering practice.* Wiley, New York.

Townsend, F., Bloomquist, D., Shiau, J.-M., Martinez, R., and Rubin, H. (1988). Analytical and experimental evaluation of piping and filter design for sands. Technical report, Department of Civil Engineering, University of Florida, Gainesville.

Townsend, F., Schmertmann, J., Logan, T., Pietrus, T., and Wong, Y. (1981). An analytical and experimental investigation of a quantitative theory for piping in sand. Technical report, Department of Civil Engineering, College of Engineering, University of Florida, Gainesville.

Townsend, F. and Shiau, J.-M. (1986). Analytical and experimental evaluation of piping and filter design for sands. Technical report, Department of Civil Engineering College of Engineering, University of Florida, Gainesville.

U.S. Department of the Interior Bureau of Reclamation and U.S. Army Corps of Engineers (2015). Internal Erosion Risks for Embankments and Foundations. In *Best practives in dam and levee safety risk analysis.*

van Beek, V. (2015). *Backward erosion piping: initiation and progression.* PhD thesis, Delft University of Technology, Delft.

van Beek, V., Bezuijen, A., and Schemkeveld, F. (2012a). Piping in loose sands- the importance of geometrical fixation of grains. In Bezuijen, A., Lottum, and Dijkstra, editors, *2nd European conference on pysical modelling in geotechnics (Eurofuge)*, pages 1–10. TU Delft.

van Beek, V., Bezuijen, A., and Sellmeijer, J. (2013). Backward Erosion Piping. In Bonelli, S. and Nicot, F., editors, *Erosion in Geomechanics Applied to Dams and Levees*, pages 193–269. John Wiley & Sons, Inc., Hoboken.

van Beek, V., Bezuijen, A., and Zwanenburg, C. (2010a). Piping: Centrifuge experiments on scaling effects and levee stability. In Springman, S., Laue, J., and Seward, L., editors, *Physical modelling in geotechnics (ICPMG)*, volume 1, pages 183–189, London. Taylor & Francis Group.

van Beek, V., Knoeff, J. G., de Bruijn, H. T. J., and Sellmeijer, J. (2009). Influence of sand characteristics on the piping process- small-scale experiments. In *International workshop in internal erosion in dams and foundations*, page 9, St. Petersburg.

van Beek, V., Knoeff, J. G., Rietdijk, J., Sellmeijer, J., and Lopez De La Cruz, J. (2010b). Influence of sand and scale on the piping process - Experiments and multivariate analysis. In Springman, S., Laue, J., and Seward, L., editors, *Physical modelling in geotechnics (ICPMG)*, volume 2, pages 1221–1226, London. Taylor & Francis Group.

van Beek, V., Knoeff, J. G., and Sellmeijer, J. (2011a). Observations on the process of backward piping by underseepage in cohesionless soils in small, medium and full-scale experiments. *European Journal of Environmental and Civil Engineering, Erosion in Geomaterials*, 15(8):1115–1137.

van Beek, V., Koelewijn, A., Kruse, G., Sellmeijer, J., and Barends, F. (2008). Piping phenomena in heterogeneous sands- experiments and simulations. In Sekiguchi, H., editor, *4th International Conference on Scour and Erosion*, pages 453–459, Tokyo. The Japanese Geotechnical Society.

van Beek, V., Rietdijk, J., Luijendijk, M., and Barends, F. (2011b). Influence of vertical loading on underseepage piping in uniform sand. In *Internal erosion in embankment dams and their foundations, Proceedings of the Institute of Water Structures, FCE, BUT, Brno, Vol.13*, pages 233–234.

van Beek, V., Vandenboer, K., and Bezuijen, A. (2014a). Influence of sand type on pipe development in small- and medium-scale experiments. In Cheng, L., Draper, S., and An, H., editors, *Proceedings of the 7th International Conference on Scour and Erosion*, pages 111–120, Perth. CRC Press.

van Beek, V., Vandenboer, K., van Essen, H., and Bezuijen, A. (2014b). Investigation of the backward erosion mechanism in small scale experiments. In Gaudin, C. and White, D., editors, *Physical Modelling in Geotechnics (ICPMG)*, pages 855–861, London. Taylor & Francis Group.

van Beek, V., Yao, Q., Van, M., and Barends, F. (2012b). Validation of Sellmeijer's model for backward piping under dikes on multiple sand layers. In *International Conference on Scour and Erosion*, pages 543–550, Paris.

van der Zee, R. (2011). *Influence of sand characteristics of the piping process- research to the influence of grain size and other sand characteristics on the critical head of piping.* Masters thesis, Delft University of Technology, Delft.

van Rhee, C. and Bezuijen, A. (1992). Influence of seepage of stability of sandy slope. *Journal of Geotechnical Engineering*, 118(8).

van Rijn, L. (2014). Review of piping processes and models. Report for deltares, www.leovanrijn-sediment.com.

Vandenboer, K., Bezuijen, A., and van Beek, V. (2014a). 3D character of backward erosion piping: Small-scale experiments. In Cheng, L., Draper, S., and An, H., editors, *Proceedings of the 7th International Conference on Scour and Erosion*, pages 81–86, Perth. CRC Press.

Vandenboer, K. and van Beek, V. (2013). Physical erosion mechanism of the progression of backward erosion piping. In *EWGIE Annual Meeting*, Vienna.

Vandenboer, K., van Beek, V., and Bezuijen, A. (2014b). 3D finite element method (FEM) simulation of groundwater flow during backward erosion piping. *Frontiers of Structural and Civil Engineering*, 8(2):160–166.

Wan, C. F. and Fell, R. (2007). Investigation of internal erosion by the process of suffusion in embankment dams and their foundations. In Fell, R. and Fry, J., editors, *Internal erosion of dams and their foundations*, pages 219–234. Taylor & Francis, London.

Weijers, J. B. A. and Sellmeijer, J. (1993). A new model to deal with the piping mechanism. In Brauns, J., Schuler, U., and Heibaun, M. H., editors, *Filters in Geotechnical and Hydraulic Engineering: proceedings of the first international conference "Geo-Filters"*, pages 349–355, Karlsruche Germany. Balkema.

White, C. (1940). The equilibrium of grains on the bed of a stream. *Proceedings of the Royal Society of London. Series A, Mathematical and Physical Sciences*, 174:322–338.

Wolff, T. F. (2002). Performance of levee underseepage controls: a critical review. Report ERDC/GSL TR-02-19, US Army Corps of Engineers, Engineer Research and Development Center, East Lansing.

Yalin, M. and Karahan, E. (1979). Inception of sediment transport. *Journal of the Hydraulics Division*, 105(HY11):1433–1443.

Yao, Q., Ding, L., Sun, D., Liu, C., and Zhang, Q. (2007). Experimental studies on piping in single-and-two-stratum dike foundations. *Water Resources and Hydropower Engineering*, 38(2):19–22.

Zhou, X.-j., Jie, Y.-x., and Li, G.-x. (2012). Numerical simulation of the developing course of piping. *Computers and Geotechnics*, 44:104–108.

Glossary & acronyms

BEP Backward erosion piping.

Channel A space void of soil, as a result of erosion, forming a long, shallow and narrow corridor along which eroded soil is transported downstream. Also referred to as a pipe (and as a slit by Sellmeijer (1988)).

Critical channel length Length of channel when critical head is needed.

Critical gradient Critical head divided by the total seepage length (may also be referred to as the *global* critical gradient). This is usually the maximum global gradient applied during an experiment.

Critical head Minimum hydraulic head difference required to progress the channel through to the upstream end. This is usually the maximum hydraulic head difference applied during an experiment.

d/s Downstream.

Exit Outlet at the downstream end where particles are transported out of and where the backward eroding channel starts.

FEM Finite element analysis.

Global gradient Change in hydraulic head from upstream to downstream divided by the seepage length.

Heave gradient Local gradient which causes zero effective stress throughout a vertical shaft of soil (when, at the base of a vertical shaft of soil, the weight of soil above it is equal and opposite to the seepage force below it). Defined by Terzaghi and Peck (1948) as $\rho'/\rho_w \approx 1$. Throughout literature, this is commonly referred to as the 'critical gradient' but referred to here as the heave gradient to differentiate it from the critical gradient required for backward erosion piping.

Initiation gradient Initiation head divided by the total seepage length (may also be referred to as the *global* initiation gradient).

Initiation head Minimum hydraulic head difference required to trigger the onset of particles leaving the sand matrix, at the exit, and start the backward eroding channel.

Local critical gradient Local gradient into the tip of the channel required to progress the channel past the critical channel length and through to the upstream end.

Local gradient Change in hydraulic head between two points divided by the seepage length between said points.

Local initiation gradient Local gradient at the exit required to start the backward eroding channel.

POI 'Points of interest' included 25, 50, 70, 80 and 90% of the seepage length.

Progression head Minimum hydraulic head required to continue tip progression at a given location (and was therefore a function of channel length).

Sheet flow A mode of sample failure in experiments whereby the top surface of soil suddenly slipped downstream across a wide area. Also referred to as surface slip. This was not a process of backward erosion piping.

UoF University of Florida.

u/s Upstream.

USACE United States Army Corps of Engineers

WRL Water Research Laboratory

Notation and Units

Table 1: Notation and units

Symbol	Units	Description
c	-	erosion coefficient
C_G	-	Schmertmann's gradient correction factor for parallel flow
C_L	-	Schmertmann's length correction factor
C_S	-	Schmertmann's grain size correction factor
C_u	-	Coefficient of uniformity $= d_{60}/d_{10}$
C_γ	-	Schmertmann's density correction factor
D	m	Flume or erodible layer depth
d	m	Particle diameter
dx	mm	Grid spacing in numerical model
f	-	Friction factor
g	m/s^2	Gravity
H or h	m	Hydraulic head
i	-	Hydraulic gradient
i_{pmt}	-	Critical local gradient in UoF test set-up (also referred to as $i_{local,UoF}$)
k or K	m/s	Permeability
KAS	-	Roundness of particle
L	m	Seepage length
l	m	Channel length
n	-	porosity
Q	m^3/s	Flow
q	m^3/s	Flux
R^2	-	Coefficient of determination
RD	-	Relative density (%)
Re	-	Reynolds number
u	kPa	Pore pressure
v	m/s	velocity
W	m (or -)	Flume width (or depth to length correction factor in Subsection 11.2.3 only)

Table 1: Notation and units (continued)

Symbol	Units	Description
x	m	Distance in x-direction (or generic unknown)
y	m	Distance in y-direction
z	m	Distance in x-direction
γ	kN/m^3	Unit weight
Δ	-	Difference in OR relative density = $(\rho_p/\rho_w - 1)$
δ	-	Partial derivative
η	-	White's coefficient
θ or θ_r	$^\circ$	angle of repose or bedding angle
κ	m^2	Intrinsic permeability
ν	m^2/s	Kinematic viscosity
ρ	kg/m^3	Density
σ	kPa	Total stress
τ	kPa	Shear stress
∇	-	Del operator
Subscripts		
10		10% of the soil by weight is finer than
50		50% of the soil by weight is finer than
60		60% of the soil by weight is finer than
70		70% of the soil by weight is finer than
c		critical
exp		Experiment
i		initiation
L		Loss
m		mean
p		particle
UoF		University of Florida
w		water
x		in x-direction
y		in y-direction
z		in z-direction
$*$		dimensionless

Appendix A: Test data and reports

This appendix firstly contains a brief account of Tests 1 to 15 in Table A. These tests were unsuccessful for reasons explained in the table. Test data sheets and reports of all remaining tests can be found in the enclosed USB disk.

The following abbreviations were used in test data sheets:

ae after exit

ab1/ab2/ab3/ab4 after bar 1, 2, 3 or 4

123–124 A 3 digit number (in square brackets) referring to a photo identification number given by the camera (this labelling was only used for first 10 or so experiments)

See happy snap or CHS A photo was taken of the observation made with the Canon IXUS 105 camera

RHS Right-hand-side looking downstream

LHS Left-hand-side looking downstream

The 'after bar 1/2/3/4' abbreviations were used to describe locations, particularly of the tip. This is because it was easier to measure a distance from the closest restraining bar than from the exit each time. The direction of 'after' was upstream, i.e. after bar 1 meant upstream of bar 1, because that was the direction of tip progression. Figure A.1 denotes the bar numbering convention.

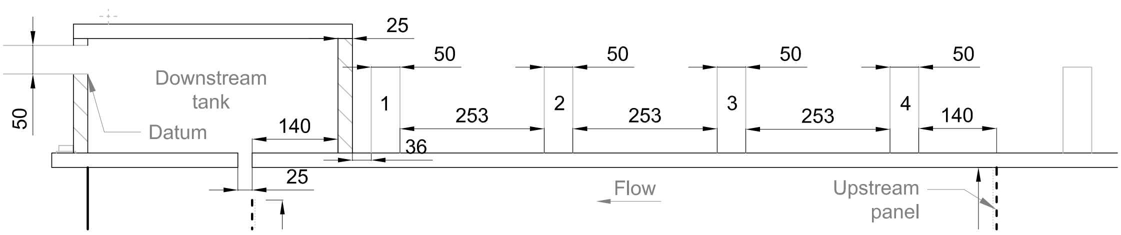

Figure A.1: Bar numbering convention used in test notes

Table A.1: Test 1 to 15

Test	Improvement made	Head (mm) Initiated	Head (mm) Progressed	Concern
1	-	-	-	Sample flushed out due to inability to control head & flow and slope instability
2	Added air valves in lid to release air bubbles flow and slope instability	-	-	Sample flushed out due to inability to control head
3	Perforated slope weir, changed to gate valve for more flow control, added bypass hose so flume could be filled in from both ends	-	-	Unable to keep head low during saturation and sugar in starter channel dissolved too quickly
4	Moved air valves so positioned over highest points, raised slope weir for flatter slope, greatly reduced inflow with constant head tank gate valve	268	615	Unable to keep head low during test and starter channel closed because sugar dissolved too quickly so channel formed along flume edge
5	Added bilge pump to underside of inner pipe in constant head tank, created starter channel with dowel, raised d/s hose so could achieve smaller head difference	263	?	Dowel broke and stayed in sample. Channels would block and new channel would form. Despite increasing head up to 642mm channels would not progress to u/s end. Suspect channels were stopping on air bubbles.
6	Delrin dowel (instead of wooden)	180	?	Tips would stop on air bubbles and channels would block. Then a new channel would form or a previous channel would unblock and re-initiate. Couldn't progress any channel further than 50
7	-	258	523	Bubble in starter channel. Tips would stop on air bubbles and channels would block. Then a new channel would form or a previous channel would unblock and re-initiate.
8	Tried using 3m bladder pressure (to see if it would reduce channel blockage) & saturated even slower (over 36 hours).	253	410	Tip slowed then stopped on air bubbles. New channel also slowed on air bubbles but reached the upstream end.

Table A.1: (continued)

Test	Improvement made	Head (mm) Initiated	Progressed	Concern
9	Used CO_2 flushing.	156	<156	Slope slipped forming a small scarp. Gas pressure built up in u/s chamber during saturation and pushed gas bubbles along flume edges, damaging sample. When dowel removed the entire sand sample flowed d/s and filled in starter channel. Channel formed along LHS edge.
10	Added gas release valve & hose in upstream chamber	142	?	Slope slipped when sand fell through crack between flume and slope panel (panel slot stopped 30mm short of the panel top corresponding to original panel height of only 120mm). This likely to be happening in previous tests but couldn't be seen until this test when a viewing space had been cut into the lid coating. Sand moved when plug pulled out of d/s standpipe (pressure had built up and was released suddenly). Started test for demonstration at sponsors meeting but didn't finish due to sample damage.
11	Raised panel slot to prevent loosing sand down sides. Added valve on standpipe so could release pressure slowly.	94	?	Slope slipped forming a small scarp. Once saturated the top of slope retreated leaving the dowel sticking out. Gas pressure built up in u/s chamber because water in gas outlet hose (sitting in sag in hose) was preventing gas escape. Gas bubbles travelled d/s through sample and damaged sides. Particle transport occurred along LHS edge with no discernable channel tip. Within 5-10min transport occurring along entire seepage length. Suspect this was concentrated leak erosion instead of BEP.

Table A.1: (continued)

Test	Improvement made	Head (mm) Initiated	Head (mm) Progressed	Concern
12	Inflated bladder after saturation in an attempt to reduce sample movement. Fixed u/s gas outlet hose above flume to ensure no sags. Filled with water much slower (approx. 1.5 days) by opening ball valve to smallest degree possible (to try minimise slope disturbance). Bypass hose not used.	389	446	Pore pressure escaping when bladder inflated disturbed sand and left channel-like patterns along flume edges. Air bubbles appeared after bladder inflation. Tip slowed on air bubbles and channel blocked. New channel formed along RHS edge.
13	Inflated bladder before saturation	486	$\leq$ 486	No detachment or transport occurred in the starter channel. Instead a channel formed along the RHS edge.
14	Compacted sand in (by tamping) in an effort to keep slope from retreating, prevent channels along flume edges and achieve a more uniform density. Also placed dowel further in (to account for slope retreat).	1105	1626	Channel blocked. Left overnight to allow time for it to unblock itself but it didn't. With increases in head to 1626mm two new channels formed along both edges and reached upstream end.
15	Nil (repeated test 14 with denser sand)	<1863	?	Flow from d/s hose restricted (not sure why, may be related to geofabric over d/s outlet). No erosion occurred despite holding the maximum head difference overnight.

Backward erosion piping test data sheet

see test 17

Test #	16	weight of can	0.08077 kg
Date	4-7-13	weight of can & soil	kg
Soil	Sydney sand	weight of soil	- kg
exit type	slope	volume of can	8.50E-04 m^3
starter dowel type	1/4' Ø	density of soil	- kg/m^3
starter dowel length	0.1524 m	unit weight of soil	- kN/m^3
seepage length	1.3 m	relative density of soil	
head in bladder tank	5 m	~~time seepage to fill can~~	~~s~~
bladder pressure	50 kPa	flow rate (ΔH=10cm)	~~#DIV/0! m^3/s~~

@ 10.5cm 0.17 L/min

time	head (cm)	observation
10.35	10.7	pulled dowel out
10.41		dowel came out successfully. Starter channel tip just on u/s side of bar 1. starter channel 22cm long (longer than test 14+15).
10.43	↑ 15.0	particles seen moving at tip and along starter channel but deposited in starter channel. I think I'm seeing the start of the starter channel infilling (I hope I am).
10.59		no more particle movement observed for past 5-8min or so.
10.59	↑ 17.7-19.0	more particles moved into starter channel + deposited. Particles moved for a few minutes + stopped again.
11.21	↑ 20.0	tip is 2.5cm abl. I'm not sure if this is where the dowel was before it was removed and so I'm just looking at disturbed sand where it was or if the tip has progressed. Infilling of the starter channel is now continuous.
11.29		the infilling has reached the back line I marked as being the top of the slope.
11.37		once the starter channel had filled in particle movement stopped.

time	head (cm)	observation
11.38	↑ 20.2	
11.42		the tip is now at 3.5ab1 so I'm gonna
		call this initiation
11.44		tip 6cm ab1
11.54		~~starts~~ channel d/s of bar 1 ±1cm
		wide and 5-10 particles ~~high~~ deep.
11.55		tip 10.5cm ab1
12.04		tip 12cm ab1
12.14		tip 17cm ab1
12.23		tip 18cm ab1
12.36		tip 20cm ab1
12.49		tip 23cm ab1
12.57		tip at bar 2
1.52		tip 9cm ab2
2.12		tip 21.5cm ab2
2.29		tip 25cm ab2
2.40		tip underneath bar 3.
		D/s end has blocked. Particles are still
		being detached + transported but are
		being deposited at blockage.
2.53		tip 2cm ab3. Blocked zone to about ~~8~~
		7cm u/s of original top of slope.
3.26		tip 11 ab3. Blocked zone extends
		13cm u/s of top of slope.
3.46		tip 21cm ab3. Blocked zone extends to
		about 10cm ab1.
4.37		tip underneath b4. Blocked zone up to
		bar 2.
4.39		d/s flow ~~[illegible]~~ 50ml = 7.2, 7.9, 5.3, 6.25.
5-7		
10.42		the sample + channel look no
		different.
10.43	↑ 21.1	no particle movement.
11.06	↑ 27.0	
12.03		just replaced the head tank filter.
		because the water wasn't rising as
		fast as it used to (even with gate
		valve opened 3 turns the water level
		was hardly rising).
12.04		tip now advancing again
12.06		tip 4cm ab4
12.09		blockage now up to halfway between
		bars 2 + 3.
12.13		particle movement has been
		constant since having replaced the
		filter.
12.28		first noticed the channel had

time	head (cm)	observation
		reached the upstream end.
12.33		Q 100mL = 8.1s , 50mL = 5.2, 6.6, 4.4, 5.1

time	head (cm)	observation

Test 16 report

Test 16 was a repeat of test 14 and 15 without the geofabric over the d/s outlet. The aim was to show repeatability by getting the same result as test 14.

Sand started to move into and deposit in the starter channel at a head of 15cm. Sand had been deposited along the full length of the starter channel by a head of 20cm. To compare this with test 14- sand started to move into the starter channel at 24cm and had deposited along the full length by 103cm. So on the plus side, sand moving into the starter channel happened in both experiments but on the down side it happened at much greater heads in test 14.

The starter channel started to advance at 20.2cm (initiation). In test 14 initiation was at 110.5cm.

The channel tip progressed at 20.2cm until it reached bar 3 when the d/s end of the channel blocked. With increases in head the tip continued to advance even though the d/s end was blocked. Particles that had been detached at the tip were deposited at the blockage causing the area of blockage to grow upstream. The tip reached the upstream end at a head of 27cm.

Channels blocked in test 14 as well however in test 14 blockage meant the channel tip stopped advancing and a new channel started.

As I mentioned in my previous email today, levels in the d/s standpipe in test 14 were much greater than datum however, with the geofrabirc removed from the over the d/s outlet, levels in the d/s standpipe in test 16 stayed just a little above datum. This suggests that excessive head was being lost at the outlet (I think the geofabric was trapping air/gas pockets). Excessive head loss at the outlet meant that the hydraulic gradient across the flume was reduced and hence flow was reduced, which is why a much greater head tank level was required to drive flows large enough to detach and transport particles. This is why I think heads in test 14 were greater than test 16.

My intention is to repeat test 16, i.e. without the geofrabic across the outlet, in hopes I will get the same results and demonstrate repeatability.

these #s should be on test 16

Backward erosion piping test data sheet

Test #	17	weight of ~~can~~ dry sand 373	~~0.08077~~ kg
Date	12-7-13	~~weight of can & soil~~	~~kg~~
Soil	Sydney sand	~~weight of soil~~	~~- kg~~
exit type	slope	volume of ~~can~~	~~8.50E-04 m^3~~ 0.22 m^3
starter dowel type	1/4' Ø	avg dry flume density of soil	- 1695.5 kg/m^3
starter dowel length	0.1524 m	unit weight of soil	- 16.6 kN/m^3
seepage length	1.3 m	relative density of soil	
head in bladder tank	5 m	time for 50mL	17.5 s
bladder pressure	50 kPa	flow rate (ΔH=10cm)	2.86e-6 m^3/s 0.17 L/min

time	head (cm)	observation
10.01	10	pulled dowel out without mishap. tip
		beneath bail.
10.04	↑ 12.5	particles moved into starter channel.
		it looked as though particles might
		have been detached from the sides
		(not the tip).
10.16		about 35 particles are moving into +
		settling in starter channel every
		75 or so. The infilled region of the
		starter channel ranges from bail
		to 5cm towards to d/s end.
10.39		infilled region now 5.5cm back from bl
11.02		" " " 5.8cm " " "
11.53		" " " 6.5cm " " "
12.01		left experiment running without
		supervision.
2.33		infilled region 7cm. If I could
		leave it overnight I would but
		it's a friday so I'm going to fh.
2.44	↑ 15	Initially with head increase a
		constant 'stream' of particles where
		being moved into + deposited in
		starter channel however before long
		(a few minutes) it was about 10
		particles every 20s or so. So I
		could wait but will fh. infill region

Test 17

time	head (cm)	observation
		10cm. Particle movement now like
		10particles every 10s.
2.58	↑ 17.5	
2.58		Again, initially there was a constant
		flow of particles but after a few
		minutes it slowed down to about
		50 particles every 30s or so.
2.59	↑ 19.9	
3.03		infilled section now full length of
		starter channel (18cm)
3.04		tip seen advancing past bar1. INITIATION.
3.13		tip 2.5cm ab1.
3.27		tip 3.5 ab1
4.01		tip 4.8cm ab1
4.13		tip 4.8cm ab1
		Going to leave it running @ 19.9 over
		weekend. Photos being taken every
		1 hour.
		- from photo observations -
5.37		tip ≑ 12cm ab1
6.37		tip ≑ 21.5cm ab1
		there the tip stayed all weekend and
		is still there Monday morning.
		the channel is well defined at
		~~[illegible]~~ widths between ≑ 5-13mm
		and maybe 10-20 particles deep. I also
		note that the tip has digressed
		toward the RHS (see happy snap
		photo). Perhaps in an effort to keep
		progressing.
15-7		
10.18	↑ 21.0	no movement
10.25	↑ 22.1	" " . I knocked on glass +
		saw a few particles move but only
		about 5 particles + then no more.
10.45	↑ 23.3	~~I [illegible] to~~
10.49		tip reinitiated but the LHS fork tip.
10.53		particles taking maybe 7-9s to
		travel from bar 2 to 1
10.54		tip 24cm ab1
10.57		tip at bar 2
11.14		tip 2cm ab2
11.21		" " ". detachment @ tip seems
		to have stopped but scour is ongoing.
		this is when I think it's at risk of
		clogging but I don't want to ↑h too

Test 17

time	head (cm)	observation
		quickly increase tip is just v. slow but not
		totally stopped
11.28		tip is still moving but in well-time-spaced
		increments. It's now at 3cm ab1.
11.48		tip 3.5cm ab1
12.01		tip 6.5cm ab1
12.10		tip 10.5cm ab1. This is about halfway. ab2
12.19		tip 12.5 " ".
12.29		tip 14.5 " ".
1.00		tip 21 " "
1.19		tip under bar 3
1.29		tip 2cm ab3
2.02		tip 10cm ab3. Region btw slope +
		bar 1 now blocked however particle
		detachment + transport still occurring
		but all u/s of bar 1.
2.27		tip 16.5cm ab3. blocked zone ~~about~~
		btw slope + 5cm ab1.
2.52		tip 24.5cm ab3. blocked ≐ 5cm bb2.
		Estimate Q to be 10s between bars 4
		and 3 and 9s btw bars 3 and 2.
3.16		tip underneath bar 4. blocked zone
		up to bar 2. No movement can been
		seen but will leave longer.
3.54		still no movement.
4.25		" " " . will leave overnight.
16-7		
10.14		I left the camera taking hourly shots
		overnight but the battery went
		flat after it's first shot at 5.32pm.
		the tip has progressed 5cm ab4 but
		I don't know when it happened.
		I've noticed air bubbles have entered
		into gaps in the blocked zone [see
		happy snap pic]. I don't know why or
		where from.
11.39		I think the tip has moved a cm. So now
		6cm ab4.
11.43		blocked zone extends to halfway btw
		bars 2 + 3.
12.22		tip 7cm ab4
2.30		" " "
4.19		tip 7.8cm ab4
5.07		" " ". leave overnight.
17-7		
9.54		tip hasn't moved. It's still 7.8cm ab4.
		Bladder tank still a bit above 5m.

Test 17

time	head (cm)	observation
		More air has moved into the d/s
		portion of the channel [16-18]. I don't
		know why or where the air is
		coming from.
9.57	↑ 24.4	u/s standpipe = 24.6, D/S = 4mm.
10.14	↑ 27.0	tip reactivated. Sediment detachment +
		transport continuous. Tip 8.4cm abt.
10.22		now movement infrequent
10.23		tip 8.5cm abt
11.57		" " "
11.57	↑ 28.3	tip reinitiated
11.59		tip 10cm abt
1.58		tip 18cm abt (about 1cm away from
		u/s panel).
2.30		at u/s panel. Test finished. Test
		used to try measuring particle speed +
		water speed

Test 17 report

Test 17 was a repeat of test 16 with the aim to show repeatability and I think I showed it!

		Test 16	Test 17
Starter channel partially in-filled with sand	Start head (cm)	15	12.5
	Finish head (cm)	20	19.9
Initiation (starter channel started to progress)	Initiation head (cm)	20.2	19.9
Channel grew until the d/s end blocked	Btw heads (cm)	20.2-20.2	19.9-23.3
	Length (cm)	75.4	90.4
The same channel reached the u/s end (even though it was still blocked at the d/s end)	Maximum Head (cm)	27	28.3

I've done a chart (attached) to pictorially show the results.

How test 17 differed is I left the experiment running for longer periods of time (allowed more time for the tip to progress). Test 16 was completed over 2 days where as test 17 was completed over 6 days (2 of them being a weekend over which nothing happened). Running test 17 for a longer period of time didn't make much difference (heads at which stuff happened about the same).

To summarise what happened in test 17:

- particles started moving into the starter channel at 12.5cm and had partially filled in the starter channel for its full length by 19.9cm.
- Once the tip started to progress (still at a head of 19.9cm) it stopped 2.5hours later after having grown 26.3cm (21.5cm after bar 1- total length of 41.3cm).
- It stopped late Friday night and didn't move all weekend indicating that if the head is insufficient, more time won't make a difference.
- To reinitiate the tip I needed to increase 3.3cm (to 23.3cm).
- At 23.3cm the tip progressed 49.1cm before blocking at the downstream end.
- The tip continued to progress even though the d/s was blocked. Particles would be detached from the tip or sides, transported along the channel and deposited in the blockage.
- After the d/s end had been blocked for about an hour, the speed of tip progression slowed down. The avg speed of tip progression went from 16cm/hour (σ=7.4) to 0.8cm/hour (σ=0.7).
- I left the head at 23.3 overnight but the tip had stopped
- I increased the head by 3.7cm (to 27cm) and the tip progressed 0.7cm in the first 9minutes but then stayed stationary for an hour and a half so I increased head by 1.3cm (to 28.3cm) and it reached the u/s end (another 11.2cm) in 2.5 hours.

As for comparing these two tests with UoF's results

- What's similar:
  - Initiation heads (within 3cm of each other)
  - One channel with a meandering pattern near the middle of the flume
  - Maximum heads are similar if I compare with UoF's test 2 but there's up to 8cm difference if I compare them with UoF's test 3
  - Blockages at the d/s end of the channel occurred
- What's different:
  - UoF don't say where along the flume the tip was when they reached the maximum head but if it was close to the middle of the flume (where the Dutch says it occurs) then this is different to what I observed. My maximum heads occurred when the tip was almost at the end of the flume. However I wonder if this happened only because the d/s end of the channels became blocked. The blockage reduced the flow through the channel (and at its tip) which is why I had to increase the total gradient to keep the flows high enough for erosion. UoF cleared the blockages as they occurred so the piping would continue without need for head increase. Perhaps if I could do the same I wouldn't have needed to increase the head either.

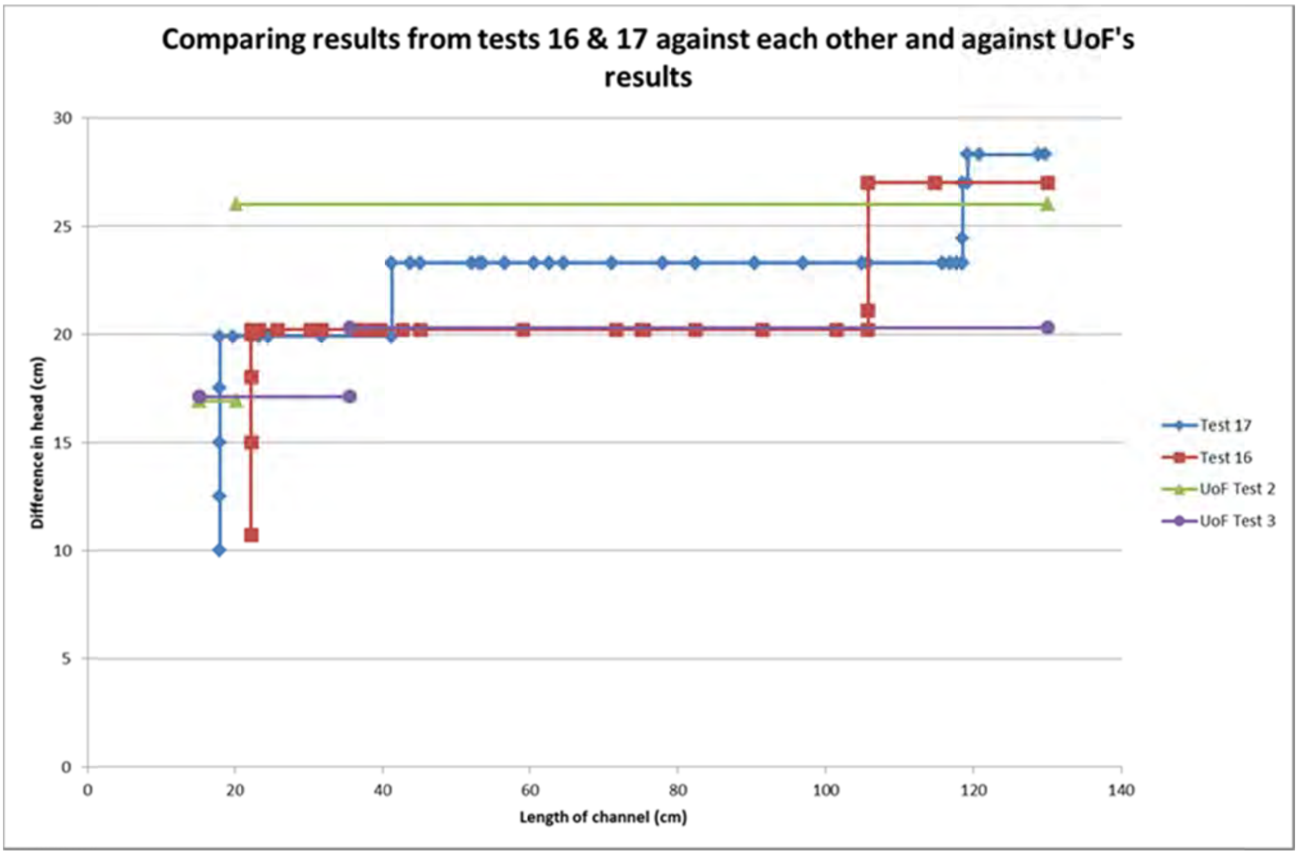

Note that I don't know what the length of the channel was when they reached the maximum head difference so I've drawn a line at the maximum head across the full length.

In short, I think have a verified UoF results close enough. Do you agree?

When plotting the results I also wanted to see:

1. if there was a connection between the head and tip speed.
2. If UoF tip progression was faster than mine.
3. Did I progress the tip slower in test 16 than test 17

Refer to graphs below. I think the answer is no to all 3 questions.

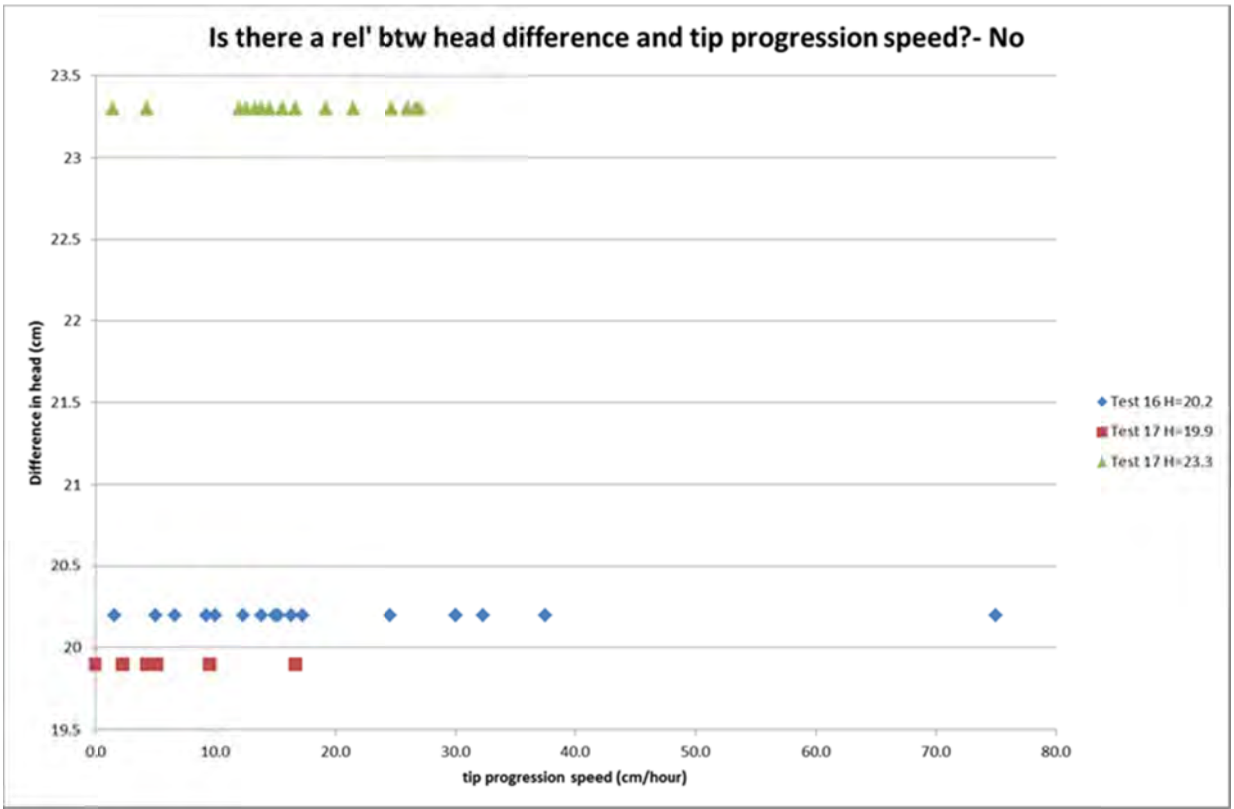

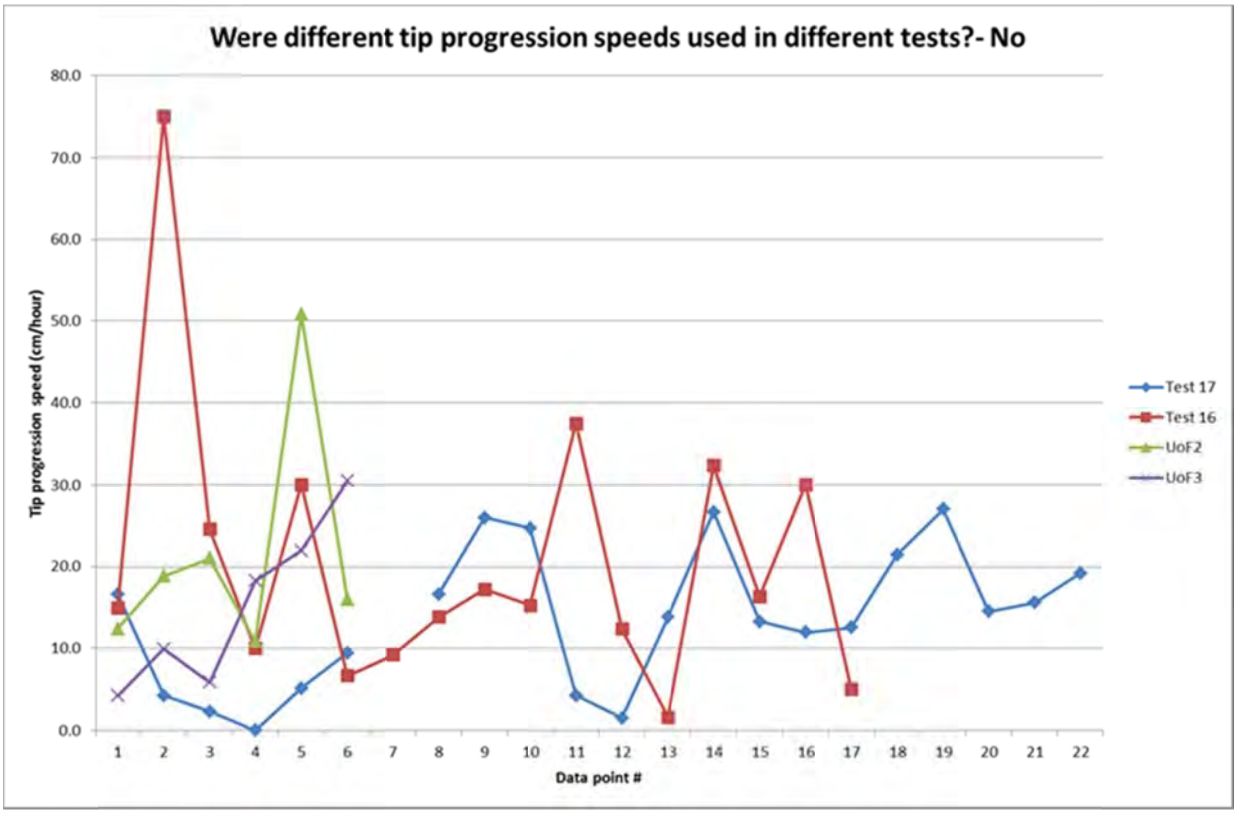

Plan for next test (Test 18)- repeat test 17 (while I’m waiting for circular exit flume to be up and ready) and find head difference across filter, experiment with different ways to measure the speed of particles and or channel flow, check I get repeatability again.

Backward erosion piping test data sheet

Test #	18	mass of soil & water	kg
Date	29-7-13	flume volume	0.22 m^3
Soil	Sydney sand	bulk unit weight	0 kN/m^3
exit type	slope	moisture content	%
starter dowel type	1/4' Ø	void ratio	#DIV/0! -
starter dowel length	0.1524 m	relative density	#DIV/0! -
seepage length	1.3 m	fill from d/s hose	50 mL
head in bladder tank	5 m	avg. time to fill	s
bladder pressure	50 kPa	flow rate @ ΔH = 10cm	#DIV/0! L/min

time	head (cm)	observation
11·22		removed dowel.
11·24		came out with sudden movement so
		a length of 6·5cm back from where I
		had filled in with sand instantly.
		A length of 13cm of open starter
		channel is remaining.
11·27	↑ 13·5	
11·30		the head tank pump died. So turned
		inflow off.
11·38		At about 11·35 I knocked the d/s hose
		off the midway bessar block. I
		didn't think anything of it and
		put it back. However at 11·38 I
		noticed the starter channel was
		all filled in + disturbed.
		[54-56] I think it was a sudden
		flow of water back into the flume
		from the hose that caused it. See
		sketch. The other thing I did was
		opened the u/s sand standpipe.
		I observed a disturbance of sand
		around the standpipe. I think it's
		more likely that the raised d/s hose
		disturbed the starter channel more
		so than opening the standpipe but
		both could have done it.

time	head (cm)	observation
12.08	6.3	head dropped whilst water was
		turned off to replace pump. Pump
		now replaced.
12.09	↑ 10cm	no movement
12.20	↑ 11.2	" "
12.22		u/s tank standpipe 11.3 . u/s sand
		standpipe 54.5 above perspex. Equiv. above
		perspex at u/s tank standpipe = 43.3 btw
		perspex + datum + 11.3 = 54.6 . Therefore
		there is 1mm head drop across filter.
		D/s standpipe 8mm.
12.32	↑ 13.7	no movement
12.47	↑ 16.1	" "
12.50	↑ 17.7-19	" "
1.01	↑ 21.0	" "
1.38	↑ ~~22~~ 23.4	" "
1.46	↑ 26.0	starter channel opened up/washed open
1.48		tip now at ab1.
1.53		u/s tank standpipe 26.1 above datum
		u/s sand " 69.2
		∴ difference = 2mm
2.44		tip 25cm ab1
2.58		tip 1cm ab2
3.06		" 3cm ab2 } check I have bar #'s correct
3.12		" 5cm ab2
3.21		" 11cm ab2
3.46		" 12cm ab2
3.58		tip progression/detachment has slowed right
		down
4.15		tip 20cm ab3
4.22		" 22cm ab3. D/s end pretty much
		blocked because channel bends on itself
		and sediments don't make it round the
		bend
		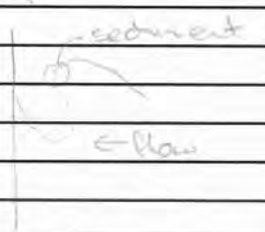
4.26		left to run over night
30-7		
11.06		tip has not moved overnight. It's still at
		22cm ab3 (more like 30cm). It is blocked
		from d/s end to about 3cm ab2.
11.58		The camera remote trigger battery had died
		so I had to get another before continuing

Test 18

time	head (cm)	observation
		test.
11.59	↑28.4	tip reactivated
12.05		now at ~~at~~ bar 4
12.24		tip now 4cm a/dt
12.32		tip 5.5cm a/dt
12.41		tip at same position. It may have stopped-
		I saw no movement
2.00		no movement
2.00	↑29.7	" "
2.11	↑31.0	tip reactivated
2.34		tip 7cm a/dt.
2.46		" " "
3.05		" " "
3.05	↑32.2	tip reactivated
3.15		tip 8.5cm a/dt
4.26		tip 11cm a/dt. Blocked zone up to bar 4.
4.55		tip 18cm
5.25		tip reached u/s panel.
5.25		I've just noticed the ~~chann~~ blocked
		channel is flowing again btw d/s end
		and bar 3.
~~5~~.29		unblocked tip now btw bars 3+4
5.31		the unblocking tip now connected with
		open channel at U/S end but it's
		blocked again (under b1 this time).
5.33		end of test.

Test 18

time	head (cm)	observation

Test 18 report

Test 18 was a repeat of test 16 and 17 except with a standpipe added just downstream of the upstream panel and more coloured sand was used. The aims of test 18 were to:

1. find head loss across filter
2. experiment with different ways to measure the speed of particles and or channel flow
3. check I get repeatability again

At the start of the test the starter channel became suddenly filled in with sand. I'm not certain why/when it happened. There are 2 possibilities, 1) when I accidently knocked besser block over from underneath the d/s hose the d/s end to raised and flow travelled backwards into flume or 2) when I opened the new standpipe (located just downstream of the upstream panel) sand around the standpipe was disturbed and flowed toward the standpipe.

I think possibility 1 is more likely to be the cause. To prevent this from happening again I tied the hose to its besser block.

The starter channel re-opened at a head of 260mm and the tip progressed, so I call this initiation. Compared to tests 16 and 17 (of 202 and 199 respectively) this initiation was greater. I think this is because the starter channel had suddenly completely filled in with sand.

When the channel tip had progressed 1024mm (220 after bar 3) the channel blocked at its downstream end. A similar thing happened in tests 16 and 17 (blocked when tip at 754 and 904mm respectively).

When the channel blocked at its downstream end the tip stopped progressing. I left it overnight to make sure it had stopped. With four more head increases (up to 322mm) the tip reached the upstream end.

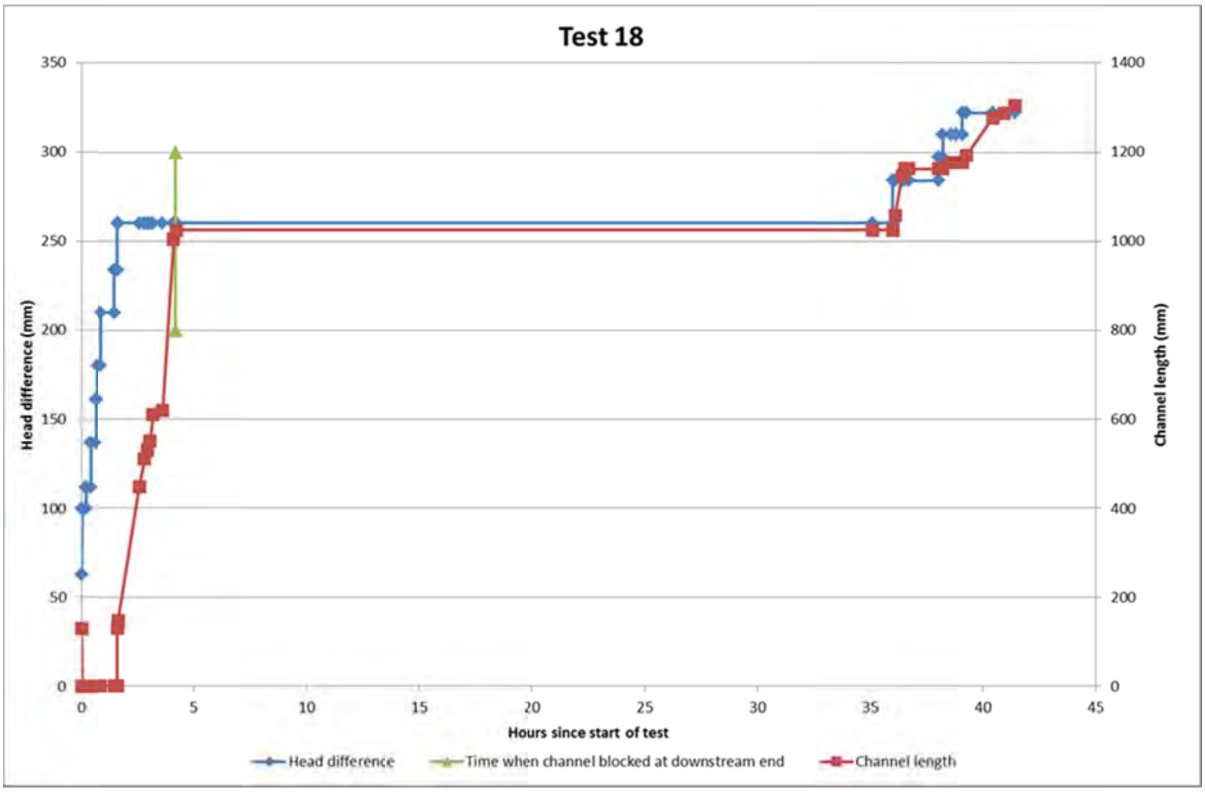

In response to my 3 aims for test 18:

1. The head loss across the upstream filter was btw 1 to 2mm, i.e. very small
2. I added more coloured sand with close up high-res pics to try measure the speed of particles travelling in the channel. It's not easy and is time consuming. I have attached a presentation file showing how I estimated the speed- if you have a suggestion as to how to make this easier that would be great. I estimated the particles were travelling at 1mm/sec (when head difference= 284mm.
3. Achieve repeatability? Kind of. It behaved in a similar way but the initiation head was a fair bit higher than tests 16 and 17. Likely to be because the starter channel filled in with sand when I knocked the besser block over.

As per Bill's request I have amended the plots I provided in the last test report for tests 16 and 17 with time on the x axis.

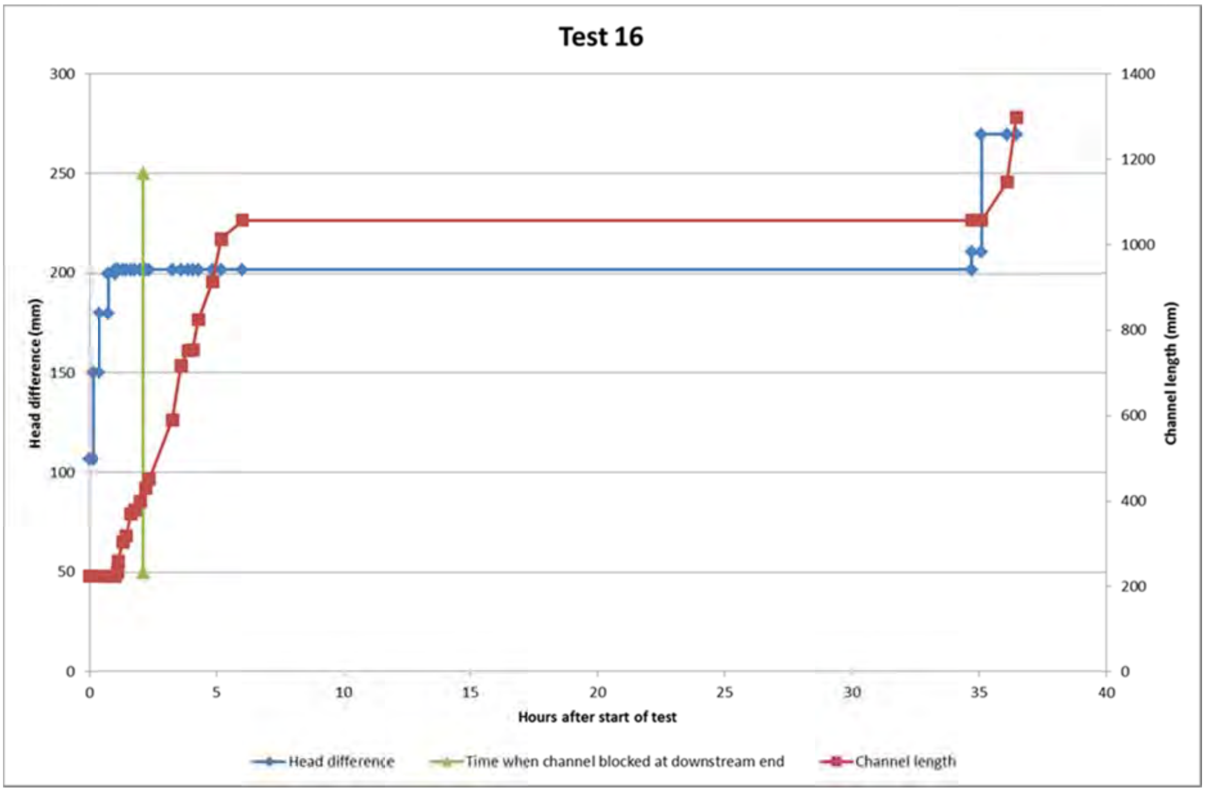

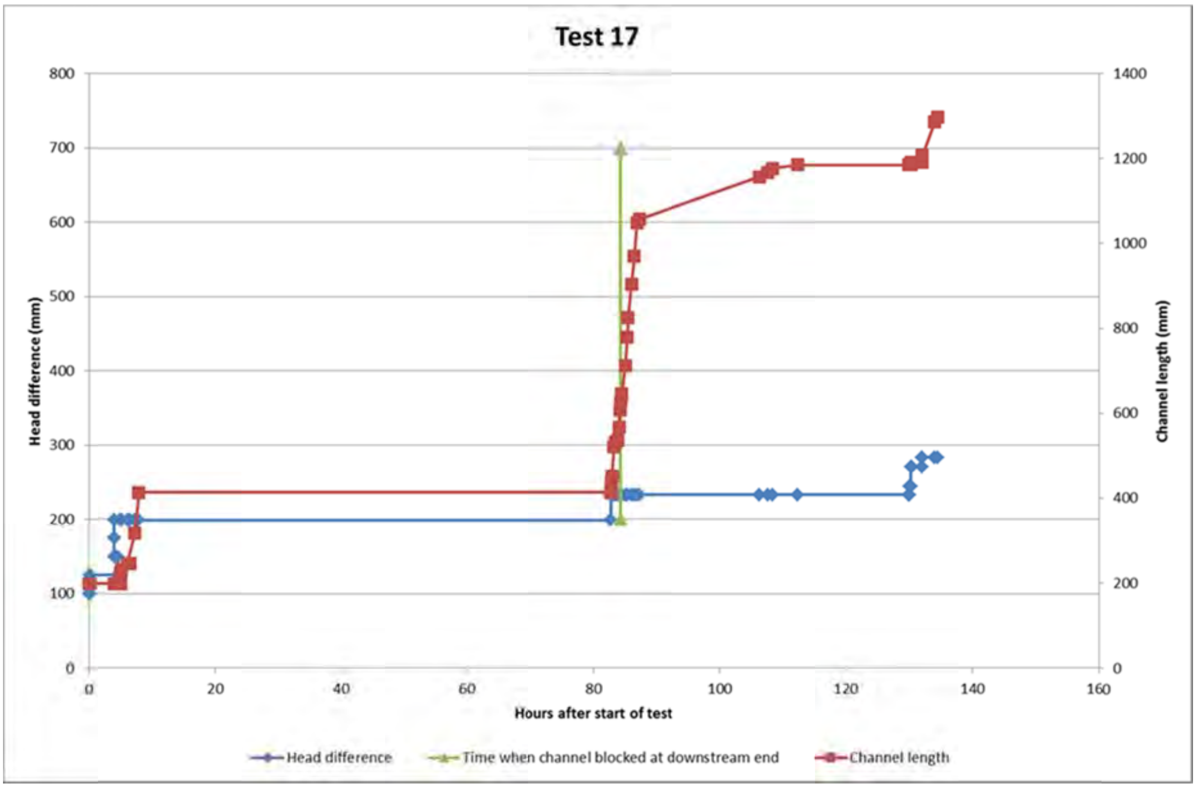

I've also added to this graph:

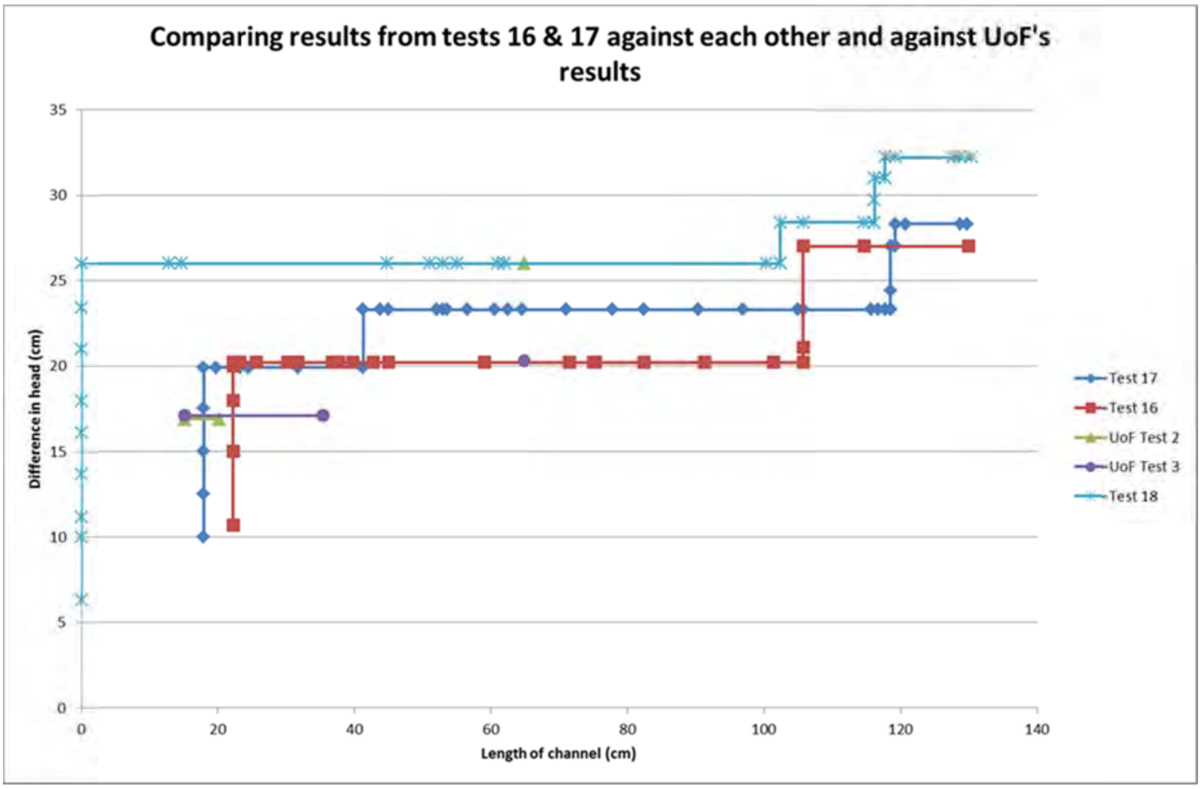

What I take from these 4 graphs is:

- Sometimes the tip continues to progress after the channel blocks at its downstream end and sometimes it doesn't- I can't see a pattern here yet.
- When the tip is progressing the slope of the time vs. displacement curve, i.e. velocity is fairly constant
- Increases in head are needed to progress the tip only in the last 200-300mm

With respect to my last point, it's my hypothesis that if the channel didn't block at its downstream end I wouldn't need to increase the head and so initiation head would equal critical head. I think this because my head that maintained tip progression matched UoF's critical heads and I think UoF cleared buildup at the downstream end, in their test 3, instead of increasing the head (their downstream end was open so they could reach in and clear sand blockages with a pen or something). But I'm not 100% sure this was the case. They say:

> 2. Sand buildup at downstream slope was cleared to continue piping. Pipes rerouted at exit point due to buildup.

But it's possible they just mean the experiment on its own accord would clear the sand buildup.

Backward erosion piping test data sheet

Test #	19	mass of soil & water	0 kg
Date	28/08/2013	flume volume	m^3
Soil	Sydney sand	moisture content	%
exit type	circle f3	dry unit weight	#DIV/0! kN/m^3
starter dowel type	-	void ratio	#DIV/0! -
starter dowel length	- m	relative density	#DIV/0! -
seepage length	1.3 m	fill from d/s hose	mL
head in bladder tank	5 m	avg. time to fill	s
bladder pressure	50 kPa	flow rate @ ΔH = 10cm	#DIV/0! L/min

time	head (cm)	observation
12.00		Water level in d/s tank according to
		the tape stuck on the side is 13.6-13.9cm
		(difficult to tell exactly). I'm not sure
		if this is the max it will reach or if
		it could go higher. I think this is the
		max it will reach. The water level is ≈
		26cm above the outlet invert. For this
		test I'm going to make this level
		datum. The equivalent level is
		marked on the head tank (level in
		standpipe at the moment. Level in
		headtank (nominated as datum for
	10.9=0	this test) is 10.9cm. All subsequent
		readings will be relative to 10.9. Eg
		I read of 11.2cm then it's 11.2-10.9 = 0.3cm
		above datum.
12.08		Sand boiling seen in hole around
		its circumference in about 4 areas.
		See photos + video.
12.11		Channels around hole were present
		when I came in this morning (occurred
		overnight during water filling).
		Most prominent
		channel ≈ 5cm long
		and ≈ 45° from

centreline towards RHS.

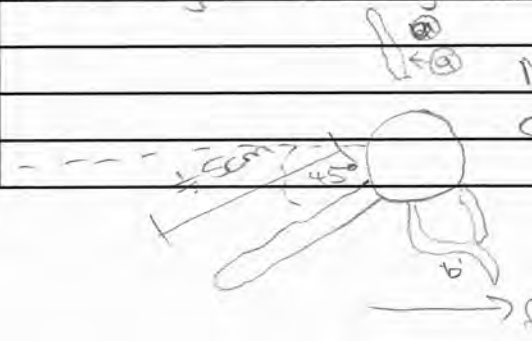

time	head (cm)	observation
		so initiation started at head lower
		than this.
12.16		I note I can hear water trickling
		through d/s hose so there must be
		a very small head on the
		system but it's hard to tell.
12.19	↑ 13.3	no movement (in channel)
12.24	↑ 16.1	" "
12.30	↑ 18.8	particles moved toward the hole from
		the most prominent channel and
		region (a) (see sketch). Different movement
~~12.36~~		occurred for ≈ 1 min after head increase
		+ then stopped.
12.36		tip of prominent channel ≈ 15.5 − 10.5cm
		from u/s edge of hole (see happy snap
		pic)
12.39	↑ 20.1	Both channels activated (prominent + 'a').
~~12.42~~		but channel 'a' stopped after ≈ 1m after
		head increase where as prominent
		channel kept going.
12.44		tip ≈ 20.5 − 10.5cm from hole.
12.46		tip same place. movement has slowed
		right down now.
12.53		tip same place, no movement.
1.28		" " " " " "
1.28	↑h 21.4	both tips reactivated. Sand now
		on top of lid (see pic)
1.32		very little movement now. Wait I take it
		back. Main tip still moving. Tip now
		≈ 22.0 − 10.5cm.
1.44		tip now underneath tank edge + more
		sand on top of lid.
1.47		I noticed a short period (30s or so) of
		increased activity. All channel tips
		were activated (main, 'a' and 'b') and
		more boiling. During this time I couldn't
		hear the pump gurgling. I wonder if
		for a short period the drain
		cylinder was flooded. I'm not sure.
		But movement slowed down +
		gurgling noise returned. Now only main
		tip activated.
1.58		tip still underneath tank edge
2.01		there's about 10-20 particles moving
		about every 30-60 seconds. So v.
		slow but still moving.
2.27		tip still not through the other side of
		tank wall

time	head (cm)	observation
2.31	↑h 22.3	tip reactivated
2.39		tip seen on other side ~~o~~f tank wall
2.53		tip not moved since 2.39pm it's ≑1cm beyond
		tank wall
3.03		tip not moved.
3.04	↑ 23.7	tip reactivated
3.13		tip reached b1
3.27		tip otherside of b1
3.40		tip 4cm ab1
3.41		the channel underneath tip has formed
		some kind of 'back-turn' containing
		an eddy. See happy snap + video
		cam.
4.02		tip 5cm ab1
4.26		tip 6.5cm ab1
4.33		tip 7cm ab1
4.58		tip 8.5cm ab1
5.14		tip 9cm ab1. left on overnight with
		photos being taken every 30min
29-8		
9.31		tip 10.5cm ab1. Whilst it's possible that
		it's still moving ultra slowly I think it's
		more likely that it kept moving at the
		same rate as it was yesterday
		≑ 0.5cm/15min and so would have
		stopped at 10.5cm maybe about 7pm-ish
		last night. ∴ I'm going to raise head.
9.34	↑ 24.9	tip reactivated. The tip is meandering
		a fair bit (taking a 90° turn). So still
		at 10.5cm
9.48		tip 12cm ab1
9.55		" " "
10.09		tip 12.5cm ab1
10.24		tip 13.5cm ab1
11.06		tip 14.5cm ab1
11.22		tip 16cm ab1
11.52		tip 16.5cm ab1
12.15		tip 17cm ab1
12.39		tip 20cm ab1
12.54		tip 21.5cm ab1
1.09		tip reached b2 (25.2cm ab1)
1.30		tip 6cm ab2
2.20		Tip 21.5cm ab2
3.15		Tip 17cm ab3
3.55		Tip 5cm ab4
4.36		reached u/s end

time	head (cm)	observation

Test 19 report

Test 19 was the first test with a hole exit.

Channelling began whilst it first filled with water. The longest channel was about 50mm.

Pic before test started:

The 50mm long channel tip reinitiated at a head of 92mm. The head required incremental increases to keep the tip going. Once at a length of 363mm (about 30% of seepage length) and a head of 140mm the tip progressed through to the upstream side without any further head increases.

Sand boiling could be seen at the exit from the start of the test. The boiling activity increased with increases in head.

Pic of sand boil when channel had reached the upstream end:

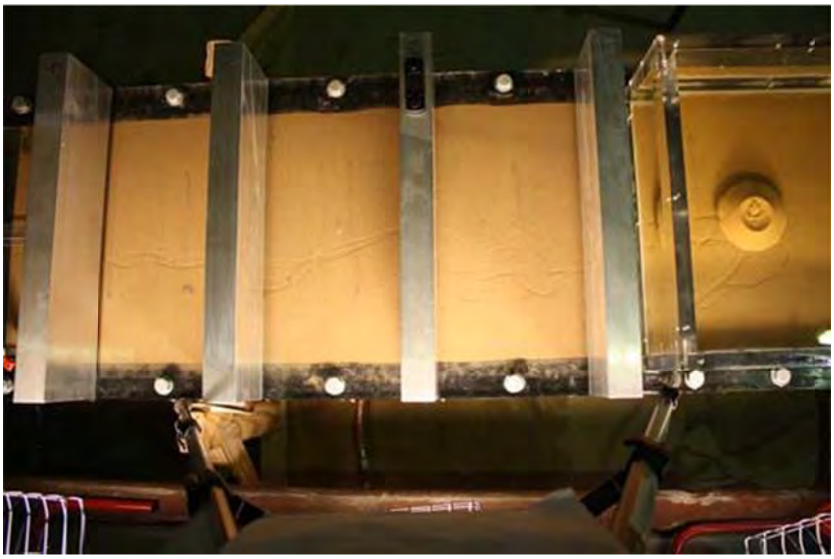

After the channel had reached the upstream end I left the test running overnight.

Pic of sand boil after leaving overnight after test complete:

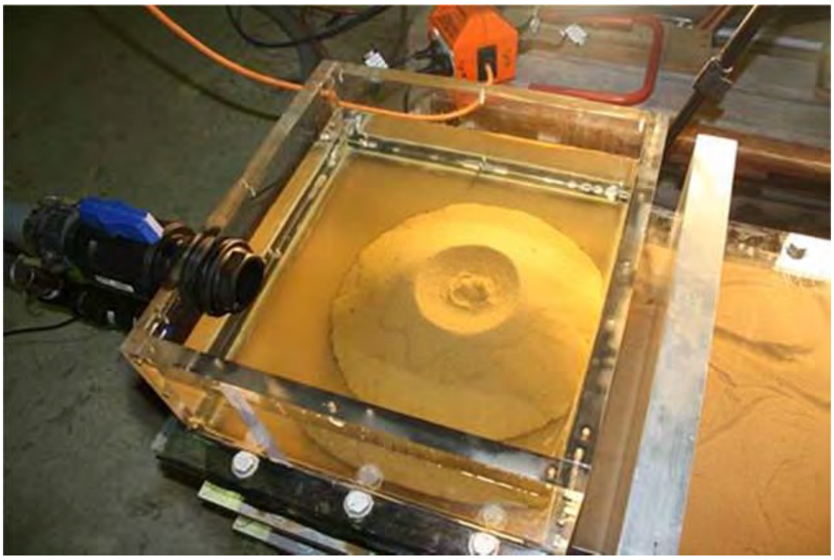

I had predicted the initiation and critical gradients between the different exits to look a little like this:

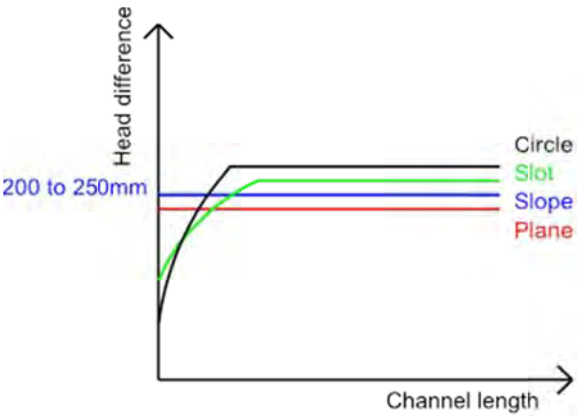

What did happen as predicted:

- Circle initiation head < slope initiation head
- For the circle the head needed increasing to progress the channel

What happened different to the prediction:

- The circle critical head < the slope critical head

At this point I'm not sure why this happened.

And so for test 19 compared to the slope tests it looked more like this:

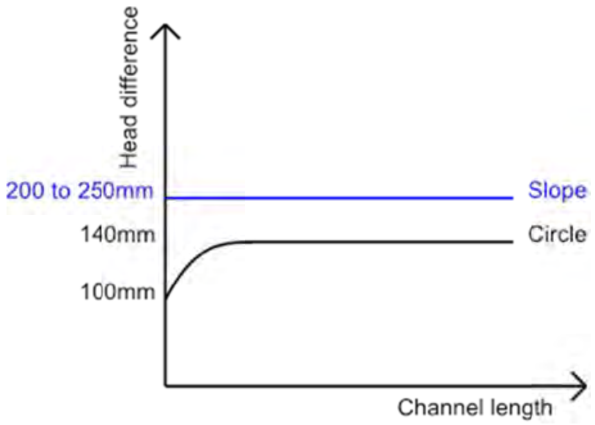

The actual data from which I've simplified this chart from is:

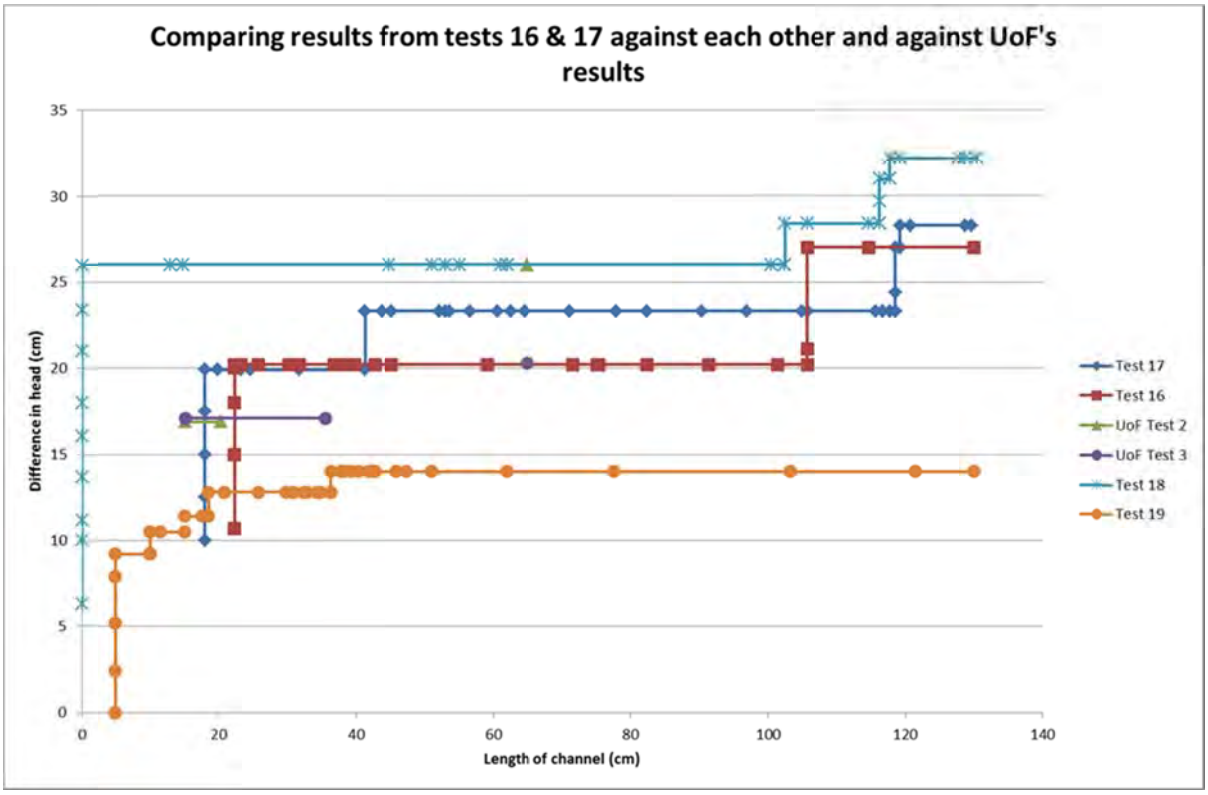

The head and channel length with time for test 19 is:

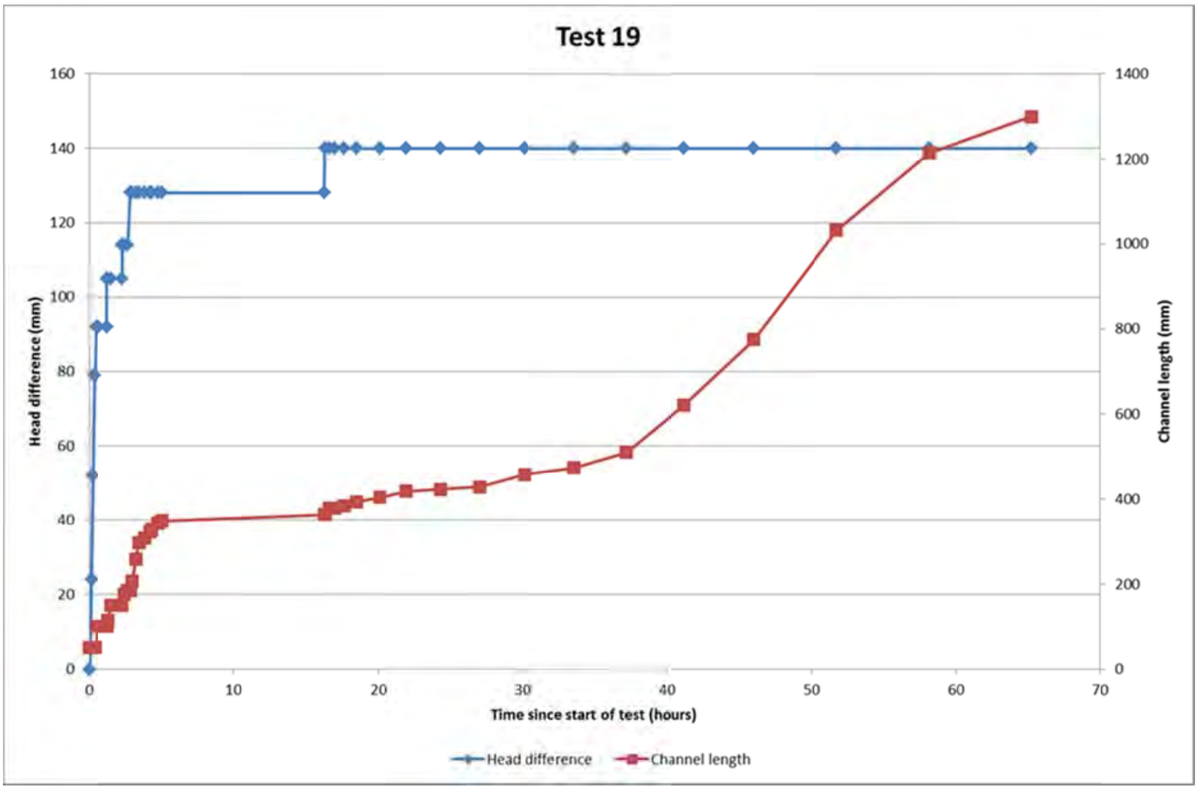

From this you can see that at the critical head the speed of the tip increased as it approached the u/s end.

A video of the sand boil is [here](#).

At the end of the test I stuck my finger through the boil. I felt no resistance- I could push my finger to the circle very easily, i.e. I felt no build-up- the sand movement was vigorous enough that I don't think it ever blocked.

The next test in flume 2 will be a repeat of this test for repeatability.

Backward erosion piping test data sheet

Test #	20	mass of soil & water	0 kg
Date	9/09/2013	flume volume	m^3
Soil	Sydney sand	moisture content	%
Flume	~~2~~ 3	dry unit weight	#DIV/0! kN/m^3
Exit type	circle	void ratio	#DIV/0! -
seepage length	1.3 m	relative density	#DIV/0! -
head in bladder tank	5 m	fill from d/s hose	mL
bladder pressure	50 kPa	avg. time to fill	s
		flow rate @ ΔH = 10cm	#DIV/0! L/min

time	head (cm)	observation
11.28	0	Channels were created during
		the saturation process.
		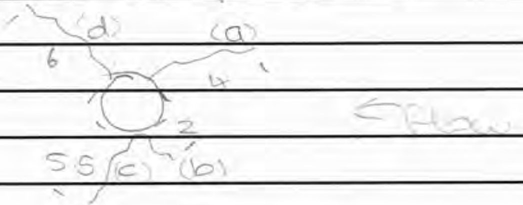
		d/s level = 2.2 below datum
11.36	↑ 2	fluidisation in hole
11.39	↑ 4.1	no movement in channels
11.52	↑ 7	d/s level = 0.6 below. no movement in
		channels
12.05	↑ 9.8	all tips momentarily activated but
		stopped again before tip progressed
		much. Channel (a) ≐ 17-11cm.
12.28	↑ 12.5	all tips reactivated except (b).
		tip (c) only moved for a bit then
		stopped. Tip (d) moved to 10cm
		long + then stopped. D/s level @
		datum.
12.33		tip (a) at ≥18-11cm. Doesn't seem to move anymore
12.34		took happy snap shot.
12.45		tip (a) ≐ 19-11cm. then no movement.
1.48	↑ 15.0	All tips reactivated. Sand in boil now
		depositing on top of lid. Tips (d) + (c) stopped.
1.52		tip (a) 21-11cm.

Test 20

time	head (cm)	observation
1.53		tip 23-11cm
1.55		tip underneath tank wall
2.03		tip 1cm past wall
2.19		tip reached b1
2.45		tip under b1 still
3.00	↑ 16.4	d/s standpipe 17cm
3.34		tip still under b1
3.34	↑ 17.8	
4.00		tip 2cm ab1
4.24		tip 4cm ab1
4.36		5cm ab1
5.10		5cm ab1
5.25		" " leaving overnight
10-9		
9.33		tip 6cm ab1 and there's a bubble
		in the channel (see happy snap).
9.37	↑ 19.1	no movement
10.06		" " still 6cm ab1
10.06	↑ 20.5	
10.33		tip 7.3 ab1
10.57		tip 8.7 ab1
11.29		9.7 ab1
11.40		"
11.59		"
11.59	↑ 22.1	
12.20		tip 10.3 ab1
12.41		" " "
12.41	↑ 23.3	
12.46		tip 13 ab1
12.54		15 ab1
1.03		17 "
1.23		tip otherside of b2
1.35		tip 12cm ab2
1.41		18.5 ab2. d/s standpipe 24
1.47		20 ab2
1.55		reached b3
2.04		tip otherside of b3
2.10		tip 3cm ab3
2.18		7cm
2.26		7.5cm
2.34		10cm ab3
2.48		23.5cm
2.55		25
3.00		blocked zone between bars 1 + 2. Very
		little movement in channel now.
3.05		tip under b4.
3.30		" " ". no movement in channel.

time	head (cm)	observation
4.29		tip other side of b4.
4.36		tip 4.5cm ab4
4.41		tip 7cm ab4
4.44		tip 8cm ab4
4.49		tip 9.8 cm ab4
4.54		tip 10.5cm ab4
5.07		tip 11cm ab4
5.14		tip 11.5 cm ab4
5.25		tip " " leave overnight.
11-9		
9.43		tip still 11.5cm ab4. Lots of air/gas
		bubbles have entered the system. See
		happy snap shots
9.44	↑ 25.6	
11.12		no movement
11.13	↑ 28.2	" "
11.55		" ". But there is a new channel
		now 18.5cm ab1. See happy snap
12.05		new tip 22cm ab1.
12.33		" " 8cm ab2
1.16		" " under b3
2.25		" " 13cm ab3
3.09		" " under b4
3.32		" " other side of b4. And new
		channel is blocked under/around b2.
3.34		new tip 2.5cm ab4
3.50		" " 12.8cm ab4. Channel also blocked
		beyond b3.
3.51		new tip reached u/s end.

time	head (cm)	observation

Test 20 (Flume 2 hole) report

Test 20 was the second test with a hole exit.

Where ever you see green text it is results from the previous test (test 19) for quick comparison.

Channelling began whilst it first filled with water. The longest channel was about 60mm 50mm.

Pic before test started:

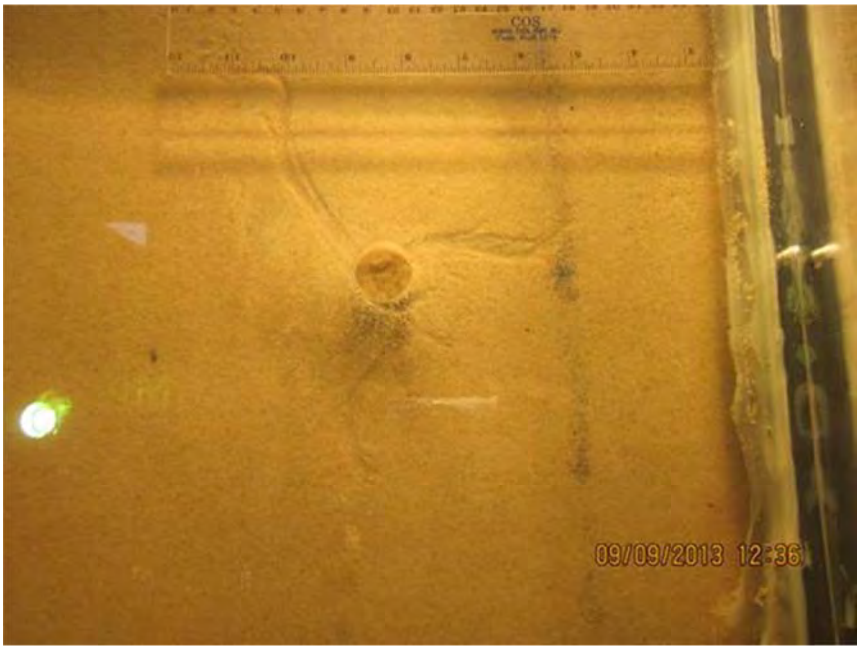

The tip of the channel facing the upstream direction continued to progress at a head of 98mm 92mm. The head required incremental increases to keep the tip going. Once at a length of 361mm 363mm (about 30% of the seepage length) and a head of 140mm 233mm the tip progressed through almost to the upstream side without any further head increases.

Sand boiling could be seen at the exit from the start of the test. The boiling activity increased with increases in head.

The tip didn't make it all the way to u/s panel- it stopped about 21mm short despite leaving it there overnight. My theory is the channel was stopped by bubbles. I first observed an air/CO2 bubble on the morning of the second day of testing.

Pic of first bubble

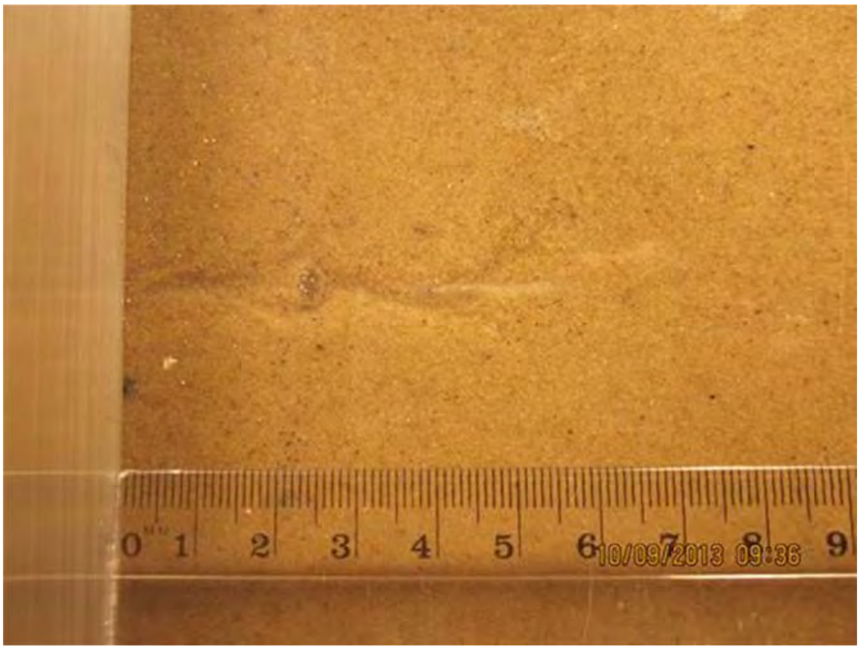

The amount of bubbles increased over time.

Pic of bubbles by end of test:

At this stage I don’t know how/why bubbles entered this system. However I have noticed that this occurs is open for an extended period of time (I had left this test open over the weekend before testing). So in the future I am going to try keep it all sealed until I know I’m definitely ready to test.

Because the channel hadn’t completely reached the upstream end I kept the experiment going. I increased the head to 256 and then 282mm which created a new channel which reach did reach the upstream end. However in my graphs and result comparison below I have only considered the first channel because I believe the first channel would have reached the upstream end if it weren’t for the bubbles.

Chart below graphs test 20 results.

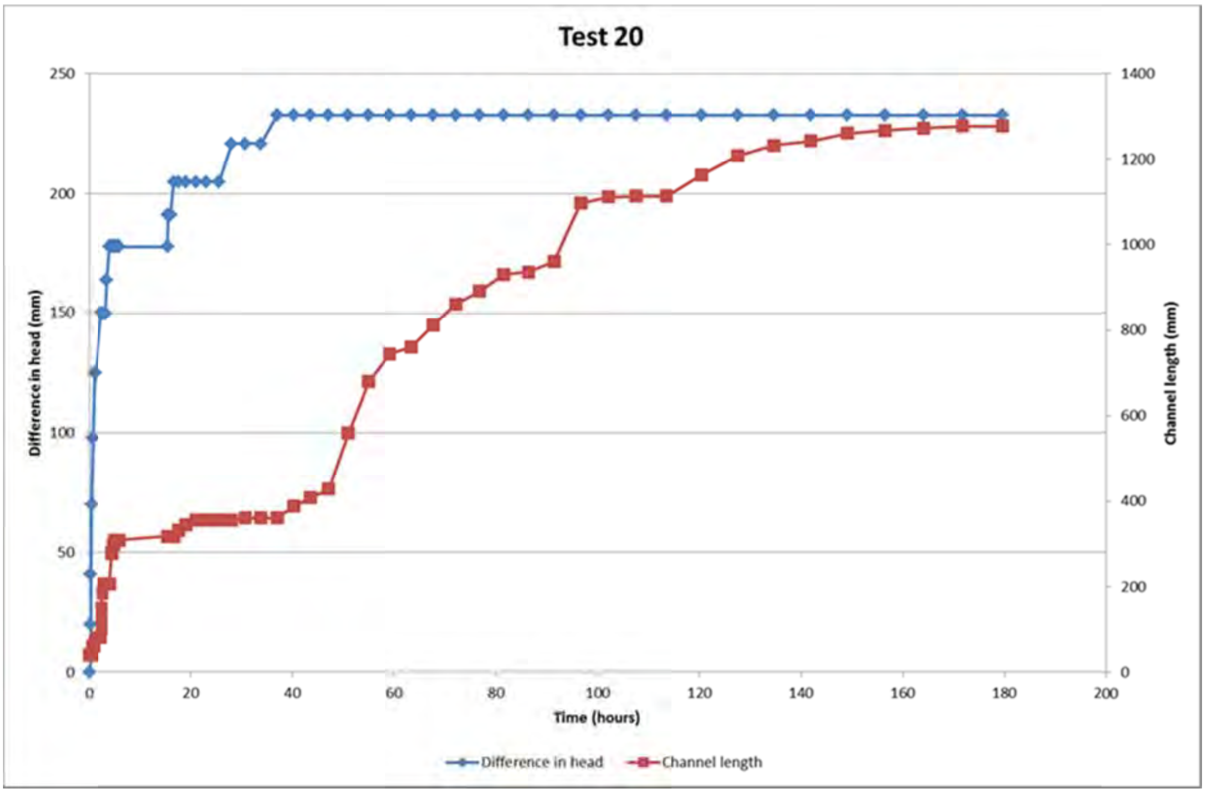

As for comparing this hole-exit test with the previous hole-exit test refer to this graph:

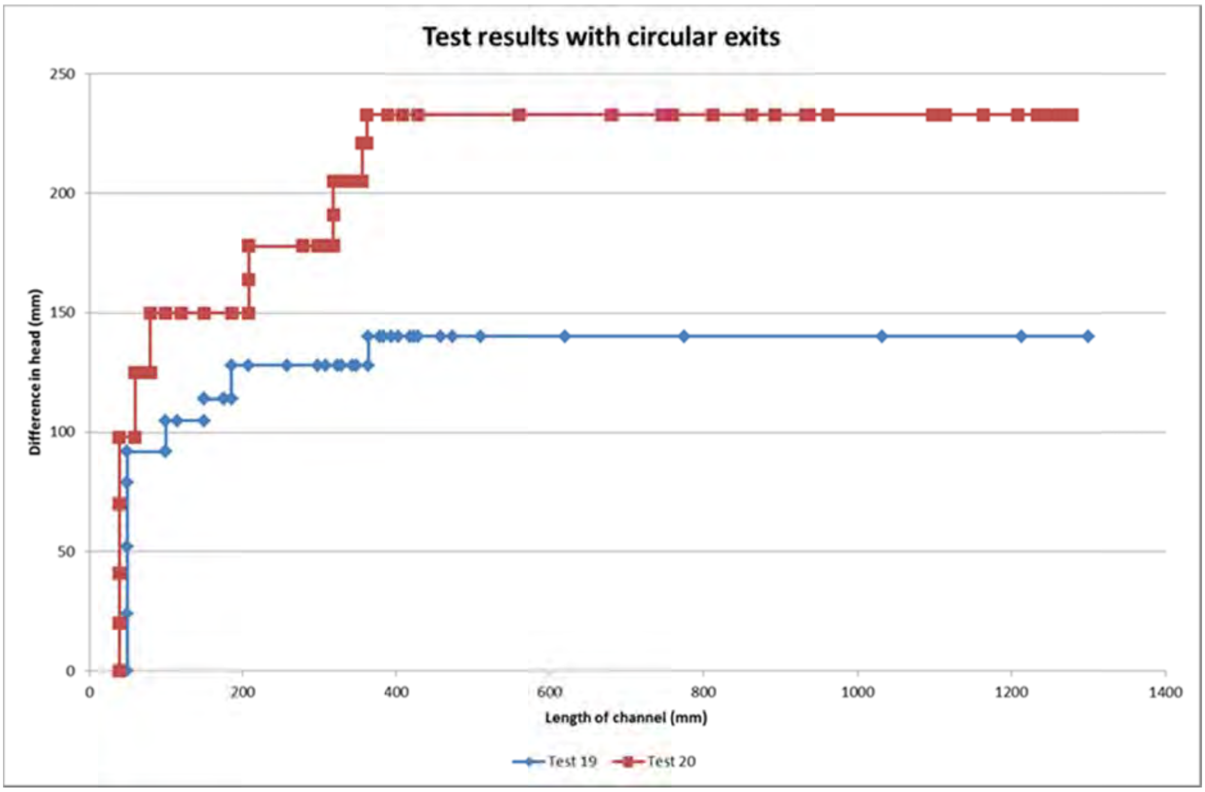

Whilst they behaved the same way in that head increases were required until the tip reached 30% of the seepage length, the critical head was 66% greater (233mm instead of 140mm). I suspect this could be for two reasons. One- the difference in head measured for test 19 wasn't correct because I hadn't yet established levels with the dumpy (it wasn't at the lab at the time) and two- bubbles which had entered test 20 had increased the head required.

I propose to do another circle-exit test which isn't opened until ready to test (less change of air/gas bubbles) and there is more certainty with difference in head levels.

Backward erosion piping test data sheet

Test #	21	mass of soil & water	0 kg
Date	16/09/2013	flume volume	m^3
Soil	Sydney sand	moisture content	%
Flume	1	dry unit weight	#DIV/0! kN/m^3
Exit type	slot	void ratio	#DIV/0! -
seepage length	1.3 m	relative density	#DIV/0! -
head in bladder tank	5 m	fill from d/s hose	50 mL
bladder pressure	50 kPa	avg. time to fill	13.8 s
		flow rate @ ΔH = 10cm	#DIV/0! L/min 0.22

time	head (cm)	observation
11.44	0	no movement.
11.45	↑14	" " . flow dripping out of
		d/s valve
11.50	↑26	no movement -
11.55	↑39	" "
12.03	↑51	" "
12.11	↑64	" "
12.21	↑80	" "
12.29	↑89	" "
12.36	↑100	d/s flow = 22.6, 14.3, 15.7, 10.5, 14.7 s
		no movement
12.45	↑115	" "
12.53	↑128	" "
1.13	↑140	" "
1.17	↑154	" "
1.29	↑170	" "
2.33	↑183	" "
2.40	↑196	" "
2.48	↑209	" "
3.03	↑223	" "
3.07	↑231	" "
3.16	↑239	" "
3.22	↑	" "
3.31	↑271	Initiation. first noticed when tip 50mm
		after bl. Channel at slot is more
		like a 'fore' from RHS edge along

Test 21

time	head (cm)	observation
		30mm. Boiling is observed along d/s
		edge of slot. Most particle
		transport occuring at RHS edge.
		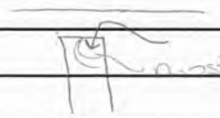 most boiling action
3.49		tip 133mm ab1
3.54		160mm ab1
3.58		195mm ab1
4.03		tip @ b2
4.05		Sand on top of lid @ RHS edge of slot.
		Channel no longer exiting at RHS edge
		but ≈ 30mm in from. No more boiling @
		RHS edge.
4.06.		there's various channels at slot
		Maybe 3.
4.08		tip 70 mm ab2
4.18		It's now boiling @ the RHS edge again.
4.20		tip 10[illegible]mm ab2
4.28		tip 160mm ab2
4.37		200mm ab2
4.43		observed small boiling along d/s of slot
		(see happy snap)
4.45		tip @ b3
4.50		channel flowing along RHS
4.57		Still under b3
5.04		" " ". A new channel has
		formed in fact there's one from either
		direction, in the middle of the
		flume width
		 See happy snap
5.09		tip other side of
		b3
5.12		tip 32mm ab3
5.17		other channel now at tank wall
5.26		" " 40mm ab1. 3 more channels
		d/s of slot (see happy snap)
5.33		2nd channel 80mm ab1
		Original channel 160mm ab3.
5.41		" " 198 mm ab3 and 2nd
		channel has joined up with original.
5.45		there's a blockage btw bars 2+3. left
		overnight.

Test 21

time	head (cm)	observation
17-9		
10:00		excessive channeling observed - i.e failure.
		" " on LHS where as
		RHS just has remenants of original
		channel. Most of the sand buildup +
		sand boiling on LHS. All flow going
		through exp (none through drain
		cylinder). See pics + vid.
		From photos
16-9		
6:15		original channel reached loc 4
6:53		" " U/S. The
		channel looked freakishly straight betw
		64 and U/S.

time	head (cm)	observation

Test 21 (flume 1 slot) report

Test 21 was the first test with a slot exit.

Initiation occurred at a head of 271mm on the RHS edge. When initiation occurred it did so quite quickly as if a resistance had been building up. Here is a photo of what I saw when I first observed initiation:

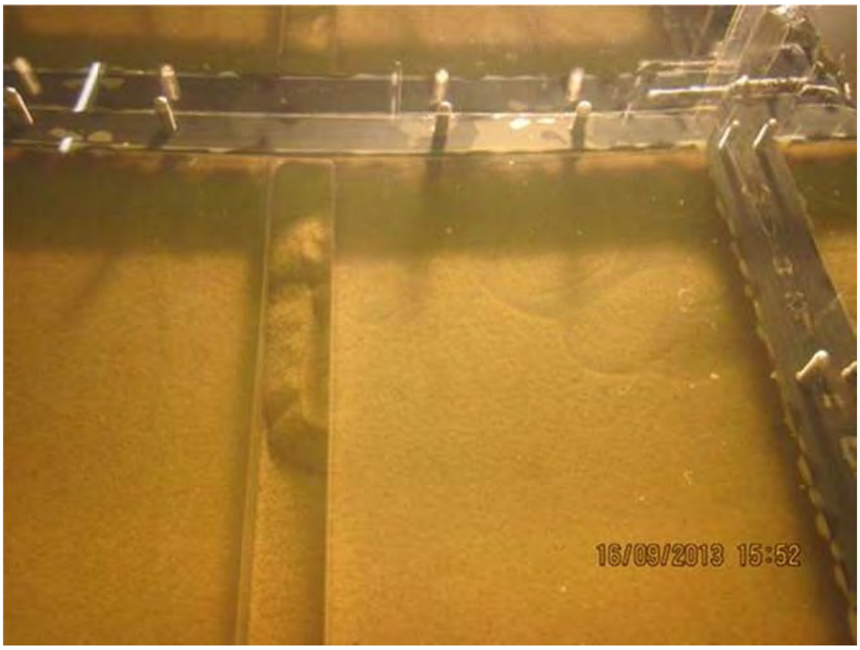

The channel progressed all the way to the upstream end at this head (271mm).

Plot of results:

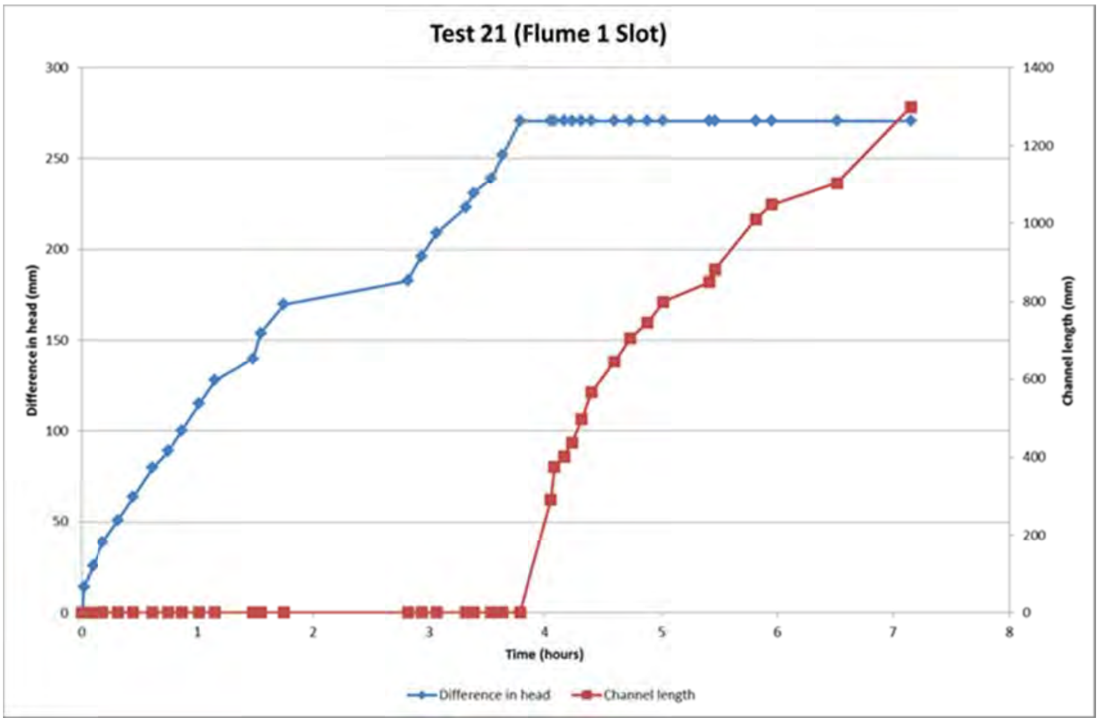

I'm concerned that the channel started at the edge. I think it started at the edge for 2 reasons:

1. friction btw sand and wall is less than friction between sand and sand
2. The slot didn't extend all the way to the inner wall of the flume as I requested (this possibly a miscommunication blunder). The slot stopped about 10mm short- in the pic below Rob is using his finger to show where the wall of the flume sits. Because the slot doesn't go all the way to the flume wall, the flow at this point concentrates and becomes more 3D (rather than purely 2D). And because the flow concentrates here I expect it to be faster than elsewhere and hence the channel will always start here.

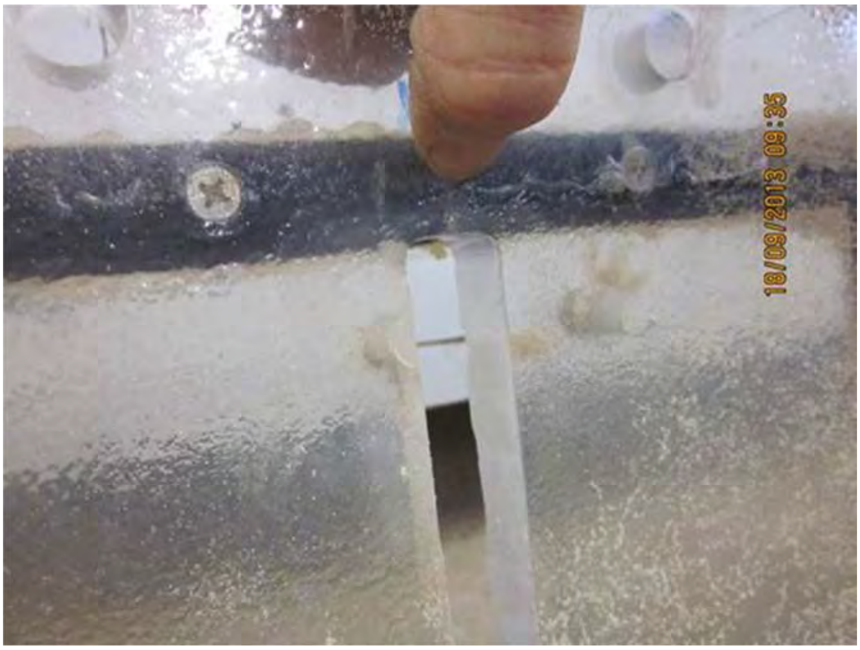

To minimise the chance of channels starting (and possibly continuing) along the edge I intend to make the following changes (in this order, only if the proceeding change doesn't work):

1. Move the d/s tank walls out so the slot can be extended to meet the inner flume walls
2. Use a small starter channel (like 20mm long) to encourage it to start in the middle
3. Coat the inner walls of the flume with the same silicon we use to coat the lid with

Do you agree with this approach?

As for comparing these results with other exit geometries, I predicted the results to look somewhat like this:

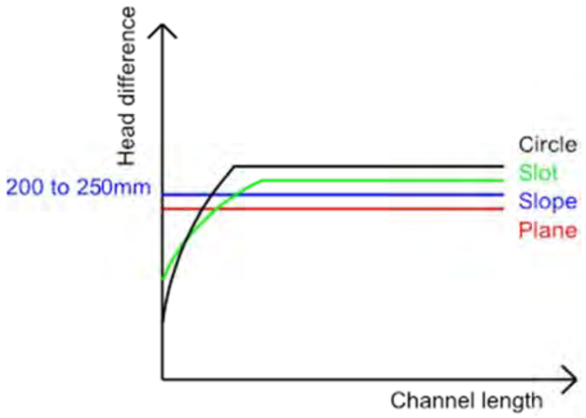

But so far they look like this (very simplified**)**:

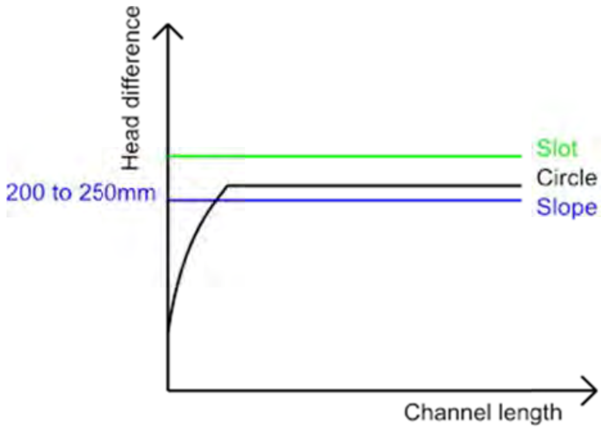

I don’t think it’s worth hypothesising why this is until I get channel not along the edge.

Backward erosion piping test data sheet

Test #	22	mass of soil & water	0 kg
Date	24/09/2013	flume volume	m^3
Soil	Sydney sand	moisture content	%
Flume	~~2~~ 3	dry unit weight	#DIV/0! kN/m^3
Exit type	circle	void ratio	#DIV/0! -
seepage length	1.3 m	relative density	#DIV/0! -
head in bladder tank	5 m	fill from d/s hose	50 mL
bladder pressure	50 kPa	avg. time to fill	15.14 s
		flow rate @ ΔH = 10cm	#DIV/0! L/min

time	head (cm)	observation
10.45	0	Because I changed the d/s
		arrangement the datum level has
		dropped a few mm. Ideally I
		would reset the datum level but
		the dumpy is unavailable so I'll
		use the existing datum but will have
		to amend the recorded levels once I
		have the dumpy to work out the
		diff btw the current + new datum
		levels.
1053		there are air/gas bubbles on the
		RHS + extending towards the middle. It
		covers a large-enough area that I think
		it is likely the tip will intercept it +
		affect results. See happy snap. I don't know
		y/how it's there except to notice that it is
		next to a part of the ~~blade~~ rubber
		that has sand on it and now/is
		leaking. So perhaps air travelled in via
		the leak (see happy snap). I'm not sure
		how to prevent it except to somehow take
		more care in preventing sand on
		the rubber.
10.58		Opened d/s valve. level dropped
		about 10mm.
11.03		2 to 3 small channels before test

Test 22

time	head (mm)	observation
		started. 
11.04	↑ 9	v small amount of fluidisation can be seen in hole. but no other movement.
11.07	↑ 27	no movement
11.16	↑ 41	" "
11.17		bladder still @ 5m.
11.20		no movement
11.29	↑ 54	" "
11.53	↑ 67	" "
11.57	↑ 80	" "
12.00	↑ 92	small intermittent movement at tips but only short lived + no progression
12.06	↑ 107	progressed tip b ≐ 5mm but then stopped and tip (a) ≐ 5mm but the stopped. Guess (a) currently 150-107mm
12.12	↓ 100	50ml @ 15.7, 16.6, 14.3, 15.9, 13.2
12.23	↑ 121	2 new channels have formed 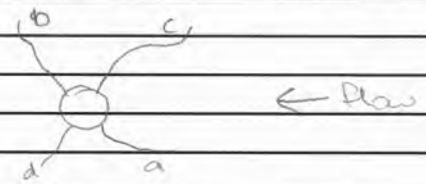
		all tips progressed initially but then stopped. the new channel (c) progressed for the longer period of time. Channel (c) moved more laterally than u/s/ds (see happy snap). Channel (c) approx 135-107mm from hole.
12.33		no longer any movement.
12.32	↑ 134	Channel (a) became more defined but didn't progress (still @ 150-107). there was movement in (c) momentarily but still only moved laterally (by a little bit < 10mm).
12.37		tip (a) on the move. Now 165-107.
12.40		" " 180-107
12.52		" " " "
12.53	↑ 148	both tips c and a reactivated.
12.54		tip (a) 195-107. tip (c) stopped.
12.55		tip (a) 210-107.
12.56		Particles on top of lid around hole.
12.57		tip (a) 230-107.
12.58		" " at d/s tank wall
1.46		" " still under tank wall
1.46	↑	tip reactivated
1.52		tip other side of tank wall

Test 22

time	head (cm)	observation
2.08		tip reached b1
2.30		still under b1 + no movement in channel
3.00	174	readjusted datum. All levels from
		now on adjusted. The datum has
		dropped 12mm so add 12mm on to
		all previous heads.
3.05		tip now other side of b1
3.21		tip 17mm ab1
3.36		tip 25 ab1
4.03		tip 33 ab1
4.44		tip still 33 ab1
4.44	↑ 186	
4.59		tip 50 ab1
25-9		
9.38		tip still 50 ab1
9.38	↑ 195	
9.40		tip reinitiated now 65 ab1
9.47		tip 100 ab1
10.00		tip 160 ab1
10.13		tip 215 ab1
10.24		217 ab1
10.46		tip underneath b2
11.02		tip 30 ab2
11.12		tip 45 ab2
11.26		" " "
11.40		tip 63 ab2
11.48		75
12.09		105
12.19		123
12.46		180
1.04		185
1.18		230
2.30		tip underneath b2
2.48		" " "
3.13		" " "
3.32		" " ", I checked head
		tank and it's now like 200.
4.20		tip underneath b2
5.13		" " "
5.26		tip otherside of b2. leaving overnight
26-9		
9.54		tip 20mm ab3
9.55	↑ 212	
10.05		tip 25 ab3
10.15	↓ to 80	because I turned tank 1 on.
10.18	↑ 212	/ tip 25 ab3
10.18	↑ 224	

time	head (cm)	observation
10.29		tip 70 ab3
10.42		113 ab3
10.45		138 ab3
10.49		190 ab3
11.29 ← check time		125 ab4 which looks to be the end
		(see happy snap). the channel has
		started to deepen. Will record
		when the deepened channel reaches
		the d/s end.

Test 22 (Flume 2 hole) report

Test 22 was the third test with a hole exit.

Channelling began whilst it first filled with water. The longest initial channel was about 50mm.

The tip of the channel facing the upstream direction continued to progress at a head of 134mm. The head required incremental increases to keep the tip going. Once at a length of 292mm (about 20% of the seepage length) and a head of 195mm the tip progressed until it was 870mm long. I then had to increase the head 2 more times (to 224mm) mm to progress the tip to the u/s side. This is summarised in this chart:

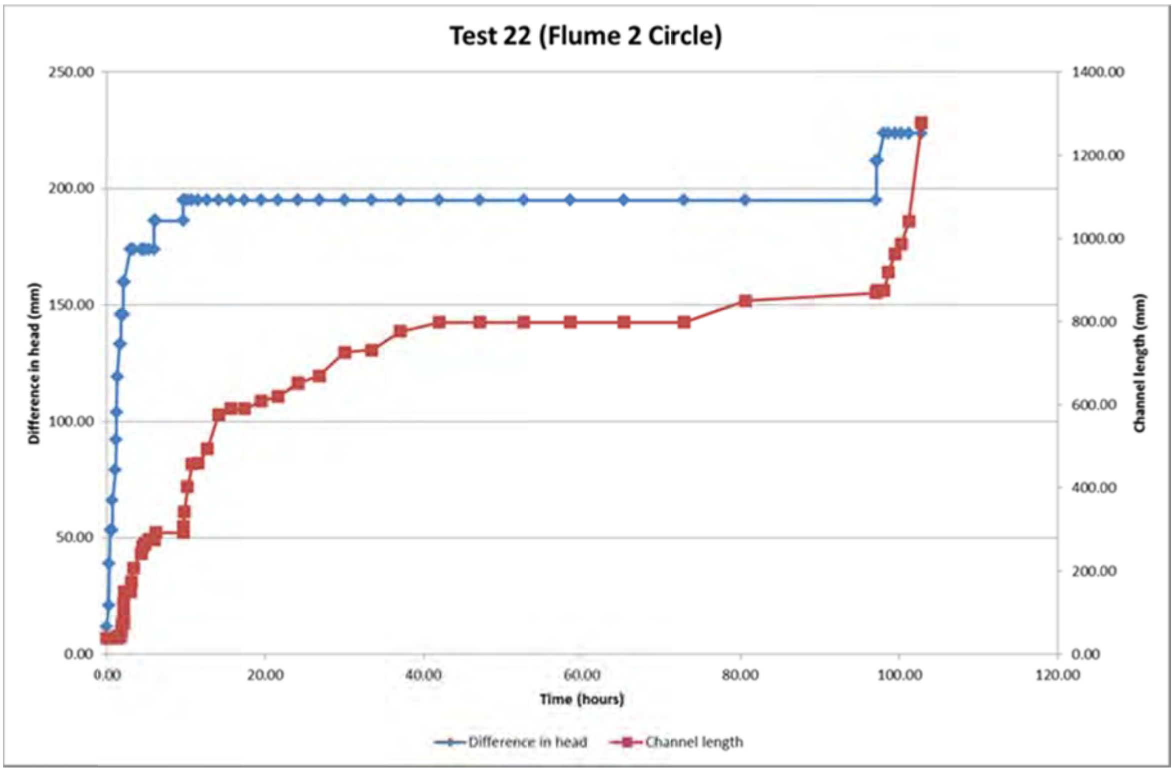

In hindsight I probably shouldn't have increased the head above 195mm because perhaps the tip was still moving, albiet painfully slow.

I left the test running until failure. When I refer to 'failure' I am referring to a sudden increase in sand boil size and a sudden increase in flow (all flow goes through the experiment and none through the head tank drain). I first saw this failure in test 21 (but forgot to mention it in test 21's report- I will report on it from now on). What happens is the channel deepens from the u/s end to the d/s end and once the deepening reaches the exit a sudden 'failure' occurs- it's best if I show you the video of this when I next see you both. In test 22 failure occurred 7 hours after the channel had reached the u/s end (still at a head of 224mm).

Air bubbles were seen in the sample- I think they had come in from the sides due to an inadequate seal. The tip didn't appear to intercept these air bubbles so I don't they affected the results. In future I will prepare the top rubber gasket before putting the lid on (clean with metho and coat with silicon grease) in order to achieve a better seal and preventing this from happening again.

Pic of air bubbles

As for comparing this test with the 2 previous circle tests refer to this chart:

As for comparing this test with the previous hole-exit tests refer to this graph:

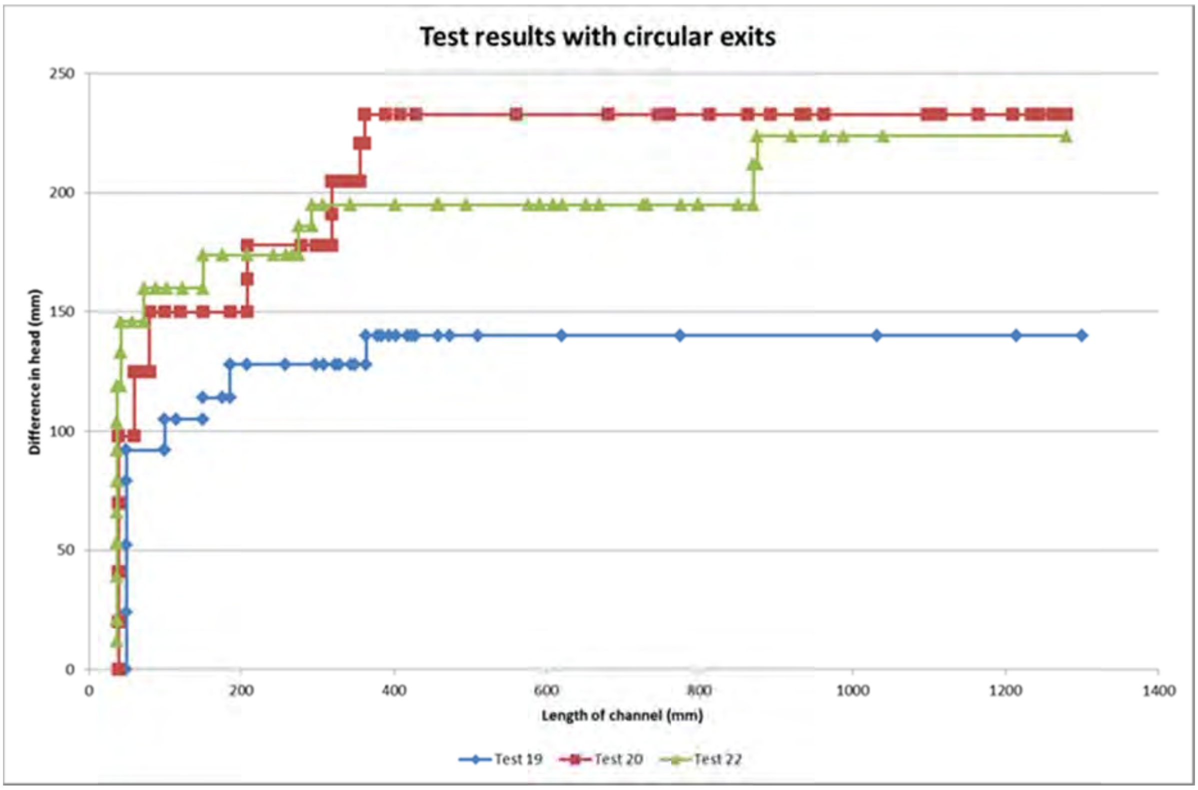

Before I compare results I need to note that:

- I’m going to ignore the fact that test 22 required increases in head at the end (because it’s possible it didn’t need increases- I just got impatient (because it moved only 20mm overnight));
- I think heads in test 19 were higher than recorded (I didn’t have the dumpy so I had to approximate); and
- Test 20 was interfered by bubbles

What is similar between tests:

- Head required increasing until channel was at between 20-30% of the seepage length and then continued to the end without further need for head increases
- The critical head for test 22 is between tests 19 and 20.

What is different between tests:

- There was a 16% drop in the critical gradient from test 20 to test 22. Is this within acceptable experimental variability?

Backward erosion piping test data sheet

Test #	23	mass of soil & water	0 kg
Date	27/09/2013	flume volume	m^3
Soil	Sydney sand	moisture content	%
Flume	1	dry unit weight	#DIV/0! kN/m^3
Exit type	slot	void ratio	#DIV/0! -
seepage length	1.3 m	relative density	#DIV/0! -
head in bladder tank	5 m	fill from d/s hose	50 mL
bladder pressure	50 kPa	avg. time to fill	14.1, 15.8, 14.7, 14.5 ~~15.14~~ s avg = 14.8 s
		flow rate @ ΔH = 10cm	0.20 L/min Ckk.

time	head (mm)	observation
10.37	9	the coloured sand that was near
		the slot has arranged itself along
		the edges (happy snap). the only
		air bubbles that can be seen
		are d/s of the slot. I have
		limited time to do this test (given
		it's a Friday) so I'm going to
		raise the head in 50mm increments
		until I get to 200mm because the
		previous slot test had a critical
		head of 271mm (was also the
		initiation head).
10.41	↑ 59	no movement
10.49	↑ 108	" "
11.17	↑ 164	" "
11.36	↑ 216	initiation. 2 channels started. One
		in the centre and one ≐ 150mm
		from the LHS. The centre one grew
		≐15mm + then appeared to stop. the one
		150mm from LHS grew ≐20mm + then seemed
		to stop. See vid + happy snap.
11.47		I checked flow because previously the
		u/s valve wasn't fully opened.
		to fill 50mL took 5.8, 6.8, 7.3, 7.9, 7.5s.
11.56		no movement
11.59	↑ 230	grain rearrangement at the tip but

Test 23

time	head (cm)	observation
		no progression. (LHS tip)
12.12	↑ 243	tip 140-113 (LHS tip)
12.22		" " " (LHS tip)
12.22	↑ 256	
12.25		middle tip progressed to 140-113
12.33		third channel first noticed. It's
		about 100mm from LHS.
12.34		3rd tip 185-113. It has 2 tips
		(see happy snap)
12.36		3rd tips have stopped but boiling
		action on going at it's end.
12.39		boiling action stopped.
12.40		a new tip off 3rd channel started.
		now 210-113.
12.41		now 236-113 (3rd channel, 3rd tip).
		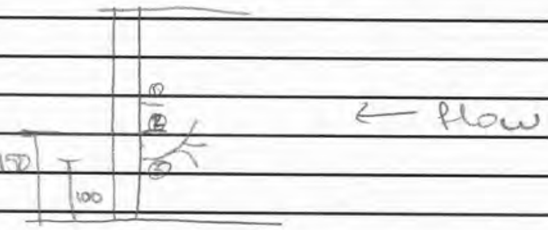
12.43		3rd channel past tank wall.
12.43		tip ~~at~~ b1
12.52		tip 85 ab1
12.54		tip 110 ab1
1.01		190 ab1. The one channel is branched
		off into many at the d/s end.
1.07		235 ab1
1.13		tip underneath b1
1.18		40 ab2. boiling action on d/s edge of
		slot.
1.23		78 ab2
1.27		120 ab2
1.32		148 ab2
1.35		tip has started moving laterally +
		slowing down (perhaps a more
		dense region).
1.36		160 ab2
1.40		198 ab2
1.50		tip under b3
1.56		60 ab3
2.05		130 ab3
2.14		190 ab3. channel has blocked under b1.
2.22		223 ab3
2.35		tip under b4. blocked zones btw b's
		2 + 3 and 1+2.
2.43		15 ab4

Test 23

time	head (cm)	observation
4.07		tip is through to u/s end. I'll have to
		check photos to work out what time it
		occured. tip is 140 abt. The camera
		battery actually died at 2.27pm
		(I hadn't noticed) so I don't know
		what time it got to the end.
4.18		I have put charged batt in camera
		+ have set to take every minute. to
		watch for failure. Will leave
		running over the weekend.
30-9		
10.17		All looks as I left it on Friday
		afternoon. the deepened channel
		is between u/s end and bar 4.
		The channel is blocked between
		bars 1 and 3. the same amount of
		sand is present at the ditch. there
		is a strange discolouration along
		the u/s edge and around the
		channel between the u/s edge and
		bar 4 (see happy snap). Not sure
		what this is about. Also, I can hear
		the pump running dry. The water
		level hasn't changed much - it's
		about 254.5. there is flow coming
		out of the drain hose as well
		as out of the flume but the flow
		out of the drain cylinder is much
		less than it was on Friday. I fully
		opened the head tank 'in' valve
		but the water level didn't change.
		So I'm thinking the filter has
		clogged up again.
12.02		washed off filter + turned water back
		on.
12.30		water off again
2.47		water on again.
2.47	↑ 275	no movement

time	head (cm)	observation

Test 23 (flume 1 slot) report

Test 23 was the second test with a slot exit.

Initiation occurred at a head of 216mm near the middle of the flume (not on the edge this time thanks to Rob having widened the slot to the edge of the flume). 2 channels formed at initiation but both stopped progressing so a 3rd channel formed at 256mm. It was the third channel that continued to progress.

Photo of 3 channels about 1 hour after initiation (the 3rd channel is underneath the ruler):

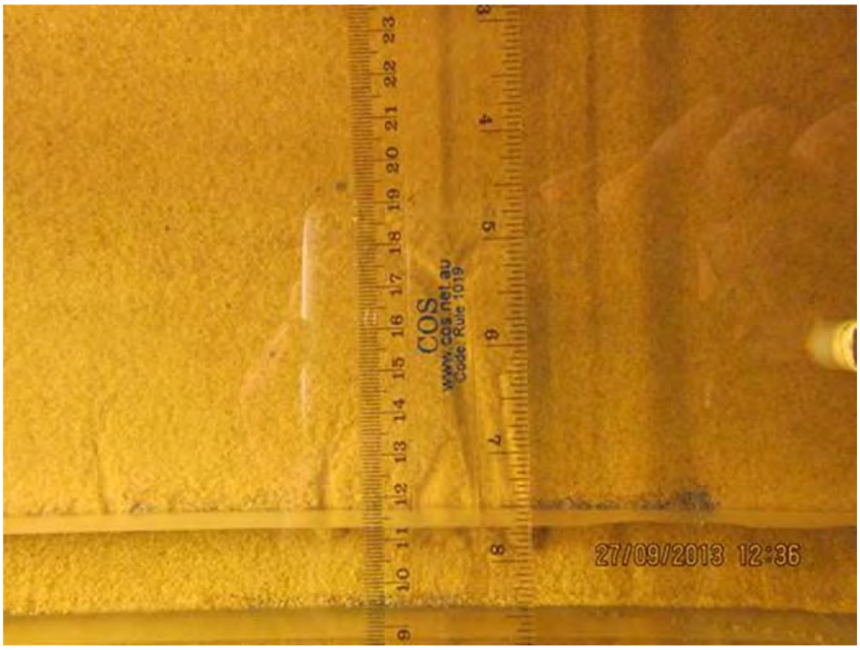

The channel progressed all the way to the upstream end at a head of 256mm.

Plot of results:

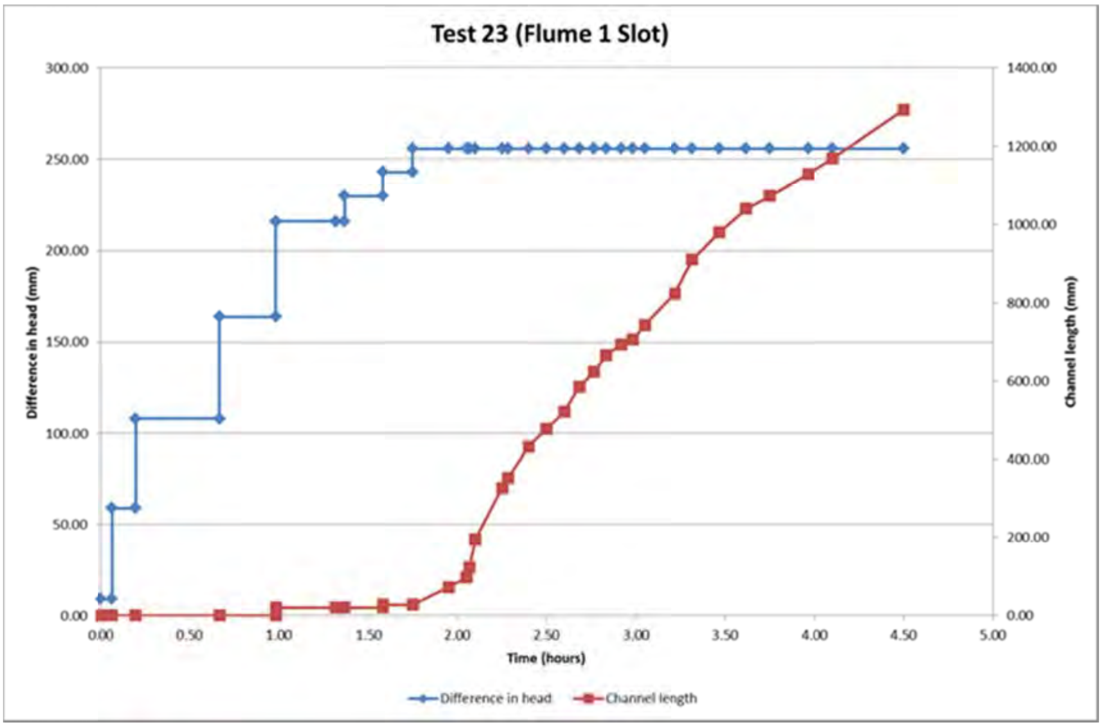

As for comparing these results with other exit geometries, I predicted the results to look somewhat like this:

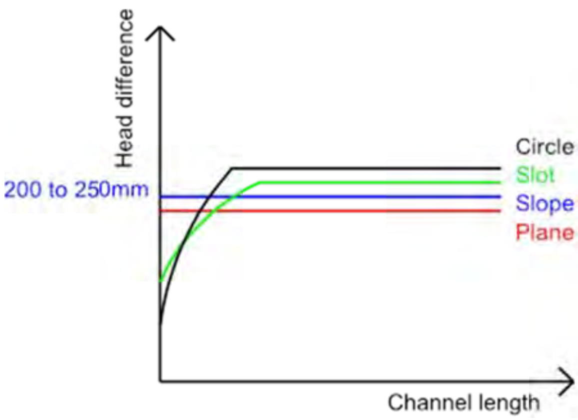

But so far they look like this (very simplified**)**:

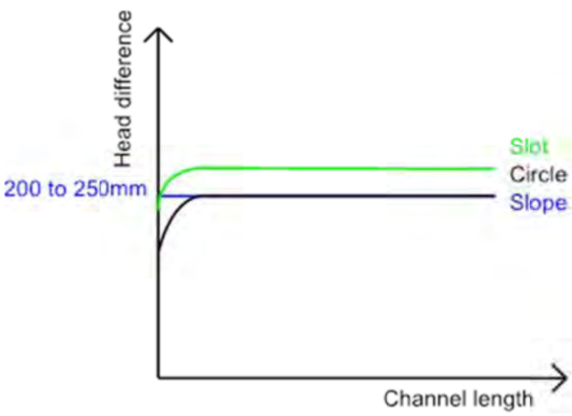

four earth-pressure-cell tests were carried out on this sample before test 24 so more dense

20 micron filter to start with & then 5 micron filter.

Backward erosion piping test data sheet

Test #	24	mass of soil & water	0 kg
Date	10/10/2013	flume volume	m^3
Soil	Sydney sand	moisture content	%
Flume	~~2~~ 3	dry unit weight	#DIV/0! kN/m^3
Exit type	circle	void ratio	#DIV/0! -
seepage length	1.3 m	relative density	#DIV/0! -
head in bladder tank	5 m	fill from d/s hose	50 mL
bladder pressure	50 kPa	avg. time to fill	15.14 s
		flow rate @ ΔH = 10cm	0.20 L/min

time	head (mm)	observation
11.59	0	no movement & no ~~start~~ initial channels
12.00	↑21	" "
12.13	↑35	" "
12.25	↑49	" "
12.36	↑70	" "
12.46	↑75	" "
12.58	↑88	" "
1.13	↑102	" ", 50mL t = 15.2, 15.9, 14.1, 15.5, 14.8
1.43	↑116	" "
2.00	↑131	" "
2.21	↑142	" "
2.43	↑155	" "
2.48	↑170	" "
3.29	↑184	" "
3.34	↑196	" "
3.41	↑211	" "
4.04	↑223	" "
4.13	↑236	a sort of initiation. There is a
		channel but it doesn't start at
		the exit (see happy snap). It exits
		into a possible depression in the sand.
4.16		190-130 mm long
4.19		the channel is growing forward in a
		fashion in that the deposition zone
		is getting closer to the exit.
4.24		190-130mm. I see a group of particles

15.15 time on camera. I think time on camera is 58' slow

time	head (cm)	observation
		leave the tip and get deposited at
		the d/s end of the channel about
		every few minutes.
5:28		190-130mm by. leave overnight
11-10		
10.00		I didn't think the channel would move
		overnight but it did - a lot. The tip
		is now 140mm ab3. However there's
		heaps of bubbles (see nappy snap).
		I suspect there's heaps of bubbles for
		the same reason I suspect CO_2 + water
		leak(ed) - sand + clumps of detached
		sealant underneath the nm gasket.
		the bubbles started to come in at
		8:33pm 1SH. I don't think the tip is going to
		progress anymore without head increase
		so I'm terminating the test. ie. its been
		compromised.
		In addition to the bubbles I don't like
		that the channel didn't start at the
		exit. I think it looked something
		like this.
		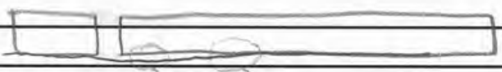
		channel started here
		local gap underneath the lid
		In short I don't think I should use
		the results from this test.
		Lessons learnt:
		1) It's crucial to make sure the top of
		sand is overfilled + screeded down
		evenly + flat.
		2) It's crucial there's nothing stuck
		underneath the nm gasket, otherwise
		air gets in + compromises the test.
10:57		test terminated.

Test 24

real	time	head (cm)	observation
			Observations from photos:
	10-10		
5.31	4.33 pm		tip to b1
7.31	6.33		tip to b2
8.31	7.33		tip halfway btw bars 2 + 3.
9.01	8.03		tip to b3. Bubbles may have started to come
10.31	9.33		tip halfway btw bars 3+4
	11-10		
	10.00		next morning tip 3+4
			halfway btw bars 3+4.
			in at this point.
			But difficult to
			see on photos.

time	head (cm)	observation

Test 24 (flume 2 circle) report

Test 24 was the 4th test with a circle exit.

I am of the opinion that this test was compromised and it's results should not be used for 2 reasons:

1. The channel did not initiate at the hole but approx. 30mm upstream of the hole; and
2. Many air bubbles entered the system from approx. 8.5hrs after the test started.

I think the channel initiated 30mm upstream of the hole because there was a gap between the lid and sand in a region around the hole, i.e. I didn't overfill the flume with sand consistently so that when I screened the surface an area of the sand was a few grains lower than its surrounds. See sketch and photo of channel when initiated first noticed:

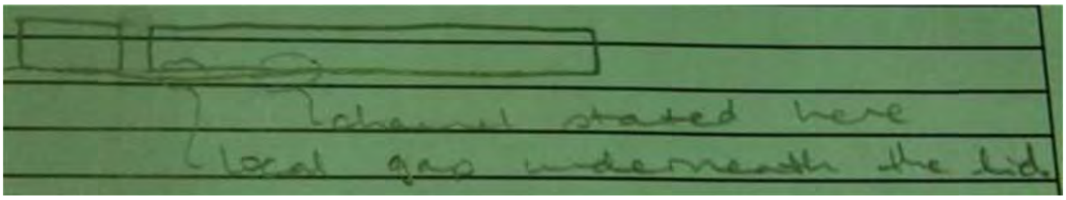

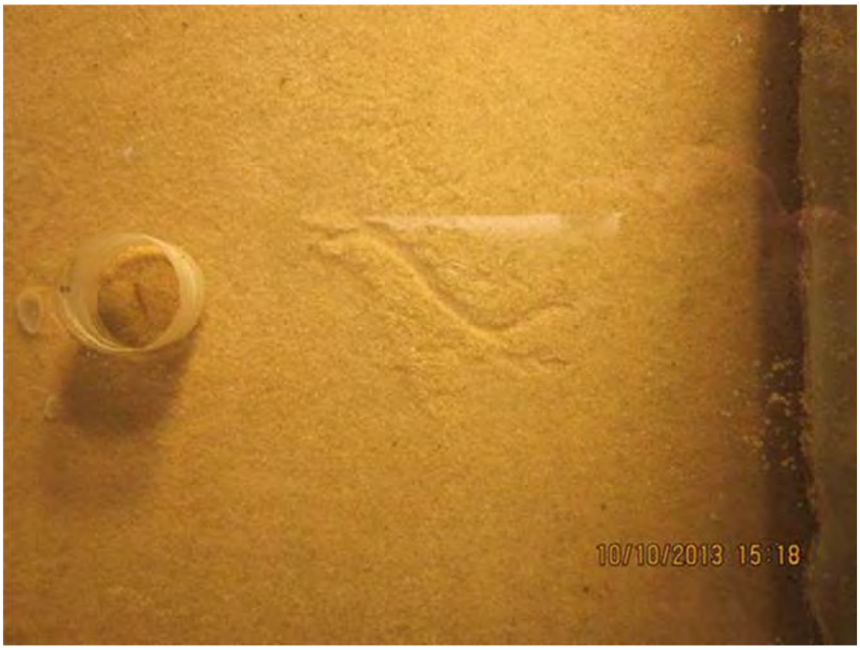

As for air bubbles entering the sample, I suspect air was getting in via gaps between the flume and the rim gasket because sand and clumps of unstuck silicon were underneath the gasket.

Pic of air bubbles:

Lessons learnt:

1. It's crucial to make sure the top of the sand if overfilled and screen down evenly and flat
2. It's important there's nothing stuck underneath the rim gasket, otherwise air gets in.

Test results:

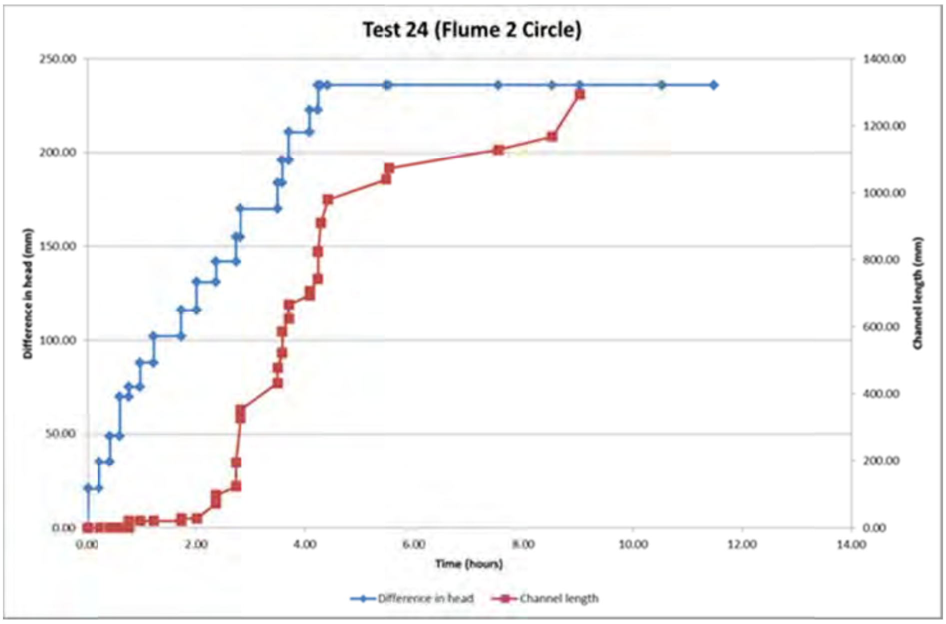

Compared with other circle tests:

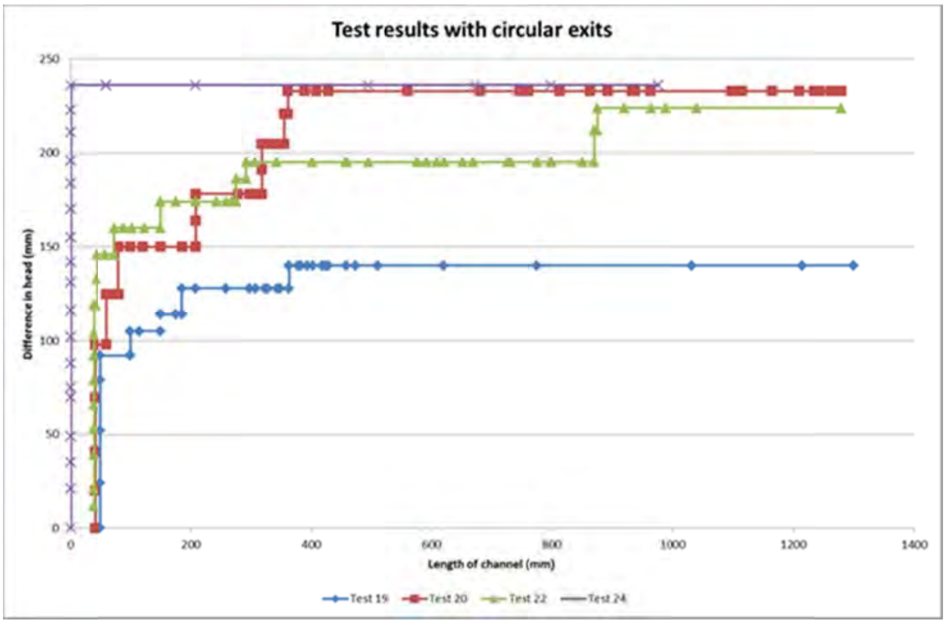

Test results with circular exits
Difference in head (mm)
Length of channel (mm)
0
50
100
150
200
250
0
200
400
600
800
1000
1200
1400
Test 19
Test 20
Test 22
Test 24

Backward erosion piping test data sheet

Test #	25	mass of soil & water	0 kg
Date	24-10-13	flume volume	m^3
Soil	Sydney sand	moisture content	%
Flume	1	dry unit weight	#DIV/0! kN/m^3
Exit type	slot	void ratio	#DIV/0! -
seepage length	1.3 m	relative density	#DIV/0! -
head in bladder tank	5 m	fill from d/s hose	50 mL
bladder pressure	50 kPa	avg. time to fill	15.14 s
		flow rate @ ΔH = 10cm	0.20 L/min

time	head (mm)	observation
9.30	0	no movement
9.31	↑ 103	flow 50mL = 17.1, 13.9, 16, 13.3, 14.1, 16.2
10.00	↑ 164	no movement
10.10	↑ 192	" "
10.22	↑ 214	" "
10.26	↑ 272	" "
10.38	↑ 244	" "
10.39		2 small sand boils on d/s edge of slot
		(see happy snap). But no movement on u/s
		edge.
10.57	↑ 257	no movement
11.07	↑ 271	
11.12		initiation. Tiny boil + tip started 120mm from RHS
		edge (see happy snap)
11.14		now 170-111mm long (once started progressed
		quickly at a width of ≈40mm + splitting into
		2 tips
11.15		One tip 120-111 mm long
11.17		tip 124-111mm
11.19		tip at tank wall
11.23		tip bl
11.2?		tip 20 abl
11.30		tip 55 abl
11.36		90 abl
11.43		150 abl
11.52		190 abl

10.14am camera is 58' slow

time	head (cm)	observation
11.57		73 ab1
11.59		b2
12.11		15 ab2
12.21		80 ab2
12.32		120 ab2
12.36		160 ab2
12.36		blocked just u/s of bar 1. New tip
		formed now 65 ab1 (call this tip tip 2).
12.49		tip 1 216 ab2. tip 2 183 ab1.
12.52		tip 1 220 ab2 tip 2 208 ab1.
1.10		tip 2 joined original channel so now
		only one channel again. essentially the
		2nd tip bypassed the blocked zone
		tip 1 now at b3.
1.52		45 ab3 and blocked from halfway btw 1 and 2
		and to 2 and 3.
2.14		45 ab3
2.26		125 ab3. Channel flowing again btw bars
		1 and 2 but still blocked btw 2 and 3.
2.3[illegible]		160 ab3. The blockage continually opens +
		reblocks (see video).
2.55		245 ab3
2.56		b4
3.08		10 ab4. A region partially blocked under b3.
3.20		80 ab4
3.34		first noticed tip @ u/s end

Test 25 (flume 1 slot) report

Test 25 was the 3rd test with a slot exit

A channel initiated approx. 120mm from the RHS at a head of 271mm. When it initiated there were 2 tips but it didn't take long before only one of the tips progressed.

ic shortly after initiation:

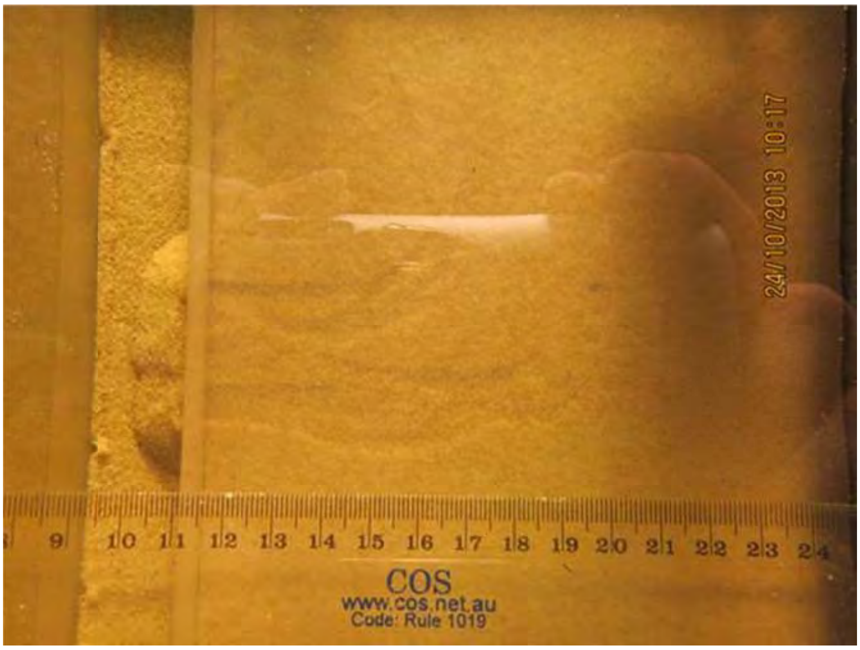

Once initiated the channel progressed relatively quickly (about 4mm/minute) until it had a reached a length of about 262mm and then slowed down a little to about 6mm/minute. Once the tip had reached 706mm a length of channel just u/s of bar 1 blocked and a new channel formed from the slot. Whilst the new channel tip progressed the original channel's tip slowed down and stopped. However eventually the 2nd tip joined the original channel, essentially bypassing the blocked zone, and the original tip reactivated and progressed at a similar speed as before (6mm/minute). Despite there being subsequent blockages along the channel length the tip continued to progress; the blockages were in a cycle of blocking and opening up.

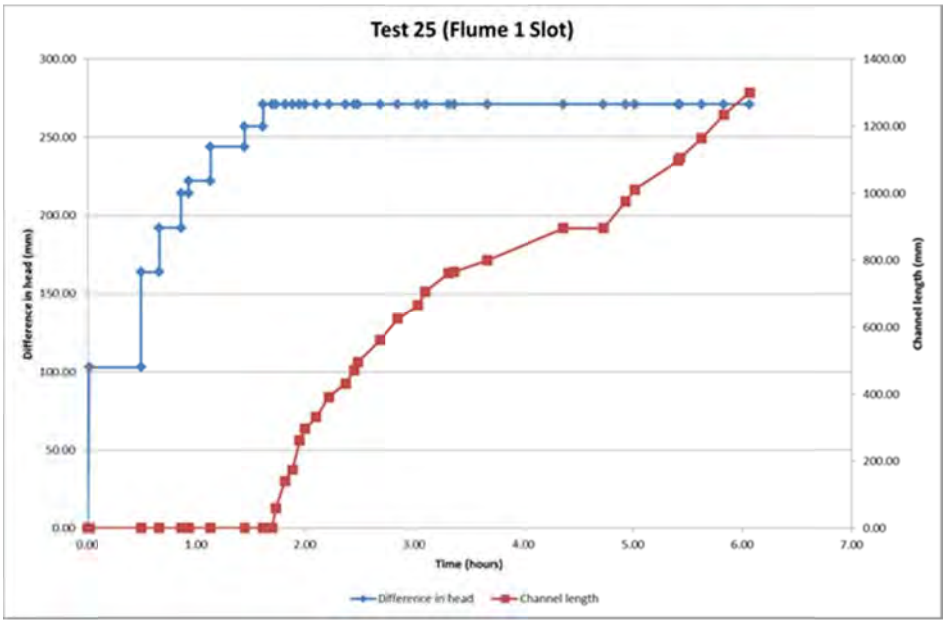

To compare these results with other slot tests:

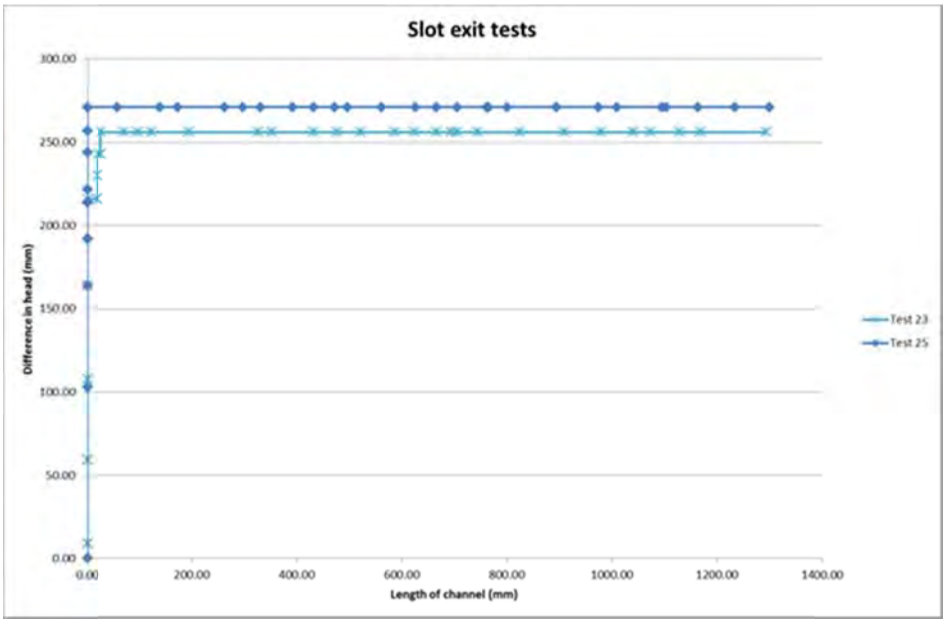

I note that:

1. I did not see the same increase in head needed near the slot as I did in test 23 and as I predicted I would need on account of the higher seepage velocity near the slot.
2. There was only a 6% variance between the critical head values

Backward erosion piping test data sheet

Test #	26	mass of soil & water	0 kg
Date	6-11-13	flume volume	m^3
Soil	Sydney sand	moisture content	%
Flume	1	dry unit weight	#DIV/0! kN/m^3
Exit type	slot	void ratio	#DIV/0! -
seepage length	1.3 m	relative density	#DIV/0! -
head in bladder tank	5 m	fill from d/s hose	50 mL
bladder pressure	50 kPa	avg. time to fill	13.1 s
water temp	19 °C	flow rate @ ΔH = 10cm	#DIV/0! L/min 0.23

tin checked on camera + correct

time	head (mm)	observation
9.55	0	A small disturbance in the outlet
		occurred when I drained the
		gas hose of water. See happy
		snap.
9.58	↑ 98	water not dripping from d/s valve yet.
10.12		water now " " " "
		Q for 50mL = 15.7, 13.5, 11.7, 11.2, 13.4.
10.13	↑ 143	no movement
10.22	↑ 171	
10.30	↑	initiation. first noticed when tip at
		tank wall. See happy snap. Flow of
		particles is consistent
10.33		tip still underneath tank wall.
10.39		tip at bl
10.45		tip under bl
10.53		tip otherside of bl
11.00		25 abl
11.09		53 abl
11.17		73 abl
11.25		83 abl
11.39		100 abl
11.48		120 abl
11.59		145 abl
12.10		177 abl
12.18		205
12.29		235

time	head (cm)	observation
12.46		245 ab1
1.10		tip under b1
1.30		tip 30 ab2
1.53		70 ab2
2.14		100 ab2
2.24		125 ab2
2.38		155 ab2
2.55		200 ab2
3.16		233 ab2
4.01		55 ab3
4.11		80 ab3
4.14		88 ab3 leaving it overnight
7-11		
10.02		tip at end. Well 100mm ab4 but that's
		the end cause it looks like sand
		sloping slightly down to panel (see
		happy snap). there's also a slight
		discolouration to the sand (crud in
		water given filter on its last legs).
		there's a blockage btw bars 3+4
		(see happy snap). the widening is
		currently up to the blockage (located
		120-190mm ab3). leaving the exp to
		run to see how long it takes to
		reach failure.
		There's also discolouration along the
		u/s portion of the deepened channel
		(see SCR). I suspect this discolouration
		has a cementing effect.
4.23		the channel is no different. It's still
		blocked btw bars 3+4. I suspect
		it hasn't moved because crud has
		cemented the sand + because the
		head is a little lower than other
		tests (and tip progression occurred
		a little slower).
4.58		having looked back at photos I can see
		that none of the channel has
		moved/changed since ≑9.50pm last
		night so it hasn't changed for ≑19
		hours. So I'm terminating the test.

1 2 3 4

254 50 146

140 25 9 50 254 50 254 50

~~158~~ + 25 + 9 + 50

time	head (cm)	observation

time	head (cm)	observation
		Notes from photos
	6-11	
	5-38 PM	best guess as to when tip reached b4
	5:58 PM	tip reached u/s end

Test 26 (flume 1 slot) report

Test 26 was the 4th test with a slot exit

A channel initiated approx. 100mm from the RHS at a head of 171mm.

Pic of when I first noticed initiation:

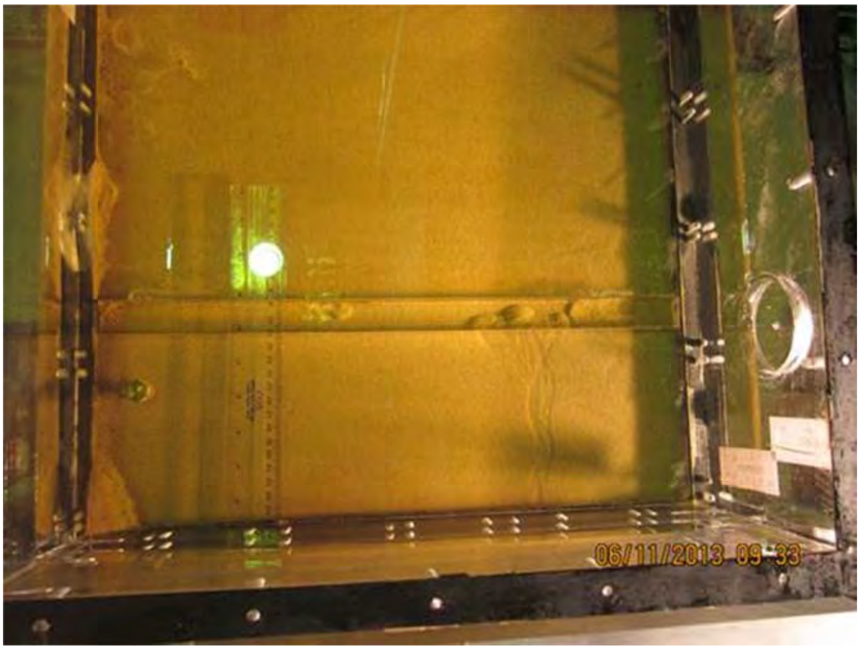

Once initiated the channel progressed relatively slowly at about 20mm/hr (compared to test 25 which progressed about 240mm/hr) until it reached the u/s end (still at a head of 171mm) 8 hrs later.

About 1.5 hrs after the tip had reached the u/s end the channel blocked for a length of approx. 70mm between bars 2 and 3.

I left the exp running for another 22 hrs but the blockage never opened up. And for the last 19 hours the channel did not change or move in any way. The channel u/s of the blockage deepened but d/s of the blockage it didn't.

Shortly after the tip reached the u/s end, sand along the u/s edge and surrounding the portion of the channel located u/s of the blockage began to become discoloured. See pic below (can also see in pic above):

I think this is 'crud' from the dam water because the filter was dirty and on its 'last legs'. I've noticed in past tests that once I saw this discolouration no/very little particle movement occurred, which was also the case in this test. I suppose the 'crud' has a binding quality to it and makes erosion more difficult. I've collected some of this discoloured sand and could look at it under a microscope (or something) but I'm not sure what I'd be looking for. In any case, I need to keep the filers as clean as possible.

Graph of test:

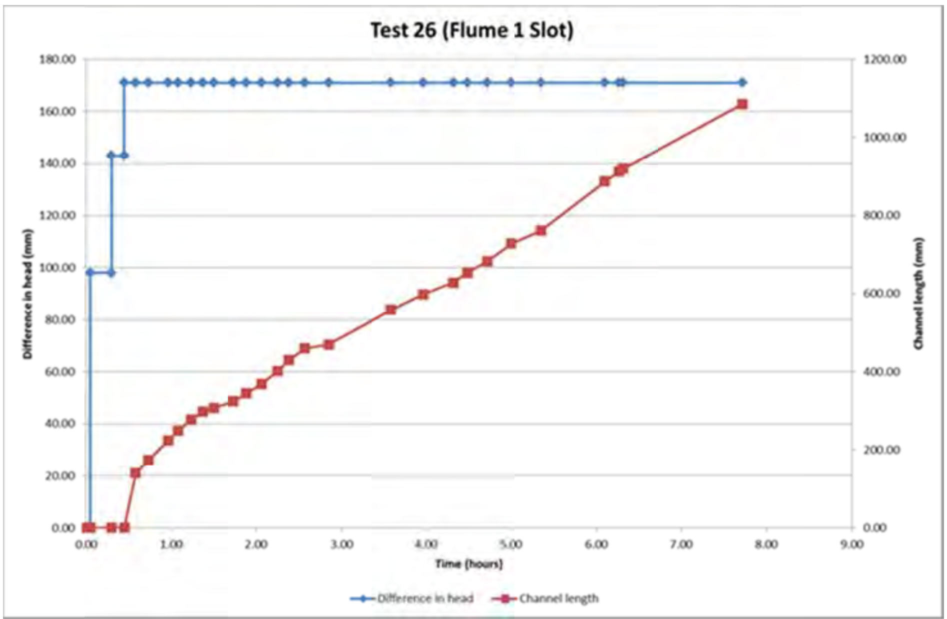

To compare these results with other slot tests:

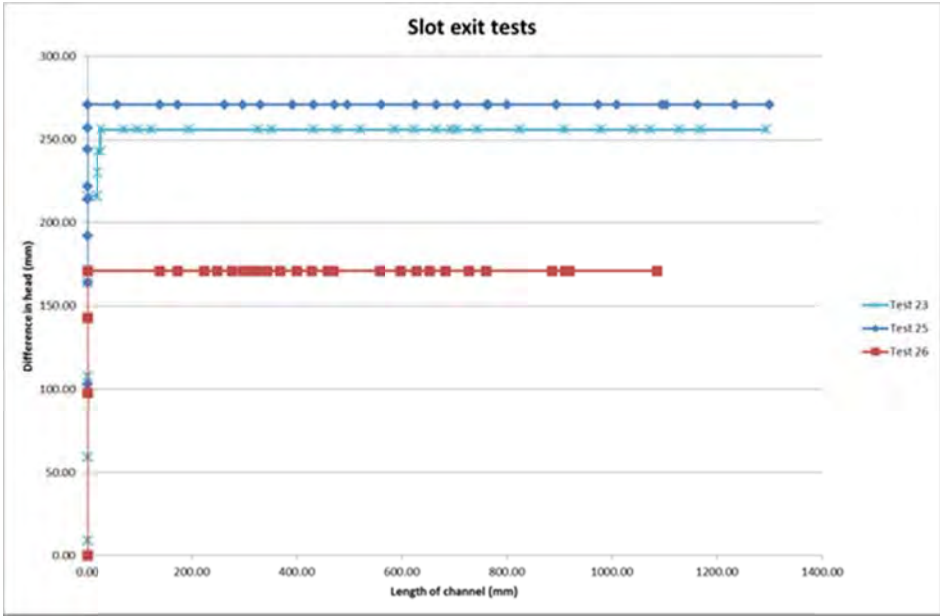

I note that:

1. This test saw a 30% decrease in critical head compared to tests 23 and 25.
2. I did not see the same increase in head needed near the slot as I did in test 23 and as I predicted I would need on account of the higher seepage velocity near the slot.

My current hypothesis as to why the critical head was much lower in this test that the others is the sand was less dense. I think the sand was less dense because Hamish compacted it and I don't think Hamish compacts it as well as I do but I don't blame him because he stands next to the flume (more tiring because more moment on ones back) whereas when I do it I stand on top of the flume and drop the rod in (and do so in a careful & repetitive pattern). I don't want to stand on top of the flume anymore because it ruins the bond between the gasket and flume, which in turn allows sand to accumulate underneath it which compromises the seal and lets CO2 out and air in. And I'm not strong/tall enough to compact with the rod without standing on top of the flume. Therefore getting the vibrator to compact is my highest priority so I can achieve more dense and consistently dense sand. At the moment I'm waiting for Larry to build a steel frame for the vibrator. Then the Wacker Neuson rep will come back with the demo to try again. I've been told the earliest Larry can do the frame is Thursday and if not Thursday then next week.

I don't want to do another slot test until I have the compaction by vibrator matter resolved because I think it has a significant impact on results. But if it takes too long to have the frame built and the vibrator bought then maybe I'll have to find a way around it (e.g. stand above the flume without standing on it and compacting with the rod myself).

Backward erosion piping test data sheet

Test #	27	mass of soil & water	0 kg
Date	14 ~~13~~/11/2013	flume volume	m^3
Soil	Sydney sand	moisture content	%
Flume	3	dry unit weight	#DIV/0! kN/m^3
Exit type	circle	void ratio	#DIV/0! -
seepage length	1.3 m	relative density	#DIV/0! -
head in bladder tank	5 m	fill from d/s hose	50 mL
bladder pressure	50 kPa	avg. time to fill	16.18 s
	19 °	flow rate @ ΔH = 10cm	#DIV/0! L/min 0.19

time	head (mm)	observation
11.12	55	There are some small channels +
		patterns around the exit (see
		happy snap) but none of them are
		on the d/s so I'm going to say
		initial channel = 0.
11.14	↑67	no movement.
11.18	↑94	
11.25	↑101	Q for 50mL = 16.8, 16.9, 15.5, 16.9, 14.8
11.30	↑120	possible initiation but channel not well
		defined. Particles detached from
		a region as opposed to a point.
		Detachment stopped about 10s after it
		started.
11.34	↑134	
11.36		tip 148-~~104~~93
11.40		tip stopped only a few minutes after
		starting so still at 148-93
11.43		tip still active
11.44		about 148-70
		2.8, 2.5, 1.7s for a group of particles to
		travel = 148-70
11.48		tip 148-60. Particles move in groups of
		about 10 to 40 particles every 15s or
		so.
11.55		tip ≑148-50
12.05		tip - 148 - 50

time	head (cm)	observation
12.30		148-50
12.55		" "
1:30		" "
2		" "
→ 2.20		148-45
2.41		148-15
2.55		148-10
3.10		" "
4.03		" "
4.49		tip at tank wall
5.50		" " " " leave overnight.
15-11		
9.41		tip in same location (at tank wall)
9.41	↑ 146	a small group of about 10 particles were
		transported.
9.54		groups of particles are moving every 30s
		or so (presumedly from the tip but
		I can't see the tip).
9.59		I timed the gap b/w groups of particles
		moving again + this time it was 1:50 mm
10.00		best approximation for time ~~to~~ for one
		particle to travel from tank wall to
		exit is 5s.
10.31		gap b/w moving particles is 1:15mm.
		But I also watched for 3min and
		nothing happened. Whilst it's possible the
		tip could still progress it's likely to
		progress at a impractical rate. So I'm
		gonna ↑h.
10.32	↑ 159	particle movement now continuous but
		tip still under tank wall
10.41		particle movement no longer continuous
		(and probably hasn't been for a good 5
		min or so).
10.45		I watched for ~~4~~ min and no movement.
10.46	↑ 172	particle movement was continuous for
		about 30s, + then moved in groups.
11.16		I watched for 3min + no movement.
11.16	↑ ≑185	
11.21		tip other side of tank wall.
11.25		particle movement has been continuous
		now since head went up at 11.16. Best
		guess on speed of particles is 3.5s
		from tank wall to exit.
11.27		tip at 61
11.34		particle movement still continuous.
11.44		about 10 particles every 15s.

150

time	head (cm)	observation
~~12.30~~		~~tip 144-50~~
~~12.55~~		~~" "~~
~~13.30~~		~~" "~~
~~14.00~~		~~" "~~
~~14-20~~		~~" 148- 45~~
12.05		about 5 particles every 1min.
12.06	↑ 200	particle movement continuous
12.11		" " still "
12.13		tip otherside of 61. + movement still
		continuous.
12.16		23 ab1
12.43		33 ab1
12.50		detachment at tip about every 45s apart
		in small groups.
1.32		50 ab1
1.57		85 ab1
2.00		about 5 particles from tip every 1.5mm
2.01	↑ 213	85 ab1
2.03		90 ab1
2.34		100 ab1
2.41		105
2.56		127 ab1
3.52		230 ab1
3.57		tip at 62
4.00		my best guess as to time it takes a
		particle from 62 to 61 is 8-10s.
4.17		tip 5 ab2
4.26		50 ab2
4.35		63 ab2
5.06		155 ab2
5.18		187 ab2
5.20	↑	~~ss~~ Th because I turned pump off (Because
		no power this weekend). I think I
		primed drain hose because now the
		head has gone back down to 213 and is
		holding steady. Scratch that. It's going up
		again.
5.25	248 and	rising
5.27	270	
5.28	290	
5.29	303	It's rising ± 19.7s for 5mm
5.31		tip at 63
5.38	~~4~~14	The head continues to rise without the
		pump so I can't keep the water
		running over the weekend. ~~so~~
5.39		water off.
5.39		35 ab3. Test terminated.

time	head (cm)	observation

150, 25, 33, 50 252,50

252,50

252,50

136

Test 27 (flume 3 circle) report

Test 27 was the 5th test with a circle exit.

Initiation began at a head of 120mm. I needed to increase the head 6 times until the channel was 348mm long (27% of the seepage length) until the channel continued to progress on its own at a head of 213mm.

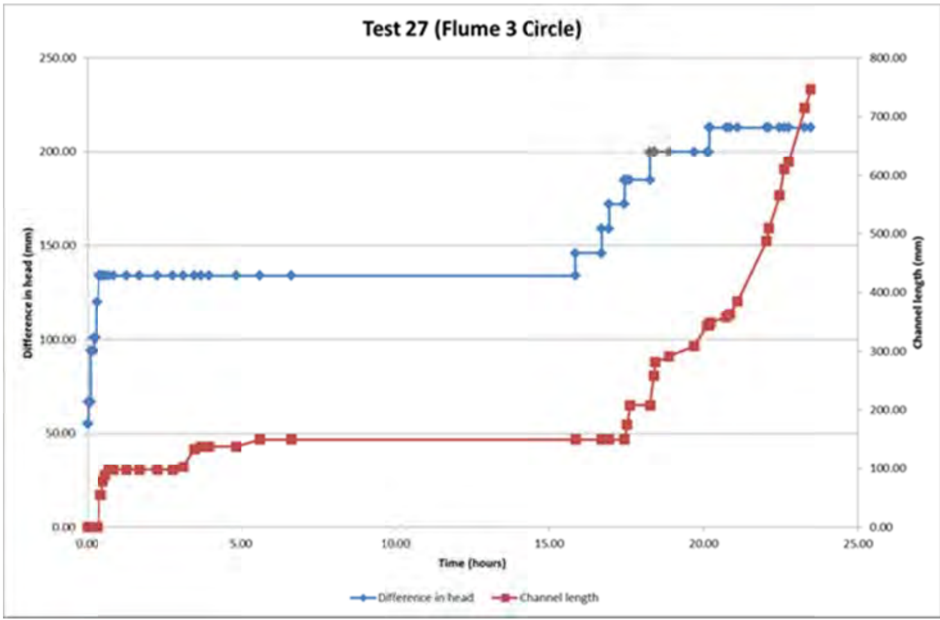

I wasn't able to complete the test. When the channel reached 747mm (57% of the seepage length) it was Friday afternoon and the power was to going to be turned off over the weekend. I was hoping the pump in the constant head tank had primed the drainage hose enough that I could turn the pump off and it would siphon itself (and therefore keep the head constant) but it didn't. Once I turned the pump off the water level drowned the internal drainage cylinder and continued to rise. The head got up to 414mm (twice was I had it at) before I gave up trying. By this stage the test had been compromised (excessive erosion near the exit created more of an eroding 'stream' rather than the one channel). So I terminated the test. I was disappointed this happened because I was hoping I could verify that no more increases in head were needed once the channel reached ~ 30% of the seepage length, but I wasn't able to do that.

To compare with other circle exit tests:

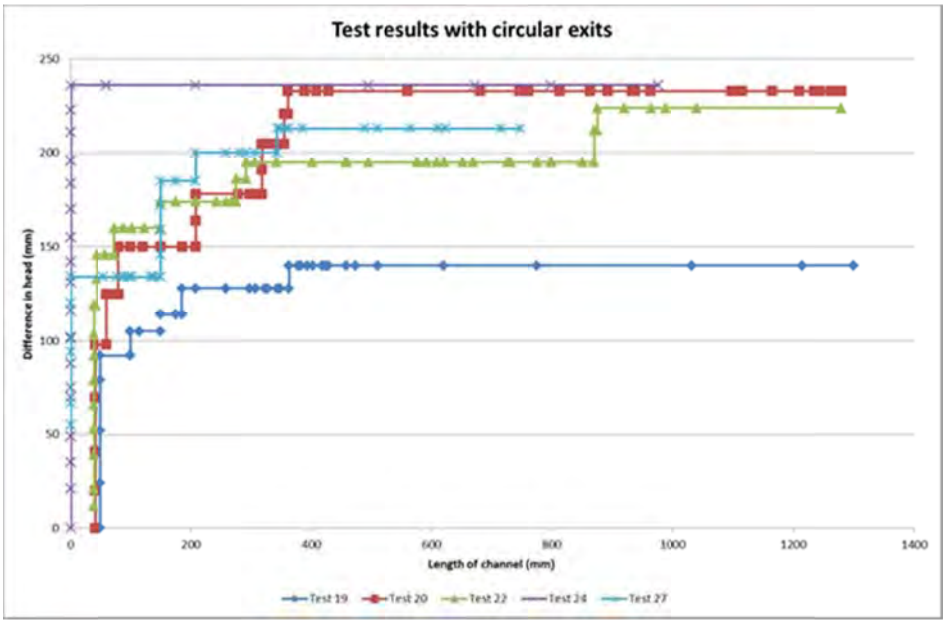

Ignoring tests 19 and 24 (see their respective reports as to why I want to ignore them) I'm becoming comfortable with a pattern in results and achieving repeatability. In the graph below the black line is the average of results.

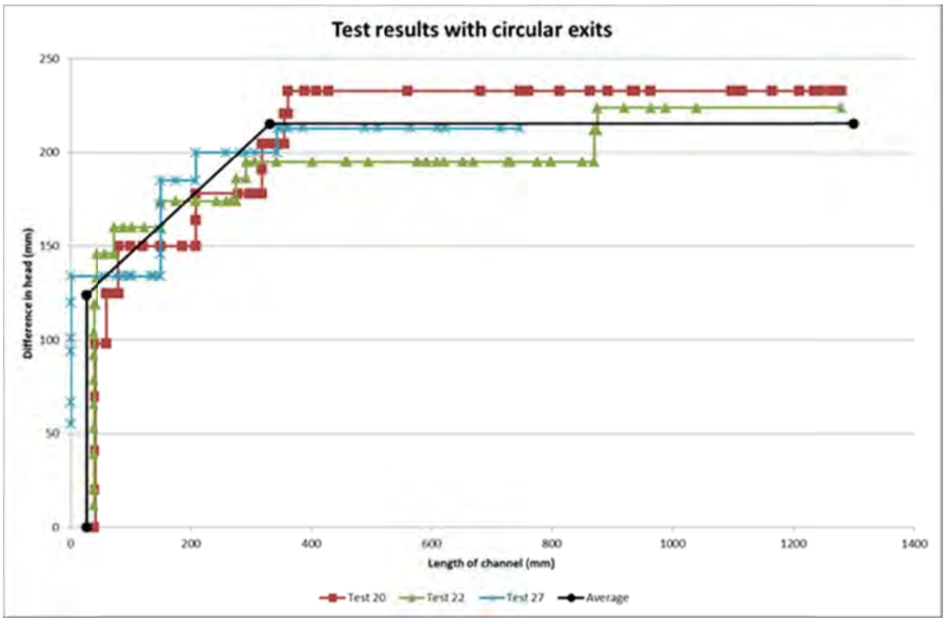

As for how this pattern compares with other exit conditions, I'll come to that when I write on email on up-to-date progress and current hypotheses.

I would appreciate another test to verify no head increase is needed past 30% but it's not critical. I'll do another circle test only if it doesn't impeded on my critical path (which is flume 4 and finishing exits plane and slope).

Backward erosion piping test data sheet

Test #	28	mass of soil & water	0 kg
Date	22/11/2013	flume volume	m^3
Soil	Sydney sand	moisture content	%
Flume	4	dry unit weight	#DIV/0! kN/m^3
Exit type	plane	void ratio	#DIV/0! -
seepage length	1.3 m	relative density	#DIV/0! -
head in bladder tank	5 m	fill from d/s hose	50 mL
bladder pressure	50 kPa	avg. time to fill	7.3 s
		flow rate @ ΔH = 10cm	#DIV/0! L/min
			0.438 L/min

time	head (mm)	observation
2.42	0 *	
2.43	↑ 50 *	no movement
2.48	↑ 92	
3.21	↑ 100	time for 50mL = 6.4, 7, 7.5, 7.5, 8.1
3.26	↑ 125	
3.43	↑ 149	
3.49	↑ 173	
3.55	↑ 197	
3.59	↑ 220	
4.02	↑ 243	
4.11	↑ 268	initiation in 3 locations. 1 in the middle
		and the other 2 roughly 50mm either
		side.
4.18		particle movement died last 10 min.
		Channel only 30-18mm long
4.22		still " " "
4.23	↑ 281	
4.26		no movement
4.31		" "
4.31	↑ 293	" "
4.33		tip now 60-18mm. Well formed channel now
4.34		100-18mm. Channel rather wide (≈30mm)
		in some places (see happy snap)
4.35		tip reached tank wall
4.36		tip reached bl
4.37		tip 25 a bl

Test 28

time	head (cm)	observation
4.42		240 ab1 and a 2nd tip at 40ab1
		(happy snap)
4.43		2nd 80ab1
4.44		1st tip 28 ab2. 2nd tip 130 ab1
4.50		1st 170 ab2 2nd 215 ab1
4.54		2nd b2
4.55		1st ab3
4.56		particle from b3 to b2 = 3.3,
4.57		2nd otherside of b2
4.59		1st 29ab3
5.08		1st 223ab3 2nd 105 ab2
5.10		1st b4 2nd 125 ab2
5.14		1st 15ab4 " " "
5.17		there's a blockage in channel 2 btw
		bars 1+2 and a 3rd tip now after b2
		(see happy)
5.18		1st 80ab4
5.19		2nd 170 ab2
5.21		3rd 105 ab2
5.22		1st reached u/s end
5.23		3rd joined 2nd.
5.25		I noticed there are 2 sand boils, one for
		each tip with the 1st tip associated with
		the largest boil. But this isn't always the
		case.
5.32		2nd 15ab3
5.41		2nd 160ab3
5.42		leaving to run over weekend to see how long
		it takes to fail.

Test 28 (flume 4 plane) report

Test 28 was the 1st test with a plane exit.

The first channel initiated at a head of 268mm. Other channels formed so that there were 2 separate tips. Two increases in head, up to 293mm, were required to reach the critical head. The critical head was reached when the channel was 12mm long (tip at 3% of seepage length). Tip 1 was the first to reach the u/s end about 1 hour after initiation.

More meandering and braiding was observed in this test than tests with other exit geometries. Also, one blockage was observed in channel 2. When the blockage occurred a branch off channel 1 formed tip 3. Tip 2 still progressed another 50mm or so before tip 3 joined channel 2 essentially bypassing the blockage. Tip 2's progression then speed up and continued.

The test failed 53 minutes after tip 1 had reached the u/s end.

This photo shows the nature of the meandering and tip 3 about to join channel 2.

Graph of test:

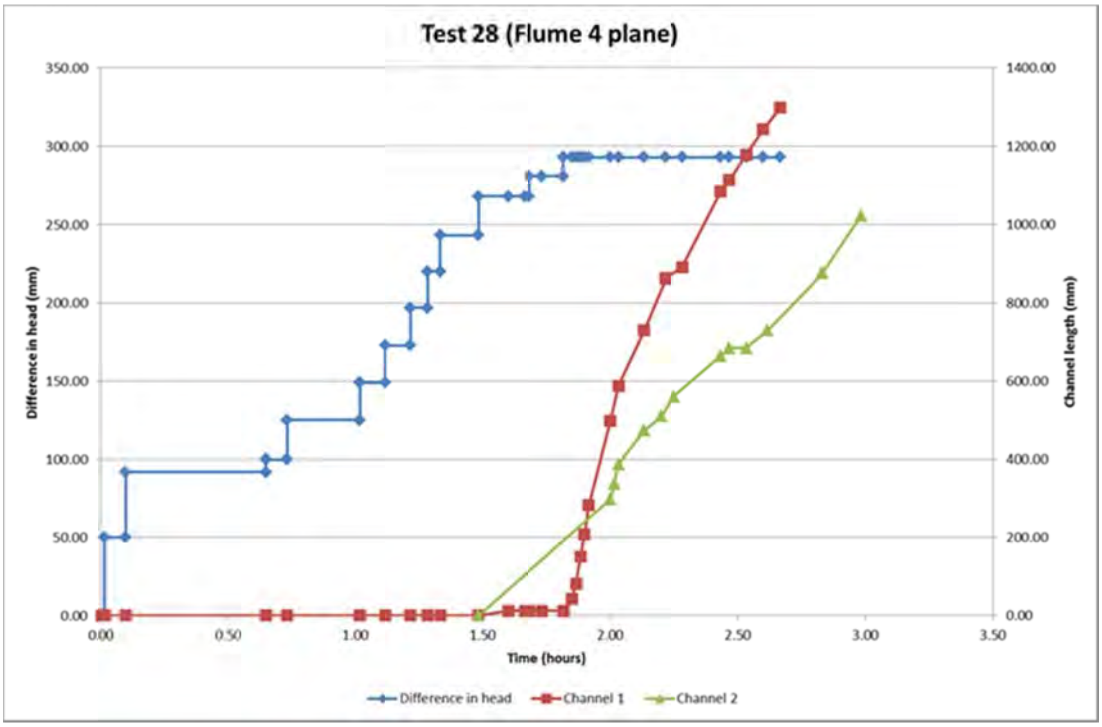
Test 28 (Flume 4 plane)
Difference in head (mm)
Channel length (mm)
Time (hours)
Difference in head
Channel 1
Channel 2

Backward erosion piping test data sheet

Test #	29	mass of soil & water	0 kg
Date	27/11/2013	flume volume	m^3
Soil	Sydney sand	moisture content	%
Flume	1	dry unit weight	#DIV/0! kN/m^3
Exit type	slot	void ratio	#DIV/0! -
seepage length	1.3 m	relative density	#DIV/0! -
head in bladder tank	5 m	fill from d/s hose	50 mL
bladder pressure	50 kPa	avg. time to fill	12.96 s
		flow rate @ ΔH = 10cm	#DIV/0! 0.231 L/min

time	head (mm)	observation
11.06	0	
11.11	↑ 66	no movement
11.14	↑ 118	" "
11.15	↓ 102	time for 50mL = 13.1, 12.9, 12.6, 13.7, 12.5s.
11.20	↑ 161	no movement
11.29	↑ 176	" "
11.35	↑ 192	" "
11.44	↑ 206	" "
11.51	↑ 218	" "
11.58	↑ 234	Initiation. In middle (see hoppy)
12.00		190-110
12.02		215-110
12.04		(still 215-110) tip more-or-less stopped but its branched
		out else where (see hoppy)
12.16		tip 0 ab1
12.18		23 ab1
12.22		70 ab1
12.27		117 ab1
12.43		225 ab1
12.54		18 ab2
1.04		190 ab2 The channel is very straight
		because I think it followed a slight
		indentation left behind from the
		screening off process.
1.13		210 ab2.
1.24		63

Test 29

	time	head (cm)	observation
			level on standpipe = 298mm
	2.13		channel blocked btw bars 1 and 2.
			tip under b3.
	2.33		" " " . still blocked.
	3.14		" " " " " .
	4.10		" " " " " .
	7.25		" " " " " .
	7.35		I can see tip just on other side of b3
			(not sure how long its been there).
	28-11		
	9.51		another channel has formed overnight.
			It's tip is currently under b2 + particle
			movement is semi-continuous. So happy.
			first tip still under b3.
	10.07		~~2~~ 2nd tip still under b2
	10.31		" " " " "
	11.06		38 ab2
	11.40		135 ab2
27.95	11.59		215 ab2
30.5	12.24		at some point tip 2 joined channel
			1 and now tip 1 is at 170 ab3.
	12.37		tip under b4
	12.50		18 ab4
	12.58		50 ab4
	1.06		first noticed tip reached u/s end.
			Also first noticed Ch2+1 blocked btw 2+3
			and just u/s of b4.
	2.32		blocking quite extensive now. Both
			channels blocked btw 2+3. Also blocked
			either side of b4.
	5.53		still blocked
	29-11		
	12.55		still blocked.
	3.00		" "
	3.44		Given it has been blocked w/ no movement
			for over 24 hours now I'm going to
			assume it won't unblock itself at this
			head. So...
	3.45	↑ 243	no movement
	3.51	↑ 257	" "
	4.47	↑ 283	" "
	5.13		there is movement but small blockages still ~~[illegible]~~
			at just d/s of b3 and u/s of b4.
	5.54		same as how it was @ 5.13
	5.54	↑ 308	
	6.24		Blockages are now 'flushed' open + if I

had of left it running over the weekend it

probably would have failed. End test.

Test 29 (flume 1 slot) report

Test 29 was the 5th test with a slot exit

The first channel initiated at a head of 234mm. No increases in head were required, i.e. initiation head = critical head. About 2.25 hours after initiation, when the tip was 782mm (60% of L), a portion of the channel blocked and the tip stopped progressing. About 7 hours later (9.42pm 27-11) a branch off channel 1 formed d/s of the blockage (tip 2). It took about 14 hours (12.10pm 28-11) for tip 2 to progress to where it joined channel 1. It joined just d/s of bar 3. After that tip 1 progressed again until it reached the u/s end an hour later.

Here is a photo shortly before tip 2 joined channel 1.

Soon after tip 1 reached the channels blocked again. I left it for over 24 hours to see whether the channel would 'deepen forward' (channel deepens from u/s end towards d/s) and lead to failure but it didn't. This may be due to contaminants in the water again, see photo of discoloured sand:

In attempt to unblock the blockages and/or fail the sample I increased the head 4 times up to 308mm and the blockages cleared. I then terminated the test but if I had of let it run over the weekend I think there is a good chance it would have failed at this head.

Graph of test:

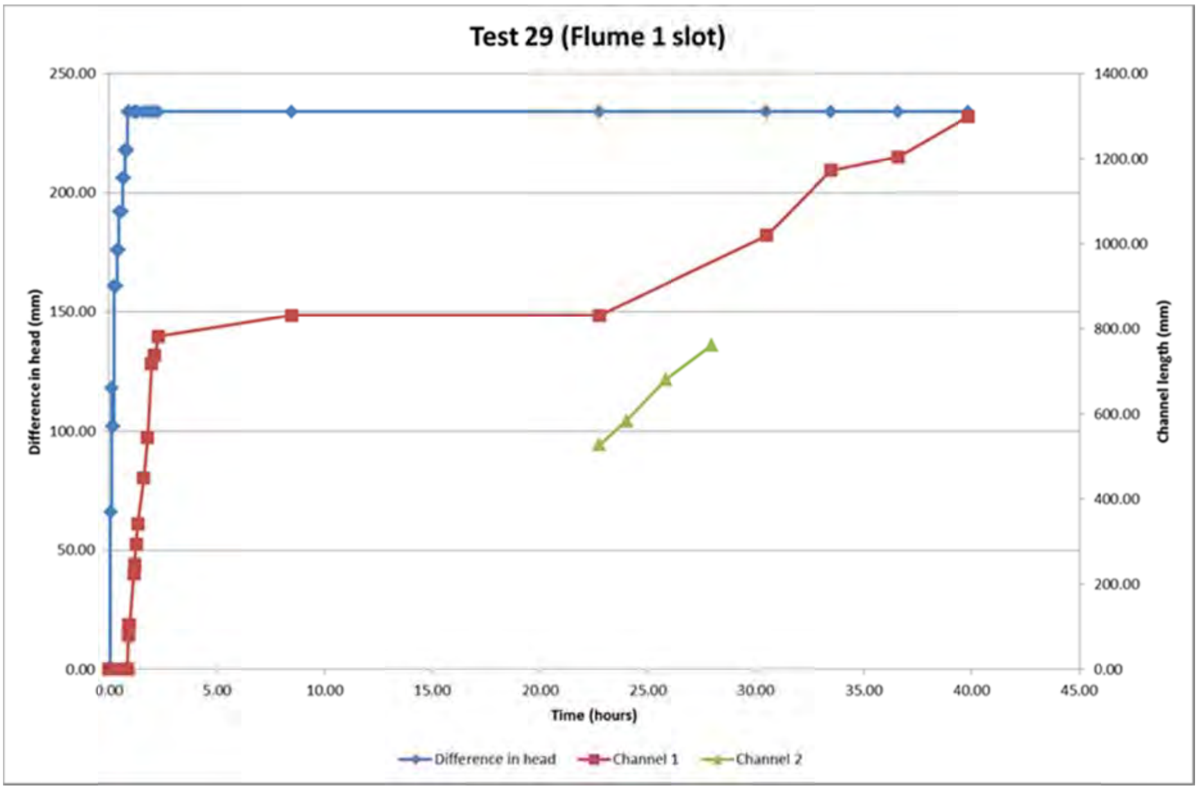

To compare this test with other slot tests:

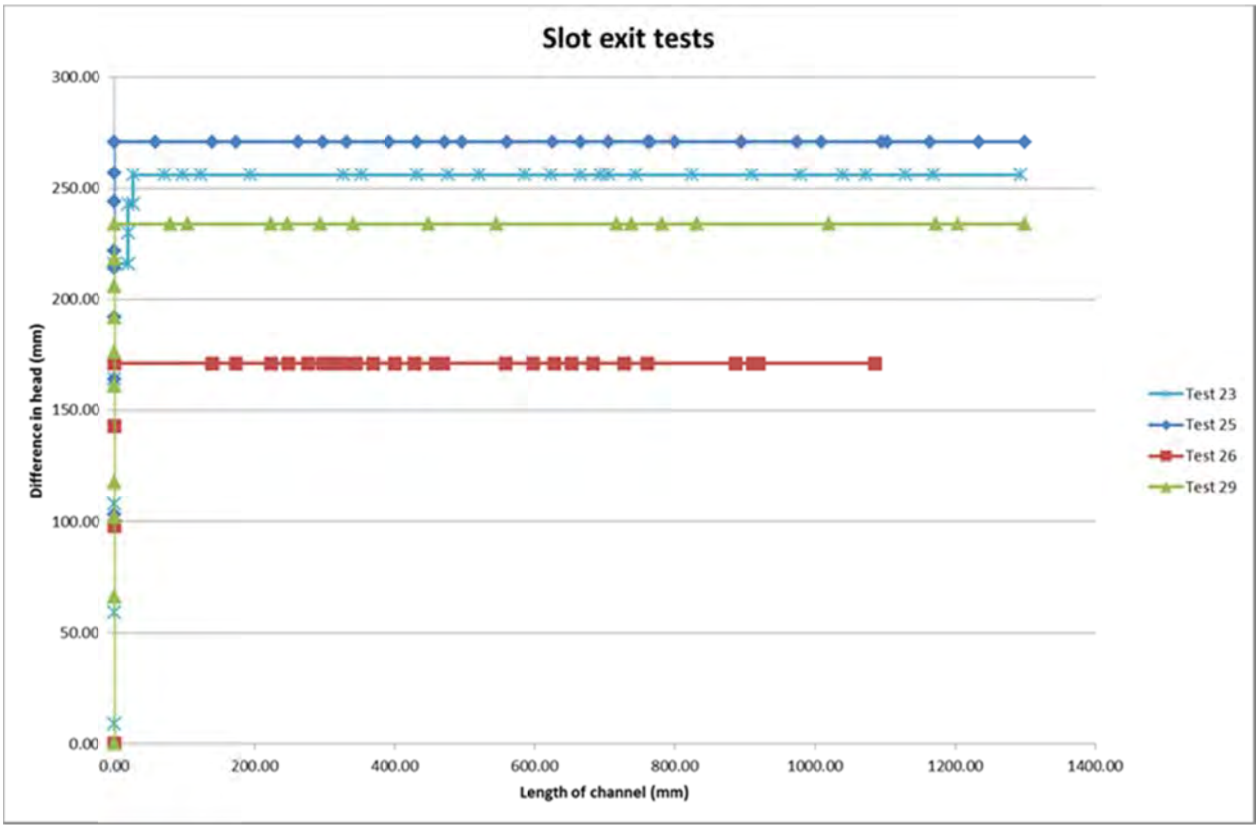

I'm happy I'm now getting a consistent slot results and will omit test 26's results (I think test 26 was different because the sand was less dense).

Backward erosion piping test data sheet

Test #	30	mass of soil & water	0 kg
Date	3/12/2013	flume volume	m^3
Soil	Sydney sand	moisture content	%
Flume	4	dry unit weight	#DIV/0! kN/m^3
Exit type	plane	void ratio	#DIV/0! -
seepage length	1.3 m	relative density	#DIV/0! -
head in bladder tank	5 m	fill from d/s hose	50 mL
bladder pressure	50 kPa	avg. time to fill	8.26 s
		flow rate @ ΔH = 10cm	#DIV/0! ~~0.656~~ L/min

time	head (mm)	observation
11.39	0	
11.40	↑ 83	
11.48	↑ 100	50mL = 7.4, 9.2, 7.3, 8.4, 8.8, 8.5s.
11.51	↑ 156	
11.59	↑ 196	no movement
12.20	↑ 217	" "
12.34	↑ 239	" "
12.39	↑ 264	" "
12.52	↑ 278	" "
1.07	↑ 289	" "
1.19	↑ 301	" "
1.44	↑ 313	initiation. Channel at RHS edge.
1.49		tip at tank wall
		Channel relatively wide, like 30mm. Tip
		moving towards middle of flume.
1.48		20 ab1
1.51		2 tip 70 ab1
1.53		furthest tip (1) 20ab2
1.55		tip 2 15ab2
1.56		Ch1 split into 2 tip 1a + 1b. Both 130ab2
1.56		tip 2 80ab2
1.59		1a at b3
2.00		1b @ b3
2.00		t2 @ 130 ab2
2.01		1a 40ab3 1b 60ab3
2.03		all movement has stopped U/s of b2.

time	head (cm)	observation
		It's all happening so quick I don't
		know why. I think there were blockages
		in ch d/s.
2·05		new tip on LHS - let this be tip 3.
2·06		tip 3 at dark wall. Ch 3 reopening. Movement
		up to 40ab2. Also channels near
		1a + 1b reopening. They might be new
		channels or they might reopening
		of existing.
2·09		Ch3 now inactive
2·10		tip 3 at 01
2·17		1a reopened up to 30ab3
2·18		t3 80 ab1
2·19		tip 1a active again @ 125 ab3
2·20		t3 130 ab1
2·27		tip 1a not move - still @ 125 ab3.
2·27		t3 250 ab1
2·28		1b active up to about 40 ab3
2·49		t3 165 ab2
2·50		1a active again. now 145 ab3
2·51		1a 150 ab3
2·53		3 185 ab2
2·53		1a 165 ab3
3·02		1a 250 ab3
3·05		1a seems to have stopped again.
3·06		1b on the move. Now 170 ab3.
3·06		3 10 ab3
3·08		1b 195 ab3
3·10		1b 200 ab3
3·11		3 50 ab3
3·12		1b 220 ab3
3·15		1a active again. Now under b4
3·17		1b 225 ab3
3·17		3 80 ab3
3·21		1b 230 ab3 . 1a still under b4. 3 95 ab3.
3·34		1a 65 ab4 . 1b 233 ab3. 3 165 ab3.
3·40		1a 85 ab4 . 1b 233 ab3. 3 190 ab3.
3·41		1b 245 ab3.
3·48		1a 85 ab4. 1b 245 ab3. 3 220 ab3.
3·52		3 - 225 ab3
4·00		1a 85 ab4. 1b 245 ab3. 3 under b4.
4·04		1a 90 ab4. " " . 3 40 ab4
4·18		first noticed 3 had reached the u/s end.
		1a 90 ab4. 1b 245 ab3
4·22		1a 110 ab4.
4·33		1a 115 ab4.
5·12		1st noticed 1a had reached u/s end

Usef ~~Arron~~

time	head (cm)	observation
4-12		
9.27		1a, ~~1b~~ + 3 have all ~~reached the u/s end~~ +
		began the deepening process. 1a's
		deepened channel is 130mm d/s of b4,
		1b is under b4 and 3 is also under b4.
		There's also significant discolouration
		around all 3 channels, particularly at the
		deepended end of 1a (see happy snap). Also,
		sand at the exit appears inactive (there's
		no sand boiling) even though flow is still
		leaving the flume + the level in the
		const head tank hasn't dropped (which
		tells me there's sufficient flow entering
		the flume, ie Qin > Qexp).
		If none of the deepened channels have
		moved by lunchtime I'll up the head.
2.02		all the same as this morning.
2.03	↑ 326	no movement
2.53	↑ 335	" "
3.32	↑ 350	" "
3.50	↑ 360	" "
4.01	↑ 371	" "
4.13	↑ 383	
4.28	↑ 393	
4.34	↑ 403	
4.45	↑ 419	
4.52	↑ 430	
5.09	↑ 442	
5.18	↑ 455	
5.28	↑ 467	
5.42		changed photo freq to 1min.
5.43	↑ 573	there was movement in Ch3 but it blocked
		itself again.
5.49	↑ 561	no movement
5.59	↑ 606	
5-11		
10.22		The 3 deepened channels are even
		more dark today. See happy snap.
		1a is 130mm d/s of b4 (not moved), 1B is
		23mm u/s of b4 (was under b4 this time
		yesterday) and 3 is also 23mm u/s of b4.
		No boiling action at exit.
10.25	↑↑↑ 7 revolutions.	
	@782	I first noticed the existing 1A and 3
		had been extended. And ~~the~~ ~~exit~~ excessive
		erosion occurred @ d/s end (see happy snap).
10.59		Even though the deepened channels
		didn't make it to d/s end I still

time	head (cm)	observation
		Consider failure to have occured because
		there was excessive d/s movement (no
		longer restricted to channels) and
		the d/s tank is half full of
		sand. End test.

Test 30 (flume 4 plane) report

Test 30 was the 2nd test with a plane exit.

The first channel initiated at a head of 313mm. Other channels formed so that there were 3 separate tips. No increases in head were required so initiation head = critical head. Tip 3 was the first to reach the u/s end about 2.5 hours after initiation.

More meandering and braiding was observed in this test than tests with other exit geometries. Also, blockages occurred frequently in this test. When a blockage occurred the tip progression either slowed right-down or stopped altogether. Most of the time a blockage would clear itself but on one occasion, whilst channels 1 and 2 were blocked, tip 3 formed at the exit and a 3rd channel was formed. Furthermore, channel 1 split into two tips (1a and 1b) when it was approximately half way.

After the first tip (tip 3) reached the u/s end I left it running, waiting for failure. Yet whilst tips 1a, 1b and 3 had all reached the u/s end and began the forwarded deepening, and the deepened channels had reached bar 4 and 130mm d/s of bar 4, the deepening progress didn't progress any further. In fact, there was no sediment movement what-so-ever, even at the exit (no boiling action). I suspect this was due to water contaminants because of the sand discolouration that formed.

I then increased the head 17 times to try force the opening of blockages and bring on failure. At a head of 513mm the blockage in ch3 opened momentarily before blocking again. At a head of 782mm excessive erosion occurred at the d/s portion of the flume (erosion no longer restricted to channels). I considered this to be failure of the sample given erosion no longer restricted to channels and excessive sand filled the d/s tank. The deepened channels didn't change/extend during failure.

This photo was taken once tips 1a and 3 had reached the u/s end. It shows the nature of the meandering, where channel 1 split, where tip 2 stopped, and where tips 1a and 3 reached the u/s end.

This photo shows the sand discolouration at the u/s end.

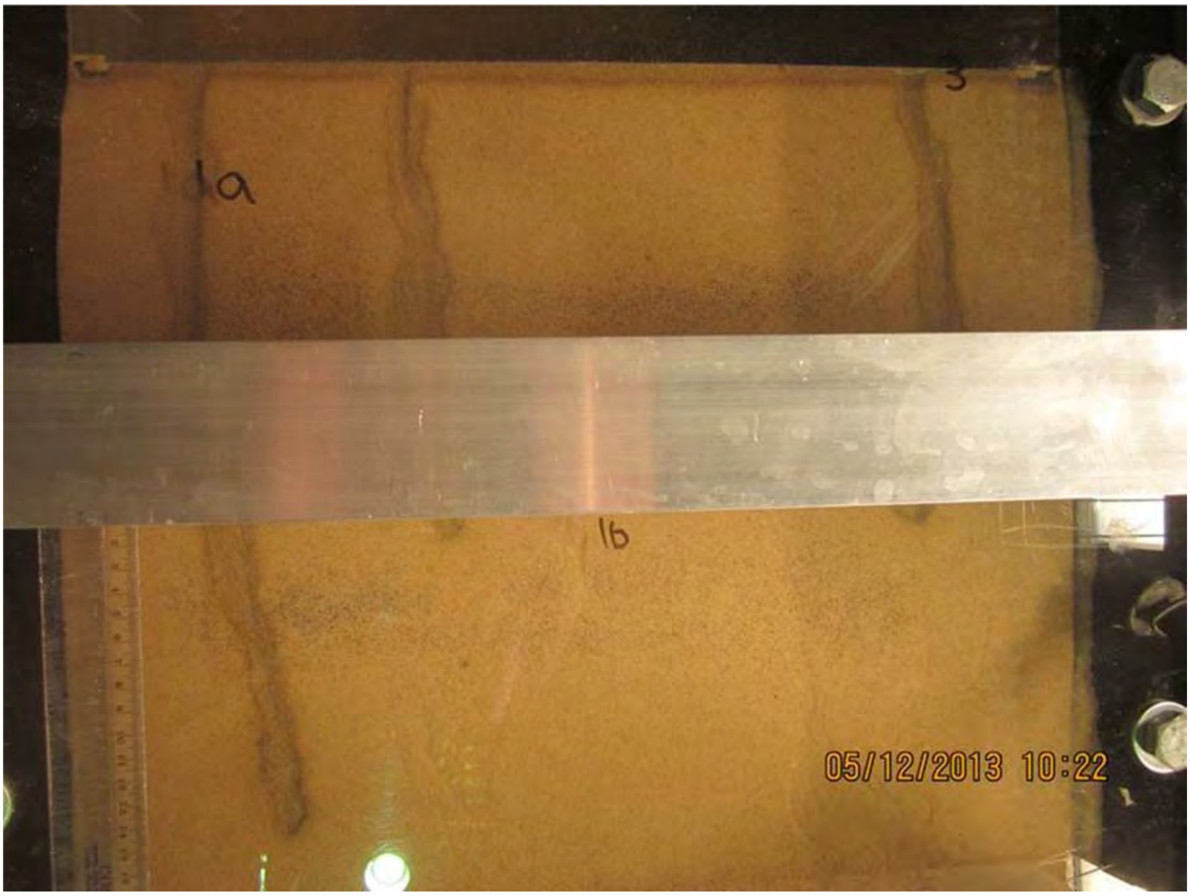

Graph of test:

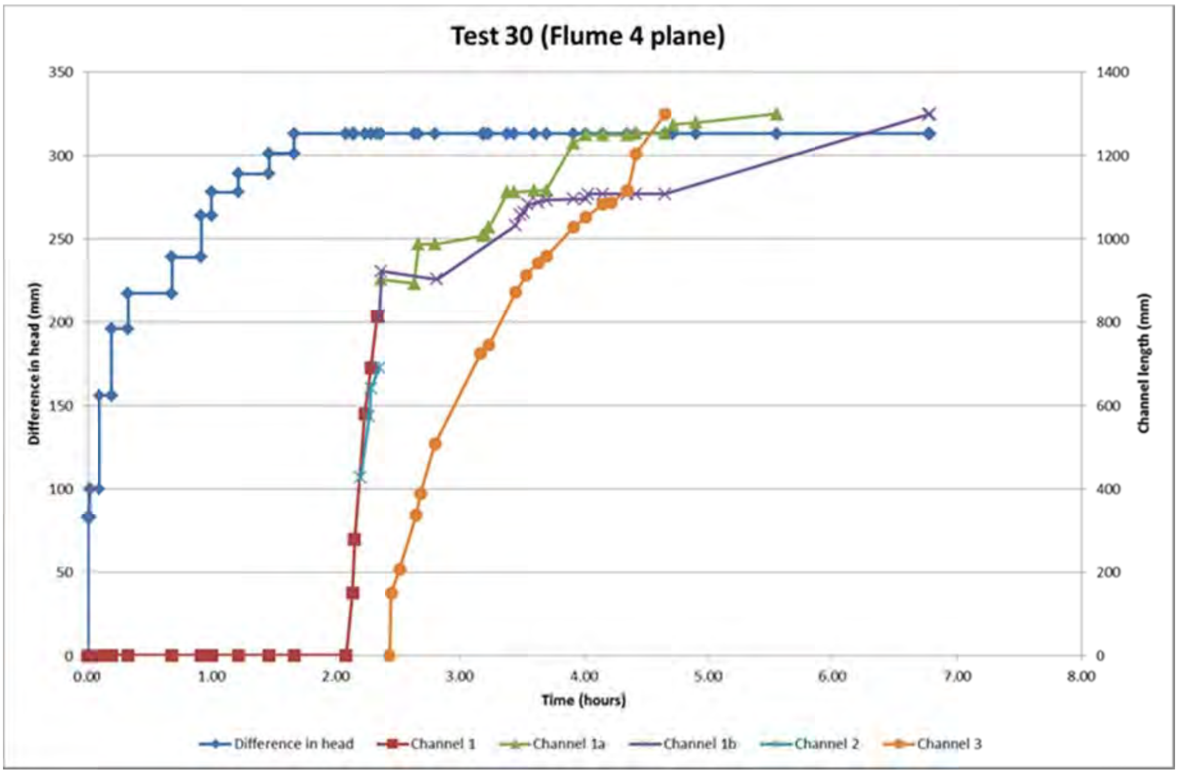

Backward erosion piping test data sheet

Test #	31	mass of soil & water	kg
Date	18/12/2013	flume volume	0.22 m^3
Soil	Sydney sand	bulk unit weight	0 kN/m^3
Flume	3	moisture content	%
Exit type	circle	void ratio	#DIV/0! -
seepage length	1.3 m	relative density	#DIV/0! -
head in bladder tank	5 m	avg. time for 50mL	16.26 s
bladder pressure	50 kPa	Q when ΔH = 0.1m	#REF! L/min
compaction	tamp & pc tests		~~0.976 L/min~~

time	head (mm)	observation
10.25	0	happy snap of starting positions of
		channels near circle. One channel
		which is about 50mm long is
		present + orientated on the
		d/s side of the hole.
10.28	↑ 37	Note there are some gas bubbles
		seen near hole (see happy snap)
		but they're not in the most likely
		path of a channel + they're
		small (and I can't wait any
		longer before testing given I'll be
		on leave in 2 days).
10.32	↑ 61	no movement
10.40	↑ 89	v. small amount of short-lived movement
10.43		just realised the u/s ball valve
		wasn't completely opened so opening
		it now. No movement in sand but
		water now flowing through d/s ball
		valve.
10.48	↑ 100	50mL = 16.8, 15.7, 17.3, 14.9, 16.6
10.54	↑ 115	no movement
10.56	↑ 129	" "
11.01	↑ 143	" " , most gas bubbles gone!!
11.04	↑ 156	boiling action enough to get the first
		grains on top of the lid.
11.11	↑ 168	initiation 183.8 - 10.5 cm.

time	head (cm)	observation
11.16		still 13.8-10.5cm
11.16	↑ ? (182)	180-105mm
11.20		" "
11.21	↑ 195	" "
11.22		180-105
11.23		230-105
11.25		It's broken into 2 tips (see nappy snap).
		One is under tank wall + one
		has veered to the left.
11.38		still under tank wall which
		surprises me cause there's particle
		movement constantly.
11.41		tip is now under bl (I didn't notice
		when it past tank wall). Perhaps
		don't dot this point until I see it
		come other side of bl.
12.07		tip other side of bl
12.12		groups of about 10 particles every
		1' 15"
12.23		18 abl
12.31		40 abl
12.37		43 abl
12.43		" "
12.46		48 abl
12.57		85 abl
12.58	↓ 183	
1.01		90 abl
1.17		93 abl
1.54		100 abl
1.59		no movement in 3min
1.59	↑ 189	
2.01		103 abl
2.02		groups of 10-50 particles every 15-30s.
2.07		110 abl
2.19		113 abl
2.25		122 abl
2.41		135 abl
2.44		135 abl
2.52		135 abl
3.11		150 abl
3.32		170 abl
3.51		173 abl
4.13		185 abl
4.30		208 abl
4.56		235 abl
5.30		35 ab2
5.49		100 ab2
5.49	↓ 170	100 ab2

Test 31

time	head (cm)	observation
5.54		103 ab2
6.02		105 ab2
6.30		106 ab2
		leave overnight
19-12		
9.25		still @ 106 ab2
9.25	↑ 180	
9.55		still @ 106 ab2
9.55	↑ 193	120 ab2
10.03		128 ab2
10.12		150 ab2
10.19		165
10.37		215
10.45		218
10.53		222
11.08		255 ab2
11.54		8 ab3
1.03		100 ab3
1.06		120 ab3
1.06	↓ 183	@ 0.75L
1.14		122 ab3
2.05		122 ab3
2.06	↑ 188	
2.10		122 ab3
2.27		122 ab3
2.28	↑ 194	
2.31		125 ab3
2.37		130 ab3
2.54		137 ab3
3.12		212 ab3
3.28		252 ab3
3.29	↓ 188	≐ 0.86L (I missed 0.8L)
4.03		it has moved a lot but I can't see by how
		much (it's under 64).
4.21		43 ab4
4.22	↓ 177	between 0.9 and 0.95L
4.50		45 ab4
5.08		53 ab4
5.25		first noticed channel @ u/s end
5.19		when reached u/s end according to photos

Test 31

time	head (cm)	observation

Test 31 (flume 3 circle) report

Test 31 was the 6th test with a circle exit and the first test with the 'decreasing head' procedure.

This was the new procedure:

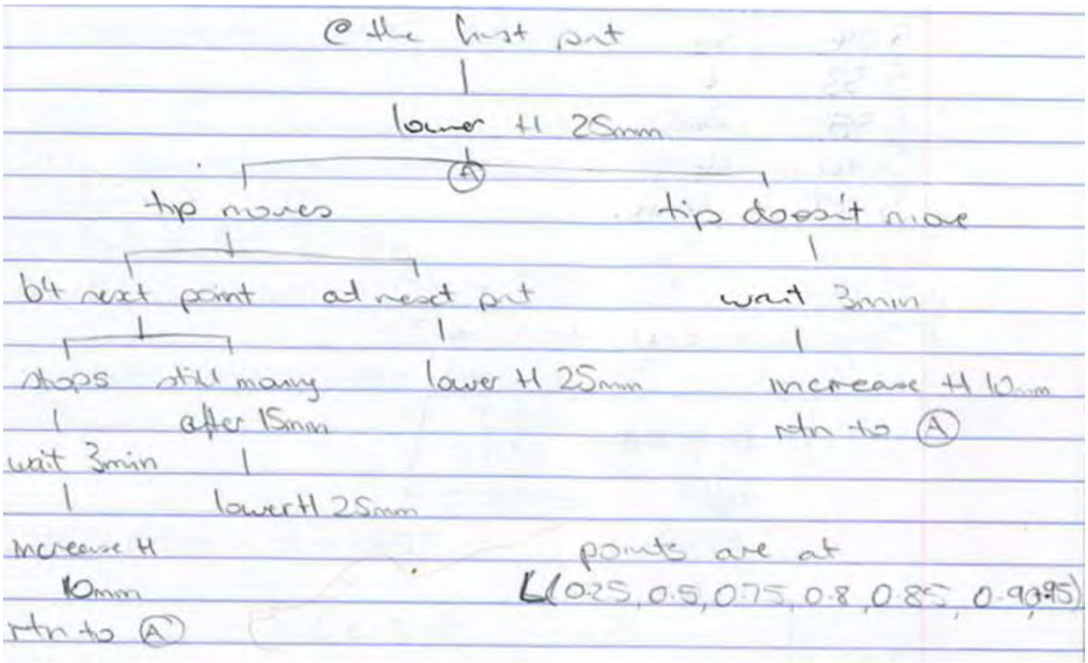

This was done to work out whether the LvsH graph went like:

or

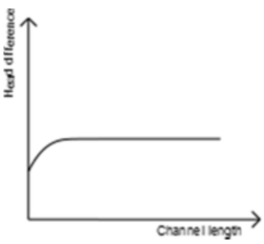

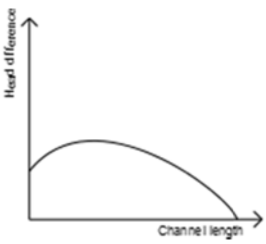

The channel initiated at a head of 168mm. Two increases in head, up to 195mm, were required to reach the critical head. The critical head was reached when the channel was 45mm long (tip at 3% of seepage length). This was much sooner than other circular tests- other circular tests reached their critical gradients when they were between 23-28% of L. One possible reason why the critical gradient was reached sooner is I needed a greater head to start initiation because the sand was more dense than other tests. It's likely the sand was more dense because a number of pressure cell tests had been carried out on the sample beforehand. However the critical gradient was similar to other tests.

Here is a summary of what happened when I reduced the head at the points of interest.

Tip @	%L	Head was	Head changed to	Tip behaviour
343	26	195	↓183	Slowed down, went another 15mm and stopped
358	28	183	↑189	Speed up, continued to next point of interest
660	51	189	↓170	Slowed down, went another 6mm and stopped
666	51	170	↑180	Didn't move
666	51	180	↑193	Started again, continued to next point of interest
982	76	193	↓183	Slowed down, went another 2mm and stopped
984	76	183	↑188	Didn't move
984	76	188	↑194	Started again, continued to next point of interest
1114	86	194	↓188	continued to next point of interest
1207	93	188	↓177	Slowed down but still continued to u/s end

Here are plots of the results:

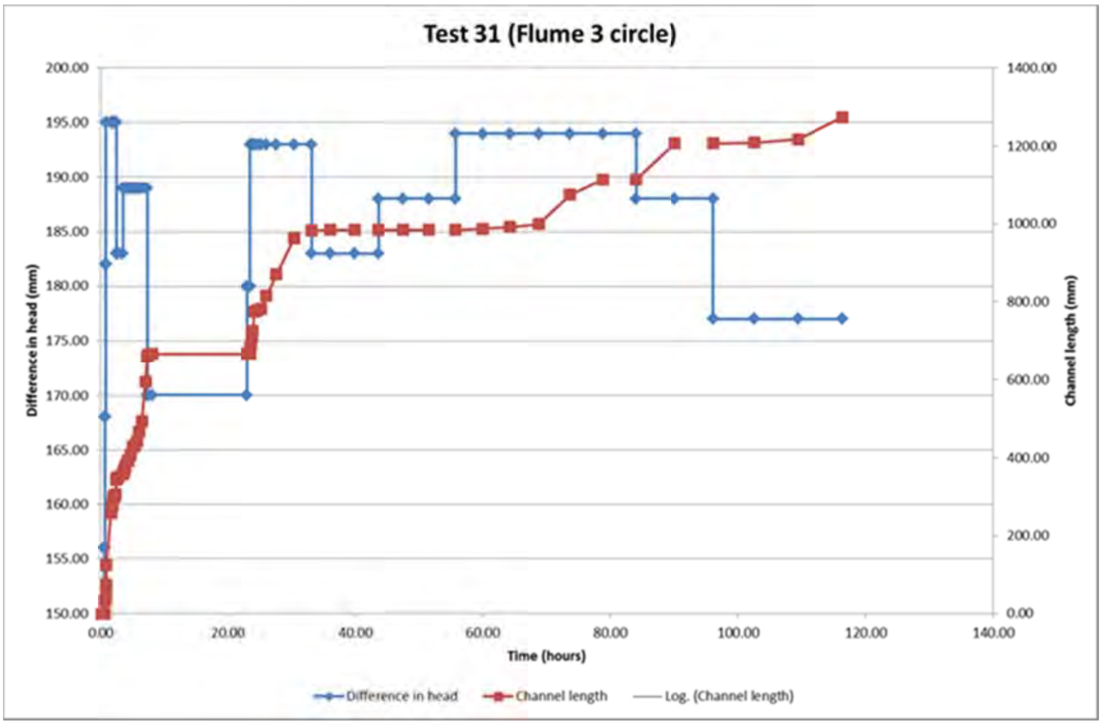

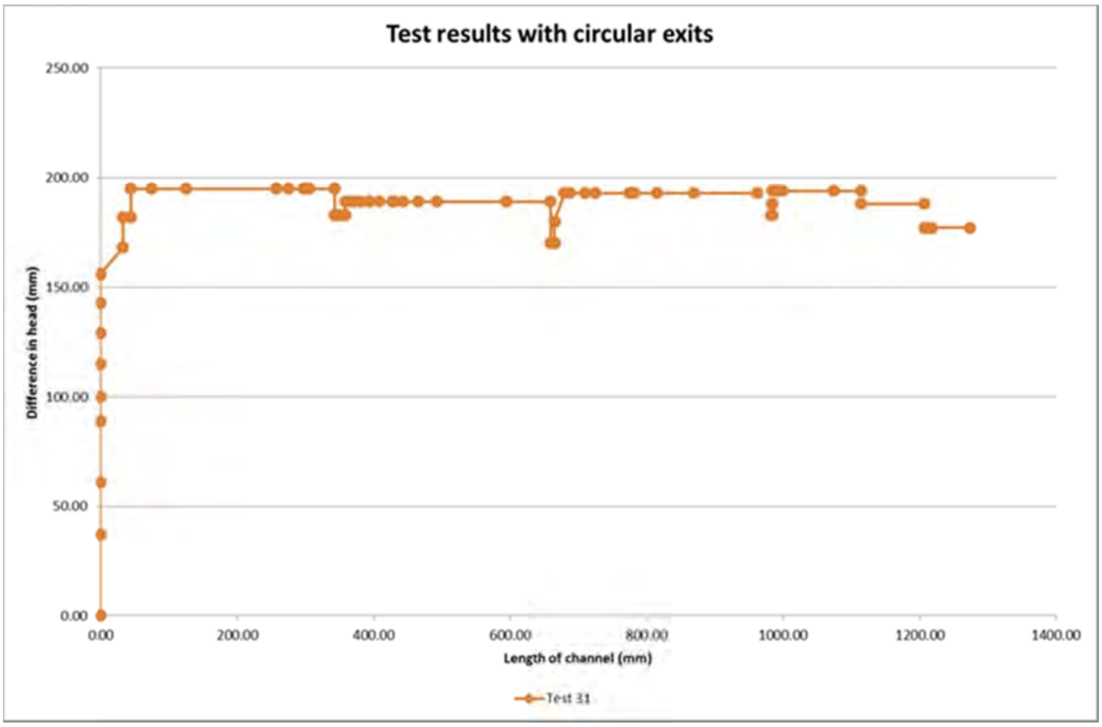

From this I deduce the tip location versus head required looks like this:

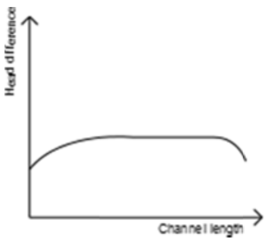

That is, the critical gradient is constant until right near the u/s end. The drop in critical gradient near the u/s end is consistent with the observation of an increased speed in tip progression near the u/s end seen in other tests.

I've also noticed (or at least I think I've noticed) that the greater the head the faster the tip progression is. I think it can be seen easier if I change the axis limits of the above graph to:

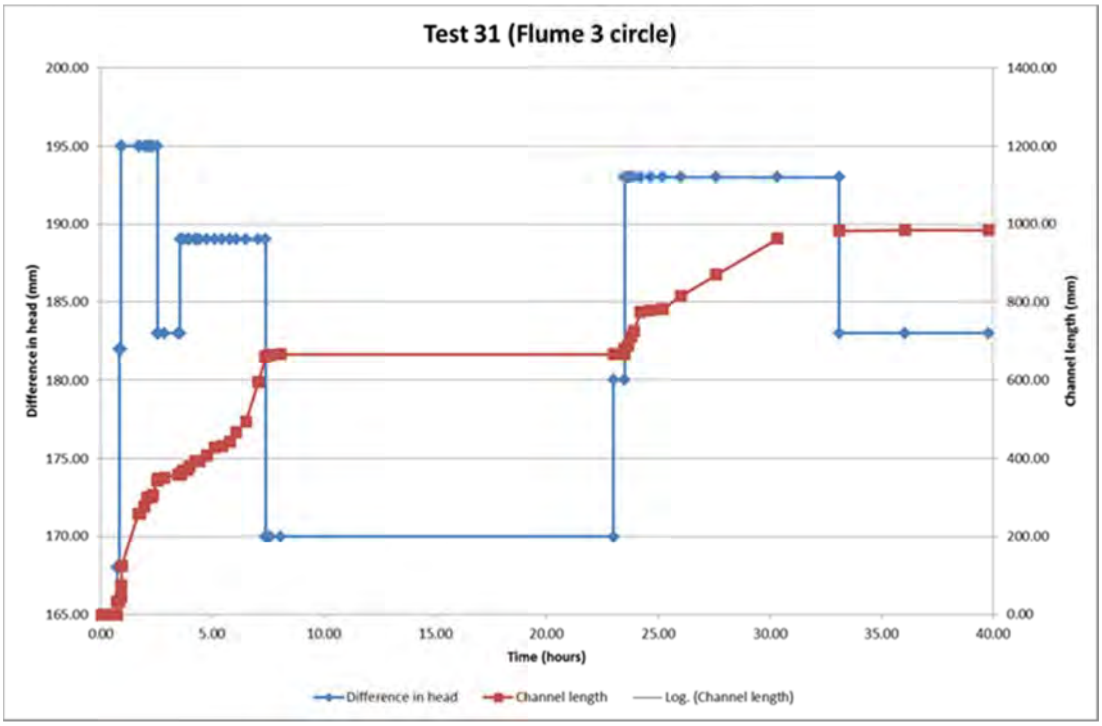

And I note that this observation only holds true in the d/s half to 2/3rds of the flume. So what I'm saying is the speed of tip progression is a function of the head such that:

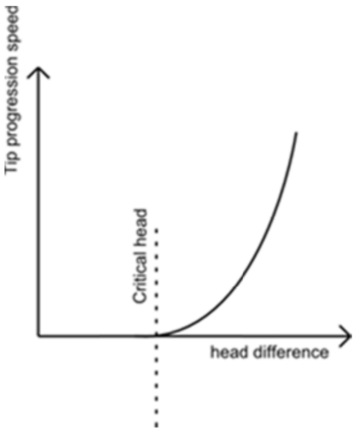

I'd need to do more tests to gain confidence in this observation.

Out of interest, this is how this test compared with other circular exit tests for which the head wasn't reduced.

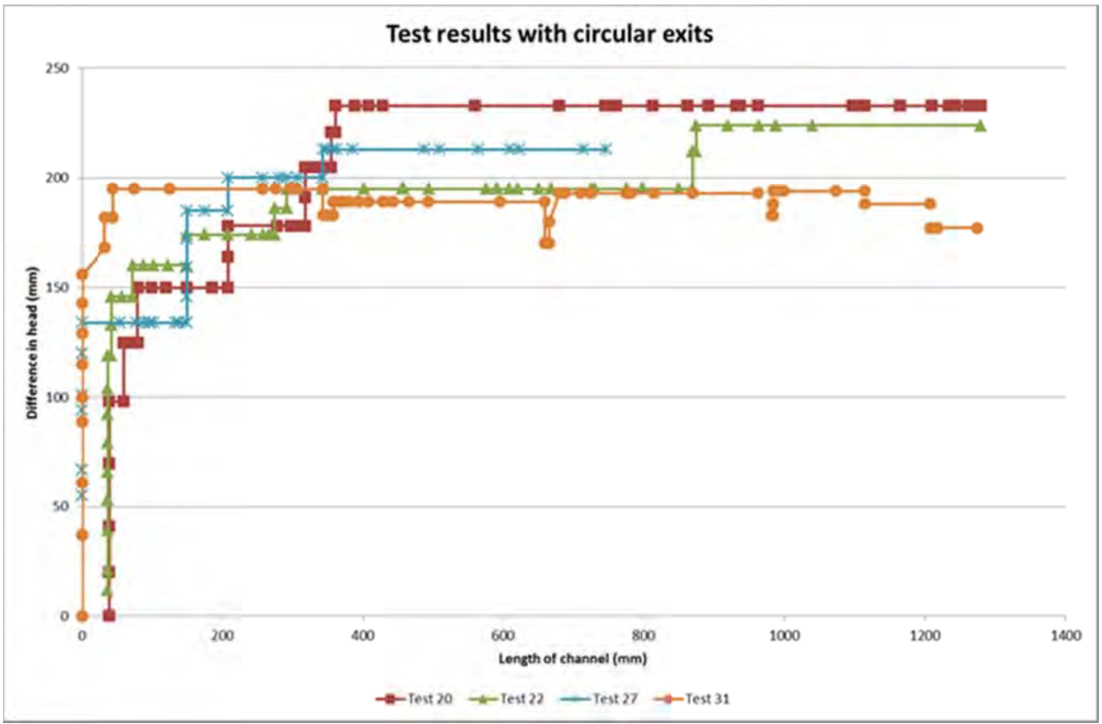

Test results with circular exits
Difference in head (mm)
Length of channel (mm)
0
50
100
150
200
250
0
200
400
600
800
1000
1200
1400
Test 20
Test 22
Test 27
Test 31

Backward erosion piping test data sheet

Test #	32	mass of soil & water	kg
Date	7/01/2014	flume volume	0.22 m^3
Soil	Sydney sand	bulk unit weight	0 kN/m^3
Flume	4	moisture content	%
Exit type	plane	void ratio	#DIV/0! -
seepage length	1.3 m	relative density	#DIV/0! -
head in bladder tank	5 m	avg. time for 50mL	s
bladder pressure	50 kPa	Q when ΔH = 0.1m	#REF! L/min
compaction	vibrator		22.5°C

only half a team

time	head (mm)	observation		
10.17	0	u/s valve opened completely		
10.18	↑ 100	50ml = 5.7, 5.7, 6.2, 6.4, 6.3		
10.26	↑ 190	no movement		
10.31	↑ 223			
10.33		very small amount of particle		
		rearrangement within coloured sand		
		zone about 30 mm d/s of exit.		
10.36	↑ 284	very small channel-type things formed		
		(see nappy snap) but not initiation yet		
		+ channels don't extend to exit.		
10.52	↑ 307	grain rearrangement.		
11.01	↑ 318			
11.15	↑ 331	initiation.		
11.17		tip 60mm but it looks as though sand		
		is struggling to come out from		
		underneath lid edge at exit.		
11.28		still 60mm		
11.52		tip 1 245ab1	tip 2 225ab1	tip 3 215ab1
11.54				at b2
11.57		30ab2		
11.59			38ab2	
11.59		83ab2		
12.01		165ab2	75ab2	0ab2
12.07			150ab2	75ab2
12.09		25ab3		
12.17		110ab3	200ab2	190ab2

time	head (cm)	observation
12.18		channel 1 blocked btw 2 and 3.
12.19		" 2 " " 1 and 2.
12.23		tip 3 45 ab3
12.24		tip 1 110 ab3 tip 2 205 ab2
12.26		190 ab3
12.26		Ch3 has partially blocked just u/s
		of b3 so tip 3b has formed trying
		to go around the blockage. (see
		happy snap).
		(3a) 230 ab3 (3b) 160 ab3
12.29		(2) 20 ab3
12.29		tips 3a + 3b joined now: 40 ab4
12.30		ch3 now blocked just d/s of b4.
12.30		88 ab4
12.31		(2) 160 ab3
12.33		(3) 103 ab4
12.33		(3) 118 ab4
12.33		(3) reached u/s end
12.35		(2) 0 ab4
12.36		Ch3 has started the ~~[illegible]~~ fwd opening.
12.36		(1) 110 ab3 (2) 75 ab4
12.37		(2) u/s end
12.46		both Chs 3 and 2 are fwd opening.
12.51		Ch1 just unblock and its tip is progressing again.
12.52		It sounded like the d/s flow just increased
		so maybe this is a 'type' of failure?
		Yep failed! catastrophically moments later.

Test 32 (flume 4 plane) report

Test 32 was the 3rd test with a plane exit.

The first channel initiated at a head of 331mm. Other channels formed so that there were 3 separate tips. No increases in head were required so initiation head = critical head. Tip 3 was the first to reach the u/s end about 1.3 hours after initiation.

Blockages occurred frequently in this test. When a blockage occurred the tip progression either slowed right-down or stopped until the blockage cleared. Most of the time a blockage would clear itself but on one occasion a branch formed in channel 3 to create a new tip which went around the blockage and re-joined the channel u/s.

Failure occurred 20minutes after channel 3 had reached the u/s end. I noticed flow increased just before failure occurred (I heard the flow out of the d/s valve increase).

I note that this test was over relatively quickly. A possible explanation for this was it required the highest critical gradient tested so far. So if tip progression is related to gradient and this test needed the highest critical gradient it seems reasonable that this was the quickest.

This photo shows the diversion in channel 3 which formed to bypass the blockage.

Graph of test:

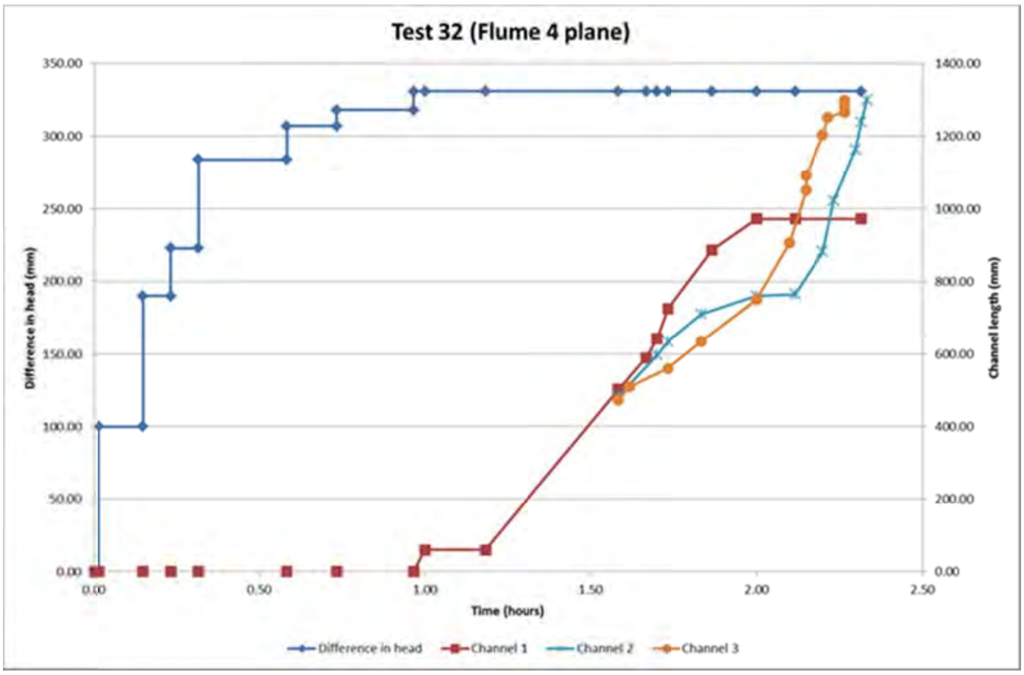

As for comparing this test with other plane tests. See below.

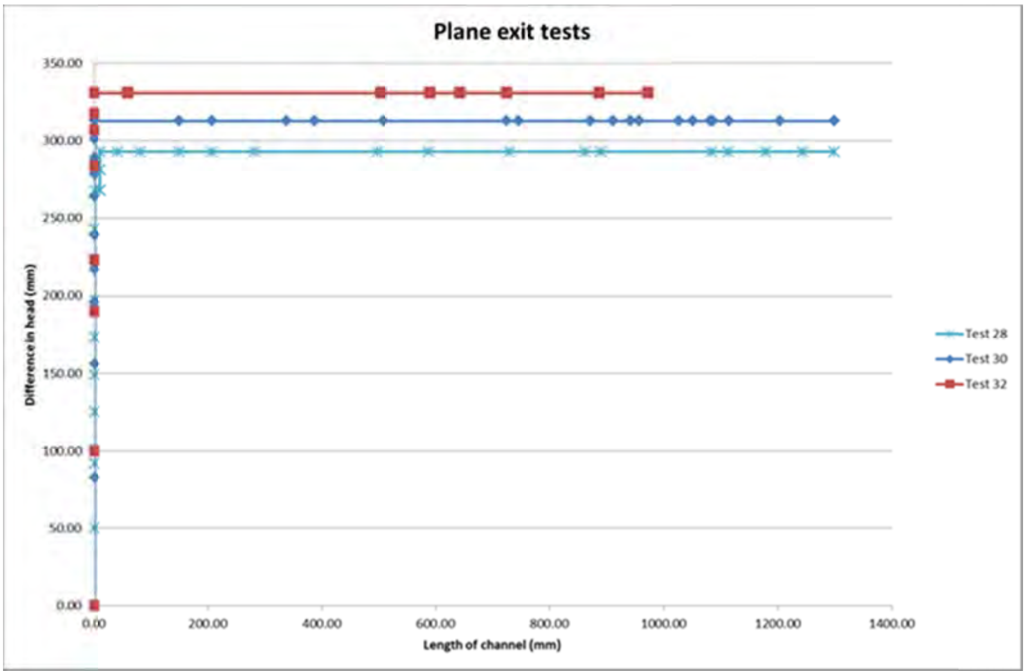

I'm happy I'm getting fairly consistent results (there's an 11% difference between max and min). And I think it's fair to say the initiation gradient = critical gradient for plane exits.

As for comparing the results from plane-exit tests with other exits see below.

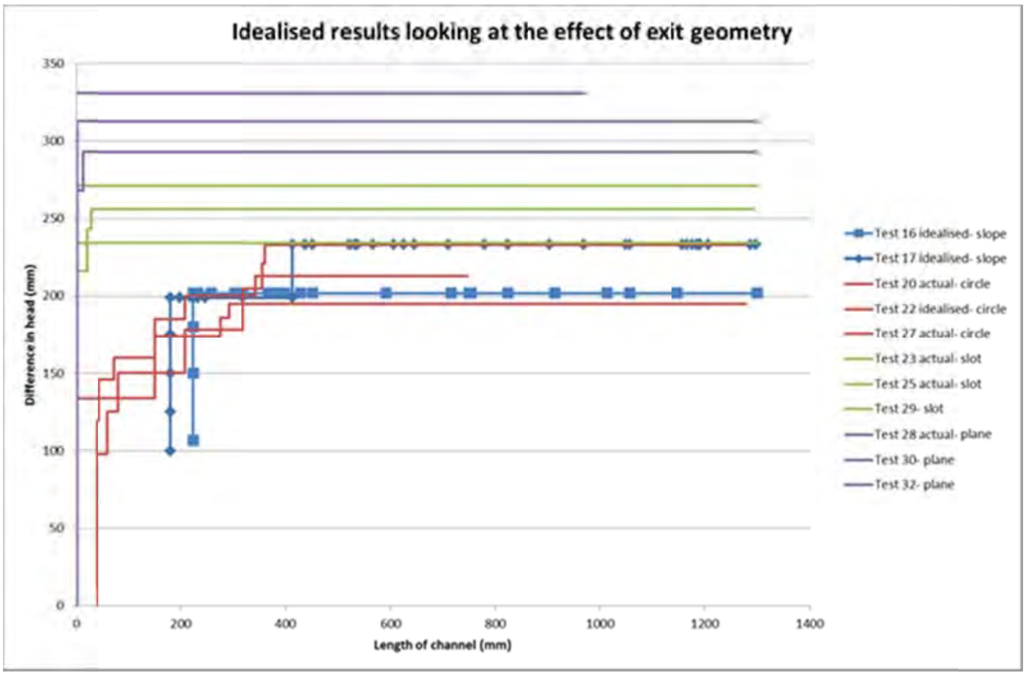

Plane requires the largest critical gradient although I'm expecting the slope to require a larger gradient again (the slopes shown on the graph above was from the original setup without the d/s tank which changes things). The more an exit concentrates the flow (i.e. the larger the seepage velocities at the exit) the lower the critical gradient.

Backward erosion piping test data sheet

Test #	33	mass of soil & water	kg
Date	14/01/2014	flume volume	0.22 m^3
Soil	Sydney sand	bulk unit weight	0 kN/m^3
Flume	3	moisture content	%
Exit type	slope	void ratio	#DIV/0! -
seepage length	1.3 m	relative density	#DIV/0! -
head in bladder tank	5 m	avg. time for 50mL	12.73 s
bladder pressure	50 kPa	Q when ΔH = 0.1m	#REF! L/min
compaction	vibrator		

time	head (mm)	observation
11.30	0	no movement
11.31	↑ 48	" "
11.39	↑ 102	50mL = 12.2, 12, 13.9, 12.8
12.02	↑ 155	no movement
12.26	↑ 207	" "
12.37	↑ 234	" " . camera fell over so pics not
1.42	↑ 260	" " regular.
2.06	↑ 288	
2.09	↑ 310	
2.13	↑ 342	it might have initiated at 310 but it
		did so along edge under sand
		sitting on lid. i.e it has initiated @
		RHS edge
2.17		tip now @ tank wall. It's moving away
		from edge.
2.19		tip @ bl
2.25		65 abl
2.29		123 abl
2.33		185 abl
2.38		8 ab2
2.42		85 ab2
2.49		190 ab2
2.54		blocked btw 2+3 (see happy snap)
2.54		8 ab3
2.57		unblocked
3.00		a new tip (B) has formed trying to

time	head (cm)	observation
		90 around blockage that keeps blocking
		+ opening, blocking + opening (see happy
		snap)
3.02		135 ab3 (1a)
3.04		tip 1b branches off 1 at about 30 d/s of bR
		and is currently 90 ab2.
3.06		210 ab3 (1a)
3.10		240 ab3 (1a)
3.10		@ b4
3.12		almost blocked btw 3+4 (see happy).
3.15		35 ab4 (1a) @ b3 (1b)
3.18		reached u/s end. See video for
		channel reaching u/s + opening up.
3.23		(1b) 60 ab3
3.42		Failed

33. Test 33 (flume 3) slope

Test 33 was the 1st test with a slope exit.

The channel initiated at 342mm at the RHS edge. The tip progressed to the u/s end at a constant speed of about 1.1m/hr. It took 1.08 hours from initiation to u/s and 24minutes from u/s to fail.

Blockages occurred but unblocked themselves in time. At one point the channel branched off in an effort to go around a blockage. Both the new tip and original tip progressed simultaneously but it was the original tip which reached the u/s end.

Test 33 graph

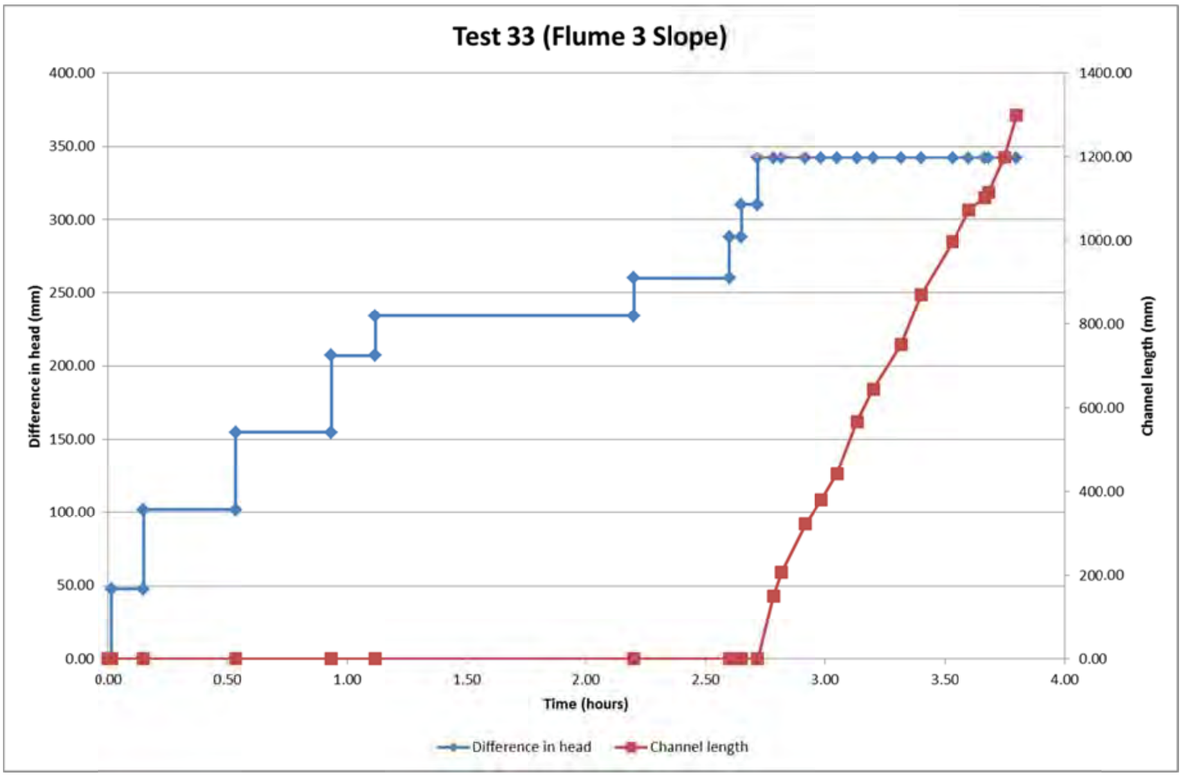

Channel branched to form new tip in an attempt to go around blockage

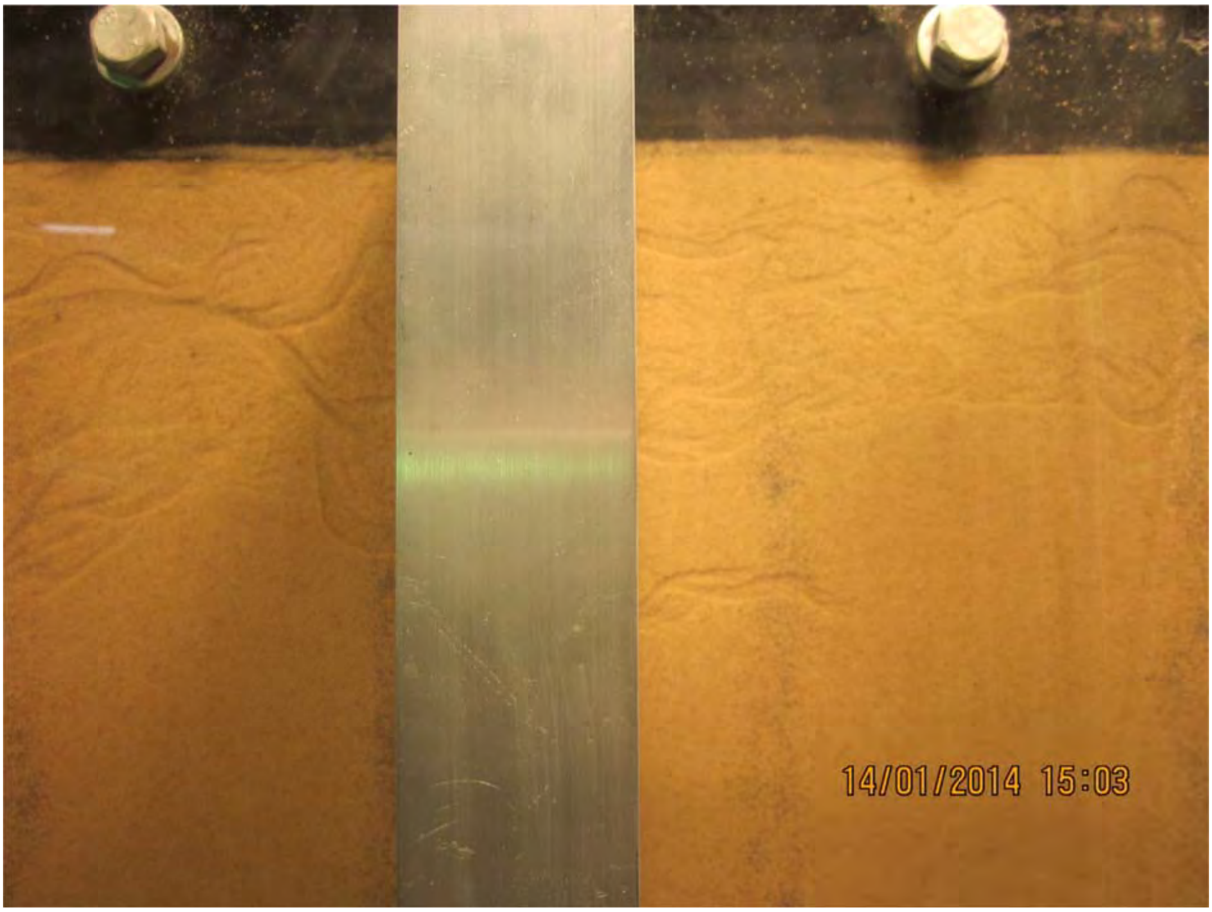

Difference in head with tip location

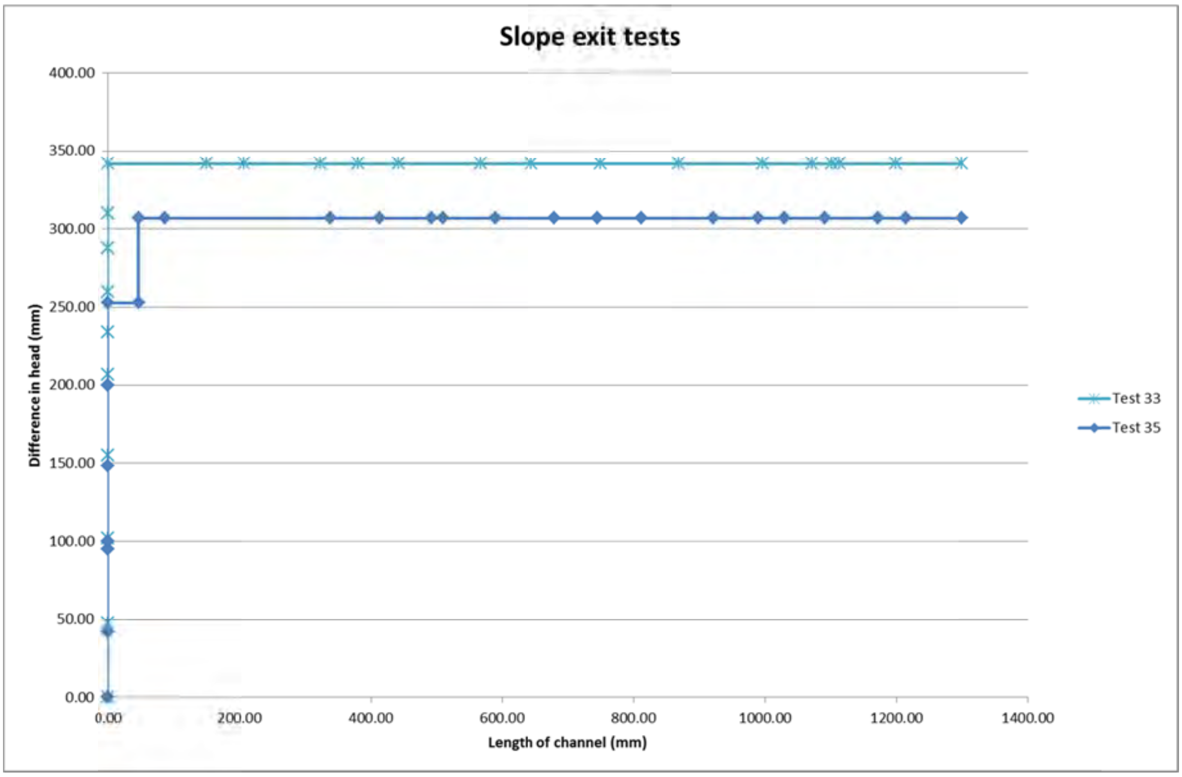

Backward erosion piping test data sheet

Test #	34	mass of soil & water	kg
Date	17/01/2014	flume volume	0.22 m^3
Soil	Sydney sand	bulk unit weight	0 kN/m^3
Flume	4	moisture content	%
Exit type	circle	void ratio	#DIV/0! -
seepage length	1.3 m	relative density	#DIV/0! -
head in bladder tank	5 m	avg. time for 50mL	12.6 s
bladder pressure	50 kPa	Q when ΔH = 0.1m	#DIV/0! L/min
compaction	vibrator		0.24

time	head (mm)	observation
10.53	0	some channeling around hole but
		still gonna say it's 0mm (see
		happy snap) because I don't think
		the larger ones are heading in this
		direction
10.55	↑ 47	
11.03		particle boiling in hole but no change
		to existing channels.
11.04	↑ 72	
11.17	↑ 96	
11.19	↑ 100	50mL = 10.9, 14.5, 12.1, 11.1, 14.3, 12.5
11.25	↑ 107	I think I should say there are 2
		channels both about 20mm (been
		there from the start)
11.28	↑ 118	
11.30	↑ 132	some particle rearrangement, particularly
		along sides of channel, but
		nothing at tip
11.33	↑ 144	again, some particle rearrangement but tips
		not moved. I'm a little concerned as
		to how the ditch in the sand next
		to the hole is affecting the flow.
		Could it be slowing down velocities
		near the hole because it's a big
		area?
11.38	↑ 155	there's a channel out to RHS of

Test 34

time	head (cm)	observation
		the side that's advancing and is
		about 50mm long (see happy snap)
		but I don't think this will be
		the main channel because it's
		out to the side.
11.42	↑ 167	
11.47		the side channel now about 70mm
11.48	↑ 180	
11.51	↑ 192	
11.54		still particles rearranging. It's trying.
		I wonder if
		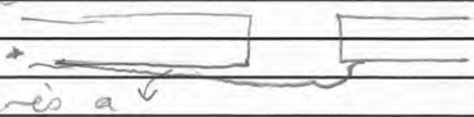
		there's a
		"void"
		here. ⟶ flow
		I see particles
		from * move but then stop in "void".
		Prob can't see but I've taken a
		happy snap. Side channel ≑ 90mm.
11.57	↑ 203	
initiation 11.59		and we're off. furthest tip now 146.40 ①
12.00		C happy snap.
12.02		146-22 ①
		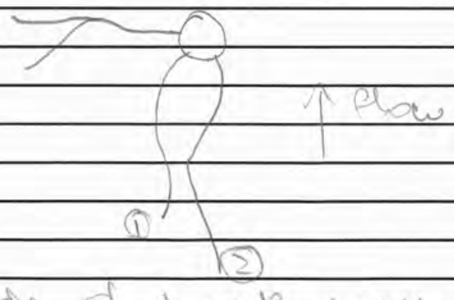
12.05		① other side of tank wall
12.06		② @ bl
12.07		no need to distinguish btw tips ① and
		② (2 was a branch off 1) so will no
		longer call it ②.
12.09		tip under bl.
12.21		" " "
12.26		" " "
12.30		" " "
12.30	↑ 215	
12.36		15 abl
12.40		40 abl
12.45		83 abl
12.47		105 abl
12.47	↓ 203	

Test 34

time	head (cm)	observation
12.49		137 ab1
12.50		160 ab1
1.02		160 ab1 and has done a 90° turn
		(see happy snap)
1.09		160 ab1
1.16		160 ab1
1.17	↑215	
1.18		there's particle movement again but the tip is struggling to move because it's done a 90° turn. Branches are trying to form off the bend.
1.20		160 ab1
1.23		160 ab1
1.34		160 ab1
1.34	↑225	
1.36		185 ab1. A tip branched off the bend (see happy snap).
1.39		225 ab1
1.41		@ b2
1.50		75 ab2
1.55		88 ab2
1.59		128 ab2
1.59	↓ 215	
2.06		153 ab2
2.10		176 ab2
2.16		188 ab2
2.19		215 ab2
2.19	↓ 204	~~22~~
2.21		225
2.28		@ b3
2.33		under b3
2.40		20 ab3
2.41	↓ 195	
2.46		20 ab3
2.57		20 ab3
3.06		40 ab3
3.11		50 ab3
3.12	↓ 180	50 ab3
3.17		50
3.22		53
3.27		53
3.39		53
3.49		53
3.49	↑ 193	53
3.54		53
4.00		67
4.05		117 ab3
4.05	↓ 183	

time	head (cm)	observation
4.10		148 ab3
4.16		154 ab3
4.21		180 ab3
4.21	↓ 170	
4.26		180
4.37		180
4.42		180 ab3
4.42	↑ 181	
4.50		180 ab3
5.03		180 ab3
5.03	↑ 193	
5.05		240 ab3
5.08		245 ab3
5.08	↓ 183	
5.14		under b4
5.19		16 ab4
5.19	↓ 170	
5.25		16 ab4
5.30		16 ab4
5.36		16 ab4
5.41		16 ab4
5.41	↑ 180	
5.43		35 ab4
5.45		88 ab4
5.45	↓ 168	
5.47		135
5.52		135
5.58		135
6.03		135
6.03	↑ 178	
6.05		there's a blockage under b4.
		It's possible it's already at the u/s edge.
		I'm not sure.
		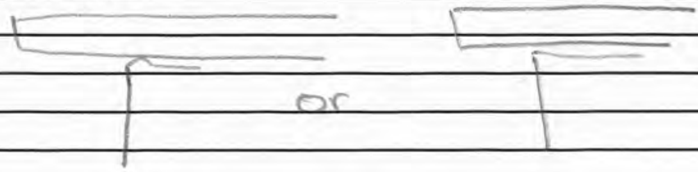
6.11		blockage now btw 3+4. the tip is so
		close to the u/s end (5mm) that I'm
		going to assume it's at the end and
		the blockage would have opened itself if
		I left it. However I can't leave it cause
		the power is being turned off tmw.
6.17		My best guess is tip at 140 abf
6.17		end of test.

22mm!!!

34. Test 34 (flume 4) circle

Test 34 was the 7th test with a circle exit and the 2nd test with the modified procedure.

The channel initiated at 181mm. Two increases in head were required to reach the critical head of 203mm. The critical head was reached when the channel was 418mm long (32% of seepage length).

No photos were taken with the canon or casio for this test. The timer remote for the canon was broken and I don't know why I didn't take any casio photos. *Note added later: I do have canon and casio photos.*

I noticed there was a 'ditch' in the sand next to the hole and made a note that perhaps this ditch was creating a larger area and therefore reducing seepage velocities in the vicinity of the exit which would require a larger head to initiate. Pic:

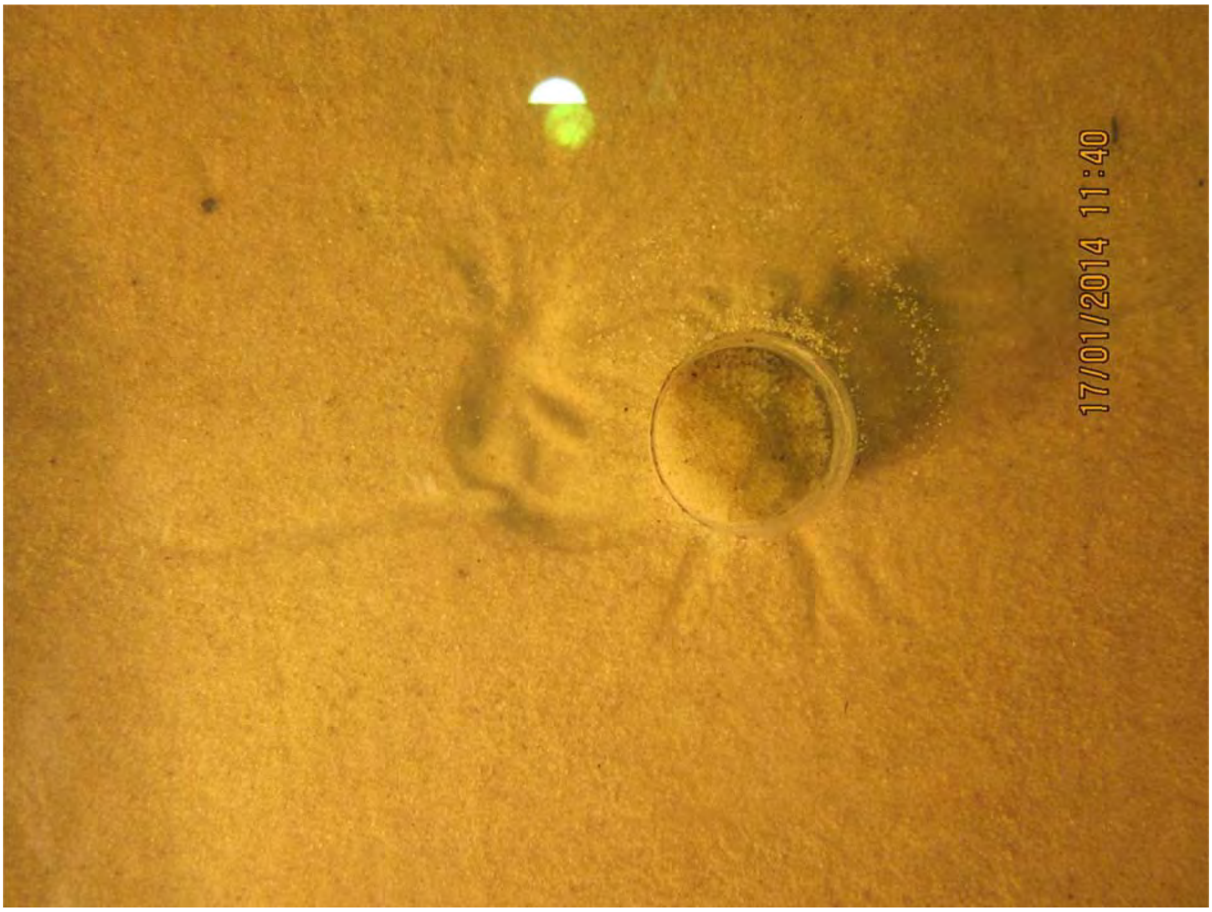

Initially there were 2 tips but they only one continued and was monitored.

At one point the channel made a 90 degree turn and new tips tried to form by branching off for a while. Eventually one was successful. Pic:

Towards the end of the test I noticed I hadn't completely opened the d/s valve so once the test had finished I measured the water level in the standpipe, fully opened the ball valve, then measured the level in the standpipe again. The difference in level in the standpipe was 22mm. I should have noted what the level in the constant head tank was at the time (because the head loss across the partially open ball valve depends on the flow passing through it) but I didn't. So all I did was subtract 22mm from all the head differences I recorded. All head differences included and graphed in this report are after this adjustment.

Test 34 graph

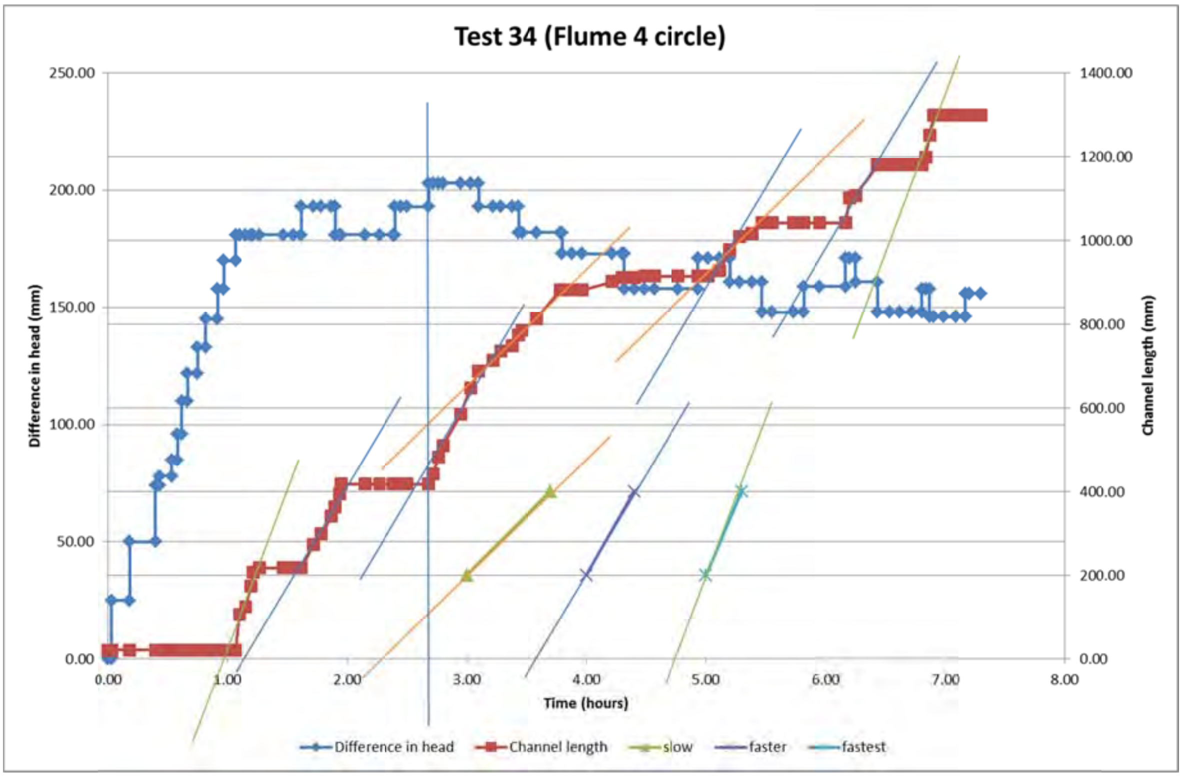

Difference in head with tip location

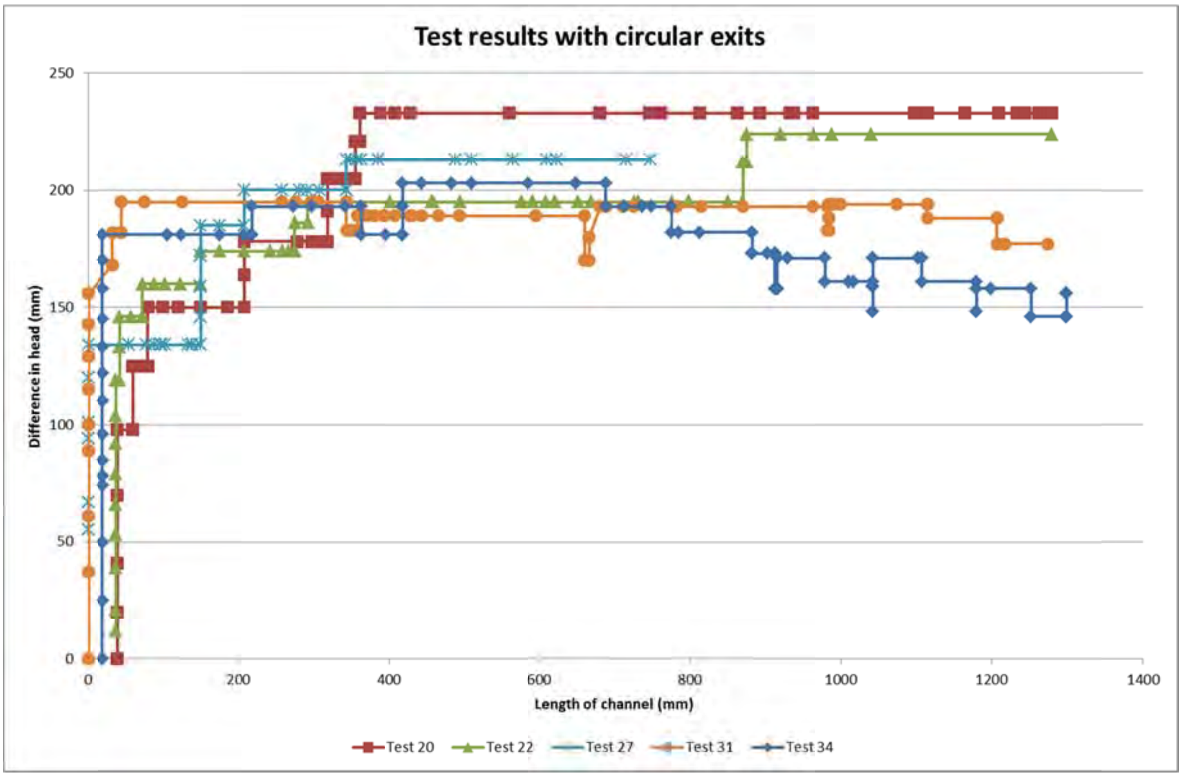

From this I deduce the tip location versus head required looks like this:

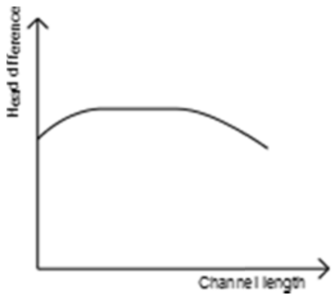

This is a bit different from what I saw in test 31 that looked more like this:

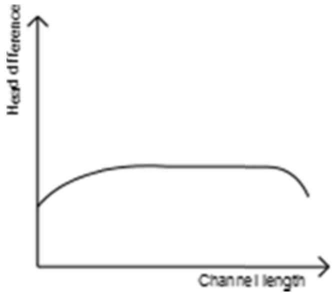

I tried looking for a pattern between head difference and speed of the tip in an effort to prove/disprove this hypothesis:

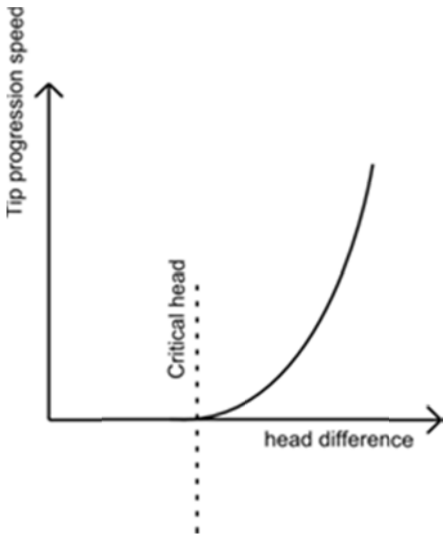

But I couldn't see any pattern.

It took 5.8 hours from initiation to u/s. I couldn't leave it to fail because the power was being turned off over the weekend.

Backward erosion piping test data sheet

Test #	35	mass of soil & water		kg
Date	29/01/2014	flume volume	0.22	m^3
Soil	Sydney sand	bulk unit weight	0	kN/m^3
Flume	3	moisture content		%
Exit type	slope	void ratio	#DIV/0!	-
seepage length	1.3 m	relative density	#DIV/0!	-
head in bladder tank	5 m	avg. time for 50mL	10.85	s
bladder pressure	50 kPa	Q when ΔH = 0.1m	#DIV/0!	L/min
compaction	vibrator		0.28	

time	head (mm)	observation
10.52	0	
10.52	↑ 42	
10.57	↑ 95	
11.00	↑ 100	for 50mL = 13.1, 9.9, 9.8, 10.6, 10.4, 11.3
11.15	↑ 148	
11.59	↑ 200	
12.03	↑ 253	
12.06	↑ 307	
12.07		initiate @ RHS so not a reliable initiation head
12.08		180-103
		190-103
12.15		80 ab1
12.17		happy snap. there r 2 tips.
12.20		155 ab1. Now 3 tips. happy snap.
12.23		I've denoted tips 'a,b,c' see happy snap.
12.23		'b' @ 235 ab1
12.24		'b' @ b1. Tips 'a' and 'c' seem to
		have stopped.
12.28		'b' 30 ab2
12.28		'c' 175 ab1. 'c' didn't stop.
12.33		'b' 120 ab2.
12.36		'b' 185 ab2. 'c' 175 ab1 - it's still moving but
		moving laterally.
12.40		'b' @ b3.
12.48		'b' 60 ab3
12.52		'b' 128 ab3

time	head (cm)	observation
12-55		168 ab3
12-59		230 ab3
1-00		whilst there's only one channel near
		tip, the channel meanders + widens
		+ branches toward d/s end.
1.03		channel blocked wide 63 See happy
		snap.
1-06		It's trying real hard to unblock
		itself.
1.07		8 ab4
1-09		50 ab4
1.14		first noticed through to u/s-end

35. Test 35 (flume 3) slope

Test 35 was the 2nd test with a slope exit.

The channel initiated at 307mm at the RHS edge. The tip progressed to the u/s end at approx. speeds of 44, 19 and 14mm/min (in that order). It took 1.1 hours from initiation to u/s. I don't think I left it running long enough to fail but if I did I didn't record it (I can't remember).

No photos were taken with the canon or casio for this test. The timer remote for the canon was broken and I don't know why I didn't take any casio photos.

13 minutes after initiation there were 3 tips. Pic:

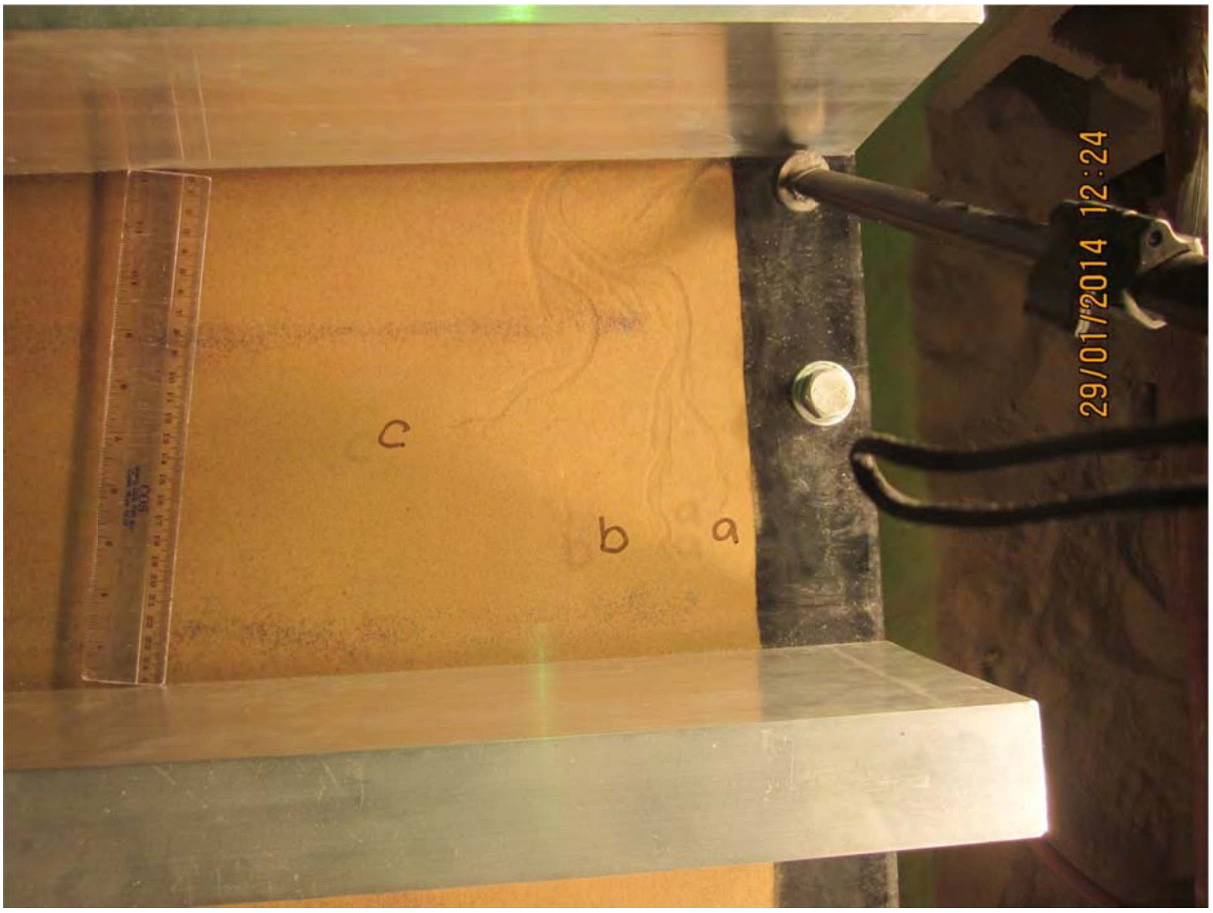

Tip 'a' stopped after a short time, and 'c' made a 90degree turn and moved laterally. Tip 'b' reached the u/s end and is the tip that is graphed.

Blockages occurred but unblocked themselves in time.

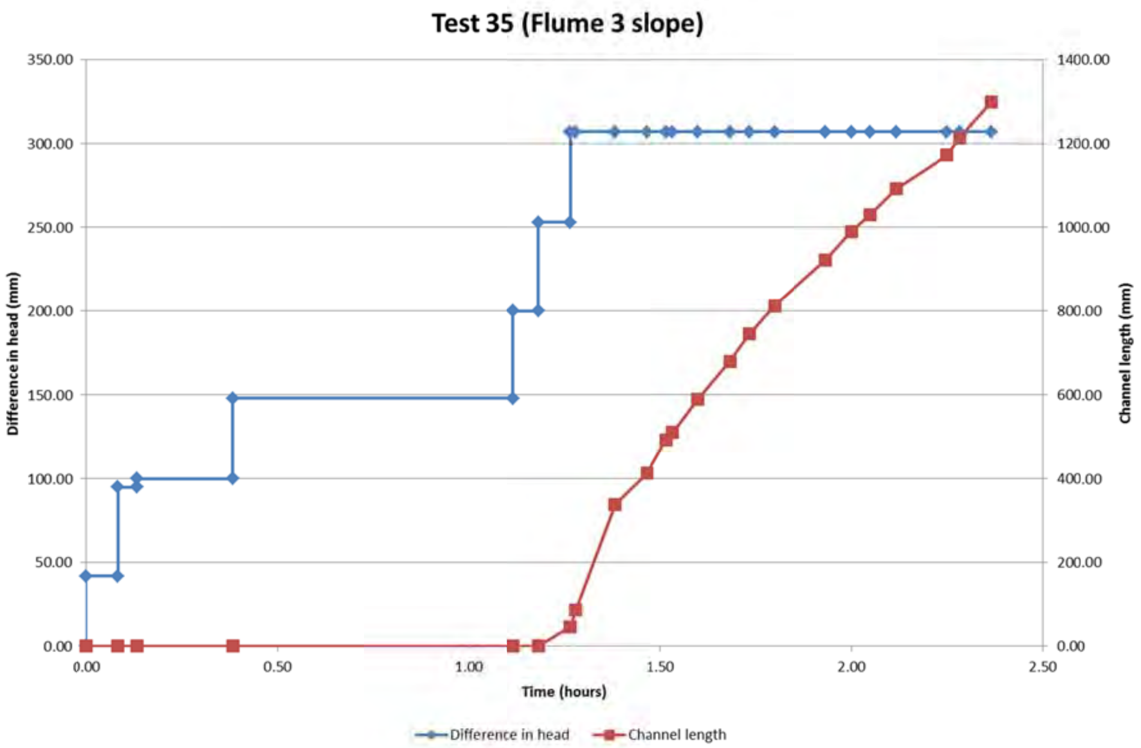

Test 35 (Flume 3 slope)
Difference in head (mm)
Channel length (mm)
Time (hours)
Difference in head
Channel length

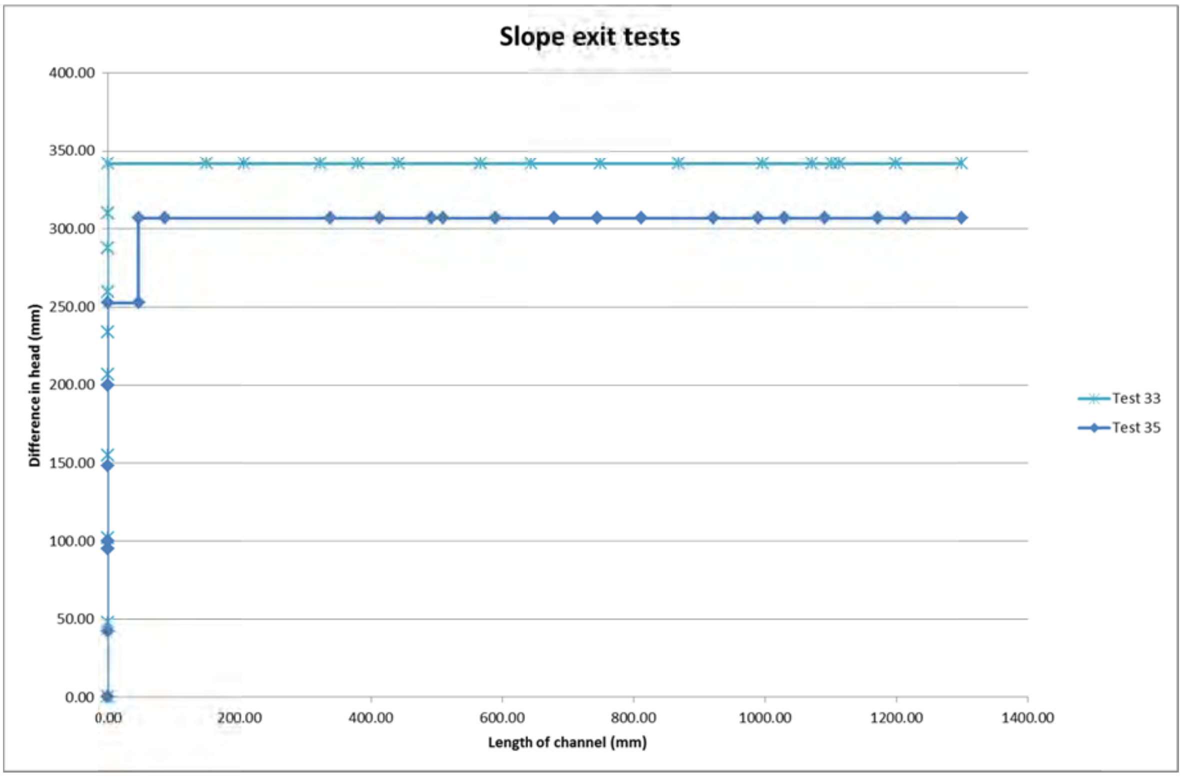

Slope exit tests
Difference in head (mm)
Length of channel (mm)
Test 33
Test 35

Backward erosion piping test data sheet

Test #	36	$m_s + m_w$ after 'drying'		kg
Date	11-2-14	m/c after 'drying'		-
Soil	Sydney sand	V_s	0	m^3
Flume	3	$V_s + V_w$ in flume	0.2065095	m^3
Exit type	slope	void ratio	#DIV/0!	-
seepage length	1.3 m	relative density	#DIV/0!	-
head in bladder tank	5 m	avg. time for 50mL	12.78	s
bladder pressure	50 kPa	Q when ΔH = 0.1m	#DIV/0!	L/min
compaction	vibrator		0.23	

time	head (mm)	observation
10.38	0	the top of the slope isn't up against
		the lid. i.e there's a gap btw the lid
		+ sand in the vicinity of the exit
		(see happy snap). I don't know why
		this happened. As for the effect it'll
		have on the experiment, it may
		mean initiation will occur @ a higher
		head than would of been because
		the flow is less concentrated &
		(slower).
10.41	↑ 65	
10.45	↑ 100	50mL Q = 14.4, 11.5, 12.9, 13.8, 11.3
10.58	↑ 157	
11.13	↑ 211	
11.56	↑ 237	
12.04	↑ 251	
12.12	↑ 265	
12.17	↑ 279	
12.22	↑ 294	some grain rearrangement toward
		RHS at exit (but not at edge;
		about 60mm from edge).
12.36	↑ 306	some particle rearrangement toward centre
		of exit.
12.43	↑ ~~÷~~320	more rearrangement. this time what
		could be considered a small channel
		has formed (see happy snap) about

time	head (~~c~~m)	observation
		60mm from RHS and it about 15mm
		long (note: slope edge about 23mm
		from exit).
12.50	↑ 335	no movement
1.43		first noticed a channel started
		≐ 40mm away from RHS (see happy
		snap).
1.44		210-100.
1.45		at tank wall.
1.48		reached b1
1.54		70 ab1
1.56		215 ab1
2.02		70 ab2
2.11		225 ab2
2.16		105 ab3
2.21		190 ab3
2.30		5 ab4
2.31		45 ab4
2.32		72 ab4
2.33		95 ab4
2.34		46 (well it turned to intercept a
		gas pocket but close enough -
		see happy snap). 110 ab4
2.35		blocked around b3.

36. Test 36 (flume 3) slope

Test 36 was the 3rd test with a slope exit.

When I formed the sand's surface I contoured the sides so they had longer seepage lengths to try keep channels from initiated along the edges. Pic:

It kind of worked. The channel initiated at the intersection of contoured edge and the top of slope. Pic:

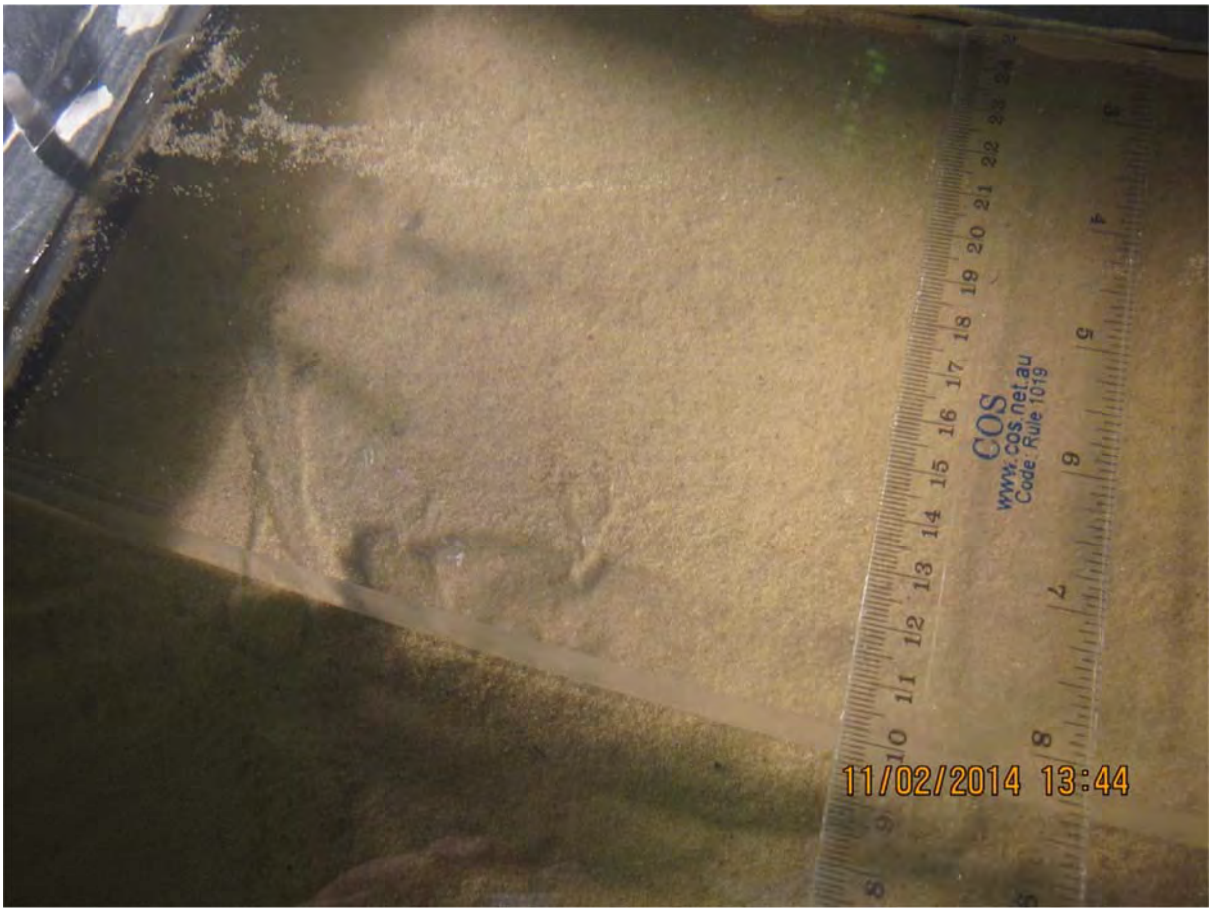

I'll contour the sides like this for all future slope tests.

Also, as you can see in the pic above, the top of the slope was in a bit from the edge of the lid. Pic:

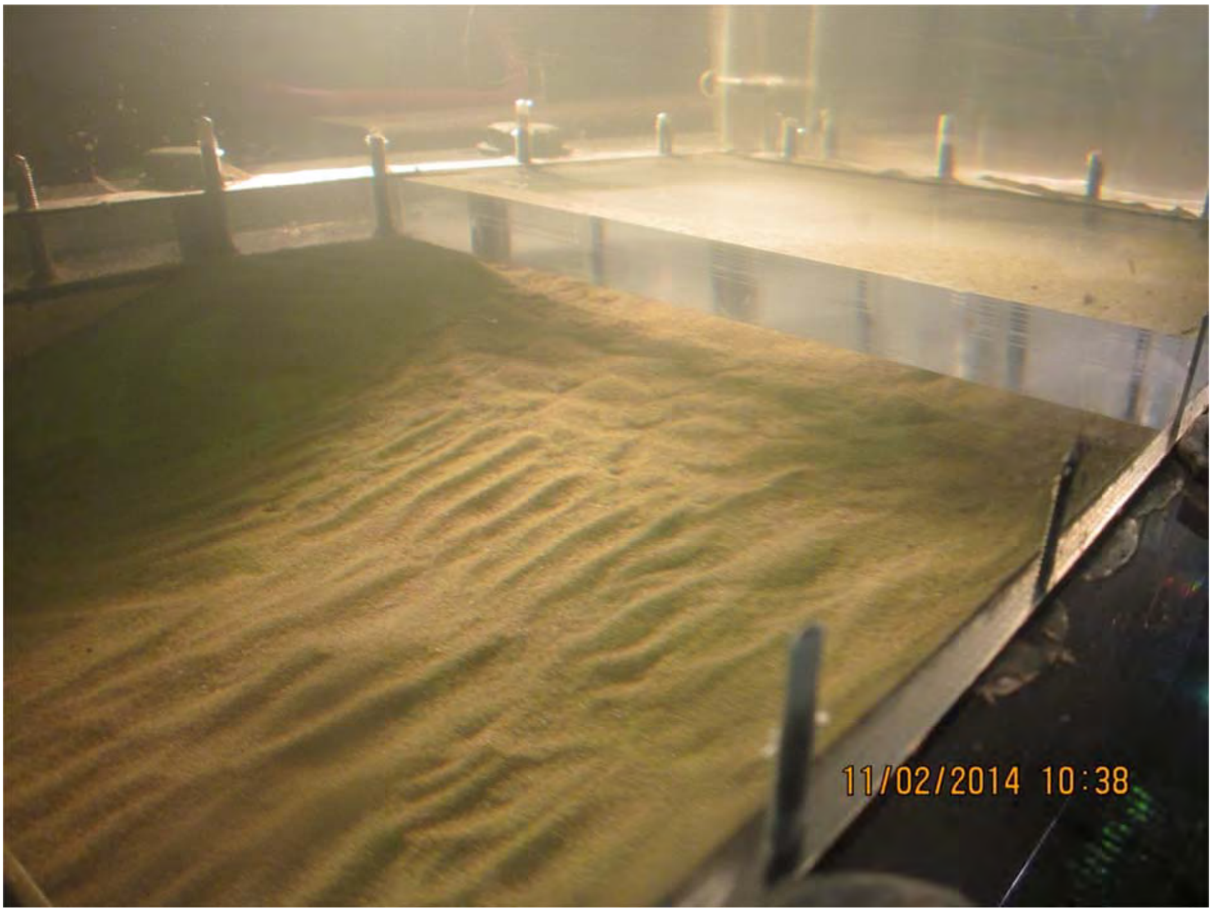

I think this happened because I just wrongly measured where the lid would end when I was forming the slope. It didn't seem to affect the test.

The channel initiated at 335mm. The tip progressed to the u/s end at approx. speeds of 1.8 and 25mm/min (in that order). It took 0.85 hours from initiation to u/s and 2.2 hours from u/s to failure.

The channel diverted slightly to a gap at the upstream end. This didn't affect the test except that during the forward deepening process gas bubbles entered the deepened pipe.

Blockages occurred but unblocked themselves in time.

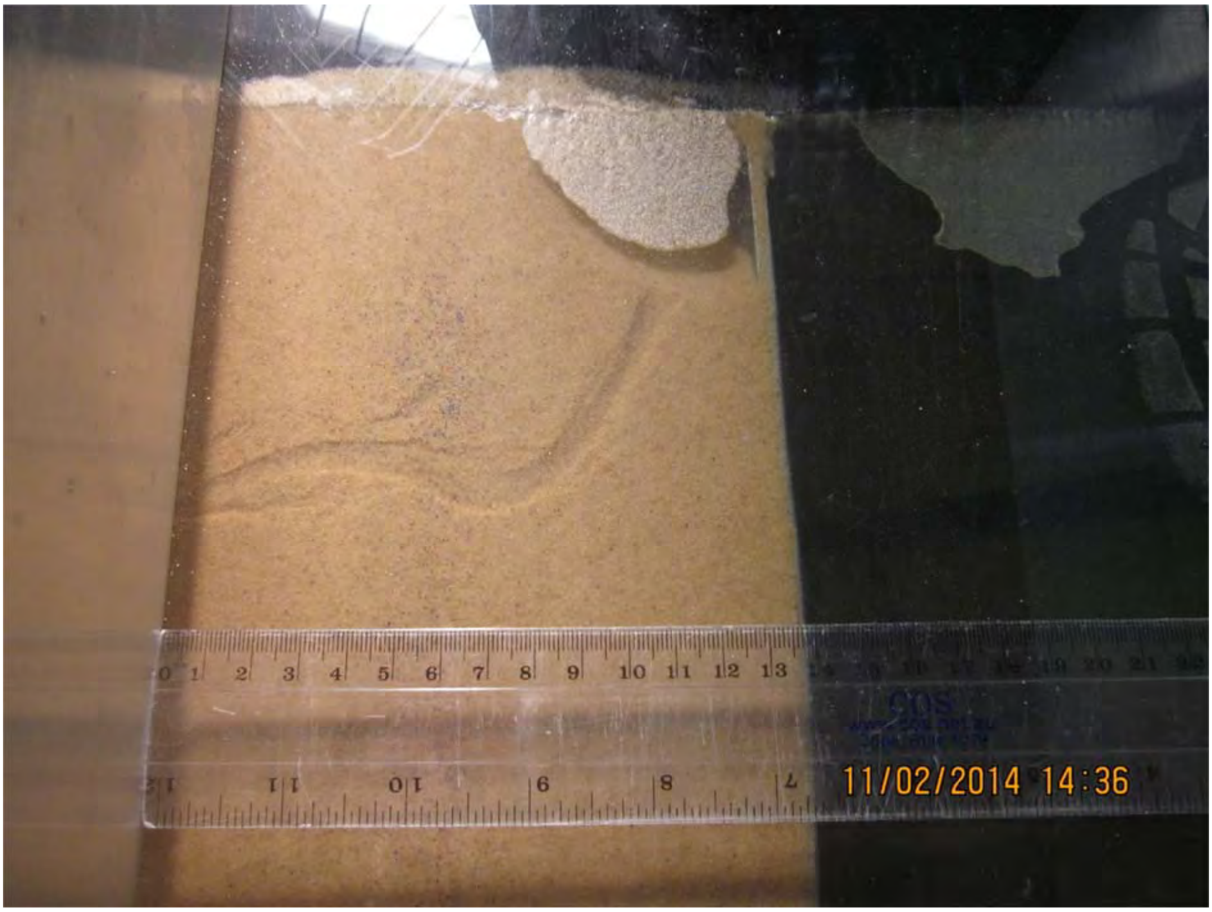
0 1 2 3 4 5 6 7 8 9 10 11 12 13
11/02/2014 14:36

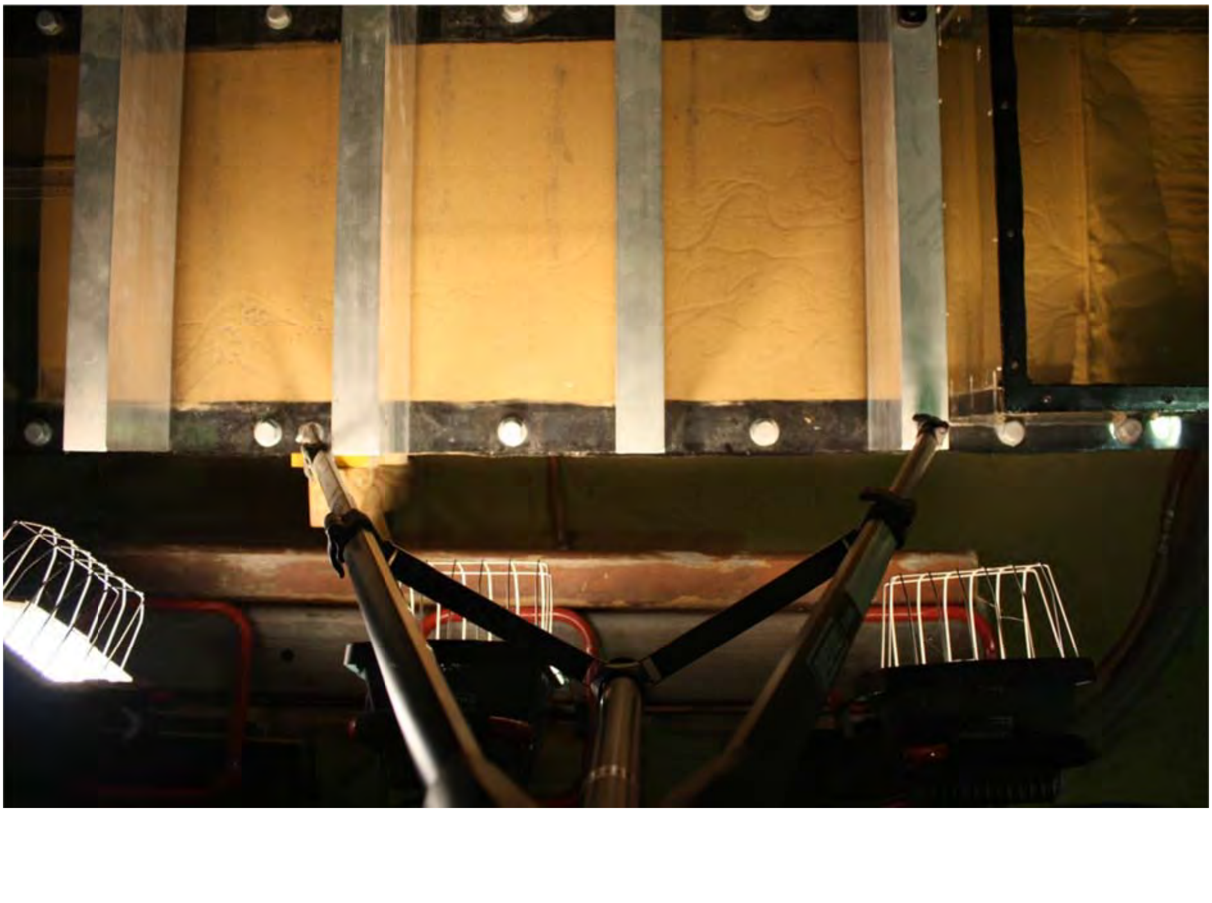

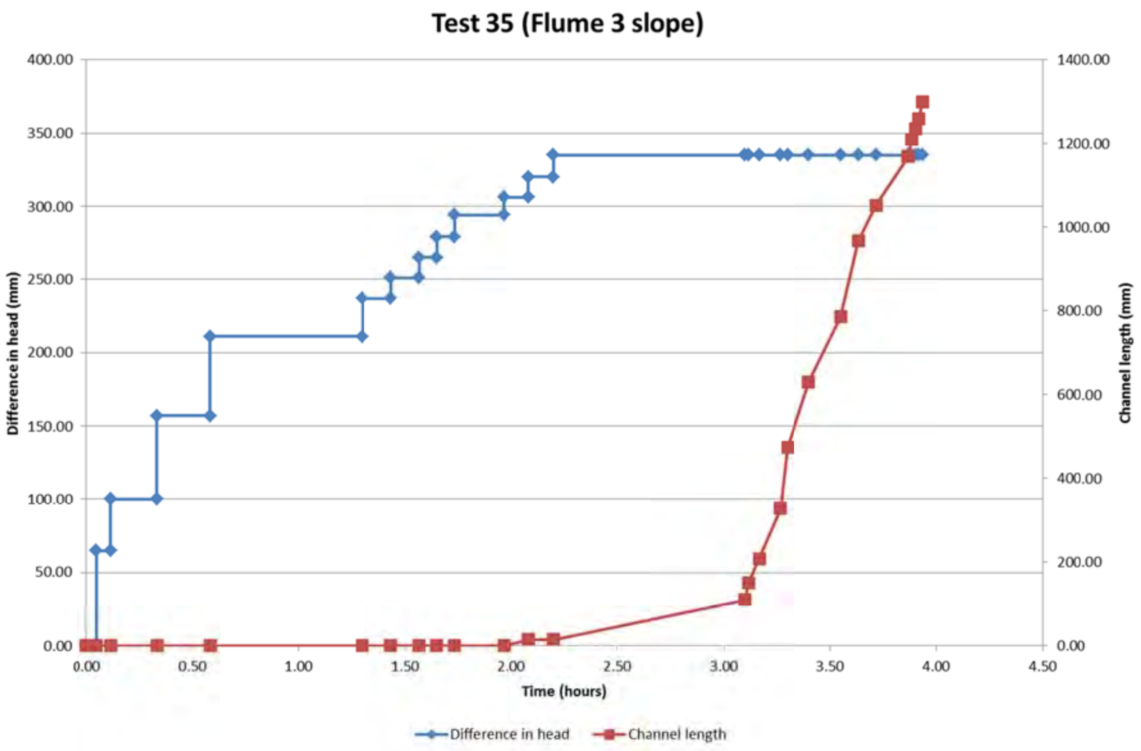
Test 35 (Flume 3 slope)
Difference in head (mm)
Channel length (mm)
Time (hours)
Difference in head
Channel length

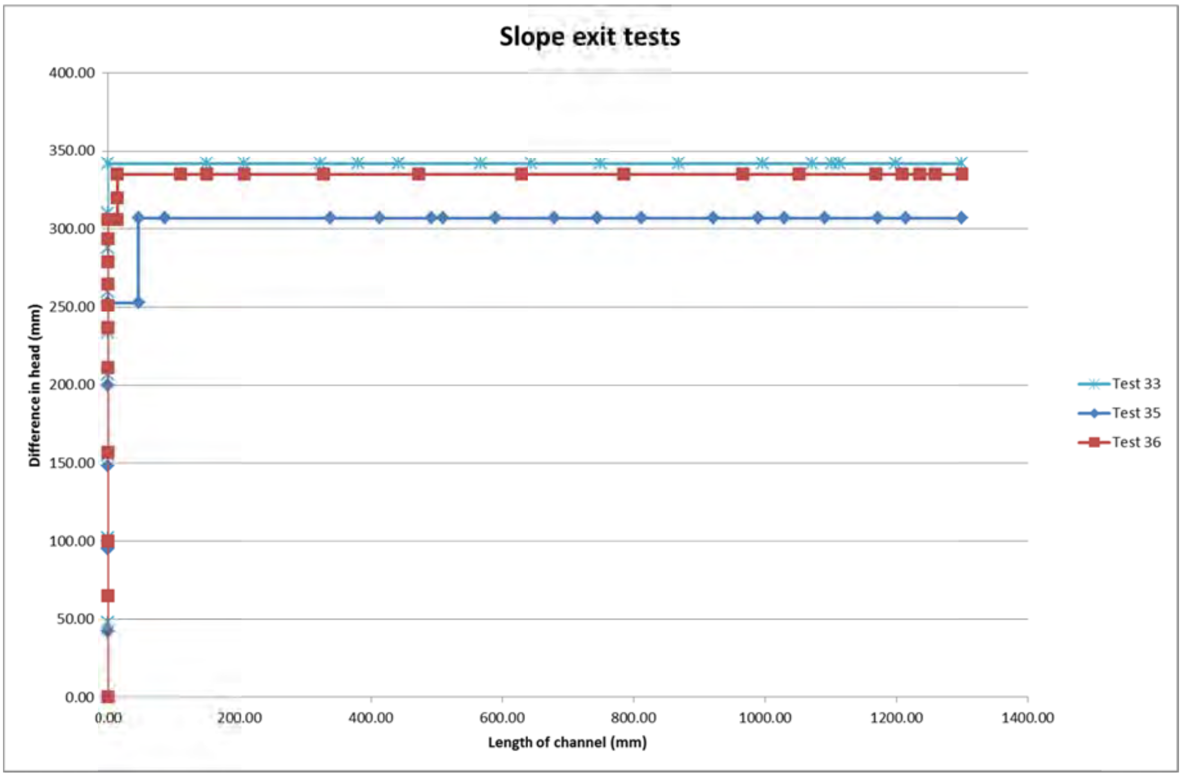
Slope exit tests
Difference in head (mm)
Length of channel (mm)
Test 33
Test 35
Test 36

Backward erosion piping test data sheet

Test #	37	$m_s + m_w$ after 'drying'		kg
Date	12-2-14	m/c after 'drying'		-
Soil	Sydney sand	V_s	0	m^3
Flume	1	$V_s + V_w$ in flume	0.2171016	m^3
Exit type	slot	void ratio	#DIV/0!	-
seepage length	1.3 m	relative density	#DIV/0!	-
head in bladder tank	5 m	avg. time for 50mL	12.3	s
bladder pressure	50 kPa	Q when ΔH = 0.1m	#DIV/0!	L/min
compaction	vibrator		0.24	

time	head (mm)	observation	
11:04	0	Normal	
11:06	54		
11:11	100	Q = 50mL ~~t = 8.6, 7.7, 7.4, 7.6, 9.5, 9.1, 8.9~~	
		t = 11.6, 11.2, 12.0, 13.6, 12.6, 13.0	
11:21	152		
11:23	185	Initiation, particle movement & chanel is being	15
		created at about mid of slot. Extended to	
		about 15mm. stopped shortly after starting.	
11:29	199	Some more particle erosion in same channel	
		Did not grow longer (maybe wider/branched out).	
11:32	212	grew to about 32 mm (straight)	32
:38	222	Very thin channel growth to about 45mm.	45
~~:43~~	~~2~~	Main thickness of channel still at 32mm.	
:43	237	88mm, rapid growth, slow growth following.	→ 2 chan openings next to each other both stem from same channel. see happy snap
11:57		Power off. Turned water off (because	
		pump not working). head dropped to 92.	
12:32	92	Power Back on. Progressive rise to 237 head.	
12:36	237	Further growth. 110 mm	
12:36	237	130mm – Greater widening of the main channel	
		about 10mm wide at widest point.	
12:52		at ab1	
1:02		ab1 23 mm	
1:05		ab1 44	→ Many channel openings
1:07		ab1 50	
1:13		ab1 70 → just past (5mm) point 1.	see happy snap
1:13	226	still have sand movement & channel growth.	

Test 37

time	head (cm)	observation
1:16	226	ab1 85
1:19		ab1 103
1:24		ab1 140
1:28	~~[illegible]~~ 237	dropped ~~[illegible]~~ head as still moving after 15 min.
		ab1 155 - accidently increased head instead of dropping
1:30	213	Dropped head ab1 160
1:34		ab1 162
1:48		ab1 162 No sand erosion
~~1:48~~		~~head dropped as no movement~~
1:49	217	head increased as no movement. sand erosion,
		but little tip erosion.
1:55		ab1 162 tip started to move immediately after this observation ~~[illegible]~~
1:58		ab1 177 ~~[illegible]~~
1:59		ab1 184
2:03		ab1 190
2:07		ab2 194
2:14		ab1 204
2:17		ab1 226
2:22		ab1 232
2:26		ab1 242
2:45		ab2 25
2:58		ab2 79
3:13		ab2 149
3:13	207	Dropped head 1/4 turn as reached point of interest. went (60mm) past but did not notice
3:18	211	↑ head as no movement of tip for 3 mins.
3:22	217	↑ head " "
3:25		ab2 153
3:31		ab2 175
4:00	↓ 133	
9:58	↑ 217	~~[illegible]~~ Tip not seeming to be moving (under
		bar 3) so will increase head by 1/2 turn
		the drop back once tip is visible.
10:11	↑ 223	" "
10:15	↑ 229	Very slow tip movement (if any) so " "
10:27	↑ 235	
10:45		ab3 3mm
10:58		moved ≈ 20mm laterally (not moving u/s) continued to move about 30 more mm ~~[illegible]~~ laterally
11:12		~~[illegible]~~ ab3 60
11:15	↓ 223	still moving ∴ lower 1/4 turn ab3 75
11:19	↑ 227	
11:27		~~120~~ ab3 120
11:27	↓ 216	
11:30		ab3 130
11:33		ab3 133
11:43		ab3 160
11:47		ab3 175
11:47	↓ 203	drop head as at poi 0.8, ab3 176
11:50		ab3 178

point 7 at ab3 105

Test 37

time	head (cm)	observation
11:51		ab3 179
11:54	↑ 208	" "
11:57		tip growing laterally. very slowly
12.22		188 ab3
12.23	↓ 197	
1.06		190 ab3
1.57		195 ab3
1.58	↑ 203	
2.06		195 ab3
2.31		195 ab3
2.32	↑ 208	
2.40		208 ab3
2.54		210 ab3
3.10		250 ab3
3.11	↓ 203	
3.29		250 ab3
3.47		under ab4
4.05		" "
4.23		" "
4.24	↑ 208	
4.40		30 ab4
4.41	↓ ~~[illegible]~~ 204	~~45 ab4~~
5.29		45 ab4
5.31	↑ 208	
5.36		1st noticed all the way through to u/s. (125 ab4)
14-2		
9.33		I left it overnight to see if it would
		fail but the biofilm clogging had
		developed so it won't.

Test 37

time	head (cm)	observation
~~[illegible]~~		~~[illegible]~~

37. Test 37 (flume 1) slot

Test 37 was the 6th test with a slot exit and the 1st test using the modified procedure.

This test was mostly logged by Bronson.

The channel initiated at 185mm at centre of slot. Four increases in head were required to reach critical of 237mm.

34 minutes after initiation the power went off for about 52minutes. Because the pump would no longer operate I turned the water off. The water level dropped to 92mm before being raised again.

The tip progressed at speeds ranging between 1.8 to 5 mm/min. It took about 13 hours from initiation to u/s. I left it overnight to fail but it didn't because biofilm clogging had occurred.

Blockages occurred but unblocked themselves in time.

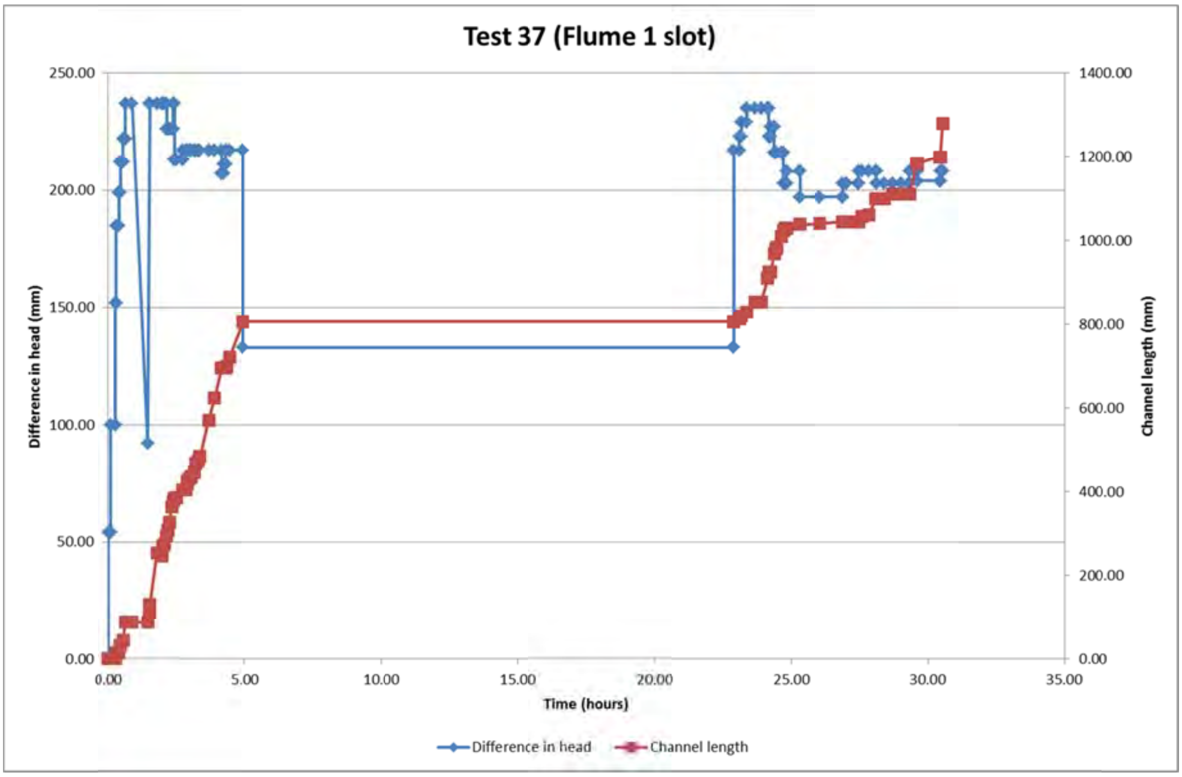

With respect to decreasing the head, it behaved like test test 31 and looked like this:

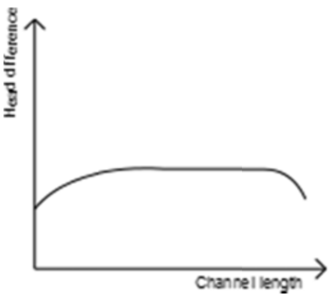

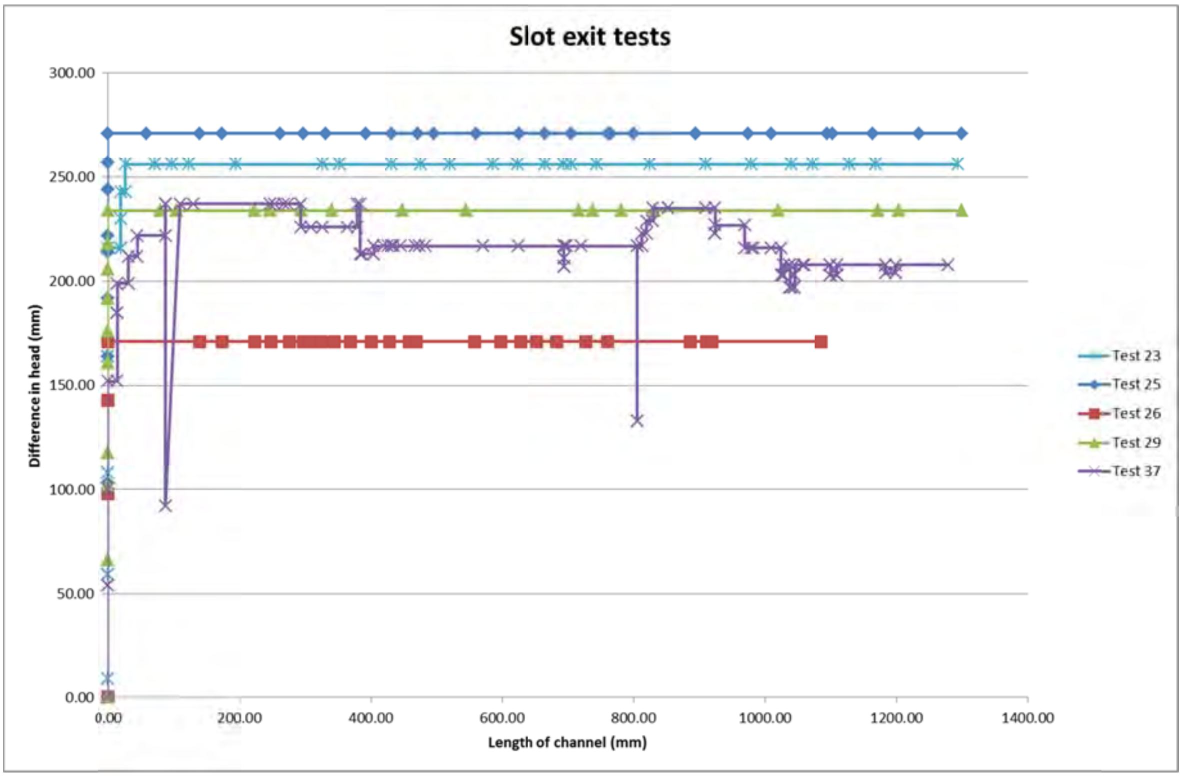

Slot exit tests
300.00
250.00
200.00
150.00
100.00
50.00
0.00
Difference in head (mm)
0.00
200.00
400.00
600.00
800.00
1000.00
1200.00
1400.00
Length of channel (mm)
Test 23
Test 25
Test 26
Test 29
Test 37

Backward erosion piping test data sheet

Test #	38	$m_s + m_w$ after 'drying'		kg
Date	20-2-14	m/c after 'drying'		-
Soil	SW-SM	V_s	0	m^3
Flume	4	$V_s + V_w$ in flume	0.2171016	m^3
Exit type	circle	void ratio	#DIV/0!	-
seepage length	1.3 m	relative density	#DIV/0!	-
head in bladder tank	5 m	avg. time for 50mL	358	s
bladder pressure	50 kPa	Q when ΔH = ~~0.1m~~ 1861-120 =1.74m	#DIV/0! .08	L/min
compaction	tamper			

time	head (mm)	observation
11.22	0	[45]
11.23	↑ 100	[47]
11.33	↑ 193	[47]
11.43	↑ 240	
11.55		[47]
11.56	↑ 290	
12.19		[50] tiny amount of boiling action
		seen in hole.
12.20	↑ 339	
12.29		[50]
12.30	↑ 386	
12.47		[53]
12.48	↑ 432	
12.59		[54]
1.00	↑ ≒ 475	(behind dip)
1.16		[56]
1.17	↑ 528	
1.46		[60]
1.47	↑ 574	
1.55		[61]
1.57	↑ 622	a plume of fine material became
		suspended above hole (see happy snap)
2.18		Water in box quite turbid. " " "
2.32		[67]
2.33	↑ 668	
2.45		[70]

time	head (cm)	observation
2.46	↑ 714	
2.59		[73]
3:00	↑ 762	
3:05		[74]
3:06	↑ 810	
3:12		[76]
3:13	↑ 856	
3:24		[78]
3:25	↑ 903	
3:30		[81]
3.31	↑ 951	
3:39		[83]
3:40	↑ 1000	
3:52		[86]
3.53	↑ 1044	It's possible I'm looking at the beginnings
		of a channel (about 40mm long) but
		not sure. See happy snap. I can't see
		any particle movement.
4.09		[90]
4.10	↑ 1093	
4.22		[94]
4.23	↑ 1143	I saw many gas bubbles leave the
		hole. This disturbed the fine grains +
		made a dune. So maybe the
		fine particles are being disturbed by
		gas particles as opposed to suffusion.
4.36		[98]
4.37	↑ 1188	
4.41		[100]
4.42	↑ 1235	
4.47		[102]
4.48	↑ 1283	
4.53		[103]
4.54	↑ 1335	
4.58	↑ 1385	(under dip)
5.03		[108]
5.04	↑ 1434	
5.08	↑ 1484	
5.13		[110]
5.14	↑ ~~1~~1582	
5.23		[115]
5.24	↑ 1680	It's now in the d/s valve but not right
		through yet.
5.33		[119]
5.34	↑ 1775	
5.47		[120]
5.51	↑ 1861	
6.06		Q = 36.5, 34.9, 35.9 [120]

time	head (cm)	observation
6.07	↑ 1865	and not many any higher (the highest it can go.
21-2 10:00		Was left at 1865mm overnight (which I confirmed by looking up-inside is the highest it can go). ~~#~~ There is considerably more boiling action in the hole (see happy snap) which is up level with the lid. But I don't think there's a channel. I can't clearly see because, whilst most of suspended material has settled overnight and the water is clearer, the material settled on the lid so I can't see through it. I've cleared a 'peep-hole' through the settled material but don't want to disturb it too much in case the water goes more murky again.
		The boiling action in the hole looks similar to the Syd sand just before initiation so I think it's close to initiating but that's really only a hunch. In short, I don't have enough head to make this BE.
		I'll leave head at this height until sponsors meeting but I'll have to turn water off so I can run other experiments. I'll need to turn it's back on every now-and-again to top it back up to its ~~its~~ current level.

Test 38

time	head (cm)	observation

38. Test 38 (flume 4) circle

Test 38 was the 1st test in SW-SM soil.

When compacting the soil in (with the tamper) some segregation was observed in the top layer. It is thought this is the case because the last soil to be placed was the last left in the soil mixer which was such a thin layer that it sat underneath the mixing paddles and so didn't contain all the coarser grains. So next time I'll have to ensure we have enough soil left over that we're not taking from the bottom of the mixer. Pic:

Also the fine 300g material did become air borne when we tamped so particulate respirator is necessary as well as not letting anyone without a respirator into lab 2 at the time. Pic:

I note that whilst CO2ing the pressure in the u/s chamber was between 1.5 to 2 PSI.

When filling with water I had the constant head tank at datum but it was taking too long for the level in d/s box to reach the d/s outlet. So I had to start the test with the level in the box not up to the d/s valve. This meant that with every constant head tank adjustment I had to also read the level in the d/s box and subtract the 2 to get the total difference in head. The level in the d/s box reached the d/s valve once the level in the constant head tank was 1.68m.

Also during water infilling I noticed many gas bubbles under the lid. It took longer for these gas bubbles to dissolve than it did in the Sydney sand. When I started the test it looked like this (bubbles u/s of the circle had dissolved but bubbles d/s of the circle had not):

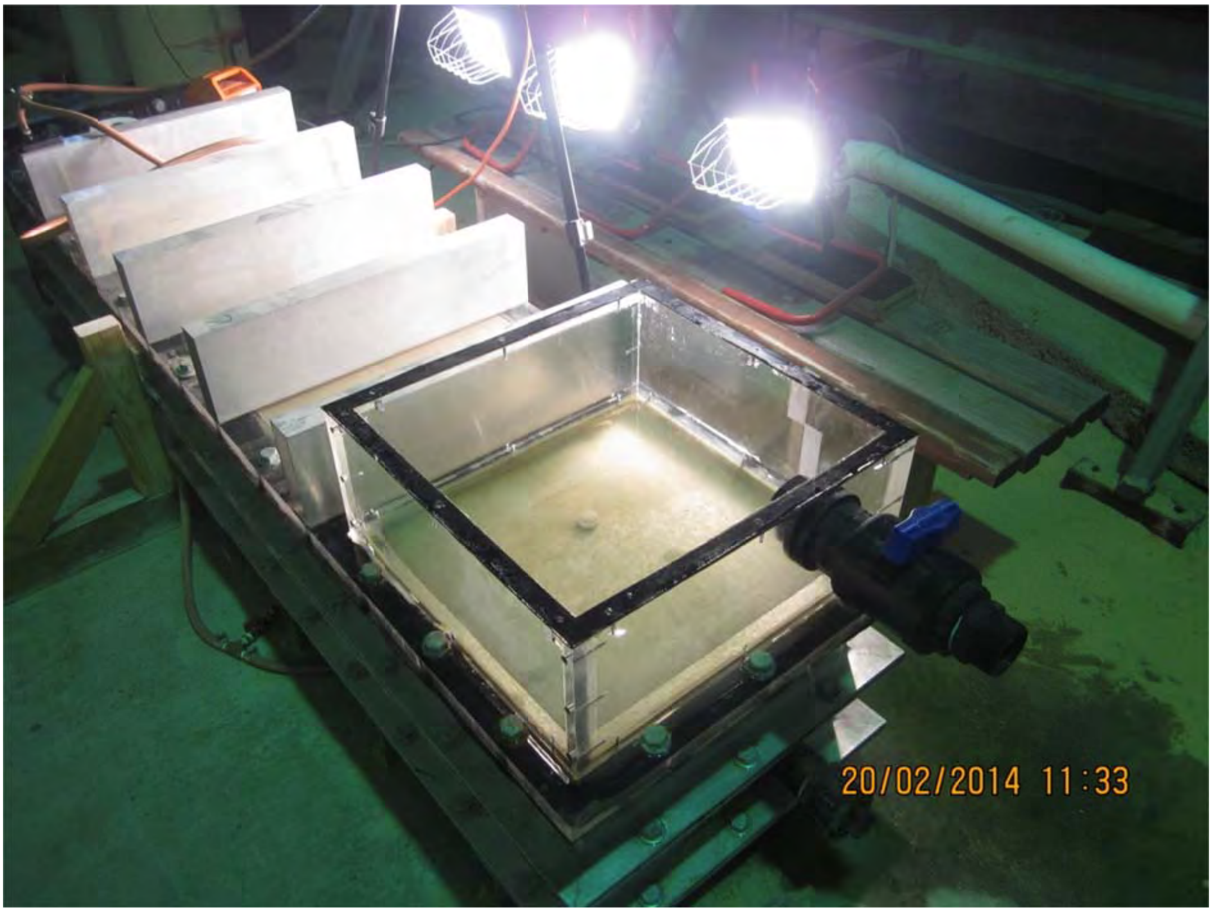
20/02/2014 11:33

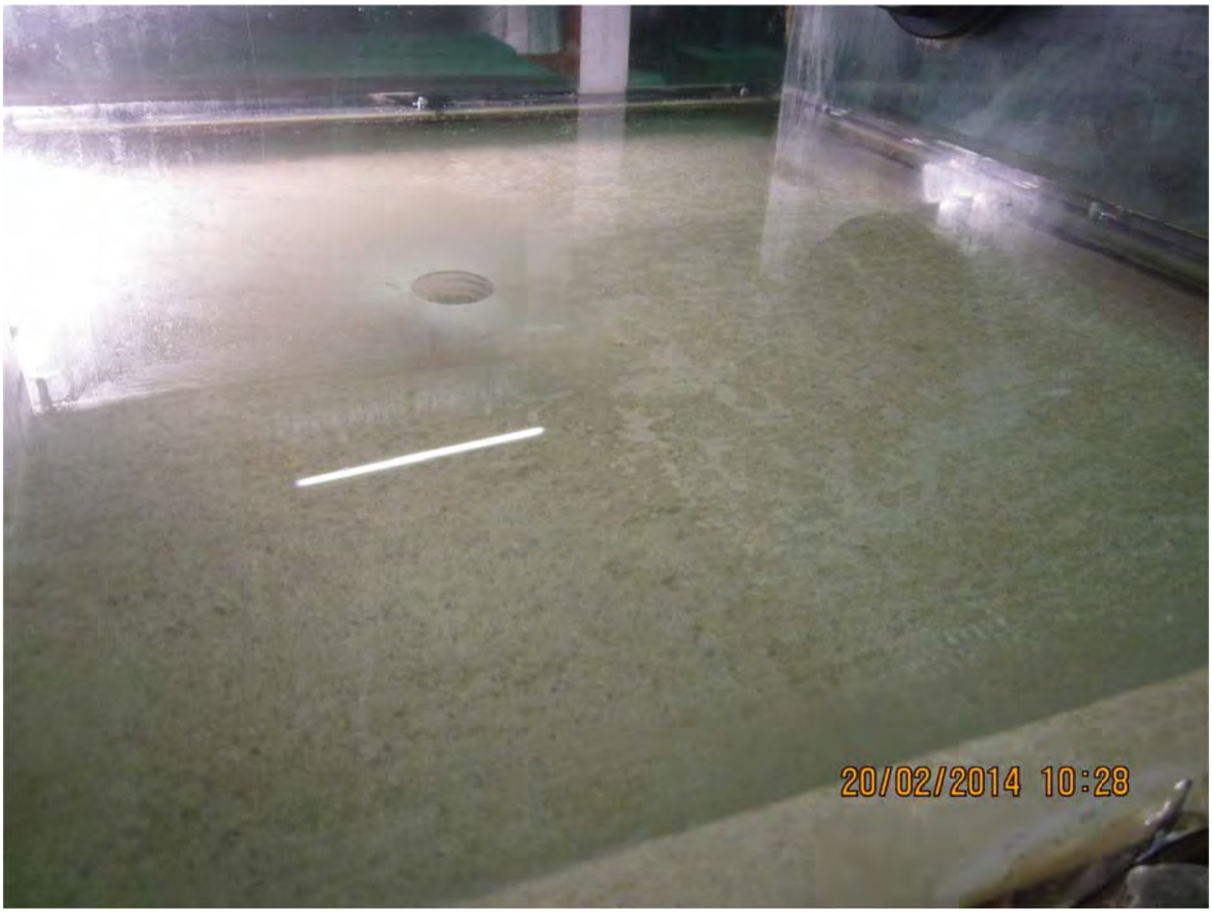
20/02/2014 10:28

During both infilling and the test the water in the d/s box became cloudy. Fine particles were becoming suspended in the water. It's not clear if this was due to erosion of the fine particles or just the fine particles on the top of the soils surface (at the circle) were becoming disturbed when gas bubbles escaped from d/s of the circle (which I did see happen). My theory is the later. The fine particles would settle overnight. Pics:

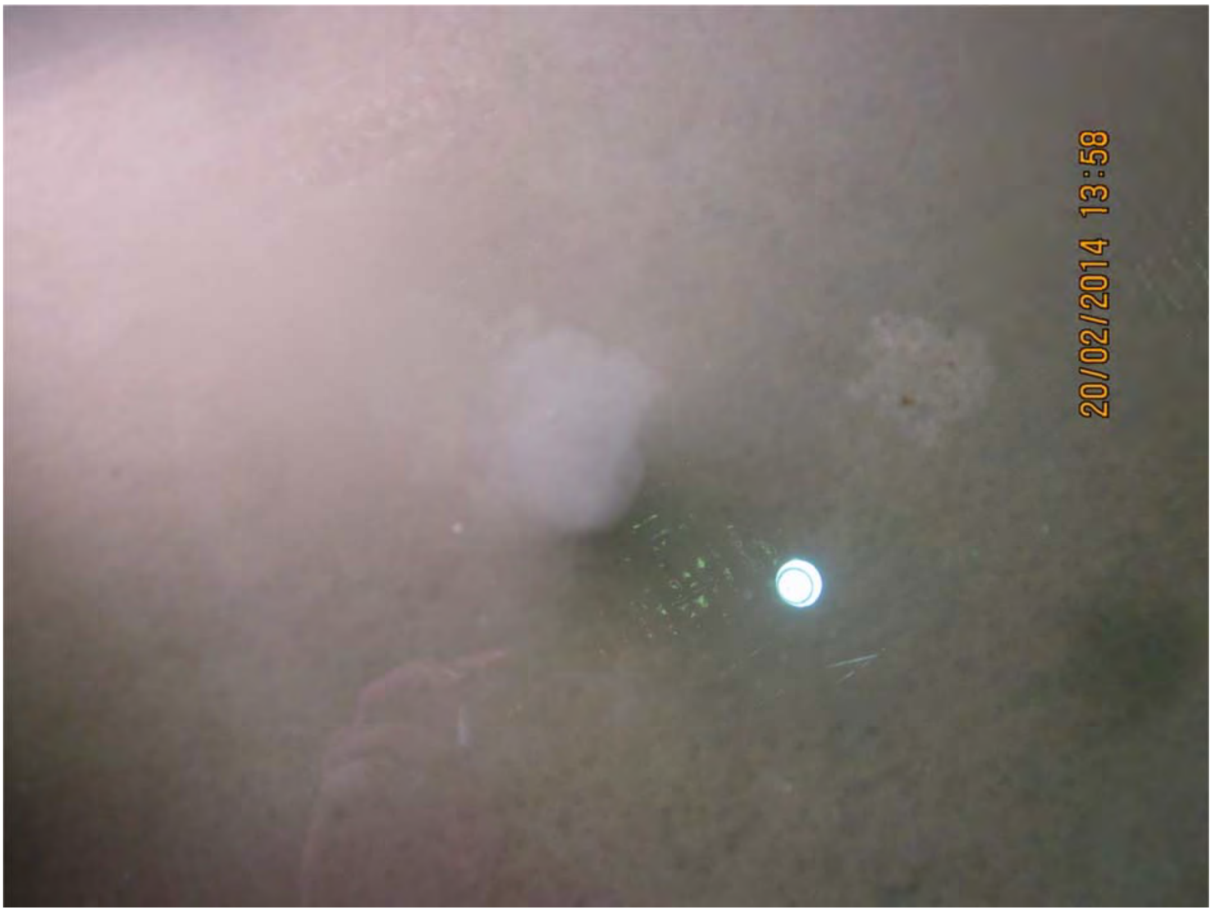

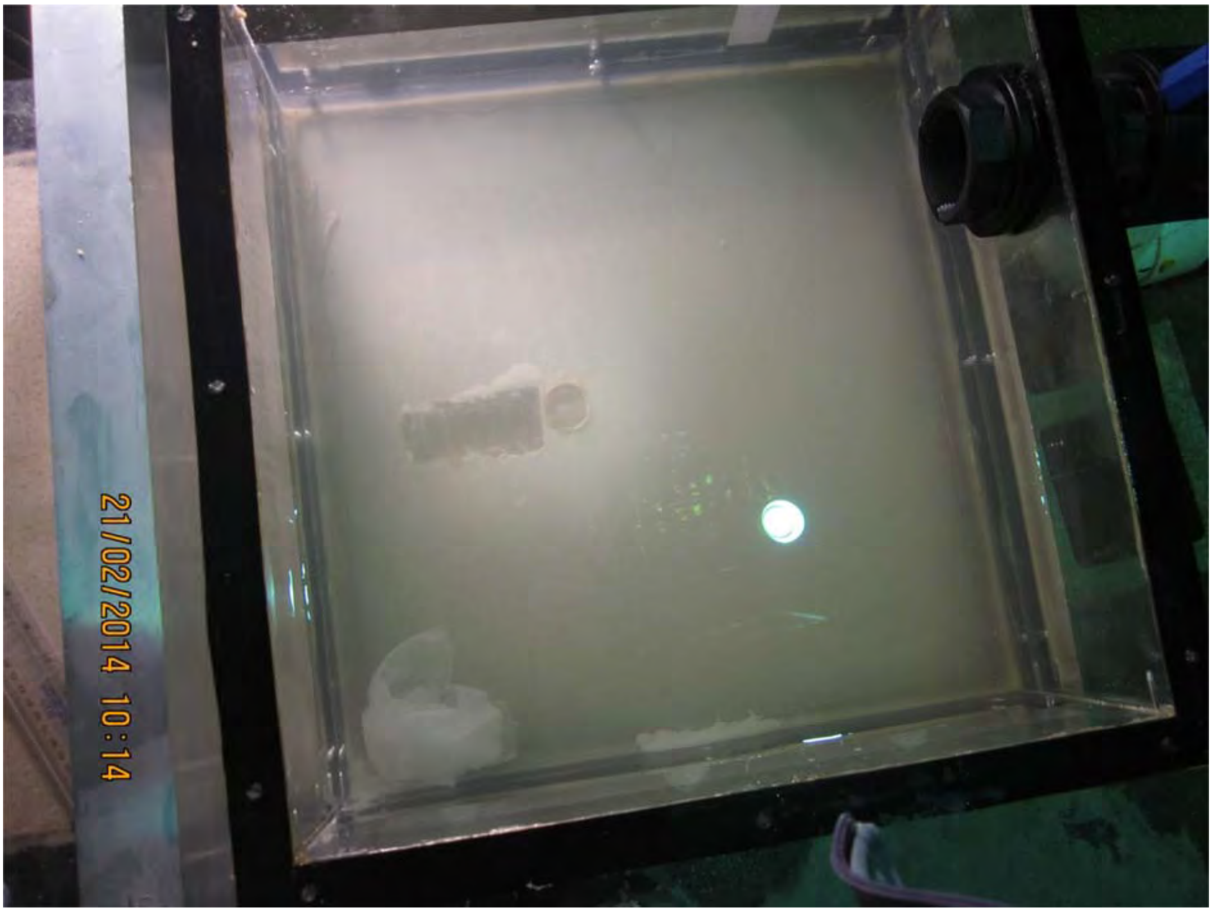

I had cleared the rectangle-shape in the settled material with the end of a ruler so I could see through the lid (to see if a channel had developed).

When the head was 290mm I started to see very small boiling action. When I had reached the maximum head possible, 1.865m, the boiling action looked similar what the boiling action in the syd sand looked like just before initiation. However backward erosion did not start. I suspect I shouldn't need to increase too much more before backward erosion would start, but I can't be sure (it's just a hunch).

In short, I need a greater gradient to initiate backward erosion in this soil.


ΔH = 1.87m
24/02/2014 18:05

Backward erosion piping test data sheet

Test #	39	$m_s + m_w$ after 'drying'		kg
Date	24-2-14	m/c after 'drying'		-
Soil	Sydney sand	V_s	0	m^3
Flume	3	$V_s + V_w$ in flume	0.2065095	m^3
Exit type	slope	void ratio	#DIV/0!	-
seepage length	1.3 m	relative density	#DIV/0!	-
head in bladder tank	~~5~~ m	avg. time for 50mL		s
bladder pressure	~~50~~ kPa	Q when ΔH = 0.1m	#DIV/0!	L/min
compaction	vibrator			

time	head (mm)	observation
6	0	
6.01	↑105	
6.02		reduced bladder pressure to 2.5
6.10	↑207	
6.19		a channel started but didn't
		start at the exit (see floppy
		snap).
6.20	↑236	
6.23		the channel grew (now 120-40mm) but
		is about 20-30mm away from the exit.
6.24	↑250	
6.26		the channel now 130-10mm) but still
		about 30mm from the exit. I'm going to
		stick a rod in there and clear btw the
		exit + the channel for the sake of
		demonstration at the sponsors
		meeting tmw.
6.30		I unblocked it and it's off.
6.40		40mm a.d.l
6.41	↓150	
6.43		50mm a.d.l
2.30	↑250	*
2.36		tip started to move again
2.40	↑265	

Test 39

9995 6822 Wendy

	time	head (cm)	observation
	2:48		150 ab1
	2:54	↓ 161	
	2:55	161	25 ab2
26/2	10:50	↑	
	10:57	↑ 248	29 ab2
	11:04		95 ab2
	11:06		105 ab2
	11:11		142 ab2
Point 2	11:26	↓ 240	~~ab3~~ 2 ab3
	11:27		12 ab3
	11:29		22 ab3
	11:34		55 ab3
	11:37		85 ab3
P3	11:40	↓ 227	120 ab3
	11:42		150 ab3
	11:44		175 ab3
P4	11:45	↓ 215	
	11:50		tip moving very slowly
	11:51		183 ab3
	11:55		188 ab3
	11:58		197 ab3
	12:01	↓	215 ab3
15min still moving →	12:02	↓ 202	220 ab3
	12:08		224 ab3
P5 →	12:15	↓ 190	242 ab3
	12:19	↑ 194	No tip progression after 4min ∴ ↑ by 1/8 turn.
	~~12:24~~		
	12:24	↑ 199	~~No tip~~ " "
	12:28		245 ab3
	12:32	↑ 200	No tip progression. Increase to 202 head
	12:34	↑ 202	" "
	12:39	↑ 205	" "
	12:45		~~———~~ Very slow tip progression
Last	12:56		45 ab4
P6	12:56	↓ 196	70 ab4
	12:58	↓ 183	92 ab4 Rapidly advancing tip ∴ ↓ by 1/4
P7 →	12:59	↓ 171	
	1:00		115ab4 – channel blocked itself at about 200 ab3
	~~1:06~~		~~No tip~~ see happy snap ☺
	1:06	↑ 176	No tip Movement ∴ ↑
	1:10	↑ 182	" "
	1:14	↑ 188	" "
	1:18		Very little tip progression. Still blocked at 200 ab3
& deepening	1:20	↑ 194	No tip movement ∴ ↑
			starting to unblock
	1:27	↑ 200	Very slow. ∴ ↑
	1:34		Unblocking. Tip progressed faster when unblocked/ing
	1:42	↑ 202	Reblocked. Tip not progressing

Test 39

time	head (cm)	observation
1:55	↓ 171	
27-2	9.40	the widening + deepening process hasn't moved since about 1pm yesterday (it's about 70mm before 104). So gonna revise head a little.
9.41	~~[illegible]~~ ↑ 176	
10.09	↑ 185	
10.45	↑ 210	

21×7
0.42
0.39

20.6 20.67 20.9 41.75 41.83

42.98 43-40.83 20.92-20.5 0.72-0.33

time	head (cm)	observation

39. Test 39 (flume 3) slope

Test 39 was the 4th test with a slope exit and the first test with a bladder pressure not equal to 5m.

I intended to fill the bladder tank to 2.5m to test the effect of bladder pressure but I accidently filled it to 5m out of habit. So before the test started I lowered the bladder tank level to 2.5m however this isn't ideal because the void ratio would be equivalent to 5m and when I lowered the tank to 2.5m the flume was already saturated so it's unlikely the void ratio would have increased (probably can consider it an undrained scenario so volume change is unlikely).

The channel initiated at 207mm but it started 20 to 30mm upstream of the exit:

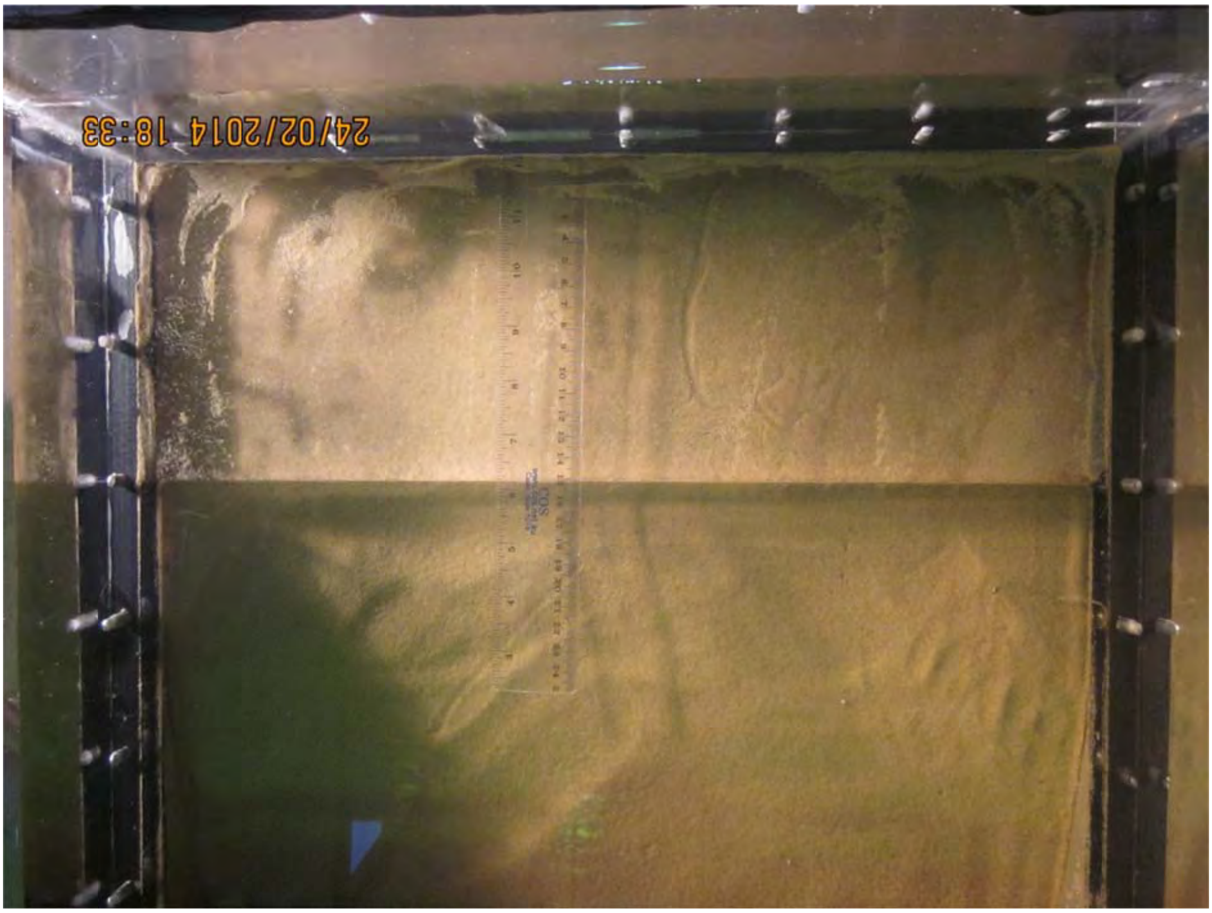

Normally I would have continued to increase the head until the channel reached the exit but this test was going to be on display for the sponsors the next day so I extended the channel to the exit with the dowel:

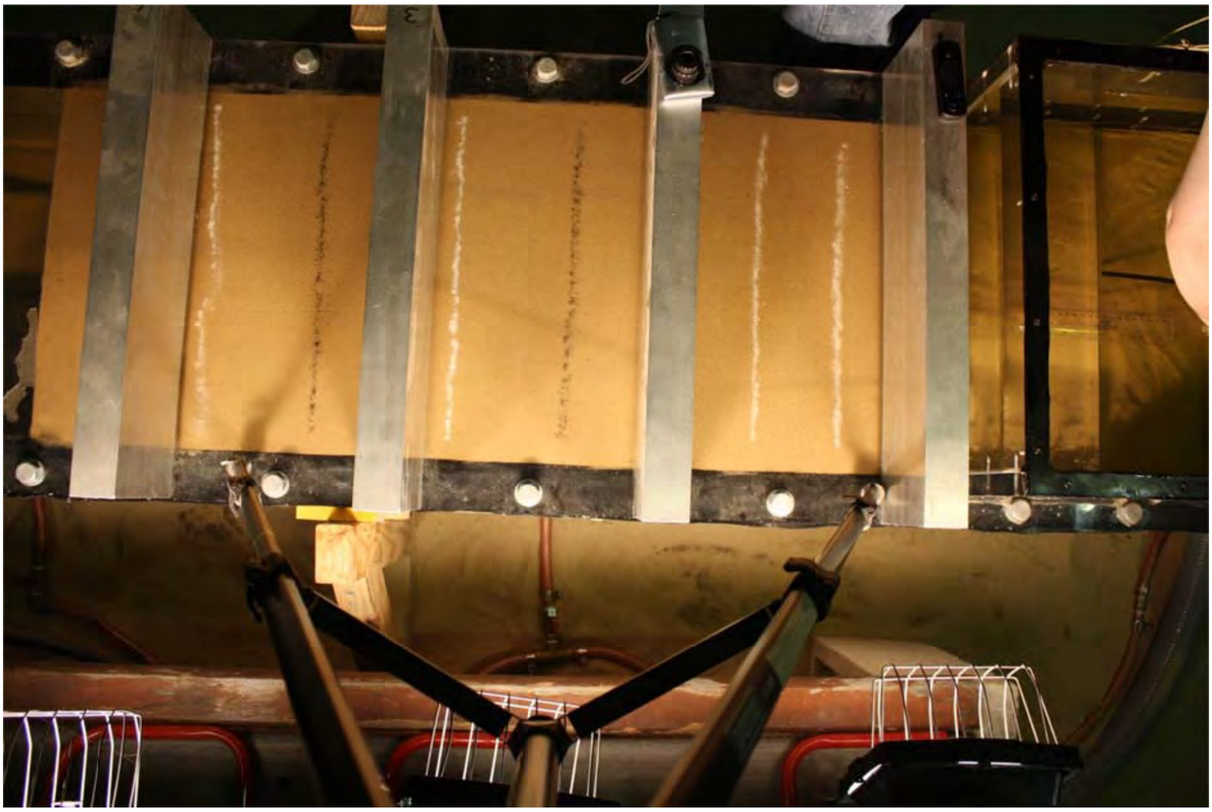

Once I had opened the channel to the exit it was off (at this point the head had been increased to 250mm).

The tip progressed at approx. speeds of 12, 11, 19, 2 and 8 mm/min (in that order). It took 3 hours from initiation to u/s. But this 3 hours was spread out over 3 days because the test was setup to show the sponsors (and the test finished the day after the sponsors meeting). I didn't record when it failed (and photos had stopped being taken) but I did watch it fail. It wasn't as obvious a failure as past tests because the flow was so small (small because filter quite clogged). I note that I had to increase the head to 210mm for the forward deepening process to continue. I don't know why this was and I think it's the first time an increase in head for failure to occur was necessary.

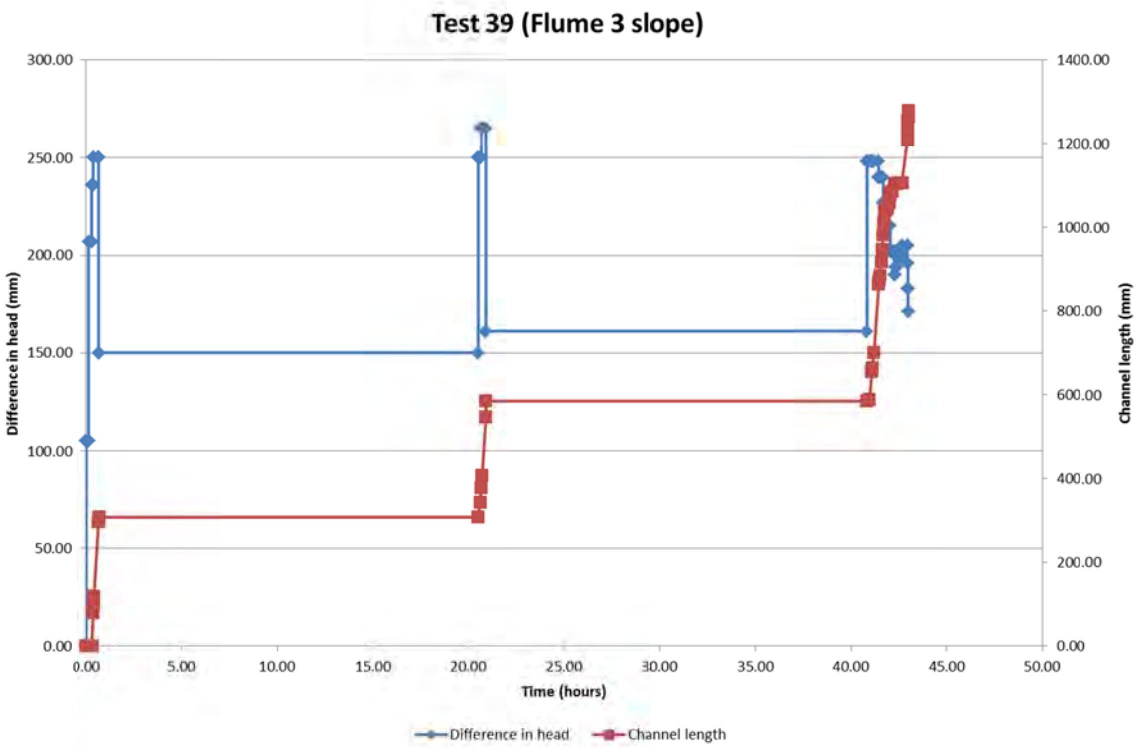

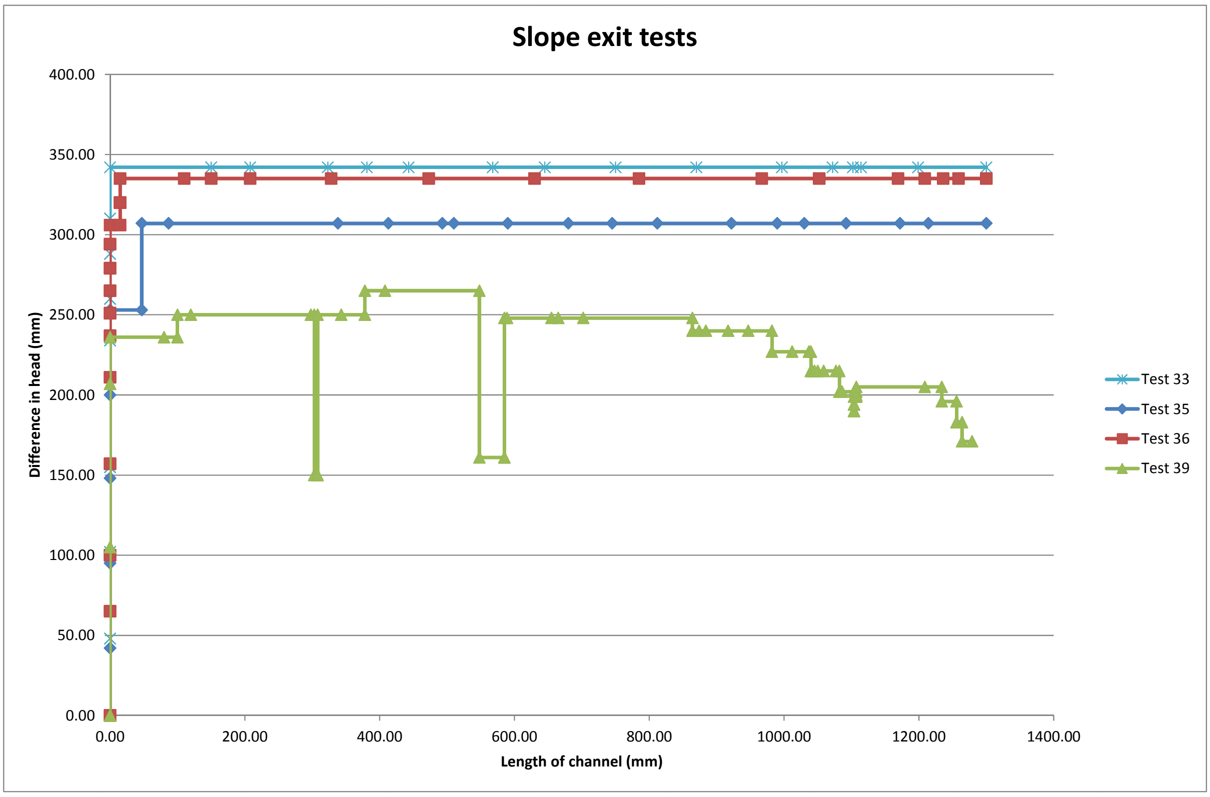

I note that test 39 has a lower crit grad than the rest of the slope tests. Perhaps this is the effect of the lower bladder pressure.

And the decreasing head pattern looks like this:

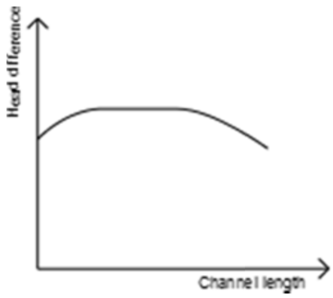

Also note this was the 2nd test (I did test 40 before I did test 39) I tried lots of different light particles. The white VTACL particles worked the best. I saw some of them float to the top of the water in the d/s tank which proves to me that they're at/less the density of water. They moved quickly through the channels and showed well in photos. Pic:

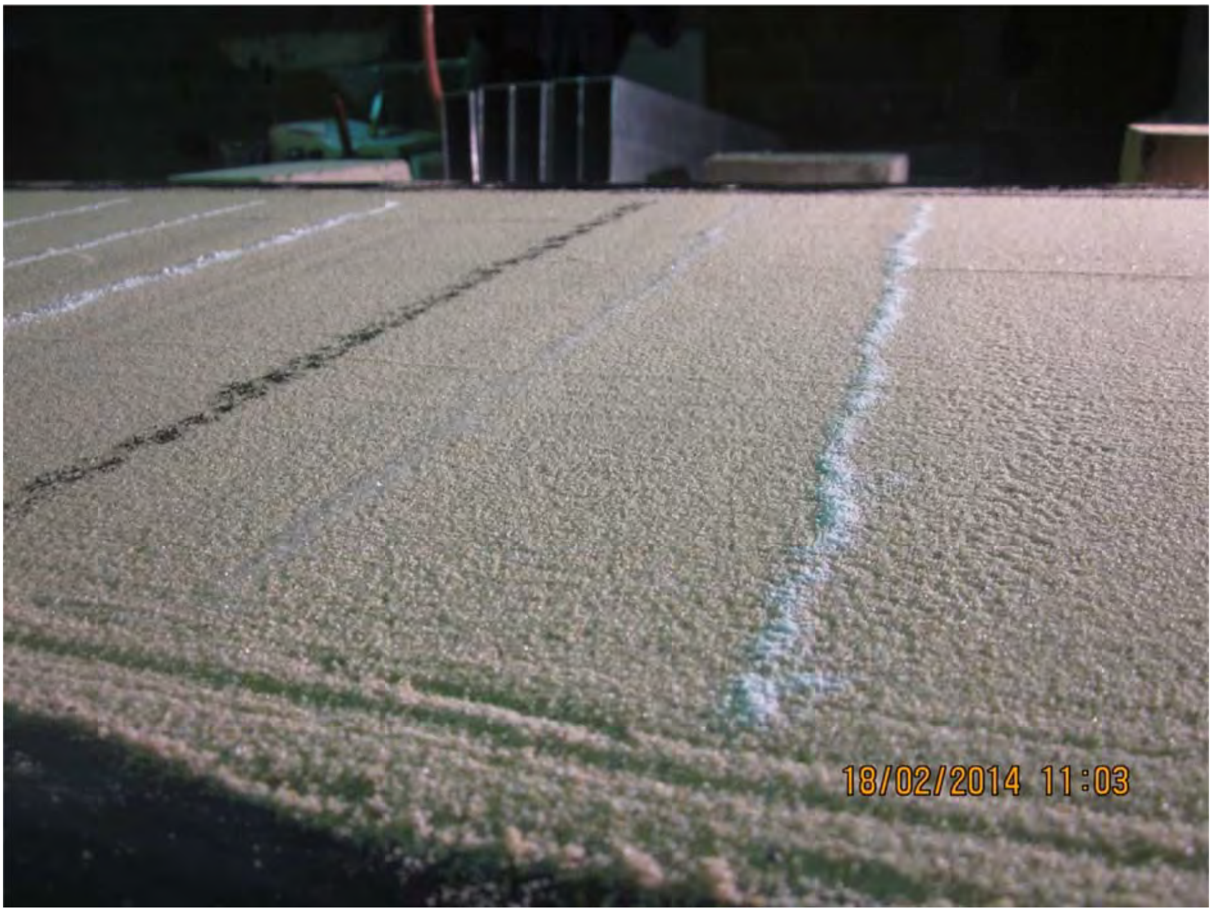

Backward erosion piping test data sheet

Test #	40	$m_s + m_w$ after 'drying'		kg
Date	21-2-14	m/c after 'drying'		-
Soil	Sydney sand	V_s	0	m^3
Flume	1	$V_s + V_w$ in flume	0.2171016	m^3
Exit type	slot	void ratio	#DIV/0!	-
seepage length	1.3 m	relative density	#DIV/0!	-
head in bladder tank	2.5 m	avg. time for 50mL	12.875	s
bladder pressure	25 kPa	Q when ΔH = 0.1m	#DIV/0! 0.23	L/min
compaction	vibrator			

time	head (mm)	observation
11.41	0	
11.42	↑ 100	Q= 14, 12.6, 14.1, 10.8 s
12.06	↑ 140	
12.11	↑ 166	
12.19	↑ 193	
12.26		possible start of a channel but
		tiny (see happy snap) (a)
12.27	↑ 207	
12.44	↑ 221	initiation in middle of slot (b)
12.47		140-110 (b)
12.56		no particle movement for 3min
12.57	↑ 227	" " " still 140-110. (b)
1.01	↑ 234	(b)
1.20		still 140-110 (b)
1.21	↑ 240	" " " (b)
1.32	↑ 247	(a) moved a little, now 130-110.
1.39		(a) 130-110 (b) 140-110
1.53	↑ 256	" "
1.57	↑ 260	" "
2.03	↑ 268	" "
2.08	↑ 273	" "
2.16		new channel (c) reached bl.
2.24		85 abl
2.28		210 abl
2.29	↓? 1/8 turn	
2.33		other side of bl

Test 40

time	head (cm)	observation
2.37		80 ab2
2.38	↓ 260	
2.47		175 ab2
2.48	↓ 254	
2.51		at b3
2.53		23 ab3
2.54	↓ 248	
2.56		28 ab3
3.01		90 ab3
3.03		130 ab3
3.04	↓ 240	
3.09		140 ab3
3.14		140 ab3
3.20		140 ab3 but it's moving laterally (see
		happy snap).
3.24		~~140 ab3~~ 140
3.25		190 ab3
3.25	↓ 235	b4
3.27	↓ 223	45 ab4
3.27		100 ab4
		a blockage under b4
3.30		I don't think im going to see the tip
		grow anymore than 100 ab4 cause
		theres a slight dropoff to the u/s
		panel (see happy snap)
		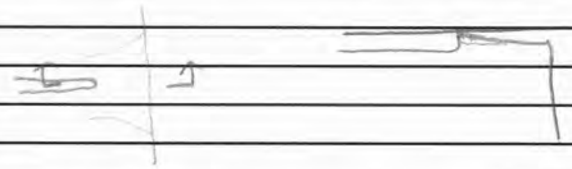
		leaving test running to see how long
		it'll take to fail at 221.
5.04		water flow increased.
5.10		failed.

2.95

3.12

3.22

150mm / 2min

40. Test 40 (flume 1) slot

Test 40 was the 7th test with a slot exit and the 2nd test with a bladder pressure < 5m.

I intended to fill the bladder tank to 2.5m to test the effect of bladder pressure but I accidently filled it to 5m out of habit. So before the test started I lowered the bladder tank level to 2.5m however this isn't ideal because the void ratio would be equivalent to 5m and when I lowered the tank to 2.5m the flume was already saturated so it's unlikely the void ratio would have increased (probably can consider it an undrained scenario so volume change is unlikely).

The channel initiated at 221mm at centre of slot. 8 increases in head were required to reach critical of 273mm.

The tip progressed at approximately 17mm/min until it took a 90degree turn (red line flattens but tip didn't stop, it just moved laterally). Eventually the channel branched so it went back on its previous trajectory and progressed to the u/s end quite quickly (about 75mm/min). Pic shortly after it branched back to towards u/s:

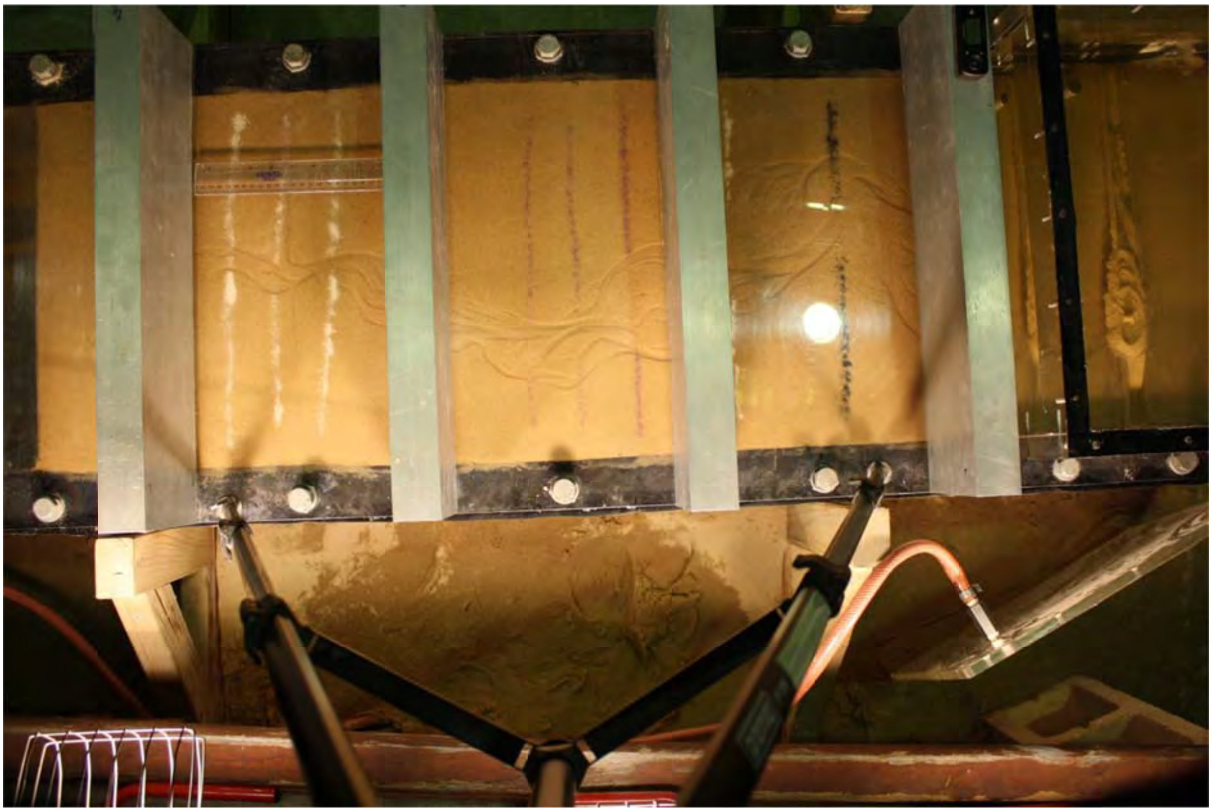

It took about 2.7 hours from initiation to u/s and 1.7 hours from u/s to failure.

Almost immediately after the tip reached the u/s end Blockages occurred but unblocked themselves in time.

I noticed the water flow increased shortly (minute or 2) before it failed.

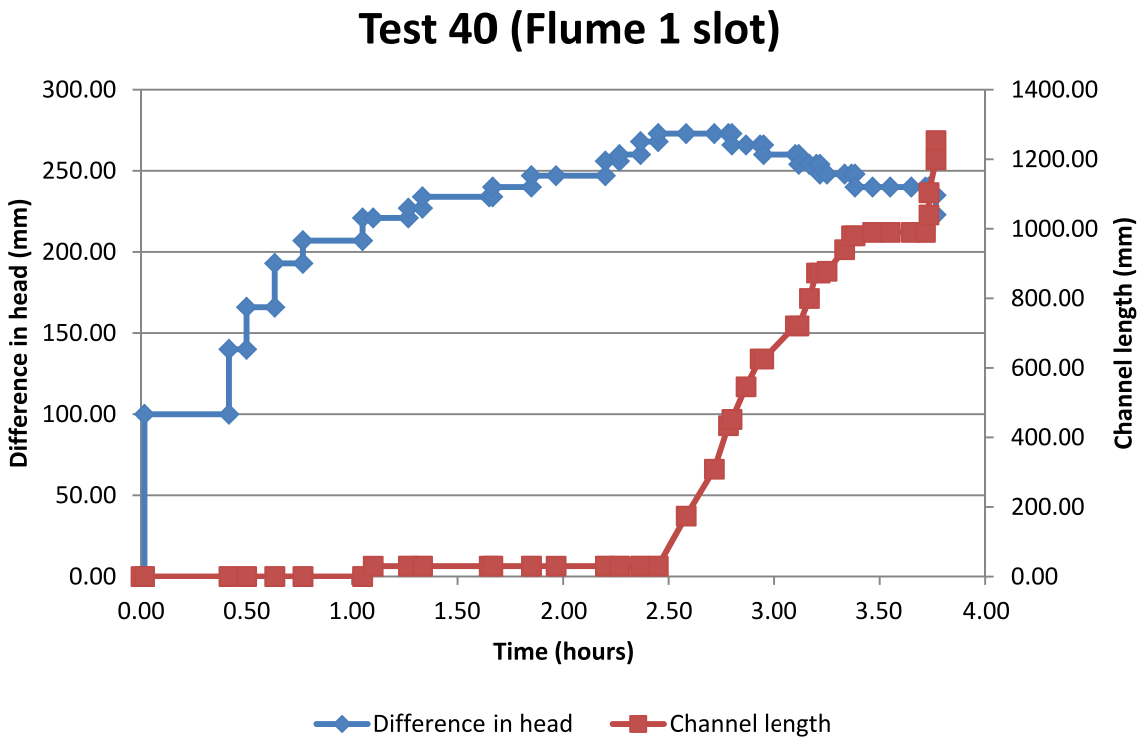

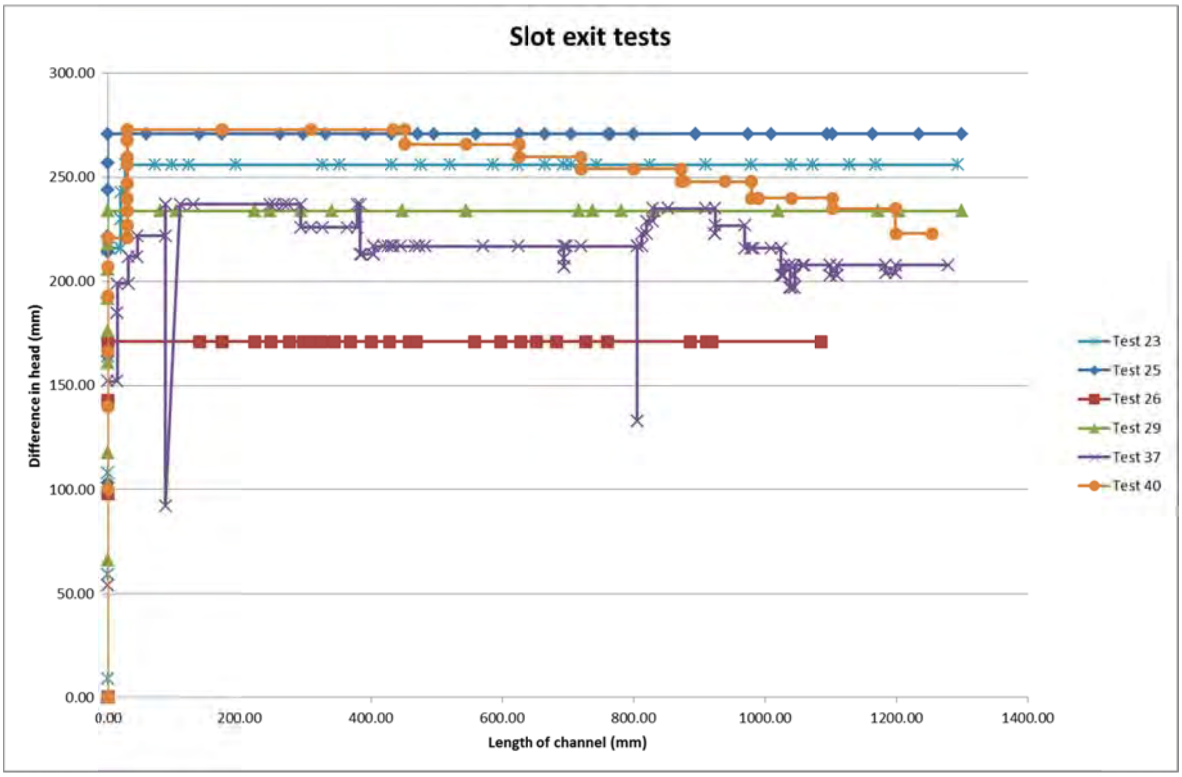

The reduced bladder pressure didn't appear to have any affect.

13-3-13 12.05 inflate bladders
17-3-13 11.45 CO2 on
5.00 CO2 off

Backward erosion piping test data sheet

Test #	41	$m_s + m_w$ after 'drying'		kg
Date	18-3-14	m/c after 'drying'		-
Soil	Sydney sand	V_s	0	m^3
Flume	~~3~~ 1+2	$V_s + V_w$ in flume	0.2171016	m^3
Exit type	~~plane~~ slot	void ratio	#DIV/0!	-
seepage length	2.6 ~~1.3~~ m	relative density	#DIV/0!	-
head in bladder tank	5 ~~2.5~~ m	avg. time for 50mL	24.6	s
bladder pressure	50 ~~25~~ kPa	Q when ΔH = 0.1m	#DIV/0!	L/min
compaction	vibrator		0.12	

time	head (mm)	observation
2.29	23	there are still some gas bubbles but
		not many (see happy snap). I'm going
		to run exp anyway (and hope they
		don't interfere).
2.32	↑ 100	Q = 29.5, 23, 25.7, 23.8, 21 for 50mL
2.55	↑ 154	
3.01	↑ 221	standpipe = 177mm
3.07	↑ 270	
3.10		SP 206
3.12		initiation first noticed @ ≈15mm long and
		roughly in middle of slot (see happy
		snap)
3.18		still 15mm long
3.19	↑ 299	
3.20		tip 145-110.
3.43		145-110
3.44	↑ 319	
3.51		145-110
3.51	↑ 346	165-110
4.00		165-110
4.01	↑ 372	
4.02		165-110
4.21		165-110
4.22	↑ 396	
4.38		SP 313
4.39		165-110

time	head (cm)	observation
4:45		the tip is growing laterally (see
		happy snap)
4:46	↓290	
19-3		
10.02	286	165-110 (see happy snap), SP230.
10.04	↑ 332	no movement
10.09	↑382	
10.11		noticed a new channel (2) right near RHS edge (see
		happy snap). It's about 150-110. It's
		showing boiling action there as the first
		channel isn't.
10.14		SP 298
10.26		both channels haven't moved.
10.27	↑ 406	
10.29		175-110 (1)
10.33		195-110 (1)
10.40		195-110 (1)
10.53		195-110 (1)
10.54	↑ 433	
10.55		215-111 (1) and other channel (2)=180-111
10.58		(1) 240-111 and (2) 195-111
11.12		I think it's still under the box wall
11.18		It looks like (2) is still moving but I
		can't clearly see where it's up to.
		It might also be under tank wall.
11.30		tips still under tank wall (I think)
11.31	↑ 446	
11.50		tips haven't moved.
11.51	↑ 461	
11.52		(1) tip now other side of tank wall
12.53		(1) at b2 (2) I can't see it so maybe it
		stayed under the tank wall
1.33		40 ab2
1.40		70 ab2
1.41	↓ 452	
1.57		130 ab2
1.58	↓ 433	
2.03		180 ab2
2.04	↓ 425	
2.18		240 ab2
2.19	↓ 411	
2.31		under b3
2.47		35 ab3
2.48	↓ 398	
3.11		190 ab3
3.12	↓ 386	
3.19		220 ab3

Test 41

time	head (~~cm~~ m)	observation
3.22	↓ 373	
3.27		250 ab3
3.28	↓ 361	
3.38		under b4
3.55	↓ 310	" "
5.23		" "
20-3		
9.39	↑ 353	still under b4.
9.57	↑ 376	" " "
10.06		" " "
10.18		20 ab4
10.30	↓ 367	85 ab4
10.35	↓ 355	120 ab4
10.51		130 ab4
10.59		130 ab4
11.21	↑ 361	130 ab4
11.31		130 ab4
11.46	↑ 363	135 ab4
11.54		channel is blocked btw b1+2. 135 ab4
12.16		135 ab4 still blocked.
1.07	↑ 390	135 ab4
1.54	↑ 417	140 ab4
2.08	↓ 407	183 ab4 (so it's moving again even though it's
		still blocked)
2.25	↑ 417	183 ab4 (still blocked)
2.42		205 ab4 SP306
2.51		205 ab4
3.14	↑ 426	" "
3.36	↑	210 ab4
~~3~~ 3.58		235 ab4
4.10		" "
4.15	↓ 331	" "
21-3		
10.12	↑ 376	235 ab4.
10.20	↑ 400	235 ab4
10.32	↑ 427	" "
10.49	↑ 455	" "
10.58		" "
11.04		first noticed a new tip. It's at b2 and
		bypasses the blocked region (see happy
		snap). Calling new tip tip (3).
11.19		(3) under b2
11.49		(3) 63 ab2
12.20		tip (3) had joined channel (1) at 180 ab2
		but then blocked itself
12.22		(1) 250 ab4. SP325.
2.01		(~~1~~) 65 ab5

time	head (cm)	observation
3.06	↑ 481	65ab5
3.32		tip under join. Blocked btw bars 2 to 5
3.52		SP343
4.18		tip still under join.
		Trying to decide what to do over
		weekend. Do I leave it @ 481 or
		bring it down? I'd like to see if
		it could unblock itself but if it
		does it means I could miss
		the rest of the test. But maybe
		it's more important to know
		whether a tork could unblock
		itself? Ok im gonna leave it + take
		photos every hour.
4.36		It's now only blocked btw bars 4+5
		(it's unblocked btw 1 and 4).
24-3		
9.36	480	tip still at join. Blocked btw bars 2+4
		and 5+6. SP 340.
9.51	↑ 501	
9.55	↓ 65	Pump stopped because water in pit low.
		So topped up.
10.12	↑ 501	still under join
10.51	↑ 527	" " "
11.25	"	SP372. Still under join.
11.26	↑ 551	
11.27		blockages have mostly opened.
11.43		blocked in sections again.
12.01	↑ 572	under join
12.24	↑ 600	" "
12.31	↓ 579	100 aj
12.37	↓ 530	10 ab7
12.44	↓ 480	98 ab7
12.50		115 ab7
12.57		115 ab7
1.01	↓ 431	213 ab7
1.10		223 ab7
1.16		223 ab7
1.33	↑ 454	222 ab7
1.38		243 ab7
1.53		243 ab7
2.23		251 ab7
2.51	↓ 431	23 ab8
3.10		23 ab8
3.27		23 ab8
3.40	↑ 445	" "
3.44		" "
3.55		" "

Test ~~40~~ 41

time	head (cm)	observation
4.07		23 ab8
4.15	↑ 452	" "
4.19		" "
4.35	↑ 461	" "
4.52		" "
4.56	↑ 470	" "
5.02		100 ab8 (reached u/s end)
25-3		
9.51		the deepening process is only 40mm
		long. The channel is btw bar 5 and ~~[illegible]~~
		u/s. see happy snap. there has been
		a new channel form overnight towards
		the CHS (see happy snap). It's tip is
		at the pin.
26-3		
9.39		no different from how it was yesterday.
		It's hard to imagine it failing at
		this head. I'm going to have to
		check for failing on at least one
		doubled flume but for now I'm
		going to end the test so I can
		go onto another.

41. Test 41 (flume 1&2) slot

Test 41 was the 8th test with a slot exit and the 1st test with seepage length >1.3m. L = 2.6m. This is also the first test I had a tenseometer installed and the first test I used chlorinated tap water.

The channel initiated at 270mm at centre of slot.

A second channel was noticed along RHS edge but didn't progress further than the box wall.

5 increases in head were required to reach "critical" of 461mm. I say "critical" because it was not the maximum head required to progress the tip. The maximum head required was 600mm when the tip was at the flume join. I wonder if perhaps this is an artefact(?) Maybe there is more area at the join because the rubber doesn't go all the way down to the sand and because there's more area the seepage speeds are lower here(?)

When the tip was progressing it did so at approximately 5 to 10 mm/min.

The channel blocked for the first time when the channel was 1270mm long. This is near the length of the single flume and I've noticed with the single length flumes the channels often blocked soon after the tip reached the u/s end. So perhaps there's something critical about this length of channel that causes it to block.

With increases in head the tip progressed despite the blockage. Later a new channel formed which went around the blockage and joined up with the original channel. However soon after joining up with the original channel it blocked again. The channel would be in a cycle of blocking and unblocking (often in sections).

The test was completed over 5 days. Overnight (or over the weekend) the head would be significantly reduced and the tip would stay stationary until the head was increased again.

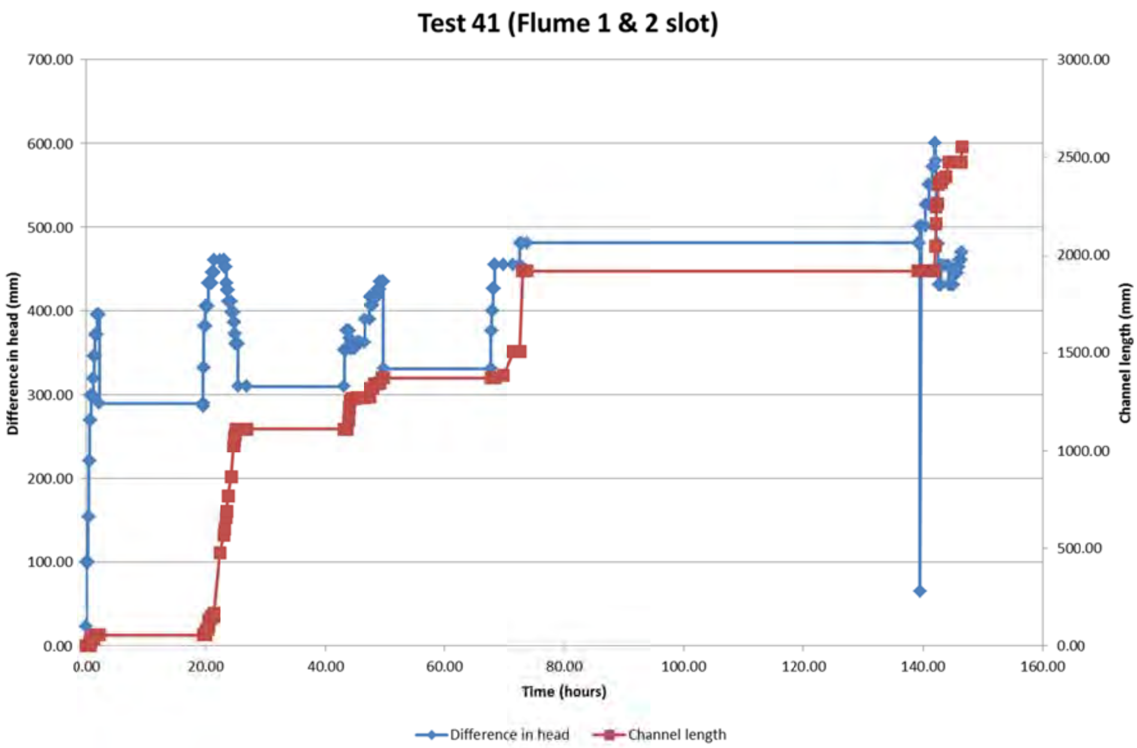

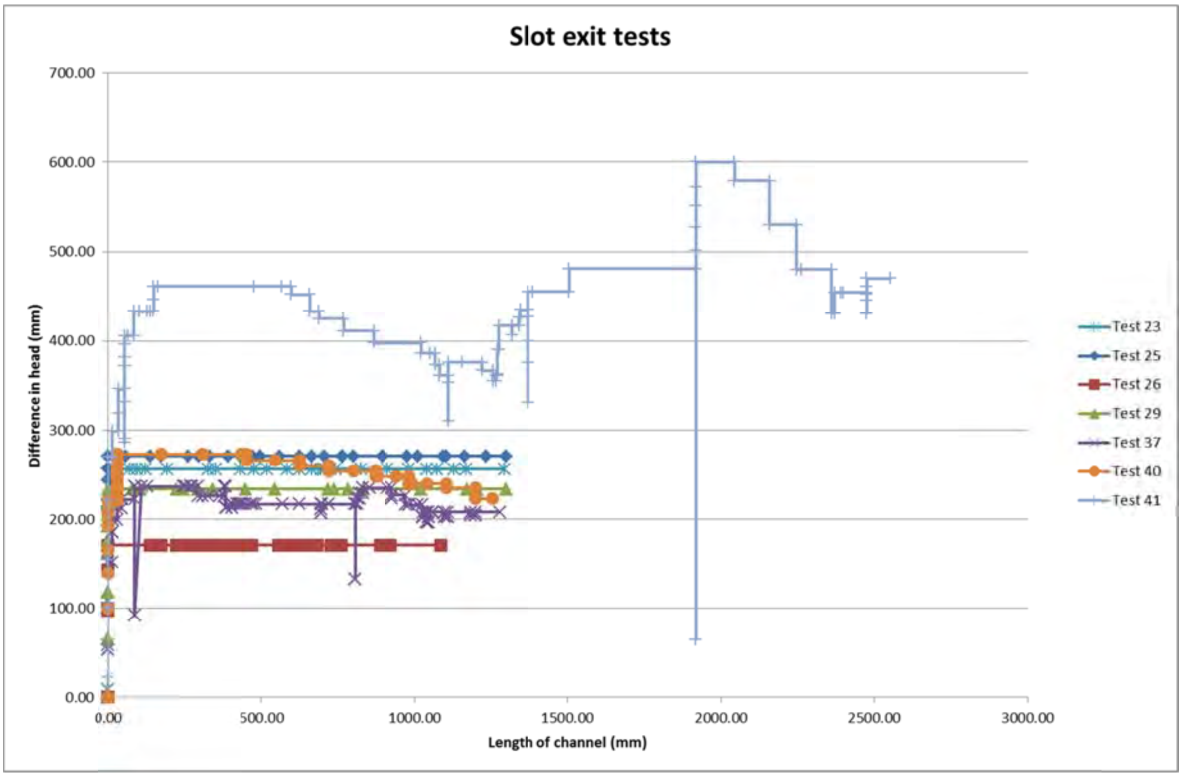

I expected the initiation and critical heads to be twice that of the single-flume results (because the seepage length is twice as long so needs twice as high a head to produce the same gradient). For the single-flumed tests the initiation head was between 200 and 270mm. For this test the initiation head was 270mm so my expectation was thwarted here. Perhaps this is because similar seepage velocities still occur at the exit regardless of the seepage length. As for the critical head- if I take it to be around 460mm (and given critical heads were around 220-260 for single-flume tests which when doubled is 440-520) then it was what I expected- double the single-flume. However it's difficult to interpret a critical head because a) the head required dropped between about 600 and 1300mm and b) the head required increasing at the join. I don't know why the head required dropped between about 600 and 1300mm and as for why the head required increasing at the join, as I mentioned before, maybe there is more area at the join because the rubber doesn't go all the way down to the sand and because there's more area the seepage speeds are lower here.

The large drop of head near the 1900mm mark was because the water level in the pit dropped too far and the pump stopped, so I had to top up the pit.

I didn't notice any bio clogging in this experiment; even though it ran over 9 days so I think using chlorinated tap water worked.

After the tip reached the u/s end I left it running for 2 more days. The deepening process was only 40mm long. Most of the channel was blocked. A new channel did form but its tip stopped at the join.

27-3 11:20 CO_2 on
" 5:20 CO_2 off
" 5:40 water on

Backward erosion piping test data sheet

Test #	42		$m_s + m_w$ after 'drying'		kg
Date	28-03		m/c after 'drying'		-
Soil	Sydney sand		V_s	0	m^3
Flume	4		$V_s + V_w$ in flume	0.2171016	m^3
Exit type	circle		void ratio	#DIV/0!	-
seepage length	1.3	m	relative density	#DIV/0!	-
head in bladder tank	0	m	avg. time for 50mL	11.12	s
bladder pressure	0	kPa	Q when ΔH = 0.1m	#DIV/0!	L/min
compaction	vibrator			0.27	

time	head (mm)	observation
11.02	0	there's a ≑40mm long channel
		already but trending d/s (see nappy
		snap).
11.07	↑100	t for 50mL = 10.7, 10.9, 11.3, 11.7, 11
11.29	↑ 143	
11.46	↑ 190	
11.48		initiation but d/s end of channel
		about 40mm u/s of exit.
11.50		tip at tank wall. There's no boiling action
		@ exit.
11.51		d/s end of channel now at exit
11.54		tip now at 61.
12.00	↓ 161	55 abl
12.03		" "
12.17		" "
12.21	↑ 175	
12.27		113 abl
12.33		155 abl
12.35		60fps set @ tip
12.36		" " "
12.46		163 abl
1.08		163 abl
1.54	↑ 156	163 abl
1.55		60fps set @ tip
1.56		" " @ 90 abl
1.57		185 abl

time	head (mm)	observation
2.31		8 ab2
2.43		30ab2
2.57	↓ 176	120 ab2
3.11	↓ 163	210 ab2
3.18		218 ab2
3.35		228 ab2
4.52	↓ 105	under b3
31-3		
10.20		the water stopped flowing over the
		weekend. I'm yet to work out if
		the water just got low or the
		pump has died. the level in the
		head tank is below the standpipe.
		The sand is unsaturated + air
		bubbles/gaps are present. I suspect
		this test has been compromised
		but once the water is flowing again
		I'll try continuing the test but I
		don't like the chances of success.
10.26	↑	Pump is fine (water had just ran too low).
2.14	0	Water brought back up to datum
		and there is air bubbles all
		throughout (see nappy snaps).
2.15	↑105	
2.17	↑ 150	
2.20	↑ 173	
2.32	↑293	tip not moved.
2.35		the channel is now active up to 150mm ab2
		Air is getting carried through the
		channel + pushed out the hole.
2.38		now active up to tip (@ b3)
2.39	↓ 210	
2.40		18 ab3
2.41		25 ab3
2.58	↓ 173	120ab 3
3.08		120ab3
3.33	↓ 150	225 ab3
3.55	↑ 163	225ab3
4.39	↑ 170	225 ab3
5.03		first noticed through to U/S and refer to
		photos for time.
1-4		
9.47		deepening up to b3 but blocked btw
		3 and 2. Going to terminate test. It
		might of failed if I had of left it
		longer but need to move on to the next
		test.

42. Test 42 (flume 4) circle

Test 42 was with the circle exit and was the 3rd test with a bladder pressure < 5m.

The bladder pressure was zero (and was not inflated at any point).

The channel initiated at 190mm but the d/s end of the channel was about 40mm u/s of the exit. However, at the same head, the d/s end grew to the exit (i.e. the channel grew in both directions).

Initiation head = critical head (190mm) which is unusual for the circle exit.

I dropped the head over the weekend (so the tip wouldn't progress and I could pick up where I left off on the Monday) but the water level in the pit get too low and the sump pump turned itself off, meaning the water stopped flowing and the head dropped below the top of the flume. This meant the soil had been desaturated. I topped up the water in the pit, turned the sump pump back on and raised the head back to datum however there were many bubbles now. Pic:

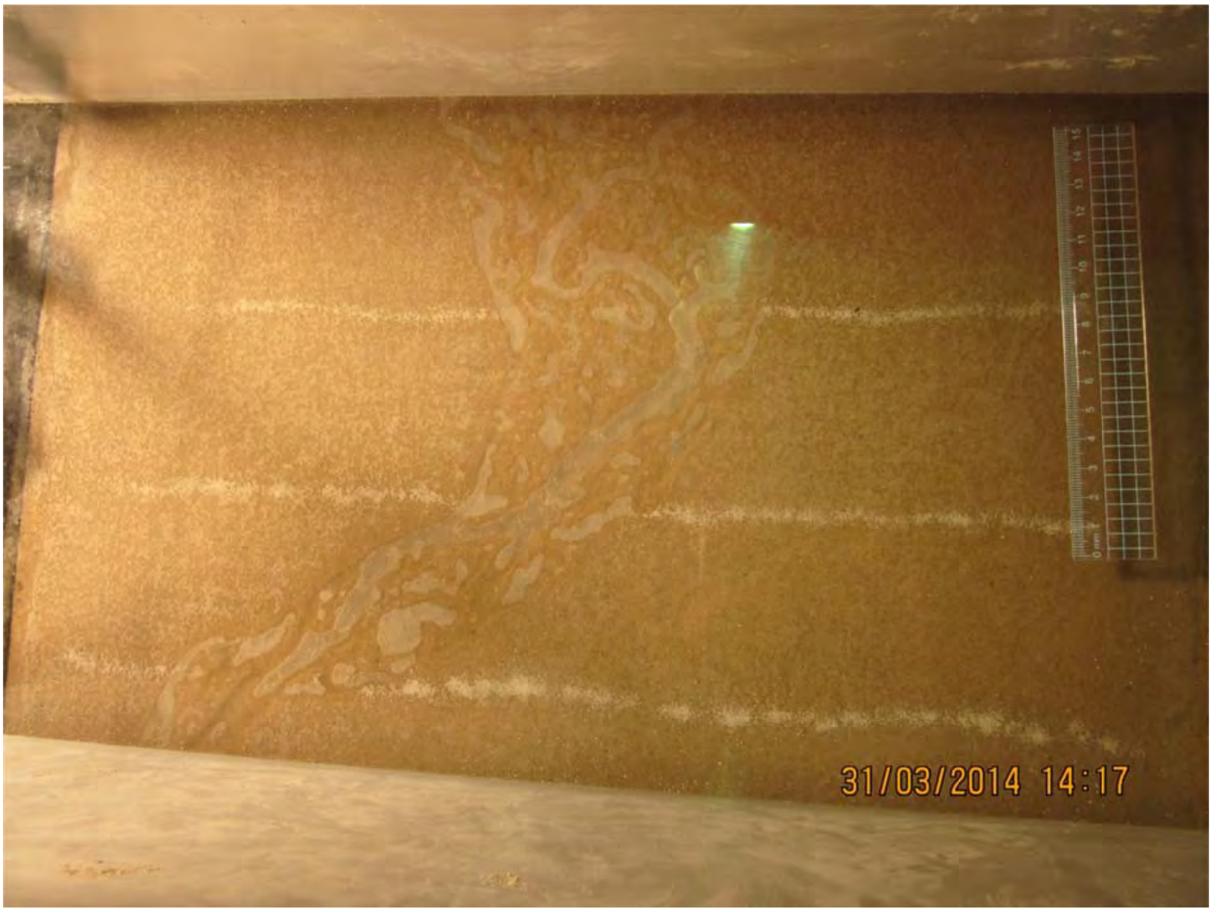

I pushed the head up to 293mm which pushed bubbles in the channel out to the exit and cleared the path for transporting sediments. The particle transport reactivated progressively backward along the channel until the tip was reactivated. Once the tip reactivated I dropped the head back down to 173mm to be in the same vicinity as it was before the weekend.

The tip progressed at speeds between 4 to 12 mm/min.

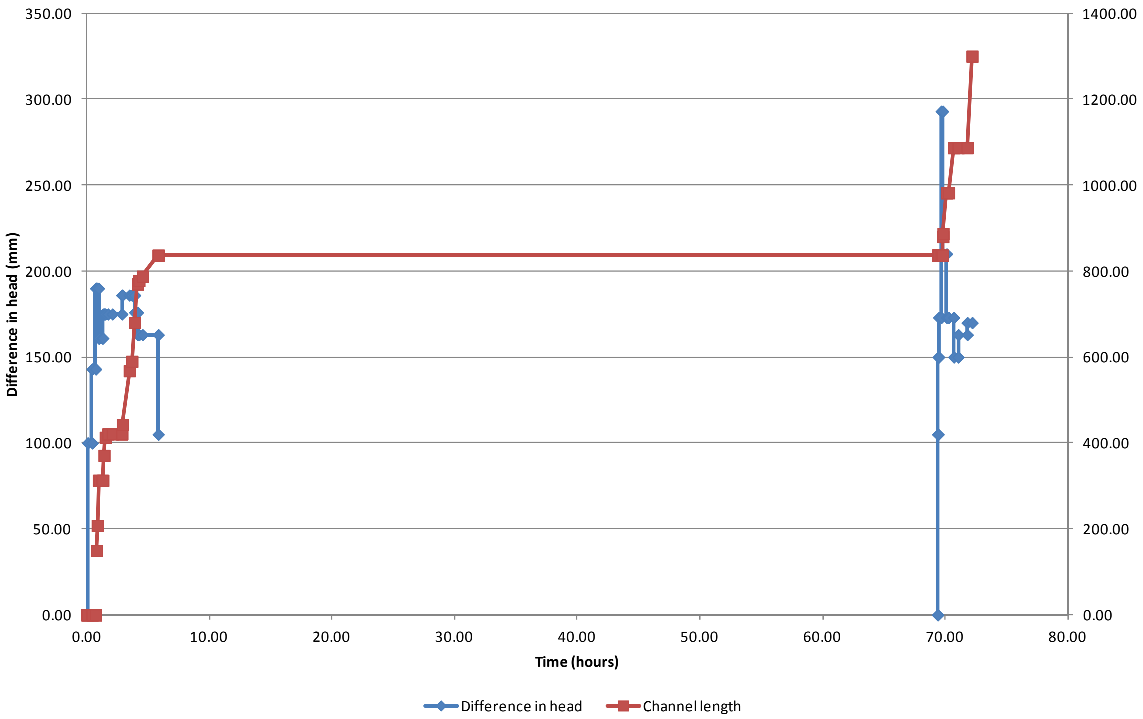

350.00
300.00
250.00
200.00
150.00
100.00
50.00
0.00
Difference in head (mm)
1400.00
1200.00
1000.00
800.00
600.00
400.00
200.00
0.00
Channel length (mm)
0.00
10.00
20.00
30.00
40.00
50.00
60.00
70.00
80.00
Time (hours)
Difference in head
Channel length

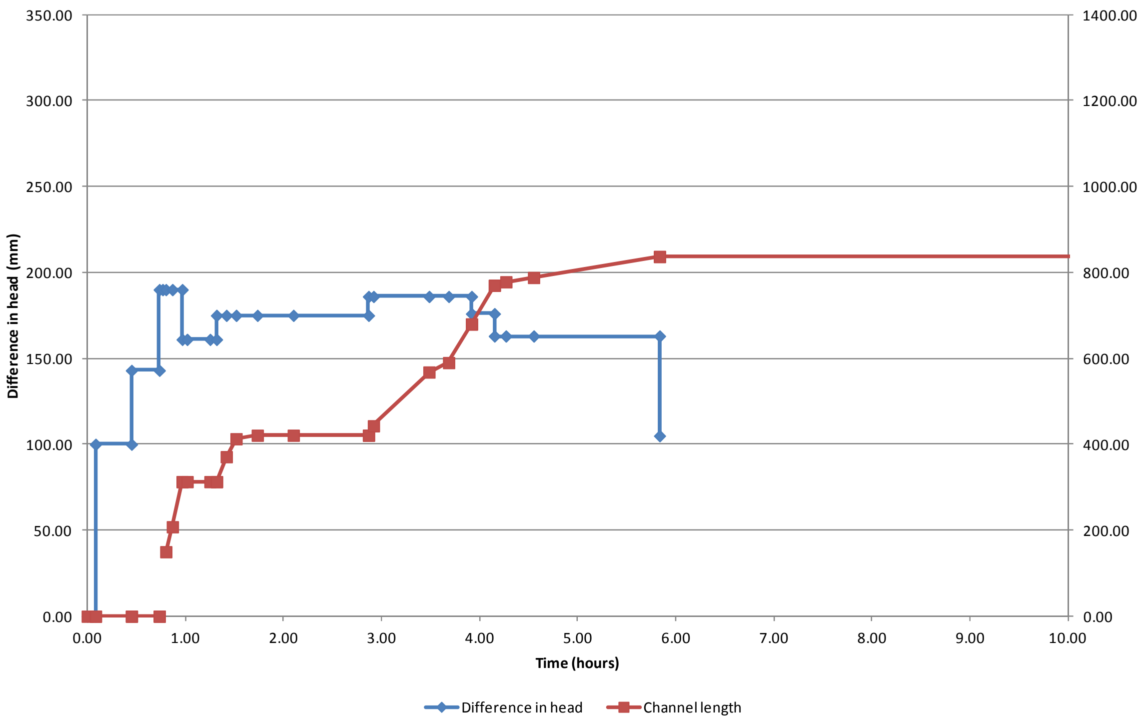

350.00
300.00
250.00
200.00
150.00
100.00
50.00
0.00
Difference in head (mm)
1400.00
1200.00
1000.00
800.00
600.00
400.00
200.00
0.00
Channel length (mm)
0.00
1.00
2.00
3.00
4.00
5.00
6.00
7.00
8.00
9.00
10.00
Time (hours)
Difference in head
Channel length

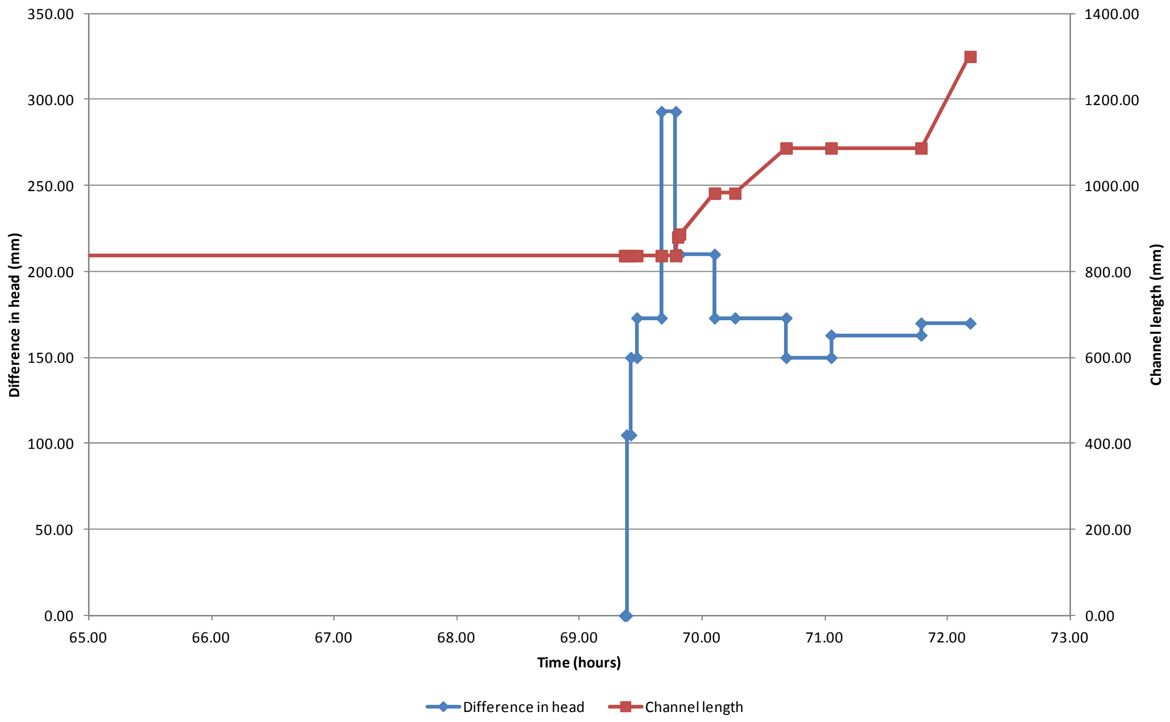

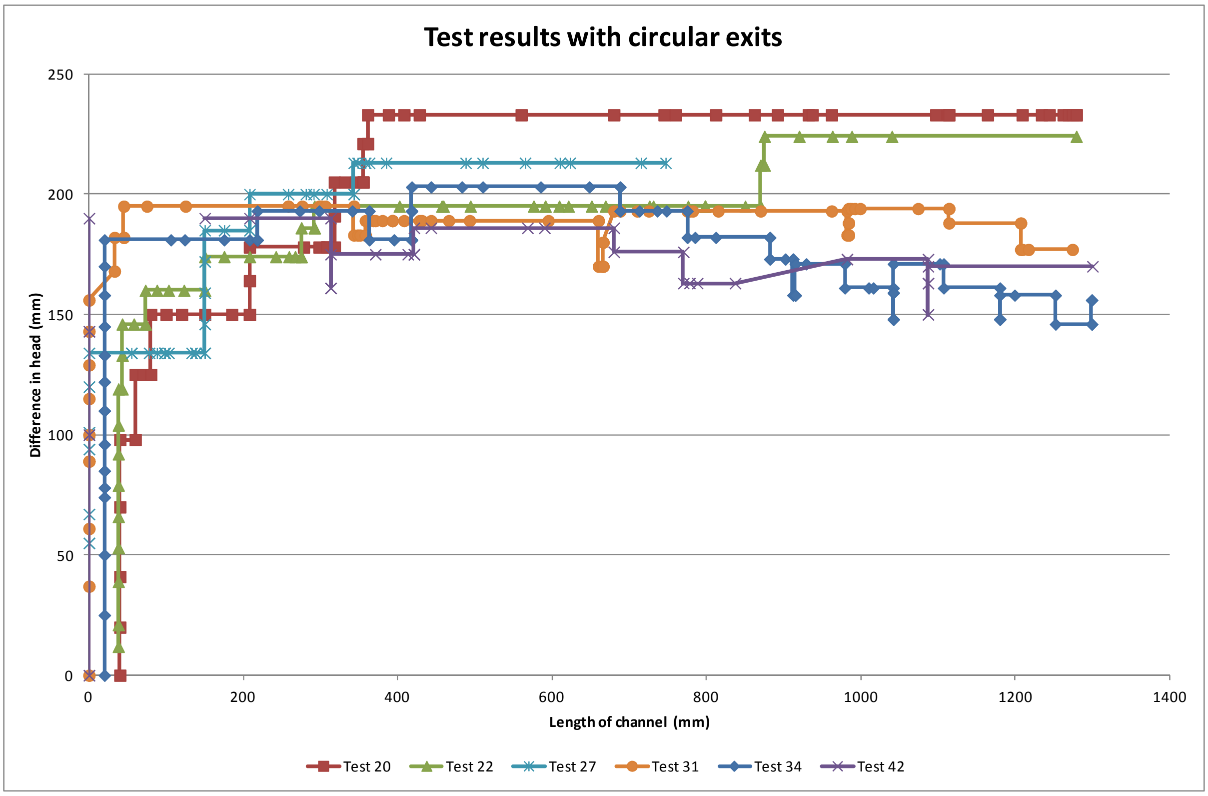

As for the effect of the zero bladder pressure- apart from the fact that initiation head = critical head, I saw no difference. This surprised me as I thought lower heads would be required because there's less effective stress so it should be easier for the flow to detach particles. Maybe the effective stress has little to do with the detachment mechanism. I note that other researchers found the bladder pressure had little effect but I don't remember them ever doing zero pressure. Maybe all the bladder does is ensure the sand is up against the Perspex lid and maybe because when I screen my sand's surface and leave a 1mm step, my sand is already pressed up against the lid without the need for the bladder.

The experiment did not fail. There was blocking (and bubbles) between bars 2 and 3. It might have failed if I had of left it longer but I wanted to move onto the next test.

Backward erosion piping test data sheet

Test #	43	$m_s + m_w$ after 'drying'		kg
Date	1/04/2014	m/c after 'drying'		-
Soil	Sydney sand	V_s	0	m^3
Flume	3	$V_s + V_w$ in flume	0.2171016	m^3
Exit type	plane	void ratio	#DIV/0!	-
seepage length	1.3 m	relative density	#DIV/0!	-
head in bladder tank	5 m	avg. time for 50mL	16.2	s
bladder pressure	50 kPa	Q when ΔH = 0.1m	#DIV/0!	L/min
compaction	vibrator & **wet**		0.19	

time	head (mm)	observation
28-3		
10.05		inflate blader
10.15		CO2 on
5.00		CO2 off
5.10		water on
1-4		
10.12	0	this is a test to see how much
		effect placing wet sand in water
		+ then CO2ing makes. the CO2ing
		left a series of channels in
		the d/s end (see happy snap).
		there's also gas/air bubbles in the
		channels but I think this is
		only because the wate
		stopped flowing over the weird
		which sucked in air. I suspect
		initiation will be quite low
		(because channels already
		formed). I also expect multiple
		channels to progress. I wouldn't
		be surprised if the critical
		gradient is lower because topmost
		sand possibly loose.
10.17	↑62	the tip of the furthest reaching
		pre-existing channel is 140 ab1 (1)

time	head (mm)	observation
		and is roughly in the middle of
		the flume
10.22	↑ 102	Q = 16.3, 16.8, 15.5 s for 50mL
11.38	↑ 154	existing channels showed particle
		transport but no tip progression.
		Transporting stopped before too long.
11.52	↑ 180	Again, particle transport in existing
		channels but not tip progression.
		The transport is occurring in
		2 channels. Transport stopped after a
		few minutes
12.22	↑ 208	
12.25		now starting to see transport u/s
		of b1.
12.57	↑ 233	
12.58		110 ab1 (2) Tip (2) has started to
		progress
12.59		(2) 130 ab1
1.01	↓ 221	(2) 200 ab1
1.02		(2) 215 ab1
1.04	↓ 208	(2) 235 ab1
1.26		(2) 83 ab2
1.28	↓ 194	" " "
1.53		(2) 90 ab2.
2.33		(2) 147 ab2
2.52	↓ 170	(2) 205 ab2
3.27	↓ 169	(2) 73 ab3
3.38		85
3.49		~~a~~ ~~a~~ the channel has braided a little (see
		happy snap)
3.50		(2) 125 ab3
4.04		180
4.40		20 ab4
5.13		(2) 20 ab4.
		Ending test here because need
		to empty constant head tank
		so it can be raised.

43. Test 43 (flume 3) plane

Test 43 was to test how much effect CO_2ing wet sand had the piping process.

During the CO_2 flushing, the gas pressure pushed water into the d/s box (there was no free water in the box before CO_2 flushing). Something created channels, perhaps water flow (because it was being pushed through) or perhaps gas flow on its own can cause backward erosion. Pics:

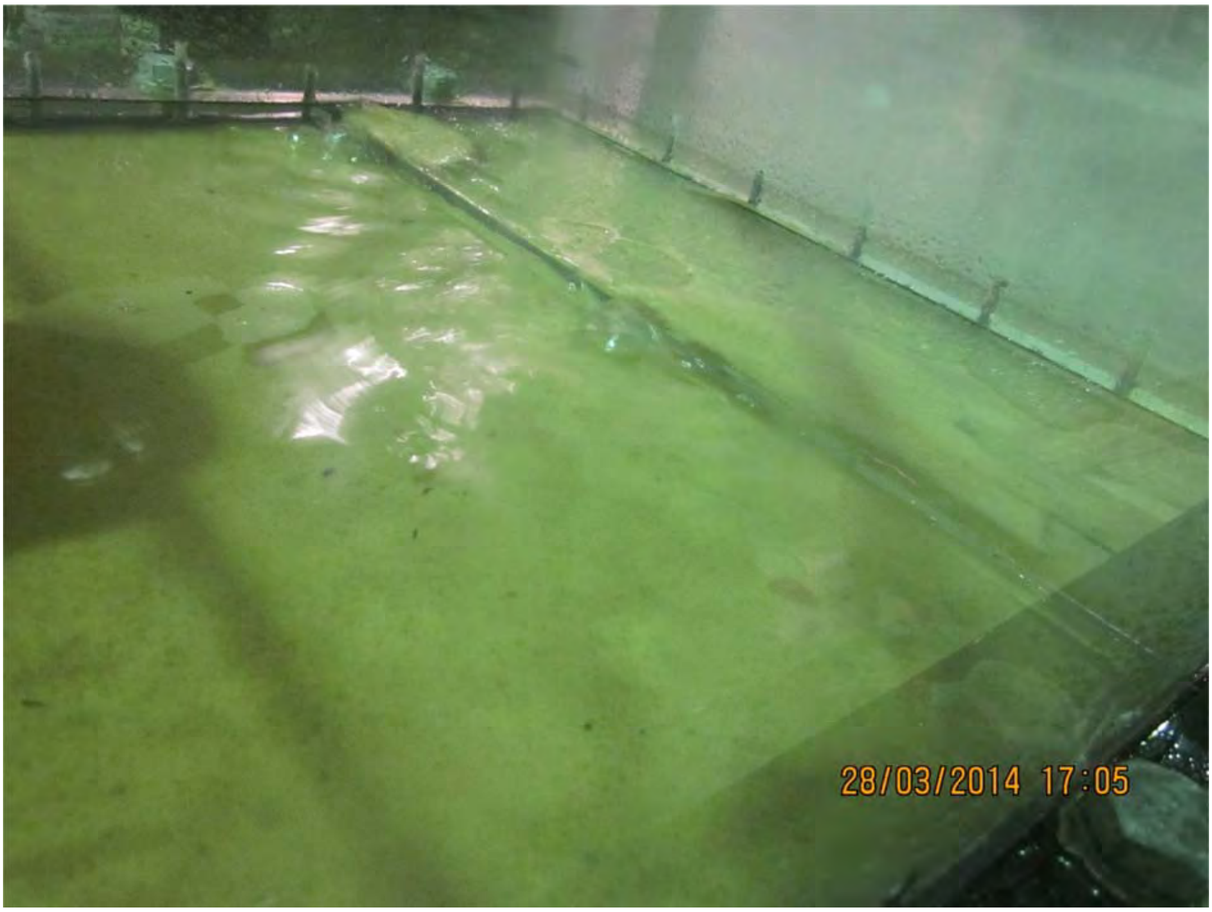

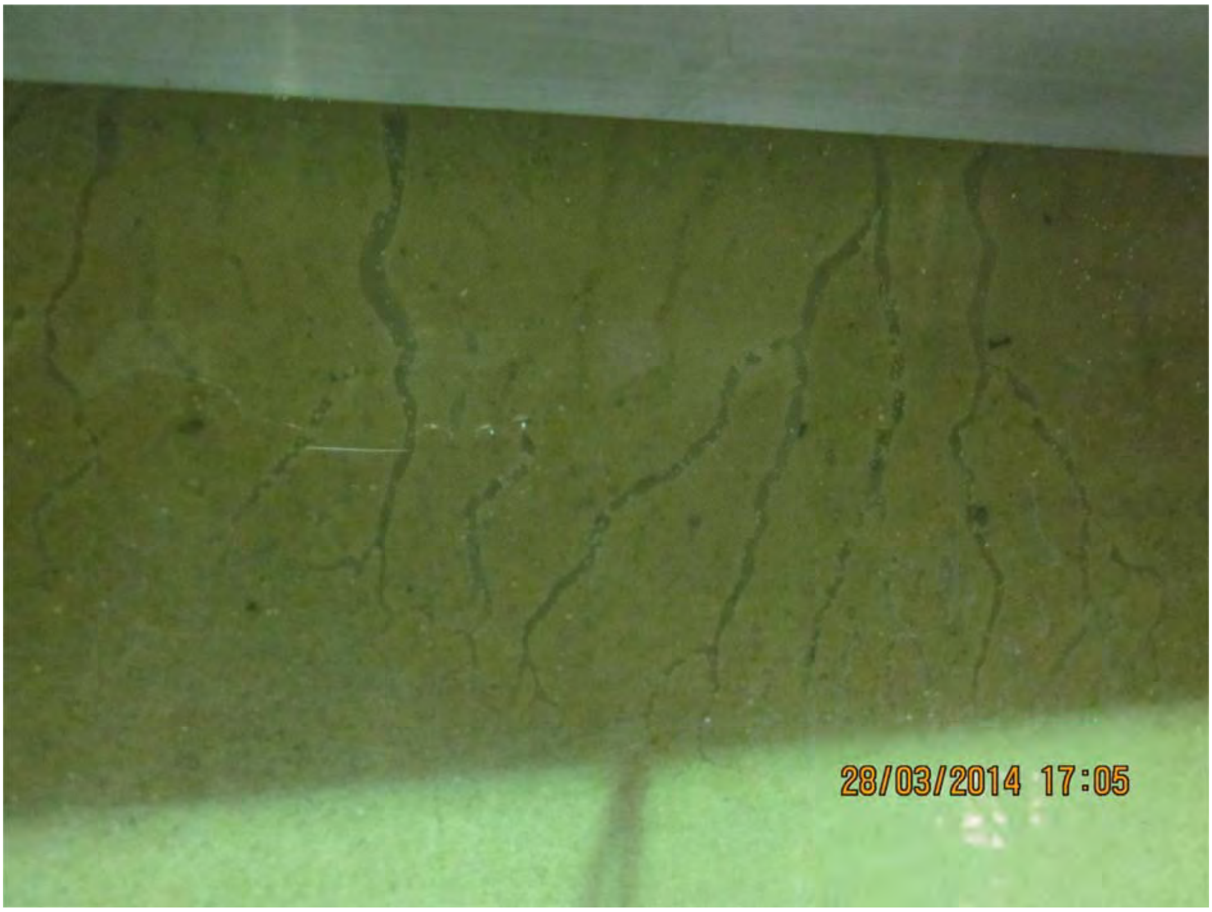

So from the onset I could see this method of saturation would prevent the initiation head from being determined (because channels were already formed). However I had hoped that once one of the pre-formed channel tips progressed, the remainder of the test would behave as the other tests did.

I turned the water on to saturate the sample on a Friday (28th March) but over the weekend the water level in the pit got too low and the sump pump turned itself off, meaning the water stopped flowing and the head dropped below the top of the flume. So on the Monday (31st March) I topped up the water in the pit, turned the sump pump back on and raised the head back to datum however there were bubbles, mostly near the exit. Pic:

I don’t think these bubbles affected the test too much because they were all d/s of the eroding tip.

As I always do I measured the flow rate leaving the d/s valve when the head difference was 100mm and I had hoped that this flow might give an indication of sand permeability/density (relative to tests whose sand wasn’t placed underwater but vibrated in dry). So I plotted all the flow rates I have:

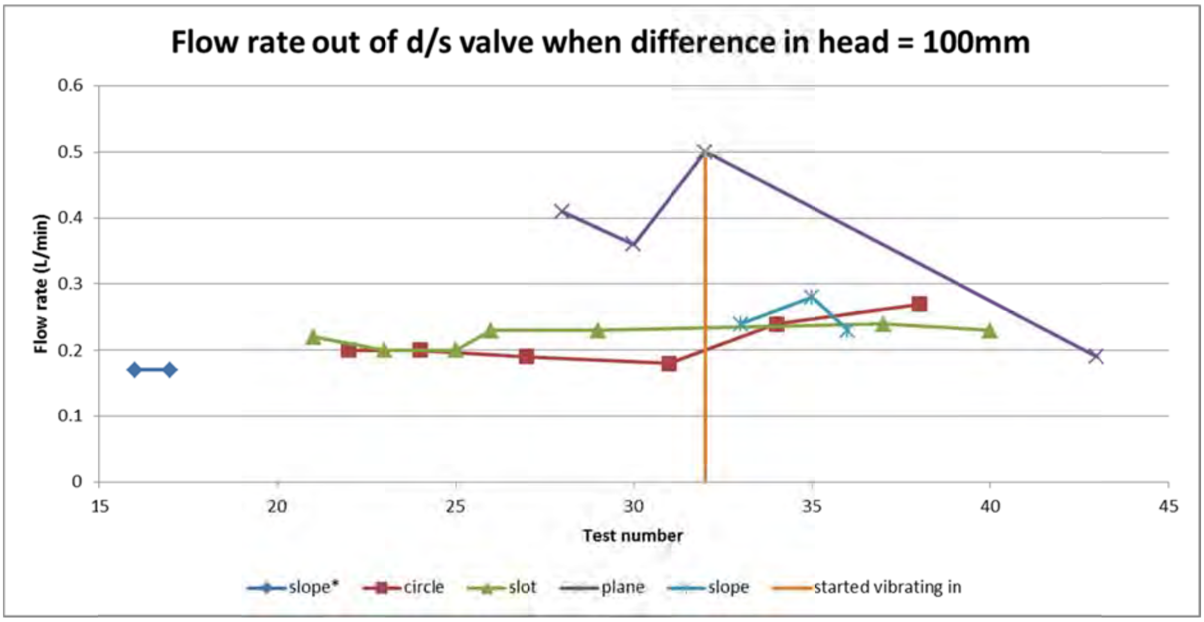

Note: the slope* indicates the slope exit I used to begin with, when I wasn’t using a d/s box.

I would expect the flow to be reduced by exit geometry in the order of slope, plane, slot and circle but this order isn't clear- don't know why. I also expected the flow rate to be lower for this test than the other tests using the plane exit because I expect the density to be lower (placed under water- although it was also vibrated) and it was- by a lot. However I'm hesitant to say this means the sand is of a lower density because the flow rate results are all over the place.

The longest pre-formed channel was numbered channel 1 and was 140ab1. However it was a channel mid-way to the RHS at 110ab1 whose tip progressed, it was named channel 2. Pic:

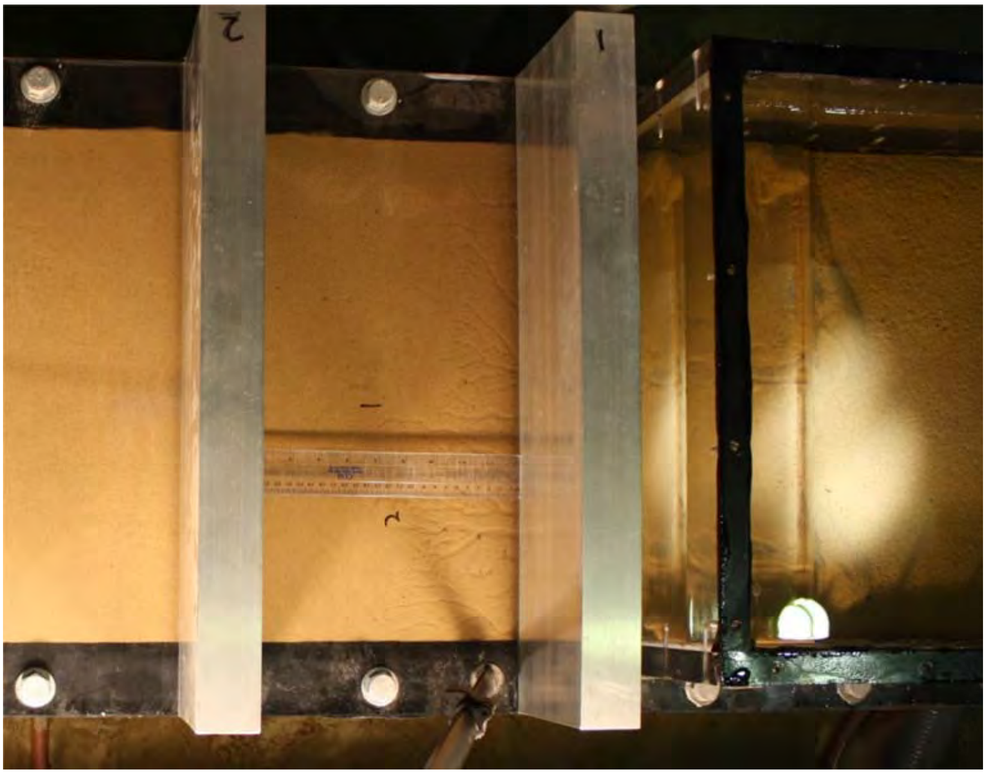

The tip progressed between around 4 to 7 mm/min.

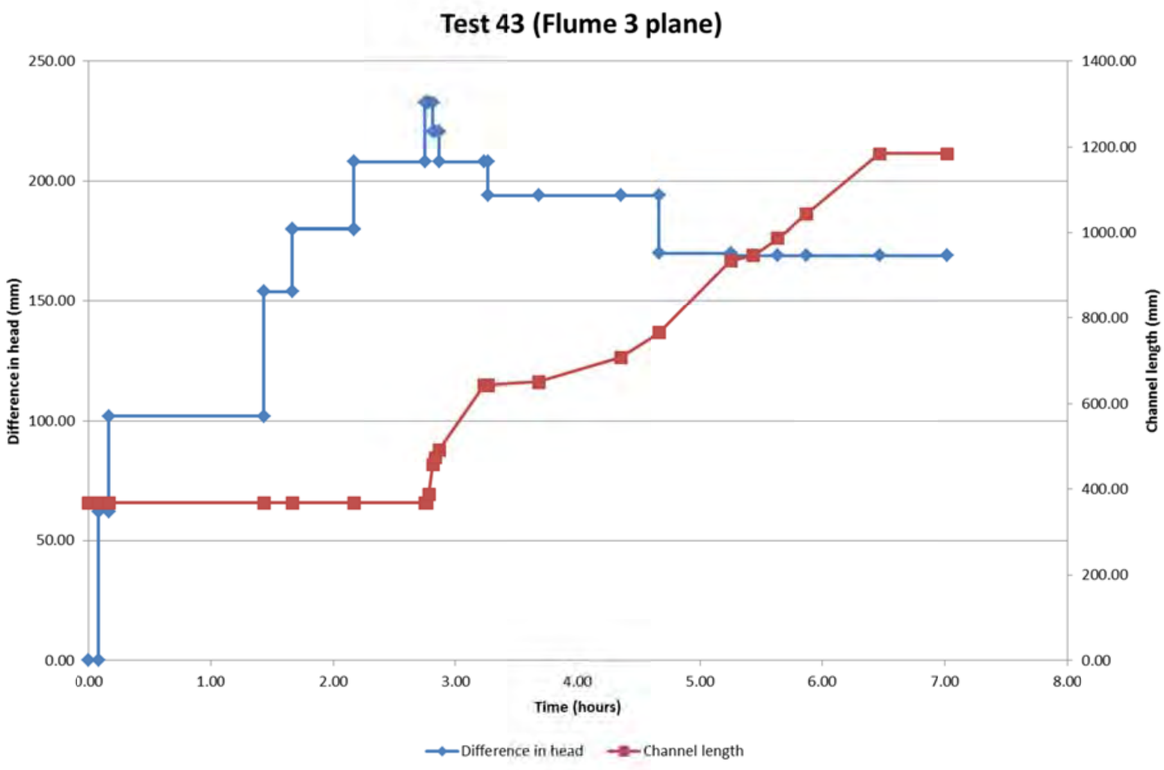

The questions is whether this test, once the tip started to progress, behaved similar to other tests, i.e. did placing the soil underwater change the results? To answer this:

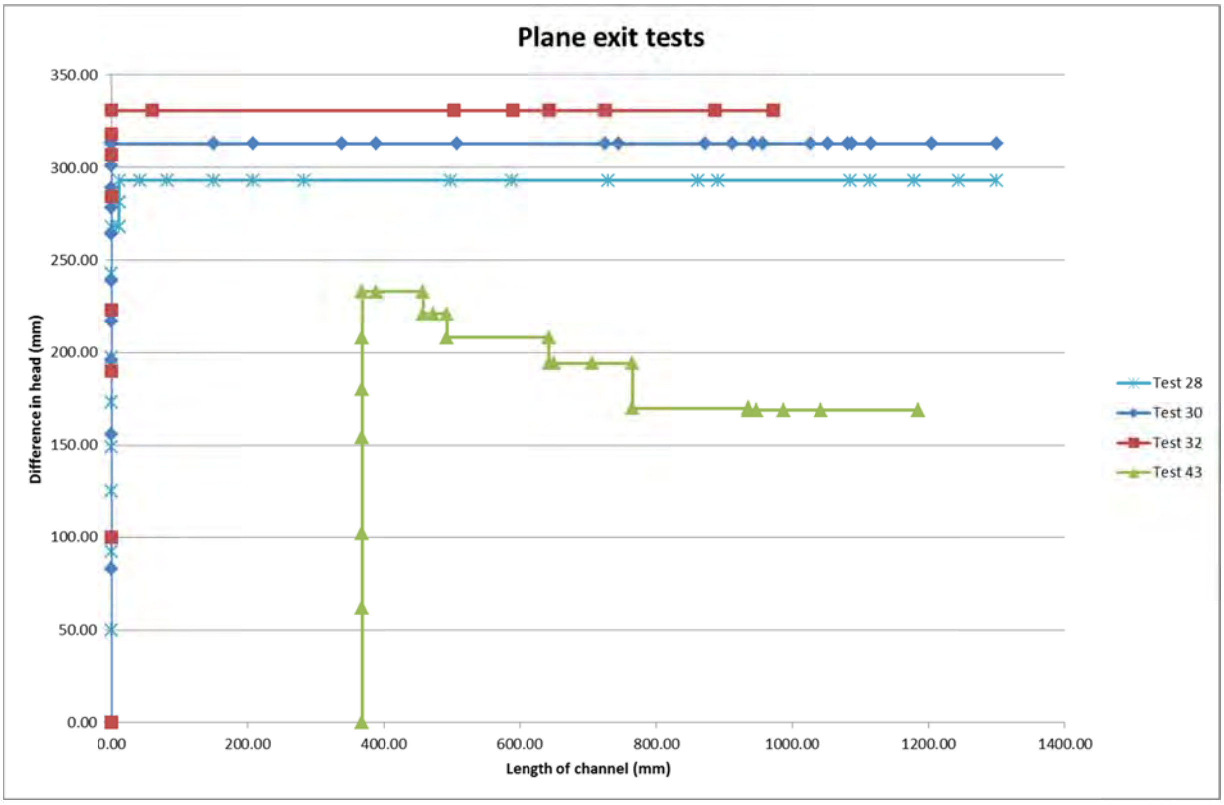

No it didn't behave the same. Yes placing under water did affect the results. The head required for progression was about 25% less at the L=400mm mark. Test 43 also looks different because the curve drops instead of remaining constant but this may just be because I didn’t reduce the head in tests 28, 30 or 32, which begs the question, what does the plane exit look like when the head is reduced?

In conclusion I don’t think pushing CO_2 through partially saturated sand is a viable method because it reduces the critical head by too much. My best guess as to why this is is the density is lower so the permeability is higher so a lower head is required to get erodible seepage velocities.

I didn’t progress the channel all the way to the u/s end or continue to failure because I needed to empty the constant head tank so Hamish could start raising it.

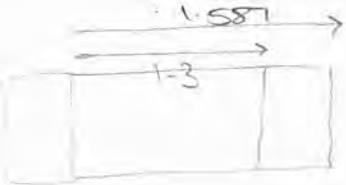

Backward erosion piping test data sheet

Test #	44	$m_s + m_w$ after 'drying'		kg
Date	8-4-14	m/c after 'drying'		-
Soil	Sydney sand	V_s	0	m^3
Flume	4	$V_s + V_w$ in flume	0.2171016	m^3
Exit type	plane	void ratio	#DIV/0!	-
seepage length	1.3 m	relative density	#DIV/0!	-
head in bladder tank	5 m	avg. time for 50mL	13.1	s
bladder pressure	50 kPa	Q when ΔH = 0.1m	#DIV/0! 0.23	L/min
compaction	vibrator & **btm 3/4wet**			

time	head (mm)	observation
7-Apr		
11:30		inflated bladder
11:40		CO2 on
4:50		CO2 off
5:00		water on
8-4		
11.17	0	no visible bubbles. I noticed that
		when I opened the d/s valve
		the water level in the box
		was higher than datum even
		though the constant head tank
		is at datum. I'm not sure
		why. But once I opened the
		valve the level dropped to datum.
11.24	↑ 100	for 50mL t = 13, 13.2, 13.7, 12.8, 12.8
11.39	↑ 143	
11.44	↑ 190	
11.56	↑ 240	Initiation. Initially d/s of channel u/s of exit but
11.58		tip @ tank wall-end it grew both ways.
		d/s end of channel now @ exit.
11.59	↓ 215	bl
12.02	↓ 193	10 abl
12.04	↓ 168	50 abl
12.05		75 abl
12.08	↓ 143	123 abl

time	head (mm)	observation
12.14		13 ab1
12.28		138 ab1
12.33		138 ab1
12.47		153 ab1
12.48	↓ 140	153 ab1
1.41	↑ 144	153 ab1
2.15	↑ 150	153 ab1
2.22		163 ab1
2.37		165 ab1
2.57		168 ab1. There's a branch (see happy snap)
3.13		169 ab1
3.28	↑ 155	169 ab1.
3.45		169 ab1 and branch still growing laterally.
		I knocked the perspex + that seemed
		to loosen particles @ the top.
4.02	↑ 159	172 ab1
4.14		178 ab1
4.47	↑ 167	178 ab1
5.18		23 ab2
5.24	↓ 81	60 ab2
5.58		60 ab2
		~~60 ab1~~
9-7		
9.58	81	60 ab2
9.59	↑ 153	" "
10.27	↑ 177	60 ab2
10.43	↓ 162	220 ab2
10.45		240 ab2
10.58	↓ 153	138 ab3
10.59		154 ab3
11.03		154 ab3
11.14	↓ 140	205 ab3
11.29		220 ab3
11.58	↓ 132	other side of b4
12.11		first noticed it through to U/S end (look
		at photos for time). The channel
		is blocked near b4 (see happy
		snap

44. Test 44 (flume 4) plane

Test 44 was to test how much effect leaving the btm ¾ worth of sand from the last test (so it was wet) but replacing the top ¼ with dry sand would have on the piping process. The btm ¾ was left from test 42. Test 42 was placed normal (filled flume with dry sand then vibrated in) but had no bladder pressure applied. This could mean that the btm ¾ was less dense than tests 28, 30 and 32 (the other plane tests I'm comparing this test with) however the bladder was inflated to 5m for this test. Is it possible that wet unsaturated sand can't compress under bladder load as much as dry sand can? And besides- I'm starting to think the bladder pressure doesn't change the density anyway (makes no diff to results).

Having the top sand dry meant that no channels were created during the CO2ing (like it did in test 43). The top sand looked even and saturated (no gas bubbles could be seen).

I did notice that after saturating the water level in the d/s box was higher than datum even though the water level in the constant head tank was at datum. I don't know why this was but after having opened the d/s valve the level in the box reduced to datum.

As I always do I measured the flow rate leaving the d/s valve when the head difference was 100mm and it plotted here:

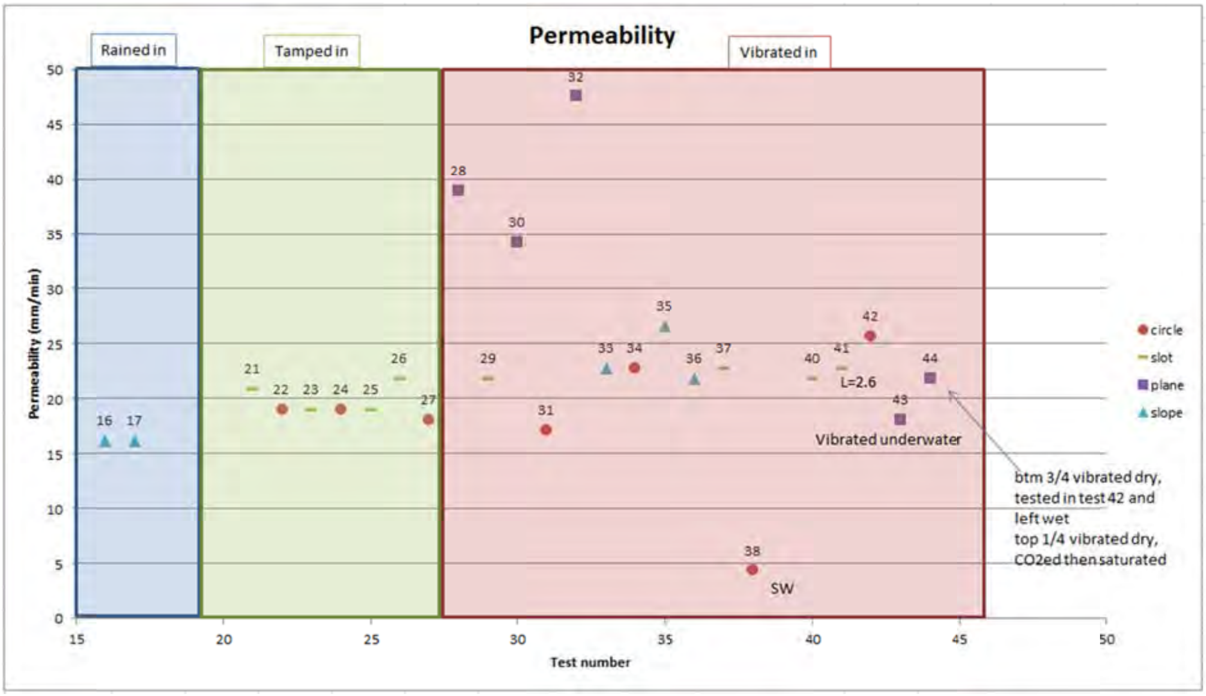

I expected the permeability to be the same as regular plane tests (because I expect the lower ¾ of the sand to be the same permeability.

The tip progressed at speeds of 22, 0.3, 5, 12, 3 and 10mm/min (in the approximate order).

The questions is whether this test behaved similar to other tests, i.e. did leaving the btm ¾ worth of sand from the last test (so it was wet) and replacing the top ¼ with dry sand change the results? To answer this:

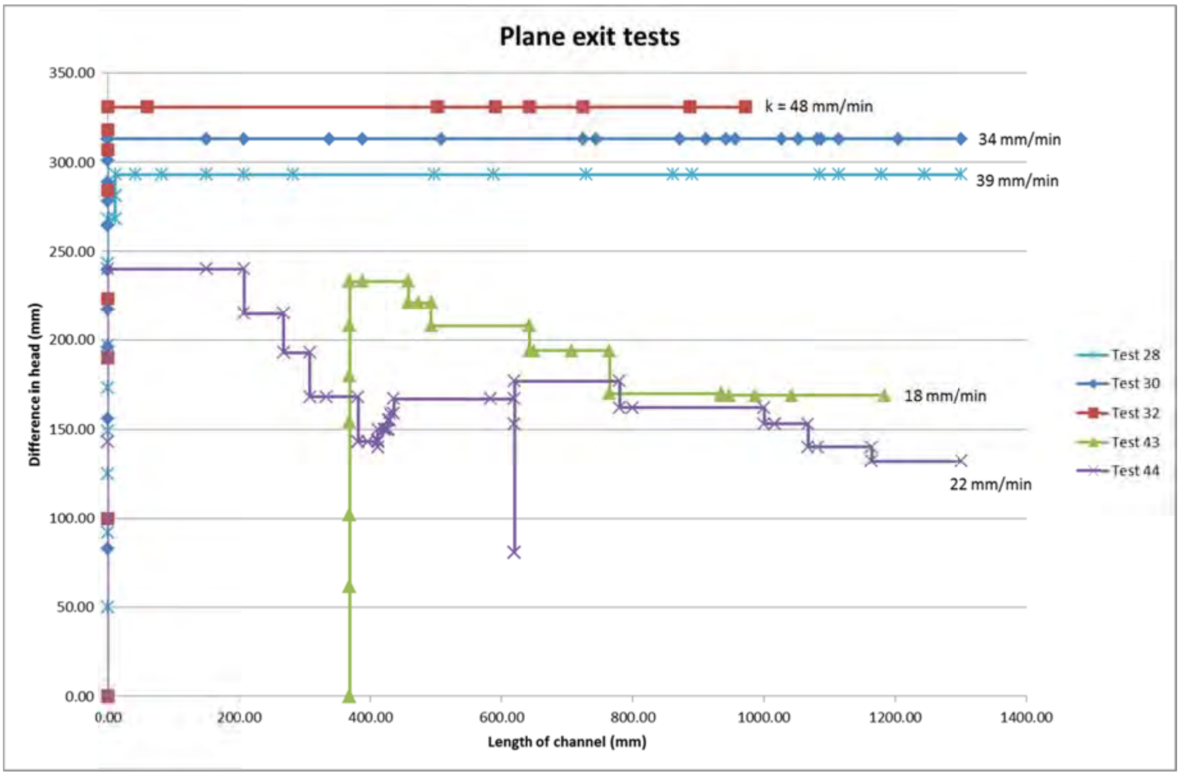

Yes it did. It reduced the initiation head by about 25%. Test 44 also looks difference because the curve drops instead of remaining constant but this may just be because I didn't reduce the head in tests 28, 30 or 32, which begs the question, what does the plane exit look like when the head is reduced?

In conclusion I don't think leaving the btm ¾ worth of sand from the last test (so it was wet) and replacing the top ¼ with dry sand is a viable method because it reduces the critical head by too much. My best guess as to why this is perhaps because the lower ¾ of the sand was less permeable (because it was more dense because it had been compacted already in previous tests) than the upper ¼ of the sand, more flow was directed through the upper ¼ and so a lower head was required to get eroding seepage velocities.

By 10-04-14 1.05pm it still hadn't failed. The forward deepening process extended from u/s to approx. 130 ab2. It was then blocked from 130 ab2 to approx. 180 ab1. It was like this for over 24 hours so I ended the test.

Backward erosion piping test data sheet

Test #	45		$m_s + m_w$ after 'drying'		kg
Date	10/06/2014		m/c after 'drying'		-
Soil	Sydney sand		V_s	0	m^3
Flume	1&2		$V_s + V_w$ in flume		m^3
Exit type	slot		void ratio		-
seepage length	3.9	m	relative density	4.705882353	-
head in bladder tank	5	m	avg. time for 50mL		s
bladder pressure	50	kPa	Q when ΔH = 0.1m	#DIV/0!	L/min
compaction	vibration				

time	head (mm)	observation
3-Jun		
11:15		inflated bladder
11:30		CO_2 on
4:30		CO_2 off
4-Jun		
10:00		water on
6-Jun		
10:00		bubbles still present at u/s side (see happy snap)
10-Jun		
11.45		bubble still present @ u/s (noless)
11.47		F2 bladder had dropped to ≐4m so
		topped up. F1 ≐ 4.5m so topped it
		up too
		I'm not expecting initiation any lower
		than 300mm and I'm expecting critical
		≈ 800mm.
11.54	0	
11.55	↑ 46	
12.05	↑ 95	
12.18	↑ 100	Q for 50mL = 34.9, 38.9, 36, 36.3
12.24	↑ 145	
12.35	↑ 198	
12.49	↑ 250	
1.03	↑ 301	small particle rearrangement (see happy snap)
1.43	↑ 312	
1.56	↑ 324	initiation. 135-110mm. 15°C. Q for 50mL = 95, 112, 98, 103, 117

Standpipe = 145mm above perspex.

Test 45

time	head (mm)	observation
2.11		135-110
2.12	↑ 333	" "
2.35	↑ 336	135-110
2.48	~~↑~~	" "
2.48	↑ 348	tip growing again 143-110.
3.05	↑ 363	143-110.
3.42	↑ 377	143-110
3.43		165-110 (joined up to a deformity already in
		sand (which is ~~y~~ how got so long so quickly)
3.46		185-110.
4.01	↑ 388	" "
4.22		195-110
4.33	↑ 399	" "
4.47	↑ 411	" "
4.49		203-110
5.04		tip @ bl
5.41		tip otherside of ~~b~~ bl
5.42	↓ 364	~~$~~ 7mm abl
11-6		
10.34		tip still at bl → well it's 7 abl.
10.35	↑ 387	7abl
10.40		detachment @ tip is occurring v. slowly.
10.49		20abl
11.00		38abl
11.08		48 abl
11.25		63 abl
11.37		73 abl
11.58		78 abl
12.14		78 abl
12.20	↑ 400	78
12.25		80
12.40	↑ 412	80
12.44		85
12.57		85
1.34	↑ 425	85
1.42		85
2.02	↑ 436	85
2.43		103 abl
3.15	↑ 449	103 abl
3.26		112
3.43	↑ 463	112 abl
3.54	↑ 476	112 abl
4.00		Scour occurring but tip not moving.
4.14	↑ 500	114 abl. The channel has branched (see
		floppy disk).
4.48	↑ 527	
5.17	↓ 479	121 abl.

45
115abl.

25
57
370
230/32

140 25
9

0.69
1.01
1.27
1.4
1.53

time	head (mm)	observation
12-06		
2.01	479	121 ab1
2.02	↑ 498	" "
2.11	↑ 525	" "
2.23	↑ 549	scour is occurring but tip not moving.
2.29	↑	
2.38		135ab1
2.52		155 ab1 (see happy snap).
2.58		165
3.06		temp = 15°
3.36		180ab1
4.44		182ab1
5.26		182ab1.
13-6		
9.42	575	187ab1
9.43	↑ 592	
10.03	↑ 652	187ab1
10.19	↑ 701	188ab1
10.23		195ab1
11.23		225ab1
11.51	↑ 726	225
12.14	↑ 749	225ab1
12.25		at b2.
12.58		98 ab2
2.19	↓ 728	153ab3
3.13		192 ab 4
3.15		2 sets @ 20ab3 plidte.
3.30		203 ab4
3.51		205 ab4
4.21		is meandering back towards middle
		(see happy snap) and has branched off.
		Furthermost tip still at 205ab4 but
		other tip now progressing.
5.15	↓ 679	210 ab4
16-6		
9.49	681	tip is about 30mm after flume join.
		There appears to be a large local
		depression or void at tip (see
		happy snap). I note this is within the
		region where coating wasn't applied (because
		it's the U/S end of the flume when in
		single-mode; it's the 'peepy hole' to see the
		inflow). So maybe this local 'void' is because
		sand can move easier along lid here. It
		could be making it more difficult for the
		tip to progress here (because seepage is
		less concentrated).

GTU1002 57509

Test 45

time	head (mm)	observation
		Because the tip got to this position at
		the weekend I have no way of
		knowing how long it's been here (time-lapse
		photography isn't being taken because the
		canon is needed on test 46).
		there's a blockage btw bars 5+6 (see
		happy snap). this may be the other
		reason the tip is stopped (if it's stopped
		at all - it could just be real slow). I do
		think it might be stopped because
		I see no particle transport. I took
		another photo of blocked zone marked
		with a marker. It'll be interesting to see
		if the blocked zone grows or not.
		I also note there are heaps of channels
		+ meandering near the d/s end (see happy
		snap).
		I also note the tip was happy to progress
		past the join without need for head
		increase.
11.56	↑ 692	the tip hasn't moved + the blocked region
		hasn't grown. No particle transport.
12.27	↑ 702	
1.41	↑ 719	tip not moved. Bladder tank 1 ≑ 4.5m.
		Bladder tank 2 ≑ 4.5m (same).
2.03	↑ 728	
2.30	↑ 738	Since this morning I've raised the head
		by 57mm but the level in the standpipe
		has only risen by 5mm. Is this because
		the higher the flow the higher the
		head loss? So the rate of head increase
		> the rate of head increase at the standpipe?
2.43	↑ 749	30 after join
2.55	↑ 761	30 after join
3.06	↑ 774	
3.15		there's particle transport again btw
		join and d/s end. The blockage is trying to
		unblock itself. I want to leave ~~it~~ it at this
		head for a while cause I reckon it'll
		unblock itself.
3.30		the blockage is more-or-less unblocked and
		I ~~[illegible]~~ can see detachment in flume 2
		occasionally but the local void seems to
		be making it hard for a tip to form.
3.38		It's blocked again (in same spot) but
		particle transport still occurring.
3.54		190 after join → it's a new tip that doesn't
		go through 'void'. See happy snap. However
		it's still blocked around bar 5. I don't

Test 45

		think I should lower the head while there's still a blockage.
4.08		tip other side of bar 7. I'm gonna lower head back to where it was before (around 692) to see if tip progresses despite the blockage
4.09	↓ 726	45 ab7
4.14		125 ab7
4.16		~~60~~ tip.
4.19	↓ 702	213 ab7. It's now blocked halfway btw 5+6 up to flume join.
4.32		13 ab8
4.50		13 ab8. blocked btws bars 6 to 7.
5.00	↑ 725	13 ab8.
5.21	↑ 736.	13 ab8
5.48		13 ab8.
5.51	↓ 637	13 ab8.
17-6		
9.30	↑ 690	13 ab8 and blocked btw ~~6~~ 5-6 and ~~7-8~~ 6-7.
10.03	↑ 713	13 ab8, still blocked in same locations + no particle transport.
11:15	↑ 724	" "
11:35	↑ 735	
11:51		Starting to unblock.
11:56		~~—~~ Unblocking
12:11		Reblocked downstream.
12:37	↑ 748	Still blocked.
1:07	↑ 760	" "
1:31		50 ab8, still blocked in same locations.
1:36		69 ab8, 2x Photos taken at 60FPS.
1:52		90 ab8,

test 45

UNSW AUSTRALIA | Civil & Environmental Engineering
Faculty of Engineering

17/6/14

	2:14		123ab8, Unblocking down stream
	2:41		205 ab8,
	2:41	↓738	Progressed 150mm ∴ drop by 25mm
	2:46		210 ab8, some particle detachment at tip.
	3:06		~260ab8 → Under Bar 9
	3:18		Particle detachment still occurring.
	3:37		110 ab9
	3:38	↓714	Reached about 0.73*L (past 0.7L critical point).
			New paths made. Also blocked themselves.
	4:05		Unblocking.
	:31		Under AB10 Blocking & Unblocking. B at bar 7 & 5
	4:38		60 FPS Photos taken
	4:40		2 ab10
	5.40	↓665	Left overnight.
18-6	11:25	↑710	No change since the day before.
	11:32	↑714	No tip progression or particle movement.
	12:12	↑727	
	12:42	↑737	
	12:57	↑749	
	1:21		" "
	1:22	↑762	
	1:38	↑1030	Pump stopped & head increased (malfunction)
			Particles began to erode
			40 ab10
	1:39	↓760	
	2:15		Unblocking, No tip progression.
	2:25	↑785	55 ab10 again.
	2:26	↓762	75 ab10 unblocking. Continous B & UB
	2:47	762	110 ab10
	3:04		120 ab10
			Blocked at Bar 8-9, 6-8, 5-6.
	4:36	↑779	130 ab10 + blocked btw 8-9, 6-8, 5-6
	4.58	↑798	130 ab10
	5:10		175 ab10

5.15		200ab10. Blockages still blocked but trp moving anyway.
5.35	↓ 698	under b11
19-6 10.00	701	20ab12. I'm not going to be able to see the channel when it goes into the u/s box cause the lid isn't very transparent + there's stuff on top of the actual lid. The channel is blocked in sections btw bars 11-12, 8-9, 6-7, 5-6.
6.22		20ab12.
20-6 11.27		channel is now below u/s box (I can't see where trp is). It's blocked btw bars 11-12, 8-9, 7-8, 5-6, 4-5
25-6 10.55		channel looks no different. It's blocked btw bars 4-5, 5-6, 6-7, 7-8, 8-9, 11-12. I think it's safe to say it's not going to fail. I'll go up ≐ 50mm to hopefully 'shock' the blockages + then if they unblock I'll drop head ↓ 50mm.
10.58	↑ 750	
4.22		there is particle transport but blocked btw 6-7, 8-9 and 11-12.

26-6	10-10	water is cloudy (both u/s + d/s) because fine sediment from S&W test in P3 got into water supply. This could mean fine sediment has gone into sand but can't tell. (see happy snap) At some point a new channel has formed. It's btw join + bar 8 (see happy snap). However it's blocked at it's d/s end. Given Hannah is going on leave next week and I'd like his help to take the lids off + empty, I'm going to end the test. I'm also concerned the cloudy water could affect things.
	10-20	end of test.

Test ~~40~~ 5

	Time	head	time for 50mL	Avg	Temp
13-6	10.44	701	5.3, 4.5, 4, 3.4, 4.2, 4.49	4.6	15
	3.18	728	5.2, 3.6, 4, 3.7, 4.8, 3.9	4.2	
16-6	10.28	681	3.6, 5.3, 2.9, 4.1, 4.6, 4.4	4.15	13
	5.49.		3.4, 3.8, 3.3, 4.1, 3, 3.6.	3.53	
17-6	10.09		3.8, 3.9, 4.2, 4.1, 4.8	4.16	13
18-6	~~1.36~~	~~head was 762~~	~~3.8, 3.5, 4, 3.5, 4.435~~		
	~~2~~				
	2:35	762	3.55, 3.59, 3.48	3.54	15
19-6	10.08		4, 3.9, 3.7, 4, 4.2	3.96	14
26-6	10.19	748	7.8, 8.4, 8.6, 8.1 for 100mL	32.9*	12

mL	t
~~550~~	~~35.7 s~~
550	38.3
500	35.5
500	35.9

Test ~~46~~5

		Row 1			Row 2			Row 3		
	Time	right	middle	left	right	middle	left	right	middle	left
	10.44	19.8								
	3.17	"								
6-6	10.31	150								
	2.05	153								
	2.34	155								
	3.08	159								
	3.17	160								
	3.38	165								
	4.14	162								
	5.49	180								
17-6	10.07	169								
	11:29	170								
	1:09	171								
18-6	11:43	150								
	1:21	155								
	3:04	170								
19-6	10.05	153								
26-6	10.20	171								
		Row 1			Row 2			Row 3		
		right	middle	left	right	middle	left	right	middle	left

45. Test 45 (flume 1&2) slot

Test 45 was the 2nd test with a seepage length >1.3m. L = 3.9m.

The CO2 dissolving took longer in this test. Usually all the co2 bubbles are gone overnight but 2 days later there were still bubbles present at the u/s end (see pic 1).

The channel initiated at 324mm near the centre of the slot.

On 2-3 occasions the channel branched off leaving the previous tip inactive (see pic 2).

This time the channel passed through the flumes join without head increase. However when the tip was about 30mm after the join several increases were needed. The need for head increases may be due to a local depression and/or channel blockage. There was a depression in the sands surface after the join (so seepage slower in this area because less concentrated so higher head was needed). This depression might be because of the ‘peepy hole’ in the Perspex- a small region that wasn’t ‘painted’ with flowable silicone (so I could see through the lid to the water inlet as the flume is first filled with water) (see pic 3). Because it’s not coated with the silicone here perhaps it’s easier for the grains to move locally which, having done so, left the slight depression. The other possible reason for tip arrest was the channel was blocked (btw bars 5 & 6) (see pic 4).

Several other blockages occurred, especially as the channel got longer. These blockages went on a cycle of blocking and unblocking itself. The tip progressed despite blockages however its possible higher heads were needed to progress the tip when blockages occurred.

Eventually (with head increases) instead of the tip going through ‘depression’ it formed a new tip and went around it (see pic 5).

I defined the tip as reaching the u/s end when it was under the u/s box however I couldn’t actually see where the tip was because there was fine sediments/build-up resting on the lid making it opaque.

I left the test running for 5 days to see if it would fail. When it didn’t seem like it would I raised the head by 50mm and left it another day but then ended the test. I ended the test because a) Hamish was going on leave so I wanted his help before he left and b) fine sediment had entered the water from flume 3 (as can be seen by the cloudy water in the u/s box- see pic 6). I was concerned that perhaps fine sediment was entering the syd sand pores making it a) less permeable and b) harder to fail.

This test was the first test I measured density with the small push tubes. I’ll need to measure a few tests before I can comment on the reliability and variability of measuring density with this method, but for this test I got:

Sample	Dry unit weight (kg/m^3)	Relative density	depth	Distance from exit (mm)	Distance from centreline (-ve is left of CL)
1	16.01	0.85	0	708	125
2	16.05	0.87	0	1273	-75
3	16.27	1.01	0	2507	-95
4	16.57	1.18	0	3647	87

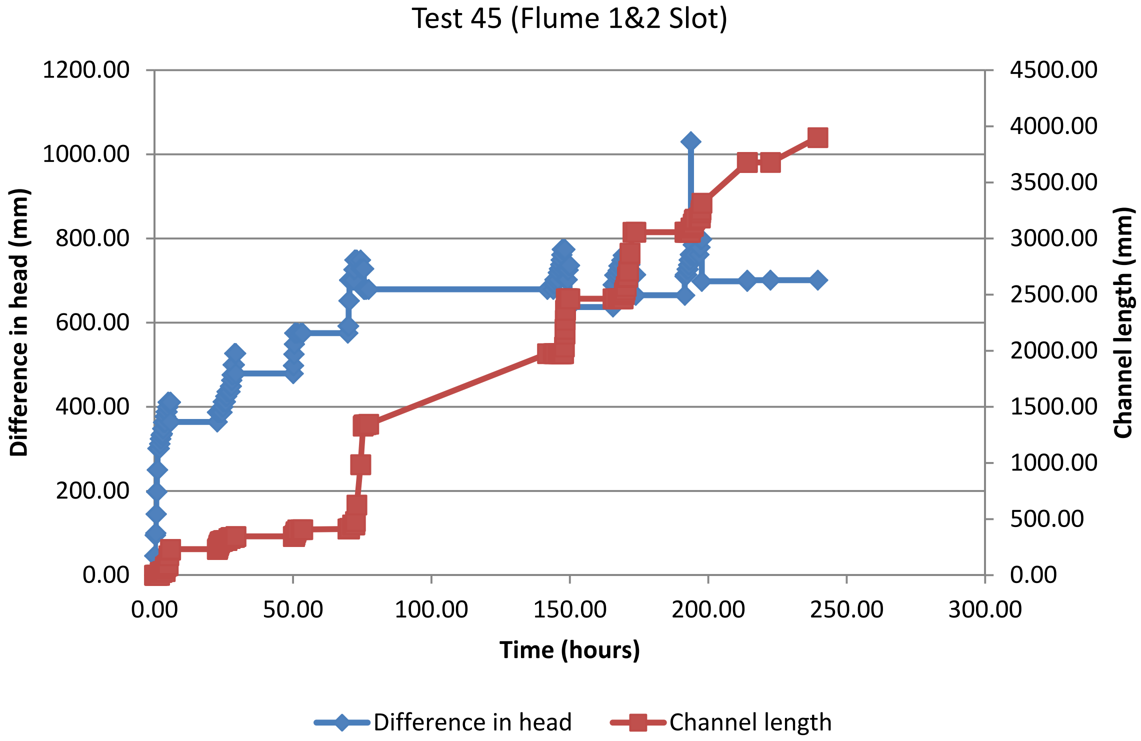

With respect to comparing it with slot tests of other lengths, it behaved as I expected: the tip progressed at similar hydraulic gradients, i.e. when the L was 3 times longer, the critical head was 3 times higher. It's possible this means the seepage velocities entering the tip required for progression is similar.

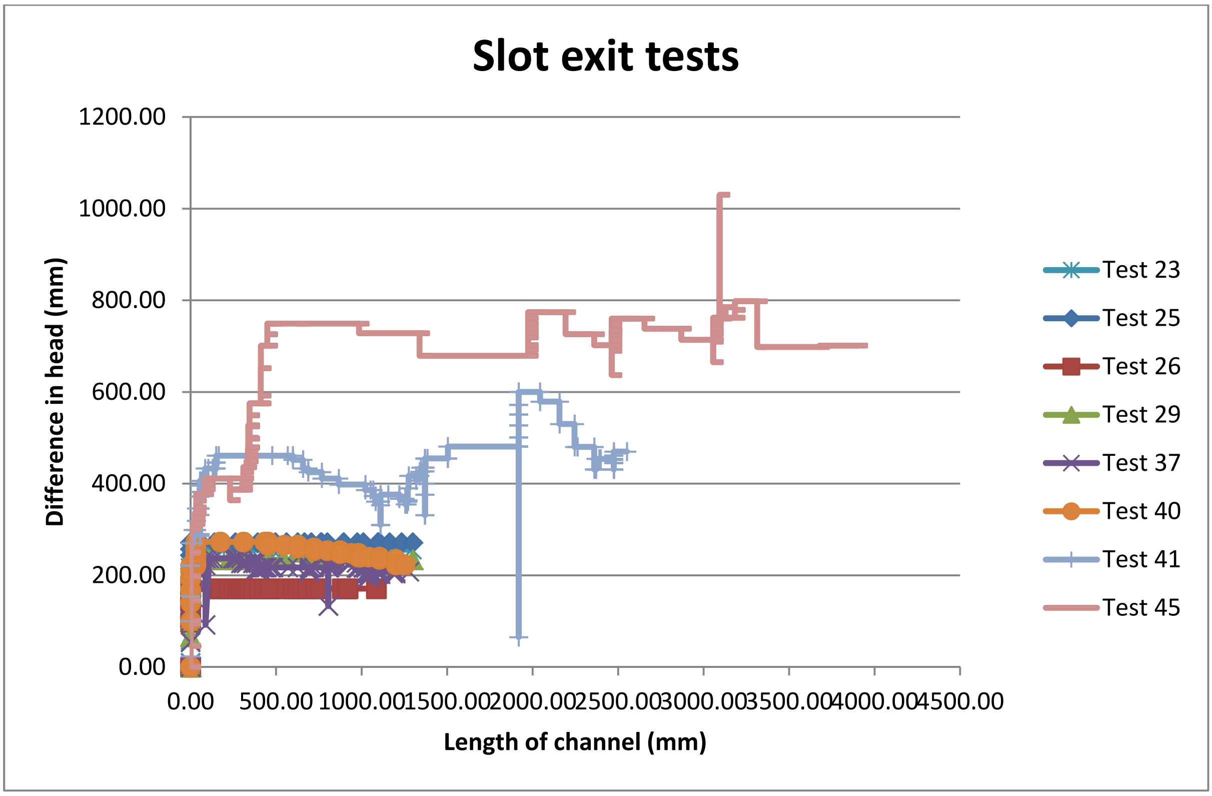

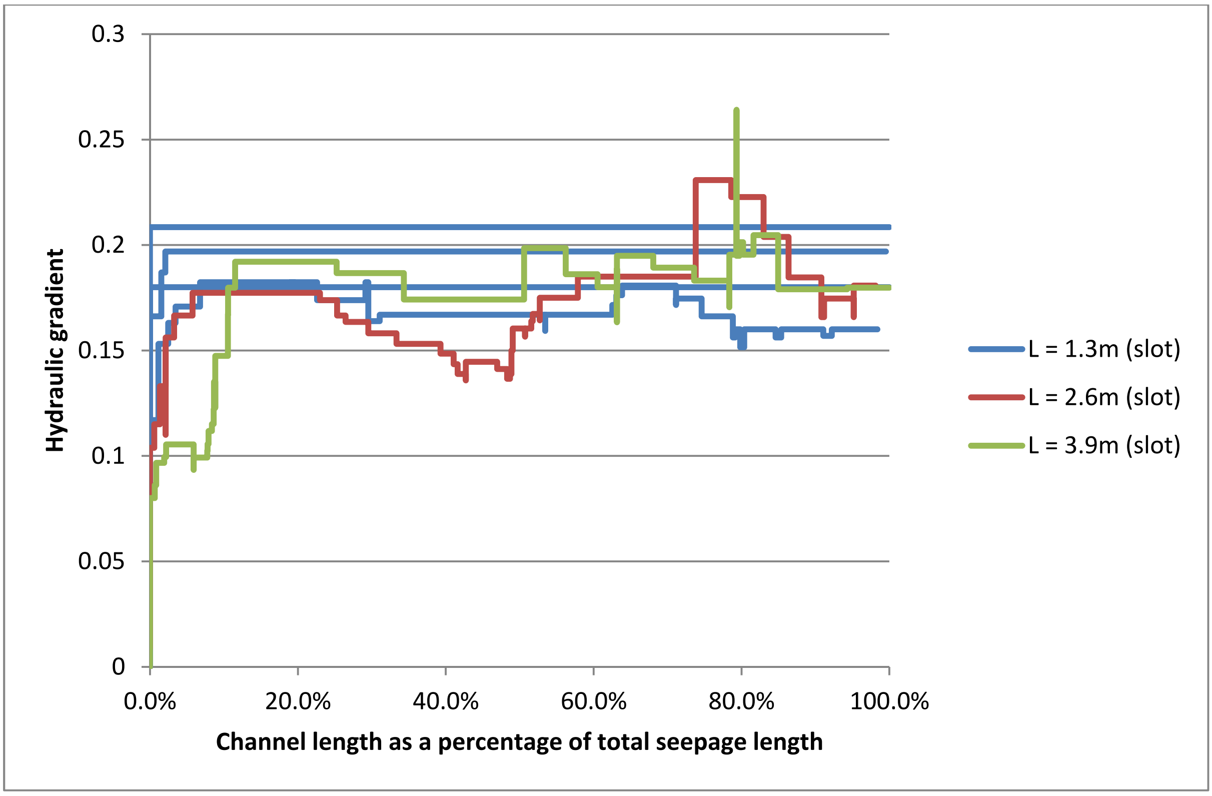

What was unexpected was an initiation gradient that was somewhat lower than the others and a slightly longer length of channel when critical head was reached.

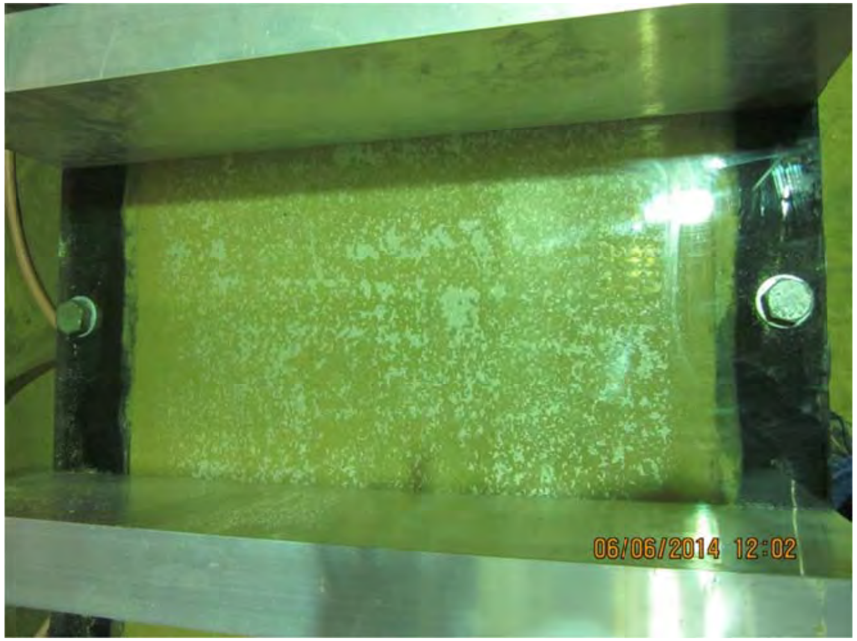

Figure 45-1 CO2 bubbles took longer to dissolve (than a L=1.3m flume)

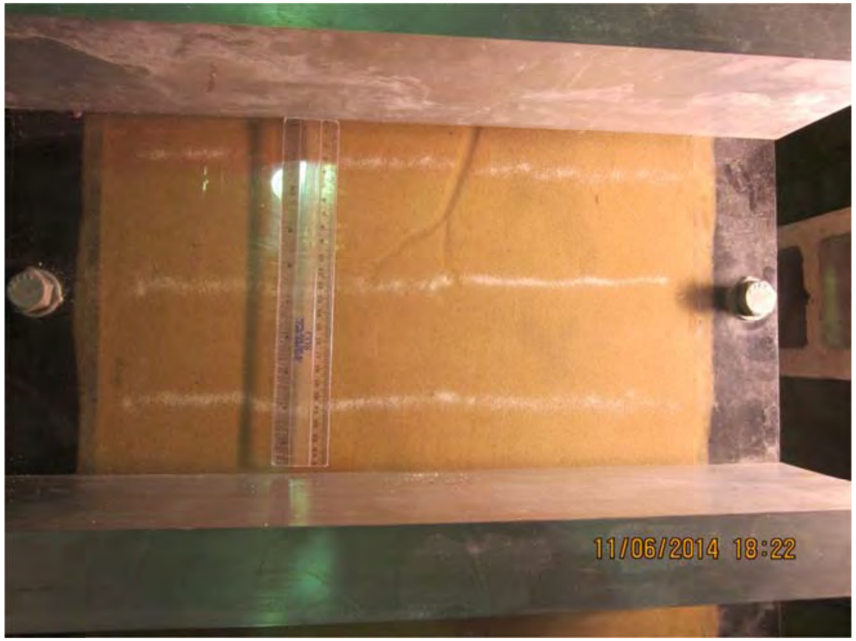

Figure 45-2 new tip branched off channel

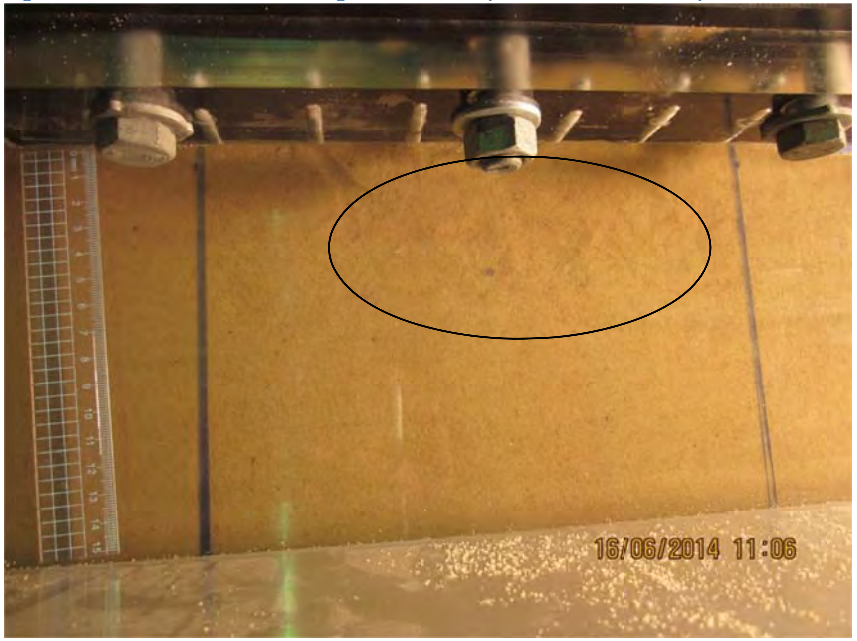

Figure 45-3 Region of perspex not coated with silicon (small depression in sand's surface)

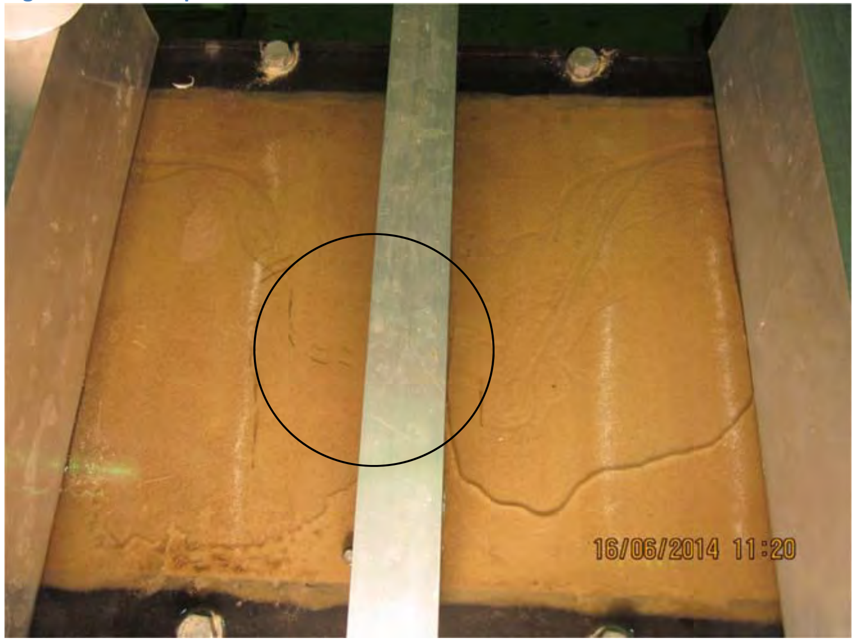

Figure 45-4 Channel blockage between bars 5 and 6

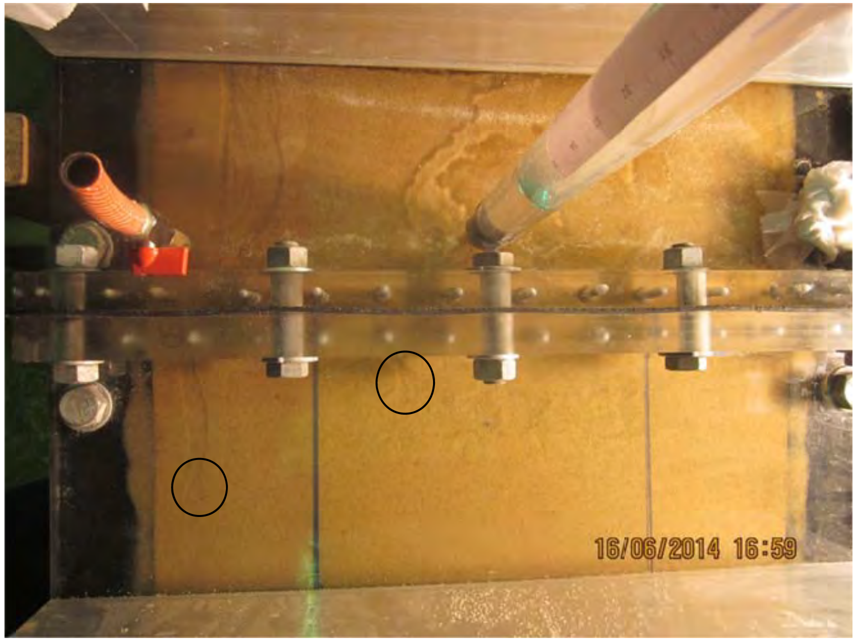

Figure 45-5 Instead of tip going through depression a new tip formed

Figure 45-6 Water cloudy from suspended fine sediments from other test

Backward erosion piping test data sheet

Test #	46	$m_s + m_w$ after 'drying'		kg
Date	11-6-14	m/c after 'drying'		-
Soil	Sydney sand	V_s	0	m^3
Flume	4	$V_s + V_w$ in flume		m^3
Exit type	circle	void ratio		-
seepage length	1.3 m	relative density	4.705882353	-
head in bladder tank	5 m	avg. time for 50mL	5.9	s
bladder pressure	50 kPa	Q when ΔH = 0.1m	#DIV/0!	L/min
compaction	rain		0.51	

50ml/5.9s
8.47ml/s
0.51 L/min

time	head (mm)	observation
4-Jun		
11:15		inflated bladder
6-Jun		
10:45		CO2 on
4ish		CO2 had run out (don't know when) so have to re-do.
10-Jun		
11:30		CO2 on
4:45		CO2 off
4.55		water on
11-Jun		
11:20	0	there's sand on top of the perspex
		around the lid. Perhaps, because
		it's so loose, sand was ejected
		during the infilling process. See
		happy snap. Handpipes (9) are
		installed + ready to be used
		for 1st time. Unfortunately I don't
		have the dummy so I've not
		been able to set datum. Instead
		I've marked where water level
		is whilst at datum.
11:30		now that I've wiped the sand from
		on top of the lid away I can
		see there are small voids
		where the sand has left from (see
		happy snap).

Test 46

time	head (mm)	observation
11.35	↑ 22	I'm expecting initiation to be btw
		50-100 and critical around 150.
11.37		Fluidisation in hole.
11.48	↑	
11.49	↓ 0	I had to take back to datum
		cause I hadn't yet put markers
		on standpipe indicating datum
		level.
12.22	↑ 20	fluidisation in hole
12.42	↑ 46	
1.42	↑ 57	
2.02	↑ 67	
2.11	↑ 79	
2.44	↑ 93	
3.00	↑ 105	
3.16	↑ 115	
3.17	↑ 128	
3.20	↓ 103	Q = for sand 6.2, 5.5, 5.7, 5.3, 6.8 s.
3.24	↑ 142	
3.45	↑ 152	
3.56	↑ 163	initiation
3.57		25.5
4.21		A channel has formed from location
		as sketched:
		
		See happy snap.
		this sand is lower
		than rest because
		it hasn't been
		pushed up by
4.22		tip 10abl. bladder (perhaps
		Effectively this is some settlement)
		behaving like a collapse
		slope exit now.
4.30		30abl
4.33		In an attempt to start a channel from the
		hole I reached in with a cable tie and
		started a channel. ~~Cha~~ Call this channel
		'B'.
4.35		B ≐ 50ae and 'A' 65abl
4.37		A 73abl and approaching wall.
4.41		B at box wall. A 78abl
4.46		A 85abl
4.52		B other side of box wall. A 90abl
5.20		A has branched (see happy snap) Furthest
		tip is 100abl. B is under RI.
5.21	↓ 115	

Test 46

time	head (mm)	observation
12-6 12-06		
2.05	115	A 110 ab1. B. under b1.
2.09	↑ 165	
2.22		A 140 ab1. B 68 ab1.
2.26	↓ 140	(~~A~~ B @ 20%.) 75 ab1
2.36		A 155 ab1. B. 79 ab1.
2.53		A 155 ab1 B. 78 ab1
2.54	↑ 153	
3.01		A 160 ab1 B. 88 ab1
3.04		temp = 16°
3.23		B 13 about 18 mm from green1.
3.24		A 160 B 148
3.25		Green1 43mm.
3.38		A160 B155
4.15		B 155
4.45		A160 B173.
4.59		B175
5.25	↓ 103	A160 B175
13-6		
9.46	100	A160 B175
9.47	↑ 149	~~B150 (going towards CHS)~~.
10.04		B180 (" " ")
10.22		B203
11.20		B at b2 and still tending
		towards CHS (see happy snaps)
11.52	↑ 165	only recording B now. at b2.
1.00		15 ab2
2.20		under b3. happy snaps taken
2.24	↓ 140	
3.20	↑ 152	under b3.
4.22	↑ 165	" "
5.13	↓ 115	
10.45 16-6	113	under b3. No particle transport.
10.53	↑ 160	
11.17	↑ 174	
11.58		68 ab3 (about 50mm away from 3CHS.
12.20		150 ab3
12.25	↓ 150.	162 ab3
12.58		162
1.35	↑ 165	162 ab3
2.14		168 ab3
2.30		173 ab3
2.45		180 ab3
2.57		218 ab3
3.07		238 ab3
3.22		250
3.38		under b4

Test 46

time	head (mm)	observation
4.02		under b4.
4.21		" "
4.56	↓135	12ab4 (@ a01.)
5.01		12ab4
5.19	↑148	12ab4
5.29		12ab4
5.52		12ab4
5.56	↓ 98	12ab4
17-6		
9.34	↑ 147	12ab4
10.17	↑ 160	12ab4
10.29		12ab4.
10.57	↑ 173	
11.04		18ab4 and 2 sets of 60 btw bars 2+3.
		↳ detachment from tip again.
11.07		23ab4
11.16		63ab4
11.21		75ab4 . 60@ tip.
11.33		first noticed through to u/s end. And there's
		a small blockage just u/s of bar4.
5 35		left it running to see if it would fail.
		The channel is blocked around b4 and
		btw bars 1+2. A new channel has
		started whose tip is about 50ab2.
		I'll leave it running overnight to see
		if it makes any progress.
18-6		
11.14		no different overnight. The ~~new~~
		original channel is blocked under b4 and
		new channel tip is btw 2+3.

Test 4~~5~~6

	Time	head	time for 50mL	Avg	Temp
	3·20	103	6·2, 5·5, 5·7, 5·3, 6·8		
12-6	3·04				16
13-6	10·40	149	3·4, 3·9, 4·8, 3·6, 4·3, 4·7, 4·2		15
	3·24	152	4·3, 4·4, 3·6, 3·7, 4·8, 4		16·5
16-6	10·51	113	6·4, 7·1, 6·2, 6·8, 6·3, 7·9		14
	5·56	148	3·6, 4·8, 4·6, 3·1, 4·8, 4·8		
17-6	10·13	147	6·1, 4·5, 3·6, 5·3, 4·8, 4·8		13
	11·18	173	4·2, 4·6, 4, 3·2, 4·3, 4·2, 3·5		
after [illegible]	11·36	173	3·7, 4, 3·6, 3·7, 4·4, 4·3, 3·8		

Test ~~45~~ 6 Upstream L = 320mm   L = ~~623~~ 625   Downstream L = ~~922~~ 925

Date	Time	Row 1 right	Row 1 middle	Row 1 left	Row 2 right	Row 2 middle	Row 2 left	Row 3 right	Row 3 middle	Row 3 left
	5.23	173	165	176	207	207	207	238	239	240
	5.30	160	154	163	182	184	183	203	204	205
13-6	10.06	172	163	175	204	205	205	235	236	237
	2.22	188	183	189	217	216	206	247	250	251
	3.28	~~15~~ 183	177	183	210	210	200	239	240	240
16-6	10.48	173	173	177	192	192	188	210	210	211
	12.22	188	190	199	221	221	216	251	251	242
	2.59	176	186	193	213	213	208	241	240	227
	5.54	173	185	193	208	208	206	232	232	221
17-6	10.15	171	185	192	206	207	205	106	105	96
		178	194	203	220	220	220	125	124	115
	11.36	174	191	204	221	222	222	128	126	118

Row 1 right	Row 1 middle	Row 1 left	Row 2 right	Row 2 middle	Row 2 left	Row 3 right	Row 3 middle	Row 3 left

46. Test 46 (flume 4) circle

Test 46 was with the circle exit and was the 1st test looking at the effect of soil density. This is also the first test I had the standpipes installed for.

I rained the soil in with the rainer held approx. 1m above the sand's surface.

Before starting the test I noticed sand on top of the Perspex around the hole as well as a void that the transported sand left (see Pics 1 and 2). Perhaps this because sand so loose it was locally transported when water first filled the top of the flume.

I also noticed that sand downstream of the hole (where the bladder pressure does not directly load the soil) was not pushed up against the lid (there was a gap) (see pic 3). Perhaps I'd gotten some settlement of the sand during saturation.

Initiation occurred at a head of 163mm but it didn't occur at the exit. It occurred near the LHS of the flume (see pic 3). Essentially the 'exit' was behaving like a slope exit on account of the gap between the sand and lid downstream of the circle. So (when channel A was 30 ab1) I artificially created a channel from the circle but pushing a cable tie in. I refer to this channel as channel 'B'. Channel B progressed to bar 1 without further head increase.

Channel A branched out shortly after bar 1 and continued to progress (with increase in head) up to 160 ab1 after which is stopped. From then on progression only occurred at tip B (see pic 4).

The results are plotted in figures 5 and 6.

The critical head was at 174mm. This is about a 17% decrease from the average critical head carried out in more dense samples (that were vibrated in). This suggests the soil density does affect the critical head and it makes sense- the less dense, the more permeable and the lower the head required to progress seepage velocities required for erosion.

I didn't leave the test running long enough for failure (don't know why).

Four density samples were taken. The results:

Volume (m^3)					Sample location (mm)		
Test	Dry Density (kg/m^3)	Dry Unit Weight (kN/m^3)	Void Ratio (e)	Relative Density (Id)	Depth	distance from d/s end	distance from centreline (-=left of centreline)
Test 46 Syd Sand	1612.910392	15.82265094	0.674814169	0.736387238	0	-117	
	1619.644882	15.88871629	0.667850285	0.777351264	0	320	
	1662.577257	16.30988289	0.624781746	1.030695611	0	1863	
	1649.108276	16.17775219	0.638052041	0.952635052	120	953	

What's encouraging is the relative densities of 0.74 and 0.78 are less than normal results but what's not encouraging is the range in results- 0.74 to 1.03. I don't think this method is very reliable.

Note the SLR photos for this test are of the standpipes (not channel progression).

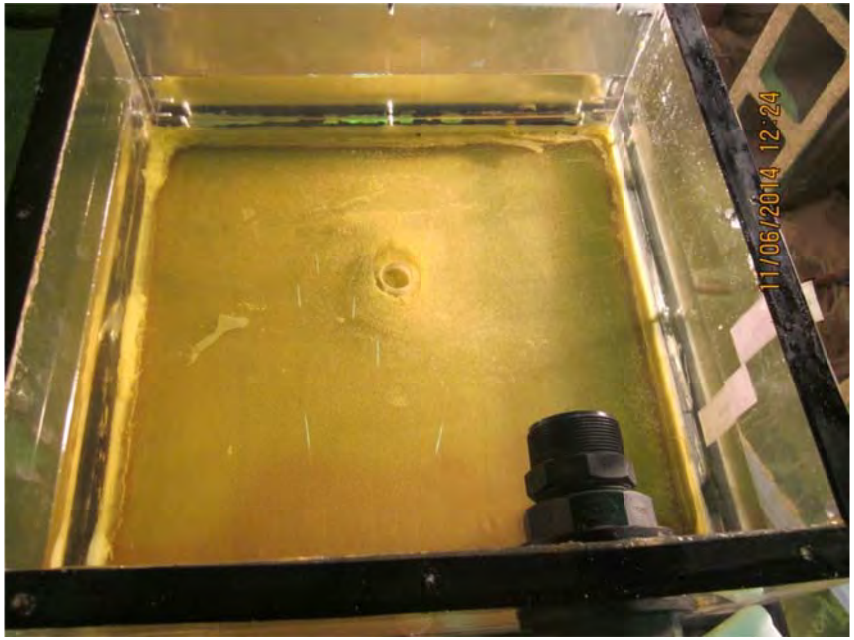

Figure 46-1 sand on top of the Perspex around the hole

Figure 46-2 void that the transported sand left

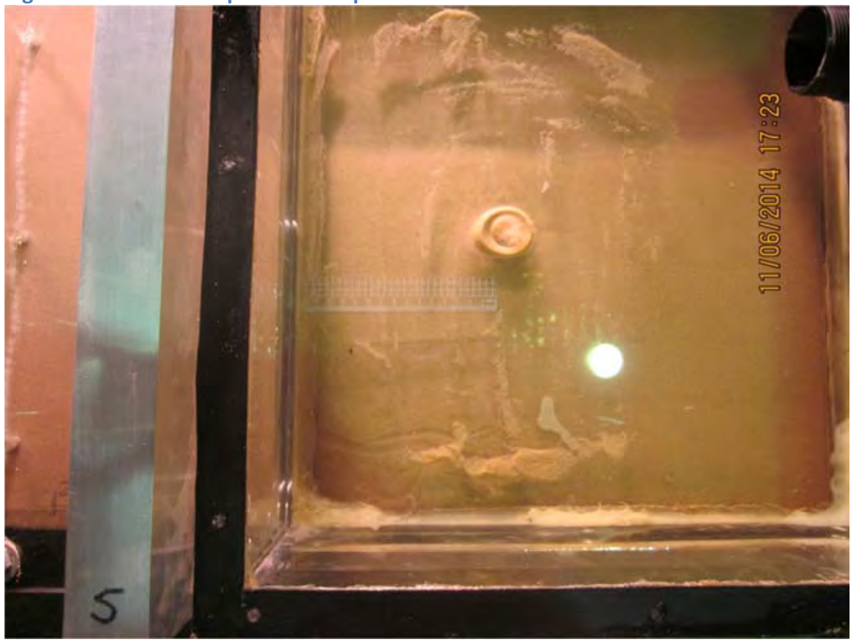

Figure 46-3 sand downstream of hole not pushed up against lid and channel ‘A’ initiated LHS (not from hole)

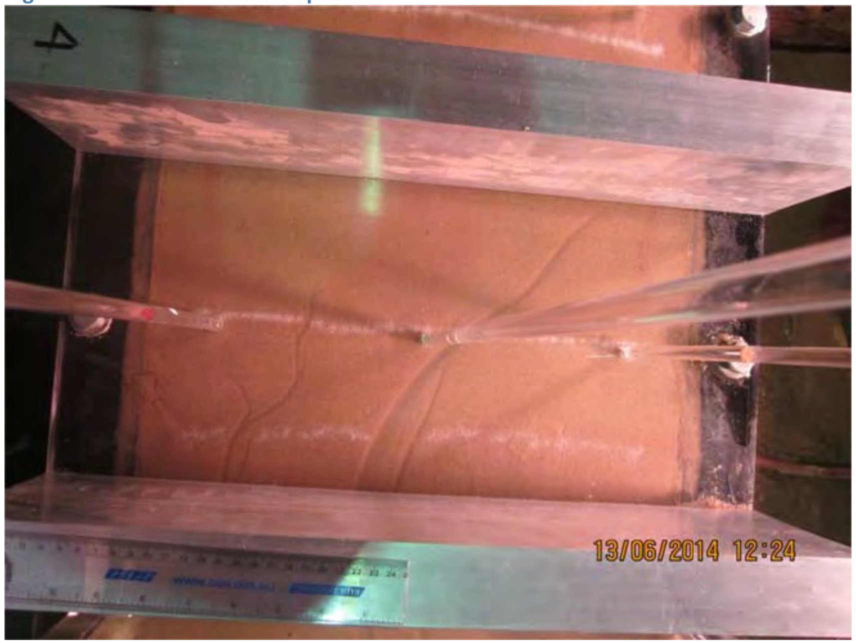

Figure 46-4 Channel A stopped at 160ab1 but channel B kept going

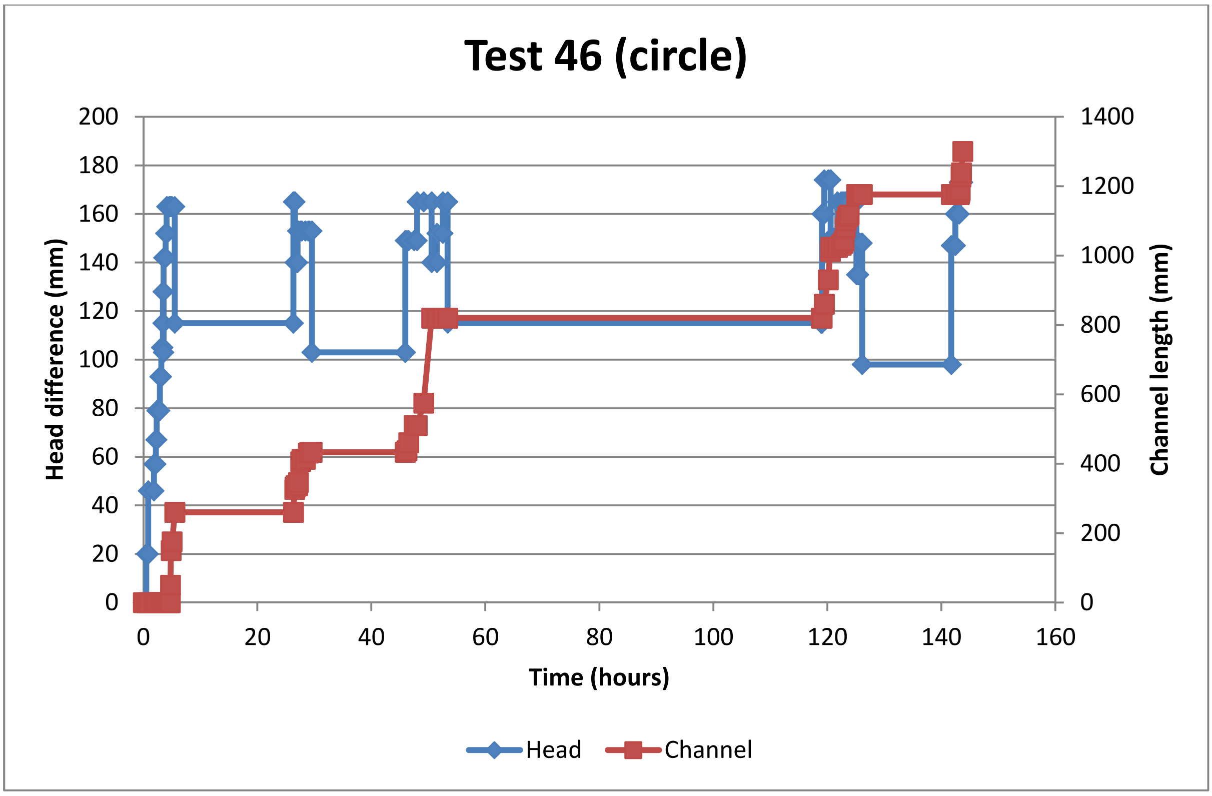

Figure 46-5 Test 46 chart

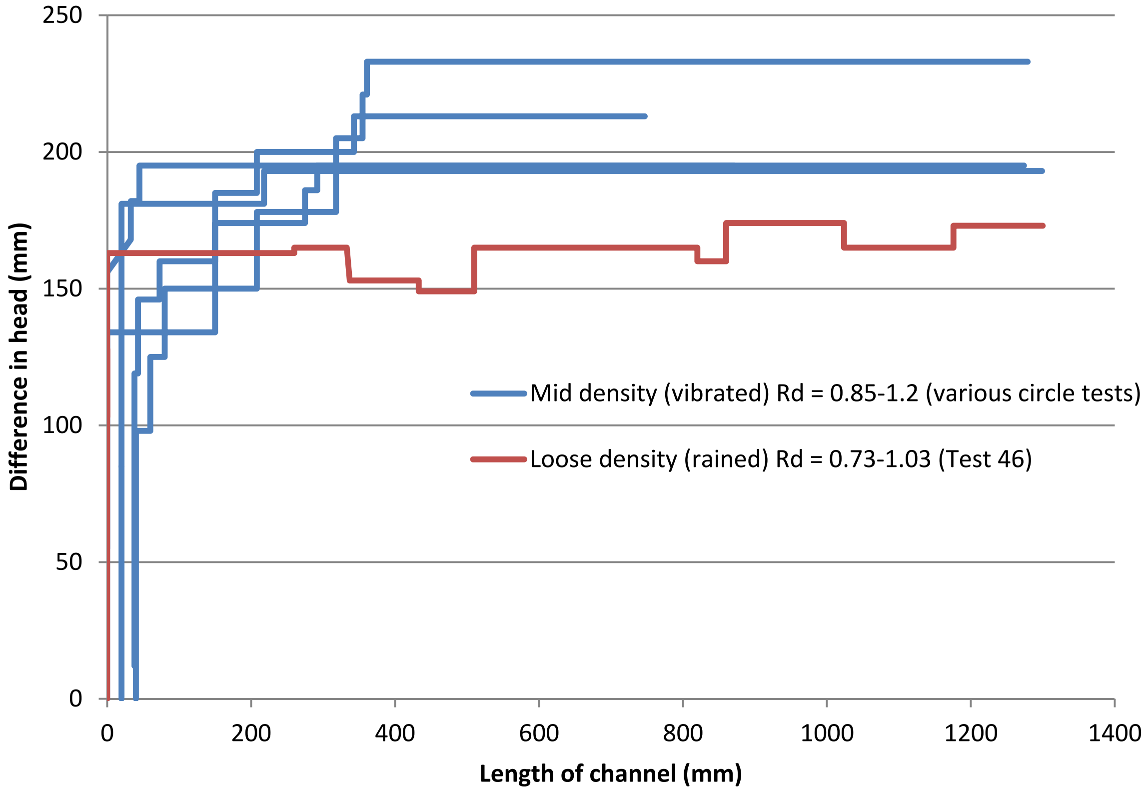

Figure 46-6 H vs CL for different densities

Backward erosion piping test data sheet

Test #	47		$m_s + m_w$ after 'drying'		kg
Date	19/06/2014		m/c after 'drying'		-
Soil	SW		V_s	0	m^3
Flume	3		$V_s + V_w$ in flume		m^3
Exit type	plane		void ratio		-
seepage length	1.3	m	relative density	4.705882353	-
head in bladder tank	5	m	avg. time for 50mL		s
bladder pressure	50	kPa	Q when $\Delta H = 0.1m$	#DIV/0!	L/min
compaction	vibrated underwater				

time	head (mm)	observation
18-Jun		
11:15		placed all soil and lid on underwater
15:30		inflated bladder
19 Jun		
11:02	0	
11:03	↑47	I won't be able to see when it
~~11:34~~	↑	initiates because I can't see
		through the water in the d/s box.
11:34	↑≐100	
11:35	↓≐50	Sand + flow was rushing along the top (see
		happy snap + video). It seems there's
		a gap btw the soil + the lid.
11:48	↑=75	~~plus~~ (video) + flow measurement.
11.50		end of test.

Test 47

above top of lid

100mL / 3.4s
29.4mL/s
1.8L/min

		u/s ~~Row 1~~			Row 2			Row 3						Q
time	head	~~right~~	middle	left	right	middle	left	right	middle	left	time for ~~50~~ 100mL	Avg	Temp	
11.20		182									2.7, 3.8, 3.4, 3.4, 3.7	3.4	15	1.8L/min
											for 200mL = 3.1, 3, 3			

47. Test 47 (flume 3) plane

Test 47 was the first test in flume 3 in the pool and the 2nd test in SW.

The placement process was:

1. Fill the flume with water up to 1/3
2. Slowly shovel SW in up to 1/3
3. Vibrate
4. Slowly shovel SW into the flume up to top (the intention was to have the water level just above/at the soil so no water was added- as soil was placed in the water the water level rose always keeping above the soil.
5. Fill pool with water so water level at/just above the flume (see pic 1)
6. Vibrate
7. Screen soil surface (see pic 2)
8. Raise water level in pool
9. Suspend lid above flume but in water and remove bubbles from underneath by wiping down with hand (see pic 3)
10. Lower lid onto flume and do up bolts
11. Lower water level in pool so top of flume can be seen
12. Inflate bladder
13. Test

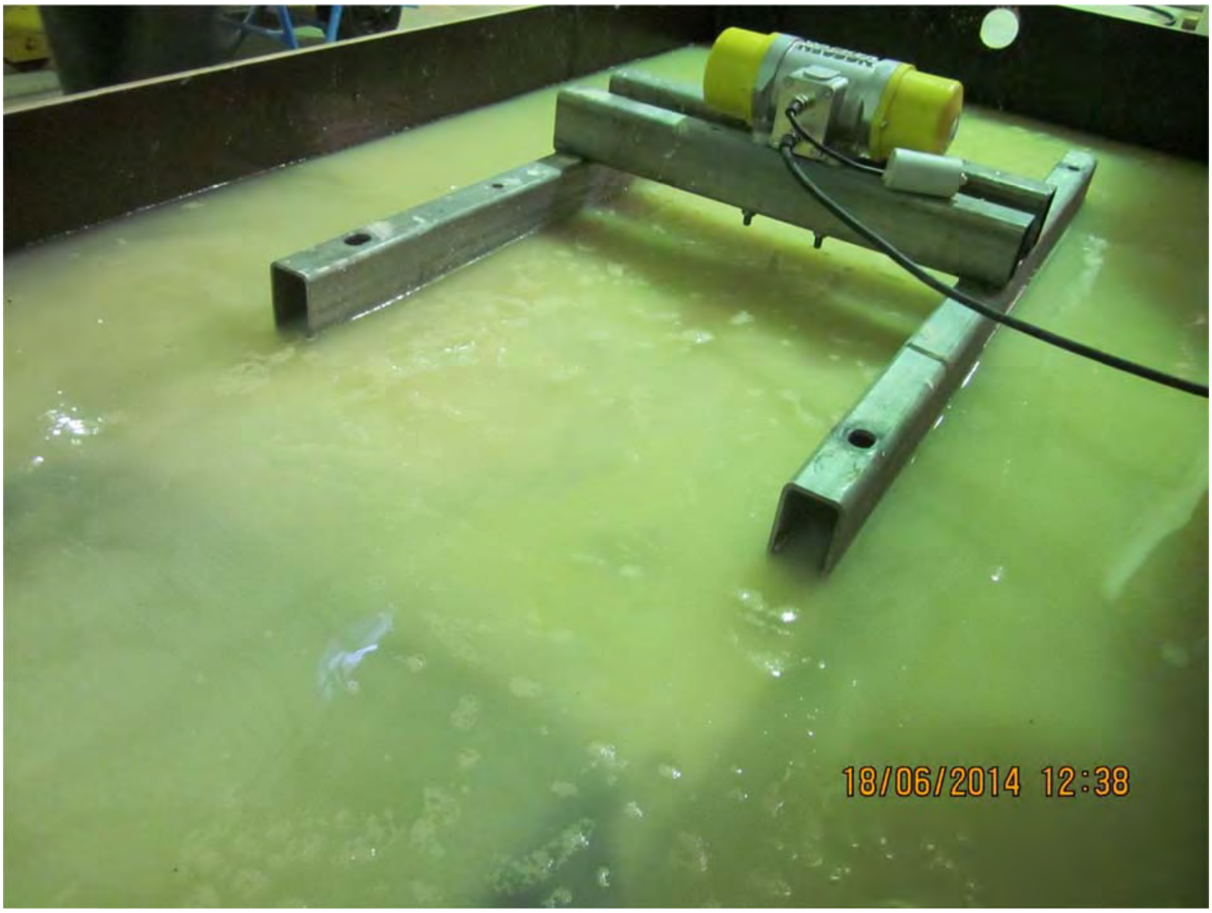

Pic 1: last vibration with flume full of soil and water just over top of flume

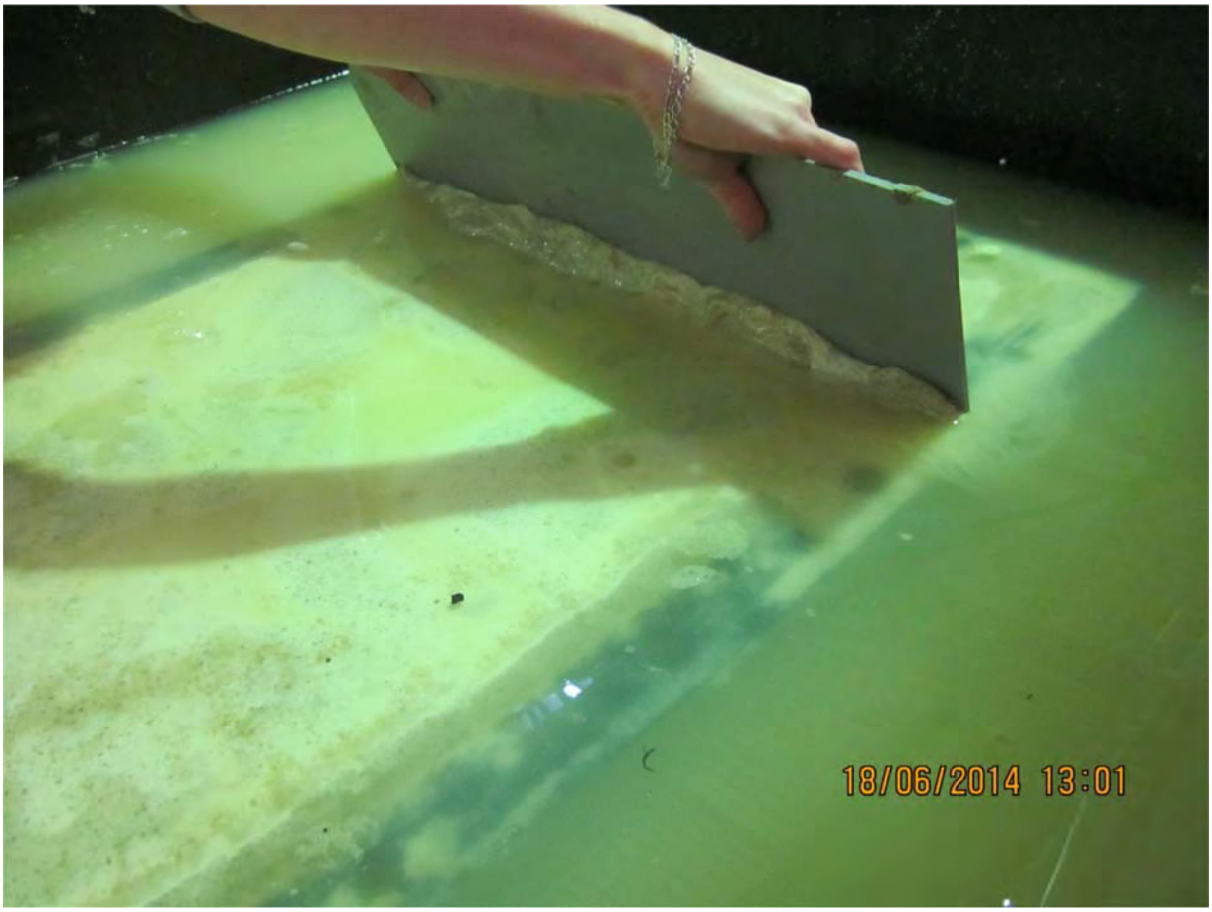

Pic 2: Screen off top surface of soil

Pic 3: Wiping bubbles away from underneath lid

Observations made during this process:

1. As soon as the first 1/3 of soil was placed in the flume the water became very cloudy. The fines suspended in the water. I filled a cup with the water to see if the soil would settle. Pic 4 is the cup first filled and Pic 5 is after 24 hours. As you can it doesn't settle. I showed this to Robin and I suggested the fines were dispersive however this surprised him because he expected the fines to be non-dispersive (silica or quartz as opposed to clay minerals) however I think my cup test suggests it is.

   This has 3 implications:

   a. The soil grading would be changed because the fines would wash out. The soil grading could go from Fig 1 to Fig 2 (assuming all the Sibelco 300g washes out). This reduces the Cu from 6.8 to 4, shifts the curve to the right (so d50 about 0.4mm) and increases the permeability.
   b. Water can't be sent down the creek. Instead it was pumped into the sewer.
   c. Because soil is removed from within the flume a gap forms between the soil and the lid and BEP is not possible.

Pic 4: water from experiment soon after lid has been placed on the flume

Pic 5: same water 4 hours later (fines don't settle)

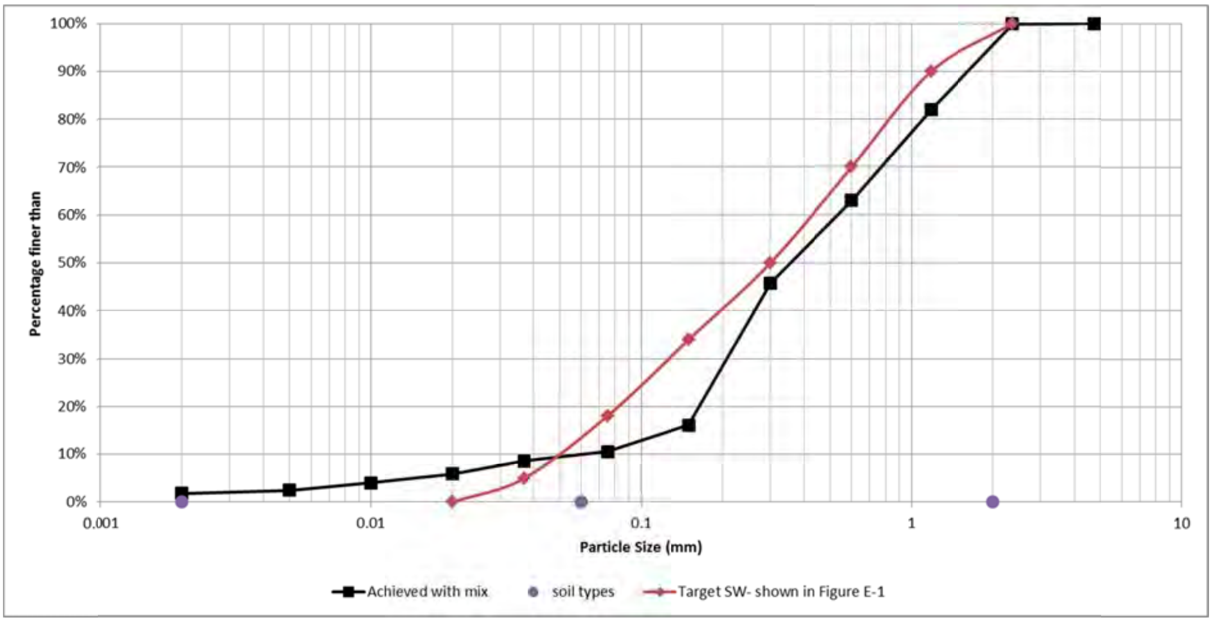

Fig 1: SW grading

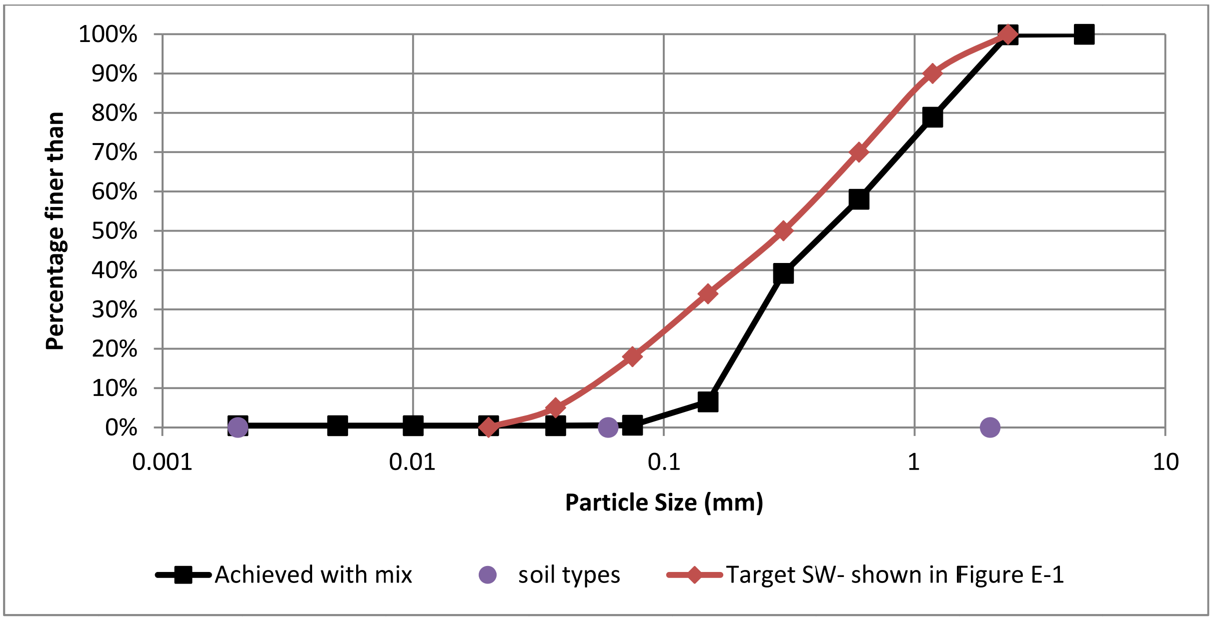

Fig 2: Remnant grading if all Sibelco 300g is washed out

2. Vibration caused fine-grained 'boils' and segregation. During the vibration I saw concentrations of light-coloured fine sediments. After vibration, when I felt these areas, they would be soft but compacted and dense elsewhere. I'm pointing to one of these spots in Pic 6. I noticed these areas were concentrated around the vibrator (as seen in Pic 7). I have this observation on video.
I suspect a high degree of segregation because afterwards, when I felt the surface of the soil, I could feel a 10mm-or-so layer of clayey soil above a coarser soil.

Pic 6: concentration of fine-grained soil

Pic 7: fine-grained concentrations at points of max vibration (under vibrator)

Once I started the test the first thing I noticed was the flow from the d/s valve was much larger than expected. It was about 1.5L/min at a head of only 50mm where as in test 38 when I used this SW last time, the flow was 0.08L/min with a head of 1.7m.

I saw no backward erosion (but note I couldn't see the exit because the water in the d/s box was turbid. So I raised the head to 100mm and saw flow moving through between the lid and the soil which gouged a depression along the centreline of the flume (Pic 8). I have videos of this.

This suggests a gap between the lid and soil was present. Therefore BEP could not occur and the test was ended.

Pic 8: Water flowing through gap between lid and soil and gouging a 'channel' through centre of flume.

Lessons learnt:

1. I can't place soil and the lid underwater when the fines suspend in the water
2. I can't vibrate graded soils

Next step: I'd appreciate your thoughts on this. I think I have one of 2 choices.

1. Create a soil whose grading is courser so no Sibelco 300g product is needed, or
2. Try tamping in moist SW and CO2ing. I have tried this before with Syd sand and concluded it didn't work because when the CO2 pushed water out a network of channels were formed at the d/s end and because I didn't get the same results as previous tests (when I CO2ed dry sand). But perhaps if I have the SW not as wet as the syd sand was (but just wet enough to prevent the fine particles becoming suspended in air) then maybe the network of channels won't form as they did in the syd sand (???).

Backward erosion piping test data sheet

Test #	48	$m_s + m_w$ after 'drying'	kg
Date	25/06/2014	m/c after 'drying'	-
Soil	SW	V_s	0 m^3
Flume	3	$V_s + V_w$ in flume	m^3
Exit type	plane	void ratio	-
seepage length	1.3 m	relative density	4.705882353 -
head in bladder tank	~~5~~ 4.8 m	avg. time for 50mL	s
bladder pressure	50 kPa	Q when ΔH = 0.1m	#DIV/0! L/min
compaction	placed loosely underwater		

time	head (mm)	observation
~~2:39~~		
2:20		bladder inflated and water flowed
		up the top RHS (b/w exit and bar
		3). The flow of water created
		a channel (see happy snap).
		I'm pretty sure this channel
		reaches the d/s end but I
		can't be sure because I can't
		see through the d/s water.
2.48	0	started
2.49	↑ 10	
2:55	↑ 35	½ turn increase as slow.
2.59	↑ 57	d/s level not @ datum yet.
3:44	↑ 80	" "
3:59	↑ 104	" " but is rising v. slowly.
4.16	↑	
4.31		water level in d/s box ≈ 5mm below
		datum. Given it's late afternoon +
		Bronson can run this test on Friday
		I'm going to drop back to datum +
		return to this test later.
4.32	↓ 16	
26-6		water level in d/s box @ datum.

Test 48

	time	head (mm)	observation
27.6.14	11:41	↑ 42	
	11:56	↑ 81	
	12:13	↑ 116	
	12:33	↑ 145	
	12:48	↑ 176	
	1:05	↑ 200	
	1:23	↑ 236	
	1:49	↑	
	2:04	↑ 312	
	2:27	↑ 352	Fixed ~~[illegible]~~ flow measuring.
	2:47	↑ 393	Pump Malfunction. Head ↑ ~550
			Some very fine particle erosion in the channel.
	3:15	↑ 444	
	3:34	↑ 494	Some air bubbles are moving.
	3:45	↑ 545	
	3:59	↑ 594	
	4:17	↑ 647	Fine particle erosion
	~~4:38~~	↑	Large particles & air bubbles eroded.
			Channel widened
	4:38	↑ 662	
	4:46	↓ 361	Dropped & left over the weekend.
	5:10	↓ 0	
30/6/14	12:56	↑ 488	
	1:14	↑ 538	Some movement of particles in channel (not tip)
	1:30	↑ 551	
	1:39	↑ 577	
	1:44	↑ 619	
	1:54	↑ 648	
	2:06	↑ 660	
	2:11	↑ 673	
	2:26	↑ 686	
	2:40	↑ 700	Some particle movement in chanel.
	2:59	↑ 713	~~Fine~~ " "
	3:08	↑ 741	Fine particle movement in channel.
	3:27	↑ 830	Pump Malfunction. → Some fines movement
	3:28	↑ 751	
	3:40	↑ 773	
	3:47	↑ 801	Fines. Large portion of channel eroded at
			~~[illegible]~~ 190 AB1
	4:05	↑ 827	
	4:21	↑ 851	Fines.
	4:34	↑ 876	channel erosion.
	4:50	↓ 0	Left overnight.
/7/14	10:50	↑ 789	
	11:05	↑ 885	Fines.
	11:18	↑ 918	Fines
	11:30	↑ 947	Fines

Test 48

	time	head (mm)	observation
1/7/14	11:46	↑ 987	Some large & fines.
	11.55	↑ 1017	
	12:00	↑ 1044	Tapped the lid near the tip ~~[illegible]~~ → large
			erosion of all particles. The larger particles
			tended to block while the fines washed
			out. Channel widened near the tip.
	12:20	↑ 1068	
Water overflowed from white container	12:38	↑ 1095	
	12:48	↑ 1120	
	12:57	↑ 1145	
	1:07	↑ 1169	
	1:13	↑ 1195	
	1:18	↑ 1219	
	1:28	↑ 1243	Channel blocked at AB1 → 30AB1
			& 110 AB1 → 170 AB1 caused by erosion
			of soil at 220 AB1
	1:40	↑ 1268	
	1:45	↑ 1293	Some erosion within channel. Still blocked.
	1 51	↑ 1318	Completely unblocked. Tips look to have
			progressed. Looking downstream, Left tip has
			progressed under bar 2, right tip (closest to wall) looks
			to have joined with channel on other side
			of bar 2. Possibly at 65AB2
			Little activity after unblocking.
	2:01	↓ 0	Left ~~[illegible]~~ overnight
2-7	10.30	0	looks very similar to how it did
			yesterday. It's difficult to determine
			where the tip is. It could be 65ab2.
			It could be 200ab2. It could even be
			≐110 ab3. this last possibility is very
			difficult to see - it could even be
			my imagination but there's "hair-line"
			channels btw bars 3 + 4. See happy
			snap. It could be that fines travel through
			first, leaving "hair-line" channels, then as
			larger particles came through, the channels
			get bigger. But what happens first???
	10.38	↑ 475	Note: no longer measuring flow constantly
			because I want to do it on 84 instead.
			I'm gonna say the tip is 200ab2 for
			recording sake but it could be in lots of
			places.
	10.55	↑ 987	Can't see anything happening.
	11.25	↑ 1187	" " " "
	11.48	↑ 1290	" " " "
	12.18	↑ 1325	" " " "
	1.35	↑ 1388	" " " "
	2.10	↑ 1438	

Test 48

time	head (mm)	observation
2:32	↑ 1488	nothing happening.
2:48	↑ 1541	
3:00	↑ 1592	
3:12	↑ 1639	
3:21	↑ 1681	
3:43	↑ 1732	
3:50	↓ water	dropped. Not sure y yet - sump pump stopped.
4:00	↑ 1732	
5:25	↓ 50	~~[illegible]~~
3-7 11:15	↑ 1640	everything looks as it did yesterday.
11:37	↑ 1737	
11:53	↑ 1786	
12:08	↑ 1833	
12:19	↑ 1885	
~~12:31~~	~~↑~~	
12:51	↑ 1933	
1:14	↑ 1981	
1:26	↑ 2030	
1:36	↑ 2079	
1:43	↑ 2130	
1:52	↑ 2177	
1:58	↑ 2227	
2:05	↑ 2276	
2:14	↑ 2325	
2:26	↑ 2374	
2:35	↑ 2423	
2:43	↑ 2474	
2:50	↑ 2526	Some erosion within channel.
3:00		Channel cleaned (widened & deepened)
		channel looks to reach to 65 ab2.
		We can say this confidently.
3:17	↑ 2577	
3:26	↑ 2630	
3:32	↑ 2691	Some channel erosion
3:40	↑ 2745	
3:45		Saw that the channel turned milky (turbid)
		and also an area on the left side (looking
		downstream) between B1 & B2. Could possibly
		be many microchannels (areas that has had
		suffusion ?) This area was about 120 mm
		wide and 250 mm long (potentially longer
		but view is obstructed towards downstream
		end).
3:48		Water is now clear in channels and that
		area.
3:58	↑ 2794	
4:01		Milky again in the described region
4:14	↑ 2845	

Channel appears to be blocked @ 50 ab1.

Note: heard a noise like a ~~[illegible]~~ bang & observed froth in the box spread towards the perimeter. could have been a pressure build up

Time	Head (mm)	Observations
4:23	↑2899	
4:36	↑2949	
4:45		~~Clouds~~ Clouds of water could be seen in the box in the ~~location~~ location of expected channels. ~~There~~ There are 4 small ones on the left & 1 large on the right. The large one is the result of the observable channel whereas the others may not have formed channels yet.

The soil leading to this area looks wetter than before. Could be microchannels or suffusion.

On the left side of the box, a mound of soil has formed about 330mm wide. Coarser material is close to lid edge and finer further

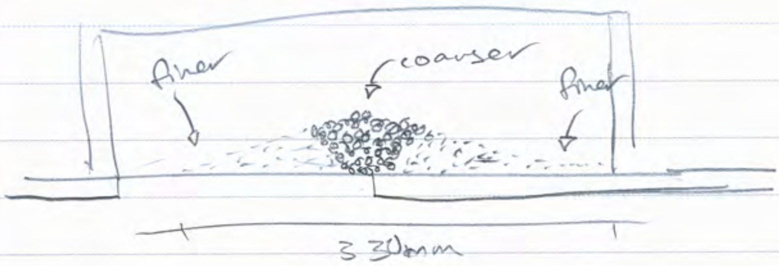

This makes sense for ~~boil~~ channel ~~erosion~~, & boil activity. (greater energy required to move larger particles so they do not travel far from channel exit.

Time	Head (mm)	Observations
4:55	↓0	
4-7		
9:42	↑3100	all looks as it did last night

11.35 I left the lab for literally 2-3 minutes + when I returned water was gushing out of the d/s valve and overflowing the d/s box. the flow was so strong it carried alot of sediment with it and deposited it outside the flume (and pool). This going to make the PSD's non-sense because the top soil was washed away. A large volume of soil is removed from the u/s end. It failed by concentrated flow along the top but I don't know why (or where) the soil 'gave way'. What else is strange is (...) emptied water from the flume + the level dropped in the d/s box but as I wrote this the water level in the box rose again + flowed out the d/s valve (without head applied at u/s end - infact water is below the lid on the u/s end).

12.30 Once the lid was cleared off I could see the likely passage of water/the likely zone of soil that gave way leading to failure. It's along the RHS about 100mm wide.
Once I deflated the bladder the soil dropped a good 20mm.
See happy snaps.

Test 48

		Row 1			Row 2			Row 3					
time	head	right	middle	left	right	middle	left	right	middle	left	time for 50mL	Avg	Temp
12:12	81	214											
12:32	116	249											
1:06	200	335											
2:10	312	447											
3:36	494	628											
4:37	647	781											
30/6/14 2:30	686	819											
4:31	851	985											
12:10	1044	1174											
4-7 10:00	6m	too high											10
1115		too high									6, 7·6, 6·6, 5·6, 5·4, 5·8		

48. Test 48 (flume 3) plane

Test 48 was the second test in flume 3 in the pool and the 3rd test in SW.

The same placement process was used as test 47 except effort was made to keep the water level no more than 50ml above the SW and the vibrator wasn't used. Pic 2 shows soil being placed into shallow water. We tried tamping the first few layers but upon tamping the plate sank and when picked up disturbed the layer even more- see pics 1 and 3.

Figure 48-1 tried tamping first few layers

Note water was still very turbid (suggesting loss of fines) but not as turbid as Test 47. See pic 4.

When we inflated the bladder water was squeezed out of the soil and concentrated to form a channel that reached about half-way between bars 2 and 3 and (probably) extended to the exit. See pic 5.

This channel did not change a lot through the experiment. It did meander slightly; carry fine and coarser particles through it; and block and unblock itself but the tip never progressed. I consider this channel to be 'concentrated leak flow' as opposed to BEP. Pic 6 shows how little the channel changed (it was taken 7 days after pic 5).

During the experiment the appearance of the soil changed slightly- either with so-called 'hair-line' channels (pictured in Pic 7) or a 'bonier' appearance (pic 8). I suspect both are a result of the fine fraction moving through the coarser fraction, i.e. suffusion. In support of the theory that suffusion was occurring, there were times through-out the test when cloudy water was seen to move through the 'hair-line' channels as shown in Pic 9.

On the 6th day of testing a build-up of soil in the d/s box was first noticed (as shown in Pic 10). This build-up was material deposited at the exit, with more coarse soil at the exit and finer material at its furthest reaches.

The head had been raised to 3.1m over 7 days (lowered to datum overnight and over weekend). The test ended suddenly with no warning when a 'strip/corridor' of soil about 100mm wide along the RHS of the flume apparently gave way. I say 'apparently' because it's difficult to know for sure what happened because a) I wasn't in the lab at the time (I'd left for about 2-3 minutes) and b) when it happened I was rushing around to stop the water and reduce the head because the flow was sufficient to not only jet from the d/s valve and jump the bucket but also to carry out a sufficient volume of soil onto the lab floor. See pic 13 for deposited soil. Pics 11 and 12 illustrate the lack of warning at a minute apart, either side of the failure.

Because there was so much flow at failure it is unlikely that density and PSD samples I take are going to representative of what was present during the test, but I'll still do them.

Once the water flow had been stopped and the top of the lid cleared off, you could see the 'corridor' along which the soil gave way (pic 14). After deflating the bladder the soil dropped a good 20mm along the relatively undisturbed LHS (pic 15- can also see that the RHS is gouged out).

According to Schmertmann's graph of critical gradient with Cu, this test should have failed (by backward erosion) at a head of about 1.4m (given this material has a cu of about 6.5 and an L of 1.3m) (assuming no geometrical corrections are required, which given my flume is so similar to UoF's, is a reasonable assumption). However this test has shown that this soil is more likely to fail by other mechanisms (suffusion and or concentrated leak) at gradients closer to 2.5.

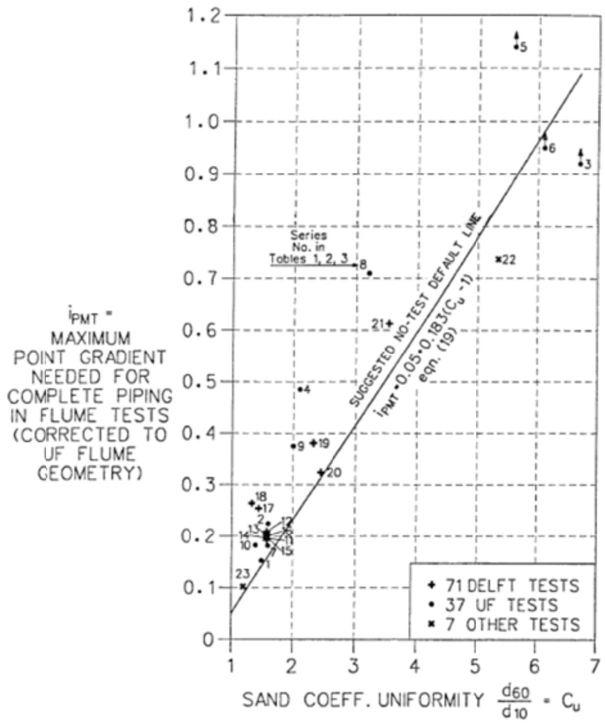

FIGURE 6 C_{DGL}-CORRECTED HORIZONTAL PIPING GRADIENTS WITH A NO-TEST DEFAULT LINE (USING UF-TEST REFERENCE L=5.0 FT AND D/L=0.20)

This is the first test I measured the flow constantly using the scale connected to the computer (mass weighed every minute). I measured the flow for the first 3 days of testing and then once (with a beaker and stop watch) on day 7. I moved the scale to test 49 after 3 days (because I wanted to see the effect a channel has on the flow). The results are given below. It shows that the permeability decreased during the experiment. This surprised me. I would have thought it would have increased, especially if suffusion was occurring. Perhaps transported fines were filling voids at the exit (???).

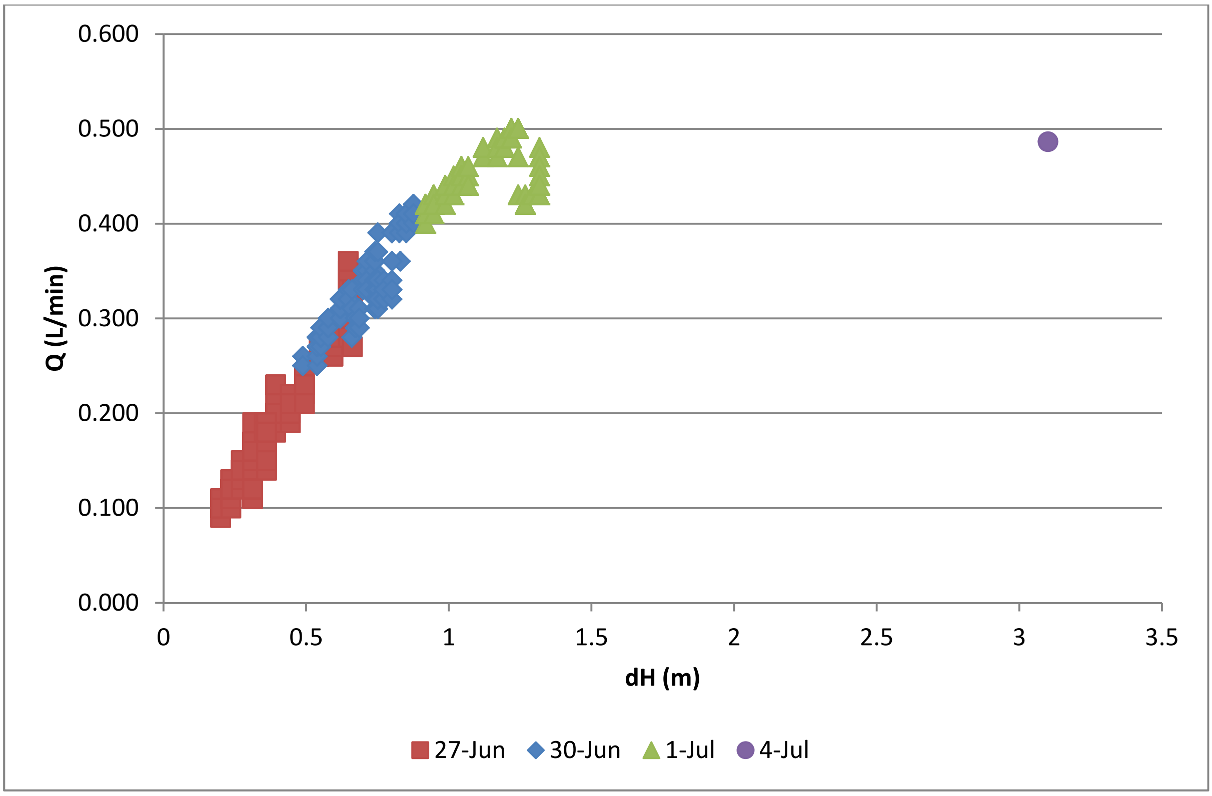

Flow with head difference (slope is related to permeability)

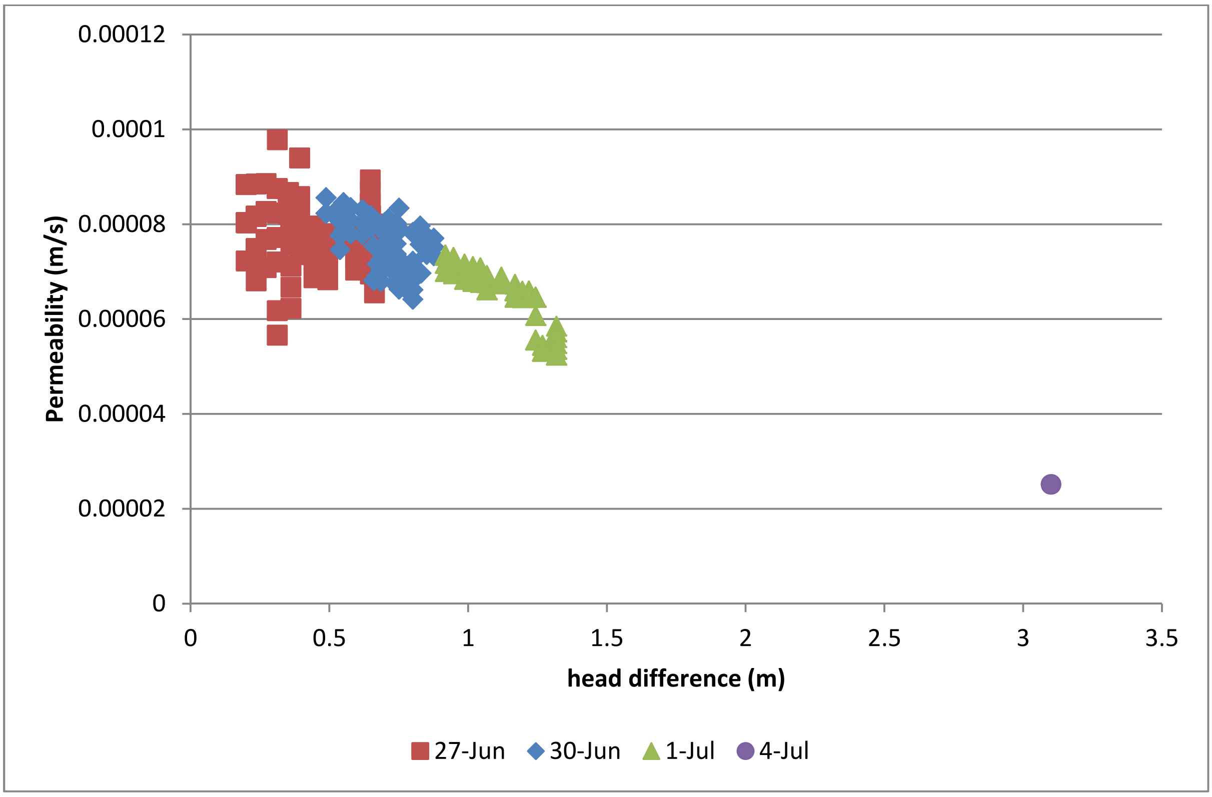

Permeability with head difference (permeability is decreasing)

Figure 48-2 soil placed slowly from shovel through very shallow water

Figure 48-3 tamper became partially buried and when removed it lifted up soil with it

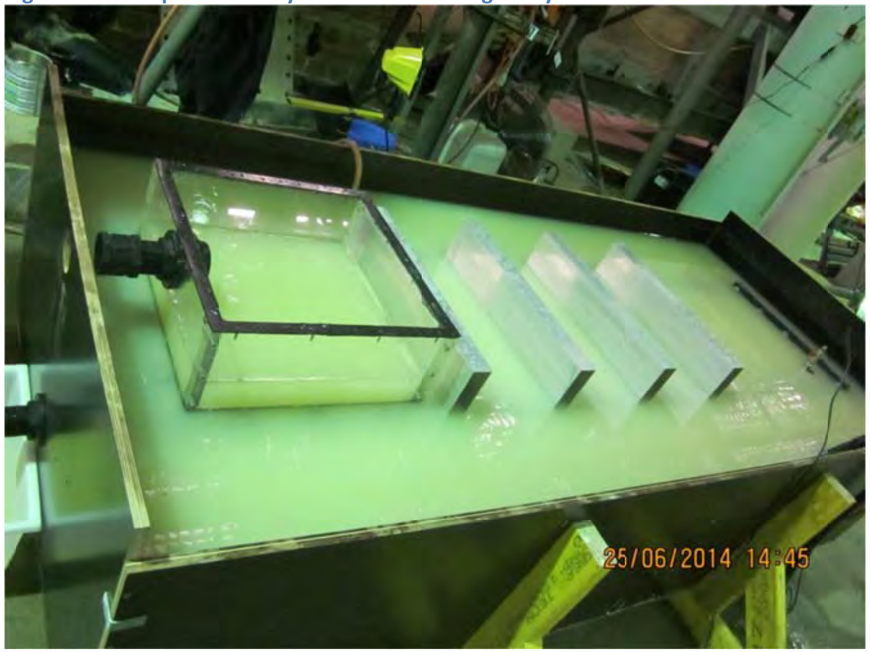

Figure 48-4 Turbid water

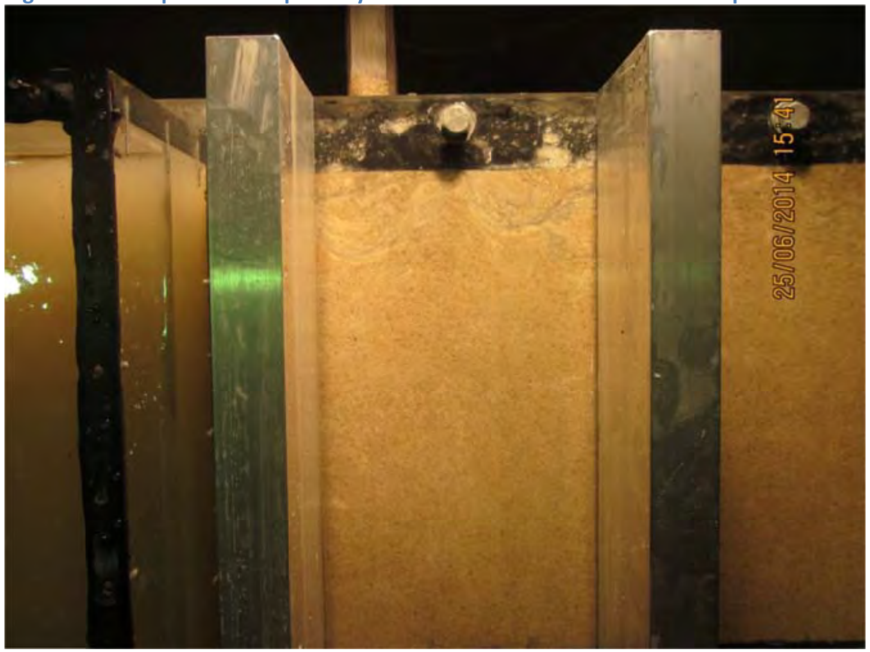

Figure 48-5 When bladder inflated water was squeezed out and created channel

Figure 48-6 channel didn't change much- this photo was taken 7 days after photo 5.

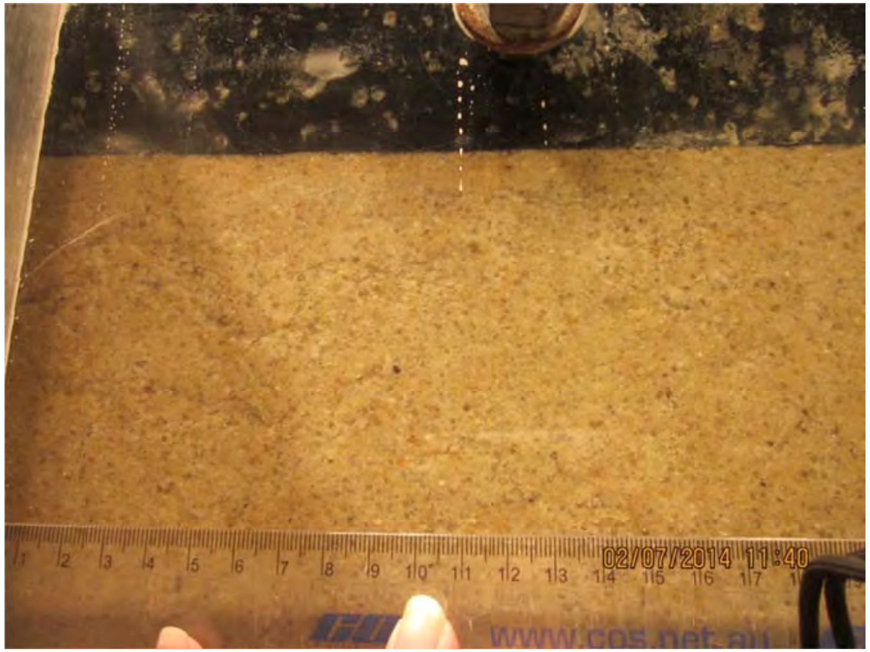

Figure 48-7 'hair-line' channels possible due to erosion of fine fraction

Figure 48-8 Coarse/"bony" appearance (possible evidence of suffusion)

Figure 48-9 Cloudy water moving through sample (possible evidence of suffusion)

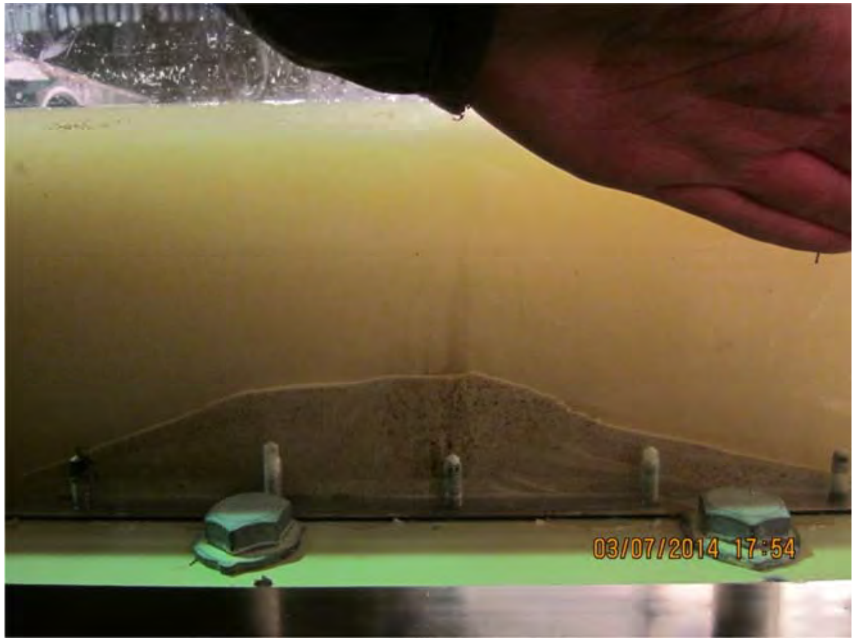

Figure 48-10 Build-up of soil at exit

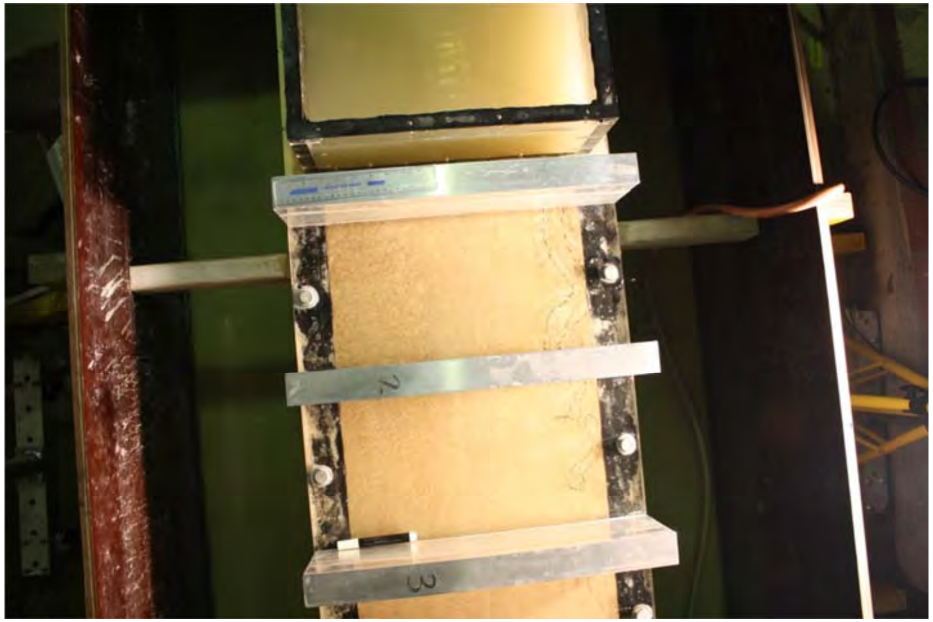

Figure 48-11 Moments before failure

Figure 48-12 After failure (1 minute after pic 11)

Figure 48-13 Soil carried out onto lab floor from flow leaving flume after failure

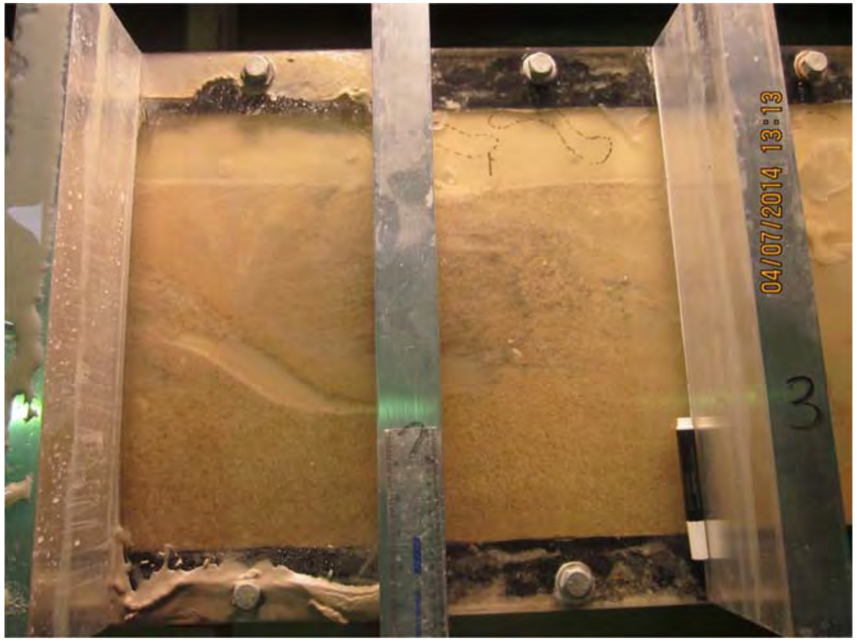

Figure 48-14 Build-up of soil at exit

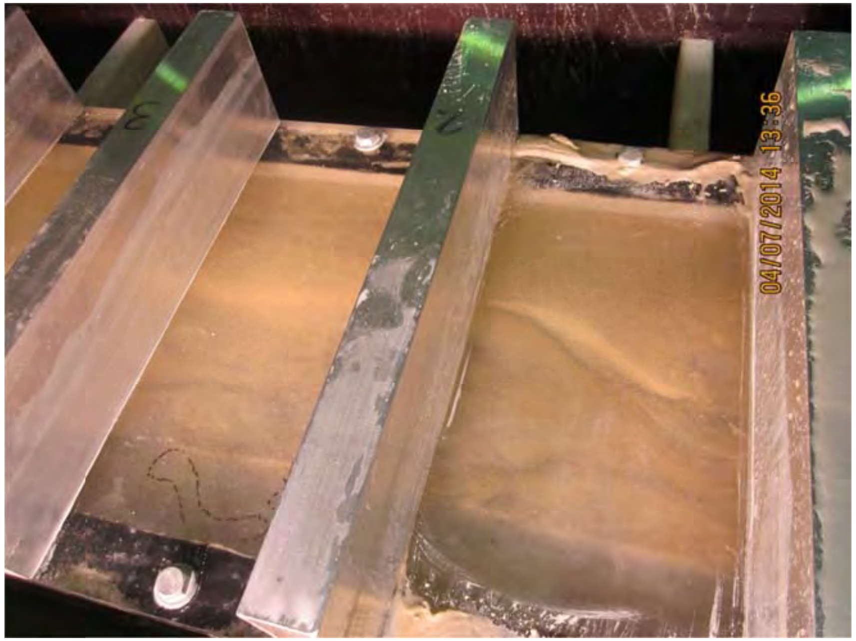

Figure 48-15 Moments before failure

Backward erosion piping test data sheet

Test #	49	$m_s + m_w$ after 'drying'		kg
Date	2/07/2014	m/c after 'drying'		-
Soil	Syd sand	V_s	0	m^3
Flume	4	$V_s + V_w$ in flume		m^3
Exit type	circle	void ratio		-
seepage length	1.3 m	relative density	4.705882353	-
head in bladder tank	5 m	avg. time for 50mL		s
bladder pressure	50 kPa	Q when ΔH = 0.1m	#DIV/0!	L/min
compaction	vibrated and tamped (as dense as possible)			

time	head (mm)	observation
11.35	0	some disturbance around hole incl.
		a ≑40mm channel in d/s direction
		+ gap on u/s side of hole (see
		happy snap). Most likely just
		local movement of sand as
		flume filled w/ water. Note: flow
		being measured w/ scale.
		I'm expecting initiation ≑ 150-200 and
		crit ≑ 230-260.
11.45	↑ 93	
11.48		boiling in hole
12.20	↑ 117	
1.35	↑ 144	initiation
1.40		180-110
2.12	↑ 156	185-110.
2.16		185-110
2.36	↑ 168	185-110
2.48		197-110
3.00	↑ 183	" "
3.02		212-110
3.04		228-110
3.21		under b!
3.50	↓ water	dropped cause sump pump stopped
3.58	178	
4.12		25 abl
4.47		73 abl

time	head (mm)	observation
5:12	↓7	73ab1
3-7 11:~~13~~35	↑	73ab1
11:50	↑103	
12:06	↑156	
12:21	↑178	
12:51	↑191	Tip progression
1:13		~~[illegible]~~ 115 ab1
1:30		2×60FPS taken. (successfully (think)
		145 ab1 Moving at 45° angle.
1:51		210 ab1 Parallel to flume.
2:10		3×60FPS
2:35		65 ab2
2:44	↓166	Reached 50% of L → 104ab2
~~2:50~~		
3:00	↑178	Tip didn't move.
3:02		Tip began to progress. Stopped.
3:17	↑190	Tip began to progress
3:23		60 FPS taken
3:28		175ab2
3:59		Channel has meandered & widened
		between ~~b1 & b2~~ b2 & the exit.
4:10	↑198	Tip didn't move for 15 mins.
		Tip is now progressing
4:12		stopped progressing at 230ab2
4:24		235 ab2. Channel branched/split
		at 220ab2. One channel is progressing
		Laterally and one at 45°
4:35		250ab2 - Lateral channel is now progressing
		Longitudinally
5:04		23ab3
5:05	↓95	Left over night.
4-7 9:51	85	28 ab3
9:52	↑180	~~28~~
10:17	↑209	28 ab3
10:45	↓188	58 ab3 @70% L
12:20		68ab3
12:35	↓165	220ab3 past 80% L
12:43		220ab3
1:00		" "
1:55		" "
2:47	↑177	" "
3:10	↓167	" "
3:40	↑177	" "
3:53	↑187	" "
4:14	↑195	223 ab3
		3 lots of 60fps sets. 1st btw b3+4 2nd btw 2+3 3rd btw 3+4

time	head (mm)	observation
4.18		235 ab3
4.30		250 ab3
5.12		First noticed tip through to U/S end.
		Also noticed channel blocked between
		loops 3+4.
5.38		Normally I'd leave it running to see if
		it fails but if it did fail the
		d/s bucket wouldn't handle the flow
		so I'll take it back to datum for
		the weekend. I'd also like to watch the
		flow rate during the forward deepening
		phase (and this can't be done unattended).
5.39	↓	

Test 49

time	head (mm)	observation

Test 49

All standpipes started btw 1-3mm below datum.
Not sure of Perhaps constant head take a few mm below datum (but don't look like it to me)
Actually it does. That's all it is. Don't adjust measurement.

3/7/14

		Row 1			Row 2			Row 3					
time	head	right	middle	left	right	middle	left	right	middle	left	time for 50mL	Avg	Temp
2:13	156	57	58		89	87		120	121	121	being measured		13
3:10	183	66	66		103	100		140	140	141	with scale.		~~[illegible]~~
1:14	191	63	•55	60	103	99		141	142	143			12
2:27	191	55	•49	55	95	•91		138	138	139			
4:06	190	54	48	54	87	•75		131	132	133			
9:58	180	56	53*	56	87	78*		125	125	125			10.5
12:42	178	55	53*	54	84	79		115	103*	116			
5:18	95	70	66	69	108	104		149	150	153			
5:19									166 ←		blockage underneath cleared		
5:20								152	170	155	channel is forward cleaning		

I've put cork back in to prevent more flow into pipe

Sand + phylite entered standpipe so I take the potter-plug (tensiometer) fell out.

49. Test 49 (flume 4) circle

Test 49 was with the circle exit and was the 2nd test looking at the effect of soil density.

I both vibrated and tamped the soil in 50mm layers in in an effort to get the sand as dense as possible. Bronson even clamped wooden planks to top of flume so when the top layer of sand was compacted in it didn't slide from the sides.

The channel initiated at 144mm and its critical was at approx. 196mm. Plots of charts in Figures 1 and 2. I have no SLR and only 2 happy snap photos of this test. I'm not sure why I have so little photos (it's not like I was doing other tests at the time).

I didn't leave it running to see when it would fail.

As can be seen in figure 2, the critical head was no different for this test than it was for tests whose soil was just vibrated in. This could mean that density has no effect on the critical head but I think it's more likely that we didn't achieve a soil any more dense than what we did when we vibrated alone. I think this because of the density sample results:

Volume (m^3)								Sample location (mm)	
			Volume (m^3)				Depth	distance from d/s end	distance from centreline (-=left of centreline)
Test	Dry Density (kg/m^3)	Dry Unit Weight (kN/m^3)	Volume water	Volum Soil	Void Ratio (e)	Relative Density (Id)			
Test 45 Syd sand	1632.272051	16.01258882	4.68E-05	7.17796E-05	0.654947885	0.853247736	0	708	125
	1635.639296	16.0456215	4.79E-05	7.19277E-05	0.65154089	0.873288884	0	1273	-75
	1658.3682	16.26859205	4.19E-05	7.29272E-05	0.628905558	1.006437896	0	2507	-95
	1688.673406	16.56588611	0.000042	7.42598E-05	0.599672955	1.17839438	0	3647	87
Test 49 Syd sand	1633.113862	16.02084699	0.0000386	7.18166E-05	0.654094819	0.858265771	0	165	-165
	1658.3682	16.26859205	0.0000393	7.29272E-05	0.628905558	1.006437896	0	480	-130
	1639.848352	16.08691234	0.0000393	7.21128E-05	0.647301822	0.898224578	0	995	-150

The range of relative densities for a test which was just vibrated in (0.85 – 1.18) were no different to the range of relative densities for this test (0.86 – 1.01) (in fact they were less). I also note there's a huge range in relative densities so my method isn't reliable.

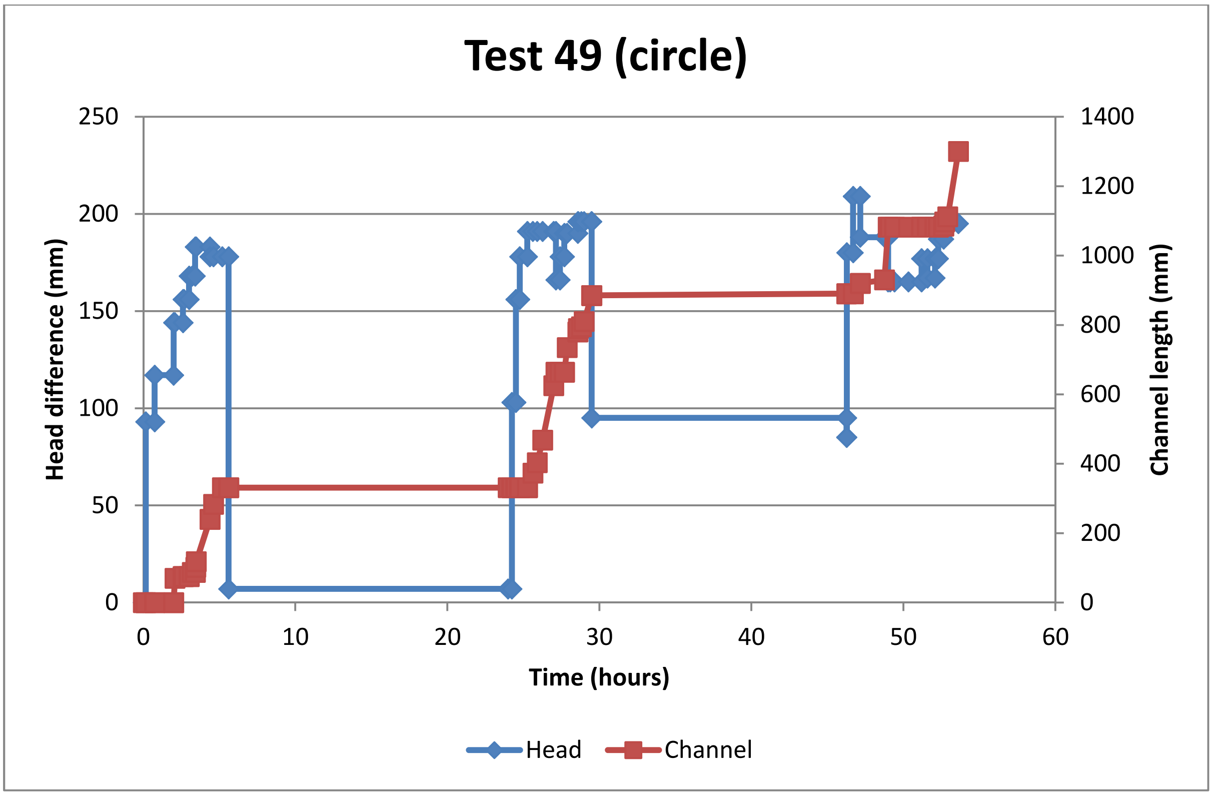

Figure 49-1 Test 49 chart

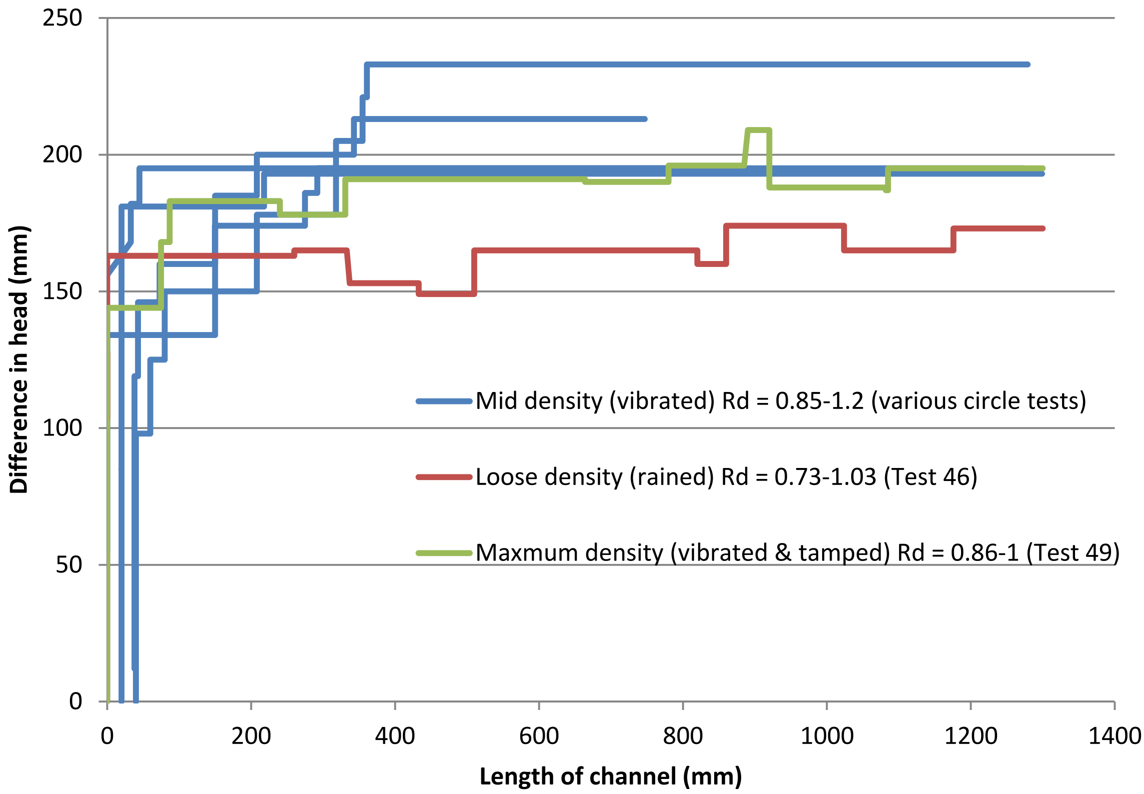

Figure 49-2 density effect on H vs CL

Backward erosion piping test data sheet

Test #	50	$m_s + m_w$ after 'drying'		kg
Date		m/c after 'drying'		-
Soil	Mix 2	V_s	0	m^3
Flume	4	$V_s + V_w$ in flume		m^3
Exit type	circle	void ratio		-
seepage length	1.3 m	relative density	4.705882353	-
head in bladder tank	5 m	avg. time for 50mL		s
bladder pressure	50 kPa	Q when ΔH = 0.1m	#DIV/0!	L/min
compaction	~~vibrated and tamped (as dense as possible)~~			

time	head (mm)	observation
18-7		
11:35		bladder inflated
12:20		CO_2 on
5:25		CO_2 off
5:40		water on
21-7		
11:38	0	
11:49	↑ 47	
11:57	↑ 94	
12:06	↑ 100	
12:12		~~100mm~~ 2 channels ~~from~~ 100 mm from exit
		& 70 mm from exit.
12:59		No progression
1:00	↑ 144	~~Possibly~~ Nothing observed.
1:19	↑ 175	Channel erosion
1:38	↑ 186	
1:59	↑ 196	Channel erosion.
2:22	↑ 210	Channel erosion
2:37	↑ 220	
2:42		~~Side of flume~~ Top of box was tapped
		with hammer to remove screw. Resulted
		in a cloud of fines billow out of
		the exit / raise from the bottom of the
		box. Channels appear unaffected.
		Still no progression.

time	head (mm)	observation
2:59	↓ 93	Box too cloudy, head dropped till
		fines settle. Left ~~[illegible]~~ overnight
4:00	↓ 45	(By Bec)
22/7 11:19	↑ 187	Channel erosion
11:35	↑ 217	
11:53	↑ 230	
12:05	↑ 242	The two channels measured ~~at~~ as 70 & 80mm from exit
12:20	↑ 255	Channel erosion
12:29	↑ 266	?
12:~~4~~44	↑ 278	Channel erosion }. Tip of right channel grew slightly
12:54	↑ 292	Another tip grew out of the right channel.
1:09	↑ 303	Channel erosion
1:20	↑ 316	
1:31	↑ 327	New tip erosion.
1:46	↑ 339	
2:00	↑ 351	
2:17	↑ 368	Channel erosion. New channel formed.
2:33	↑ 392	Channel erosion
2:50	↑ 416	Some erosion at tip.
3:04	↑ 464	Channels merged, large erosion.
3:08		Tip ~~s~~ moved ~~beyond~~ ~~box~~ to edge of
		box
3:12		~~[illegible]~~ 10 ~~[illegible]~~ mm past box
3:20	↑ 485	10mm past box
3:~~25~~		20mm past box
3:47	↑ 512	" " "
4:15	↑ 533	
4:32	↑ 571	tip is moving again. Channel is v. wide @ 40-50mm.
		Some fines suspended in d/s box water.
4:34	↓ 545	60abl. It was going way too fast so I lowered head
4:36		110abl
4:47	↑ 557	" "
5:05	↑ 569	" "
5:38	↓ 5	" "
23-7 9:57	↑ ~~5~~490	110abl
10:07	↑ 539	From what I've seen so far the tip has
		moved only after a significant jump in head
		(like 50mm instead of 2.5mm) and when it
		does it moves it moves really fast with
		a wide channel (btw 30-60mm). So it's either
		not progressing or progressing really fast
		(there's no in-between) and it seems to be
		a jump in head that starts it moving.
10:43	↑ 563	110abl
11:03	↑ 587	110abl
11:04		erosion @ tip but still 110abl

Test 50

time	head (mm)	observation
11:30	↑ 613	110ab1
11:51	↑ 635	
11:55		New tip formed. Only extends 85 ab1
		No movement of other tips. Lots of channel erosion
12:11	↑ 661	Movement of soil between the tips. Did not
		erode away. Area of about 30x30 mm^2.
		Tip progression. Quite rapid.
12:15		150 ab1
12:16	↓ 650	10 ab2. Very rapid so reduced head.
		Still rapid
12:17	↓ 642	150 ab2
12:19	↓ 590	at bar 3
12:20	[illegible]	150 ab3
12:21	↓ 545	ab4
12:21		40 ab4
12:22		120 ab4
12:22		through to u/s end.
12:27		Fail

Test 50

time	head (mm)	observation

Test 50

500mL/120.8s
4.139mL/s
Q = 4.139e-6 m³/s

		Row 1			Row 2			Row 3			500mL		
time	head	right	middle	left	right	middle	left	right	middle	left	time for ~~50mL~~	Avg	Temp
21/7 12:48	100	42	43	42	61	57	51	76	76	76	120.8 sec		
2:11	196	78	79	79	113	109	103	144	144	145	57.3 sec		
2:30	210												
22/7 12:41	266	108	108	109	152	148	142	191	192	192			
337	485	163	163	167	254	254		340	340	340			
445	545	140	120	127	254	249	242	363	364	363			
23-7 10:05	400	126	107	113	228	223	217	327	328	326			
1233	545	145	140	136	230	200	203	358	366	367			

8.726
8.726e-6 m³/s

50. Test 50 (flume 4) circle

Test 50 was the first test on mix 2 (d10=0.2mm and Cu= 4.2).

The soil was placed dry and tamped every fifth of the way up. Saturation was achieved using CO2 flushing.

Bronson's summary:

Initiation occurred at 100mm head, extending to 80 mm. At 464mm head, the channel extended to 10mm past the box. No significant movement until 571mm head with the channel moving to 60ab1. This head had the channel moving very rapidly so it was dropped to 545. By this stage it reached 110ab1 and didn't move until 661mm head. The progression was so rapid that the head was dropped several times until 545mm head at which breakthrough to the u/s end was reached. From 2.5 hours after initiation had stopped, with the head at 220mm, the top of the box was hit lightly a few times with a hammer (this was in an attempt to remove a screw that was stuck). This resulted in clouds of fines to billow out of the exit, making the box water turbid. The channels did not appear to change due to this. After 20 minutes, the box was too cloudy to observe the progression of the channel so the head was dropped overnight to allow the fines to settle. The next day, the experiment continued as normal.

Bec's summary:

Initiation occurred at lower head than I expected- at 100mm. This is 33% less than Sydney sand's average initiation head at 148mm (ranging between 98 to 190mm). it progressed at this head for 100mm before stopping. The head then needed to be raised to 464mm (a 365% increase) before progression recommenced. The tip stopped 3 more times, needing a critical head of 661mm (a 224% increase on Sydney sand's average critical head of 204mm).

Also, when the tip progressed it did so very quickly. In fact, once the critical head had been reached, it took only 9 minutes for the tip to reach the upstream end even though we dropped the head as quick as we could. Figure 4 illustrates how quick the tip progressed and we couldn't drop the head fast enough to stop the tip. It was as if the progression of this tip had only 2 speeds- stationary and very fast. There didn't appear to be an in-between speed like there was for Sydney sand.

I also noticed that when the tip progressed it did so after large head increases. When we increased the head by 25mm nothing happened, even though we did so several times, however after having grown a little impatient and increasing the head by 50mm the tip did progress. I'm not sure if this is a coincidence or the sudden change in head trigger the tip to progress.

It took only 6 minutes for the test to fail.

Figure 6 shows where this test plots on Schmertmann's graph. It plots near Schmertmann's 'no-test' line.

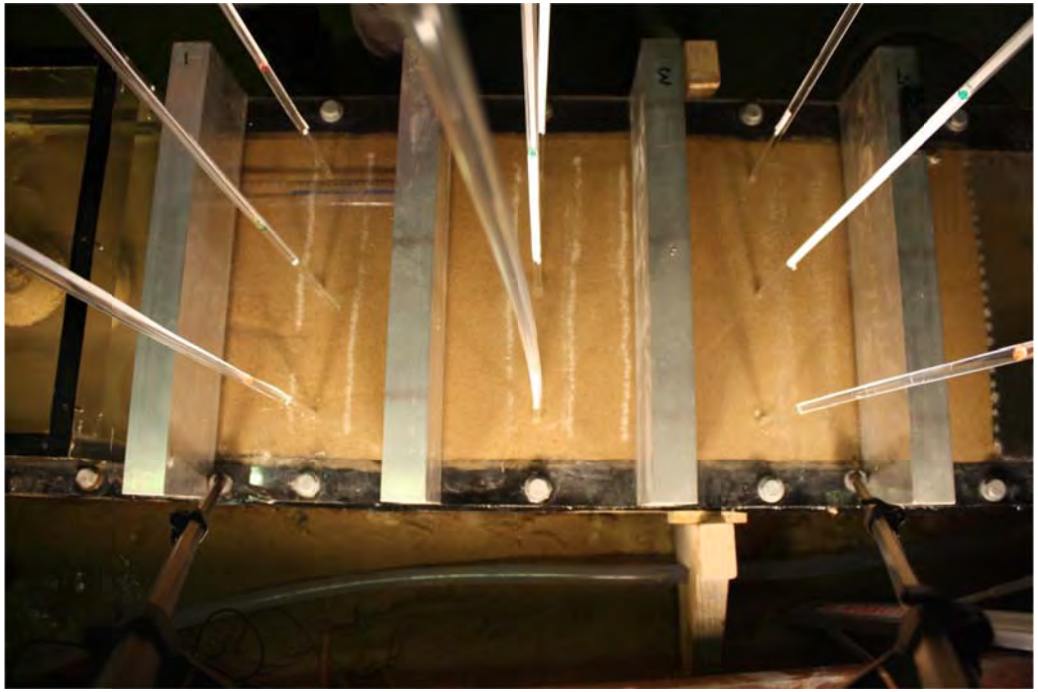

Figure 50-1 Head first at 661mm (12:12pm)

Figure 50-2 Head through to u/s end at 12:23pm (9 minutes later)

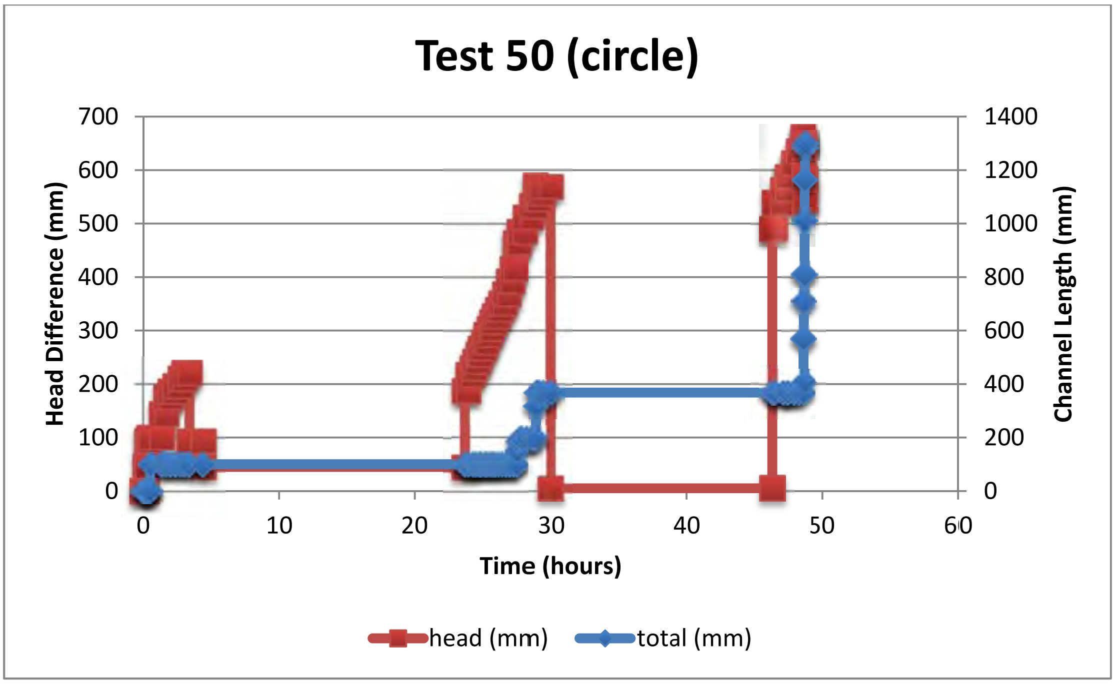

Figure 50-3 Test 50 plot

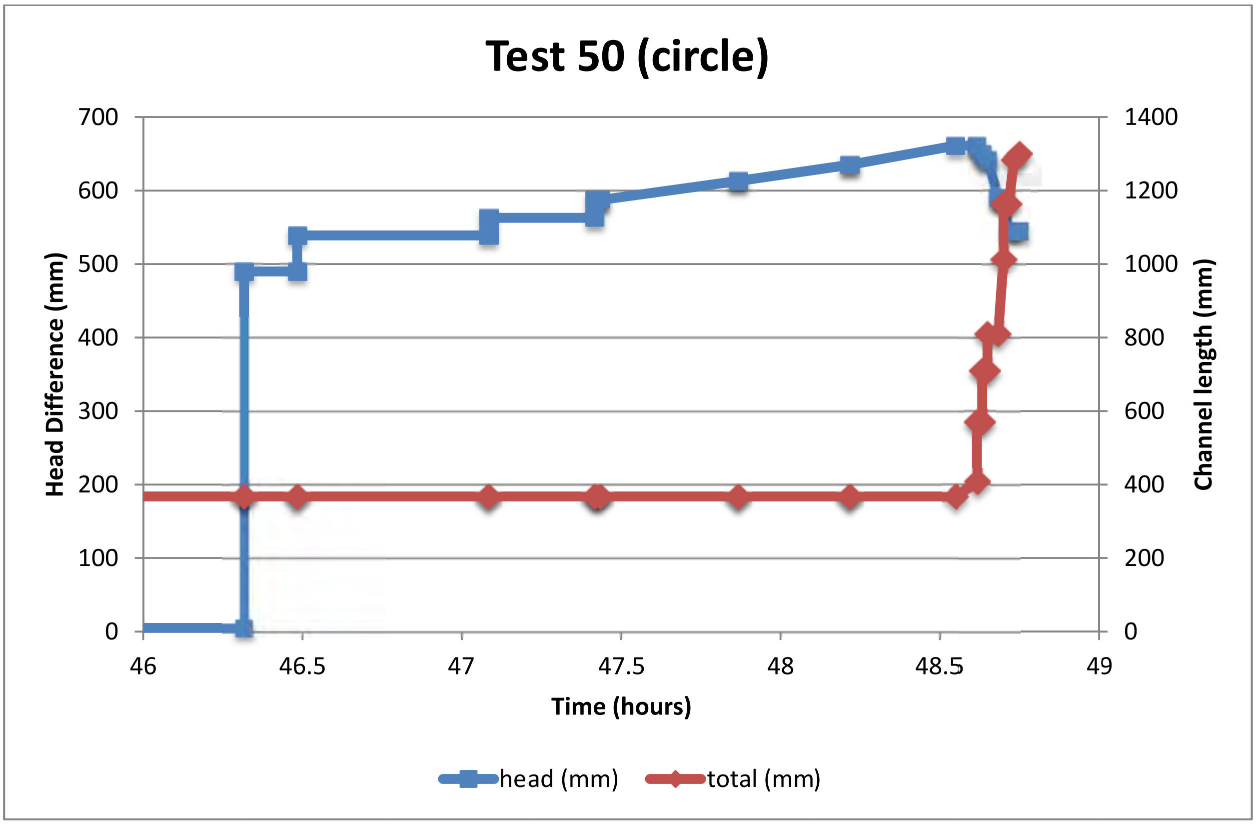

Figure 50-4 Zoom in on time scale at end of test showing how quickly tip progressed

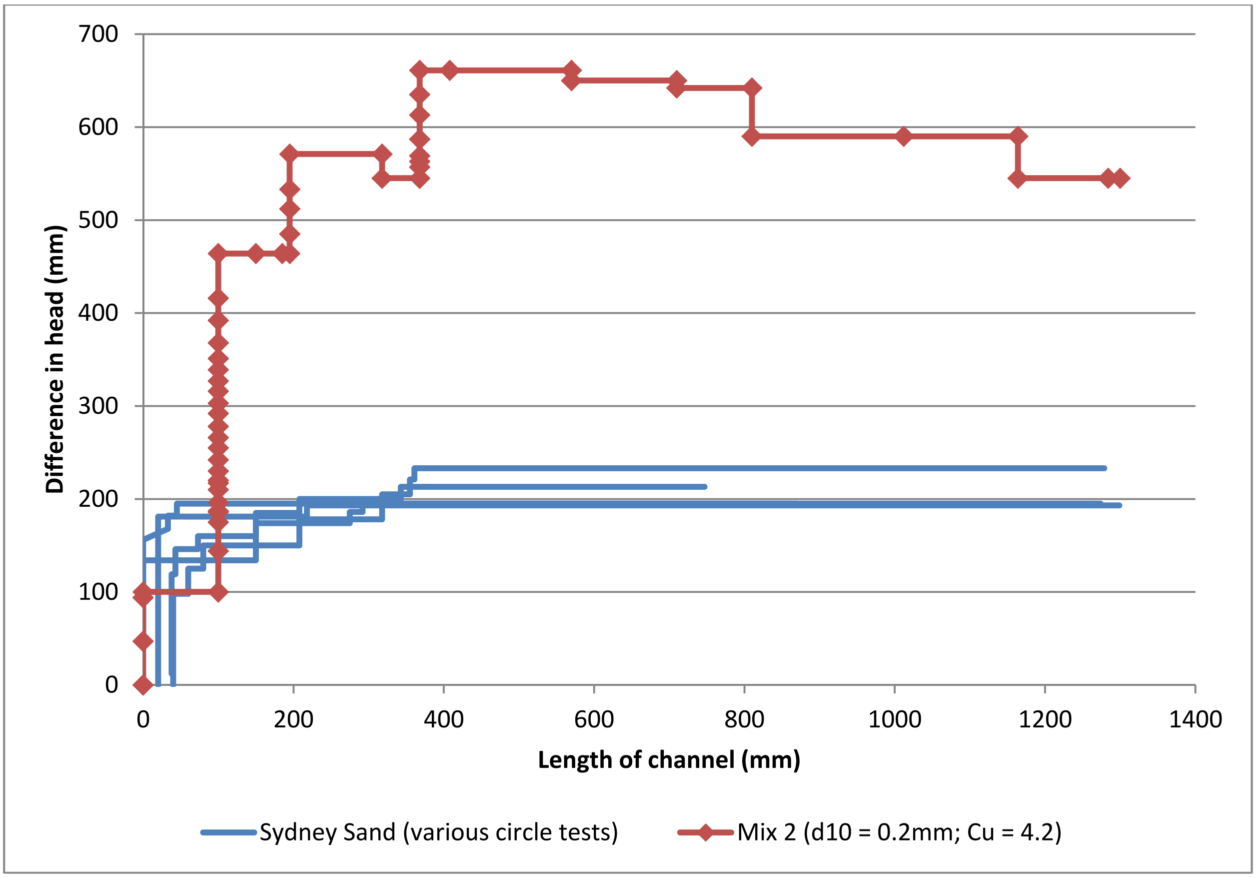

Figure 50-5 H vs CL for different soils

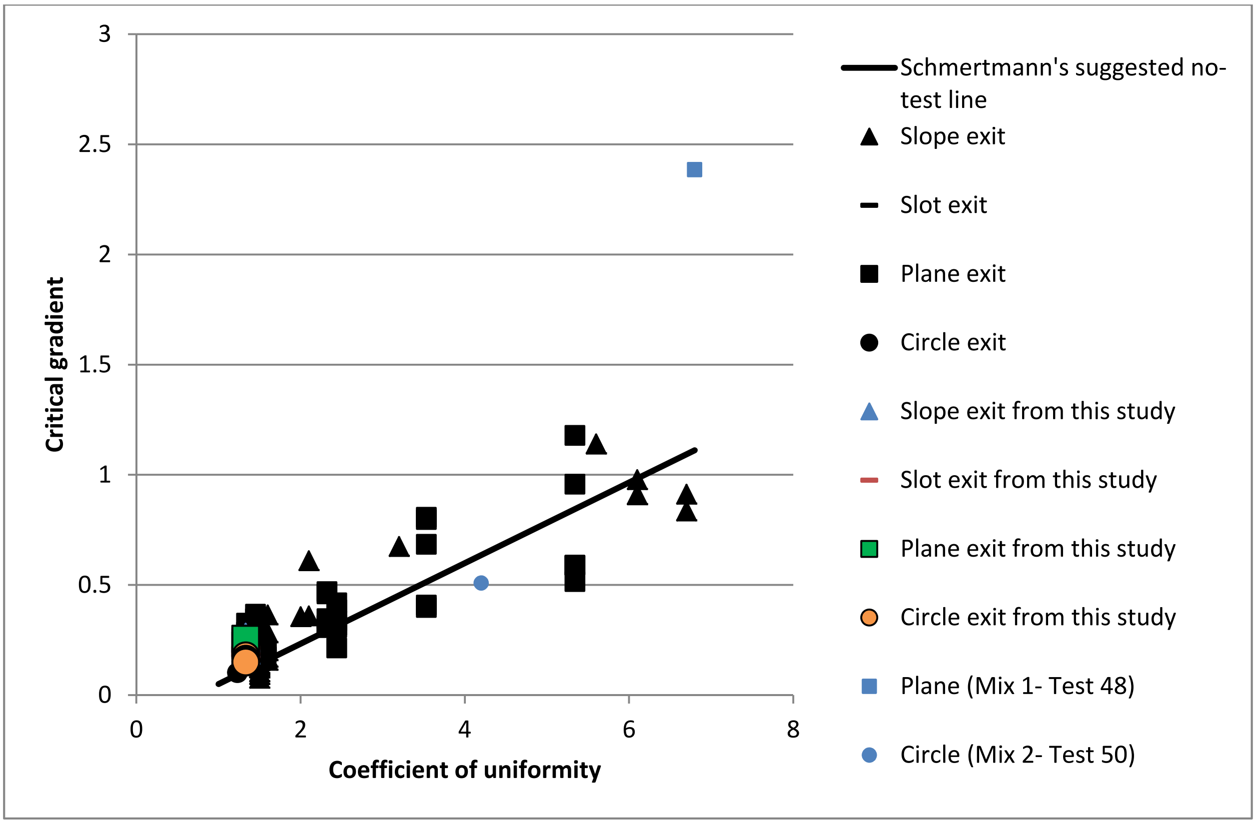

Figure 50-6 Schmertmann's graph

Backward erosion piping test data sheet

Test #	51	Exit type	circle
Date	11/08/2014	seepage length	1.3 m
Soil	Mix 3	head in bladder tank	5 m
Flume	3	compaction	tamped

time	head	observation
8-8		CO2ed
11.30		CO2ed
5		inflated bladder (should of inflated bladder
		before CO2ing but forgot to)
5:30		started infilling w/ water.
11-8		
11.24	0	I can still see some small CO2/gas
		bubbles under the lid but I'm not
		too concerned cause they're small
		and spread out. they might have
		dissolved given more time but I was
		keen to start today. Also it looks
		like the [illegible] has moved during
		infill even though I filled really slowly
~~[illegible]~~		Only moved a little though. I also
		note that the surface of the
		soil isn't as consistent or regular
		as I would like. there's small
		gaps. I don't know why -> maybe just
		caused by large grains when
		screeding surface. I don't think it'll
		effect the test.
11:37	↑ 98	
11:47	↑ 147	Initiation Tip@ ~40 mm from exit
11:54	↑ 193	Tip progressed 90 mm from exit
12.24	↑ 240	110-150 mm
12:28		other channels surrounding hole progressed
		(see happy snap) but stopped before long
		(lasted a few minutes). And it wasn't the
		channel facing u/s (it was channels

Test 51

time	head	observation
		painting to RHS. Channel facing
		u/s didn't move. Still 110-155 (ok
		so it actually moved ≈ 5mm). I
		note I only see finer-grains
		around rim of hole (and boiling
		in hole).
12:42		165-110
12:56	↑ 289	170-110 A&B 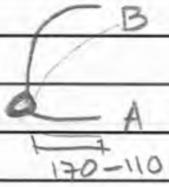
1:10	↑ 312	
1:15	↑ 338	
1:21	↑ 375	
1:29	↑ 425	Box became cloudy with fines — Coarse material is boiling now
1:30		Edge of box (A) → 250-110
		B went to 200-110
1:47	↑ 476	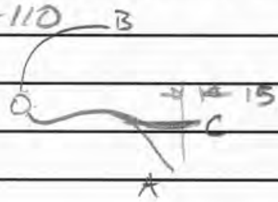
1:55	↑ 525	15 past box
2:08	↑ 577	
2:15	↑ 642	
		Possibly at 22abl → could just be
		a channel formed when screening
		Looks as though it could be joined
		to tip at 15 past box
2:26	↑ 725	
2:36	↑ 802	
2:48	↑ 876	
2:58	↑ 951	
3:09	↑ 1025	
3:17	↑ 1123	
3:27	↑ 1198	At bar 1. Tip is ~20 mm wide
~~3:41~~	~~↑~~	Washed out finer portion in the channel.
		The larger particles remain. See Happy Snap
3:41	↑ 1227	Tip shape changed. It has likely
		progressed under bar 1 but cannot see
		how far.
+50 3:55	↑ 1277	tip most likely under bl but
		could be 22abl.
maybe 3.4 turns 4:00	↓ ? ≈1077	impossible to know where tip was at cause it all happened so fast!
4:01	↓ 77	
4:05		reached u/s end

4:06 failed!

Test 51

		Row 1			Row 2			Row 3						
time	head	right	middle	left	right	middle	left	right	middle	left	time for 50mL	Avg	Temp	
1223	193	98	98	95	128	128	118	165	163	165				Q=1.12e-5
2:02	525	220	217	211	312	315	300	426	419	424				Q=?
3:32	1198	417	396	385	648	650	635	936	922	936			15	Q=9.3e-5

51. Test 51 (flume 3) circle

Test 51 was the first test on mix 3 (d10=0.2mm and Cu= 6.2).

The soil was placed dry and tamped every fifth of the way up. Saturation was achieved using CO2 flushing.

Initiation occurred at 100mm (the same as test 50 on Mix 2) and stopped after 40mm. Five increases in head (and 193mm of progression- to 233mm or 18% of L) were required to get to critical at 1277mm. Once at 1277mm the tip progressed so fast it only took 4 minutes to reach the upstream end. I tried to lower the head to stop the tip progression but I couldn't even slow it down despite dropping the head by 1200mm (to 77mm)! This critical head was a 525% increase on Sydney sand's average of 204mm.

The jumps in head didn't proceed progression for this test as it did in test 50 (I kept the head increase increment the same).

1 minute later it failed.

Figure 3 shows where this test plots on Schmertmann's graph. It plots near Schmertmann's 'no-test' line.

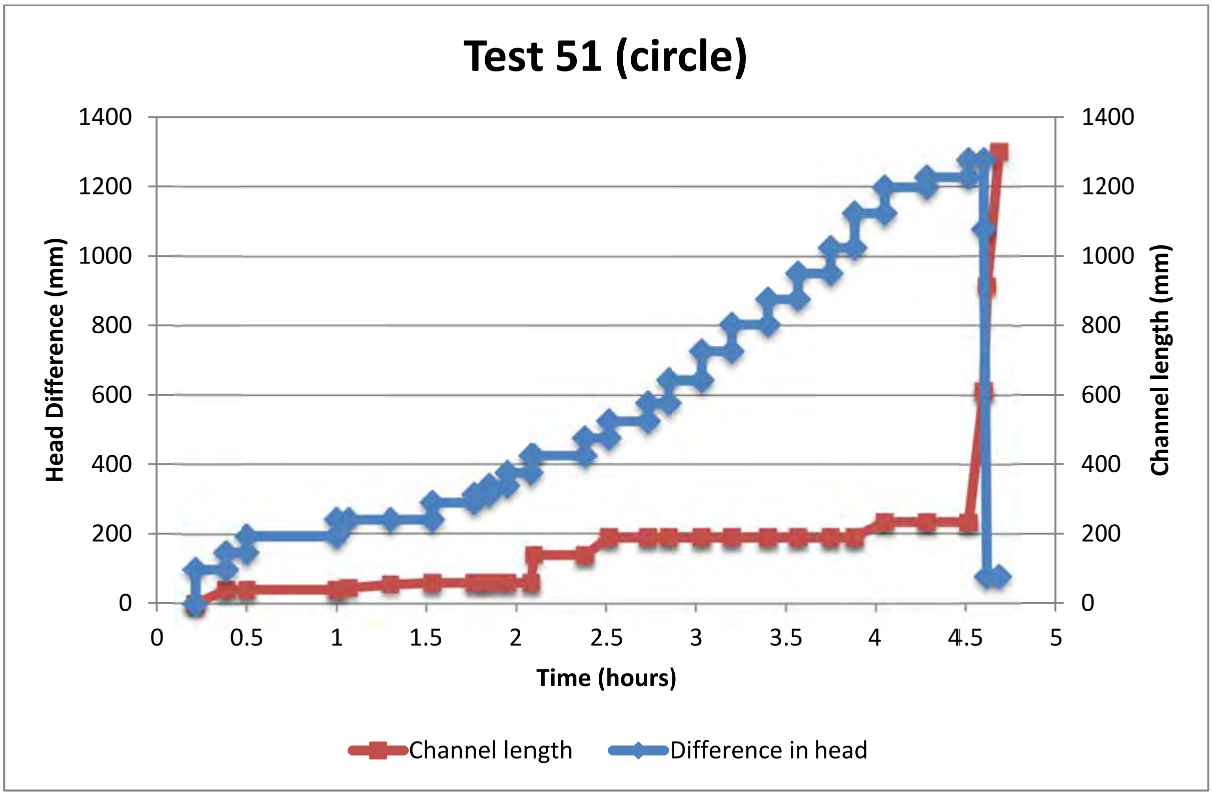

Figure 51-1 Test 51 plot

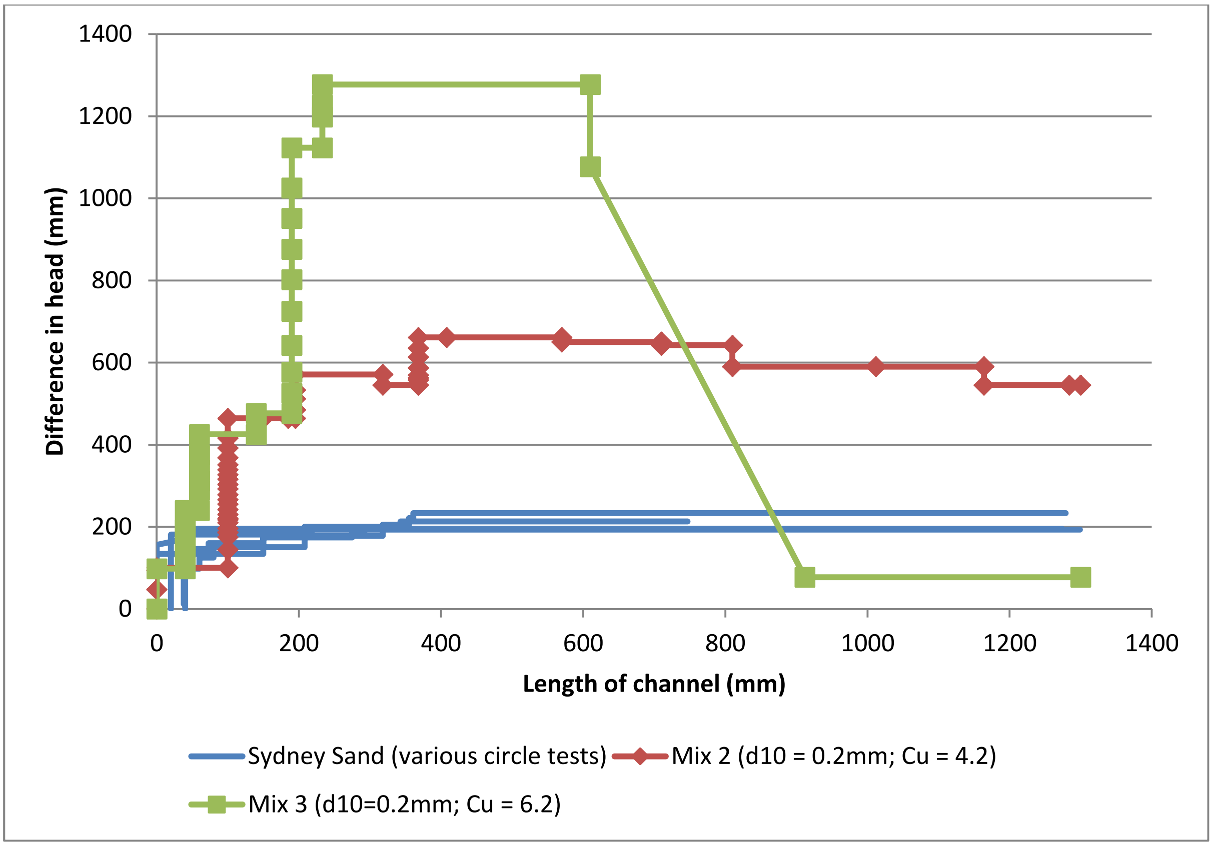

Figure 51-2 H vs CL for different soils

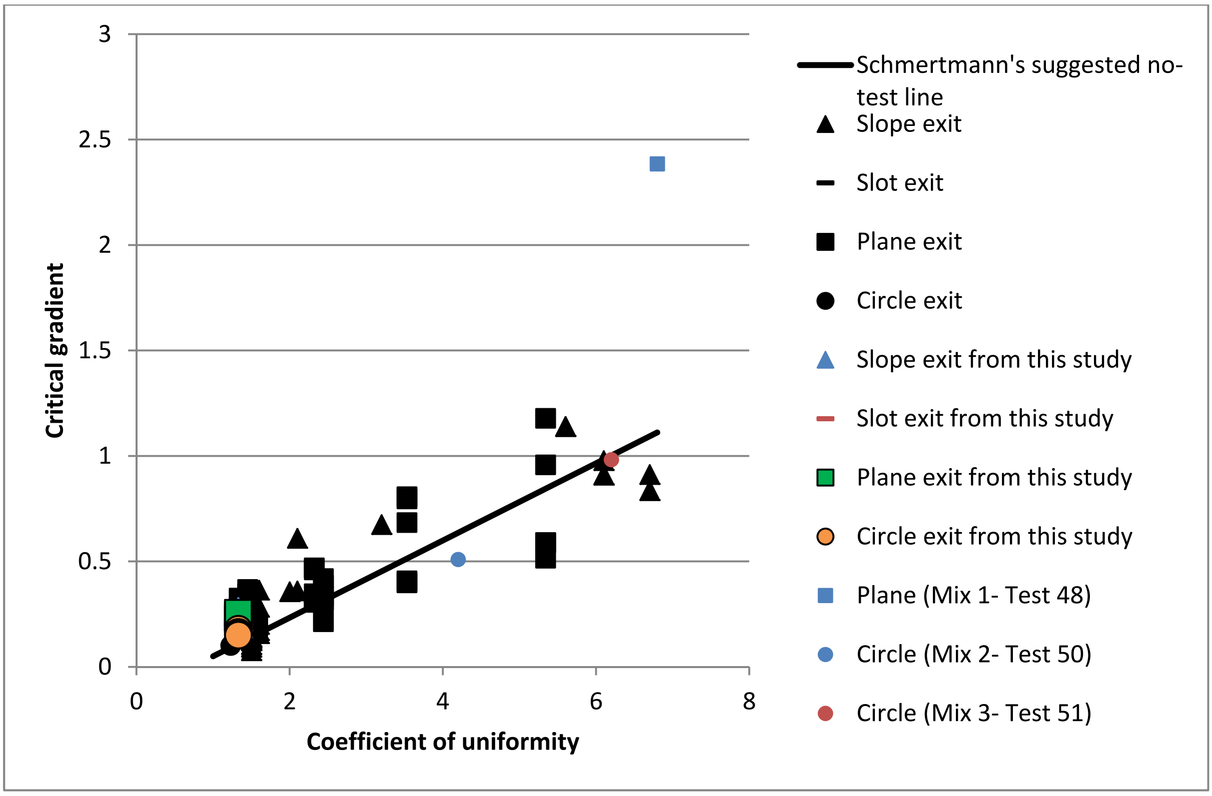

Figure 51-3 Schmertmann's graph showing test 51

Test 52

Backward erosion piping test data sheet

Test #	52	$m_s + m_w$ after 'drying'	
Date		m/c after 'drying'	
Soil	mix 4 (Cu 9.09)	V_s	
Flume	3	$V_s + V_w$ in flume	
Exit type	circle	void ratio	
seepage length	1.3 m	relative density	
head in bladder tank	5 m	avg. time for 50mL	
bladder pressure	50 kPa	Q when ΔH = 0.1m	
compaction	Tamped		

time	head (mm)	observation
~~4-Jun~~		schmertmann's graph predicts $i_{pmt} = 0.05 + 0.183(Cu-1$
~~11:15~~		~~inflated bladder~~ ∴ at $Cu = 9.09$, $i_{pmt} = 1.53$
~~6-Jun~~		with seepage length = 1.3m
~~10:45~~		~~CO2 on~~ ∴ ~~Hed~~ critical head = 1.3 × 1.53 = 1.99 m
8/9 11:05		inflated bladder
11:40		CO2 on
4:42		CO2 off
4:55	−10	began filling flume to 10mm below datum
11/ 10:13	↑ 0	brought to datum (according to VHT)
10:50	↑ 45	Datum (water started flowing out)
10:56	↑ 66	
11:00	↑ 100	
11:07	↑ 124	
13	↑ 148	~~Boiling begins~~ Just a few particles boiled then stopped.
23	↑ 174	*
28	↑ 196	
31	↑ 222	Initiation ~10mm from exit 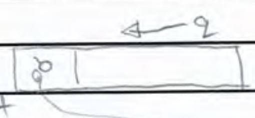 There appears to be a slight depression. Not too big and at downstream end
38	↑ 228	
46	↑ 262	
58	↑ 300	Erosion around the exit. (particle movement)
12:11	↑ 349	
12:18	↑ 404	New channels formed (some started earlier) longest is ~20mm laterally to flow direction

Boiling is now occuring (the larger particles have eroded to the exit.

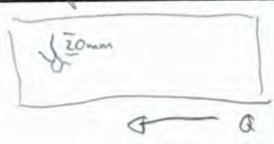

Test 52

time	head (mm)	observation
12:27	↑458	All channels have grown cannot see if grown
		towards upstream end as the soil has deposited on this
		side of the exit.
		It appears that there is a channel
		40mm past exit. ~~confirm this later~~
36	↑510	
45	↑564	60mm past exit
53	↑625	New channels formed
		(These are at 40mm past exit)
1:01	↑680	
04		70mm (the new channel has taken over
1:10	↑737	
1:22	↑779	
30	~~↑~~	Channel widened then blocked at 45mm past
		exit.
37	↑830	
42		100mm after exit. Blocked itself at 30mm shortly
		after growing.
2:04		Channel has widened massively to 80mm after exit
~~2:04~~		about 20mm wide
2:08	↑877	~~~~
23	↑935	
27		Erosion at edge of box (120mm after exit)
~~30~~	↑	but channel blocked at 90 mm
34	↑1026	
38		channel erosion
55	↑1100	
3:10	↑1171	
3:16		15 mm past box ~~( )~~
:23	↑1245	
31		Cloudy in the box.
		20 abl large channel ~ 25mm wide
38	↑1316	Fines in box have mostly settled.
51	1316	
58	↑1415	
4:19	↑	
23		70 abl blocked soon after Now at 40 abl
4:46		40 abl
4:48	↓1025	
12-9	↑	
12:00	1025	40 abl
12:08	↑1215	
12:28	↑1361	
1:26	↑1460	40 abl
1:42	↑1486	
2:16	↑ ?	40 abl

There is no page 2 — Misprinted

time	head (mm)	observation
2.25	↑ 1608	
2.30		I noticed movement btw 2+3 along RHS. Possibly some small channeling but channel doesn't appear to connect to exit / It's hard to tell but it may go btw midway btw 1 and 2 through to 3/4 from 2 towards 3. See happy snap. Soon after I noticed the movement it stopped again.
2.40	↑ 1704	
2.49	↑ 1806	
3.14	↑ 1898	
3.35	↑ 1952	
3.50	↑ 2000	
4.00		material has moved from around the tip area. See happy snap. It's hard to know where ~~to~~ to define the tip. The furthest possible hint of a tip is 170 abl but it's so faint it could be my imagination and I don't know when this hint of a tip got there. I don't want to say it was at 40 abl @ H = 1952 and then 170 abl @ . It's been so gradual I haven't noticed it. Hell it could of even been like this morning! tip = 40abl (for sake of plotting).
4.06	↑ ~~2000~~ 2050	
4.22		more material has moved from near tip. I'd say I'm real close to critical H. See happy snap. I'm gonna say tip still at 170 abl (but still a subjective call). NO WAIT. I'm gonna say tip @ 70abl now.
4.25	↑ 2075	
4.35	↑ 2097	
4.43	↑ 2147	
4.54	↑ 2195	
5.08		moved material from hole to see if it would help channel grow. See happy snap for b4 and after. Moving the boil had no effect on the channels. Only gravel at site of exit.
5.18	↑ 2245	80abl.
5.23	↑ 2295?	
5.28		I can't read it anymore (the constant head tank level). I need a taller ladder but the workshop is closed now. So I'm going to have to stop the experiment now until Monday.

time	head (mm)	observation
5.30	↓ 1807	
5.33	↓ 1289	
5.37	↓ 800	
5.40	↓ 297	tip 80 abl.

Backward erosion piping test data sheet

Test #	52	Exit type	circle
Date	11/09/2014	seepage length	1.3 m
Soil	Mix 4	head in bladder tank	5 m
Flume	3	compaction	tamped

time	head	observation
15-9	~~30~~	
11.00	300	80 abl
11.08	↑ 782	
11.15	↑ 1288	
11.40	↑ 1797	
11.48	↑ 2183	
12.12	↑ 2282	80 abl
12.23	↑ 2379	
12.42	↑ 2476	
1.17		difficult to define tip but best guess
		is 180 abl. See happy snap. Sand boil
		has grown.
1.35		180
1.55		"
2.20		" abl. See happy snap. I moved boil
		material to see if it would make
		a difference.
2.37	↑ 2525	clearing boil made no effect. the water flow
		is strong enough to suspend a 20mm Ø
		piece of gravel.
2.48	↑ 2574	
3.10	↑ ≑ 2660 ←	can't see level because in join.
3.24	↑ 2760	180 abl
[illegible]	↑ 2828	
3.42	↑ 2928	It's struggling to ~~go~~ raise the head anymore
		than this so I'm going to change the
		filter in the hope that it'll help.
4.29	↑ 3050 →	best guess on head. It's too high for
		me to read accurately. Still 180 abl
4.35		water turbid in d/s box. Easily seen
		finer grains moving through channel

time	head	observation
4.38		more material around hole (i.e. new
		boil). See happy snap.
4.46		Water level in d/s box is ≈ 50mm
		above perspex lid (it's higher than
		datum on account of the volume
		of flow leave the 50mm d/s
		value).
		It may be that finer sediments are
		locked up against coarse grains
		preventing erosion into the top.
4.47	↑3105	
4.53		It's getting too dangerous reading
		the constant head tank with
		the current ladder I'm using. I need
		a taller one but the taller ladder
		is now locked up for the day
		so I'll have to lower head +
		come back to it tmw. I don't want
		to leave it at this head over
		night incase it does fail ~~and~~
		which would flood the lab.
4.54	↓1134	
5.17	↓430	
16-9	430	
10.16	↑2417	
10.30	↑2944	
10.48	↑3044	
11.06	↑3140	
11.14	↑3233	180 abl
11.29	↑3220	
11.35	↑3450	It looks as though the existing channel
		is just getting deeper. There is new
		transported material @ exit. See
		happy.
11.45	↑3553	
12.05		I gave the top a few hits with the
		mallet to try dislodge the gravel pieces
		but no success. 180 abl.

time	head	observation
12-06	↑~~[illegible]~~3571	
12.23	↑3563	I think I've reached the limit of
		the head the pump can provide. Note
		all valves are fully opened and
		filter was new yesterday (i.e.
		maximised head (x.000). I'll raise
		inner drain cylinder to make sure
		sure (to as high as it can go).
		I wonder if the head went down
12.33	↑3570.	from 3571 to 3563 because the
		inner drain cylinder had been
		lifted and so the water by-passes.
		If so I suspect my next head
		reading will be lower still.
12.41		Yep, I've reached the max possible head.
12.42		I ~~banged~~hit the tip with the mallet
		a few more times and the channel
		spread laterally (not forward). The
		"channel" is now ≑400mm wide (see
		happy snap). Alot of sediment was
		transported out the exit - making
		the d/s box water turbid (and water
		in the overflow box turbid). And yet
		the "channel" still doesn't extend
		further than 180abl.
12.48		See happy snap for boil pic now
		that water has cleared.
12.49		I moved boil from around exit. See
		happy snap. I'll leave it running for
		a little while.
1.43		180abl + no change. hit tip w/ mallet.
1.47		180abl.
4.48	3526	180abl. Ideally I'd leave it overnight
		just incase it decided to fail but if it
		were to fail I'd flood the lab so I
		can't. Instead ~~I'll~~ ~~[illegible]~~ will end
		test.
4.51	↓↓↓	

Test 52

Looking Downstream r1 r2 r3 left ↑ Right Q

11/9/14 500mL

		Row 1			Row 2			Row 3					
time	head	right	middle	left	right	middle	left	right	middle	left	time for ~~50mL~~	Avg	temp
11:53	262	115	110	116	154	155	150	206	207	206	35.0		
1:18	737	314	300	314	420	430	427	573	575	572	12.0		16
2:41	1026	415	394	411	568	583	581	791	794	790	8.2		
3:33	1245	421	370	368	626	642	640	930	932	927	6.1		
4:42	1512	497	437	427	760	774	773	1130	1130	1127	5.0		
12.9													
12.03		340	301	292	578	525	525	764	764	760	using scale.		17
2.22		494	434	420	758	770	770	1125	1125	1123			
3.54		634	556	513	1019	1016	1018 too high for r3 to reach						
4.40		633	534	495	=1050	=1050	=1050						
6.03		88	72	65	157	147	139	222	222	220			
15.9													
11.00		87	70	64	149	145	138	220	220	220	using scale		
2.45		444	103	93			99						
4.42		501	116	114									
16.9													
11.43		561	135	134	too high →						using scale		
12.47		430	104	105	"	"							

52. Test 52 (flume 3) circle

Test 52 was the first test on mix 4 (d10=0.22mm and Cu= 9.1).

The soil was placed dry and tamped in approximately 50mm lifts. Saturation was achieved using CO2 flushing.

Initiation occurred at 222mm and stopped after 10mm. The head was continually increased over 4 days but the furthest the tip got was 180 ab1 (total of 438mm, i.e. 34% of L) at a head of 2476mm. The head was increased up to its maximum of 3577mm (the highest the submergible pump could push) but the tip stayed at 180ab1.

I moved boiled material away from the exit (at least 3 times, once when the tip was 80ab1 and the test when the tip was 180ab1) but it made no difference to the tip position (see fig 2 & 3 for before and after shots of having moved the boil). I thought perhaps the tip wasn't progressing because larger grains were barricading finer grains from eroding (see fig 4) so I tapped the Perspex lid with a mallet several times. The mallet hits did dislodge smaller grains and drastically widen the channel (from a width of approx. 200mm to a width of approximately 400mm- see fig 5) but the tip still didn't move).

I didn't bother doing a head and channel length with time graph but see Fig 1 for CL vs H for different soils. And see Fig 6 for where test 52 plots on Schmertmann's graph (note critical head wasn't reached so an arrow is needed on this data point). As can be seen it plots well above Schmertmann's line.

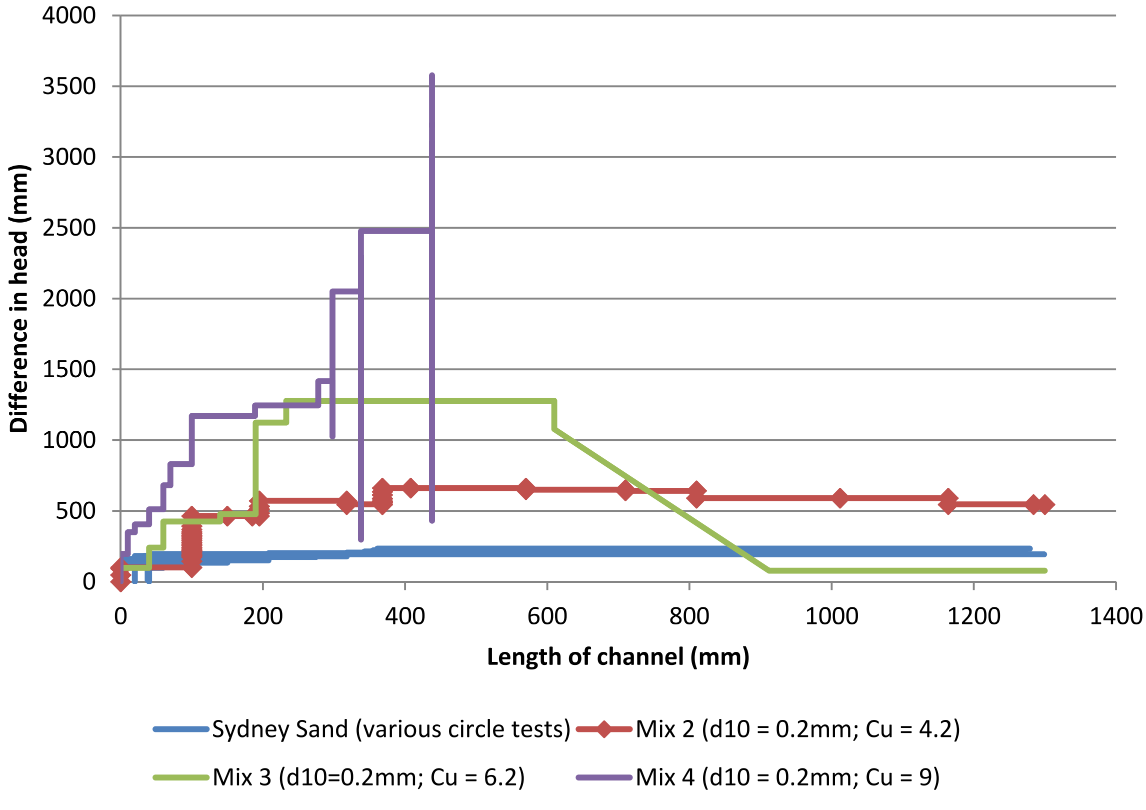

Figure 52-1 H vs CL for different soil mixes

Figure 52-2 Sand boil when tip was 80ab1

Figure 52-3 The same sand boil moved away from exit

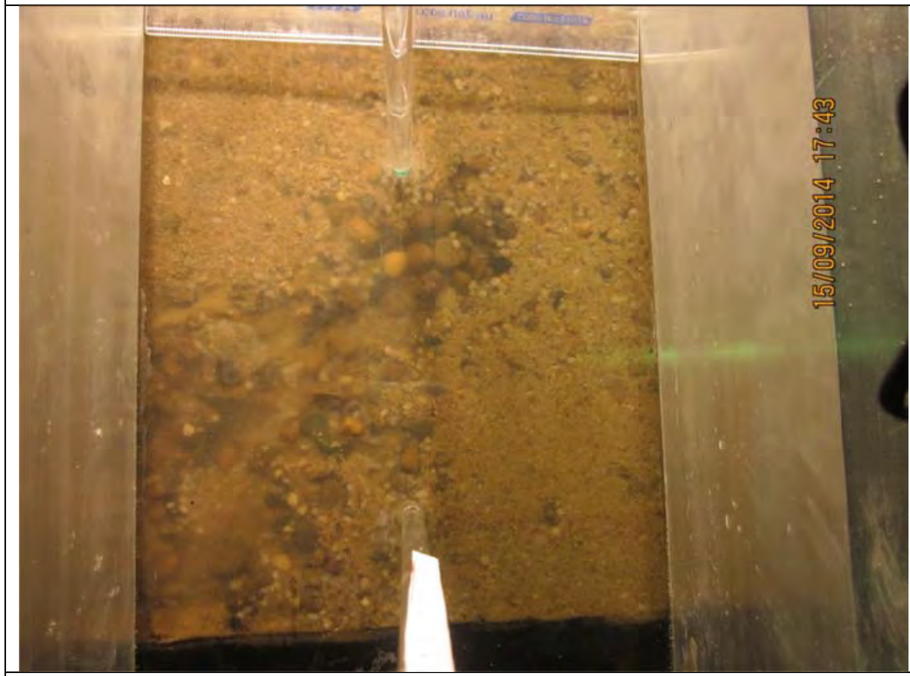

Figure 52-4 Perhaps larger particles at tip were preventing finer particles from eroding?

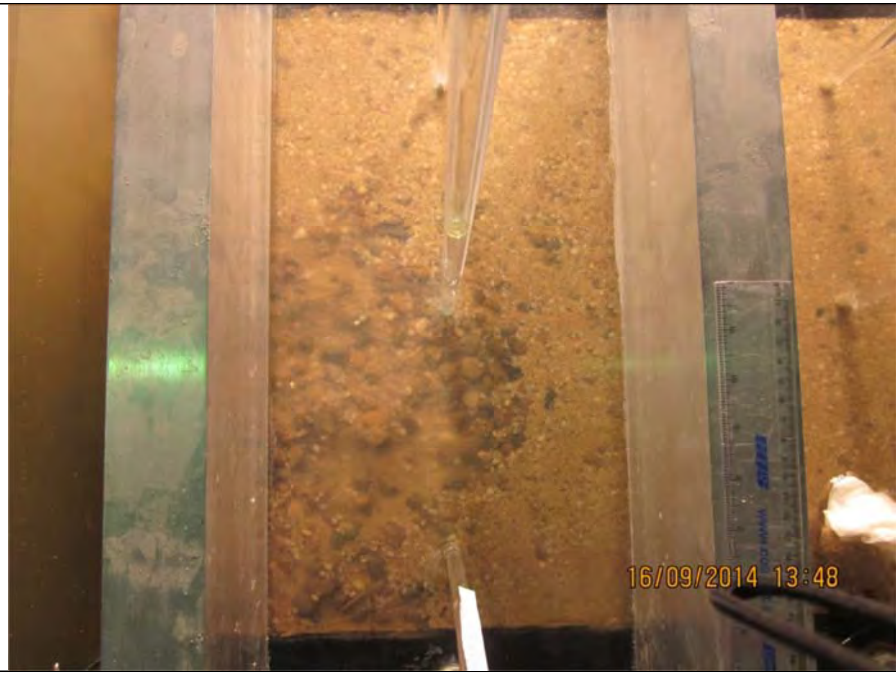

Figure 52-5 Channel doubled in width after having been tamped with mallet

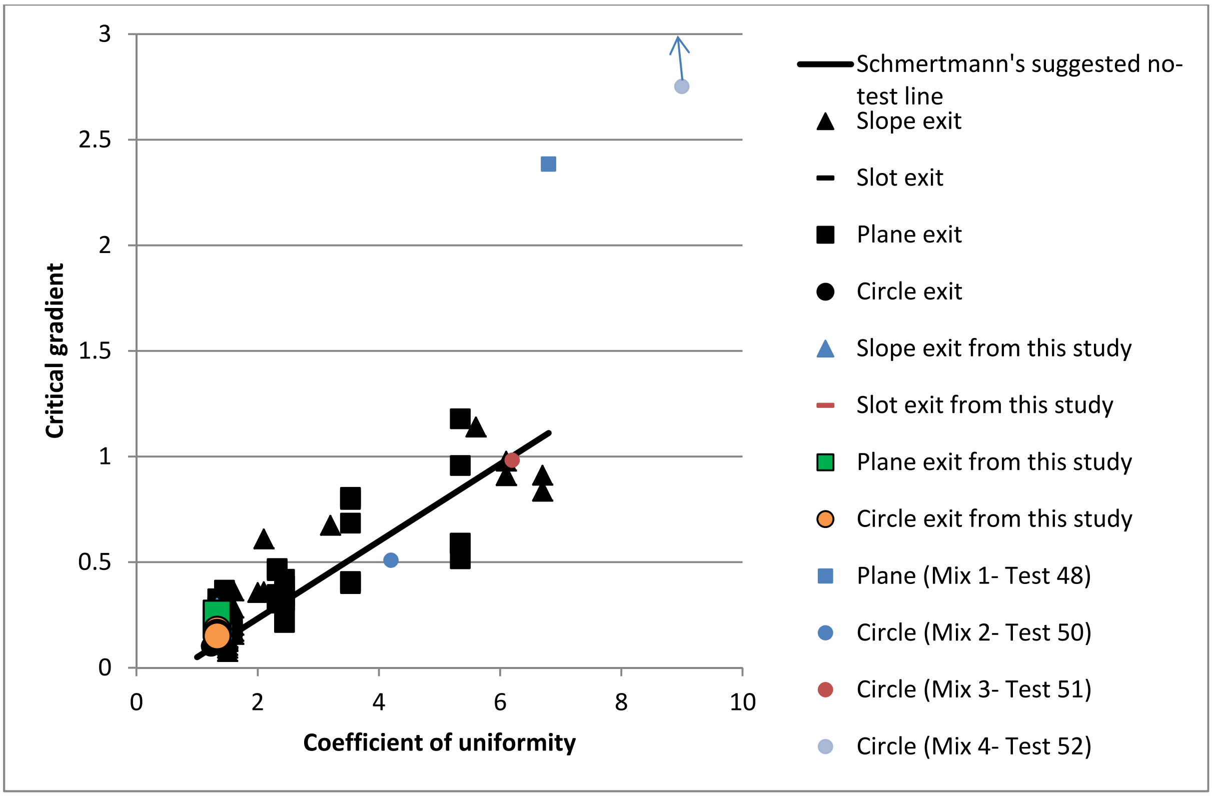

Figure 52-6 Test 52 on Schmertmann's graph

Seeing as I was measuring flow with the scales only between channel lengths 298 and 338mm, I wasn't able to get a clear indication whether the apparent permeability increased with channel length or not. Although it is suggested.

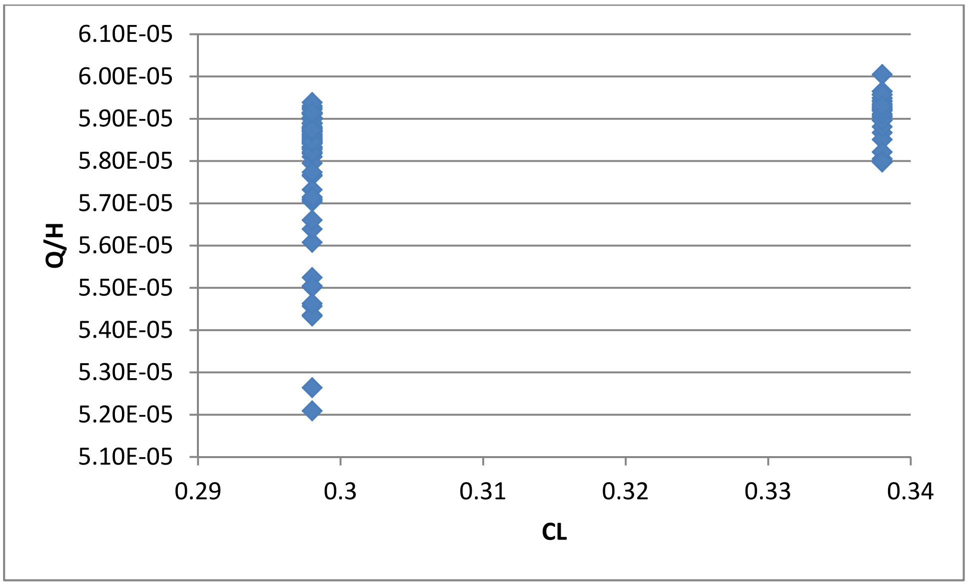

Backward erosion piping test data sheet

Test #	53	Exit type	circle
Date	22-9-14	seepage length	1.3 m
Soil	Mix 3	head in bladder tank	5 m
Flume	4	compaction	tamped

time	head	observation
18-Sep		
10:30am		co2 on
12:37		inflate bladder (opps)
4:00		co2 off
4-Jan	4.05	water on
19-9		Didn't start test because gas bubbles still around
22-9		
11.16	0	all air/gas bubbles appear to have
		gone.
		This is a repeat of test 51 but I'll
		remove + weigh + PSD material
		removed to try assess whether
		the channel gets "stuck" at 30%L
		because the sand boil is stopping it
		or not. In test 51 initiation occured
		at 100mm, then moved to 233mm ~~until~~ where
		critical head of 1277mm was reached.
11.33	↑ 90	
11.43	↑ 103	
11.49	↑ 140	
11.57	↑ 164	
12.02	↑ 188	
12.10	↑ 212	A channel has initiated but it's
		directed "downstream" so I'm not going
		to count it.
1.33	↑ 237	
1.38	↑ 291	
2.10	↑ 285	there's now 2 channels but both
		either out to side or "downstream"
2.38	↑ 332	
2.57	↑ 379	Initiation. See sketch + happy snap

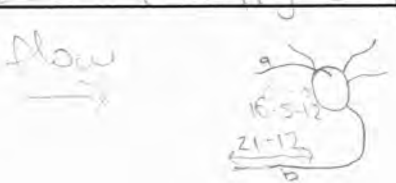

time	head	observation
3.05	↑ 403	no tips moved.
3.13		first boiled material removed. See happy.
		I tried removing the material (for a PSD)
		and I did but it was very difficult.
		I guess I got somewhere btw 60-90%
		of it.
3.22		tip a 180-110mm tip b maybe 170-110mm.
3.23	↑ 452	
3.24		tip (a) at wall. Water cloudy.
3.26		somewhere beneath b1.
3.28		tip 0 ab1
3.30	↓ 428	60 ab1 (at 25%)
4.09		60 ab1. Removed boil (see happy snap).
4.13	↑ 449	60 ab1.
5.47	↓ 0	
23-9		
9.48	0	60 ab1
9.52	↑ 372	
9.59	↑ 472	60 ab1
10.27	↑ 496	
10.53		160 ab1 under right standpipe.
10.56		removed sand boil 3.
11.26	↑ 520	160 ab1.
11.32	↑ 566	160 ab1
11.56	↑ 616	160 ab1
2.19	↑ 663	160 ab1
3.00	↑ 709	160 ab1
3.35	↑ 753	160 ab1
3.54	↑ 801	160 ab1
4.05		removed boil #4.
4.50	↑ 846	160 ab1
5.00		60 ab2 + water in d's box murky.
5.02		60 ab2 collect #5 boil.
5.06	↓ 90	overnight. 60 ab2
24-9		
9.48	90	60 ab2
9.49	↑ 795	" "

Test 53

time	head	observation
10.04	↑ 819	60ab2
10.15	↑ ?	60ab2. It's possible the channel is
		blocked btw bars 1+2. See happy
		snap.
10.51	↑ 870	60ab2
11.20	↑ 919	60ab2
≐50mm 12.33	↑ 964	60ab2
12.38	↑	
12.52		180ab3
12.55		about 10minutes ago I witnessed a....
		not sure what to call it. fluid
		erosion? Concentrated leak? A
		region that opened up along the
		u/s boundary. like a gap
		left behind as sand moved
		d/s. See happy.
12.58		180ab3
1.00		removed bail #6.
1.05		because sediment is now in water
		the filter is getting clogged. The head
		dropped down to around 800mm. So
		I had to open the head tank in
		valve more.
1.12		at the moment the head is at 1009 and
		still rising. I've fully opened the tank
		inlet but the water is struggling to get
		back up.
1.13		As I was writing the last entry the
		test failed ~~As in the~~ (I had my
		back to it. I heard it before I
		saw it) As in the channel reached
		the u/s end and forward widening
		occurred + completed all within a
		few minutes.

time	head	observation

Test 53

			Row 1			Row 2			Row 3					
	time	head	right	middle	left	right	middle	left	right	middle	left	time for 50mL	Avg	Temp
22-9	11.17	0	3	4	2	4	2	-5	3	3	4	using scales		
	12.13	212	93	94	93	124	123	119	159	156	155			
	3.03		149	150	150	206	206	204	271	266	264			
	3.28		153	150	152	226	228	226	311	304	300			
23-9	10.34		55	109	128	205	210	213	311	303	300	" "		
	5.01		60	59	135	282	288	308	500	484	477			
24-9	12.53		100	100	100	130	109	92	145	170	165	these were fluctuating		
			quickly				quickly			quickly	rising	as the channel		
				falling			falling			~~Rotated~~		moved around and		
	12.34		125	many	99	145	130	113	many	150	160	the geometry of the		
	1.10		75	69	66	89	87	65	95	100	100	channel changed		

53. Test 53 (flume 4) circle

Test 53 was a repeat of test 51 (circle test on mix 3 (d10=0.2mm and Cu= 6.2)). The aim was to test for repeatability and see if the accumulation of boiled material could be the reason why the tip get 'stuck' about a 1/3 of the way (because the boiled material adds resistance).

The soil was placed dry and tamped every fifth of the way up. Saturation was achieved using CO2 flushing.

Initiation occurred at 379mm and stopped after 45mm. Several increases in head (and progression up to 620mm- 48% of L) were required to get to critical head of 1014mm. This is notably different from test 51 (see figure 2). Test 51's critical head was 1277mm (so this was an 20% decrease) and it reached critical at a length of 18% of L (so this reached critical much further up the flume).

The boiled material was moved 6 times throughout the experiment. The material was dried and PSDed whose results are given below in figure 7. AS can been seen in the figure, the grading of the boiled material becomes larger with each boil removed. The last boil was very similar in grading to mix 3. I also notice that 2 and 3 are very similar and 4 and 5 are very similar and these boils were removed when the heads were similar (see figure 1) so it's likely the head applied affects the size of material boiled.

Whilst it is possible that the critical head was lower in this test than test 51 because the boiled material was removed, I don't think it is the case. I think this because every time I removed the boil (which I did so when the tip was stationary) the tip didn't progress any (not until much later after the head had been increased again). To illustrate this I have plotted over figure 1 when I removed the boils. So, I don't think the sand boil adds any resistance or is the reason why the channel gets 'stuck' at about 30%L.

What was also interesting was that once the critical head was reached I didn't notice the channel had moved lots until 14 minutes later. It may have been moving over that time but based on how fast it was also moving when I did notice it, I doubt this was the case. So I suspect the tip stayed stationary at the critical head for about 10minutes (my best guess) before moving (I can't check the SLR photos to verify this because that battery had gone flat over this time).

As the tip was progressing rapidly (and approaching 846mm) I noticed a gap formed along the u/s boundary (see figure 5). I think this gap opened up as sand moved into (and towards) the channel. The gap didn't seem to have any effect on the rest of the test.

Also, at critical and once the tip was rapidly progressing, the downstream water became murky (figure 6) and once this murky water was reticulated through the system I noticed the head was dropping (from 1014 to 800mm 13 minutes later). I suspect this happened because the sediment in the water was clogging the filter. So I had to fully open the tank inlet valve so there's was next-to-no head loss across it to compensate. At roughly the same time as the head dropping the tip stopped and 1 minute later after the head had gotten back up to 1009mm the tip progression recommenced (and did so rapidly). So in short, I think once the critical head was reached the tip would have rapidly progressed to the u/s end without stopping (as it has done so for previous well graded tests) if it weren't for the head dropping. The test failed a minute after the tip reached the u/s end.

Figure 3 shows where this test plots on Schmertmann's graph. It plots near Schmertmann's 'no-test' line.

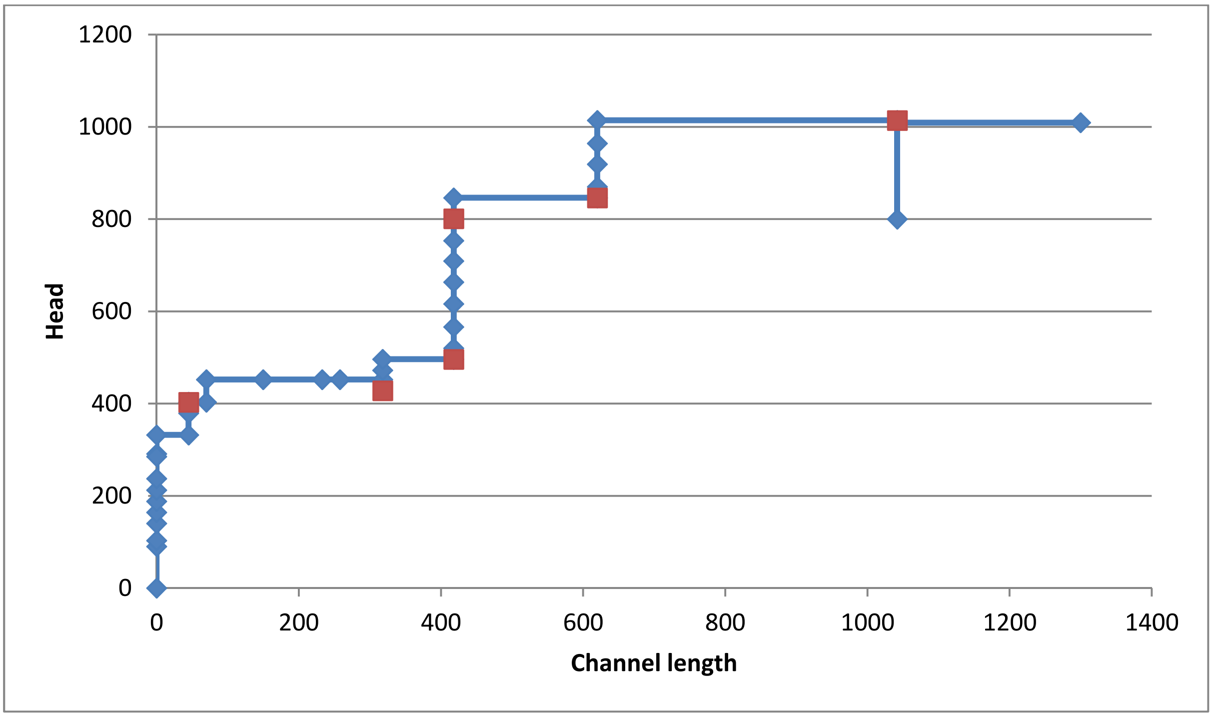

Figure 53-1 Test 53 plot (red points indicate when sand boils were removed)

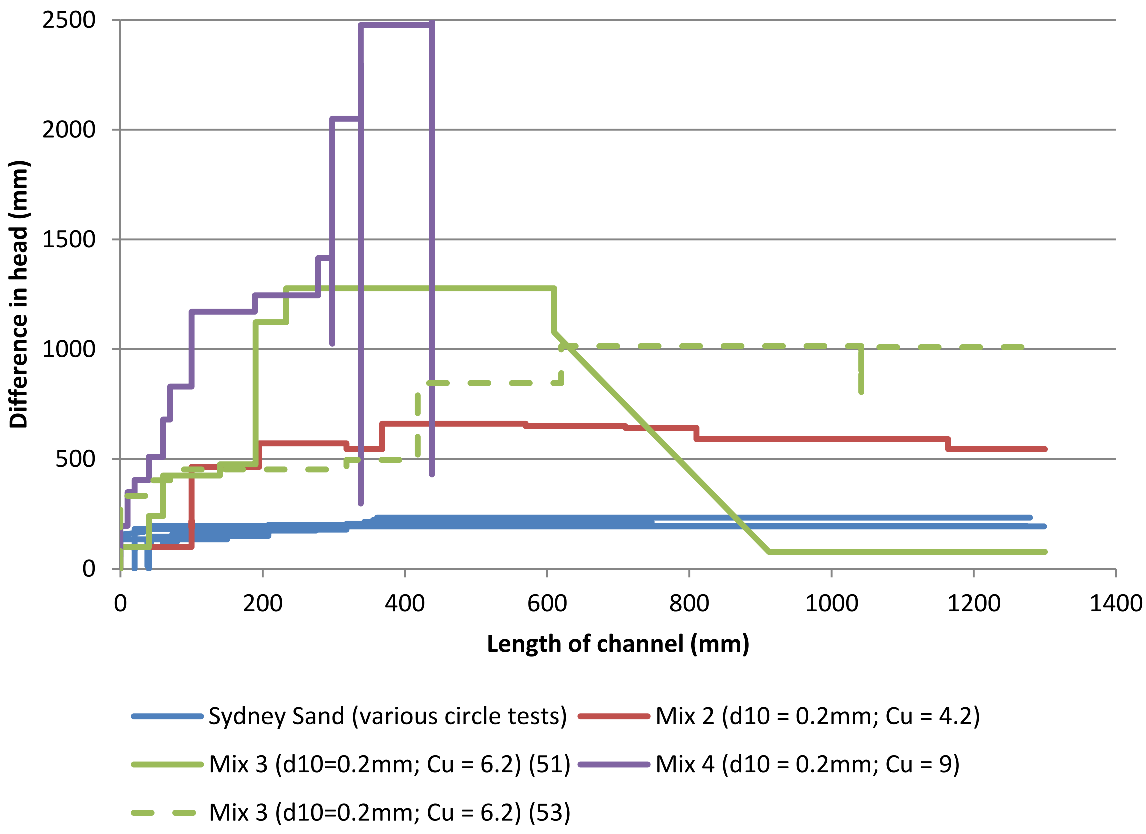

Figure 53-2 H vs L for different soils

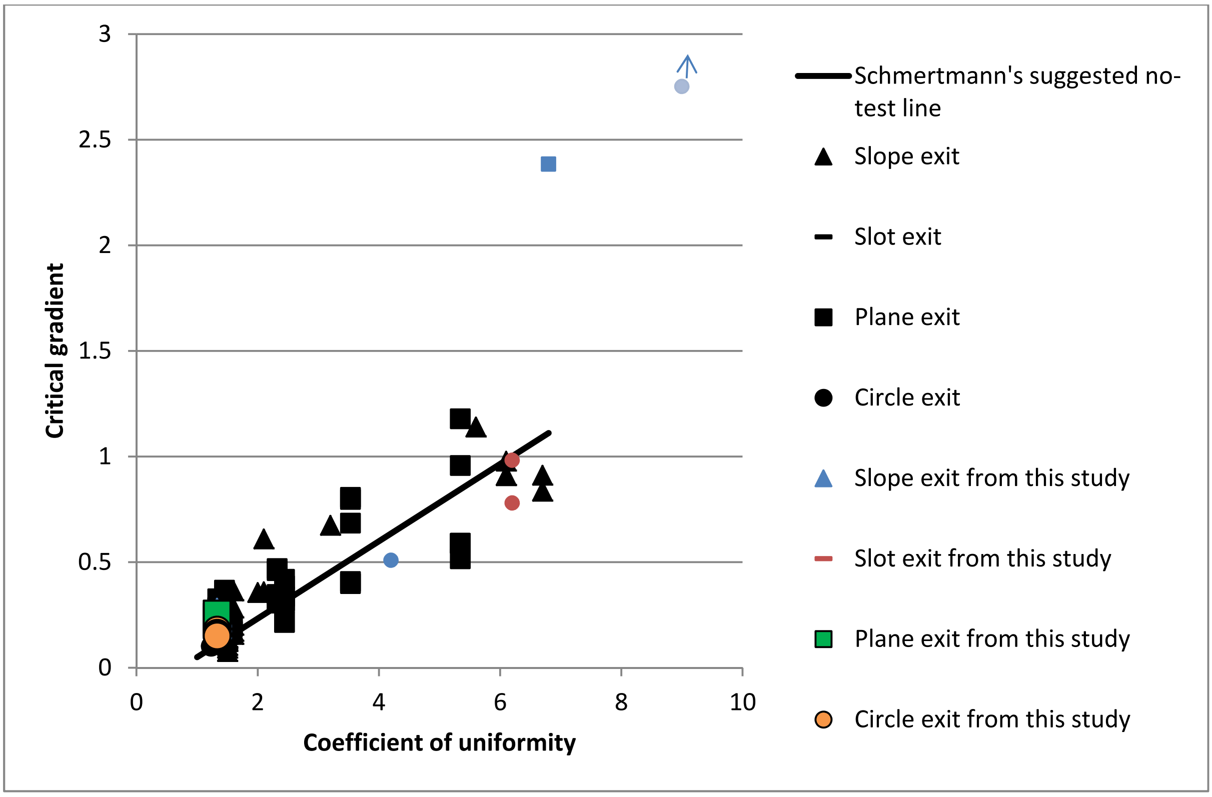

Figure 53-3 Schmertmann's graph with test 53 plotted (it is the lower red circle)

With respsect to flow, the apparent permeability increased with channel length as illustrated in Figure 4 in a similar fashion observed by Vandeboer et. al.

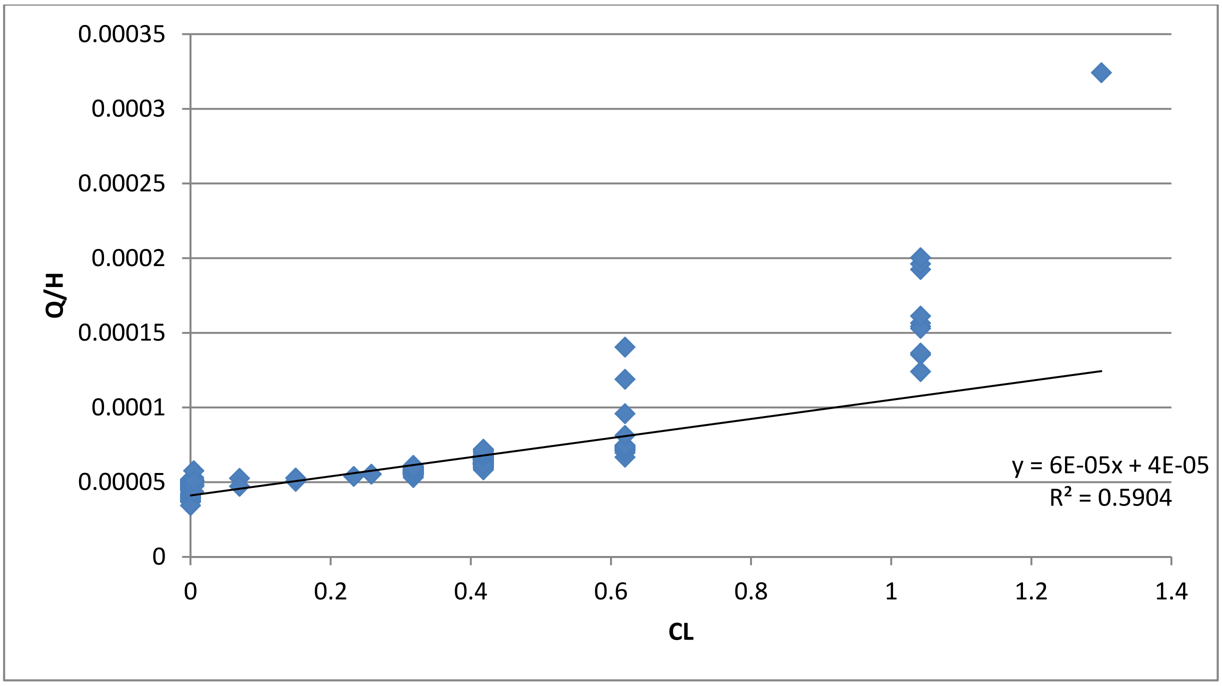

Figure 53-4 Change in apparent permeability with channel length

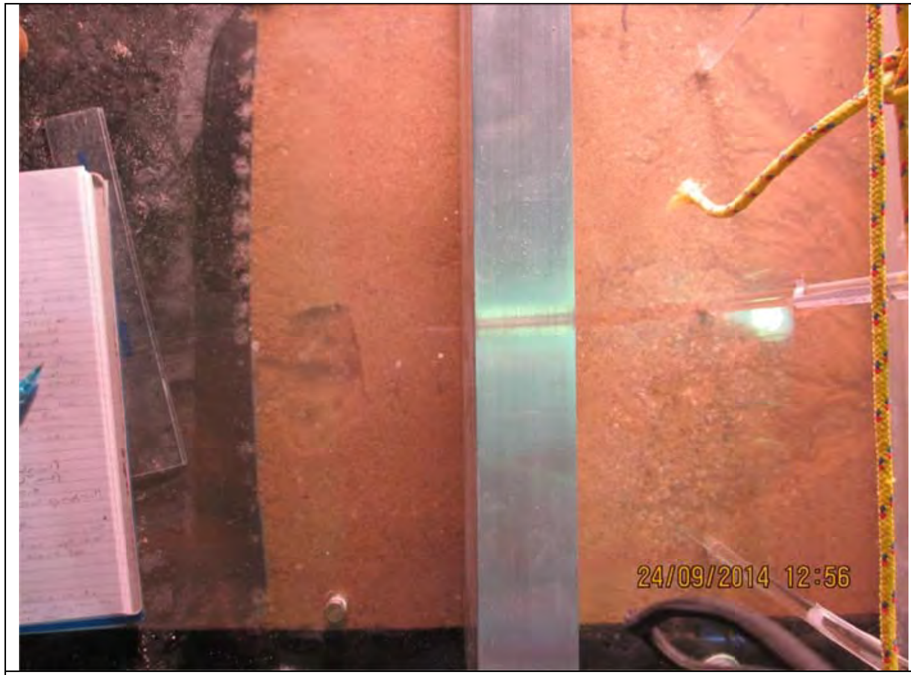

Figure 53-5 gap that opened along u/s end as sand moved towards and into the channel

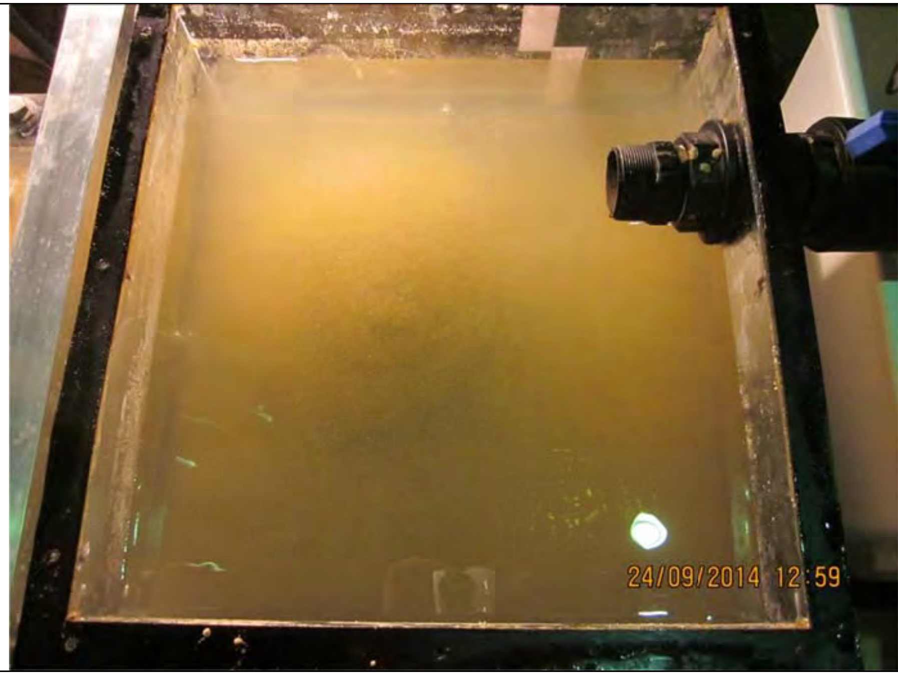

Figure 53-6 Murky water whose sediments partially blocked the filter and caused the head to drop

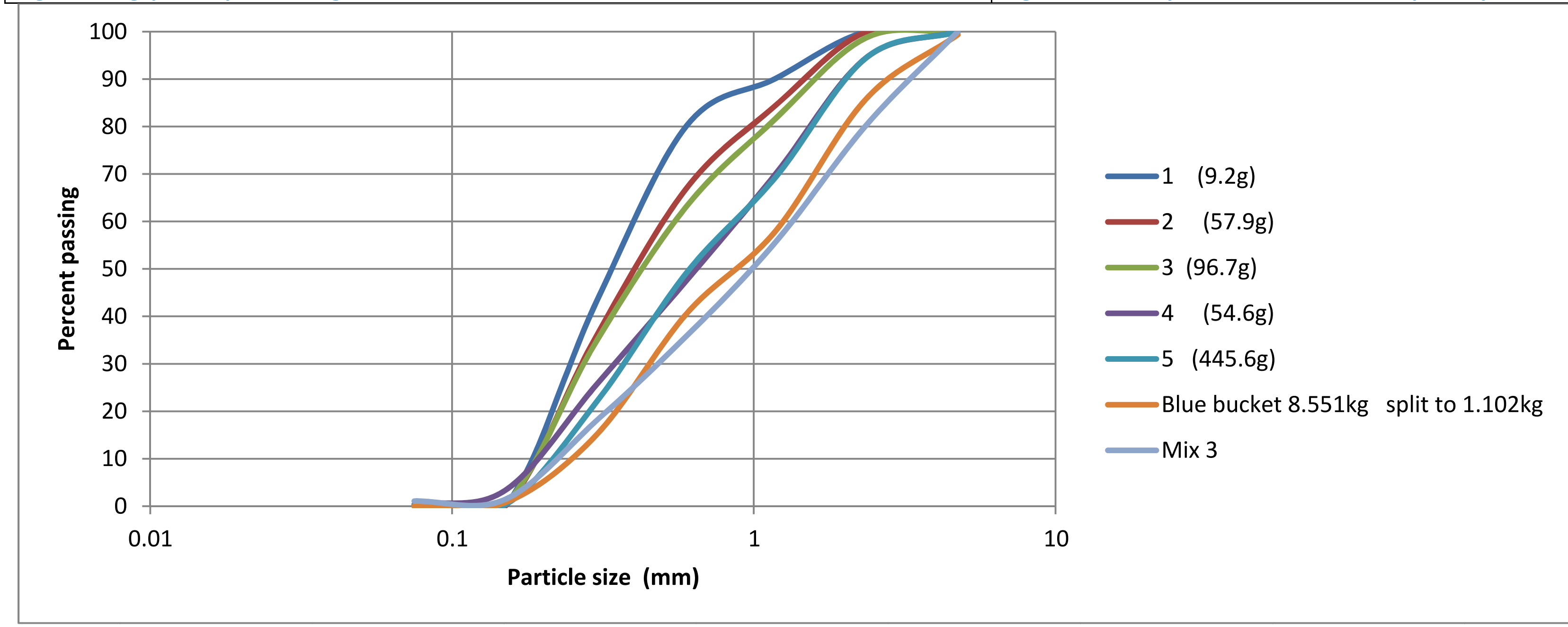

Fig 7.

Backward erosion piping test data sheet

Test #	~~53~~ 54	Exit type	circle
Date	26-9-14	seepage length	1.3 m
Soil	~~Mix 3~~ Mix 1	head in bladder tank	5 m
Flume	~~4~~ 3	compaction	~~tamped~~ placed underwater

time	head	observation
~~18-Sep~~		
~~10:30am~~		~~co2 on~~
~~12:37~~		~~inflate bladder (opps)~~
~~4:00~~		co2 off
4:15 ~~4-Jan~~		~~water on~~
26-9		
11.43	9	started to inflate bladder super
		slowly. Like 7.5cm/1minute.
12.55	9	bladder tank now full to 5m. NO
		sign of concentrated pore pressure
		release or channeling. (Yay!).
1.02	↑250	I note I can't see the exit on
		account of the turbid water.
1.57	↑493	I can see disturbance has occurred
		at the exit ~~due to~~ because I could
		see a light-coloured plume + tiny
		bubbles. It's possible initiation has
		occurred but it's impossible to know.
		I note that water isn't flowing from the
		d/s valve yet but it's very close
		(maybe 10mm).
2.54	↑694	
2.56		again, I can see a pale plume
		above exit. See happy snap.
		there are large leaks from the
		u/s chamber. This may be affecting
		the head applied to the soil. See
		happy snap. there's not a lot I can
		do about it.
3.12	↑932	

Test ~~53~~ 54

time	head	observation
2.14		movement seen in water in d/s box
		again. But no sign of a
		channel btw box and bl.
2.18		I can see, btw " " ", an
		entire region of soil slowly migrating
		d/s (like across a width about
		3/4 the flume width).
250 (I think) 3.20	↓	this "sheet flow" now extends to
		about 170mm d/s. this sheet flow
		worries me + but what's expected
		so I've dropped the head and it
		seems to have slowed it down.
		D/S water very turbid.
3.28		I think there's a channel that's
		formed in the zone where the 'sheet
		flow' occurred. Tip now at 150d/s. It's
		not easy to see as light in colour
		from turbid water.
3.32		sudden failure by sheet flow
3.33	↓↓↓↓	

54. Test 54 (flume 3) circle

Test 54 was a repeat of test 48 (mix 1) (but this time with the circle exit). Mix 1 was placed under water in small lifts with no compaction.

When I inflated the bladder I did it very slowly so that no "channel" formed like it did in test 48 (channel not by backward erosion but a deformity in the soil, like a pipe, that occurred when excess pore pressure escaping concentrated and left a pipe behind).

Again, the water in d/s box was turbid and I couldn't see the exit.

I don't know if backward erosion ever initiated but at a head of 493mm I noticed a light-coloured plume and small bubbles above the exit (suggesting sediment transport of fine material). See pic 1 for e.g. of plume.

At a head of 932mm I could see, between the box and bar 1, a region of soil slowly migrating d/s. this 'region' was across approximately ¾ of the flume. Once this 'sheet flow' extended to about 170mm after bar 1 (see pic 2) I dropped the head by approximately 250mm. This seemed to stop the sheet flow and it left behind what looked to be a channel whose tip was 150ab1 (see pic 3). However 12 minutes later the experiment slipped suddenly by sheet flow/top surface slip. Pics 4 and 5 are 1 minutes apart.

Test 48 failed the same way- sudden sheet flow/top surface slip however it happened at a head almost 3 times higher (at 3.1m). I don't know why this test failed sooner than test 48 but what I have decided is placing soil underwater leaves it too loose and will slip along the top surface before it backward erodes.

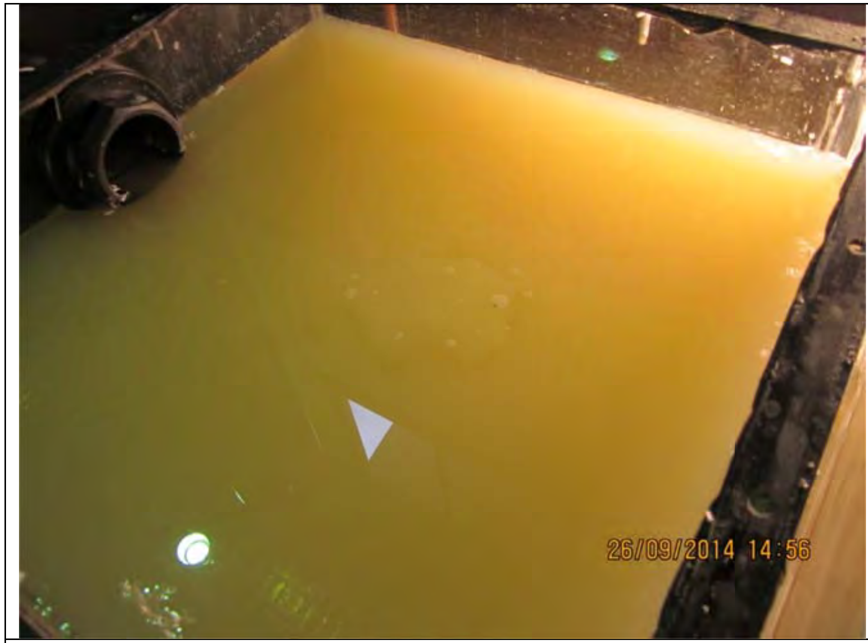

Figure 54-1 Plume and bubbles above exit- possible indication of backward erosion occurring

Figure 54-2 The start of failure by sheet flow (region indicated was slowly sliding d/s)

Figure 54-3 Possible channel left behind when 'sheet flow' stopped

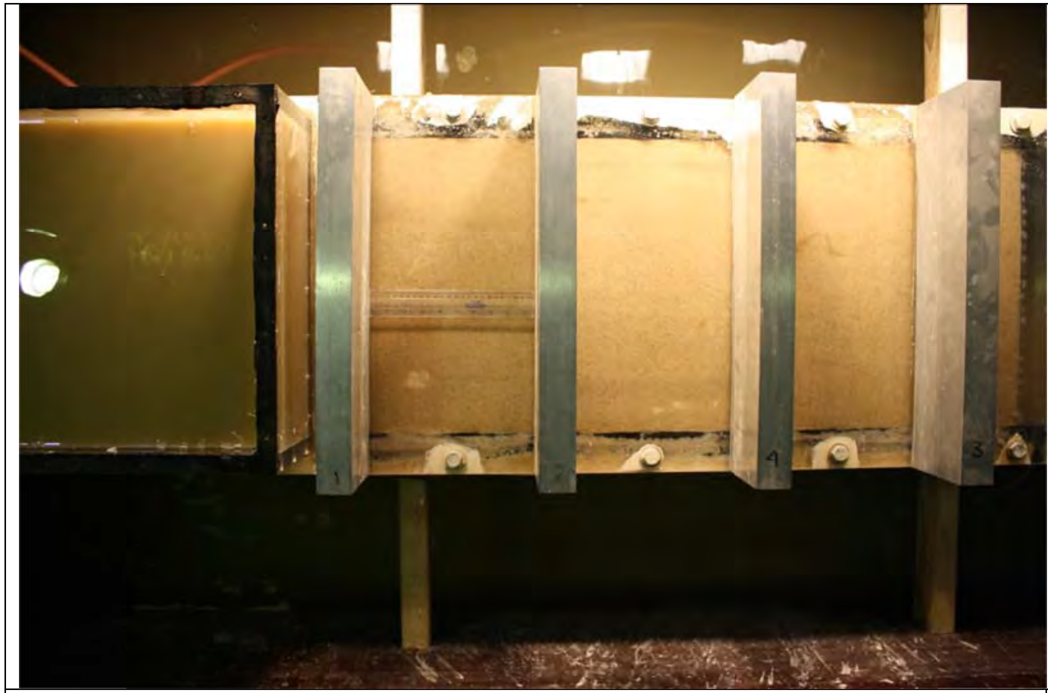

Figure 54-4 In the minute before failure

Figure 54-5 In the minute after failure

Backward erosion piping test data sheet

Test #	~~54~~ 55	Exit type	slot
Date	3/10/2014	seepage length	2.6 m
Soil	Syd sand	head in bladder tank	5 m
Flume	1&2	compaction	vibrated

time	head	observation
29-Sep		
10:15am		inflated bladder
10:15		co2 on
4:20		co2 off
4:30		water on
7-10 1:45		3 small channels present at the start
		of test (probably occured [illegible]
		head (pump issues)). See SLR.
		Based on test 41 we expect
		initiation ≐ 270mm and critical at
		461mm.
1:54	↑ 34	
2:10	↑ 89	
2:17	↑ 129	
2:24	↑ 185	
2:35	↑ 205	
2:46	↑ 232	
2:52	↑ 260	
2:58	↑ 289	[DSLR 101-9282]
3:03	↑ 309	
3:08	↑ 335	
3:13	↑ 361	First few particles detached (not sure from
		tip or base) – [DSLR 101-9284/5]
3:18	↑ 384	Very small amount of particle movement at
		the sand boil
3:23	↑ 412	Group of about 3-5 particles detached [101-9286]
3:28	↑ 439	Piping initiated. Clusters detach from tip of
		pipe
3:47		Sandboils become too large, hence the channel
		exit moves aside [101-9284 to 101-9286]

Test ~~54~~ 55

time	head	observation
cont'd		Secondary erosion is much greater than
		primary [101-9317 to 101-9321][101-9327 to 101-9329]
3:53		Primary erosion has almost completely
		stopped. Secondary erosion still occuring
		significantly. Sand exiting through two
		boils in the slit. Pipe stops at 70ab1
3:59		Primary erosion commences again in small
		clusters, but in a channel to the side.
4:02		Erosion in the channel to the side
		stops. Erosion in the main channel
		commences again [101-9331 to 101-9333]
4:05		90ab1
4:10		110ab1
4:15		DSCR [101-9334 to 101-9335]
4:20		125ab1
4:26		145ab1
4:31		150ab1
4:39		180ab1, alternating between one and two
		sand boil exits
5:40		200ab1
5:41	↓ 43	
9-10 11.20		Air bubbles are in the sample. I think it's
		because the submergable pump stopped
		(maybe because it overheated) and the
		water level dropped. So I think
		the experiment is ruined. I can see
		air gaps all throughout. But I'll
		try run it anyway. See happy snaps.
11.23	↑ 416	Sediment transport + detachment
		occuring again but still at 205ab1.
11.35		under b2.
11.48		43ab2
11.55		78 ab2
12.12	↓ 390	195 ab2 past 25%.
12.15		Yep, water had definitely emptied from
		the flume because I just found a
		large air bubble in the entire u/s
		chamber + the u/s box was empty.

Test ~~53~~ ~~54~~ 55

time	head	observation
		It was empty (despite head
		~~ato~~ ≐400mm because the was
		air pressure in it. Once I opened
		valve on top of u/s box it
		~~[illegible] pushed air~~ sucked air in
		+ equalised and ~~$~~ refilled with
		the water. I don't think the
		air gap had reached the u/s
		end of the sand.
12.18	~~[illegible]~~	222 ab2
12.25	~~[illegible]~~	225 ab2
12.30	↑ ~~[illegible]~~ 400	the hose from the d/s box has
		been siphoning a lot so flow
		measurements might not be right. I've
		hopefully fixed it now.
12.45		236 ab2
12.57		236 ab2
1.32		130 ab3
1.38		240 ab3
1.58		82 ab 4
2.08	↓ 373	180 ab4 (past 50% L)
2.10		channel appears to be blocked btw
		bars 2+3.
2.24		190ab4. still blocked btw 2+3.
2.34		218 ab4
2.57	↓ 347	250 ab4
3.24		blocked btw 2 to 4. + tip under b 5.
4.04	↑ 358	still under b5
4.27	↑ 370	" " "
4.49		" " " + still blocked btw 2 to 4.
4.55	↑ 396	
5.00		15 ab5
5.03		I've had to stop weighing flow because
		I need the bucket + pump at P3.
5.12		28 ab5
5.42		43 ab5
5.50	↑ 422	" "
6.08		212 ab5 no longer blocked.
6.14		250 ab5

Test ~~53~~ ~~54~~ 55

time	head	observation
6.23		there's a large air bubble that starts about 30ab6. the tip has reached this bubble. Air has travelled down the channel and essentially blocked it. there's no point continuing because air in the channel will prevent flow through the channel and the air bubble its self expands the middle 1/3 of the flume (so it's wide and would take a lot of work to go around) AND in flume 2 there are more large bubbles and even flow paths in the sand (see happy snap). So there's no point continuing. Test ended.

55. Test 55 (flume 1&2) slot

Test 55 was a repeat of test 41 to see if I could get a flatter CL vs H line (like I did in test 45).

After the first day of testing at some point the submergible pump switched off (maybe because it overheated) and the water level dropped to below the lid. This meant air bubbles were brought into the sample, see pic 2. Despite this I ran the test.

Backward erosion initiated at 439mm. When the head was dropped at 25% and at 50%L the tip kept progressing. Once the tip was 180 after bar 4 the channel became blocked between bars 2 & 3 but continued to progress for another 70-80mm before it stopped and I had to increase the head. Once I had increased the head by 50mm the tip recommenced and progressed another 43mm but stopped, so increased head again by another 25mm and the blockage cleared the tip progressed again.

At approx. 30mm after bar 6 a large bubble (about 1/3 of the flumes width) was present (see pic 3). When the tip reached this bubble more air entered the channel (pic 4). For this reason and because further upstream (in flume 2) there were large voids from where sand had flowed back into the upstream chamber when the water emptied (see pic 3).

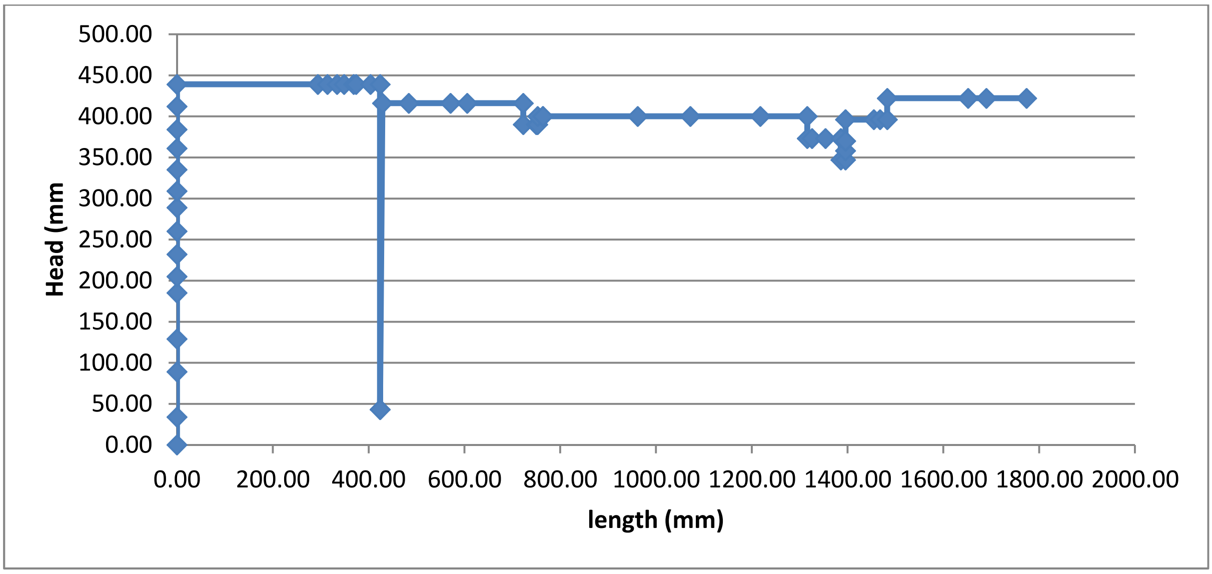

Figure 55-1 test 55

To compare this with test 41, it the H vs L curve was a little flatter but it was also a little lower. All in all I think the differences are minor and I've demonstrated repeatability and consistent critical local gradients (see f

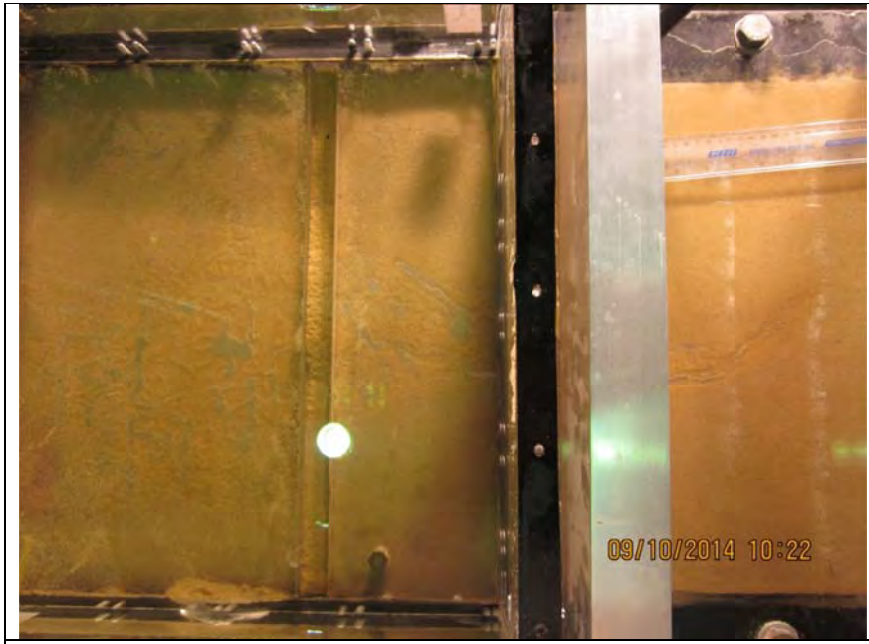

Figure 55-2 Air entered the sample when the water level dropped whilst unattended

Figure 55-3 Test ended when tip reached air bubble located at end of flume 1 (can also air and voids in flume 2)

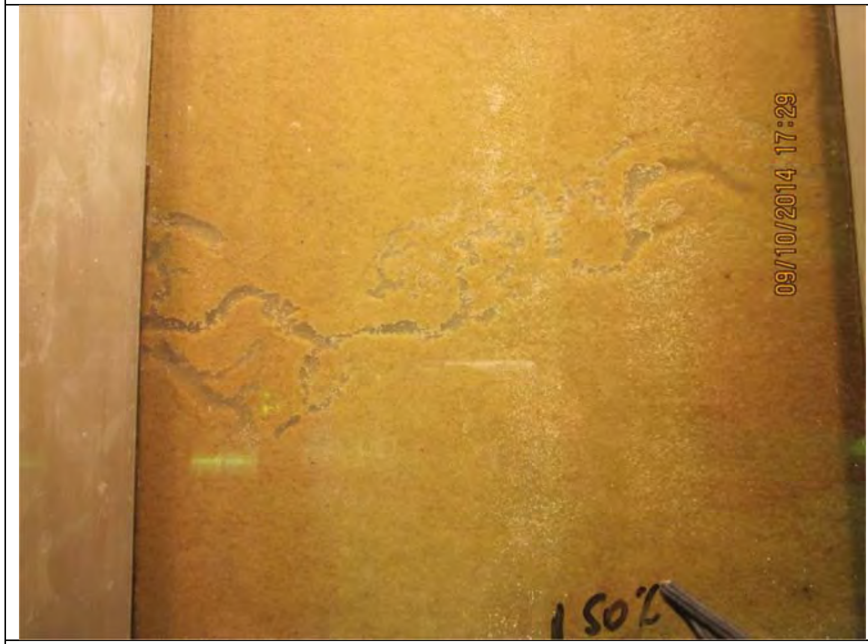

Figure 55-4 When channel reached large air bubble, air travelled down the channel

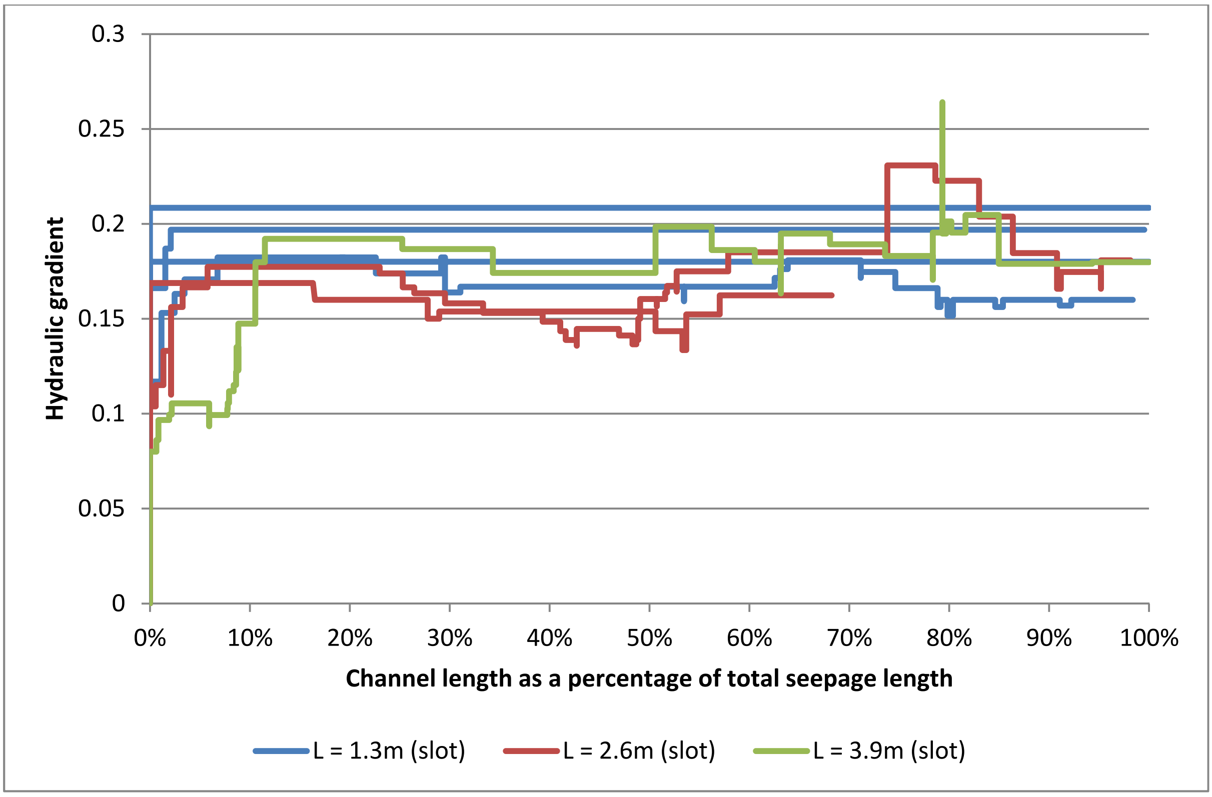

Figure 55-5 When channel reached large air bubble, air travelled down the channel

Backward erosion piping test data sheet

Test #	~~55~~ 56	Exit type	circle
Date	9-10-14	seepage length	1.3 m
Soil	mix 1 (dry)	head in bladder tank	5 m
Flume	3	compaction	tamped

time	head	observation
3-Oct		
12:00		inflated bladder
12:02		co2 on
4:30		first noticed CO2 had run out
7-Oct		
10:50		co2 on
4:30		co2 off
4:35		water on
9-10 11.27		when I first saw the exp this morning
		I thought it just hadn't been
		saturated yet. However given the
		gas bubble is so large in the u/s
		chamber and air bubbles are all
		through out the flume and it's
		been saturating 2 days, I think
		the same thing that happened to
		test 45 has happened to this.
		the submerged pump stopped so
		water ran back down to the pit
		and partially drained the flume
		(and reintroduced air). I'm going to
		run the experiment anyway just in
		case it can still work (and given
		how much effort went into filling
		it up).
11.53	40	
11.54	↑ 216	Water in standpipe is murky.
12.04		Can see that fines are being transported
		out due to murky water about exit.
		Water in d/s box ≈ ~~44~~mm above lid

40

Test ~~55~~ 56

time	head	observation
		(so not at datum yet.
12.19	↑ 314	
12.27	↑ 410	water level in d/s box now about
		46mm. (Hard to tell cause I
		can't get my eye level with
		it).
12.50	↑ 605	
1.39	↑ 705	d/s box water level = 58
2.02	↑ 810	I've noticed theres a steady head
		loss from one row of standpipes
		to the next but there's a huge
		head loss btw row 1 and the
		d/s box. Btw row 2 + 3 theres ≐ 0.1/0.3
		and btw 1 + 2 there's about the same
		but btw 1 and d/s box there's ≐ 0.5/0.2.
		And I don't know why!
		It's difficult to see if there's
		channeling but I don't think there is.
2.23	↑ 918	
3.00	↑ 1022	level in d/s tank = 75mm
3.17	↑ 1121	
3.26	↑ 1225	
4.00	↑ 1325	I can't see through d/s water at all
		now.
4.28	↑ 1415	
4.36	↑ 1538	
4.38	↑ 1644	this head increase seems to be
		pushing air/gas out of the u/s
		chamber through the sample and out
		the exit. I think this is happening
		because a) I can see a continual
		stream of air bubbles leaving the
		exit (see happy snap). b) I can see
		the air bubbles through the sample
		pulsating + moving (see vid on happy
		snap) and c) the air bubble in the u/s
		chamber has shrunk (indicated by
		the line I drew on the lid where
		the bubble/water interface was this

Test ~~55~~ 56

time	head	observation
		morning). See happy snap.
4.45		stream of bubbles leaving exit stopped.
4.58	↑1844	
5.14		It just started dripping out of the d/s
		valve.
5.43	↑2046	
5.47	↑2258	
6.11	↑2466	
6.19	↑2640-2680 (behind power).	
6.28	↑2893	
6.43	↑3118	
6.50		Flow per 50mL = 19.5, 17.8, 21.5, 15.9s. 50ml/18.6 2.68/1 2.677e-6
6.57	↑3353	
7.04		continual small bubbles coming up
		from exit. See vid on happy snap.
7.08		Closed ball to flume to remove head
		because I need to leave.
17-10 10.23	0	I can feel a boil (and almost
		see it - see happy snap). I think
		it's has a diameter of ≈150mm. But
		I don't know if that means its
		backward eroding or not. I don't know
		if there's a channel.
10.32	3353	
10.58	↑3472	
11.20	↑3583	
11.36	↑3750	
11:43	3750	failure. I didn't see it when it started
		but I caught the "tail-end" of it and
		it appeared to fail by surface slip
		again.

Test 5~~5~~50

time	head	observation

Test ~~55~~ 56

don't know why this so different when ro[illegible]

		Row 1			Row 2			Row 3					
time	head	right	middle	left	right	middle	left	right	middle	left	time for 50mL	Avg	Temp
R.Q.		≈30 below	75	30	122	128	120	178	174	165			
1.59		380	394	410	520	509	514	611	605	613			
		too high to measure											

56. Test 56 (flume 3) circle

Test 56 is a repeat of test 38 (mix 1 tamped in dry with saturation achieved with CO2 flushing). Substantial fine grained material became air born during the tamping process (see pic 1).

Over the two days of saturating at some point the submergible pump stopped (maybe because it overheated) and the water level dropped below the lid which brought air bubbles into the sample (see pic 2). So much water had emptied that a large air bubble was along the u/s edge of the sample.

Despite the sample being compromised and no longer saturated I ran the test.

At the start of the test I could see through the d/s box water (as opposed to tests that were placed wet). From early on (a head of around 200mm) I could see plumes of fine sediments being transported out of the exit.

I noticed the head drop between the standpipe rows was much less than the drop between row 1 and the d/s box (gradient of 0.1/0.3=0.3 between standpipe rows but 0.5/0.2=2.5 btw row 1 and d/s box). I don't know why this is. There is likely to be head loss around the exit but I wouldn't have thought there'd be this much.

By the time I'd raised the head to 1.325m I could no longer see through the d/s box water (too turbid).

At a head of 1644mm the air that was in the upstream chamber (shown in pic 2) was pushed through the sample. I could see air pulsated through the sample and air bubbles coming out of the exit.

On the morning of the 2nd day of testing I could feel a boil under the turbid water. It had a diameter of approximately 150mm but I can't tell if this boiled material is evidence of backward erosion or whether it was just material moved locally from around the exit.

At a head of 3.75m the sample suddenly failed by surface slip.

Air bubbles make a sample more resistant to backward erosion so it is possible that if the pump didn't stop and the water level didn't drop and bring air into the flume maybe backward erosion could have occurred at a head less than 3.75m. I will probably have to repeat this test again.

I didn't take SLR pics of this test because I was taking pics of test 55.

Figure 56-1 300g soil became airborn when tamping

Figure 56-2 The pump had stopped during saturation so the water level dropped below the lid and air was brought into the sample

Test ~~46~~ ~~56~~ 57

Backward erosion piping test data sheet

Test #	~~56~~ 57	$m_s + m_w$ after 'drying'	
Date	12-10-14	m/c after 'drying'	
Soil	50n	V_s	
Flume	4	$V_s + V_w$ in flume	
Exit type	circle	void ratio	
seepage length	1.3 m	relative density	
head in bladder tank	5 m	avg. time for 50mL	
bladder pressure	50 kPa	Q when ΔH = 0.1m	
compaction	~~rain~~ ~~60~~ tamped.		

time	head (mm)	observation
10/10		CO2 on
~~10~~ 12/10 10:50		Upstream at datum, d/s ~40mm below
		datum. ∴ ~~a loss of 40 mm~~
11:04	40	Boiling ~~observed~~. about 40 mm wide
16	↑ 67	
29	↑ 87	Initiation.
40		A channel growing ~~...~~ perpendicular &
~~45~~		downstream. ~80 mm long.
41	↑ 108	
54	↑ 126	2 channels growing perpendicular.
		100 & 90 mm in length.
4 12:09		60 after exit (a.e)
10	↑ 140	
13		80 ae
24		3 channels  100 ae, 65 ae, 30 ae
26	↑ 160	
35		130ae, 70ae, 35ae
42	↑ 172	
52		160 ae, 70 ae, 40 ae
54	↑ 193	
1:03		20 after box
1:15	↑ 217	under bar 1
29	↑ 241	
36		15 abl
46		20 abl

Test ~~46~~ 57

time	head (mm)	observation
1:47	↑ 265	
52		60 ab1
2:03		107 ab1 Reached 25% but
		as tip is moving very slowly the
		head will not be dropped.
08		120 ab1
09	↓ 253	changed my mind.
10		140 ab1
20		170 ab1
32		195 ab1
33	↓ 242	
43		205 ab1 Very slow tip progression.
52		210 ab1
2:53	↓ 0	Dropped to datum to be left overnight
13/10 11:30		Realised that the entry valve was only
		partially open. Likely that this
		caused a head loss between the
		VHT and the flume. ∴ need to measure
		this and adjust heads recorded.

time	VHT	Standpipe	Observations
11:39	↑ 50	40	210 ab1
12:15	↑ 73	61	
19	↑ 96	85	
22	↑ 121	110	
26	↑ 144	133	
31	↑ 168	157	
35	↑ 192	180	
39	↑ 215	203	
12:54	↑ 215	205	Valve is opened fully
57	↑ 239		
1:10	↑ 251		
23		~~215~~	215 ab1
33			220 ab1
35	↑ 263		~~[illegible]~~
45			233 ab1
52			At bar 2 (250 ab1)
2:12			3ab2
22			15ab2
23	↑ 276		Progression too slow
28			40ab2
42			85ab2
48			95ab2
57	↑ 288		Too slow.
3:15	↓		155 ab2
30			160 ab2
~~31~~	~~↓~~		

Only 2mm head loss

Test ~~46~~ ~~56~~ 57

time	head (mm)	observation
3:31	↓ 239	head dropped, will then increase
		half this drop to see the impact
		of an increase by 25 mm. (have only been increasing by 12mm lately)
35	↑ 264	~~No effect. Tip~~
44		No movement of tip. ∴ No effect.
45	↑ 300	
54		170 ab2
55	↑ 324	
4:05		195 ab2
4:07		210 ab2
12		245 ab2
26		10 ab3
27	↓ 0	
14-10 10.58	0	15ab3
10.59	↑ 284	
11.14	↑ 306	
11.20		28ab3
11.23		42ab3
11.38	↓ 283	103ab3 past 70%L
11.45	↓ 260	133ab3
11.53		155 ab3
12.04		163ab3
12.24	↓ 250	214 ab3
12.31		" ab3
12.49		230 ab3
1.10		under b4
1.31		" "
2.00	↓ 212	20ab4 (has moved laterally by about 50mm).
		(up to 90%L)
2.22		27ab4
2.47		53ab4
3.07		123ab4. There's a discolouration along
		the u/s bndry.
3.08		140ab4. I'm going to say it has reached
		the u/s end here because the
		channel is locally blocked (suggesting
		a flow surge) and the u/s side of the
		channel appears deeper (forward
		deepening has started). See happy
		snap.
3.14		the channel doesn't appear to be
		blocked anywhere else
5.14		The fwd deepening is up to 80 ab3.
		I don't want to leave it at this head
		incase it fails overnight so ↓H overnight.
5.45	↓ 25	I note there's usually a region ≈ 50mm
		ahead of the deepening that's blocked.
		i.e there's usually a blocked btw the
time	head (mm)	observation regular channel + the deepened channel.

15-10 9.45 fwd deepening still up to ≈ 50 ab3.

2.10 ↑h 9.46

5.47 fwd deepening up to 130 ab 3/2
Blockage extends b/tw 130 ab 3/2
and 170 abl. has been at this
position for a few hours.
Need to ~~take~~ head back
down to zero for overnight.

H = 27mm

16-10 1.55 27 All as I left it.
9.56 ↑210
11.17 ↑237 It's now been close to 24hr since
the channelling has changed any
so I'm going to ↑H a little
+ drop it back if it unblocks.
12.04 fwd deepening now progressing
again. blockage now only ≈ 20mm
~~Now~~ fwd deepening now inside 1o2.
5.39 ↓ turn it off for overnight.

17-10 10.26 ↑257
5.12 ↓

20-10 9.49 ↑260

57. Test 57 (flume 4) circle

Test 57 was the first test carried out on the Sibelco 50n soil. It was tamped in dry and flushed with CO2 before saturation.

Initiation occurred at 126mm. At a channel length of 278mm (21% L) an 'apparent' critical head of 265mm was reached however at a channel length of 563mm (43% L) the head needed raising up to a max of 324mm. This behaviour was unusual; usually the max head was around 20-30%L when critical first reached. I don't have any suggestions as to why it happened this way. I'm going to define the critical head as 324mm. See figure 1 for plot.

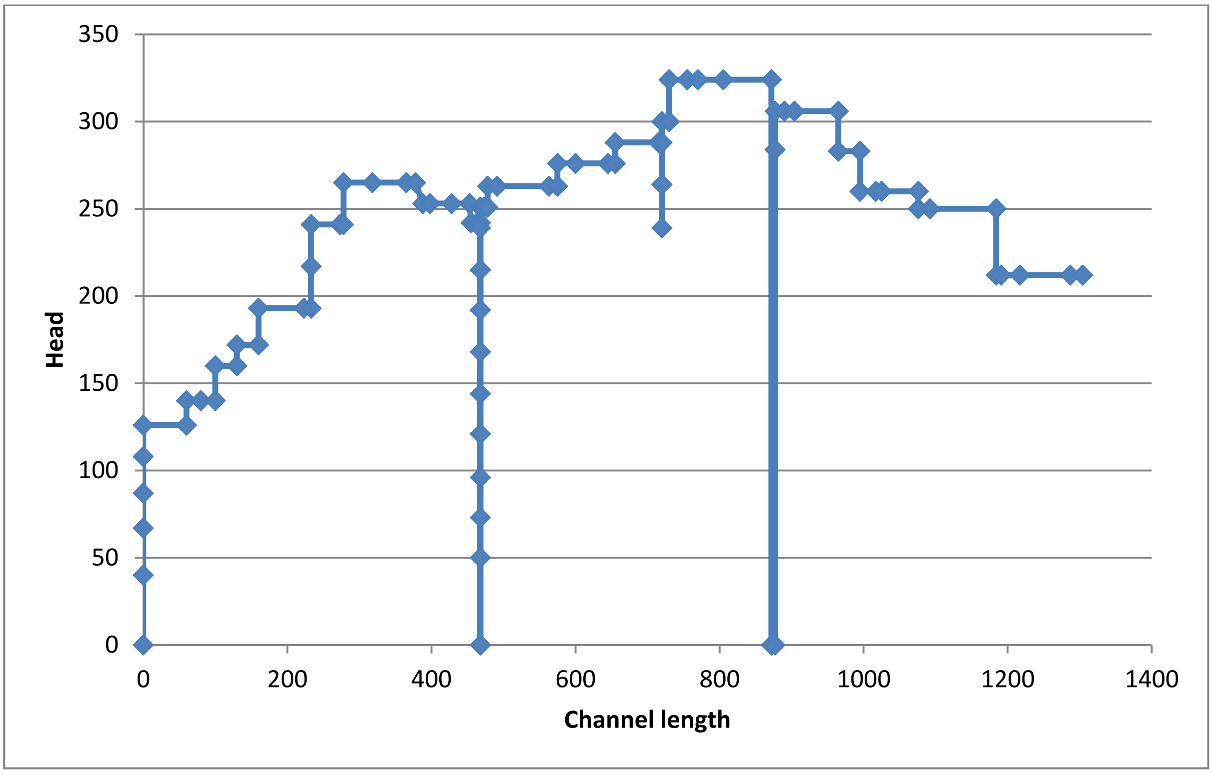

Figure 57-1 Test 57 plot

After 2-3 days of testing I noticed the sand become discoloured, probably due to bio-film (see pic 6) but it didn't appear to affect the experiment (erosion didn't seem to be impeded).

The forward deepening process in this test was interesting. There was always a blockage in between the deepened channel and the regular channel as seen in pic 7. My theory is when a channel is deepened so much sediment is suddenly pulled down the channel that the channel becomes blocked. Regular backward erosion removes the blocked sediment slowly (from the d/s end of the blockage). Once enough of the blockage has been removed the pressure in the deepened channel pushes what's left of the blockage downstream unblocks the channel causing another sudden cluster of erosion, reblocking the channel, and the process repeats. After about 0.5 days of forward deepening the channel didn't change for about 24hours so I raised the head by 27mm to 237mm and the forward deepening process continued. It took another 2 days (about) for the forward deepening to reach the d/s end and cause failure (the head was reduced back down to datum overnights and over the weekend). I captured the forward deepening process on the SLR and have made a time lapse video of it.

As for how the results of this test compared to others, see plots 2 and 3.

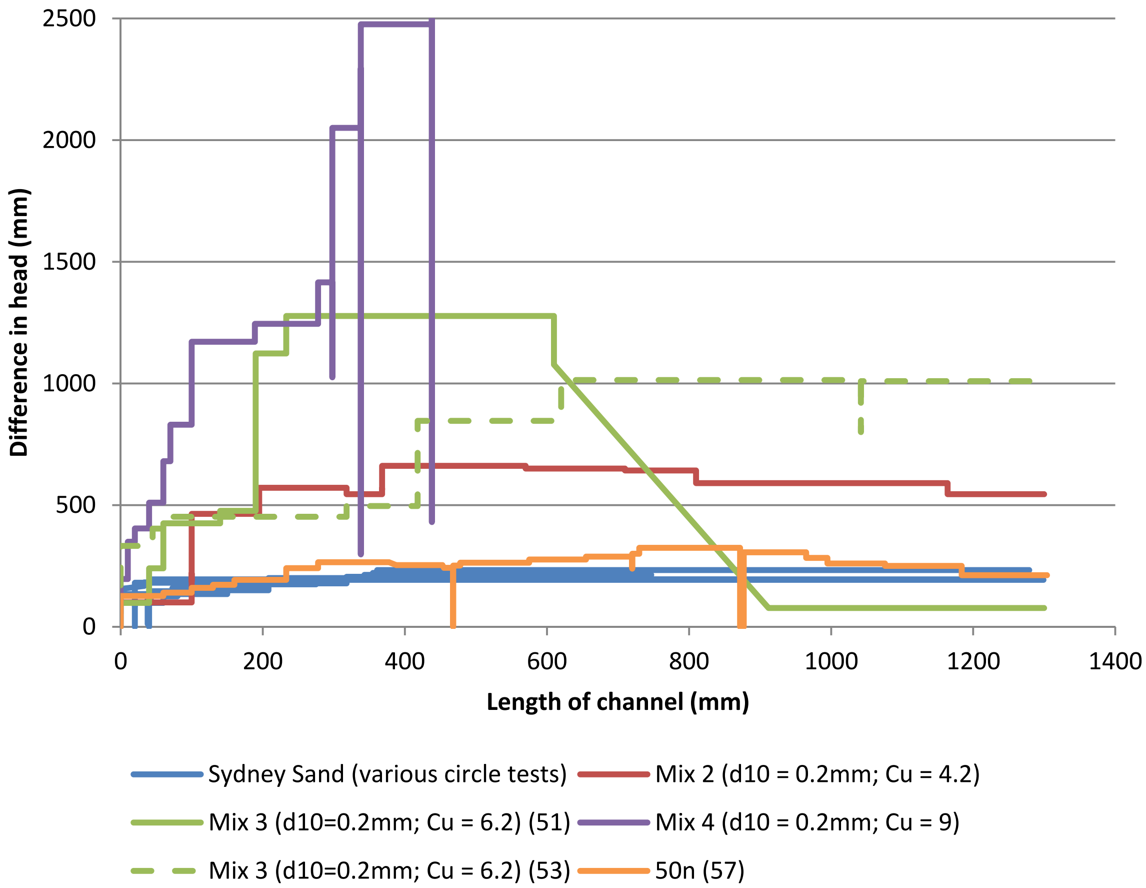

Figure 57-2 CL with H for different soils

I was expecting the critical head of this test to be higher than it was because I thought a smaller permeability would require a larger head to achieve erosive forces but this wasn't the case. This motivated me to compare permeability's of the soils, wondering if perhaps the permeability of 50n wasn't all that much smaller than Sydney Sand's. Figure 3 shows the comparison.

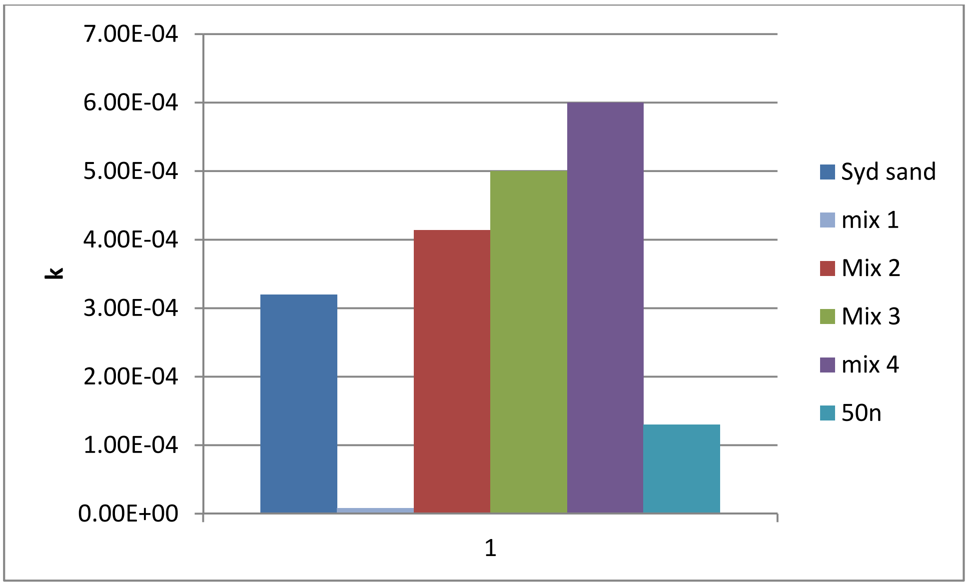

Figure 57-3 Estimated permeabilities

So the k of 50n *is* significantly smaller than syd sand. Therefore there must be something going on here other than a pure permeability dependence. To investigate further I plotted ic against k.

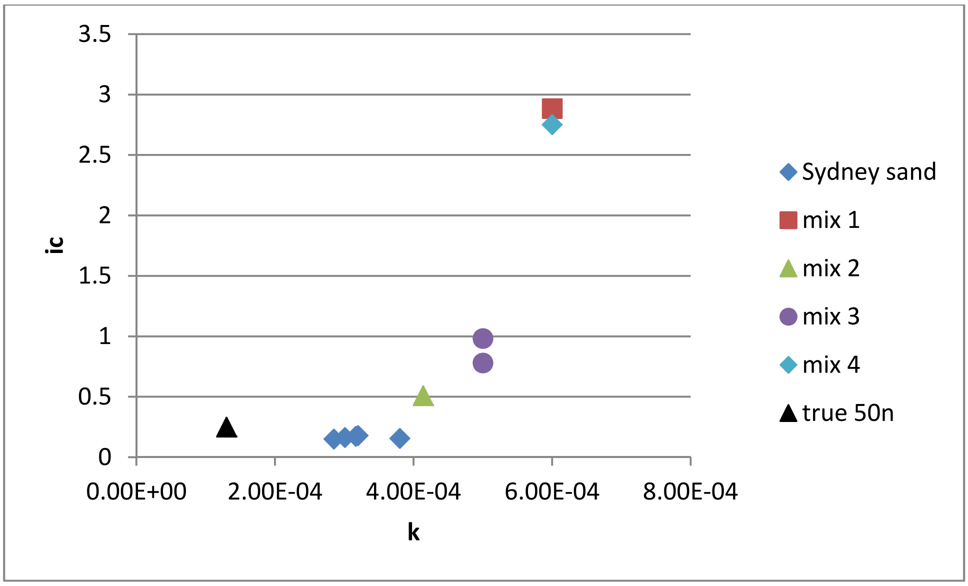

Figure 57-4 Critical gradient with permeability

If it weren't for the results from this test there might be a nice exponential relationship here. It's worth keeping an eye on this plot as further results are produced.

As for Schmertmann's plot, Sibelco 50n lies right on his line. See below.

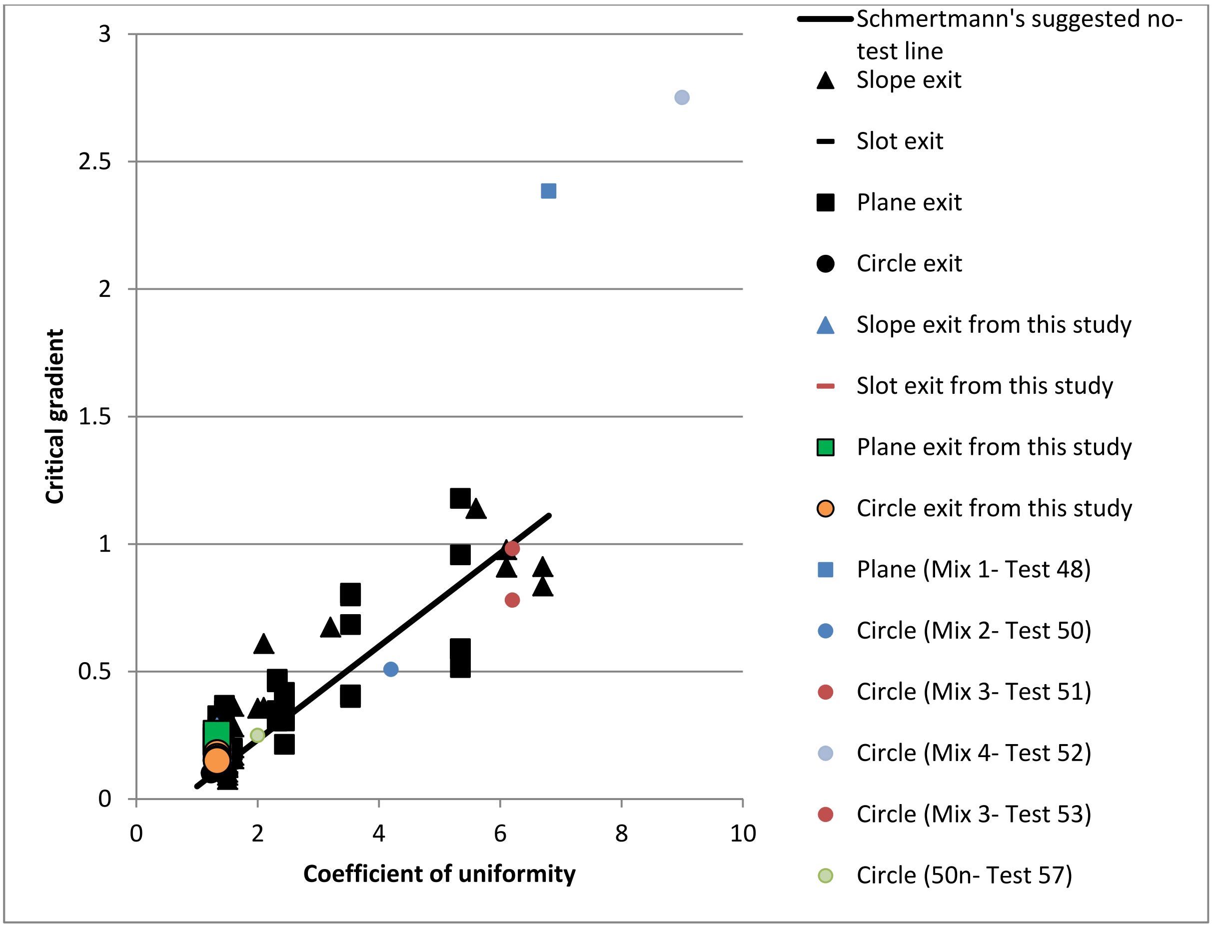

Figure 57-5 Schmertmann's graph after test 57 on sibelco 50n

Figure 57-6 Discolouration along u/s edge

Figure 57-7 Blockage between forward deepening & regular channel

Backward erosion piping test data sheet

Test #	~~57~~ 58	Exit type	circle
Date	13-10-14	seepage length	1.3 m
Soil	mix 5	head in bladder tank	5 m
Flume	3	compaction	tamped

time	head	observation
12-Oct		
10:30		inflated bladder
10:45		co2 on
15:00		co3 off
13/10 12:15	↑ 30	
25	↑ 55	
32	↑ 77	
54	↑ 102	
1:03	↑ 122	Some particle movement at the exit.
		Not boiling yet.
1:11	↑ 151	
1:23	↑ 176	Very slight boiling
34	↑ 202	
46	↑ 227	
51		The downstream box is a bit cloudy.
		Boiling has deposited soil about 10mm
		surrounding the exit.
2:15		1st Sample of boil taken
18	↑ 250	
26	↑ 274	
43	↑ 310	
51	↑ 346	There looks to be a channel that
		has blocked itself [d1]
3:09	↑ 382	it may have just been fines moving through coarser soil
27		2nd Sample taken
30	↑ 419	
34		Area surrounding exit has eroded away.
		(not just fines but larger particles too)
		Longest grain size in boil is about 5mm diameter
40	↑ 455	
56	↑ 492	

Test ~~57~~ 58

	time	head	observation
	4:07	492	
	23	492	Stopped boiling
	25	↓ ~~[illegible]~~ 0	
4-10	11.18	0	
	11.19	↑ 418	
	11.37	↑ 466	
	11.48	↑ 425	
	11.49		I've found the bladder tank drained.
			there's maybe 0.5m left in it. I
			think the inlet was left open.
	12.24		Starting filling bladder tank up
			again (slowly).
	2.28		Q for 300mL = 3.8 and 3.9s.
	2.29	↑ 415	
	2.43	↑	I think the filter is clogged.
	2.49		just finished filling bladder tank
			to 5m
	3.14	481	
	3.15	↑ 520	
	4.37	↓ 72	collected boil. 3rd sample. Changed
			filter.
15-10	9.53	~~↑~~ ~~[illegible]~~ 260	
	9.54	↑ 500	
	10.27	↑ 577	
	10.43	↑ 585	
	11.11	↑ 787	
	11.28	↑ 848	
			as mentioned previously there's an
			area surrounding the exit that
			has eroded away. It's possible some
			of this area could be the start of
			a potential channel but it's very
			wide + doesn't look like a channel
			(see happy snap). If I called it a
			channel I'd say the tip is ≑ 50cm.
	1.51	↑ 832	
	2.07	↑ 1027	
	2.22		~~under 62~~! 250 and very wide. btw

i didn't mean for it to go up this far. It happened because i had turned the inner cylinder pump off whilst i removed the filter + forgot to turn it back on

Test ~~57~~ 58

time	head	observation
		R0 to 60mm wide (see happy snap).
		Large boil # 4 collected
2.48	↑ 1147	
3:00		Soil is being detached from the
		bed of the channel in intermitten
		surges. But tip not moving.
3.24	↑ 1175	
3.53		I'm often finding the water level in
		the tank lower than expected. I think
		this is because the flow out of the
		exp is > than Qin.
3.58		the inlet to the CHT is now fully
		open
4.16	915	channel all looks the same. Head
		gone down by itself.
4.17	0	removed filter to increase flow.
4.22	back up	again. filter removed.
4.23		occasional detachment from tip but
		not enough to progress.
		Note water level in d/s ~~box~~ above
		datum
4.25	→ 1280	tip jumped to bar 4. But stopped
4.26	↓ 1049	because the channel blocked under
		b2. (see happy snap).
4.32		Naturally when the channel jumped
		to b4 I got a large boil again.
		I haven't moved this boil because
		a) it's so large and b) I'm confident it'll
		have good representation of all
		max 5 sizes.
4.59	↑ 1070	Still @ b4
5.10	↑ 1098	" " " + still blocked beneath b2
5.18	↑ 1124	" " " " " " "
5.29	↑ 1150	" " " " " "
5.41	122	" " " " " "
16-10 9.59	↑ 893	
10.11	↑ 994	
10.48	↑ 1094	

Test ~~57~~ 58

time	head	observation
11.04	↑ 1147	channel width varies btw 220 and 60
		mm. the tip is about 600mm wide.
11.17	↑ 1202	still @ b4 + still blocked ~~btw~~
		under b2.
11.28	↑ 1254	" " "
11.37	↑ 1306	" " "
11.49	↑ 1356	" " "
12.04	↑ 1408	" " "
12.15	↑ 1459	
12.31	↑ 1506	Water level in the d/s box almost
		level with the top of the outlet
		(see happy snaps).
2.39	↑ 1560	Still @ b4 and still blocked beneath b2
3.22	↑ 1615	
4.59		first noticed the ~~the~~ channel was
		through to the u/s end. See
		happy snap. I didn't get the
		sudden increase in flow that I
		was expecting once the channel had
		read the u/s end. I thought I'd
		hear it. There are no visible blockages.
		I've drawn the channel on the lid.
		See happy snap. Width of channel
		varies from btw 300 to 160mm.
5.10		I've just noticed that the levels
		in the standpipes are all a) fairly
		equal and b) level with the CHT.
		See happy snap. this means there's
		a ~~trapping~~ large gradient btw row 1
		+ the d/s box like 1.5/0.2 = !!
		And there's no ripples in the top
		of water in the d/s box anymore.
		Q = 5.4, 5.6, 5.8s/800mL which is
		much less than the 2.1 measured this
		morning whilst at a lower head.
		All I can think of is the circle exit
		is blocked and the head loss is
		all concentrated there. So I'm going
		to reach in + try unblock it to

see what happens. Yep that did trick. See video.

5.37 I just found the bladder tank completely empty! It's outlet was open! Aghhh.

Test ~~57~~ 58

13/10

		Row 1			Row 2			Row 3			500		
time	head	right	middle	left	right	middle	left	right	middle	left	time for ~~50mL~~	Avg	Temp
3:20	382	205	205	208	259	252	258	315	327	327	6.8 s 500/6.8 73.53/1 7.35e-5		22°C
4:10	492	260	259	262	329	322	328	402	417	416	5.1 500/5.1 98/1 9.8e-5		
15-10													
10-12	500	236	235	240	313	304	310	391	~~405~~	405			
2.41	1027	88	125	222	390	389	420	658	409 ~~698~~	695	3s/800mL 266.67/1 2.67e-4		
4.36	1049	110	115	220	378	474	421	573	562	616	2.4s/800mL 333.3/1 3.33e-4		20°C
5.31		120	124	238	407	510	455	623	611	668			
16-10													
11.33	1254	123	128	241	373	527	470	643	632	696	2.1s/800mL 380.95/1 3.81e-4		20°C

58. Test 58 (flume 3) circle

Test 58 was the first test carried out on mix 5. Bronson designed mix 5 to test a soil with the same Cu as mix 3 but with a larger grain size (and therefore higher permeability).

It was tamped in dry and flushed with CO2 before saturation.

Initiation was difficult to define because the 'channel' was more an eroded 'region' than a channel. See pic 7. I defined it at a head of 419mm because it was first time when particles of all sizes moved (that just fines through the coarse matrix).

From there the tip progressed in 3 sudden bursts as shown in graph 1. I've defined the critical head as 1280mm even though the max head was 1615mm because I think I needed to go above 1280mm only due to a blockage of gravel. The blockage occurred when a heap of material was moved down the channel. It was so much material for 2 reasons 1) because the tip progressed from 508mm to 1114mm in a matter of minutes (maybe even less than 1min) and 2) the channel was always wide. Pic 8 shows the blockage and Pic 9 shows the width of the channel.

In short, mix 5 produced fast, sudden and wide channels.

Throughout the test I collected the boiled material from on the top of the lid. I wanted to see if there was a change in the size of particles transported out to the boil. I don't know where the results of these went. Ask Hamish on Monday.

During the test I noticed the water level in the CHT was dropping on its own. This was because the flow through the experiment was larger than the flow coming into the CHT even with the in-valve to the CHT completely opened. So I took the filter out so Qin > Qexp. When I took the filter out I turned the inner drain cylinder's pump off but forgot to turn it back on again. So the water level went a little higher than I intended- it went from 1175mm to 1280mm quite quickly (not in steps like I would have liked). This means that critical could have been less than 1280mm (but greater than 1175mm).

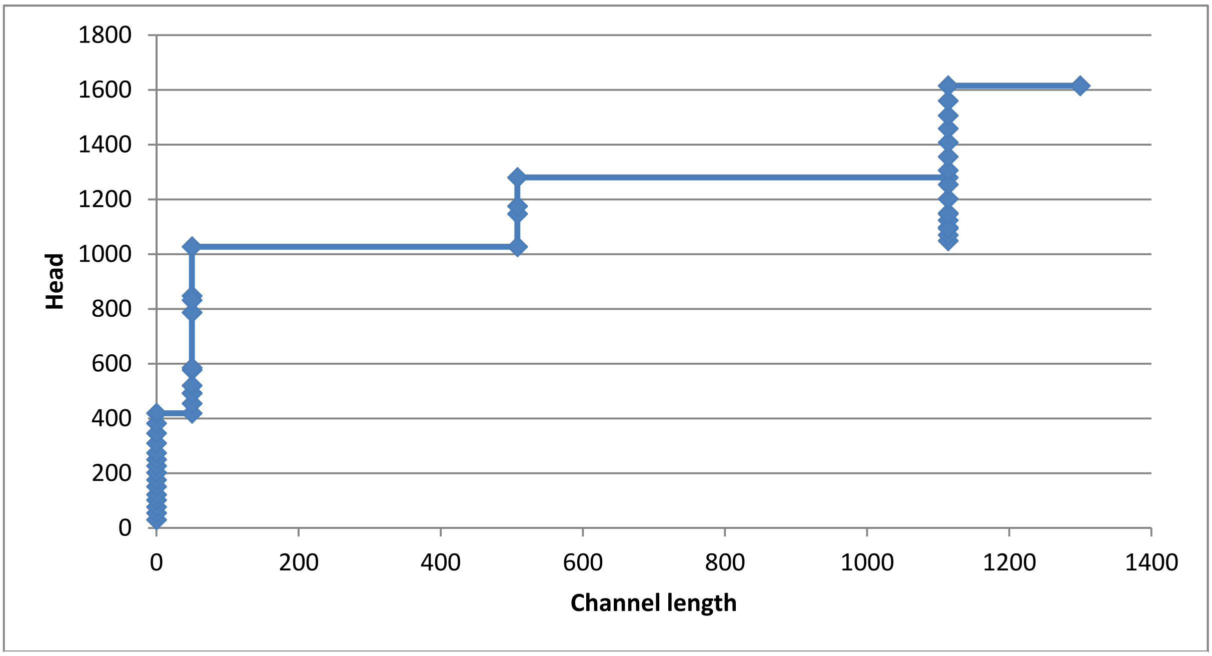

Figure 58-1 test 58 chart

Additionally, flow through the experiment was so high that the 50mm downstream valve wasn't large enough to release enough water to keep the water level in the downstream tank at datum. The water level was up near the top of the outlet (see Pic 10). Technically this meant the head level from the CHT should have been subtracted by about 50mm (d/s no longer at datum) but it's a relatively small adjustment so I didn't bother.

Once the tip reached the u/s end I expected it to fail quickly but it didn't. Instead I noticed the levels in the standpipes were all fairly similar and almost level with the constant head tank. I also noticed the flow had reduced. This happened because gravel had interlocked at the exit and most of the head loss was concentrated at the exit. Pic 9 suggests the size of the flow coming through boil (by the ripples in the water's surface) as compared to pic 10 showing no ripples and relatively little flow coming through boil. This means that the head loss across the actual soil sample was small. I looked at piezo levels throughout exp (Figure 6) in case I could see when the blockage at the exit occurred. But I couldn't, probably because the last piezometer reading I took was a good 5 hours before the blockage happened. I couldn't measure the piezo's when they were all almost level with the CHT (too high). Perhaps when the tip reached the upstream end there was a surge of particle movement in the channel which blocked the exit.

Once I released the gravel under the exit (by sticking my finger in) flow jumped drastically and the experiment failed. Pic 11 shows test after failure.

Also, it should be assumed that for most of this test there was no pressure in the bladder. This is because twice I found the bladder tank empty because the drainage was accidently left open.

To compare the results of mix 5 was other tests see below. It's interesting to note that despite mix 5 being more permeable than mix 3 (and therefore I expected its critical head to be lower) the critical head was the same.

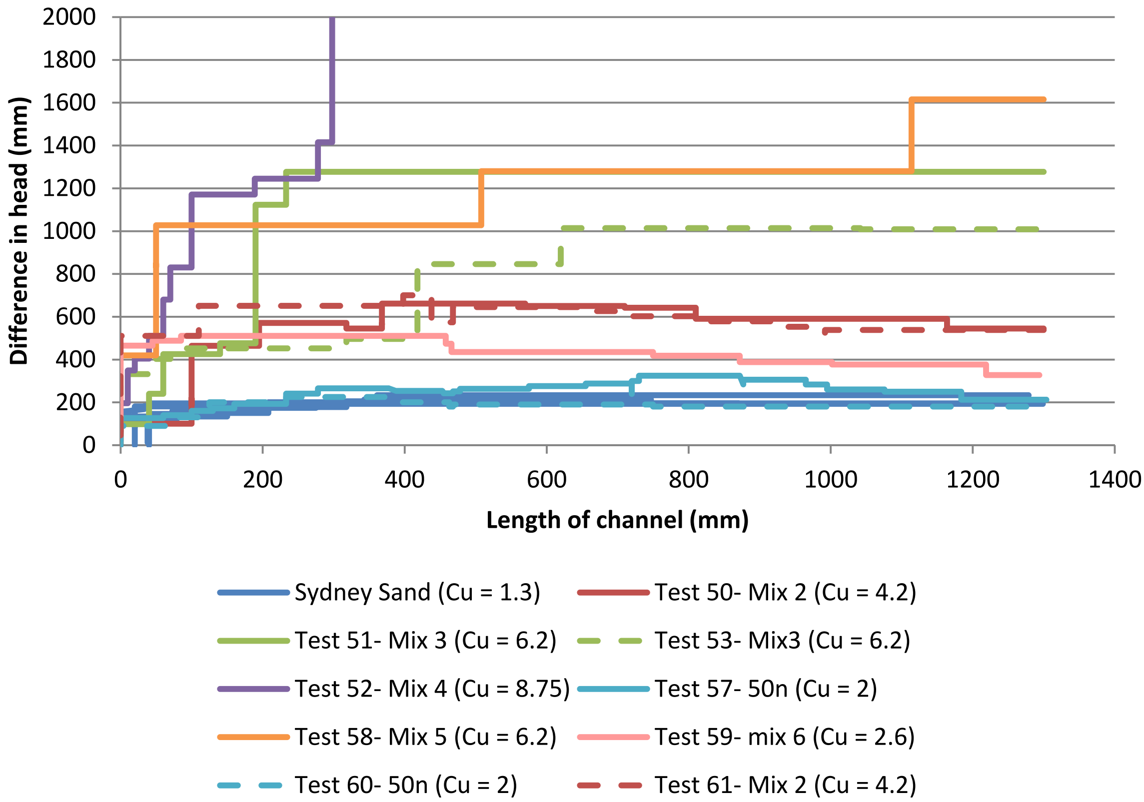

Figure 58-2 head against channel length

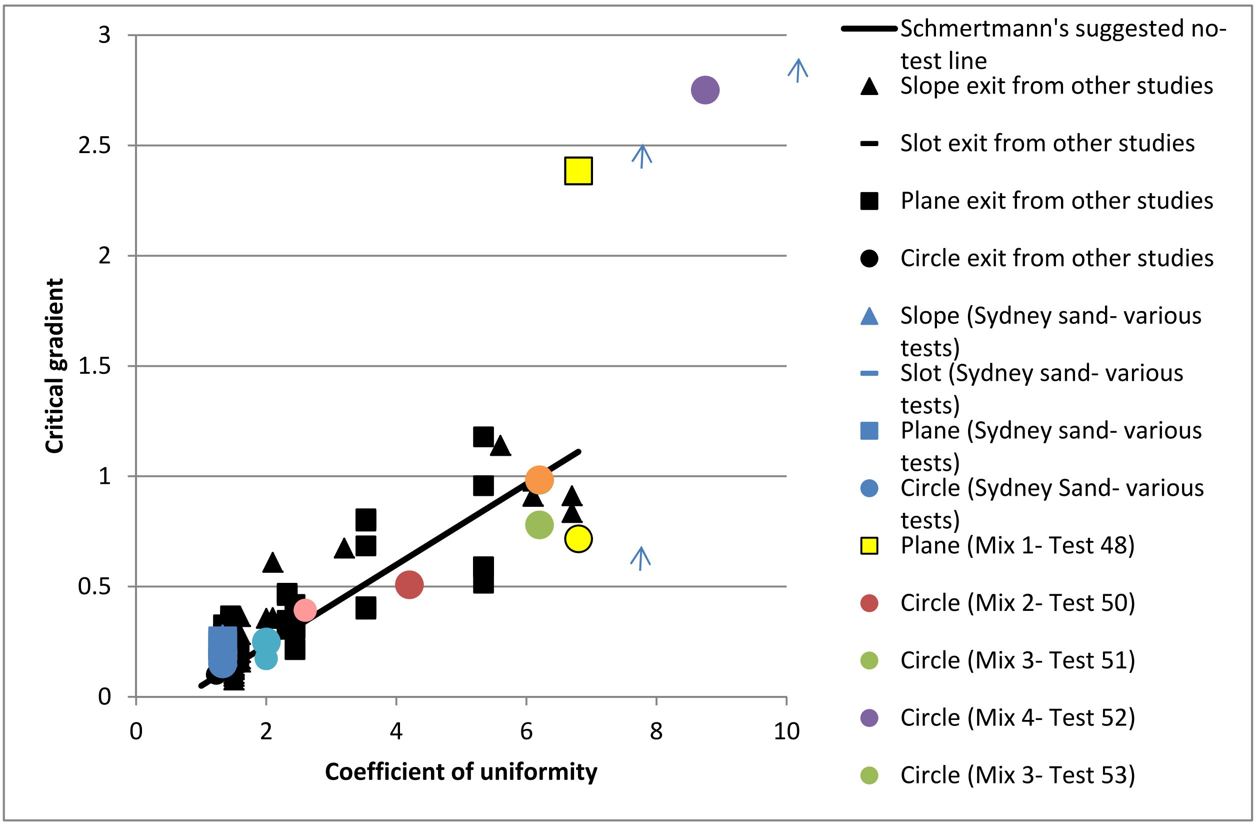

Figure 58-3 Schmertmann's graph (orange dot)

In additional, both mix 3 and mix 5 plotted near each other on Schmertmann's graph.

To get a feel for difference in permeability:

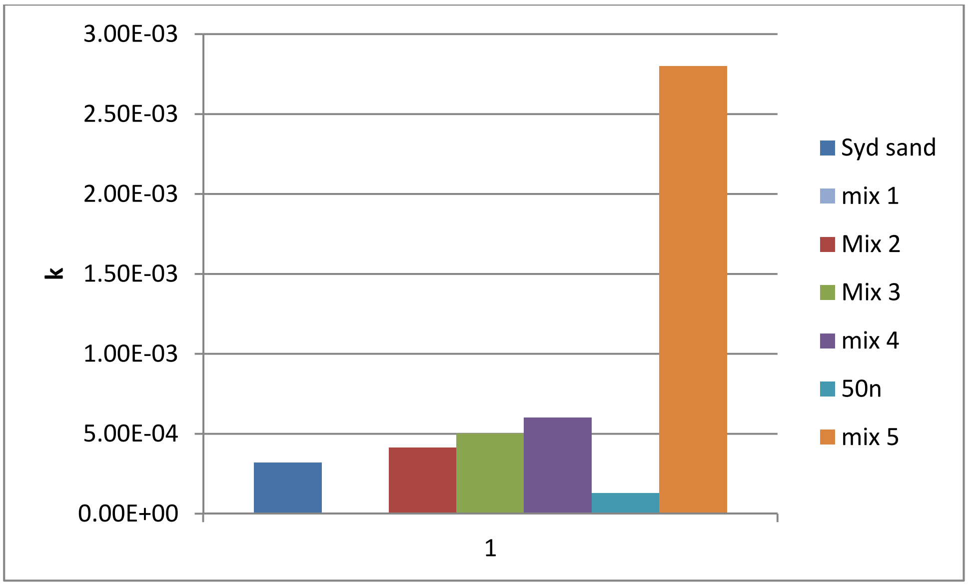

Figure 58-4 different permeabilites

If I look at the critical gradient with permeability again I now get this:

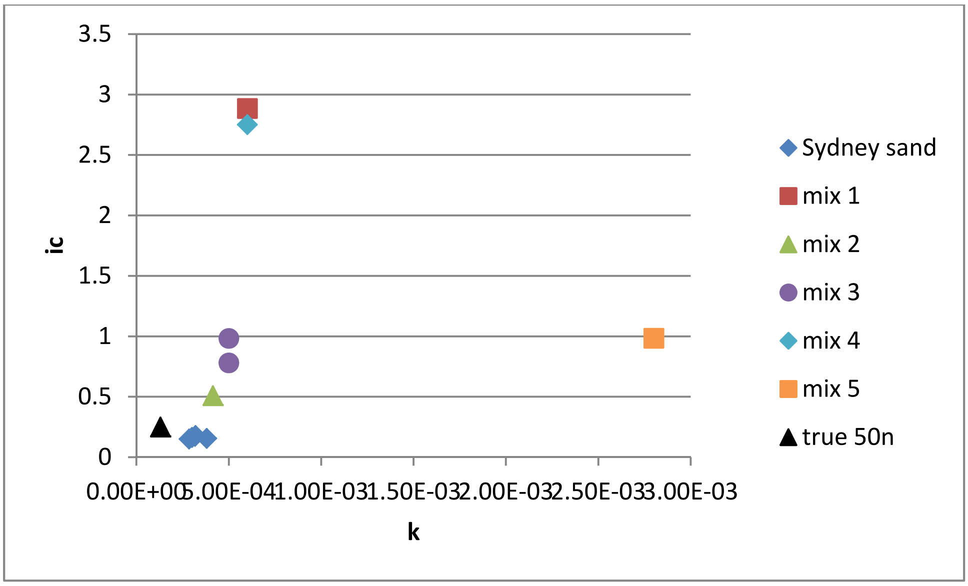

Figure 58-5 critical gradient with permeability

Which has totally ruined my theory of an exponential relationship. Maybe an exponential relationship exists for soils of similar d10's or within a range of permeability values(?) Either way, this demonstrates that there's more going on than just a permeability relationship.

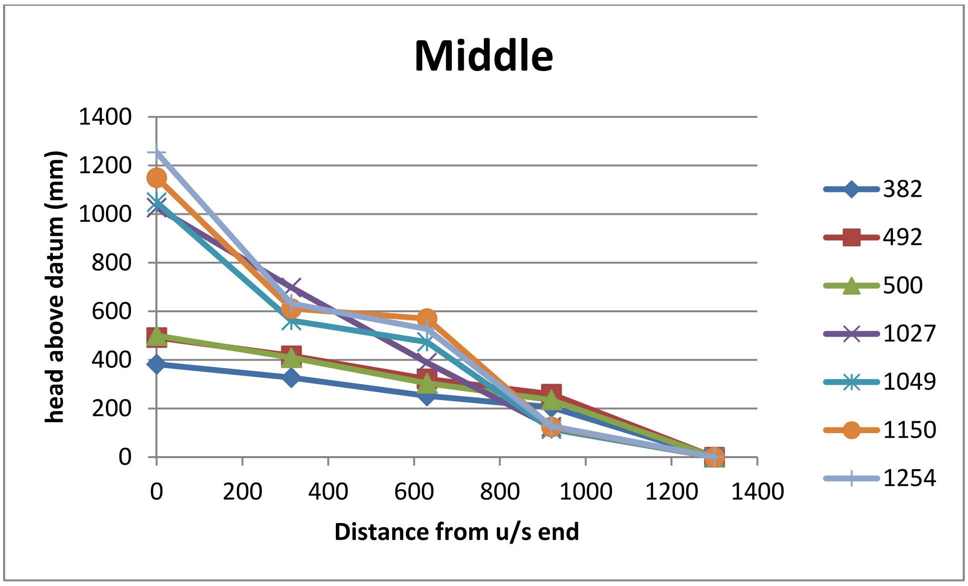

Figure 58-6 piezometer levels

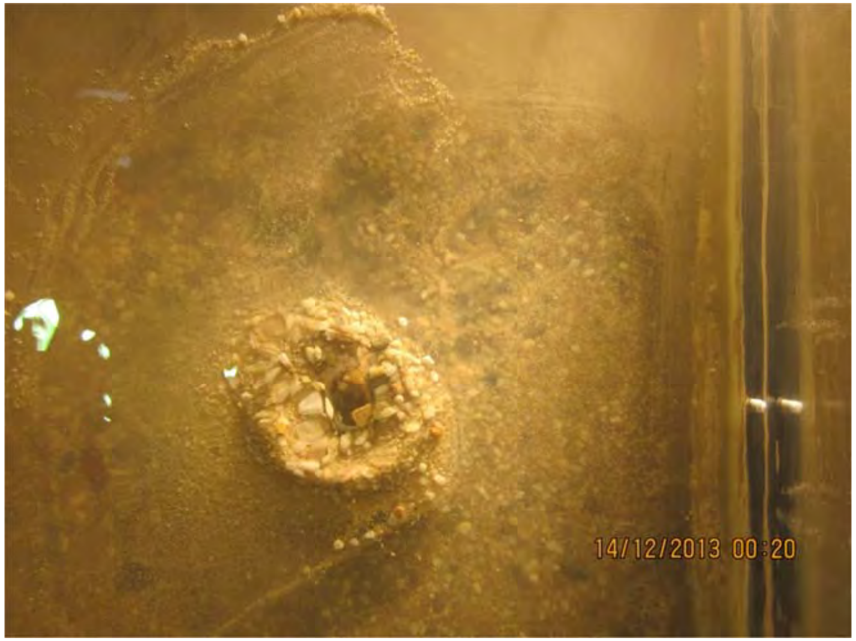

Figure 58-7 ‘channel’ was so wide it didn’t look like a channel but was

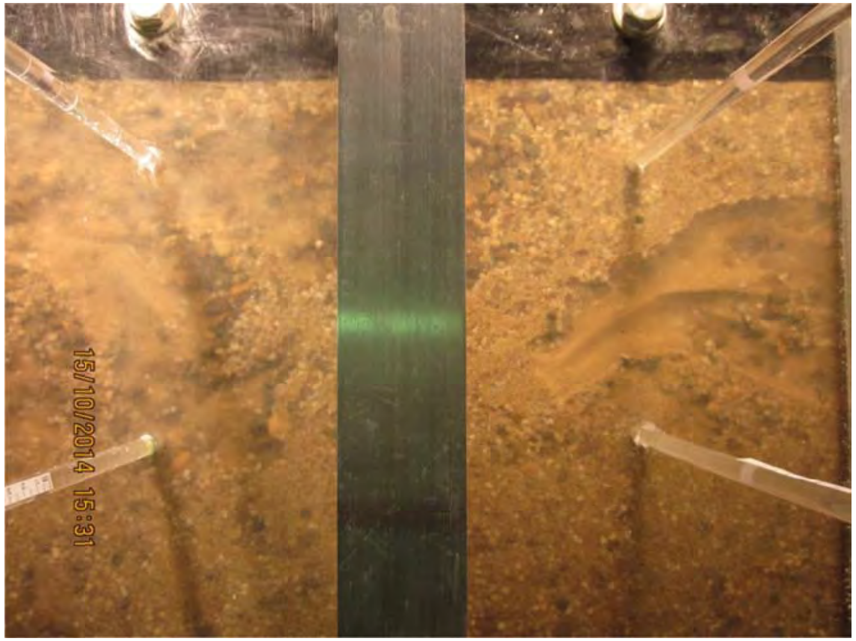

Figure 58-8 Blockage in channel

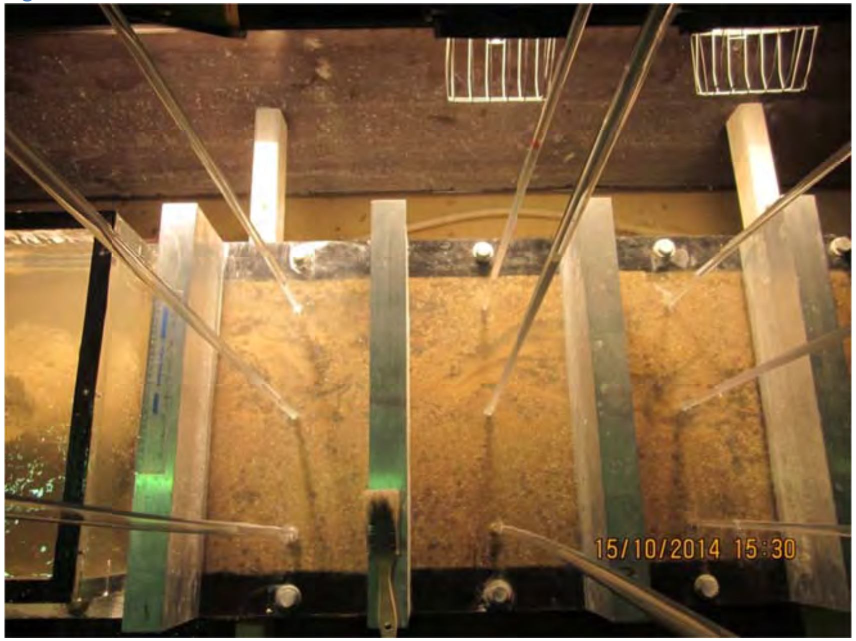

Figure 58-9 ‘channel’ was wide so a lot of material transported down channel

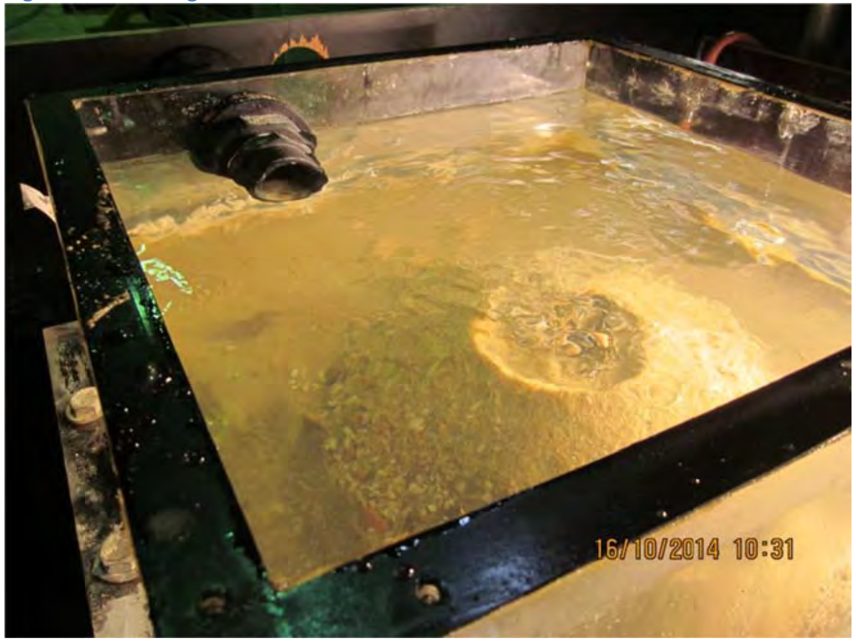

Figure 58-10 water level in d/s box almost to top of outlet

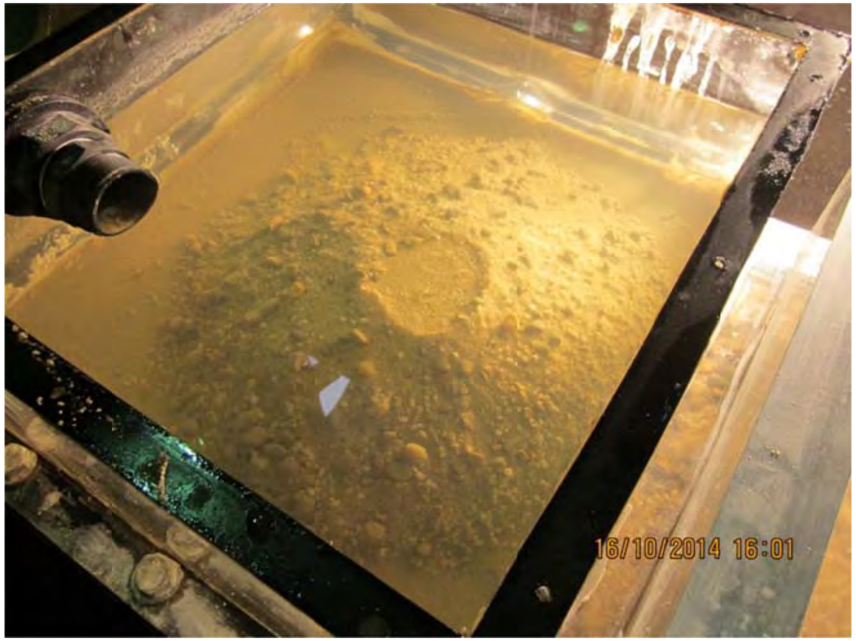

Figure 58-11 flow greatly reduced as evident by still water

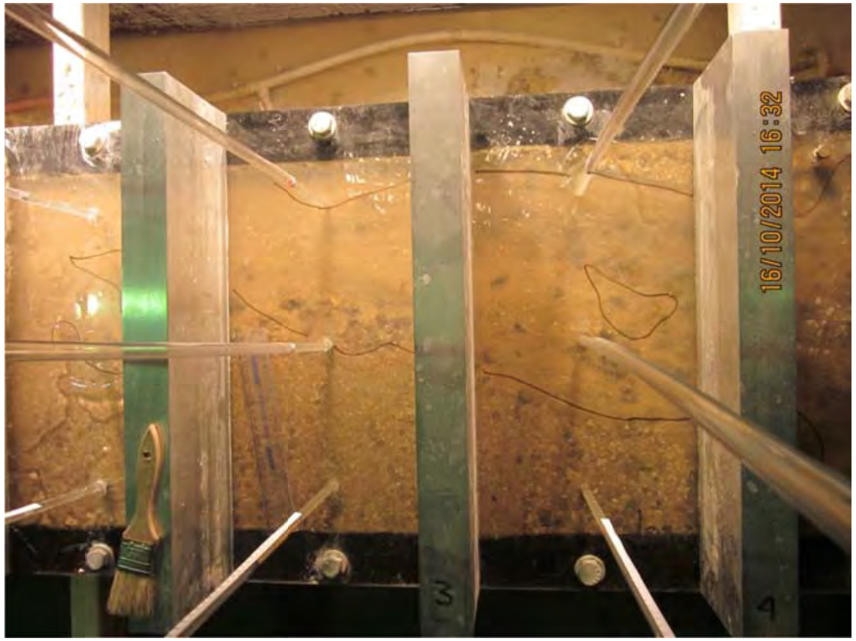

Figure 58-12 after failure

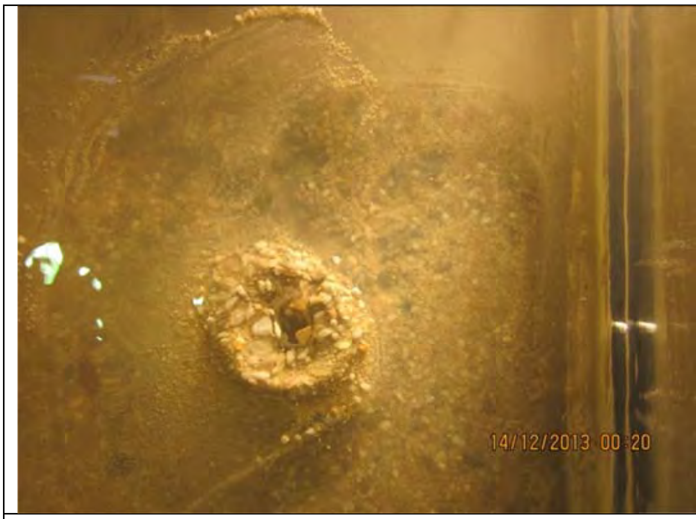

Figure 58-13 'channel' was so wide it didn't look like a channel but was

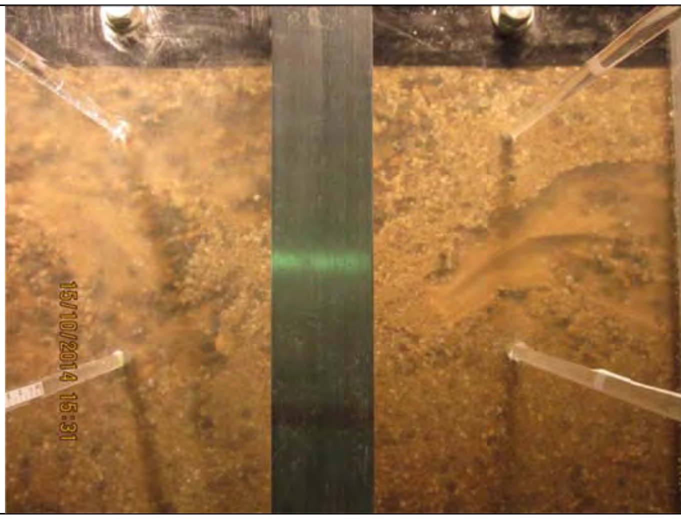

Figure 58-14 Blockage in channel

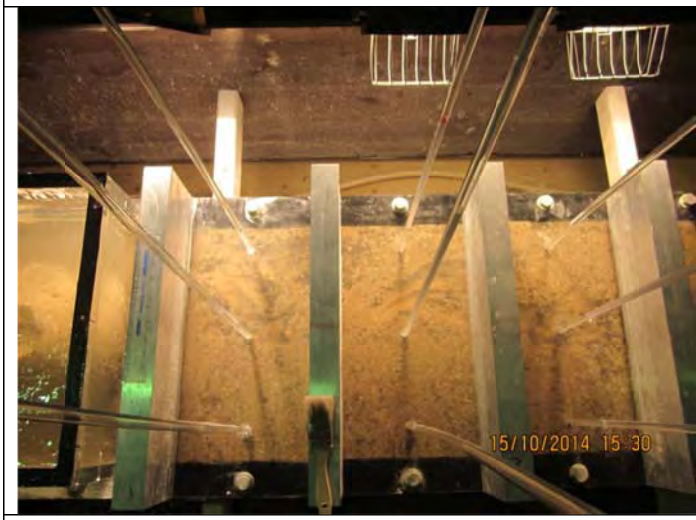

Figure 58-15 'channel' was wide so a lot of material transported down channel

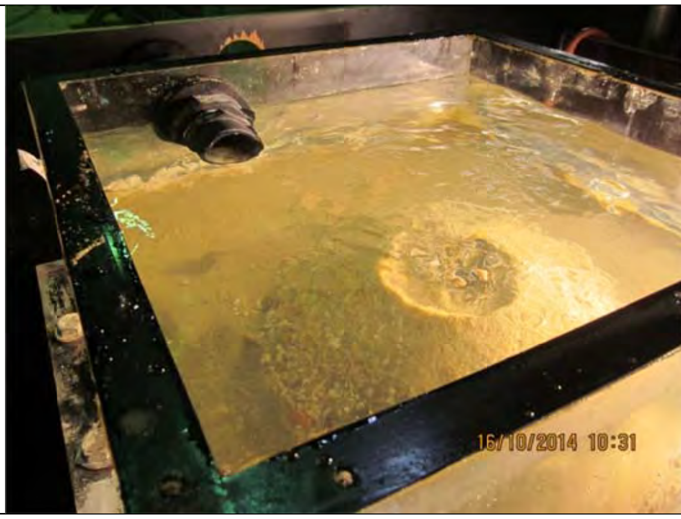

Figure 58-16 water level in d/s box almost to top of outlet

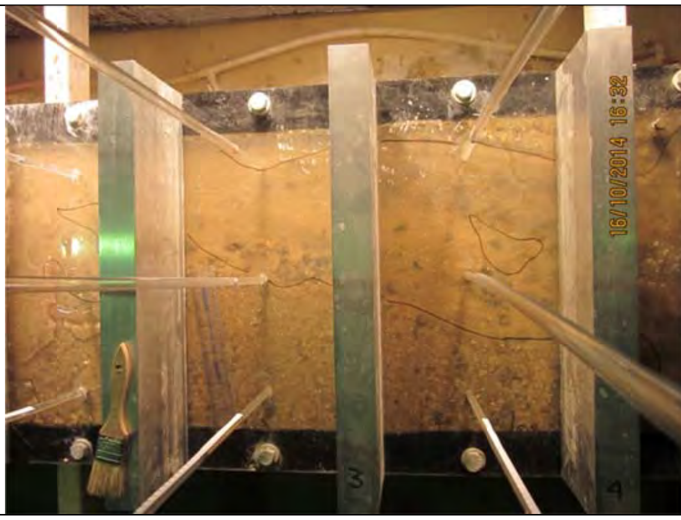

Backward erosion piping test data sheet

Test #	59	Exit type	circle
Date	10 ~~7~~/11/2014	seepage length	1.3 m
Soil	mix 6	head in bladder tank	5 m
Flume	3	compaction	tamped

time	head mm	observation
9.47	20	strange squiggle pattern in sand btw
		bars 1 + 2. See happy snap.
		Can also other distortions/patterns
		but I think it's just from coating
		on underside of lid.
		Test with 50m behaved similar
		to sugd sand initiation = 100m
		criti was around 200-300mm.
		However flow with 7% 300g I'm
		not sure what to predict. Decided
		to go up in 50mm.
9.55	↑ 72	
		I note there's soil on top of lid
		around hole that happened during
		saturation. See happy snap.
10.03		I just cleared away more soil from
		top of lid at exit and see bubbles
		and eroded voids around exit. See
		happy snap. The eroded voids occurred
		during saturation but not sure why/
		when the bubbles occurred. I don't
		think they should affect the exp too
		much cause there aren't many of
		them and I suspect they'll move out
		through the exit once the flow increases.
10.27	↑ 124	
10.30		Starting to boil,
10.47	↑ 174	
10.52		Boiling getting more rapid
11.09	↑ 227	
11.23	↑ 270	

time	head	observation
11·34	↑ 320	
12·12	↑ 365	
12·55	↑ 414	
13.15		Possible channel forming? took happy snap
13·16	↑ 465	
13·20		channel tip - 145 - 100
13·35	↑ 488	
13·41		tip at 185 - 100
14·05	↑ 510	
14·15		tip at 195 - 100
14·45		Very cloudy - Tip at 5 ab1
15·05		~~tip at 195~~ ab1
"	↓ 474	
		tip at 200 ab1
15·18	↓ 435	
15·23		tip at 215 ab1
3·30		at bar 2
3·50		30 ab2
4·20	↓ 48	190 ab2 (past 50%L)
4·25		210 ab2
4·59		under b3
5·17	↓ 28	10 ab3
11-11 10·19	28	10 ab3. Can see through water in walls [illegible]
		tank. Took happy snaps.
10·20	↑ 360	10 ab3
10·40	↑ 388	10 ab3
10·51		95 ab3
11·03	↓ 377	140 ab3
11·17		165 ab3
11·47		under b4
12·13	↓ 327	55 ab4 in ~~two~~ 3 places. See happy snap.
12·15		87 ab4
12·19		The channel is struggling to form u/s of
		b4 in that, whilst there's sediment
		transport, there's not a clear path for it.
		It's as if there's so much ~~[illegible]~~ particles
		being moved it's always on the verge
		of becoming blocked (cont. [illegible])

time	head	observation
12.21		100 ab4
12.24		130ab4 (U/S end). But this channel now blocked it self so other 2 tips are now advancing. See happy snap.
4.06		fwd deepening upto b2 and blocked btw 1-2. No more SCR (batt flat).
5.05	↓35	
12-11 9.50	↑325	
1.27	↑330	
13-11 10.04	330	exp was left running at 330 overnight. This morning the forward deepened channel is discoloured along its full length - presumedly bio clogging. Although I think Hamish put chlorine in the water not long ago so bio clogging surprises me. & Also I don't have the 5um filter in (there's no filter) so the discolouration could also just be 'rusty' water from pit/pump/hoses. Either way, it looks to me like it would have a cementicous effect + therefore the forward deepening is unlikely to continue at this head so I'm ending the experiment here. See happy snap. Hey Hamish did put chlorine in the water a few days ago. I note the water in the pit looks quite dirty.

Test 59

Note 6-3-15. I think I MIGHT have left + right swapped.

			Row 1			Row 2			Row 3					
	time	head	right	middle	left	right	middle	left	right	middle	left	time for 50mL	Avg	Temp
10-11	12.14	365	150	148	148	225	220	213	—	295	297	Using scales		
	13.38	488	195	190	193	295	288	280	—	390	393			
	3.34		147	140	116	243	235	227	—	338	340			22
	4.26		131	123	98	218	204	175	—	312	313			
11-11	10.38		104	97	82	170	158	124	—	253	253			
	11.04		119	111	100	188	174	146	—	252	266			
	11.48		116	109	101	190	178	152	—	258	266			20
	12.26		109	103	102	173	163	141		234	251			
	4.01		142	135	142	226	231	260		295	294			

59. Test 59 (flume 3) circle

Test 59 was the first test carried out on mix 6. Mix 6 was 7% Sibelco 300g and 93% Sibelco 50n as suggested by Robin. Robin suggested it because it models soils he often comes across in practice which are reasonably uniform but with a fine grained "tail". This fine "tail" slightly increases Cu.

It was expected that given its drop in permeability it would require a much higher head than when it was 50n alone (test 57). It was also expected that the result would lie well above Schmertmann's line.

It initiated at 465mm and continually progressed at 510mm as shown in figure 1. This critical head was 57% greater than test 57 as expected, but the result was still on schmertmann's line. Figure 2 shows the relative permeabilities of 50n and mix 6 and figure 58-3 shows where mix 6 plotted on Schmertmann's graph (light pink point). Figure 58-2 shows comparison between different soils.

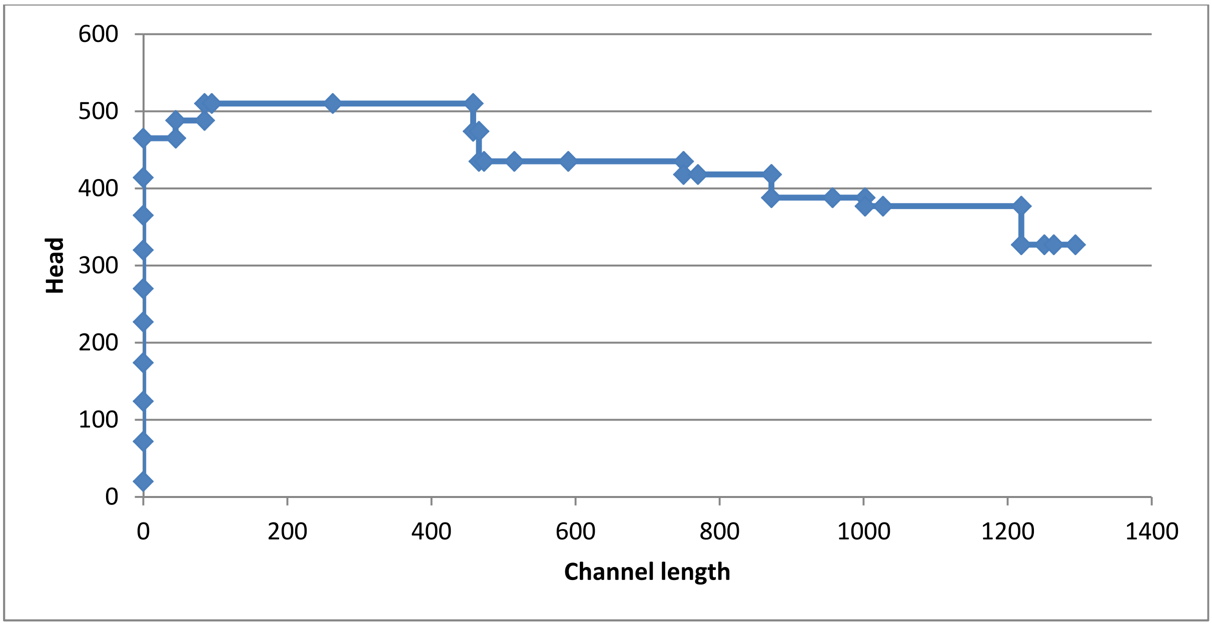

Figure 59-1 Test 59 plot

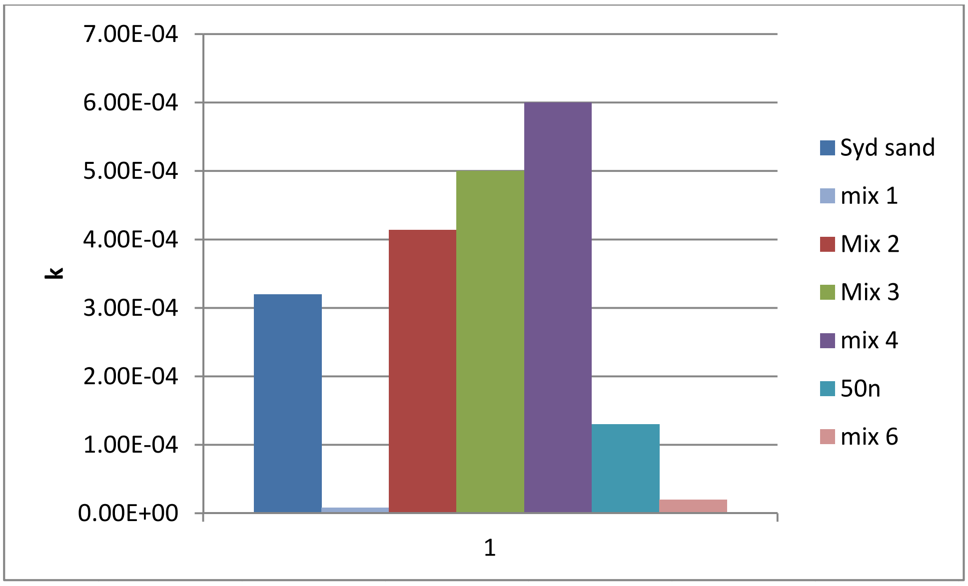

Figure 59-2 relative permeabilities (with mix 5 removed)

After the tip had reached the u/s end the exp was left running to wait for failure. At the end of the day the forward deepening was up to b2 and it was left overnight. However the next morning the deepened channel was discoloured (pics 3 and 4). This may have been bioclogging but Hamish had treated the water with chlorine only a few days prior. It might have also been rust (from pump, valves, etc) and other sediments in the water 'sticking' on the deepened channel because no filter was used for this test (it hadn't been replaced since test 58). Either way, the discolouration seemed to have a cementitious effect and therefore forward deepening and failure were unlikely to occur (at the same head) so the test was terminated.

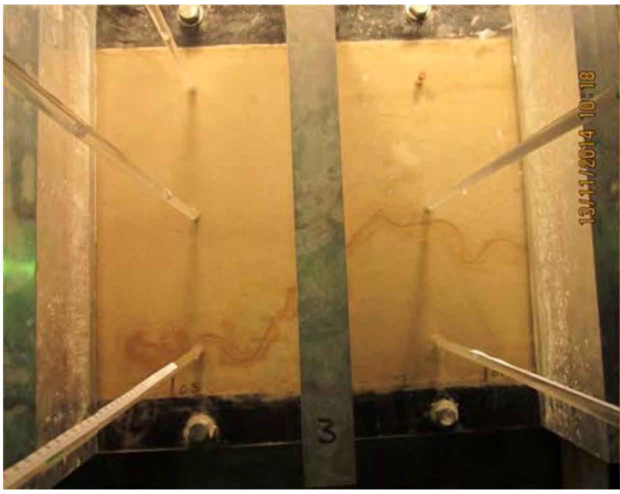

Figure 59-3 Forward deepened channel discoloured

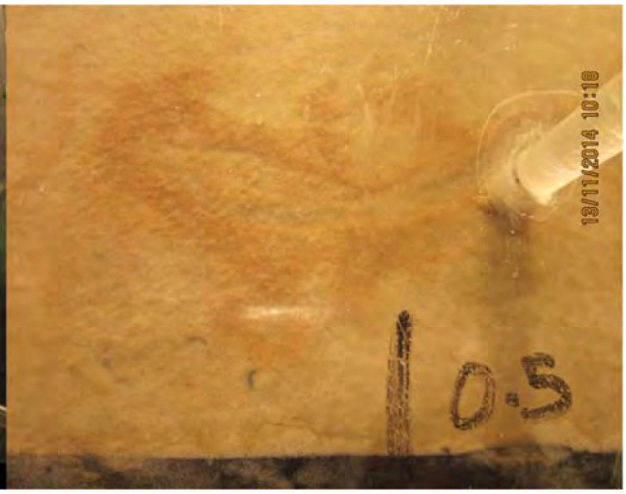

Figure 59-4 Forward deepened channel discoloured

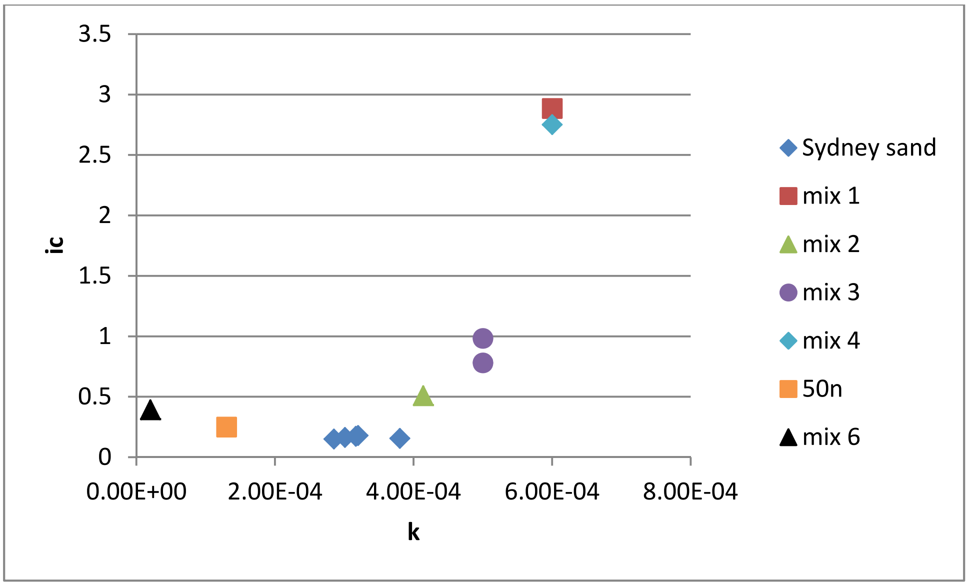

Figure 59-5 critical gradient with permeability

Backward erosion piping test data sheet

Test #	60	Exit type	circle
Date	21/11/2014	seepage length	1.3 m
Soil	50n	head in bladder tank	5 m
Flume	3	compaction	tamped

	time	head	observation
24/11	1:55	20	Start test.
	2.00	"	slight sand bubbling from circle
	2.04		1) L 20 M 20 R 20 2) L 25 M 20 R 20 3) L 35 M 25 R 25
	2.10		changed filter
	2.13	30 ↑	bubbling increasing
	2.30	40 ↑	
	2.35	60 ↑	
	2.55	90 ↑	
	3.05	110 ↑	tip 70 mm
	3.25	130 ↑	
	3.30	155 ↑	tip 120 mm
	3.35	175 ↑	
	3.45	200 ↑	tip 125
	3.50		stop for night
25/11	8.25	240 ↑	Start up. Tip under 1ST Bar
	8.46	200 ↓	
	8.50		1) L 80 M 80 R 80 2) L 120 M 120 R 120 3) L 170 M 160 R 160
	9.45	225 ↑	
	9.57		35 ab1
	10.07		50 ab1
	10.17		100 ab1
	10.18	200 ↓	120 ab1
	11.37		205 ab1
	11.37	180 ↓	~~210 ab1~~
	12.00		210 ab1
	12.30	190 ↑	210 ab1
	12.55	200	250 ab1
	1.15		Somewhere und ab2
	1.35	190	Can't find tip (under b2)
	2.00		30 ab2
	2.18		55 ab2

Test 60

	time	head	observation
25/11	2:30		70 ab2
	3.04		95 ab2
	3.40		120 ab2
	3.40	190	1) L 65 M 60 R 65 2) L 100 M 85 R 102 3) L 145 M 145 R 150
	3.45		stop test back to 0 for night
26/11	8.07	190	Restart test
	8.30	190	140 ab2
	9.05	180 ↓	190 ab2
	9.05		1) L 63 M 58 R 65 2) L 95 M 82 R 100 3) L 145 M 140 R 140
	9.33	180	210 ab2
	9.47	"	232 ab2
	10.00		240 ab2
	10.00	"	250 ab2
	10.30		20 ab3
	10.55	"	50 ab3
	11.06		60 ab3
	11.45		120 ab3
	12.17		155 ab3
	12.38		162 ab3
	1.08		180 ab3
	1.40	180	220 ab3
	1:40		1) L 65 M 57 R 65 2) L 93 M 92 R 100 3) L 130 M 130 R 142
	2.15		tip under b4.
	3.15	↓ 163	75 ab4
	3.33	↑ 175	75 ab4
	4.04	↑ 180	75ab4. I note water isn't touching
			the lid over the u/s chamber
			(see happy snap). I'm not sure
			why this is, it might be because
			we're turning the pump off each
			night and some water leaked out
			of the flume overnight. It doesn't
			appear to have affected the exp
			because the sand still looks to
			be saturated (no air entered
			the sand).
	5.00		113 ab4
	5.49		122 ab4
	5.50		closed CHT invalve. let head slowly

drop to datum on it's own. Left overnight.

HAMISH: If you could ~~[illegible]~~ open invalve + turn pumps back on it will go to H=180 on its own.

Test 60

27/11

time	head	observation
7.58	180	122 ab4
9.05	190 ↑	122 ab4
9.46		130 ab4
9.47		1) 75, 70, 75 2) 105 110 110 3) 140 142 154
9.59		TIP at the end 100%
5.34		the exp had been left running
		to wait for forward deepening
		but air from the u/s chamber
		has entered the channel (see
		happy snap). No point continuing.
		Exp ended.

Test 60

			Row 1			Row 2			Row 3					
	time	head	right	middle	left	right	middle	left	right	middle	left	time for 50mL	Avg	Temp
26-11	335		67	61	64	100	95	93	134	129	127	using scales		

60. Test 60 (flume 3) circle

Test 60 was a repeat of test 57 on 50n.

Initiation occurred at 90mm and progressed at 225mm. See figure 1.

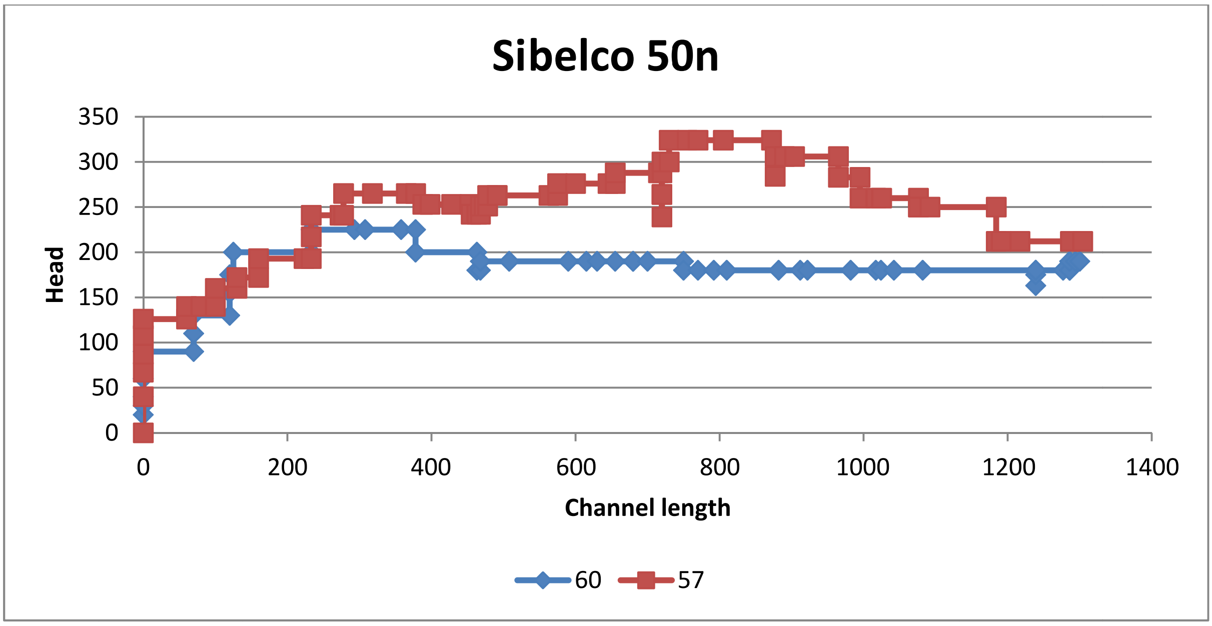

Figure 60-1 Test 60 chart and comparison with test 57

I notice the difference between the 2 progression heads is 30% which is greater than expected experimental variance. I can't see a reason for the difference although I do think the results of test 60 are more typical than test 57 because critical gradient occurred at 20%L.

Hamish ran the test for first 3 days and I took over on the 3rd day. When I took over I noticed there was air underneath the lid at the u/s chamber (see fig 2). I'm not sure why this was. Perhaps because the sump pump had been turned off overnight maybe the water level dropped below the lid at some point. However the air didn't appear to affect the experiment, i.e. the sand sample looked to still be saturated. Well, not until the forward deepening phase that is. Once the channel reached the u/s end air from the u/s chamber entered the channel so forward deepening was not possible (or at least would have required an increase in head). Therefore the test was ended once air entered the channel.

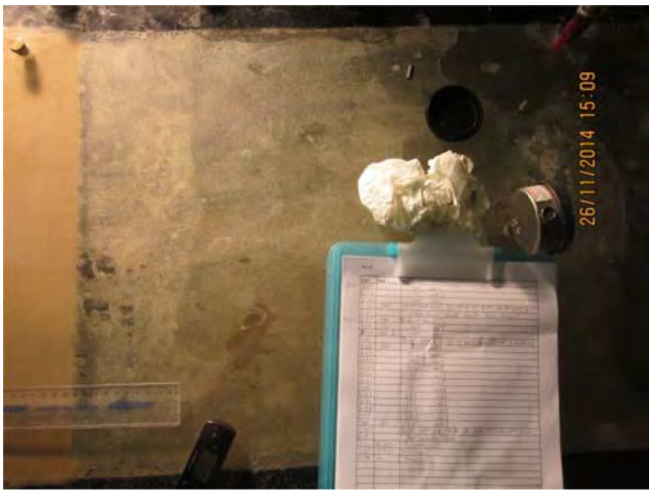

Figure 60-2 Air under lid in u/s chamber

See figures 58-2 and 58-3 for graphs of CL with H for different soils and Schmertmann's graph (test 60 is lower blue dot on Schmertmann's chart). Results as expected.

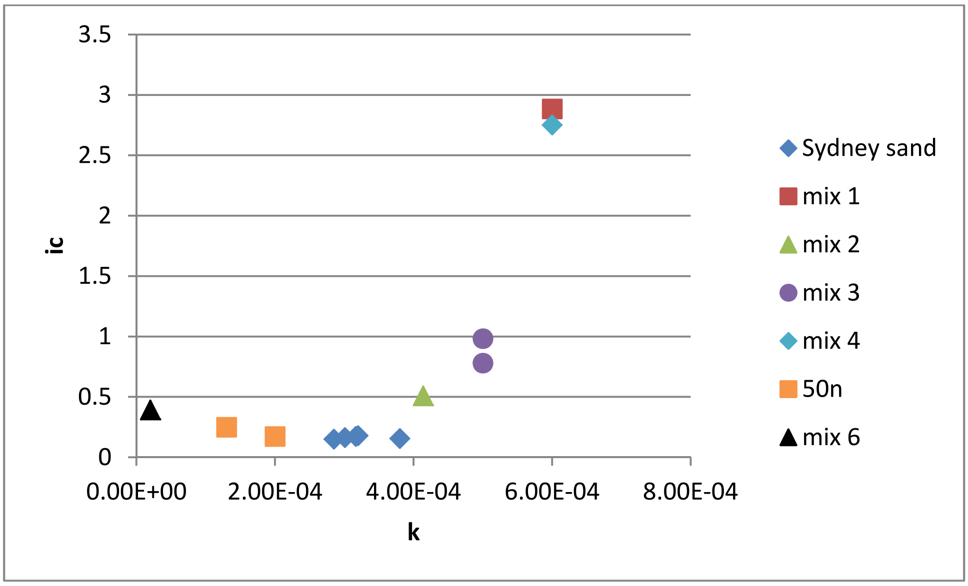

Figure 60-3 i critical versus k

Backward erosion piping test data sheet

Test #	61	Exit type	circle
Date	2/12/14	seepage length	1.3 m
Soil	M1X2	head in bladder tank	5 m
Flume	4	compaction	tamped

	time	head	observation
2/12	11·00	0	Start saturation -
	2·20	60·	start test
	2·25	↑ 80	
	2·26		Looks like a tip from 0-15 unsure (happysnap)
	2·30	↑ 104	
	3·00		shut down for day - no tip.
			Bring head back down to 0.
4/12	10·30	104	test startup
	10·35	↑ 144	
	10·46	↑ 169	
	10·54	↑ 193	Still no obvious tip.
	10·59	↑ 215	"
	11·22	↑ 240	
	11·38	↑ 264	
NOON	12·00	↑ 287	
	12·20	↑ 310	
	12·50	↑ 338	See happysnap - maybe a tip deepening unsure?
	12·51		Same sand coming from downward flow
	1·00		back to 0 End of the day.
5/12	10·12	338	test startup
	10·15	↑ 360	
	10·24	↑ 389	Happysnap / See tips increasing downstream
	10·42	↑ 416	
	10·49	↑ 440	
	11·06	↑ 462	
	11·29	↑ 510	
	11·30		Tip 210 - 100
	11·39	↑ 532	
	11·48	↑ 557	
	12·08	↑ 602	2 TIPS now 210 - 100 / 160 - 100 upstream
	12·10	↑ 651	

PTO continued.

Test 61

	time	head	observation
5/12	12.15	↑ 700	140 ab1 too fast.
	12.16	↓ 574	180 ab1
	12.19	574	210 ab1
	12.21		Have trouble holding slow sand flow
	12.25	↑ 595	210 ab1 Hold now
	12.30	↑ 620	Happysnap.
	12.35	↑ 645	
	12.36	↓ 626	tip 110 ab2 too fast
	12.38	↓ 602	tip 150 ab2
	12.41	↓ 578	tip 250 ab2
	12.42	↓ 553	tip 55 ab3
	12.45		tip 120 ab3
	12.45		Shut down for weekend.
/12	9.08	↓ 525	Start up Monday am
			tip 130 ab3
	9.18		See happy video! Tip 130 ab3.
	9.27	"	tip still 130ab3 - but quite a lot of Sand movement
			down-stream (around b2)
	9.32	↑ 538	
	9.33		tip 190 ab3 big change in sand movement.
	9.34		tip 200 ab3
	9.35		tip 210 ab3
			tip 90 ab4. Very Rapid sand movement
			for 1 min then seemed to stop.
	9.51	538	tip 90 ab4 → 150 ab4 total
			length 100% channeled out.
	10.08		TEST FAILED —

61. Test 61 (flume 4) circle

Test 61 was a repeat of test 50 on Mix 2.

Initiation occurred at 510mm and progressed at 651mm. Although the maximum head difference recorded was 700mm, it was kept at that head for a length of only 40mm so I think it's more accurate to nominate the 651mm head as critical. See Fig 1.

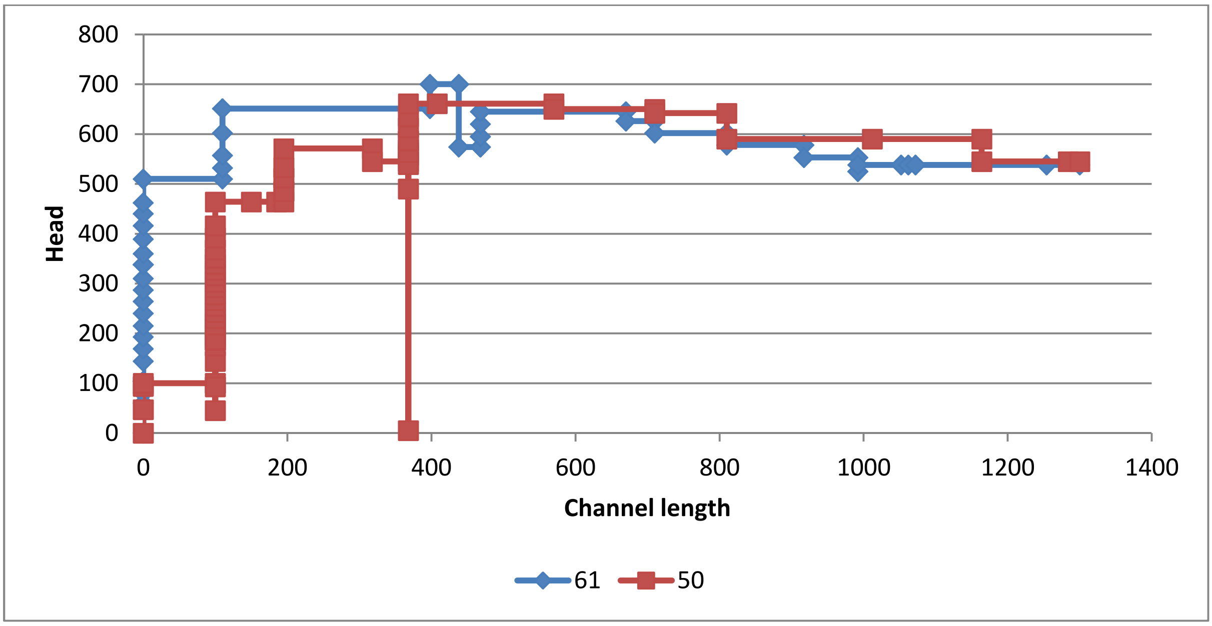

Figure 61-1 Test 61 plot

As can be seen the results were quite similar to test 50. Although test 61 did behave more typically in that the initiation head was around 80% of the critical head (as opposed to 15% of the critical as was the case in test 50).

As was the case in other tests on well graded soils, it was difficult to keep the tip progression slow. It was either stationary or progressing quite fast (like 200mm in a minute).

Forward deepening took about 10minutes to complete and cause failure.

Whilst the scale was being used to measure the flow the time set on the computer was wrong so I can't correlate flows with head levels.

See figure 58-2 for CL with head chart across different soils.

Backward erosion piping test data sheet

Test #	62	Exit type	circle
Date	16/12/2014	seepage length	1.3 m
Soil	mix 8	head in bladder tank	5 m
Flume	3	compaction	tamped

time	head	observation
3.49	0	as this test was being saturated
		over the weekend the water in
		the pit drained away + lowered
		so the pump turned off +
		emptied from the flume. So
		this test is no longer saturated.
		However I will try run the
		test anyway + see how it
		goes.
		~~[illegible]~~ Water in u/s
		chamber isn't up to lid
		(see happy snap).
		Some 300g product has
		come up through hole exit
		+ deposited on lid (see happy
		snap).
3.52		water level in d/s chamber ≈ 45mm
		above lid. Or about 75mm below datum.
		Haven't weighed outflow or took S&R
		photos because doing test 63 at
		same time (and this test likely to not
		count).
3.54	↑ 33	Not tested this soil before so difficult
		to predict but expecting initiation
		≐ 500mm and progression ≐ 600mm based
		on results from test 59 on mix 6.
		However given sample isn't saturated
		I'm also expected bubbles to
		interfer.
3.57	↑ 224	
4.03	↑ 370	

time	head	observation
4.15		boiling at exit. See happy snap.
		300g covered lid so wiped away.
		standpipe row 2 left full of
		sediment with channel from
		standpipe. See happy snaps.
4.21		flow of fine particles so constant
		that even when I wipe it off lid ~~the~~
		~~sew~~ plume continues and covers
		lid up again. So I'm not going to
		be able to see initiation. Also
		there are gas bubbles coming
		out of hole periodically. Gas
		bubbles disperse 300g material
		even more.
4.25		level in d/s chamber ≐ 75mm below
		datum. I'll wait a while to see
		if a channel ~~is~~ is seen d/s of
		box.
5.27		Going to leave head at 370 overnight.
		If water in pit drops then ~~s~~new
		oneway valve should stop the
		flow from sump back into pit and
		water level shouldn't drop below datum.
		No sign of channel b/w box and WL.
		Can't see if there's a channel under
		box.
17/12 10.10	↑ 418	Re-start test
10.15	↑ 444	
10.30	↑ 468	
10.41	↑ 514	No tip visable
10.49	↑ 563	
11.10	↑ 611	
11.30	↑ 660	
11.43	↑ 708	
11.51	↑ 758	〃
12.41	↑ 808	
12.52	↑ 854	
1.02	↑ 904	
1.15	↑ 952	

Test 62

time	head	observation
1.30	↑ 1001	
2.06	↑ 1055	
2.09	↑ 1108	
2.13	↑ 1159	
2.26	↑ 1212	
2.35	↑ 1264	
2.40	↑ 1315	
2.48	↑ 1367	
2.57		Rapid erosion 120 ab 2
		tip now 200 ab 2
3:03		tip 140 ab 3
3:05	↓ 1210	brought down to reduce erosion.
3.19		test failed

Test 62

time	head	observation

Test 62

		Row 1			Row 2			Row 3					
time	head	right	middle	left	right	middle	left	right	middle	left	time for 50mL	Avg	Temp
3:49	0	-10	-35	-15	-2	-5	-103	10	1	-5			
4:25		172	64	135	256	252	238	322	409	317			
17/12 ~~1316~~ 3:45	1316	535	535	532	795	780	790	1065	1072	1072			

62. Test 62 (flume 3) circle

Test 62 was the first test carried out on mix 8. Mix 8 was 13% Sibelco 300g and 87% Sibelco 50n. Robin suggested this mix in order to test soils typical of Australian conditions- a fine grained sand with a silty 'tail'. See fig 1 for PSD's.

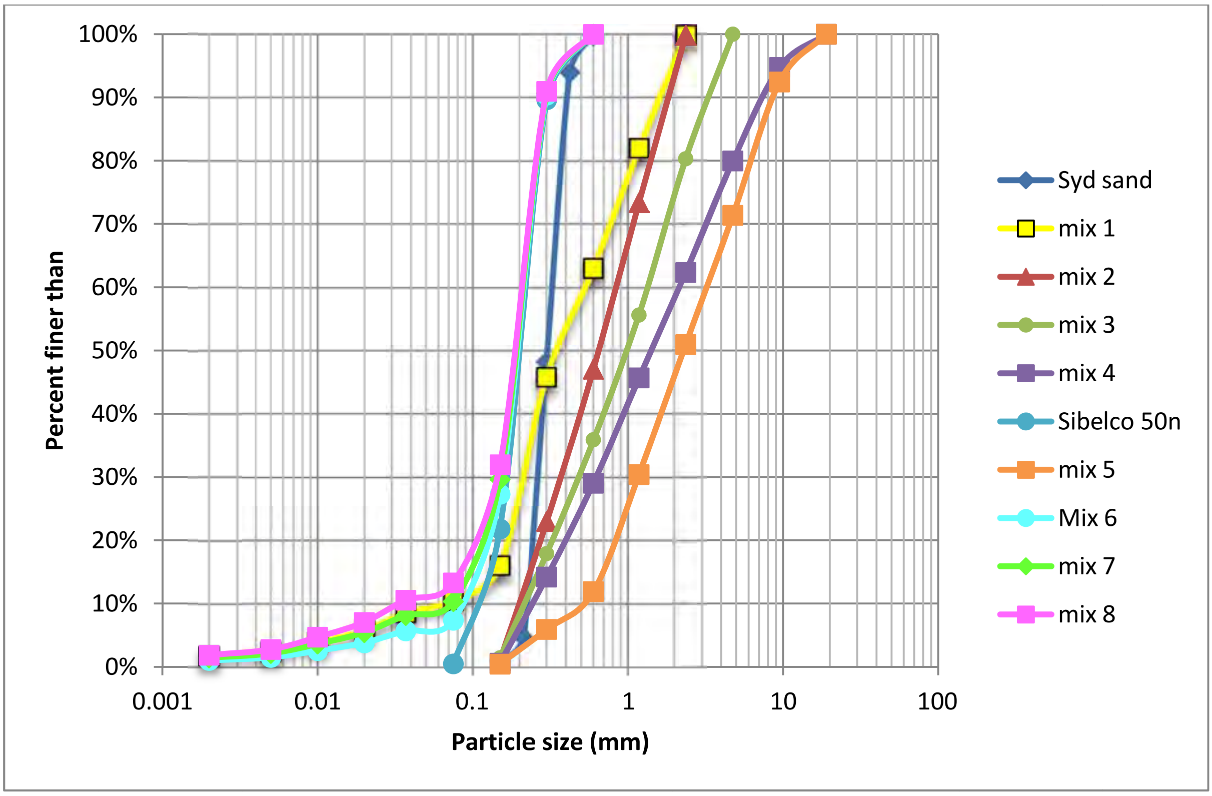

Figure 62-1 PSD's

It was expected that given its drop in permeability it would require a much higher head than when it was 50n alone (test 57 & 60). It was also expected that the result would lie well above Schmertmann's line.

The test was left to saturate over the weekend however the water level dropped in the pit causing the sump pump to switch off the water level to drop in the flume and the sand to unsaturate. Given the time spent on preparing the test I still ran it despite the fact that the air bubbles would probably affect the results.

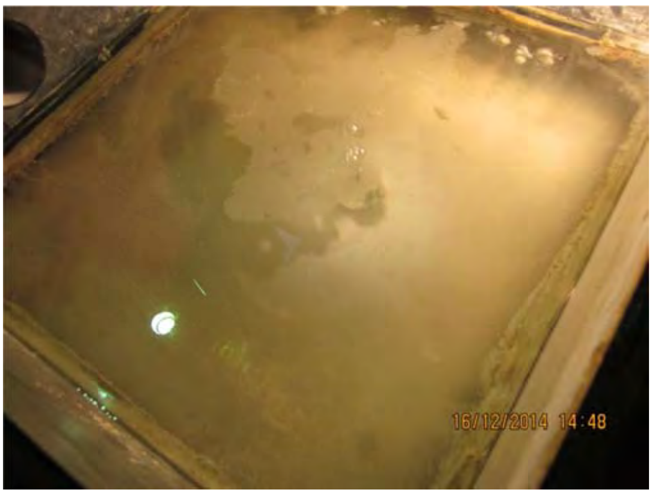

Figure 62-2 300g material on top of lid at start of test and bubbles came up through exit

Prior to starting the test some 300g product was up on the lid and bubbles came up through the exit (fig 2).

Within about 30min of the test starting the water in the d/s box became cloudy from the 300g soil. So point of initiation was unknown. However at a head of 1367mm a channel was observed and very quickly progressed to the u/s end (the full length in about 15 minutes). This fast behaviour was unexpected and unlike test 59 which was relatively slow (test 59 was done on the similar mix 6).

CL with H given in Fig 3 Note how much difference there is between tests 59 and this test despite the only difference being 7% versus 13% of 300g soil.

Even though it was expected this result would lie well above Schmertmann's line, it didn't- it's right on the line (see fig 4).

I think forward deepening and failure occurred but I'm not sure because not recorded by Hamish and no photos.

Note: I didn't take any SLR photos or weigh the flow because the test was damaged by desaturation.

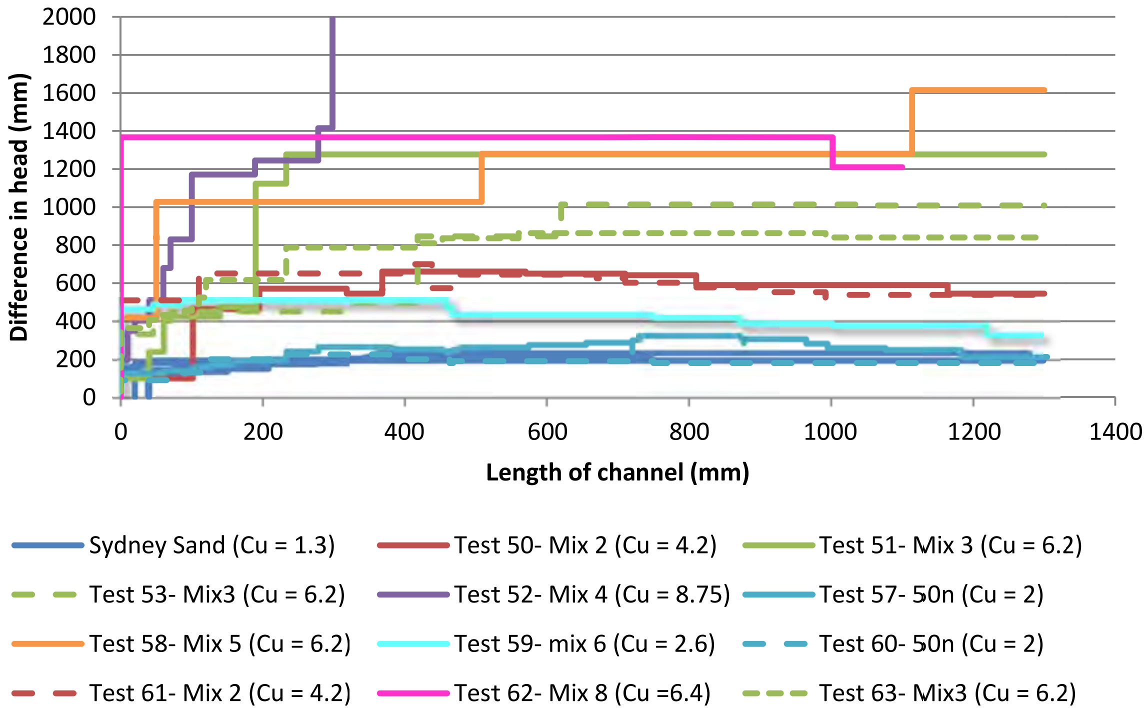

Figure 62-3 CL with head (test 62 is pink)

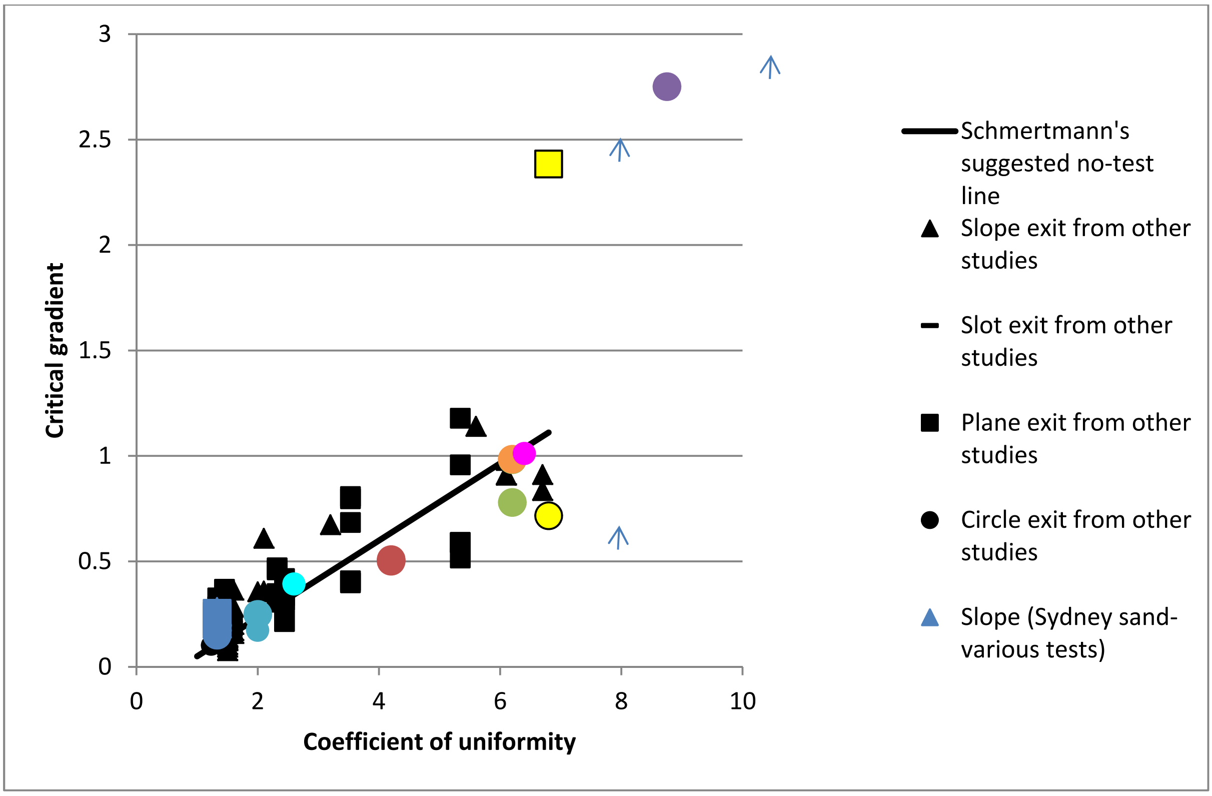

Figure 62-4 Schmertmann's graph- test 62 is bright pink dot

Backward erosion piping test data sheet

Test #	63	Exit type	circle
Date	17/12/2014	seepage length	1.3 m
Soil	mix 3	head in bladder tank	5 m
Flume	4	compaction	tamped

17/12

time	head	observation HS.
10.00	↑ 30	Start test
10.04	↑ 56	No sand movement
10.06	↑ 100	"
10.11	↑ 146	"
10.12		Very slight sand movement at exit.
10.14	↑ 170	
10.16	↑ 219	
10.30	↑ 265	
10.38	↑ 314	
10.44	↑ 363	Still only very slight sand movement
10.49	↑ 407	tip 140 – 100 in box
10.54		tip 150 – 100 "
11.10		Sand movement stopped
11.30	↑ 432	
11.45		tip 170 – 100 in box
11.52	↑ 455	tip moving 190 – 100 "
11.55		fair bit more movement now
11.58		tip 200 – 100
12.43	↑ 475	
12.44		tip 210 – 100 Movement around 210 area.
12.53	↑ 501	
1.02	↑ 525	tip still 210 but branching out.
1.15		tip 220 – 100
1.16	↑ 551	
1.17	↑ 573	channel deepening
1.30	↑ 617	
1.32		Tip under bar 1
2.06	↑ 645	"
2.08	↑ 665	
2.13	↑ 691	
2.26	↑ 715	

time	head	observation
2.27	↑ [illegible]74	/
2.35	↑ 764	
2.39	↑ 787	
2.42		tip 160 ab1 Rapid erosion for 10 secs.
~~2.48~~		
2.52	↑ 810	
2.59	814	Tip 185 ab1
3.20	↑ 836	tip 195 ab1
3.32	↑ 863	Rapid erosion – ab2
3.34	↓ 840	Tip 130 ab3 try to slow down
3.35	840	Reach 100% finish line
3.39		test failed

63. Test 63 (flume 4) circle

Test 63 was a repeat of tests 51 and 53 on mix 3. The aim was to test for repeatability because results of tests 51 and 53 were quite different.

Initiation occurred at 407mm and progressed at 863mm. See fig 1 below. Test 63 behaved more like test 53 (difference in critical heads within 15%). Therefore I'm going to consider test 63 to have demonstrated repeatability and consider test 51 to be an erroneous outlier.

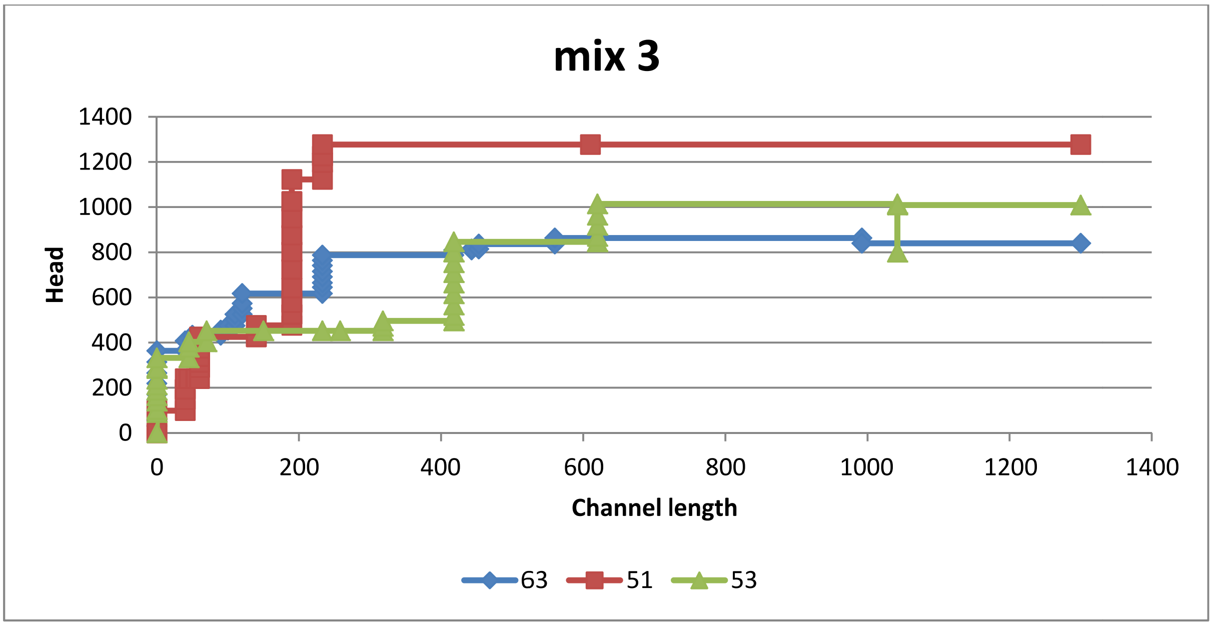

Figure 63-1 Head with CL for mix 3 tests

When the channel progressed it did so quite quickly. Once the channel reached a length of 560mm progression was very fast. To demonstrate Pics in Fig 2 and 3 are spaced only a minute apart.

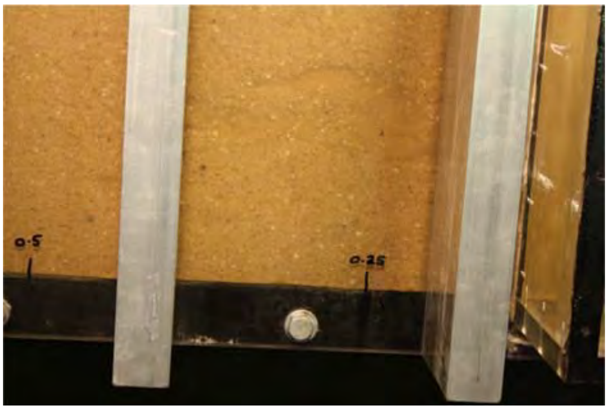

Figure 63-2 Channel length at 560mm

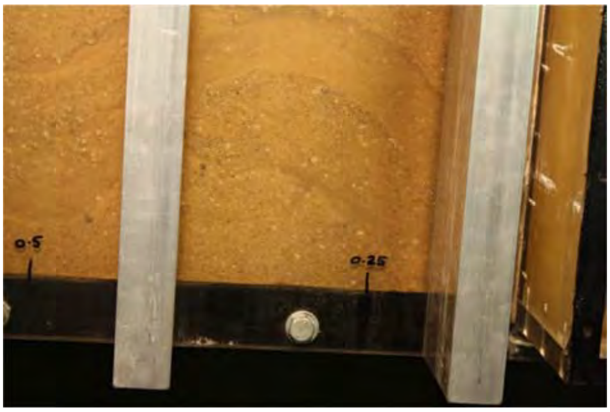

Figure 63-3 1 minute after fig 2 (progression was very fast)

It took only 4 minutes for forward deepening and failure to occur.

I note that test 63 is quite low below Schmertmann's line (see fig 3).

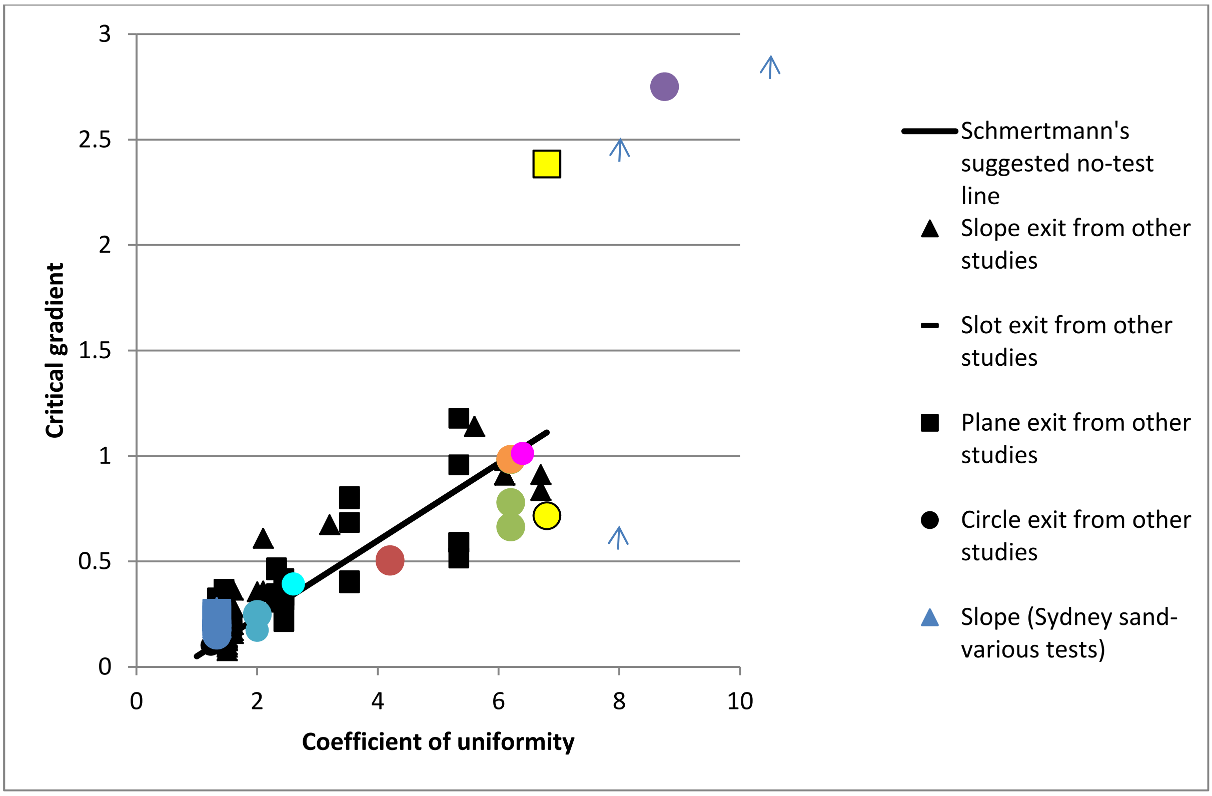

Figure 63-4 Schmertmann's plot- test 63 is the btm green dot

Backward erosion piping test data sheet

Test #	64	Exit type	circle
Date	16-01-15	seepage length	1.3 m
Soil	mix 8	head in bladder tank	5 m
Flume	4	compaction	tamped

	time	head	observation
16/01	12.30	35	Water level 45mm above lid - in box.
			Air ~~near~~ hole in box.
			this is the 1st test on Mix8 (well it isn't
upstream pipe			but the previous test on mix 8 was ruined) so
			it's difficult to predict when this test
			will initiate.
110	12.56	↑ 114	.
204	1.48	↑ 208	
	2.12	↑ 305	Water level 48mm above lid - in box
400	2.37	↑ 401	
	3.05		Sand starting starting to bubble
498	3.13	↑ 499	Water level. 57mm above lid in box
—	3.27	↑ 594	Unable to see a tip - due to murky water.
-	3.45	↑ 688	Water level. 62mm above lid in box
			Weekend left at 688 Head.
19/01	9.01	↑ 729	Box now overflowing - No visable tip, weighing water.
	10.10	↑ 777	.
	10.46	↑ 827	
	10.56	↑ 873	
	11.29	↑ 925	No visable tip - Water in box still murky
	11.49	↑ 971	Cytronine added this morning
	12.00		2 Happy snaps of upstream edge - Soil discoloured?
	1.02	↑ 1028	
—	1.12	*	Tip at 90 ab1
	1.17		Tip at 190 ab1
	1.30		tip at 230 ab1
	1.37		Tip under b2.
	1.40		Tip ~~un~~ at 50 ab2
	1.45		tip at 78 ab2
	1.51		Tip at 120 ab2
	2.12		Tip under b3

time	head	observation
2.38	1028	tip at 38 ab3
		tip at 120 ab3
2.55		tip at 140 ab3
3.13		Happy snap of Tip
3.23	"	tip at 148 ab3
3.25		Water overflow - 2:32 152 (5.2105 LT/hr)
3.30		tip at 225 ab3
3.38		tip at ~~240~~ 235 ab3
3.40	"	check Constant Head tank - still on 5.
3.46	"	tip at 238 ab3
3.48		New tip noticed on Westside at box.
# 3.51	↓ 110 →	Drop Headtank down to 110 for overnight shutdown
10/01 8.43	↑ 1028	
9.00	1028	Very little sand movement at Tip - 238 ab3
9.15		Tip under b4 - More Sand movement now.
		Sand movement near tip - increases / decreases.
9.26	1028	tip at 40 ab4
9.36		tip channel widening - and to the east side
10.00		2:46 166 (4.771 LT/hr Water Outflow)
10.14		tip appears to have stopped moving.
11.40	↑ 1045	
# 12.02		tip reached 100%
1.32	↑ 1097	No Sand movement last 1.5 hrs.
1.42	↑ 1150	
2.05	↑ 1206	
# 2.13		TEST FAILED.

Test 64

16/01/15

to measure loss through CHT + flume

for accurate readings adjust to levels drawn on standpipes.

upstream pipe	time	head	Row 1 right	Row 1 middle	Row 1 left	Row 2 right	Row 2 middle	Row 2 left	Row 3 right	Row 3 middle	Row 3 left	time for 50mL	Avg	Temp
34	12.42	35	5	4	3	10	22	15	20	13	15	used scales.	or in	
~~34~~	~~12.42~~	~~35~~	~~10~~	~~22~~	~~15~~							notes.		
304	2.14	305	128	112	120	170	171	176	229	203	221			
498	3.15	494	179	171	173	265	270	263	367	341	356			
–	3.45	688	264	247	252	378	384	375	505	483	490			
19/01/15	9.03	729	224	220	222	348	356	351	486	474	478			
	11.30	925	289	282	287	454	461	457	637	621	627			
	2.12	1029	308	314	343	515	518	495	721	715	707			
	3.40	1029	305	308	298	520	529	514	725	718	687			
20/01	8.45	1028	215	197	270	328	373	462	608	471	682			
	9.04	1028	306	300	308	505	527	499	736	710	724			
	1.45	1150	341	346	379	597	598	565	849	849	876			

64. Test 64 (flume 4) circle

Test 64 was a repeat of test 62- the circle exit with mix 8, but this time the sample remained saturated.

Water in the d/s box became murky so the tip couldn't be seen until it was past the box. Therefore it is unknown at what head it initiated.

The channel appeared on the LHS of the flume and remained along the LHS of the flume for its full length. The tip progressed at a head of 1028mm for nearly the full length of the flume (a small increase was needed right towards the end).

The test failed (by forward deepening) approximately 2 hours after the channel had reached the upstream end.

On the 19th Jan (the test started on the 16th Jan) soil discolouration was seen at the upstream end (see fig 1) Therefore chlorine was added to the water in case it was bioclogging.

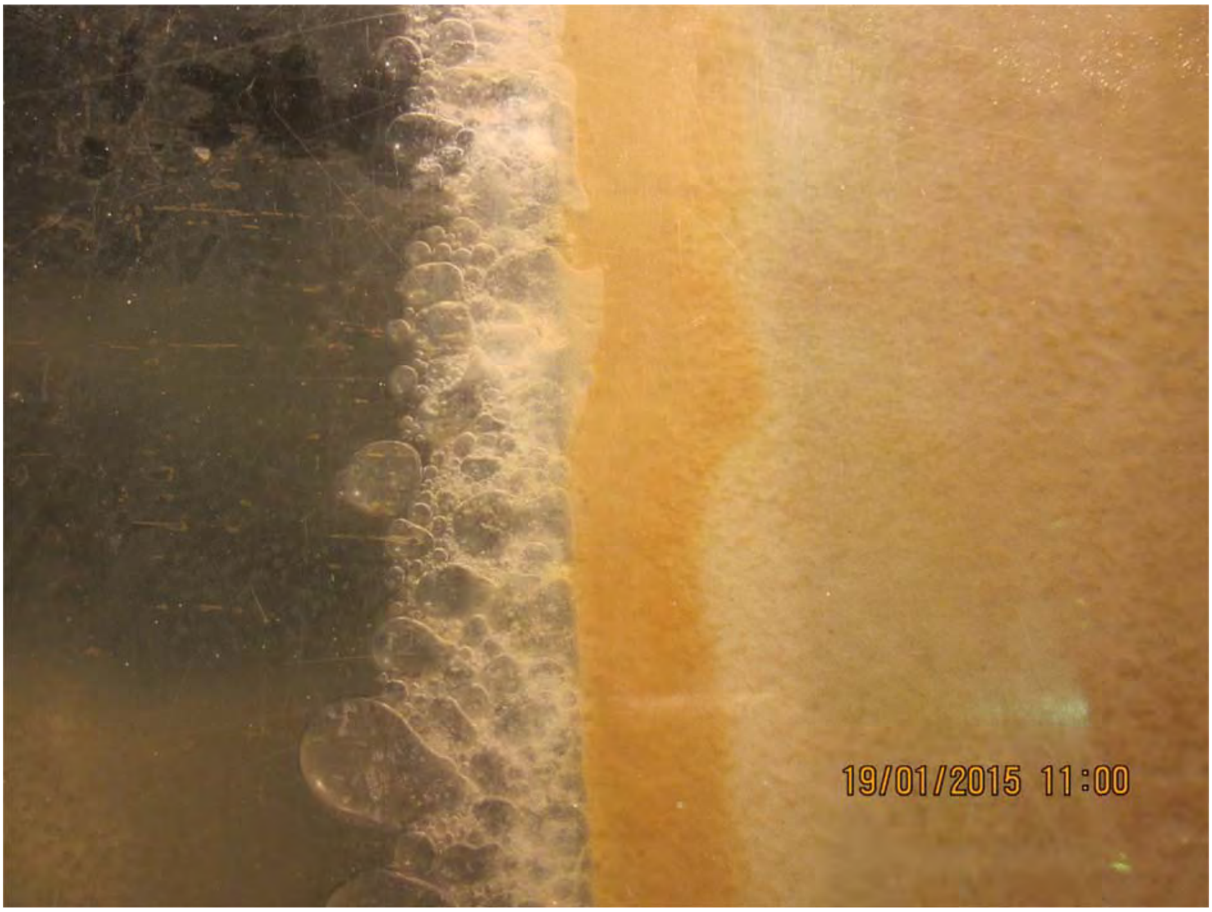

Figure 64-1 Soil discolouration along the upstream end

When compared to test 62, the progression head was about 25% lower. I suspect this is because test 62 was unsaturated and had air bubbles. See fig 2.

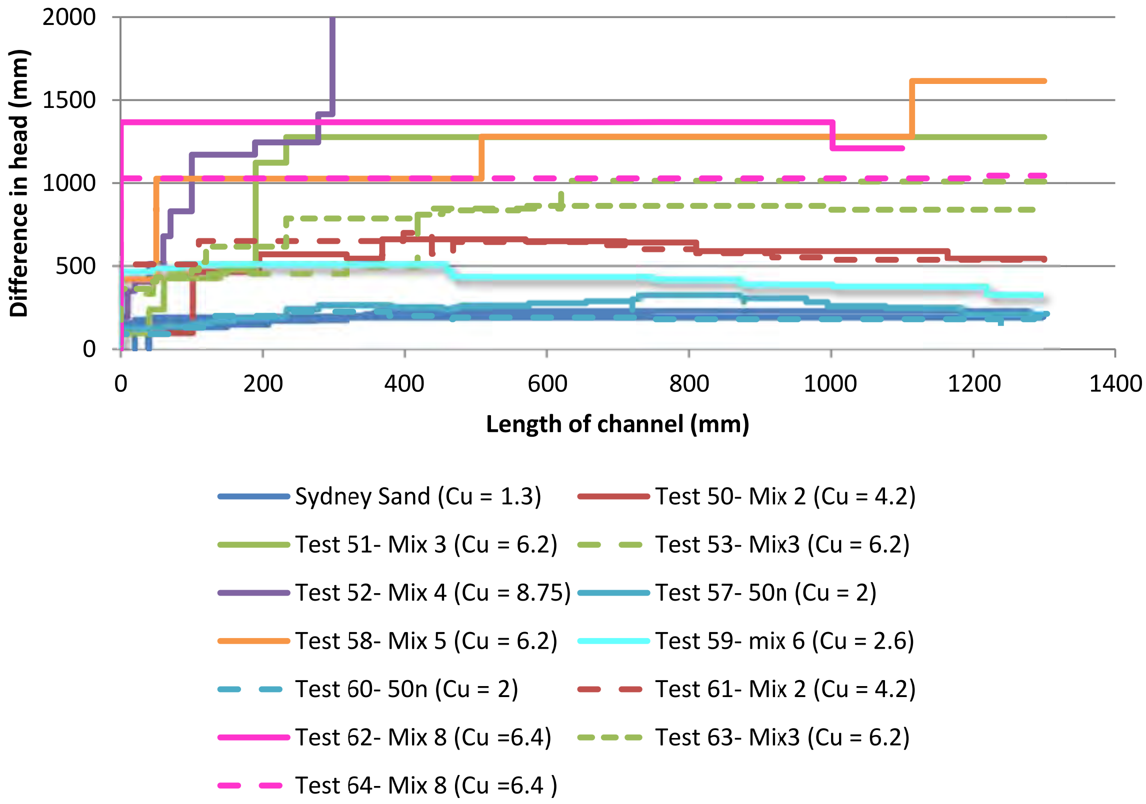

Figure 64-2 CL with head for different soils

The test plotted below (but not too far away from) Schmertmann's line (see fig 3).

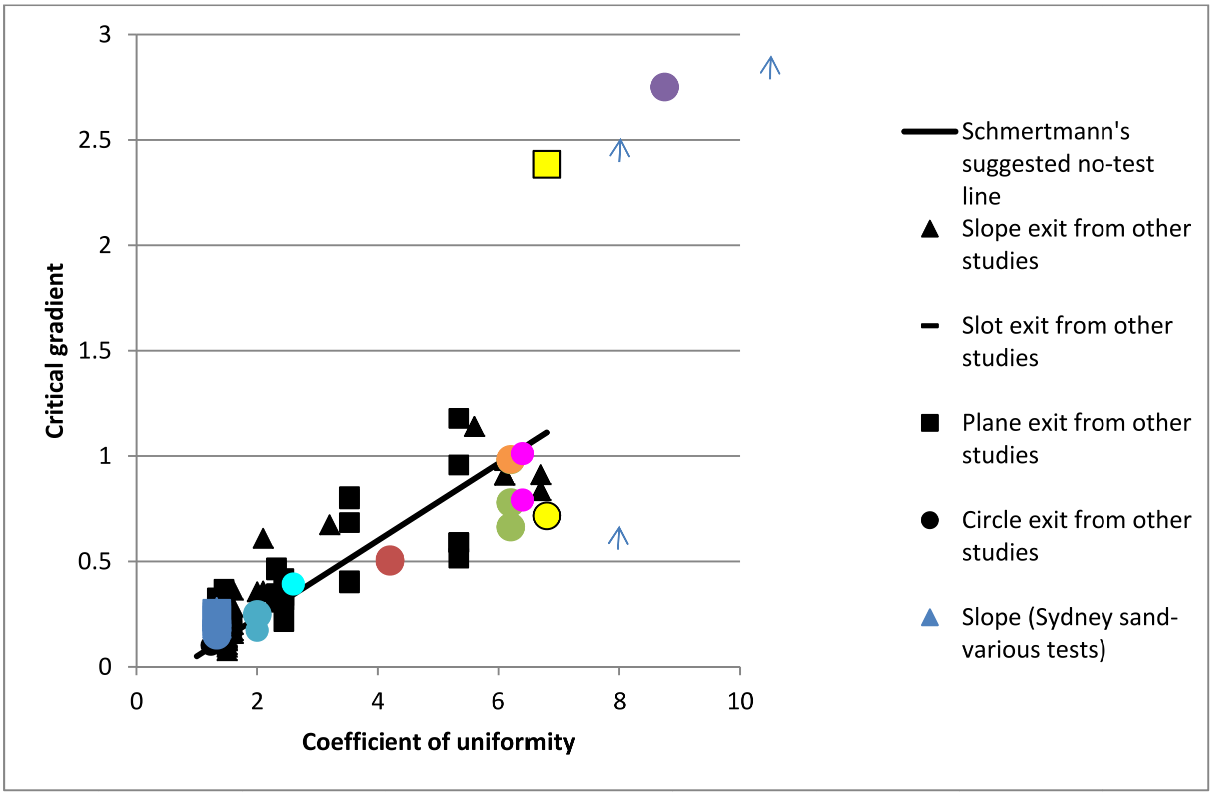

Figure 64-3 Schmertmann's plot (test 64 is the lower pink dot)

Backward erosion piping test data sheet

Test #	65	Exit type	slot
Date	23/01/2015	seepage length	3.9 m
Soil	sydney sand	head in bladder tank	5 m
Flume	1&2	compaction	vibrated

	time	head	observation
23/01	12·40	0	No water overflow yet.
	12·41	↑38	
	1·03	↑88	No sand movement, no water over flow yet.
	1·18		Water Overflow started.
	1·25		Start Recording water weight
	1·25		Camera on.
	1·30	↑139	
	1·55	↑190	No visable sand movement.
	2·23	↑240	
	2·34	↑292	
	3·00	↑342	
	3·23	↑394	
	3·45		Turned Camera/computer etc off for W/E
			Left Head tank at 394.
27/01	9·03	394	Re-Start test
	9·05	↑439	start Camera, balances, etc. (tip 185mm?)
	9·40	↑490	
	9·45	↓445	tip at 40 ab1
	9·47		Happy snap of tip.
	9·50		tip at 70 ab1
	10·08	445	tip at 150 ab1
	10·12		tip at 185 ab2
	10·15		" " 215 ab2
	10·15	↓420	try to slow tip down
	10·45		tip under bar 2.
	11·12	420	tip at 50 ab2
	11·13		Happy snap of slot opening
	11·25		tip at 70 ab2
	12·07		tip at 105 ab2
	12·37		tip at 145 ab2
	1·03		tip at 157 ab2

time	head	observation
1.12	420	tip at 194 ab2
1.34		tip at 223 ab2
1.51		" " 225 "
2.17		" " 235 "
2.35		Tip under b3
2.59		tip at 12 ab3
3.40		" " 20 ab3
3.41	↓ 0	Dropped Head level to 0 for night.
28/01 10.32	420	tip at 20 ab3
10.55	↑ 430	
11.33	430	tip at 25 ab3
11.35	↑ 444	
12.05	↑ 455	
12.15		tip at 30 ab3
12.57	↑ 480	
1.32		" " 43 ab3
1.50		" " 45 ab3
2.03		" " 48 ab3
2.03	↑ 498	
2.10		" 48 ab3
2.28	↑ 527	
2.50		144 ab3 Another tip to West has formed.
2.52		170 "
3.02		190 ab3
3.24	527	tip under ab4.
3.29		tip at 10 ab4
3.42		" " 25 ab4
3.54		" " 45 ab4
3.55	↓ 154	Dropped Head for Overnight.
29/01 7.52	↑ 527	Start up - tip at 45 ab4
7.57		tip at 52 ab4
8.25		" " 130 ab4
8.57	↑ 530	" " 200 ab4
9.07		" " 25 ab4
9.11		" under ab5
9.41		tip at 80 ab5
9.43		84 Happy snaps taken
9.55		tip at 120 ab5
10.13		" " 180 ab5

	time	head	observation
29/01	10.31	530	tip at 5 mm ab6.
	10.56		" " 115 ab6 (tip is at Centre tube)
	1.27		120 ab6 and channel is blocked
			btw bars 5+6 and 3+4.
	2.29	↑ 570	Seems to be ~~bt~~ stopped at Raise pipe?
	2.57	↑ 618	
	4.50		I think the tip is under the join.
			If I leave it @ 618 overnight and
			the tip keeps then I'll miss
			the opportunity to see if H=530
			is adequate to keep it going
			once it's past the join. Note -
			I saw a cluster of sediment
			transport through the channel
			+ deposit on blockage (now
			btw bars 5+6) so I think
			detachment is still occurring
			from the tip (it's just
			super slow).
	5.00	↓ 573	Hamish: in morning raise head up
			by 1 revolution + continue (unless
			tip has progressed past join → then
			leave the head as is). And turn Camera on.
			Note the channel is blocked btw
			5+6 and 3+4.
30/	8.21	↑ 632	
	9.45	↑ 700	
	10.33	↑ 752	Sand movement now through the blocked sections.
	10.52		tip at 220 ab6
	10.56		tip at 350 ab6
	10.57	↓ 703	tip under b7 (Getting blocked again between b5-b6
	11.45	↓ 683	tip at 150 ab7
	11.56		" " 180 ab7
	12.12		" " 220 ab7
	1.06	↑ 708	tip not moving.
	1.40	↑ 739	~~tip at 230 ab7~~
	2.07		tip at 230 ab7
	2.30		tip at 250 ab7
	2.37		" under b8

Test 65

	time	head	observation
30/01	2:38	744	tip under bar 8 - 2 tips.
	3.07		tip at 60 ab8
	3.20		tip at 120 ab8
	3.50		" " 155 ab8
	3.57	↓ 380	Head lowered for weekend to 380 (7 turns)
2/02	8.55	↑ 744	tip at 155 ab8. Monday start-up.
	9.58	↑ 775	
	10.28		tip at 220 ab8
	10.44		" " 250 ab8
	11.01		tip under bar 9
	11.51		tip at 120 ab9
	12.04		" " 130 ab9
	12.42	↑ 801	" " 137 ab9
	1.08		" " 185 ab9
	1.10	↑ 827	~~" 210 ab9~~
	1.17		" " 210 ab9
	1.45		tip under bar 10.
	2.06	↑ 852	
	2.28		tip at 10 ab10
	2.39	855.	tip at 45 ab10
	2.44		" " 55 ab10
	3.15		" " 170 ab10
	3.21	↑ 880	tip at 175 ab10
	3.42		" " 190 ab10
	3.43	↓ 460	Dropped Head Down for night (8 turns)
3/02	8.10	↑ 880	~~tip at 215 ab10~~
	8.39		tip at 215 ab10
	8.44	↑ 915	Sand Bubbling seems to have stopped.
	9.18	↑ 943	tip at 220 ab10
	10.45	↑ 969	tip sitting at 220 ab10
	1.02	↑ 994	
	1.55	↑ 1020	Blocked back at bar 7
	3.04	↑ 1073	
	3.26	↓ 525	Down for night (10 turns).
4/02	8.19	↑ 1075	
	9.38	↑ 1117	
	10.26	↑ 1170	tip still not moving.
	11.34		" at 230 ab10
	1.50		Down for night (10 turns).

Test 65

	time	head	observation
5/02	8.13	↑ 1180	tip at 230 ab10
	10.13	↑ 1230	
	10.50	↑ 1280	
	3.19	↑ 1335	
	3.30	↓ ~~[illegible]~~ 610	Down for night (10 turns)
/02	8.58	↑ 1335	Sand bubbling straight away
	9.06		tip under bar11 now
	9.15		A lot of Sand Movement between b1 - ~~b5~~ b6
	9.35		tip at ~~[illegible]~~ 15 ab11 - Sandmovement b1 - b4 Increasing.
	9.50		Seems to have blocked all the Way b1 - b6.
	10.56	↑ 1385	
	12.54	↑ 1430	
	4.08	↓ 311	I'm going to have it over the weekend
			incase it fails and makes a
			great mess. Tip 10 ab11. No boiling
			at exit.
/02	8.58	↑ 1430	
	9.54	↑ 1503	tip not moving, at 10 ab11
	11.38	↑ 1558	
	1.41	↑ 1610	
	1.53	↑ 1658	
	2.15	↑ 1710	
	3.00	↑ 1754	
	4.00	↓ 740	No tip movement all Day (15 turns.) down.
0/02	~~10.00~~ 8.50	↑ 1765	
	9.03	↑ 1812	
	10.06	↑ 1862	
	11.25	↑ 1880	
	2.42		- ~~She~~ Removed sand from Exit box
			this started a lot of Sand movement from
			b1 - b3.
	2.51		b1 - b5 A lot of Sand moving
	3.05		More sand Removed (another 10 kgs).
	3.06		Sand movement to b8
	3.28		tip now at 35 ab11
	3.36		" " 55 ab11
	3.39		" " 110 ab11
	3.52		" " 200 ab11
	3.54		" Under b12 (under box).

TIP movement stops | starts | stops | starts

~~3-10 s / 30cm~~
30cm / 3-10s

	time	head	observation
10/02	3.55	1880	tip under b12 (Under box).
	4.07		Test failed.

date	time	head	observation
	1·30	95	CENTRE TUBE READING.
	2·55	157	
	~~2·58~~		~~Empty water tub.~~
	3·24	187	
	3·45	211	
27/01	9·35	242	
	9·52	249	
	10·45	224	
	1·03	212	
	2·59	~~[illegible]~~ 205	
28/01	10·24	~~[illegible]~~ 23	Head 10.
	10·32	174	" 420
	10·50	203	420
	11·37	208	" 444
	2·10	~~[illegible]~~ 234	" 498
	2·28	238	" 498
	3·25	253	" 527
29/01	7·57	229	" 527
	9·43	256	530
30/01	9·46	305	" 700
	10·38	347	" 752
2/02	12·30	356.	" 801
	2·08	390	" 852
	3·22	405	" 880
/02	8·45	437	" 915
	9·20	522	" 943
	10·45	556	" 969

65. Test 65 (flume 1&2) slot

Test 65 was a repeat of test 45 in order to demonstrate repeatability. It was of a slot exit, on Sydney sand and a seepage length of 3.9m. Hamish ran this test.

Initiation occurred at 342mm. It's difficult to define the progression head because it appeared to be different in flume 1 (around a head of 500mm) than it was in flume 2 (around 750mm). See figure 1.

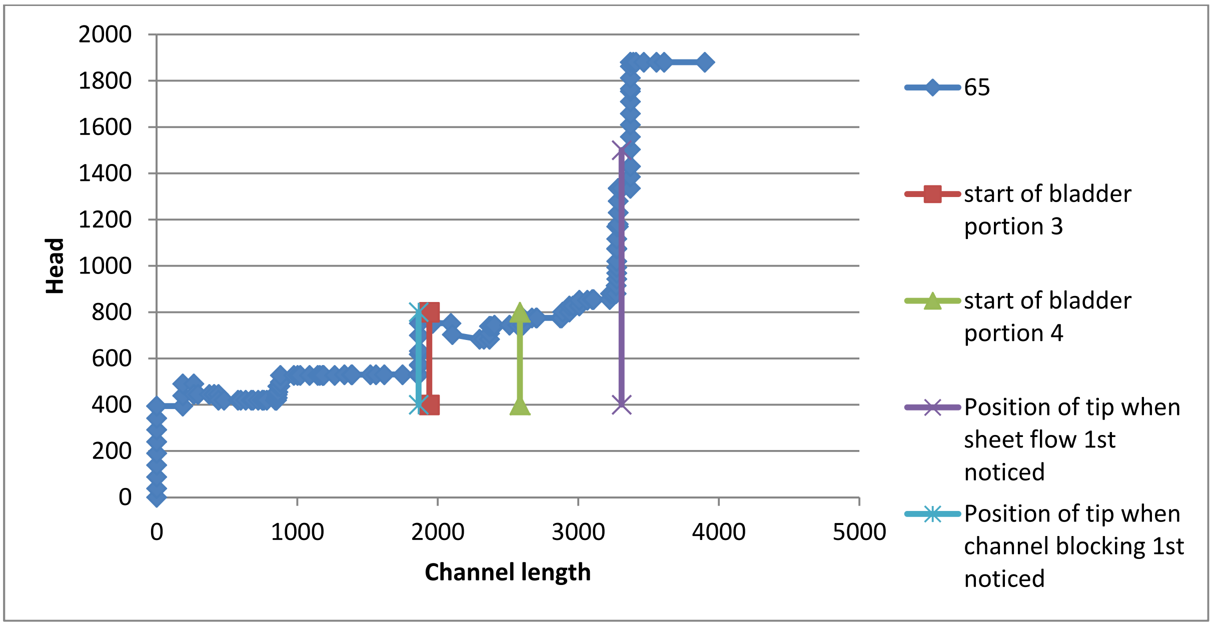

Figure 65-1 test 65 plot

I don't know why this is. I can think of 4 reasons.

1. Perhaps it was due to bladder pressures. I know I've shown that bladder pressure makes little difference to progression head but if bladder pressures differ across a seepage length surely it would affect things (but note: Hamish was unsure he agrees).

   When using both flumes 1 & 2 there are 4 separate bladder pressure portions- portions 1 and 2 in flume 1 and portions 3 and 4 in flume 2. After saturation (but before start of test) I noticed the inlet tap to either portion 3 or 4 was closed (I can't remember which tap it was). The tap was then opened before running the test. It's possible that inflating this portion of the bladder after saturation caused less effective stress in this region compared to other regions (but not by much- see below for calcs). But I would have thought if the effective stress was less then less head would have been needed to progress the tip- and yet more was needed. So I don't think this explains anything.

2. The other alternative is pressure from flume 1 was leaking so didn't stay at 50kPa. Hamish didn't record checking it. However this bladder hasn't shown a tendency to leak (not like bladder 4 has).

3. Another alternative is a higher head was needed once the channel blocked at any point along its length. I first noticed the channel was blocking at the same time a higher head was needed (see plot above).

4. There may have been a gap between the sand and the gasket where the flumes join. A gap means lower water velocities so higher heads needed to progress the tip.

So in short, I don't know why flume 2 needed a higher head than flume 2. But I think reason 3 is the most likely.

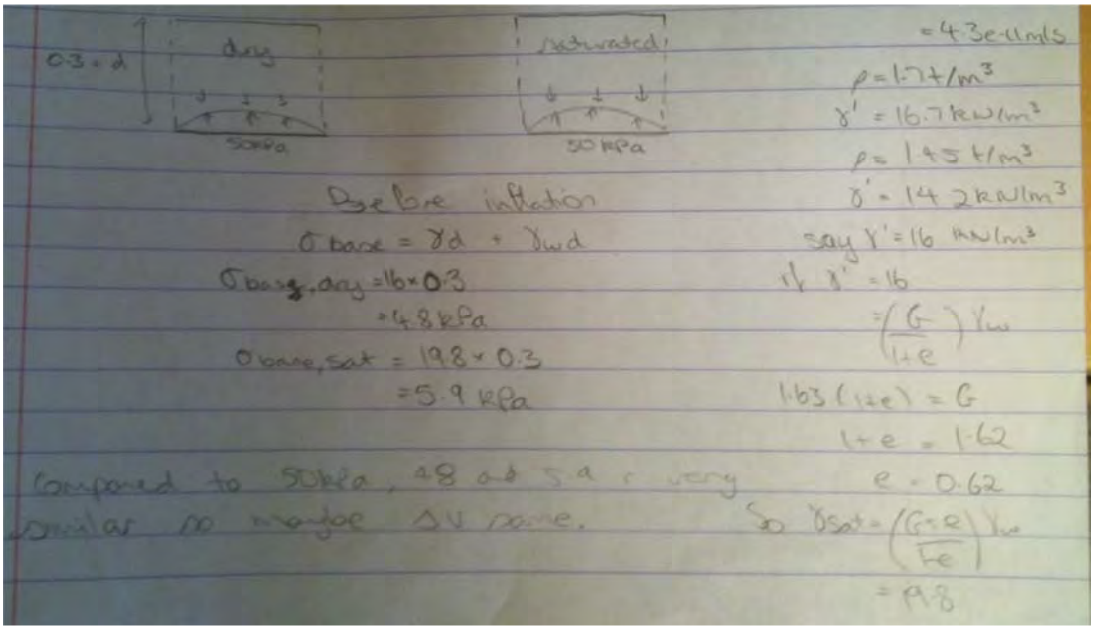

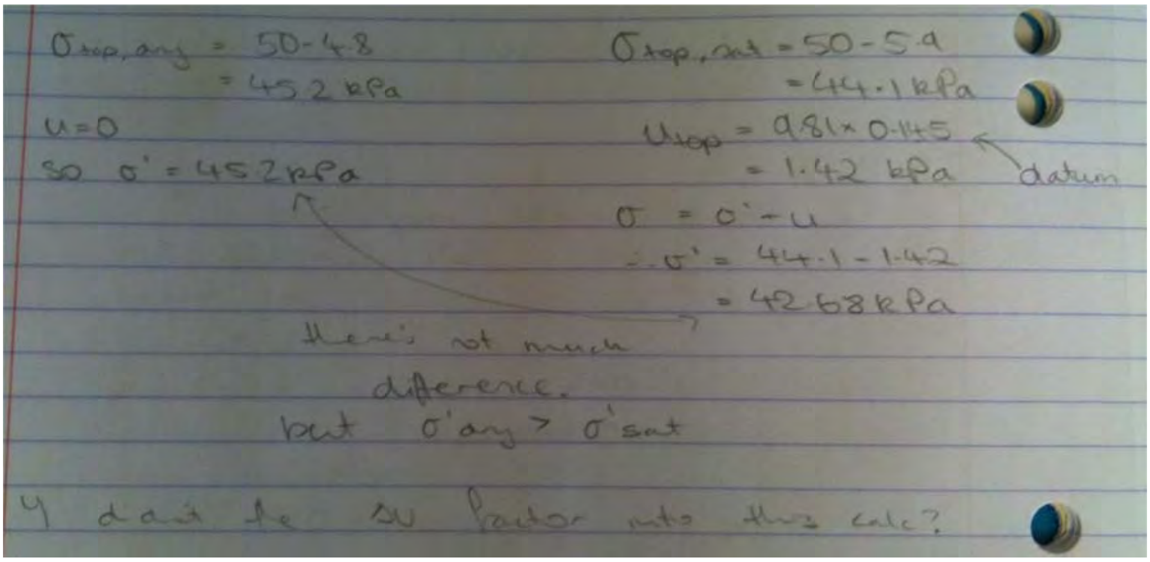

At a channel length of 3270mm and a head of 880mm another large step in head was needed to progress the tip. An increase in head from 880mm to 1335mm only saw the tip progress 15mm. The only suggestion I have as to why this happened was a blockage of accumulated sand at the exit caused excessive head loss at the exit (and therefore less head gradient across the flume) (note: this location didn't correspond with a bladder edge). This would support Hamish's observation that boiling at the exit stopped when the head was 880mm. Perhaps if sand had been removed the exit at this time the tip could of progressed without further need for head increase but we didn't think of it at the time so Hamish continued to raise the head.

Whilst the head was at 1335mm Hamish noticed a sudden burst of a lot of sand movement between bars 1 to 6. This sand movement was not restricted to channels, instead it appeared to flow along large zones spaced out across the full width of the flume. See video for example (it's difficult to show with photos). I'm referring to this as sheet flow because it flowed more like a sheet than a channel. This sheet flow wiped the channel out and lasted for about 30min before stopping. During this time the tip progressed about 90mm but stopped about 15mm after bar 11. The head was increased from 1335mm to 1880mm but the tip didn't move so Hamish removed sand that had accumulated at the exit (about 10kg) (in case this sand was adding resistance to piping). This removal reinitiated the sheet flow but did not affect the tip. After about 5-10min or so the sheet flow stopped so Hamish removed more sand from the exit (another 10kg). This time the tip did progress in a stop/start fashion until it reached the end. Note the sheet flow only occurred in flume 1 (it never extended to flume 2).

Sample failure occurred about 10 minutes after the channel reached the upstream end however it didn't do so by forward deepening, it did so by incremental surface slippage which started at the downstream end and worked backwards at a rate of around 30cm/3-10s.

In summary I suspect the channel could have reached the upstream end at a head of 880mm (or even 750mm) if we had of removed build-up from the exit. If the channel had of reached the end at a head of 750mm this would have given a result more similar to test 45. Plot below shows comparison of seepage lengths.

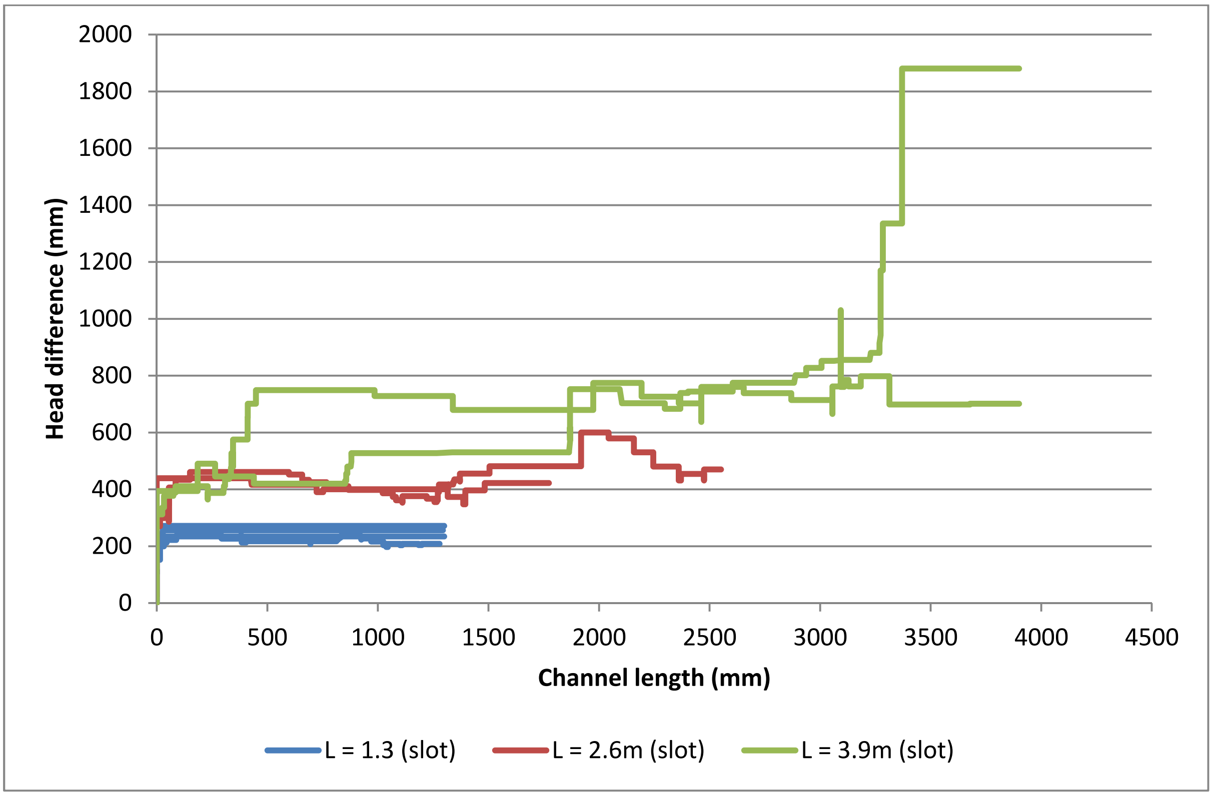

Figure 65-2 Comparison of different seepage lengths

This test has not demonstrated repeatability (it was quite different to test 45). Therefore I will need to do it again. Next time, when the channel blocks, I want to try removing the sand build-up at the exit and wait longer before raising the head.

Backward erosion piping test data sheet

Test #	66	Exit type	slope
Date	17/02/2015	seepage length	1.3 m
Soil	sydney sand	head in bladder tank	2.5 m
Flume	3	compaction	vibrated

time	head	observation
17/02 11.09	↑224	Some air traped on Water entry side
11.16		Water flowing.
11.27	↑292	
11.51	↑363	
12.19	↑386	
		Some sand bubbling and tip under bar 1
12.49	↓365	so decided to drop Head (tip 200 from Exit)
1.16	↓336	tip at 230 ab1
2.40		Sand still bubbling. tip 240 ab1
2.45	↑376	
2.53		tip under b2
2.56		tip at 30 ab2
3.17	↓160	tip at 240 ab2 = shut down for night
18/02 10.14	↑376	tip under b3
10.26		tip at 25 ab3
10.33		" " 135 ab3
10.34	↓339	In attempt to slow tip down.
10.35		Happy snap of Exit
10.51		Tip under b4
10.56		" @ 80ab4
10.58		" " 115 ab4
10.59		" " 135 THE END
11.00		Sand blocked around b3
11.10		unblocked " " now
11.14		Air bubbles (from 2" TAP) are blocking in tracks
11.45		Shut test down due to air
		trapped in tracks.

66. Test 66 (flume 3) slope

Test 66 was a repeat of test 39- a slope exit with a pressure bladder of 2.5m. This repeat was done because test 39 behaved differently (lower head) than other tests that were carried out bladder pressures less than 5m (tests done on other exits). It is unlikely that the slope causes the bladder pressure to affect results so the test was repeated.

Before starting the test air was observed in the sample. See pic 1 (although the air isn't clear in this photo it was the best one I had). It is not known how this air entered the sample. Whilst Hamish did observe the water had dropped below datum overnight- it was still above the lid. The water level must have dropped below the lid at some point for some reason.

Despite the desaturation we ran the test. Results are shown in fig 2 below. Both the initiation and progression heads were above previous tests (about a 20% increase on the average initiation head and 11% increase on the average progression head). Given the significant increase in heads I am considering this test to have been compromised by the desaturation and will need to repeat it.

Figure 66-1 Air entered into sample

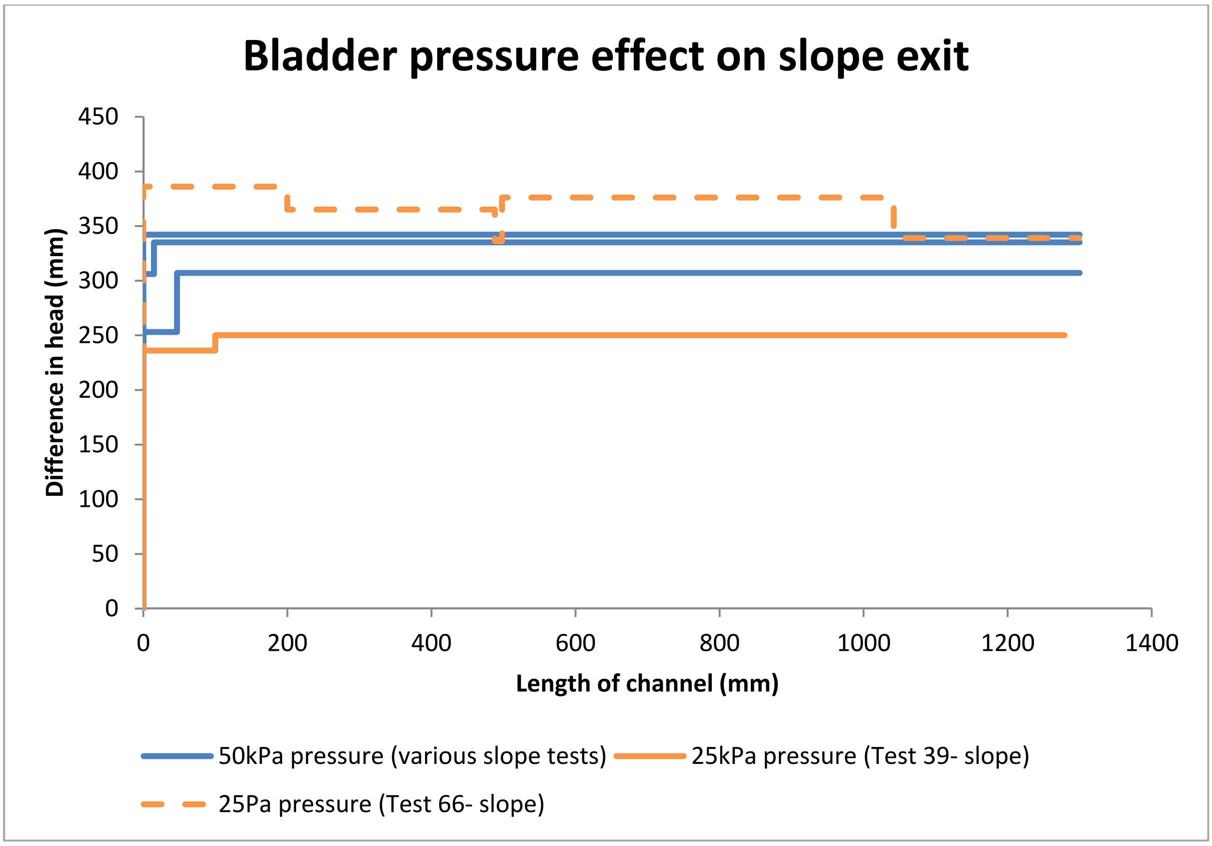

Figure 66-2 Test 66 compared to other slope results

Backward erosion piping test data sheet

Test #	67 H.S.	Exit type	circle
Date	25/02/15	seepage length	1.3 m
Soil	Mix ~~8~~ ?7	head in bladder tank	5 m
Flume	4	compaction	tamped

If datum 145mm above sand then top of lid 120mm below datum

	time	head	observation
			Water needs 115 to start flowing.
25/2	10.54	95	Water level in box 32 mm
	11.12	↑143	" " 3~~6~~3 "
	11.51	↑170	Some sand bubbling. " " 36
	12.59	↑215	" " 4~~0~~1
	1.45	↑290	46
	2.10	↑335	" " 48
	2.36	↑350	" " 51
26/2	8.30		Water is now dripping into tub.
			Sand Bubbling.
	8.45	↑388	
	9.06	↑438	
	9.13	↑485	
	9.55	↑535	
	10.09	↑581	
	10.55	↑632	
	11.40	↑677	Can't see a tip yet, very cloudy water.
	12.40		Looks like there maybe a tip about 60mm from Exit circle??
	2.44		tip at 100 from Circle
	2.58	↑705	
	3.28	↓537	4 turns.
27/02	8.16	↑705	tip at 105 from Circle exit
	9.08	↑751	
	9.22	↑776	
	9.42	↑827	
	10.37	↑877	
	11.10	↓805	a lot more bubbling at Sand. Tip now under b1
	11.40	805	Tip at 95 ab1
	11.52		Tip at 145 ab1
	12.30		tip at 150 ab1
	12.50		start Recording water flow – computer.
	1.20		tip at 155 ab1

So $\Delta h = 95 + (120 - 32)$

1.6E5

Test 67

	time	head	observation
	3.00	805	180 ab1 tip.
	3.26	↓460	" " " 7 turns
2/03	9.16	↑ 805	
	9.46	↑ 827	tip still 180 ab1
	11.25	↑ 853	tip is unusually wide (70mm).
	12.21		tip at 25 ab2
	12.46	↓ 815	tip at 90 ab3 (Decided to turn head down).
	2.41	↑ 832	tip isn't moving.
	3.40	↓ 486.	7 turns.
3/03	8.45	↑ 832	
	12.43	↑ 856	
	1.19		Tip under b4.
	1.32		Quik Rapid erosion – still Tip under b4
	1.35		tip at 35 ab4
	1.48		Tip Reached the End.
	2.41		FAILED SHUT DOWN.

R= 1.7e-5

Test 67

			Row 1			Row 2			Row 3					
	time	head	right	middle	left	right	middle	left	right	middle	left	time for 50mL	Avg	Temp
25/2	10.50	95	About	10mm	V o	12	25	18	47	42	39			
	1.00	170	56	56	52	99	112	105	152.	147	146			
	1.46	215	79	79	75	124	135	130	183	180	176			
26/2	8.45	350	135	137	135	201	213	208	275	271	275	220 ml 6.10 310 2.1405 L/hr		25
6.7e-7	10.05	535	209	210	209	313	325	320	427	424	427			
8.8e-7	11.37	6.32	240	241	243	360	372	368	484	479	483			
9.7e-7	12.44	677	264	264	264	392	406	403	527	520	526			
27/2	9.06	705	246	246	246	380	384	389	522	518	523	220 ml 3.10 4.168 L/hr		
	10.43	877	299	299	301	468	484	480	649	646	653			
	11.43	805	237	242	250	414	428	424	586	582	590	220 ml 2.45 4.8 L/hr		
2/3	9.48	805	230	235	246	391	409	403	551	548	555			
3/3	12.38	832	255	255	~~5~~260	395	410	407	547	543	551			
	1.19	856	178	188	240	344	363	367	525.	523	530			

67. Test 67 (flume 4) circle

Test 67 was the first test to be carried out on mix 7. Mix 7 is 90% 50n and 10% 300g with Cu = 3.2.

I initiated at 677mm and progressed at 877mm.

As expected the results were midway between mix 6 and mix 8 (see figure 1).

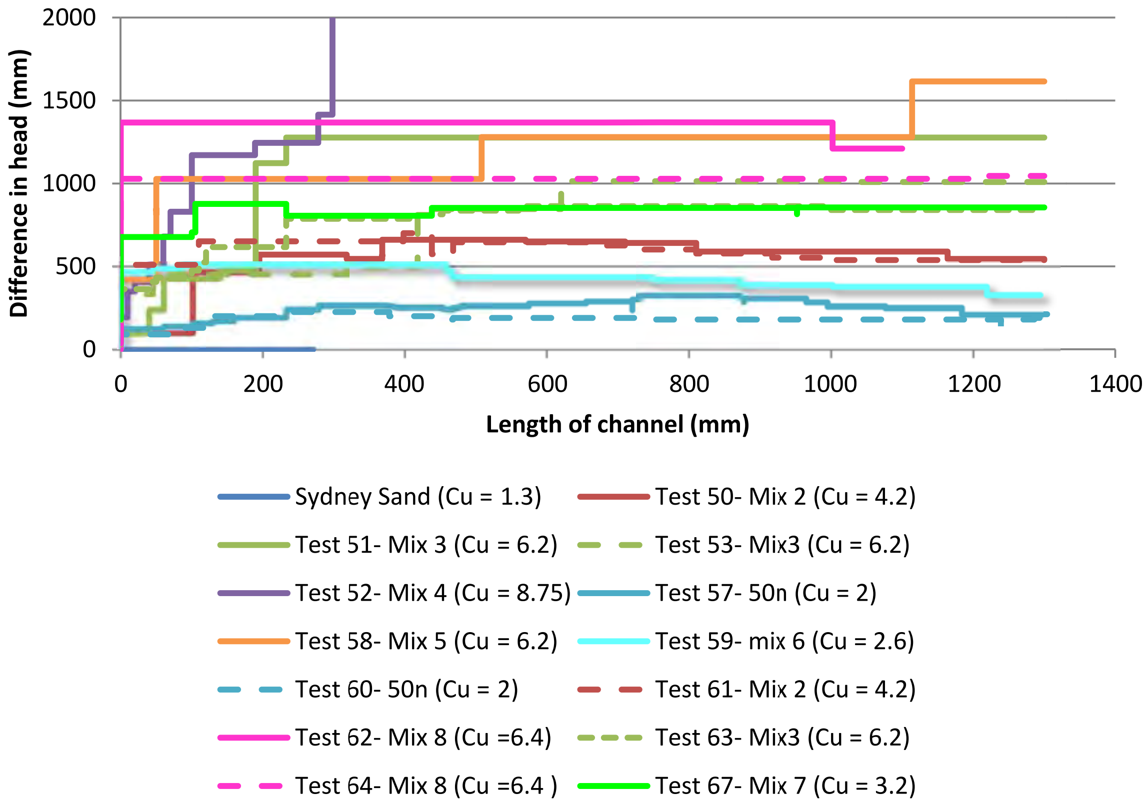

Figure 67-1 Test 67 compared to other soils

The channel was relatively wide for such a fine sand, at its widest it was 70mm. See pic 2. I'm not sure why this was.

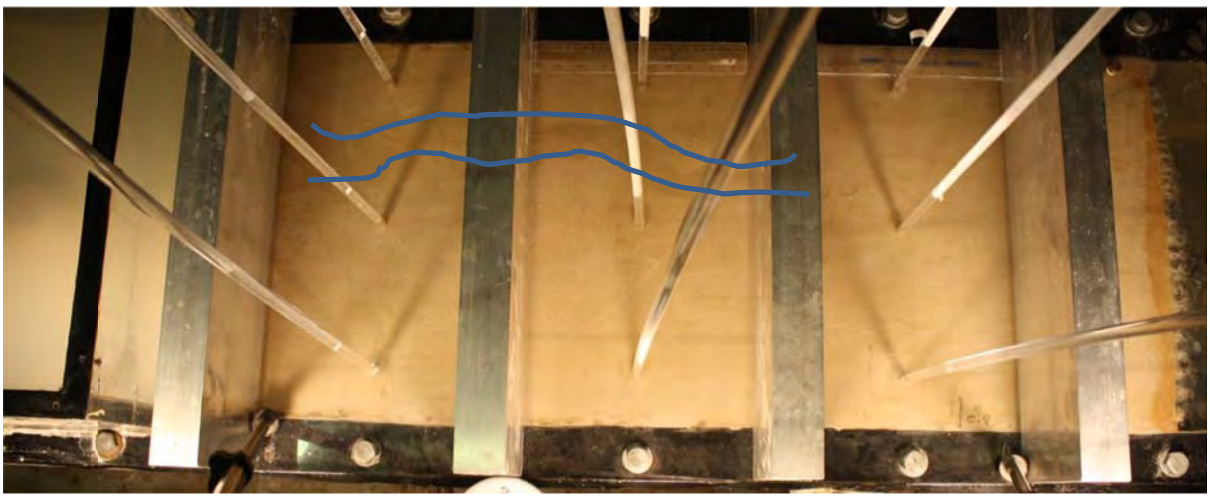

Figure 67-2 channel relatively wide for such a fine soil

Failure occurred about an hour after the tip reached the upstream end.

On Schmertmann's chart mix 7 lies near but above the line. See fig 3.

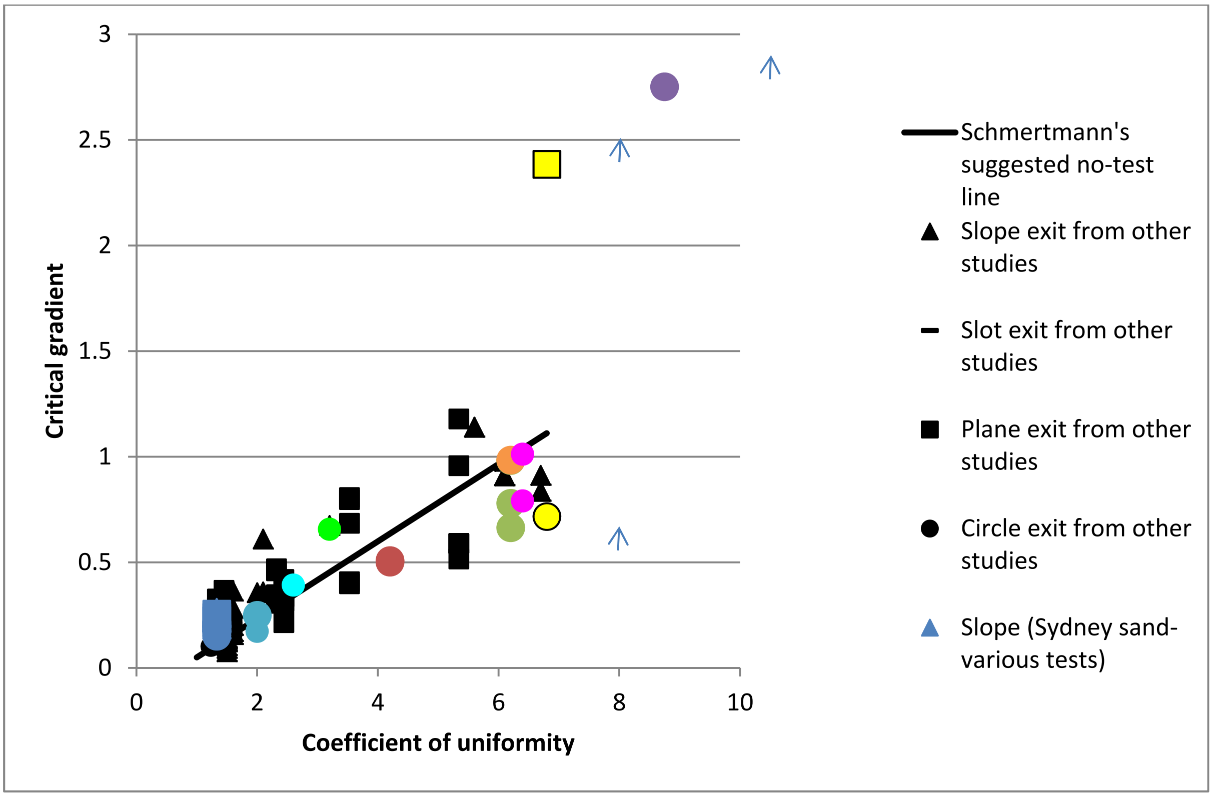

Figure 67-3 Test 67 on Schmertmann's chart (bright green dot)

Backward erosion piping test data sheet

Test #	68	Exit type	slot
Date	4/03/2015	seepage length	3.9 m
Soil	Syd sand	head in bladder tank	5 m
Flume	1&2	compaction	vibrated

time	head	observation
10.29	0	Note: chlorine added this morning.
10.30	↑ 100	
10.39	↑ 150	
10.44	↑ 196	No flow through d/s valve yet.
10.52		I've just realised the u/s valve isn't
		fully open so it won't have 200mm
		head on it & that explains why
		no flow is leaving d/s valve yet.
10.53	↓ 43	
10.57		Just noticed bladder tank #2 is
		down to ≐ 1.5m. Re inflated to 5m.
11.00		opened u/s valve fully
11.01	↑ 98	
11.11	↑ 150	
11.23	↑ 196	
11.45	↑ 250	
12.03	↑ 303	
12.23	↑ 349	
12.37	↑ 402	
12.39		Standpipe 312mm above lid. Water temp
		23°C.
12.49	↑ 452	
1.33	↑ 504	
1.41	[illegible]	Standpipe 374mm above lid.
1.42	↑ 558	
1.54	↑ 608	first boiling action @ exit seen. Possible
		initiation - only maybe 12mm
2.21		12mm
2.22	↑ 634	"
2.32	↑ 660	"
3.21	↑ 690	"

1.4E-4

Test 68

time	head	observation
3:33		channel started on RHS-edge tip
		now under bl. Happy snap.
		Standpipe ~~[illegible]~~ 463mm.
3.59	↓ 658	65 ab1. Happy snap.
4.07	↓ 636	145 ab1
4.13	↓ 612	202 ab1
4.20		231 ab1
4.33	↓ 586	0 ab2
4.48	↓ 560	45 ab2
5.07	↓ 535	60 ab2
5.30		60 ab2. Standpipe 374mm above lid
5.58		" "
6.07		75 ab2
6.22		81 ab2
6.40	↓ 507	92 ab2
6.51		" . leave overnight.
5-3 9.36	507	92 ab2
9.42	↑ 526	"
10.01		92 ab2
10.14	↑ 556	"
10.40		103 ab2
10.52		"
12.16		245 ab2
1.27	↓ 533	105 ab3
2.09		105 ab3
2.28		" " moved laterally about 10mm
2.48	↑ 544	107 ab3
3.01		" "
3.24		112 ab3
3.38		" "
3.50		" "
4.21	↑ 55~~7~~	" "
4.35		114 ab3
4.42		116 ab3 (moved about 30mm laterally)
5.08		121 ab3
5.28		" " . leave overnight. Standpipe 354mm above lid

Test 68

t-3

time	head	observation
9.51	557	125 ab3 and moved laterally
		to almost centre of flume.
		Perhaps there's some form of
		resistance here making it harder
		for the tip to advance straight.
		See Happy snap.
9.58	↑578	125ab3
10.17		125ab3
10.50	↑607	125ab3
10.53		a region under 62 looks relatively
		shallow + wide + looks as though
		it could be more susceptible to
		blocking so keep an eye on it.
		See happy snap.
10.55		145ab3 + still moving laterally towards
		centre. See HS. Large amount of
		continual sediment transport.
		Channel about 15mm wide ≑ 150mm
		downstream of tip and stays at
		about that width.
11.15		150ab3. Bladder tank # 2 ≑ 1.5m so
		increased back up to 5m.
11.19		155ab3
11.28		160 ab3. Channel in its widest section
		30mm. See HS. But usually 15-20mm wide.
12.02		160 ab3
12.19		" "
1.27	↑634	" "
1.43		" "
1.53		" " , standpipe 383mm
2.29	↑663	" "
2.37		" "
3.23	↑687.	" "
3.25		one of the branches has taken off.
		@145ab3 c HS. After I knocked on the
		lid a fair few times.
		New tip now 175 ab3.
3.27	↓637	" " " 193 ". Tip moving fast
3.3[illegible]		and possible blockage setting up in

but didn't

time	head	observation
		btw b1 + 2 so ↓H. CHS.
3.28		250 ab3
3.33	↓611	35 ab4
		58 ab4
3.41	↓587	98 ab4
3.54	↓560	160 ab4
3.59		180 ab4
4.10	↓534	227 ab4
4.13		250 . Standpipe 335.
4.39		I think the tip is just on the other side
		of b5 (say 0 ab5). It's difficult to
		see. And it looks like the channel
		might be running laterally. CHS.
		I note that H=533 last time it moved
		laterally like this. I've managed to not
		got any blockages yet which is
		great - usually I would have by now
		(the first blockage often occurs when
		the channel = 1.3m).
5.16		5 ab5.
5.30		" ". I'm going to leave it at this head
		over the weekend. I don't think the tip
		will grow but want to be sure.
		There are still no blockages however there
		is considerable buildup at the exit so
		I will remove it. CHS 4 b4 and after
		shots. Note though that sand boiling is
		still taking place as is sediment
		transport through the channel (presumeably
		from scour). I've reduced the frequency
		of photos to 1/hr and stopped the
		flow measurements.
5.57		I had one last look before I left and
		the tip had moved! To 30 ab5. So I'm
		↓H.
5.58	↓507	
9-3 10.34	507	tip 20 after join. Channel blocked
		btw b2-4. Standpipe 336mm.

Backward erosion piping test data sheet

Test #	68	Exit type	slot
Date	4/03/2015	seepage length	3.9 m
Soil	Syd sand	head in bladder tank	5 m
Flume	1&2	compaction	vibrated

9-3

time	head	observation
10.47		head tank 4 bladder 2 ≑ 1.5m so
		raised back up to 5m. head tank 4
		bladder 1 ≑ 4.5m so raised to
		5m.
10.52		bad boiling at exit but raised small
		building just in case. CHS
10.55		tip moving. despite channel still blocked,
		60 aj. (after jam). Transported sand
		from tip being deposited at blockage
		btw bars 3+4. Maybe moving sand from
		exit helped?
10.57		There's a small transverse indent in
		the sand's surface where the tip now
		is. CHS. The dent looks to be a
		similar depth as the channel. This
		dent may impede tip growth as
		velocities slow down at tip given increased
		area. Will wait + see.
11.41		Blockages have moved. It's now btw 4 and
		5 as well as 1+2. Tip still 60aj.
12.28	↑ 561	still 60 aj. Blocked btw 4-5 and 1-2.
1.37	↑ 610	" "
1.52	↑ 664	" "
1.53		Saw particle transport along ditch
		(perpendicular to tip). Gave ditch a
		few taps with mallet to try persuade
		a new tip from ditch but no luck.
2.13	↑ 714	took H.S. + vid at tip. Only blockage btw
		2+3. Standpipe 435mm. Hit with mallet again.
2.39	↓ 612	100 aj. tip moving fast. Blockage btw 4+5.
2.41		tip stopped.

time	head	observation
3.05	↑ 637	10 aj.
4.06	↑ 665	" "
4.38	↓ 642	175 ab7. Blockage btw 5+6
4.54		177 ab7
		" "
5.16	↓ 486	Down 3 revolutions. I would have liked
		to have left it at 642 but I won't be
		here tmw and I'm not satisfied that
		the tip has stopped (like I was on
5.19	↑ 505.	Fri).
10-3 9.30		177 ab7 + blocked btw 5+6 & and 2+3
1+3 11.29		177 ab7. blocked btw 5+6 and 2+3.
		Still boiling @ exit. Moved buildup from
		exit. See before shot on H.S. Standpipe 364mm.
11.43	↑ 611	177 ab7.
12.14	↑ 662	" "
12.15		Detachment at tip occurring now But not
		continuously Maybe about 50 or so
		particles every 1-2 minutes. Blocked
		btw bw 7 to end of flume!.
12.32	↑ 691	Detachment from the tip is only short
		lived + not enough to progress the tip.
		So still 177ab7. Note that despite the
		tip not moving there's still considerable
		sediment transport downstream. Esp
		from b3 to the exit.
12.50		185 ab7
1.14		187 ab7
1.46		250 ab7
2.09	↓ ≑ 670	40 ab8. Blockages btw 6+7 and 4+5
		1+2. Because blocked btw 1+2 a new
		channel has formed near LH's & HS.
		It's about 100 ab2.
2.34		70 ab8
2.58		" " . Moved build up at exit. And
		there now appears to be 2 possible
		new channels, neither of which have

Test 68

time	head	observation
		joined the existing channel d/s.
		See H.S.
3.16		70 ab8
3.34	↑ 694	" "
3.41		110 ab8. Only blocked btw 6+7.
4.01		135 ab8 and moving laterally
		C.H.S.
4.34		140 ab8
5.34		145 ab8. removed buildup @ exit. There
		are multiple boiling points. C.H.S.
6.33		145 ab8, leave at this head overnight.
12-3 9.52		130 ab10, a lot of buildup @ exit
		but still boiling. Blocked btw 8+9 & 6+7 & 4+5
10.57		130 ab10 and no longer boiling at
		exit so cleared exit. ~~Sediment~~
11.02		Sediment transport continuous -
		plentiful d/s of 64. Standpipe 446mm.
11.10		140 ab10
11.56		178 ab10
1.40		180 ab10
2.11		" "
2.31		" " and removed buildup from
		exit.
5.36		180 ab10. leave overnight.
13-3 9.47		a new channel branched off the
		existing channel near 68 and is
		now 250 ab10. The channel is
		blocked btw 8+9, 6+7, 5+6, 4+5, 3+4.
		There's no boiling at the exit + alot
		of buildup. There's no sediment transport
		along channels even @ d/s end.
11.56		tip just under b11. Removed d/s buildup.
12.02		Sediment transport now recommenced
		through channel d/s of 65. And
		boiling @ exit.
4.53	↓ 133	tip still under b11. Going to drop
		head to datum for weekend.

	time	head	observation
6-3	11.03	134	2nd tip under b11. 1st tip 193 ab10.
			Blockages btw 8+9, 6+7, 5+6. No
			boiling at exit. Buildup removed.
	11.07	↑634	Boiling @exit again.
	12.28	↑680	tips not moved.
	2.38	↑705	″ ″ ″ 1st tip now under b11
			(Perhaps I shouldn't have raised the
			head but I did because I only
			looked at the 2nd tip and saw it
			hadn't moved). I noticed the 1st tip
			had moved after I raised the head.
	3.28		both tip under b11.
	4.29	↓695	107 ab11
	5.26	↓≑670	107 ab11, leave overnight.
7-3	10.03		I think tip is through to u/s
			end. C H.S. And I think forward
			deepening has begun and is up
			to just d/s of the u/s box (It's
			difficult to see through u/s box).
			The channel appears to be
			blocked (perhaps a surge of
			particle transport occurred when
			it opened into u/s edge) and is
			reasonably wide (btw 15 to 40mm).
			C H.S. Channel is blocked btw
			b9 to u/s box, just u/s of flume join,
			and a small region btw 4+5. No
			boiling at exit so removed buildup.
			Standpipe @446mm.
	10.14		Will leave exp at this head to see if
			it fails.
8-3	10.05		Sample has failed. from u/s to d/s. It
			looks like fwd deepening occurred
			all the way through leading to failure
			but I can't be sure. C H.S. D/S box is
			full of sand and flow is applied into
			weighing box. Took exp down.
			Bladder tank 2 @ about 1.5m when I

emptied. And tank 1 ≑1m.

68. Test 68 (flume 1&2) slot

Test 68 was a repeat of tests 45 and 65 in order to demonstrate repeatability. It was of a slot exit, on Sydney sand and a seepage length of 3.9m.

I ran this test and I did it a little differently. I:

1. Didn't wait until the channel had reached 25,50,78,89,90% of L before lower the head. Instead I lowered the head once the tip was moving (except if it moved overnight) repeatedly until it stopped.
2. Waited much longer whilst the tip wasn't moving before I raised the head. Instead of the approx. 15 minutes of no movement I waited at least an hour (and even more on occasions when I left the head overnight).
3. Periodically removed sand build up from the exit (especially before raising the head and/or when boiling was no longer seen).

The CL versus H is in figure 1 below.

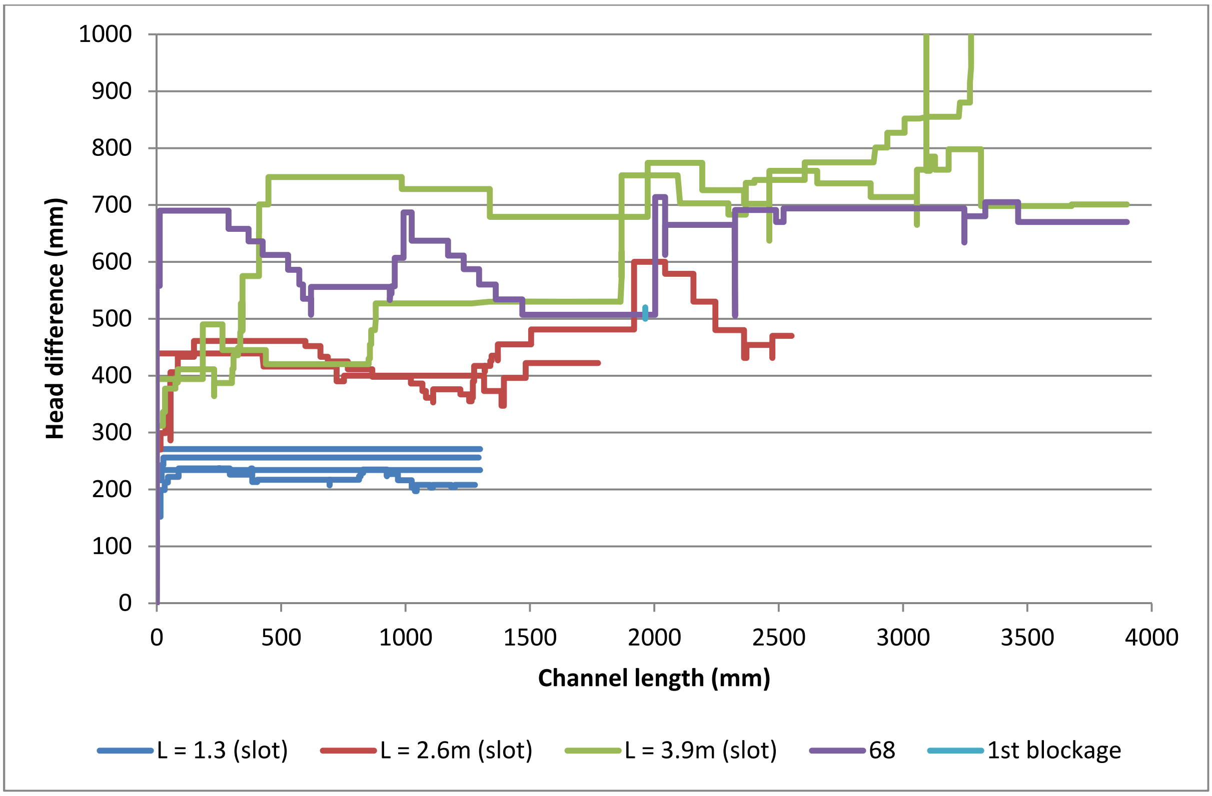

Figure 68-1 CL with H for different seepage lengths

Initiation occurred at 690mm which was about 45% higher than tests 45 & 65. Once the tip was moving I continuously reduced the head until it stopped. The tip stopped approximately 6 times. The head at which they stopped seemed to depend on whether a section of the channel was blocked or not. Prior to first blockage the tip stopped twice at heads of 535 and 557mm (approx. 22% less than the estimated progression head). Whereas after first blockage the tip stopped at heads of 665, 670 and 680mm (btw 4 to 2% less than the estimate progression head).

The first blockage was sighted when the channel was 1964mm long (45mm after the flume join) (shown as a short blue line in figure 1). This was later than previous tests which first blocked when the channels were around 1.3m long. I attribute this to continuously dropping the head during tip progression and waiting longer before raising the head (less head, less sediment transport and therefore less likely to block). Once the first blockage formed there was always at least 1 (sometimes 2-3) blockages along the channel which moved over time.

When the tip stopped it (pre blockages) it moved laterally before stopping. See fig 2.

Because the head needed increasing to around 690mm each time it stopped and was able to maintain slow (incremental) tip progression despite channel blockages I am going to identify this as the progression/critical head.

Note that the large increase in head shortly after the first blockage was observed may not have just on account of the blockage but probably also had to do with a dent/impression in the sands surface perpendicular to the channel. This impression would have caused velocities to slow down in this region (and so needed extra higher heads). See fig 3.

During the exp about 2 or 3 times new channels formed either off the existing channel or from the exit. Fig 4 shows an example. However it was the original channel that reached the u/s end.

Several times throughput the experiment I removed built up sand from the exp (I'm guessing around 10 times). The volume of soil removed almost filled one of the 15L containers (I they're 15L). See fig 5 for full container. Sometimes there was enough sand buildup to prevent boiling. Sometimes when I removed the buildup it enabled the tip to progress a little further but it never meant that I didn't have to raise the head. In other words, I don't think removing the buildup meant the progression head was reduced, I think it just meant the tip progressed a little further before stopping and may have helped with less blockages.

At one point boiling at the exit occurred right at the edge which meant I could see what the centre of the boil looked like. I took a short video of it.

By the end of the 17th March forward deepening only went for a length of about 200mm but by the next morning the experiment had failed. It looked as though failure occurred in the 'normal' way (i.e. after forward deepening had reached the d/s end) because the corridor of washed out sand extending to the u/s end (instead of a surface slip occurring for the entire length of the flume from starting from the d/s end). But I can't be sure because it happened overnight without photos. If it did fail in the 'normal' way then this was the first time it did so across the seepage length.

As for comparing this test with other tests, the two large "step downs" appear to make it quite different to the 2 previous tests but the steps are only because I reduced the head as soon as the tip was moving. So I don't consider this an inconsistency among tests. Given test 45's critical head was about 730mm (5% difference) I consider this test has demonstrated repeatability when compared with test 45. I consider test 65 to be an erroneous outlier.

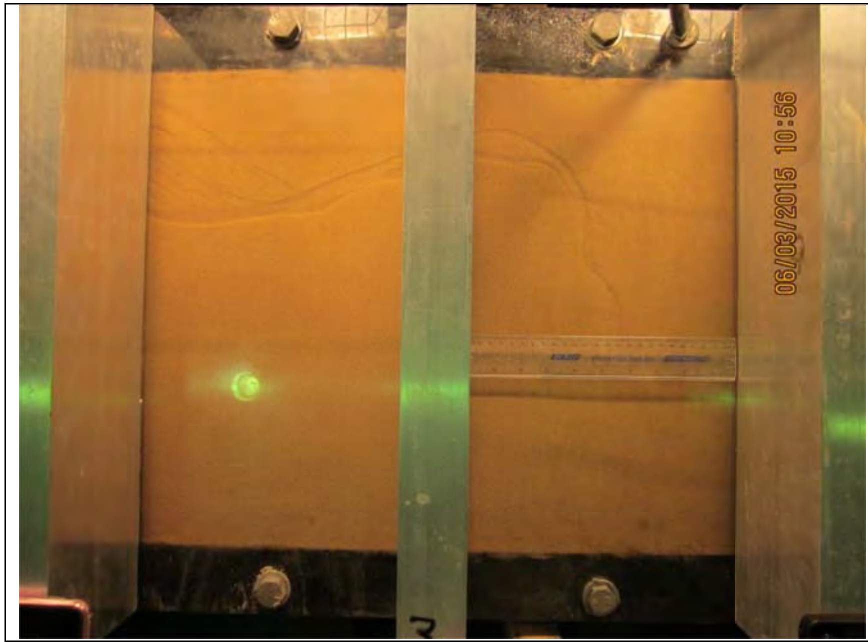

Figure 68-2 Channel moves laterally when tip stops

Figure 68-3 dent/impression in sand surface that slowed tip down

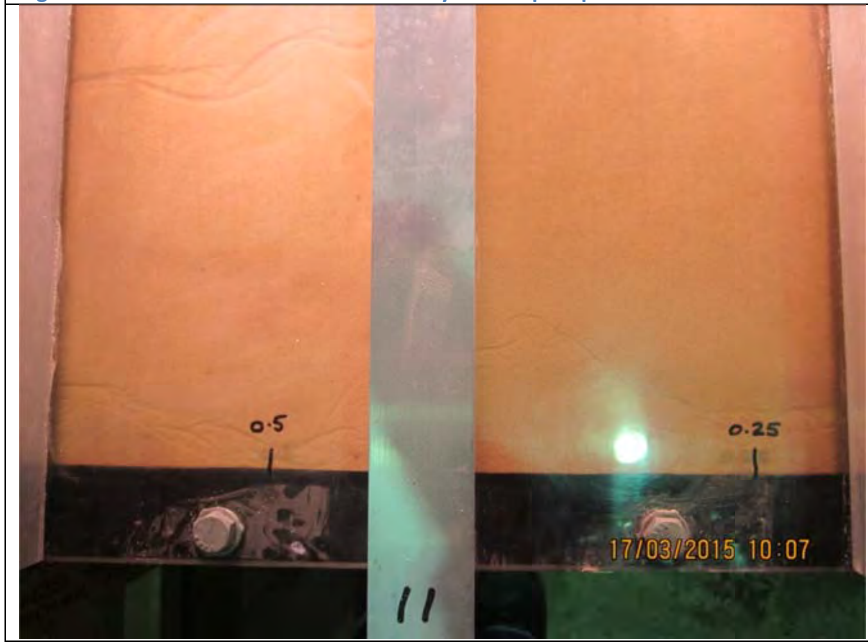

Figure 68-4 Additional channels formed (original channel along LHS and new channel in middle)

Figure 68-5 At end of exp showing the container full of sand removed from the exit (sand in the d/s box at time of pic was due to failure overnight)

Backward erosion piping test data sheet

Test #	69	Exit type	circle
Date	30/03/2015	seepage length	1.3 m
Soil	mix 7	head in bladder tank	5 m
Flume	4	compaction	tamped

	time	head	observation
30/03	10.23	80	water level in d/s box 75 mm
			from top of lid.
	10.04		large amount of material around
			exit (soiled "boiled" up and left
			exit during CO2 filling). C.M.S.
			I tried moving material so I
			could see through lid to sample
			but water still just murky enough
			that I can't quite see. There would
			have to be a void around exit
			(made vacant by "boiled" material).
			Based on test 67, expecting initiation
			≑ 670mm and critical ≑ 850mm.
	11.16	↑ 124	Small boil @ exit.
	11.38	↑ 173	
	12.08	↑ 223	d/s box water level 80mm above lid
	12.44	↑ 272	
	1.39		I can see bubbles near the
			exit possibly where soil left during
			CO2.
	1.40	↑ ?	
	2.07	↑ 371	
	2.38		Water level in d/s box 96mm above lid.
	2.42	↑ 420	
	3.07	↑ 468	
	3.23	↑ 490	Water level in d/s box 103mm above lid
	3.54	↑ ~~5?~~ 544	Water in d/s box quite murky. ow.
			Can't see through to sample at all.
	4.45	↑ 595	no sign of a channel. leave here
~~31/03~~	~~10.05~~	↑	overnight. Now flowing from d/s box.
31/03	10.05	↑ 610	

1.9E-5

Test 69

	time	head	observation
31/03	10.44	↑646	
	11.12	↑670	Water outflow 3.2195 LT/hr
	11.18		Started Recording waterweights - com
	11.46	↑ 697	
	1.46	↑ 725	Seems to be a tip formed in the box - Hard to see.
	2.28	↑ 752	
	3.50	↓ 651	Down for night.
/04	8:37	↑ 754	Seems to be 4 or 5 braided tips - still in box
	9.45	↑ 787	
	10.49		tip ≑ 40mm d/s of d/s box wall.
			took pic with phone (H.S. not working).
	10.57	↑ 807	
	11.37		tip might be ≑ 30mm d/s of wall but
			hard to tell.
	11.38	↑ 833	
	12.08	↑ 860	tip may be same spot (difficult to see).
	12.20	↑ 886	" " " " " " " "
	2.19	↑ 901	
			tip appears to be moving laterally..
	2.53	↑ 927	tip not moved.
	3.27	↑ 951	" " "
	4.16	↑ 979	
	4.40	↑ 1001	
	5.03	↑ 1028	
	5.22	↑ 1058	
	5.36	↑ 1081	
	6.04	↑ 1105	
	6.05	↓ 1001	under bl (also noticed water in d/s box became more turbid).
	6.06	↓ 899	40 abl
	6.07		80 abl
	6.09		130 abl at middle standpipe
	6.11	↓ 845	there's about 3-4 different channels
			(see iphone). but furthest still 130 abl.
	6.14		another channel now approaching
			(HS standpipe (row 1). Call channel 2.
	6.17	↓ 795	channel 2 now 160 abl It tends to
			behave a little differently at the tip.
			Instead of ~~more~~ particles movement being
			concentrated at the tip. ~~the~~ a region

Test 69

time	head	observation
		about 20mm upstream of developed
		channel seems to slide d/s
		together.
6.21	↓ 743	200 ab1.
6.26		230 ab1
6.28	↓ 690	tip under b2
6.36		there's still plenty of sediment transport
		in channel even though tip is
		still under b2. I'm gonna have to
		drop H overnight to make sure
		the channel stops.
6.37	↓ 484	
6.38		10 ab2.
6.40		30 ab2
6.46		" " and I can't see any
		particle transport so here's hoping
2/04 8.40	↑ 532	the tip has stopped.
10.04	↑ 583	tip where I left it last night.
10.14		50 ab2.
10.28		62 ab2
10.41		can't see any sediment transport.
11.13	↑ 636	62 ab2
11.26		85 ab2
11.37		103 ab2
12.29	↑ 659	103 ab2
1.15	↑ 682	
1.49	↑ 696	
2.30	↑ 725	
3.16	↑ 770	+ moved build up @ exit C.H.S.
3.38	↓745	103 ab2
3.41	↑ 802	on the move again.
3.42		115 ab2
3.43		130 ab2
3.59		164 ab2
4.18	↓↓ 194	250 ab2
7-4 10.17	186	under b3. no boiling @ exit so
10.19	↑ 283	moved build-up.
10.45	↑ 391	

$\gamma_w = 9810\ kg/m^3$
$\rho = 1000\ kg/m^3$

~~TxE~~/m³

Test 69

time	head	observation
11.08	↑ 499	no movement in channel but there is
		boiling at exit. Outflow too small to
		measure.
11.27	↑ 594	
12.07	↑ 700	particle transport can be seen in
		channel d/s of b2 but not btw b3-2.
		tip still under b3.
12.28		tip 20ab3. Channel usually ≑ 5-7mm
		wide.
1.09		20ab3
2.06	↑ 754	20ab3
2.54	↑ 808	bladder tank = 4.5m. 20ab3
3.38		30ab3. Channel is intermittently blocking
		& unblocking itself.
3.44		Channel that branched from main channel
		tip is now at middle row 2 standpipe
		has reactivated but stopped before growing.
4.15		43ab3. Channel blocked btw bars 1-3m
		sections.
4.35		43ab3
5.23	↓ 697	53ab3
8-4 11.35	698	tip could be 75ab3 or 100ab3 it's
		difficult to tell. C.H.S.
11.44		There's build up at exit so removed
		C.H.S.
12.50		125ab3 (tip at middle row 3 standpipe).
		CH.S. No blockages anymore.
1.00		Channel blocked u/s of b3. But open
		everywhere else.
1.45	↓ 672	185 ab3
2.45		200 ab3 CH.S.
3.52	↑ 697	200ab3. Since having moved down to 672
		the channel has moved laterally a
		little and there are 3 possible places
		tip could progress from CHS.
5.34	↓ 592	205 ab3
9-4 10.31	594	205 ab3

285

Backward erosion piping test data sheet

Test #	69	Exit type	circle
Date	30/03/2015	seepage length	1.3 m
Soil	mix 7	head in bladder tank	5 m
Flume	4	compaction	tamped

time	head	observation
10.59	↑ 697	moved build up @ exit CHS.
12.50	↑ 751	205 ab3. channel appears to be
		open for entire length (not blocked).
1.20		205 ab3
1.59		214 ab3
2.25		250 ab3
3.37		under b~~3~~4
4.03		channel is going through cycles of
		blocking + unblocking. see for video.
4.52		13 ab4
5.48	↓ 643	70 ab4
6.05	↓	(I don't want it to finish overnight).
13-4 11.00	566	70 ab4 but all clogged so hard to see.
		Channel blocked from tip to b3 (but
		open btw 3 and exit). Build up at
		exit removed CHS.
11.07	↑ 593	
11.26	↑ 654	
11.47		channel open btw standpipe + b3 but
		still blocked u/s
1.35		133 ab4 Sand discoloured along u/s edge
		CHS.
~~2.10~~		
2.20		Sample failed. See photos for when ~~the~~
		channel reach u/s end and how
		long failure took

5 of

[illegible] adjust [illegible] levels according to markings.

Test 69

can't be sure 0 at datum [illegible] each time.

	time	head	Row 1 right	Row 1 middle	Row 1 left	Row 2 right	Row 2 middle	Row 2 left	Row 3 right	Row 3 middle	Row 3 left	time for 50mL	Avg	Temp
415														
76	11.12		4	÷-20	8	30	39	35	49	40	44	not flowing yet		
172	12.07		25	0	30	91	101	95	125	116	118			
370	2.40		129	88	126	225	235	229	287	278	280			
468	3.23		161	117	159	285	294	289	364	354	356			
496	3.52		190	145	188	313	323	315	395	388	381			
610	31/03 10.10		223	227	226	335	344	338	451	438	443	"		
725	2.00		262	265	266	396	404	398	535	520	525	see scale info.		
754	1/04 9.34		270	272	274	413	420	413	557	544	547			
1-4	10.55		280	284	283	430	437	430	578	565	568			
901	2.21		315	321	321	485	491	485	658	640	645			
	5.20		364	370	371	560	566	559	756	740	744			
	6.09		318	150*	304	498	494	484	664	667	648			
	6.23		227	86 old channel	122*	380	378	367	534	530	518			
2/04	2.39	725	189	73 old c	79*	325	323	313	476	462	464			
7-4	10.18		44	37 oc	40*	59	67	62*	79	70	74			
	12.31		133	72 oc	91*	236	200	172*	383	362	363			
	3.39		165	65 oc	108*	286	248	202*	456	437	432			
8-4	11.43		118	61 oc	69*	211	155	118*	364	333	340			

Test 69

			Row 1			Row 2			Row 3					
	time	head	right	middle	left	right	middle	left	right	middle	left	time for 50mL	Avg	Temp
8-4	12.59		127	65*	88*	230	195*	170*	377	291*	355			
9-4	2.26		142	78*	103	245	218*	194	394	285*	360	→ flowing ~~under~~ next to		
	2.27									245		→ as channel moved directly under		
	2.30								355	300	386	→ as channel moved away		
13-4	11.06		102	57*	60*	176	132	114*	307	278B	286B	and stopped flowing on		
												account of blockage.		

* = open channel near BS
B = blocked " "

69. Test 69 (flume 4) circle

Test 69 was a repeat of test 67 on mix 7 in order to demonstrate repeatability of mix 7.

Mix 7 is 90% 50n and 10% 300g with Cu = 3.2.

During CO2ing a large amount of soil boiled up and deposited on lid (see fig 2). I couldn't see through the lid to see the void it would have left behind (water was murky) but it was likely to be there. I have no record of and don't recall this happening in test 67 so I don't know why it happened this time. Also, I started the test before the water level in the d/s box had reached the outlet so I just recorded the level so I could correct the head difference later (if need be).

Initiation was difficult to judge because the tip couldn't be seen under the box (murky water) and because there was a large void around the exit. I'm going to say initiation occurred at a head of 725mm because that's when Hamish first though he spotted a channel. This initiation head is only 7% more than test 67 however I needed to raise the head up to 1105mm to keep the tip progressing.

1105mm was the maximum head required and was 25% higher than test 67. However I think this higher maximum was only due to the void in the soil around the exit (greater "channel" area, slower speeds and therefore higher heads to detach particles). *Note added 17-12-15: No longer agree with this. At H=1105 and CL=120m. Void would have to be this large and doubt it was.*

Once the tip was properly moving I reduced the head in steps straight away right down to 484mm where it stopped. This large step makes it look different to test 67 but it's just a difference in test procedure- I didn't reduce the head straight away or as regularly as I did in this test.

Having then increased the head again in steps the tip stopped twice more until it was at a head of 802mm. I'm going to call this the progression head as this happened twice (tip kept stopping until head was at 802mm). This progression head is similar to the progression head in test 67 of 853mm (6% difference). Therefore I consider this test to have demonstrated repeatability of mix 7.

See fig 1 for chart.

The channel width was smaller than test 67. It varied between 3 and 13mm (but was usually around 5-7mm). But it did exhibit the same zone around the channel of previously disturbed soil as in test 67. See fig 3 for e.g.

There were occasions when there were 3-4 channel (see pic 4) but there first channel was always the furthest).

Many times during the experiment I moved the build up at the exit.

The channel would be in a repeating cycle of blocking, clear, tip progress and reblock, particularly once the tip was past bar 3. I have a video of this. .

I got interesting standpipe reading when the channel was moving underneath and way from the it.

Failure occurred about an hour after the tip reached the upstream end.

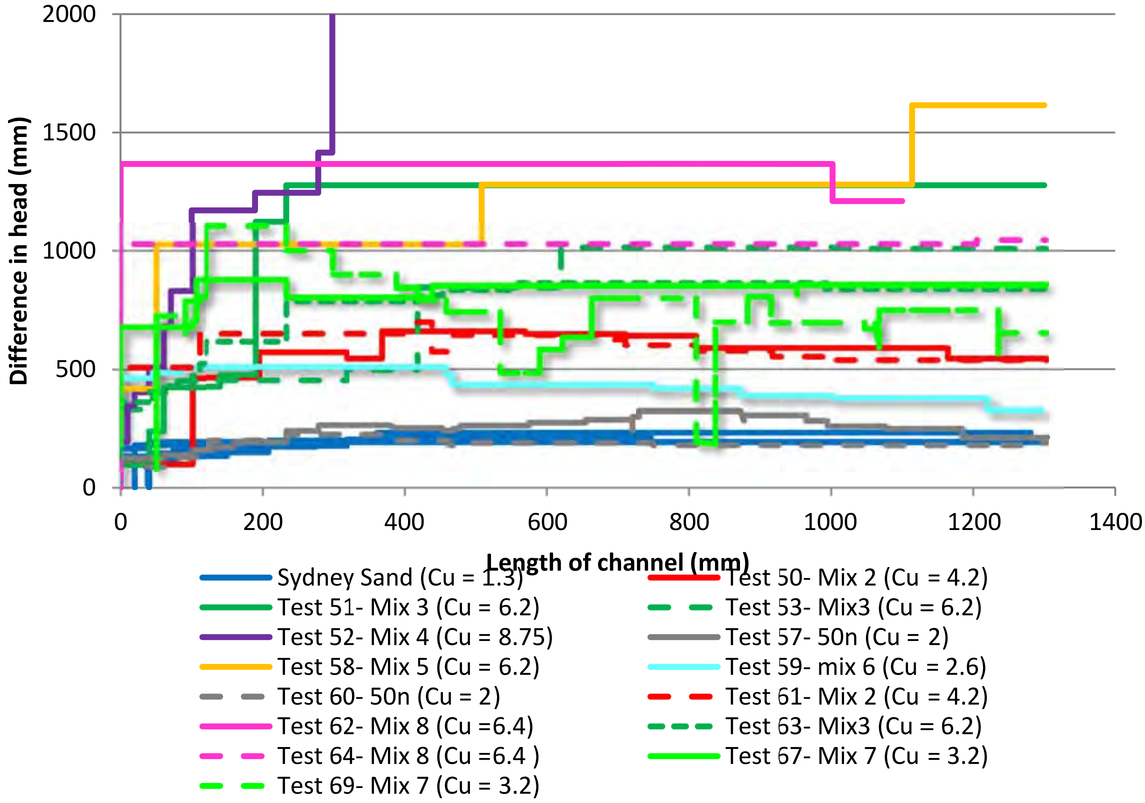

Figure 69-1 CL with H for different soils

Figure 69-2 sand boiled out of lid during CO2ing

Figure 69-3 zone around channel indicating where channel has been

Figure 69-4 multiple channels

Initialled inflated to 5m then dropped to 2.5m 64 saturation

Backward erosion piping test data sheet

Test #	70	Exit type	slope
Date	2/04/2015	seepage length	1.3 m
Soil	syd sand	head in bladder tank	2.5 m
Flume	3	compaction	vibrated

time	head	observation
12.24	45	already a channel. Not sure when
		it formed. Tip is ≈ 220-105 from
		exit. C H.S.
12.30	↑ 101	
1.15	↑ 145	Water flow rate 23.29 LT/hr
1.49	↑ 180	stand pipe 220
1.51		Water flow 30.46 LT/hr
2.30	↑ 229	Sand starting to move inside box.
2.33	↓ 204	brought down because rapid Sand movement.
2.34		Tip under b1. Water flow rate 36 LT/hr
2.37		Stand pipe 246
2.41		tip at 20 ab1
2.54	↓ 182	tip at 150 ab1
3.15		163 ab1. Standpipe 183
3.36		under b2
3.37		0 ab2.
3.40	↓ 158	60 ab2
3.44		72 ab2
4.01		77 ab2
4.18		77 ab2
4.20	↓ 20	
7-4 10.27	5	77 ab2
10.28	↑ 57	
10.47		220mL/1min 4s. 77 ab2.
10.48	↑ 105	
11.06	↑ 128	Checked bladder tank and it's still at
		2.5m.
11.37	↑ 153	77 ab2. Standpipe 153
12.16		79 ab2. 220mL/26.7s.
12.17	↑ 165	

Test 70

	time	head	observation
	12:35		82ab2. Standpipe = 166
	1.10		82ab2.
	2.06	↑ 176	82ab2
	2.14		85ab2. There's intermittent detachment
			from tip.
	2:35	↓ 154	190ab2
	3:21		190ab2
	4.12	↑ 164	" "
	4:34		202ab2
	5:23		202ab2. ~~leave it here overnight~~.
	5.27	↓ 105	207ab2
3-4	11:35	105	207ab2
	11:36	↑ 154	
	12 49	↑ 165	207ab2
			222ab2
	1.44	↓ 159	10ab3 . 220mL / 233 s
	2.45	↓ 145	0ab4
	3.51		23ab4
	5.33	↓ 106	23ab4
9-4	10 22		It failed overnight! CHS. I don't know
			how long it took the channel to
			reach the U/S end or how long it
			took for bed deepening to occur.
			As I went to empty flume by
			lowering the inner cylinder as low
			as poss I realised the pump in the
			CHT is no longer working. It's possible
			the pump stopped working during the
			night, the head rose and caused the
			sample to fail this morning the head
			was at 106 ~~[illegible]~~
			~~[illegible]~~ (I think - I didn't check
			but there was a constant flow out
			of the d/s end).

70. Test 70 (flume 3) slope

This test was a repeat of tests 39, 40 and 66 which were slope tests with bladder pressures less than the standard (i.e. to 2.5m). It was repeated because I haven't achieved the same results as I did with a 50kPa pressure (as I would expect).

However the bladder was accidently inflated to 5m before being dropped to 2.5m (miscommunication between Hamish and I). This is likely to mean that a small gap was formed btw the sand and lid. To explain:

When the bladder is inflated its increase in volume is limited by the decrease of the soil (which occurs as a result of 50kPa of surcharge). Therefore, during bladder inflation, I can use the unconsolidated void ratio with effective stress chart to visualise the drop in void ratio. However, when the bladder is deflated, its decrease in volume has no relation to the soil. The bladder volume will simply decrease as a result of the drop in pressure and will do elastically. Due to the drop in total stress the soil will expand but will do so plastically. That is, the bladder volume will decrease more than the soil volume will increase. This will cause *a gap* in between the soil and the lid, or in other words, a larger void ratio than what's in the soil.

It's important to recognise that the void ratio between the soil and the lid is different to the void ratio in the soil. If I didn't then my explanation above wouldn't hold. The 'unconsolidated void ratio with effective stress chart' shows the soil's void ratio to be *less* when the bladder is inflated incorrectly (up to 5m then down to 2.5m) than when it's inflated correctly (straight to 2.5m). So, whilst it's true that the void ratio in the soil is less when the bladder is inflated incorrectly, there is a larger void ratio between the soil and lid. Also note that when the bladder is inflated correctly the void ratio between the sand and the lid is the same as the void ratio in the soil.

So $e_{soil,incorrect} < e_{soil,correct} = e_{soil\text{-}lid,correct} < e_{soil\text{-}lid,incorrect}$

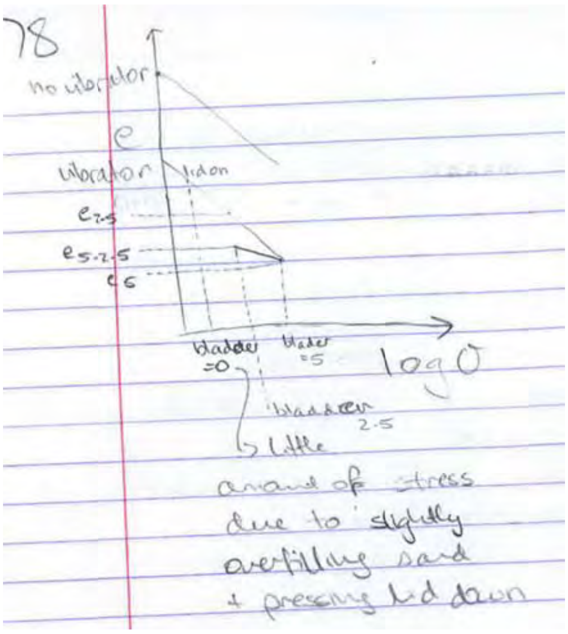

And it is the void ratio at the soil-lid interface that counts because that's where the backward erosion occurs.

I predicted that a gap under the lid would cause a lower gradient than the 50kPa tests and this was the case. Refer to Fig 1 below.

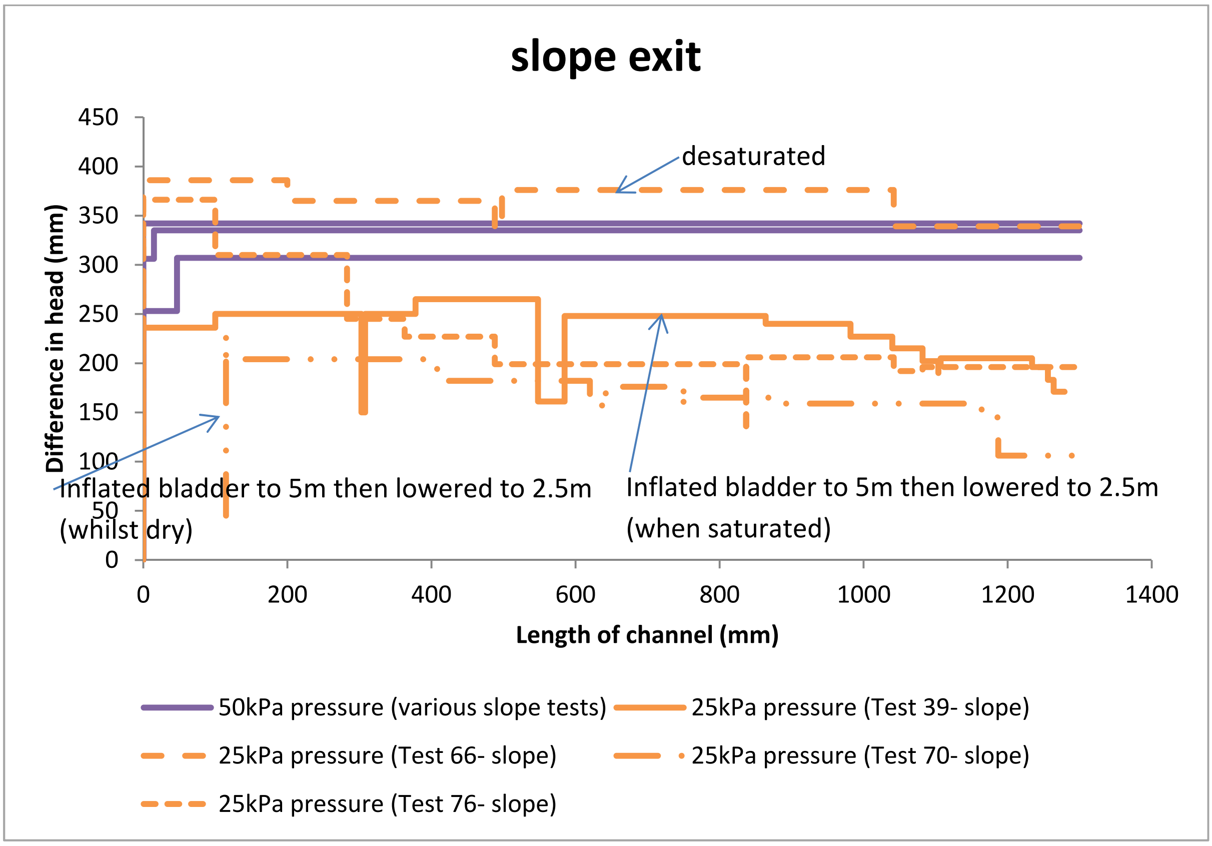

Figure 70-1 CL with head for test 70 and other slope tests

As the labels on Fig 1 indicate, bladders in both tests 39 and 70 were inflated incorrectly (up to 5m then down to 2.5m). This made both their critical heads less than their 5m counterparts.

I notice that the critical head of test 39 is greater than test 70. I think this is because the bladder was deflated in test 39 after saturation where as it was done before saturation, whilst it was still dry, in test 70. Once the soil is saturated it would expand more than if it were dry because pore pressure is available to 'push soil particles apart'. So even though the bladder would still decrease more than the soil volume would increase, the soil volume would increase more and hence less of a gap would be left under the lid. I'm not sure whether this is right but it's my postulation.

I'm taking both initiation and progression heads to be 204mm. It's interesting that the head required continued to drop. Perhaps this is because head for initiation > head for progression in slope exits. Other slope exit results exhibited similar behaviour if the head was reduced.

Backward erosion piping test data sheet

Test #	71	Exit type	circle
Date	27/04/2015	seepage length	1.3 m
Soil	mix 1	head in bladder tank	5 m
Flume	4	compaction	tamped

time	head	observation
	61	there's no 300g in the d/s box
		yet. It's clear. this surprises me,
		usually the water is cloudy
		whenever I use 300g.
11.16	↑255	there are some gas bubbles seen
		under the lid. Maybe they'll go
		as water starts to flow or maybe
		it's because I stopped the CO_2 after
		4 hours (instead of 5). CHS
11.24	↑448	now I can see some 300g rising out of
		exit CH.S.
11.48	↑640	
12.38	↑834	
1.04	↑1043	
1.58		there's a slight hint of a
		channel but it's so slight I
		could be imagining it. If I had to
		guess a length I'd say 50mm but
		I'm not sure it's even a channel. CHS.
		the 300g flow stops about 10-15 min
		after head is risen.
2.01	↑1253	
3.06	↑1411	can't see through water in d/s box
		anymore so can't see if a channel
		has formed.
3.37	↑1557	
4.25	↑1710	
5.19		left here overnight.
28-4 10.05		there's a channel 215-100 long. CHS.
		300g has settled so I can see

time	head	observation
		through water + there's larger soils
		boiled up onto exit.
10.46	↑ 1800	
12.20	↑ 1890	
1.52	↑ 1964	
2.22	↑ 2050	
2.33	↑ 2129	
3.35	↑ 2213	A lot more cloudy now
4.00	↓ 1240	Com. date - 27/09/06 4.06 am
9/4 9.00	↑ 2238	
9.46	↑ 2340	
10.44	↑ 2437	
11.32	↑ 2533	
11.59	↑ 2625	large boil erupted. CHS. No channel
		past box thayn yet.
2.35		I think there's been a zone at the
		upstream end (from the U/S end to
		just past the 3rd row of standpipes)
		where the soil is no longer pressed
		up against the lid. The bladder
		tank is still at 5m so that
		can't be why. CHS. I don't know why.
		Also, I took the cap off a row 1
		standpipe to see where the water
		level would go up to and it spilled
		over the top! So there's a huge
		gradient (like a 1.8m/0.04m) drop
		btw row 1 and the exit. I've seen
		this once before - I eventually
		stuck my finger down the hole to
		free coarse grains blocking the hole
		(and hence a large head drop at
		the hole). So I'm wondering if this has
		happened again. Although mix 1 doesn't
		have the gravel sizes that the last mix
		that did this had so I'll be surprised
		if it is the same thing occurring. However
		before I stick my finger in there to
		release the possible blockage I want to

time	head	observation
		decrease the head. Otherwise, if I'm
		right and I release a blockage
		at the exit, the sample will
		probably fail ~~with~~ by sudden short
		flow. I'll take the head down
		to around 1.5m because that's
		the limit of ~~when~~ other soils have
		failed and I expect mix 1 to ~~fail~~
		have a critical head higher than
		all the other soils I've done.
2.55	↓1548	
3.10	↓1295	standpipe level drops are(?)
		constant. there's a bigger drop btw
		~~bars~~ rows 2+3 than there is
		btw rows 1+2. I think this also
		suggests there's a blockage at the
		exit.

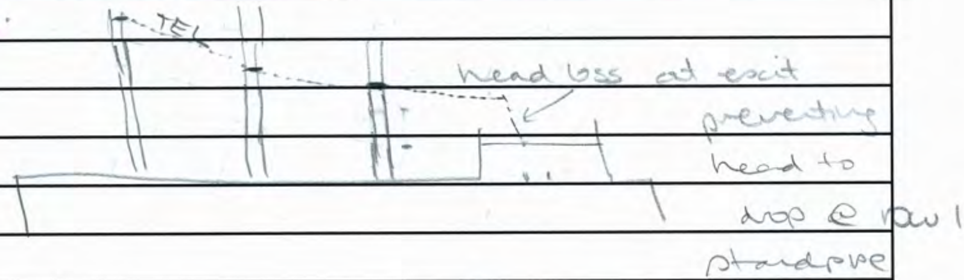

time	head	observation
3.22		stuck finger in. It didn't make much
		of a difference to the row 1 levels.
		there's still more of a drop btw
		bars 3+2 than there is btw 2+1. CHS.
		I couldn't feel a blockage but I tried to
		loosen the material anyway. Interestingly
		it also felt warmer - like there was
		warm water coming through the flume ->
		which it's not happening so not sure
		why I could feel it.
3.54	↑2058	
4.19	↑2317	
4.52	↑2560	
5.16	↑2762	
5.46	↓492	

	time	head	observation
30-4	10.07	↑ 2759	I think the line of "pushed soil" has crept d/s. CHS.
	11.32	↑ 2905	
	11.58	↑ 3004	
	12.36	↑ 3104	each time I raise the head I get a new "cloud" of 300g leaving the exit.
	2.12	↑ 3258	
	3.04	↑ 3416	
	3.34	↑ 3574	
	3.59	↑ 3730	
	4.35	⇊	
1-5	11.21	⇈ 3710	
	11.52		now a 2nd line of transverse settlement btw bays 2+3. CHS.
	11.55		just noticed a possible channel whose top may be ≈80 abs2 But I don't think it's continuous. It looks more like a network of unconnected channels. CHS. I can't see any sediment transport ~~around the~~ through them.
	12.47		possible channel looks the same
	12.48	↑ as high	as it could go. Maybe ≈ 3.9
	1ish		suddenly failed. I didn't see it happen but I suspect it failed to top "sheet" slip. See SLR pics.

Test 71

remember to adjust levels

$\rho = \frac{kg}{m^3}$

			Row 1			Row 2			Row 3					
	time	head	right	middle	left	right	middle	left	right	middle	left	time for 50mL	Avg	Temp
58	1114	61	11	13	11	25	33	48	39	31	35	too slow to		
446	1146	448	138	149	165	244	251	243	327	316	333	measure.		
-	12:32		219	237	264	365	374	373	479	464	482	scales on		
	2:20		543	582	626	786	795	789	995	976	986.			
	3:04		559	600	642	794	802	797	999	982	994			
284			too high too measure											16

71. Test 71 (flume 4) circle

Test 71 was on mix 1. It was a repeat of tests 38 and 56 because the CHT wasn't high enough for test 38 and the soil became unsaturated in test 56.

Initially there were a reasonable amount of bubbles left behind (see fig 3). I'm not sure why this was- perhaps because I ran the co2 flushing for 4 hours instead of 5, however by the next day the bubbles were greatly reduced (if not totally gone) so I don't think the bubbles affected the results.

I'm taking initiation head to be 1043mm but progression head (critical or maximum head) wasn't obtained.

On the 3rd day of testing I noticed a zone from u/s end to just past the 3rd row of standpipes that wasn't pressed up against the lid (see fig 4). I don't know why this occurred. This zone 'grew' indicated by a 'tension crack' type of line that moved d/s. The next day (day 4 of test) the line was d/s of row 3 (see fig 5) and by day 5 a second line formed approx. mid-way btw bars 2 and 3 (see fig 6).

Also on day 3 I took the cap off the row 1 standpipes to see what the gradient was like between here and the exit. And the standpipe overflowed! So there was a huge gradient > 1.8m/0.04m = 45! I had seen something like this before- a large gradient btw the exit and row 1- and it was because gravel pieces had jammed in the exit so after having stuck my finger in to release the jam, the gradient between row 1 and the exit reduced. However this time it was in mix 1 which doesn't have gravel sizes, so I wasn't expecting the same scenario here, but I still tried it. Although before sticking my finger in I dropped the head to 1.5m. When I stuck my finger in I couldn't feel any blockage but I tried loosening the material anyway. This made no difference to the water level in row 1. There was still a higher gradient between 1 and the exit than btw rows 2 and 3. See Fig 7.

When the channel was 640mm long the maximum head of 3710mm I wasn't able to progress the channel any further. It is the yellow line in the chart below. Note however that whilst I've said the tip was at 640mm, the tip location was quite difficult to define because the channel wasn't continuous but more like a network of disconnected channels. I haven't got a good pic showing this unfortunately.

Once the head had been at the max for about 1hr and a half the sample failed suddenly. I didn't see it happen but from the SLR pictures (in Figures 8, 9 and 10) it looks as though a continuous channel formed with its tip almost up to bar 2 and at the same time, the settled region slipped d/s. This all occurred in the space of 2 minutes.

Notes added later: there are good SLR photos of failure that I didn't realise I had when I wrote this report. See IMG-7604 to 606. It looks like a continuous channel formed almost up to b2 and the void region slipped d/s at the same time. All in the space of 2 minutes.

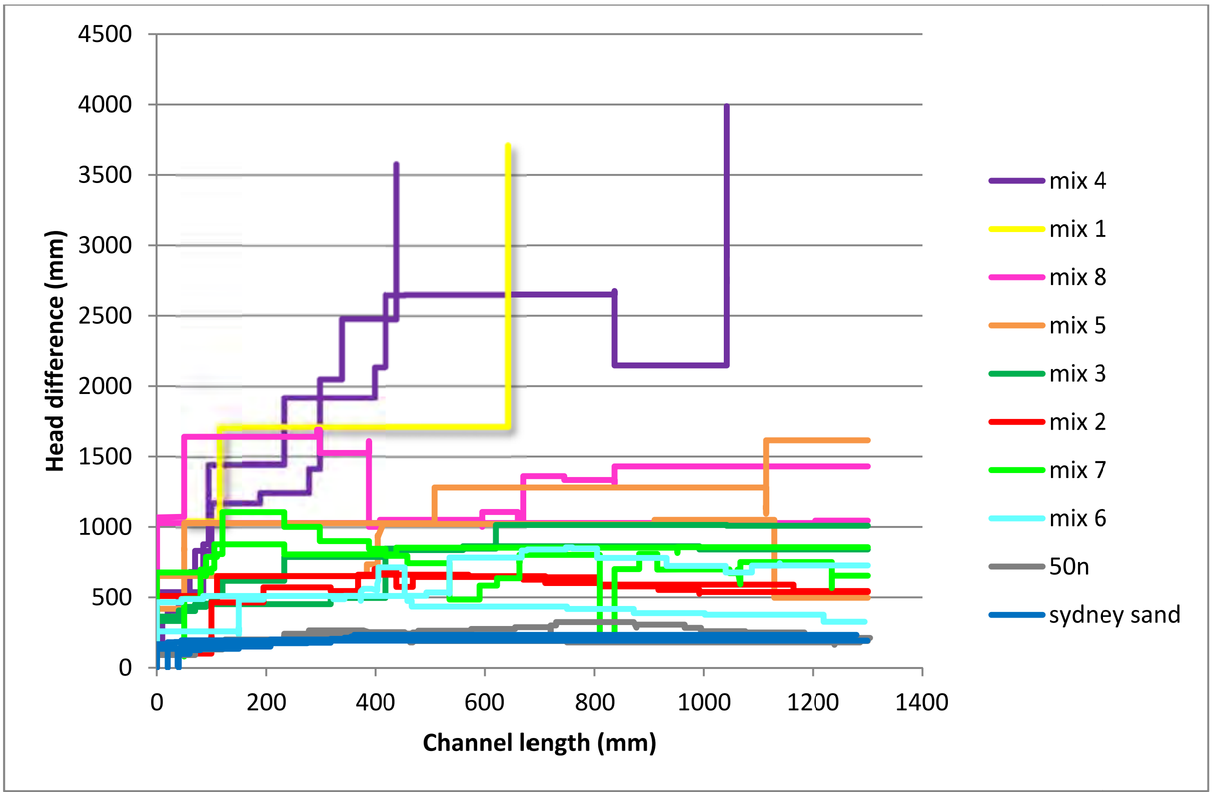

Figure 71-1 CL with head for different soils

As expected the heads are approximately between mixes 4 and 8 (because so is the coefficient of uniformity). Schmertmann's relationship clearly fails for this soil. See below.

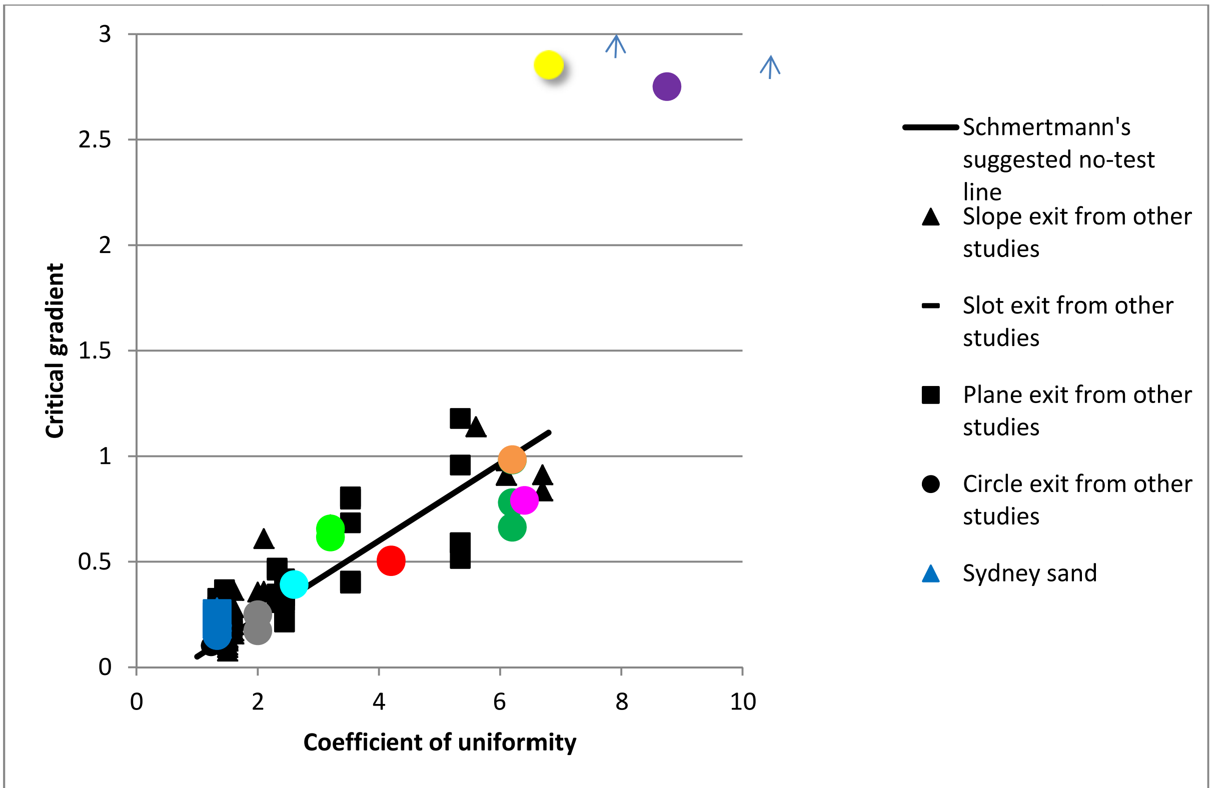

Figure 71-2 Schmertmann's chart- mix 1 is the yellow marker

Figure 71-3 Bubbles in sample initially

Figure 71-4 zone from u/s edge to row 3 standpipes that wasn't pressed up against the lid

Figure 71-5 day 4-'tension crack' line had moved d/s

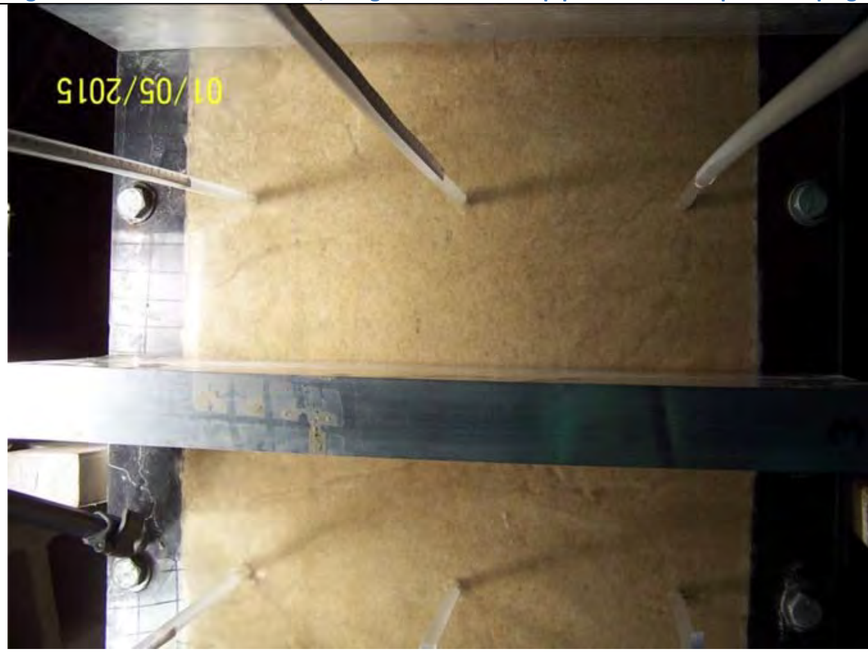

Figure 71-6 day 5- 2 'tension crack' lines

Figure 71-7 tape measure shows gradient btw rows 3 and 2 and my hand indicates level in row 1.

Figure 71-8 2 minutes before failure (discontinuous channel with "tip" at 640mm)

Figure 71-9 1 minutes before failure

Figure 71-10 failure

Backward erosion piping test data sheet

Test #	72	Exit type	circle
Date	1/05/2015	seepage length	1.3 m
Soil	mix 6	head in bladder tank	5 m
Flume	~~1~~ 2	compaction	tamped

time	head	observation
2.40	53	last mix 6 test (test 59) initiated at
		465mm and progressed at 510mm
		so expecting round there again.
		the bladder on F2 leaks so
		head is down to ≐3.5m even
		though it was initially inflated
		to 5m. So topped up to 5m.
		There's a small mound around exit
		that would have occured during
		CO_2/saturation. CHS. Also, the
		water level in the d/s box is 61mm
		above the lid.
3.00	↑158	
3.17	↑258	boiling @ exit.
3.35		channel tip beneath d/s box wall
		(i.e. 150 from exit). level in d/s box
		is 68mm.
3.51	~~3.45~~ [illegible]	still beneath d/s box wall but can
		see occasional sediment transport
		through channel.
5.07	↑284	still beneath d/s box wall.
5.45	↓33	
4-5 11.03	30	tip still under d/s box wall.
11.04	↑233	water level in d/s box was @
		datum
11.09		blader tank @ ≐ 3m so increased
		back up to 5m.
11.39	↑283	there are bubbles in and around
		the exit. CHS. Not sure why but
		no more bubbles are visible from ≐ 50min

Test 72

	time	head	observation
			Walls of the exit
	12.05	↑ 331	
	12.24	↑ 383	
	12.52	↑ 434	
	1.32	↑ 483	transport along channel
	1.43		tip ≑ 20mm past d/s box wall.
	2.09	↑ 510	" " " " " "
	2.21		tip under bl.
	2.30	↓ 487	65abl
	2.39		85abl
	2.54		" "
	3.20	↑ 499	" "
	3.45	↑ 511	" "
	3.48		100 abl
	3.57		113abl
	4.37		115 abl
	6.00		" "
	6.04	↓ 115	
5/5	11.05	↑ 475	
	12.04	↑ 485	" "
	12.44	↑ 515	
	1.57	↑ 541	
	2.38	↑ 561	120 abl
	2.51		135 " tip widened slowly during day
	3.36	↓ 120	145 "
/5	8.42	↑ 548	Bladder had gone down to 4.0 overnight
	9.38	↑ 570	
	10.04	↑ 596	
	10.34	↑ 621	147 abl. There's bubbles along side the
			channel. I don't know how/why
			CHS. I can't see any at tip so I
			don't think they'd be inhibiting
			progression.
	11.40	↑ 648	147abl
	12.14	↑ 687	
	12.45	↑ 713	
	2.13		195abl
	2.14	↓ 511	
	2.15		223abl

	time	head	observation
	2:38		235 ab1
	2.55		" "
	3.42	↑535	
	3.46	↓525	Under bar 2.
	4.16		" " "
	5.00	↑535	" " "
	5.47	↓340	
7/5	8.14	↑537	(note: Bladder was down at 4.0) (& topped up)
	9.10	↑548	
	10.04	↑563	still under b2.
	10.34	↑582	
	10.57	↑606	
	11.19	↑632	
	11.40	↑655	
	11.55		channel is blocked under b1. CHS.
	12.19	↑684	
	12.53	↑708	
	1.28	↑733	
	1.58	↑759	
	2.21	↑782	
	3.06		107 ab2. there's a 2nd channel
			formed from the exit. It's tip (tip B) is
			68mm ab1. CHS. Also, the original
			channel (channel A) is blocked btw.
			b1 and ≑150 ab1 CHS. There appears
			to be no transport through either
			channel and tips appear stationary.
	3.57	↑808	107 ab2 and b=70 ab1.
	4.34	↑832	" "
	4.53		a=116 ab2 "
	5.16		" "
	5.40	↓245	
8/5	8.03	↑840	118 ab2
	9.12	↑855	188 ab2
	9.46	↓847	200 ab2
	9.54	↓780	245 ab2 channel a
	9.56		under bar 3
	10.08	↓723	70 ab3
	10.14	↓677	178 ab3 . Channel b=235 ab1

time	head	observation
		channel a blocked btw for almost
		entire length but tip moves periodically
		in bursts. Because it moves abt all
		at once there's a lot of sediment
		transport which probably blocks it
		again. Have channel b isn't blocked
		at all.
10.50		a) 193 ab3 b) 230 ab1
11.40	↑ 702	a) 226 ab3. b) under b1
12.39	↑ 725	" " ?
12.58		a) under b4 b) "
1.59	↑ 737	" "
2.39	↑ 743	
2.58		b 25 ab2
3.00		a) under b4 b) 80 ab2
3.05		a) " b) 175 ab2
3.09		" b) 235 ab2
3.10		b) Under b3
3.15		" b) 70 ab3
3.25	↓ 255	Lowered for W/E - Test to be Re-started Monday
11/5 8.42	↑ 727	Bladder was on 3.5 over W/E
8.56		a) under b4 b) 133 ab3
		Quite a lot of Sandmovement between b1 + b3 on both tips
9.12		a) " b) 198 ab3
9.34		a) 115 ab4 b) 245 ab3
9.49		a) 120 ab4 b) Under b4 Alot of sandmovement b1/b2
9.55		Almost "sheet flow" btw b1 + 2 but
		channel a) is fwd deepening (tip is
		btw 2+3. It's as if the sheet flow
		leaves space for the fwd deepening
		to "flow" into. The fwd deepening
		occurred in little bursts. Channel b)
		tip got up to beneath b4.

72. Test 72 (flume 2) circle

Test 72 was a repeat of test 59 on mix 6.

The flume 2 bladder leaks so each morning I would find the bladder tank at like 3-4m so it had to be topped up to 5m each morning. I don't expect this to affect the test too much because I don't expect it to affect the void ratio (either within the soil or between the soil and lid) too much. So long as it took considerable time for the head to drop back down to 3-4m (like overnight) otherwise I might have still been running the test (later in the day) with the bladder less than 5m. I don't know how long it takes for the bladder tank to drop from 5 to 3-4m.

The channel started at a head of 258mm.

When the channel was 150mm I noticed bubbles around the exit (fig 1) and when it was 405mm I noticed bubbles alongside of the channel (fig 2). I'm not sure how/why these bubbles were present but I don't think they affected results because they seemed to appear along the channel once it was already formed (and wasn't upstream of the channel waiting to impede the tip progression).

When the channel was 535mm long I noticed a blockage under bar 1. However the tip kept progressing. In fact the channel remained blocked for much of the remainder of the test but the tip kept progressing. The tip progressed in short sudden 'bursts' and this is probably why the channel was always blocked: a sudden large volume of sediment was moved down the channel (more than the channel could accommodate) so it blocked.

When the channel was at 667mm a 2nd channel (dubbed channel 'b') was noticed (presumably originating from the exit). Both tips continued to progress but channel 'a' reached upstream first. Channel 'b' reached under bar 4.

Fig 2 shows the 2 channels as well as the progressive blockage in channel 'a'.

The maximum head required was 847mm. See fig 5. Forward deepening took about 30 minutes to complete and lead to failure. The SLR photos showing forward deepening are quite good. See fig 4.

As can be seen in fig 5 the 2 mix 6 tests were rather different. The critical head for this test was 66% increase. And this test plots a fair bit higher than Schmertmann's line (see fig 6).

One reason why tests 59 and 72 may be different is the bladder leaking. I said above that I didn't expect the leaking bladder to affect the results because I made sure it was back up to 5m each morning, however maybe the difference in results proves otherwise. Maybe the bladder head tank dropped during the day and this created a small gap between the sand and lid like described in test 70. A gap between the sand and lid would cause in an decrease in head required to backward erode. Note that test 59 was done in flume 3 whose bladder doesn't leak.

Another theory as to why the two tests are different is channel blocking. The channel didn't block in test 59 but did so in 72. This could explain why 72 needed a higher head. But why would 72 block and 59 not? I don't know. I'll need to repeat mix 6 test and I won't do it in flume 2. I'll do it in a flume whose bladder doesn't leak.

Figure 72-1 bubbles around channel

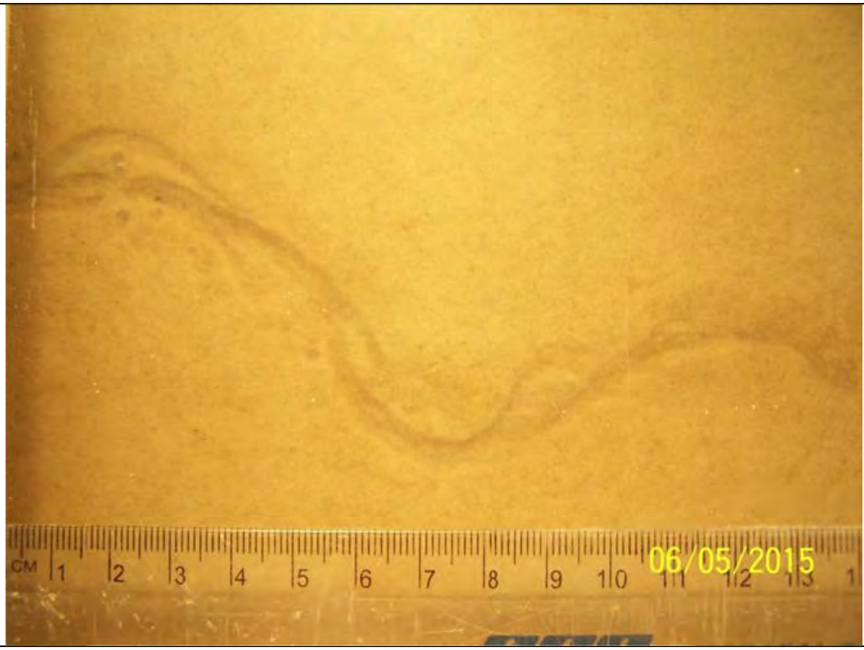

Figure 72-2 bubbles alongside channel

Figure 72-3 two channels and channel ‘a’ blocked for most of it

Figure 72-4 bubbles alongside channel

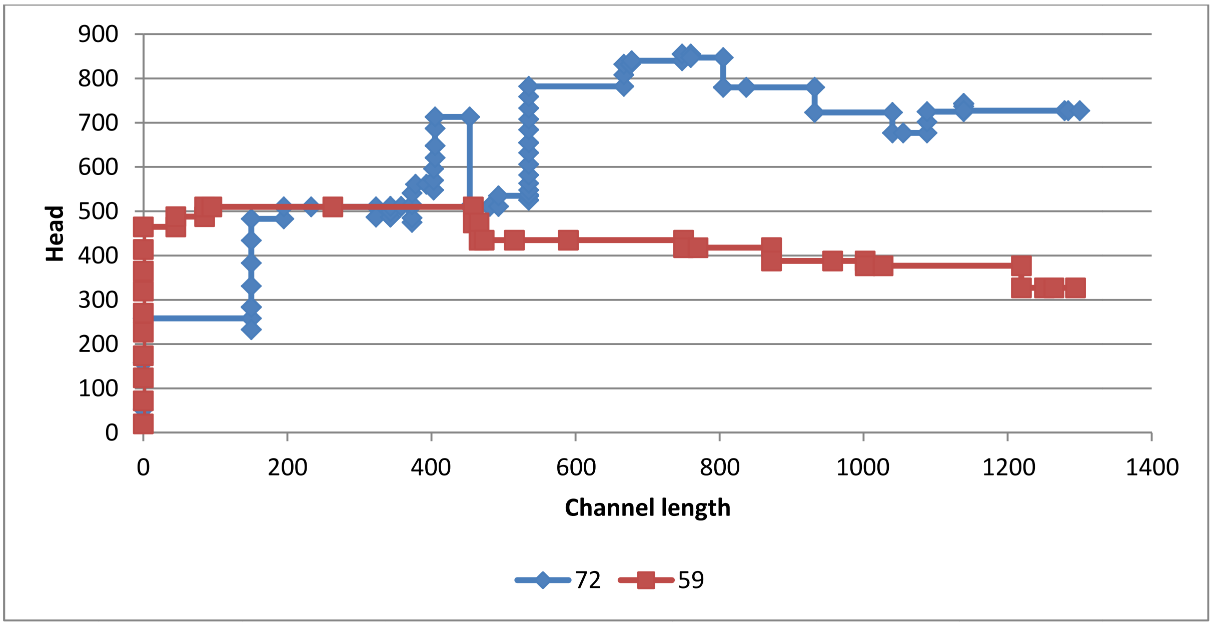

Figure 72-5 test 72 chart and mix 6 comparison

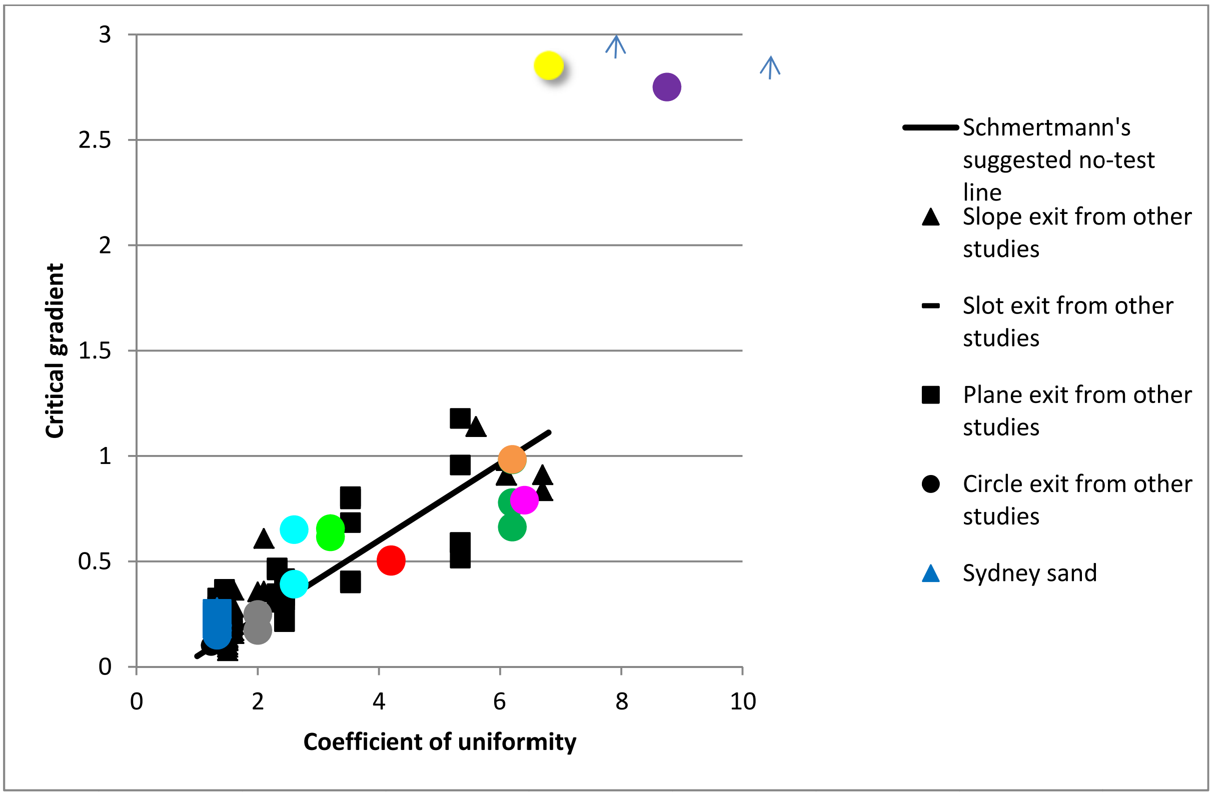

Figure 72-6 test 72 is the highest light blue point

Backward erosion piping test data sheet

Test #	73	Exit type	circle
Date	11/05/2015	seepage length	1.3 m
Soil	mix 4	head in bladder tank	5 m
Flume	4	compaction	tamped

time	head	observation
11.14		water in d/s box not at outlet yet.
		It looks as though at some point
		the gravel pieces were dragged
		u/s because there's gaps left
		behind them (see HS.)
11.20		the last mix 4 I did was test 52.
		It initiated at 196mm. I couldn't get
		it to progress any further than
		440mm (even at a ~~[illegible]~~ max head
		of 3553).
11.22	↑ 148	
11.53	↑ 245	
12.29	↑ 334	fine grains boiling at exit.
12.49	↑ 441	
1.43	↑ 537	
2.56	↑ 727	channel 145-60. Tip at a gravel
		piece. CHS. Also, fine gravel-sized
		particles now boiling.
4.05	↑ 877	
4.25		tip 145-50. Channel is ~~[illegible]~~
		~~&~~ moving around towards right-hand-side.
		CHS.
12/05 8.29	↑ 971	
11.52	↑ 1080	
12.56	↑ 1195	
1.30	↑ 1315	
3.15	↑ 1440	
3.35	↓ 565	for Overnight.
13/05 7.57	↑ 1445	
9.11	↑ 1570	Tip under bar 1
10.43	↑ 1670	

Test 73

	time	head	observation
	11.15	↑ 1783	
	12.44	↑ 1918	
	1.09	↑ 2045	tip at 140 abl
	3.39	↓ 485	
14/05	8.15	↑ 2045	
	10.04		cleared bowl.
	10.45	↑ 2136	140 abl
	11.41	↑ 2234	160 abl
	12.06	↑ 2336	" "
	12.25	↑ 2440	" "
	1.31	↑ 2544	" "
	2.05	↑ 2647	" "
	3.09		195 abl. It's very difficult to define the
			tip because there are many channel-looking
			paterns and they're not well defined. CHS.
			So 195 abl a best guess but is
			subjective.
	5.09	↓ 165	maybe 195 abl.
5/05	8.15	↑ 2650	~~ti~~
	11.30	↑ 2675	tip under b3 732 h/hr.
			tip maybe betwee 3 + 4 ?
	3.40	↓ 280	Weekend
8/5	8.15	↑ 2147	
	11.19		It's very difficult to tell where the
			tip is. My best guess is 10ab3.
			Howevere there's a channel-looking
			~~gap~~ depression in btw bars 3+4 which
			if it is a part of the channel the tip
			would be ≑180ab3. But this
			depression appears isolated. As if
			there's just been local transport
			around large gravel pieces. But if
			there was particle transport where
			were they transported to? CHS.
			Also, the "channel" is quite discontinuous
			(not joined) + difficult to define. In
			some locations it's ≑ 50mm wide
			and in others it's hardly noticable
			except for a region of removed

	time	head	observation
			finer sediments (just coarse left
			behind).
	11.57	↑2470	
	12.42	↑2664	
	2.42	↑2766	"channel" remained unchanged
	3.21	↓(50)	
19/5	8.15	↑2736	878 KT/hr
	9.58	↑2800	
	11.05	↑2972	
	1.08		Some sand pulled away from
			U/S 50mm across face
	3.50	↓(50)	
20/05	8.20	↑2920	
	10.17	↑3064	
	12.12	↑3220	
	12.53		Q = 2.44L / 9.4, 9.6s.
	12.55	↑3374	
	1.31	↑3525	
	1.58	↑3675	
	2.53	↑3825	→ approx head (now too high for me to read).
	3.26	↑3975	
	4.01	↑3988	MAX HEAD.
	6.13		It's now been at the max head for
			2 hours. The "tip" is still at ≑180abs.
			But as mentioned before the
			"channel" is very discontinuous and
			I just can't see it progressing. I can't
			see any particle transport. And I
			can't feel any blockage at the
			exit (it's quite loose). So I'm going
			to terminate the test. I also note that
			there's a region along the U/S panel
			that has slipped (up to ≑ 50mm) but
			this slippage has been here for a while
			and isn't moving.
			Q = 2.44L / 7.9, 7.6s.
	6.21	↓↓↓	

time	head	observation

Test 73

remember to adjust levels w/ corrections

			Row 1			Row 2			Row 3					
	time	head	right	middle	left	right	middle	left	right	middle	left	time for 50mL	Avg	Temp
11-5	1157	245	67	72	78	109	119	114	158	155	158	using scales		
	1248	334	97	102	113	157	168	160	225	222	227			
			206	216	239	334	346	334	477	473	486	putting plugs in		
												standpipes now		
												to keep them from sagging		
												w/ weight.		

73. Test 73 (flume 4) circle

Test 73 was a repeat of test 52 on mix 4.

Before starting the test is was noticed that gaps downstream of the gravel pieces were present. Perhaps the lid was dragged a little over the soil to position it in place. See pic 2.

Initiation occurred at 537mm.

Throughout the test it was difficult to define the channel and tip position because the channel wasn't well defined. There were many disconnected channel-looking patterns, sometimes up to 50mm and other times barely noticeable (just hint of finer grains having been removed through coarser). See pic 3 for example.

When the channel tip was at 1042mm (keeping in mind the location of the tip was a subjective judgment call) the head was raised to max (to 3988mm) and left there for 2 hours but didn't move.

During the test there was a region along the u/s panel that looked as if it had slipped or settled. Once this zone formed it didn't change through the test. I didn't note when it formed. See pic 4.

Figure 1 compares this test with test 52. As can be seen initiation and progression heads were similar. I consider this to have demonstrated repeatability. What is different is the distance the channel progressed before it couldn't be progressed any further. I'm not sure why this is. One possibility is the tip wasn't actually at 1042mm; it was somewhere downstream of this but was identified incorrectly (was hard to define where the tip was). Another possibility is the voids downstream of the gravel pieces made it easier for the tip to progress (so it progressed further than test 52.

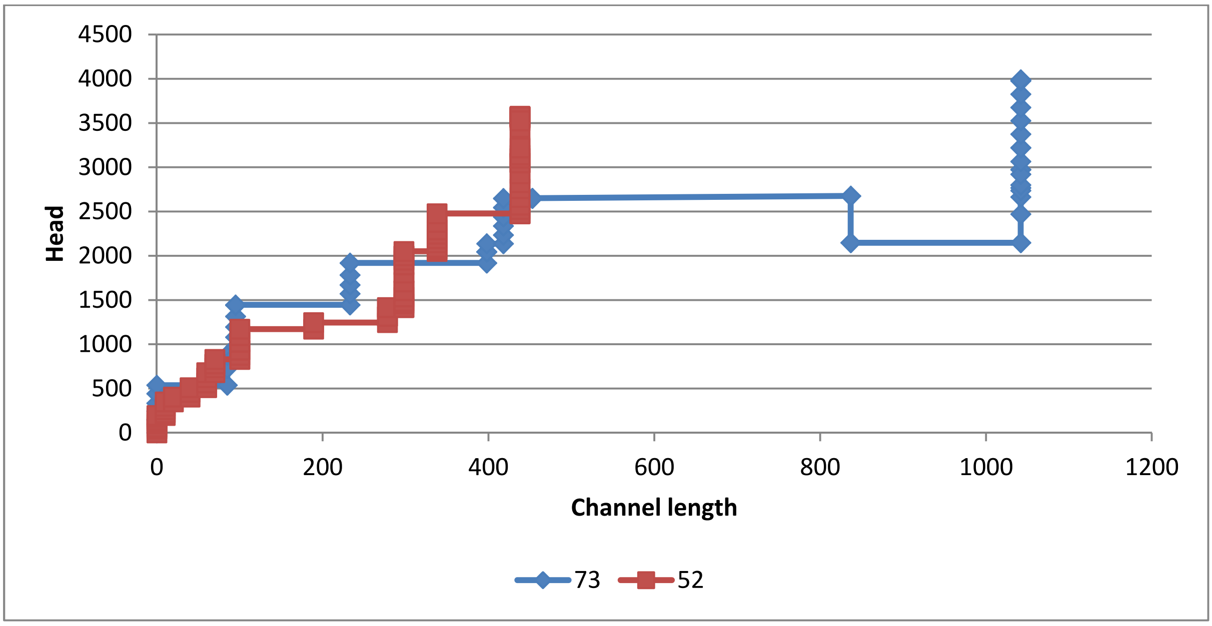

Figure 73-1 test 73 and comparing it with test 52

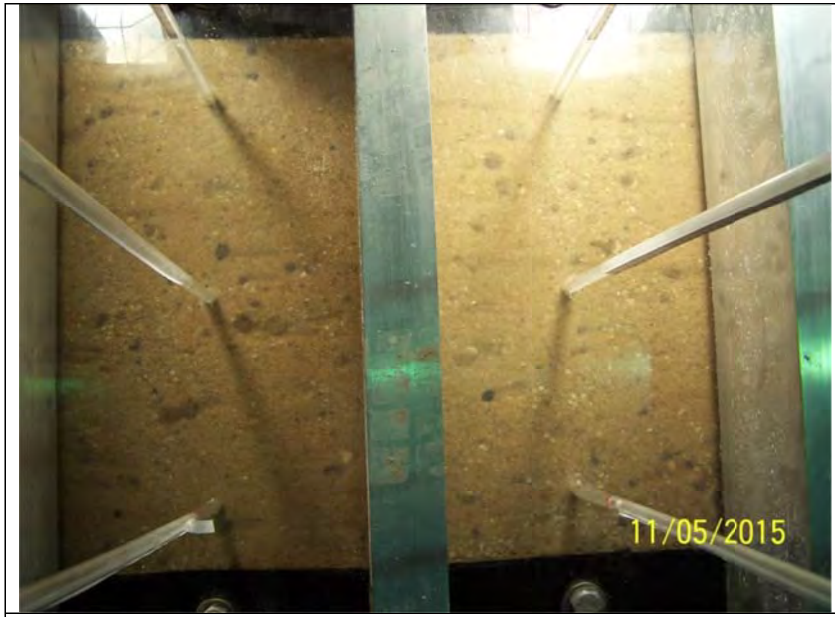

Figure 73-2 gaps behind gravel pieces from having dragged the lid

Figure 73-3 channel and tip were difficult to define.

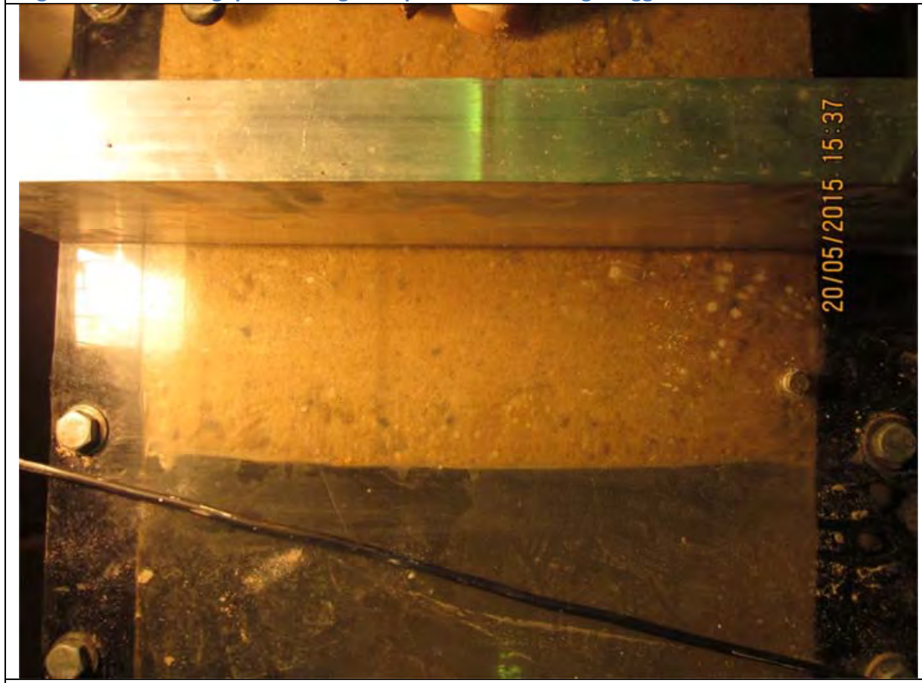

Figure 73-4 zone along u/s panel that slipped or settled.

Both tests 52 and 73 plotted well above Schmertmann's line and demonstrate that Schmertmann's line isn't applicable to a soil with a Cu of 8.75. See below.

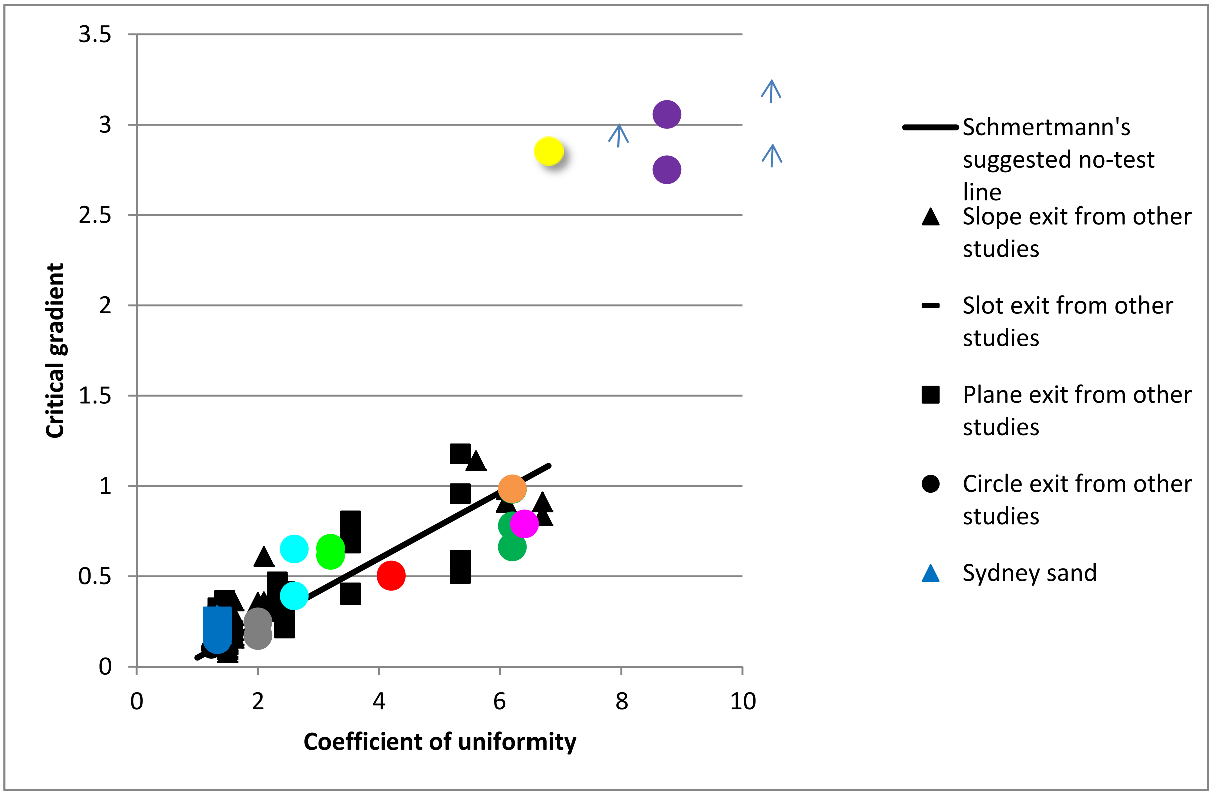

Figure 73-5 Schmertmann's chart- test 73 is the highest purple point

Backward erosion piping test data sheet

Test #	74	Exit type	circle
Date	13/05/2015	seepage length	1.3 m
Soil	mix 5	head in bladder tank	5 m
Flume	1	compaction	tamped

	time	head	observation	Qm³/s
	10.26	100	Out flow started. 853.8 ml/m	1.42E-5
	10.40	↑170	boiling @ exit. ~~2.64 L/m~~ 158.4 L/hr	4.4..
	10.58	↑208		
	11.16	↑300	271 L/hr	7.53..
	11.41	↑406		
	12.43	↑535	517 LT/hr	1.44E-4
	1.00	↑652		
	1.29	↑735	tip now 160 ab1 798 LT/hr	
	3.38	↓245		
14/05	8.15	↑735	tip at 180 ab1 878 L/hr	
	10.01		" " " ", cleared boil and	
			any gravel pieces ~~at~~ stuck beneath	
			exit. Made no immediate difference.	
	10.44	↑798		
	11.40	↑853	180 ab1	
	12.05	↑913	" "	
	12.23	↑940	the level in the d/s box is only	
			25mm from the top of the outlet CHS	
	1.30	↑936		
	2.05	↑928	~~190 ab1~~ 180 ab1	
	3.01	↑1021	190 ab1 (I had to open in valve a little.	
			The filter must be getting clogged and increasing	
			head loss).	
	3.32		75 ab2. cleared boil. I couldn't feel	
			any gravel blockage in exit. Also	
			channel btw 100-200mm wide.	
	5.08	↓385	75ab2	
15/05	8:16	↑1020	tip under b2	
	11.20	↑1050	tip 60 ab2	
	12.00		" 70 ab2	
	12.44		225 ab2 1,254 L/hr.	

	time	head	observation
	2.04		tip under b3
	3.40	↓ 205	Weekend
18/5	8.05	↑ 497	(tip is through to u/s end. Bed
			deepening might be up to ≐
			200ab3.)
	11.59		→ CHS. There's also a lot
			of air/gas bubbles through-out
			sample but don't appear to be in
			channel. Hamish tells me this
			channel at the u/s end wasn't here
			this morning so it's happened since
			then. Also, ~~apart from the cha~~ the
			"channel" btw bars 2+4 are
			very difficult to define: they look
			more like 'zones' that have had
			their finer grains removed with
			coarser stuff left behind, CHS. So
			maybe the "tip" was further than
			b3 on friday afternoon but it was
			difficult for Hamish to see. Maybe.
			Also, the air/gas bubbles seem
			to have been introduced by a
			large air bubble in the u/s
			chamber. I opened the u/s chamber
			valve to release most of it. Not
			sure how it got there in the
			first place. Will leave it running
			at this head to see if bed
			deepening occurs but I doubt
			it will cause the head is much
			lower than the critical of ≐ 1m.
	3.20		Bed deepening still ≐ 200ab3.
19/05	8.15	↑ 493	732 LT/hr
	9.58	↑ 510	
	10.30	↑ 525	
	1.08	↑ 535	
	3.45	↓ (7) 177	
20/05	8.23	↑ 525	
	9.45	↑ 809	

time	head	observation
1016	↑892	
11.57	↑1068	Q= 2.44 L / 7.1, 6.6, 6.2s.
6.40	⇓45	
245 9.49	↑ 1041	
10.05		failed by sudden flush-through i.e.
		didn't fluid deepen but a group of
		particles must have slipped triggering
		failure of the whole sample.

time	head	observation

74. Test 74 (flume 1) circle

Test 74 was a repeat of test 58 on mix 5.

Initiation occurred at 652mm and I'm defining progression head as 1020mm. See fig 1.

Again, as was the case for mix 4, the channel wasn't well defined and the position of the tip is unclear and subjective.

The last stretch at head of 497mm isn't reliable data because many confusing things happened. Firstly, on Monday morning, Hamish moved the head up from 205mm to 497mm, presumably because the tip was still under bar 3. However when I came and looked about 4 hours later the channel was through to the upstream end. It seems unlikely that the channel would have progressed at this low head so maybe the channel was already through to the u/s end before the weekend but Hamish didn't notice it because the channel wasn't well defined. But I can't be sure.

Also, when I came back 4 hours later, I noticed bubbles in the sample. See fig 2. The bubbles were at the upstream end and had entered the sample from the large bubble in the upstream chamber. I opened the u/s chamber release valve to release most of the bubble. This bubble in the u/s chamber (which then enters the sample when the channel reaches the u/s end) usually occurs when the head is dropped below the lid at some point. Perhaps this happened over the weekend (power turned off or something) but I can't be sure and even if the pump had been turned off the one-way valve should have prevented the flume from emptying. So I don't why/how this happened. Having said all this, I don't think the bubbles affected the results because I think they entered the sample after the channel had reached the u/s end.

The head had to be raised to 1041mm to trigger failure. It failed by sudden flush-through (not forward deepening). I don't have SLR pics for this test so didn't see it happen.

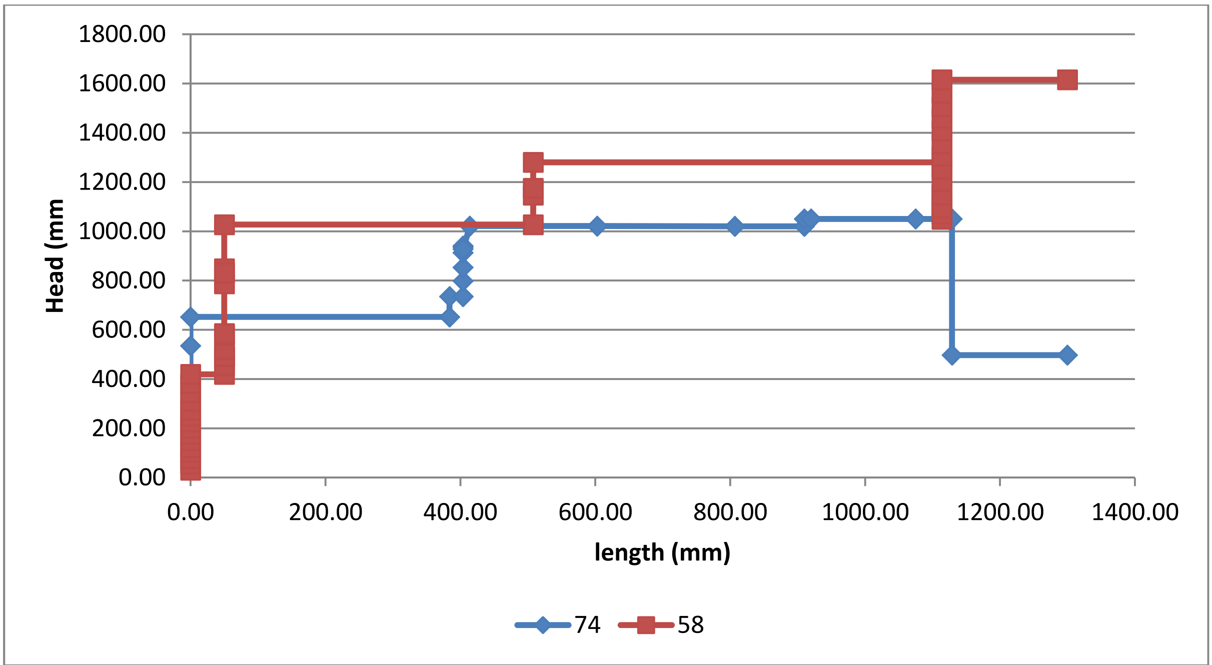

Figure 74-1 test 74 and comparing it to test 58

As for comparing the results with test 58: depending on what I interpret as being the critical gradient, results were within 20% of each other. I would preferred results were closer together but given they lie approximately where I would expect with respect to the other soils and on Schmertmann's graph, I'm going to consider this to have demonstrated sufficient repeatability. Also mix 5 is less important to me (it was Bronson's request).

Figure 74-2 bubbles in sample at u/s end

Backward erosion piping test data sheet

Test #	75	Exit type	circle
Date	29/05/2015	seepage length	1.3 m
Soil	mix 8	head in bladder tank	5 m
Flume	2	compaction	tamped

time	head	observation
9.30	412	Height of Water in box 94mm
10.04	↑520	
10.25	↑624	
11.08	↑788	" 100mm
11.33	↑900	" 104mm
11.55	↑935	" 108
12.36	↑987	Some bubbling from Exit hole " 115
1.10	↑1026	" 122
1.24		" 123
1.27	↑1049	
1.40		Water starts to overflow out top exit
2.25	↑1067	
3.12		Water flowrate 2.64 LT/hr
3.40	↓415	for the Weekend
1/06 8.37	↑1072	Tip 50mm - inside the box
9.43	↑1103	bladder pressure had dropped to 3.5
		so topped up to 5.
10.02	↑1165	still 50mm.
10.29	↑1215	
10.53	↑1273	
11.23	↑1317	
11.35	↑1353	
11.45		Started weighing water
12.00	↑1393	
12.37	↑1430	Note: Tip has gone right over to side of box.
1.00	↑1480	
1.22	↑1535	Very murky water - Hard to see tip
1.44	↑1587	
2.00	↑1640	
2.15		*Tip under bar 1
2.49	↑1690	Sheet movement - West side - 35mm abl

time	head	observation
2.52	↓ 1525	brought head down as movement was rapid
		Tip is hard to see – Maybe 35-40 ab1
3.00		Tip is about 80 ab1 – Hard to see
3.15		" 130 "
3.40		" "
3.50	↓ 490	for night.
2/06 8.20	↑ 1525	tip may extend to b2 – Hard to see
10.30	↑ 1568	
12.25	↑ 1610	
12.40		fair amount of sand movement between b1 + 120
1.55	↓1000	I brought down to 1m to test my
		theroey that it's moving as it is
		because there's so much sediment
		transport it's in a continual cycle
		of block + unblock. I'm hoping that
		with a reduced head there'll be
		less sediment transport so it'll
		be able to travel the full
		length of the channel without
		blocking. In doing so I'm hoping
		I'll see more channel-like
		behaviour + continual progression.
		At the moment it's not really
		typical channel behaviour
		because there's a region btw
		b1 + 2 approx. 80mm wide that
		stops + starts particle flow
		along many simultaneous "flow
		paths". It's as if d/s material
		slides d/s + soil u/s of it slides
		~~en masse~~ in a group into the space
		it left + then all blocks up +
		doesn't move for ages until a
		new group of d/s material slides.
		~~This~~
2.03		raised bladder ≑ 0.5m.
2.05		already I can see a better formed
		channel. CHS. Tip is 150 ab1.
3.27	↑ 1051	

Test 75

Seems to be some sheet erosion 35 ab2 ?

	time	head	observation
	3.56	↓ 470	for night.
3/06	8.26	↑ 1000	Bladder was 3.5 M.
	11.32	↑ 1033	
	12.07	↑ 1056	
	12.55		Yes, definetly a tip at 35 ab2.
	1.45	↑ 1081	Quite a bit sand movement around 160 ab1
	2.18	↑ 1106	
	2.45		tip at 87 ab2.
	3.20	↓ 490	
4/06	8.10	↑ 1050	tip at 100 ab2
	9.42	↑ 1076	" " 110 "
	11.33	↑ 1100	More defined tip at 33 ab2 but region of
	12.45	↑ 1126	previous movement up to 110 ab2.
	2.33	↑ 1157	
	3.09	↑ 1206	
	3.50	↓ 456	
5/06	7.55	↑ 1206	
	8.34	↑ 1256	
	10.47	↑ 1306	
	12.44	↑ 1361	
	1.38		tip at 150 ab2. After knocking
			a large group of particles moved into
			channel. More like a "sheet flow." This
			material filled the newly-formed channel
			in so that now it's all blocked.
			~~Once the channel was refilled nearly~~
			~~all activity stopped.~~ About 2 minutes
			later channel flow recommenced.
	1.45		170 ab2
	1.53	↓ 1333	185 ab2
	1.54		120 ab2
	2.28	↓ 1306	under 63.
	3.50	↓	(12 turns). for Weekend.
10-6	10.39	598	erosion up to under 63 but well formed
			channel up to 165 ab3.
	10.40	↑ 746	13°C. Moved boil away from exit.
	10.57	↑ 893	
	11.04	↑ 1046	

time	head	observation
11.15	↑ 1203	
11.38	↑ 1304	
11.39		bladder tank dropped to ≑3m so
		raised to 5m.
11.44		there's is movement around b2 but
		there are alot of blockages + the
		channel isn't continous so movement
		doesn't translate to tip progression.
1.17	↑ 1357	
1.36	↑ 1383	
2.04	↑ 1410	
2.26		a small sand cone has returned to
		the exit so there must be transport
		of the system from somewhere. And
		I can c movement btw 1-2 (it's trying
		to sustain a channel) but just
		stops on blockages.
2.30	↑ 1430	
2.57		there's been alot of action whilst I wasn't
		looking. My best guess is the tip is 215ab3
		but it's not very clear. CHS.
2.58		Now its under 54 Circles on HS.
		It's moving like sheet flow on mass
		(not just at tip). And continually
		opening itself + blocking itself.
3.05		30ab4. see handycam.
3.07		through 2 u/s end.
3.12		Sample fail.

75. Test 75 (flume 2) circle

Test 75 was a repeat of tests 64 and 62 on mix 8. The repeat was carried out because tests 64 and 62 gave slightly different results.

The test was carried out in Flume 2 whose bladder slowly leaks. This leak is discussed in test 72 report. You can actually see the dripping from the bladder into a puddle of the ground in the SLR time-lapse video. The purple points on fig 3 indicate when the bladder tank was topped up to 5m. I plotted these points to see if it always preceded progression with low heads (which would support my theory that a gap between the lid and sand results in the need for higher heads). However as can be seen in fig 3 this was not always the case.

Throughout this test it was often difficult to define where the tip was because it didn't behave like typical channel behaviour. Instead there was often a widish region (100-150mm wide) through which many simultaneous flows paths moved in a stop-start fashion. It was if d/s material would suddenly slide and then groups of particles u/s of it would slide into the space left behind. Once blocked the eroding region wouldn't move until, sometimes up to a few hours and after several head increases, a new group of d/s material would slide, u/s soil would replace the gap and it would be blocked again. This can be seen well in the time-lapse video. I've also got good handy cam videos of the un-channel-like behaviour, including a good video as it approached the upstream end. See fig 1 for an example of when many flow paths were eroding.

It was difficult to define the tip because it could have been taken as one of the many hints of channels through the 'disturbed' region or it could have been taken as the slight discolouration indicating extent of u/s soil that had previously slipped. In most occasions Hamish defined the tip as the later.

I came to see how the experiment was going when the channel was 388mm long (Hamish was running the test) and I saw this un-channel-like behaviour. My theory as to why it was behaving this way was the head was too high (it was a fair bit higher than previous tests) and if I reduced the head then there'd be less sediment transport so it'd be able to travel the full length of the channel without blocking. To test this theory I reduced the head from 1568mm to 1000m (because test 64 progressed at 1m). This worked for a while; the channel had more definition to it, behaved more like a channel and progressed from 388mm to 595mm at a head of 1m. See fig 2 for comparison. However it then stopped progressing and the head to be raised up to 1383mm before it would complete its progression to the u/s end. Once higher than 1m it reverted back to the non-channel behaviour observed before.

I did not mention this unlike-channel behaviour in test report 62 or 64 so I think this is the first time I have seen this behaviour. I do not know why it behaved like this when previous tests didn't.

It took 5 minutes for forward deepening to lead to failure.

As can be seen in fig 3, all three mix 8 tests have behaved rather differently, keeping in mind that test 62 unsaturated. If I have the time and materials I would like to repeat it.

Figure 75-1 unchannel-like behaviour

Figure 75-2 channel better defined once head dropped

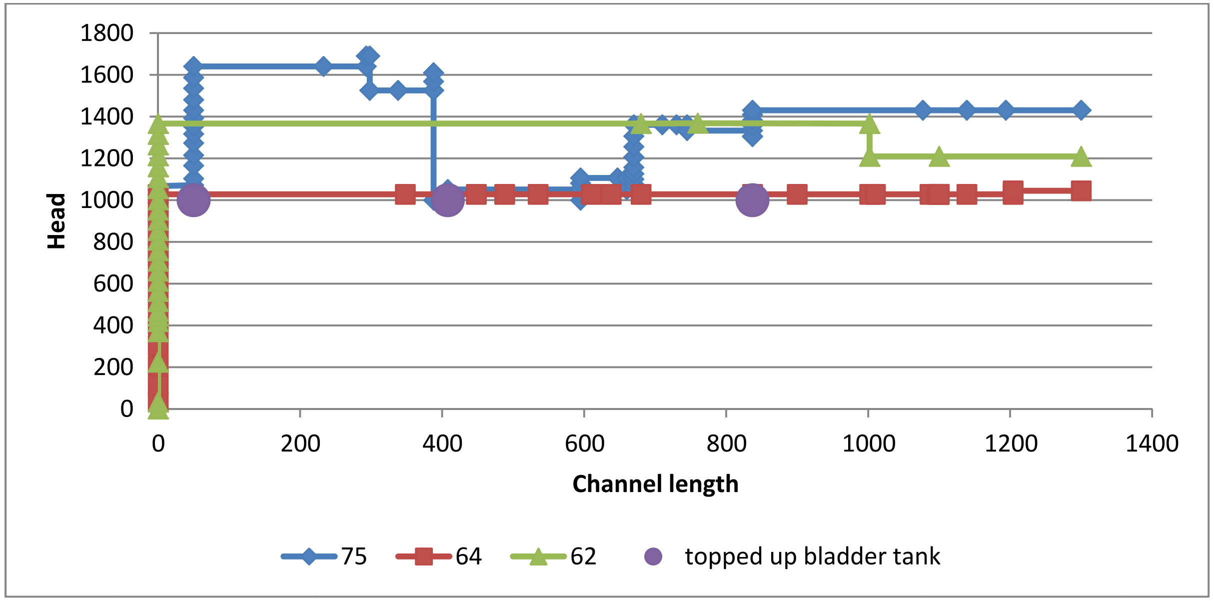

Figure 75-3 test 75 and comparison with other mix 8 tests

Falnash St

Backward erosion piping test data sheet

Test #	76	Exit type	slope
Date	1/06/2015	seepage length	1.3 m
Soil	syd sand	head in bladder tank	2.5 m
Flume	3	compaction	vibrated

time	head	observation
		Slope experiments @ 50kPa initiated
		btw 253-342mm and progressed btw
		307-342mm. I expected a bladder
		pressure of 25kPa to make no
		difference.
11.35	41	105mm Water height in box - not at Outlet yet.
11.45	↑ 125	
11.51		Water now at Exit pipe
12.00	↑ 175	
12.39	↑ 264	Water outflow 36 lt/hr
1.00	↑ 314	
1.22	↑ 366	
1.25	↓ 310	Tip Started - 100mm (in box) - photo
1.28		Tip between box and bar 1.
1.36		Tip under b1 Water flow - 46.5 l/hr
1.39	↓ 245	Tip at 25 ab1 - A little too fast
1.41	245	2 Tips A - 60 ab1 B - 65 ab1 Photo
1.44	↓ 227	Tip A - 105 ab1 Tip B - 85 ab1
1.49		" 160 " " 100 "
2.00	↓ 199	" 230 " " 125 "
2.03		" under b2 " 130 " photo
2.11		" 35 ab2 " " "
2.18		" 60 " " photo
2.34		" 145 " " photo
2.50		" 205 " " photo
3.00		" 240 " " photo
3.15		" under bar3 - Tip B has joined tip A. Photo
3.35		" " Water flow 34.4 l/hr
3.50	↓ 130	for night.
2/06 8.20	↑ 206	
8.55		Tip A 30 ab3

time	head	observation
9.05	↓ 192	tip at 180 ab3 photo
9.55	↑ 196	tip at 220 ab3 Water flow 31.6 l/hr
10.12	~~235~~	" 230 ab3
10.16		" under b4
10.23		" 15 ab4
10.32		" 60 " Water - 36 l/hr photo x 2
10.36		" 110 "
10.38		Tip reached the End. photo
11.00		Sand blocked between b1+2, b3+4
11.45		4 photos taken in order.
12.20		Test failed. THE END

76. Test 76 (flume 3) slope

This test was a repeat of tests 39, 40, 66 and 70 which were slope tests with bladder pressures less than the standard (i.e. to 2.5m). It was repeated because I haven't achieved the same results as I did with a 50kPa pressure (as I would expect). Results are shown in Fig 1 below.

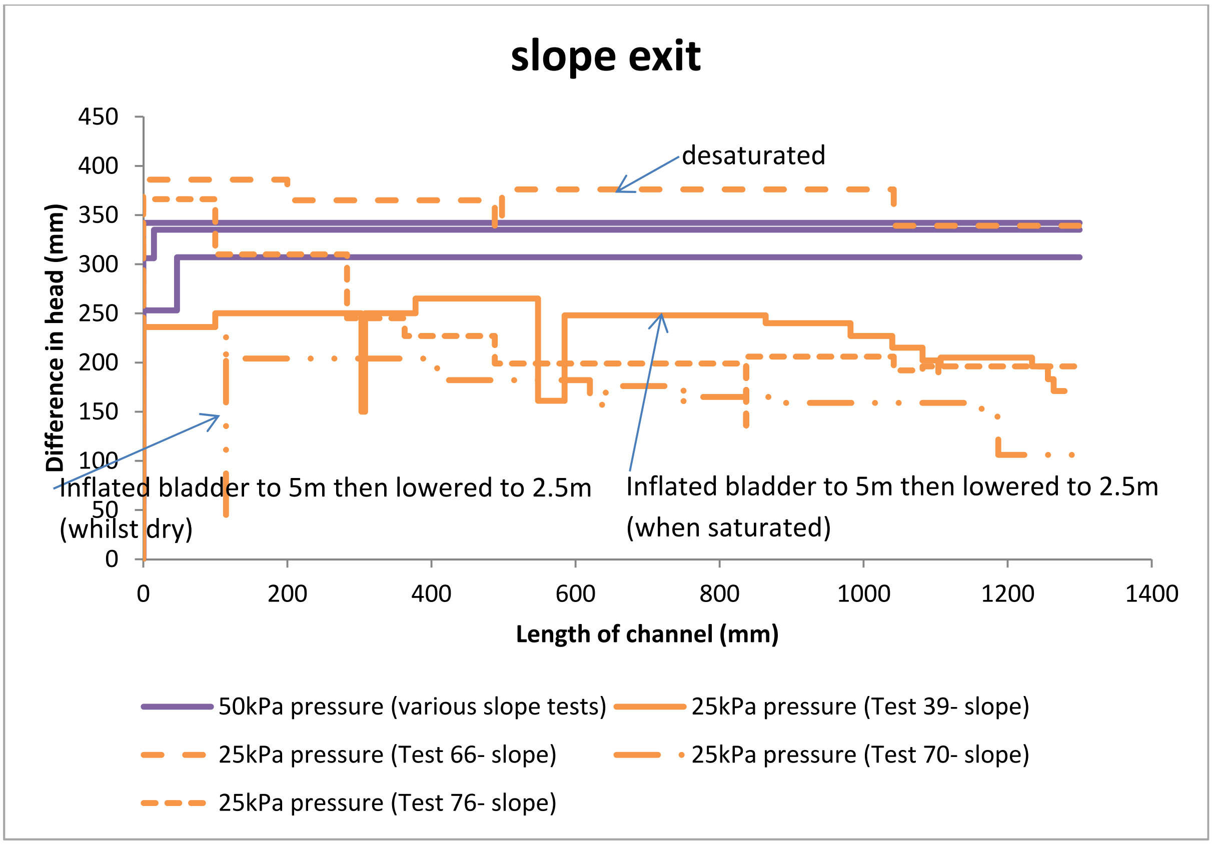

Figure 76-1 CL with head for test 76 and other slope tests

I'm taking initiation head to be 366mm. This is a little larger than the 50kPa tests (17% larger) but I consider it to be within experimental error (given the 50kPa tests had range of 26%).

The head required for progression continued to decrease as seems to be typical for slope exits. This makes the test 76 result look quite different from the 50kPa tests but this is only because I didn't reduce head in the 50kPa tests. So, because the initiation head is similar to the 50kPa tests, I consider this test to have shown similar results to the 50kPa tests indicating that different bladder pressures do not affect the initiation or progression gradients.

When the channel was after bar 1 it split into 2 channels. The 2 channels joined up again after bar 3.

The forward deepening took about 1hr 45min to complete and led to failure.

Backward erosion piping test data sheet

Test #	77	Exit type	circle
Date	23/06/2015	seepage length	1.3 m
Soil	syd sand	head in bladder tank	5 m
Flume	4	compaction	vibrated

	time	head	observation
	1.00	↑ 98	Sand bubbling immediately, Water at 95mm in box.
	1.05		Tip started moving
	1.06		Tip under b1
	1.~~0~~12		Tip at 70 after b1
	1.24	↓ 50	+ Collected Sand boil No.1
	2.15		Water started overflowing
24/6	8.30	↑ 90	Started Recording Water flow.
	10.01	↑ 119	
	10.29	↑ 140	
	11.07	↑ 166	
	12.55	↑ 194	
	1.45	↑ 219	
	1.55	↑ 243	
	2.11		tip at 80 ab1
	2.35	↑ 269	" " 95 "
	2.40		" " 130 "
	2.49	↓ 135	" " 200 " Reached another 130 (2nd) mm for the day
26/6	8.25	↑ 166	Tip still at 200 ab1
	8.49	↑ 190	
	9.05	↑ 215	
	9.29	↑ 240	
	10.06	↑ 265	
	10.25		Tip at 220 ab1
	11.05		" under b2
	11.27		Tip at 5 ab2
	11.32		" " 35 ab2
	11.33	↓ 130	Drop head because we've reached '3rd point' - collected Sand.
29/06	8.20	↑ 164	
	8.57	↑ 189	
	9.12	↑ 212	
	9.32	↑ 240	Tip at 47 ab2

+ collect Sand No.2

	time	head	observation
29/6	9.52	↑ 266	Now a lot of Sand movement close to exit.
	9.58		Tip at 60 ab2
	10.06		" " 95 ab2
	10.21		" " 105 ab2
	10.51	↓ 131	Reached 180 ab2 (another 130) took sand 4th Sample.
30/6	7.58	↑ 164	
	8.12	↑ 188	
	8.31	↑ 212	Tip still at 180 ab2
	8.45	↑ 236	
	9.09	↑ 261	Sand movement now near exit
	9.13		Tip at 185 ab2
	9.28		Tip at 225 ab2
	9.34		Tip at 235 ab2
	9.43		" under bar 3
	9.45	↓ ~~130~~ 0	Reached 5th - 130mm point - took sand 5th sample.
1/07	11.15	↑ 20	No sand bubbling
	11.17	↑ 40	Sand started to bubble
	11.19	↑ 60	
	11.23	↑ 95	
	11.27	↑ 118	
	11.34	↑ 141	
	11.46	↑ 165	
	12.49	↑ 190	
	1.04	↑ 215	
	1.16	↑ 232	Some sand movement close to exit
	1.26	↑ 253	
	1.55		tip at 15 ab3
	2.15		" " 53 ab3
	2.22		" " 80 ab3
	2.30		" " 115 ab3
	2.38	↓ 0	Tip at 135 ab3 (130mm point - took sand 6th Sample).
2/07	10.16	↑ 19	
	10.18	↑ 39	Sand started to bubble
	10.20	↑ 67	Sand bubbling is very responsive to Head raise - immediate.
	10.35	↑ 92	
	10.37	↑ 118	
	10.40	↑ 140	
	10.43	↑ 165	
	10.53	↑ 188	

Test 77

time	head	observation
2/07 10.56	↑ 215	
10.59	↑ 237	starting to see sand movement in the box near exit.
11.00		Tip still at 135 ab3
11.20	↑ 250	
11.20		Tip at 140 ab3
11.25		" " 150 ab3
11.32		" " 155 "
11.34		" " 173 "
11.39		" " 188 "
11.48		" " 220 "
11.51		" " 240 "
11.52	↓ 0	" " 250 ab3 (Under b4) Took Sandsample 7.
3/07 9.39	↑ 20	No bubbling.
9.49	↑ 24	Very slight ~~Sand bubbling~~ in exit hole
9.51	↑ 44	Sand bubbling increasing
9.54	↑ 68	
9.58	↑ 116	
10.05	↑ 140	
10.10	↑ 165	
10.30	↑ 189	
10.45	↑ 213	
11.10	↑ 232	Sand starting to move near exit.
11.23	↑ 235	Tip under bar 4.
11.32	[illegible]	" at 50 ab4
11.42		" " 82 "
11.46		" " 143 " THE END. Sand Sample 8 Taken
12.30		Getting sand blockages around b3 mark.
12.52		TEST FAILED.

Test 77

* closest pipe to tip

			Row 1			Row 2			Row 3					
	time	head	right	middle	left	right	middle	left	right	middle	left	time for 50mL	Avg	Temp
23/06	1.45	50	10	10	10	18	29	25	29	20	25			
24/06	10.38	143	37	35	36	61	72	67	88	81	84			
	2.39	269	*65	64	68	115	125	121	165	160	162			
26/06	9.34	240	*48	51	55	*92	103	97	132	125	130			
29/6	9.54	266	*45	49	56	*92	105	101	140	135	139			
30/6	9.28	261	*45	48	54	*65	100	96	135	130	134			
1/7	1.19	232	*37	40	44	*60	86	85	120	115	118			

77. Test 77 (flume 4) circle

Test 77 was the first test in group 5- cyclic loading. The procedure was to raise the head in small increments until boiling was first observed (and note boiling head) then continue to raise the head (probably in larger increments) until initiation (or progression) occurred, then hold the head until the channel progressed 130mm. The 130mm length was rather arbitrary- I chose it because it's 10% of the seepage length and would create a sensible number of cycles- 10. Once the channel progressed 130mm I lowered the head down to datum and collected the sand boil (material sitting above the lid- not material inside the exit shaft). I waited at least 24 hours before repeating.

The idea was to impose repeated 'floods' on the test. I wanted to see if a) the head required to start boiling changed b) the head required to progress the channel changed and c) the size of the boil grew with each 130mm channel length. I did this to investigate USACE's observation that more boiling activity occurred with successive lower floods. I also wanted to know whether boiled material could help me back calculate the volume of each 130mm channel length and how much of the boiled material was from the newly created 130mm channel and how much was scour from older portions of the channel.

However for the first 4 cycles I wasn't lowering the head back to datum (I was lowering to 50% of whatever the head was at the time) or recording when boiling occurred. Because these steps were added to the procedure halfway through the test.

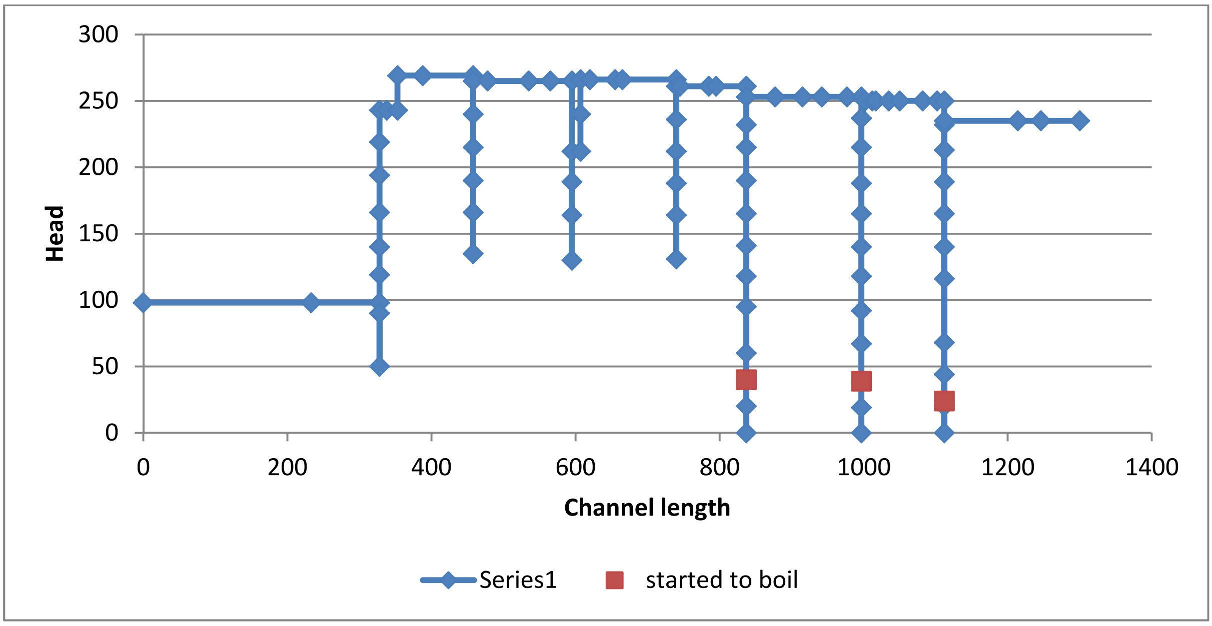

Initiation occurred at 98mm and progressed for 328mm. This was a relatively low initiation head and progressed surprisingly far. There was no indication as to why this was.

The head required to progress the tip decreased slightly with each channel portion, from 269mm to 235mm (a 13% reduction). The head required to start boiling decreased slightly in the last 3 cycles: 40, 39 and 24mm.

Hamish ran this test and noted that when he was at one head raised before progression he noticed transport in the downstream portion of the channel (usually under the d/s box).

Hamish also noticed the channel blocked during the forward deepening stage. The forward deepening stage took about 1hr to complete and fail the sample.

As for sand boil sizes, the graph below plots the dry sand weight of each boil and the channel length segment length prior to it being collected. It shows that the boil did *not* increase in size with each 130mm segment, but it did vary, the largest boils being collected when the channel was 740 and 997mm long.

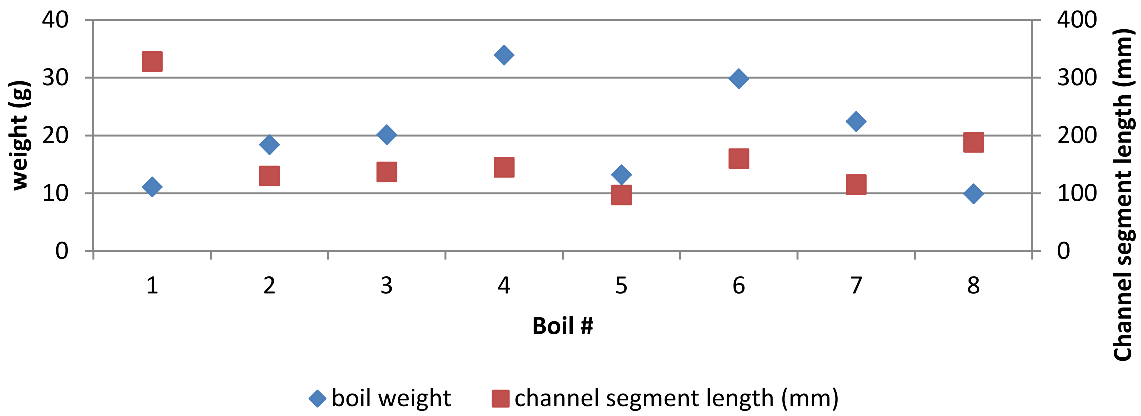

However it's noticed that the boil size is sensitive to the length of channel segment eroded prior to boil collection (effort was made to keep every channel segment close to 130mm but factors such as the restraining bar locations meant that a constant segment length couldn't always be kept). Therefore the boil size was expressed as a ratio of the segment length, in g/mm and plotted against the total channel length resulting in the following graph.

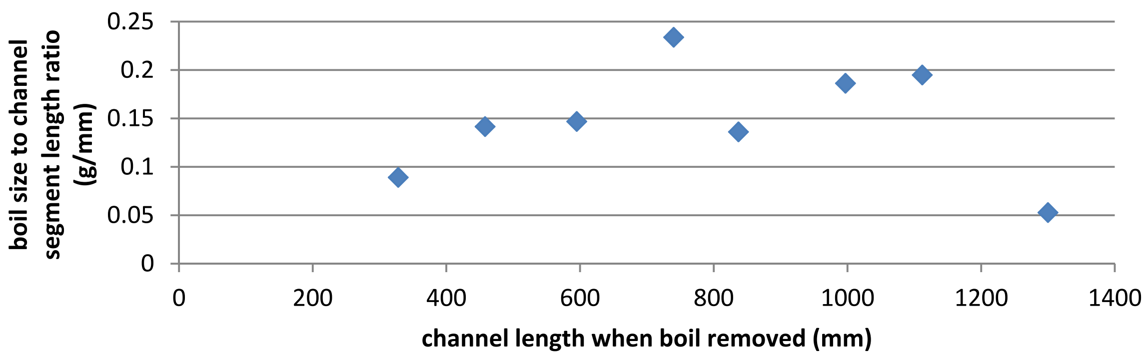

This tells a slightly different story. Now it does look like there is a trend of increasing boil size with a few exceptions.

With respect to whether the boil weight could tell me anything about the primary to secondary erosion proportions (by back calculating the volume of each 130mm channel length and how much of the boiled material was from the newly created 130mm channel and how much was scour from older portions of the channel), this was very difficult because it all depends on what I assumed the channel geometry to be which was subject to a lot of uncertainty and variability.

If I assume that:

1. the first boil collected was only primary erosion (because there were no downstream portions of channel from which secondary erosion could be drawn from yet);
2. I include weight of sand which would have been left behind in the hole shaft in the first sand boil (assuming it was at the loosest dry density of 1.475e-3 g/mm3);
3. a channel depth;
4. the channel has a rectangular cross-section;
5. the channel dimensions remain constant through the experiment; and
6. sand was at 1.6e-3 g/mm3 when it was in the channel (a density btw loosest and densest but closer to densest).

Then I vary the channel depth and back calculate a channel width until I get something sensible. Thereby giving me feel for probable channel dimensions. If I divide the initial sand boil weight by the initial channel length then I can estimate primary erosion as a g/mm and assume that this primary erosion rate remains constant and any additional erosion is secondary. This gives me the table and chart below.

volume mm3	depth	length	width	primary erosion (g/mm)
18125	1	328	55.2591463	0.08841463
18125	2	328	27.6295732	0.08841463
18125	3	328	18.4197154	0.08841463
18125	4	328	13.8147866	0.08841463
18125	5	328	11.0518293	0.08841463

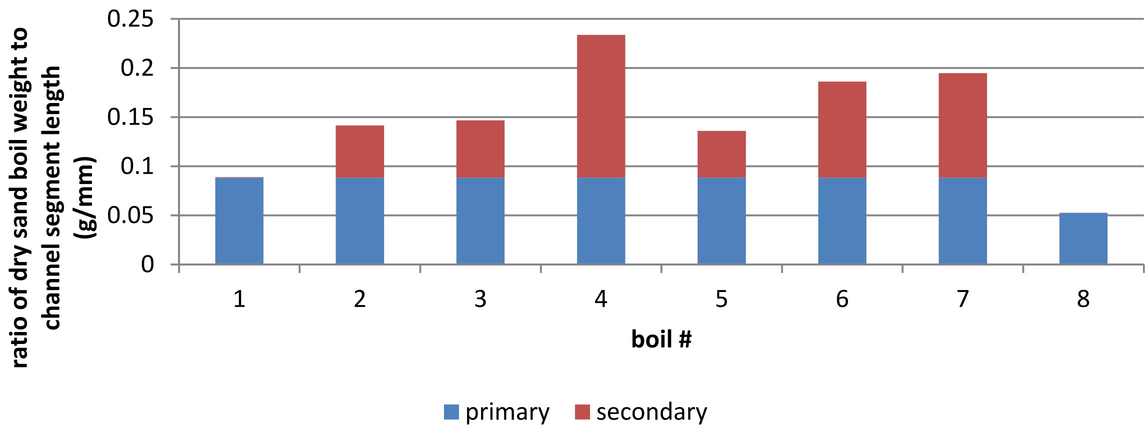

I expected the portion of secondary erosion to increase with each boil because the channel length, from which scour is removed, increases. And whilst this is the overall trend, there are exceptions, namely boils 4, 5 and 8 so the trend is not convincing.

All possible measurements were made during this test including flow rate with scales, pliolite particle speeds and standpipe levels.

UNSW Australia | Civil & Environmental Engineering
Faculty of Engineering

Test 78 — Circle
7-7-15 — 1.3m
mix 6 — 5m
Flume 3 — tamped

11.05	~~5~~ .77	There's still a patch btw b1+2 that looks unsaturated but I can't see any gas/air bubbles ~~so~~ and the patch is small so will start test anyway. CHS. Also there's a boil that occurred during oozing or saturation. CHS. There's also boiling so will reduce H to determine when boiling starts.
11.07	↓32	still small amount of boiling (I moved boil away)
11.11	↓7	boiling stopped.
11.13	↑15	no boiling
11.14	↑25	" "
11.17	↑28	" "
11.18	↑32	Smallest hint of ~~a~~ boiling
11.24	↑123	
11.27		having wiped 300g from lid I can now see voids/bubbles in/around exit - presumably voids from boiled material. No sign of any channel. CHS. Water 11°C.
11.59	↑220	
12.27	↑267	
12.49	↑317	
1.27	↑364	
2.12	↑412	
3.02	↑460	

test 78

3.35	↓435	120ab1
3.50	↓412	230ab1
4.26	↓389	90ab2
4.38		140ab2. So channel is on verge of blocking but not quite.
4.41	↓363	
5.04	↓335	178 ab2
5.25	↓316	240ab2
5.52	↓↓30	under b3
8-7		
10.26	30	there are bubbles in the channel. CHS. I don't how/why they got there. Perhaps if I ever do mix 6 again I'll coz it for longer - or let it soak for longer. these bubbles may interfer with results. It depends if there are bubbles at or u/s of the tip. [illegible] Also, I moved boiled material. See happy snap.
10.32		It's difficult to see whether it's boiling or not (cloudy water). OK it is boiling - I just saw it. Try ↓
10.34	↓27	no boiling
1035	↑28	" "
10.46	↑29	" "
10.50	↑31	boiling
10.51	↑124	
11.19	↑220	
11.39	↑268	
12.31	↑316	
12.57	↑364	getting transport through channel

test 78

up to midway btw b2+3. There are a lot of bubbles midway btw 2+3; the channel might even be blocked here. CHS.

1.15 the transport lasted for only a few minutes when I last raised the head. All seems still now but I'll wait a little longer.

2.16 There's transport through the channel again → up to midway btw b2+3. I think if the channel can manages to form itself around air bubbles + transport bubbles away, and can do this all the way the tip, I think progression would recommence. There's transport up to around 110mm after b2.

3.27 Channel is well defined btw 1+2 but not btw 2+3. CHS. Bubbles everywhere. I'm starting to think this has been ~~ruind~~ ruined. I wish I know where/how the bubbles entered.

4.26 a new tip has formed from a brach btw b2+3. There's less bubbles in this newly branched channel + the tip is progressing slowley. It's 230ab2 CHS.

4.52 new tip now under b3.

5.52 " " 208 ab3 (oops I should have come look sooner).

5.53 ↓↓30 unfortunately more bubbles will probably come in over night like they did last night (for goodness-knows-why)

Page 3 of 4

test 78

9-7		
10.25	30	thankfully there aren't bubbles in the latest channel-branch-off. Moved boiled material. No boiling.
10.27	↑31	no boiling.
10.29	↑36	" "
10.31	↑39	" "
10.32	↑43	boiling.
10.33	↑147	
10.42	↑245	210 ab3
11.37	↑293	" "
11.49	↑317	
12.00	↑340	
12.32	↑364	the channel is well formed (no blockages) and there is a hint of sediment transport periodically but I can't see it occuring from tip.
12.55	↓316	10ab4
12.57		16ab4
12.58	↓268	22ab4
" "		33ab4
1.45		first noticed channel through to u/s (refer to SLR for time it occured). Channel is blocked btw 6&4.
5.27	↓30	forward deepening reaches midway btw 2&3 (where bubbles start).
10-7		
10.56	↑268	
4.56		the forward deepening has not moved all day and is stopped on the bubbles so I'm going to conclude that fwd deeping will not occur.

 End of test.

78. Test 78 (flume 3) circle

Test 78 was the third test on mix 6 (tests 59 and 72 was the previous tests). It was done because the results of 59 and 72 were reasonably different. The 2 theories as to why they were different was 1) because the bladder in test 72 was leaking, so even though it was topped up each morning it would deflate slightly during the day, enough to form a small gap between the soil and lid and 2) the channel blocked in 72 and not in 59 (although I have no theories as to why it would block in one and not the other).

Prior to starting the test there was boiled material, probably from CO_2 or saturation, see pic 1. When I moved the boiled material away I could see voids/bubbles in and around the exit, presumably left behind by boiled material, see pic 2.

Channel initiated at 460mm.

I found the start of boiling each morning. They were 32, 31, and 43mm. So no, they didn't decrease.

On the 2nd day of testing I came in to find lots of bubbles in the channel. Not sure why. It's possible I hadn't achieved full saturation in the first place because before I started the test there was a patch the looked unsaturated, see pic 3. Maybe I should have let it CO_2 or soak for longer(?). I note there were also bubbles in test 72 but not 59. Not sure why.

Sediment transport occurred up to the bubbles but not beyond. I left the head at 268mm (where it had progressed the previous day) for a full day and by late afternoon a branch formed off the bubble-riddled channel, see pic 4. I thought bubbles would enter newly branched off channel overnight but they didn't and the channel remained well formed (no bubbles or blockages) for the remainder of the test.

I'm defining the progression head as 475mm but it continually decreased throughout the experiment. See plot in fig 5.

The channel did block soon after it reached the u/s end. Forward deepening reached the bubbled zone but didn't go any further so I ended the test there.

As can been seen in figure 5 this test result was similar to test 59 (only a 7% difference in progression head) so I consider this to have demonstrated repeatability. I also now consider test 72 to be untrustworthy.

Test 78 plotted very close to Schmertmann's graph. See fig 6.

Figure 78-1 boiled at start of test

Figure 78-2 void/bubbles in around exit

Figure 78-3 patch the didn't look saturated at start of test

Figure 78-4 branched off bubble-ridden section of channel

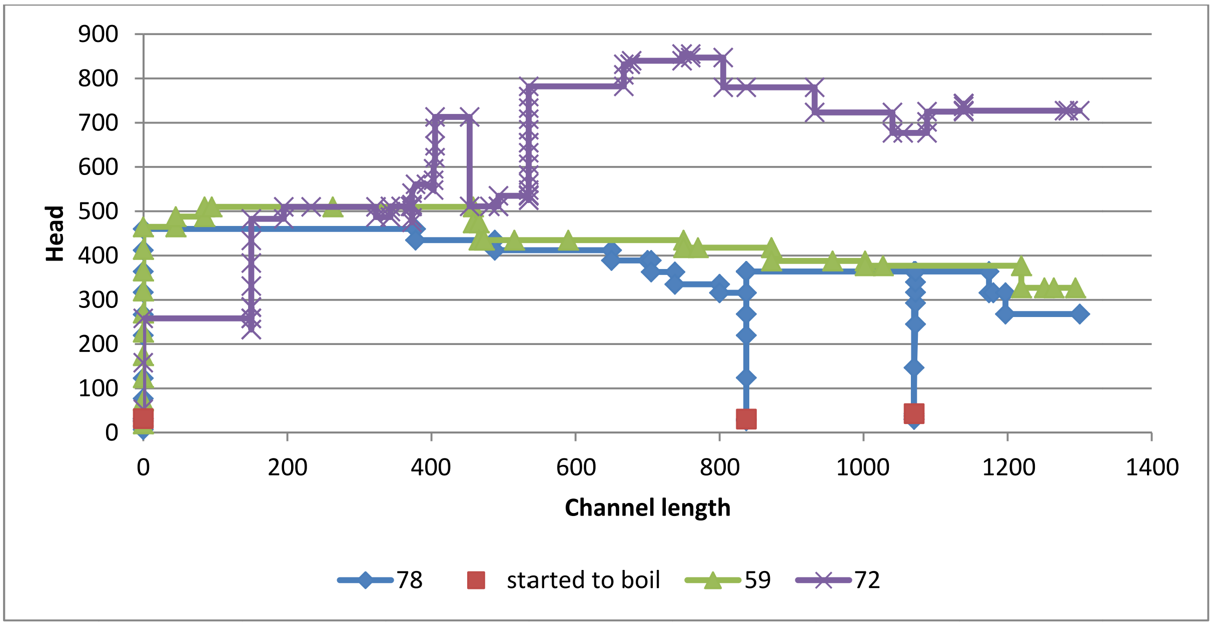

Figure 78-5 test 78 plot

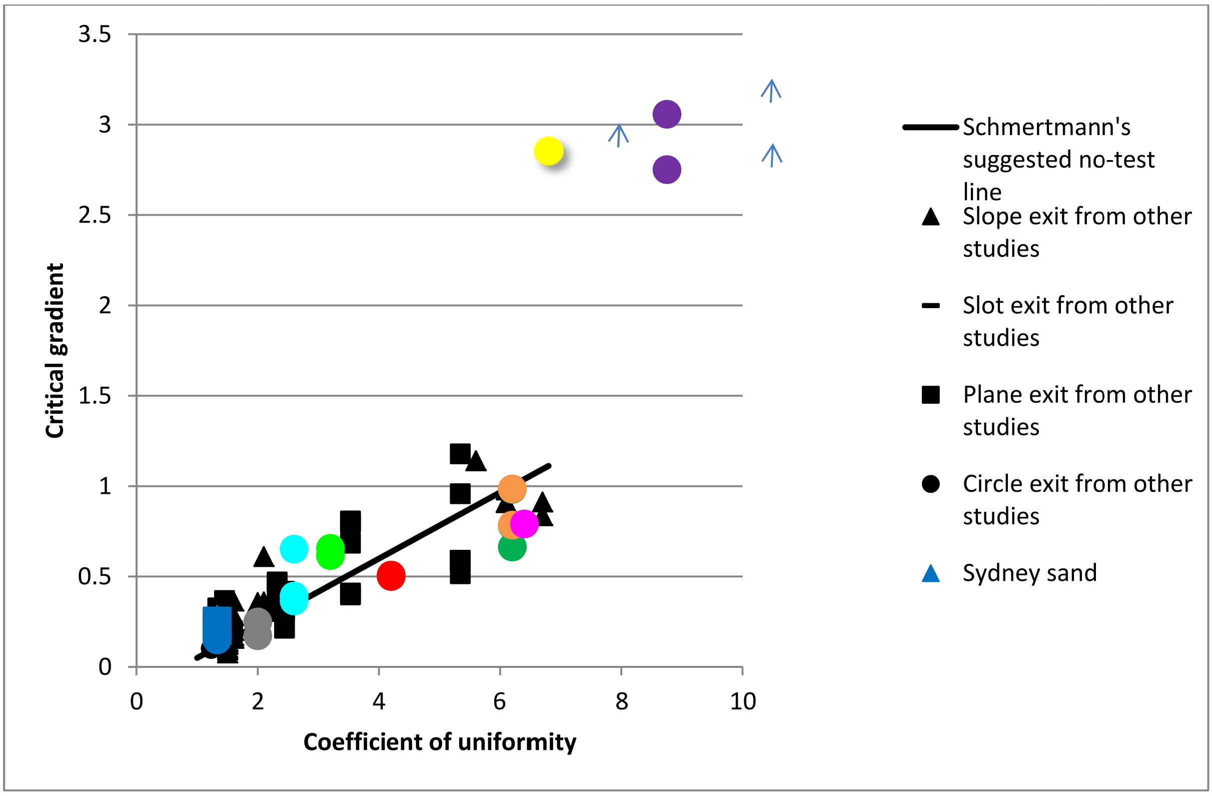

Figure 78-6 test 78 on schmertmann chart (lower light blue)

Test <u>79</u> circle.
9-7-15 1.3m
Syd sand 5m
flume 1 vibrated

11.40	-3	no boiling.
11.41	↑ 17	" "
11.44	↑ 32	" "
11.46	↑ 40	" "
11.47	↑ 49	" "
11.50	↑ 60	
11.53	↑	
11.55	↑ 89	
11.57	↑ 100	
11.59	↑ 114	
12.02	↑ 127	started overflowing d/s.
12.04	↑ 141	
12.06	↑ 152	
12.12	↑ 168	
12.30	↑ 181	
12.37	↑ 194	
12.42	↑ 206	
12.45	↑ 220	
12.48	↑ 234	
12.51	↑ 247	there's still no boiling action or initiation. But there's material mounded up around the edge of the exit. CHS.
2.02	↑ 260	I can see very occasional sediment movement that moves for a few mm. In a region about 40mm d/s of exit. CHS. It's possible there's a slight void d/s of the exit (sand not right up against lid). this would explain why the head is high. No boiling at exit. I wouldn't call this initiation. there's no channel yet.
2.15	↑ 272	there's a slightest hint of channel btw 50 to 90mm (tip at 90mm and d/s "end" at 50mm. CHS.

		I think once the channel is well formed to the exit I'll be able to reduce the head alot to be more like previous tests (here's hoping).
2.35	↑283	
2.36		135-30 (tip). 2 Channels now @ exit LHS, + boiling action.
2.37		tip now at ~~tank~~ tank wall.
2.38	↓19	
2.43		can't see tip. I presume it's under the d/s tank wall. No more boiling. No boil to collect (no sand on top of lid).
13-7		
10.48	8	tip under d/s box wall (I assume).
10.50	↑13	no boiling
11.04	↑24	" "
11.06	↑37	" "
11.07	↑43	boiling. Where the 2 channels meet the exit. See video on H.S.
11.09	↑116	
11.13	↑?	plenty of boiling until no movement
11.16	↑170	in channel.
11.37	↑201	Sediment transport in channel for about 30 sec. looked as if it was coming from d/s and of channel.
11.43	↑212	
11.45	↑241	Continual transport through channel now. Still can't see tip. Checked bladder tank + it's still at 5m.
11.50		can't see transport in channel anymore. SCRAP that. I can, just only a small volume of sand + only in ~~occasional~~ intermitten groups. Water 11°C.
12.20	↓12	60 abl. Collected boil 1. Very difficult to collect all of it. I'd guess I got maybe 80-90% of it.

14/07

1·00 ↑ 29 ~~As~~ Sand bubbling just starting

1·02 ↑ 66

1·06 ↑ 88 tip still at 60 abl

1·13 ↑ 113 Can't see any sand movement except exit hole.

1·15 ↑ 135

1·18 ↑ 168

1·20 ↑ 187

1·51 ↑ 220 Sand movement in the box

2·00 ↓ 210 Some reason in went down on its own

2·02 ↑ 242

2·03 ↓ 230 tip at 63 abl

2·08 " " 67 "

2·12 " " 74 "

2·15 " " 80 "

2·28 " " 105 " Casio × 3 . (130 abl

2·36 " " 140 "

2·42 " " 150 "

2·45 " " 155 "

2·52 ↓ 24 168 2nd ~~Next~~ Red marker

15/07 2·19 ↑ 35

2·24 Sand started to bubble (after 5 mins,

2·25 ↑ 72 Bubbling stopped, then started agai

2·37 ↑ 120

~~2·54~~ ↑ 150

2·56 ↑ 176

3·09 ↑ 204 Sand starting to move near exit in bo

3·15 Tip at 173 abl

3·17 ↑ 217

3·19 " " 182 " the stopped

3·29 ↑ 226 tip now moving towards west

3·37 tip at 191 abl

3·41 " " 212 "

3·42 Casio shot × 3 at (220 abl)

3·44 Tip at 224 abl

3·46 " " 249 abl

3·53 Tip under b2 and Reached 3rd marker.

3·55 ↓ 5

7/07		
9.50	↑ 15	No sand bubbling
9.51	↑ 23	" " "
9.53	↑ 34 *	Sand starting to bubble.
9.54	↑ 70	
10.15	↑ 95	
10.20	↑ 120	
10.27	↑ 146	
10.29	↑ 172	
10.31	↑ 188	
10.34	↑ 202 *	Sand starting to move near exit (in box)
10.46		fair amount of sand moment near tip then it stopped.
10.49	↑ 220	Tip still under b2
11.06	↑ 233	
11.09		Tip at 10 ab2
11.11		" " 35 ab2 *(Casio multishot x2) shot taken midway betwn b1 + b2
11.04		Casio multishot x 1
11.16		" " 39 ab2
11.31	↑ 239	" " 43 ab2
11.39		" " 62 "
11.40		" " 67 "
11.44		" " 75 "
11.47		" " 93 "
11.51		" " 118 "
11.52	↓ 2	" " 125 " * Reached <u>4th</u> marker.
20/7		
10.51	↑ 14	
10.53	↑ 20	
10.54	↑ 29	
10.56	↑ 35 *	Sand started to bubble after 1 minute delay
10.58	↑ 121	
11.06	↑ 171	Started to weigh water.
11.08	↑ 189	
11.16	↑ 225 *	Some sand movement in box near exit.
11.22		Tip at 140 ab2 now.
11.25		" " 155 "
11.27		" " 175 "
11.29		" " 185 "

20/07	Head	
11·32	225	Tip at 185 ab2
11·37		" " 200 "
11·40		tip at 205 Casio multishot X3 between b1 + b2
11·44		tip at 215 ab2
11·46		" " 230 "
11·57		" " 235 "
12·05		" " 250 " (start bar3) Reached* 5th marker.
12·05	↓ 0	
21/07		
12·56	↑ 16	
12·59	↑ 26	
1·00	↑ 34	
1·02	↑ 42	* Sand bubbling started.
1·05	↑ 122	
1·07	↑ 173	
1·26	↑ 207	* Sand starting to move between Exit + b2.
1·35	↑ 220	Tip still under bar3 (start of).
1·50		Tip has moved but still under b3.
2·17	↑ 230	
2·29		tip at 10 ab3
2·43		" " 30 "
2·44		1x Casio multi shot (between b1 + b2)
2·47		1x " " " "
3·02		" " " "
3·18		tip at 40 ab3
3·39	↓ 10	" " 60 ab3 6th Marker.

Note: channels seem to deepen, then tip moves along, then stops, and channels deepen again.

went to printed sheets.

Test 79

time	head	observation
24-7		
3.25	8	removed sand boil #6.
3.29	↑ 18	no boiling.
3.32	↑ 30	" "
3.34	↑ 44	boiling
3.35	↓ 37	"
3.36	↓ 34	no boiling
3.37	↑ 36	boiling
~~3.36~~		~~boiling~~
3.40	↑ 73	
3.53	↑ 123	
4.00	↑ 174	
4.09	↑ 203	movement in channel from btw 2-3
		to exit for only about 30s and
		then stopped.
4.20		still some movement in channel d/s
		of b2 only.
4.26	↑ 217	Still, movement from halfway btw 2 3
		to exit. Tip still 68 ab3.
4.42		75 ab3 (~~movement~~ detachment now
		occuring from tip
4.45		60fps midway btw 42.
4.47		78 ab3
5.10		89 ab3
4.28		120 ab3
4.22		145 ab3
5.33		160 ab3
6.04		220 ab3
6.04	↓ 2	237 ab3
27-7	2	removed sand boil #7. no boiling.
4.22		tip still at 237 ab3.
4.24	↑ 15	no boiling
4.25	↑ 29	" "
4.26	↑ 34	boiling
4.28	↓ 32	"
4.29	↓ 30	"
4.30	↓ 29	no boiling

Test 79

time	head	observation
4.32	↑ 72	
4.36	↑ 122	for some reason the water level
		in the CHT is going ≑ 25mm
		above the inner pipe level before
		dropping down to inner pipe. I'm
		not sure why.
4.45	↑ 149	no movement.
4.59	↑ 174	there was momentary movement
		because the head raised above
		the inner pipe b4 dropping back
		down again. But once the head
		lowered movement stopped.
5.13	↑ 187	sediment transport up to tip. But
		took a while to get there.
5.21		
		sediment transport appeared to
		other at the d/s end of the
		channel + work it's way upstream.
5.28		250 ab3.
		However the transport isn't constant.
		It's intermittent.
5.30		now I see no transport anywhere.
5.31		now there is. 252 ab3.
5.33		now there isn't.
5.37	↓ 14	I imagine the tip could progress at this
		head just slowly. However, unfortunately,
		I've left it too late to start the test
		and need to go now so I will
		drop the head + recommence tmrw.
28-7		
2.22		tip still 252 ab3. There is boiled
		material that I would ordinarily
		remove but seeing as I didn't
		progress the channel the full
		130mm I was supposed to I'm not
		going to remove it. However I will
		just brush some of the sand
		back into the hole so that

Test 79

time	head	observation
		the hole is full and has the
		whole 25mm height of sand
		as would have been the case
		when I've determined the
		boiling head previously.
2.28	↑30	no boiling
2.30	↑31	" " . Checked bladder tank
		and still right on 5m.
2.33	↑34	the smallest hint of boiling (like
		maybe area of 5 particles boiling).
2.34	↑95	
2.41	↑123	
2.53	↑149	
3.18	↑175	
3.35	↑188	transport stops + starts in
		channel up to b3.
3.55	↑196	I've seen transport up to mid-way
		btw b3+4 but I don't think
		it's any further. Although it's
		hard to know how long to
		watch for.
4.06	↑202	transport now full length of channel
		and I'm assuming from tip also (it's
		under b4 so can't see tip). Transport
		presumably from tip about every minute
		or so.
4.27		23 ab4.
4.30	↓	40 ab4. At last marker. Collect last
		boil # 8.
		SEE PAGE 126 of book
		4 for wax + caliper measurement

Time	Downstream row 1			midstream row 2			upstream row 3		
	left	mid	right	left	mid	right	left	mid	right
11.38	114	115	115	112	114	114	112	113	114
12.28	184	187	187	213	215	215	244	246	246
13-7 11.41	194	195	198	228	229	229	265	265	265
4/7 1.57	204	200	206	240	239	244	280	280	280
7/7 11.49	201	191	195	240	235*	239	286	287	288
24-7 4.22	185	174* HS.	182	215	216 HS.	217	257	257	258
28-7 4.28	184	177	182	211	198	204	250	242*	250

All measurements from top of perspex lid.

79. Test 79 (flume 1) circle

Test 79 was the second test in group 5- cyclic loading and was on Sydney sand.

The first boiling did not occur until after initiation. Initiation occurred at a relatively high head of 283mm and did so from 50mm upstream of the exit (see pic2). This suggests sand wasn't pressed up against the exit and there was a local void. This explains why boiling occurred after initiation (because a concentration of low at a point at the exit is needed to boil sand and the void was keeping this from happening) and why the initiation head was so high. Once the d/s end of the channel reached the exit boiling occurred and the channel became well formed, with 2 tips.

The next 130mm segment reinitiated at a much lower head of 212mm (25% less), probably because there was now a channel connected to the exit. Remaining 130mm segments all reinitiated at similar heads within 202 to 239mm, but didn't always decrease as was the case in Test 77. See fig 1.

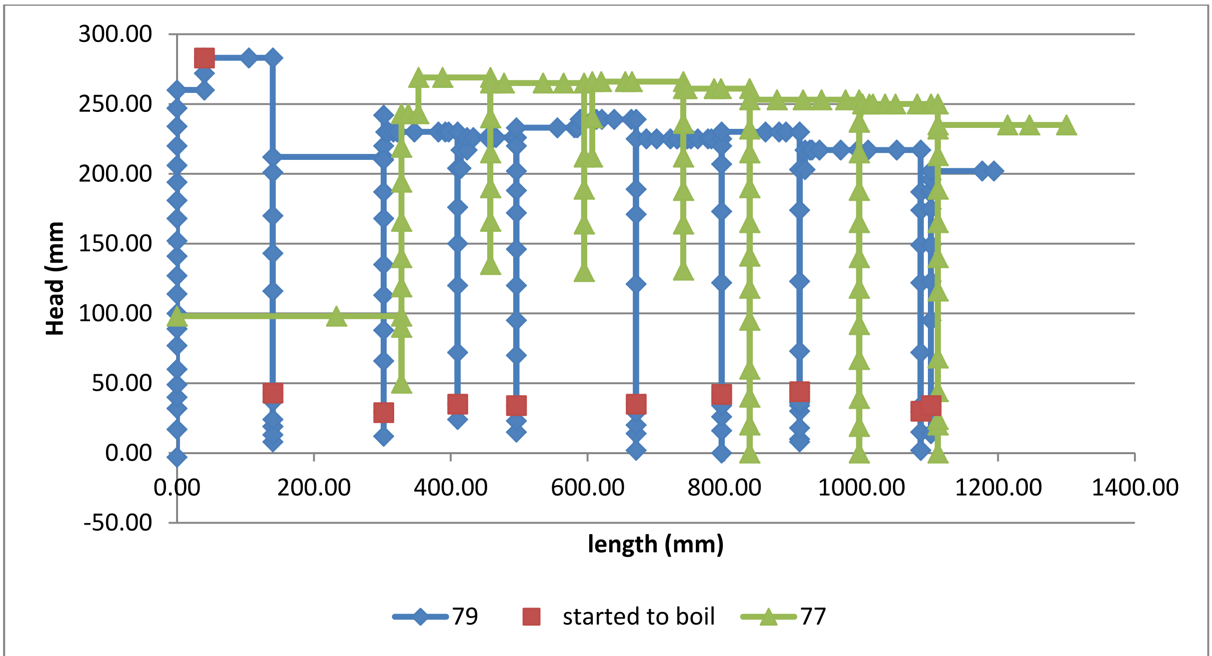

Figure 79-1 Test 79 plot

Hamish and I often observed sediment transport along the d/s portion of the channel at a head level just prior to the head level needed to reinitiate the channel. In other words, the first sign that the head level was approaching critical was sediment transport along the downstream end of the channel. Perhaps this is suggesting that erosion occurs from the downstream end of the channel and works its way backwards as bed load moving along as if on a conveyor belt. Erosion at the tip occurs when this 'conveyor belt' of erosion reaches the toe of the tip slope. But if erosion always started from the d/s end of the channel wouldn't it be significantly deeper/wider at the d/s end? And I don't think I see this. The channel geometry doesn't change that much. Maybe sand transported from upstream settles in downstream portions which is why the channel geometry doesn't change much.

With respect to boil sizes. See chart below.

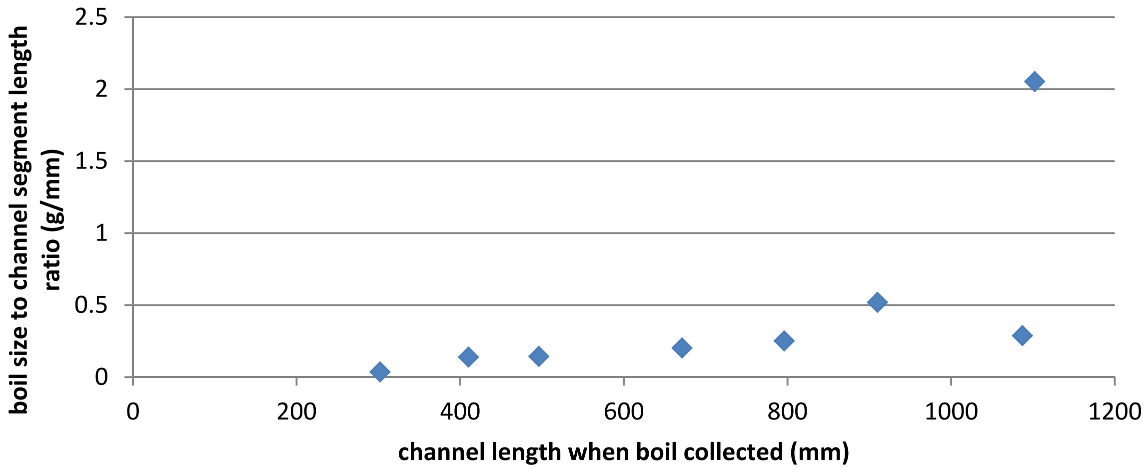

As was the case in Test 77, it appears the boil increases in size with increasing total channel length, with a few exceptions (this time the last 2 boils are the exceptions).

With respect to whether the boil weight could tell me anything about the primary to secondary erosion proportions, I made the same assumptions and used the same technique as done for Test 77 to produce this table and graph:

volume mm3	depth	length	width	primary erosion (g/mm)
6812.5	1	302	22.55795	0.036093
6812.5	2	302	11.27897	0.036093
6812.5	3	302	7.519316	0.036093
6812.5	4	302	5.639487	0.036093
6812.5	5	302	4.511589	0.036093

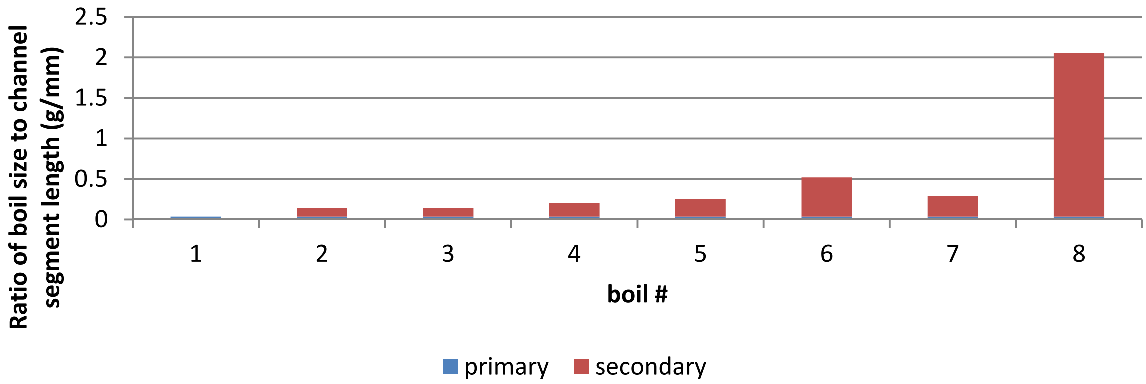

As expected the portion of secondary erosion increases with each boil because the channel length, from which scour is removed, increases. Having looked back at timelapse video I was hoping to see more meandering during the last segment to explain the jump in boil size but I didn't so I can't explain the jump.

The test was stopped after the last 130mm marker so forward deepening or failure weren't observed.

After the test I lowered the water level in the flume and pulled out standpipes which had the channel positioned beneath them. I then melted wax and tried pouring wax into the hole in the hope that it would run into the channel and set providing me with a mould of the channel I could directly measure the depth of. But the wax was too viscous to allow air to pass up through it so air in the channel prevented wax from flowing into it. I then tried using a self-priming syphon (bought from a pet shop to syphon water out of fish tanks with) as a plunger to push wax in. This managed to fill the channel in for a length of about 50mm but no further because again, trapped air would prevent wax to flow in (see pic 3 and 4). Also wax set in the plunger so it couldn't be used again.

So I took the lid off and just poured wax into the channel. This was less ideal because without the lid or bladder pressure the channel depth may have changed. I tried resting something on top of the sand and tried pouring wax underneath it (to mimic the boundary of the lid) but I found it was better just to pour without anything on top of the sand and let the wax overflow the channel. This way I could measure the depth of the channel as the difference between the thickest wax and the thickness of the overflow (see pic 5 and 6). I measured the wax with a calliper. I also tried measuring the channel bare with the calliper but this was also difficult because it was hard to extend the rod into the channel just enough to touch the bed of the channel without moving and penetrating the sand. See page 126 of book 4 for measurements. Channel depths varied between 1 to 5mm. I have kept the piece of wax poured without a cover.

Figure 79-2 **channel initiated 50mm upstream of exit**

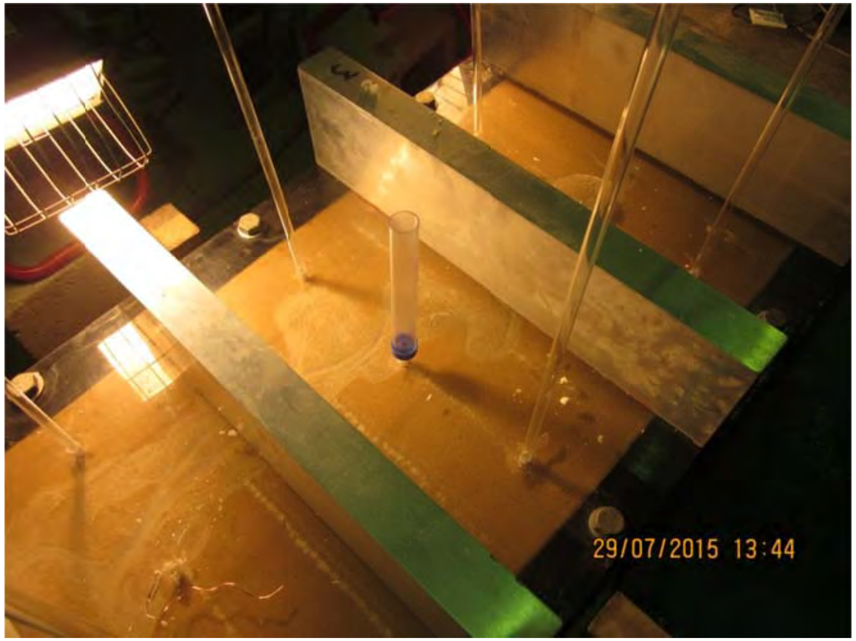

Figure 79-3 **3 middle holes filled with wax. Row 1 and 3 failed and 2 has plunger ready to try**

Figure 79-4 **Plunger pushed wax into channel for about 50mm**

Figure 79-5 **Lid off. Poured wax under plastic and with no cover**

Figure 79-6 Measuring bare channel with calliper and fry pan in background

Backward erosion piping test data sheet

Test #	80	Exit type	circle
Date	3-8 ~~31/07~~/2015	seepage length	1.3 m
Soil	syd sand	head in bladder tank	5 m
Flume	4	compaction	vibrated

time	head	observation
4.50	~5	pressure bladder still @ 5m.
4.52	↑ 3	no boiling
4.54	↑ 6	" "
4.57	↑ 8	boiling. area about 10 grain-sizes.
		See video on happy snap.
5.00	↑ 55	
5.09	↑ 103	
5.33	↑ 128	
5.46	↑ 153	I can see some particle arrangement
		immediately u/s of exit so I expect
		I'm close to initiation.
5.57	↑ 177	initiation.
5.59		170-110
6.02		220-110. Channel has meandered left.
		CHS. Tip has slowed right down.
6.06		A new tip is trying to branch off
~~[illegible]~~		the channel where it starts to
		turn left.
6.10		220-110 still. I expect it could continue
		at this head but need to go so will
		shut down.
6.12	↓ 5	
6-8		
2.50	5	tip still 220-110. Negligible material at
		top of lid.
2.51	↑ 32	boiling
2.52	↓ 22	no boiling
2.53	↑ 24	exit shaft maybe half full of sand.
		boiling. See happy snap vid. Stopped boiling
		once I was videoing.

time	head	observation
2.56	↑ 27	boiling again.
2.59	↑ 78	
3-08	↑ 103	
3.13	↑ 127	
3.19	↑ 151	
3.27	↑ 164	
3.35	↑ 177	there was particle transport through
		channel for about first 15s after
		head increase and then stopped.
3.42	↑ 190	particles detached from tip and from
		branch-off at bend for about 1 minute
		after head increase + then stopped.
4.03	↑ 200	particle detachment is occurring intermittently
		from tip but progressive laterally.
4.34		still 220-110 + no movement in
		channel.
4.35	↑ 212	
4.52	↑ 224	H's trying to progress. there are now
		2-3 tips trying to form off the
		channel. c HS. About 20-30 particles
		move right on head increase + then
		stop.
5.25	↓ 7	tip now midway btw box + bar 1
		∴ ↓H.
11/08 8.55	↑ 27	
8.57	↑ 41	very small amount of bubbling.
8.59	↑ 127	
9.02	↑ 175	
9.10	↑ 207	
9.20	↑ 225	
9.25	↑ 234	Sand starting to move near exit.
10.06	↑ 238	
10.19	↑ 244	
11.02	↑ 256	
11.15	↑ 268	
11.28		Tip at 20 abl
11.47		" " 32 "
11.59		" " 52 "
12.07	↓ 0	" " 73 " Shut down for day

1ST SAND SAMPLE

Test 80

	time	head	observation
12/08	1.15	↑ 18	
	1.17	↑ 31	
	1.19	↑ 44	Sand starts to bubble
	1.20	↑ 127	
	1.22	↑ 176	
	1.24	↑ 209	tip at 75 abl
	1.29	↑ 218	
	1.40	↑ 236	
	1.44	↑ 245	
	2.07	↑ 265	tip at 81 abl
	2.21	↑ 287	Sand moving better now near exit
	2.30		tip at 90 abl
	2.45		" " 98 " then stopped
	3.08	↑ 302	
	3.27		" " 118 " then stopped
	3.30	↑ 319	
	4.04	↑ 366	
	4.10	↓ 12	* Sand Sample #2
14/08	9.04	↑ 21	
	9.06	↑ 40	
	9.08	↑ 54	
	9.09	↑ 62	Sand starts to bubble (took 25 secs).
	9.10	↑ 125	
	9.12	↑ 200	
	9.14	↑ 229	
	9.16	↑ 249	
	9.17	↑ 266	
	9.21	↑ 293	
	9.25	↑ 306	
	9.29	↑ 320	
	9.34	↑ 334	
	9.38	↑ 348	Getting some sand movement near exit.
	9.52	↑ 360	
	10.00		Erosion around tip - Deepening/widening only.
	10.21		tip at 220
	10.38		" " 250
	10.43		" under bar 2
	10.55		" at 12 ab2 - Casio Multishot @ 110 abl
	11.01	↓ 5	tip at 30 ab2 * Sand Sample # 3

Test 80

	time	head	observation
7/08	9.26	↑ 17	
	9.28	↑ 35	
	9.29	↑ 52	
	9.32	↑ 70	started bubbling –
	9.33	↑ 196	
	9.42	↑ 227	
	9.44	↑ 270	
	9.56	↑ 319	
	9.59	↑ 334	
	10.02	↑ 345	
	10.05	↑ 354	
	10.08	↑ 365	Some sand movement now near exit
	10.14	↑ 373	
	10.42		tip at 35 ab2.
	11.00		" " 110 ab2
	11.03		2x Casio Multishots taken @ 110 ab1
	11.04		tip at 130 ab2
	11.08		" " 145 ab2
	11.19	↓ 12	~~Down~~ " " 170 ab2 *SAND SAMPLE # 4.
8/08	1.49	↑ 26	
	1.51	↑ 39	
	1.53	↑ 52	
	1.55	↑ 62	
	1.56	↑ 70	Sand starts to bubble – Progressively higher each day?
	1.57	↑ 177	
	1.58	↑ 257	
	1.59	↑ 298	
	2.14	↑ 329	
	2.16	↑ 355	Some Sand movement near exit.
	2.27	↑ 374	
	2.36	↑ 380	
	2.50	↑ 387	
	2.59	↑ 398	
	3.09		tip at 195 ab2
	3.14		" " 210 "
	3.15		2x Casio multishots taken @ 110 ab1
	3.21		tip at 225 ab2
	3.24		" " 235 "
	3.29	↓ 15	Somewhere under b3 * SAND SAMPLE # 5

Page 5. TEST # 80

8 8.05 ↑ 40
8.06 ↑ 56
8.07 ↑ 68
* 8.09 ↑ 79 Sand starts to bubble
8.10 ↑ 221
8.14 ↑ 322.
8.32 ↑ 372
* 8.36 ↑ 380 Some sand movement now – near exit.
8.45 ↑ 395 No tip movement.
8.59 ↑ 405
9.17 tip at 15 ab3
9.28 ↓ 9 tip at 130 ab3 * Sand Sample #6.
21/08 1.42 ↑ 24
1.44 ↑ 33
1.45 ↑ 49
1.46 ↑ 66
* 1.48 Sand starts to bubble
1.49 ↑ 245
1.50 ↑ 300
1.56 ↑ 343
2.04 ↑ 360
2.13 ↑ 374
* 2.15 ↑ 385
2.16 Some sand movement now – near exit.
2.23 ↑ 391
2.39 2x Casio multi-shots @ 120 ab1
2.40 ↑ 404 Raised as can't see tip moving.
2.47 tip at 150 ab3
3.04 " " 165 ab3
3.40 Some air under lid – I think this has affected tip movement?!
4.10 ↓ 8 Tip reached 250 ab3 * SAND SAMPLE #7

Page 6

24/08 10·05 ↑ 20
10·07 ↑ 30
10·08 ↑ 45
10·09 ↑ 52
* 10·11 ↑ 68 Sand bubbling starts.
10·12 ↑ 205
10·14 ↑ ~~2~~325
10·25 ↑ 354
10·29 ↑ 370
* 10·47 ↑ 389 Sand Movement now near exit.
10·59 ↑ 399
11·30 ↑ 409 Tip somewhere under bar 4?
11·45 tip at 10 ab4 (Some air around this area)
11·49 " " 20 "
11·51 " " 50 " Air getting trapped in channels (mainly between b3 + b4).
11·55 ↓ shut Test down.
↓ 10

End of Test

See photo for position of pieces

Wax measurements.

Piece ① under bar 2.21mm
next 2 " 2.58 – 1.07mm 1.51

piece ② 4.82 – 2.18 2.64
4.85 – 3.17 1.68
3.73 – 2.4 1.33

piece ③ 3.3 – 2.5 0.8
4.83 – 3.03 1.8
4.87 – 2.8 2.07
7.5 – 3.4 4.1

Test 80

R= 3.3E-4

	time	head	Row 1			Row 2			Row 3						
	time	head	right	middle	left	right	middle	left	right	middle	left	time for 50mL	Avg	Temp	Q
3-8	6.00	177	60	60	58	83	91	88	106	150	115				2.75E6
6-8	3.22	151	46	45	43	64	73	69	83	125	91				
12-8	1.45	245	53	52	55	80	89	85	110	147	104				4E-6
17-8	11.07	373	60	48*	54	92	79*	95	132	175	140				?
21-8	3.47	404	56	52	57	84	82	90	121	160	131				

80. Test 80 (flume 4) circle

Test 80 was the third test in group 5- cyclic loading and was on Sydney sand.

Initiation occurred at 177mm. The first 6 channel segment needed a higher head to reinitiate each time (head needed for the last 4 segments remained reasonably consistent) (see fig 1). At a channel length of 400mm the head required jumped significantly. In fact, the head needed was a minimum of approximately 40% higher than Tests 77 and 79. The only sign why this might have occurred is bubbles were seen in the sample, but not until the channel was 1027mm long. So it doesn't explain why the head was higher between 400 and 1027mm, not unless these bubbles were a sign of other bubbles just beneath the surface. Most bubbles were between bars 3 and 4 (see pic 2).

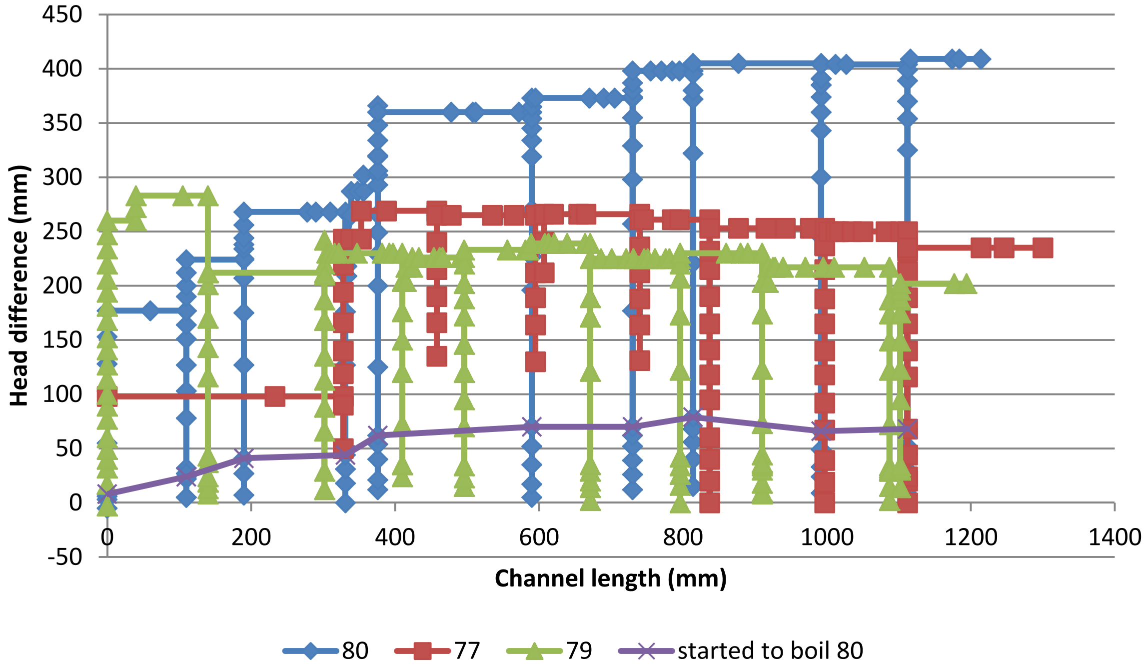

Figure 80-1 Test 80 chart

Head required to start boiling in the exit appears to increase.

With respect to boil sizes. See chart below.

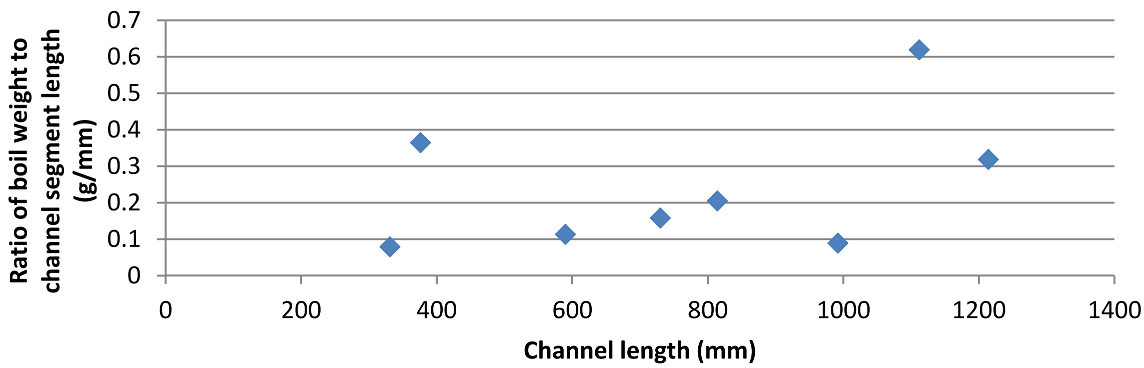

As was the case in Test 77 and 79, it appears the boil increases in size with increasing total channel length, but the trend isn't clear and there are exceptions.

With respect to whether the boil weight could tell me anything about the primary to secondary erosion proportions, I made the same assumptions and used the same technique as done for Test 77 to produce this table and graph:

volume mm3	depth	length	width	primary erosion (g/mm)
16250	1	331	49.0936556	0.07915408
16250	2	331	24.5468278	0.07915408
16250	3	331	16.3645519	0.07915408
16250	4	331	12.2734139	0.07915408
16250	5	331	9.81873112	0.07915408

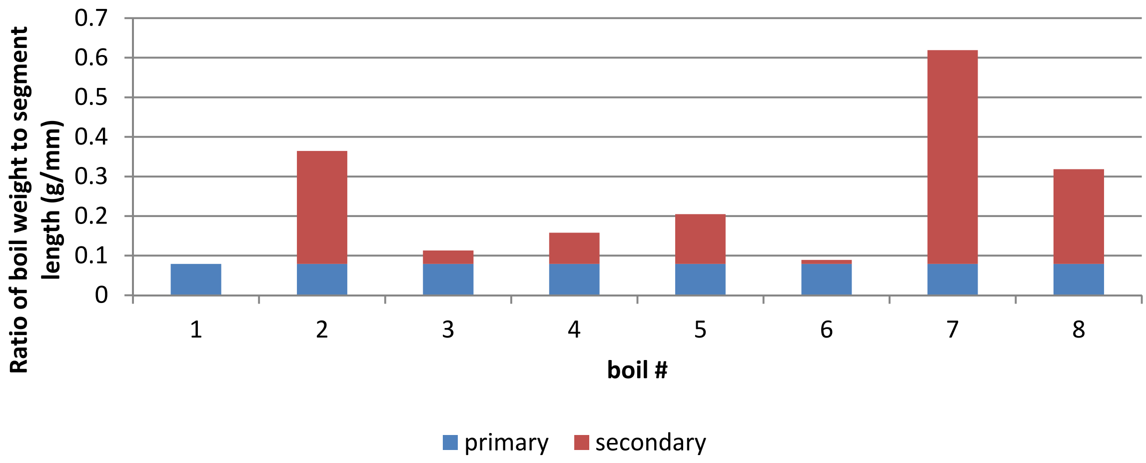

With the exception of boils 3-5, the expected trend of increasing secondary erosion with channel length isn't demonstrated. I'm not surprised boil 7 is the largest because this was the boil when the bubbles were encountered and the bubbles would have slowed tip progression down causing the channel to meander a lot. But this is the only deviation from expected trend that I can explain.

The test was stopped after the last 130mm marker so forward deepening or failure weren't observed.

I tried pouring wax into the standpipe holes again, this time in a smaller steady stream of wax with the hope that escaping air could travel up out of the hole past the wax so wax would be able to flow into the channel. But it didn't work. Wax would still fill the hole before flowing into the channel (see pic 3). So I removed the lid and poured wax both underneath restraining bars resting on the sand and without any cover (see pic 4). See pic 5 for underside of a wax mould showing the channel. Again, the wax pieces were measured using a calliper. Measured depths ranged between 0.8 and 4.1mm and are recorded at the end of the last lab sheet.

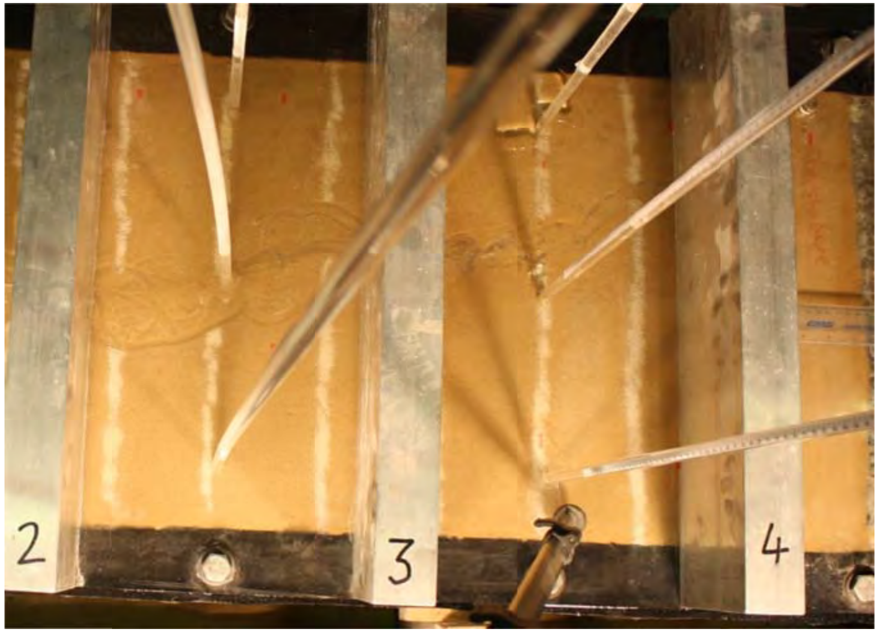

Figure 80-2 Bubbles that appeared in channel between bars 3 and 4

Figure 80-3 Wax filled hole and didn't flow into channel.

Figure 80-4 Wax poured beneath lid restraints and without cover

Figure 80-5 Example of channel mould

Backward erosion piping test data sheet

Test #	81	Exit type	circle
Date	1/09/2015	seepage length	1.3 m
Soil	mix 6	head in bladder tank	5 m
Flume	1	compaction	tamped

	time	head	observation
1/09	9.52	0	Water level 55mm high - inside box
	9.57	↑ 34	
	11.21		" " 59mm " "
	11.22	↑ 84	Sand bubbling starting out @ Exit.
	11.50	↑ 144	Water level 60mm inside box.
	12.55	↑ 171	" " 64 " "
	1.52		" " 73 " "
	1.53	↑ 228	
	2.18	↑ 243	" " 77 " "
	~~3~~ 2.52	↑ 314	" " 83 " "
	3.31	↑ 346	" " 90 " "
	3.54	↓ 0	" " 96 * Tip at 80mm from exit
3/09	11.53	↑ 19	
	11.54	↑ 37	
	11.56	↑ 63	
*	11.57	↑ 92	
	11.59		Sand Bubbling starts. Water level 104mm in box.
	12.03	↑ 162	
	12.24	↑ 190	
	2.28	↑ 240	Hard to see if tip is moving in cloudy water.
	2.29		Water level - 120mm in box.
	3.09	↑ 295	Water now coming out overflow pipe
→	3.15	↑ 348	
	3.55	↓ 10	Tip at 100 mm in box.
7/09	9.03	↑ 25	
	9.04	↑ 54	
	9.09	↑ 92	
	9.20	↑ 125	Sand starts to bubble at exit.
	9.21	↑ 248	
	9.58	↑ 307	
	10.11	↑ 383	

Unable to see tip movement until cleared the next day.

Test 81

	time	head	observation	
	10.46	↑ 415		
	11.02	↑ 447	tip seems to be widening near exit (not extending).	
	1.04	↑ 490		
	2.03	↑ 547		
	2.20	↑ 622		
	2.46	↑ 667		
	3.19	↓ 2.	Water in box very cloudy, can see tip	
			just between box and bar 1, so shut down	
			for day. * Sand Sample #1 Taken.	
9/09	7.55	↑ 37		
	7.56	↑ 87		
	8.19	↑ 141	Sand bubbling at exit	
	8.55	↑ 250		
	9.34	↑ 351		
	9.51	↑ 434		
	10.20	↑ 467	Tip under bar 1	
	10.59	↑ 497		
	11.25	↑ 540		
	11.41	↑ 575		2+3
little too high →	1.15	↑ 626		as tip
	1.47	↓ 17.	Tip now at 170 ab3 *Sand Sample #3.	moved
10/09	1.28	↑ 95	· starts to bubble -	so
	1.30	↑ 303		fast.
	1.39	↑ 464		
	2.13	↑ 568		
	2.44	↑ 596		
	3.02	↓ 26.	Tip under bar 2 - Tip as a sheet 30-40mm wide	
11/09	1.20	↑ 91	Sand bubbling at exit.	
	1.21	↑ 245		
	1.25	↑ 456		
	1.30	↑ 551	Some sand movement between b1 + b2	
	1.53		Tip A at 35 ab2 / tip b at 140 ab1	
	2.04		tip A at 132 ab2	
	2.05	↓ 5	tip A at 135 ab2. For Weekend.	
14/09	9.05	↑ 87	Tip A " " * Sand Sample #4.	
	9.09	↑ 245	Tip B at 130 ab1	
	9.18	↑ 348		
	9.45	↑ 480	Water measurement started.	
	10.12		Tip A at 182 ab2.	

Test 81

Seems to be just right gradient
↑ for slow sand movement.

	time	head	observation	
	10.17	480	TipA at 220 ab2. / Tipb at 160 ab1	
	10.20		TipA at 250 ab2 * Sand Sample #6.	5?
	10.21	↓ 15		
15/09	8.49	↑ 51	Moving up in small incriments to see when	
	8.50	↑ 75	Sand bubbles - Hard to see, trying to keep	
	8.51	↑ 145.	* Sand bubbling now water clear/undisurbed.	
	8.55	↑ 305		
	9.00	↑ 412.		
✓→	9.32	↑ 479	* Sand movement now between b2 + b3	
	9.37		tip A at 40 ab3, tip b at 175 ab1	
	9.40		" " 70 "	
	9.50	↓ 28	" " 80 " * Sand Sample #7.	6?
16/	9.10	↑ 87	Sand starts bubbling - very small.	
	9.12	↑ 352		
	9.30	↑ 433	Some sand movement now between b1 + b2.	
	9.40		" " " " " b2 + b3	
	9.49		" " " " " b3 + b4	
	10.02		Tip A starting to move, @ 82 ab3.	
✓→	10.18	↑ 466	Lifted head as sand movement stopped.	
	10:26		Tip A at 160 ab3 (Tip b as joined A @ 30 ab2)	
	10.30	↓ 12	" " 208 " * Sand sample #8	7?
17/09	9.04	↑ 40		
	9.06	↑ 68	Sand bubbling after 3 minutes	
	9.15	↑ 316		
	9.18	↑ 428		
	10.15	↑ 465		
	10.21		Sand movement now, mainly between b1 + b3.	
	10.39		Tip A at 12 ab4.	
	10.50		tip A " 30 ab4	
	10.52		Another Tip formed (tip C) brached out at 100 ab3	
			headed westward. now at 235 ab3.	
	11.09		Tip A at ~~30~~ 38 ab4 / TipC ~~at~~ under b4.	
	11.34	↑ 480	Sand movement seems to have stopped.	
	11.52	↑ 518		
	12.03	↑ 582	Tip A at 30 ab4 / TipC at 32 ab4	
	12.20		" " 47 "	
	12.36		" " 52 "	
	12.51	↓ 7	" " 80 " * Sand Sample #9	8?
			Very Hard to see where tip is	

as there is sheet Erosion which appears to be lower down than surface? HS.

Test 81

K = 2.2E-5

using 4x2 Wood.

Q

	time	head	Row 1			Row 2			Row 3			time for 50mL	Avg	Temp	
			right	middle	left	right	middle	left	right	middle	left				
1/09	1.00	171	179	171*	171	212	211	208	251	252	251				
7/09	10.14	383	266	261*	257	344	344	338	428	429	242				7.6E-7
9/09	11.45	575	334	329*	322	453	451	450	580	580	579				1.3E-6
14/09	9.47	480	228	270*	263	355	350	353	489	489	487				1.3E-6
15/09	9.36	479	240	270*	282	374	377	379	489	486	484				
17/09	10.53	465	226	205*	232	331	315	328	461	456	465				

81. Test 81 (flume 1) circle

Test 81 was the first test in group 5- cyclic loading carried out on Mix 6.

Test 81 initiated at a head of 346mm or less. ‘Or less’ because initiation couldn’t be seen through the turbid water. The first channel segment of 80mm was only seen the next day once 300g product had settled.

The third cycle, once the tip had reached 120mm, required a large jump in head, from 346 to 667mm. There was no indication as to why this was. From there the head required to reinitiate each segment gradually reduced down to a head of around 480mm for the last 4 segments. When the channel was only 116mm from the upstream end it stopped progressing and needed a significant head increase to reach the upstream end. Perhaps this was on account of a channel blockage because at around the same time the channel was seen to widen significantly (to almost 1/3 of the flume’s width) and look more like sheet flow than channel flow. See pic 2.

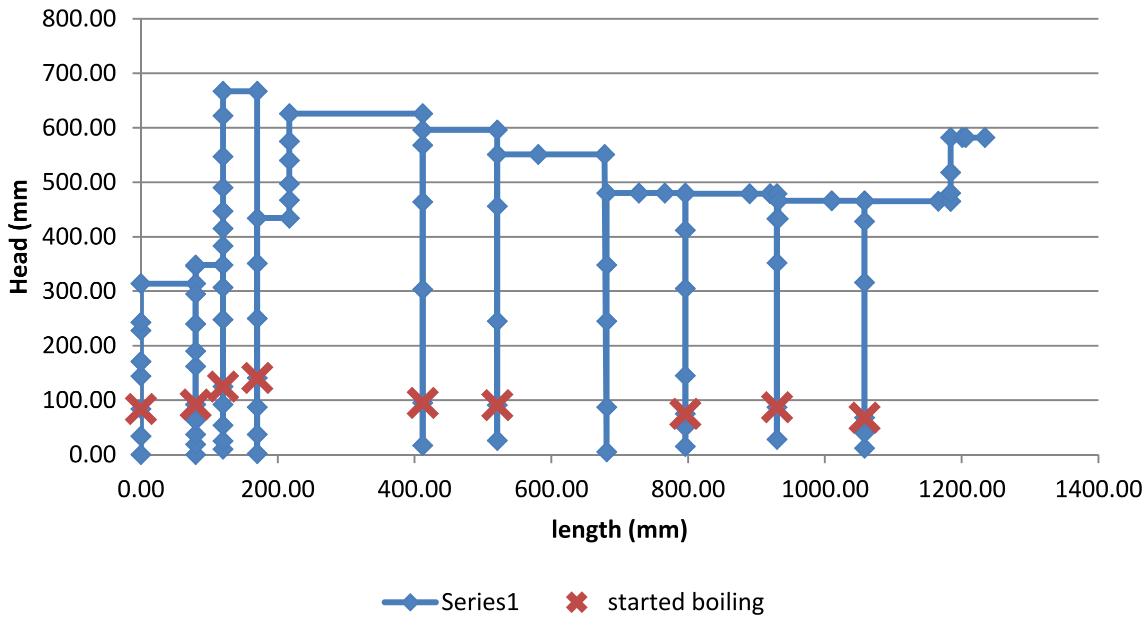

Figure 81-1 Test 81 plot

Throughout the experiment Hamish often noted that sediment transport could be seen in downstream portions of the channel prior to the tip reinitiating.

3 distinct channel tips formed during the experiment but it was the first tip that reached the upstream end.

The head at start of boiling was noted however it was difficult to define because it was difficult to see through the turbid water. As can be seen in fig 1 the head required for boiling increased with each channel segment at the start of the test but then levelled out to be much the same for the remaining segments.

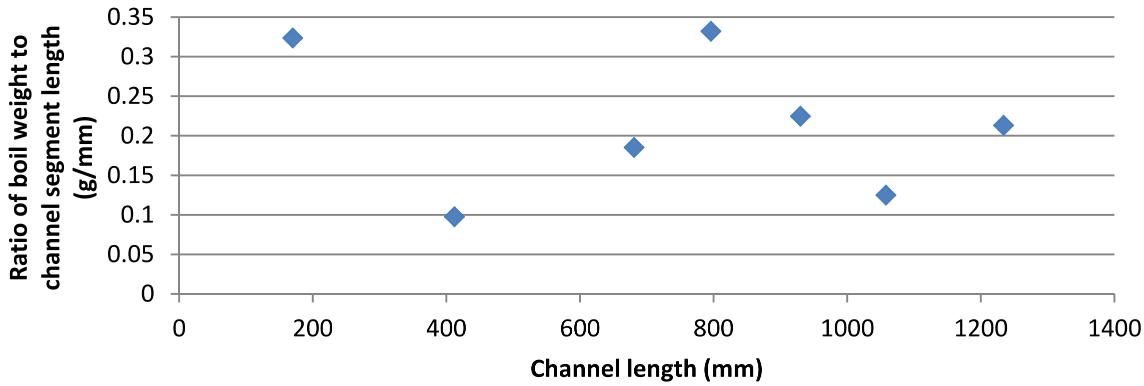

This shows there was no clear trend or pattern with successive boil weights.

The first boil weight was reported to be 37g (not including any soil left in the exit shaft). But I don't believe this because a) all other first boils were between 2-11g, b) the channel segment when the boil was removed was much shorter than all other tests (170mm where others were around 300mm) c) it doesn't look like 37g worth- see pic 3 and d) when I enter 37g into table below I get channel widths that are too wide.

volume mm3	depth	length	width	primary erosion (g/mm)
21764.71	1	170	128.0277	0.323529
21764.71	2	170	64.01384	0.323529
21764.71	3	170	42.67589	0.323529
21764.71	4	170	32.00692	0.323529
21764.71	5	170	25.60554	0.323529

If I can't trust the first sand boil weight I have then I can't do the primary to secondary portion chart I've done for previous tests.

The test was stopped after the last 130mm marker so forward deepening or failure weren't observed.

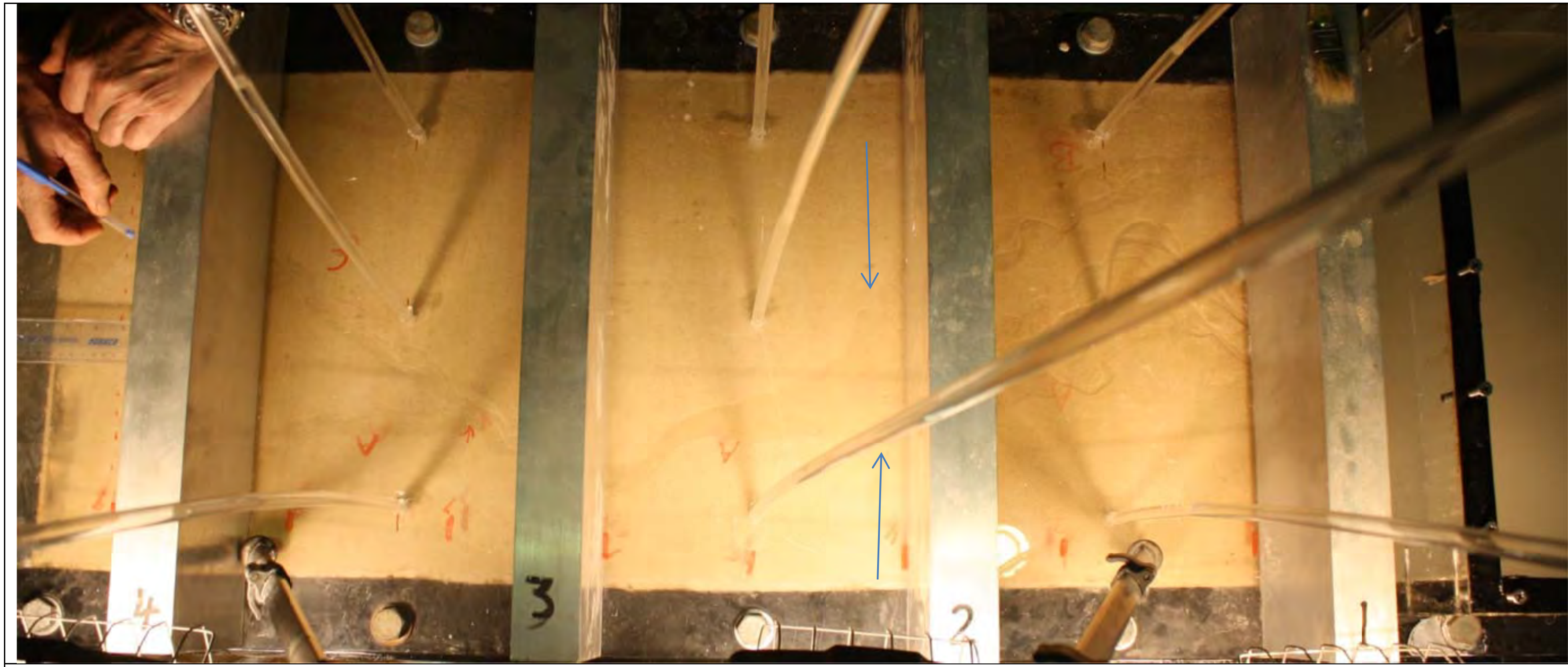

Figure 81-2 Approximately when head needed substantial increasing- possible channel blocking shown btw bars 2 and 3

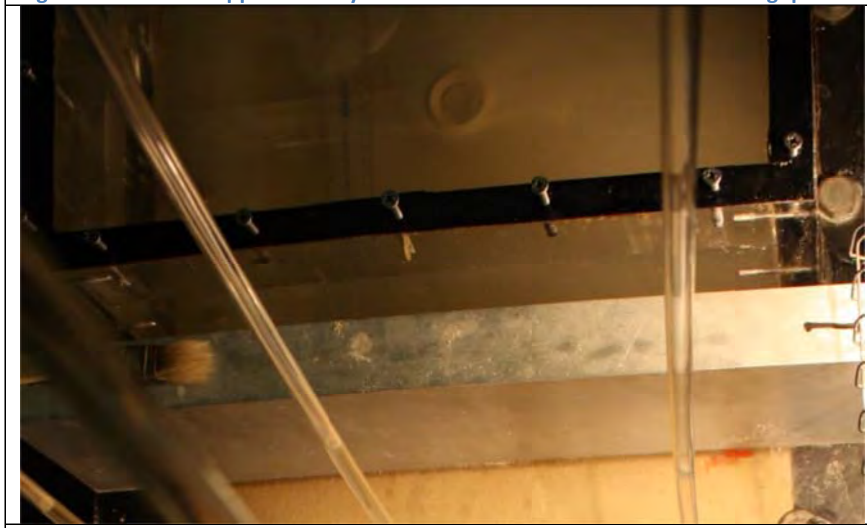

Figure 81-3 First boil. Unlikely that it was 37g as records indicate.

Figure 81-4 Example of a boil from Test 79 that was reported to be 35g

Backward erosion piping test data sheet

Test #	82	Exit type	circle
Date	23/09/15	seepage length	1.3 m
Soil	mix 6	head in bladder tank	5 m
Flume	4	compaction	tamped

	time	head	observation
23/09	8.45	−15	Water level @ 90 mm inside box
	8.46	↑ 13	
	9.44	↑ 64	" " 93 "
	10.44	↑ 146	" " 95 "
	11.26	↑ 233	" " 100 "
	12.50	↑ 296	" " 115 "
	1.50	↑ 324	Water now out Exit pipe
	2.59	↑ 403	
	3.55	↓ 22	Tip at edge of box somewhere *Sand Sample 1
24/09	2.24	↑ 126	
	2.27	↑ 240	
	2.29	↑ 342	No sand bubbling yet.
	2.34	↑ 445	
	2.56	↑ 525	Sand starting to move between exit + b1
	3.12	↑ 618	Sand movement has stopped
	3.15	↑ 677	
	3.27	↑ 741	
	3.34		Tip at 35 ab1
	3.36		" " 40 "
	3.38		" " 65 "
	3.39	↓ 36	" " 75 " *Sand sample #2.
25/09	1.31	↑ 159	Sand starting to bubble after 1 min.
	1.34	↑ 526	
	1.49		Tip at 140 ab1
	2.04		" " 180 "
			" " 205 " *Sand sample # 3
	2.05	↓ 22	
28/09	9.17	↑ 110	
	9.20		Sand Started to bubble.
	10.08	↑ 323	
	10.11	↑ 501	Sand starting to move near exit.

	time	head	observation
28/09	10.14	501	Sand moving between b1 + b2
	10.15		Tip at 240 ab1
	10.19		" " 240 "
	10.21		" Under b2
	10.26		" at 15 ab2
	10.28	↓ 18	" " 65 ab2 * Sand sample # 4.
29/09	11.43	↑ 137	Sand bubbling after 1 min
	11.45	↑ 472	Some sand movement between b1 + b2.
	12.58	↓ 33	Tip at 200 ab2. * Sand Sample # 5.
30/09	2.23	↑ 166	Sand started bubbling.
	2.28	↑ 429	Tip at 235 ab2
	2.49	↑ 525	
	3.25	↑ 567	Tip under b3
	3.42	↓ 34	Tip @ 10 ab3 * Sand Sample # 6.
/10	1.52	↑ 84	Sand started to bubble
	1.54	↑ 256.	
	2.05	↑ 507	
	2.30		Tip @ 55 ab3
	2.54		tip @ 70 "
	3.04		" " 95 "
	3.12	↓ 29	Tip @ 155 " * Sand Sample # 7
/10	10.12	↑ 84	
	10.14	↑ 121	Sand bubbling after 1 min
	10.16	↑ 397	
	10.35	↑ 506	Tip now 160 ab3
	10.40		" 175 "
	10.49		" 215 "
	11.03	↓ 24	" 245 " * Sand Sample # 8.
19-10	11.34		Even though there's 1 more 450mm
			'leg' to go I'm going to finish
			the experiment here because it's
			been sitting for 17 days + could be
			effected by bio-clogging (although
			I can't see discolouring) and I'd
			like to dismantle + move ASAP. So
			end of test.

Test 82

k=2.3E-5

Q

			Row 1			Row 2			Row 3						
	time	head	right	middle	left	right	middle	left	right	middle	left	time for 50mL	Avg	Temp	
23/09	12.54	296	~~200~~ 81	~~195~~ 200	~~[illegible]~~ 76	146	155	~~[illegible]~~ 152	205	249	212				
24/09	3.22	677	223.	344	220	364	367	368	498	541	507				1.5E-6
1/10	3.04	507	94	–	88	162	1:53	1:57	255	280	265				

82. Test 82 (flume 4) circle

Test 82 was the second test in group 5- cyclic loading carried out on Mix 6.

Test 82 initiated at a head of 403mm. The 2nd cycle required a much larger head at 741mm (84% increase). From there the critical head decreased for the next 3 cycles until the channel reached 795mm in length. Then the critical head increased a small amount although this increase might not have been necessary because I notice Hamish increased the head from 429 to 525mm which skipped the head it was progressing at in the previous cycle of 462mm. So it could have progressed at a smaller or similar head. Also, it was increased again to 567mm but the tip was under the bar at the time so it might have still been progressing but just slowly. In the remaining cycles the head needed 'levelled out' to a head of around 500mm. See fig 1.

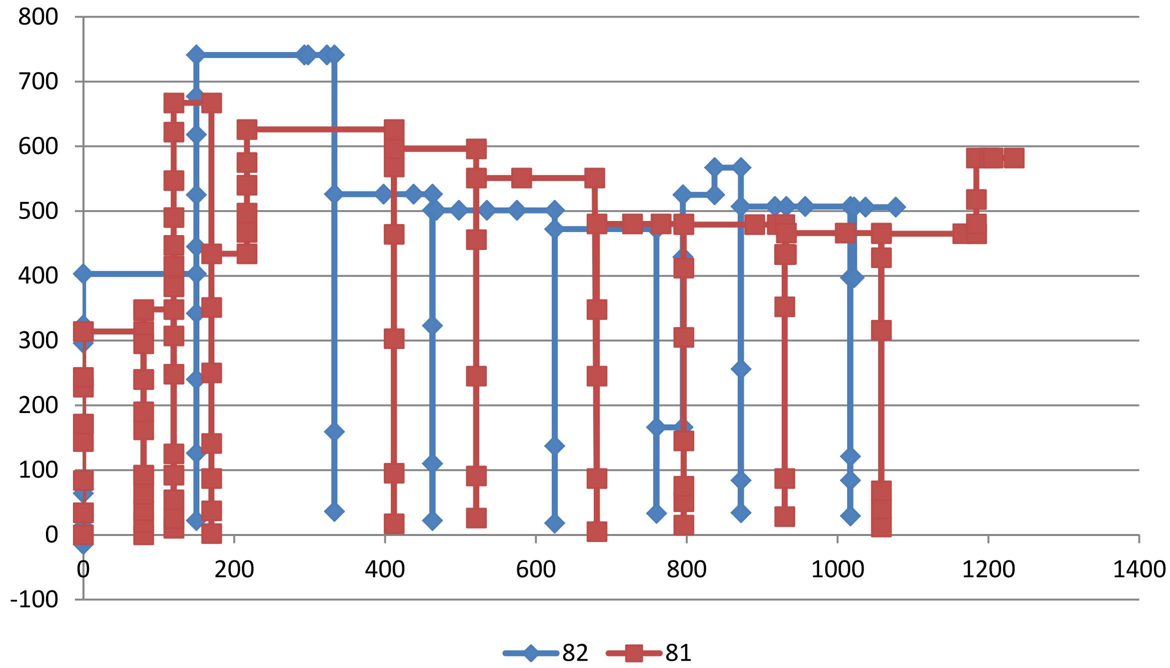

Figure 82-1 Test 82 plot

Throughout the experiment Hamish often noted that sediment transport could be seen in downstream portions of the channel prior to the tip reinitiating.

Whilst first sand boiling was noted by Hamish, he increased head in large steps so it wasn't known whether boiling would have commenced at lower heads.

The last 130mm segment wasn't tested because 17 days had passed between Hamish's last day and me returning. I was concerned that after 17 days the soil could be affected by bio clogging (although I couldn't see any discolouration) and I was keen to dismantle the test and move on. This also means that forward deepening or failure were not observed.

With respect to boil sizes. See chart below.

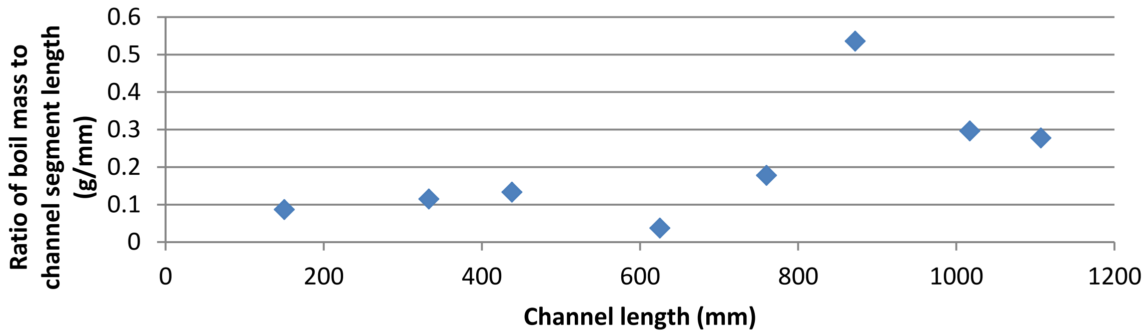

As was the case in Test 77 and 79, it appears the boil increases in size with increasing total channel length, but the trend isn't clear and there are exceptions.

With respect to whether the boil weight could tell me anything about the primary to secondary erosion proportions, I made the same assumptions and used the same technique as done for Test 77 and 80 except that I assumed the densities of Mix 6 was 1.5E-3 g/mm3 min and 1.7E-3 g/mm3 max. I didn't have lab tests carried out on Mix 6, only Mix 8, so these densities are an estimate between Sydney sand and Mix 8. This is the resulting table and graph:

volume mm3	depth	length	width	primary erosion (g/mm)
7647.05882	1	150	50.9803922	0.08666667
7647.05882	2	150	25.4901961	0.08666667
7647.05882	3	150	16.9934641	0.08666667
7647.05882	4	150	12.745098	0.08666667
7647.05882	5	150	10.1960784	0.08666667

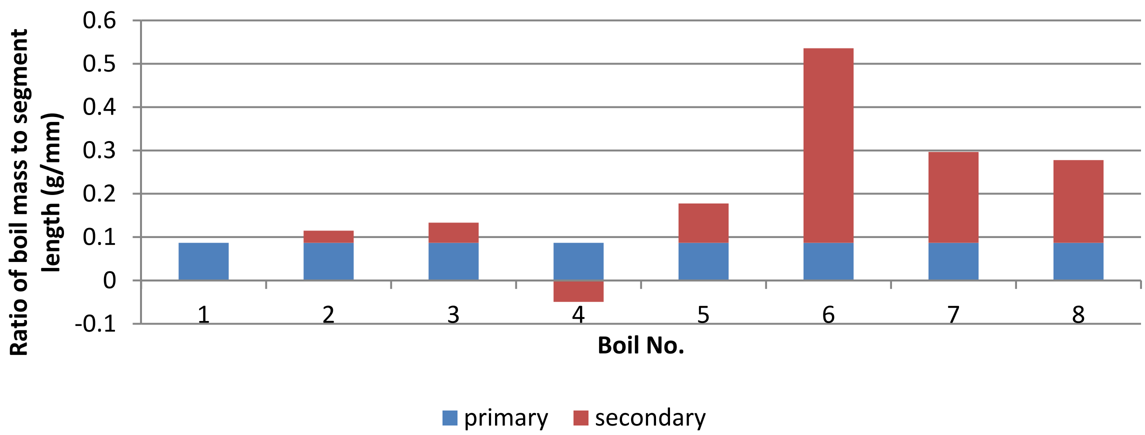

Normally I assume the exit shaft was full of sand when the first boil was removed so I add 18g to the first boil weight however I didn't in this case. In fact I didn't add any mass to it because given the channel length was only 150mm it is unlikely the full shaft was full yet and it doesn't appear to be full in pic 2 (although it's not a good photo) and when I did add mass onto the first boil the calculated channel width became too wide and unlikely to be correct.

The expected trend of increasing secondary erosion with channel length is somewhat demonstrated, although there are exceptions to this trend and it is not clear, as has been the case for other cyclic tests.

Figure 82-2 first sand boil before it was collected showing exit shaft was not full of sand

avg crit 208
$\frac{208}{347} = 167\%$

Backward erosion piping test data sheet

Test #	83	Exit type	circle
Date	2/11/2015	seepage length	1.3 m
Soil	Syd sand	head in bladder tank	5 m
Flume	1	compaction	vibrated

time	head	observation
10:55	datum 0	
11.10	↑ 347	
11.12		130 ab1. Sheet flow.
11.14		210 ab1. 3 tips but one is ~~so~~
		longer than the others.
11.14		@ b2, tip a split into 2.
11.15		20 ab2
11.16		80 ab2
		tip C slowed significantly
11.17		140 ab2.
		channels split & converge repeatedly. [High speed photos @ midway b/w B2 & B3]
11.18		@ B3.
11.19		Tip C progression stopped
		Tip B @ B2.
11.20		Tip B 10 AB2
~~11~~		Tip A 20 AB3.
11.21		100 AB3 Tip A.
11.22		High speed photos [AB2 || BB3]
		High speed photos [AB3 ↑ BB4]
11.23		80 AB2 Tip B
		180 AB3 Tip A1 } Tip A split into 2
		120 AB3 Tip A2 }
11:25		Tip A1 At B4
11:26		5 AB4
11:27		25 AB4
11:28		Tip A1 splitting - split did not progress
		Tip A1 90 AB4
		Close to blocking b/ween B2 & B3
11:29		110 AB4
11:30		A2 @ B4

11

ab1 = after bar 1

CHS = see happy snap

Test No. 83

time	head	observation
11:30		130 AB4 (Tip A2)
11:31		@ u/s but moving laterally due to panel.
11:34		not sure fwd deepening gonna
		occur because u/s panel pushed
		up against lid preventing channel
		from opening into u/s chamber.
11:38		Some deepening of channels near b4
		~~b4&~~ close to blockage b/ween b3 & b4.
		Some blockage near b3.
11:48		gap made near u/s filter
Standpipe levels		
R1	~~left~~	218
	mid	206
	right	218
R2	left	280
	mid	270
	right	282
R3	left	371
	mid	382
	right	371
3:01		failed.

Test 83 (flume 1) circle

Prepared by Angela Greenlees

Test 83 was the first of the amplified loading tests. All of these tests will be performed on uniform Sydney sand with a circle exit.

The camera was set up to take photos at intervals of 1 minute which was too far apart for this test speed.

The upstream filter was taped over the edges of the internal plate, which was extremely bulky and pressed against the lid. This seemed to prevent failure to some extent by restricting the flow considerably; however the flow during piping did not seem to be affected.

The head was raised to 347mm (167% of critical) and it took 36 minutes for the pipe to reach the upstream end.

There was significant branching early in the piping process;

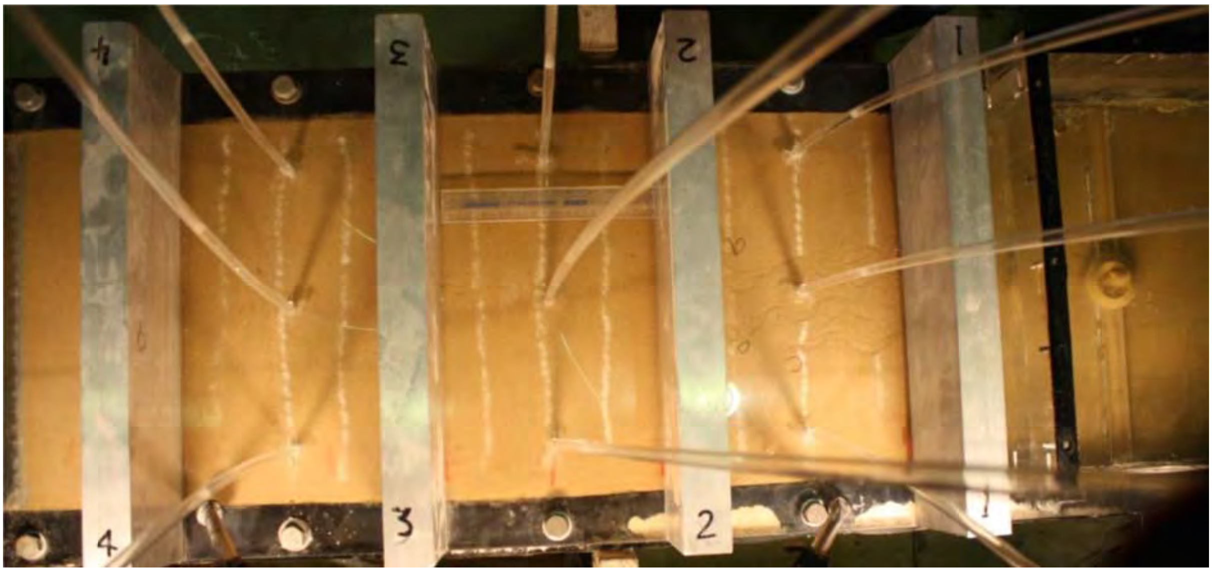

However, the number of branches reduced as the pipe travelled upstream.

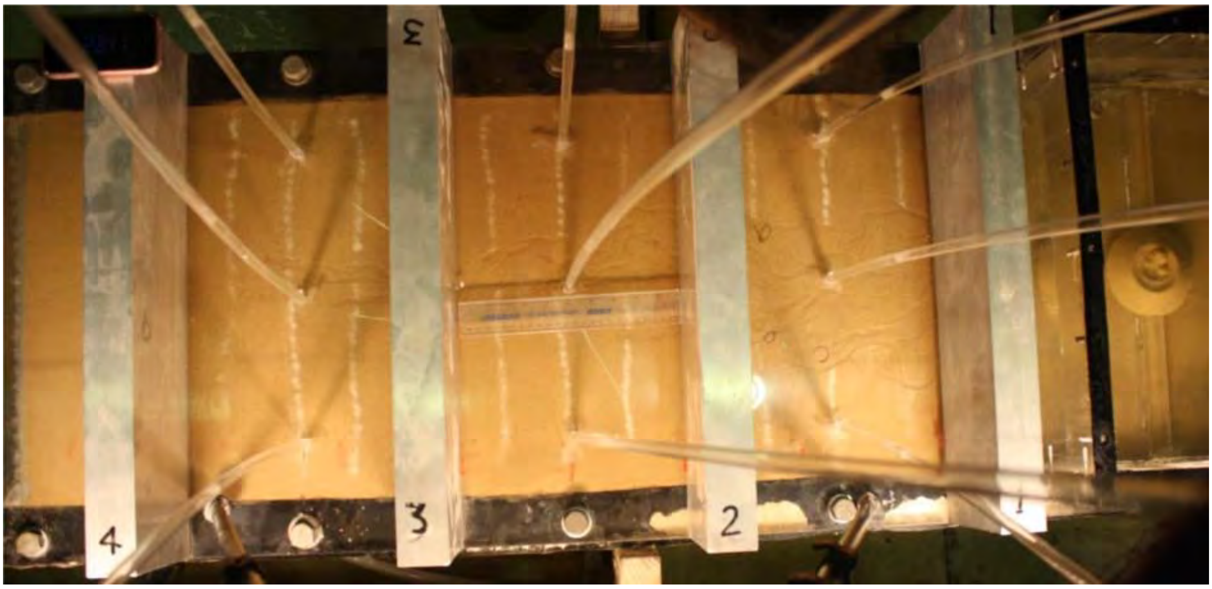

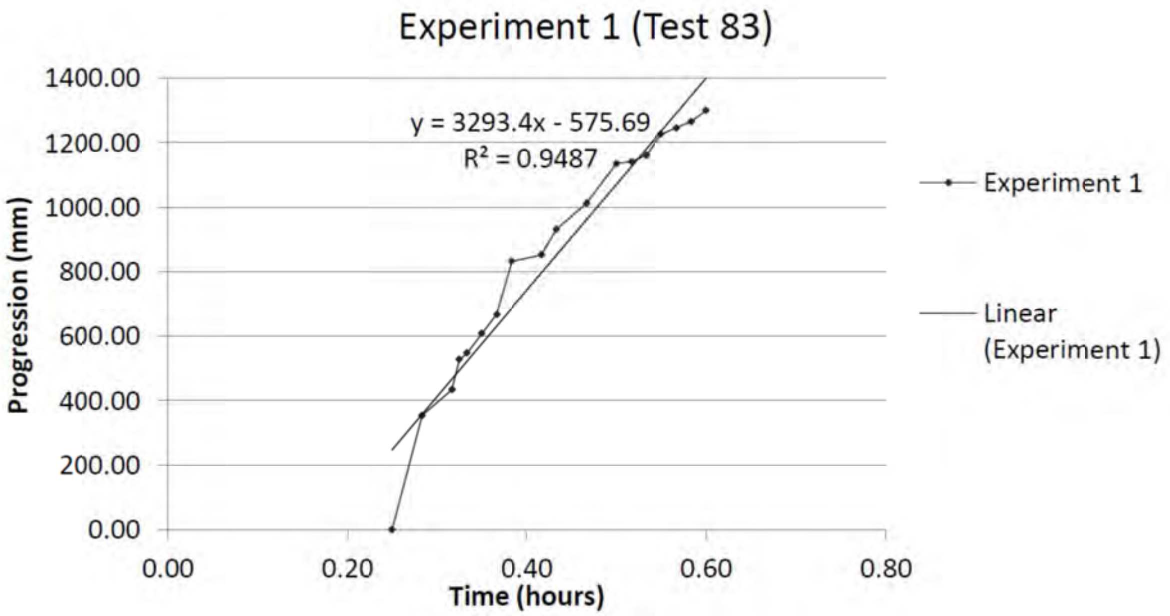

The gradient of the line of best fit shows the tip speed of the pipe, which was 3293.4mm/hour or 0.915mm/s.

There was significant sheet flow at the beginning of the experiment which may indicate that sheet failure will occur along the length of the flume at higher heads.

Backward erosion piping test data sheet

Test #	84	Exit type	circle
Date	27/11/2015	seepage length	1.3 m
Soil	Syd sand	head in bladder tank	5 m
Flume	1	compaction	vibrated

ST.
measured in [illegible] for [illegible]

time	head	observation
		Note that there are air bubbles present in sample. [CHS]
		~~[illegible]~~
		~~[illegible]~~
~~[illegible]~~		
13:45	0(datum)	
13:46	100	
13:47	200	
13:48	300	
13:49	36~~7~~	Initiation
0:31		~~ab~~ @b1 (2 channels)
1:28		30mm ~~@~~ AB1
2:30		70mm AB1
3:54		2a 160mm AB1
		1b 130mm AB1
		1a 80mm AB1
		2b 80mm AB1
6:12		3 70 AB1
		2a 240AB1
		1b 190 AB1
7:26		2a 10AB2
		2b ~~stopped~~ @ 90 AB1
		1a slowing 180 AB1
		1b slowing 240AB1
8:40		2a 40mm AB2
		4 240mm AB2
10:00		~~8~~ 2b 80mm AB2
10:50		2a 130mm AB2
		2b 110mm AB2
		4 @ B3
13:30		2b 230mm AB2
		2a 180mm AB2

time	head	observation
		1B 80mm AB2
		2A stopped @ 220mm AB1
		4 stopped @ B3
16:00		2b 10 mm AB3
17:30		2b 50mm AB3
		1b slowing 140mm AB2.
18:40		2b 120mm AB3.
20:00		2b 170mm AB3
21:20		2b 210mm AB3.
		1b tip slowed
22:00		2b 245mm AB3
22:40		2a 40mm AB3
23:30		2a 70 mm AB3
24:05		2a & 2b joined at SP3m.
24:40		2 10mm AB4.
25:10		2 50mm AB4
25:40		105mm AB4
26:00		u/s
		forward deepening begins
28:11		" " at B4
1:32:14		failure.

Test 84

		Row 1			Row 2			Row 3					
time	head	right	middle	left	right	middle	left	right	middle	left	time for 50mL	Avg	Temp
			.										
1:54		229	210	237	316	307	303	395	392	389			
12:00		222	226	208 [a]	304	288	295	387	385	383			
33:00		229	225	220	311	304	314	419	476 [b]	418			
1:00:57		288	278	281	395	471	390	444	483	454			
1:32													

a) Tip 3 underneath

b) ~~find~~ deepening underneath

Test 84 (flume 1) circle

Prepared by Angela Greenlees

Test 84 was the second of the amplified loading tests. The camera was reset to take photos at intervals of 30 seconds, which worked well for this test.

The upstream geotextile was replaced and trimmed back from the edges of the plate to prevent the filter pressing against the lid, which fix the problem that occurred in the previous test.

The head was raised to 367mm (176% of critical) and it took 30 minutes for the pipe to reach the upstream end and 1 hour 36 minutes to fail.

There were small air bubbles between Bar 1 and Bar 2, and to the left and right hand sides of the exit. The central standpipe between Bar 2 and Bar 3 leaked slightly however it is unlikely that this affected the test.

Again, there was significant branching early in the piping process;

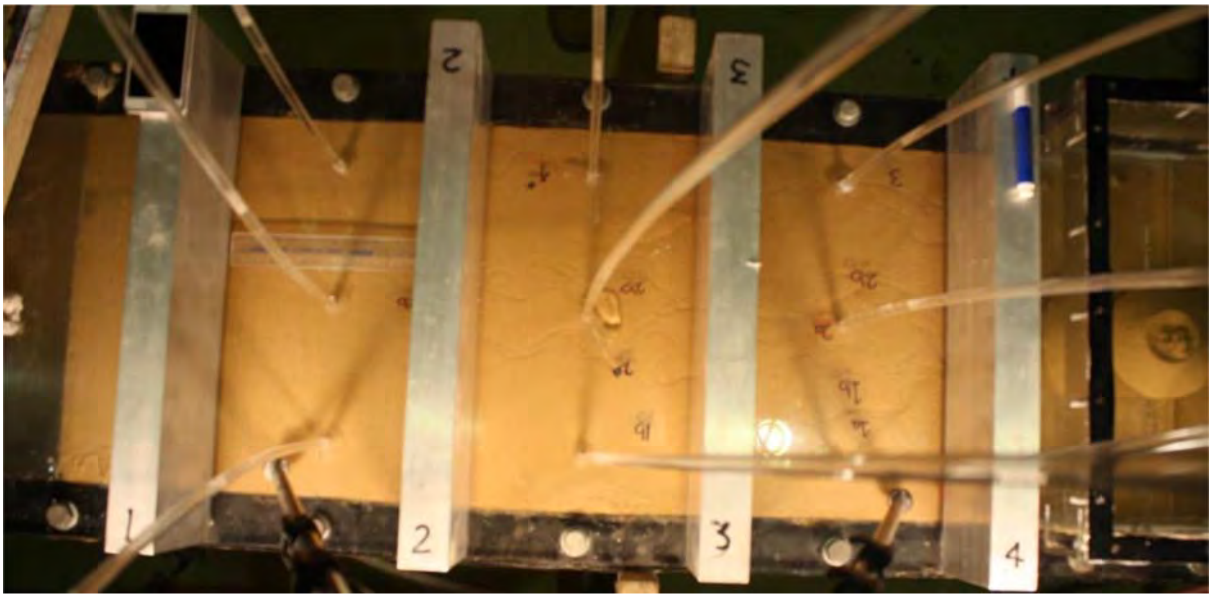

It should be noted that “pipe 4” appears to have formed along the LHS wall of the flume, likely due to the bladder being a curved surface of pressure that results in lower pressure at the edges of the flume.

The branching continued until after Bar 3, where the pipes converged to the upstream section. Forward deepening was fairly straight and failure occurred quickly.

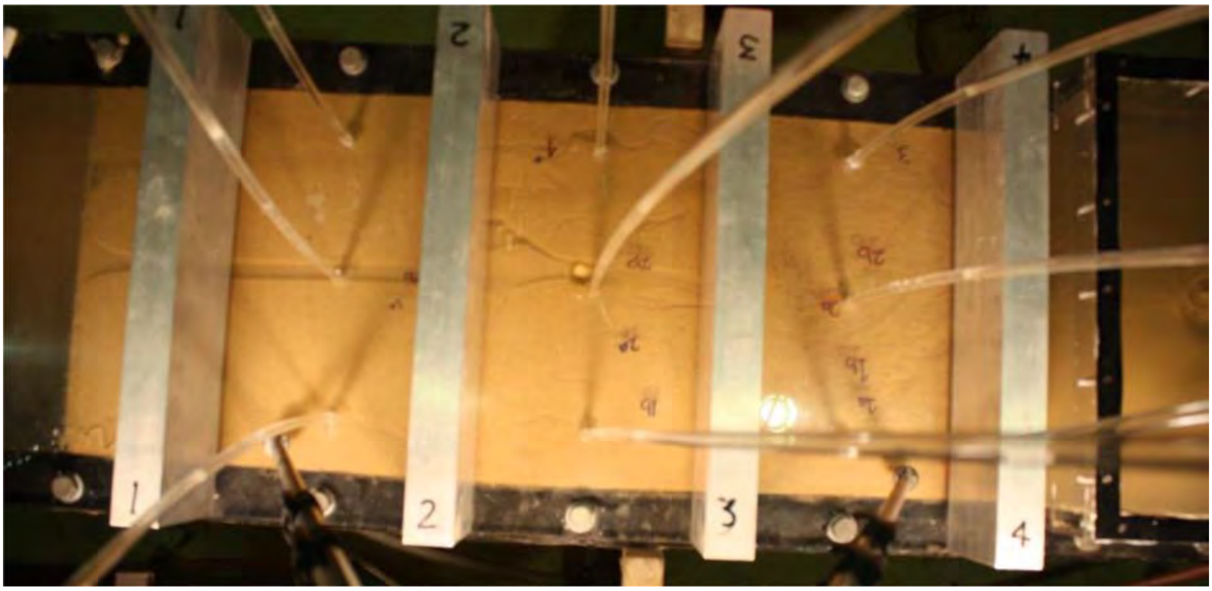

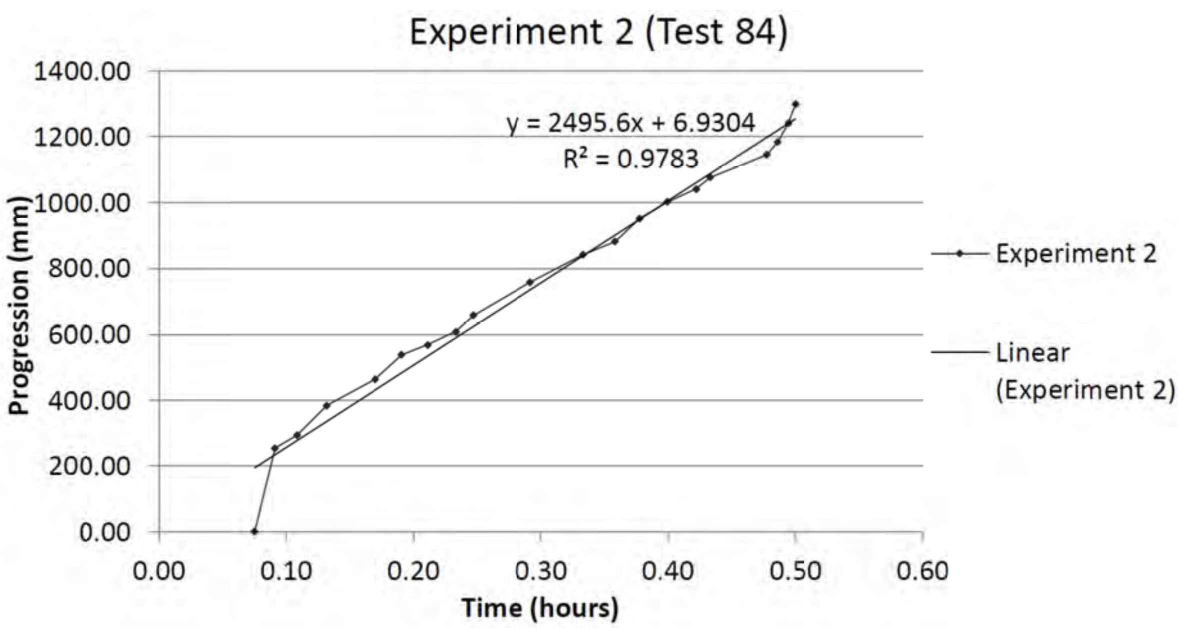

The gradient of the line of best fit shows the tip speed of the pipe, which was 2495.6mm/hour or 0.693mm/s.

Backward erosion piping test data sheet

Test #	85	Exit type	circle
Date	3-12-157	seepage length	1.3 m
Soil	Syd sand	head in bladder tank	5 m
Flume	1	compaction	vibrated

head increase due to piping failure

time	head	observation
B:02	0	
46	95	boiling
53	100	
1:23	150	movement 5cm upstream
1:53	200	initiation
2:32	300	4 tips, longest under tank wall
3:39	314	1 50 ab1
4:44		1 110 ab1
5:11		2 80 ab1
		1 140 ab1
5:30		1 160 ab1
5:46		1 170 ab1
6:18		high speed photos of 1 & 2
6:32		1 200 ab1
7:38		1a 240 ab1
		1b 220 ab1
		2 120 ab1
8:54	440	1a 20 ab2
9:10		1a 60 ab2
9:46		1b 50 ab2
		1a 100 ab2
10:05	313	
11:00		1a 130 ab2
	325	1b 70 ab2
11:30	333	1a 160 ab2
11:51	313	2 stopped
12:22		1a 170 ab2
13:10		1a 170 ab2
	322	1b 70 ab2
13:56		1a slowing down & picking back up
14:18	326	1a 210 ab2

Test 85

time	head	observation
		1c stopped
14:42	313	1a 240 ab2
		1b 80 ab2
15:05		1c Started again
		1b 90 ab2
		1a 240 ab2
15:45		1a & 1c joined
16:00		1a 250 ab2
16:50	324	1b 90 ab2
17:03	313	1a 20 ab3
18:00	324	1a 40 ab3
18:15	313	1a 50 ab3
18:30		1b 120 ab2
18:50		1a 90 ab3
19:15		1a 130 ab3
19:30		1a 170 ab3
		2 joined 1
20:00		1a 170 ab3
		1b 160 ab2
20:30		1a 170 ab3
21:30		1a 180 ab3
24:00		1a 200 ab3
		1b 210 ab2
25:00		1b 240 ab3
26:00		1a @ b4
		1b @ b3
27:22		1a downstream blockages
		1a 50 @ b4
27:45	335	1a 70 ab4
		1b 10 ab3
28:09		1a 80 ab4
28:25	313	1a 100 ab4
28:45		1a 130 ab4
29:00		u/s
29:40	345	forward deepening
29:47	313	
2:07pm		failure

Test 85

		Row 1			Row 2			Row 3					
time	head	right	middle	left	right	middle	left	right	middle	left	time for 50mL	Avg	Temp
13:25	313	219	208	213	274	254	262	348	336	345			

Test 85 (flume 1) circle

Prepared by Angela Greenlees

Test 85 was the third of the amplified loading tests. There were no time lapse photos recording this test due to the timer attachment running out of battery.

The head was raised to 313mm (150% of critical) and it took 28.8 minutes for the pipe to reach the upstream end and 1 hour 5 minutes to fail.

It is important to note with this test that the bilge pump in the constant head tank stopped working during this test, meaning the head jumped to 440mm which was observed as the pipe head reached Bar 2. The head was manually dropped back to 313mm however it jumped to 326 again before the pipe head reached Bar 3. For the rest of the test, the head did not reach more than 315mm before being immediately dropped. It is estimated that the average head for this test was 330mm (159% of critical).

The head jump was noticed when the pipe began moving very quickly and not much branching was observed. Once the head was dropped, the pipe progressed slower than in previous tests, but it must be questioned whether this data point is valid due to the uncertainties about the head.

There were two distinct branches during piping progression, and each of these continued to branch. The overall progression was not straight or direct.

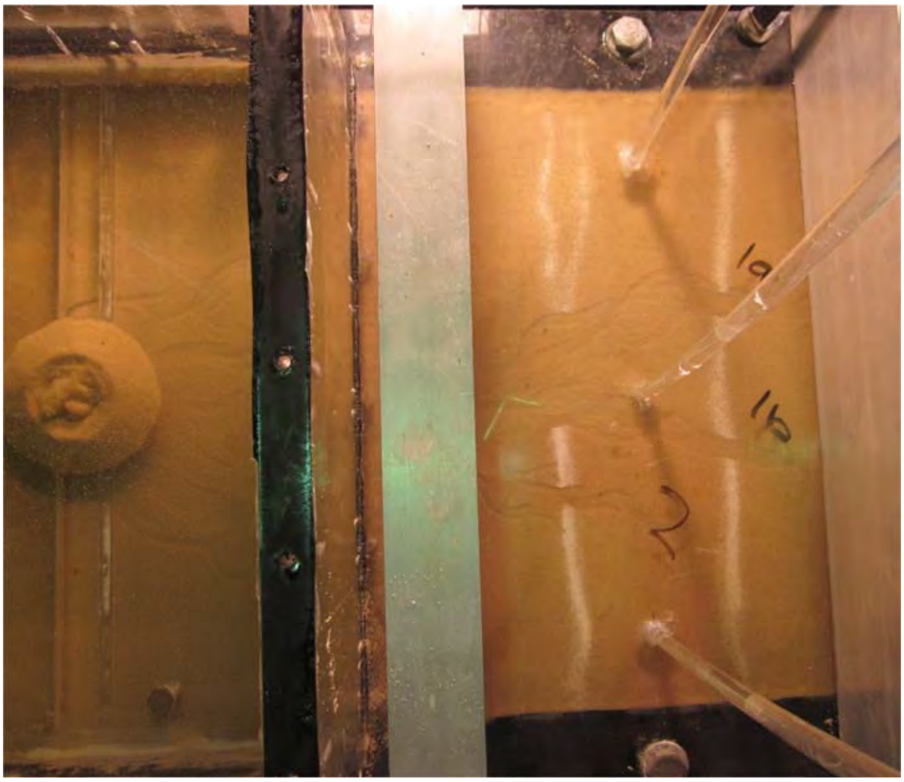

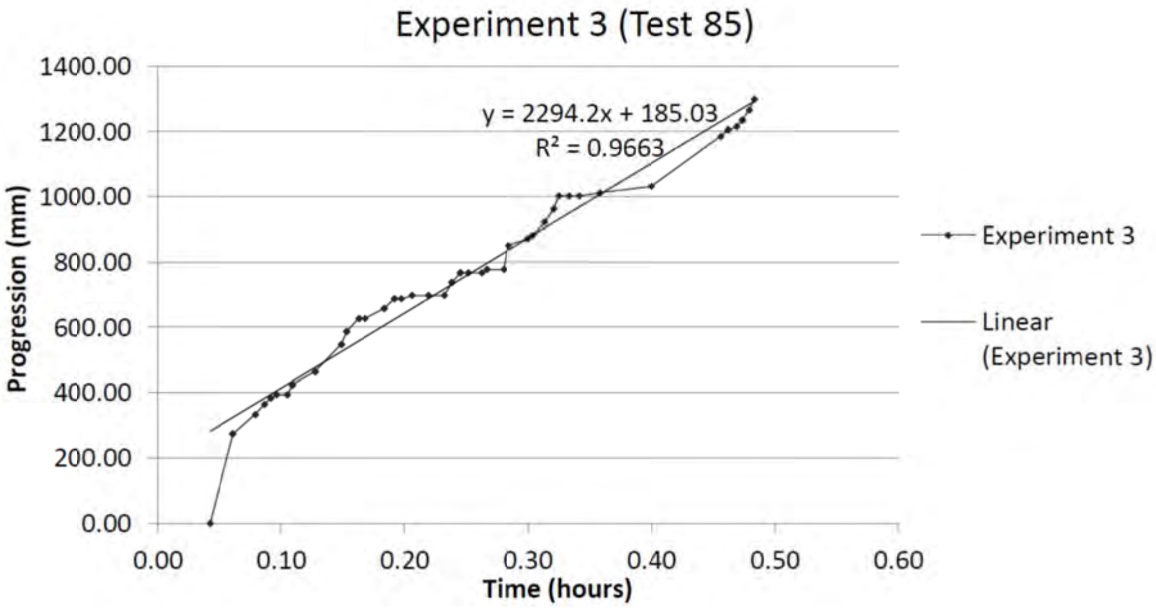

The gradient of the line of best fit shows the tip speed of the pipe, which is 2294.2mm/hour or 0.637mm/s.

Backward erosion piping test data sheet

Test #	86	Exit type	circle
Date	14/12/2015	seepage length	1.3 m
Soil	Syd sand	head in bladder tank	5 m
Flume	1	compaction	vibrated

Note: Bladder dropped to 3m before exp.

	time	head	observation
	10:26	0	
	10:27	100	
	10:28	200	tip progression
	1:20	304	
	1:52	305	happy snap :)
	2:50		at bar 1
31	3:00		30 ab1 [HS2]
	3:45		2 tips formed
			70 ab1
	4:30		100 ab1 (both tips)
33	5:00		120 ab1
	5:30		150 ab1
34	6:00		160 ab1
	6:30		175 ab1 (3 tips)
35	7:00		185 ab1
	7:30		205 ab1
36	8:00		230 ab1
	8:30		250 ab1
	9:00		260 ab1
	9:30		270 ab1
	10:00		280 ab1
	10:30		290 ab1
39	11:00		10 ab2
	11:30		15
	12:00		20
	12:30		30
	13:00		40
	13:30		50
	14:00		65
	14:30		75
	15:00		80

time	head	observation
16:00		115 ab2
17:00		155 ab2
18:00		175 ab2
19:00		195 ab2
20:30		240 ab2
21:00		245 ab2
23:00		20 ab3
~~24~~ 24:46		30 ab3 High speed photos.
26:00		55 ab3
27:00		85 ab3
28:20		155 ab3
29:30		195 ab3
30:00		220 ab3
30:46		250 ab3.
33:00		10 ab4
33:30		appears to be fwd deepening at bar 4 –
		sand possibly not compressed due to bladder?
		[ü snap] of fwd deepening
		& [ü snap] of no apparent tip after b4
		Forward deepening strong on 2 tips

Test 86 (flume 1) circle

Prepared by Angela Greenlees

Test 86 was the fourth of the amplified loading tests. There were no time lapse photos recording this test.

This was the first test in which a straight edge was used to pour the Pliolite particles onto the sand. A uniformly thick and straight line was achieved but it is questionable whether the thickness affects the erosion at the pipe head.

The head was raised to 305mm (147% of critical) and it took 36 minutes for the pipe to reach the upstream end and 1 hour 16.2 minutes to fail.

The bilge pump in the constant head tank was replaced before this test was run and it worked consistently throughout the entire experiment, however the bladder head tank level had dropped to 3m before the experiment began.

The pipe progression appeared to only reach 1146mm before forward deepening began, and it is likely that this was due to the deflation of the bladder causing the sand at the upstream end to sink away from the lid.

Three distinct progression tips formed during this test and there was significant branching during progression.

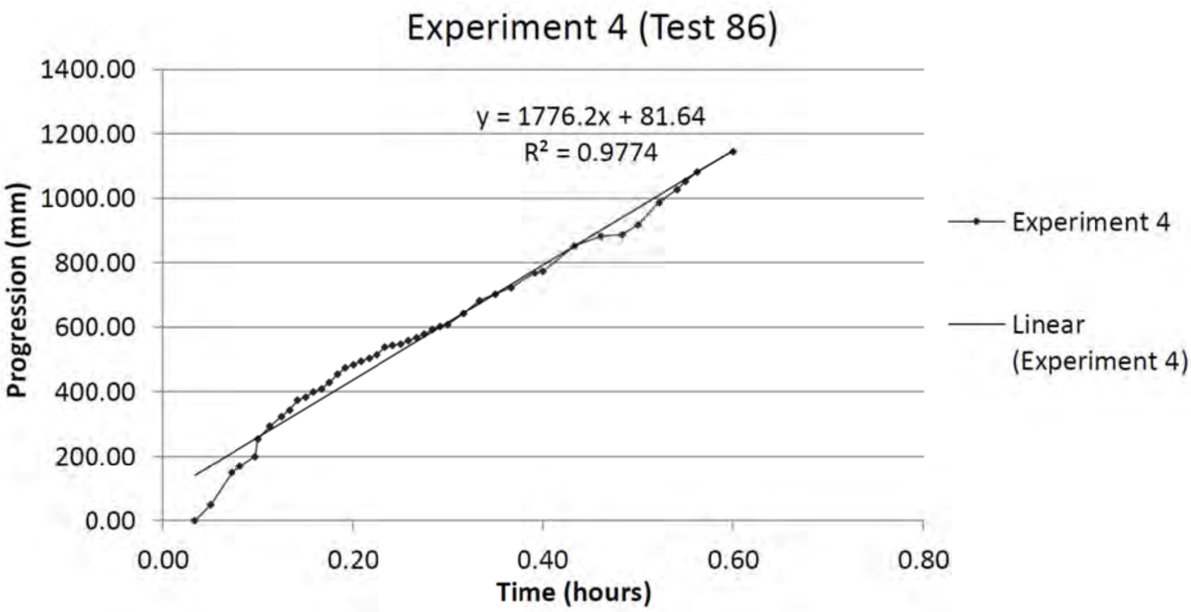

The gradient of the line of best fit shows the tip speed of the pipe, which is 1776.2mm/hour or 0.493mm/s.

Backward erosion piping test data sheet

Test #	87	Exit type	circle
Date	18/12/2015	seepage length	1.3 m
Soil	Syd sand	head in bladder tank	5 m
Flume	3	compaction	vibrated

time	head	observation
1:05pm	0	
0:45	100	
1:03	180	initiation
1:20	250	tip at d/s wall
2:35	312	tip 60 ab1
3:22	314	
3:36	314	111 ab1
4:10		155ab1
4:56		185ab1
5:37		220ab1
6:09	315	at b2
7:50		15ab2
8:32		40ab2
9:12	309	[illegible]
10:42		120ab2 slight u/s flow ab3
12:15		155ab2
12:54		165ab2 [HSP]
15:00		250ab2
17:46		30 ab3
18:48		85ab3
19:13		100ab3
22:24		175ab3
23:00		220ab3
25:12		10ab4
25:40		25ab4
26:48		35ab4
27:32		45ab4
28:00		55ab4
28:24		80ab4
28:50		100ab4
29:15		u/s

2:18pm failure

Test 87

		Row 1			Row 2			Row 3					
time	head	right	middle	left	right	middle	left	right	middle	left	time for 50mL	Avg	Temp
16:35		106	100	101	162	153	160	229	229	235			
47:30		117	92	100	174	166	170	249	291*	260			

* fwd deepening under pipe

Test 87 (flume 3) circle

Prepared by Angela Greenlees

Test 87 was the fifth of the amplified loading tests.

This was the first of the amplified loading tests done in flume 3. Flume 3 did not manage to seal as tightly or easily as flume 1, however this may simply be from lack of constant use.

This was the second test in which a straight edge was used to pour the Pliolite particles onto the sand. It results in reasonably clear high speed photographs however it is still unknown whether the thickness of the pour is affecting the progression path.

The head was raised to 309mm (149% of critical) and it took 29 minutes and 15 seconds for the pipe to reach the upstream end and 1 hour 13 minutes to fail.

For the most part, the tip progressed in a reasonably straight line along the centre of the flume without much branching.

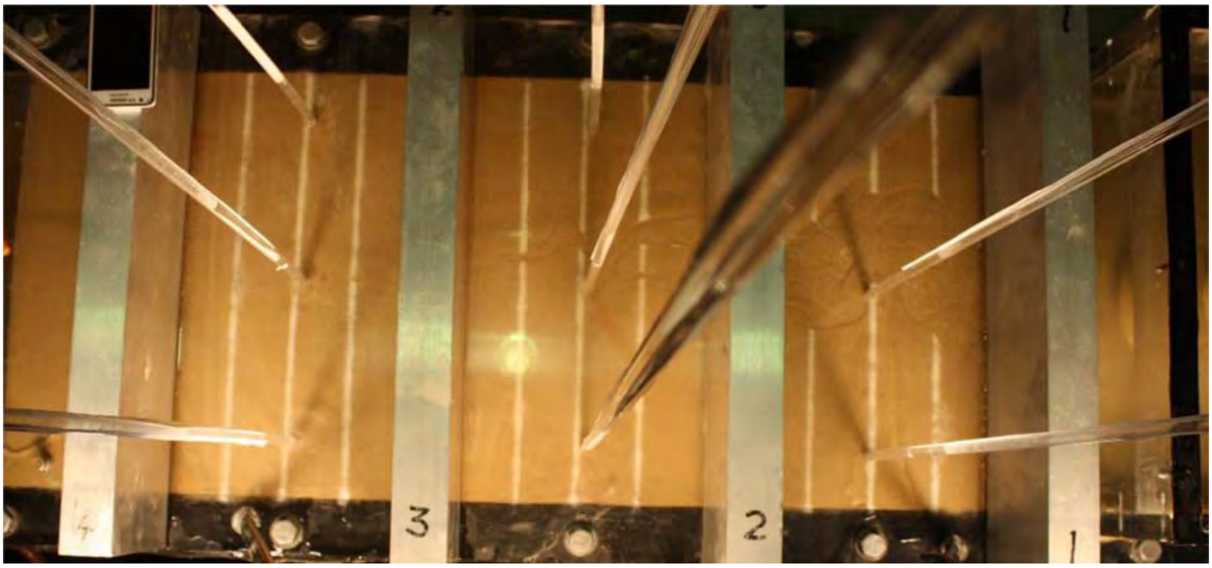

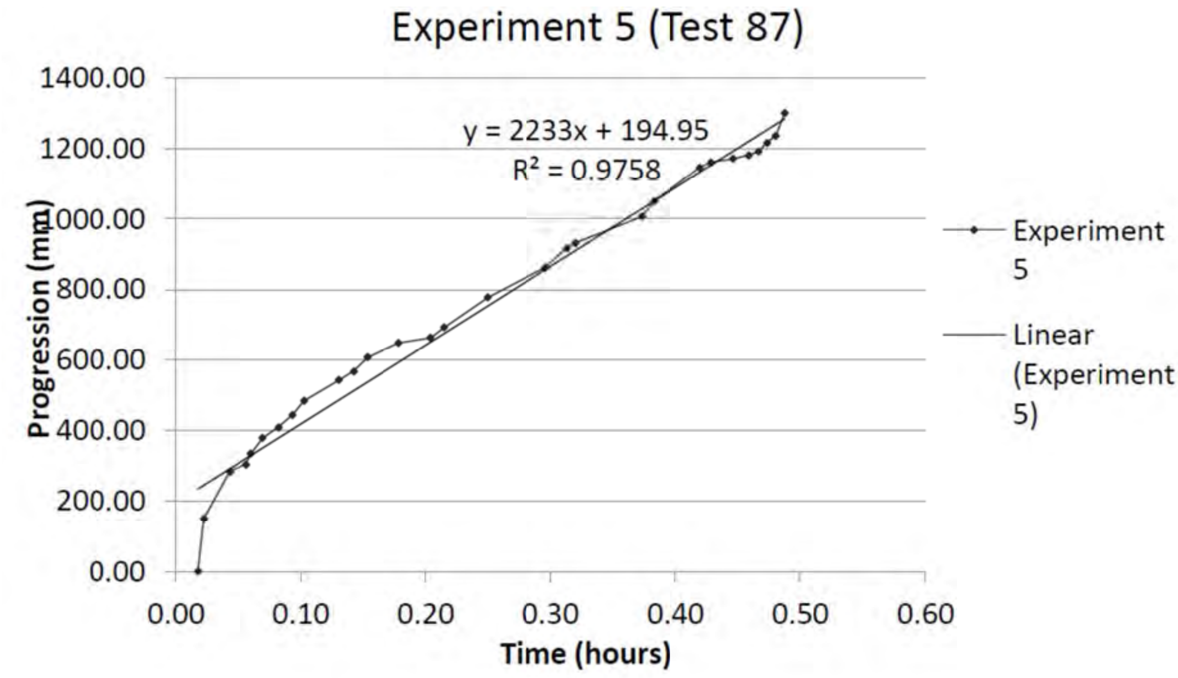

The gradient of the line of best fit shows the tip speed of the pipe, which is 2333mm/hour or 0.620mm/s.

Backward erosion piping test data sheet

Test #	88	Exit type	circle
Date	11/01/2016	seepage length	1.3 m
Soil	Syd sand	head in bladder tank	5 m
Flume	1	compaction	vibrated

*Aiming for 130% Hp = 262.6mm

time	head	observation
12:27	0	
0:38	50	
1:25	100	
2:11	150	progression at exit
2:46	200	
3:50	271	@b1
4:22		15ab1
5:00		70ab1
5:30		100ab1 (3 tips)
6:00		130ab1
6:30		145ab1
7:30		170ab1
8:00		230 ab1
8:30		250 ab1
9:00		255ab1
11:00		10ab2
11:30		20 ab2
12:00		30 ab2
12:30		30 ab2
13:00		45ab2
14:00		60 ab2
15:00		65ab2
16:00		65ab2
17:00		65ab2
17:30		70ab2
18:00		80ab2
19:00		95ab2
20:00		115ab2
21:00		130ab2
21:30		150ab2
22:00		170 ab2

	time	head	observation
	23:00		180 ab2
	24:00		180 ab2
	25:00		190 ab2
	26:00		230 ab2
	27:00		240 ab2
	27:25		250 ab2
	33:00		little progression of central tip
			LHS Tip has progressed a small amount.
			Movement is slow but present.
02:45 PM	35:45		10 ab3
	37:00		20 ab3
	38:00		25 ab3
	40:00		25 ab3
	41:00		35 ab3
	42:00		40 ab3
1:10	43:00		50 ab3
	44:00		65 ab3
	44:30		80 ab3
	45:30		85 ab3
	46:00		100 ab3
	47:00		100 ab3
	48:00		100 ab3
	48:30		105 ab3
:16	49:00		110 ab3
	50:00		130 ab3
	51:00		145 ab3
	52:00		160 ab3
	53:00		170 ab3
	54:00		190 ab3
	55:00		210 ab3
	56:00		230 ab3
-23:30	56:30		250 ab3
	63:00		10 ab4
	64:00		10 ab4 [smaller than normal sand boil?
	65:00		25 ab4 See HSP]
	66:00		30 ab4
	67:00		35 ab4
	68:00		40 ab4
	69:00		70 ab4

time	head	observation
69:30		85ab4
70:00		120ab4
72:00		140ab4 (u/s)
72:30		forward deepening.
2:51:14 pm		Failure.

Test 88

		Row 1			Row 2			Row 3					
time	head	right	middle	left	right	middle	left	right	middle	left	time for 50mL	Avg	Temp
6:50	271	204	193	203	266	264	262	324	321	317			
14:00		no change.											
35:00		no change											
66:00		no change											

Test 88 (flume 1) circle

Prepared by Angela Greenlees

Test 88 was the sixth of the amplified loading tests.

This was the third test in which a straight edge was used to pour the Pliolite particles onto the sand. The thickness of the pour does not seem to affect the progression tip however some of the Pliolite particles tend to stick to the surface of the lid while the tip continues underneath.

There was some sliding of sand through the upstream filter which meant that the “upstream” boundary was not at the total 1300mm and was measured at 1276mm.

The head was raised to 271mm (130% of critical) and it took 1 hour and 12 minutes for the pipe to reach the upstream end and 2 hours 24 minutes to fail.

There were several points in the middle of the flume where the pipe blocked and progression stopped for one to three minutes, however overall the progression was fairly consistent.

One of the points where progression stopped is shown in the photo below.

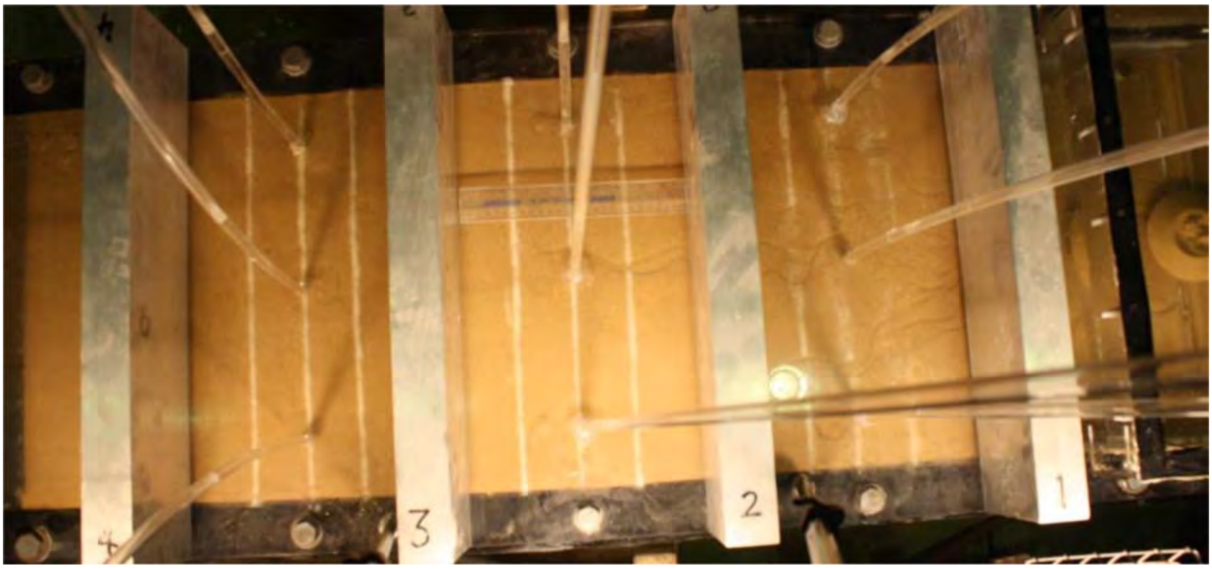

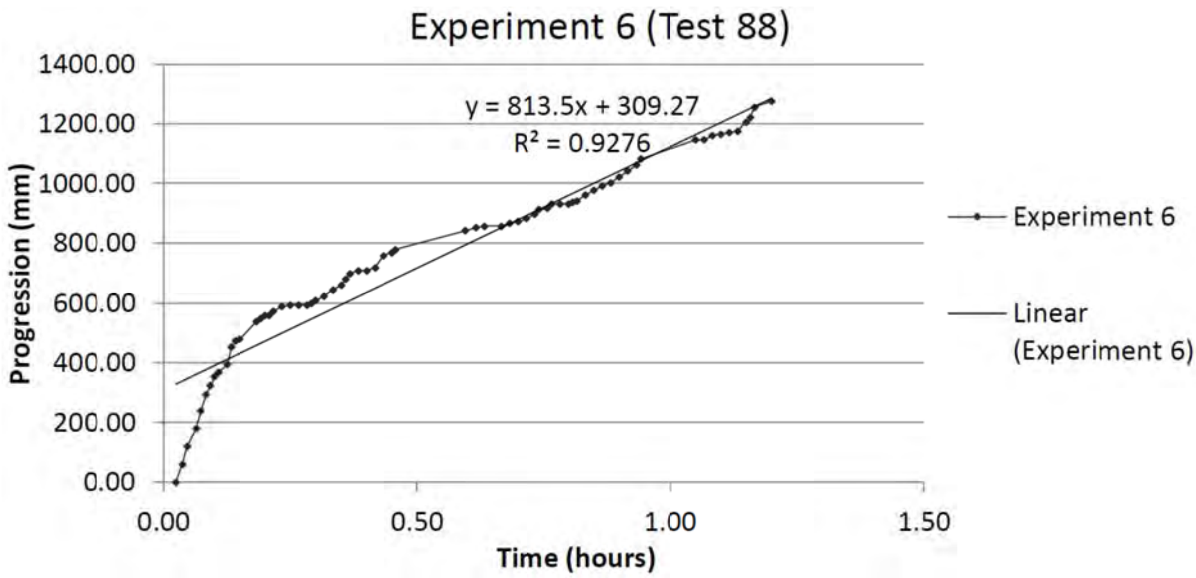

The gradient of the line of best fit shows the tip speed of the pipe, which is 813.5mm/hour or 0.226mm/s.

Backward erosion piping test data sheet

Test #	89	Exit type	circle
Date	14/01/2016	seepage length	1.3 m
Soil	Syd sand	head in bladder tank	5 m
Flume	3	compaction	vibrated

time	head	observation
12:40	0	
1:07	100	
1:32	200	
1:45	220	80ae
2:35	259	120ae (edge of box) small air bubble AB1 (see " snap)
4:15		170ae (at B1)
6:00		10ab1
6:15		25ab1
6:45		75ab1 tip has surrounded air bubble (see " snap)
7:45		90ab1
9:15		130ab1
9:45		145ab1
10:45		170ab1
11:55		210ab1
13:00		235ab1
13:25		250 ab1
16:15		10 ab2
17:15		20ab2
18:15		20ab2
19:15		25ab2
20:45		50ab2
21:45		70 ab2
22:45		95ab2
23:45		125ab2
24:45		150ab2
25:45		170ab2
27:00		210ab2
28:00		225ab2
28:25		movement 70mm ahead of tip. Tip under b3 250ab2
32:15		80ab3
33:25		80ab3

time	head	observation
35:25		~~180ab3~~ 90ab3
36:15		~~170ab3~~ 150 ab3
36:45		~~205ab3~~ 170 ab3
38:00		~~220ab3~~ 205 ab3
38:45		~~240ab3~~ 220 ab3
39:15		~~8 ab4~~ 240 ab3
43:15		~~20ab4~~ 5 ab4
43:45		~~35ab4~~ 20 ab4
44:15		~~40ab4~~ 35 ab4
44:45		~~55ab4~~ 40 ab4
45:45		~~65ab4~~ 55 ab4
46:00		~~80ab4~~ 65 ab4
46:15		~~95ab4~~ 80 ab4
46:30		~~100ab4~~ 95 ab4
46:45		~~115ab4~~ 100 ab4
47:15		~~u/s~~ 115 ab4
47:28		u/s
1:24:49		failure.

Test 89 time on computer = 1:20 AM 26/9/06 = 1:36 pm 14/1/16

		Row 1			Row 2			Row 3					
time	head	right	middle	left	right	middle	left	right	middle	left	time for 50mL	Avg	Temp
14:00	259	100	91	110	157	150	125	197	201	203			
32:00		92	81	102	139	122	113	193	196	198			

Test 89 (flume 3) circle

Prepared by Angela Greenlees

Test 89 was the seventh of the amplified loading tests, and the second conducted in flume 3.

This was the fourth test in which a straight edge was used to pour the Pliolite particles onto the sand.

The head was raised to 259mm (125% of critical) and it took 47 minutes and 28 seconds for the pipe to reach the upstream end and 1 hour 25 minutes to fail.

Again, there were several points in the middle of the flume where the pipe blocked and progression stopped, however each of these were for less than two minutes. Progression was fairly consistent, but noticeably faster than the previous test, even though the lower head level should have indicated a slower result.

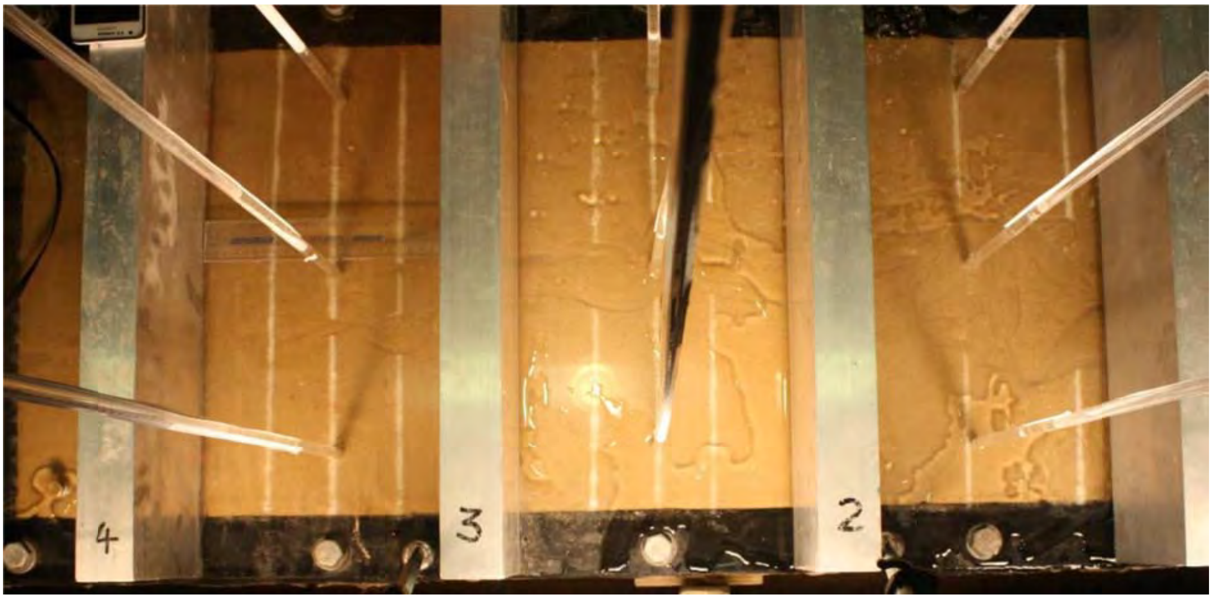

While the path of the tip was reasonably straight and direct, there was one point just after Bar 4 where the pipe encountered an obstruction and branched off on the left.

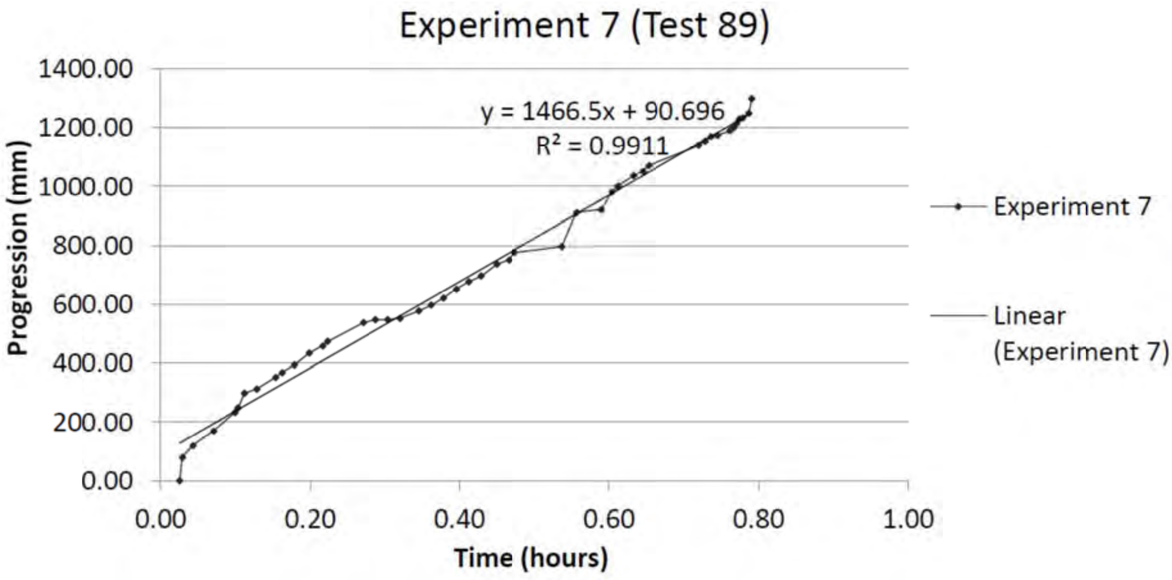

The gradient of the line of best fit shows the tip speed of the pipe, which is 1466.5mm/hour or 0.407mm/s.

Backward erosion piping test data sheet

Test #	90	Exit type	circle
Date	8/02/2016	seepage length	1.3 m
Soil	Syd sand	head in bladder tank	5 m
Flume	1	compaction	vibrated

time	head	observation
2:25PM	0	
1:45	100	movement at exit
2:25	200	boiling
2:49	230	100ae
4:00		10ab1
4:30		20ab1
5:00		45ab1 tip width 4mm, 45ab1 10mm
5:30		80ab1
6:00		120ab1
6:30		150ab1
7:00		175ab1 tip width 3mm, 130ab1 5mm
7:30		210ab1
8:00		225ab1 #Notes for this experiment:
8:30		240ab1 - tip is progressing in a fairly
9:00		260ab1 straight, central line
10:00		10ab2 - minimal branching
10:30		30ab2 - no secondary tips forming
11:00		30ab2 from exit.
11:30		30ab2
14:00		65ab2
15:30		75ab2
16:00		90ab2
17:00		150ab2 2mm@tip, 7mm@80ab2
18:00		180ab2
18:30		190ab2
19:00		200ab2
19:30		210ab2
20:15		225ab2
22:00		235ab2 5mm@tip, 7mm@190ab2
25:30		10ab3 1mm@tip, 7mm@240ab2
26:30		70ab3

time	head	observation
28:00		100ab3
29:00		140ab3
30:00		190ab3
31:00		forward deepening appears to have begun at bar4
		blockage in the channel is sitting under
		the middle standpipe & little concentrated
		movement is observed after bar 4.
		possible causes are that the sand AB4 is not
		sitting against the acrylic or that water through
		the u/s screen is not flowing at the top of
		the flume.
		the "drag lines" that typically appear at the
		u/s screen have manifested at 20mm ab4.
		Conclusion: u/s should be considered as 20mm ab4

Test 90

		Row 1			Row 2			Row 3					
time	head	right	middle	left	right	middle	left	right	middle	left	time for 50mL	Avg	Temp
21:00	230	201	196	210	254	232	251	304	306	310			

Test 90 (flume 1) circle

Prepared by Angela Greenlees

Test 90 was the eighth of the amplified loading tests.

This was the fifth test in which a straight edge was used to pour the Pliolite particles onto the sand.

The head was raised to 230mm (111% of critical) and it took 31 minutes for the pipe to reach the upstream end and 45 minutes to fail.

There was one point after Bar 2 where the pipe blocked and progression stopped for one minute, however the progression was fairly continuous after that. The lower head level has seemed to result in a mostly straight pipe with minimal branching, and a pattern of fewer branches has been noticed as the head levels have dropped.

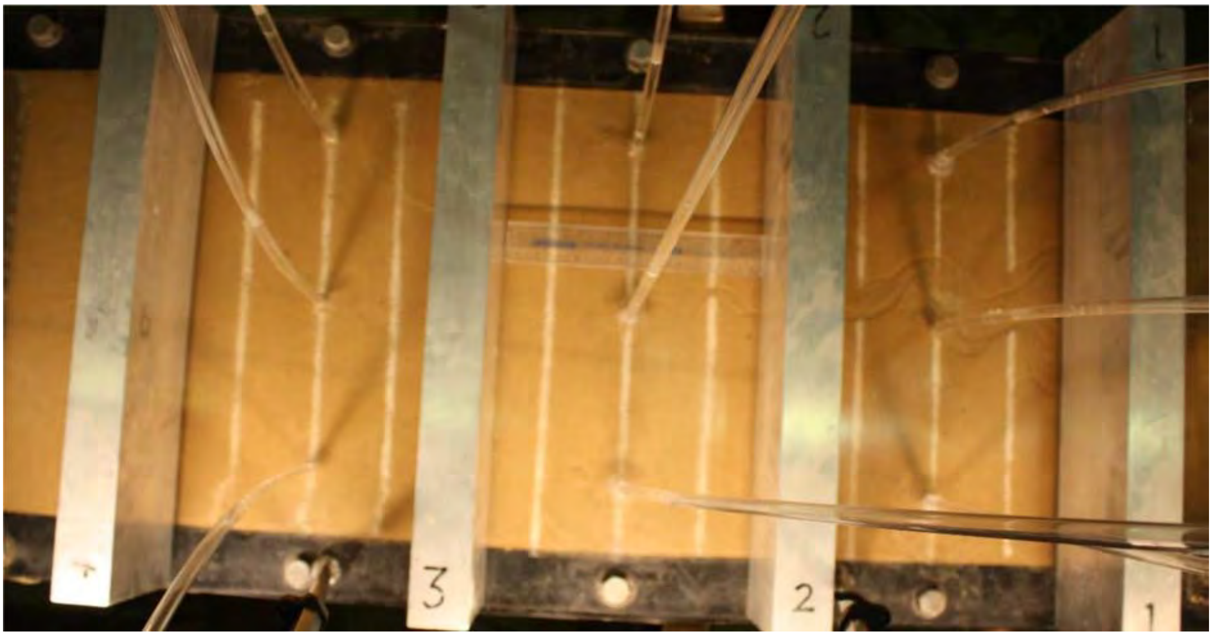

It must be noted in this experiment that there seemed to be issues with the sand levels at the upstream end after Bar 4, as it was observed that forward deepening started from underneath Bar 4. This will be taken as the upstream boundary (1112mm) and calculations may be scaled and extrapolated.

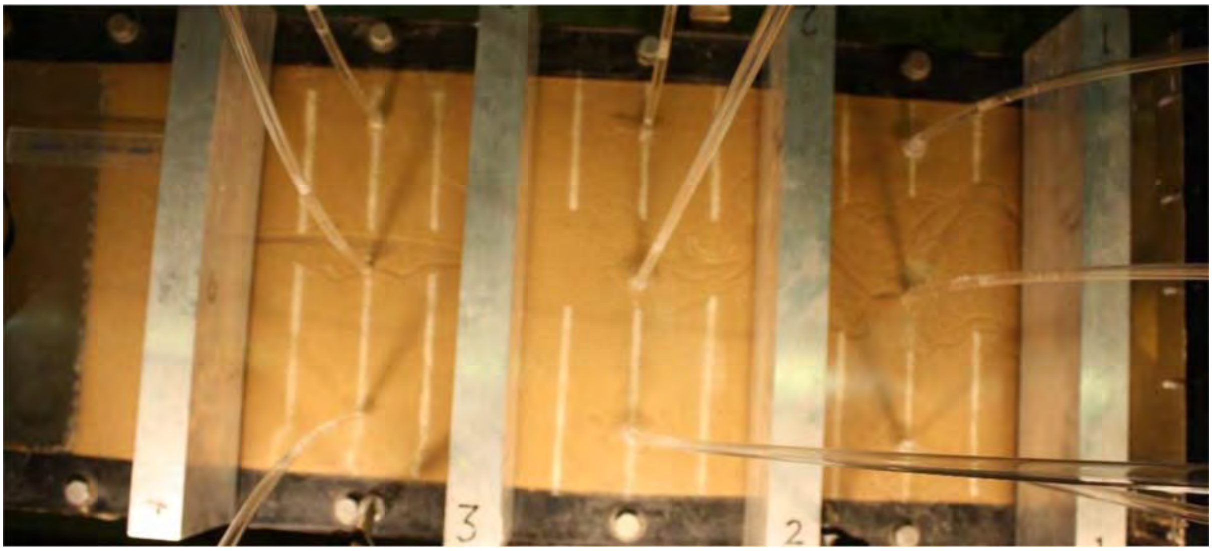

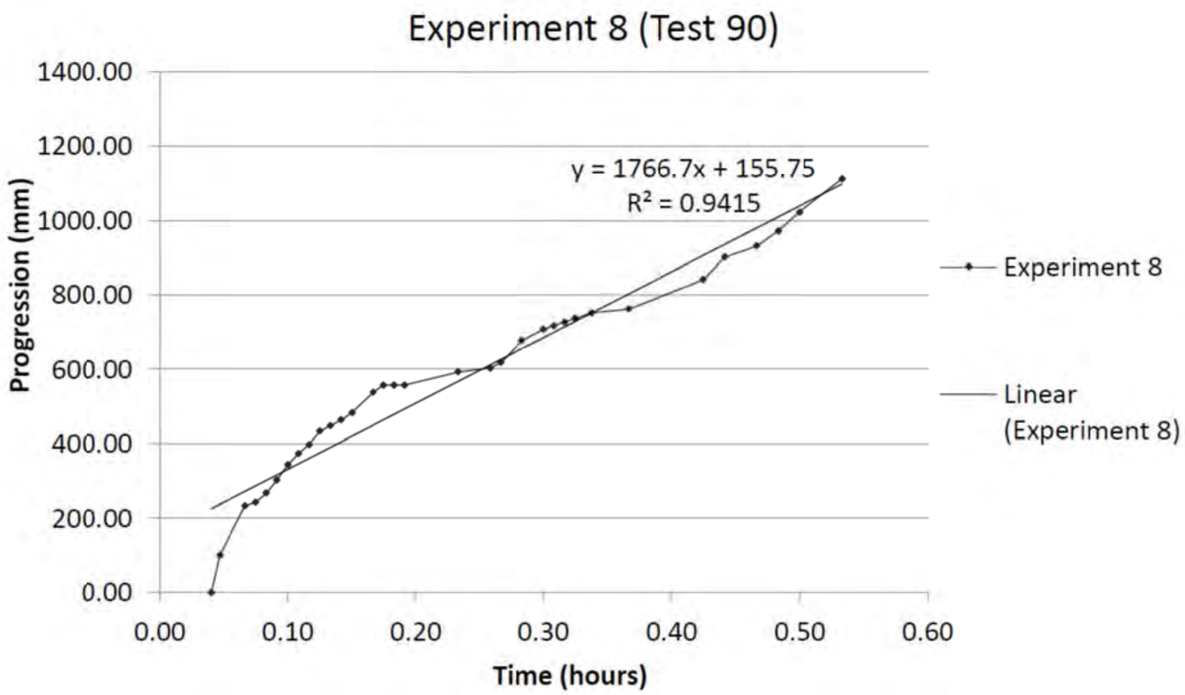

The gradient of the line of best fit shows the tip speed of the pipe, which is 1766.7mm/hour or 0.491mm/s.

Backward erosion piping test data sheet

Test #	91	Exit type	circle
Date	17/02/2016	seepage length	1.3 m
Soil	Syd sand	head in bladder tank	5 m
Flume	3	compaction	vibrated

time	head	observation
		large number & distribution of small air
		bubbles from exit to b3. (see !! snaps)
		None visible after B3 though.
		Leaking is noticeable on the inner edge (towards
		wall) of flume.
		small leak at standpipe: Row 1 RHS
10:28	0	
10:29:15	150	
10:30:10	200	90 after exit
10:31:40	216	reasonably quickly (around 32:00)
10:38:00		channel has reached B1, but yet to appear on
		u/s side. I am concerned this is due to the air
		bubbles. Quite a deep channel has formed between
		the exit & B1 (see !! snap)
10:43:30		25ab1
10:45:30		35ab1
10:49:00		50ab1
10:51:00		60ab1
11:06:00		70ab1 air bubbles have moved to the LHS
11:07:30		100ab1 d/s end of the flume. Most are out
11:10:00		110ab1 of the path of the tip! [See !! snap]
11:15:30		120ab1
11:20:00		140ab1 1mm @ tip. 5mm @ 80ab1
11:22:00		160ab1
11:33:00		165ab1
11:35:00		170ab1
11:43:00		180ab1
11:47:00		185ab1
11:50:00		200ab1
12:10:00		205ab1
12.19		under b2

time	head	observation
12.35		57 ab2
12.44		115 ab2 (I think it closer to H=218)
12.52		136 ab2 tip = hard to tell ≑ 4mm } active widths
		220 ab1 ≑ 5mm
		50 ab1 ≑ 5mm
		It's possible channel is progressing
		along side edge of underside coating.
1.03		165 ab2
1.22		under b3
1.54		118 ab3
2.12		210 ab3. Significant meandering +
		braiding d/s of b2.
2.13		60fps shots taken from tip.
2.16		225 ab3
2.31		under b4
2.41		35 ab4 tip ≑ 4mm } active widths
		mid-way b3-4 ≑ 6mm
		" b2-3 ≑ 7mm
		" b1-2 ≑ 7mm
2.53		53 ab4. Channel has branched
		from somewhere just d/s of b2
		so that now a new tip has
		formed which is 153 ab2. It
		looks as though it might rejoin
		original channel but I'll see.
3.02		85 ab4. Yep new tip joined original
		channel. Both ch1 + 2 are blocked
		underneath b2.
3.17		first noticed through to u/s end. See
		SLR pics for time it occurred. And
		deepening may be up to b4.
		There's a blockage btw reg +
		deepended channel (spanning
		midway btw 3-4 to 4). Also still
		blocked under b2.
4.57		all is at it was at 3.17. I'm going
		to ↓H back to datum and might
		start-up again on Friday.
4.59	↓0	

Hamchenin

time	head	observation
19-2		
9.56		all looks as I left it on Wed
		arvo. fwd deepening up to d/s of
		b4. Blocked btw deepened + regular
		channel. And blocked d/s of b2.
9.58	↑	The submersible pump isn't working.
		When turned on it triggers the
		Circuit breaker in the orange box.
		I need to replace the pump w/ one
		of the pumps Hamish used at the
		GBE tests for which I'd like Angela's
		help so I'll end the test here.

Test 91

		Row 1			Row 2			Row 3					
time	head	right	middle	left	right	middle	left	right	middle	left	time for 50mL	Avg	Temp
10:41	216	92	86	98	129	128	138	169	168	176			
12:44		*83	80	88*	126	122	124*	166	170	172			
1:54		90	83	100	128	123	128*	167	168	165			
3:19		82	66	79	122	120	132	166	170	168			

Test 91 (flume 3) circle

Prepared by Angela Greenlees

Test 91 was the ninth of the amplified loading tests, and the third conducted in flume 3.

This was the sixth test in which a straight edge was used to pour the Pliolite particles onto the sand.

The head was raised to 216mm (103.8462105% of critical) and it took 4 hours and 51 minutes for the pipe to reach the upstream end. This experiment ran for an extended period without failing- the head levels were dropped to datum overnight, however there was no movement when the test was resumed the next morning and the submersible pump failed to work. An approximate failure time may need to be interpolated from the other results.

The tip travelled fairly close to the right hand side of the flume, which may indicate an easier path due to the curve of the bladder at the base of the flume.

There were a significant number of small air bubbles along the underside of the lid, as shown in the picture on the following page. These air bubbles seemed to move along the flume ahead of the tip progression so it is unlikely they affected the movement of sand.

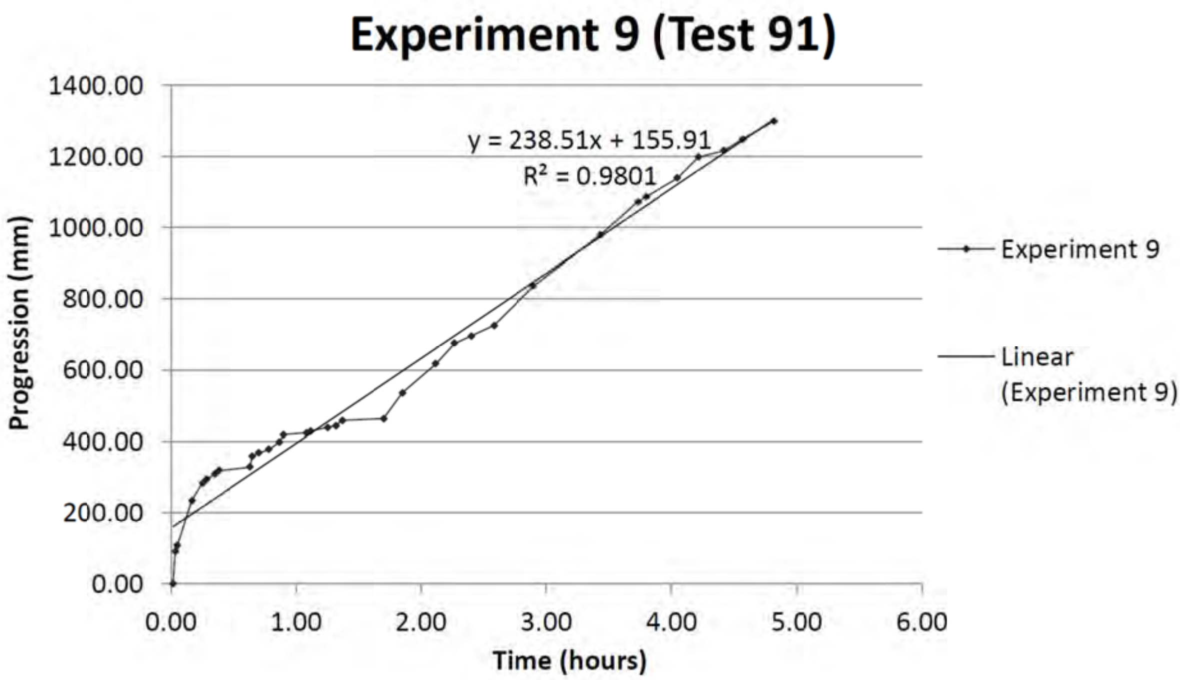

The gradient of the line of best fit shows the tip speed of the pipe, which is 238.51mm/hour or 0.066mm/s.

Backward erosion piping test data sheet

Test #	92	Exit type	circle
Date	6/04/2016	seepage length	1.3 m
Soil	Syd sand	head in bladder tank	5 m
Flume	1	compaction	vibrated

aiming for 110% ≑ 222mm.

time	head	observation
1:36	0	no major air bubbles. Sample seems normal
		A good seal while CO_2-ing.
		Head tank is filling very slowly - first run w/ new
		pump.
1:40	25	Boiling @ exit
1:55	133	
1:58	170	Piping started
2:03	180	150 ae.
2:07	215	5ab1
2:09	225	55ab1
2:11		95ab1 Single tip, fairly straight central pipe
2:12		120ab1 forming
2:16		155ab1
2:19		170ab1
2:23		190ab1
2:25		230ab1 Channel has straightened out
2:29		5ab2
2:30		25ab2
2:32		50ab2
2:34		70ab2
2:36		90ab2
2:42		140ab2
2:43		155ab2
2:44		170ab2
2:46		195ab2
2:47		210ab2
2:50		230ab2
2:52		250ab2
3:11		10ab3

time	head	observation
3:14		45ab3
3:16		70ab3
3:17		90ab3
3:20		120ab3
3:22		130ab3
3:30		150ab3
3:34		170ab3
3:36		195ab3
3:40		210ab3
3:42		220ab3
3:43		230ab3
3:45		240ab3
3:49		restarted scales 2:46AM 26/09/2006 .
4:02		15ab4
4:03		50ab4
4:05		70ab4
4:06		110ab4
4:07		130ab4 (U/S)
7/4 10:42		Exp stopped 9:38pm 26/09/06 on laptop
		10:42 am 7/04/16 real time
		Hard to say if "failure" occured as no sheet
		failure visible, however water flow was observed with
		no sand movement.
		Will need to check camera times for failure.

Test 92

		Row 1			Row 2			Row 3					
time	head	right	middle	left	right	middle	left	right	middle	left	time for 50mL	Avg	Temp
2:15	225	210	190	206	255	252	252	298	296	295			

Test 92 (flume 1) circle

Prepared by Angela Greenlees

Test 92 was the tenth of the amplified loading tests, and the seventh conducted in flume 1.

This was the seventh test in which a straight edge was used to pour the Pliolite particles on the sand.

The upstream geotextile was replaced prior to this test and succeeded in reducing the amount of sand falling through the filter during the compaction process.

The pump that supplied the constant head tank failed after the previous experiment and was replaced with a pump with half the flow capacity. This meant that the head increase took twice as long, and this allowed for more measurements at the exit during the increase.

The head was raised to 225mm (108% of critical) and it took 2 hours and 31 minutes for the pipe to reach the upstream end. The time to failure was 5 hours and 38 minutes.

The progression occurred in a single tip that began from the downstream exit and continued in a mostly straight line after 490mm until reaching the upstream end.

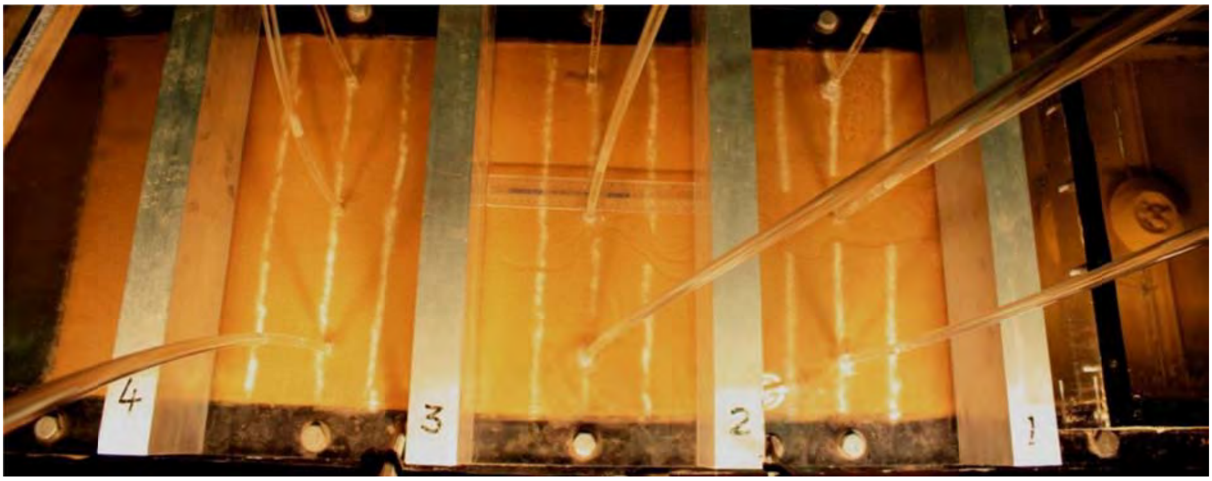

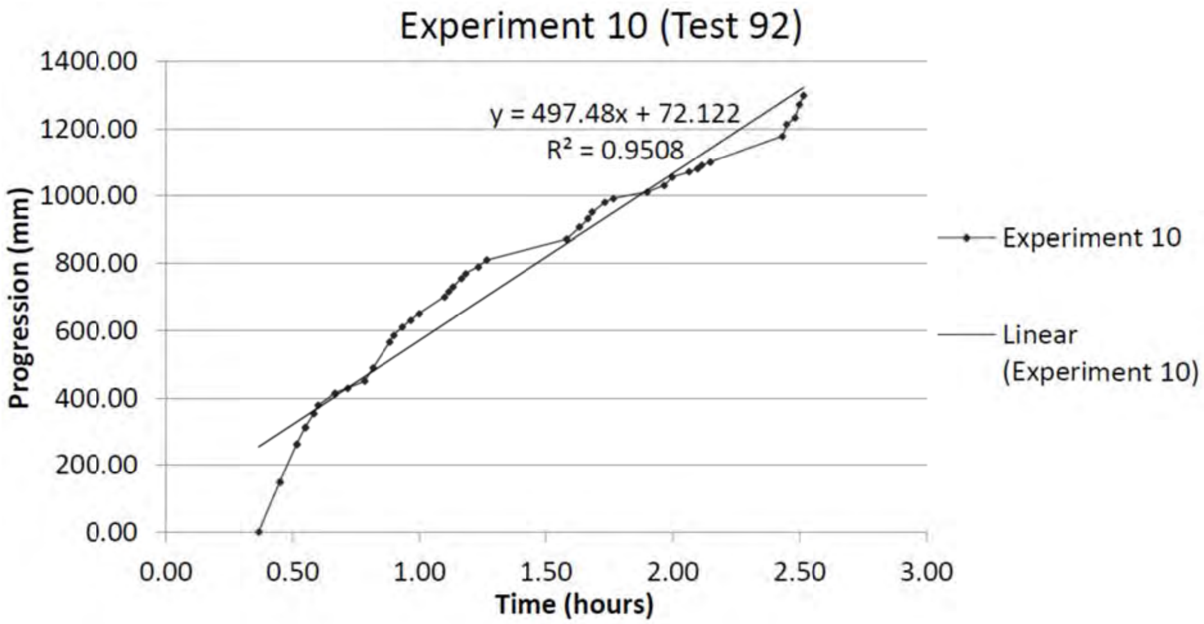

The gradient of the line of best fit shows the average tip speed of the pipe, which is 497.48mm/hour or 0.138mm/s.

Appendix B: Data used in model reviews

B.1 Data used in the review of the Schmertmann (2000) model

Table B.1: Data used in the review of the Schmertmann (2000) model

Test series	Reference	Test No. in ref.	D (m)	L (m)	$1/C_D$	$1/C_L$	Exit	C_G	Soil	RD	$1/C_\gamma$	C_u	d_{10} (mm)	$1/C_S$	H (m)	i_{exp}	K (m/s)
1	Pietrus (1981)	1	0.30	1.52	1	1	slope*	0.95	Reid Bedford	-	1	1.5	0.14	1.07	0	0.00	-
1	Pietrus (1981)	2	0.30	1.52	1	1	slope*	0.95	Reid Bedford	-	1	1.5	0.14	1.07	0.3048	0.20	-
1	Pietrus (1981)	3	0.30	1.52	1	1	slope*	0.95	Reid Bedford	-	1	1.5	0.14	1.07	0.238252	0.16	-
1	Pietrus (1981)	4	0.30	1.52	1	1	slope*	0.95	Reid Bedford	-	1	1.5	0.14	1.07	0.20955	0.14	-
1	Pietrus (1981)	5	0.30	1.52	1	1	slope*	0.95	Reid Bedford	-	1	1.5	0.14	1.07	0.270002	0.18	-
1	Pietrus (1981)	6	0.30	1.52	1	1	slope*	0.95	Reid Bedford	-	1	1.5	0.14	1.07	0.225552	0.15	-
1	Pietrus (1981)	7	0.30	1.52	1	1	slope*	0.95	Reid Bedford	-	1	1.5	0.14	1.07	0.2286	0.15	-
1	Pietrus (1981)	8	0.30	1.52	1	1	slope*	0.95	Reid Bedford	-	1	1.5	0.14	1.07	0.1524	0.10	-
1	Pietrus (1981)	9	0.30	1.52	1	1	slope*	0.95	Reid Bedford	-	1	1.5	0.14	1.07	0.193802	0.13	-
1	Pietrus (1981)	10	0.30	1.52	1	1	slope*	0.95	Reid Bedford	-	1	1.5	0.14	1.07	0.2413	0.16	-
1	Pietrus (1981)	11	0.30	1.52	1	1	slope*	0.95	Reid Bedford	-	1	1.5	0.14	1.07	0.270002	0.18	-
1	Pietrus (1981)	12	0.30	1.52	1	1	slope*	0.95	Reid Bedford	-	1	1.5	0.14	1.07	0.2159	0.14	-
1	Townsend (1986)	1	0.30	1.52	1	1	slope*	0.95	Reid Bedford	-	1	1.5	0.14	1.07	0.206502	0.14	-
1	Schmertmann (1995)	1	0.30	1.52	1	1	slope*	0.95	Reid Bedford	-	1	1.5	0.14	1.07	0.185166	0.12	-
2	Townsend (1986)	2	0.30	1.52	1	1	slope*	0.95	20/30	-	1	1.6	0.63	0.79	0.28956	0.19	-
2	Townsend (1986)	3	0.30	1.52	1	1	slope*	0.95	20/30	-	1	1.6	0.63	0.79	0.454152	0.30	-
2	Townsend (1986)	4	0.30	1.52	1	1	slope*	0.95	20/30	-	1	1.6	0.63	0.79	0.583692	0.38	-
2	Townsend (1986)	5	0.30	1.52	1	1	slope*	0.95	20/30	-	1	1.6	0.63	0.79	0.252984	0.17	-
2	Townsend (1986)	6	0.30	1.52	1	1	slope*	0.95	20/30	-	1	1.6	0.63	0.79	0.323088	0.21	-
3	Townsend (1986)	7	0.30	1.52	1	1	slope*	0.95	WG	-	1	6.7	0.24	0.96	1.46304	0.96	-
3	Townsend (1986)	8	0.30	1.52	1	1	slope*	0.95	WG	-	1	6.7	0.24	0.96	1.34112	0.88	-
4	Townsend (1986)	9	0.30	1.52	1	1	slope*	0.95	8/30	-	1	2.1	0.8	0.76	0.978408	0.64	-
4	Townsend (1986)	10	0.30	1.52	1	1	slope*	0.95	8/30	-	1	2.1	0.8	0.76	0.577596	0.38	-
5	Townsend (1986)	11	0.30	1.52	1	1	slope*	0.95	Gap I	-	1	5.6	0.16	1.05	1.8288	1.20	-
5	Townsend (1986)	12	0.30	1.52	1	1	slope*	0.95	Gap I	-	1	5.6	0.16	1.05	1.8288	1.20	-
6	Townsend (1986)	13	0.30	1.52	1	1	slope*	0.95	Gap II	-	1	6.1	0.28	0.93	1.56972	1.03	-
6	Townsend (1986)	14	0.30	1.52	1	1	slope*	0.95	Gap II	-	1	6.1	0.28	0.93	1.458468	0.96	-
6	Townsend (1986)	15	0.30	1.52	1	1	slope*	0.95	Gap II	-	1	6.1	0.28	0.93	1.459992	0.96	-
7	Schmertmann (1995)	?	0.30	1.52	1	1	slope*	0.95	?	-	1	1.6	0.23	0.97	0.28956	0.19	-
8	Schmertmann (1995)	2	0.30	1.52	1	1	slope*	0.95	site stratum 3	-	1	3.2	0.062	1.26	0.93726	0.62	-
8	Schmertmann (1995)	3B	0.30	1.52	1	1	slope*	0.95	site stratum 3	-	1	3.2	0.062	1.26	1.143	0.75	-
8	Schmertmann (1995)	3C	0.30	1.52	1	1	slope*	0.95	site stratum 3	-	1	3.2	0.062	1.26	0.908304	0.60	-
8	Schmertmann (1995)	7	0.30	1.52	1	1	slope*	0.95	site stratum 3	-	1	3.2	0.062	1.26	1.118616	0.73	-
9	Schmertmann (1995)	5	0.30	1.52	1	1	slope*	0.95	site tailings	-	1	2	0.13	1.09	0.606552	0.40	-
9	Schmertmann (1995)	6	0.30	1.52	1	1	slope*	0.95	site tailings	-	1	2	0.13	1.09	0.51054	0.34	-
10	Schmertmann (1995)	4	0.30	1.52	1	1	slope*	0.95	UF 50/50	-	1	1.4	0.17	1.03	0.292608	0.19	-
11	Silvis (1991)	4	6.00	6.00	1.28	1.32	slot	0.67	Marsdiepzand	0.65	0.98	1.58	0.144	1.07	1.053	0.18	5.10E-05
12	Silvis (1991)	2	6.00	9.00	1.21	1.43	slot	0.64	Marsdiepzand	0.65	0.98	1.58	0.144	1.07	1.689	0.19	5.10E-05
13	Silvis (1991)	3	6.00	12.00	1.16	1.51	slot	0.67	Marsdiepzand	0.65	0.98	1.58	0.144	1.07	2.16	0.18	5.10E-05
14	de Wit (1984)	220880-VI-1	1.50	2.40	1.20	1.10	plane	0.86	beach	0.88	0.90	1.33	0.167	1.04	0.415	0.17	2.00E-04
14	de Wit (1984)	220880-VI-2	1.50	2.40	1.20	1.10	plane	0.86	beach	0.83	0.92	1.33	0.167	1.04	0.352	0.15	1.90E-04
14	de Wit (1984)	220880-VI-3	1.50	2.40	1.20	1.10	plane	0.86	beach	0.68	0.97	1.33	0.167	1.04	0.414	0.17	2.40E-04
14	de Wit (1984)	220880-VI-4	1.50	2.40	1.20	1.10	plane	0.86	beach	0.66	0.98	1.33	0.167	1.04	0.444	0.19	2.30E-04
14	de Wit (1984)	220880-VI-5	1.50	2.40	1.20	1.10	plane	0.86	beach	0.57	1.01	1.33	0.167	1.04	0.36	0.15	2.90E-04
14	de Wit (1984)	220880-VI-6	1.50	2.40	1.20	1.10	plane	0.86	beach	0.49	1.05	1.33	0.167	1.04	0.381	0.16	3.00E-04
14	de Wit (1984)	220880-VI-7	1.50	2.40	1.20	1.10	plane	0.86	beach	0.4	1.09	1.33	0.167	1.04	0.285	0.12	3.50E-04
15	de Wit (1984)	220881-40-1	1.50	4.50	1.09	1.24	plane	0.89	beach	0.81	0.92	1.33	0.167	1.04	0.809	0.18	2.20E-04
15	de Wit (1984)	220881-40-2	1.50	4.50	1.09	1.24	plane	0.89	beach	0.71	0.96	1.33	0.167	1.04	0.715	0.16	3.10E-04
15	de Wit (1984)	220881-40-3	1.50	4.50	1.09	1.24	plane	0.89	beach	0.62	0.99	1.33	0.167	1.04	0.624	0.14	3.10E-04
16	de Wit (1984)	220881-40-4	1.50	1.20	1.29	0.95	plane	0.80	beach	0.74	0.95	1.33	0.167	1.04	0.307	0.26	2.10E-04
16	de Wit (1984)	220881-40-5	1.50	1.20	1.29	0.95	plane	0.80	beach	0.74	0.95	1.33	0.167	1.04	0.189	0.16	2.10E-04
16	de Wit (1984)	220881-40-6	1.50	1.20	1.29	0.95	plane	0.80	beach	0.74	0.95	1.33	0.167	1.04	0.288	0.24	2.10E-04
16	de Wit (1984)	220881-40-7	1.50	1.20	1.29	0.95	plane	0.80	beach	0.74	0.95	1.33	0.167	1.04	0.2	0.17	2.10E-04

Table B.1: Data used in the review of the Schmertmann (2000) model (continued)

Test series	Reference	Test No. in ref.	D (m)	L (m)	$1/C_D$	$1/C_L$	Exit	C_G	Soil	RD	$1/C_\gamma$	C_u	d_{10} (mm)	$1/C_S$	H (m)	i_{exp}	K (m/s)
17	de Wit (1984)	220880-I-1	0.50	0.80	1.20	0.88	plane	0.78	Dune	0.85	0.91	1.48	0.143	1.07	0.33	0.41	1.10E-04
17	de Wit (1984)	220880-I-2	0.50	0.80	1.20	0.88	plane	0.78	Dune	0.9	0.89	1.48	0.143	1.07	0.364	0.46	8.90E-05
17	de Wit (1984)	220880-I-3	0.50	0.80	1.20	0.88	plane	0.78	Dune	0.89	0.90	1.48	0.143	1.07	0.331	0.41	1.10E-04
17	de Wit (1984)	220880-I-4	0.50	0.80	1.20	0.88	plane	0.78	Dune	0.73	0.95	1.48	0.143	1.07	0.239	0.30	1.50E-04
17	de Wit (1984)	220880-I-5	0.50	0.80	1.20	0.88	plane	0.78	Dune	0.64	0.98	1.48	0.143	1.07	0.269	0.34	1.50E-04
17	de Wit (1984)	220880-I-6	0.50	0.80	1.20	0.88	plane	0.78	Dune	0.81	0.92	1.48	0.143	1.07	0.272	0.34	1.80E-04
17	de Wit (1984)	220880-I-7	0.50	0.80	1.20	0.88	plane	0.78	Dune	0.53	1.03	1.48	0.143	1.07	0.201	0.25	2.50E-04
17	de Wit (1984)	220880-I-8	0.50	0.80	1.20	0.88	plane	0.78	Dune	0.37	1.10	1.48	0.143	1.07	0.166	0.21	2.70E-04
17	de Wit (1984)	220880-I-9	0.50	0.80	1.20	0.88	plane	0.78	Dune	0.45	1.06	1.48	0.143	1.07	0.222	0.28	3.30E-04
17	de Wit (1984)	220883-39-1	0.50	0.80	1.20	0.88	plane	0.78	Dune	0.55	1.02	1.48	0.143	1.07	0.237	0.30	2.60E-04
17	de Wit (1984)	220883-39-2	0.50	0.80	1.20	0.88	plane	0.78	Dune	0.55	1.02	1.48	0.143	1.07	0.195	0.24	2.60E-04
17	de Wit (1984)	220883-39-3	0.50	0.80	1.20	0.88	plane	0.78	Dune	0.55	1.02	1.48	0.143	1.07	0.214	0.27	2.20E-04
18	de Wit (1984)	220880-V-1	0.50	0.80	1.20	0.88	plane	0.78	beach	0.91	0.89	1.33	0.167	1.04	0.266	0.33	1.60E-04
18	de Wit (1984)	220880-V-2	0.50	0.80	1.20	0.88	plane	0.78	beach	0.83	0.92	1.33	0.167	1.04	0.303	0.38	1.90E-04
18	de Wit (1984)	220880-V-3	0.50	0.80	1.20	0.88	plane	0.78	beach	0.74	0.95	1.33	0.167	1.04	0.234	0.29	2.10E-04
18	de Wit (1984)	220880-V-4	0.50	0.80	1.20	0.88	plane	0.78	beach	0.66	0.98	1.33	0.167	1.04	0.244	0.31	2.60E-04
18	de Wit (1984)	220880-V-5	0.50	0.80	1.20	0.88	plane	0.78	beach	0.57	1.01	1.33	0.167	1.04	0.208	0.26	2.40E-04
18	de Wit (1984)	220880-V-6	0.50	0.80	1.20	0.88	plane	0.78	beach	0.49	1.05	1.33	0.167	1.04	0.25	0.31	2.90E-04
18	de Wit (1984)	220880-V-7	0.50	0.80	1.20	0.88	plane	0.78	beach	0.4	1.09	1.33	0.167	1.04	0.244	0.31	3.40E-04
18	de Wit (1984)	220880-VII-1	0.50	0.80	1.20	0.88	plane	0.78	beach	0.95	0.88	1.33	0.167	1.04	0.28	0.35	1.40E-04
18	de Wit (1984)	220880-VII-2	0.50	0.80	1.20	0.88	plane	0.78	beach	0.83	0.92	1.33	0.167	1.04	0.241	0.30	1.80E-04
18	de Wit (1984)	220880-VII-3	0.50	0.80	1.20	0.88	plane	0.78	beach	0.66	0.98	1.33	0.167	1.04	0.241	0.30	2.20E-04
19	de Wit (1984)	220880-III-1	0.50	0.80	1.20	0.88	plane	0.78	River 1A	0.72	0.95	2.1	0.208	0.99	0.3	0.38	3.70E-04
19	de Wit (1984)	220880-III-2	0.50	0.80	1.20	0.88	plane	0.78	River 1A	0.61	1.00	2.1	0.208	0.99	0.392	0.49	3.70E-04
19	de Wit (1984)	220880-III-3	0.50	0.80	1.20	0.88	plane	0.78	River 1A	0.51	1.04	2.1	0.208	0.99	0.364	0.46	3.80E-04
19	de Wit (1984)	220880-III-4	0.50	0.80	1.20	0.88	plane	0.78	River 1A	0.38	1.10	2.1	0.208	0.99	0.284	0.36	4.60E-04
19	de Wit (1984)	220880-III-5	0.50	0.80	1.20	0.88	plane	0.78	River 1A	0.27	1.15	2.1	0.208	0.99	0.322	0.40	5.30E-04
19	de Wit (1984)	220880-III-6	0.50	0.80	1.20	0.88	plane	0.78	River 1A	0.16	1.21	2.1	0.208	0.99	0.202	0.25	6.90E-04
20	de Wit (1984)	220880-II-1	0.50	0.80	1.20	0.88	plane	0.78	River	0.84	0.91	2.3	0.23	0.97	0.302	0.38	3.70E-04
20	de Wit (1984)	220880-II-2	0.50	0.80	1.20	0.88	plane	0.78	River	0.75	0.94	2.3	0.23	0.97	0.45	0.56	3.90E-04
20	de Wit (1984)	220880-II-3	0.50	0.80	1.20	0.88	plane	0.78	River	0.6	1.00	2.3	0.23	0.97	0.3	0.38	5.20E-04
20	de Wit (1984)	220880-II-4	0.50	0.80	1.20	0.88	plane	0.78	River	0.48	1.05	2.3	0.23	0.97	0.445	0.56	6.10E-04
20	de Wit (1984)	220880-II-5	0.50	0.80	1.20	0.88	plane	0.78	River	0.36	1.11	2.3	0.23	0.97	0.34	0.43	6.60E-04
20	de Wit (1984)	220880-II-6	0.50	0.80	1.20	0.88	plane	0.78	River	0.24	1.17	2.3	0.23	0.97	0.225	0.28	7.50E-04
21	de Wit (1984)	220884-26-1	0.50	0.80	1.20	0.88	plane	0.78	coarse	0.19	1.20	3.85	0.283	0.93	0.394	0.49	1.60E-03
21	de Wit (1984)	220884-26-2	0.50	0.80	1.20	0.88	plane	0.78	coarse	0.34	1.12	3.85	0.283	0.93	0.391	0.49	1.10E-03
21	de Wit (1984)	220884-26-3	0.50	0.80	1.20	0.88	plane	0.78	coarse	0.48	1.05	3.85	0.283	0.93	0.783	0.98	8.90E-04
21	de Wit (1984)	220884-26-4	0.50	0.80	1.20	0.88	plane	0.78	coarse	0.18	1.20	3.85	0.283	0.93	0.792	0.99	1.10E-03
21	de Wit (1984)	220884-26-5	0.50	0.80	1.20	0.88	plane	0.78	coarse	0.33	1.12	3.85	0.283	0.93	0.66	0.83	8.00E-04
22	Kohno (1987)	3-1	0.10	1.50	0.81	1.00	unknown	0.81	sand	-	1.00	5.34	0.17	1.03	2.4	1.60	-
22	Kohno (1987)	3-2	0.10	1.50	0.81	1.00	unknown	0.81	sand	-	1.00	5.34	0.17	1.03	1.95	1.30	-
22	Kohno (1987)	3-4	0.10	1.50	0.81	1.00	unknown	0.81	sand	-	1.00	5.34	0.17	1.03	1.05	0.70	-
22	Kohno (1987)	3-7	0.10	1.50	0.81	1.00	unknown	0.81	sand	-	1.00	5.34	0.17	1.03	1.2	0.80	-
22	Kohno (1987)	3-8	0.10	1.50	0.81	1.00	unknown	0.81	sand	-	1.00	5.34	0.17	1.03	1.2	0.80	-
22	Kohno (1987)	3-9	0.10	1.50	0.81	1.00	unknown	0.81	sand	-	1.00	5.34	0.17	1.03	1.2	0.80	-
23	Muller-Kirchenbauer (1993)	on fig 6	0.24	0.72	1.09	0.86	circle	0.75	medium sand A	-	1.00	1.23	0.25	0.96	0.1224	0.17	-
N/A	de Wit (1984)	220880-IV-1	1.50	2.40	1.20	1.10	plane	0.86	Dune	0.92	0.89	1.48	0.143	1.07	0.838	0.35	1.40E-04
N/A	de Wit (1984)	220880-IV-2	1.50	2.40	1.20	1.10	plane	0.86	Dune	0.82	0.92	1.48	0.143	1.07	0.374	0.16	1.70E-04
N/A	de Wit (1984)	220880-IV-3	1.50	2.40	1.20	1.10	plane	0.86	Dune	0.73	0.95	1.48	0.143	1.07	0.409	0.17	1.90E-04
N/A	de Wit (1984)	220883-35-1	1.50	2.40	1.20	1.10	plane	0.86	coarse	0.18	1.20	3.85	0.283	0.93	0.88	0.37	1.80E-03
N/A	de Wit (1984)	220883-35-2	1.50	2.40	1.20	1.10	plane	0.86	coarse	0.2	1.19	3.85	0.283	0.93	0.96	0.40	1.50E-03
N/A	de Wit (1984)	220883-35-3	1.50	2.40	1.20	1.10	plane	0.86	coarse	0.21	1.18	3.85	0.283	0.93	0.8	0.33	1.50E-03
N/A	de Wit (1984)	220883-35-4	1.50	2.40	1.20	1.10	plane	0.86	coarse	0.35	1.11	3.85	0.283	0.93	0.68	0.28	1.10E-03
N/A	de Wit (1984)	220883-35-5	1.50	2.40	1.20	1.10	plane	0.86	coarse	0.35	1.11	3.85	0.283	0.93	0.714	0.30	1.00E-03
N/A	de Wit (1984)	220883-35-6	1.50	2.40	1.20	1.10	plane	0.86	coarse	0.36	1.11	3.85	0.283	0.93	0.885	0.37	1.00E-03
N/A	de Wit (1984)	220883-35-7	1.50	2.40	1.20	1.10	plane	0.86	coarse	0.48	1.05	3.85	0.283	0.93	0.626	0.26	8.30E-04
N/A	de Wit (1984)	220883-35-8	1.50	2.40	1.20	1.10	plane	0.86	coarse	0.48	1.05	3.85	0.283	0.93	1.04	0.43	7.50E-04

Table B.1: Data used in the review of the Schmertmann (2000) model (continued)

Test series	Reference	Test No. in ref.	D (m)	L (m)	$1/C_D$	$1/C_L$	Exit	C_G	Soil	RD	$1/C_\gamma$	C_u	d_{10} (mm)	$1/C_S$	H (m)	i_{exp}	K (m/s)
N/A	de Wit (1984)	220883-35-9	1.50	2.40	1.20	1.10	plane	0.86	coarse	0.48	1.05	3.85	0.283	0.93	0.94	0.39	7.30E-04
N/A	van Beek (2011)	I-137	0.10	0.33	1.08	0.74	plane	0.88	Enschede	0.98	0.87	1.6	0.265	0.95	0.26	0.79	3.10E-04
N/A	van Beek (2011)	I-138	0.10	0.33	1.08	0.74	plane	0.88	Enschede	0.97	0.87	1.6	0.265	0.95	0.28	0.85	2.80E-04
N/A	van Beek (2011)	Ijkfs01	3.00	15.00	1.00	1.58	plane	0.92	Fine Ijkdijk	0.6	1.00	1.6	0.1	1.15	2.3	0.15	8.00E-05
N/A	van Beek (2011)	Ijkfs02	2.85	15.00	0.99	1.58	plane	0.92	coarse Ijkdijk	0.75	0.94	1.8	0.125	1.10	1.75	0.12	1.40E-04
N/A	van Beek (2011)	Ijkfs03	3.00	15.00	1.00	1.58	plane	0.92	Fine Ijkdijk	0.6	1.00	1.6	0.1	1.15	2.1	0.14	8.00E-05
N/A	van Beek (2011)	Ijkfs04	2.85	15.00	0.99	1.58	plane	0.92	coarse Ijkdijk	0.7	0.96	1.8	0.125	1.10	2	0.13	1.20E-04
N/A	de Wit (1984)	220885-10-1	0.50	0.90	1.18	0.90	slot	0.80	beach	0.49	1.05	1.33	0.167	1.04	0.204	0.23	-
N/A	de Wit (1984)	220885-10-2	0.50	0.90	1.18	0.90	slot	0.80	beach	0.83	0.92	1.33	0.167	1.04	0.206	0.23	-
N/A	de Wit (1984)	220885-10-3	0.50	0.90	1.18	0.90	slot	0.80	beach	0.49	1.05	1.33	0.167	1.04	0.144	0.16	-
N/A	de Wit (1984)	220885-10-4	0.50	0.90	1.18	0.90	slot	0.80	beach	0.83	0.92	1.33	0.167	1.04	0.227	0.25	-
N/A	de Wit (1984)	220885-10-5	0.50	0.90	1.18	0.90	slot	0.80	beach	0.49	1.05	1.33	0.167	1.04	0.15	0.17	-
N/A	de Wit (1984)	220885-10-6	0.50	0.90	1.18	0.90	slot	0.80	beach	0.83	0.92	1.33	0.167	1.04	0.267	0.30	-
N/A	de Wit (1984)	220885-10-1	1.50	2.70	1.18	1.12	slot	0.81	beach	0.83	0.92	1.33	0.167	1.04	0.397	0.15	-
N/A	de Wit (1984)	220885-10-2	1.50	2.70	1.18	1.12	slot	0.81	beach	0.83	0.92	1.33	0.167	1.04	0.392	0.15	-
N/A	de Wit (1984)	220885-10-3	1.50	2.70	1.18	1.12	slot	0.81	beach	0.83	0.92	1.33	0.167	1.04	0.332	0.12	-
N/A	de Wit (1984)	220883-4-1	1.50	2.40	1.20	1.10	circle	0.57	beach	0.74	0.95	1.33	0.167	1.04	0.47	0.20	1.80E-04
N/A	de Wit (1984)	220883-4-2	1.50	2.40	1.20	1.10	circle	0.63	beach	0.74	0.95	1.33	0.167	1.04	0.456	0.19	1.90E-04
N/A	de Wit (1984)	220883-4-3	1.50	4.50	1.09	1.24	circle	0.71	beach	0.74	0.95	1.33	0.167	1.04	0.862	0.19	1.80E-04
N/A	de Wit (1984)	220883-4-4	1.50	4.50	1.09	1.24	circle	0.76	beach	0.74	0.95	1.33	0.167	1.04	0.78	0.17	1.60E-04
N/A	Hanses (1985)	21	0.24	0.70	1.10	0.86	circle	0.75	Sand A	1	0.86	1.3	0.265	0.95	0.126	0.18	4.00E-04
N/A	Hanses (1985)	22	0.24	0.70	1.10	0.86	circle	0.75	Sand A	1	0.86	1.3	0.265	0.95	0.128	0.18	4.00E-04
N/A	Hanses (1985)	23	0.24	0.70	1.10	0.86	circle	0.75	Sand A	1.02	0.86	1.3	0.265	0.95	0.127	0.18	3.90E-04
N/A	Hanses (1985)	24	0.24	0.70	1.10	0.86	circle	0.75	Sand A	1.05	0.85	1.3	0.265	0.95	0.127	0.18	3.70E-04
N/A	Hanses (1985)	25	0.24	0.70	1.10	0.86	circle	0.75	Sand A	1	0.86	1.3	0.265	0.95	0.126	0.18	4.00E-04
N/A	Hanses (1985)	26a	0.24	0.70	1.10	0.86	circle	0.75	Sand A	0.96	0.87	1.3	0.265	0.95	0.107	0.15	4.20E-04
N/A	Hanses (1985)	51	0.08	0.60	0.93	0.83	circle	0.89	Sand A	0.99	0.87	1.3	0.265	0.95	0.206	0.34	4.00E-04
N/A	Hanses (1985)	52	0.08	0.60	0.93	0.83	circle	0.89	Sand A	0.87	0.90	1.3	0.265	0.95	0.2	0.33	4.70E-04
N/A	Hanses (1985)	53	0.08	0.60	0.93	0.83	circle	0.89	Sand A	0.92	0.89	1.3	0.265	0.95	0.17	0.28	4.40E-04
N/A	Hanses (1985)	71	0.33	2.60	0.92	1.11	circle	0.88	Sand A	0.87	0.90	1.3	0.265	0.95	0.276	0.11	4.70E-04
N/A	Hanses (1985)	73	0.33	2.60	0.92	1.11	circle	0.88	Sand A	0.8	0.93	1.3	0.265	0.95	0.275	0.11	5.10E-04
N/A	van Beek (2015)	B115	0.10	0.30	1.09	0.72	circle	0.75	Baskarp 1	0.89	0.90	1.54	0.095	1.16	0.08	0.27	5.40E-05
N/A	van Beek (2015)	B118	0.10	0.30	1.09	0.72	circle	0.75	Baskarp 1	0.89	0.90	1.54	0.095	1.16	0.08	0.27	6.30E-05
N/A	van Beek (2015)	W130	0.10	0.30	1.09	0.72	circle	0.75	Hoherstall Waalre	0.65	0.98	1.58	0.24	0.96	0.106	0.35	5.10E-04
N/A	van Beek (2015)	W131	0.10	0.30	1.09	0.72	circle	0.75	Hoherstall Waalre	0.65	0.98	1.58	0.24	0.96	0.086	0.29	5.40E-04
N/A	van Beek (2015)	B132	0.10	0.30	1.09	0.72	circle	0.75	Baskarp 1	0.65	0.98	1.54	0.095	1.16	0.065	0.22	9.30E-05
N/A	van Beek (2015)	B133	0.10	0.30	1.09	0.72	circle	0.75	Baskarp 1	0.65	0.98	1.54	0.095	1.16	0.065	0.22	9.50E+05
N/A	van Beek (2015)	o140	0.10	0.30	1.09	0.72	circle	0.75	Oostelijke	0.65	0.98	2.06	0.12	1.11	0.095	0.32	2.00E-04
N/A	van Beek (2015)	o141	0.10	0.30	1.09	0.72	circle	0.75	Oostelijke	0.65	0.98	2.06	0.12	1.11	0.09	0.30	2.10E-04
N/A	van Beek (2015)	b142	0.10	0.30	1.09	0.72	circle	0.75	Baskarp 1	0.91	0.89	1.54	0.095	1.16	0.08	0.27	6.20E-05
N/A	van Beek (2015)	b143	0.10	0.30	1.09	0.72	circle	0.79	Baskarp 1	0.91	0.89	1.54	0.095	1.16	0.084	0.28	5.50E-05
N/A	van Beek (2015)	B144	0.10	0.30	1.09	0.72	circle	0.79	Baskarp 1	0.91	0.89	1.54	0.095	1.16	0.085	0.28	5.30E-05
N/A	van Beek (2015)	b145	0.10	0.30	1.09	0.72	circle	0.79	Baskarp 1	0.65	0.98	1.54	0.095	1.16	0.069	0.23	8.00E-05
N/A	van Beek (2015)	b146	0.10	0.30	1.09	0.72	circle	0.79	Baskarp 1	0.65	0.98	1.54	0.095	1.16	0.07	0.23	8.00E-05
N/A	van Beek (2015)	e150	0.10	0.30	1.09	0.72	circle	0.75	Enschede	1	0.86	1.6	0.265	0.95	0.099	0.33	4.10E-04
N/A	van Beek (2015)	o163	0.10	0.30	1.09	0.72	circle	0.75	Oostelijke	0.94	0.88	2.06	0.12	1.11	0.185	0.62	1.30E-04
N/A	van Beek (2015)	I164	0.10	0.30	1.09	0.72	circle	0.75	Itterbeck 125-250	0.97	0.87	1.7	0.125	1.10	0.113	0.38	1.30E-04
N/A	van Beek (2015)	I165	0.10	0.30	1.09	0.72	circle	0.75	Itterbeck 125-250	0.93	0.88	1.7	0.125	1.10	0.096	0.32	1.40E-04
N/A	van Beek (2015)	I166	0.10	0.30	1.09	0.72	circle	0.75	Itterbeck mix1	1	0.86	2.43	0.08	1.20	0.21	0.70	4.60E-05
N/A	van Beek (2015)	I167	0.10	0.30	1.09	0.72	circle	0.75	Itterbeck mix2	0.93	0.88	3.17	0.055	1.29	0.152	0.51	3.70E-05
N/A	van Beek (2015)	I168	0.10	0.30	1.09	0.72	circle	0.75	Itterbeck mix2	0.89	0.90	3.17	0.055	1.29	0.205	0.68	2.70E-05
N/A	van Beek (2015)	E169	0.10	0.30	1.09	0.72	circle	0.75	Enschede	0.94	0.88	1.6	0.265	0.95	0.09	0.30	3.20E-04
N/A	van Beek (2015)	S170	0.10	0.30	1.09	0.72	circle	0.75	Sterksel	0.89	0.90	2.25	0.1	1.15	0.35	1.17	7.60E-05
N/A	van Beek (2015)	B171	0.10	0.30	1.09	0.72	circle	0.75	Baskarp 1	0.9	0.89	1.54	0.095	1.16	0.079	0.26	6.80E-05
N/A	van Beek (2015)	E172	0.10	0.30	1.09	0.72	circle	0.75	Enschede	0.94	0.88	1.6	0.265	0.95	0.085	0.28	3.40E-04
N/A	van Beek (2015)	Ims18	0.40	1.30	1.08	0.97	circle	0.76	Itterbeck 0.33	0.87	0.90	2.1	0.24	0.96	0.33	0.25	3.50E-04
N/A	van Beek (2015)	Bms1	0.40	1.30	1.08	0.97	circle	0.76	Baskarp 2	0.94	0.88	1.5	0.095	1.16	0.21	0.16	8.00E-05

Table B.1: Data used in the review of the Schmertmann (2000) model (continued)

Test series	Reference	Test No. in ref.	D (m)	L (m)	$1/C_D$	$1/C_L$	Exit	C_G	Soil	RD	$1/C_\gamma$	C_u	d_{10} (mm)	$1/C_S$	H (m)	i_{exp}	K (m/s)
N/A	van Beek (2015)	Ims20	0.40	1.30	1.08	0.97	circle	0.76	Itterbeck 0.33	0.91	0.89	2.1	0.24	0.96	0.194	0.15	3.90E-04
N/A	van Beek (2011)	B19	0.10	0.34	1.07	0.74	Slope	0.93	Baskarp	0.64	0.98	1.54	0.095	1.16	0.114	0.34	1.50E-04
N/A	van Beek (2011)	B23	0.10	0.34	1.07	0.74	Slope	0.93	Baskarp	0.98	0.87	1.54	0.095	1.16	0.193	0.57	5.90E-05
N/A	van Beek (2011)	B24	0.10	0.34	1.07	0.74	Slope	0.93	Baskarp	0.97	0.87	1.54	0.095	1.16	0.172	0.51	6.80E-05
N/A	van Beek (2011)	B28	0.10	0.34	1.07	0.74	Slope	0.93	Baskarp	0.37	1.10	1.54	0.095	1.16	0.071	0.21	2.70E-04
N/A	van Beek (2011)	D31	0.10	0.33	1.07	0.74	Slope	0.93	Dekzand Nunspeet	0.65	0.98	2.6	0.07	1.23	0.179	0.54	6.20E-05
N/A	van Beek (2011)	D32	0.10	0.33	1.07	0.74	Slope	0.93	Dekzand Nunspeet	0.65	0.98	2.6	0.07	1.23	0.138	0.42	8.30E-05
N/A	van Beek (2011)	B35	0.10	0.34	1.07	0.74	Slope	0.93	Baskarp	0.64	0.98	1.54	0.095	1.16	0.135	0.40	1.30E-04
N/A	van Beek (2011)	B36	0.10	0.33	1.07	0.74	Slope	0.93	Baskarp	0.63	0.99	1.54	0.095	1.16	0.137	0.41	1.10E-04
N/A	van Beek (2011)	D37	0.10	0.33	1.07	0.74	Slope	0.93	Dekzand Nunspeet	0.98	0.87	2.6	0.07	1.23	0.265	0.79	3.90E-05
N/A	van Beek (2011)	D38	0.10	0.34	1.07	0.74	Slope	0.93	Dekzand Nunspeet	0.92	0.89	2.6	0.07	1.23	0.165	0.49	5.90E-05
N/A	van Beek (2011)	D39	0.10	0.33	1.07	0.74	Slope	0.93	Dekzand Nunspeet	0.92	0.89	2.6	0.07	1.23	0.139	0.42	5.40E-05
N/A	van Beek (2011)	B40	0.10	0.33	1.07	0.74	Slope	0.93	Baskarp	0.91	0.89	1.54	0.095	1.16	0.148	0.45	5.30E-05
N/A	van Beek (2011)	B41	0.10	0.33	1.07	0.74	Slope	0.93	Baskarp	0.92	0.89	1.54	0.095	1.16	0.153	0.46	7.30E-05
N/A	van Beek (2011)	O43	0.10	0.33	1.07	0.74	Slope	0.93	Oostelijke	0.75	0.94	2.06	0.12	1.11	0.099	0.30	4.20E-04
N/A	van Beek (2011)	I45	0.10	0.33	1.07	0.74	Slope	0.93	Itterbeck Boxtel	0.72	0.95	2.2	0.08	1.20	0.203	0.61	8.80E-05
N/A	van Beek (2011)	I46	0.10	0.34	1.07	0.74	Slope	0.93	Itterbeck Boxtel	0.7	0.96	2.2	0.08	1.20	0.155	0.46	1.10E-04
N/A	van Beek (2011)	I47	0.10	0.34	1.07	0.74	Slope	0.93	Enschede	0.75	0.94	1.6	0.265	0.95	0.087	0.26	7.30E-04
N/A	van Beek (2011)	I48	0.10	0.34	1.07	0.74	Slope	0.93	Enschede	0.76	0.94	1.6	0.265	0.95	0.079	0.23	1.10E-03
N/A	van Beek (2011)	I49	0.10	0.34	1.07	0.74	Slope	0.93	Hoherstall Waalre	0.76	0.94	1.58	0.24	0.96	0.069	0.20	8.00E-04
N/A	van Beek (2011)	I50	0.10	0.33	1.07	0.74	Slope	0.93	Hoherstall Waalre	0.73	0.95	1.58	0.24	0.96	0.047	0.14	2.20E-03
N/A	van Beek (2011)	I51	0.10	0.34	1.07	0.74	Slope	0.93	Sandr	0.7	0.96	1.5	0.125	1.10	0.112	0.33	1.70E-04
N/A	van Beek (2011)	I52	0.10	0.33	1.07	0.74	Slope	0.93	Hoherstall Waalre	0.71	0.96	1.58	0.24	0.96	0.092	0.28	7.00E-04
N/A	van Beek (2011)	I53	0.10	0.33	1.08	0.73	Slope	0.93	Sandr	0.74	0.95	1.5	0.125	1.10	0.128	0.39	1.10E-04
N/A	van Beek (2011)	B54	0.10	0.33	1.08	0.74	Slope	0.93	Baskarp	0.79	0.93	1.54	0.095	1.16	0.18	0.55	7.40E-05
N/A	van Beek (2011)	B55	0.10	0.33	1.08	0.73	Slope	0.93	Baskarp	0.71	0.96	1.54	0.095	1.16	0.141	0.43	8.80E-05
N/A	van Beek (2011)	I56	0.10	0.34	1.07	0.74	Slope	0.93	Scheemda	0.69	0.97	1.3	0.125	1.10	0.1	0.30	1.30E-04
N/A	van Beek (2011)	B57	0.10	0.33	1.08	0.74	Slope	0.93	Baskarp	0.75	0.94	1.54	0.095	1.16	0.132	0.40	8.80E-05
N/A	van Beek (2011)	B58	0.10	0.35	1.07	0.74	Slope	0.93	Baskarp	0.7	0.96	1.54	0.095	1.16	0.182	0.53	1.00E-04
N/A	van Beek (2011)	B61	0.10	0.35	1.07	0.74	Slope	0.93	Baskarp	0.73	0.95	1.54	0.095	1.16	0.114	0.33	9.90E-05
N/A	van Beek (2011)	I62	0.10	0.33	1.08	0.73	Slope	0.93	Scheemda	0.63	0.99	1.3	0.125	1.10	0.099	0.30	2.00E-04
N/A	van Beek (2011)	S63	0.10	0.34	1.07	0.74	Slope	0.93	Sterksel	0.75	0.94	2.25	0.1	1.15	0.125	0.37	2.40E-04
N/A	van Beek (2011)	S64	0.10	0.34	1.07	0.74	Slope	0.93	Sterksel	0.75	0.94	2.25	0.1	1.15	0.12	0.36	1.70E-04
N/A	van Beek (2011)	B82	0.10	0.34	1.07	0.74	Slope	0.93	Baskarp	0.85	0.91	1.54	0.095	1.16	0.139	0.41	5.90E-05
N/A	van Beek (2011)	B83	0.10	0.33	1.07	0.74	Slope	0.93	Baskarp	0.85	0.91	1.54	0.095	1.16	0.139	0.42	6.00E-05
N/A	van Beek (2011)	B84	0.10	0.33	1.07	0.74	Slope	0.93	Baskarp	0.53	1.03	1.54	0.095	1.16	0.098	0.29	9.70E-05
N/A	van Beek (2011)	B85	0.10	0.34	1.07	0.74	Slope	0.93	Baskarp	0.53	1.03	1.54	0.095	1.16	0.118	0.35	7.70E-05
N/A	van Beek (2011)	B86	0.10	0.34	1.07	0.74	Slope	0.93	Baskarp	0.43	1.07	1.54	0.095	1.16	0.098	0.29	1.00E-04
N/A	van Beek (2011)	B87	0.10	0.34	1.07	0.74	Slope	0.93	Baskarp	0.42	1.08	1.54	0.095	1.16	0.046	0.14	1.80E-04
N/A	van Beek (2011)	B101	0.10	0.31	1.09	0.73	Slope	0.93	Baskarp	0.31	1.13	1.54	0.095	1.16	0.08	0.26	1.00E-04
N/A	van Beek (2011)	B103	0.10	0.32	1.08	0.73	Slope	0.93	Baskarp	0.09	1.26	1.54	0.095	1.16	0.08	0.25	1.60E-04
N/A	van Beek (2011)	B104	0.10	0.31	1.09	0.73	Slope	0.93	Baskarp	0.09	1.26	1.54	0.095	1.16	0.08	0.26	-
N/A	van Beek (2011)	B105	0.10	0.34	1.07	0.74	Slope	0.93	Baskarp	0.83	0.92	1.54	0.095	1.16	0.16	0.48	7.60E-05
N/A	van Beek (2011)	B107	0.10	0.33	1.07	0.74	Slope	0.93	Baskarp	0.88	0.90	1.54	0.095	1.16	0.18	0.54	6.10E-05
N/A	van Beek (2011)	B121	0.10	0.34	1.07	0.74	Slope	0.93	Baskarp	0.13	1.23	1.54	0.095	1.16	0.09	0.27	1.80E-04
N/A	van Beek (2011)	B122	0.10	0.34	1.07	0.74	Slope	0.93	Baskarp	0.12	1.24	1.54	0.095	1.16	0.08	0.24	1.60E-04
N/A	van Beek (2011)	B123B	0.10	0.33	1.07	0.74	Slope	0.93	Baskarp	0.12	1.24	1.54	0.095	1.16	0.13	0.39	9.50E-05
N/A	van Beek (2011)	BMS1	0.40	1.37	1.07	0.98	Slope	0.94	Baskarp	0.6	1.00	1.54	0.095	1.16	0.28	0.20	1.20E-04
N/A	van Beek (2011)	BMS2	0.40	1.45	1.06	0.99	Slope	0.94	Baskarp	0.5	1.04	1.54	0.095	1.16	0.37	0.26	1.40E-04
N/A	van Beek (2011)	IMS3	0.40	1.46	1.06	0.99	Slope	0.94	Itterbeck 125-250	0.64	0.98	1.7	0.125	1.10	0.26	0.18	2.00E-04
N/A	van Beek (2011)	IMS4	0.40	1.46	1.06	0.99	Slope	0.94	Itterbeck 125-250	0.51	1.04	1.7	0.125	1.10	0.2	0.14	3.70E-04
N/A	van Beek (2011)	IMS5	0.40	1.42	1.06	0.99	Slope	0.94	Itterbeck 125-250	0.75	0.94	1.7	0.125	1.10	0.29	0.20	2.20E-04
N/A	van Beek (2011)	BMS7	0.40	1.30	1.08	0.97	Slope	0.94	Baskarp	0.64	0.98	1.54	0.095	1.16	0.29	0.22	1.50E-04
N/A	van Beek (2011)	BMS8	0.40	1.33	1.07	0.97	Slope	0.94	Baskarp	0.5	1.04	1.54	0.095	1.16	0.19	0.14	2.60E-04
N/A	van Beek (2011)	IJKMS9	0.40	1.46	1.06	0.99	Slope	0.94	Itterbeck 333	0.5	1.04	2.1	0.155	1.05	0.345	0.24	2.30E-04
N/A	van Beek (2011)	IJKMS1	0.40	1.43	1.06	0.99	Slope	0.94	Itterbeck 431	0.47	1.05	2.6	0.16	1.05	0.26	0.18	1.60E-04
N/A	van Beek (2011)	IMS11	0.40	1.48	1.05	0.99	Slope	0.94	Itterbeck 333	0.65	0.98	2.1	0.155	1.05	0.59	0.40	4.73E-03

Table B.1: Data used in the review of the Schmertmann (2000) model (continued)

Test series	Reference	Test No. in ref.	D (m)	L (m)	$1/C_D$	$1/C_L$	Exit	C_G	Soil	RD	$1/C_\gamma$	C_u	d_{10} (mm)	$1/C_S$	H (m)	i_{exp}	K (m/s)
N/A	van Beek (2011)	IMS12	0.40	1.44	1.06	0.99	Slope	0.94	Itterbeck 431	0.65	0.98	2.6	0.16	1.05	0.39	0.27	4.00E-04
N/A	van Beek (2011)	IMS13	0.40	1.45	1.06	0.99	Slope	0.94	coarse Ijkdijk	0.55	1.02	1.8	0.125	1.10	0.37	0.26	4.60E-04
N/A	van Beek (2011)	IMS14	0.40	1.46	1.06	0.99	Slope	0.94	Fine Ijkdijk	0.5	1.04	1.6	0.1	1.15	0.48	0.33	3.80E-04
N/A	Yao et al (2007)	?1	0.60	1.40	1.14	0.98	circle	0.71	?1	-	1	3.5	0.8	0.76	0.2996	0.21	-
N/A	Yao et al (2007)	?2	0.60	1.40	1.14	0.98	plane	0.84	?2	-	1	3.5	0.8	0.76	0.3892	0.28	-
N/A	this study	20	0.31	1.30	1.03	0.97	Circle	0.83	Syd sand	-	1	1.3	0.24	0.96	0.233	0.18	-
N/A	this study	21	0.31	1.30	1.03	0.97	Slot	0.83	Syd sand	-	1	1.3	0.24	0.96	0.271	0.21	3.42E-04
N/A	this study	22	0.31	1.30	1.03	0.97	Circle	0.83	Syd sand	-	1	1.3	0.24	0.96	0.195	0.15	3.11E-04
N/A	this study	23	0.31	1.30	1.03	0.97	Slot	0.83	Syd sand	-	1	1.3	0.24	0.96	0.256	0.20	3.11E-04
N/A	this study	24	0.31	1.30	1.03	0.97	Circle	0.83	Syd sand	-	1	1.3	0.24	0.96	0.236	0.18	3.11E-04
N/A	this study	25	0.31	1.30	1.03	0.97	Slot	0.83	Syd sand	-	1	1.3	0.24	0.96	0.271	0.21	3.11E-04
N/A	this study	27	0.31	1.30	1.03	0.97	Circle	0.83	Syd sand	-	1	1.3	0.24	0.96	0.213	0.16	2.95E-04
N/A	this study	28	0.31	1.30	1.03	0.97	Plane	0.90	Syd sand	-	1	1.3	0.24	0.96	0.293	0.23	6.37E-04
N/A	this study	29	0.31	1.30	1.03	0.97	Slot	0.83	Syd sand	-	1	1.3	0.24	0.96	0.234	0.18	3.57E-04
N/A	this study	30	0.31	1.30	1.03	0.97	Plane	0.90	Syd sand	-	1	1.3	0.24	0.96	0.313	0.24	5.59E-04
N/A	this study	31	0.31	1.30	1.03	0.97	Circle	0.83	Syd sand	-	1	1.3	0.24	0.96	0.195	0.15	2.80E-04
N/A	this study	32	0.31	1.30	1.03	0.97	Plane	0.90	Syd sand	-	1	1.3	0.24	0.96	0.331	0.25	7.77E-04
N/A	this study	33	0.31	1.30	1.03	0.97	Slope	0.92	Syd sand	-	1	1.3	0.24	0.96	0.342	0.26	3.73E-04
N/A	this study	34	0.31	1.30	1.03	0.97	Circle	0.83	Syd sand	-	1	1.3	0.24	0.96	0.203	0.16	3.73E-04
N/A	this study	35	0.31	1.30	1.03	0.97	Slope	0.92	Syd sand	-	1	1.3	0.24	0.96	0.307	0.24	4.35E-04
N/A	this study	36	0.31	1.30	1.03	0.97	Slope	0.92	Syd sand	-	1	1.3	0.24	0.96	0.335	0.26	3.57E-04
N/A	this study	37	0.31	1.30	1.03	0.97	Slot	0.83	Syd sand	-	1	1.3	0.24	0.96	0.237	0.18	3.73E-04
N/A	this study	40	0.31	1.30	1.03	0.97	Slot	0.83	Syd sand	-	1	1.3	0.24	0.96	0.273	0.21	3.57E-04
N/A	this study	41	0.31	2.60	0.91	1.11	Slot	0.83	Syd sand	-	1	1.3	0.24	0.96	0.481	0.19	3.73E-04
N/A	this study	42	0.31	1.30	1.03	0.97	Circle	0.83	Syd sand	-	1	1.3	0.24	0.96	0.186	0.14	4.19E-04
N/A	this study	45	0.31	3.90	0.84	1.21	Slot	0.83	Syd sand	-	1	1.3	0.24	0.96	0.73	0.19	1.24E-04
N/A	this study	49	0.31	1.30	1.03	0.97	Circle	0.83	Syd sand	-	1	1.3	0.24	0.96	0.196	0.15	2.90E-04
N/A	this study	50	0.31	1.30	1.03	0.97	Circle	0.83	Mix 2	-	1	4.2	0.2	1.00	0.661	0.51	3.90E-04
N/A	this study	52	0.31	1.30	1.03	0.97	Circle	0.83	Mix 4	-	1	8.8	0.24	0.96	2.476	1.90	6.50E-04
N/A	this study	53	0.31	1.30	1.03	0.97	Circle	0.83	Mix 3	-	1	6.2	0.21	0.99	1.014	0.78	7.10E-04
N/A	this study	55	0.31	2.60	0.91	1.11	Slot	0.83	Syd sand	-	1	1.3	0.24	0.96	0.439	0.17	-
N/A	this study	57	0.31	1.30	1.03	0.97	Circle	0.83	50n	-	1	1.9	0.11	1.13	0.324	0.25	1.00E-04
N/A	this study	58	0.31	1.30	1.03	0.97	Circle	0.83	Mix 5	-	1	6.1	0.51	0.83	1.28	0.98	2.90E-03
N/A	this study	59	0.31	1.30	1.03	0.97	Circle	0.83	Mix 6	-	1	2.44	0.081	1.20	0.51	0.39	2.90E-05
N/A	this study	60	0.31	1.30	1.03	0.97	Circle	0.83	50n	-	1	1.9	0.11	1.13	0.225	0.17	1.60E-04
N/A	this study	61	0.31	1.30	1.03	0.97	Circle	0.83	Mix 2	-	1	4.2	0.2	1.00	0.651	0.50	-
N/A	this study	62	0.31	1.30	1.03	0.97	Circle	0.83	Mix 8	-	1	6.36	0.033	1.43	1.315	1.01	-
N/A	this study	63	0.31	1.30	1.03	0.97	Circle	0.83	Mix 3	-	1	6.2	0.21	0.99	0.863	0.66	-
N/A	this study	64	0.31	1.30	1.03	0.97	Circle	0.83	Mix 8	-	1	6.36	0.033	1.43	1.028	0.79	1.50E-05
N/A	this study	66	0.31	1.30	1.03	0.97	Slope	0.92	Syd sand	-	1	1.3	0.24	0.96	0.386	0.30	2.50E-04
N/A	this study	67	0.31	1.30	1.03	0.97	Circle	0.83	Mix 7	-	1	2.92	0.065	1.25	0.853	0.66	1.60E-05
N/A	this study	68	0.31	3.90	0.84	1.21	Slot	0.83	Syd sand	-	1	1.3	0.24	0.96	0.69	0.18	1.40E-04
N/A	this study	69	0.31	1.30	1.03	0.97	Circle	0.83	Mix 7	-	1	2.92	0.065	1.25	0.802	0.62	1.90E-05
N/A	this study	71	0.31	1.30	1.03	0.97	Circle	0.83	Mix 1	-	1	6.8	0.075	1.22	3.71	2.85	2.90E-05
N/A	this study	73	0.31	1.30	1.03	0.97	Circle	0.83	Mix 4	-	1	8.8	0.24	0.96	2.675	2.06	6.00E-04
N/A	this study	74	0.31	1.30	1.03	0.97	Circle	0.83	Mix 5	-	1	6.1	0.51	0.83	1.02	0.78	2.40E-03
N/A	this study	75	0.31	1.30	1.03	0.97	Circle	0.83	Mix 8	-	1	6.36	0.033	1.43	1.64	1.26	7.00E-06
N/A	this study	76	0.31	1.30	1.03	0.97	Slope	0.92	Syd sand	-	1	1.3	0.24	0.96	0.366	0.28	4.20E-04
N/A	this study	78	0.31	1.30	1.03	0.97	Circle	0.83	Mix 6	-	1	2.44	0.081	1.20	0.475	0.37	-
N/A	this study	79	0.31	1.30	1.03	0.97	Circle	0.83	Syd sand	-	1	1.3	0.24	0.96	0.239	0.18	3.40E-04

B.2 Data used in the review of the Sellmeijer et al. (2011) model

Table B.2: Data used in the review of the Sellmeijer et al. (2011) model

Reference	Test	Exit	Soil	Hc (m)	L (m)	i_c (-)	η (-)	γ'_p (N/m^3)	γ_u (N/m^3)	d_{50} (m)	θ (°)	RD (%)	U (-)	KAS (%)	FR	d_{70} (m)	K (m/s)	μ (Ns/m^2)	κ (m^2)	FS	D (m)	FG	i_c (-)
de Wit (1984)	220880-I-1	Plane	Dune	0.33	0.8	0.413	0.25	16187	9810	0.0002	37	85	1.48	49.8	0.320	0.0002	1.10E-04	1.E-03	1.12E-11	1.009	0.50	1.062	0.343
de Wit (1984)	220880-I-2	Plane	Dune	0.364	0.8	0.455	0.25	16187	9810	0.0002	37	90	1.48	49.8	0.327	0.0002	8.90E-05	1.E-03	9.07E-12	1.083	0.50	1.062	0.375
de Wit (1984)	220880-I-3	Plane	Dune	0.331	0.8	0.414	0.25	16187	9810	0.0002	37	89	1.48	49.8	0.325	0.0002	1.10E-04	1.E-03	1.12E-11	1.009	0.50	1.062	0.348
de Wit (1984)	220880-I-4	Plane	Dune	0.239	0.8	0.299	0.25	16187	9810	0.0002	37	73	1.48	49.8	0.304	0.0002	1.50E-04	1.E-03	1.53E-11	0.910	0.50	1.062	0.293
de Wit (1984)	220880-I-5	Plane	Dune	0.269	0.8	0.336	0.25	16187	9810	0.0002	37	64	1.48	49.8	0.290	0.0002	1.50E-04	1.E-03	1.53E-11	0.910	0.50	1.062	0.280
de Wit (1984)	220880-I-6	Plane	Dune	0.272	0.8	0.340	0.25	16187	9810	0.0002	37	81	1.48	49.8	0.315	0.0002	1.80E-04	1.E-03	1.83E-11	0.856	0.50	1.062	0.286
de Wit (1984)	220880-I-7	Plane	Dune	0.201	0.8	0.251	0.25	16187	9810	0.0002	37	53	1.48	49.8	0.271	0.0002	2.50E-04	1.E-03	2.55E-11	0.767	0.50	1.062	0.221
de Wit (1984)	220880-I-8	Plane	Dune	0.166	0.8	0.208	0.25	16187	9810	0.0002	37	37	1.48	49.8	0.239	0.0002	2.70E-04	1.E-03	2.75E-11	0.748	0.50	1.062	0.190
de Wit (1984)	220880-I-9	Plane	Dune	0.222	0.8	0.278	0.25	16187	9810	0.0002	37	45	1.48	49.8	0.256	0.0002	3.30E-04	1.E-03	3.36E-11	0.699	0.50	1.062	0.190
de Wit (1984)	220880-II-1	Plane	Dune	0.302	0.8	0.378	0.25	16187	9810	0.0002	37	84	2.3	49.8	0.338	0.0002	3.70E-04	1.E-03	3.77E-11	0.673	0.50	1.062	0.241
de Wit (1984)	220880-II-2	Plane	Dune	0.45	0.8	0.563	0.25	16187	9810	0.0002	37	75	2.3	49.8	0.325	0.0002	3.90E-04	1.E-03	3.98E-11	0.662	0.50	1.062	0.228
de Wit (1984)	220880-II-3	Plane	Dune	0.3	0.8	0.375	0.25	16187	9810	0.0002	37	60	2.3	49.8	0.300	0.0002	5.20E-04	1.E-03	5.30E-11	0.601	0.50	1.062	0.192
de Wit (1984)	220880-II-4	Plane	Dune	0.445	0.8	0.556	0.25	16187	9810	0.0002	37	48	2.3	49.8	0.278	0.0002	6.10E-04	1.E-03	6.22E-11	0.570	0.50	1.062	0.168
de Wit (1984)	220880-II-5	Plane	Dune	0.34	0.8	0.425	0.25	16187	9810	0.0002	37	36	2.3	49.8	0.251	0.0002	6.60E-04	1.E-03	6.73E-11	0.555	0.50	1.062	0.148
de Wit (1984)	220880-II-6	Plane	Dune	0.225	0.8	0.281	0.25	16187	9810	0.0002	37	24	2.3	49.8	0.218	0.0002	7.50E-04	1.E-03	7.65E-11	0.532	0.50	1.062	0.123
de Wit (1984)	220880-III-1	Plane	River sand 1A	0.3	0.8	0.375	0.25	16187	9810	0.0004	37	72	2.1	49.8	0.316	0.00048	3.70E-04	1.E-03	3.77E-11	0.934	0.50	1.062	0.313
de Wit (1984)	220880-III-2	Plane	River sand 1A	0.392	0.8	0.490	0.25	16187	9810	0.0004	37	61	2.1	49.8	0.298	0.00048	3.70E-04	1.E-03	3.77E-11	0.934	0.50	1.062	0.296
de Wit (1984)	220880-III-3	Plane	River sand 1A	0.364	0.8	0.455	0.25	16187	9810	0.0004	37	51	2.1	49.8	0.280	0.00048	3.80E-04	1.E-03	3.87E-11	0.925	0.50	1.062	0.275
de Wit (1984)	220880-III-4	Plane	River sand 1A	0.284	0.8	0.355	0.25	16187	9810	0.0004	37	38	2.1	49.8	0.253	0.00048	4.60E-04	1.E-03	4.69E-11	0.868	0.50	1.062	0.233
de Wit (1984)	220880-III-5	Plane	River sand 1A	0.322	0.8	0.403	0.25	16187	9810	0.0004	37	27	2.1	49.8	0.224	0.00048	5.30E-04	1.E-03	5.40E-11	0.828	0.50	1.062	0.197
de Wit (1984)	220880-III-6	Plane	River sand 1A	0.202	0.8	0.253	0.25	16187	9810	0.0004	37	16	2.1	49.8	0.187	0.00048	6.90E-04	1.E-03	7.03E-11	0.758	0.50	1.062	0.150
de Wit (1984)	220880-IV-1	Plane	Dune	0.838	2.4	0.349	0.25	16187	9810	0.0002	37	92	1.48	49.8	0.329	0.0002	1.40E-04	1.E-03	1.43E-11	0.645	1.50	1.062	0.226
de Wit (1984)	220880-IV-2	Plane	Dune	0.374	2.4	0.156	0.25	16187	9810	0.0002	37	82	1.48	49.8	0.316	0.0002	1.70E-04	1.E-03	1.73E-11	0.605	1.50	1.062	0.203
de Wit (1984)	220880-IV-3	Plane	Dune	0.409	2.4	0.170	0.25	16187	9810	0.0002	37	73	1.48	49.8	0.304	0.0002	1.90E-04	1.E-03	1.94E-11	0.583	1.50	1.062	0.188
de Wit (1984)	220880-V-1	Plane	Beach	0.266	0.8	0.333	0.25	16187	9810	0.0002	37	91	1.33	49.8	0.323	0.0002	1.60E-04	1.E-03	1.63E-11	0.904	0.50	1.062	0.310
de Wit (1984)	220880-V-2	Plane	Beach	0.303	0.8	0.379	0.25	16187	9810	0.0002	37	83	1.33	49.8	0.313	0.0002	1.90E-04	1.E-03	1.94E-11	0.853	0.50	1.062	0.284

Table B.2: Data used in the review of the Sellmeijer et al. (2011) model (continued)

Reference	Test	Exit	Soil	Hc (m)	L (m)	i_c (-)	η (-)	γ'_p (N/m^3)	γ_u (N/m^3)	d_{50} (m)	θ (°)	RD (%)	U (-)	KAS (%)	FR	d_{70} (m)	K (m/s)	μ (Ns/m^2)	κ (m^2)	FS	D (m)	FG	i_c (-)
de Wit (1984)	220880-V-3	Plane	Beach	0.234	0.8	0.293	0.25	16187	9810	0.0002	37	74	1.33	49.8	0.301	0.0002	2.10E-04	1.E-03	2.14E-11	0.825	0.50	1.062	0.264
de Wit (1984)	220880-V-4	Plane	Beach	0.244	0.8	0.305	0.25	16187	9810	0.0002	37	66	1.33	49.8	0.289	0.0002	2.60E-04	1.E-03	2.65E-11	0.769	0.50	1.062	0.236
de Wit (1984)	220880-V-5	Plane	Beach	0.208	0.8	0.260	0.25	16187	9810	0.0002	37	57	1.33	49.8	0.275	0.0002	2.40E-04	1.E-03	2.45E-11	0.789	0.50	1.062	0.230
de Wit (1984)	220880-V-6	Plane	Beach	0.25	0.8	0.313	0.25	16187	9810	0.0002	37	49	1.33	49.8	0.260	0.0002	2.90E-04	1.E-03	2.96E-11	0.741	0.50	1.062	0.205
de Wit (1984)	220880-V-7	Plane	Beach	0.244	0.8	0.305	0.25	16187	9810	0.0002	37	40	1.33	49.8	0.243	0.0002	3.40E-04	1.E-03	3.47E-11	0.703	0.50	1.062	0.181
de Wit (1984)	220880-VI-1	Plane	Beach	0.415	2.4	0.173	0.25	16187	9810	0.0002	37	88	1.33	49.8	0.320	0.0002	2.00E-04	1.E-03	2.04E-11	0.582	1.50	1.062	0.197
de Wit (1984)	220880-VI-2	Plane	Beach	0.352	2.4	0.147	0.25	16187	9810	0.0002	37	83	1.33	49.8	0.313	0.0002	1.90E-04	1.E-03	1.94E-11	0.592	1.50	1.062	0.197
de Wit (1984)	220880-VI-3	Plane	Beach	0.414	2.4	0.173	0.25	16187	9810	0.0002	37	68	1.33	49.8	0.292	0.0002	2.40E-04	1.E-03	2.45E-11	0.547	1.50	1.062	0.170
de Wit (1984)	220880-VI-4	Plane	Beach	0.444	2.4	0.185	0.25	16187	9810	0.0002	37	66	1.33	49.8	0.289	0.0002	2.30E-04	1.E-03	2.34E-11	0.555	1.50	1.062	0.170
de Wit (1984)	220880-VI-5	Plane	Beach	0.36	2.4	0.150	0.25	16187	9810	0.0002	37	57	1.33	49.8	0.275	0.0002	2.90E-04	1.E-03	2.96E-11	0.514	1.50	1.062	0.150
de Wit (1984)	220880-VI-6	Plane	Beach	0.381	2.4	0.159	0.25	16187	9810	0.0002	37	49	1.33	49.8	0.260	0.0002	3.00E-04	1.E-03	3.06E-11	0.508	1.50	1.062	0.140
de Wit (1984)	220880-VI-7	Plane	Beach	0.285	2.4	0.119	0.25	16187	9810	0.0002	37	40	1.33	49.8	0.243	0.0002	3.50E-04	1.E-03	3.57E-11	0.483	1.50	1.062	0.124
de Wit (1984)	220880-VII-1	Plane	Beach	0.28	0.8	0.350	0.25	16187	9810	0.0002	37	95	1.33	49.8	0.328	0.0002	1.40E-04	1.E-03	1.43E-11	0.945	0.50	1.062	0.329
de Wit (1984)	220880-VII-2	Plane	Beach	0.241	0.8	0.301	0.25	16187	9810	0.0002	37	83	1.33	49.8	0.313	0.0002	1.80E-04	1.E-03	1.83E-11	0.869	0.50	1.062	0.289
de Wit (1984)	220880-VII-3	Plane	Beach	0.241	0.8	0.301	0.25	16187	9810	0.0002	37	66	1.33	49.8	0.289	0.0002	2.20E-04	1.E-03	2.24E-11	0.813	0.50	1.062	0.249
de Wit (1984)	220881-40-1	Plane	Beach	0.809	4.5	0.180	0.25	16187	9810	0.0002	37	81	1.33	49.8	0.310	0.0002	2.20E-04	1.E-03	2.24E-11	0.457	1.50	1.200	0.170
de Wit (1984)	220881-40-2	Plane	Beach	0.715	4.5	0.159	0.25	16187	9810	0.0002	37	71	1.33	49.8	0.296	0.0002	2.10E-04	1.E-03	2.14E-11	0.464	1.50	1.200	0.165
de Wit (1984)	220881-40-3	Plane	Beach	0.624	4.5	0.139	0.25	16187	9810	0.0002	37	62	1.33	49.8	0.283	0.0002	2.10E-04	1.E-03	2.14E-11	0.464	1.50	1.200	0.157
de Wit (1984)	220881-40-4	Plane	Beach	0.307	1.2	0.256	0.25	16187	9810	0.0002	37	74	1.33	49.8	0.301	0.0002	2.10E-04	1.E-03	2.14E-11	0.721	1.50	0.968	0.210
de Wit (1984)	220881-40-5	Plane	Beach	0.189	1.2	0.158	0.25	16187	9810	0.0002	37	74	1.33	49.8	0.301	0.0002	2.10E-04	1.E-03	2.14E-11	0.721	1.50	0.968	0.210
de Wit (1984)	220881-40-6	Plane	Beach	0.288	1.2	0.240	0.25	16187	9810	0.0002	37	74	1.33	49.8	0.301	0.0002	2.10E-04	1.E-03	2.14E-11	0.721	1.50	0.968	0.210
de Wit (1984)	220881-40-7	Plane	Beach	0.2	1.2	0.167	0.25	16187	9810	0.0002	37	74	1.33	49.8	0.301	0.0002	2.10E-04	1.E-03	2.14E-11	0.721	1.50	0.968	0.210
de Wit (1984)	220883-35-1	Plane	Coarse	0.88	2.4	0.367	0.25	16187	9810	0.0008	37	18	3.85	49.8	0.211	0.0014	1.80E-03	1.E-03	1.83E-10	0.584	1.50	1.062	0.131
de Wit (1984)	220883-35-2	Plane	Coarse	0.96	2.4	0.400	0.25	16187	9810	0.0008	37	20	3.85	49.8	0.218	0.0014	1.50E-03	1.E-03	1.53E-10	0.621	1.50	1.062	0.144
de Wit (1984)	220883-35-3	Plane	Coarse	0.8	2.4	0.333	0.25	16187	9810	0.0008	37	21	3.85	49.8	0.222	0.0014	1.50E-03	1.E-03	1.53E-10	0.621	1.50	1.062	0.147
de Wit (1984)	220883-35-4	Plane	Coarse	0.68	2.4	0.283	0.25	16187	9810	0.0008	37	35	3.85	49.8	0.266	0.0014	1.10E-03	1.E-03	1.12E-10	0.689	1.50	1.062	0.194
de Wit (1984)	220883-35-5	Plane	Coarse	0.714	2.4	0.298	0.25	16187	9810	0.0008	37	35	3.85	49.8	0.266	0.0014	1.00E-03	1.E-03	1.02E-10	0.711	1.50	1.062	0.201
de Wit (1984)	220883-35-6	Plane	Coarse	0.885	2.4	0.369	0.25	16187	9810	0.0008	37	36	3.85	49.8	0.268	0.0014	1.00E-03	1.E-03	1.02E-10	0.711	1.50	1.062	0.203

Table B.2: Data used in the review of the Sellmeijer et al. (2011) model (continued)

Reference	Test	Exit	Soil	Hc (m)	L (m)	i_c (-)	η (-)	γ'_p (N/m^3)	γ_u (N/m^3)	d_{50} (m)	θ (°)	RD (%)	U (-)	KAS (%)	FR	d_{70} (m)	K (m/s)	μ (Ns/m^2)	κ (m^2)	FS	D (m)	FG	i_c (-)
de Wit (1984)	220883-35-7	Plane	Coarse	0.626	2.4	0.261	0.25	16187	9810	0.0008	37	48	3.85	49.8	0.297	0.0014	8.30E-04	1.E-03	8.46E-11	0.757	1.50	1.062	0.238
de Wit (1984)	220883-35-8	Plane	Coarse	1.04	2.4	0.433	0.25	16187	9810	0.0008	37	48	3.85	49.8	0.297	0.0014	7.50E-04	1.E-03	7.65E-11	0.783	1.50	1.062	0.247
de Wit (1984)	220883-35-9	Plane	Coarse	0.94	2.4	0.392	0.25	16187	9810	0.0008	37	48	3.85	49.8	0.297	0.0014	7.30E-04	1.E-03	7.44E-11	0.790	1.50	1.062	0.249
de Wit (1984)	220883-39-1	Plane	Dune	0.237	0.8	0.296	0.25	16187	9810	0.0002	37	55	1.48	49.8	0.275	0.0002	2.60E-04	1.E-03	2.65E-11	0.757	0.50	1.062	0.221
de Wit (1984)	220883-39-2	Plane	Dune	0.195	0.8	0.244	0.25	16187	9810	0.0002	37	55	1.48	49.8	0.275	0.0002	2.60E-04	1.E-03	2.65E-11	0.757	0.50	1.062	0.221
de Wit (1984)	220883-39-3	Plane	Dune	0.214	0.8	0.268	0.25	16187	9810	0.0002	37	55	1.48	49.8	0.275	0.0002	2.20E-04	1.E-03	2.24E-11	0.801	0.50	1.062	0.234
de Wit (1984)	220883-4-1	Circle	Beach sand	0.47	2.4	0.196	0.25	16187	9810	0.0002	37	74	1.33	49.8	0.301	0.0002	1.80E-04	1.E-03	1.83E-11	0.602	1.50	1.062	0.192
de Wit (1984)	220883-4-2	Circle	Beach sand	0.456	2.4	0.190	0.25	16187	9810	0.0002	37	74	1.33	49.8	0.301	0.0002	1.90E-04	1.E-03	1.94E-11	0.592	1.50	1.062	0.189
de Wit (1984)	220883-4-3	Circle	Beach sand	0.862	4.5	0.192	0.25	16187	9810	0.0002	37	74	1.33	49.8	0.301	0.0002	1.80E-04	1.E-03	1.83E-11	0.489	1.50	1.200	0.176
de Wit (1984)	220883-4-4	Circle	Beach sand	0.78	4.5	0.173	0.25	16187	9810	0.0002	37	74	1.33	49.8	0.301	0.0002	1.60E-04	1.E-03	1.63E-11	0.508	1.50	1.200	0.183
de Wit (1984)	220884-26-1	Plane	Coarse	0.394	0.8	0.493	0.25	16187	9810	0.0008	37	19	3.85	49.8	0.215	0.0014	1.60E-03	1.E-03	1.63E-10	0.877	0.50	1.062	0.200
de Wit (1984)	220884-26-2	Plane	Coarse	0.391	0.8	0.489	0.25	16187	9810	0.0008	37	34	3.85	49.8	0.263	0.0014	1.10E-03	1.E-03	1.12E-10	0.993	0.50	1.062	0.277
de Wit (1984)	220884-26-3	Plane	Coarse	0.783	0.8	0.979	0.25	16187	9810	0.0008	37	48	3.85	49.8	0.297	0.0014	8.90E-04	1.E-03	9.07E-11	1.066	0.50	1.062	0.336
de Wit (1984)	220884-26-4	Plane	Coarse	0.792	0.8	0.990	0.25	16187	9810	0.0008	37	18	3.85	49.8	0.211	0.0014	1.10E-03	1.E-03	1.12E-10	0.993	0.50	1.062	0.222
de Wit (1984)	220884-26-5	Plane	Coarse	0.66	0.8	0.825	0.25	16187	9810	0.0008	37	33	3.85	49.8	0.260	0.0014	8.00E-04	1.E-03	8.15E-11	1.105	0.50	1.062	0.305
de Wit (1984)	220885-10-1	Slot	Beach sand	0.204	0.9	0.227	0.25	16187	9810	0.0002	37	49	1.48	49.8	0.264	0.0002	1.80E-04	1.E-03	1.83E-11	0.835	0.50	1.084	0.239
de Wit (1984)	220885-10-1	Slot	Beach sand	0.397	2.7	0.147	0.25	16187	9810	0.0002	37	83	1.48	49.8	0.317	0.0002	1.80E-04	1.E-03	1.83E-11	0.579	1.5	1.084	0.199
de Wit (1984)	220885-10-2	Slot	Beach sand	0.206	0.9	0.229	0.25	16187	9810	0.0002	37	83	1.48	49.8	0.317	0.0002	1.80E-04	1.E-03	1.83E-11	0.835	0.50	1.084	0.287
de Wit (1984)	220885-10-2	Slot	Beach sand	0.392	2.7	0.145	0.25	16187	9810	0.0002	37	83	1.48	49.8	0.317	0.0002	1.80E-04	1.E-03	1.83E-11	0.579	1.5	1.084	0.199
de Wit (1984)	220885-10-3	Slot	Beach sand	0.144	0.9	0.160	0.25	16187	9810	0.0002	37	49	1.48	49.8	0.264	0.0002	1.80E-04	1.E-03	1.83E-11	0.835	0.50	1.084	0.239
de Wit (1984)	220885-10-3	Slot	Beach sand	0.332	2.7	0.123	0.25	16187	9810	0.0002	37	83	1.48	49.8	0.317	0.0002	1.80E-04	1.E-03	1.83E-11	0.579	1.5	1.084	0.199
de Wit (1984)	220885-10-4	Slot	Beach sand	0.227	0.9	0.252	0.25	16187	9810	0.0002	37	83	1.48	49.8	0.317	0.0002	1.80E-04	1.E-03	1.83E-11	0.835	0.50	1.084	0.287
de Wit (1984)	220885-10-5	Slot	Beach sand	0.15	0.9	0.167	0.25	16187	9810	0.0002	37	49	1.48	49.8	0.264	0.0002	1.80E-04	1.E-03	1.83E-11	0.835	0.50	1.084	0.239
de Wit (1984)	220885-10-6	Slot	Beach sand	0.267	0.9	0.297	0.25	16187	9810	0.0002	37	83	1.48	49.8	0.317	0.0002	1.80E-04	1.E-03	1.83E-11	0.835	0.50	1.084	0.287
Hanses (1985)	21	Circle	Sand A	0.126	0.72	0.175	0.25	16187	9810	0.0003	37	100	1.3	49.8	0.333	0.0004	4.00E-04	1.E-03	4.08E-11	0.835	0.24	1.200	0.334
Hanses (1985)	22	Circle	Sand A	0.128	0.72	0.178	0.25	16187	9810	0.0003	37	100	1.3	49.8	0.333	0.0004	4.00E-04	1.E-03	4.08E-11	0.835	0.24	1.200	0.334
Hanses (1985)	23	Circle	Sand A	0.127	0.72	0.176	0.25	16187	9810	0.0003	37	102	1.3	49.8	0.336	0.0004	3.90E-04	1.E-03	3.98E-11	0.842	0.24	1.200	0.339
Hanses (1985)	24	Circle	Sand A	0.127	0.72	0.176	0.25	16187	9810	0.0003	37	105	1.3	49.8	0.339	0.0004	3.70E-04	1.E-03	3.77E-11	0.857	0.24	1.200	0.349

Table B.2: Data used in the review of the Sellmeijer et al. (2011) model (continued)

Reference	Test	Exit	Soil	Hc (m)	L (m)	i_c (-)	η (-)	γ'_p (N/m^3)	γ_u (N/m^3)	d_{50} (m)	θ (°)	RD (%)	U (-)	KAS (%)	FR	d_{70} (m)	K (m/s)	μ (Ns/m^2)	κ (m^2)	FS	D (m)	FG	i_c (-)
Hanses (1985)	25	Circle	Sand A	0.126	0.72	0.175	0.25	16187	9810	0.0003	37	100	1.3	49.8	0.333	0.0004	4.00E-04	1.E-03	4.08E-11	0.835	0.24	1.200	0.334
Hanses (1985)	51	Circle	Sand A	0.206	0.66	0.312	0.25	16187	9810	0.0003	37	99	1.3	49.8	0.332	0.0004	4.00E-04	1.E-03	4.08E-11	0.860	0.08	1.499	0.428
Hanses (1985)	52	Circle	Sand A	0.2	0.66	0.303	0.25	16187	9810	0.0003	37	87	1.3	49.8	0.317	0.0004	4.70E-04	1.E-03	4.79E-11	0.815	0.08	1.499	0.388
Hanses (1985)	53	Circle	Sand A	0.17	0.66	0.258	0.25	16187	9810	0.0003	37	92	1.3	49.8	0.324	0.0004	4.40E-04	1.E-03	4.49E-11	0.833	0.08	1.499	0.404
Hanses (1985)	71	Circle	Sand A	0.276	2.64	0.105	0.25	16187	9810	0.0003	37	87	1.3	49.8	0.317	0.0004	4.70E-04	1.E-03	4.79E-11	0.513	0.33	1.501	0.244
Hanses (1985)	73	Circle	Sand A	0.275	2.64	0.104	0.25	16187	9810	0.0003	37	80	1.3	49.8	0.308	0.0004	5.10E-04	1.E-03	5.20E-11	0.499	0.33	1.501	0.231
Hanses (1985)	26a	Circle	Sand A	0.107	0.72	0.149	0.25	16187	9810	0.0003	37	96	1.3	49.8	0.328	0.0004	4.20E-04	1.E-03	4.28E-11	0.822	0.24	1.200	0.324
Silvis (1991)	2	Slot	Marsdiepzar	1.053	9	0.117	0.25	16187	9810	0.0002	37	65	1.57	49.8	0.294	0.0002	5.10E-05	1.E-03	5.20E-12	0.618	6.00	1.050	0.191
Silvis (1991)	3	Slot	Marsdiepzand	1.689	12	0.141	0.25	16187	9810	0.0002	37	65	1.57	49.8	0.294	0.0002	5.10E-05	1.E-03	5.20E-12	0.562	6.00	1.105	0.182
van Beek et al. (2011a)	B101	Slope	Baskarp	0.08	0.31	0.258	0.25	16187	9810	0.0001	37	31	1.54	49.8	0.226	0.0002	1.00E-04	1.E-03	1.02E-11	1.257	0.10	1.208	0.343
van Beek et al. (2011a)	B103	Slope	Baskarp	0.08	0.32	0.250	0.25	16187	9810	0.0001	37	9	1.54	49.8	0.147	0.0002	1.60E-04	1.E-03	1.63E-11	1.063	0.10	1.217	0.190
van Beek et al. (2011a)	B105	Slope	Baskarp	0.16	0.335	0.478	0.25	16187	9810	0.0001	37	83	1.54	49.8	0.319	0.0002	7.60E-05	1.E-03	7.75E-12	1.342	0.10	1.229	0.526
van Beek et al. (2011a)	B107	Slope	Baskarp	0.18	0.333	0.541	0.25	16187	9810	0.0001	37	88	1.54	49.8	0.326	0.0002	6.10E-05	1.E-03	6.22E-12	1.447	0.10	1.227	0.578
van Beek et al. (2011a)	B121	Slope	Baskarp	0.09	0.335	0.269	0.25	16187	9810	0.0001	37	13	1.54	49.8	0.167	0.0002	1.80E-04	1.E-03	1.83E-11	1.007	0.10	1.229	0.206
van Beek et al. (2011a)	B122	Slope	Baskarp	0.08	0.335	0.239	0.25	16187	9810	0.0001	37	12	1.54	49.8	0.162	0.0002	1.60E-04	1.E-03	1.63E-11	1.047	0.10	1.229	0.209
van Beek et al. (2011a)	B123B	Slope	Baskarp	0.13	0.332	0.392	0.25	16187	9810	0.0001	37	12	1.54	49.8	0.162	0.0002	9.50E-05	1.E-03	9.68E-12	1.250	0.10	1.226	0.249
van Beek et al. (2011a)	B19	Slope	Baskarp	0.114	0.34	0.335	0.25	16187	9810	0.0001	37	64	1.54	49.8	0.291	0.0002	1.50E-04	1.E-03	1.53E-11	1.065	0.10	1.233	0.382
van Beek et al. (2011a)	B23	Slope	Baskarp	0.193	0.338	0.571	0.25	16187	9810	0.0001	37	98	1.54	49.8	0.338	0.0002	5.90E-05	1.E-03	6.01E-12	1.456	0.10	1.231	0.606
van Beek et al. (2011a)	B24	Slope	Baskarp	0.172	0.338	0.509	0.25	16187	9810	0.0001	37	97	1.54	49.8	0.337	0.0002	6.80E-04	1.E-03	6.93E-11	0.645	0.10	1.231	0.267
van Beek et al. (2011a)	B28	Slope	Baskarp	0.071	0.335	0.212	0.25	16187	9810	0.0001	37	37	1.54	49.8	0.241	0.0002	2.70E-04	1.E-03	2.75E-11	0.880	0.10	1.229	0.260
van Beek et al. (2011a)	B35	Slope	Baskarp	0.135	0.335	0.403	0.25	16187	9810	0.0001	37	64	1.54	49.8	0.291	0.0002	1.30E-04	1.E-03	1.33E-11	1.122	0.10	1.229	0.402
van Beek et al. (2011a)	B36	Slope	Baskarp	0.137	0.334	0.410	0.25	16187	9810	0.0001	37	63	1.54	49.8	0.290	0.0002	1.10E-04	1.E-03	1.12E-11	1.188	0.10	1.228	0.423

Table B.2: Data used in the review of the Sellmeijer et al. (2011) model (continued)

Reference	Test	Exit	Soil	Hc (m)	L (m)	i_c (-)	η (-)	γ'_p (N/m^3)	γ_u (N/m^3)	d_{50} (m)	θ (°)	RD (%)	U (-)	KAS (%)	FR	d_{70} (m)	K (m/s)	μ (Ns/m^2)	κ (m^2)	FS	D (m)	FG	i_c (-)
van Beek et al. (2011a)	B40	Slope	Baskarp	0.148	0.332	0.446	0.25	16187	9810	0.0001	37	91	1.54	49.8	0.330	0.0002	5.30E-05	1.E-03	5.40E-12	1.518	0.10	1.226	0.614
van Beek et al. (2011a)	B41	Slope	Baskarp	0.153	0.334	0.458	0.25	16187	9810	0.0001	37	92	1.54	49.8	0.331	0.0002	7.30E-05	1.E-03	7.44E-12	1.362	0.10	1.228	0.553
van Beek et al. (2011a)	B54	Slope	Baskarp	0.18	0.33	0.545	0.25	16187	9810	0.0001	37	79	1.54	49.8	0.314	0.0002	7.40E-05	1.E-03	7.54E-12	1.361	0.10	1.225	0.523
van Beek et al. (2011a)	B55	Slope	Baskarp	0.141	0.325	0.434	0.25	16187	9810	0.0001	37	71	1.54	49.8	0.302	0.0002	8.80E-05	1.E-03	8.97E-12	1.291	0.10	1.221	0.476
van Beek et al. (2011a)	B57	Slope	Baskarp	0.132	0.33	0.400	0.25	16187	9810	0.0001	37	75	1.54	49.8	0.308	0.0002	8.80E-05	1.E-03	8.97E-12	1.285	0.10	1.225	0.485
van Beek et al. (2011a)	B58	Slope	Baskarp	0.182	0.345	0.528	0.25	16187	9810	0.0001	37	70	1.54	49.8	0.301	0.0002	1.00E-04	1.E-03	1.02E-11	1.213	0.10	1.237	0.451
van Beek et al. (2011a)	B61	Slope	Baskarp	0.114	0.345	0.330	0.25	16187	9810	0.0001	37	73	1.54	49.8	0.305	0.0002	9.90E-05	1.E-03	1.01E-11	1.217	0.10	1.237	0.459
van Beek et al. (2011a)	B82	Slope	Baskarp	0.139	0.336	0.414	0.25	16187	9810	0.0001	37	85	1.54	49.8	0.322	0.0002	5.90E-05	1.E-03	6.01E-12	1.459	0.10	1.230	0.577
van Beek et al. (2011a)	B83	Slope	Baskarp	0.139	0.334	0.416	0.25	16187	9810	0.0001	37	85	1.54	49.8	0.322	0.0002	6.00E-05	1.E-03	6.12E-12	1.454	0.10	1.228	0.574
van Beek et al. (2011a)	B84	Slope	Baskarp	0.098	0.334	0.293	0.25	16187	9810	0.0001	37	53	1.54	49.8	0.273	0.0002	9.70E-05	1.E-03	9.89E-12	1.239	0.10	1.228	0.415
van Beek et al. (2011a)	B85	Slope	Baskarp	0.118	0.336	0.351	0.25	16187	9810	0.0001	37	53	1.54	49.8	0.273	0.0002	7.70E-05	1.E-03	7.85E-12	1.335	0.10	1.230	0.448
van Beek et al. (2011a)	B86	Slope	Baskarp	0.098	0.336	0.292	0.25	16187	9810	0.0001	37	43	1.54	49.8	0.254	0.0002	1.00E-04	1.E-03	1.02E-11	1.224	0.10	1.230	0.381
van Beek et al. (2011a)	B87	Slope	Baskarp	0.046	0.336	0.137	0.25	16187	9810	0.0001	37	42	1.54	49.8	0.251	0.0002	1.80E-04	1.E-03	1.83E-11	1.006	0.10	1.230	0.311
van Beek et al. (2011a)	BMS1	Slope	Baskarp	0.28	1.37	0.204	0.25	16187	9810	0.0001	37	60	1.54	49.8	0.285	0.0002	1.20E-04	1.E-03	1.22E-11	0.721	0.40	1.235	0.254
van Beek et al. (2011a)	BMS2	Slope	Baskarp	0.37	1.45	0.255	0.25	16187	9810	0.0001	37	50	1.54	49.8	0.267	0.0002	1.40E-04	1.E-03	1.43E-11	0.672	0.40	1.250	0.224
van Beek et al. (2011a)	BMS7	Slope	Baskarp	0.29	1.3	0.223	0.25	16187	9810	0.0001	37	64	1.54	49.8	0.291	0.0002	1.50E-04	1.E-03	1.53E-11	0.681	0.40	1.221	0.242
van Beek et al. (2011a)	BMS8	Slope	Baskarp	0.19	1.33	0.143	0.25	16187	9810	0.0001	37	50	1.54	49.8	0.267	0.0002	2.60E-04	1.E-03	2.65E-11	0.563	0.40	1.227	0.184
van Beek et al. (2011a)	D31	Slope	Dekzand Nunspeet	0.179	0.332	0.539	0.25	16187	9810	0.0001	37	65	2.6	49.8	0.314	0.0002	6.20E-05	1.E-03	6.32E-12	1.574	0.10	1.226	0.605
van Beek et al. (2011a)	D32	Slope	Dekzand Nunspeet	0.138	0.332	0.416	0.25	16187	9810	0.0001	37	65	2.6	49.8	0.314	0.0002	8.30E-05	1.E-03	8.46E-12	1.428	0.10	1.226	0.549

Table B.2: Data used in the review of the Sellmeijer et al. (2011) model (continued)

Reference	Test	Exit	Soil	Hc (m)	L (m)	i_c (-)	η (-)	γ'_p (N/m^3)	γ_u (N/m^3)	d_{50} (m)	θ (°)	RD (%)	U (-)	KAS (%)	FR	d_{70} (m)	K (m/s)	μ (Ns/m^2)	κ (m^2)	FS	D (m)	FG	i_c (-)
van Beek et al. (2011a)	D37	Slope	Dekzand Nunspeet	0.265	0.334	0.793	0.25	16187	9810	0.0001	37	98	2.6	49.8	0.362	0.0002	3.90E-05	1.E-03	3.98E-12	1.833	0.10	1.228	0.815
van Beek et al. (2011a)	D38	Slope	Dekzand Nunspeet	0.165	0.335	0.493	0.25	16187	9810	0.0001	37	92	2.6	49.8	0.354	0.0002	5.90E-05	1.E-03	6.01E-12	1.595	0.10	1.229	0.694
van Beek et al. (2011a)	D39	Slope	Dekzand Nunspeet	0.139	0.331	0.420	0.25	16187	9810	0.0001	37	92	2.6	49.8	0.354	0.0002	5.40E-05	1.E-03	5.50E-12	1.649	0.10	1.226	0.716
van Beek et al. (2011a)	I-137	Plane	Enschede	0.26	0.33	0.788	0.25	16187	9810	0.0004	37	98	1.6	49.8	0.340	0.0004	3.10E-04	1.E-03	3.16E-11	1.274	0.10	1.225	0.530
van Beek et al. (2011a)	I-138	Plane	Enschede	0.28	0.33	0.848	0.25	16187	9810	0.0004	37	97	1.6	49.8	0.339	0.0004	2.80E-04	1.E-03	2.85E-11	1.318	0.10	1.225	0.547
van Beek et al. (2011a)	I45	Slope	Itterbeck Boxtel	0.203	0.332	0.611	0.25	16187	9810	0.0002	37	72	2.2	49.8	0.318	0.0002	8.80E-05	1.E-03	8.97E-12	1.429	0.10	1.226	0.557
van Beek et al. (2011a)	I46	Slope	Itterbeck Boxtel	0.155	0.337	0.460	0.25	16187	9810	0.0002	37	70	2.2	49.8	0.315	0.0002	1.10E-04	1.E-03	1.12E-11	1.320	0.10	1.230	0.511
van Beek et al. (2011a)	I47	Slope	Itterbeck Enschede	0.087	0.34	0.256	0.25	16187	9810	0.0004	37	75	1.6	49.8	0.310	0.0004	7.30E-04	1.E-03	7.44E-11	0.948	0.10	1.233	0.362
van Beek et al. (2011a)	I48	Slope	Itterbeck Enschede	0.079	0.34	0.232	0.25	16187	9810	0.0004	37	76	1.6	49.8	0.311	0.0004	1.10E-03	1.E-03	1.12E-10	0.827	0.10	1.233	0.317
van Beek et al. (2011a)	I49	Slope	Hoherstall Waalre	0.069	0.34	0.203	0.25	16187	9810	0.0003	37	76	1.58	49.8	0.310	0.00040	8.00E-04	1.E-03	8.15E-11	0.893	0.10	1.233	0.342
van Beek et al. (2011a)	I50	Slope	Hoherstall Waalre	0.047	0.332	0.142	0.25	16187	9810	0.0003	37	73	1.58	49.8	0.306	0.00040	2.20E-03	1.E-03	2.24E-10	0.642	0.10	1.226	0.241
van Beek et al. (2011a)	I51	Slope	Itterbeck Sandr	0.112	0.335	0.334	0.25	16187	9810	0.0002	37	70	1.5	49.8	0.300	0.00020	1.70E-04	1.E-03	1.73E-11	1.128	0.10	1.229	0.415
van Beek et al. (2011a)	I52	Slope	Hoherstall Waalre	0.092	0.331	0.278	0.25	16187	9810	0.0003	37	71	1.58	49.8	0.303	0.00040	7.00E-04	1.E-03	7.14E-11	0.942	0.10	1.226	0.350
van Beek et al. (2011a)	I53	Slope	Itterbeck Sandr	0.128	0.325	0.394	0.25	16187	9810	0.0002	37	74	1.5	49.8	0.306	0.00020	1.10E-04	1.E-03	1.12E-11	1.317	0.10	1.221	0.491
van Beek et al. (2011a)	I56	Slope	Itterbeck Scheemda	0.1	0.335	0.299	0.25	16187	9810	0.0002	37	69	1.3	49.8	0.293	0.00018	1.30E-04	1.E-03	1.33E-11	1.181	0.10	1.229	0.425
van Beek et al. (2011a)	I62	Slope	Itterbeck Scheemda	0.099	0.325	0.305	0.25	16187	9810	0.0002	37	63	1.3	49.8	0.283	0.00018	2.00E-04	1.E-03	2.04E-11	1.033	0.10	1.221	0.358
van Beek et al. (2011a)	Ijkfs01	Plane	Fine Ijkdijk	2.3	15	0.153	0.25	16187	9810	0.0001	37	60	1.6	49.8	0.286	0.0002	8.00E-05	1.E-03	8.15E-12	0.395	3.00	1.345	0.152
van Beek et al. (2011a)	Ijkfs02	Plane	Coarse Ijkdijk	1.75	15	0.117	0.25	16187	9810	0.0002	37	75	1.8	49.8	0.314	0.0003	1.40E-04	1.E-03	1.43E-11	0.380	2.85	1.361	0.163
van Beek et al. (2011a)	Ijkfs03	Plane	Fine Ijkdijk	2.1	15	0.140	0.25	16187	9810	0.0001	37	60	1.6	49.8	0.286	0.0002	8.00E-05	1.E-03	8.15E-12	0.395	3.00	1.345	0.152

Table B.2: Data used in the review of the Sellmeijer et al. (2011) model (continued)

Reference	Test	Exit	Soil	Hc (m)	L (m)	i_c (-)	η (-)	γ'_p (N/m^3)	γ_u (N/m^3)	d_{50} (m)	θ (°)	RD (%)	U (-)	KAS (%)	FR	d_{70} (m)	K (m/s)	μ (Ns/m^2)	κ (m^2)	FS	D (m)	FG	i_c (-)
van Beek et al. (2011a)	Ijkfs04	Plane	Coarse Ijkdijk	2	15	0.133	0.25	16187	9810	0.0002	37	75	1.8	49.8	0.314	0.0003	1.20E-04	1.E-03	1.22E-11	0.400	2.85	1.361	0.171
van Beek et al. (2011a)	IJKMS1	Slope	Itterbeck 431	0.26	1.43	0.182	0.25	16187	9810	0.0003	37	47	2.6	49.8	0.280	0.0005	1.60E-04	1.E-03	1.63E-11	1.034	0.40	1.246	0.361
van Beek et al. (2011a)	IJKMS9	Slope	Itterbeck 333	0.345	1.46	0.236	0.25	16187	9810	0.0003	37	50	2.1	49.8	0.278	0.0004	2.30E-04	1.E-03	2.34E-11	0.789	0.40	1.252	0.275
van Beek et al. (2011a)	IMS11	Slope	Itterbeck 333	0.59	1.48	0.399	0.25	16187	9810	0.0003	37	65	2.1	49.8	0.305	0.0004	4.30E-04	1.E-03	4.38E-11	0.637	0.40	1.256	0.244
van Beek et al. (2011a)	IMS12	Slope	Itterbeck 431	0.39	1.44	0.271	0.25	16187	9810	0.0003	37	65	2.6	49.8	0.314	0.0005	4.00E-04	1.E-03	4.08E-11	0.760	0.40	1.248	0.298
van Beek et al. (2011a)	IMS13	Slope	Coarse Ijkdijk	0.37	1.45	0.255	0.25	16187	9810	0.0002	37	55	1.8	49.8	0.282	0.0003	4.60E-04	1.E-03	4.69E-11	0.557	0.40	1.250	0.196
van Beek et al. (2011a)	IMS14	Slope	Fine Ijkdijk	0.48	1.46	0.329	0.25	16187	9810	0.0001	37	50	1.6	49.8	0.269	0.0002	3.80E-04	1.E-03	3.87E-11	0.511	0.40	1.252	0.172
van Beek et al. (2011a)	IMS3	Slope	Itterbeck 125-250	0.26	1.455	0.179	0.25	16187	9810	0.0002	37	64	1.7	49.8	0.295	0.0002	2.00E-04	1.E-03	2.04E-11	0.675	0.40	1.251	0.249
van Beek et al. (2011a)	IMS4	Slope	Itterbeck 125-250	0.2	1.455	0.137	0.25	16187	9810	0.0002	37	51	1.7	49.8	0.273	0.0002	3.70E-04	1.E-03	3.77E-11	0.549	0.40	1.251	0.187
van Beek et al. (2011a)	IMS5	Slope	Itterbeck 125-250	0.29	1.415	0.205	0.25	16187	9810	0.0002	37	75	1.7	49.8	0.312	0.0002	2.20E-04	1.E-03	2.24E-11	0.660	0.40	1.244	0.256
van Beek et al. (2011a)	O43	Slope	Oostelijke	0.099	0.332	0.298	0.25	16187	9810	0.0002	37	75	2.06	49.8	0.320	0.0003	4.20E-04	1.E-03	4.28E-11	1.003	0.10	1.226	0.394
van Beek et al. (2011a)	S63	Slope	Hoherstall Sterksel	0.125	0.34	0.368	0.25	16187	9810	0.0002	37	75	2.25	49.8	0.324	0.0003	2.40E-04	1.E-03	2.45E-11	1.189	0.10	1.233	0.474
van Beek et al. (2011a)	S64	Slope	Hoherstall Sterksel	0.12	0.335	0.358	0.25	16187	9810	0.0002	37	75	2.25	49.8	0.324	0.0003	1.70E-04	1.E-03	1.73E-11	1.340	0.10	1.229	0.533
van Beek (2015)	B115	Circle	Baskarp 1	0.08	0.344	0.233	0.25	16187	9810	0.0001	37	89	1.54	49.8	0.327	0.0002	5.40E-05	1.E-03	5.50E-12	1.491	0.10	1.236	0.603
van Beek (2015)	B118	Circle	Baskarp 1	0.08	0.344	0.233	0.25	16187	9810	0.0001	37	89	1.54	49.8	0.327	0.0002	6.30E-05	1.E-03	6.42E-12	1.416	0.10	1.236	0.572
van Beek (2015)	B132	Circle	Baskarp 1	0.065	0.344	0.189	0.25	16187	9810	0.0001	37	65	1.54	49.8	0.293	0.0002	9.30E-05	1.E-03	9.48E-12	1.244	0.10	1.236	0.450
van Beek (2015)	B133	Circle	Baskarp 1	0.065	0.344	0.189	0.25	16187	9810	0.0001	37	65	1.54	49.8	0.293	0.0002	9.50E-05	1.E-03	9.68E-12	1.235	0.10	1.236	0.447
van Beek (2015)	b142	Circle	Baskarp 1	0.08	0.344	0.233	0.25	16187	9810	0.0001	37	91	1.54	49.8	0.330	0.0002	6.20E-05	1.E-03	6.32E-12	1.424	0.10	1.236	0.580
van Beek (2015)	b143	Circle	Baskarp 1	0.084	0.344	0.244	0.25	16187	9810	0.0001	37	91	1.54	49.8	0.330	0.0002	5.50E-05	1.E-03	5.61E-12	1.482	0.10	1.236	0.604
van Beek (2015)	B144	Circle	Baskarp 1	0.085	0.344	0.247	0.25	16187	9810	0.0001	37	91	1.54	49.8	0.330	0.0002	5.30E-05	1.E-03	5.40E-12	1.500	0.10	1.236	0.611
van Beek (2015)	b145	Circle	Baskarp 1	0.069	0.344	0.201	0.25	16187	9810	0.0001	37	65	1.54	49.8	0.293	0.0002	8.00E-05	1.E-03	8.15E-12	1.308	0.10	1.236	0.474
van Beek (2015)	b146	Circle	Baskarp 1	0.07	0.344	0.203	0.25	16187	9810	0.0001	37	65	1.54	49.8	0.293	0.0002	8.00E-05	1.E-03	8.15E-12	1.308	0.10	1.236	0.474

Table B.2: Data used in the review of the Sellmeijer et al. (2011) model (continued)

Reference	Test	Exit	Soil	Hc (m)	L (m)	i_c (-)	η (-)	γ'_p (N/m^3)	γ_u (N/m^3)	d_{50} (m)	θ (°)	RD (%)	U (-)	KAS (%)	FR	d_{70} (m)	K (m/s)	μ (Ns/m^2)	κ (m^2)	FS	D (m)	FG	i_c (-)
van Beek (2015)	Bms1	Circle	Baskarp 2	0.21	1.3	0.152	0.25	16187	9810	0.0001	37	94	1.5	49.8	0.332	0.0002	8.00E-05	1.E-03	8.15E-12	0.835	0.40	1.219	0.338
van Beek (2015)	e150	Circle	Enschede sand	0.099	0.344	0.288	0.25	16187	9810	0.0004	37	100	1.6	49.8	0.342	0.0004	4.10E-04	1.E-03	4.18E-11	1.145	0.10	1.236	0.484
van Beek (2015)	E169	Circle	Enschede sand	0.09	0.344	0.262	0.25	16187	9810	0.0004	37	94	1.6	49.8	0.335	0.0004	3.20E-04	1.E-03	3.26E-11	1.243	0.10	1.236	0.515
van Beek (2015)	I164	Circle	Itterbeck 125-250	0.113	0.344	0.328	0.25	16187	9810	0.0002	37	97	1.7	49.8	0.341	0.0003	1.30E-04	1.E-03	1.33E-11	1.409	0.10	1.236	0.594
van Beek (2015)	I165	Circle	Itterbeck 125-250	0.096	0.344	0.279	0.25	16187	9810	0.0002	37	93	1.7	49.8	0.336	0.0003	1.40E-04	1.E-03	1.43E-11	1.374	0.10	1.236	0.571
van Beek (2015)	I166	Circle	Itterbeck Mix 1	0.21	0.344	0.610	0.25	16187	9810	0.0002	37	100	2.43	49.8	0.361	0.0002	4.60E-05	1.E-03	4.69E-12	1.824	0.10	1.236	0.815
van Beek (2015)	I167	Circle	Itterbeck Mix 2	0.152	0.344	0.442	0.25	16187	9810	0.0001	37	93	3.17	49.8	0.365	0.0002	3.70E-05	1.E-03	3.77E-12	1.889	0.10	1.236	0.851
van Beek (2015)	I168	Circle	Itterbeck Mix 2	0.205	0.344	0.596	0.25	16187	9810	0.0001	37	89	3.17	49.8	0.359	0.0002	2.70E-05	1.E-03	2.75E-12	2.098	0.10	1.236	0.931
van Beek (2015)	Ims18	Circle	Itterbeck 0.33mm	0.33	1.3	0.238	0.25	16187	9810	0.0003	37	87	1.6	49.8	0.326	0.0004	3.50E-04	1.E-03	3.57E-11	0.759	0.40	1.219	0.302
van Beek (2015)	Ims20	Circle	Itterbeck 0.33mm	0.194	1.3	0.140	0.25	16187	9810	0.0003	37	91	1.6	49.8	0.331	0.0004	3.90E-04	1.E-03	3.98E-11	0.733	0.40	1.219	0.296
van Beek (2015)	O140	Circle	Oostelijke	0.095	0.344	0.276	0.25	16187	9810	0.0002	37	65	2.06	49.8	0.304	0.0003	2.00E-04	1.E-03	2.04E-11	1.270	0.10	1.236	0.477
van Beek (2015)	O141	Circle	Oostelijke	0.09	0.344	0.262	0.25	16187	9810	0.0002	37	65	2.06	49.8	0.304	0.0003	2.10E-04	1.E-03	2.14E-11	1.249	0.10	1.236	0.470
van Beek (2015)	O163	Circle	Oostelijke	0.185	0.344	0.538	0.25	16187	9810	0.0002	37	94	2.06	49.8	0.346	0.0003	1.30E-04	1.E-03	1.33E-11	1.466	0.10	1.236	0.627
van Beek (2015)	S170	Circle	Sterksel	0.35	0.344	1.017	0.25	16187	9810	0.0002	37	89	2.25	49.8	0.344	0.0003	7.60E-05	1.E-03	7.75E-12	1.737	0.10	1.236	0.738
van Beek (2015)	W130	Circle	Hoherstall waalre	0.106	0.344	0.308	0.25	16187	9810	0.0003	37	65	1.58	49.8	0.294	0.0004	5.10E-04	1.E-03	5.20E-11	1.033	0.10	1.236	0.375
van Beek (2015)	W131	Circle	Hoherstall waalre	0.086	0.344	0.250	0.25	16187	9810	0.0003	37	65	1.58	49.8	0.294	0.0004	5.40E-04	1.E-03	5.50E-11	1.014	0.10	1.236	0.368
this study	20	Circle	SS	0.233	1.3	0.179	0.25	16187	9810	0.0003	37	50	1.3	49.8	0.261	0.0004	3.40E-04	1.E-03	3.47E-11	0.720	0.31	1.292	0.243
this study	21	Slot	SS	0.271	1.3	0.208	0.25	16187	9810	0.0003	37	50	1.3	49.8	0.261	0.0004	3.40E-04	1.E-03	3.47E-11	0.720	0.31	1.292	0.243
this study	22	Circle	SS	0.195	1.3	0.150	0.25	16187	9810	0.0003	37	50	1.3	49.8	0.261	0.0004	3.10E-04	1.E-03	3.16E-11	0.742	0.31	1.292	0.251
this study	23	Slot	SS	0.256	1.3	0.197	0.25	16187	9810	0.0003	37	50	1.3	49.8	0.261	0.0004	3.10E-04	1.E-03	3.16E-11	0.742	0.31	1.292	0.251
this study	24	Circle	SS	0.236	1.3	0.182	0.25	16187	9810	0.0003	37	50	1.3	49.8	0.261	0.0004	3.10E-04	1.E-03	3.16E-11	0.742	0.31	1.292	0.251
this study	25	Slot	SS	0.271	1.3	0.208	0.25	16187	9810	0.0003	37	50	1.3	49.8	0.261	0.0004	3.10E-04	1.E-03	3.16E-11	0.742	0.31	1.292	0.251
this study	27	Circle	SS	0.213	1.3	0.164	0.25	16187	9810	0.0003	37	50	1.3	49.8	0.261	0.0004	3.00E-04	1.E-03	3.06E-11	0.750	0.31	1.292	0.253
this study	28	Plane	SS	0.293	1.3	0.225	0.25	16187	9810	0.0003	37	50	1.3	49.8	0.261	0.0004	3.30E-04	1.E-03	3.36E-11	0.727	0.31	1.292	0.246
this study	29	Slot	SS	0.234	1.3	0.180	0.25	16187	9810	0.0003	37	50	1.3	49.8	0.261	0.0004	3.57E-04	1.E-03	3.64E-11	0.708	0.31	1.292	0.239
this study	30	Plane	SS	0.313	1.3	0.241	0.25	16187	9810	0.0003	37	50	1.3	49.8	0.261	0.0004	3.30E-04	1.E-03	3.36E-11	0.727	0.31	1.292	0.246
this study	31	Circle	SS	0.195	1.3	0.150	0.25	16187	9810	0.0003	37	50	1.3	49.8	0.261	0.0004	2.80E-04	1.E-03	2.85E-11	0.768	0.31	1.292	0.259
this study	32	Plane	SS	0.331	1.3	0.255	0.25	16187	9810	0.0003	37	50	1.3	49.8	0.261	0.0004	3.30E-04	1.E-03	3.36E-11	0.727	0.31	1.292	0.246
this study	33	Slope	SS	0.342	1.3	0.263	0.25	16187	9810	0.0003	37	50	1.3	49.8	0.261	0.0004	3.73E-04	1.E-03	3.80E-11	0.698	0.31	1.292	0.236
this study	34	Circle	SS	0.203	1.3	0.156	0.25	16187	9810	0.0003	37	50	1.3	49.8	0.261	0.0004	3.73E-04	1.E-03	3.80E-11	0.698	0.31	1.292	0.236
this study	35	Slope	SS	0.307	1.3	0.236	0.25	16187	9810	0.0003	37	50	1.3	49.8	0.261	0.0004	4.35E-04	1.E-03	4.43E-11	0.663	0.31	1.292	0.224
this study	36	Slope	SS	0.335	1.3	0.258	0.25	16187	9810	0.0003	37	50	1.3	49.8	0.261	0.0004	3.57E-04	1.E-03	3.64E-11	0.708	0.31	1.292	0.239
this study	37	Slot	SS	0.237	1.3	0.182	0.25	16187	9810	0.0003	37	50	1.3	49.8	0.261	0.0004	3.73E-04	1.E-03	3.80E-11	0.698	0.31	1.292	0.236
this study	40	Slot	SS	0.273	1.3	0.210	0.25	16187	9810	0.0003	37	50	1.3	49.8	0.261	0.0004	3.57E-04	1.E-03	3.64E-11	0.708	0.31	1.292	0.239
this study	41	Slot	SS	0.481	2.6	0.185	0.25	16187	9810	0.0003	37	50	1.3	49.8	0.261	0.0004	3.73E-04	1.E-03	3.80E-11	0.554	0.31	1.518	0.220
this study	42	Circle	SS	0.186	1.3	0.143	0.25	16187	9810	0.0003	37	50	1.3	49.8	0.261	0.0004	4.19E-04	1.E-03	4.27E-11	0.671	0.31	1.292	0.227
this study	45	Slot	SS	0.73	3.9	0.187	0.25	16187	9810	0.0003	37	50	1.3	49.8	0.261	0.0004	3.30E-04	1.E-03	3.36E-11	0.504	0.31	1.672	0.220
this study	49	Circle	SS	0.196	1.3	0.151	0.25	16187	9810	0.0003	37	50	1.3	49.8	0.261	0.0004	2.90E-04	1.E-03	2.96E-11	0.759	0.31	1.292	0.256
this study	50	Circle	2	0.661	1.3	0.508	0.25	16187	9810	0.0006	37	50	4.15	49.8	0.304	0.0011	3.90E-04	1.E-03	3.98E-11	1.087	0.31	1.292	0.427
this study	52	Circle	4	2.476	1.3	1.905	0.25	16187	9810	0.0014	37	50	8.75	49.8	0.335	0.003	6.50E-04	1.E-03	6.63E-11	1.370	0.31	1.292	0.593
this study	53	Circle	3	1.014	1.3	0.780	0.25	16187	9810	0.001	37	50	6.19	49.8	0.320	0.0018	7.10E-04	1.E-03	7.24E-11	1.084	0.31	1.292	0.449

Table B.2: Data used in the review of the Sellmeijer et al. (2011) model (continued)

Reference	Test	Exit	Soil	Hc (m)	L (m)	i_c (-)	η (-)	γ'_p (N/m^3)	γ_u (N/m^3)	d_{50} (m)	θ (°)	RD (%)	U (-)	KAS (%)	FR	d_{70} (m)	K (m/s)	μ (Ns/m^2)	κ (m^2)	FS	D (m)	FG	i_c (-)
this study	55	Slot	SS	0.439	2.6	0.169	0.25	16187	9810	0.0003	37	50	1.3	49.8	0.261	0.0004	3.30E-04	1.E-03	3.36E-11	0.577	0.31	1.518	0.229
this study	57	Circle	50n	0.324	1.3	0.249	0.25	16187	9810	0.0002	37	50	1.9	49.8	0.275	0.0002	1.00E-04	1.E-03	1.02E-11	0.931	0.31	1.292	0.330
this study	58	Circle	5	1.28	1.3	0.985	0.25	16187	9810	0.0024	37	50	6.08	49.8	0.319	0.0046	2.90E-03	1.E-03	2.96E-10	0.987	0.31	1.292	0.407
this study	59	Circle	6	0.51	1.3	0.392	0.25	16187	9810	0.0002	37	50	2.59	49.8	0.286	0.0002	2.90E-05	1.E-03	2.96E-12	1.406	0.31	1.292	0.519
this study	60	Circle	50n	0.225	1.3	0.173	0.25	16187	9810	0.0002	37	50	1.9	49.8	0.275	0.0002	1.60E-04	1.E-03	1.63E-11	0.796	0.31	1.292	0.282
this study	61	Circle	2	0.651	1.3	0.501	0.25	16187	9810	0.0006	37	50	4.15	49.8	0.304	0.0011	3.90E-04	1.E-03	3.98E-11	1.087	0.31	1.292	0.427
this study	62	Circle	8	1.315	1.3	1.012	0.25	16187	9810	0.0002	37	50	6.36	49.8	0.321	0.0002	1.50E-05	1.E-03	1.53E-12	1.752	0.31	1.292	0.727
this study	63	Circle	3	0.863	1.3	0.664	0.25	16187	9810	0.001	37	50	6.19	49.8	0.320	0.0018	7.10E-04	1.E-03	7.24E-11	1.084	0.31	1.292	0.449
this study	64	Circle	8	1.028	1.3	0.791	0.25	16187	9810	0.0002	37	50	6.36	49.8	0.321	0.0002	1.50E-05	1.E-03	1.53E-12	1.752	0.31	1.292	0.727
this study	66	Slope	SS	0.386	1.3	0.297	0.25	16187	9810	0.0003	37	50	1.3	49.8	0.261	0.0004	2.50E-04	1.E-03	2.55E-11	0.797	0.31	1.292	0.269
this study	67	Circle	7	0.853	1.3	0.656	0.25	16187	9810	0.0002	37	50	3.23	49.8	0.294	0.0002	1.60E-05	1.E-03	1.63E-12	1.714	0.31	1.292	0.652
this study	68	Slot	SS	0.69	3.9	0.177	0.25	16187	9810	0.0003	37	50	1.3	49.8	0.261	0.0004	3.30E-04	1.E-03	3.36E-11	0.504	0.31	1.672	0.220
this study	69	Circle	7	0.802	1.3	0.617	0.25	16187	9810	0.0002	37	50	3.23	49.8	0.294	0.0002	1.90E-05	1.E-03	1.94E-12	1.619	0.31	1.292	0.615
this study	73	Circle	4	2.675	1.3	2.058	0.25	16187	9810	0.0014	37	50	8.75	49.8	0.335	0.003	6.00E-04	1.E-03	6.12E-11	1.407	0.31	1.292	0.609
this study	74	Circle	5	1.02	1.3	0.785	0.25	16187	9810	0.0024	37	50	6.08	49.8	0.319	0.0046	2.40E-03	1.E-03	2.45E-10	1.051	0.31	1.292	0.434
this study	75	Circle	8	1.64	1.3	1.262	0.25	16187	9810	0.0002	37	50	6.36	49.8	0.321	0.0002	7.00E-06	1.E-03	7.14E-13	2.258	0.31	1.292	0.938
this study	76	Slope	SS	0.366	1.3	0.282	0.25	16187	9810	0.0003	37	50	1.3	49.8	0.261	0.0004	4.20E-04	1.E-03	4.28E-11	0.671	0.31	1.292	0.227
this study	78	Circle	6	0.475	1.3	0.365	0.25	16187	9810	0.0002	37	50	2.59	49.8	0.286	0.0002	3.40E-04	1.E-03	3.47E-11	0.619	0.31	1.292	0.229
this study	79	Circle	SS	0.239	1.3	0.184	0.25	16187	9810	0.0003	37	50	1.3	49.8	0.261	0.0004	3.40E-04	1.E-03	3.47E-11	0.720	0.31	1.292	0.243